A Survey of Stellar Families: Multiplicity of Solar-Type Stars

A Dissertation

Presented in Partial Fulfillment of Requirements for the Degree of

Doctor of Philosophy

in the College of Arts and Sciences

Georgia State University

2009

by

Deepak Raghavan

Committee:

Dr. Harold A. McAlister, Chair

Dr. Douglas R. Gies, Member

Dr. Todd J. Henry, Member

Dr. David W. Latham, Member

Dr. Brian D. Mason, Member

Dr. A. G. Unil Perera, Member

Dr. Russel J. White, Member

Date

Dr. H. Richard Miller, Chair
Department of Physics & Astronomy

A Survey of Stellar Families: Multiplicity of Solar-Type Stars

by

Deepak Raghavan

Under the Direction of Harold A. McAlister

Abstract

I present the results of a comprehensive assessment of companions to solar-type stars. The sample of 454 stars, including the Sun, was selected from the *Hipparcos* catalog with $\pi > 40$ mas, $\sigma_\pi/\pi < 0.05$, $0.5 \leq B - V \leq 1.0$, and positioned on an HR diagram within a band extending 1.5 magnitudes below and 2 magnitudes above an iterative best-fit main sequence. The resulting sample is an exhaustive set of stars with V-band flux between 0.1 and 10 times that of the Sun, providing a physical basis for the term "solar-type". New observational aspects of this work include a survey for separated fringe packet companions with long-baseline interferometry at the Center for High Angular Resolution Astronomy (CHARA) Array, blinking multi-epoch archival images to identify wide common proper motion companions, and speckle interferometry. Apart from evaluating companion information from the various catalogs covering many different techniques, I also obtained and included unpublished results

from extensive radial velocity monitoring programs. The many sources leveraged enable a thorough search and evaluation for stellar and brown dwarf companions.

The results presented here include eight new companion discoveries, four of which are wide common proper motion pairs discovered by blinking archival images, and four more are from the spectroscopic data. The overall observed fractions of single, double, triple, and higher order systems are $57\% \pm 3\%$, $33\% \pm 2\%$, $8\% \pm 1\%$, and $3\% \pm 1\%$, respectively. If all candidate companions identified are found to be real, the percentages would be $54\% \pm 2\%$, $34\% \pm 2\%$, $9\% \pm 2\%$, and $3\% \pm 1\%$, respectively. The incompleteness analysis indicates that only a few undiscovered companions remain for this well-studied sample. Including these missed companions and estimating the percentage of candidates that are real leads to multiplicity fractions of $55\% \pm 3\%$, $34\% \pm 2\%$, $9\% \pm 2\%$, and $2\% \pm 1\%$ for single, binary, triple, and higher order systems. These results include all stellar and brown dwarf companions, and show that a majority of the solar-type stars are single, in contrast to earlier expectations. This large sample enables a check of the dependence of multiplicity on various physical parameters. Bluer, more massive stars are more likely to have companions than redder, less massive ones, consistent with the trend seen over the entire spectral range, but showing a steeper drop at solar-type stars than previously believed. Consistent with prior studies, younger, more active stars are seen as more likely to have companions than older, less active ones, suggesting that companions may be stripped over time by dynamical interactions. A preliminary, but important indication seen here is that brown dwarfs, like planets, seem to prefer stars with higher metallicity, tentatively suggesting that brown dwarfs may form like

planets, at least when they are companions to stars.

The period distribution derived is unimodal and roughly Gaussian with a peak and median value of 300 years. The period-eccentricity relation shows the expected circularization for periods below 12 days, followed by a roughly flat distribution. The mass-ratio distribution shows a clear discontinuity near a value of one, indicating a preference for twins, which are not confined to short orbital periods. The period-mass-ratio relationship shows that multiple formation mechanisms are likely responsible for the formation of stellar systems – fission for like pairs and fragmentation or random associations for longer-period systems of all mass ratios. This distribution also shows a paucity of low-mass companions, confirming that the brown dwarf desert extends out to wide separations. The ratio of planet hosts among single, binary, and multiple systems are statistically indistinguishable, suggesting that planets are as likely to form around single stars as they are around components of binary or multiple systems. Hence, the common occurrence of binary systems is likely to increase the real-estate available for planets, and perhaps life.

INDEX WORDS: Stellar multiplicity, Binary stars, Solar-type stars, Solar neighborhood, Exoplanet systems, Brown dwarfs, Survey, Long baseline interferometry, Radial velocity

A Survey of Stellar Families: Multiplicity of Solar-Type Stars

by

Deepak Raghavan

A Dissertation Presented in Partial Fulfillment of Requirements for the Degree of

Doctor of Philosophy

in the College of Arts and Sciences

Georgia State University

2009

Copyright by
Deepak Raghavan
2009

A Survey of Stellar Families: Multiplicity of Solar-Type Stars

by

Deepak Raghavan

Major Professor:	Harold A. McAlister
Committee:	Douglas R. Gies
	Todd J. Henry
	David W. Latham
	Brian D. Mason
	A. G. Unil Perera
	Russel J. White

Electronic Version Approved:

Office of Graduate Studies
College of Arts & Sciences
Georgia State University
May 2009

To my parents

Thank you for inculcating the spirit of learning in me

Acknowledgments

When I decided to pursue a doctorate in astronomy more than six years ago, it was not with complete certainty, but with a sense of curiosity, wonder, and yes, some apprehension. I had decided to chart a unique course for myself, and to travel down a path with few footsteps, especially given where I was coming from. I would not have been able to complete this journey without the steadfast support of my family and friends, and I would like to extend my most sincere gratitude to them.

I could not have done this without the support of my dear wife, Priya, who has not only always stood by me, but also been such a tremendous source of support and wisdom, letting me probe and explore, while always being there when I needed a listening ear or a supporting hand. My children, Anjan and Aditi, while sometimes curious, and sometimes worried as to what daddy was doing back in school, never wavered in their implicit support.

I thank my parents and siblings for inculcating the spirit of learning in me, which has become a significant driver of my life. My mother led by example, completing her own Ph.D. in Hinduism in 2007. I am very proud of her accomplishment and inspired by it. I appreciate my friends for their indulgence when I would excitedly talk about astronomy and for allowing me to miss parties or leave them early to go to AROC for observing.

My thanks also go out to my committee members and the astronomy faculty members for the invaluable support and guidance they have provided me throughout the process. Special

thanks to Todd Henry for directing my master's work on exoplanet systems, for the idea of this thesis work, and for his consistently insightful feedback. I have truly enjoyed working with my advisor, Hal McAlister, and would like to recognize his consistent encouragement, support, and direction, not to mention his pioneering efforts in making the CHARA Array a reality and providing us graduate students with copious observing time on such a world-class instrument. Special thanks to Dave Latham for allowing my work to benefit from his meticulous radial velocity monitoring over 30 years and for being so supportive, gathering new data as required and reducing the data on hundreds of stars to enhance the results of this effort. Thanks to Brian Mason for always knowing the answer to any question about double stars and for taking me along on the speckle observing runs; and to Doug Gies, whose consistent advice and ideas enabled me to give a better shape to this effort.

This work would not have been possible without the help extended by astronomers around the world, who responded to my persistent requests with support and encouragement. Geoff Marcy graciously allowed me access to his treasure trove of the highest precision radial velocities, enabling me to derive more robust statistics. Artie Hatzes, Bill Cochran, Hugh Jones, and Jason Wright also helped me improve the radial velocity coverage. Bill Hartkopf, Andrei Tokovinin, Dimitri Pourbaix, and Richard Gray were very helpful with their insights and analysis on specific stellar systems.

My fellow graduate students enriched this journey with their humor, wit, and open acceptance of a who some might have considered "an outsider", for which I am indebted to them. Special thanks to Rajesh Deo and Justin Cantrell for taking care of our computers

while working on their own research, and to Alvin Das for creating a template that made it easier to navigate the LaTeX dissertation jungle. Thanks also to the staff at the CHARA Array for keeping such a sophisticated instrument working so well that it seemed like I was witnessing science fiction come alive.

I am grateful to have grown up in India, whose society gave me a strong foundation, built with a desire to learn and accomplish. I am also proud to call the the Unites States of America home, and am thankful to my fellow citizens for accepting and embracing me beyond my wildest expectations. There is no other country in the world where I could have traveled the paths I did, charting a uniquely individual course for my life, without once having to justify or explain the twists and turns I decided to take. May India and the USA always be beacons of freedom, innovation, and accomplishment.

This work could not have been possible without various grants and resources, which I acknowledge here. Research at the CHARA Array is supported by the College of Arts and Sciences at Georgia State University and by the National Science Foundation through NSF grant AST-0606958. This research has made use of the SIMBAD literature database, operated at CDS, Strasbourg, France; NASA's Astrophysics Data System; multi-epoch images from the Digitized Sky Survey, which was produced at the Space Telescope Science Institute under U.S. Government grant NAG W-2166; and data products from the Two Micron All Sky Survey (2MASS), which is a joint project of the University of Massachusetts and the Infrared Processing and Analysis Center/California Institute of Technology, funded by the National Aeronautics and Space Administration and the National Science Foundation.

Table of Contents

Acknowledgments . . . . . **v**

List of Tables . . . . . **xii**

List of Figures . . . . . **xiv**

Abbreviations and Acronyms . . . . . **xliii**

1 Introduction and Background 1

1.1 Motivation 1

1.2 History of Double Star Observations 5

1.3 Previous Multiplicity Surveys 9

1.3.1 Early Multiplicity Surveys 10

1.3.2 The Duquennoy & Mayor Survey 15

1.3.3 Multiplicity Results Since DM91 17

1.4 Multiplicity Among Stars with Planets 24

2 Sample and Survey Methods 26

2.1 The Sample of Solar-Type Stars 26

2.1.1 Sample Selection from the Hipparcos Catalog 27

2.1.2 Comparison with DM91 Sample 54

2.1.3 A New Reduction of the *Hipparcos* Data 57

2.1.4 Sample Analysis & Bias 62

2.2 Survey Methods 65

3 Long-Baseline Interferometric Results 68

3.1 Survey of Separated Fringe Packet Binaries 73

3.1.1 SFP Data Reduction and Results 76
3.1.2 Astrometry from Separated Fringe Packets 100
3.2 Visual Orbits Derived using the CHARA Array 103
3.2.1 The Visual Orbit of σ^2 CrB (HD 146361) 104
3.2.2 The Visual Orbit of HD 8997 105
3.2.3 The Visual Orbit of HD 45088 108
3.2.4 The Visual Orbit of HD 223778 111

4 Common Proper Motion Results 116

4.1 Identification and Confirmation of CPM Companions 116
4.2 Linear Motion of Field Stars 149

5 Other Astrometric Results 160

5.1 The *Hipparcos* Double Stars 160
5.1.1 Component Solutions 162
5.1.2 Accelerating Proper Motions 165
5.1.3 Orbital Solutions 171
5.1.4 Stochastic Solutions 172
5.2 Visual Orbits 172
5.3 The Washington Double Star Catalog 182
5.4 The Fourth Interferometric Catalog 187
5.5 The Catalog of Nearby Stars 188

6 Spectroscopic and Photometric Results 190

6.1 Constant Radial Velocity Stars 191
6.2 Stellar Companions 208
6.2.1 Single-lined Spectroscopic Binaries 208
6.2.2 Double-lined Spectroscopic Binaries 213
6.2.3 Radial Velocity Variations Without Orbits 221
6.3 Planetary Companions 223

6.4 Eclipsing Binaries 224

7 Synthesis of Results 227

7.1 Nomenclature 227

7.2 Results for Each of the 454 Systems 229

7.3 Observed Stellar Multiplicity 243

7.4 Notes on Individual Systems 248

8 Discussion and Analysis 285

8.1 Comparison with DM91 Multiplicity Statistics 285

8.2 Incompleteness Analysis & True Stellar Multiplicity 292

8.2.1 Missing Spectroscopic Companions 294

8.2.2 Missing Visual Companions 298

8.2.3 Very Low-Mass Companions 300

8.2.4 Results from DM91 Incompleteness Analysis 303

8.2.5 Missed Companions and True Multiplicity 304

8.3 Multiplicity Dependency on Physical Parameters 306

8.3.1 Multiplicity by Spectral Type and Color 307

8.3.2 Multiplicity by Chromospheric Activity 311

8.3.3 Multiplicity by Metallicity 312

8.4 The Distribution of Orbital Elements 316

8.4.1 Period Distribution 316

8.4.2 Period-Eccentricity Relationship 320

8.4.3 Mass-Ratio Distribution 322

8.5 Multiplicity in Exoplanetary Systems 327

8.6 Hierarchy of Multiple Systems 329

8.7 Conclusions 330

References 343

Appendices **363**

A Physical Parameters for Primaries and Companions **364**

B SFP Investigation Plots for Individual Systems **392**

C IDL Programs **611**

C.1 CHARA Observations Planning Tool for Survey Projects 612

C.1.1 Example Input File 612

C.1.2 IDL code 613

C.2 Example Output File 635

C.3 SFP Detection 636

C.4 Blinking Archival Images 650

C.5 Deriving a Visual Orbit From Interferometric Visibilities 655

C.5.1 Deriving the Best-fit Orbit 655

C.5.2 Example Input File of Calibrated Visibilities 661

C.5.3 Example Input File of Orbital Elements 662

C.5.4 Calculating Interferometric Visibility for Given Parameters 663

C.5.5 Estimating Parameter Uncertainties 666

D Two Suns in the Sky: Stellar Multiplicity in Exoplanet Systems . . **669**

E The Visual Orbit σ^2 Coronae Borealis **690**

List of Tables

1.1 Results of Previous Multiplicity Surveys 23

2.1 Volume-Limited Sample of 454 Solar-Type Stars 32
2.2 Stars Excluded Due to Large Parallax Errors 51
2.3 Stars Excluded Due to Large Offset from the Main Sequence 53
2.4 Stars excluded from sample, but qualifying in FvL07 data 60
2.5 Sample stars outside selection criteria based on FvL07 data 61

3.1 Observing Nights for the SFP Survey 77
3.2 SFP Observations and Results 83
3.3 Summary of SFP Results 94
3.4 Projected Separations for SFP Measurements 102
3.5 Interferometric Visibilities for HD 8997 105
3.6 Visual Orbit Solution for HD 8997 107
3.7 Interferometric Visibilities for HD 45088 109
3.8 Visual Orbit Solution for HD 45088 111
3.9 Interferometric Visibilities for HD 223778 112
3.10 Visual Orbit Solution for HD 223778 113

4.1 Archival Image Blink Results 125
4.2 Photometry of CPM Candidates 148
4.3 Optical WDS Entries 151

5.1 *Hipparcos* Component Solutions 163
5.2 Accelerating Proper Motion Solutions 169
5.3 *Hipparcos* Orbital Solutions 171
5.4 Visual Orbit Solutions 178
5.5 WDS companions confirmed by photometry 184
5.6 WDS pairs demonstrating orbital motion 186

6.1 Stars with no Evidence of Radial Velocity Variations 193
6.2 SB1 Orbits 211
6.3 SB2 Orbits 217
6.4 Stars with Possible RV Variations 222
6.5 Planetary Companions 225

7.1 Stellar and Planetary Companions 233
7.2 Observed Multiplicity Statistics 243
7.3 Classification of Confirmed Companions 246
7.4 Classification Including Candidate Companions 247

8.1 Comparison of Multiplicity Statistics with DM91 290
8.2 Multiplicity Statistics by Spectral Type and Color 308

A.1 Physical Parameters of the Sample Stars 365
A.2 Spectral Type and Mass of the Companions 383

List of Figures

2.1 *Hipparcos* main sequence 27

2.2 *Hipparcos* distance-limited sample 28

2.3 *Hipparcos* distance-limited sample close to the main sequence 29

2.4 Volume-limited sample of solar-type stars from *Hipparcos* 31

2.5 DM91 sample selected from *Gliese* and *Hipparcos* catalogs 55

2.6 The current sample plotted along the same axes as Figure 2.5 58

2.7 The current sample from *Hipparcos* and FvL07 59

2.8 Color-Magnitude diagram of *Hipparcos* and FvL07 samples 60

2.9 Apparent and absolute magnitude distribution of the sample 63

2.10 Distance distribution of the sample 64

2.11 $B - V$ color distribution of the sample 65

2.12 Spectral type distribution of the sample 66

2.13 Correlation between spectral type and color 66

3.1 Intensity of diffraction patterns 70

3.2 Schematic of a basic interferometer 71

3.3 Beam combining at CHARA Classic 73

3.4 Examples of separated fringe packets 75

3.5 Example fringe envelopes for a separated fringe packet binary 80

3.6 Example fringe envelopes for a single fringe packet star 81

3.7 Triangulation of SFP measures 102

3.8 Calibrated visibility measurements for HD 8997 106

3.9 Calibrated visibility measurements for HD 45088 110
3.10 Calibrated visibility measurements for HD 223778 115

4.1 Example of DSS images 117
4.2 Epoch distribution of the images used for blinking 118
4.3 Distribution of the time interval between images blinked 119
4.4 Distribution of the motion seen on blinking 121
4.5 Distribution of the search space for CPM companions 123
4.6 New CPM companion to HD 4391 145
4.7 New CPM companion to HD 43162 146
4.8 New CPM companion to HD 157347 146
4.9 New CPM companion to HD 218868 147
4.10 Examples of the linear motion of unrelated field stars 150

6.1 Number and time coverage of CfA RV measurements 201
6.2 Error profiles of the CfA RV measurements 203
6.3 $P(\chi^2)$ distribution for constant RV stars 205
6.4 $P(\chi^2)$ distribution for constant RV stars as a function of the number of observations 207
6.5 Error distributions as a function of $P(\chi^2)$ for constant RV stars 208
6.6 Single-lined spectroscopic orbits of HD 10307 and HD 17382 213
6.7 Single-lined spectroscopic orbits of HD 24409 and HD 32850 213
6.8 Single-lined spectroscopic orbits of HD 54371 and HD 79028 214
6.9 Single-lined spectroscopic orbits of HD 101206 and HD 112758A 214
6.10 Single-lined spectroscopic orbits of HD 121370 and HD 128642 215
6.11 Single-lined spectroscopic orbits of HD 142267 and HD 185414 215
6.12 Single-lined spectroscopic orbit of HD 224465 216

6.13 Double-lined spectroscopic orbits of HD 8997 and HD 13974 219
6.14 Double-lined spectroscopic orbits of HD 45088 and HD 80715 220
6.15 Double-lined spectroscopic orbits of HD 111312 and HD 148704 220
6.16 Double-lined spectroscopic orbits of HD 223778 221

7.1 Illustration of companion nomenclature according to the WMC standards 230
7.2 The observed frequency single, binary, triple, and quadruple systems. . . . 244

8.1 The DM91 frequency single, binary, triple, and quadruple systems. 286
8.2 HR diagram for the DM91 sample 292
8.3 Number and time coverage of CCPS RV measurements 296
8.4 External error distribution in the CCPS RV measurements 297
8.5 Multiplicity statistics by color 309
8.6 Multiplicity statistics by spectral type 310
8.7 Distribution of chromospheric activity by $B-V$ Color 312
8.8 Multiplicity statistics by chromospheric activity 313
8.9 Multiplicity statistics by metallicity 314
8.10 Planet metallicity correlation 316
8.11 Period distribution for the 258 confirmed companions 318
8.12 Period-eccentricity relationship 321
8.13 Eccentricity distribution 323
8.14 Mass-ratio distribution 324
8.15 Mass-ratio – period relation 325
8.16 Secondary mass distribution 327
8.17 Mobile diagrams of triple systems (1 of 3) 338
8.18 Mobile diagrams of triple systems (2 of 3) 339
8.19 Mobile diagrams of triple systems (3 of 3) 340

8.20 Mobile diagrams of quadruple systems 341
8.21 Mobile diagrams of quintuple and higher order systems 342

B.1 SFP inspection for HD 000166 with S1-E1 on UT 2007/07/29, seq 001 . . 392
B.2 SFP inspection for HD 000166 with S1-E1 on UT 2007/08/14, seq 001 . . 393
B.3 SFP inspection for HD 000166 with S1-W1 on UT 2007/08/14, seq 002 . . 393
B.4 SFP inspection for HD 001461 with S1-E1 on UT 2008/07/22, seq 001 . . 393
B.5 SFP inspection for HD 001461 with S1-W1 on UT 2008/07/27, seq 001 . . 394
B.6 SFP inspection for HD 001461 with S2-W1 on UT 2007/09/17, seq 001 . . 394
B.7 SFP inspection for HD 001562 with S1-E1 on UT 2007/08/16, seq 002 . . 394
B.8 SFP inspection for HD 001562 with S1-E1 on UT 2008/07/09, seq 001 . . 395
B.9 SFP inspection for HD 001562 with S1-W1 on UT 2007/08/16, seq 001 . . 395
B.10 SFP inspection for HD 001562 with S1-W1 on UT 2008/07/08, seq 001 . . 395
B.11 SFP inspection for HD 003196 with S1-E1 on UT 2007/08/14, seq 003 . . 396
B.12 SFP inspection for HD 003196 with S1-E1 on UT 2008/07/22, seq 001 . . 396
B.13 SFP inspection for HD 003196 with S1-W1 on UT 2007/08/14, seq 004 . . 396
B.14 SFP inspection for HD 003196 with S1-W1 on UT 2008/07/07, seq 001 . . 397
B.15 SFP inspection for HD 003196 with S2-E2 on UT 2007/09/27, seq 001 . . 397
B.16 SFP inspection for HD 003196 with S2-W1 on UT 2007/09/17, seq 001 . . 397
B.17 SFP inspection for HD 003651 with S1-E1 on UT 2007/07/29, seq 001 . . 398
B.18 SFP inspection for HD 003651 with S1-E1 on UT 2007/08/14, seq 001 . . 398
B.19 SFP inspection for HD 003651 with S1-W1 on UT 2007/08/14, seq 002 . . 398
B.20 SFP inspection for HD 003765 with S1-E1 on UT 2007/08/16, seq 002 . . 399
B.21 SFP inspection for HD 003765 with S1-E1 on UT 2008/07/09, seq 001 . . 399
B.22 SFP inspection for HD 003765 with S1-W1 on UT 2007/08/16, seq 001 . . 399
B.23 SFP inspection for HD 003765 with S1-W1 on UT 2008/07/08, seq 001 . . 400

B.24 SFP inspection for HD 004256 with S1-E1 on UT 2007/08/14, seq 001 . . 400
B.25 SFP inspection for HD 004256 with S1-W1 on UT 2007/08/14, seq 002 . . 400
B.26 SFP inspection for HD 004628 with S1-E1 on UT 2007/08/14, seq 001 . . 401
B.27 SFP inspection for HD 004628 with S1-W1 on UT 2007/08/14, seq 002 . . 401
B.28 SFP inspection for HD 004635 with S1-E1 on UT 2007/09/16, seq 002 . . 401
B.29 SFP inspection for HD 004635 with S1-W1 on UT 2007/09/16, seq 001 . . 402
B.30 SFP inspection for HD 004635 with S2-E1 on UT 2007/08/20, seq 001 . . 402
B.31 SFP inspection for HD 004813 with S1-W1 on UT 2008/07/27, seq 001 . . 402
B.32 SFP inspection for HD 004915 with S1-W1 on UT 2008/07/27, seq 001 . . 403
B.33 SFP inspection for HD 004915 with S2-W1 on UT 2007/09/17, seq 001 . . 403
B.34 SFP inspection for HD 007590 with S1-E1 on UT 2007/02/04, seq 001 . . 403
B.35 SFP inspection for HD 007590 with S1-E1 on UT 2007/02/04, seq 002 . . 404
B.36 SFP inspection for HD 007590 with S1-E1 on UT 2007/08/16, seq 002 . . 404
B.37 SFP inspection for HD 007590 with S1-E1 on UT 2008/07/09, seq 001 . . 404
B.38 SFP inspection for HD 007590 with S1-W1 on UT 2007/08/16, seq 001 . . 405
B.39 SFP inspection for HD 007590 with S1-W1 on UT 2008/07/08, seq 001 . . 405
B.40 SFP inspection for HD 007924 with S1-E1 on UT 2007/09/16, seq 002 . . 405
B.41 SFP inspection for HD 007924 with S1-W1 on UT 2007/09/16, seq 001 . . 406
B.42 SFP inspection for HD 008997 with S1-E1 on UT 2008/07/23, seq 001 . . 406
B.43 SFP inspection for HD 008997 with S1-W1 on UT 2008/07/07, seq 001 . . 406
B.44 SFP inspection for HD 008997 with S2-E2 on UT 2007/09/18, seq 001 . . 407
B.45 SFP inspection for HD 008997 with S2-W1 on UT 2007/09/17, seq 001 . . 407
B.46 SFP inspection for HD 010008 with S2-E2 on UT 2007/09/27, seq 001 . . 407
B.47 SFP inspection for HD 010008 with S2-W1 on UT 2007/09/17, seq 001 . . 408
B.48 SFP inspection for HD 010086 with S1-E1 on UT 2007/08/16, seq 002 . . 408
B.49 SFP inspection for HD 010086 with S1-W1 on UT 2007/08/16, seq 001 . . 408

B.50 SFP inspection for HD 010476 with S1-E1 on UT 2007/07/29, seq 001 . . 409
B.51 SFP inspection for HD 010476 with S1-E1 on UT 2007/08/16, seq 001 . . 409
B.52 SFP inspection for HD 010476 with S1-W1 on UT 2007/08/14, seq 001 . . 409
B.53 SFP inspection for HD 010780 with S1-E1 on UT 2007/09/16, seq 002 . . 410
B.54 SFP inspection for HD 010780 with S1-W1 on UT 2007/09/16, seq 001 . . 410
B.55 SFP inspection for HD 010780 with S2-E1 on UT 2007/08/20, seq 002 . . 410
B.56 SFP inspection for HD 010780 with S2-W1 on UT 2008/06/24, seq 001 . . 411
B.57 SFP inspection for HD 012051 with S1-E1 on UT 2007/01/26, seq 001 . . 411
B.58 SFP inspection for HD 012051 with S2-E2 on UT 2007/09/18, seq 001 . . 411
B.59 SFP inspection for HD 012051 with S2-E2 on UT 2007/09/18, seq 002 . . 412
B.60 SFP inspection for HD 012051 with S2-W1 on UT 2007/09/17, seq 001 . . 412
B.61 SFP inspection for HD 012846 with S2-E2 on UT 2007/09/18, seq 001 . . 412
B.62 SFP inspection for HD 012846 with S2-W1 on UT 2007/09/17, seq 001 . . 413
B.63 SFP inspection for HD 016160 with S1-E1 on UT 2007/08/15, seq 001 . . 413
B.64 SFP inspection for HD 016160 with S2-E2 on UT 2007/09/18, seq 001 . . 413
B.65 SFP inspection for HD 016160 with S2-W1 on UT 2007/09/17, seq 001 . . 414
B.66 SFP inspection for HD 016287 with S1-E1 on UT 2007/08/15, seq 001 . . 414
B.67 SFP inspection for HD 016287 with S1-E1 on UT 2007/10/31, seq 001 . . 414
B.68 SFP inspection for HD 016673 with S1-E1 on UT 2007/08/15, seq 001 . . 415
B.69 SFP inspection for HD 016673 with S2-E2 on UT 2007/09/27, seq 001 . . 415
B.70 SFP inspection for HD 016765 with S1-E1 on UT 2007/08/15, seq 001 . . 415
B.71 SFP inspection for HD 016765 with S1-E1 on UT 2007/10/31, seq 001 . . 416
B.72 SFP inspection for HD 016765 with S1-W1 on UT 2007/10/31, seq 002 . . 416
B.73 SFP inspection for HD 016765 with S2-E2 on UT 2007/09/27, seq 001 . . 416
B.74 SFP inspection for HD 016765 with S2-W1 on UT 2007/09/17, seq 001 . . 417
B.75 SFP inspection for HD 017382 with S1-W1 on UT 2008/07/07, seq 001 . . 417

B.76 SFP inspection for HD 017382 with S1-W1 on UT 2008/07/08, seq 001 . . 417
B.77 SFP inspection for HD 017382 with S2-E2 on UT 2007/09/18, seq 001 . . 418
B.78 SFP inspection for HD 017382 with S2-W1 on UT 2007/09/17, seq 001 . . 418
B.79 SFP inspection for HD 018143 with S1-E1 on UT 2007/10/31, seq 001 . . 418
B.80 SFP inspection for HD 018143 with S1-E1 on UT 2008/07/23, seq 001 . . 419
B.81 SFP inspection for HD 018143 with S1-W1 on UT 2007/11/01, seq 001 . . 419
B.82 SFP inspection for HD 018143 with S2-W1 on UT 2007/09/17, seq 001 . . 419
B.83 SFP inspection for HD 018632 with S1-E1 on UT 2007/11/01, seq 001 . . 420
B.84 SFP inspection for HD 018632 with S1-W1 on UT 2007/11/01, seq 002 . . 420
B.85 SFP inspection for HD 018757 with S1-E1 on UT 2007/09/16, seq 003 . . 420
B.86 SFP inspection for HD 018757 with S1-W1 on UT 2007/09/16, seq 002 . . 421
B.87 SFP inspection for HD 018757 with S2-E1 on UT 2007/08/20, seq 001 . . 421
B.88 SFP inspection for HD 018803 with S2-E2 on UT 2007/09/18, seq 001 . . 421
B.89 SFP inspection for HD 018803 with S2-W1 on UT 2007/09/17, seq 001 . . 422
B.90 SFP inspection for HD 019994 with S1-E1 on UT 2007/11/01, seq 001 . . 422
B.91 SFP inspection for HD 019994 with S1-W1 on UT 2007/11/01, seq 002 . . 422
B.92 SFP inspection for HD 019994 with S2-E2 on UT 2007/09/27, seq 001 . . 423
B.93 SFP inspection for HD 019994 with S2-E2 on UT 2007/09/27, seq 002 . . 423
B.94 SFP inspection for HD 019994 with S2-E2 on UT 2007/09/27, seq 003 . . 423
B.95 SFP inspection for HD 020165 with S1-E1 on UT 2007/11/01, seq 001 . . 424
B.96 SFP inspection for HD 020165 with S1-W1 on UT 2007/11/01, seq 002 . . 424
B.97 SFP inspection for HD 020619 with S1-E1 on UT 2007/11/01, seq 001 . . 424
B.98 SFP inspection for HD 020619 with S1-W1 on UT 2007/11/01, seq 002 . . 425
B.99 SFP inspection for HD 022049 with S2-E2 on UT 2007/09/27, seq 001 . . 425
B.100 SFP inspection for HD 022049 with S2-E2 on UT 2007/09/27, seq 002 . . 425
B.101 SFP inspection for HD 022879 with S1-E1 on UT 2007/11/01, seq 001 . . 426

B.102 SFP inspection for HD 022879 with S2-E2 on UT 2007/09/27, seq 002 . . 426
B.103 SFP inspection for HD 022879 with S2-E2 on UT 2007/09/27, seq 003 . . 426
B.104 SFP inspection for HD 024238 with S1-E1 on UT 2007/09/16, seq 002 . . 427
B.105 SFP inspection for HD 024238 with S1-W1 on UT 2007/09/16, seq 001 . . 427
B.106 SFP inspection for HD 024409 with S1-E1 on UT 2007/09/16, seq 002 . . 427
B.107 SFP inspection for HD 024409 with S1-W1 on UT 2007/09/16, seq 001 . . 428
B.108 SFP inspection for HD 024409 with S2-E1 on UT 2007/08/20, seq 001 . . 428
B.109 SFP inspection for HD 024496 with S1-E1 on UT 2007/10/31, seq 001 . . 428
B.110 SFP inspection for HD 024496 with S1-W1 on UT 2007/10/31, seq 002 . . 429
B.111 SFP inspection for HD 024496 with S2-E2 on UT 2007/09/26, seq 001 . . 429
B.112 SFP inspection for HD 024496 with S2-E2 on UT 2007/09/27, seq 001 . . 429
B.113 SFP inspection for HD 025457 with S1-E1 on UT 2007/10/31, seq 001 . . 430
B.114 SFP inspection for HD 025457 with S1-W1 on UT 2007/10/31, seq 002 . . 430
B.115 SFP inspection for HD 025457 with S2-E2 on UT 2007/09/26, seq 001 . . 430
B.116 SFP inspection for HD 025457 with S2-E2 on UT 2007/09/27, seq 001 . . 431
B.117 SFP inspection for HD 025457 with S2-E2 on UT 2007/09/27, seq 002 . . 431
B.118 SFP inspection for HD 025665 with S1-E1 on UT 2007/09/16, seq 002 . . 431
B.119 SFP inspection for HD 025665 with S1-W1 on UT 2007/09/16, seq 001 . . 432
B.120 SFP inspection for HD 026913 with S1-E1 on UT 2007/10/31, seq 001 . . 432
B.121 SFP inspection for HD 026913 with S1-W1 on UT 2007/10/31, seq 002 . . 432
B.122 SFP inspection for HD 026913 with S2-E2 on UT 2007/09/26, seq 001 . . 433
B.123 SFP inspection for HD 026923 with S1-E1 on UT 2007/10/31, seq 001 . . 433
B.124 SFP inspection for HD 026923 with S1-W1 on UT 2007/10/31, seq 002 . . 433
B.125 SFP inspection for HD 026923 with S2-E2 on UT 2007/09/26, seq 001 . . 434
B.126 SFP inspection for HD 029883 with S2-E2 on UT 2007/09/18, seq 001 . . 434
B.127 SFP inspection for HD 029883 with S2-W1 on UT 2007/09/17, seq 001 . . 434

B.128 SFP inspection for HD 032850 with S1-E1 on UT 2007/10/31, seq 001 . . 435
B.129 SFP inspection for HD 032850 with S1-W1 on UT 2007/10/31, seq 002 . . 435
B.130 SFP inspection for HD 032923 with S1-E1 on UT 2007/02/25, seq 001 . . 435
B.131 SFP inspection for HD 032923 with S1-E1 on UT 2007/02/25, seq 002 . . 436
B.132 SFP inspection for HD 032923 with S1-E1 on UT 2007/03/11, seq 001 . . 436
B.133 SFP inspection for HD 032923 with S1-E1 on UT 2007/10/31, seq 001 . . 436
B.134 SFP inspection for HD 032923 with S1-W1 on UT 2007/10/31, seq 002 . . 437
B.135 SFP inspection for HD 032923 with S2-E2 on UT 2007/09/26, seq 001 . . 437
B.136 SFP inspection for HD 032923 with S2-E2 on UT 2007/09/27, seq 001 . . 437
B.137 SFP inspection for HD 035112 with S1-E1 on UT 2007/10/31, seq 001 . . 438
B.138 SFP inspection for HD 035112 with S1-W1 on UT 2007/10/31, seq 002 . . 438
B.139 SFP inspection for HD 037008 with S1-E1 on UT 2007/01/25, seq 001 . . 438
B.140 SFP inspection for HD 037008 with S1-W1 on UT 2007/11/01, seq 002 . . 439
B.141 SFP inspection for HD 037008 with S2-E2 on UT 2007/11/19, seq 001 . . 439
B.142 SFP inspection for HD 037008 with S2-E2 on UT 2007/11/19, seq 002 . . 439
B.143 SFP inspection for HD 037008 with S2-E2 on UT 2007/11/27, seq 001 . . 440
B.144 SFP inspection for HD 037394 with S1-E1 on UT 2007/01/25, seq 001 . . 440
B.145 SFP inspection for HD 037394 with S1-E1 on UT 2007/01/26, seq 002 . . 440
B.146 SFP inspection for HD 037394 with S1-E1 on UT 2007/04/14, seq 001 . . 441
B.147 SFP inspection for HD 037394 with S1-W1 on UT 2007/11/01, seq 001 . . 441
B.148 SFP inspection for HD 037394 with S2-E2 on UT 2007/11/19, seq 003 . . 441
B.149 SFP inspection for HD 037394 with S2-E2 on UT 2007/11/19, seq 004 . . 442
B.150 SFP inspection for HD 037394 with S2-E2 on UT 2007/11/19, seq 005 . . 442
B.151 SFP inspection for HD 037394 with S2-E2 on UT 2007/11/27, seq 001 . . 442
B.152 SFP inspection for HD 038230 with S1-E1 on UT 2007/01/25, seq 001 . . 443
B.153 SFP inspection for HD 038230 with S1-W1 on UT 2007/11/01, seq 001 . . 443

B.154 SFP inspection for HD 038230 with S2-E2 on UT 2007/11/19, seq 002 . . 443
B.155 SFP inspection for HD 038230 with S2-E2 on UT 2007/11/27, seq 001 . . 444
B.156 SFP inspection for HD 038858 with S1-E1 on UT 2007/10/31, seq 001 . . 444
B.157 SFP inspection for HD 038858 with S1-W1 on UT 2007/10/31, seq 002 . . 444
B.158 SFP inspection for HD 038858 with S2-E2 on UT 2007/09/26, seq 001 . . 445
B.159 SFP inspection for HD 040397 with S1-W1 on UT 2007/11/01, seq 001 . . 445
B.160 SFP inspection for HD 040397 with S2-E2 on UT 2007/09/26, seq 001 . . 445
B.161 SFP inspection for HD 041593 with S1-E1 on UT 2007/10/31, seq 001 . . 446
B.162 SFP inspection for HD 041593 with S1-W1 on UT 2007/11/01, seq 001 . . 446
B.163 SFP inspection for HD 041593 with S2-E2 on UT 2007/09/26, seq 002 . . 446
B.164 SFP inspection for HD 042618 with S1-E1 on UT 2007/10/31, seq 001 . . 447
B.165 SFP inspection for HD 042618 with S1-W1 on UT 2007/11/01, seq 001 . . 447
B.166 SFP inspection for HD 042618 with S2-E2 on UT 2007/09/26, seq 001 . . 447
B.167 SFP inspection for HD 046588 with S1-E1 on UT 2007/04/14, seq 001 . . 448
B.168 SFP inspection for HD 046588 with S1-E1 on UT 2007/09/16, seq 001 . . 448
B.169 SFP inspection for HD 046588 with S1-W1 on UT 2008/04/26, seq 001 . . 448
B.170 SFP inspection for HD 051419 with S1-E1 on UT 2007/02/05, seq 002 . . 449
B.171 SFP inspection for HD 051419 with S1-E1 on UT 2007/02/05, seq 003 . . 449
B.172 SFP inspection for HD 051419 with S1-W1 on UT 2008/04/26, seq 001 . . 449
B.173 SFP inspection for HD 051866 with S1-E1 on UT 2007/01/25, seq 001 . . 450
B.174 SFP inspection for HD 051866 with S1-W1 on UT 2007/11/01, seq 002 . . 450
B.175 SFP inspection for HD 051866 with S2-E2 on UT 2007/11/19, seq 001 . . 450
B.176 SFP inspection for HD 051866 with S2-E2 on UT 2007/11/19, seq 002 . . 451
B.177 SFP inspection for HD 054371 with S1-E1 on UT 2007/02/04, seq 001 . . 451
B.178 SFP inspection for HD 054371 with S1-E1 on UT 2008/04/25, seq 001 . . 451
B.179 SFP inspection for HD 054371 with S1-W1 on UT 2007/11/01, seq 002 . . 452

B.180 SFP inspection for HD 054371 with S1-W1 on UT 2008/04/26, seq 001 . . 452
B.181 SFP inspection for HD 055575 with S1-E1 on UT 2007/01/26, seq 001 . . 452
B.182 SFP inspection for HD 055575 with S1-E1 on UT 2007/02/03, seq 001 . . 453
B.183 SFP inspection for HD 055575 with S1-W1 on UT 2007/11/01, seq 001 . . 453
B.184 SFP inspection for HD 055575 with S2-E2 on UT 2007/11/20, seq 001 . . 453
B.185 SFP inspection for HD 055575 with S2-E2 on UT 2007/11/27, seq 002 . . 454
B.186 SFP inspection for HD 059747 with S1-W1 on UT 2007/11/01, seq 001 . . 454
B.187 SFP inspection for HD 063433 with S1-E1 on UT 2007/03/20, seq 001 . . 454
B.188 SFP inspection for HD 063433 with S1-E1 on UT 2008/04/13, seq 001 . . 455
B.189 SFP inspection for HD 063433 with S1-W1 on UT 2007/11/01, seq 001 . . 455
B.190 SFP inspection for HD 063433 with S1-W1 on UT 2008/04/12, seq 001 . . 455
B.191 SFP inspection for HD 065430 with S1-W1 on UT 2008/04/26, seq 001 . . 456
B.192 SFP inspection for HD 065583 with S1-E1 on UT 2008/04/13, seq 001 . . 456
B.193 SFP inspection for HD 065583 with S1-W1 on UT 2008/04/26, seq 001 . . 456
B.194 SFP inspection for HD 067228 with S1-E1 on UT 2007/02/06, seq 002 . . 457
B.195 SFP inspection for HD 067228 with S1-E1 on UT 2007/02/25, seq 001 . . 457
B.196 SFP inspection for HD 067228 with S1-E1 on UT 2007/02/25, seq 002 . . 457
B.197 SFP inspection for HD 067228 with S2-E2 on UT 2007/11/29, seq 003 . . 458
B.198 SFP inspection for HD 068017 with S1-E1 on UT 2008/04/13, seq 001 . . 458
B.199 SFP inspection for HD 068017 with S1-E1 on UT 2008/04/25, seq 001 . . 458
B.200 SFP inspection for HD 068017 with S1-W1 on UT 2008/04/12, seq 001 . . 459
B.201 SFP inspection for HD 068255 with S1-E1 on UT 2007/02/25, seq 002 . . 459
B.202 SFP inspection for HD 068255 with S1-E1 on UT 2007/02/25, seq 003 . . 459
B.203 SFP inspection for HD 079096 with S1-E1 on UT 2007/02/06, seq 003 . . 460
B.204 SFP inspection for HD 079096 with S1-E1 on UT 2007/02/25, seq 001 . . 460
B.205 SFP inspection for HD 079096 with S1-E1 on UT 2007/02/25, seq 002 . . 460

B.206 SFP inspection for HD 079096 with S1-E1 on UT 2007/03/09, seq 001 . . 461
B.207 SFP inspection for HD 079096 with S1-E1 on UT 2007/03/09, seq 002 . . 461
B.208 SFP inspection for HD 079096 with S1-E1 on UT 2007/03/10, seq 001 . . 461
B.209 SFP inspection for HD 079096 with S1-E1 on UT 2007/03/11, seq 001 . . 462
B.210 SFP inspection for HD 079096 with S1-E1 on UT 2008/04/14, seq 001 . . 462
B.211 SFP inspection for HD 079096 with S1-E1 on UT 2008/04/14, seq 002 . . 462
B.212 SFP inspection for HD 079096 with S1-E1 on UT 2008/04/14, seq 003 . . 463
B.213 SFP inspection for HD 079096 with S1-W1 on UT 2008/04/12, seq 001 . . 463
B.214 SFP inspection for HD 079096 with S2-E2 on UT 2007/11/29, seq 002 . . 463
B.215 SFP inspection for HD 079969 with S1-E1 on UT 2007/02/06, seq 001 . . 464
B.216 SFP inspection for HD 079969 with S1-E1 on UT 2007/02/25, seq 001 . . 464
B.217 SFP inspection for HD 079969 with S1-E1 on UT 2008/04/13, seq 001 . . 464
B.218 SFP inspection for HD 079969 with S1-W1 on UT 2008/04/12, seq 001 . . 465
B.219 SFP inspection for HD 079969 with S2-E2 on UT 2007/11/29, seq 001 . . 465
B.220 SFP inspection for HD 080715 with S1-E1 on UT 2008/04/13, seq 001 . . 465
B.221 SFP inspection for HD 080715 with S1-W1 on UT 2008/04/26, seq 001 . . 466
B.222 SFP inspection for HD 082443 with S1-E1 on UT 2007/02/06, seq 001 . . 466
B.223 SFP inspection for HD 082443 with S1-E1 on UT 2008/04/13, seq 001 . . 466
B.224 SFP inspection for HD 082443 with S1-E1 on UT 2008/04/13, seq 002 . . 467
B.225 SFP inspection for HD 082443 with S1-W1 on UT 2008/04/12, seq 001 . . 467
B.226 SFP inspection for HD 082443 with S2-E2 on UT 2007/11/29, seq 001 . . 467
B.227 SFP inspection for HD 082885 with S1-E1 on UT 2007/01/26, seq 003 . . 468
B.228 SFP inspection for HD 082885 with S1-W1 on UT 2007/04/24, seq 001 . . 468
B.229 SFP inspection for HD 082885 with S1-W1 on UT 2008/04/26, seq 001 . . 468
B.230 SFP inspection for HD 082885 with S2-E2 on UT 2007/11/29, seq 001 . . 469
B.231 SFP inspection for HD 087883 with S1-E1 on UT 2007/02/06, seq 001 . . 469

B.232 SFP inspection for HD 087883 with S1-W1 on UT 2008/04/26, seq 001 . . 469
B.233 SFP inspection for HD 087883 with S2-E2 on UT 2007/11/29, seq 001 . . 470
B.234 SFP inspection for HD 089269 with S1-E1 on UT 2007/05/17, seq 002 . . 470
B.235 SFP inspection for HD 089269 with S1-W1 on UT 2007/04/24, seq 001 . . 470
B.236 SFP inspection for HD 090343 with S1-E1 on UT 2008/06/25, seq 001 . . 471
B.237 SFP inspection for HD 090343 with S2-W1 on UT 2008/06/24, seq 001 . . 471
B.238 SFP inspection for HD 094765 with S1-E1 on UT 2008/04/14, seq 001 . . 471
B.239 SFP inspection for HD 094765 with S1-W1 on UT 2008/04/15, seq 001 . . 472
B.240 SFP inspection for HD 096064 with S1-E1 on UT 2008/04/14, seq 001 . . 472
B.241 SFP inspection for HD 096064 with S1-W1 on UT 2008/04/15, seq 001 . . 472
B.242 SFP inspection for HD 097334 with S1-E1 on UT 2008/04/12, seq 002 . . 473
B.243 SFP inspection for HD 097334 with S1-W1 on UT 2008/04/12, seq 001 . . 473
B.244 SFP inspection for HD 097658 with S1-E1 on UT 2008/04/13, seq 001 . . 473
B.245 SFP inspection for HD 097658 with S1-E1 on UT 2008/04/14, seq 001 . . 474
B.246 SFP inspection for HD 098230 with S1-E1 on UT 2007/02/06, seq 001 . . 474
B.247 SFP inspection for HD 098230 with S1-E1 on UT 2007/03/08, seq 001 . . 474
B.248 SFP inspection for HD 098230 with S1-E1 on UT 2007/03/08, seq 002 . . 475
B.249 SFP inspection for HD 098230 with S1-E1 on UT 2007/05/17, seq 001 . . 475
B.250 SFP inspection for HD 098230 with S1-E1 on UT 2007/05/17, seq 002 . . 475
B.251 SFP inspection for HD 098230 with S1-E1 on UT 2007/05/17, seq 003 . . 476
B.252 SFP inspection for HD 098230 with S1-E1 on UT 2008/04/13, seq 001 . . 476
B.253 SFP inspection for HD 098230 with S1-W1 on UT 2007/04/24, seq 001 . . 476
B.254 SFP inspection for HD 098230 with S1-W1 on UT 2007/05/28, seq 001 . . 477
B.255 SFP inspection for HD 098230 with S1-W1 on UT 2007/06/01, seq 001 . . 477
B.256 SFP inspection for HD 098230 with S1-W1 on UT 2007/06/01, seq 002 . . 477
B.257 SFP inspection for HD 098230 with S1-W1 on UT 2007/06/01, seq 003 . . 478

B.258 SFP inspection for HD 098230 with S1-W1 on UT 2008/04/12, seq 001 . . 478
B.259 SFP inspection for HD 098281 with S1-E1 on UT 2008/04/14, seq 001 . . 478
B.260 SFP inspection for HD 098281 with S1-W1 on UT 2008/04/15, seq 001 . . 479
B.261 SFP inspection for HD 099028 with S1-E1 on UT 2007/02/06, seq 003 . . 479
B.262 SFP inspection for HD 099491 with S1-E1 on UT 2007/03/08, seq 001 . . 479
B.263 SFP inspection for HD 099491 with S1-E1 on UT 2008/04/14, seq 001 . . 480
B.264 SFP inspection for HD 099491 with S1-E1 on UT 2008/04/14, seq 002 . . 480
B.265 SFP inspection for HD 099491 with S1-W1 on UT 2008/04/15, seq 001 . . 480
B.266 SFP inspection for HD 099492 with S1-W1 on UT 2008/04/15, seq 001 . . 481
B.267 SFP inspection for HD 100180 with S1-E1 on UT 2007/02/06, seq 001 . . 481
B.268 SFP inspection for HD 100180 with S1-E1 on UT 2007/03/08, seq 001 . . 481
B.269 SFP inspection for HD 100180 with S1-W1 on UT 2007/04/24, seq 001 . . 482
B.270 SFP inspection for HD 101177 with S1-E1 on UT 2007/05/17, seq 001 . . 482
B.271 SFP inspection for HD 101177 with S1-W1 on UT 2007/04/24, seq 001 . . 482
B.272 SFP inspection for HD 101206 with S1-E1 on UT 2008/04/12, seq 002 . . 483
B.273 SFP inspection for HD 101206 with S1-W1 on UT 2008/04/12, seq 001 . . 483
B.274 SFP inspection for HD 104304 with S1-E1 on UT 2008/04/14, seq 001 . . 483
B.275 SFP inspection for HD 104304 with S1-W1 on UT 2008/04/15, seq 001 . . 484
B.276 SFP inspection for HD 105631 with S1-E1 on UT 2007/05/17, seq 001 . . 484
B.277 SFP inspection for HD 105631 with S1-W1 on UT 2007/04/24, seq 001 . . 484
B.278 SFP inspection for HD 105631 with S1-W1 on UT 2007/06/01, seq 001 . . 485
B.279 SFP inspection for HD 105631 with S1-W1 on UT 2008/04/26, seq 001 . . 485
B.280 SFP inspection for HD 108954 with S1-E1 on UT 2007/04/11, seq 001 . . 485
B.281 SFP inspection for HD 108954 with S1-E1 on UT 2007/04/11, seq 002 . . 486
B.282 SFP inspection for HD 108954 with S1-W1 on UT 2007/04/24, seq 001 . . 486
B.283 SFP inspection for HD 110833 with S1-E1 on UT 2007/04/14, seq 001 . . 486

B.284 SFP inspection for HD 110833 with S1-E1 on UT 2007/07/28, seq 001 . . 487
B.285 SFP inspection for HD 110833 with S1-W1 on UT 2007/04/17, seq 001 . . 487
B.286 SFP inspection for HD 110833 with S1-W1 on UT 2007/04/17, seq 002 . . 487
B.287 SFP inspection for HD 110833 with S1-W1 on UT 2007/05/28, seq 002 . . 488
B.288 SFP inspection for HD 112758 with S1-E1 on UT 2008/04/14, seq 001 . . 488
B.289 SFP inspection for HD 112758 with S1-W1 on UT 2008/04/15, seq 001 . . 488
B.290 SFP inspection for HD 113449 with S1-E1 on UT 2008/04/14, seq 001 . . 489
B.291 SFP inspection for HD 113449 with S1-W1 on UT 2008/04/15, seq 001 . . 489
B.292 SFP inspection for HD 114783 with S1-E1 on UT 2008/04/13, seq 001 . . 489
B.293 SFP inspection for HD 114783 with S1-E1 on UT 2008/04/25, seq 001 . . 490
B.294 SFP inspection for HD 114783 with S1-W1 on UT 2008/04/13, seq 002 . . 490
B.295 SFP inspection for HD 115404 with S1-E1 on UT 2007/02/06, seq 001 . . 490
B.296 SFP inspection for HD 115404 with S1-E1 on UT 2007/02/06, seq 002 . . 491
B.297 SFP inspection for HD 115404 with S1-E1 on UT 2007/03/08, seq 001 . . 491
B.298 SFP inspection for HD 115404 with S1-W1 on UT 2007/04/24, seq 001 . . 491
B.299 SFP inspection for HD 116442 with S1-E1 on UT 2007/03/12, seq 002 . . 492
B.300 SFP inspection for HD 116442 with S1-W1 on UT 2007/06/01, seq 001 . . 492
B.301 SFP inspection for HD 116443 with S1-E1 on UT 2007/03/12, seq 001 . . 492
B.302 SFP inspection for HD 116443 with S1-W1 on UT 2007/06/01, seq 001 . . 493
B.303 SFP inspection for HD 116956 with S1-E1 on UT 2007/04/03, seq 001 . . 493
B.304 SFP inspection for HD 116956 with S1-E1 on UT 2007/04/03, seq 003 . . 493
B.305 SFP inspection for HD 116956 with S1-E1 on UT 2008/06/25, seq 001 . . 494
B.306 SFP inspection for HD 116956 with S1-W1 on UT 2007/05/28, seq 001 . . 494
B.307 SFP inspection for HD 116956 with S1-W1 on UT 2008/04/26, seq 001 . . 494
B.308 SFP inspection for HD 116956 with S2-W1 on UT 2008/06/24, seq 001 . . 495
B.309 SFP inspection for HD 119332 with S1-E1 on UT 2007/04/03, seq 002 . . 495

B.310 SFP inspection for HD 119332 with S1-E1 on UT 2008/04/12, seq 002 . . 495
B.311 SFP inspection for HD 119332 with S1-W1 on UT 2008/04/12, seq 001 . . 496
B.312 SFP inspection for HD 121560 with S1-E1 on UT 2007/02/05, seq 001 . . 496
B.313 SFP inspection for HD 121560 with S1-E1 on UT 2007/02/05, seq 002 . . 496
B.314 SFP inspection for HD 121560 with S1-E1 on UT 2007/03/08, seq 001 . . 497
B.315 SFP inspection for HD 121560 with S1-W1 on UT 2007/04/24, seq 001 . . 497
B.316 SFP inspection for HD 124292 with S1-E1 on UT 2007/03/12, seq 002 . . 497
B.317 SFP inspection for HD 124292 with S1-E1 on UT 2008/04/13, seq 001 . . 498
B.318 SFP inspection for HD 124292 with S1-E1 on UT 2008/04/25, seq 001 . . 498
B.319 SFP inspection for HD 124292 with S1-W1 on UT 2008/04/13, seq 002 . . 498
B.320 SFP inspection for HD 124850 with S1-E1 on UT 2007/02/16, seq 001 . . 499
B.321 SFP inspection for HD 124850 with S1-E1 on UT 2007/03/23, seq 001 . . 499
B.322 SFP inspection for HD 124850 with S1-E1 on UT 2008/04/25, seq 001 . . 499
B.323 SFP inspection for HD 124850 with S1-E2 on UT 2007/05/31, seq 001 . . 500
B.324 SFP inspection for HD 124850 with S1-E2 on UT 2008/06/08, seq 001 . . 500
B.325 SFP inspection for HD 124850 with S1-E2 on UT 2008/06/08, seq 002 . . 500
B.326 SFP inspection for HD 124850 with S1-W1 on UT 2008/07/08, seq 001 . . 501
B.327 SFP inspection for HD 124850 with S2-W2 on UT 2008/06/09, seq 001 . . 501
B.328 SFP inspection for HD 125455 with S1-E1 on UT 2007/03/12, seq 001 . . 501
B.329 SFP inspection for HD 125455 with S1-E1 on UT 2008/04/14, seq 001 . . 502
B.330 SFP inspection for HD 125455 with S1-E1 on UT 2008/04/25, seq 001 . . 502
B.331 SFP inspection for HD 125455 with S1-W1 on UT 2008/04/14, seq 002 . . 502
B.332 SFP inspection for HD 127334 with E1-W1 on UT 2007/04/26, seq 001 . . 503
B.333 SFP inspection for HD 127334 with S1-E1 on UT 2007/04/14, seq 001 . . 503
B.334 SFP inspection for HD 127334 with S1-W1 on UT 2007/04/17, seq 001 . . 503
B.335 SFP inspection for HD 127334 with S1-W1 on UT 2007/04/17, seq 002 . . 504

B.336 SFP inspection for HD 128165 with E1-W1 on UT 2007/04/26, seq 001 . . 504
B.337 SFP inspection for HD 128165 with S1-E1 on UT 2007/04/14, seq 001 . . 504
B.338 SFP inspection for HD 128165 with S1-E1 on UT 2007/07/28, seq 001 . . 505
B.339 SFP inspection for HD 128165 with S1-W1 on UT 2007/05/28, seq 001 . . 505
B.340 SFP inspection for HD 128311 with S1-E1 on UT 2008/04/13, seq 001 . . 505
B.341 SFP inspection for HD 128311 with S1-E1 on UT 2008/04/25, seq 001 . . 506
B.342 SFP inspection for HD 128311 with S1-W1 on UT 2008/04/13, seq 002 . . 506
B.343 SFP inspection for HD 128642 with S1-E1 on UT 2008/06/25, seq 001 . . 506
B.344 SFP inspection for HD 128642 with S1-E1 on UT 2008/06/25, seq 002 . . 507
B.345 SFP inspection for HD 128642 with S1-W1 on UT 2008/04/26, seq 001 . . 507
B.346 SFP inspection for HD 128642 with S1-W1 on UT 2008/04/26, seq 002 . . 507
B.347 SFP inspection for HD 128642 with S2-W1 on UT 2008/06/24, seq 001 . . 508
B.348 SFP inspection for HD 130004 with S1-E1 on UT 2007/03/10, seq 001 . . 508
B.349 SFP inspection for HD 130004 with S1-E1 on UT 2008/04/13, seq 001 . . 508
B.350 SFP inspection for HD 130004 with S1-E1 on UT 2008/04/25, seq 001 . . 509
B.351 SFP inspection for HD 130004 with S1-W1 on UT 2007/05/28, seq 001 . . 509
B.352 SFP inspection for HD 130004 with S1-W1 on UT 2008/04/13, seq 002 . . 509
B.353 SFP inspection for HD 130307 with S1-E1 on UT 2008/04/13, seq 001 . . 510
B.354 SFP inspection for HD 130307 with S1-W1 on UT 2008/04/13, seq 002 . . 510
B.355 SFP inspection for HD 132142 with S1-E1 on UT 2008/04/12, seq 002 . . 510
B.356 SFP inspection for HD 132142 with S1-E1 on UT 2008/06/25, seq 001 . . 511
B.357 SFP inspection for HD 132142 with S1-W1 on UT 2008/04/12, seq 001 . . 511
B.358 SFP inspection for HD 132142 with S2-W1 on UT 2008/06/24, seq 001 . . 511
B.359 SFP inspection for HD 132254 with E1-W1 on UT 2007/04/26, seq 001 . . 512
B.360 SFP inspection for HD 132254 with S1-E1 on UT 2007/04/11, seq 001 . . 512
B.361 SFP inspection for HD 132254 with S1-W1 on UT 2007/04/24, seq 001 . . 512

B.362 SFP inspection for HD 135204 with S1-E1 on UT 2007/03/08, seq 001 . . 513
B.363 SFP inspection for HD 135204 with S1-E1 on UT 2008/06/23, seq 001 . . 513
B.364 SFP inspection for HD 135204 with S1-E1 on UT 2008/07/05, seq 001 . . 513
B.365 SFP inspection for HD 135204 with S1-E1 on UT 2008/07/05, seq 002 . . 514
B.366 SFP inspection for HD 135204 with S1-E2 on UT 2007/05/31, seq 001 . . 514
B.367 SFP inspection for HD 135204 with S1-W1 on UT 2008/06/22, seq 001 . . 514
B.368 SFP inspection for HD 135204 with S1-W1 on UT 2008/06/22, seq 002 . . 515
B.369 SFP inspection for HD 135204 with S1-W1 on UT 2008/07/08, seq 001 . . 515
B.370 SFP inspection for HD 135204 with S1-W1 on UT 2008/07/08, seq 002 . . 515
B.371 SFP inspection for HD 135204 with S2-W2 on UT 2008/06/09, seq 001 . . 516
B.372 SFP inspection for HD 135599 with S1-E1 on UT 2007/03/08, seq 001 . . 516
B.373 SFP inspection for HD 135599 with S1-E2 on UT 2007/05/31, seq 001 . . 516
B.374 SFP inspection for HD 136202 with S1-E1 on UT 2007/02/16, seq 001 . . 517
B.375 SFP inspection for HD 136202 with S1-E1 on UT 2007/03/08, seq 001 . . 517
B.376 SFP inspection for HD 136202 with S1-E1 on UT 2008/04/13, seq 001 . . 517
B.377 SFP inspection for HD 136202 with S1-E2 on UT 2007/05/31, seq 001 . . 518
B.378 SFP inspection for HD 136202 with S1-E2 on UT 2007/06/01, seq 001 . . 518
B.379 SFP inspection for HD 136202 with S1-W1 on UT 2008/04/13, seq 002 . . 518
B.380 SFP inspection for HD 136713 with S1-E1 on UT 2008/04/25, seq 001 . . 519
B.381 SFP inspection for HD 136713 with S1-W1 on UT 2008/04/14, seq 001 . . 519
B.382 SFP inspection for HD 136923 with S1-E1 on UT 2008/04/13, seq 001 . . 519
B.383 SFP inspection for HD 136923 with S1-W1 on UT 2008/04/13, seq 002 . . 520
B.384 SFP inspection for HD 137763 with S1-E1 on UT 2008/04/25, seq 001 . . 520
B.385 SFP inspection for HD 137763 with S1-E1 on UT 2008/06/23, seq 001 . . 520
B.386 SFP inspection for HD 137763 with S1-W1 on UT 2008/04/14, seq 001 . . 521
B.387 SFP inspection for HD 137763 with S1-W1 on UT 2008/06/22, seq 001 . . 521

B.388 SFP inspection for HD 137763 with S1-W1 on UT 2008/07/07, seq 001 . . 521
B.389 SFP inspection for HD 137763 with S1-W1 on UT 2008/07/07, seq 002 . . 522
B.390 SFP inspection for HD 137763 with S2-W2 on UT 2008/06/09, seq 001 . . 522
B.391 SFP inspection for HD 137778 with S1-E1 on UT 2008/04/25, seq 001 . . 522
B.392 SFP inspection for HD 137778 with S1-W1 on UT 2008/04/14, seq 001 . . 523
B.393 SFP inspection for HD 137778 with S1-W1 on UT 2008/06/22, seq 001 . . 523
B.394 SFP inspection for HD 137778 with S1-W1 on UT 2008/07/07, seq 001 . . 523
B.395 SFP inspection for HD 137778 with S1-W1 on UT 2008/07/07, seq 002 . . 524
B.396 SFP inspection for HD 139323 with S1-E1 on UT 2008/04/12, seq 002 . . 524
B.397 SFP inspection for HD 139323 with S1-W1 on UT 2008/04/12, seq 001 . . 524
B.398 SFP inspection for HD 139341 with E1-W1 on UT 2007/04/26, seq 002 . . 525
B.399 SFP inspection for HD 139341 with S1-E1 on UT 2007/04/14, seq 001 . . 525
B.400 SFP inspection for HD 139341 with S1-W1 on UT 2007/04/17, seq 001 . . 525
B.401 SFP inspection for HD 139341 with S1-W1 on UT 2007/04/17, seq 002 . . 526
B.402 SFP inspection for HD 139341 with S1-W1 on UT 2007/04/17, seq 004 . . 526
B.403 SFP inspection for HD 139777 with S1-E1 on UT 2007/04/14, seq 001 . . 526
B.404 SFP inspection for HD 139777 with S1-W1 on UT 2007/05/28, seq 001 . . 527
B.405 SFP inspection for HD 139777 with S1-W1 on UT 2008/04/26, seq 001 . . 527
B.406 SFP inspection for HD 139777 with S2-W1 on UT 2008/06/24, seq 001 . . 527
B.407 SFP inspection for HD 139813 with S1-E1 on UT 2008/06/25, seq 001 . . 528
B.408 SFP inspection for HD 139813 with S1-W1 on UT 2008/04/26, seq 001 . . 528
B.409 SFP inspection for HD 139813 with S2-W1 on UT 2008/06/24, seq 001 . . 528
B.410 SFP inspection for HD 141272 with S1-E1 on UT 2008/04/25, seq 001 . . 529
B.411 SFP inspection for HD 141272 with S1-W1 on UT 2008/04/14, seq 001 . . 529
B.412 SFP inspection for HD 142267 with S1-E1 on UT 2007/08/15, seq 001 . . 529
B.413 SFP inspection for HD 142267 with S1-E1 on UT 2008/04/13, seq 001 . . 530

B.414 SFP inspection for HD 142267 with S1-E2 on UT 2007/06/01, seq 001 . . 530
B.415 SFP inspection for HD 142267 with S1-W1 on UT 2008/04/13, seq 002 . . 530
B.416 SFP inspection for HD 144287 with S1-E1 on UT 2008/04/13, seq 001 . . 531
B.417 SFP inspection for HD 144287 with S1-W1 on UT 2008/04/12, seq 001 . . 531
B.418 SFP inspection for HD 145675 with E1-W1 on UT 2007/04/26, seq 001 . . 531
B.419 SFP inspection for HD 145675 with S1-E1 on UT 2007/05/17, seq 001 . . 532
B.420 SFP inspection for HD 145675 with S1-W1 on UT 2007/04/24, seq 001 . . 532
B.421 SFP inspection for HD 146233 with S1-E1 on UT 2007/03/08, seq 001 . . 532
B.422 SFP inspection for HD 146233 with S1-E1 on UT 2008/04/25, seq 001 . . 533
B.423 SFP inspection for HD 146233 with S1-E1 on UT 2008/06/23, seq 001 . . 533
B.424 SFP inspection for HD 146233 with S1-W1 on UT 2008/04/14, seq 001 . . 533
B.425 SFP inspection for HD 146233 with S1-W1 on UT 2008/06/22, seq 001 . . 534
B.426 SFP inspection for HD 148653 with S1-E1 on UT 2007/02/04, seq 001 . . 534
B.427 SFP inspection for HD 149661 with S1-E1 on UT 2007/03/08, seq 002 . . 534
B.428 SFP inspection for HD 149661 with S1-E2 on UT 2007/05/31, seq 001 . . 535
B.429 SFP inspection for HD 149806 with S1-E1 on UT 2008/04/25, seq 001 . . 535
B.430 SFP inspection for HD 149806 with S1-W1 on UT 2008/04/13, seq 001 . . 535
B.431 SFP inspection for HD 149806 with S1-W1 on UT 2008/04/14, seq 001 . . 536
B.432 SFP inspection for HD 151541 with S1-E1 on UT 2008/06/25, seq 001 . . 536
B.433 SFP inspection for HD 151541 with S1-W1 on UT 2008/04/26, seq 001 . . 536
B.434 SFP inspection for HD 151541 with S2-W1 on UT 2008/06/24, seq 001 . . 537
B.435 SFP inspection for HD 153557 with S1-E1 on UT 2008/06/25, seq 001 . . 537
B.436 SFP inspection for HD 153557 with S1-W1 on UT 2007/05/30, seq 001 . . 537
B.437 SFP inspection for HD 153557 with S1-W1 on UT 2007/08/21, seq 001 . . 538
B.438 SFP inspection for HD 153557 with S1-W1 on UT 2008/04/12, seq 001 . . 538
B.439 SFP inspection for HD 153557 with S2-W1 on UT 2008/06/24, seq 001 . . 538

B.440 SFP inspection for HD 154345 with E1-W1 on UT 2007/04/26, seq 001 . . 539
B.441 SFP inspection for HD 154345 with S1-E1 on UT 2007/04/14, seq 001 . . 539
B.442 SFP inspection for HD 154345 with S1-W1 on UT 2007/04/17, seq 001 . . 539
B.443 SFP inspection for HD 154345 with S1-W1 on UT 2007/04/17, seq 002 . . 540
B.444 SFP inspection for HD 155712 with S1-E1 on UT 2008/04/25, seq 001 . . 540
B.445 SFP inspection for HD 155712 with S1-W1 on UT 2008/04/13, seq 001 . . 540
B.446 SFP inspection for HD 155712 with S1-W1 on UT 2008/04/14, seq 001 . . 541
B.447 SFP inspection for HD 155712 with S2-W1 on UT 2007/09/17, seq 001 . . 541
B.448 SFP inspection for HD 157347 with S1-E1 on UT 2008/04/25, seq 001 . . 541
B.449 SFP inspection for HD 157347 with S1-W1 on UT 2008/04/13, seq 001 . . 542
B.450 SFP inspection for HD 157347 with S1-W1 on UT 2008/04/14, seq 001 . . 542
B.451 SFP inspection for HD 158614 with S1-E1 on UT 2008/04/25, seq 001 . . 542
B.452 SFP inspection for HD 158614 with S1-E2 on UT 2007/06/01, seq 001 . . 543
B.453 SFP inspection for HD 158614 with S1-W1 on UT 2008/04/14, seq 001 . . 543
B.454 SFP inspection for HD 158633 with S1-E1 on UT 2007/04/14, seq 001 . . 543
B.455 SFP inspection for HD 158633 with S1-W1 on UT 2007/04/17, seq 001 . . 544
B.456 SFP inspection for HD 158633 with S1-W1 on UT 2007/04/17, seq 002 . . 544
B.457 SFP inspection for HD 158633 with S1-W1 on UT 2007/04/17, seq 003 . . 544
B.458 SFP inspection for HD 159062 with S1-E1 on UT 2007/04/14, seq 001 . . 545
B.459 SFP inspection for HD 159062 with S1-E1 on UT 2008/06/25, seq 001 . . 545
B.460 SFP inspection for HD 159062 with S1-W1 on UT 2007/08/21, seq 002 . . 545
B.461 SFP inspection for HD 159062 with S1-W1 on UT 2008/04/12, seq 001 . . 546
B.462 SFP inspection for HD 159062 with S2-W1 on UT 2008/06/24, seq 001 . . 546
B.463 SFP inspection for HD 159222 with S1-E1 on UT 2007/05/17, seq 002 . . 546
B.464 SFP inspection for HD 159222 with S1-E1 on UT 2008/06/26, seq 001 . . 547
B.465 SFP inspection for HD 159222 with S1-W1 on UT 2008/04/12, seq 001 . . 547

B.466 SFP inspection for HD 159222 with S2-W1 on UT 2008/06/24, seq 001 . . 547
B.467 SFP inspection for HD 160346 with S1-E1 on UT 2007/07/22, seq 003 . . 548
B.468 SFP inspection for HD 160346 with S1-W1 on UT 2007/07/22, seq 001 . . 548
B.469 SFP inspection for HD 161198 with S1-E1 on UT 2008/04/25, seq 001 . . 548
B.470 SFP inspection for HD 161198 with S1-W1 on UT 2007/05/30, seq 001 . . 549
B.471 SFP inspection for HD 161198 with S1-W1 on UT 2008/04/13, seq 001 . . 549
B.472 SFP inspection for HD 161198 with S1-W1 on UT 2008/04/14, seq 001 . . 549
B.473 SFP inspection for HD 161198 with S2-W1 on UT 2007/09/17, seq 001 . . 550
B.474 SFP inspection for HD 164922 with S1-E1 on UT 2007/05/17, seq 001 . . 550
B.475 SFP inspection for HD 164922 with S1-E2 on UT 2007/05/31, seq 001 . . 550
B.476 SFP inspection for HD 165401 with S1-E1 on UT 2007/07/22, seq 002 . . 551
B.477 SFP inspection for HD 165401 with S1-E1 on UT 2008/04/25, seq 001 . . 551
B.478 SFP inspection for HD 165401 with S1-E1 on UT 2008/06/21, seq 001 . . 551
B.479 SFP inspection for HD 165401 with S1-E1 on UT 2008/06/23, seq 001 . . 552
B.480 SFP inspection for HD 165401 with S1-E1 on UT 2008/07/05, seq 001 . . 552
B.481 SFP inspection for HD 165401 with S1-E1 on UT 2008/07/05, seq 002 . . 552
B.482 SFP inspection for HD 165401 with S1-W1 on UT 2007/07/22, seq 001 . . 553
B.483 SFP inspection for HD 165401 with S1-W1 on UT 2008/06/22, seq 001 . . 553
B.484 SFP inspection for HD 165401 with S1-W1 on UT 2008/07/07, seq 001 . . 553
B.485 SFP inspection for HD 165401 with S1-W1 on UT 2008/07/07, seq 002 . . 554
B.486 SFP inspection for HD 166620 with E1-W1 on UT 2007/04/26, seq 001 . . 554
B.487 SFP inspection for HD 166620 with S1-E1 on UT 2007/04/14, seq 001 . . 554
B.488 SFP inspection for HD 166620 with S2-E2 on UT 2007/09/18, seq 001 . . 555
B.489 SFP inspection for HD 166620 with S2-W1 on UT 2007/09/17, seq 001 . . 555
B.490 SFP inspection for HD 175742 with S1-E1 on UT 2008/06/21, seq 001 . . 555
B.491 SFP inspection for HD 175742 with S1-E1 on UT 2008/06/23, seq 001 . . 556

B.492 SFP inspection for HD 175742 with S1-E2 on UT 2007/05/29, seq 001 . . 556
B.493 SFP inspection for HD 175742 with S1-W1 on UT 2008/04/13, seq 001 . . 556
B.494 SFP inspection for HD 175742 with S1-W1 on UT 2008/04/14, seq 001 . . 557
B.495 SFP inspection for HD 175742 with S2-E2 on UT 2007/09/18, seq 003 . . 557
B.496 SFP inspection for HD 175742 with S2-W1 on UT 2007/09/17, seq 001 . . 557
B.497 SFP inspection for HD 175742 with S2-W1 on UT 2008/06/24, seq 001 . . 558
B.498 SFP inspection for HD 176377 with S1-E1 on UT 2007/04/14, seq 001 . . 558
B.499 SFP inspection for HD 176377 with S1-E1 on UT 2008/06/21, seq 001 . . 558
B.500 SFP inspection for HD 176377 with S1-E1 on UT 2008/06/23, seq 001 . . 559
B.501 SFP inspection for HD 176377 with S1-E1 on UT 2008/06/26, seq 001 . . 559
B.502 SFP inspection for HD 176377 with S1-W1 on UT 2008/04/13, seq 001 . . 559
B.503 SFP inspection for HD 176377 with S2-W1 on UT 2007/09/17, seq 001 . . 560
B.504 SFP inspection for HD 176377 with S2-W1 on UT 2008/06/24, seq 001 . . 560
B.505 SFP inspection for HD 178428 with S1-E2 on UT 2007/05/29, seq 001 . . 560
B.506 SFP inspection for HD 178428 with S1-E2 on UT 2007/06/01, seq 001 . . 561
B.507 SFP inspection for HD 178428 with S1-W1 on UT 2007/05/30, seq 001 . . 561
B.508 SFP inspection for HD 179957 with S1-E1 on UT 2007/07/25, seq 002 . . 561
B.509 SFP inspection for HD 179957 with S1-W1 on UT 2007/05/30, seq 001 . . 562
B.510 SFP inspection for HD 179957 with S1-W1 on UT 2007/08/18, seq 001 . . 562
B.511 SFP inspection for HD 179957 with S1-W1 on UT 2007/08/21, seq 002 . . 562
B.512 SFP inspection for HD 179957 with S2-E1 on UT 2007/08/20, seq 001 . . 563
B.513 SFP inspection for HD 179958 with S1-W1 on UT 2007/05/30, seq 002 . . 563
B.514 SFP inspection for HD 180161 with S1-E1 on UT 2007/04/14, seq 001 . . 563
B.515 SFP inspection for HD 180161 with S1-E1 on UT 2007/09/16, seq 002 . . 564
B.516 SFP inspection for HD 180161 with S1-W1 on UT 2007/08/21, seq 001 . . 564
B.517 SFP inspection for HD 180161 with S1-W1 on UT 2007/09/16, seq 001 . . 564

B.518 SFP inspection for HD 180161 with S2-E1 on UT 2007/08/20, seq 001 . . 565
B.519 SFP inspection for HD 182488 with S1-E1 on UT 2007/04/14, seq 001 . . 565
B.520 SFP inspection for HD 182488 with S1-W1 on UT 2007/08/18, seq 001 . . 565
B.521 SFP inspection for HD 182488 with S2-E2 on UT 2007/09/18, seq 001 . . 566
B.522 SFP inspection for HD 182488 with S2-W1 on UT 2007/09/17, seq 001 . . 566
B.523 SFP inspection for HD 184385 with S1-E2 on UT 2007/05/29, seq 001 . . 566
B.524 SFP inspection for HD 184385 with S1-W1 on UT 2007/05/30, seq 001 . . 567
B.525 SFP inspection for HD 185144 with E1-W1 on UT 2007/04/26, seq 001 . . 567
B.526 SFP inspection for HD 185144 with S1-E1 on UT 2007/07/28, seq 001 . . 567
B.527 SFP inspection for HD 185144 with S1-E1 on UT 2007/09/16, seq 002 . . 568
B.528 SFP inspection for HD 185144 with S1-W1 on UT 2007/05/28, seq 001 . . 568
B.529 SFP inspection for HD 185144 with S1-W1 on UT 2007/09/16, seq 001 . . 568
B.530 SFP inspection for HD 185144 with S2-E1 on UT 2007/08/20, seq 001 . . 569
B.531 SFP inspection for HD 185414 with S1-E1 on UT 2007/04/14, seq 001 . . 569
B.532 SFP inspection for HD 185414 with S1-W1 on UT 2007/05/28, seq 001 . . 569
B.533 SFP inspection for HD 189340 with S1-E1 on UT 2008/06/21, seq 001 . . 570
B.534 SFP inspection for HD 189340 with S1-E1 on UT 2008/06/23, seq 001 . . 570
B.535 SFP inspection for HD 189340 with S1-E1 on UT 2008/06/23, seq 002 . . 570
B.536 SFP inspection for HD 189340 with S1-W1 on UT 2008/06/22, seq 001 . . 571
B.537 SFP inspection for HD 189340 with S2-W2 on UT 2008/06/09, seq 001 . . 571
B.538 SFP inspection for HD 189340 with S2-W2 on UT 2008/06/09, seq 002 . . 571
B.539 SFP inspection for HD 189733 with S1-E1 on UT 2007/07/24, seq 001 . . 572
B.540 SFP inspection for HD 189733 with S1-W1 on UT 2007/05/30, seq 001 . . 572
B.541 SFP inspection for HD 189733 with S2-W1 on UT 2007/09/17, seq 001 . . 572
B.542 SFP inspection for HD 190067 with S1-E1 on UT 2007/07/22, seq 002 . . 573
B.543 SFP inspection for HD 190067 with S1-E1 on UT 2007/07/24, seq 003 . . 573

B.544 SFP inspection for HD 190067 with S1-W1 on UT 2007/07/22, seq 001 . . 573
B.545 SFP inspection for HD 190404 with S1-E1 on UT 2007/07/24, seq 001 . . 574
B.546 SFP inspection for HD 190404 with S1-W1 on UT 2007/07/24, seq 002 . . 574
B.547 SFP inspection for HD 190470 with S1-E1 on UT 2007/07/24, seq 001 . . 574
B.548 SFP inspection for HD 190470 with S1-E1 on UT 2007/08/18, seq 002 . . 575
B.549 SFP inspection for HD 190470 with S1-W1 on UT 2007/07/24, seq 002 . . 575
B.550 SFP inspection for HD 190470 with S1-W1 on UT 2007/08/17, seq 001 . . 575
B.551 SFP inspection for HD 190470 with S1-W1 on UT 2007/08/18, seq 001 . . 576
B.552 SFP inspection for HD 190771 with S1-E1 on UT 2007/04/14, seq 001 . . 576
B.553 SFP inspection for HD 190771 with S1-E1 on UT 2007/08/18, seq 002 . . 576
B.554 SFP inspection for HD 190771 with S1-W1 on UT 2007/08/18, seq 001 . . 577
B.555 SFP inspection for HD 190771 with S1-W1 on UT 2007/08/21, seq 001 . . 577
B.556 SFP inspection for HD 190771 with S2-E1 on UT 2007/08/20, seq 001 . . 577
B.557 SFP inspection for HD 191499 with S1-E1 on UT 2007/07/22, seq 002 . . 578
B.558 SFP inspection for HD 191499 with S1-E1 on UT 2007/07/24, seq 001 . . 578
B.559 SFP inspection for HD 191499 with S1-W1 on UT 2007/07/22, seq 001 . . 578
B.560 SFP inspection for HD 191499 with S1-W1 on UT 2007/07/24, seq 002 . . 579
B.561 SFP inspection for HD 191785 with S1-E1 on UT 2007/07/22, seq 001 . . 579
B.562 SFP inspection for HD 191785 with S1-E1 on UT 2007/07/24, seq 001 . . 579
B.563 SFP inspection for HD 191785 with S1-W1 on UT 2007/07/24, seq 002 . . 580
B.564 SFP inspection for HD 192263 with S1-E1 on UT 2007/08/15, seq 002 . . 580
B.565 SFP inspection for HD 192263 with S1-E1 on UT 2008/04/25, seq 001 . . 580
B.566 SFP inspection for HD 192263 with S1-E1 on UT 2008/06/23, seq 001 . . 581
B.567 SFP inspection for HD 192263 with S1-E1 on UT 2008/07/06, seq 001 . . 581
B.568 SFP inspection for HD 192263 with S1-E1 on UT 2008/07/06, seq 002 . . 581
B.569 SFP inspection for HD 192263 with S1-W1 on UT 2008/06/22, seq 001 . . 582

B.570 SFP inspection for HD 192263 with S1-W1 on UT 2008/07/07, seq 001 . . 582
B.571 SFP inspection for HD 192263 with S1-W1 on UT 2008/07/07, seq 002 . . 582
B.572 SFP inspection for HD 195564 with S1-E1 on UT 2008/06/23, seq 001 . . 583
B.573 SFP inspection for HD 195564 with S1-W1 on UT 2008/06/22, seq 001 . . 583
B.574 SFP inspection for HD 195564 with S2-W2 on UT 2008/06/09, seq 001 . . 583
B.575 SFP inspection for HD 195564 with S2-W2 on UT 2008/06/09, seq 002 . . 584
B.576 SFP inspection for HD 197076 with S1-E1 on UT 2007/07/22, seq 002 . . 584
B.577 SFP inspection for HD 197076 with S1-E1 on UT 2007/07/24, seq 001 . . 584
B.578 SFP inspection for HD 197076 with S1-W1 on UT 2007/07/22, seq 001 . . 585
B.579 SFP inspection for HD 197076 with S1-W1 on UT 2007/07/24, seq 002 . . 585
B.580 SFP inspection for HD 198425 with S1-E1 on UT 2007/08/14, seq 001 . . 585
B.581 SFP inspection for HD 198425 with S1-E1 on UT 2008/07/23, seq 001 . . 586
B.582 SFP inspection for HD 198425 with S1-W1 on UT 2007/08/17, seq 001 . . 586
B.583 SFP inspection for HD 198425 with S1-W1 on UT 2008/07/08, seq 001 . . 586
B.584 SFP inspection for HD 200560 with S1-E1 on UT 2007/07/28, seq 001 . . 587
B.585 SFP inspection for HD 200560 with S1-E1 on UT 2007/08/18, seq 002 . . 587
B.586 SFP inspection for HD 200560 with S1-W1 on UT 2007/08/18, seq 001 . . 587
B.587 SFP inspection for HD 200560 with S2-E1 on UT 2007/08/20, seq 001 . . 588
B.588 SFP inspection for HD 202751 with S1-E1 on UT 2007/07/22, seq 001 . . 588
B.589 SFP inspection for HD 202751 with S1-W1 on UT 2007/07/24, seq 001 . . 588
B.590 SFP inspection for HD 202751 with S2-W1 on UT 2007/09/17, seq 001 . . 589
B.591 SFP inspection for HD 208038 with S1-E1 on UT 2007/07/24, seq 002 . . 589
B.592 SFP inspection for HD 208038 with S1-E1 on UT 2007/08/14, seq 001 . . 589
B.593 SFP inspection for HD 208038 with S1-W1 on UT 2007/08/14, seq 002 . . 590
B.594 SFP inspection for HD 208313 with S1-E1 on UT 2007/07/25, seq 001 . . 590
B.595 SFP inspection for HD 208313 with S1-E1 on UT 2007/08/14, seq 001 . . 590

B.596 SFP inspection for HD 208313 with S1-W1 on UT 2007/08/14, seq 002 . . 591
B.597 SFP inspection for HD 210277 with S1-E1 on UT 2008/06/23, seq 001 . . 591
B.598 SFP inspection for HD 210277 with S1-E1 on UT 2008/07/06, seq 001 . . 591
B.599 SFP inspection for HD 210277 with S1-E1 on UT 2008/07/06, seq 002 . . 592
B.600 SFP inspection for HD 210277 with S1-W1 on UT 2008/06/22, seq 001 . . 592
B.601 SFP inspection for HD 210277 with S1-W1 on UT 2008/07/07, seq 001 . . 592
B.602 SFP inspection for HD 210277 with S1-W1 on UT 2008/07/07, seq 002 . . 593
B.603 SFP inspection for HD 210277 with S2-W1 on UT 2007/09/17, seq 001 . . 593
B.604 SFP inspection for HD 210667 with S1-E1 on UT 2007/07/26, seq 001 . . 593
B.605 SFP inspection for HD 210667 with S1-E1 on UT 2007/07/28, seq 001 . . 594
B.606 SFP inspection for HD 210667 with S1-W1 on UT 2007/07/26, seq 002 . . 594
B.607 SFP inspection for HD 211472 with S1-E1 on UT 2007/07/26, seq 001 . . 594
B.608 SFP inspection for HD 211472 with S1-E1 on UT 2007/07/28, seq 001 . . 595
B.609 SFP inspection for HD 211472 with S1-W1 on UT 2007/07/26, seq 002 . . 595
B.610 SFP inspection for HD 215152 with S1-E1 on UT 2008/07/06, seq 001 . . 595
B.611 SFP inspection for HD 215152 with S1-W1 on UT 2008/07/07, seq 001 . . 596
B.612 SFP inspection for HD 215152 with S2-W1 on UT 2007/09/17, seq 001 . . 596
B.613 SFP inspection for HD 216520 with S1-E1 on UT 2007/07/26, seq 001 . . 596
B.614 SFP inspection for HD 216520 with S1-E1 on UT 2007/09/16, seq 002 . . 597
B.615 SFP inspection for HD 216520 with S1-W1 on UT 2007/09/16, seq 001 . . 597
B.616 SFP inspection for HD 217107 with S1-E1 on UT 2007/08/14, seq 001 . . 597
B.617 SFP inspection for HD 217107 with S1-W1 on UT 2007/08/14, seq 002 . . 598
B.618 SFP inspection for HD 217813 with S1-E1 on UT 2007/07/22, seq 001 . . 598
B.619 SFP inspection for HD 217813 with S1-E1 on UT 2007/08/14, seq 001 . . 598
B.620 SFP inspection for HD 217813 with S1-W1 on UT 2007/08/14, seq 002 . . 599
B.621 SFP inspection for HD 218868 with S1-E1 on UT 2007/07/26, seq 001 . . 599

B.622 SFP inspection for HD 218868 with S1-E1 on UT 2007/07/28, seq 002 . . 599
B.623 SFP inspection for HD 218868 with S1-E1 on UT 2008/06/25, seq 001 . . 600
B.624 SFP inspection for HD 218868 with S1-E1 on UT 2008/07/21, seq 001 . . 600
B.625 SFP inspection for HD 218868 with S1-W1 on UT 2007/07/26, seq 002 . . 600
B.626 SFP inspection for HD 219134 with S1-E1 on UT 2007/07/26, seq 002 . . 601
B.627 SFP inspection for HD 219134 with S1-W1 on UT 2007/07/26, seq 003 . . 601
B.628 SFP inspection for HD 219538 with S1-E1 on UT 2007/08/14, seq 001 . . 601
B.629 SFP inspection for HD 219538 with S1-W1 on UT 2007/08/14, seq 002 . . 602
B.630 SFP inspection for HD 219623 with S1-E1 on UT 2007/08/18, seq 002 . . 602
B.631 SFP inspection for HD 219623 with S1-W1 on UT 2007/08/18, seq 001 . . 602
B.632 SFP inspection for HD 219623 with S2-E1 on UT 2007/08/20, seq 001 . . 603
B.633 SFP inspection for HD 220140 with S1-E1 on UT 2007/09/16, seq 002 . . 603
B.634 SFP inspection for HD 220140 with S1-W1 on UT 2007/09/16, seq 001 . . 603
B.635 SFP inspection for HD 220182 with S1-E1 on UT 2007/08/18, seq 002 . . 604
B.636 SFP inspection for HD 220182 with S1-W1 on UT 2007/08/18, seq 001 . . 604
B.637 SFP inspection for HD 220339 with S1-E1 on UT 2008/07/06, seq 001 . . 604
B.638 SFP inspection for HD 220339 with S1-W1 on UT 2008/07/07, seq 001 . . 605
B.639 SFP inspection for HD 221354 with S1-E1 on UT 2007/09/16, seq 002 . . 605
B.640 SFP inspection for HD 221354 with S1-W1 on UT 2007/09/16, seq 001 . . 605
B.641 SFP inspection for HD 221354 with S2-E1 on UT 2007/08/20, seq 002 . . 606
B.642 SFP inspection for HD 221851 with S1-E1 on UT 2007/08/18, seq 002 . . 606
B.643 SFP inspection for HD 221851 with S1-W1 on UT 2007/08/18, seq 001 . . 606
B.644 SFP inspection for HD 222143 with S1-E1 on UT 2007/07/27, seq 001 . . 607
B.645 SFP inspection for HD 222143 with S1-E1 on UT 2007/08/18, seq 002 . . 607
B.646 SFP inspection for HD 222143 with S1-W1 on UT 2007/08/18, seq 001 . . 607
B.647 SFP inspection for HD 222143 with S2-E1 on UT 2007/08/20, seq 001 . . 608

B.648 SFP inspection for HD 222404 with S1-E1 on UT 2007/09/16, seq 003 . . 608
B.649 SFP inspection for HD 222404 with S1-E1 on UT 2008/06/25, seq 001 . . 608
B.650 SFP inspection for HD 222404 with S1-W1 on UT 2007/09/16, seq 002 . . 609
B.651 SFP inspection for HD 222404 with S1-W1 on UT 2008/04/26, seq 001 . . 609
B.652 SFP inspection for HD 222404 with S2-W1 on UT 2008/06/24, seq 001 . . 609
B.653 SFP inspection for HD 224465 with S1-E1 on UT 2007/08/18, seq 002 . . 610
B.654 SFP inspection for HD 224465 with S1-W1 on UT 2007/08/18, seq 001 . . 610
B.655 SFP inspection for HD 224465 with S2-E1 on UT 2007/08/20, seq 001 . . 610

Abbreviations and Acronyms

AO	Adaptive Optics
CHARA	Center for High Angular Resolution Astronomy
CCPS	California and Carnegie Planet Search
CIV	Calibrated Interferometric Visibility
CfA	The Harvard-Smithsonian Center for Astrophysics
CNS	Catalogs of Nearby Stars
CPM	Common Proper Motion
EB	Eclipsing Binary
FIC	Fourth Catalog of Interferometric Measurements of Binary Stars
GSU	Georgia State University
HST	Hubble Space Telescope
IMF	Initial Mass Function
SB	Spectroscopic Binary
SB1	Single-Lined Spectroscopic Binary
SB1VB	Single-Lined Spectroscopic Binary with a Visual Orbit
SB2	Double-Lined Spectroscopic Binary
SB2VB	Double-Lined Spectroscopic Binary with a Visual Orbit
SB9	The 9th Catalogue of Spectroscopic Binary Orbits

SED spectral Energy Distribution

SFP Separated Fringe Packet

SNR Signal-to-Noise Ratio

SSS SuperCOSMOS Sky Survey

IAU International Astronomical Union

IDL Interactive Data Language

IMF Initial Mass Function

IR Infrared

LBI Long-Baseline Interferometry

NASA National Aeronautic and Space Administration

NLTT New Luyten Catalogue of Stars With Proper Motions Larger than Two Tenths of an Arcsecond

OPLE Optical Path-Length Equalizer

PMS Pre-Main-Sequence

PTI Palomar Testbed Interferometer

POP Pipes of Pan, the fixed-delay offsets at the CHARA Array

SFP Separated Fringe Packets

SFR Star Formation Regions

SMARTS Small and Moderate Aperture Research Telescope System

USNO United States Naval Observatory

WDS Washington Double Star Catalog

VB	Visual Binary
VBO	Visual Binary Orbit
VB6	Sixth Catalog of Orbits of Visual Binary Stars
VLMC	Very Low Mass Companion(s)
WDS	Washington Double Star Catalog
WMC	Washington Multiplicity Catalog
ZAMS	Zero-Age Main Sequence
2MASS	Two Micron All Sky Survey

Sometimes I think we're alone in the universe, and sometimes I think we're not. In either case, the idea is quite staggering.

—— Arthur C. Clark

– 1 –

Introduction and Background

This dissertation presents the results of a comprehensive multiplicity survey of solar-type stars in the solar neighborhood. In this chapter, I discuss my motivation for undertaking this effort, outline the history of double star observations, and summarize the results of prior surveys. Chapter 2 describes my sample selection, compares it with those of significant prior efforts, and outlines the survey methods for identifying and characterizing the various types of companions. Chapters 3–6 detail the results obtained from the individual observing techniques and Chapter 7 synthesizes the results and presents the overall statistics. Finally, Chapter 8 presents an analysis of the results and discusses their implications.

1.1 Motivation

Humans have always been fascinated by the night sky. A view of the sky on a clear night, far from city lights, seems filled with countless stars and is sure to evoke a feeling of amazement and wonder. Indeed, we wonder if among what we are looking at, there might be someone who is looking back at us! This question has always fascinated me: is our Earth the only place in the Universe with life, or is the Universe, like our home planet, teeming with life? The vastness of space and time and the minuscule part of it that we occupy make it very hard for us to experimentally answer this question. Speaking of time, if we imagine the Universe to be one year old and it began with the Big Bang on January 1, the Sun and Earth formed

in early September, and life was flourishing on Earth by late September. However, humans arrived very late in the game, at around 9 p.m. on December 31, and the entire human civilization has played out in just the last 30 seconds! Similarly, speaking of space, if the observable Universe was the size of the Earth, galaxies would only stretch from the end-zone to midfield on a typical football field and would be separated by some 500 miles of nothingness. Stars would be invisible specs about 2 mm apart, and the Earth would be a millionth of the size of a typical bacteria! So, even though we do not have any evidence for life outside Earth, Carl Sagan's words "*absence of evidence is not evidence of absence*" is very relevant in this context.

Our innate curiosity does not allow us to abandon hard problems. If we cannot study something directly and in its entirety, we study it indirectly and break it up into manageable chunks. The most accepted attempt of this technique for the study of alien life is the Drake Equation (Equation (1.1) below), which takes a probabilistic approach to determining N, the number of civilizations in the Galaxy whose electromagnetic emissions are detectable.

$$N = R_* f_p n_e f_l f_i f_c L, \tag{1.1}$$

where R_* is the rate of star formation in the Galaxy, f_p is the fraction of those stars with planetary systems, n_e is the number of planets per solar system with conditions suitable for life, f_l is the fraction of suitable planets where life actually begins, f_i is the fraction of life-bearing planets on which intelligent life emerges, f_c is the fraction of civilizations that develop technologies which emit detectable signs of their existence into space, and L is the length of time for which such civilizations emit their signal into space.

My thesis effort aims to make a very small contribution to one factor in Equation (1.1), namely f_p, the fraction of stars that are suitable planet hosts. This work is a survey of the habitats of solar-type stars, aiming to better understand the types of objects (planets, brown dwarfs, or other stars) that inhabit their immediate environs. Until recently, it was believed that close binary systems are not conducive environments for planet formation, but more recent observational efforts (e.g., Raghavan et al. 2006; Eggenberger et al. 2007) have shown that planets are quite common in binary systems despite selection biases, and recent theoretical work (e.g., Boss 2006) now suggests that stellar companions as close as $\sim$ 50 AU may actually trigger the formation of gas giant planets out to $\sim$ 20 AU by inducing clumping through gravitational instability. With two-thirds of Sun-like stars thought to live in binary or higher-order multiple systems (Duquennoy & Mayor 1991, hereafter DM91), a better understanding of any relations between stellar and substellar companions to Sun-like stars is critical in better estimating the fraction of planet-host stars, thus impacting the number of potentially habitable places in the Universe.

In addition to this motivation for better understanding life in the Universe, the study of stellar multiplicity has many other important benefits. First, knowing whether a star is single or not is important for many astronomical researches, such as for the selection of calibration stars, which typically need to be single. Second, studies of stellar multiplicity ratios contribute valuable clues about star formation and evolution. It has been a long-established belief that the majority of stars live in systems of more than one star (e.g., Heintz 1969; Abt & Levy 1976, DM91), and more recent work suggests a dependence of

binary fraction on mass (DM91, Henry & McCarthy 1990; Fischer & Marcy 1992; Mason et al. 1998a; Burgasser et al. 2003), and on age (Mason et al. 1998b). Third, a very valuable result of studying stellar multiplicity is the determination of dynamical masses of the component stars. According to the Vogt-Russell theorem, composition and mass are the most important physical parameters of stars, and binary stars remain the only direct means of obtaining accurate masses, enabling an observational basis of testing stellar structure and evolution models.

Yes, stellar multiplicity studies have many benefits, but is yet another effort in this subject warranted at this time? Do we by now not have access to robust multiplicity statistics? Indeed, DM91 represents the seminal work on the multiplicity of solar-type stars, as evidenced by over a thousand citations since publication. Science, however, represents an evolving process of learning, and there are benefits in revisiting important topics from time to time in order to ratify or revise our understanding, as warranted by the new facts available to us. My dissertation is a humble effort at a modern update to DM91, leveraging a larger sample selected using modern measures and the great volume of other multiplicity studies that are constantly evolving our knowledge of this field. Most notably, even though my observational efforts do not focus on substellar companions, a great amount of excellent work is being done in this area, enabling a modern statistical analysis to include these results.

1.2 History of Double Star Observations

The first mention of the term "double star" was made in Ptolemy's Star Catalog (2nd century AD), to identify ν_1 and ν_2 Sagittarii as $\delta\iota\pi\lambda o\upsilon\varsigma$ (Heintz 1978). While this pair, separated by $14'$ in our sky, is not physically related, its appearance as a double star is consistent with the modern definition of the term. In fact, when astronomers began telescopically studying double stars, starting with Galileo's observations of the double star Mizar in about the year 1617, which was independently measured and published by Riccioli in 1650, they presumed that these stars were *not* physical associations, but rather chance alignments of stars separated by a great distance along the line of sight. In 1767, John Mitchell first argued that the law of probabilities suggested that double stars are likely to be gravitationally bound (Aitken 1964). The earliest organized studies of double stars were initiated by Christian Mayer and Sir William Herschel in the last quarter of the eighteenth century. Mayer published the first catalog of double stars in his 1779 book, and Herschel undertook a systematic search for double stars at around the same time. Once again, these astronomers assumed that they were studying chance alignments of stars separated by large distances, and they hoped to measure differential proper motions to derive a parallax to the nearer star, as was proposed by Galileo. In any case, this began an era of careful measurements of the separations between double stars using micrometers. By 1802, Herschel, based on his own observations, and the persistent input from Mitchell, separated his observations into optical double stars (chance alignments of unbound stars) and binary stars (gravitationally bound pairs), and his publication in the following year demonstrated that orbital motion was the only reasonable

choice in describing his observations for six pairs, including *Castor*.

Double star astronomy continued over the ages through stalwarts such as Sir John Herschel (William's son), Sir James South, and Sherburne W. Burnham to F. G. Wilhelm Struve, who is credited with taking this science to a new level with the publication of the *Mensurae Micrometricae*, a fundamental catalog of double stars, in 1837. In this catalog, Struve adopted John Herschel's earlier suggestions of recording the epoch of each observation, and measuring the position angle of the pair's separation in degrees from 0 to 360, starting at north and going towards east. These conventions are followed for double star work to this day. The early work of double star astronomy continued with other legends in this field such as Otto Struve, (Wilhelm's son), W. R. Dawes, and Admiral W. H. Smythe through the mid 1800s, and by this time, methods had been developed to derive orbital elements from the observations of Visual Binaries (VB).

The modern era of double star astronomy was heralded by S. W. Burnham, who, over an active 40-year career beginning around 1870, made remarkable contributions to all of the modern developments in double star astronomy, including the discovery and observation of spectroscopic binaries, the demonstration that variable stars are eclipsing binary systems, and the application of photographic methods to the measurement of visual double stars, all while discovering 1,340 new double stars and contributing many thousands of high-quality measures (Aitken 1964). Notably, Burnham measured pairs with separations down to $0\farcs2$ and ones with large brightness differences between the components. In 1895, Robert G. Aitken started working in this field and conducted the first systematic study of double stars

for the purpose of deriving multiplicity statistics. Visual double star worked flourished in the coming decades with significant contributions from Gerard Kuiper, Robert Jonckheere, Paul Couteau, and Charles Worley (H. McAlister 2008, private communication). Worley transferred the Lick "Index Catalog" to the United States Naval Observatory (USNO), creating the Washington Double Star Catalog[1] (WDS), a current online double star resource that is continually updated under the direction of Brian Mason at the USNO. Meanwhile, lunar occultation events had been used for over a hundred years to determine the angular diameters of stars (Evans 1950, 1952) and vector separations of close binaries (Innes 1901; Nather & Evans 1970; Edwards et al. 1980). Observations of double stars in the southern hemisphere were started in the late nineteenth century by Robert Innes, and continued with significant contributions by Willem van den Bos, William S. Finsen, and Richard Rossiter. Recent notable contributors to visual double stars include Willem Luyten, who systematically measured proper motions of fast-moving stars and discovered about 2,000 common proper motion pairs, Antoine Labeyrie, who introduced the technique of speckle interferometry, and Harold McAlister, who used this technique to discover almost 300 new pairs and contributed about 35,000 double star measures. Recent adaptive optic surveys have enabled the detection of doubles with a very high brightness difference between the components, enabling the detection of substellar companions such as brown dwarfs (e.g., Liu et al. 2002).

The history of double stars traced above relates to visual doubles, one in which the two components of the system are resolved and their angular separation, or a component thereof, measured. As noted, these can be optical or physical. There are however, other techniques of

[1] $http://ad.usno.navy.mil/wds/$

identifying and characterizing binaries, and these involve studying periodic variations in the spectral lines or apparent brightnesses. The first spectroscopic binary was discovered by E. C. Pickering, with the announcement of Mizar as a double-lined spectroscopic binary (SB2) in 1889, in which the spectral lines of an apparently single star were seen as a pair of lines which moved relative to each other in a periodic manner due to the Doppler effect. Essentially, what Pickering saw was the shifting of the light from the components of the binary as they orbited each other, moving towards shorter wavelength (blue-shift) when a component moved towards us, and towards longer wavelengths (red-shift) when the component moved away from us. As the stars orbit their center-of-mass, when one star moves towards us, the other moves away, and so the characteristic pattern of movement is very telling and can be used to deduce characteristics of the stars and their orbits. Many astronomers and observatory programs have contributed to the study of spectroscopic binaries, notable among them, Roger Griffin, who pioneered the field by developing a technique for measuring stellar velocities to 1 $\mathrm{km\,s^{-1}}$ precision (Griffin 1967) and recently published his 200^{th} paper using this technique (Griffin 2008), the CORAVEL survey (Baranne et al. 1979, DM91), and Carney & Latham (1987).

As early as 1782, John Goodricke had discovered that *Algol* (β Persei) showed periodic variations in its apparent brightness and explained this behavior as a partial eclipse by an unseen darker companion in orbit around the brighter primary. In 1889, H. C. Vogel confirmed this theory by demonstrating that the spectral lines of this star showed a periodic shift consistent with the brightness changes. Due to the relative faintness of the companion,

its spectral lines were not seen, so only one set of spectral lines moved periodically towards shorter and longer wavelengths, consistent with the eclipses. Hence *Algol* was the first star to be seen as a single-lined spectroscopic binary (SB1).

Studying planets around stars other that the Sun is a relatively new field in astronomy, and the most fruitful techniques involve the detection and characterization of planets by studying minute shifts in the parent star's spectral lines as a result of its wobble around the center of mass of its solar system, or by studying the tiny drop in its brightness due to eclipses from an unseen planet. Radial velocities are now routinely being measured to a few $\mathrm{m\,s^{-1}}$ (Baranne et al. 1996; Butler et al. 1996) and have enabled the detection of almost 300 planets around other stars[2], enabling statistical analyses of orbital and physical properties (Marcy et al. 2005; Udry & Santos 2007). On the other hand, detecting planets via eclipses or transits requires photometric precision below 1% and is recently gaining momentum, with over 50 planets detected to-date, either as a follow-up of spectroscopically identified planets (Charbonneau et al. 2000) or through photometric surveys (e.g., Udalski et al. 2002), some of which are run with robotic telescopes (Bakos et al. 2002; Pollacco et al. 2006) or from space (Moutou et al. 2008).

1.3 Previous Multiplicity Surveys

While double star astronomers have focused on the discovery and characterization of pairs since William Herschel in the late eighteenth century, it was Robert Aitken who launched

[2] *http://exoplanet.eu/catalog.php*

the first systematic survey in 1895, aimed at deriving multiplicity statistics, vastly increasing the number of pairs discovered. Several noteworthy efforts followed, and, as expected, the quality of the results has improved over the years, enabled by better observing instruments and techniques as well as by more robust statistical analyses. Before discussing the seminal work of DM91 on the multiplicity of solar-type stars (§ 1.3.2), let us first review the efforts leading up to it.

1.3.1 Early Multiplicity Surveys

The early double star observers, from William Herschel in the late 1700s to Robert Aitken about a hundred years later, focused on discovering and cataloging thousands of visual double stars. Aitken's Double Star Catalog (Aitken & Doolittle 1932) lists over 3,000 double stars, over 30% of which have angular separations $< 0\farcs5$, and over half have separations $< 1''$, confirming the improved capabilities, and increasing the confidence in a physical relationship due to proximity. Given the nascent nature of these surveys, however, there is little discussion of orbital elements or multiplicity statistics until a few years later.

With the evidence for a physical association among double stars mounting because of the large number of close doubles discovered, attention turned toward treating them as bound systems whose orbital properties could be studied. Hertzsprung (1922) developed an empirical method of estimating the orbital period of visual binaries by deriving a relationship between the orbital period and the ratio of the radius vector to yearly orbital motion, based on his studies of 13 pairs within 10 pc of the Sun with known orbits. He also noted that of the 15,000 known double stars at that time, only 50 had reliable orbits and an additional

1,000 showed hints of orbital motion. A few years later, Luyten (1927) used matching proper motion measurements of the components of double stars to argue for a physical association. Luyten (1930a) noted that the results of Hertzsprung (1922) are incomplete and arbitrary, and developed a more rigorous statistical method for the estimation of orbital period based on Kepler's Third Law. He measured separation at one epoch, estimated masses from measured luminosities, and statistically estimated the orbital eccentricity and inclination. He also provided observational support for this method by testing it on 15 binaries with known orbits (Luyten 1930b). In perhaps the earliest statistical analysis of a volume-limited sample, Luyten (1930b) presented a tally of 47 visual doubles, 15 of which had reliable orbits, and 5 spectroscopic binaries for the 10 pc sample, which included 105 stars (Luyten & Shapley 1930). Estimating the periods of the visual doubles without orbits, Luyten (1930b) developed a period distribution of the complete sample of known binaries within 10 pc, concluding that the $\log P$ distribution was unimodal with a mean of 2.5 and a dispersion of 1.7, noting that any undetected binaries were likely to have periods larger than the derived mean.

Kuiper (1935a,b) proposed a variety of problems that could be studied with double stars, and addressed some of them, deriving a companion fraction of 80%, i.e. for the 465 primaries studied, he estimated a total of 372 companions. These results were based on an observed companion fraction of 33%, which was adjusted to account for the incompleteness of the survey for large Δmag pairs. Further, he noted a roughly Gaussian distribution of the semi-major axis, with a peak at about 20 AU. In a follow up work, Kuiper (1942) reported raw

multiplicity statistics for a sample of 254 stars with parallax $\geq 0\farcs095$. He presented multiplicity by spectral type and by total mass. For A-K stars, the Single:Double:Triple:Quadruple (S:D:T:Q) ratios were 44:23:5:1, which yields a companion fraction of 49%. This is significantly higher than his earlier work's results of 33%, but no incompleteness analysis was performed in the later effort. The semi-major axis distribution was confirmed to be Gaussian, but the peak had moved out to 50 AU. Kuiper noted the incompleteness of the survey and suggested that a sample selected from a larger volume of space along with the completion of spectroscopic and visual surveys would provide more reliable results. Heintz (1969) studied 100 stellar systems and presented a companion fraction of 1.0 to 1.1, i.e. the 100 systems contained 200–210 stars. Based on spectroscopic and visual binaries, his work identified 30 single, 47 binary, and 23 multiple systems, with an asymmetric distribution of semi-major axis peaked at 45 AU. However, Heintz also noted that the statistics were limited by selection effects, primarily the discovery probability and confirmation of physical pairs.

Focusing on spectroscopic binaries, Jaschek & Jaschek (1957) derived an observed binary ratio of approximately 12% for F-K stars by studying about 200 stars of varying spectral types and luminosity classes. Binaries were identified as pairs with known orbits, those noted as spectroscopic binaries in earlier efforts, or those with mean velocity differences between observatories of more than 20 $\mathrm{km\,s^{-1}}$. This threshold was independent of spectral type or mass, and, to account for the dependence of velocity semi-amplitude on mass, they applied a correction factor and reported a corrected spectroscopic binary fraction of about 30%, noting that it was roughly constant along the main sequence, a conclusion earlier noted by Kuiper

for visual binaries. Petrie (1960) studied the probable error distributions of radial velocities and estimated that $\sim 51\%$ of F-M stars showed radial velocity variations, higher than previous estimates, but once again confirmed a roughly flat distribution across the main sequence. However, Petrie's work assumed a Gaussian distribution for the observational errors of constant velocity stars, which was later showed to be incorrect (Kirillova & Pavlovskaya 1963). Jaschek & Gómez (1970) reviewed these prior efforts and presented an updated percentage of variable radial velocity stars as about 45% for F-M stars based on 350 stars, once again noting similar results across all spectral types.

Abt & Levy (1976) attempted a comprehensive systematic effort for the multiplicity statistics of solar-type stars based on a sample of 135 F3–G2 IV or V bright field stars ($V < 5.5$ mag) and about 20 radial velocity measurements for each star. Their results were S:D:T:Q = 42:46:9:2 with a median period of 14 years, considerably shorter than the estimates of 320 years obtained by Luyten (1930b) or 79 years by Kuiper (1935a,b). Based on an incompleteness analysis aimed at accounting for missed binaries, they derived a a companion fraction of 1.4 companions for each primary, and concluded that two-thirds of solar-type stars have stellar companions and the remaining one-third have substellar companions. However, their results have been called into question based on selection effects and the validity of the binaries reported. As analyzed by Branch (1976), their magnitude limited sample suffers from a serious selection effect favoring binaries with bright companions, because unresolved binaries are intrinsically brighter than single stars and will be counted out to a larger volume of space (the Malmquist bias). Further, Morbey & Griffin (1987) pointed out that 24 of the

25 new binaries reported by Abt & Levy are not statistically supported by their data and showed that 21 of these are likely not binaries at all. Another important conclusion of Abt & Levy (1976) was the bimodal distribution of mass-ratio, which they use as evidence of two formation mechanisms of binaries – fission for close systems and cloud fragmentation for wider systems. However, several authors have pointed out that these results are dominated by selection effects and that the true distribution of mass-ratio is unimodal with frequencies increasing towards lower mass-ratios (Scarfe 1986; Trimble 1987, 1990).

Zinnecker (1984) reviewed binary statistics and the distribution of mass-ratios, discussing the various selection effects that hampered such studies and suggesting that none of the binary formations mechanisms (fission, fragmentation, capture, and disintegration of small clusters) could be ruled out. Halbwachs (1986) studied the multiplicity statistics of the stars in the 4th edition of the Yale Catalog of Bright Stars (Hoffleit & Jaschek 1982) and its supplement (Hoffleit et al. 1983). Accounting for selection biases, he reported that the sample of 2591 dwarfs contained 52% single stars, 36% binaries, and 12% multiple systems. Based on an estimation of missed binaries, he concluded that at most 23% of stars are truly single. Halbwachs (1987) analyzed the mass-ratio distribution among spectroscopic binaries in the 7th Catalog of Spectroscopic Binaries (Batten et al. 1978), and concluded that there was no peak at $q \sim 1$ as suggested by Abt & Levy (1976) but rather a possible peak near $q \sim 0.4$. Further, he concluded that there is no difference in the mass-ratio distribution between close-period spectroscopic systems and the long-period visual binaries, suggesting that all binaries may be formed by a single mechanism.

1.3.2 The Duquennoy & Mayor Survey

In the most comprehensive and systematic treatment of the multiplicity of solar-type stars to date, DM91 studied an unbiased sample of 164 stars. In order to minimize selection effects that plagued prior efforts, they chose a volume-limited sample with trigonometric parallaxes from Gliese (1969) $\geq 0.045''$. Choosing to focus on solar-type stars, they limited spectral types to F7–G9 and luminosity classes to IV-V, V, and VI. While they included companions of all known types for statistical analyses, their primary observing program resulted in about 4200 radial velocity measurements obtained over 13 years with a precision of 0.3 $\mathrm{km\,s^{-1}}$. The location of their observing facility at Haute-Provence Observatory imposed a final restriction on their sample, namely, declination north of $-15°$. In addition to the 164 primaries in their sample, they could obtain radial velocity observations for 17 of the 30 wide Common Proper Motion (CPM) companions, and included them in the analysis as well.

In all, DM91 presented 82 orbits with derivable orbital periods, 52 of which had spectroscopic orbital solutions, including 6 new orbits, 2 revisions to existing orbits, 17 preliminary orbital solutions, and 12 independent orbits corresponding to existing orbits in the Batten et al. (1989) catalog. The 82 orbits for 164 primaries implies an average of 0.5 companions per primary, significantly lower than the earlier estimates presented above. They also noted that their S:D:T:Q = 57:38:4:1 indicate much fewer multiple systems (triples or higher order) than the 25–50% of binaries found by prior studies (Mayor & Mazeh 1987; Mazeh 1990). They explained the deficiency of multiple systems as additional components that had so far been missed. Including stars without definitive orbits, but with evidence of radial velocity

variations, their statistics change to 51:40:7:2. Accounting for an estimation of undetected binaries, they concluded that 57% of solar-type stars have companions with $q > 0.1$, and about one-third may be real single stars, i.e. with no companion above 0.01 $M_\odot$. This compares to 0% reported in Abt & Levy (1976) and a 23% upper-limit in Halbwachs (1986).

The primary results of DM91 for $M_2/M_1 > 0.1$ are: (i) The orbital period distribution is unimodal and roughly Gaussian, with a median period of 180 years. (ii) The eccentricity distribution follows three different patterns depending on the period: for periods below $\sim$ 11 days, the orbits are circularized due to tidal interactions; for $11 < P < 1000$ days, the mean eccentricity is 0.31 ± 0.04; and for $P > 1000$ days, the distribution follows $f(e) = 2e$. (iii) The mass-ratio distribution is independent of period and is not peaked at $q \sim 1$, but rather rises toward smaller ratios to at least $q \sim 0.3$.

For systems with $M_2/M_1 < 0.1$, DM91 used simulations to identify a binary percentage of $8\% \pm 6\%$. They also drew the following conclusions from the 11 SB they found with very low mass companions (VLMC) among CORAVEL data for the International Astronomical Union (IAU) standard stars and M dwarfs plus 7 published astrometric binaries with VLMC candidates: (i) Approximately 10% of IAU standard stars may contain brown dwarf companions, similar to the G dwarf sample. (ii) The mean eccentricity for these VLMC binaries for $11 < P < 1000$ days is 0.34 ± 0.07, similar to the G dwarf sample, implying a similar formation mechanism of stellar and brown dwarf companions, but one different from the formation of planets, given the low eccentricities of Solar System gas giant planets.

1.3.3 Multiplicity Results Since DM91

While DM91 remains the most comprehensive multiplicity survey of solar-type stars, several efforts have looked at multiplicity statistics and analyzed patterns among orbital and physical elements as well as compared the results of subsamples or disparate samples to those of DM91. A brief description of some of these follows.

Analyzing short-period systems ($P < 3000$ days) from DM91, Mazeh et al. (1992) showed that the mass-ratio distribution monotonically increases from $q = 0$ to 1. However, with only 23 systems analyzed, their results should be considered preliminary, and a flat or a decreasing function is still consistent with their data (Halbwachs et al. 2003). In any case, this distribution being considerably different than that of DM91 suggests that the mass-ratio distribution might indeed be dependent on the orbital period, as mentioned by Abt & Levy (1976). Heacox (1995) developed a statistical approach to adequately analyze SB1 pairs, and found that the distribution was roughly independent of spectral type. His reanalysis of DM91 data (Heacox 1995, 1998) showed a clear peak around $q \sim 0.2$ and the detection difficulty of lower mass-ratios might imply a rise all the way to $q = 0$. He also noted a second peak at $q = 1$, but one of limited statistical significance. Bimodal distributions were also seen in several prior analyses as noted above, but they were generally explained by selection effects alone (Halbwachs 1987). Nevertheless, as noted by Halbwachs et al. (2003), bimodal distributions were also seen in the photometric study of binaries in open clusters (Kähler 1999), but these results could be contaminated by triple systems.

Other studies seem to indicate that the DM91 work might have underestimated the true

multiplicity among solar-type stars. Studies of *Hipparcos* (Perryman & ESA 1997) double stars (more on this in § 5.1) seem to indicate a significantly higher binary fraction. Quist & Lindegren (2000) modeled the reliability of *Hipparcos* double stars identifications and concluded that a companion fraction of 0.9–1.2 is implied, as compared to 0.67 of DM91. Söderhjelm (2000) studied *Hipparcos* doubles and once again concluded that the implied multiplicity is about twice as found by DM91. In an effort to recover the primordial binary fraction of intermediate-mass stars, Kouwenhoven et al. (2007) studied the nearby, young Scorpius OB2 association and combined multi-technique observational results with Monte Carlo simulations to determine a binary fraction of at least 70% for intermediate-mass stars, with a fraction of 100% providing the best fit with the data. They also stated that the log-normal period distribution of DM91 agrees with the fraction of VB but significantly underpredicts the number of SB, and a related effort (Kouwenhoven 2006) derives a binary fraction of $\sim 93\%$ for solar-type stars.

Woitas et al. (2001) studied T Tauri binary systems in four nearby star forming regions using near-infrared speckle interferometry and derived mass ratios, concluding that the mass distribution was roughly flat for $q > 0.2$ even though the results depend on the evolutionary model used. They do not find any relationship between mass-ratio and the primary's mass or the components' separation. Goldberg et al. (2003) studied 129 SBs with periods 1–2500 days and concluded that the mass-ratio distribution showed a high asymmetric peak at $q \sim 0.2$ characterized by a sharp drop below 0.2 and a slower drop to a minimum at around $q \sim 0.55$, followed by an increase to a lower peak $q \sim 0.8$. An analysis of subsamples

confirms a similar distribution among disk stars, but not among halo stars. The distributions also seem to depend on the primary's mass, with the lower mass ($M_p < 0.67$ $M_\odot$) sample showing the two peaks, but the higher mass sample showing an increasing trend towards lower mass-ratios. Halbwachs et al. (2003) studied SBs with orbital periods up to 10 years and saw a mass-ratio distribution with a broad, shallow peak from $q \sim 0.2 - 0.7$ and a sharp high peak for $q > 0.8$. Combining this with the finding that large mass-ratio systems (twins) have lower eccentricity that other binaries at all periods, they speculated that this points to a different formation mechanism for twins. The relative abundance of twin systems was earlier seen by Tokovinin (2000) and confirmed for *Hipparcos* visual binaries by Söderhjelm (2007). However, Mazeh et al. (2003) obtained infrared spectroscopic observations of 62 disk binaries, including 43 double-lined systems, and derived a flat distribution of mass ratios from $q \sim 0.3 - 1.0$ and a possible increase at lower ratios. They suggested that earlier distributions showing the peaks might be influenced by selection effects.

Meanwhile, surveys based on specific observing techniques have contributed to our growing understanding of binaries. Mason et al. (1998a) surveyed Galactic O-stars via speckle interferometry and found that $> 75\%$ of the O-stars in clusters and associations had spectroscopic or visual companions, but the percentages were lower for field and runaway stars. This suggests that most massive stars form in binary systems which may lose companions via dynamic interactions. In a follow-up effort, Mason et al. (2009a) confirmed these findings, once again concluding that at least 75% of the O-type stars in clusters and associations are part of binary or multiple systems. Kobulnicky & Fryer (2007) compared the observed

radial velocity of early-type stars in the Cygnus OB2 association with expectations from Monte-Carlo models to conclude that binary fractions are likely greater than 80% and that the companion mass distribution follows the Initial Mass Function (IMF) for only 60% of the companions, with the remainder having $q \sim 1$. At the other end of the main sequence, Fischer & Marcy (1992) find a smaller binary fraction of 42% ± 9% among M-dwarfs, consistent with the earlier efforts of Henry & McCarthy (1990), and smaller than the DM91 results for solar type stars. Thus, multiplicity frequency appears to drop with the mass of the primary, perhaps in part due to the shrinking mass available for companions.

Mason et al. (1998b) used speckle interferometry to suggest a decreasing binary fraction from 17.9% ± 4.6% for chromospherically active and presumably young (1 Gyr) stars to 8.5% ± 2.7% for inactive and older (4 Gyr) stars, a result confirmed in a follow-up survey of a large volume-limited sample (B. Mason 2008, private communication). In a progress report of an adaptive optics (AO) survey looking for faint companions to solar-type stars within 25 pc, Turner et al. (2001) reported five faint companions, including three new detections. In spectroscopic surveys of high proper motion stars, Goldberg et al. (2002) presented 34 SB2 orbits and Latham et al. (2002) presented 171 SB1 orbits, noting that that binary characteristics such as frequency and period distribution are similar for the halo and the disk populations. In the first of an intended series of papers, Abt & Willmarth (2006) presented the results of a spectroscopic survey of 167 solar-type stars in the solar-neighborhood. While this work presents 39 SB1 and 12 SB2 orbits, analysis of orbital elements has been left to follow-up efforts, yet to come.

Other efforts have studied multiplicity frequencies in specific populations of stars like globular clusters or open clusters. Albrow et al. (2001) conducted a photometric survey using the *Hubble Space Telescope* (HST) in the core of the globular cluster 47 Tucanae, deriving overall percentages of 13% ± 6% detached binaries and 14% ± 4% W UMa-type contact binaries. In a theoretical effort, Ivanova et al. (2005) predicted that dynamical interactions in the core of clusters would rapidly deplete binary populations, estimating that a cluster starting as 100% binaries would eventually be left with a maximum of ∼ 5–10% binary fraction. They revised the incompleteness analysis of Albrow et al. (2001), primarily questioning the assumption of a flat period distribution, and showed that the resulting expectations are more consistent with recent HST observations. In a recent HST effort, Sollima et al. (2007) used color-magnitude diagram morphologies to estimate the minimum percentage of binaries in 13 low-density clusters, obtaining values of around 6%, larger than estimates for dense clusters, presumably due to the lower level of dynamical interactions. Their analysis of the radial distribution of binaries indicates a concentration towards the core, and a comparison of the results for the individual clusters implies a depletion of binary frequency with age from 6–12 Gyr.

Early multiplicity studies of low-mass (roughly solar-mass and lower) in star forming regions (SFR) yielded significantly higher percentages, suggesting that pre-main-sequence (PMS) stars have a much higher fraction of binaries than nearby solar-type stars (Ghez et al. 1993, 1997; Leinert et al. 1993). Brandner & Koehler (1998) studied 114 weak-line T Tauri stars in the nearby Scorpius-Centaurus OB association to demonstrate that separate

populations exist with different separation distributions, which are more peaked than field star samples, but peak at different values correlated with the number of massive stars in the population. They invoked this finding to explain that binary fractions among T Tauri stars may not be very different compared to older field stars, and results indicating such a conclusion could have extrapolated a sharp peak out to wider ranges of separations. More recent studies have indeed confirmed similar binary fractions among T Tauri and solar-neighborhood samples (e.g., Melo 2003). Moving up the evolutionary stage to open clusters, Patience et al. (2002a) conducted a high-angular resolution multiplicity survey of two open clusters and presented the following results: (a) For companions identifiable by their survey, they found a binary ratio consistent with field G-dwarfs, implying that binary ratios do not change appreciably over a few times 10^7 years; (b) The cluster binary separation peaks at $4^{+1}_{-1.5}$ AU, significantly smaller than for field or T Tauri stars, supporting the notion of sub-populations with different sharply peaked separation distributions; (c) The binary fraction in clusters increases with decreasing primary mass, and the mass-ratio distribution increases towards lower values for higher-mass stars, while it is reasonably flat for lower-mass stars; and, (d) solar-type primaries with close companions have higher rotational velocities, suggesting that companions affect the rotational evolution of young stars.

Searching for additional companions to known SBs using AO, Tokovinin et al. (2006) reported 12 new tertiary companions and several interesting conclusions for multiple systems: (a) the period distribution for SBs with and without tertiary companions is significantly different, strongly indicating that binaries without additional companions exist; (b) the

mass-ratio distributions for binary and triple systems are identical; (c) While 63% of SB pairs have tertiary companions, there is a strong dependence on period, with 96% of the close ($P < 3$ days) pairs having tertiary companions, suggesting an angular momentum exchange; (d) The SB primaries are more massive than the tertiary companion in 83% $\pm$ 4% of the systems. In a follow-up effort, Tokovinin (2008) studied a large sample of triple and quadruple systems, concluding that the properties of multiple stars do not correspond to dynamical decay of small clusters, but are rather consistent with a cascading rotationally driven fragmentation followed by a migration of the orbits.

Table 1.1 summarizes the multiplicity statistics of the comprehensive surveys discussed above. It is clear that, while multiplicity studies can offer important clues to star formation and evolution, the results available vary significantly based on the samples, observing techniques, and incompleteness analyses. My Ph.D. effort is able to leverage all these prior efforts, and based on a systematic approach, aims to further improve our understanding of stars through a study of their multiplicity.

TABLE 1.1: Results of Previous Multiplicity Surveys

Survey (1)	Sample Description (2)	Sample Size (3)	Observed S:D:T:Q (4)	Multiplicity Ratio[a] Observed (5)	Corrected (6)	Comment (7)
Luyten (1930b)	10 pc sample	105	...	50%	...	...
Kuiper (1935b)	33 pc sample	465	...	33%	80%	...
Kuiper (1942)	10.5 pc sample	465	44:23:5:1	40%	...	1
Heintz (1969)	Large sample	...	30:47:23	70%	...	2
Jaschek & Gómez (1970)	Diverse sample	350	...	45%	...	3
Abt & Levy (1976)	Magnitude limited F3-G2 IV-V	135	42:46:9:2	58%	66%	4
Halbwachs (1986)	Large sample of bright dwarfs	2591	52:36:12	48%	77%	5
Duquennoy & Mayor (1991)	Volume-limited F7-G9 IV-VI	164	57:38:4:1	43%	67%	6
Söderhjelm (2000)	*Hipparcos* Double Stars	...	...	70%	100%	7

NOTES.— Column 7 abridged notes (see § 1.3 for more information): (1) Noted by the author as limited and based on incomplete surveys. The ratios reported are for A–K stars. M star and white dwarf results are not included. (2) The ratio is for Single:Double:Multiple systems. At least 1/3 of the non-single stars are estimated to be multiple (more than two components). (3) Estimated binary fraction includes only spectroscopic binaries and stars showing radial-velocity variations. (4) Recognized to suffer from selection effects favoring binaries, and most new binaries reported were

later refuted. (5) Corrected multiplicity ratio is based on the upper-limit of 23% for single stars. (6) Corrected multiplicity ratio is based on the estimated 33% single stars, i.e. stars with no companions with mass greater than 0.01 $M_{\odot}$. (7) The reference suggests that multiplicity implied by *Hipparcos* is twice that of DM91. Further, Kouwenhoven (2006) estimates a 93% multiplicity ratio for solar-type stars.

[a] Multiplicity Ratio is the percentage of non-single stars in a sample.

1.4 Multiplicity Among Stars with Planets

As a majority of the stars are thought to have stellar companions, any attempt to comprehend the availability of habitable real estate in the Universe is incomplete without an understanding of the nature of planetary systems in binaries and multiple star systems. While the stability of planets in binary systems has long been theoretically established (e.g., Harrington 1977; Holman & Wiegert 1999; Pilat-Lohinger et al. 2003; Musielak et al. 2005; Verrier & Evans 2007), observational investigations of planets around tight binaries are very difficult. Hence, most planet-hunting programs avoid close binaries (e.g., Marcy & Butler 1996), and while a couple of nascent programs specifically tackle this problem (Konacki 2005; Muterspaugh 2005), they have yet to produce concrete results. Nevertheless, searches for stellar companions around planet-host stars have produced positive results (e.g., Patience et al. 2002b; Eggenberger et al. 2004; Udry et al. 2004; Mugrauer et al. 2005,and references therein). My 2006 publication (Raghavan et al. 2006), undertaken based on a suggestion by Todd Henry and completed with the help of my collaborators, reported on a comprehensive assessment of stellar companions to exoplanet systems, showing that even against selection biases, at least 23% of the exoplanet systems had stellar companions. As this work was performed as a part of my thesis, I have reproduced this Astrophysical Journal publication in *Appendix* D. While this effort remains the most comprehensive statistical assessment to-

date, the number of radial velocity-detected planets has since risen from 131 to 251, and additional efforts have continued to enhance our understanding of specific aspects of planets in binary systems (e.g., Bonavita & Desidera 2007; Desidera & Barbieri 2007; Eggenberger et al. 2007; Fabrycky & Tremaine 2007; Takeda et al. 2008).

Who are we? We find that we live on an insignificant planet of a humdrum star lost in a galaxy tucked away in some forgotten corner of a universe in which there are far more galaxies than people.

—— *Carl Sagan*

– 2 –

Sample and Survey Methods

2.1 The Sample of Solar-Type Stars

The Milky Way galaxy is just one of perhaps a trillion galaxies in the universe, and this galaxy alone contains about 200 billion stars. My thesis is aimed at enhancing our understanding of the habitats of solar-type stars in our galaxy, of which there are about 30 billion. I have chosen a sample of 454 primary stars to study comprehensively, from which the results can be extrapolated to the galactic population. In order to minimize selection effects, I have chosen a volume-limited sample, consistent with the approach of DM91. The selection criteria for solar-type stars in the solar neighborhood are as follows:

Solar-type stars: The luminosity of stars in the main-sequence ranges from about 10^{-4} to 10^{+4} $L_\odot$. I limit the selection of solar-type stars to the range 10^{-1} to 10^{+1} $L_\odot$, and further restrict them to a band around the main sequence to include luminosity classes IV, V, and VI, but exclude evolved and degenerate stars. This band extends 1.5 magnitudes below a best-fit main sequence and two magnitudes above it. The wider range above the main sequence avoids discrimination against binaries. As we will see in § 2.1.1, these conditions conveniently translate to a color range of $0.5 < B - V < 1.0$.

Solar neighborhood: As pointed out by DM91, a volume-limited sample is free of selection effects that plague magnitude-limited samples. Accordingly, I chose a spherical volume of space around the Sun, out to a radius of 25 pc, using *Hipparcos* parallaxes as

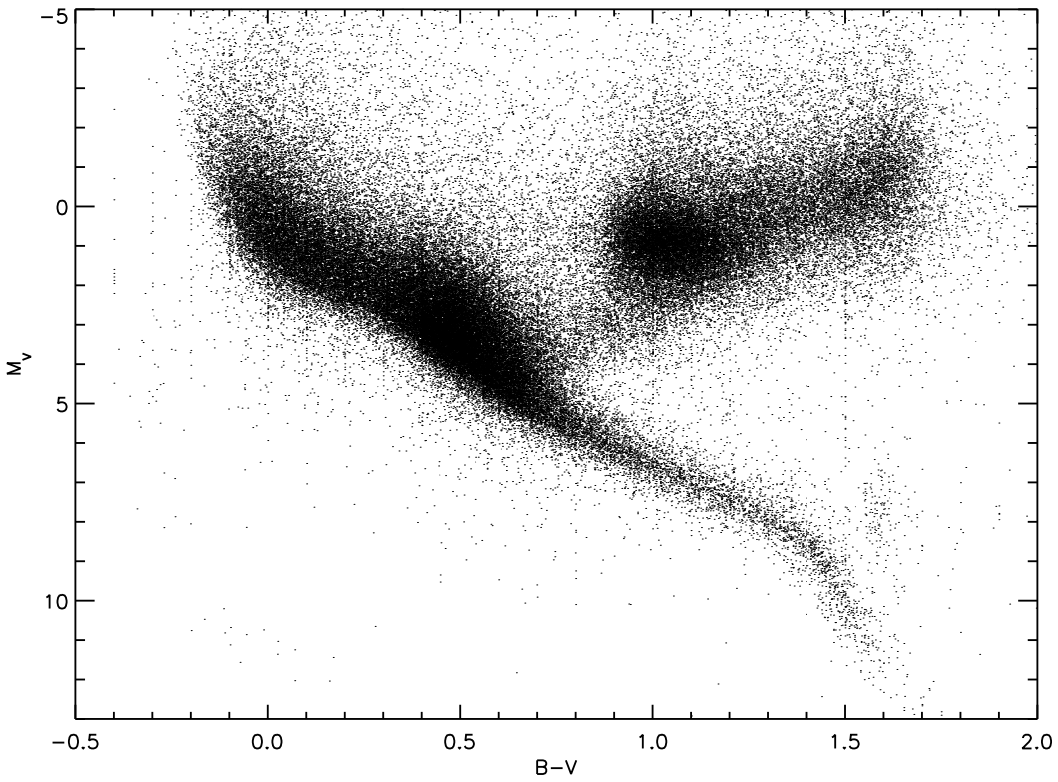

FIGURE 2.1: Color-Magnitude diagram of stars in the *Hipparcos* catalog.

described below.

2.1.1 Sample Selection from the Hipparcos Catalog

The *Hipparcos* mission conducted unprecedented astrometry on over 100,000 stars, and the resulting catalog contains accurate information on a large volume of stars. Hence, this became the natural source for my sample selection. Figure 2.1 plots all the stars in the *Hipparcos* catalog on a color-magnitude diagram. Applying the distance selection first, I included all stars in the catalog with parallax $\pi \geq 40$ mas with uncertainty $\sigma_\pi/\pi \leq 0.05$, resulting in the selection of 1 231 stars. In making this selection, I leveraged Söderhjelm (1999),

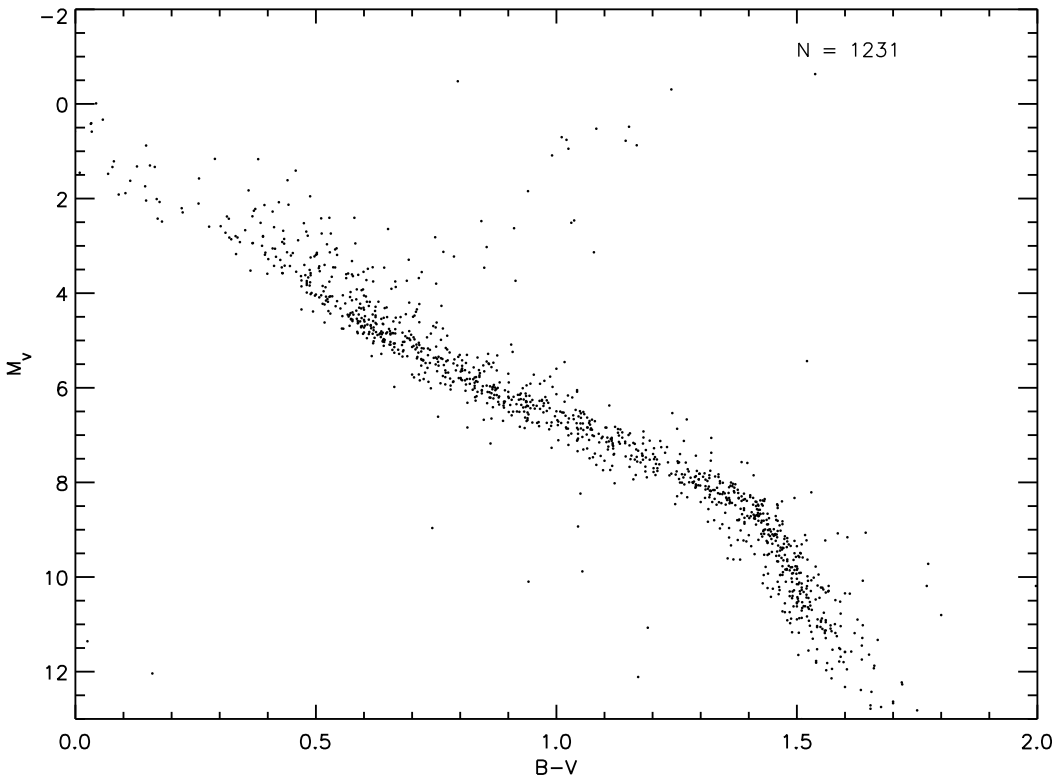

FIGURE 2.2: Color-Magnitude diagram of stars within 25 pc of the Sun from the *Hipparcos* catalog.

an effort that improved the *Hipparcos* parallax for close binaries by combining *Hipparcos* and ground-based observations, resulting in the inclusion of three stars, one (HD 98230, ξ UMa) due to a high-quality parallax estimate where *Hipparcos* had none, and two (HIP 40167 and HD 219834) as a result of revised parallax estimates just above the 40 mas threshold. This effort also resulted in the exclusion of one star (HD 108799), whose parallax was moved just below the 40 mas threshold. Figure 2.2 shows the resulting subset of distance-limited stars on a color-magnitude diagram. HD 219834, included due to the Söderhjelm (1999) effort above was nevertheless later left out of the final sample because it lies too far above the main

sequence, and HIP 40167, which represents a close triple system in *Hipparcos* was included through its primary, HD 68257.

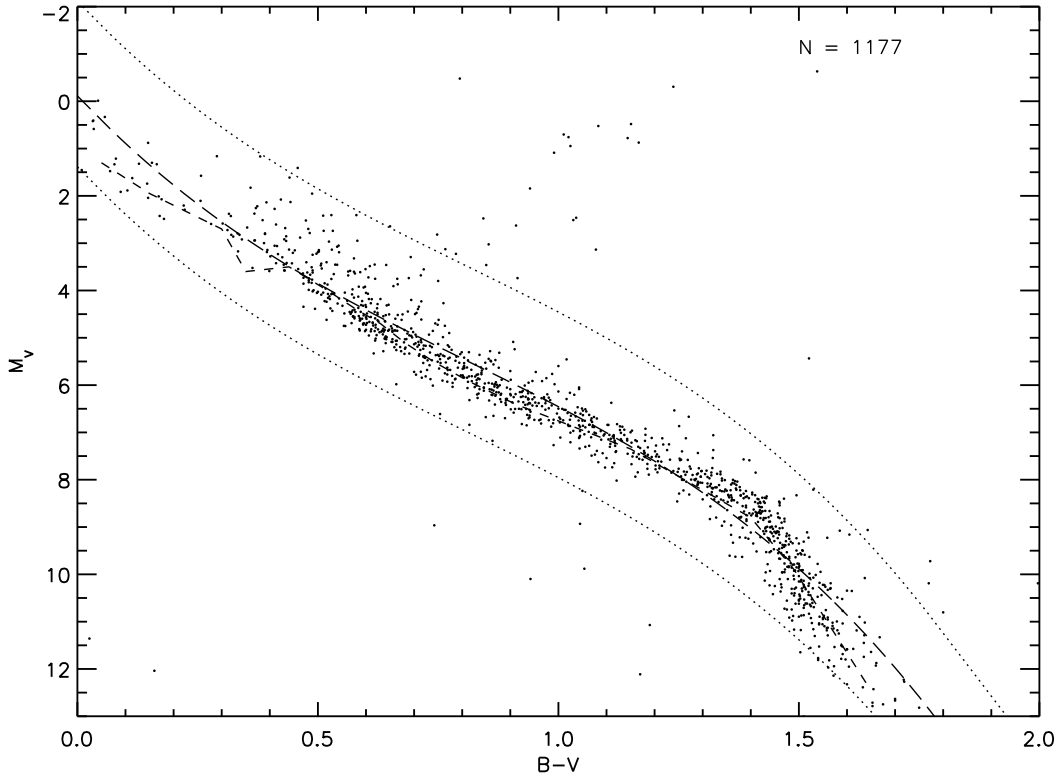

FIGURE 2.3: Selection of *Hipparcos* stars within 25 pc of the Sun and within 2 magnitudes above or 1.5 magnitudes below (dotted lines) a best-fit main sequence (long dashed line). The short dashed line is the main sequence based on data from Cox (2000).

Next, I generated a recursive best-fit main-sequence curve fitted to this selection of stars, the first fit using all the distance-limited stars, and the second one excluding the outliers, i.e. all points two magnitudes or more above or below the first fit. The selection of luminosity classes IV, V, and VI was then accomplished by including stars within 1.5 magnitudes below or 2 magnitudes above this main sequence, resulting in 1 177 stars (Figure 2.3). The final sample of 462 solar-type stars in the solar neighborhood was obtained by applying a color

filter of $0.5 \leq B-V \leq 1.0$, as seen in Figure 2.4. The two small triangles in the figure marked by "x" do not contain any stars, confirming that the above criteria are equivalent to selecting all stars within 2.5 magnitudes, i.e. within a factor of 10 in luminosity, of the Sun. Thus, the term "solar-type" has a physical basis connected to intrinsic luminosity of stars. Nine of the 462 stars selected above are companions to other stars in the sample, yielding a final sample of 454 primaries, including the Sun. Table 2.1 lists the final sample of solar-type primaries, in ascending order of right ascension. Columns 5–8 are from the *Hipparcos* catalog, with the exception of a few updated parallaxes from Söderhjelm (1999) as described in the previous paragraph. Columns 9–10 list the parallax and its error from van Leeuwen (2007b), a recent effort that updated *Hipparcos* astrometry based on a new reduction of the raw data (more on this in § 2.1.3). Column 11 lists the spectral type from Gray et al. (2003, 2006), or when not available from these sources, from *Hipparcos*, respectively coded as G03, G06, and HIP in Column 12.

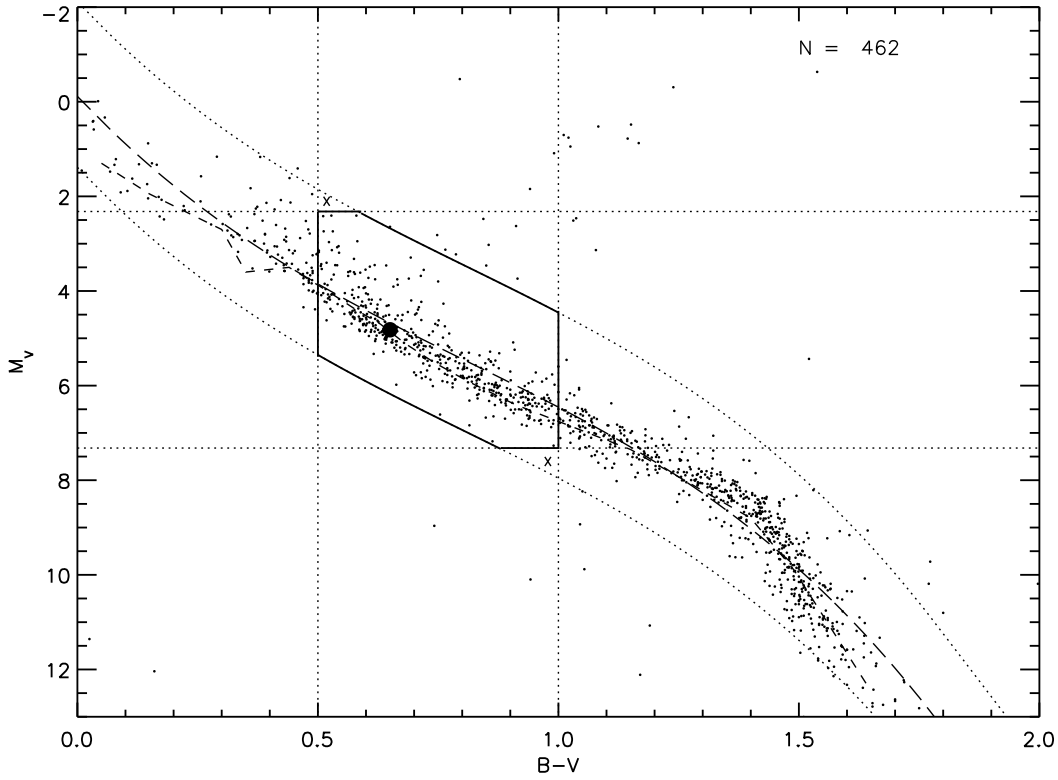

FIGURE 2.4: The volume-limited sample of solar-type stars from the *Hipparcos* catalog. The symbols for the main-sequence curves are the same as in Figure 2.3. The dotted vertical lines mark the $B - V$ color limits of the sample, and the dotted horizontal lines mark the magnitudes corresponding to one-tenth and ten times the luminosity of the Sun. The two triangles marked by "X" do not contain any stars, confirming that the color-based selection is equivalent to a selection based on luminosity. The solid outline defines the boundary of the final sample of 462 stars, and the large filled circle inside it marks the position of the Sun.

TABLE 2.1: Volume-Limited Sample of 454 Solar-Type Stars

						Hipparcos		**FvL07**			
R.A. (J2000.0) (1)	**Decl. (J2000.0) (2)**	**HIP Name (3)**	**HD Name (4)**	V **(5)**	$B-V$ **(6)**	π **(mas) (7)**	σ_π **(mas) (8)**	π **(mas) (9)**	σ_π **(mas) (10)**	**Spec Type (11)**	**Ref (12)**
...	...	Sun	...	...	0.650	...	...	...	...	G2V	...
00 02 10.16	+27 04 56.1	000171	224930	5.80	0.690	80.63	3.03	82.17	2.23	G3V	HIP
00 06 15.81	+58 26 12.2	000518	000123	5.98	0.687	49.30	1.05	46.56	0.65	G5V	HIP
00 06 36.78	+29 01 17.4	000544	000166	6.07	0.752	72.98	0.75	73.15	0.56	K0V	HIP
00 12 50.25	−57 54 45.4	001031	000870	7.22	0.775	49.18	0.78	49.53	0.58	K0V	G06
00 16 12.68	−79 51 04.3	001292	001237	6.59	0.749	56.76	0.53	57.15	0.31	G8.5V	G06
00 16 53.89	−52 39 04.1	001349	001273	6.84	0.655	43.45	1.19	44.25	0.62	G5V	G06
00 18 41.87	−08 03 10.8	001499	001461	6.47	0.674	42.67	0.85	43.02	0.51	G0V	HIP
00 20 00.41	+38 13 38.6	001598	001562	6.97	0.640	40.25	0.81	40.33	0.59	G0	HIP
00 20 04.26	−64 52 29.2	001599	001581	4.23	0.576	116.38	0.64	116.46	0.16	F9.5V	G06
00 22 51.79	−12 12 34.0	001803	001835	6.39	0.659	49.05	0.91	47.93	0.53	G5V	G06
00 24 25.93	−27 01 36.4	001936	002025	7.92	0.940	55.53	1.08	54.87	0.86	K3V	G06
00 25 45.07	−77 15 15.3	002021	002151	2.82	0.618	133.78	0.51	134.07	0.11	G0V	G06
00 35 14.88	−03 35 34.2	002762	003196	5.20	0.567	47.51	1.15	47.05	0.67	F8V...	HIP
00 37 20.70	−24 46 02.2	002941	003443	5.57	0.715	64.38	1.40	64.93	1.85	G7V	G06
00 39 21.81	+21 15 01.7	003093	003651	5.88	0.850	90.03	0.72	90.42	0.32	K0V	HIP
00 40 49.27	+40 11 13.8	003206	003765	7.36	0.937	57.90	0.98	57.71	0.80	K2V	HIP
00 44 39.27	−65 38 58.3	003497	004308	6.55	0.655	45.76	0.56	45.34	0.32	G6V	G06
00 45 04.89	+01 47 07.9	003535	004256	8.03	0.983	45.43	0.95	46.37	0.62	K2V	HIP
00 45 45.59	−47 33 07.2	003583	004391	5.80	0.635	66.92	0.73	65.97	0.39	G5V	G06
00 48 22.98	+05 16 50.2	003765	004628	5.74	0.890	134.04	0.86	134.14	0.51	K2.5V	G06
00 48 58.71	+16 56 26.3	003810	004676	5.07	0.502	41.80	0.75	42.64	0.27	F8V...	HIP
00 49 06.29	+57 48 54.7	003821	004614	3.46	0.587	167.99	0.62	167.98	0.48	G0V	HIP

Continued on Next Page...

TABLE 2.1 – Continued

R.A. (J2000.0) (1)	Decl. (J2000.0) (2)	HIP Name (3)	HD Name (4)	V (5)	$B-V$ (6)	*Hipparcos* π (mas) (7)	*Hipparcos* σ_π (mas) (8)	FvL07 π (mas) (9)	FvL07 σ_π (mas) (10)	Spec Type (11)	Ref (12)
00 49 26.77	−23 12 44.9	003850	004747	7.15	0.769	53.09	1.02	53.51	0.53	G9V	G06
00 49 46.48	+70 26 58.1	003876	004635	7.75	0.900	46.47	0.70	46.23	0.53	K0	HIP
00 50 07.59	−10 38 39.6	003909	004813	5.17	0.514	64.69	1.03	63.48	0.35	F7IV-V	HIP
00 51 10.85	−05 02 21.4	003979	004915	6.98	0.663	45.27	0.97	46.47	0.66	G0	HIP
00 53 01.13	−30 21 24.9	004148	005133	7.15	0.936	71.01	0.78	70.56	0.61	K2.5V	G06
00 53 04.20	+61 07 26.3	004151	005015	4.80	0.540	53.85	0.60	53.35	0.33	F8V	HIP
01 08 16.39	+54 55 13.2	005336	006582	5.17	0.704	132.40	0.60	132.38	0.82	K1V	G03
01 15 00.99	−68 49 08.1	005842	007693	7.22	1.000	47.36	1.25	46.20	0.82	K2+V	G06
01 15 11.12	−45 31 54.0	005862	007570	4.97	0.571	66.43	0.64	66.16	0.24	F9V	G06
01 16 29.25	+42 56 21.9	005944	007590	6.59	0.594	42.30	0.75	43.11	0.45	G0-V	G03
01 21 59.12	+76 42 37.0	006379	007924	7.17	0.826	59.46	0.59	59.49	0.46	K0	HIP
01 29 04.90	+21 43 23.4	006917	008997	7.74	0.966	43.16	0.93	42.13	0.68	K2.5V	G03
01 33 15.81	−24 10 40.7	007235	009540	6.97	0.766	51.27	0.88	52.49	0.46	G8.5V	G06
01 34 33.26	+68 56 53.3	007339	009407	6.52	0.686	47.65	0.60	48.41	0.40	G6.5V	G03
01 35 01.01	−29 54 37.2	007372	009770	7.11	0.909	42.29	1.47	46.24	3.07	K2V	G06
01 36 47.84	+41 24 19.7	007513	009826	4.10	0.536	74.25	0.72	74.12	0.19	F8V	HIP
01 37 35.47	−06 45 37.5	007576	010008	7.66	0.797	42.35	0.96	41.75	0.74	G9V	G03
01 39 36.02	+45 52 40.0	007734	010086	6.60	0.690	46.73	0.80	46.79	0.60	G5V	G03
01 39 47.54	−56 11 47.0	007751	010360	5.76	0.880	122.75	1.41	127.84	2.19	K2V	G06
01 41 47.14	+42 36 48.1	007918	010307	4.96	0.618	79.09	0.83	78.50	0.54	G1V	G03
01 42 29.32	−53 44 27.0	007978	010647	5.52	0.551	57.63	0.64	57.36	0.25	F9V	G06
01 42 29.76	+20 16 06.6	007981	010476	5.24	0.836	133.91	0.91	132.76	0.50	K0V	G03
01 44 04.08	−15 56 14.9	008102	010700	3.49	0.727	274.17	0.80	273.96	0.17	G8.5V	G06
01 47 44.83	+63 51 09.0	008362	010780	5.63	0.804	100.24	0.68	99.33	0.53	G9V	G03
01 59 06.63	+33 12 34.9	009269	012051	7.14	0.773	40.74	0.90	40.03	0.58	G9V	G03

Continued on Next Page...

TABLE 2.1 – Continued

R.A. (J2000.0) (1)	Decl. (J2000.0) (2)	HIP Name (3)	HD Name (4)	V (5)	$B-V$ (6)	*Hipparcos* π (mas) (7)	*Hipparcos* σ_π (mas) (8)	FvL07 π (mas) (9)	FvL07 σ_π (mas) (10)	Spec Type (11)	Ref (12)
02 06 30.24	+24 20 02.4	009829	012846	6.89	0.662	43.14	0.94	43.91	0.57	G2V-	G03
02 10 25.93	−50 49 25.4	010138	013445	6.12	0.812	91.63	0.61	92.74	0.32	K1V	G06
02 17 03.23	+34 13 27.2	010644	013974	4.84	0.607	92.20	0.84	92.73	0.39	G0V	HIP
02 18 01.44	+01 45 28.1	010723	014214	5.60	0.588	40.04	0.92	41.06	0.49	G0IV-	G03
02 18 58.50	−25 56 44.5	010798	014412	6.33	0.724	78.88	0.72	78.93	0.35	G8V	G06
02 22 32.55	−23 48 58.8	011072	014802	5.19	0.608	45.60	0.82	45.53	0.82	G0V	G06
02 36 04.89	+06 53 12.7	012114	016160	5.79	0.918	138.72	1.04	139.27	0.45	K3V	G03
02 36 41.76	−03 09 22.1	012158	016287	8.10	0.944	41.09	1.25	41.44	0.97	K2.5V	G03
02 40 12.42	−09 27 10.3	012444	016673	5.79	0.524	46.42	0.82	45.96	0.41	F8V	G03
02 41 14.00	−00 41 44.4	012530	016765	5.72	0.511	46.24	1.31	44.27	0.84	F7V	G03
02 42 14.92	+40 11 38.2	012623	016739	4.91	0.582	40.52	1.25	41.34	0.43	F9IV-V	G03
02 42 33.47	−50 48 01.1	012653	017051	5.40	0.561	58.00	0.55	58.25	0.22	F9V	G06
02 44 11.99	+49 13 42.4	012777	016895	4.10	0.514	89.03	0.79	89.87	0.22	F7V	HIP
02 48 09.14	+27 04 07.1	013081	017382	7.56	0.820	44.71	1.15	40.59	1.28	K0V	G03
02 52 32.13	−12 46 11.0	013402	017925	6.05	0.862	96.33	0.77	96.60	0.40	K1.5V	G06
02 55 39.06	+26 52 23.6	013642	018143	7.52	0.953	43.71	1.26	42.57	0.84	K2IV	G03
03 00 02.81	+07 44 59.1	013976	018632	7.97	0.926	42.66	1.22	41.00	1.12	K2.5V	G03
03 02 26.03	+26 36 33.3	014150	018803	6.62	0.696	47.25	0.89	48.45	0.47	G6V	G03
03 04 09.64	+61 42 21.0	014286	018757	6.64	0.634	43.74	0.84	41.27	0.58	G1.5V	G03
03 09 04.02	+49 36 47.8	014632	019373	4.05	0.595	94.93	0.67	94.87	0.23	F9.5V	G03
03 12 04.53	−28 59 15.4	014879	020010	3.80	0.543	70.86	0.67	70.24	0.45	F6V	G06
03 12 46.44	−01 11 46.0	014954	019994	5.07	0.575	44.69	0.75	44.29	0.28	F8.5V	G03
03 14 47.23	+08 58 50.9	015099	020165	7.83	0.861	44.96	1.09	44.15	0.83	K1V	G03
03 15 06.39	−45 39 53.4	015131	020407	6.75	0.586	41.05	0.59	41.34	0.40	G5V	G06
03 18 12.82	−62 30 22.9	015371	020807	5.24	0.600	82.79	0.53	83.11	0.19	G0V	G06

Continued on Next Page...

TABLE 2.1 – Continued

R.A. (J2000.0) (1)	Decl. (J2000.0) (2)	HIP Name (3)	HD Name (4)	V (5)	$B-V$ (6)	*Hipparcos* π (mas) (7)	*Hipparcos* σ_π (mas) (8)	FvL07 π (mas) (9)	FvL07 σ_π (mas) (10)	Spec Type (11)	Ref (12)
03 19 01.89	−02 50 35.5	015442	020619	7.05	0.655	40.52	0.98	39.65	0.74	G2V	G03
03 19 21.70	+03 22 12.7	015457	020630	4.84	0.681	109.18	0.78	109.41	0.27	G5Vvar	HIP
03 19 55.65	−43 04 11.2	015510	020794	4.26	0.711	165.02	0.55	165.47	0.19	G8V	G06
03 21 54.76	+52 19 53.4	015673	232781	9.05	0.990	44.03	1.24	42.81	1.03	K3.5V	G03
03 23 35.26	−40 04 35.0	015799	021175	6.90	0.840	58.53	1.04	57.40	0.67	K1V	G06
03 32 55.84	−09 27 29.7	016537	022049	3.72	0.881	310.75	0.85	310.94	0.16	K2V	G03
03 36 52.38	+00 24 06.0	016852	022484	4.29	0.575	72.89	0.78	71.62	0.54	F9V	HIP
03 40 22.06	−03 13 01.1	017147	022879	6.68	0.554	41.07	0.86	39.12	0.56	F9V	HIP
03 43 55.34	−19 06 39.2	017420	023356	7.10	0.927	71.17	0.91	71.69	0.67	K2.5V	G06
03 44 09.17	−38 16 54.4	017439	023484	6.99	0.870	61.63	0.67	62.39	0.52	K2V	G06
03 54 28.03	+16 36 57.8	018267	024496	6.81	0.719	48.36	1.02	48.95	0.70	G7V	G03
03 55 03.84	+61 10 00.5	018324	024238	7.84	0.831	46.95	0.95	47.59	0.84	K2V	G03
03 56 11.52	+59 38 30.8	018413	024409	6.53	0.698	46.74	0.96	45.49	0.62	G3V	G03
04 02 36.74	−00 16 08.1	018859	025457	5.38	0.516	52.00	0.75	53.10	0.32	F7V	G03
04 03 15.00	+35 16 23.8	018915	025329	8.51	0.863	54.14	1.08	54.68	0.92	K3Vp	G03
04 05 20.26	+22 00 32.1	019076	025680	5.90	0.620	59.79	0.84	59.04	0.33	G1V	G03
04 07 21.54	−64 13 20.2	019233	026491	6.37	0.636	43.12	0.50	42.32	0.28	G1V	G06
04 08 36.62	+38 02 23.0	019335	025998	5.52	0.520	46.87	0.77	47.63	0.26	F8V	G03
04 09 35.04	+69 32 29.0	019422	025665	7.70	0.952	54.17	0.79	53.33	0.71	K2.5V	G03
04 15 16.32	−07 39 10.3	019849	026965	4.43	0.820	198.24	0.84	200.62	0.23	K1V	G03
04 15 28.80	+06 11 12.7	019859	026923	6.32	0.570	47.20	1.08	46.88	0.47	G0IV-V	G03
04 43 35.44	+27 41 14.6	021988	029883	8.00	0.907	44.74	0.99	45.61	0.81	K5III	HIP
04 45 38.58	−50 04 27.2	022122	030501	7.58	0.875	48.90	0.64	47.93	0.45	K2V	G06
04 47 36.29	−16 56 04.0	022263	030495	5.49	0.632	75.10	0.80	75.32	0.36	G1.5V	G06
04 49 52.33	−35 06 27.5	022451	030876	7.49	0.901	55.59	0.71	56.35	0.48	K2V	HIP

Continued on Next Page...

TABLE 2.1 – Continued

R.A. (J2000.0) (1)	Decl. (J2000.0) (2)	HIP Name (3)	HD Name (4)	V (5)	$B-V$ (6)	*Hipparcos* π (mas) (7)	*Hipparcos* σ_π (mas) (8)	FvL07 π (mas) (9)	FvL07 σ_π (mas) (10)	Spec Type (11)	Ref (12)
05 02 17.06	−56 04 49.9	023437	032778	7.02	0.636	44.94	0.58	44.48	0.36	G7V	G06
05 05 30.66	−57 28 21.7	023693	033262	4.71	0.526	85.83	0.46	85.87	0.18	F9V	G06
05 06 42.22	+14 26 46.4	023786	032850	7.74	0.804	41.70	1.14	42.24	0.92	G9V	G03
05 07 27.01	+18 38 42.2	023835	032923	4.91	0.657	63.02	0.93	64.79	0.33	G1V	G03
05 18 50.47	−18 07 48.2	024786	034721	5.96	0.572	40.11	0.76	39.96	0.40	F9-V	G06
05 19 08.47	+40 05 56.6	024813	034411	4.69	0.630	79.08	0.90	79.17	0.28	G1V	G03
05 22 33.53	+79 13 52.1	025110	033564	5.08	0.506	47.66	0.52	47.88	0.21	F7V	G03
05 22 37.49	+02 36 11.5	025119	035112	7.76	0.980	50.24	1.52	49.44	1.17	K2.5V	G03
05 24 25.46	+17 23 00.7	025278	035296	5.00	0.544	68.19	0.94	69.51	0.38	F8V	G03
05 26 14.74	−32 30 17.2	025421	035854	7.70	0.946	55.76	0.76	56.27	0.61	K3-V	G06
05 27 39.35	−60 24 57.6	025544	036435	6.99	0.755	51.10	0.52	52.08	0.45	G9V	G06
05 28 44.83	−65 26 54.9	025647	036705	6.88	0.830	66.92	0.54	65.93	0.57	K2V	G06
05 36 56.85	−47 57 52.9	026373	037572	7.95	0.845	41.90	1.74	39.82	1.36	K1.5V	G06
05 37 09.89	−80 28 08.8	026394	039091	5.65	0.600	54.92	0.45	54.60	0.21	G0V	G06
05 38 11.86	+51 26 44.7	026505	037008	7.74	0.834	48.72	1.00	49.60	0.72	K1V	G03
05 41 20.34	+53 28 51.8	026779	037394	6.21	0.840	81.69	0.83	81.45	0.54	K0V	G03
05 46 01.89	+37 17 04.7	027207	038230	7.34	0.833	48.60	1.03	45.76	0.76	K0V	G03
05 48 34.94	−04 05 40.7	027435	038858	5.97	0.639	64.25	1.19	65.89	0.41	G2V	G03
05 54 04.24	−60 01 24.5	027887	040307	7.17	0.935	77.95	0.53	76.95	0.37	K2.5V	G06
05 54 22.98	+20 16 34.2	027913	039587	4.39	0.594	115.43	1.08	115.43	0.27	G0IV-V	G03
05 54 30.16	−19 42 15.7	027922	039855	7.51	0.700	43.86	1.19	42.43	0.99	G8V	G06
05 58 21.54	−04 39 02.4	028267	040397	6.99	0.720	43.10	0.93	42.46	0.63	G7V	G03
06 06 40.48	+15 32 31.6	028954	041593	6.76	0.814	64.71	0.91	65.48	0.67	G9V	G03
06 10 14.47	−74 45 11.0	029271	043834	5.08	0.714	98.54	0.45	98.06	0.14	G7V	G06
06 12 00.57	+06 46 59.1	029432	042618	6.85	0.642	43.26	0.87	42.55	0.55	G3V	G03

Continued on Next Page...

TABLE 2.1 – Continued

R.A. (J2000.0) (1)	Decl. (J2000.0) (2)	HIP Name (3)	HD Name (4)	V (5)	$B-V$ (6)	*Hipparcos* π (mas) (7)	*Hipparcos* σ_π (mas) (8)	FvL07 π (mas) (9)	FvL07 σ_π (mas) (10)	Spec Type (11)	Ref (12)
06 13 12.50	+10 37 37.7	029525	042807	6.43	0.663	55.20	0.96	55.71	0.44	G5V	G03
06 13 45.30	−23 51 43.0	029568	043162	6.37	0.713	59.90	0.75	59.80	0.49	G6.5V	G06
06 17 16.14	+05 06 00.4	029860	043587	5.70	0.610	51.76	0.78	51.95	0.40	G0V	G03
06 22 30.94	−60 13 07.2	030314	045270	6.53	0.614	42.56	0.49	42.05	0.27	G0Vp	G06
06 24 43.88	−28 46 48.4	030503	045184	6.37	0.626	45.38	0.63	45.70	0.40	G1.5V	G06
06 26 10.25	+18 45 24.8	030630	045088	6.78	0.938	68.20	1.10	67.89	1.53	K3V	G03
06 38 00.36	−61 32 00.2	031711	048189	6.15	0.624	46.15	0.64	46.96	0.81	G1V	G06
06 46 05.05	+32 33 20.4	032423	263175	8.80	0.964	40.02	1.22	38.11	1.01	K3V	G03
06 46 14.15	+79 33 53.3	032439	046588	5.44	0.525	56.02	0.53	55.95	0.27	F8V	G03
06 46 44.34	+43 34 38.7	032480	048682	5.24	0.575	60.56	0.73	59.82	0.30	F9V	G03
06 55 18.67	+25 22 32.5	033277	050692	5.74	0.573	57.89	0.90	58.00	0.41	G0V	G03
06 58 11.75	+22 28 33.2	033537	051419	6.94	0.620	41.25	0.88	40.60	0.53	G5V	G03
06 59 59.66	−61 20 10.3	033690	053143	6.81	0.786	54.33	0.54	54.57	0.34	K0IV-V	G06
07 01 13.74	−25 56 55.4	033817	052698	6.71	0.882	68.42	0.72	68.27	0.61	K1V	G06
07 01 38.59	+48 22 43.2	033852	051866	7.98	0.986	48.96	0.97	49.79	0.84	K3V	G03
07 03 30.46	+29 20 13.5	034017	052711	5.93	0.595	52.37	0.84	52.27	0.41	G0V	G03
07 03 57.32	−43 36 28.9	034065	053705	5.56	0.624	61.54	1.05	60.55	1.04	G0V	G06
07 08 04.24	+29 50 04.2	034414	053927	8.32	0.907	44.92	1.43	44.93	0.97	K2.5V	G03
07 09 35.39	+25 43 43.1	034567	054371	7.09	0.700	40.68	1.02	39.73	0.54	G6V	G03
07 15 50.14	+47 14 23.9	035136	055575	5.54	0.576	59.31	0.69	59.20	0.33	F9V	G03
07 17 29.56	−46 58 45.3	035296	057095	6.70	0.975	67.69	0.86	68.52	0.56	K2.5V	G06
07 27 25.47	−51 24 09.4	036210	059468	6.72	0.694	44.43	0.53	44.10	0.36	G6.5V	G06
07 29 01.77	+31 59 37.8	036357	...	7.73	0.923	56.98	1.24	56.63	0.93	K2.5V	G03
07 30 42.51	−37 20 21.7	036515	059967	6.66	0.641	45.93	0.58	45.84	0.37	G2V	G06
07 33 00.58	+37 01 47.4	036704	059747	7.68	0.863	50.80	1.29	50.60	0.94	K1V	G03

Continued on Next Page...

TABLE 2.1 – Continued

R.A. (J2000.0) (1)	Decl. (J2000.0) (2)	HIP Name (3)	HD Name (4)	V (5)	$B-V$ (6)	*Hipparcos* π (mas) (7)	*Hipparcos* σ_π (mas) (8)	FvL07 π (mas) (9)	FvL07 σ_π (mas) (10)	Spec Type (11)	Ref (12)
07 34 26.17	−06 53 48.0	036827	060491	8.16	0.900	40.32	1.26	40.73	1.00	K2.5V	G03
07 39 59.33	−03 35 51.0	037349	061606	7.18	0.891	70.44	0.94	70.37	0.64	K3-V	G03
07 45 35.02	−34 10 20.5	037853	063077	5.36	0.589	65.79	0.56	65.75	0.51	F9V	G06
07 49 55.06	+27 21 47.4	038228	063433	6.90	0.682	45.84	0.89	45.45	0.53	G5V	G03
07 51 46.30	−13 53 52.9	038382	064096	5.16	0.600	59.98	0.95	60.59	0.59	G0V	G06
07 54 34.18	−01 24 44.1	038625	064606	7.43	0.739	52.01	1.85	49.78	1.85	K0V	G03
07 54 54.07	+19 14 10.8	038657	064468	7.76	0.950	50.05	1.05	48.33	0.86	K2.5V	G03
07 56 17.23	+80 15 55.9	038784	062613	6.55	0.719	58.67	0.57	58.17	0.36	G8V	HIP
07 57 46.91	−60 18 11.1	038908	065907	5.59	0.573	61.76	0.51	61.71	0.21	F9.5V	G06
07 59 33.93	+20 50 38.0	039064	065430	7.68	0.833	43.21	0.96	42.15	0.71	K0V	G03
08 00 32.13	+29 12 44.5	039157	065583	6.97	0.716	59.52	0.77	59.64	0.56	K0V	G03
08 02 31.19	−66 01 15.4	039342	067199	7.18	0.872	57.88	0.58	57.76	0.41	K2V	G06
08 07 45.86	+21 34 54.5	039780	067228	5.30	0.642	42.86	0.97	42.94	0.30	G2IV	G03
08 11 38.64	+32 27 25.7	040118	068017	6.78	0.679	46.05	0.92	45.90	0.55	G3V	G03
08 12 12.73	+17 38 52.0	040167	068257	4.67	0.531	41.10[a]	0.90[a]	39.87	0.82	F8V	G03
08 18 23.95	−12 37 55.8	040693	069830	5.95	0.754	79.48	0.77	80.04	0.35	G8+V	G06
08 19 19.05	+01 20 19.9	040774	...	8.35	0.901	42.89	1.32	43.61	1.26	G5	HIP
08 27 36.79	+45 39 10.8	041484	071148	6.32	0.624	45.89	0.84	44.94	0.46	G1V	G03
08 32 51.50	−31 30 03.1	041926	072673	6.38	0.780	82.15	0.66	81.91	0.46	G9V	G06
08 34 31.65	−00 43 33.8	042074	072760	7.32	0.791	45.95	1.01	47.31	0.72	K0-V	G03
08 37 50.29	−06 48 24.8	042333	073350	6.74	0.655	42.32	1.04	41.71	0.70	G5V	G03
08 39 07.90	−22 39 42.8	042430	073752	5.05	0.720	50.20	0.98	51.55	0.63	G5IV	G06
08 39 11.70	+65 01 15.3	042438	072905	5.63	0.618	70.07	0.71	69.66	0.37	G1.5Vb	HIP
08 39 50.79	+11 31 21.6	042499	073667	7.61	0.832	53.98	1.04	55.13	0.71	K2V	G03
08 42 07.52	−42 55 46.0	042697	074385	8.11	0.904	44.73	0.79	43.73	0.55	K2+V	G06

Continued on Next Page...

TABLE 2.1 – Continued

R.A. (J2000.0) (1)	Decl. (J2000.0) (2)	HIP Name (3)	HD Name (4)	V (5)	$B-V$ (6)	*Hipparcos* π (mas) (7)	*Hipparcos* σ_π (mas) (8)	FvL07 π (mas) (9)	FvL07 σ_π (mas) (10)	Spec Type (11)	Ref (12)
08 43 18.03	−38 52 56.6	042808	074576	6.58	0.917	89.78	0.56	89.76	0.37	K2.5V	G06
08 52 16.39	+08 03 46.5	043557	075767	6.57	0.640	41.42	1.19	41.64	1.03	G1.5V	G03
08 52 35.81	+28 19 50.9	043587	075732	5.96	0.869	79.80	0.84	81.03	0.75	K0IV-V	G03
08 54 17.95	−05 26 04.1	043726	076151	6.01	0.661	58.50	0.88	57.52	0.39	G3V	G06
08 58 43.93	−16 07 57.8	044075	076932	5.80	0.521	46.90	0.97	47.54	0.31	G2V	G06
09 08 51.07	+33 52 56.0	044897	078366	5.95	0.585	52.25	0.87	52.11	0.33	G0IV-V	G03
09 12 17.55	+14 59 45.7	045170	079096	6.49	0.731	48.83	0.92	49.11	0.54	G9V	G03
09 14 20.54	+61 25 23.9	045333	079028	5.18	0.605	51.12	0.72	51.10	0.32	G0IV-V	G03
09 17 53.46	+28 33 37.9	045617	079969	7.20	0.992	57.05	1.08	57.92	0.76	K3V	G03
09 22 25.95	+40 12 03.8	045963	080715	7.69	0.987	41.19	1.08	40.10	0.64	K2.5V	G03
09 30 28.09	−32 06 12.2	046626	082342	8.31	0.985	51.71	0.91	51.79	0.85	K3.5V	G06
09 32 25.57	−11 11 04.7	046816	082558	7.82	0.933	54.52	0.99	53.70	0.84	K0	HIP
09 32 43.76	+26 59 18.7	046843	082443	7.05	0.779	56.35	0.89	56.20	0.60	G9V	G03
09 35 39.50	+35 48 36.5	047080	082885	5.40	0.770	89.45	0.78	87.96	0.32	G8+V	G03
09 42 14.42	−23 54 56.1	047592	084117	4.93	0.534	67.19	0.73	66.61	0.21	F8V	G06
09 48 35.37	+46 01 15.6	048113	084737	5.08	0.619	54.26	0.74	54.44	0.28	G0IV-V	G03
10 01 00.66	+31 55 25.2	049081	086728	5.37	0.676	67.14	0.83	66.46	0.32	G4V	G03
10 04 37.66	−11 43 46.9	049366	087424	8.15	0.891	43.14	1.11	41.61	0.95	K2V	G06
10 08 43.14	+34 14 32.1	049699	087883	7.56	0.965	55.37	0.94	54.93	0.54	K2.5V	G03
10 13 24.73	−33 01 54.2	050075	088742	6.38	0.592	43.98	0.72	43.77	0.41	G0V	G06
10 17 14.54	+23 06 22.4	050384	089125	5.81	0.500	44.01	0.75	43.85	0.36	F6V	G03
10 18 51.95	+44 02 54.0	050505	089269	6.66	0.653	48.45	0.85	49.41	0.50	G4V	G03
10 23 55.27	−29 38 43.9	050921	090156	6.92	0.659	45.26	0.75	44.74	0.49	G5V	G06
10 28 03.88	+48 47 05.6	051248	090508	6.42	0.610	42.45	0.77	43.65	0.43	G0V	G03
10 30 37.58	+55 58 49.9	051459	090839	4.82	0.541	77.82	0.65	78.25	0.28	F8V	G03

Continued on Next Page...

TABLE 2.1 – Continued

R.A. (J2000.0) (1)	Decl. (J2000.0) (2)	HIP Name (3)	HD Name (4)	V (5)	$B-V$ (6)	*Hipparcos* π (mas) (7)	*Hipparcos* σ_π (mas) (8)	FvL07 π (mas) (9)	FvL07 σ_π (mas) (10)	Spec Type (11)	Ref (12)
10 31 21.82	−53 42 55.7	051523	091324	4.89	0.500	45.72	0.51	45.85	0.19	F9V	G06
10 35 11.27	+84 23 57.6	051819	090343	7.29	0.819	47.55	0.60	48.24	0.49	K0	HIP
10 36 32.38	−12 13 48.4	051933	091889	5.71	0.528	40.67	0.68	39.88	0.37	F8V	G06
10 42 13.32	−13 47 15.8	052369	092719	6.79	0.622	42.73	0.82	41.97	0.47	G1.5V	G06
10 43 28.27	−29 03 51.4	052462	092945	7.72	0.873	46.36	0.84	46.73	0.69	K1.5V	G06
10 56 30.80	+07 23 18.5	053486	094765	7.37	0.920	56.98	1.03	57.79	0.87	K2.5V	G03
10 59 27.97	+40 25 48.9	053721	095128	5.03	0.624	71.04	0.66	71.11	0.25	G0V	HIP
11 04 41.47	−04 13 15.9	054155	096064	7.64	0.770	40.57	1.40	38.06	0.99	G8+V	G03
11 08 14.01	+38 25 35.9	054426	096612	8.35	0.942	43.91	1.03	44.29	0.84	K3-V	G03
11 12 01.19	−26 08 12.0	054704	097343	7.05	0.760	46.22	0.84	45.16	0.50	G8.5V	G06
11 12 32.35	+35 48 50.7	054745	097334	6.41	0.600	46.04	0.90	45.61	0.44	G1V	G03
11 14 33.16	+25 42 37.4	054906	097658	7.76	0.845	46.95	0.97	47.36	0.75	K1V	G03
11 18 10.95	+31 31 45.7	055203	098230	3.79	0.606	119.70[a]	0.80[a]	...	...	G0V	HIP
11 18 22.01	−05 04 02.3	055210	098281	7.29	0.732	45.48	1.00	46.36	0.64	G8V	HIP
11 26 45.32	+03 00 47.2	055846	099491	6.49	0.778	56.59	1.40	56.35	0.75	K0IV	HIP
11 31 44.95	+14 21 52.2	056242	100180	6.27	0.570	43.42	1.10	42.87	1.22	F9.5V	G03
11 34 29.49	−32 49 52.8	056452	100623	5.96	0.811	104.84	0.81	104.61	0.37	K0-V	G06
11 38 44.90	+45 06 30.3	056809	101177	6.29	0.566	42.94	0.95	43.01	0.73	F9.5V	G03
11 38 59.72	+42 19 43.7	056829	101206	8.22	0.980	50.61	1.15	50.19	1.03	K5V	HIP
11 41 03.02	+34 12 05.9	056997	101501	5.31	0.723	104.81	0.72	104.04	0.26	G8V	G03
11 46 31.07	−40 30 01.3	057443	102365	4.89	0.664	108.23	0.70	108.45	0.22	G2V	G06
11 47 15.81	−30 17 11.4	057507	102438	6.48	0.681	56.26	0.77	57.23	0.41	G6V	G06
11 50 41.72	+01 45 53.0	057757	102870	3.59	0.518	91.74	0.77	91.50	0.22	F8V	HIP
11 52 58.77	+37 43 07.2	057939	103095	6.42	0.754	109.21	0.78	109.99	0.41	K1V	G03
11 59 10.01	−20 21 13.6	058451	104067	7.92	0.974	48.04	1.03	47.47	0.90	K3-V	G06

Continued on Next Page...

TABLE 2.1 – Continued

R.A. (J2000.0) (1)	Decl. (J2000.0) (2)	HIP Name (3)	HD Name (4)	V (5)	$B-V$ (6)	*Hipparcos* π (mas) (7)	*Hipparcos* σ_π (mas) (8)	FvL07 π (mas) (9)	FvL07 σ_π (mas) (10)	Spec Type (11)	Ref (12)
12 00 44.45	−10 26 45.6	058576	104304	5.54	0.760	77.48	0.80	78.35	0.31	G8IV-V	G03
12 09 37.26	+40 15 07.4	059280	105631	7.46	0.794	41.07	0.98	40.77	0.66	G9V	G03
12 30 50.14	+53 04 35.8	061053	108954	6.20	0.568	45.58	0.62	45.92	0.35	F9V	G03
12 33 31.38	−68 45 20.9	061291	109200	7.13	0.836	61.83	0.63	61.82	0.48	K1V	G06
12 33 44.54	+41 21 26.9	061317	109358	4.24	0.588	119.46	0.83	118.49	0.20	G0V	G03
12 41 44.52	+55 43 28.8	061946	110463	8.27	0.955	43.06	0.82	42.78	0.81	K3V	HIP
12 44 14.55	+51 45 33.5	062145	110833	7.01	0.936	66.40	0.78	67.20	0.66	K3V	HIP
12 44 59.41	+39 16 44.1	062207	110897	5.95	0.557	57.57	0.64	57.55	0.32	F9V	G03
12 45 14.41	−57 21 28.8	062229	110810	7.82	0.937	49.71	0.95	48.79	0.88	K2+V	G06
12 48 32.31	−15 43 10.1	062505	111312	7.93	0.946	47.19	1.93	41.96	3.00	K2.5V	G06
12 48 47.05	+24 50 24.8	062523	111395	6.29	0.703	58.23	0.99	59.06	0.45	G7V	G03
12 59 01.56	−09 50 02.7	063366	112758	7.54	0.769	47.60	0.86	47.87	0.90	K2V	G03
12 59 32.78	+41 59 12.4	063406	112914	8.60	0.940	41.36	1.48	39.71	1.00	K3-V	G03
13 03 49.66	−05 09 42.5	063742	113449	7.69	0.847	45.20	1.27	46.10	0.81	K1V	G03
13 11 52.39	+27 52 41.5	064394	114710	4.23	0.572	109.23	0.72	109.54	0.17	G0V	HIP
13 12 03.18	−37 48 10.9	064408	114613	4.85	0.693	48.83	0.79	48.38	0.29	G4IV	G06
13 12 43.79	−02 15 54.1	064457	114783	7.56	0.930	48.95	1.06	48.78	0.59	K1V	G03
13 13 52.23	−45 11 08.9	064550	114853	6.93	0.643	40.87	0.84	40.95	0.56	G1.5V	G06
13 15 26.45	−87 33 38.5	064690	113283	7.11	0.710	40.52	0.56	40.70	0.38	G5V	G06
13 16 46.52	+09 25 27.0	064792	115383	5.19	0.585	55.71	0.85	56.95	0.26	G0Vs	HIP
13 16 51.05	+17 01 01.9	064797	115404	6.49	0.926	89.07	0.99	90.32	0.74	K2.5V	G03
13 18 24.31	−18 18 40.3	064924	115617	4.74	0.709	117.30	0.71	116.89	0.22	G7V	G06
13 23 39.15	+02 43 24.0	065352	116442	7.06	0.780	62.41	1.41	64.73	1.33	G9V	G03
13 25 45.53	+56 58 13.8	065515	116956	7.29	0.804	45.76	0.72	46.31	0.51	G9V	G03
13 25 59.86	+63 15 40.6	065530	117043	6.50	0.739	46.86	0.55	47.24	0.31	G6V	HIP

Continued on Next Page...

TABLE 2.1 – Continued

						Hipparcos		FvL07			
R.A. (J2000.0)	**Decl. (J2000.0)**	**HIP Name**	**HD Name**			π	σ_π	π	σ_π	**Spec Type**	**Ref**
(1)	**(2)**	**(3)**	**(4)**	V **(5)**	$B-V$ **(6)**	**(mas) (7)**	**(mas) (8)**	**(mas) (9)**	**(mas) (10)**	**(11)**	**(12)**
13 28 25.81	+13 46 43.6	065721	117176	4.97	0.714	55.22	0.73	55.60	0.24	G5V	HIP
13 41 04.17	−34 27 51.0	066765	118972	6.92	0.855	64.08	0.81	63.88	0.49	K0V	G06
13 41 13.40	+56 43 37.8	066781	119332	7.77	0.830	42.12	0.76	40.59	0.53	K0IV-V	HIP
13 47 15.74	+17 27 24.9	067275	120136	4.50	0.508	64.12	0.70	64.03	0.19	F7V	HIP
13 51 20.33	−24 23 25.3	067620	120690	6.43	0.703	50.20	0.85	51.35	0.45	G5+V	G06
13 51 40.40	−57 26 08.4	067655	120559	7.97	0.663	40.02	1.00	39.42	0.97	G7V	G06
13 52 35.87	−50 55 18.3	067742	120780	7.37	0.891	60.86	0.95	58.55	0.68	K2V	G06
13 54 41.08	+18 23 51.8	067927	121370	2.68	0.580	88.17	0.75	87.75	1.24	G0IV	HIP
13 55 49.99	+14 03 23.4	068030	121560	6.16	0.518	41.28	0.79	40.22	0.37	F6V	HIP
14 03 32.35	+10 47 12.4	068682	122742	6.27	0.733	60.24	0.78	58.88	0.62	G6V	G03
14 11 46.17	−12 36 42.4	069357	124106	7.93	0.865	43.35	1.40	42.76	1.22	K1V	G06
14 12 45.24	−03 19 12.3	069414	124292	7.05	0.733	44.89	1.01	45.35	0.54	G8+V	G03
14 15 38.68	−45 00 02.7	069671	124580	6.31	0.596	47.51	0.78	47.13	0.42	G0V	G06
14 16 00.87	−06 00 02.0	069701	124850	4.07	0.511	46.74	0.87	44.97	0.19	F7V	HIP
14 19 00.90	−25 48 55.5	069965	125276	5.87	0.518	56.23	0.94	55.45	0.82	F9V	G06
14 19 34.86	−05 09 04.3	070016	125455	7.58	0.867	48.12	1.11	47.89	0.81	K1V	HIP
14 23 15.28	+01 14 29.6	070319	126053	6.25	0.639	56.82	1.04	58.17	0.53	G1.5V	G03
14 29 22.30	+80 48 35.5	070857	128642	6.88	0.774	51.04	0.58	50.27	0.48	G5	HIP
14 29 36.81	+41 47 45.3	070873	127334	6.36	0.702	42.43	0.59	42.12	0.38	G5V	G03
14 33 28.87	+52 54 31.6	071181	128165	7.24	0.997	74.50	0.69	75.65	0.42	K3V	HIP
14 36 00.56	+09 44 47.5	071395	128311	7.48	0.973	60.35	0.99	60.60	0.83	K3-V	G03
14 39 36.50	−60 50 02.3	071683	128620	−0.01	0.710	742.12	1.40	754.81	4.11	G2V	G06
14 40 31.11	−16 12 33.4	071743	128987	7.24	0.710	42.43	0.97	42.23	0.54	G8V	G06
14 41 52.46	−75 08 22.1	071855	128400	6.73	0.707	49.15	0.64	50.01	0.43	G5V	G06
14 45 24.18	+13 50 46.7	072146	130004	7.87	0.931	51.20	0.98	52.92	0.82	K2.5V	G03

Continued on Next Page...

TABLE 2.1 – Continued

R.A. (J2000.0) (1)	Decl. (J2000.0) (2)	HIP Name (3)	HD Name (4)	V (5)	$B-V$ (6)	*Hipparcos* π (mas) (7)	*Hipparcos* σ_π (mas) (8)	FvL07 π (mas) (9)	FvL07 σ_π (mas) (10)	Spec Type (11)	Ref (12)
14 47 16.10	+02 42 11.6	072312	130307	7.76	0.893	50.84	1.04	51.62	0.79	K2.5V	G03
14 49 23.72	−67 14 09.5	072493	130042	7.26	0.836	41.69	1.24	40.11	0.89	K1V	G06
14 50 15.81	+23 54 42.6	072567	130948	5.86	0.576	55.73	0.80	55.03	0.34	G2V	HIP
14 51 23.38	+19 06 01.7	072659	131156	4.54	0.720	149.26	0.76	148.98	0.48	G7V	G03
14 53 23.77	+19 09 10.1	072848	131511	6.00	0.841	86.69	0.81	86.88	0.46	K0V	G03
14 53 41.57	+23 20 42.6	072875	131582	8.65	0.934	43.66	1.20	42.47	1.12	K3V	HIP
14 55 11.04	+53 40 49.2	073005	132142	7.77	0.785	41.83	0.63	42.76	0.45	K1V	HIP
14 56 23.04	+49 37 42.4	073100	132254	5.63	0.533	40.25	0.54	39.83	0.26	F8-V	G03
14 58 08.80	−48 51 46.8	073241	131923	6.34	0.708	40.79	0.86	41.93	0.83	G4V	G06
15 03 47.30	+47 39 14.6	073695	133640	4.83	0.647	78.39	1.03	79.95	1.56	G2V	HIP
15 10 44.74	−61 25 20.3	074273	134060	6.29	0.623	41.41	0.77	41.32	0.45	G0V	G06
15 13 50.89	−01 21 05.0	074537	135204	6.58	0.763	57.80	0.85	56.59	0.49	G9V	G03
15 15 59.17	+00 47 46.9	074702	135599	6.92	0.830	64.19	0.97	63.11	0.70	K0V	G03
15 19 18.80	+01 45 55.5	074975	136202	5.04	0.540	40.46	0.81	39.40	0.29	F8III-IV	HIP
15 21 48.15	−48 19 03.5	075181	136352	5.65	0.639	68.70	0.79	67.51	0.39	G2-V	G06
15 22 36.69	−10 39 40.0	075253	136713	7.97	0.970	45.83	1.41	45.22	1.12	K3IV-V	G03
15 22 46.83	+18 55 08.3	075277	136923	7.16	0.804	49.67	0.92	51.01	0.64	G9V	G03
15 23 12.31	+30 17 16.1	075312	137107	4.99	0.577	53.70	1.24	55.98	0.78	G2V	HIP
15 28 09.61	−09 20 53.1	075718	137763	6.89	0.788	50.34	1.11	48.58	1.33	G9V	G03
15 29 11.18	+80 26 55.0	075809	139777	6.57	0.665	45.32	0.57	45.77	0.37	G1.5V(n)	G03
15 36 02.22	+39 48 08.9	076382	139341	6.78	0.906	45.85	0.79	44.83	0.60	K1V	G03
15 44 01.82	+02 30 54.6	077052	140538	5.86	0.684	68.16	0.87	68.22	0.66	G5V	HIP
15 46 26.61	+07 21 11.1	077257	141004	4.42	0.604	85.08	0.80	82.48	0.32	G0IV-V	G03
15 47 29.10	−37 54 58.7	077358	140901	6.01	0.715	65.60	0.77	65.13	0.40	G7IV-V	G06
15 48 09.46	+01 34 18.3	077408	141272	7.44	0.801	46.84	1.05	46.97	0.80	G9V	G03

Continued on Next Page...

TABLE 2.1 – Continued

R.A. (J2000.0) (1)	Decl. (J2000.0) (2)	HIP Name (3)	HD Name (4)	V (5)	$B-V$ (6)	*Hipparcos* π (mas) (7)	*Hipparcos* σ_π (mas) (8)	FvL07 π (mas) (9)	FvL07 σ_π (mas) (10)	Spec Type (11)	Ref (12)
15 52 40.54	+42 27 05.5	077760	142373	4.60	0.563	63.08	0.54	62.92	0.21	G0V	G03
15 53 12.10	+13 11 47.8	077801	142267	6.07	0.598	57.27	0.88	57.64	0.54	G0IV	HIP
16 01 02.66	+33 18 12.6	078459	143761	5.39	0.612	57.38	0.71	58.02	0.28	G0V	G03
16 01 53.35	+58 33 54.9	078527	144284	4.01	0.528	47.79	0.54	47.54	0.12	F8IV-V	HIP
16 04 03.71	+25 15 17.4	078709	144287	7.10	0.771	46.56	0.89	45.01	0.79	G8+V	G03
16 04 56.79	+39 09 23.4	078775	144579	6.66	0.734	69.61	0.57	68.87	0.33	K0V	G03
16 06 29.60	+38 37 56.1	078913	144872	8.58	0.963	42.57	0.86	42.55	0.77	K3V	G03
16 09 42.79	−56 26 42.5	079190	144628	7.11	0.856	69.66	0.90	68.17	0.64	K1V	G06
16 10 24.31	+43 49 03.5	079248	145675	6.61	0.877	55.11	0.59	56.91	0.34	K0IV-V	G03
16 13 18.45	+13 31 36.9	079492	145958	6.68	0.764	41.05	1.58	42.40	1.12	G9V	G03
16 13 48.56	−57 34 13.8	079537	145417	7.53	0.815	72.75	0.82	72.01	0.68	K3V	G06
16 14 11.93	−31 39 49.1	079578	145825	6.55	0.646	45.73	0.95	46.40	0.62	G2V	G06
16 14 40.85	+33 51 31.0	079607	146361	5.23	0.599	46.11	0.98	47.44	1.22	G1IV-V	G03
16 15 37.27	−08 22 10.0	079672	146233	5.49	0.652	71.30	0.89	71.94	0.37	G2V	G03
16 24 01.29	−39 11 34.7	080337	147513	5.37	0.625	77.69	0.86	78.26	0.37	G1V	G06
16 24 19.81	−13 38 30.0	080366	147776	8.40	0.950	46.44	1.20	46.46	1.06	K3-V	G06
16 28 28.14	−70 05 03.8	080686	147584	4.90	0.555	82.61	0.57	82.53	0.52	F9V	G06
16 28 52.67	+18 24 50.6	080725	148653	6.98	0.848	51.20	1.49	50.87	0.80	K2V	G03
16 31 30.03	−39 00 44.2	080925	148704	7.24	0.858	40.60	1.75	40.77	2.01	K1V	G06
16 36 21.45	−02 19 28.5	081300	149661	5.77	0.827	102.27	0.85	102.55	0.40	K0V	G03
16 37 08.43	+00 15 15.6	081375	149806	7.09	0.828	49.63	0.92	49.18	0.62	K0V	G03
16 39 04.14	−58 15 29.5	081520	149612	7.01	0.616	46.13	0.91	44.54	0.54	G5V	G06
16 42 38.58	+68 06 07.8	081813	151541	7.56	0.769	41.15	0.57	39.97	0.45	K1V	HIP
16 52 58.80	−00 01 35.1	082588	152391	6.65	0.749	59.04	0.87	57.97	0.66	G8+V	G03
16 57 53.18	+47 22 00.1	083020	153557	7.76	0.980	55.71	1.21	54.63	0.61	K3V	G03

Continued on Next Page...

TABLE 2.1 – Continued

						Hipparcos		FvL07			
R.A. (J2000.0)	**Decl. (J2000.0)**	**HIP Name**	**HD Name**			π	σ_π	π	σ_π	**Spec Type**	**Ref**
(1)	**(2)**	**(3)**	**(4)**	V **(5)**	$B-V$ **(6)**	**(mas) (7)**	**(mas) (8)**	**(mas) (9)**	**(mas) (10)**	**(11)**	**(12)**
17 02 36.40	+47 04 54.8	083389	154345	6.76	0.728	55.37	0.55	53.80	0.32	G8V	HIP
17 04 27.84	−28 34 57.6	083541	154088	6.59	0.814	55.31	0.89	56.06	0.50	K0IV-V	G06
17 05 16.82	+00 42 09.2	083601	154417	6.00	0.578	49.06	0.89	48.39	0.40	F9V	G03
17 10 10.35	−60 43 43.6	083990	154577	7.38	0.889	73.07	0.91	73.41	0.70	K2.5V	G06
17 12 37.62	+18 21 04.3	084195	155712	7.95	0.941	48.69	1.03	47.70	0.93	K2.5V	G03
17 15 20.98	−26 36 10.2	084405	155885	4.33	0.855	167.08	1.07	168.54	0.54	K1.5V	G06
17 19 03.83	−46 38 10.4	084720	156274	5.47	0.764	113.81	1.36	113.61	0.69	M0V	HIP
17 20 39.57	+32 28 03.9	084862	157214	5.38	0.619	69.48	0.56	69.80	0.25	G0V	HIP
17 22 51.29	−02 23 17.4	085042	157347	6.28	0.680	51.39	0.85	51.22	0.40	G3V	G03
17 25 00.10	+67 18 24.1	085235	158633	6.44	0.759	78.14	0.51	78.11	0.30	K0V	HIP
17 30 16.43	+47 24 07.9	085653	159062	7.22	0.737	44.77	0.59	44.91	0.50	G9V	G03
17 30 23.80	−01 03 46.5	085667	158614	5.31	0.715	60.80	1.42	61.19	0.68	G8IV-V	HIP
17 32 00.99	+34 16 16.1	085810	159222	6.52	0.639	42.20	0.56	41.81	0.35	G1V	G03
17 34 59.59	+61 52 28.4	086036	160269	5.23	0.602	70.98	0.55	70.47	0.37	G0V	HIP
17 39 16.92	+03 33 18.9	086400	160346	6.53	0.959	93.36	1.25	90.91	0.67	K2.5V	G03
17 41 58.10	+72 09 24.9	086620	162004	5.81	0.530	44.80	1.94	43.36	0.51	G0V	HIP
17 43 15.64	+21 36 33.1	086722	161198	7.51	0.752	42.45	0.98	44.15	0.89	G9V	G03
17 44 08.70	−51 50 02.6	086796	160691	5.12	0.694	65.46	0.80	64.47	0.31	G3IV-V	G06
17 46 27.53	+27 43 14.4	086974	161797	3.42	0.750	119.05	0.62	120.33	0.16	G5IV	HIP
17 53 29.94	+21 19 31.1	087579	...	8.50	0.940	40.22	1.04	41.06	1.04	K2.5V	G03
18 02 30.86	+26 18 46.8	088348	164922	7.01	0.799	45.61	0.71	45.21	0.54	G9V	G03
18 05 27.29	+02 30 00.4	088601	165341	4.03	0.860	196.62	1.38	196.72	0.83	K0-V	G03
18 05 37.46	+04 39 25.8	088622	165401	6.80	0.610	41.00	0.88	41.82	0.59	G0V	G03
18 06 23.72	−36 01 11.2	088694	165185	5.94	0.615	57.58	0.77	56.97	0.48	G0V	G06
18 07 01.54	+30 33 43.7	088745	165908	5.05	0.528	63.88	0.55	63.93	0.34	F7V	HIP

Continued on Next Page...

TABLE 2.1 – Continued

R.A. (J2000.0) (1)	Decl. (J2000.0) (2)	HIP Name (3)	HD Name (4)	V (5)	$B-V$ (6)	*Hipparcos* π (mas) (7)	*Hipparcos* σ_π (mas) (8)	FvL07 π (mas) (9)	FvL07 σ_π (mas) (10)	Spec Type (11)	Ref (12)
18 09 37.42	+38 27 28.0	088972	166620	6.38	0.876	90.11	0.54	90.71	0.30	K2V	G03
18 10 26.16	−62 00 07.9	089042	165499	5.47	0.592	56.32	0.68	56.78	0.52	G0V	G06
18 15 32.46	+45 12 33.5	089474	168009	6.30	0.641	44.08	0.51	43.82	0.29	G1V	G03
18 19 40.13	−63 53 11.6	089805	167425	6.17	0.584	43.64	0.72	43.39	0.39	F9.5V	G06
18 31 18.96	−18 54 31.7	090790	170657	6.81	0.861	75.71	0.89	75.46	0.70	K2V	G06
18 38 53.40	−21 03 06.7	091438	172051	5.85	0.673	77.02	0.85	76.43	0.47	G6V	G06
18 40 54.88	+31 31 59.1	091605	...	8.54	0.865	41.88	1.59	42.48	1.11	K2.5V	G03
18 55 18.80	−37 29 54.1	092858	175073	7.98	0.857	41.84	1.19	41.31	0.98	K1V	G06
18 55 53.22	+23 33 23.9	092919	175742	8.16	0.910	46.64	1.03	46.74	0.85	K0V	HIP
18 57 01.61	+32 54 04.6	093017	176051	5.20	0.594	66.76	0.54	67.24	0.37	G0V	HIP
18 58 51.00	+30 10 50.3	093185	176377	6.80	0.606	42.68	0.64	41.94	0.47	G1V	G03
19 06 25.11	−37 03 48.4	093825	177474	4.23	0.523	55.89	1.94	57.79	0.75	F8V	G06
19 06 52.46	−37 48 38.4	093858	177565	6.15	0.705	58.24	0.91	58.98	0.47	G6V	G06
19 07 57.32	+16 51 12.2	093966	178428	6.08	0.705	47.72	0.77	46.66	0.48	G5IV-V	G03
19 12 05.03	+49 51 20.7	094336	179957	5.85	0.666	40.16	0.83	40.90	0.58	G3V	G03
19 12 11.36	+57 40 19.1	094346	180161	7.04	0.804	50.00	0.54	49.96	0.32	G8V	HIP
19 21 29.76	−34 59 00.6	095149	181321	6.48	0.628	47.95	1.28	53.10	1.41	G1V	G06
19 23 34.01	+33 13 19.1	095319	182488	6.37	0.804	64.54	0.60	63.45	0.35	G9+V	G03
19 24 58.20	+11 56 39.9	095447	182572	5.17	0.761	66.01	0.77	65.89	0.26	G8IVvar	HIP
19 31 07.97	+58 35 09.6	095995	184467	6.60	0.859	59.84	0.64	58.96	0.65	K2V	G03
19 32 06.70	−11 16 29.8	096085	183870	7.53	0.922	55.50	0.90	56.73	0.72	K2.5V	G06
19 32 21.59	+69 39 40.2	096100	185144	4.67	0.786	173.41	0.46	173.77	0.18	G9V	G03
19 33 25.55	+21 50 25.2	096183	184385	6.89	0.745	49.61	0.94	48.64	0.63	G8V	G03
19 35 55.61	+56 59 02.0	096395	185414	6.73	0.636	41.24	0.49	41.48	0.30	G0	HIP
19 41 48.95	+50 31 30.2	096895	186408	5.99	0.643	46.25	0.50	47.44	0.27	G1.5V	G03

Continued on Next Page...

TABLE 2.1 – Continued

R.A. (J2000.0) (1)	Decl. (J2000.0) (2)	HIP Name (3)	HD Name (4)	V (5)	$B-V$ (6)	*Hipparcos* π (mas) (7)	*Hipparcos* σ_π (mas) (8)	FvL07 π (mas) (9)	FvL07 σ_π (mas) (10)	Spec Type (11)	Ref (12)
19 45 33.53	+33 36 07.2	097222	186858	7.68	1.000	49.09	1.43	47.34	0.82	K3+V	G03
19 51 01.64	+10 24 56.6	097675	187691	5.12	0.563	51.57	0.77	52.11	0.29	F8V	HIP
19 59 47.34	−09 57 29.7	098416	189340	5.87	0.598	40.75	1.35	45.04	0.99	F9V	G03
20 00 43.71	+22 42 39.1	098505	189733	7.67	0.932	51.94	0.87	51.41	0.69	K2V	G03
20 02 34.16	+15 35 31.5	098677	190067	7.15	0.714	51.71	0.83	52.71	0.65	K0V	G03
20 03 37.41	+29 53 48.5	098767	190360	5.73	0.749	62.92	0.62	63.06	0.34	G7IV-V	G03
20 03 52.13	+23 20 26.5	098792	190404	7.28	0.815	64.17	0.85	63.43	0.57	K1V	G03
20 04 06.22	+17 04 12.6	098819	190406	5.80	0.600	56.60	0.76	56.28	0.35	G0V	G03
20 04 10.05	+25 47 24.8	098828	190470	7.82	0.924	46.28	0.91	45.56	0.77	K2.5V	G03
20 05 09.78	+38 28 42.4	098921	190771	6.18	0.654	52.99	0.55	53.22	0.36	G2V	G03
20 05 32.76	−67 19 15.2	098959	189567	6.07	0.648	56.45	0.74	56.41	0.44	G2V	G06
20 07 35.09	−55 00 57.6	099137	190422	6.26	0.530	43.08	0.79	42.68	0.45	F9V	G06
20 08 43.61	−66 10 55.4	099240	190248	3.55	0.751	163.73	0.65	163.71	0.17	G8IV	G06
20 09 34.30	+16 48 20.8	099316	191499	7.56	0.810	41.07	1.18	42.26	0.99	G9V	G03
20 11 06.07	+16 11 16.8	099452	191785	7.34	0.830	48.83	0.91	49.04	0.65	K0V	G03
20 11 11.94	−36 06 04.4	099461	191408	5.32	0.868	165.24	0.90	166.25	0.27	K2.5V	G06
20 13 59.85	−00 52 00.8	099711	192263	7.79	0.938	50.27	1.13	51.77	0.78	K2.5V	G03
20 15 17.39	−27 01 58.7	099825	192310	5.73	0.878	113.33	0.89	112.22	0.30	K2+V	G06
20 17 31.33	+66 51 13.3	100017	193664	5.91	0.602	56.92	0.52	56.92	0.24	G0V	G03
20 27 44.24	−30 52 04.2	100925	194640	6.61	0.724	51.50	0.82	51.22	0.54	G8V	G06
20 32 23.70	−09 51 12.2	101345	195564	5.66	0.689	41.26	0.87	40.98	0.33	G2V	G03
20 32 51.64	+41 53 54.5	101382	195987	7.08	0.796	44.99	0.64	45.35	0.43	G9V	G03
20 40 02.64	−60 32 56.0	101983	196378	5.11	0.544	41.33	0.73	40.55	0.27	G0V	G06
20 40 11.76	−23 46 25.9	101997	196761	6.36	0.719	68.28	0.82	69.53	0.40	G8V	G06
20 40 45.14	+19 56 07.9	102040	197076	6.43	0.611	47.65	0.76	47.74	0.48	G1V	G03

Continued on Next Page...

TABLE 2.1 – Continued

R.A. (J2000.0) (1)	Decl. (J2000.0) (2)	HIP Name (3)	HD Name (4)	V (5)	$B-V$ (6)	*Hipparcos* π (mas) (7)	*Hipparcos* σ_π (mas) (8)	FvL07 π (mas) (9)	FvL07 σ_π (mas) (10)	Spec Type (11)	Ref (12)
20 43 16.00	−29 25 26.1	102264	197214	6.95	0.671	44.57	0.87	44.83	0.91	G6V	G06
20 49 16.23	+32 17 05.2	102766	198425	8.25	0.939	42.23	0.98	41.58	0.83	K2.5V	G03
20 56 47.33	−26 17 47.0	103389	199260	5.70	0.507	47.61	0.95	45.52	0.38	F6V	G06
20 57 40.07	−44 07 45.7	103458	199288	6.52	0.587	46.26	0.81	45.17	0.46	G2V	G06
21 02 40.76	+45 53 05.2	103859	200560	7.69	0.970	51.65	0.72	51.36	0.63	K2.5V	G03
21 07 10.38	−13 55 22.6	104239	200968	7.12	0.901	56.67	1.18	56.90	0.60	G9.5V	G06
21 09 20.74	−82 01 38.1	104436	199509	6.98	0.619	41.28	0.58	41.95	0.37	G1V	G06
21 09 22.45	−73 10 22.7	104440	200525	5.67	0.590	53.38	2.18	50.59	1.52	F9.5V	G06
21 14 28.82	+10 00 25.1	104858	202275	4.47	0.529	54.11	0.85	54.09	0.66	F7V	G03
21 18 02.97	+00 09 41.7	105152	202751	8.15	0.990	52.03	1.23	50.46	1.03	K3V	G03
21 18 27.27	−43 20 04.7	105184	202628	6.75	0.637	42.04	0.90	40.95	0.46	G1.5V	G06
21 19 45.62	−26 21 10.4	105312	202940	6.56	0.737	53.40	1.09	55.65	0.62	G7V	G06
21 24 40.64	−68 13 40.2	105712	203244	6.98	0.723	48.86	0.81	48.97	0.68	G8V	G06
21 26 58.45	−56 07 30.9	105905	203850	8.65	0.924	43.12	1.17	43.47	1.01	K2.5V	G06
21 27 01.33	−44 48 30.9	105911	203985	7.49	0.876	42.52	1.29	42.54	1.32	K2III-IV	G06
21 36 41.24	−50 50 43.4	106696	205390	7.14	0.879	67.85	0.92	68.40	0.58	K1.5V	G06
21 40 29.77	−74 04 27.4	107022	205536	7.07	0.755	45.17	0.67	45.41	0.52	G9V	G06
21 44 08.58	+28 44 33.5	107310	206826	4.49	0.512	44.64	0.69	44.97	0.43	F6V	G03
21 44 31.33	+14 46 19.0	107350	206860	5.96	0.587	54.37	0.85	55.91	0.45	G0IV-V	G03
21 48 00.05	−40 15 21.9	107625	207144	8.62	0.960	42.12	1.06	42.20	0.93	K3V	G06
21 48 15.75	−47 18 13.0	107649	207129	5.57	0.601	63.95	0.78	62.52	0.35	G0V	G06
21 53 05.35	+20 55 49.9	108028	208038	8.18	0.937	41.71	0.98	43.40	0.75	K2.5V	G03
21 54 45.04	+32 19 42.9	108156	208313	7.73	0.911	49.21	0.93	50.11	0.80	K2V	G03
22 09 29.87	−07 32 55.1	109378	210277	6.54	0.773	46.97	0.79	46.38	0.48	G8V	G03
22 11 11.91	+36 15 22.8	109527	210667	7.23	0.812	44.57	0.79	43.67	0.53	G9V	G03

Continued on Next Page...

TABLE 2.1 – Continued

R.A. (J2000.0) (1)	Decl. (J2000.0) (2)	HIP Name (3)	HD Name (4)	V (5)	$B-V$ (6)	*Hipparcos* π (mas) (7)	*Hipparcos* σ_π (mas) (8)	FvL07 π (mas) (9)	FvL07 σ_π (mas) (10)	Spec Type (11)	Ref (12)
22 14 38.65	−41 22 54.0	109821	210918	6.23	0.648	45.19	0.71	45.35	0.37	G2V	G06
22 15 54.14	+54 40 22.4	109926	211472	7.50	0.810	46.62	0.67	46.43	0.50	K0V	G03
22 18 15.62	−53 37 37.5	110109	211415	5.36	0.614	73.47	0.70	72.54	0.36	G0V	G06
22 24 56.39	−57 47 50.7	110649	212330	5.31	0.665	48.81	0.61	48.63	0.34	G2IV-V	G06
22 25 51.16	−75 00 56.5	110712	212168	6.12	0.599	43.39	0.96	43.39	0.50	G0V	G06
22 39 50.77	+04 06 58.0	111888	214683	8.48	0.938	44.10	1.12	41.49	0.76	K3V	G03
22 42 36.88	−47 12 38.9	112117	214953	5.99	0.584	42.47	0.72	42.31	0.40	F9.5V	G06
22 43 21.30	−06 24 03.0	112190	215152	8.11	0.966	46.46	1.31	46.47	0.90	K3V	G03
22 46 41.58	+12 10 22.4	112447	215648	4.20	0.502	61.54	0.77	61.36	0.19	F7V	HIP
22 47 31.87	+83 41 49.3	112527	216520	7.53	0.867	50.15	0.64	50.83	0.44	K0V	G03
22 51 26.36	+13 58 11.9	112870	216259	8.29	0.849	47.56	1.18	46.99	1.01	K2.5V	G03
22 57 27.98	+20 46 07.8	113357	217014	5.45	0.666	65.10	0.76	64.07	0.38	G3V	G03
22 58 15.54	−02 23 43.4	113421	217107	6.17	0.744	50.71	0.75	50.36	0.38	G8IV-V	G03
23 03 04.98	+20 55 06.9	113829	217813	6.65	0.620	41.19	0.87	40.46	0.57	G1V	G03
23 10 50.08	+45 30 44.2	114456	218868	6.98	0.750	42.65	0.74	41.15	0.54	G8V	G03
23 13 16.98	+57 10 06.1	114622	219134	5.57	1.000	153.24	0.65	152.76	0.29	K3V	G03
23 16 18.16	+30 40 12.8	114886	219538	8.07	0.871	41.33	0.97	41.63	0.72	K2V	G03
23 16 42.30	+53 12 48.5	114924	219623	5.58	0.556	49.31	0.58	48.77	0.26	F7V	HIP
23 16 57.69	−62 00 04.3	114948	219482	5.64	0.521	48.60	0.60	48.69	0.33	F6V	G06
23 19 26.63	+79 00 12.7	115147	220140	7.53	0.893	50.65	0.64	52.07	0.47	K2V	G03
23 21 36.51	+44 05 52.4	115331	220182	7.36	0.801	45.63	0.83	46.46	0.53	G9V	G03
23 23 04.89	−10 45 51.3	115445	220339	7.80	0.881	51.37	1.25	52.29	0.86	K2.5V	G03
23 31 22.21	+59 09 55.9	116085	221354	6.76	0.839	59.31	0.67	59.06	0.45	K0V	G03
23 35 25.61	+31 09 40.7	116416	221851	7.90	0.845	42.63	0.93	42.00	0.72	K1V	G03
23 37 58.49	+46 11 58.0	116613	222143	6.58	0.665	43.26	0.80	42.86	0.42	G3V	G03

Continued on Next Page...

TABLE 2.1 – Continued

						Hipparcos		FvL07			
R.A. (J2000.0) **(1)**	**Decl. (J2000.0)** **(2)**	**HIP Name** **(3)**	**HD Name** **(4)**	V **(5)**	$B-V$ **(6)**	π **(mas)** **(7)**	σ_π **(mas)** **(8)**	π **(mas)** **(9)**	σ_π **(mas)** **(10)**	**Spec Type** **(11)**	**Ref** **(12)**
23 39 37.39	−72 43 19.8	116745	222237	7.09	0.989	87.72	0.64	87.56	0.51	K3+V	G06
23 39 51.31	−32 44 36.3	116763	222335	7.18	0.802	53.52	0.86	53.85	0.63	G9.5V	G06
23 39 57.04	+05 37 34.6	116771	222368	4.13	0.507	72.51	0.88	72.92	0.15	F7V	HIP
23 52 25.32	+75 32 40.5	117712	223778	6.36	0.977	92.68	0.55	91.82	0.30	K3V	G03
23 56 10.67	−39 03 08.4	118008	224228	8.24	0.973	45.28	1.11	45.52	0.93	K2.5V	G06
23 58 06.82	+50 26 51.6	118162	224465	6.72	0.694	41.35	0.76	40.77	0.49	G4V	G03

NOTES.—Column 12 lists the source of the spectral types and has the following values: G03=Gray et al. (2003), G06=Gray et al. (2006), HIP=The *Hipparcos* catalog.

[a] The parallax is from Söderhjelm (1999).

Table 2.2 lists the 24 stars that were left out of the sample because their parallax error was greater than 5% of the corresponding parallax value. All columns have the same meaning as Table 2.1. Only four of these stars have a parallax larger than 40 mas to a 3-σ significance, and these were also left out of the sample so as to only include "good-quality" parallax measures from *Hipparcos*. Table 2.3 lists the 15 stars excluded from the final sample due to a large offset from the best-fit main sequence, i.e. being over 2 magnitudes above or 1.5 magnitudes below it. Columns 1–8 have the same meaning as in Table 2.1, Column 9 lists the derived absolute V magnitude from the apparent magnitude and parallax, and Column 10 lists the absolute magnitude of the best-fit main sequence corresponding to the $B-V$ color of the star.

TABLE 2.2: Stars Excluded Due to Large Parallax Errors ($\sigma_\pi/\pi \geq 0.05$)

						Hipparcos	
R.A. (J2000.0)	**Decl. (J2000.0)**	**HIP Name**	**HD Name**	V	$B-V$	π **(mas)**	σ_π **(mas)**
00 22 23.61	−27 01 57.3	001768	001815	8.30	0.888	44.57	7.12
01 49 23.36	−10 42 12.8	008486	011131	6.72	0.654	43.47	4.48
02 15 42.55	+67 40 20.2	010531	013579	7.13	0.920	42.46	2.51
02 57 14.71	−24 58 10.2	013772	018455	7.33	0.863	44.49	2.55
03 47 02.12	+41 25 38.2	017666	023439	7.67	0.796	40.83	2.24
04 29 44.87	−29 01 37.4	020968	...	11.42	0.646	120.70	56.47
04 30 12.58	+05 17 55.8	021000	...	9.83	0.600	84.76	4.74
05 44 56.79	+09 14 31.5	027111	247168	11.35	0.699	44.67	14.98
07 03 58.92	−43 36 40.8	034069	053706	6.83	0.779	66.29	6.81
08 35 51.27	+06 37 22.0	042173	072946	7.25	0.710	42.71	4.61
10 04 50.59	−31 05 28.0	049376	...	11.99	0.938	41.59	3.13
12 29 55.04	+36 26 42.1	060970	...	11.91	0.800	43.42	3.62
12 31 18.92	+55 07 07.7	061100	109011	8.08	0.941	42.13	3.11
12 59 18.98	+06 30 33.7	063383	...	10.69	0.515	45.19	44.19

Continued on Next Page...

TABLE 2.2 – Continued

R.A. (J2000.0)	**Decl. (J2000.0)**	**HIP Name**	**HD Name**	V	$B-V$	***Hipparcos*** π **(mas)**	σ_π **(mas)**
13 33 18.71	−77 34 24.6	066125	...	9.31	0.914	52.09	39.91
15 31 54.05	+09 39 26.9	076051	...	9.80	0.787	44.59	20.41
15 38 39.95	−08 47 41.0	076602	139460	6.56	0.520	44.21	4.72
15 38 40.08	−08 47 29.4	076603	139461	6.45	0.505	40.19	3.62
16 19 31.52	−30 54 06.7	079979	146835	7.29	0.585	56.82	23.38
22 06 11.82	+10 05 28.7	109119	...	10.20	0.668	93.81	66.11
22 12 59.72	−47 23 11.1	109670	...	11.48	0.660	44.20	16.43
22 26 34.28	−16 44 31.7	110778	212697	5.55	0.618	49.80	2.54
23 01 51.54	−03 50 55.4	113718	217580	7.48	0.943	59.04	3.40
23 44 07.36	−27 11 45.8	117081	222834	9.01	0.535	58.45	47.16

TABLE 2.3: Stars Excluded Due to Large Offset from the Main Sequence

R.A. (J2000.0)	**Decl. (J2000.0)**	**HIP Name**	**HD Name**	V	$B-V$	***Hipparcos*** π **(mas)**	***Hipparcos*** σ_π **(mas)**	M_V	**MS** M_V
00 49 09.90	+05 23 19.0	003829	...	12.37	0.554	226.95	5.35	14.15	4.21
01 55 57.47	−51 36 32.0	009007	011937	3.69	0.844	57.19	0.62	2.48	5.72
03 43 14.90	−09 45 48.2	017378	023249	3.52	0.915	110.58	0.88	3.74	6.08
05 16 41.36	+45 59 52.8	024608	034029	0.08	0.795	77.29	0.89	−0.48	5.48
07 34 27.43	+62 56 29.4	036834	...	10.40	0.942	87.01	2.17	10.10	6.22
07 42 57.10	−45 10 23.2	037606	062644	5.04	0.765	41.43	0.81	3.13	5.33
07 45 18.95	+28 01 34.3	037826	062509	1.16	0.991	96.74	0.87	1.09	6.47
16 41 17.16	+31 36 09.8	081693	150680	2.81	0.650	92.63	0.60	2.64	4.73
18 21 18.60	−02 53 55.8	089962	168723	3.23	0.941	52.81	0.75	1.84	6.22
19 55 18.79	+06 24 24.4	098036	188512	3.71	0.855	72.95	0.83	3.03	5.78
19 55 50.36	−26 17 58.2	098066	188376	4.70	0.748	42.03	0.94	2.82	5.24
20 06 21.77	+35 58 20.9	099031	191026	5.38	0.850	41.34	0.54	3.46	5.75
20 45 17.38	+61 50 19.6	102422	198149	3.41	0.912	69.73	0.49	2.63	6.07
21 58 24.52	+75 35 20.6	108467	...	10.56	0.742	47.95	1.08	8.96	5.21
23 19 06.67	−13 27 30.8	115126	219834	5.20	0.787	40.28[a]	1.51[a]	3.23	5.44

[a] The parallax is from Söderhjelm (1999).

2.1.2 Comparison with DM91 Sample

In order to minimize selection effects, DM91 chose a volume-limited sample out to 22 pc based on (Gliese 1969) parallaxes. The *Hipparcos* mission, whose results were published well after the DM91 effort, greatly improved the accuracy and completeness of parallaxes. As pointed out by Halbwachs et al. (2003), the Gliese (1969) data becomes increasingly incomplete for parallaxes below 53 mas, and I will show that a sample selected using DM91's criteria from *Hipparcos* is significantly different than their sample.

As described in § 1.3.2, the DM91 volume-limited sample of solar-type stars included 164 primaries. Selecting an equivalent sample, subject to the same criteria but from the *Hipparcos* catalog, results in the selection of 148 primaries, but only 92 of these overlap with the DM91 sample. This indicates that 72 (44%) of the DM91 sample is now known to lie outside their selection criteria, and 56 (38%) of the stars meeting their criteria are not included in their sample. Figure 2.5 plots the 164 stars of the DM91 sample (circles) based on their *Hipparcos* parallax and $B - V$ color. The filled circles represent stars that still match their selection criteria based on the *Hipparcos* data, while the open circles identify stars that are now known to violate their criteria.

Figure 2.5 illustrates several points: (i) As expected, the density of stars in the plot drops off with proximity due to the cubed relation of volume to distance. I will use this in § 2.1.4 to test the completeness of the current sample. (ii) Many stars included by DM91 based on Gliese parallaxes are now known to reside beyond their distance limit of 22 pc. In fact, the updated *Hipparcos* parallaxes alone account for as many as 68 of the 72 stars

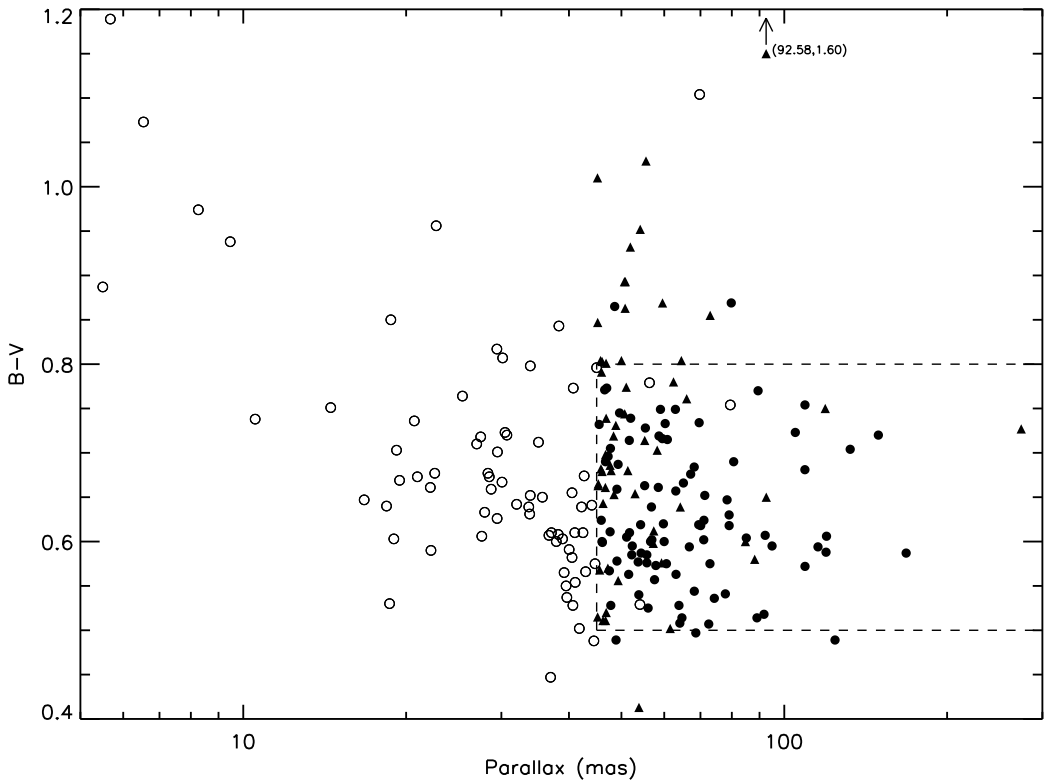

FIGURE 2.5: The DM91 multiplicity survey sample and the sample selected according to their criteria from the *Hipparcos* catalog are plotted against *Hipparcos* parallaxes and $B-V$ colors. Filled circles represent DM91 sample stars that still match their criteria based on the *Hipparcos* data while open circles identify DM91 sample stars that no longer fit their criteria. Filled triangles represent stars that were not part of the DM91 sample but meet their criteria based on *Hipparcos* data. The vertical dashed line marks the parallax limit of 45 mas of the DM91 study, and the horizontal dashed lines mark $B-V$ colors of 0.5 and 0.8, which roughly correspond to the DM91 spectral-type limits of F7–G9.

in the DM91 sample that no longer fit their criteria. Most of these distant stars (five have *Hipparcos* parallaxes of less than 10 mas) are likely to be evolved stars. (iii) The *Hipparcos* data indicates that the DM91 sample was fairly incomplete, as evidenced by the number of filled triangles inside the DM91 criteria "window" outlined by the dashed lines, the vertical line corresponding to a parallax of 45 mas and the horizontal lines to $B-V$

color limits of 0.5 and 0.8, which roughly correspond to the DM91 spectral-type limits of F7–G9 (Cox 2000). The filled triangles represent the 56 stars that were not part of the DM91 sample but consistent with their criteria. One outlier (HIP 84123) is not included in the figure because its very red $B-V$ color of 1.6 is beyond the plot's range, but consistent with its spectral type of M3V (Gray et al. 2006). It was however selected as matching the DM91 criteria because of an erroneous *Hipparcos* spectral type of G. (iv) Most of the stars lying outside the DM91 criteria window due to their color are red rather than blue, i.e. there are many more points above the window than below. Furthermore, most of these outliers were not part of the DM91 sample, but their *Hipparcos* spectral types indicate G-dwarfs, which appears incorrect based on their colors. This might be suggestive of the fact that a sample selection based on spectral types in these catalogs may be error-prone. The current sample selection is based on the *Hipparcos* $B-V$ color, and we will compare these colors to recent independent assessment of their spectral types in § 2.1.4 to check the quality of the *Hipparcos* colors.

We have thus seen that there are substantial differences between the samples selected according to DM91 criteria from Gliese (1969) and *Hipparcos*. The key question, however, is whether these differences introduce biases that would taint their results. One such aspect explored by Halbwachs et al. (2003) was whether the incompleteness of the CNS catalog at farther distances implied that fainter stars were less studied hence not fully represented in the catalog. If this were true, there would be a bias towards binaries due to a similar reasoning as the Malmquist bias, i.e. single stars would be included to a smaller volume of

space than binaries. However, Halbwachs et al. (2003) showed that the samples of stars from CNS and *Hipparcos* have similar distributions around the main sequence, arguing against any magnitude bias.

My thesis effort attempts to verify whether the DM91 results were biased due to this sampling difference and obtain updated multiplicity statistics based on a larger sample chosen using the more accurate *Hipparcos* catalog. It also leverages current studies on stellar and substellar companions to solar-type stars, enabling the exploration of a key aspect of my motivation, namely, the correlations between stellar and substellar companions to solar-type stars. While no substellar companions were confirmed before the DM91 effort, well over 300 such companions have been published to-date, offering a wealth of observational results to conduct this analysis. Figure 2.6 plots the thesis sample of 454 primaries based on their *Hipparcos* parallax and $B - V$ color.

2.1.3 A New Reduction of the *Hipparcos* Data

van Leeuwen (2007a) recently published the results of a new reduction of the *Hipparcos* raw data based on an improved model of the satellite attitude, yielding improved astrometry but making no updates to the photometry. A more recent update was posted online[1] (van Leeuwen 2007b, hereafter FvL07), which corrected some errors relating to the goodness of fit calculation in the original work. While these results came well after my sample construction and bulk of the observational work, I discuss below their possible effects on the multiplicity statistics derived in this work. Selecting the thesis sample using the FvL07 results yields 459

[1] $http://webviz.u-strasbg.fr/viz-bin/VizieR-3$

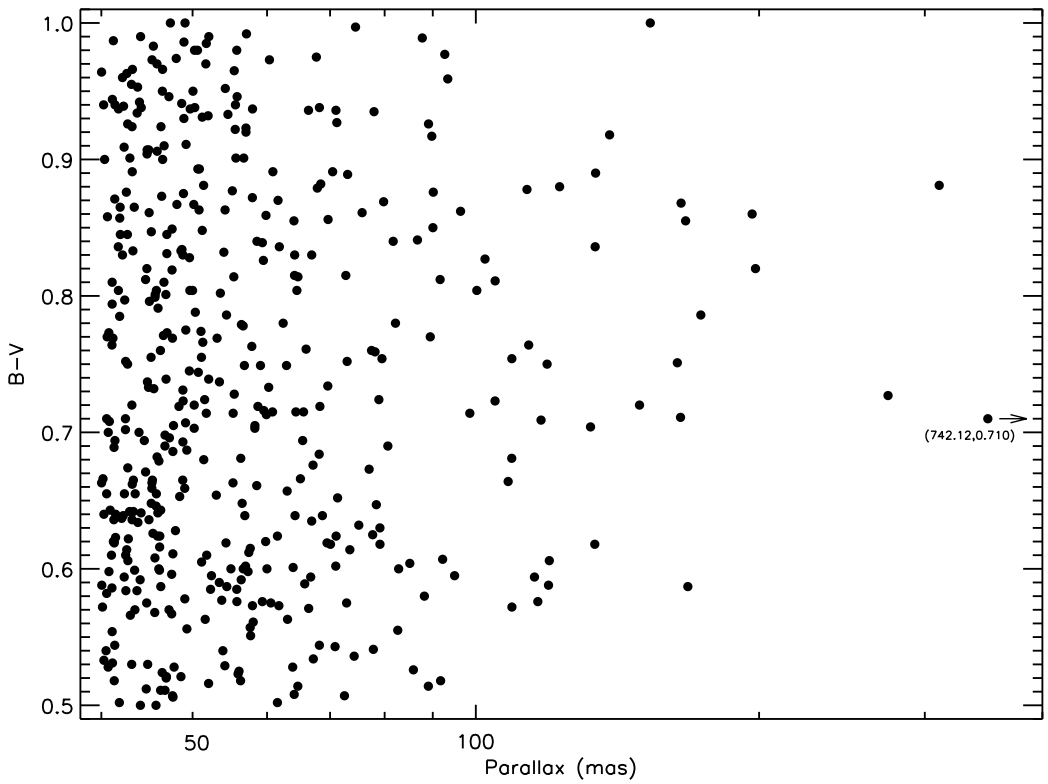

FIGURE 2.6: The current sample plotted along the same axes as Figure 2.5

stars compared to the 462 selected from *Hipparcos*. Both these samples include the same nine stars that are removed from the sample of primaries because they are companions to other primary stars in the sample. Thus, the final sample of stars selected from FvL07 would contain 451 primary stars including the Sun, compared to the *Hipparcos*-based sample of 454 stars. The total number of stars in both samples is almost the same, and a check of specific stars reveals the 15 new stars that would have been included, and the 18 stars that would have been left out if the sample were selected using FvL07data. Tables 2.4 and 2.5 list these specific stars with the individual reasons for exclusion or inclusion. Compared to the sample size, these differences are small, and most of them are due to small changes

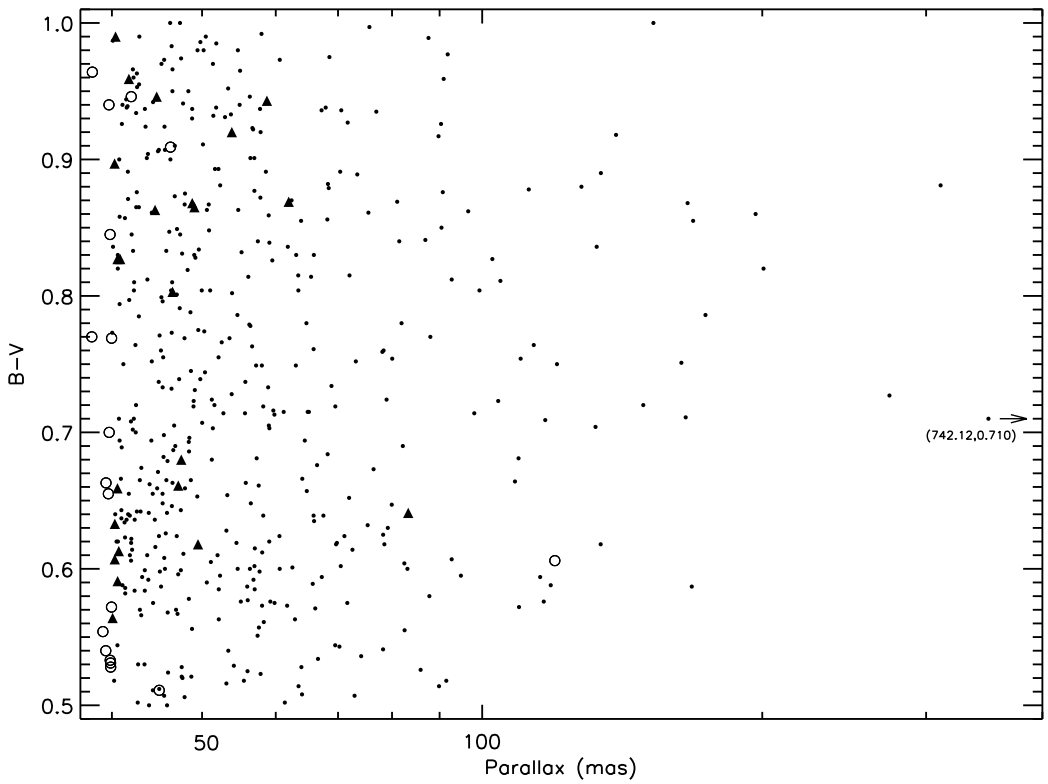

FIGURE 2.7: The current sample plotted using the updated FvL07 parallaxes. Solid circles identify stars of the current sample that qualify selection using FvL07, open circles identify the ones which do not qualify selection using the updated data, and filled triangles are stars not in the current sample but match the criteria based on the FvL07 data. The size of the solid circles have been suppressed to enable easier spotting of the other symbols. Tables 2.4 and 2.5 detail these two sets of stars.

in the parallax value near the 40 mas limit. Accordingly, while the updated work presents improved astrometry which will be used in the determination of orbital parameters and mass determinations, they are not expected to have a significant impact on the derived multiplicity statistics. Figure 2.7 compares the *Hipparcos* and FvL07 samples by parallax and color, and Figure 2.8 shows these stars on a color-magnitude diagram, demonstrating that the two samples are largely consistent for statistical analyses. One star included in the

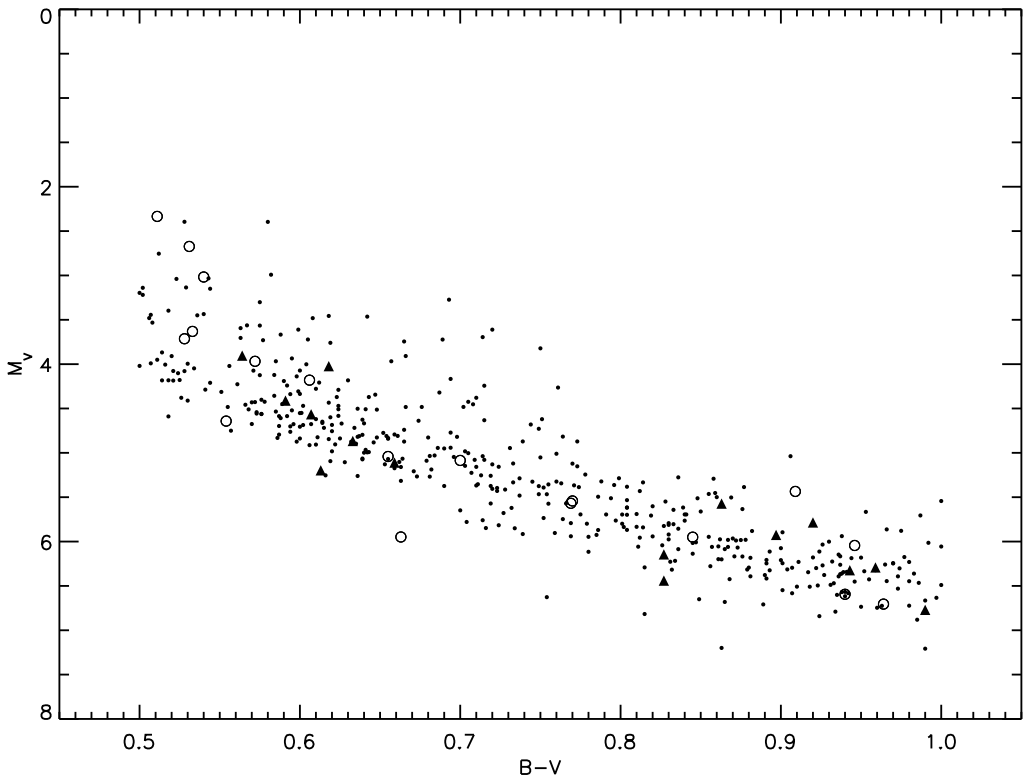

FIGURE 2.8: Color-Magnitude diagram for the current sample using *Hipparcos* and FvL07 data. Symbols have the same meaning as in Figure 2.7.

thesis sample, HIP 55203, was selected based on Söderhjelm (1999) parallax but does not exist in *Hipparcos* or FvL07 catalogs and hence is plotted in the figure using its Söderhjelm (1999) parallax.

TABLE 2.4: Stars excluded from sample, but qualifying in FvL07 data

HIP		***Hipparcos***		**FvL07**		**Reason for**
Name	$B-V$	π **(mas)**	σ_π **(mas)**	π **(mas)**	σ_π **(mas)**	**Exclusion**
003170	0.564	39.26	0.56	40.07	0.34	1
010531	0.920	42.46	2.51	53.82	1.74	2
013388	0.827	38.45	0.90	40.83	0.74	1
013772	0.863	44.49	2.55	44.51	2.09	2

Continued on Next Page...

TABLE 2.4 – Continued

HIP Name	$B-V$	*Hipparcos* π (mas)	*Hipparcos* σ_π (mas)	FvL07 π (mas)	FvL07 σ_π (mas)	Reason for Exclusion
017336	0.659	38.75	0.99	40.55	1.11	1
021223	0.990	39.93	0.93	40.36	0.78	1
030862	0.613	38.98	0.90	40.69	0.62	1
034950	0.827	39.72	1.29	40.56	0.90	1
035872	0.959	39.91	1.14	41.72	0.86	1
042418	0.897	39.28	1.21	40.27	1.14	1
060994	0.591	39.6[a]	0.9[a]	40.57	0.60	3
088945	0.633	39.62	0.68	40.29	0.49	1
110778	0.618	49.80	2.54	49.50	1.23	2
113718	0.943	59.04	3.40	58.70	0.92	2
114378	0.607	38.67	0.83	40.28	0.53	1

NOTES.—Column 7 notes: (1) = *Hipparcos* parallax less than the 40 mas threshold, (2) = *Hipparcos* parallax error greater than the 5% threshold, (3) = Parallax from Söderhjelm (1999) less than the 40 mas threshold.

[a] The parallax is from Söderhjelm (1999).

TABLE 2.5: Sample stars outside selection criteria based on FvL07 data

HIP Name	$B-V$	*Hipparcos* π (mas)	*Hipparcos* σ_π (mas)	FvL07 π (mas)	FvL07 σ_π (mas)	Reason for Exclusion
007372	0.909	42.29	1.47	46.24	3.07	1
015442	0.655	40.52	0.98	39.65	0.74	2
017147	0.554	41.07	0.86	39.12	0.56	2
024786	0.572	40.11	0.76	39.96	0.40	2
026373	0.845	41.90	1.74	39.82	1.36	2
032423	0.964	40.02	1.22	38.11	1.01	2
034567	0.700	40.68	1.02	39.73	0.54	2
040167	0.531	39.11	1.38	39.87	0.82	2
051933	0.528	40.67	0.68	39.88	0.37	2
054155	0.770	40.57	1.40	38.06	0.99	2
055203	0.606	119.70[a]	0.80[a]	...	...	3

Continued on Next Page...

TABLE 2.5 – Continued

HIP Name	$B-V$	*Hipparcos* π (mas)	*Hipparcos* σ_π (mas)	FvL07 π (mas)	FvL07 σ_π (mas)	Reason for Exclusion
062505	0.946	47.19	1.93	41.96	3.00	1
063406	0.940	41.36	1.48	39.71	1.00	2
067655	0.663	40.02	1.00	39.42	0.97	2
069701	0.511	46.74	0.87	44.97	0.19	4
073100	0.533	40.25	0.54	39.83	0.26	2
074975	0.540	40.46	0.81	39.40	0.29	2
081813	0.769	41.15	0.57	39.97	0.45	2

NOTES.—Column 7 notes: (1) = FvL07 parallax error greater than the 5% threshold, (2) = FvL07 parallax less than the 40 mas threshold, (3) = Not in *Hipparcos* or FvL07 catalogs. Selected based on Söderhjelm (1999) parallax, (4) = More than 2 magnitudes above FvL07 main-sequence.

[a] The parallax is from Söderhjelm (1999).

2.1.4 Sample Analysis & Bias

The targets for this survey were selected as a distance-limited sample from the *Hipparcos* catalog to minimize selection effects. In this section, I analyze the sample based on parallax, magnitude, color, and spectral type as a way of of determining the sample completeness and discussing any remaining biases. Söderhjelm (2000) analyzed the completeness of the *Hipparcos* catalog based on brightness and presented V magnitude limits based on the $V-I$ color and galactic latitude. These relations indicate that the catalog is complete to $V \sim 9$ for solar-type stars with galactic latitudes of at least 40°and to $V \sim 8.2$ for all latitudes. Figure 2.9 shows the distribution of apparent (solid) and absolute (dashed) V magnitudes of the sample. The largest apparent V magnitude is 9.05 and only 30 of the 454 stars have

$V > 8.2$, indicating that the sample is fairly complete. As an additional check, Figure 2.10 shows the sample's distance distribution along with a curve representing the theoretical cubed-dependence of the number of stars in a given volume of space based on distance, using the number of stars within 11 pc as the reference (dotted line). The actual distribution of stars closely follows the expected curve out to the distance-limit of 25 pc, improving the confidence in the completeness of the sample.

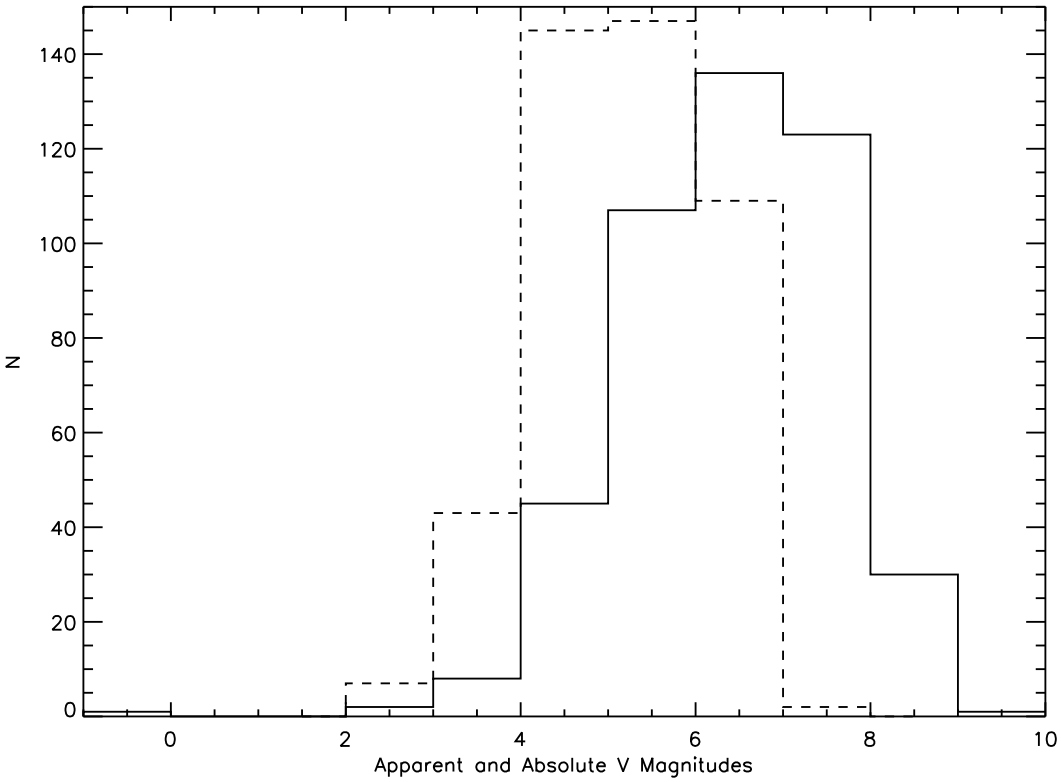

FIGURE 2.9: Apparent magnitude (solid line) and absolute magnitude (dashed line) distributions of the sample.

Unlike DM91's sample selection based on spectral type, I used the *Hipparcos* $B-V$ color. Figure 2.11 shows the color-distribution of the sample, indicating a peak around $B-V = 0.6$,

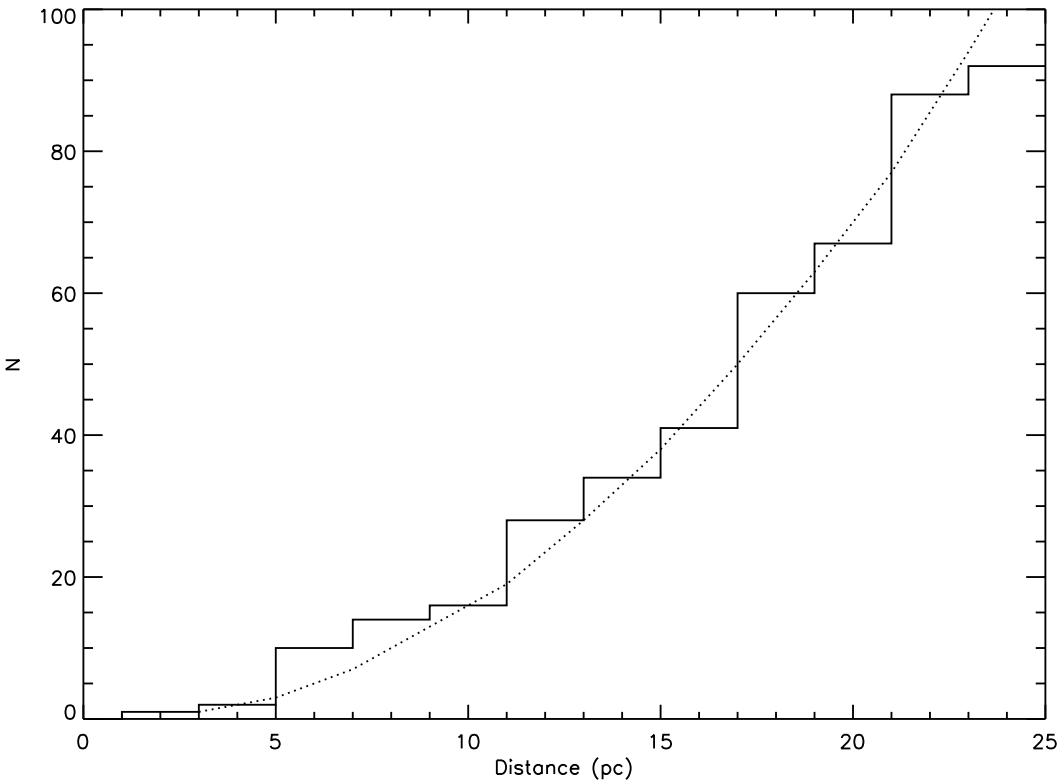

FIGURE 2.10: Distance Distribution of the Sample. The dotted line represents the theoretical distribution of the number of stars in a given volume of space, based on its cubed relation to distance. The number of sample stars within 11 pc is used as the reference for this curve.

just blueward of the Sun with a tapering distribution out to the limit of 1.0. In contrast, Figure 2.12 shows a double-peaked distribution with a strong peak at K2 and a smaller peak at G0. To further analyze this, Figure 2.13 shows the correlation between color and spectral type. While the figure indicates a fairly good correlation between these parameters, the range of colors for many spectral types is quite broad. These figures suggest that while color is determined directly from photometric measurements, spectral identifications are more complex and involve the interpretation of spectral lines, which may not always be easy. The

difficulty in identifying certain spectral types is likely responsible for the low counts for the mid-G stars and a high count for K2.

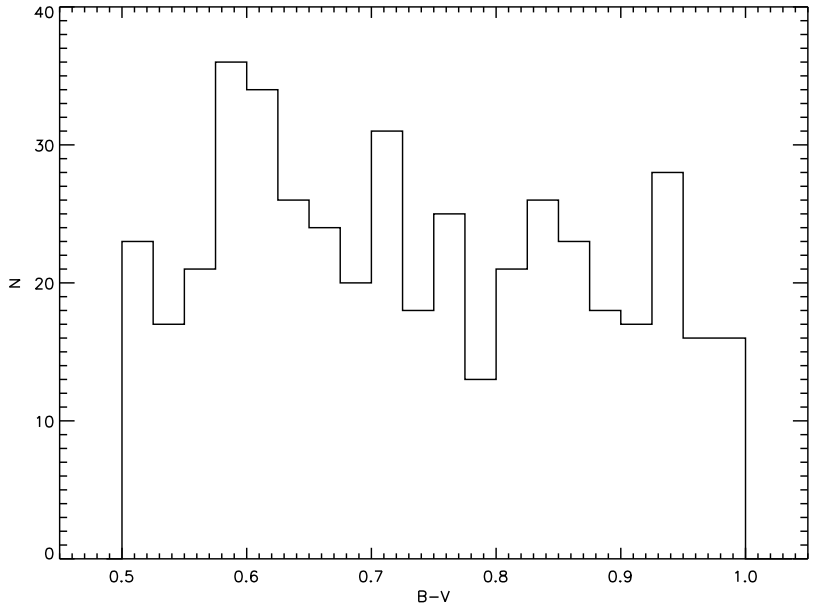

FIGURE 2.11: $B - V$ Color Distribution of the Sample.

2.2 Survey Methods

The primary observational efforts of this work include a survey for Separated Fringe Packet (SFP) companions using long baseline interferometry (LBI) at the Center for High Angular Resolution Astronomy (CHARA) Array, a search for wide CPM companions by blinking multi-epoch archival images, follow-up photometry for the candidates thus revealed, and speckle interferometric observations to achieve a near 100% completion using this technique. The CHARA Array was also used to develop visual orbits for select short-period spectroscopic binaries. The results of the LBI efforts are covered in Chapter 3. The search for wide CPM

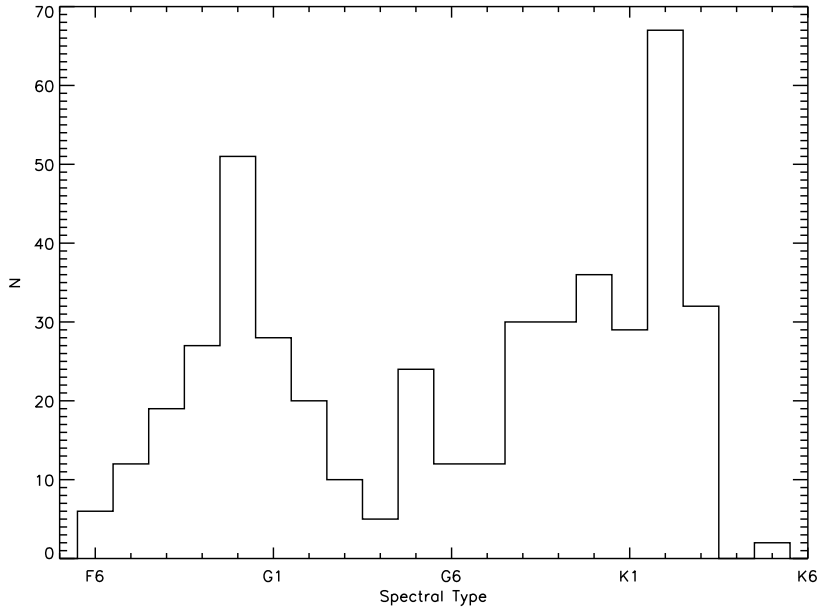

FIGURE 2.12: Spectral type distribution of the sample.

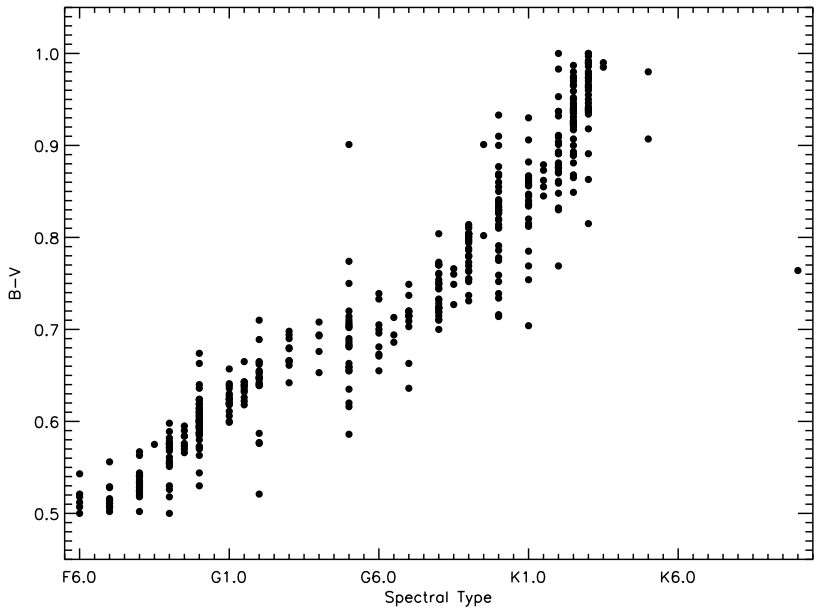

FIGURE 2.13: Correlation between spectral type and color for the sample of stars.

companions and the follow-up photometry are discussed in Chapter 4, which also covers the

evaluation of entries in the Washington Double Star Catalog[2] (WDS) as CPM pairs or chance alignments of optical pairs.

Apart from the targeted observations, this survey benefits from the tremendous amount of attention these nearby solar-type stars have garnered over the years. A comprehensive synthesis effort brings together information about previously known and suspected companions, which are evaluated individually. Chapter 5 addresses astrometric companions discovered by the *Hipparcos* mission, the resolved-pair and photocentric-motion visual binaries cataloged in the Sixth Catalog of Orbits of Visual Binary Stars[3] (VB6), visual resolutions cataloged in the WDS and the Fourth Catalog of Interferometric Measurements of Binary Stars[4] (FIC), and the CPM as well as spectroscopic binaries listed in the Catalogs of Nearby Stars (Gliese 1969; Gliese & Jahreiß 1979, 1991, hereafter CNS). Finally, Chapter 6 covers the spectroscopic companions from publications as well as from the unpublished data made available to this effort. This chapter also mentions the few eclipsing binaries in the sample of stars of this study.

[2] *http* : *//ad.usno.navy.mil/wds/*
[3] *http* : *//ad.usno.navy.mil/wds/orb*6.*html*
[4] *http* : *//ad.usno.navy.mil/wds/int*4.*html*

If it was easy, someone would have already done it!

—— Harold A. McAlister

– 3 –

Long-Baseline Interferometric Results

The primary observing method of this thesis effort aims to leverage the high resolving power of interferometers, especially the world's longest baselines for optical and near-infrared interferometry of the CHARA Array. A brief overview of the technique and instrument is outlined below. For a more complete description, see ten Brummelaar et al. (2005).

Ever since the days of William Herschel, visual observers have continually been in pursuit of better angular resolution. For single-aperture techniques, the resolution limit or Rayleigh Criterion (θ) depends on the wavelength of light collected (λ) and the aperture of the telescope (D), and is given, in radians, by $\theta = 1.22\,\lambda/D$, which corresponds to the situation when the first diffraction minimum of one source coincides with the maximum of another. The actual resolution of observations can, at best, equal the above limit, but is often worse due to atmospheric and instrumental effects. Techniques such as AO and speckle interferometry have been successfully used to mitigate astrometric effects and approach the resolution limit. The pursuit of even higher resolutions has led to the use of innovative techniques such as Long-Baseline Interferometry (LBI), which involve the simultaneous observation of a target with two or more telescopes. By leveraging multiple telescopes, this technique effectively uses the distance between the telescopes, or *baseline*, in place of aperture in the above relationship to get far better resolutions than the single telescopes for resolved stellar disks (see Michelson 1890, 1920). Further, Michelson also showed that unresolved point sources

could be detected at a resolving power of 2.4 times the above value. This resolution of an interferometer is related to the wavelength (λ) and baseline (B) as

$$\theta_{\rm int} = \lambda/2B \tag{3.1}$$

Let us look at the above in a bit more detail. From Chapter 3 of Lawson (2000), the intensity of an image after diffraction though a circular aperture of diameter D for a wavelength λ is given by

$$I_{\rm tel}(\theta) = \left[\frac{2J_1(\pi\theta D/\lambda)}{\pi\theta D/\lambda}\right]^2 D^2, \tag{3.2}$$

where J_1 is the first-order Bessel function and θ, the independent variable, is the angle from the peak intensity in the center. This intensity function is plotted in Figure 3.1 as the solid outer envelope. The condition corresponding to the Rayleigh Criterion is when the peak of one source coincides with the first zero of another, and this corresponds to $\theta_{\rm tel} = 1.22\lambda/D$ as seen in the figure. Now, when we use two apertures of diameter D, separated by a distance B, the resultant intensity function for an interferometer becomes (Lawson 2000)

$$I_{\rm int}(\theta) = 2I_{\rm tel}(\theta)\left[1 + \cos(2\pi\theta B/\lambda)\right] \tag{3.3}$$

Figure 3.1 also plots this function for $B = 3D$ as the narrow-inner fringe envelope. Similar to the discussion above, the resolution of an interferometer is considered to be the first zero of this function, which corresponds to $\theta_{\rm int} = \lambda/2B$ or $\theta_{\rm int} = \lambda/6D$ as seen in the figure.

While long baseline interferometers can, in general, use any number of telescopes greater than one, this effort used only two-telescope interferometry, and so the discussion here will be limited to this situation. In order to obtain interferometric fringes, light wavefronts from the

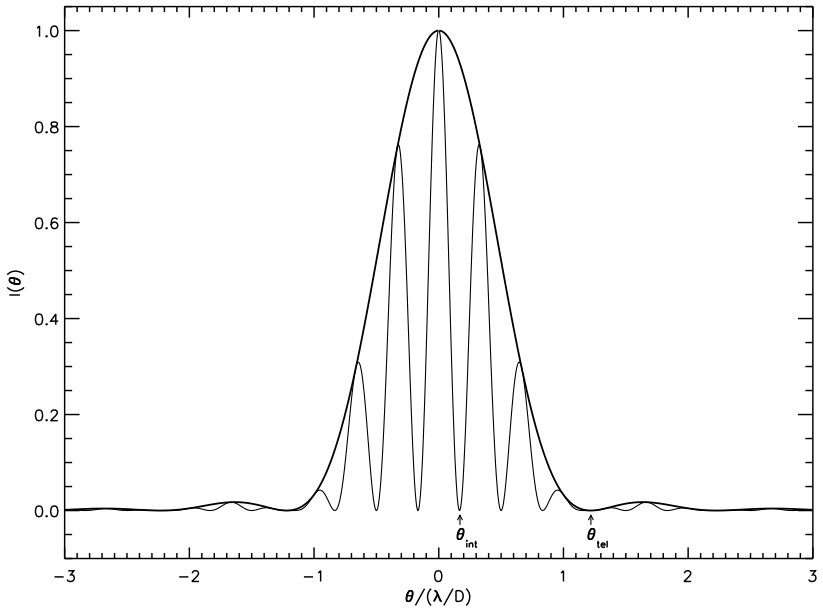

FIGURE 3.1: Intensity of the diffraction patterns from single and two-telescope images. The broad, thick envelope represents a single-telescope diffraction pattern and the narrow fringes are for a two-telescope setup with $B = 3D$. The single aperture and interferometer resolution limits are marked.

two telescopes must be combined, or allowed to interfere. One aspect that makes this difficult is the fact that while the difference in distance from the star to the two telescopes is negligible when compared to the distance to either telescope, it is not zero. Hence, a wavefront from the star reaches one telescope a bit sooner than it does the other. Interferometers are designed to compensate for this delay to sub-micron precision to generate the fringe. A simple pictorial depiction of this is shown in Figure 3.2. CHARA uses a two-stage delay compensation method including Pipes of Pan (POP) mirrors which offer one of five fixed delays for each telescope between 0 and 143 meters in roughly 37-meter increments, and Optical Path-Length Equalizer (OPLE) carts that run on 46-m rails to compensate for the delay in real-time to a precision of about 10-nm (ten Brummelaar et al. 2005). Because the

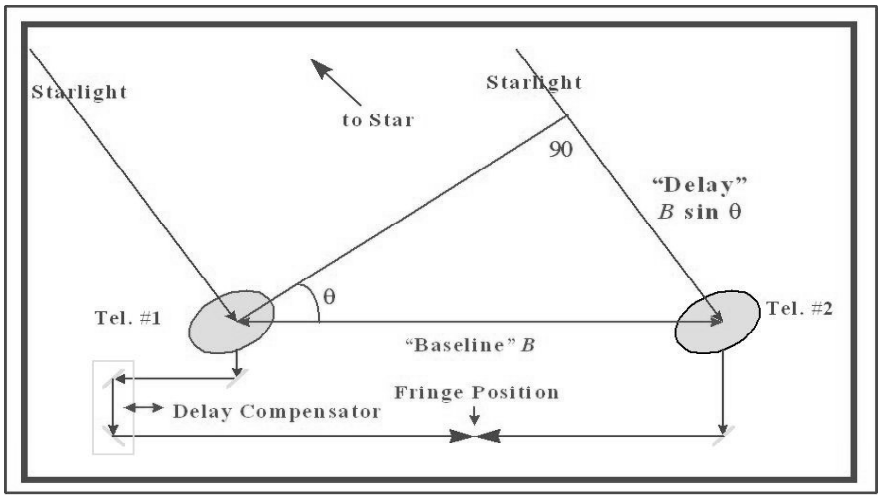

FIGURE 3.2: Schematic of a basic interferometer showing the delay compensation (diagram by H. McAlister).

target star is rising or setting during an observation, its differential distance to the telescopes changes constantly, and the carts move actively during an observation to keep up with this change.

The final step in generating interference fringes is combining the delay-compensated beams from the two telescopes. The beam combiner used in this effort, CHARA Classic, is a pupil-plane interferometer, which passes the light from the two telescopes through the two sides of a half-reflecting and half-transmitting piece of glass to enable interference, producing two beams with the interference pattern, one obtained by combining the reflected light from one telescope and the transmitted light from the other, and the other with the transmitted light from the first telescope and the reflected light from the second. This technique of beam combination is referred to as a *Michelson* interferometer because it uses the same method as used by Michelson in 1893 to demonstrate that the speed of light is independent of the observer's motion. When a fringe is found and tracked, the observations need to record a

sampling of the fringe pattern over a range of delay space around the peak of the fringe. This is accomplished by an oscillating mirror (Dither mirror) that changes the path length of the light from one telescope with respect to the other over a range of roughly 80 microns for "short-scan" mode to 160 microns for "long-scan" sample at a velocity of about 0.3 $\mathrm{mm\,s^{-1}}$. Figure 3.3 shows a picture of the CHARA Classic beam combination setup, with captions and lines representing the light beams added for clarity. For the Classic setup, the two telescope beams are sent along beams 5 and 6 of the six-telescope arrangement, and as seen in the figure, beam 5 is reflected off the Dither mirror before combination. Fringe data are then recorded from both the interferences (B5R+B6T and B5T+B6R) at a sampling rate of 250 Hz, 500 Hz, 750 Hz, or 1000 Hz, which is typically 5 times the fringe frequency to adequately sample each fringe and is observer-selected based on seeing conditions. In the above notations, "T" stands for transmitted light, and "R" for reflected light.

Using Equation (3.1), observations at the K' band of 2.15 microns with the longest CHARA baseline of 330 meters have a resolution of 0.7 mas. However, the definition of the first zero corresponding to the resolution is somewhat arbitrary, and simulations show resolution capabilities down to about 0.4 mas for binaries (H. McAlister 2008, private communication). These resolutions are valuable for resolving short-period double-lined spectroscopic pairs, and for periods less than about 10 days, the Array's longest baselines are uniquely suited. This technique has been utilized to resolve some short-period binaries as discussed in § 3.2. First, § 3.1 below covers the survey effort in the search for new companions at wider separations (10–120 mas) using the Separated Fringe Packet (SFP) approach.

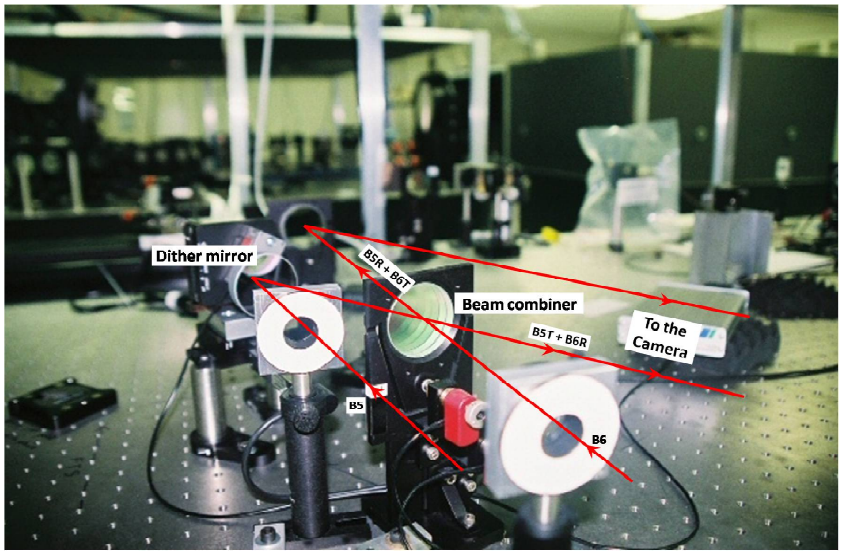

FIGURE 3.3: A picture of the beam combining equipment at CHARA Classic. Captions and lines representing light beams have been added for clarity. B5 and B6 represent light from the two telescopes, which are sent along beams 5 and 6 of a six-telescope arrangement, and the interference pattern emerging from both sides of the beam combiner are labeled with suffixes R and T representing reflected and transmitted light, respectively.

3.1 Survey of Separated Fringe Packet Binaries

A hypothesis tested by this survey effort via SFP analysis is whether this technique, leveraging the long baselines of the CHARA Array, can address a gap in binary separations between spectroscopic techniques and traditional visual methods. While spectroscopic efforts are suited to short-period systems, typically from hours to a few dozen years, visual techniques are ideal for more widely separated systems with orbital periods of many-tens to thousands of years. Speckle interferometry using 4-m class telescopes routinely resolve binaries with separations down to 30 mas (Horch et al. 2008; Mason et al. 2009a) and AO can resolve high Δmag binaries to sub-arcsec separations (e.g., Tokovinin et al. 2006; Turner

et al. 2008). However, as seen above, LBI allows us to probe closer-in on visual binaries. While the resolution limits of LBI described in the preceding section are for *overlapping* fringe envelopes separated at least by θ_{int} in Figure 3.1, wider binaries may have spatially *separated* fringe packets that fit within the delay-space scanning window. This technique was first demonstrated as a viable means of studying binary stars by Dyck et al. (1995) and later used with the CHARA Array to derive a precise orbit and component masses for 12 Persei (Bagnuolo et al. 2006).

While SFP studies of binary stars are an effective way of characterizing orbits and the component stars, they are especially suited to searching a large list of stars for new companions. In contrast to Calibrated Interferometric Visibility (CIV) measurements (more on this in § 3.2), SFP analysis can identify a companion with just a single observation and can confirm the absence of a companion within detection limits with just two observations taken over a short time gap, one each along orthogonal baselines. The CHARA Array can detect SFPs for binaries with separations of 10–120 mas (Bagnuolo et al. 2006) and is sensitive to $\Delta K' \leq 2.5$. Figure 3.4 shows some theoretical examples of separated fringes for various separations and intensity ratios.

Targets for the SFP survey were selected from the *Hipparcos* sample of 462 stars (including 9 companions), based on the magnitude and declination limits of CHARA. Specifically, the Array can reach targets north of a declination of -10° and has magnitude limits of $V \leq 9$ for tip-tilt tracking of the target and $K' \leq 6$ for fringe recording in moderate seeing conditions. These criteria selected 288 of the 462 targets, 92 of which were being observed by

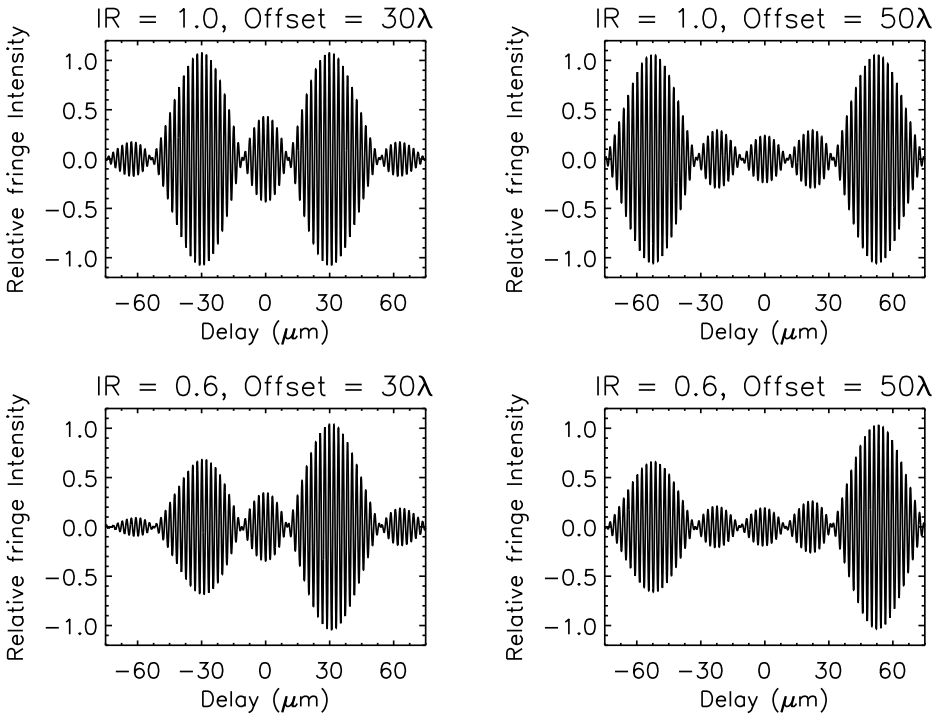

FIGURE 3.4: Examples of theoretical separated fringe packets for different values of intensity ratios (IR above the figures) and separations (offsets above the figures in units of wavelength).

Chris Farrington as part of his Ph.D. effort (Farrington 2008) with the same instrument and technique, leaving me with 196 targets. The observations for this survey were carried out between 2007 January and 2008 July. Following the loss of allocated time in the Fall of 2006 due to camera issues at the Array, make-up time was assigned during 2007 January–March, the normal maintenance time due to unfavorable weather conditions on Mount Wilson, as a shared pool to various survey projects of Georgia State University (GSU) graduate students, enabling about 20 nights of data-gathering. Additionally, the equivalent of approximately 60 nights were awarded in total to this survey during the observing seasons of 2007 April–August, 2007 September–December, and 2008 April–August, allowing for the completion of a majority of the survey. The individual observing nights along with some notes regarding

observing conditions are included in Table 3.1. All but 12 (6%) of the 196 targets have so far been observed at least once, and 161 (82%) have been observed on orthogonal baselines and are hence considered done.

3.1.1 SFP Data Reduction and Results

The CHARA Classic observing software was changed to generate FITS files beginning 2008, before which, text files in a proprietary format were generated. The reduction code for 2007 data used a text file output containing some header information and three arrays for each observation. Each array entry represents an interpolated sampling of the readout to correspond to a frequency of 1000 Hz. So, for every millisecond, the arrays record the dither mirror position offset and the intensity of the light of the interference pattern on each side of the beam combiner as shown in Figure 3.3. The FITS files generated since 2008 contain similar information, but in a more standard form, and with an added array containing the time offset for every sampling interval. This is required because the data captured now corresponds to the actual sampling rate rather than an interpolated fixed rate. Also, the FITS files parse the data into two-dimensional arrays with the each row representing a particular scan of delay space, i.e. the motion of the Dither mirror from one end to the other, and the columns corresponding to the sampling step within the scan. The observing software records data until 200 good Signal-to-Noise Ratio (SNR) scans, as described below, are recorded, so a typical data packet contains over 200 scans.

TABLE 3.1: Observing Nights for the SFP survey

UT Date (1)	Share (2)	Observer (3)	Data Sets Recorded Total (4)	Data Sets Recorded SFP (5)	Baseline(s) (6)	Comment (7)
2007-01: April–August 2007						
04/10/2007	H	DR	...	...	...	High winds
04/11/2007	H	DR	16	4	S1(1)-E1(5)	Poor, variable seeing early
04/12/2007	H	DR	...	...	...	High winds
04/13/2007	H	DR	...	...	...	High winds
04/14/2007	H	DR	27	17	S1(1)-E1(5)	Worked well mostly!
04/15/2007	H	DR	...	...	...	Clouds
04/16/2007	H	DR	...	...	...	Clouds
04/17/2007	H	PJ	17	11	S1(1)-W1(5)	Variable seeing
04/18/2007	H	PJ	...	...	...	High RH, terrible seeing
04/19/2007	H	PJ	...	...	...	Wind, Dust, Ash
04/20/2007	H	PJ	...	...	...	Clouds
04/21/2007	H	CF	...	...	...	Clouds
04/22/2007	H	CF	...	...	...	Clouds, Rain, Snow
04/23/2007	H	CF	...	...	...	Clouds
04/24/2007	H	DR	14	12	S1(1)-W1(5)	Variable seeing
04/25/2007	H	DR	...	...	...	Network issues
04/26/2007	H	DR	25	8	E1(5)-W1(5)	Variable seeing
05/16/2007	F	DR	3	3	E1(1)-S1(1)	Many issues, little data
05/17/2007	F	DR	36	9	E1(1)-S1(1)	11 brackets + 9 SFP
05/27/2007	H	CF	26	...	E2(4)-S1(1)	6 brackets of HD 146361
05/28/2007	H	CF	23	8	W1(5)-S1(1)	Clear & nice!
05/29/2007	H	PJ	26	3	E2(4)-S1(1)	Includes 6 brackets of HD 146361
05/30/2007	H	DR	19	7	W1(1)-S1(1)	Good weather
05/31/2007	H	DR	10	6	W1(1)-S1(1)	Windy, some dust, bright moon, jet stream?
06/01/2007	H	DR	23	10	W1(5)-S1(2); E2(1)-S1(2)	Light cloud cover
07/22/2007	H	CF	26	12	W1(1)-S1(5); S1(5)-E1(1)	Calm, cool
07/23/2007	H	CF	1	...	...	Clouds all night, drizzle later
07/24/2007	H	PJ	27	16	S1(5)-E1(1); S1(5)-W1(1)	Partly cloudy, variable seeing
07/25/2007	H	DR	8	3	S1(1)-E1(1)	Many technical issues
07/26/2007	H	DR	18	9	S1(1)-E1(5); W1(5)-S1(1)	Many Tip-Tilt issues
07/27/2007	H	DR	8	1	S1(1)-E1(4)	Delayed start due to MIRC offsets
07/28/2007	H	DR	16	7	S1(1)-E1(4)	Thin, high clouds, poor to moderate seeing
07/29/2007	H	DR	16	3	S1(1)-E1(1)	Includes 6 brackets of HD 146361
08/14/2007	F	DR	25	22	S1(1)-E1(1); W1(1)-S1(1)	Few hours spent on ToO Nova Vul 07
08/15/2007	F	DR	14	6	S1(5)-E1(1)	Few hours spent on ToO Nova Vul 07
08/16/2007	F	DR	17	9	S1(5)-E1(1); S1(5)-W1(1)	Clear but hazy, steady stream of particulates
08/17/2007	F	DR	3	2	W1(5)-S1(5)	Little data due to time on ToO & smoke later
08/18/2007	F	DR	19	19	W1(5)-S1(5); S1(5)-E1(5)	Clear & nice!
08/19/2007	H	CF	4	...	...	Smoke, Haze, Clouds later
08/20/2007	H	CF	21	13	S2(2)-E1(5)	Clear & nice!
08/21/2007	H	PJ	22	5	W1(4)-S1(2)	Spent some time on ToO Nova Vul 07
2007-02: September–December 2007						
09/16/2007	F	CF	26	26	W1(5)-S1(1); S1(1)-E1(5)	Clear & nice!
09/17/2007	F	CF	23	23	W1(5)-S2(5)	Cool & dry, light winds
09/18/2007	F	PJ	12	12	E2(5)-S2(5)	Clear
09/24/2007	F	CF	...	...	...	Fog, Clouds, High RH
09/25/2007	F	NT	...	...	...	MIRC offsets and E1 metrology issues
09/26/2007	F	TB	9	9	S2(1)-E2(1)	Late start due to weather & technical issues
09/27/2007	F	NT	13	13	E2(1)-S2(1)	Mostly clear, passing clouds
10/31/2007	F	DR	22	22	S1(5)-E1(5), S1(5)-W1(5)	High RH early, CA fires subsided, no smoke
11/01/2007	F	DR	24	21	E2(1)-W1(5); S1(5)-E1(5); S1(5)-W1(5)	Spent some time on ToO Comet Holmes
11/18/2007	Q	DR	64	...	E2(4)-S2(1)	Very smooth, observed Yamina & Ellyn's targets
11/22/2007	Q	PJ	7	...	E2(4)-S2(1)	Clear
11/24/2007	Q	YT	...	...	E2(4)-S2(1)	High winds, Malibu fire restarts!

Continued on Next Page...

TABLE 3.1 – Continued

UT Date (1)	Share (2)	Observer (3)	Data Sets Recorded Total (4)	Data Sets Recorded SFP (5)	Baseline(s) (6)	Comment (7)
11/25/2007	Q	DR	...	...	E2(4)-S2(1)	Power outage on the mountain!
11/26/2007	Q	EB	...	...	E2(4)-S2(1)	Power issues and bad weather
11/27/2007	Q	EB	25	4	E2(4)-S2(1)	Cloudy in the latter part of the night
11/28/2007	Q	TB	...	...	E2(4)-S2(1)	Clouds
11/29/2007	Q	TB	25	6	E2(4)-S2(1)	Clouds for half the night
11/30/2007	F	PJ	...	...	...	Clouds
12/01/2007	F	DR	...	...	...	Clouds
12/02/2007	F	DR	...	...	...	High humidity
2008-01: April–August 2008						
04/12/2008	F	DR	21	21	S1(1)-W1(1); S1(1)-E1(1)	Clear & nice
04/13/2008	F	DR	32	32	S1(1)-E1(1); S1(1)-W1(1)	Clear & nice
04/14/2008	F	DR	26	26	S1(5)-E1(1); S1(5)-W1(1)	Clear & nice
04/15/2008	F	DR	8	8	S1(5)-W1(1); S1(5)-E1(1)	E1 light pipe vignetting
04/24/2008	F	DR	...	...	S1(5)-E1(1)	High RH, then windy & dusty
04/25/2008	F	DR	21	21	S1(5)-E1(1)	Hard to find/keep fringes for half the night
04/26/2008	F	DR	21	21	S1(1)-W1(5)	Hard to find/keep fringes for half the night
04/27/2008	F	DR	...	...	...	Smoke at the base of the mountain
06/21/2008	F	DR	4	4	S1(5)-E1(1)	Too dusty in the first half-night
06/22/2008	F	DR	23	10	S1(5)-W1(1); S1(5)-S2(5)	Clear, windy, dusty
06/23/2008	F	DR	25	10	S1(5)-E1(1); S1(5)-S2(5)	Clear, windy
06/24/2008	F	DR	19	14	S2(1)-W1(5)	Clear
06/25/2008	F	DR	14	11	S1(1)-E1(5); S1(1)-S2(1)	Clear & nice
06/26/2008	F	PJ	35	2	S1(1)-S2(1)	Hazy, high thin clouds
07/05/2008	F	DR	4	4	S1(5)-E1(1)	Dust & ash
07/06/2008	F	DR	52	6	S1(5)-E1(1); S1(5)-S2(5)	Nice night
07/07/2008	F	DR	47	15	S1(5)-W1(1); S1(5)-S2(5)	Nice night
07/08/2008	F	DR	8	8	S1(5)-W1(3)	VPN issues throughout the night
07/09/2008	F	DR	3	3	S1(1)-E1(5)	Clouds & dust!
07/26/2008	F	DR	...	...	...	OPLE issues all night
07/27/2008	F	DR	57	3	S1(5)-W1(1); S1(5)-S2(5)	Clear & nice

NOTES.—Column 2 denotes the fraction of the night allocated to the SFP survey: F = Full night, H = Half-night, Q = Quarter-night. Column 3 observer codes are: CF = C. Farrington, DR = D. Raghavan, EB = E. Baines, NT = N. Turner, PJ = PJ Goldfinger, TB = T. Boyajian, YT = Y. Touhami. Counts in Column 5 are data files obtained for this survey and are sometimes less than Column 4 values because some data was obtained for CIV work or for other observers. Column 6 contains the baseline(s) used during the night. The numbers within the brackets are the POP setting for the telescopes.

The reduction process involves using the shutter sequences to subtract dark noise and balance the beams from each telescope, combining the beams from both sides of the beam combiner after normalization, then taking a Fourier transform of the data to work in frequency domain. Next, "good" fringes are identified by comparing the integrated power in a bandwidth around the fringe frequency to the power off the fringe, and the qualifying scans are low-pass and band-pass filtered to reduce noise. Then, fringe envelopes are fitted to each fringe. The detection of a second separated fringe packet is enabled by three summary fringe envelope plots, described below, as well as a visual inspection of each fringe envelope. The Interactive Data Language (IDL) code written for this reduction process is included in § C.3. The three summary fringe envelope plots are – (1) a normalized shift-and-add plot which determines the shift by cross-correlating each fringe with a reference fringe. (2) a normalized sum of the autocorrelation of each fringe envelope, which produces a symmetric plot with a central peak, and when there is a separated fringe, a second peak on either side, and (3) a simple normalized shift-and-add plot by aligning the peaks of each fringe envelope. While all three plots serve the same purpose, i.e., to enable detection of a second fringe when present, they have some differences, and experience has shown it useful to inspect all three. For example, when two fringes are found, the third plot above is the best for follow-up astrometry as it best preserves the directional orientation of the fringes allowing for differential brightness assessments and elimination of the 180° ambiguity of the other methods. However, the simple shift-and-add plot is often better at noise cancellation of weak side-lobes that are not separate fringes, while the cross correlation plots tends to accentuate them. Figures 3.5

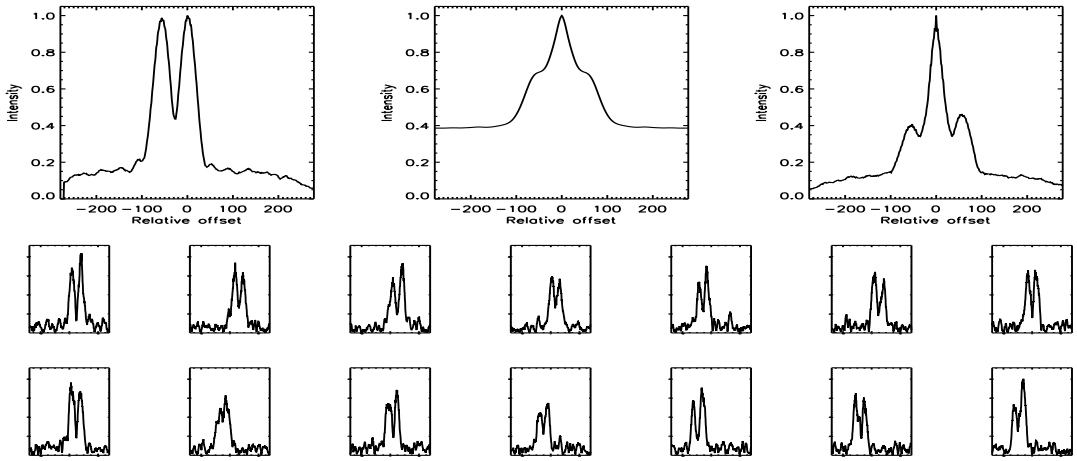

FIGURE 3.5: Example fringe envelopes for a separated fringe packet binary HD 79096. The observation was made on UT 20070309 on the S1-E1 baseline. The summary plots in the top panel from left to right are the cross-correlation shifted sum, the autocorrelation sum, and the peak-align shifted sum. The bottom panels shows the 14 strongest individual fringe envelopes as determined by the integrated power in a bandwidth around the fringe frequency when compared to off-fringe power. The X-axis of all plots is the relative offset in the dither mirror position as represented by the count of the sampling interval bin, the Y-axis is the relative intensity of the fringe envelope. While all plots clearly show the double fringe envelopes, and the top left plot is most effective at identifying the magnitude difference and resolving the 180° ambiguity of the companion's position angle.

and 3.6 show examples of the plot included in *Appendix* B for each target observed in this effort. Figure 3.5 is an example of a star with separated fringe packets and Figure 3.6 is an example of an apparently single star. The top three panels of the plots show the summary plots discussed above and the bottom panels shows the individual envelopes corresponding to the 14 strongest fringes as determined by the integrated power method described above.

Overall, this effort largely yielded null results, with only a few resolutions of known pairs and no new detections. Table 3.2 lists the results of the SFP data reduction for each observation and Table 3.3 identifies the status of each target on every baseline observed. Only three stars showed definitive evidence of separated fringes – HD 3196 on 5 observations

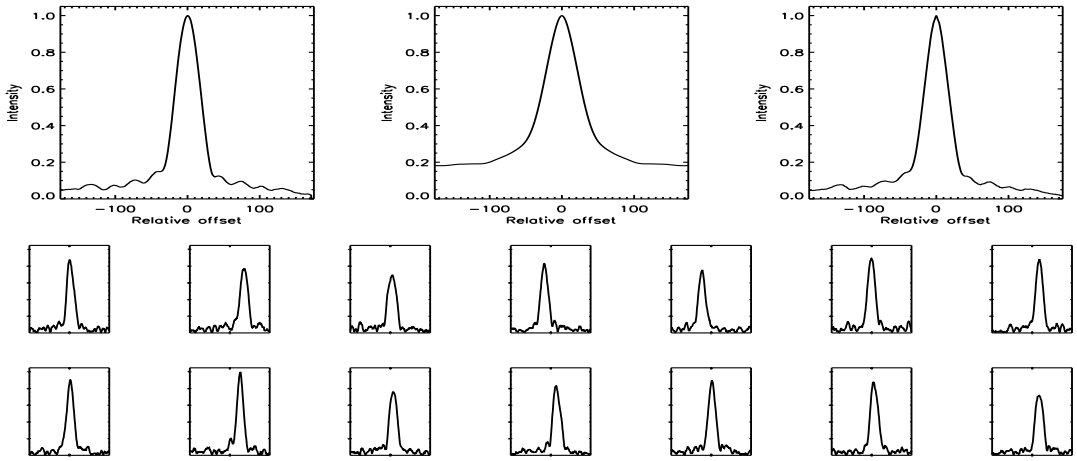

FIGURE 3.6: Example fringe envelopes for a single fringe packet star HD 1461 observed on UT 20080727 on the S1-W1 baseline, in the same format as Figure 3.5. These plots do not show any evidence of a separated fringe packet.

over two baselines, HD 79096 on 10 observations along the S-E baseline, three of which were too wide to fit in the scan window, and HD 137763 on three observations along S1-W1, two of which were too wide to fit in the scan window. All detections pertain to known binary systems (HD 3196 is a 6.9-year SB2VB, HD 79096 is a 2.6-year SB2VB, and HD 137763 is a 2.4-year SB2VB), so no new companions were discovered by this survey. Additionally, HD 98230 (ξ UMa) is a quadruple system with a wide 1.″6 separation pair, each component of which is a single-lined spectroscopic binary. Upon searching wide for fringes by moving the OPLE carts around the first fringe, the widely separated fringe was seen on several occasions, but they were always only a single fringe, indicating that the magnitude difference of a single-lined spectroscopic binary is perhaps too large for detection by the Array. Additionally, Bagnuolo et al. (2006) derived a visual orbit for HD 16739 (12 Per) using SFP detection at CHARA and C. Farrington detected SFPs for three more stars of this sample Farrington (2008) –

HD 4676 and 202275, which are known SB2VBs, and HD 131511, which is a known SB1 with a photocentric-motion orbit for which Farrington saw a second fringe on one of three observations (Figure B.24 in Farrington (2008)).

TABLE 3.2: SFP Observations and Results

HD Name	Obs UT Date	S	Baseline	Obs	Red	Date Reduced	S	Fringe Scans Good	Total	FF	⟨FW⟩	σ_{FW}	Reduction Notes
000166	07/29/2007	1	E1–S1	DR	DR	11/09/2007	S	200	200	102	18.4	11.1	...
000166	08/14/2007	1	E1–S1	DR	DR	11/09/2007	S	198	198	156	21.8	8.8	...
000166	08/14/2007	2	W1–S1	DR	DR	11/09/2007	S	181	198	156	3.5	2.1	Weaker fringes than on E1-S1
001461	09/17/2007	1	W1–S2	CF	DR	11/14/2007	D?	241	241	65	14.0	9.7	Prominent twin peak in many scans
001461	07/22/2008	1	E1–S1	TB	DR	07/24/2008	S	167	333	150	2.5	1.6	...
001461	07/27/2008	1	W1–S1	DR	DR	10/07/2008	S	202	202	150	29.4	13.1	High SNR
001562	08/16/2007	1	W1–S1	DR	DR	11/12/2007	S?	169	441	102	0.9	0.5	Low SNR, Weak, choppy FE; asymmetric SFE
001562	08/16/2007	2	E1–S1	DR	DR	11/12/2007	S?	208	327	102	1.3	0.6	Weak, choppy FE, double-peaked SFE
001562	07/08/2008	1	W1–S1	DR	DR	07/08/2008	S	125	346	100	2.0	1.1	...
001562	07/09/2008	1	E1–S1	DR	DR	07/20/2008	S	82	472	100	1.4	0.4	...
003196	08/14/2007	3	E1–S1	DR	DR	11/09/2007	D	198	198	156	14.8	7.3	...
003196	08/14/2007	4	W1–S1	DR	DR	11/09/2007	D	197	198	156	9.8	6.3	Reference scan at edge, causing ACOR plot to have two peaks
003196	09/17/2007	1	W1–S2	CF	DR	11/14/2007	D	201	205	102	11.7	6.1	...
003196	09/27/2007	1	E2–S2	NT	DR	11/14/2007	D	198	198	65	19.0	7.7	...
003196	07/07/2008	1	W1–S1	DR	DR	07/07/2008	D	200	200	150	23.6	12.3	Clear double fringes
003196	07/22/2008	1	E1–S1	TB	DR	07/24/2008	S	165	359	150	2.5	1.8	No evidence of companion on this observation!
003651	07/29/2007	1	E1–S1	DR	DR	11/09/2007	S	197	200	102	11.5	7.2	...
003651	08/14/2007	1	E1–S1	DR	DR	11/09/2007	S	198	198	156	19.1	9.7	...
003651	08/14/2007	2	W1–S1	DR	DR	11/09/2007	S	184	198	156	3.9	2.9	...
003765	08/16/2007	1	W1–S1	DR	DR	11/12/2007	S?	201	314	102	1.3	0.7	Choppy FE, double-peaked SFE
003765	08/16/2007	2	E1–S1	DR	DR	11/12/2007	S?	205	257	102	2.2	1.4	Choppy FE, asymmetric SFE
003765	07/08/2008	1	W1–S1	DR	DR	07/08/2008	S	143	340	150	2.1	1.3	...
003765	07/09/2008	1	E1–S1	DR	DR	07/20/2008	S	148	312	100	1.7	0.6	...
004256	08/14/2007	1	E1–S1	DR	DR	11/09/2007	S	179	198	156	2.5	1.3	...
004256	08/14/2007	2	W1–S1	DR	DR	11/09/2007	S	119	198	156	1.3	0.8	Poor SNR, choppy FE
004628	08/14/2007	1	E1–S1	DR	DR	11/09/2007	S	191	198	156	15.0	10.0	...
004628	08/14/2007	2	W1–S1	DR	DR	11/09/2007	S	197	198	156	13.0	6.2	...
004635	08/20/2007	1	E1–S2	CF	DR	11/12/2007	S	207	207	65	10.1	5.8	Multi-peaked FE in several scans
004635	09/16/2007	1	W1–S1	CF	DR	11/12/2007	S	210	273	102	2.1	1.6	...
004635	09/16/2007	2	E1–S1	CF	DR	11/12/2007	S	207	259	102	1.8	1.0	...
004813	07/27/2008	1	W1–S1	DR	DR	10/07/2008	S	200	201	150	55.9	28.1	High SNR
004915	09/17/2007	1	W1–S2	CF	DR	11/14/2007	S	208	264	102	2.6	2.0	...
004915	07/27/2008	1	W1–S1	DR	DR	10/07/2008	S	202	206	150	8.3	5.3	High SNR
007590	02/04/2007	1	E1–S1	CF	DR	05/09/2007	S?	198	257	155	...	...	...
007590	02/04/2007	2	E1–S1	CF	DR	05/09/2007	S?	196	239	155	...	...	...
007590	08/16/2007	1	W1–S1	DR	DR	11/12/2007	S?	206	341	102	1.3	0.7	Choppy FE; asymmetric SFE
007590	08/16/2007	2	E1–S1	DR	DR	11/12/2007	S	199	202	102	5.1	2.8	Asymmetric SFE
007590	07/08/2008	1	W1–S1	DR	DR	07/08/2008	S	141	390	150	2.3	1.1	Weak fringe
007590	07/09/2008	1	E1–S1	DR	DR	07/20/2008	S	99	571	100	1.4	0.4	...
007924	09/16/2007	1	W1–S1	CF	DR	11/12/2007	S	210	225	102	5.4	4.8	...
007924	09/16/2007	2	E1–S1	CF	DR	11/12/2007	S	209	235	102	3.2	2.2	Multi-peaked FE in several scans; asymmetric SFE
008997	09/17/2007	1	W1–S2	CF	DR	11/14/2007	S	254	254	65	6.5	3.6	Asymmetric sum SFE
008997	09/18/2007	1	E2–S2	PJ	DR	11/14/2007	S?	208	619	102	0.9	0.6	Asymmetric or twin-peaked SFE
008997	07/07/2008	1	W1–S1	DR	DR	07/07/2008	S	112	432	150	1.6	0.5	Weak fringe
008997	07/23/2008	1	E1–S1	TB	DR	07/24/2008	S	106	264	100	1.8	0.7	...
010008	09/17/2007	1	W1–S2	CF	DR	11/14/2007	S	262	262	65	6.5	3.7	Asymmetric SFE plots
010008	09/27/2007	1	E2–S2	NT	DR	11/14/2007	S?	159	265	65	1.2	0.6	Asymmetric SFE plots
010086	08/16/2007	1	W1–S1	DR	DR	11/12/2007	S	129	198	102	1.4	0.8	Asymmetric SFE plots
010086	08/16/2007	2	E1–S1	DR	DR	11/12/2007	S	198	198	102	9.1	2.8	Multi-peaked FE in several scans
010476	07/29/2007	1	E1–S1	DR	DR	11/09/2007	S	198	198	102	14.4	6.7	...
010476	08/14/2007	1	W1–S1	DR	DR	11/09/2007	S	189	198	156	5.4	3.6	...
010476	08/16/2007	1	E1–S1	DR	DR	11/12/2007	S	198	198	102	59.9	20.3	...
010780	08/20/2007	2	E1–S2	CF	DR	11/12/2007	S	199	199	102	24.1	13.2	...
010780	09/16/2007	1	W1–S1	CF	DR	11/12/2007	S?	209	254	102	12.9	13.3	...
010780	09/16/2007	2	E1–S1	CF	DR	11/12/2007	S	199	199	102	15.7	8.6	...
010780	06/24/2008	1	W1–S2	DR	CB	06/30/2008	S	206	219	100	12.9	10.3	...
012051	01/26/2007	1	E1–S1	EB	DR	05/09/2007	S?	188	807	155	...	...	Very noisy data
012051	09/17/2007	1	W1–S2	CF	DR	11/14/2007	S	207	207	65	21.3	13.0	Multi-peaked FE in several scans
012051	09/18/2007	1	E2–S2	PJ	DR	11/14/2007	S	207	278	102	1.7	0.9	...
012051	09/18/2007	2	E2–S2	PJ	DR	11/14/2007	S	213	286	102	1.3	0.9	...

Continued on Next Page...

TABLE 3.2 – Continued

HD Name	Obs UT Date	S	Baseline	Obs	Red	Date Reduced	S	Fringe Scans Good	Total	FF	⟨FW⟩	σ_{FW}	Reduction Notes
012846	09/17/2007	1	W1–S2	CF	DR	11/14/2007	S	199	199	65	12.0	6.4	Multi-peaked FE in most scans; asymmetric SFE
012846	09/18/2007	1	E2–S2	PJ	DR	11/14/2007	S	194	251	102	1.6	0.8	Multi-peaked FE in most scans; asymmetric SFE
016160	08/15/2007	1	E1–S1	DR	DR	11/12/2007	S	198	198	102	44.1	21.6	...
016160	09/17/2007	1	W1–S2	CF	DR	11/14/2007	S	198	199	156	10.6	6.1	...
016160	09/18/2007	1	E2–S2	PJ	DR	11/14/2007	S	203	207	102	5.8	4.6	...
016287	08/15/2007	1	E1–S1	DR	DR	11/12/2007	D?	207	232	102	2.8	1.8	Noticeable double peaks in SFE plots
016287	10/31/2007	1	E1–S1	DR	DR	11/14/2007	S?	230	607	102	0.9	0.5	Low SNR, weak fringe
016673	08/15/2007	1	E1–S1	DR	DR	11/12/2007	D?	198	198	102	30.6	15.4	Bumpy FE, multi-peaked SFE
016673	09/27/2007	1	E2–S2	NT	DR	11/14/2007	S	199	199	65	14.3	5.7	Multi-peaked FE in several scans; asymmetric SFE
016765	08/15/2007	1	E1–S1	DR	DR	11/12/2007	S	198	198	102	25.6	16.1	...
016765	09/17/2007	1	W1–S2	CF	DR	11/14/2007	S	206	206	65	23.0	15.2	...
016765	09/27/2007	1	E2–S2	NT	DR	11/14/2007	S	205	206	65	11.7	5.0	Multi-peaked FE in several scans; asymmetric SFE
016765	10/31/2007	1	E1–S1	DR	DR	11/14/2007	S	205	359	156	1.2	0.8	...
016765	10/31/2007	2	W1–S1	DR	DR	11/14/2007	S	208	216	102	5.3	4.7	...
017382	09/17/2007	1	W1–S2	CF	DR	11/14/2007	S	232	232	65	9.9	5.8	...
017382	09/18/2007	1	E2–S2	PJ	DR	11/14/2007	S?	180	452	102	0.9	0.5	Multi-peaked FE in most scans; two peaks in SFE
017382	07/07/2008	1	W1–S1	DR	DR	07/07/2008	S	154	246	150	2.6	1.2	...
017382	07/08/2008	1	W1–S1	DR	DR	07/08/2008	S	146	324	150	2.3	1.4	...
018143	09/17/2007	1	W1–S2	CF	DR	11/14/2007	S	206	206	65	11.1	5.8	Multi-peaked FE in most scans; asymmetric SFE
018143	10/31/2007	1	E1–S1	DR	DR	11/14/2007	S?	230	258	102	2.2	1.0	Multi-peaked FE in several scans; double-peaked SFE
018143	11/01/2007	1	W1–S1	DR	DR	11/15/2007	S?	210	307	102	1.5	1.0	Multi-peaked FE in several scans; asymmetric SFE
018143	07/23/2008	1	E1–S1	TB	DR	07/24/2008	S	160	224	100	2.5	1.1	...
018632	11/01/2007	1	E1–S1	DR	DR	11/15/2007	S?	157	355	102	1.1	0.7	Low SNR; Multi-peaked FE in several scans; asymmetric SFE
018632	11/01/2007	2	W1–S1	DR	DR	11/15/2007	S	228	338	102	1.5	0.9	Multi-peaked FE in several scans; asymmetric SFE
018757	08/20/2007	1	E1–S2	CF	DR	11/12/2007	S	202	272	102	4.5	3.8	...
018757	09/16/2007	2	W1–S1	CF	DR	11/12/2007	S	205	216	102	4.9	4.0	Multi-peaked FE in several scans
018757	09/16/2007	3	E1–S1	CF	DR	11/12/2007	S	203	229	102	2.9	2.0	Multi-peaked FE in several scans
018803	09/17/2007	1	W1–S2	CF	DR	11/14/2007	S	217	239	102	2.7	1.7	...
018803	09/18/2007	1	E2–S2	PJ	DR	11/14/2007	S	185	206	102	2.5	1.3	...
019994	09/27/2007	1	E2–S2	NT	DR	11/14/2007	S	199	199	65	24.1	11.5	Multi-peaked FE in several scans
019994	09/27/2007	2	E2–S2	NT	DR	11/14/2007	S	199	199	102	32.2	16.9	...
019994	09/27/2007	3	E2–S2	NT	DR	11/14/2007	S	198	198	102	32.7	18.2	...
019994	11/01/2007	1	E1–S1	DR	DR	11/15/2007	S	213	273	102	3.1	2.8	Multi-peaked FE in several scans; asymmetric SFE
019994	11/01/2007	2	W1–S1	DR	DR	11/15/2007	S	198	200	102	11.8	9.0	...
020165	11/01/2007	1	E1–S1	DR	DR	11/15/2007	S	175	371	102	1.1	0.7	Low SNR; Multi-peaked FE in several scans; asymmetric SFE
020165	11/01/2007	2	W1–S1	DR	DR	11/15/2007	S	216	450	102	1.1	0.7	Multi-peaked FE in several scans; asymmetric SFE
020619	11/01/2007	1	E1–S1	DR	DR	11/15/2007	S	243	243	65	6.3	3.8	Multi-peaked FE in several scans; asymmetric SFE
020619	11/01/2007	2	W1–S1	DR	DR	11/15/2007	S	213	283	102	1.9	1.3	Multi-peaked FE in several scans
022049	09/27/2007	1	E2–S2	NT	DR	11/14/2007	S	201	208	156	3.4	1.5	Multi-peaked FE in several scans; asymmetric SFE
022049	09/27/2007	2	E2–S2	NT	DR	11/14/2007	S	199	199	102	11.7	6.7	...
022879	09/27/2007	2	E2–S2	NT	DR	11/14/2007	S	196	202	102	6.2	3.3	Multi-peaked FE in several scans
022879	09/27/2007	3	E2–S2	NT	DR	11/14/2007	S	211	220	102	4.5	2.6	Multi-peaked FE in several scans; asymmetric SFE
022879	11/01/2007	1	E1–S1	DR	DR	11/15/2007	S?	247	247	65	8.4	6.5	Multi-peaked FE in several scans;
024238	09/16/2007	1	W1–S1	CF	DR	11/12/2007	S?	200	309	102	1.6	1.2	Asymmetric SFE
024238	09/16/2007	2	E1–S1	CF	DR	11/12/2007	S?	208	359	102	1.3	0.8	Asymmetric SFE
024409	08/20/2007	1	E1–S2	CF	DR	11/12/2007	S	200	201	102	7.3	4.0	...
024409	09/16/2007	1	W1–S1	CF	DR	11/12/2007	S	198	225	102	3.5	2.6	...
024409	09/16/2007	2	E1–S1	CF	DR	11/12/2007	S?	197	226	102	2.7	2.0	Asymmetric SFE
024496	09/26/2007	1	E2–S2	TB	DR	11/14/2007	S?	199	222	156	2.7	1.4	Multi-peaked FE in several scans; asymmetric SFE
024496	09/27/2007	1	E2–S2	NT	DR	11/14/2007	S?	206	252	102	1.9	1.0	Multi-peaked FE in several scans; asymmetric SFE
024496	10/31/2007	1	E1–S1	DR	DR	11/14/2007	S	199	199	102	4.6	1.5	...
024496	10/31/2007	2	W1–S1	DR	DR	11/14/2007	S	202	203	102	9.2	6.6	...
025457	09/26/2007	1	E2–S2	TB	DR	11/14/2007	S	198	200	156	11.1	5.2	...
025457	09/27/2007	2	E2–S2	NT	DR	11/14/2007	S	196	198	102	7.0	5.4	Clouds during after-shutter sequence
025457	10/31/2007	1	E1–S1	DR	DR	11/14/2007	S	218	278	102	5.8	4.8	...
025457	10/31/2007	2	W1–S1	DR	DR	11/14/2007	S	203	203	102	17.5	14.1	...
025665	09/16/2007	1	W1–S1	CF	DR	11/12/2007	S	200	233	102	2.7	1.9	Asymmetric SFE
025665	09/16/2007	2	E1–S1	CF	DR	11/12/2007	S?	211	287	102	1.9	1.4	Asymmetric SFE
026913	09/26/2007	1	E2–S2	TB	DR	11/14/2007	S	196	219	156	3.2	1.9	Multi-peaked FE in several scans; asymmetric SFE
026913	10/31/2007	1	E1–S1	DR	DR	11/14/2007	S	203	212	102	3.4	1.7	...
026913	10/31/2007	2	W1–S1	DR	DR	11/14/2007	S	196	203	102	7.5	4.3	...
026923	09/26/2007	1	E2–S2	TB	DR	11/14/2007	S	198	304	156	1.6	1.1	Multi-peaked FE in several scans; asymmetric SFE

Continued on Next Page...

TABLE 3.2 – Continued

HD Name	Obs UT Date	S	Baseline	Obs	Red	Date Reduced	S	Fringe Scans Good	Total	FF	⟨FW⟩	σ_{FW}	Reduction Notes
026923	10/31/2007	1	E1–S1	DR	DR	11/14/2007	S	213	218	102	4.2	2.3	...
026923	10/31/2007	2	W1–S1	DR	DR	11/14/2007	S	205	250	102	6.8	5.9	...
029883	09/17/2007	1	W1–S2	CF	DR	11/14/2007	S	219	219	65	5.9	3.5	Multi-peaked FE in most scans; asymmetric SFE
029883	09/18/2007	1	E2–S2	PJ	DR	11/14/2007	S	201	343	102	1.3	0.7	...
032850	10/31/2007	1	E1–S1	DR	DR	11/14/2007	S	204	249	102	1.9	1.0	Asymmetric SFE
032850	10/31/2007	2	W1–S1	DR	DR	11/14/2007	S	197	202	102	4.9	2.6	...
032923	02/25/2007	1	E1–S1	TB	DR	05/09/2007	S	200	201	155	...	...	Good SNR
032923	02/25/2007	2	E1–S1	TB	DR	05/09/2007	S	202	206	155	...	...	Good SNR
032923	03/11/2007	1	E1–S1	DR	DR	05/09/2007	S	204	238	155	...	...	...
032923	09/26/2007	1	E2–S2	TB	DR	11/14/2007	S	198	198	156	19.4	8.8	...
032923	09/27/2007	1	E2–S2	NT	DR	11/14/2007	S	197	198	102	10.0	5.8	Multi-peaked FE in several scans; asymmetric SFE
032923	10/31/2007	1	E1–S1	DR	DR	11/14/2007	S	199	199	102	19.9	12.1	...
032923	10/31/2007	2	W1–S1	DR	DR	11/14/2007	S	198	198	102	61.7	27.8	...
035112	10/31/2007	1	E1–S1	DR	DR	11/14/2007	S?	243	333	102	1.5	0.8	Multi-peaked FE in several scans; asymmetric/double-peaked SFE
035112	10/31/2007	2	W1–S1	DR	DR	11/14/2007	S	200	203	102	5.6	3.0	...
037008	01/25/2007	1	E1–S1	EB	DR	05/09/2007	D?	210	643	155	...	...	Second peak (0.95) at $\sim +25$, one more small bump (0.4) $\sim +55$
037008	11/01/2007	2	W1–S1	DR	DR	11/15/2007	S	217	240	102	2.8	1.6	Multi-peaked FE in several scans
037008	11/19/2007	1	E2–S2	CF	DR	12/05/2007	S	201	206	102	7.0	3.6	...
037008	11/19/2007	2	E2–S2	CF	DR	12/05/2007	S	195	222	102	2.9	1.8	...
037008	11/27/2007	1	E2–S2	EB	DR	12/05/2007	S	185	275	102	1.5	1.0	Poor SNR, bad PS
037394	01/25/2007	1	E1–S1	EB	DR	05/09/2007	D?	210	268	155	...	...	Distinct second peak in SFE plots
037394	01/26/2007	2	E1–S1	EB	DR	05/09/2007	D?	220	588	155	...	...	Weak fringe, shutter seq very uneven, but clear double peak seen!
037394	04/14/2007	1	E1–S1	DR	DR	05/09/2007	S?	224	252	155	...	...	No secondary seen in SFE here!
037394	11/01/2007	1	W1–S1	DR	DR	11/15/2007	S	198	199	102	15.5	10.5	Multi-peaked FE in several scans
037394	11/19/2007	3	E2–S2	CF	DR	12/05/2007	S	198	198	102	26.5	11.8	...
037394	11/19/2007	5	E2–S2	CF	DR	12/05/2007	S	198	198	102	16.8	8.5	...
037394	11/27/2007	1	E2–S2	EB	DR	12/05/2007	S	204	220	102	8.3	5.4	...
038230	01/25/2007	1	E1–S1	EB	DR	05/09/2007	D?	206	292	155	...	...	Shows close double peak like other observations of this night
038230	11/01/2007	1	W1–S1	DR	DR	11/15/2007	S	201	204	102	5.7	3.3	Multi-peaked FE in several scans
038230	11/19/2007	2	E2–S2	CF	DR	12/05/2007	S	198	198	102	6.7	3.8	...
038230	11/27/2007	1	E2–S2	EB	DR	12/05/2007	S	222	266	102	2.3	1.5	...
038858	09/26/2007	1	E2–S2	TB	DR	11/14/2007	S	201	293	156	2.0	1.5	Multi-peaked FE in several scans; asymmetric SFE
038858	10/31/2007	1	E1–S1	DR	DR	11/14/2007	S	203	203	102	15.0	8.9	...
038858	10/31/2007	2	W1–S1	DR	DR	11/14/2007	S	200	214	102	26.4	16.9	...
040397	09/26/2007	1	E2–S2	TB	DR	11/14/2007	S?	213	373	156	1.2	0.7	Low SNR; Multi-peaked FE in several scans; asymmetric SFE
040397	11/01/2007	1	W1–S1	DR	DR	11/15/2007	S	199	200	102	5.0	2.8	...
041593	09/26/2007	2	E2–S2	TB	DR	11/14/2007	S	196	217	156	2.7	1.4	Asymmetric SFE
041593	10/31/2007	1	E1–S1	DR	DR	11/14/2007	S?	204	205	102	9.5	5.7	Asymmetric SFE; double-peaked CCORR plot
041593	11/01/2007	1	W1–S1	DR	DR	11/15/2007	S	200	202	102	6.5	4.0	...
042618	09/26/2007	1	E2–S2	TB	DR	11/14/2007	S	198	280	156	1.5	0.9	Multi-peaked FE in several scans; asymmetric SFE
042618	10/31/2007	1	E1–S1	DR	DR	11/14/2007	S?	224	543	102	1.0	0.7	Low SNR; Multi-peaked FE in several scans; asymmetric SFE
042618	11/01/2007	1	W1–S1	DR	DR	11/15/2007	S	200	204	102	4.7	2.8	Multi-peaked FE in several scans
046588	04/14/2007	1	E1–S1	DR	DR	05/09/2007	S	211	234	155	...	...	...
046588	09/16/2007	1	E1–S1	CF	DR	11/12/2007	S	198	198	102	10.7	8.0	...
046588	04/26/2008	1	W1–S1	DR	CB	06/05/2008	S	312	870	100	2.2	3.8	...
051419	02/05/2007	2	E1–S1	EB	DR	05/09/2007	S	195	370	155	...	...	...
051419	02/05/2007	3	E1–S1	EB	DR	05/09/2007	S	210	461	155	...	...	Poor SNR, weak fringe in many scans
051419	04/26/2008	1	W1–S1	DR	CB	06/05/2008	S	231	688	100	1.4	2.5	...
051866	01/25/2007	1	E1–S1	EB	DR	05/09/2007	S?	197	208	155	...	...	Weak fringes; hint of secondary peak in SFE
051866	11/01/2007	2	W1–S1	DR	DR	11/15/2007	S	211	261	102	2.4	1.6	Multi-peaked FE in several scans
051866	11/19/2007	1	E2–S2	CF	DR	12/05/2007	S	201	214	102	3.2	2.0	...
051866	11/19/2007	2	E2–S2	CF	DR	12/05/2007	S	210	291	102	1.7	1.0	Weak fringe; ...
054371	02/04/2007	1	E1–S1	CF	DR	05/09/2007	S	203	256	155	...	...	...
054371	11/01/2007	2	W1–S1	DR	DR	11/15/2007	S	198	203	102	6.6	4.6	...
054371	04/25/2008	1	E1–S1	DR	CB	06/04/2008	S	145	658	100	0.6	0.7	CCORR has sub-peaks close to primary, but OK farther out
054371	04/26/2008	1	W1–S1	DR	CB	06/05/2008	S	272	417	100	2.5	2.4	Asymmetric SFE
055575	01/26/2007	1	E1–S1	EB	DR	05/09/2007	S?	206	362	155	...	...	Hint of second peak (0.4) at ± 20 like other obs of this night
055575	02/03/2007	1	E1–S1	CF	DR	05/09/2007	S	203	253	155	...	...	...
055575	11/01/2007	1	W1–S1	DR	DR	11/15/2007	S	200	200	102	20.5	14.7	Multi-peaked FE in several scans
055575	11/20/2007	1	E2–S2	PJ	DR	12/05/2007	S	199	265	156	1.9	1.4	Poor SNR, many scans have a weak fringe
055575	11/27/2007	2	E2–S2	EB	DR	12/05/2007	S	207	214	102	5.9	4.0	...
059747	11/01/2007	1	W1–S1	DR	DR	11/15/2007	S	207	232	102	3.1	2.1	...

Continued on Next Page...

TABLE 3.2 – Continued

HD Name	Obs UT Date	S	Baseline	Obs	Red	Date Reduced	S	Fringe Scans Good	Total	FF	⟨FW⟩	σ_{FW}	Reduction Notes
063433	03/20/2007	1	E1–S1	TB	DR	05/09/2007	S?	195	331	155	...	...	Hint of secondary peak in SFE
063433	11/01/2007	1	W1–S1	DR	DR	11/15/2007	S	200	204	102	6.9	4.6	...
063433	04/12/2008	1	W1–S1	DR	DR	04/21/2008	S	158	349	150	1.2	1.2	Double-peaked PS
063433	04/13/2008	1	E1–S1	DR	DR	04/21/2008	S	167	256	100	2.2	2.1	...
065430	04/26/2008	1	W1–S1	DR	CB	06/05/2008	S	245	659	100	1.0	1.3	...
065583	04/13/2008	1	E1–S1	DR	DR	04/21/2008	S	141	317	150	1.3	1.1	...
065583	04/26/2008	1	W1–S1	DR	CB	06/05/2008	S	284	433	100	3.7	4.1	...
067228	02/06/2007	2	E1–S1	EB	DR	05/09/2007	S	202	220	155	...	...	Uneven shutter sequence
067228	02/25/2007	1	E1–S1	TB	DR	05/09/2007	S?	203	205	155	...	...	Hint of a bulge at sep ~ -40 in CCOR
067228	02/25/2007	2	E1–S1	TB	DR	05/09/2007	S	200	221	155	...	...	...
067228	11/29/2007	3	E2–S2	TB	DR	12/05/2007	S	197	240	156	2.7	1.9	...
068017	04/12/2008	1	W1–S1	DR	DR	04/21/2008	S	128	357	150	1.0	0.9	Noisy PS
068017	04/25/2008	1	E1–S1	DR	CB	06/04/2008	S	242	381	100	2.5	2.5	...
068255	02/25/2007	2	E1–S1	TB	DR	05/09/2007	S	206	215	155	...	...	Clearly single
068255	02/25/2007	3	E1–S1	TB	DR	05/09/2007	S?	207	571	155	...	...	Poor SNR and weak fringe
079096	02/06/2007	3	E1–S1	EB	DR	05/09/2007	D?	194	407	155	...	...	Hint of a comp close to primary
079096	02/25/2007	1	E1–S1	TB	DR	05/09/2007	D	199	468	155	...	...	Companion clearly seen
079096	02/25/2007	2	E1–S1	TB	DR	05/09/2007	D				...	...	Companion clearly seen
079096	03/09/2007	1	E1–S1	DR	DR	05/09/2007	D	199	201	155	...	...	Companion clearly seen
079096	03/09/2007	2	E1–S1	DR	DR	05/09/2007	D	217	499	155	...	...	Companion clearly seen
079096	03/10/2007	2	E1–S1	DR	DR	05/09/2007	S	208	381	155	...	...	No comp seen at this epoch!! Probably too wide
079096	03/11/2007	1	E1–S1	DR	DR	05/09/2007	D				...	...	Companion clearly seen
079096	11/29/2007	2	E2–S2	TB	DR	12/05/2007	D	221	268	102	2.5	1.6	Many scans have only one fringe
079096	04/12/2008	1	W1–S1	DR	DR	04/21/2008	S	164	281	150	1.7	1.5	...
079096	04/14/2008	1	E1–S1	DR	DR	04/21/2008	S	183	221	150	3.7	3.0	Double fringes too wide – this is A
079096	04/14/2008	1	E1–S1	DR	DR	04/21/2008	S	182	232	150	2.9	2.6	Double fringes too wide – this is A
079096	04/14/2008	1	E1–S1	DR	DR	04/21/2008	S	185	230	150	2.7	2.1	Double fringes too wide – this is B
079969	02/06/2007	1	E1–S1	EB	DR	05/10/2007	S	192	269	155	...	...	ACOR flat part a little wavy
079969	02/25/2007	1	E1–S1	TB	DR	05/10/2007	S	203	323	155	...	...	Slight hint of comp peak in SFE
079969	11/29/2007	1	E2–S2	TB	DR	12/05/2007	S	210	267	102	1.9	1.2	...
079969	04/12/2008	1	W1–S1	DR	DR	04/21/2008	S	202	334	100	1.8	1.7	...
079969	04/13/2008	1	E1–S1	DR	DR	04/21/2008	S	153	297	150	1.5	1.5	...
080715	04/13/2008	1	E1–S1	DR	DR	04/21/2008	S	165	269	150	1.8	1.8	...
080715	04/26/2008	1	W1–S1	DR	CB	06/05/2008	S	311	768	100	1.5	2.3	...
082443	02/06/2007	1	E1–S1	EB	DR	05/10/2007	S	186	264	155	...	...	...
082443	11/29/2007	1	E2–S2	TB	DR	12/05/2007	S	206	215	102	3.3	1.7	...
082443	04/12/2008	1	W1–S1	DR	DR	04/21/2008	S	223	321	100	3.1	3.1	...
082443	04/13/2008	1	E1–S1	DR	DR	04/21/2008	S	168	241	150	2.8	2.7	...
082443	04/13/2008	1	E1–S1	DR	DR	04/21/2008	S	153	291	100	1.4	1.4	...
082885	01/26/2007	3	E1–S1	EB	DR	05/10/2007	S?	200	209	155	...	...	Spurious double peak, similar to other observations of this date
082885	04/24/2007	1	W1–S1	DR	DR	05/10/2007	S	230	305	155	...	...	...
082885	11/29/2007	1	E2–S2	TB	DR	12/05/2007	S	201	202	102	12.9	8.9	Strong fringe
082885	04/26/2008	1	W1–S1	DR	CB	06/05/2008	S	289	386	100	13.8	16.6	...
087883	02/06/2007	1	E1–S1	EB	DR	05/10/2007	S?	204	244	155	...	...	Small bump (0.35) at ± 65 in ccorr sum
087883	11/29/2007	1	E2–S2	TB	DR	12/05/2007	S?	229	393	102	1.4	1.0	Weak fringe; ...
087883	04/26/2008	1	W1–S1	DR	CB	06/05/2008	S	243	823	100	0.8	1.4	...
089269	04/24/2007	1	W1–S1	DR	DR	05/10/2007	S	218	290	155	...	...	...
089269	05/17/2007	2	E1–S1	DR	DR	05/21/2007	S	213	259	155	...	...	Slight asymmetry on the right on both shift-and-add plots
090343	06/24/2008	1	W1–S2	DR	CB	06/30/2008	S	200	235	100	5.4	4.7	...
090343	06/25/2008	1	E1–S1	DR	CB	07/01/2008	S	157	303	100	1.2	1.1	...
094765	04/14/2008	1	E1–S1	DR	DR	04/21/2008	S	189	247	150	3.0	2.6	...
094765	04/15/2008	1	W1–S1	DR	DR	04/21/2008	S	217	219	150	16.7	11.0	...
096064	04/14/2008	1	E1–S1	DR	DR	04/21/2008	S	192	246	150	2.4	1.7	A component, no fringe found for B
096064	04/15/2008	1	W1–S1	DR	DR	04/21/2008	S	230	244	150	6.4	4.5	...
097334	04/12/2008	1	W1–S1	DR	DR	04/21/2008	S	215	424	100	1.9	2.6	...
097334	04/12/2008	2	E1–S1	DR	DR	04/21/2008	S	164	329	150	1.4	1.5	...
097658	04/13/2008	1	E1–S1	DR	DR	04/21/2008	S	165	277	150	1.6	1.3	...
097658	04/14/2008	1	E1–S1	DR	DR	04/21/2008	S	173	352	150	1.4	1.5	...
098230	02/06/2007	1	E1–S1	EB	DR	05/10/2007	S	198	203	155	...	...	...
098230	02/21/2007	1	E1–S1	DR	DR	05/10/2007	S	206	245	155	...	...	Primary fringe on the right end of window
098230	02/21/2007	2	E1–S1	TB	DR	05/10/2007	S	199	218	155	...	...	Primary fringe on the left end of window
098230	03/08/2007	1	E1–S1	DR	DR	05/10/2007	S?	199	279	155	...	...	...

Continued on Next Page...

TABLE 3.2 – Continued

HD Name	Obs UT Date	S	Baseline	Obs	Red	Date Reduced	S	Fringe Scans Good	Total	FF	⟨FW⟩	σ_{FW}	Reduction Notes
098230	03/08/2007	2	E1–S1	DR	DR	05/10/2007	S?	198	198	155	...	...	Hint of peak in SFE
098230	04/24/2007	1	W1–S1	DR	DR	05/10/2007	D?	205	208	155	...	...	Hint of peak in SFE
098230	05/17/2007	1	E1–S1	DR	DR	05/21/2007	S	214	217	155	...	...	Primary fringe at left edge
098230	05/17/2007	2	E1–S1	DR	DR	05/21/2007	S?	212	215	155	...	...	Primary fringe at right edge
098230	05/17/2007	3	E1–S1	DR	DR	05/21/2007	S	213	215	155	...	...	Servo-tracked primary fringe
098230	05/28/2007	1	W1–S1	CF	DR	06/27/2007	S	210	213	156	27.0	16.5	...
098230	06/01/2007	1	W1–S1	DR	DR	06/27/2007	S?	217	524	156	1.1	0.9	Comp1; weak fringe,
098230	06/01/2007	2	W1–S1	DR	DR	06/27/2007	S	211	214	156	10.6	9.2	Comp2
098230	06/01/2007	3	W1–S1	DR	DR	06/27/2007	S?	208	213	156	17.7	13.5	Comp2
098230	04/12/2008	1	W1–S1	DR	DR	04/21/2008	S	255	359	100	15.7	17.0	...
098230	04/13/2008	1	E1–S1	DR	DR	04/21/2008	S	160	270	100	2.0	2.0	...
098281	04/14/2008	1	E1–S1	DR	DR	04/21/2008	S	205	216	150	4.7	2.8	...
098281	04/15/2008	1	W1–S1	DR	DR	04/21/2008	S	214	248	150	8.5	6.9	...
099491	03/08/2007	1	E1–S1	DR	DR	05/10/2007	S?	200	302	155	...	...	Hint of second peak in SFE
099491	04/14/2008	1	E1–S1	DR	DR	04/21/2008	S	184	215	150	4.1	2.9	A component
099491	04/15/2008	1	W1–S1	DR	DR	04/21/2008	S	223	226	150	28.7	18.6	...
099492	04/14/2008	1	E1–S1	DR	DR	04/21/2008	S	202	204	150	12.4	6.8	B component (99492)
099492	04/15/2008	1	W1–S1	DR	DR	04/21/2008	S	219	225	150	13.5	9.2	...
100180	02/06/2007	1	E1–S1	EB	DR	05/10/2007	S	203	331	155	...	...	...
100180	03/08/2007	1	E1–S1	DR	DR	05/10/2007	S	206	276	155	...	...	...
100180	04/24/2007	1	W1–S1	DR	DR	05/10/2007	S	212	234	155	...	...	...
101177	04/24/2007	1	W1–S1	DR	DR	05/10/2007	S	226	306	155	...	...	...
101177	05/17/2007	1	E1–S1	DR	DR	05/21/2007	S	213	269	155	...	...	Slight asymmetry on the right on both shift-and-add plots
101206	04/12/2008	1	W1–S1	DR	DR	04/21/2008	S	226	322	100	2.2	1.9	Bumpy PS
101206	04/12/2008	2	E1–S1	DR	DR	04/21/2008	S	115	407	150	0.8	0.8	Noisy data
104304	04/14/2008	1	E1–S1	DR	DR	04/21/2008	S	209	235	150	14.0	11.4	...
104304	04/15/2008	1	W1–S1	DR	DR	04/21/2008	S	233	237	150	34.1	25.5	...
105631	04/24/2007	1	W1–S1	DR	DR	05/10/2007	S	222	356	155	...	...	...
105631	05/17/2007	1	E1–S1	DR	DR	05/21/2007	S	204	459	155	...	...	Noisy data, weak fringe
105631	06/01/2007	1	W1–S1	DR	DR	06/27/2007	S?	207	401	156	1.2	0.9	Weak fringe, poor PS, SFE shows double-peak
105631	04/26/2008	1	W1–S1	DR	CB	06/05/2008	S	215	309	100	1.9	1.4	...
108954	04/11/2007	1	E1–S1	DR	DR	05/10/2007	S?	226	268	155	...	...	Slight asymmetry of shifted FE sum plots
108954	04/11/2007	2	E1–S1	DR	DR	05/10/2007	S	221	244	155	...	...	...
108954	04/24/2007	1	W1–S1	DR	DR	05/10/2007	S	219	269	155	...	...	...
110833	04/14/2007	1	E1–S1	DR	DR	05/10/2007	S?	237	343	155	...	...	Slight asymmetry & secondary peak in SFE
110833	04/17/2007	1	W1–S1	PJ	DR	05/10/2007	S?	235	278	155	...	...	Slight bump in SFE
110833	04/17/2007	2	W1–S1	PJ	DR	05/10/2007	S	223	240	155	...	...	...
110833	05/28/2007	2	W1–S1	CF	DR	06/27/2007	S	213	226	155	3.9	2.4	...
110833	07/28/2007	1	E1–S1	DR	DR	11/09/2007	S	222	372	156	1.4	1.0	Poor SNR, Multi-peaked FE in several scans
112758	04/14/2008	1	E1–S1	DR	DR	04/21/2008	S	174	321	150	1.4	1.3	...
112758	04/15/2008	1	W1–S1	DR	DR	04/21/2008	S	244	281	150	4.6	4.0	...
113449	04/14/2008	1	E1–S1	DR	DR	04/21/2008	S	187	288	150	1.7	1.3	...
113449	04/15/2008	1	W1–S1	DR	DR	04/21/2008	S	214	225	150	6.1	3.9	...
114783	04/13/2008	2	W1–S1	DR	DR	04/21/2008	S	196	257	100	5.0	4.6	...
115404	02/06/2007	1	E1–S1	EB	DR	05/10/2007	S	199	209	155	...	...	...
115404	02/06/2007	2	E1–S1	EB	DR	05/10/2007	S?	201	208	155	...	...	Hint of second peak in SFE
115404	03/08/2007	1	E1–S1	DR	DR	05/10/2007	S	197	202	155	...	...	...
115404	04/24/2007	1	W1–S1	DR	DR	05/10/2007	S	227	242	155	...	...	...
116442	03/12/2007	2	E1–S1	CF	DR	05/10/2007	S	197	216	155	...	...	...
116442	06/01/2007	1	W1–S1	DR	DR	06/27/2007	S	185	355	156	1.3	1.0	Weak fringe, poor PS
116443	03/12/2007	1	E1–S1	CF	DR	05/10/2007	S	199	290	155			...
116443	06/01/2007	1	W1–S1	DR	DR	06/27/2007	S	187	326	156	1.3	0.9	Weak fringe, poor PS
116956	04/03/2007	1	E1–S1	PJ	DR	05/10/2007	S	196	207	155	...	...	...
116956	04/03/2007	3	E1–S1	PJ	DR	05/10/2007	S	198	225	155	...	...	...
116956	05/28/2007	1	W1–S1	CF	DR	06/27/2007	S?	214	797	156	0.8	0.6	Noisy data; Second peak in SFE
116956	04/26/2008	1	W1–S1	DR	CB	06/05/2008	S?	223	289	100	3.0	2.6	SFE shows multiple peaks, similar to other obs of the night
116956	06/24/2008	1	W1–S2	DR	CB	06/30/2008	S	160	271	100	1.5	1.2	...
116956	06/25/2008	1	E1–S1	DR	CB	07/01/2008	S	166	267	100	2.6	2.7	...
119332	04/03/2007	2	E1–S1	PJ	DR	05/10/2007	S?	204	298	155	...	...	Hint of a second peak in SFE
119332	04/12/2008	1	W1–S1	DR	DR	04/21/2008	S	192	267	150	2.8	2.5	...
119332	04/12/2008	2	E1–S1	DR	DR	04/21/2008	S	144	336	150	1.0	0.9	...
121560	02/05/2007	1	E1–S1	EB	DR	05/10/2007	S?	198	245	155	...	...	Hint of a second peak in SFE

Continued on Next Page...

TABLE 3.2 – Continued

HD Name	Obs UT Date	S	Baseline	Obs	Red	Date Reduced	S	Fringe Scans Good	Fringe Scans Total	FF	⟨FW⟩	σ_{FW}	Reduction Notes
121560	02/05/2007	2	E1–S1	EB	DR	05/10/2007	S	200	283	155	...	...	...
121560	03/08/2007	1	E1–S1	DR	DR	05/10/2007	S	204	260	155	...	...	...
121560	04/24/2007	1	W1–S1	DR	DR	05/10/2007	S	233	298	155	...	...	...
124292	03/12/2007	2	E1–S1	CF	DR	05/10/2007	S	195	231	155	...	...	...
124292	04/13/2008	2	W1–S1	DR	DR	04/21/2008	S	208	218	100	15.1	9.5	...
124292	04/25/2008	1	E1–S1	DR	CB	06/04/2008	S	272	452	100	1.8	1.8	...
124850	02/16/2007	1	E1–S1	DR	DR	05/10/2007	S	199	202	155	...	...	Big low freq variation! Small second peak in SFE
124850	03/23/2007	1	E1–S1	TB	DR	05/10/2007	S	213	635	155	...	...	Ref scan has peak on the left edge
124850	05/31/2007	1	W1–S1	DR	DR	06/27/2007	S	210	222	156	6.9	5.8	...
124850	04/25/2008	1	E1–S1	DR	CB	06/04/2008	S	312	338	100	6.2	5.6	Several FE show double-peak
124850	06/08/2008	1	E2–S1	EB	CB	07/01/2008	S	271	348	100	3.2	3.1	...
124850	06/08/2008	2	E2–S1	EB	CB	07/01/2008	S	274	349	100	3.9	4.3	...
124850	06/09/2008	1	W2–S2	EB	CB	07/01/2008	S	210	217	100	25.9	21.1	...
124850	07/08/2008	1	W1–S1	DR	DR	07/08/2008	S	200	201	150	56.2	24.0	...
125455	03/12/2007	1	E1–S1	CF	DR	05/10/2007	S	200	263	155	...	...	...
125455	04/14/2008	1	W1–S1	DR	DR	04/21/2008	S	200	201	150	14.8	6.8	...
125455	04/25/2008	1	E1–S1	DR	CB	06/04/2008	S	255	492	100	1.3	1.3	...
127334	04/14/2007	1	E1–S1	DR	DR	05/10/2007	S	218	278	155	...	...	...
127334	04/17/2007	1	W1–S1	PJ	DR	05/10/2007	S	229	441	155	...	...	...
127334	04/17/2007	2	W1–S1	PJ	DR	05/10/2007	S?	226	233	155	...	...	Small second peak in SFE
127334	04/26/2007	1	W1–E1	DR	DR	05/10/2007	S	220	229	155	...	...	Small second peak in SFE
128165	04/14/2007	1	E1–S1	DR	DR	05/10/2007	S?	218	274	155	...	...	Mini shoulders in SFE plots
128165	04/26/2007	1	W1–E1	DR	DR	05/10/2007	S?	216	247	155	...	...	Small peaks in SFE, probably just noise
128165	05/16/2007	1	E1–S1	DR	DR	05/21/2007	S?	230	393	155	...	...	Slight asymmetries, but nothing more
128165	05/28/2007	1	W1–S1	CF	DR	06/27/2007	S	210	220	156	4.4	2.6	...
128165	07/28/2007	1	E1–S1	DR	DR	11/09/2007	S	214	332	102	1.7	1.2	Poor SNR, Multi-peaked FE in several scans
128311	04/13/2008	2	W1–S1	DR	DR	04/21/2008	S	215	219	100	23.1	15.3	...
128311	04/25/2008	1	E1–S1	DR	CB	06/04/2008	D?	352	547	100	2.3	2.3	SFE shows multiple peaks - similar to other obs of the night
128642	04/26/2008	1	W1–S1	DR	CB	06/05/2008	D?	246	310	100	3.0	2.2	SFE shows multiple peaks - similar to other obs of the night
128642	04/26/2008	2	W1–S1	DR	CB	06/05/2008	S?	259	318	100	3.4	2.8	SFE shows multiple peaks - similar to other obs of the night
128642	06/24/2008	1	W1–S2	DR	CB	06/30/2008	D?	191	219	100	10.4	8.6	SFE shows multiple peaks
128642	06/25/2008	1	E1–S1	DR	CB	07/01/2008	S	117	425	150	0.8	0.7	Used higher frequency
128642	06/25/2008	2	E1–S1	DR	CB	07/01/2008	S	184	245	100	2.7	2.3	...
130004	03/10/2007	1	E1–S1	DR	DR	05/14/2007	S	195	433	155	...	...	Slight broadening at base in SFE plots
130004	05/28/2007	1	W1–S1	CF	DR	06/27/2007	S?	229	690	156	0.8	0.5	Very noisy data.
130004	04/13/2008	1	E1–S1	DR	DR	04/21/2008	S?	180	242	100	2.4	1.9	Noisy data, asymmetric sum plots
130004	04/13/2008	2	W1–S1	DR	DR	04/21/2008	S	207	238	100	10.4	8.2	...
130004	04/25/2008	1	E1–S1	DR	CB	06/04/2008	D?	326	788	100	1.1	1.4	SFE shows multiple peaks - similar to other obs of the night
130307	04/13/2008	1	E1–S1	DR	DR	04/21/2008	S	173	241	100	2.0	1.5	...
130307	04/13/2008	2	W1–S1	DR	DR	04/21/2008	S	198	223	100	12.0	8.3	...
132142	04/12/2008	1	W1–S1	DR	DR	04/21/2008	S	188	326	150	1.8	1.8	...
132142	04/12/2008	2	E1–S1	DR	DR	04/21/2008	S?	144	341	150	1.1	0.9	Hint of second peak in SFE
132142	06/24/2008	1	W1–S2	DR	CB	06/30/2008	S	170	241	100	2.6	2.0	...
132142	06/25/2008	1	E1–S1	DR	CB	07/01/2008	S	125	398	100	0.9	1.0	...
132254	04/11/2007	1	E1–S1	DR	DR	05/14/2007	S	216	235	155	...	...	Latter part of signal scans drop in intensity - passing clouds?
132254	04/24/2007	1	W1–S1	DR	DR	05/14/2007	S	211	226	155	...	...	Weird low freq oscillation in Beam 5 data
132254	04/26/2007	1	W1–E1	DR	DR	05/14/2007	S	224	235	155	...	...	...
135204	03/08/2007	1	E1–S1	DR	DR	05/14/2007	S	198	198	155	...	...	...
135204	05/31/2007	1	W1–S1	DR	DR	06/27/2007	S	224	241	156	3.8	2.5	...
135204	04/25/2008	1	E1–S1	DR	CB	06/04/2008	S	358	403	100	5.0	3.9	...
135204	06/09/2008	1	W2–S2	EB	CB	07/01/2008	S	198	252	150	2.5	1.9	...
135204	06/23/2008	1	E1–S1	DR	CB	06/30/2008	D?	225	295	100	4.7	5.2	...
135204	07/05/2008	1	E1–S1	DR	DR	07/05/2008	S	220	237	100	11.4	8.2	...
135204	07/05/2008	2	E1–S1	DR	DR	07/05/2008	S	209	264	100	13.2	9.8	...
135204	07/08/2008	1	W1–S1	DR	DR	07/08/2008	S	198	222	150	4.4	3.0	...
135404	07/08/2008	2	W1–S1	DR	DR	07/08/2008	S	192	204	150	5.1	3.0	...
135599	03/08/2007	1	E1–S1	DR	DR	05/14/2007	S	199	199	155	...	...	...
135599	05/31/2007	1	W1–S1	DR	DR	06/27/2007	S	212	240	156	3.4	2.0	...
136202	02/16/2007	1	E1–S1	DR	DR	05/14/2007	S?	197	432	155	...	...	Low SNR; SFE plots show hint of second peak
136202	03/08/2007	1	E1–S1	DR	DR	05/14/2007	S?	198	198	155	...	...	...
136202	05/31/2007	1	W1–S1	DR	DR	06/27/2007	S	198	270	156	11.5	10.6	...
136202	06/01/2007	1	E2–S1	DR	DR	06/27/2007	S?	216	315	156	1.9	1.6	Poor PS, CCORR plot shows sub-peak at $\sim +35$

Continued on Next Page...

TABLE 3.2 – Continued

HD Name	Obs UT Date	S	Baseline	Obs	Red	Date Reduced	S	Fringe Scans Good	Total	FF	⟨FW⟩	σ_{FW}	Reduction Notes
136202	04/13/2008	1	E1–S1	DR	DR	04/21/2008	S	200	218	100	6.9	5.1	...
136202	04/13/2008	2	W1–S1	DR	DR	04/21/2008	S	213	218	100	60.0	43.7	...
136713	04/14/2008	1	W1–S1	DR	DR	04/21/2008	S	201	202	150	10.8	4.9	...
136713	04/25/2008	1	E1–S1	DR	CB	06/04/2008	S	271	384	100	2.4	2.1	...
136923	04/13/2008	1	E1–S1	DR	DR	04/21/2008	S	192	237	100	2.3	1.7	...
136923	04/13/2008	2	W1–S1	DR	DR	04/21/2008	S	158	275	100	6.6	8.3	...
137763	04/14/2008	1	W1–S1	DR	DR	04/21/2008	D?	199	205	150	12.9	10.1	Two peaks seen in SFE
137763	04/25/2008	1	E1–S1	DR	CB	06/04/2008	S	262	405	100	3.3	4.8	...
137763	06/09/2008	1	W2–S2	EB	CB	07/01/2008	S	195	303	100	1.8	1.5	...
137763	06/23/2008	1	E1–S1	DR	CB	06/30/2008	S	222	315	100	2.8	2.9	...
137763	07/07/2008	1	W1–S1	DR	DR	07/07/2008	S	196	211	150	9.4	7.4	Fringe 1 of a wide SFP – too wide to fit in window
137763	07/07/2008	2	W1–S1	DR	DR	07/07/2008	S	203	208	150	11.9	7.0	Fringe 2 of a wide SFP – too wide to fit in window
137778	04/14/2008	1	W1–S1	DR	DR	04/21/2008	S	200	200	150	13.7	6.5	...
137778	04/25/2008	1	E1–S1	DR	CB	06/04/2008	S?	277	328	100	3.8	3.0	SFE shows multiple peaks - similar to other obs of the night
137778	07/07/2008	1	W1–S1	DR	DR	07/07/2008	S	201	203	150	12.3	6.8	...
137778	07/07/2008	2	W1–S1	DR	DR	07/07/2008	S	200	202	150	13.5	7.6	...
139323	04/12/2008	1	W1–S1	DR	DR	04/21/2008	S	173	325	150	1.7	1.9	...
139323	04/12/2008	2	E1–S1	DR	DR	04/21/2008	S	131	334	100	1.1	1.1	...
139341	04/14/2007	1	E1–S1	DR	DR	05/14/2007	S?	117	338	155	...	...	Poor SNR, scan stopped midway; weak fringe, noisy envelopes
139341	04/17/2007	1	W1–S1	PJ	DR	05/14/2007	S?	223	350	155	...	...	Hint of peak in SFE
139341	04/17/2007	4	W1–S1	PJ	DR	05/14/2007	S	222	440	155	...	...	VB comp of a=0.8" not seen!
139341	04/26/2007	2	W1–E1	DR	DR	05/14/2007	S	225	303	155	...	...	VB comp of a=0.8" not seen!
139777	04/14/2007	1	E1–S1	DR	DR	05/14/2007	S	224	278	155	...	...	Mini sub-peak (0.3) at +45
139777	05/28/2007	1	W1–S1	CF	DR	06/27/2007	S	216	260	156	2.6	1.7	...
139777	04/26/2008	1	W1–S1	DR	CB	06/05/2008	S	234	416	100	2.5	3.0	...
139777	06/24/2008	1	W1–S2	DR	CB	06/30/2008	S	203	219	100	14.0	11.1	...
139813	04/26/2008	1	W1–S1	DR	CB	06/05/2008	S	218	329	100	1.8	1.6	...
139813	06/24/2008	1	W1–S2	DR	CB	06/30/2008	S	196	279	100	6.0	6.3	...
139813	06/25/2008	1	E1–S1	DR	CB	07/01/2008	S	202	292	100	2.3	2.1	...
141272	04/14/2008	1	W1–S1	DR	DR	04/21/2008	S	201	202	150	19.8	8.6	...
141272	04/25/2008	1	E1–S1	DR	CB	06/04/2008	S	256	325	100	3.5	3.2	...
142267	06/01/2007	1	E2–S1	DR	DR	06/27/2007	S	210	332	156	1.5	1.2	Big spike in PS
142267	08/15/2007	1	E1–S1	DR	DR	11/12/2007	S?	124	198	102	1.5	1.0	Noisy data, poor PS, assym SFE
142267	04/13/2008	1	E1–S1	DR	DR	04/21/2008	S	194	233	100	4.6	3.4	...
142267	04/13/2008	2	W1–S1	DR	DR	04/21/2008	S	209	212	100	38.2	26.5	...
144287	04/12/2008	1	W1–S1	DR	DR	04/21/2008	S	199	273	150	3.0	3.2	...
144287	04/13/2008	1	E1–S1	DR	DR	04/21/2008	S	175	258	100	2.1	1.8	...
145675	04/24/2007	1	W1–S1	DR	DR	05/14/2007	S?	222	245	155	...	...	Weird low-freq noise in beam 5
145675	04/26/2007	1	W1–E1	DR	DR	05/14/2007	S	233	347	155	...	...	...
145675	05/17/2007	1	E1–S1	DR	DR	05/21/2007	S	212	241	155	...	...	...
146233	03/08/2007	1	E1–S1	DR	DR	05/14/2007	S?	201	219	155	...	...	Hint of subpeak (0.2) at +60
146233	04/14/2008	1	W1–S1	DR	DR	04/21/2008	S	201	201	150	73.1	28.8	...
146233	04/25/2008	1	E1–S1	DR	CB	06/04/2008	S?	265	285	100	14.1	11.8	SFE shows multiple peaks - similar to other obs of the night
146233	06/23/2008	1	E1–S1	DR	CB	06/30/2008	S	246	279	100	10.4	10.0	...
146361	05/17/2007	1	E1–S1	DR	DR	06/27/2007	S	214	216	156	13.4	8.1	...
146361	05/17/2007	2	E1–S1	DR	DR	06/27/2007	S	214	219	156	16.2	10.5	...
146361	05/17/2007	3	E1–S1	DR	DR	06/27/2007	S	216	218	156	13.6	9.0	...
146361	05/17/2007	4	E1–S1	DR	DR	06/27/2007	S	218	222	156	9.7	6.6	...
146361	05/17/2007	5	E1–S1	DR	DR	06/27/2007	S	216	239	156	7.3	5.5	...
146361	05/17/2007	6	E1–S1	DR	DR	06/27/2007	S	206	220	156	7.6	5.3	...
146361	05/17/2007	7	E1–S1	DR	DR	06/27/2007	S	208	227	156	5.4	4.0	...
146361	05/17/2007	9	E1–S1	DR	DR	06/27/2007	S	209	211	156	30.5	15.2	...
146361	05/17/2007	10	E1–S1	DR	DR	06/27/2007	S	205	214	156	29.0	13.4	...
146361	05/17/2007	12	E1–S1	DR	DR	06/27/2007	S	212	215	156	26.8	11.3	...
146361	05/17/2007	14	E1–S1	DR	DR	06/27/2007	S	216	234	156	4.2	2.2	...
146361	05/27/2007	1	E2–S1	CF	DR	06/27/2007	S	212	224	156	8.3	6.4	...
146361	05/27/2007	2	E2–S1	CF	DR	06/27/2007	S	211	214	156	8.1	5.3	...
146361	05/27/2007	3	E2–S1	CF	DR	06/27/2007	S	219	230	156	6.5	4.9	...
146361	05/27/2007	4	E2–S1	CF	DR	06/27/2007	S	205	226	156	4.3	3.8	...
146361	05/27/2007	5	E2–S1	CF	DR	06/27/2007	S	194	325	156	1.6	1.2	...
146361	05/27/2007	6	E2–S1	CF	DR	06/27/2007	S	240	914	156	0.7	0.5	Tiny fringe, very noisy data
146361	05/29/2007	1	E2–S1	PJ	DR	06/27/2007	S	212	247	156	3.2	2.2	...

Continued on Next Page...

TABLE 3.2 – Continued

HD Name	Obs UT Date	S	Baseline	Obs	Red	Date Reduced	S	Fringe Scans Good	Total	FF	⟨FW⟩	σ_{FW}	Reduction Notes
146361	05/29/2007	2	E2–S1	PJ	DR	06/27/2007	S	211	256	156	2.9	2.1	...
146361	05/29/2007	3	E2–S1	PJ	DR	06/27/2007	S	223	268	156	2.4	1.7	...
146361	05/29/2007	4	E2–S1	PJ	DR	06/27/2007	S	211	274	156	2.3	1.6	...
146361	05/29/2007	6	E2–S1	PJ	DR	06/27/2007	S	231	474	156	1.1	0.7	Weak fringe
146361	05/29/2007	7	E2–S1	PJ	DR	06/27/2007	S	231	629	156	0.9	0.6	Weak fringe
146361	07/29/2007	1	E1–S1	DR	DR	11/09/2007	S	206	218	105	9.7	9.9	...
146361	07/29/2007	2	E1–S1	DR	DR	11/09/2007	S	204	261	105	6.1	7.2	...
146361	07/29/2007	3	E1–S1	DR	DR	11/09/2007	S?	217	394	105	1.3	1.0	Double-peaked SFE
146361	07/29/2007	5	E1–S1	DR	DR	11/09/2007	S	199	219	105	7.7	6.5	Many weak fringes
146361	07/29/2007	6	E1–S1	DR	DR	11/09/2007	S	174	303	105	5.8	8.7	Many weak fringes
146361	07/29/2007	7	E1–S1	DR	DR	11/09/2007	S	200	202	105	13.7	10.5	...
146361	07/29/2007	10	E1–S1	DR	DR	11/09/2007	S	199	204	105	12.3	9.4	...
146361	11/01/2007	1	E2–W1	DR	DR	11/15/2007	S?	215	515	105	1.1	0.9	Very weak fringes; very low SNR
148653	02/04/2007	1	E1–S1	CF	DR	05/14/2007	S	203	305	155	...	...	...
149661	03/08/2007	2	E1–S1	DR	DR	05/14/2007	S	198	198	155	...	...	...
149661	05/31/2007	1	W1–S1	DR	DR	06/27/2007	S	201	230	156	4.0	3.1	...
149806	04/13/2008	1	W1–S1	DR	DR	04/21/2008	S	202	266	100	9.4	10.7	...
149806	04/14/2008	1	W1–S1	DR	DR	04/21/2008	S	200	202	150	25.3	9.5	...
149806	04/25/2008	1	E1–S1	DR	CB	06/04/2008	S	238	270	100	5.4	3.9	...
151541	04/26/2008	1	W1–S1	DR	CB	06/05/2008	S	192	348	100	1.5	1.5	...
151541	06/24/2008	1	W1–S2	DR	CB	06/30/2008	S	192	227	100	4.8	3.5	...
151541	06/25/2008	1	E1–S1	DR	CB	07/01/2008	S	129	358	100	1.0	1.2	...
153557	05/30/2007	1	W1–S1	DR	DR	06/27/2007	S?	193	285	156	1.5	0.8	Widening ACOR plot
153557	08/21/2007	1	W1–S1	PJ	DR	11/12/2007	S	161	198	156	2.0	1.0	Multi-peaked FE in several scans
153557	04/12/2008	1	W1–S1	DR	DR	04/21/2008	S	197	299	100	2.3	2.2	...
153557	06/24/2008	1	W1–S2	DR	CB	06/30/2008	S	184	251	100	2.8	2.4	...
154345	04/14/2007	1	E1–S1	DR	DR	05/14/2007	S	215	217	155	...	...	...
154345	04/17/2007	1	W1–S1	PJ	DR	05/14/2007	S	217	229	155	...	...	...
154345	04/17/2007	2	W1–S1	PJ	DR	05/14/2007	S	218	230	155	...	...	...
154345	04/26/2007	1	W1–E1	DR	DR	05/14/2007	S	217	235	155	...	...	...
155712	09/17/2007	1	W1–S2	CF	DR	11/14/2007	S?	224	224	65	6.6	2.8	Additional weak peaks in SFE
155712	04/13/2008	1	W1–S1	DR	DR	04/21/2008	S	209	231	100	11.6	8.7	...
155712	04/14/2008	1	W1–S1	DR	DR	04/21/2008	S	199	202	150	8.0	3.9	...
155712	04/25/2008	1	E1–S1	DR	CB	06/04/2008	S	158	488	100	0.9	0.9	Poor fringe quality, multi-peaked FE in several scans
157347	04/13/2008	1	W1–S1	DR	DR	04/21/2008	S	212	219	100	24.7	19.5	...
157347	04/14/2008	1	W1–S1	DR	DR	04/21/2008	S	201	202	150	33.5	14.4	...
157347	04/25/2008	1	E1–S1	DR	CB	06/04/2008	S	260	311	100	6.8	6.5	...
158614	06/01/2007	1	E2–S1	DR	DR	06/27/2007	S?	72	407	156	0.6	0.4	Weak fringe, few good scans
158614	04/14/2008	1	W1–S1	DR	DR	04/21/2008	S	201	205	150	40.2	18.7	...
158614	04/25/2008	1	E1–S1	DR	CB	06/04/2008	S	256	305	100	4.3	4.6	...
158633	04/14/2007	1	E1–S1	DR	DR	05/14/2007	S	218	219	155	...	...	...
158633	04/17/2007	1	W1–S1	PJ	DR	05/14/2007	S	225	306	155	...	...	...
158633	04/17/2007	3	W1–S1	PJ	DR	05/14/2007	S	222	222	155	...	...	...
159062	04/14/2007	1	E1–S1	DR	DR	05/14/2007	S	215	240	155	...	...	Hint of additional peaks in SFE
159062	08/21/2007	2	W1–S1	PJ	DR	11/12/2007	S	146	198	156	1.6	0.9	Multi-peaked FE in several scans
159062	04/12/2008	1	W1–S1	DR	DR	04/21/2008	S	173	293	150	2.0	2.1	...
159062	06/24/2008	1	W1–S2	DR	CB	06/30/2008	S	189	232	100	4.0	3.3	...
159222	05/17/2007	2	E1–S1	DR	DR	05/21/2007	S	216	223	155	...	...	...
159222	04/12/2008	1	W1–S1	DR	DR	04/21/2008	S	204	284	150	3.4	3.6	...
159222	06/24/2008	1	W1–S2	DR	CB	06/30/2008	S	196	220	100	11.9	9.2	...
159222	06/26/2008	1	E1–S1	DR	CB	07/01/2008	S	180	690	100	0.7	0.7	Poor SNR
160346	07/22/2007	1	W1–S1	CF	DR	11/08/2007	S	197	255	156	3.0	2.8	...
160346	07/22/2007	3	E1–S1	CF	DR	11/08/2007	S	198	198	156	9.1	5.0	...
161198	05/30/2007	1	W1–S1	DR	DR	06/27/2007	S?	200	350	156	1.2	0.8	Widening ACOR plot
161198	09/17/2007	1	W1–S2	CF	DR	11/14/2007	S	217	217	65	11.9	7.5	Multi-peaked FE in most scans; asymmetric SFE
161198	04/13/2008	1	W1–S1	DR	DR	04/21/2008	S	197	230	100	7.6	6.6	...
161198	04/14/2008	1	W1–S1	DR	DR	04/21/2008	S?	194	217	150	4.9	3.5	Side lobes on both sides of fringe in both sum plots
161198	04/25/2008	1	E1–S1	DR	CB	06/04/2008	S	186	339	100	1.7	1.6	...
164922	05/17/2007	1	E1–S1	DR	DR	05/21/2007	S	221	228	155	...	...	...
164922	05/31/2007	1	W1–S1	DR	DR	06/27/2007	S	211	250	156	2.2	1.3	...
165401	07/22/2007	1	W1–S1	CF	DR	11/08/2007	S?	230	608	156	1.0	0.7	Poor SNR, broadened ACOR, hint of second peak in shift plot
165401	07/22/2007	2	E1–S1	CF	DR	11/08/2007	S	199	213	156	2.8	1.5	...

Continued on Next Page...

TABLE 3.2 – Continued

HD Name	Obs UT Date	S	Baseline	Obs	Red	Date Reduced	S	Fringe Scans Good	Total	FF	⟨FW⟩	σ_{FW}	Reduction Notes
165401	04/25/2008	1	E1–S1	DR	CB	06/04/2008	S	226	269	100	3.7	3.1	...
165401	06/21/2008	1	E1–S1	DR	CB	06/30/2008	S	264	506	100	1.3	1.3	Several FE are double peaked
165401	06/23/2008	1	E1–S1	DR	CB	06/30/2008	S	208	385	100	1.7	1.8	...
165401	07/05/2008	1	E1–S1	DR	DR	07/05/2008	S	172	369	100	2.3	1.4	Weak fringes, double-peaked FE in many scans
165401	07/05/2008	2	E1–S1	DR	DR	07/05/2008	S	173	353	100	2.2	1.4	Weak fringes, double-peaked FE in many scans
165401	07/07/2008	1	W1–S1	DR	DR	07/07/2008	S	199	205	150	15.3	9.6	...
165401	07/07/2008	2	W1–S1	DR	DR	07/07/2008	S	200	206	150	14.2	8.9	...
166620	04/14/2007	1	E1–S1	DR	DR	05/14/2007	S	221	224	155	...	...	...
166620	04/26/2007	1	W1–E1	DR	DR	05/14/2007	S	222	231	155	...	...	...
166620	09/17/2007	1	W1–S2	CF	DR	11/14/2007	S?	93	289	102	0.9	0.8	Multi-peaked FE in most scans; asymmetric SFE; few good scans
166620	09/18/2007	1	E2–S2	PJ	DR	11/14/2007	S	206	214	102	4.0	2.5	...
175472	06/21/2008	1	E1–S1	DR	CB	06/30/2008	S	235	431	100	2.1	2.4	...
175742	05/29/2007	1	E2–S1	PJ	DR	06/27/2007	S?	222	312	156	1.5	0.8	Weak fringe, strong side-lobes
175742	09/17/2007	1	W1–S2	CF	DR	11/14/2007	S?	210	210	65	9.8	6.0	Twin-peaked SFE
175742	04/13/2008	1	W1–S1	DR	DR	04/21/2008	S	181	255	100	2.9	2.8	...
175742	04/14/2008	1	W1–S1	DR	DR	04/21/2008	S	158	257	150	1.8	1.6	...
175742	06/21/2008	1	E1–S1	DR	CB	06/30/2008	S?	127	615	100	0.6	0.6	Poor SNR
175742	06/23/2008	1	E1–S1	DR	CB	06/30/2008	S	74	821	100	0.4	0.4	...
175742	06/24/2008	1	W1–S2	DR	CB	06/30/2008	S	169	306	100	1.7	1.6	...
176377	04/14/2007	1	E1–S1	DR	DR	05/14/2007	S	209	226	155	...	...	...
176377	09/17/2007	1	W1–S2	CF	DR	11/14/2007	S	213	213	65	15.4	10.9	Multi-peaked FE in most scans; asymmetric SFE
176377	04/13/2008	1	W1–S1	DR	DR	04/21/2008	S	203	242	100	5.7	5.4	...
176377	06/23/2008	1	E1–S1	DR	CB	06/30/2008	S	149	407	100	0.9	0.9	...
176377	06/24/2008	1	W1–S2	DR	CB	06/30/2008	S	176	249	100	2.5	2.3	...
178428	05/29/2007	1	E2–S1	PJ	DR	06/27/2007	S	209	215	156	5.1	3.5	...
178428	05/30/2007	1	W1–S1	DR	DR	06/27/2007	S	207	212	156	15.1	8.5	...
178428	06/01/2007	1	E2–S1	DR	DR	06/27/2007	S?	193	299	156	1.6	1.2	Double-peaked SFE
179957	05/30/2007	1	W1–S1	DR	DR	06/27/2007	S?	221	376	156	1.3	0.9	...
179957	07/25/2007	2	E1–S1	DR	DR	11/09/2007	S	208	285	156	1.6	0.9	...
179957	08/18/2007	1	W1–S1	DR	DR	11/12/2007	S	208	283	156	2.4	1.8	...
179957	08/20/2007	1	E1–S2	CF	DR	11/12/2007	S	221	379	102	1.2	0.7	Weak fringe
179957	08/21/2007	2	W1–S1	PJ	DR	11/12/2007	S	118	198	102	1.5	1.3	Low SNR
179958	05/30/2007	2	W1–S1	DR	DR	06/27/2007	S?	215	286	156	1.8	1.0	...
180161	04/14/2007	1	E1–S1	DR	DR	05/14/2007	S	229	252	155	...	...	Slight asymmetry at base of peak on left
180161	08/20/2007	1	E1–S2	CF	DR	11/12/2007	S	198	199	102	5.9	2.8	...
180161	08/21/2007	1	W1–S1	PJ	DR	11/12/2007	S?	120	198	102	1.4	0.8	Asymmetric SFE
180161	09/16/2007	1	W1–S1	CF	DR	11/12/2007	S	205	224	102	3.1	2.4	...
180161	09/16/2007	2	E1–S1	CF	DR	11/12/2007	S	205	219	102	4.4	3.0	...
182488	04/14/2007	1	E1–S1	DR	DR	05/14/2007	S	212	221	155	...	...	...
182488	08/18/2007	1	W1–S1	DR	DR	11/12/2007	S	195	224	156	3.0	2.2	...
182488	09/17/2007	1	W1–S2	CF	DR	11/14/2007	S	210	221	102	7.7	6.3	Multi-peaked FE in most scans; asymmetric SFE
182488	09/18/2007	1	E2–S2	PJ	DR	11/14/2007	S	207	237	102	2.3	1.4	...
184385	05/29/2007	1	E2–S1	PJ	DR	06/27/2007	S	208	225	156	3.3	1.8	...
184385	05/30/2007	1	W1–S1	DR	DR	06/27/2007	S	215	219	156	6.0	3.0	...
185144	04/26/2007	1	W1–E1	DR	DR	05/14/2007	S	228	236	155	...	...	...
185144	05/28/2007	1	W1–S1	CF	DR	06/27/2007	S	208	208	156	23.7	15.6	...
185144	07/28/2007	1	E1–S1	DR	DR	11/09/2007	S?	213	344	102	8.2	13.7	Hint of low second peak in SFE
185144	08/20/2007	1	E1–S2	CF	DR	11/12/2007	S	197	200	102	12.5	9.5	...
185144	09/16/2007	1	W1–S1	CF	DR	11/12/2007	S	198	198	102	29.5	21.3	...
185144	09/16/2007	2	E1–S1	CF	DR	11/12/2007	S	203	250	102	6.5	5.6	...
185414	04/14/2007	1	E1–S1	DR	DR	05/14/2007	S	223	245	155	...	...	...
185414	05/28/2007	1	W1–S1	CF	DR	06/27/2007	S	213	310	156	2.4	2.0	...
189340	06/09/2008	1	W2–S2	EB	CB	07/01/2008	S?	166	329	151	1.5	1.5	Poor SNR
189340	06/09/2008	2	W2–S2	EB	CB	07/01/2008	S	196	235	100	3.4	2.5	...
189340	06/21/2008	1	E1–S1	DR	CB	06/30/2008	S	253	420	100	1.6	1.4	...
189340	06/23/2008	1	E1–S1	DR	CB	06/30/2008	S	250	866	100	0.9	1.4	...
189340	06/23/2008	2	E1–S1	DR	CB	06/30/2008	S	228	702	100	0.9	1.2	...
189733	05/30/2007	1	W1–S1	DR	DR	06/27/2007	S	215	232	156	3.6	2.4	...
189733	07/24/2007	1	E1–S1	PJ	DR	11/08/2007	S	203	228	156	2.4	1.3	...
189733	09/17/2007	1	W1–S2	CF	DR	11/14/2007	S	208	208	65	11.9	8.0	Multi-peaked FE in most scans; asymmetric SFE
190067	07/22/2007	1	W1–S1	CF	DR	11/08/2007	S	200	209	102	7.2	3.7	...
190067	07/22/2007	2	E1–S1	CF	DR	11/08/2007	S	201	217	156	13.5	6.4	...

Continued on Next Page...

TABLE 3.2 – Continued

HD Name	Obs UT Date	S	Baseline	Obs	Red	Date Reduced	S	Fringe Scans Good	Total	FF	⟨FW⟩	σ_{FW}	Reduction Notes
190067	07/24/2007	3	E1–S1	PJ	DR	11/08/2007	S	206	248	156	2.7	1.9	...
190404	07/24/2007	1	E1–S1	PJ	DR	11/08/2007	S	198	206	156	5.1	2.8	...
190404	07/24/2007	2	W1–S1	PJ	DR	11/08/2007	S	193	198	102	6.5	3.7	...
190470	07/24/2007	1	E1–S1	PJ	DR	11/08/2007	S	200	243	156	2.1	1.2	...
190470	07/24/2007	2	W1–S1	PJ	DR	11/08/2007	S	211	496	156	1.1	1.1	Poor fringe quality, multi-peaked FE in several scans
190470	08/17/2007	1	W1–S1	DR	DR	11/12/2007	S	198	198	156	3.9	1.3	Multi-peaked FE in several scans
190470	08/18/2007	1	W1–S1	DR	DR	11/12/2007	S	201	214	102	3.4	1.7	...
190470	08/18/2007	2	E1–S1	DR	DR	11/12/2007	S	239	239	65	4.0	1.4	Weak, choppy fringe; asymmetric summary SFE
190771	04/14/2007	1	E1–S1	DR	DR	05/14/2007	S	223	235	155	...	...	...
190771	08/18/2007	1	W1–S1	DR	DR	11/12/2007	S	198	198	102	16.7	8.7	...
190771	08/18/2007	2	E1–S1	DR	DR	11/12/2007	S	200	205	102	5.1	2.6	...
190771	08/20/2007	1	E1–S2	CF	DR	11/12/2007	S	233	254	102	2.6	1.6	Asymmetric SFE
190771	08/21/2007	1	W1–S1	PJ	DR	11/12/2007	S	200	200	102	11.6	5.7	...
191499	07/22/2007	1	W1–S1	CF	DR	11/08/2007	S	197	198	102	5.2	2.0	Broad ACOR plot
191499	07/22/2007	2	E1–S1	CF	DR	11/08/2007	S	198	198	156	7.1	2.3	...
191499	07/24/2007	1	E1–S1	PJ	DR	11/08/2007	S	208	260	156	2.0	1.2	Low fringe quality
191499	07/24/2007	2	W1–S1	PJ	DR	11/08/2007	S	161	198	102	2.5	1.9	Multi-peaked FE in several scans
191785	07/22/2007	1	E1–S1	CF	DR	11/08/2007	S	198	198	156	9.6	4.0	...
191785	07/24/2007	1	E1–S1	PJ	DR	11/08/2007	S	205	224	156	3.8	2.4	Multi-peaked FE in several scans
191785	07/24/2007	2	W1–S1	PJ	DR	11/08/2007	S	181	198	102	4.5	3.5	...
192263	08/15/2007	2	E1–S1	DR	DR	11/12/2007	S?	134	198	102	1.9	1.4	Noisy data, poor PS, assym SFE
192263	04/25/2008	1	E1–S1	DR	CB	06/04/2008	S	191	470	100	1.1	1.1	...
192263	06/22/2008	1	W1–S1	DR	CB	06/30/2008	S?	89	547	100	0.5	0.5	The fringes are very very messy, this is inconclusive data
192263	06/23/2008	1	E1–S1	DR	CB	06/30/2008	S	115	1016	100	0.4	0.5	...
192263	07/06/2008	1	E1–S1	DR	DR	07/07/2008	S	190	237	150	3.8	2.2	...
192263	07/06/2008	2	E1–S1	DR	DR	07/07/2008	S	174	228	150	3.6	2.3	...
192263	07/07/2008	1	W1–S1	DR	DR	07/07/2008	S	198	217	150	12.9	9.1	...
192263	07/07/2008	2	W1–S1	DR	DR	07/07/2008	S	202	214	150	11.1	8.2	...
195564	06/09/2008	1	W2–S2	EB	CB	07/01/2008	S	206	213	151	7.1	5.2	...
195564	06/09/2008	2	W2–S2	EB	CB	07/01/2008	S	212	240	100	8.4	7.3	...
195564	06/22/2008	1	W1–S1	DR	CB	06/30/2008	S?	241	246	100	6.8	4.5	Double peaked CCORR
195564	06/23/2008	1	E1–S1	DR	CB	06/30/2008	S	248	349	100	2.7	2.7	...
197076	07/22/2007	1	W1–S1	CF	DR	11/08/2007	S	199	211	156	4.4	2.5	...
197076	07/22/2007	2	E1–S1	CF	DR	11/08/2007	S	198	198	156	16.8	6.5	...
197076	07/24/2007	1	E1–S1	PJ	DR	11/08/2007	S	203	229	156	3.8	2.8	...
197076	07/24/2007	2	W1–S1	PJ	DR	11/08/2007	S	198	198	156	7.8	4.6	Flat-topped FE peak in several scans
198425	08/14/2007	1	E1–S1	DR	DR	11/09/2007	S	176	198	156	2.0	0.8	...
198425	08/17/2007	1	W1–S1	DR	DR	11/12/2007	S?	273	273	65	3.6	1.3	Poor-quality data, very low SNR, weird PS
198425	07/08/2008	1	W1–S1	DR	DR	07/08/2008	S	142	522	150	1.8	0.8	...
198425	07/23/2008	1	E1–S1	TB	DR	07/24/2008	S	65	279	100	1.8	0.9	...
200560	07/28/2007	1	E1–S1	DR	DR	11/09/2007	S	199	213	102	2.9	1.4	...
200560	08/18/2007	1	W1–S1	DR	DR	11/12/2007	S	197	198	102	5.3	2.0	...
200560	08/18/2007	2	E1–S1	DR	DR	11/12/2007	S	211	231	102	2.3	1.1	...
200560	08/20/2007	1	E1–S2	CF	DR	11/12/2007	S?	126	411	102	0.8	0.5	Weak choppy fringe
202751	07/22/2007	1	E1–S1	CF	DR	11/08/2007	S	198	199	156	5.1	2.0	...
202751	07/24/2007	1	W1–S1	PJ	DR	11/08/2007	S	178	198	156	2.8	1.6	Multi-peaked FE in several scans
202751	09/17/2007	1	W1–S2	CF	DR	11/14/2007	S?	228	229	65	8.5	5.3	Asymmetric or twin-peaked SFE plots
208038	07/24/2007	2	E1–S1	PJ	DR	11/08/2007	S	213	309	156	1.6	1.0	Multi-peaked FE in several scans
208038	08/14/2007	1	E1–S1	DR	DR	11/09/2007	S	168	198	156	2.0	1.1	Weak fringe
208038	08/14/2007	2	W1–S1	DR	DR	11/09/2007	S	132	198	156	1.4	0.9	...
208313	07/25/2007	1	E1–S1	DR	DR	11/09/2007	S	201	264	156	1.7	1.0	Multi-peaked FE in several scans
208313	08/14/2007	1	E1–S1	DR	DR	11/09/2007	S	183	198	156	2.7	1.5	...
208313	08/14/2007	2	W1–S1	DR	DR	11/09/2007	S	181	198	156	2.5	1.2	...
210277	09/17/2007	1	W1–S2	CF	DR	11/14/2007	S	198	199	102	12.3	6.2	...
210277	06/23/2008	1	E1–S1	DR	CB	06/30/2008	S	193	697	100	0.7	0.8	...
210277	07/06/2008	1	E1–S1	DR	DR	07/07/2008	S	191	225	150	4.2	3.1	...
210277	07/06/2008	2	E1–S1	DR	DR	07/07/2008	S	186	218	150	5.1	4.2	...
210277	07/07/2008	1	W1–S1	DR	DR	07/07/2008	S	201	211	150	7.8	6.5	...
210277	07/07/2008	2	W1–S1	DR	DR	07/07/2008	S	205	217	150	7.6	5.7	...
210667	07/26/2007	1	E1–S1	DR	DR	11/09/2007	S	199	203	156	4.8	2.1	...
210667	07/26/2007	2	W1–S1	DR	DR	11/09/2007	S	211	270	156	2.4	1.7	...
210667	07/28/2007	1	E1–S1	DR	DR	11/09/2007	S?	189	258	102	1.6	0.8	...

Continued on Next Page...

TABLE 3.2 – Continued

HD Name	Obs UT Date	S	Baseline	Obs	Red	Date Reduced	S	Fringe Scans Good	Total	FF	⟨FW⟩	σ_{FW}	Reduction Notes
211472	07/26/2007	1	E1–S1	DR	DR	11/09/2007	S	184	259	156	2.1	1.7	...
211472	07/26/2007	2	W1–S1	DR	DR	11/09/2007	S	198	243	156	2.1	1.3	...
211472	07/28/2007	1	E1–S1	DR	DR	11/09/2007	S?	203	373	156	1.2	0.7	...
215152	09/17/2007	1	W1–S2	CF	DR	11/14/2007	S	198	203	102	4.1	1.8	Multi-peaked FE in most scans; asymmetric SFE
215152	07/06/2008	1	E1–S1	DR	DR	07/07/2008	S	166	313	150	2.3	1.2	...
215152	07/07/2008	1	W1–S1	DR	DR	07/07/2008	S	167	279	150	2.6	1.9	...
216520	07/26/2007	1	E1–S1	DR	DR	11/09/2007	S?	219	323	156	1.5	0.9	Poor SNR; multi-peaked FE in several scans
216520	09/16/2007	1	W1–S1	CF	DR	11/12/2007	S	204	234	102	2.9	2.4	...
216520	09/16/2007	2	E1–S1	CF	DR	11/12/2007	S	197	222	102	4.4	3.1	Multi-peaked FE in several scans
217107	08/14/2007	1	E1–S1	DR	DR	11/09/2007	S	192	198	156	6.3	4.3	...
217107	08/14/2007	2	W1–S1	DR	DR	11/09/2007	S	197	198	156	7.4	3.4	...
217813	07/22/2007	1	E1–S1	CF	DR	11/08/2007	S?	198	233	102	19.6	12.2	Beam intensities weird during fringes; few scans show two peaks
217813	08/14/2007	1	E1–S1	DR	DR	11/09/2007	S	192	198	156	4.9	2.8	...
217813	08/14/2007	2	W1–S1	DR	DR	11/09/2007	S	198	198	156	6.3	2.2	...
218868	07/26/2007	1	E1–S1	DR	DR	11/09/2007	S	200	223	156	5.7	3.1	...
218868	07/28/2007	2	E1–S1	DR	DR	11/09/2007	S	203	224	102	2.6	1.3	Multi-peaked FE in several scans
218868	06/25/2008	1	E1–S1	DR	CB	07/01/2008	S	70	616	100	0.4	0.5	...
218868	07/21/2008	1	E1–S1	TB	DR	07/24/2008	S	197	218	150	6.4	4.1	...
219134	07/26/2007	2	E1–S1	DR	DR	11/09/2007	S	198	198	156	35.7	12.1	Good SNR
219134	07/26/2007	3	W1–S1	DR	DR	11/09/2007	S	198	198	156	18.4	11.2	Good SNR
219538	08/14/2007	1	E1–S1	DR	DR	11/09/2007	S	159	198	156	1.9	1.0	...
219538	08/14/2007	2	W1–S1	DR	DR	11/09/2007	S	172	198	156	1.9	0.9	Weak fringe, Choppy FE
219623	08/18/2007	1	W1–S1	DR	DR	11/12/2007	S	198	198	102	26.0	11.9	...
219623	08/18/2007	2	E1–S1	DR	DR	11/12/2007	S	199	199	102	27.2	8.6	...
219623	08/20/2007	1	E1–S2	CF	DR	11/12/2007	S	205	236	102	2.2	1.2	Noisy data
220140	09/16/2007	1	W1–S1	CF	DR	11/12/2007	S	199	214	102	3.9	3.1	...
220140	09/16/2007	2	E1–S1	CF	DR	11/12/2007	S	197	205	102	5.3	3.1	...
220182	08/18/2007	1	W1–S1	DR	DR	11/12/2007	S	202	213	102	4.9	2.6	...
220182	08/18/2007	2	E1–S1	DR	DR	11/12/2007	S	200	201	102	4.1	1.7	...
220339	07/06/2008	1	E1–S1	DR	DR	07/07/2008	S	149	443	150	2.0	1.1	Weak fringe
220339	07/07/2008	1	W1–S1	DR	DR	07/07/2008	S	159	257	150	3.1	2.1	...
221354	08/20/2007	2	E1–S2	CF	DR	11/12/2007	S	201	201	65	9.6	6.0	Multi-peaked FE in several scans
221354	09/16/2007	1	W1–S1	CF	DR	11/12/2007	S	199	210	102	5.0	3.6	...
221354	09/16/2007	2	E1–S1	CF	DR	11/12/2007	S	201	204	102	3.4	1.5	Multi-peaked FE in several scans
221851	08/18/2007	1	W1–S1	DR	DR	11/12/2007	S	188	189	102	1.5	1.0	...
221851	08/18/2007	2	E1–S1	DR	DR	11/12/2007	S	201	208	102	4.2	2.2	Multi-peaked FE in several scans
222143	07/27/2007	1	E1–S1	DR	DR	11/09/2007	S	79	610	102	1.3	4.3	Poor SNR, but fringes strong when seen
222143	08/18/2007	1	W1–S1	DR	DR	11/12/2007	S	198	198	102	10.6	4.2	...
222143	08/18/2007	2	E1–S1	DR	DR	11/12/2007	S	198	198	102	8.4	3.3	...
222143	08/20/2007	1	E1–S2	CF	DR	11/12/2007	S	137	137	65	4.0	1.9	Very choppy fringe
222404	09/16/2007	2	E1–S1	CF	DR	11/12/2007	S	199	200	156	14.0	7.6	...
222404	09/16/2007	3	E1–S1	CF	DR	11/12/2007	S	201	239	156	2.4	1.5	Tiny fringes, weak PS
222404	04/26/2008	1	W1–S1	DR	CB	06/05/2008	S	242	351	100	6.0	7.3	...
222404	06/24/2008	1	W1–S2	DR	CB	06/30/2008	S	209	223	100	13.8	12.7	...
224465	08/18/2007	1	W1–S1	DR	DR	11/12/2007	S	200	207	102	9.0	4.2	...
224465	08/18/2007	2	E1–S1	DR	DR	11/12/2007	S	201	201	102	9.1	4.0	...
224465	08/20/2007	1	E1–S2	CF	DR	11/12/2007	S	154	253	102	1.3	0.6	...

NOTES.— Column 5 observer codes are: CF = C. Farrington, DR = D. Raghavan, EB = E. Baines, NT = N. Turner, PJ = PJ Goldfinger, TB = T. Boyajian. Column 6 reducer codes are DR as above and CB = C. Black. The last column contains notes made when data were reduced and analyzed. It contains some abbreviations that stand for: ACOR = Autocorrelation summary plot, CCORR = Cross-correlation shifted summary plot, FE = Fringe envelope, PS = Power spectrum, and SFE = Summary fringe envelope. When secondary fringes are mentioned, their intensity relative to the primary fringe is given parenthetically, and the offset in sampling interval unit is given as a positive or negative number, indicating the position of the secondary fringe relative to the primary.

TABLE 3.3: Summary of SFP Results

HD Name	Total Obs	======= S-E Baselines ======				======= S-W Baselines ======				======= E-W Baselines ======			
		Single	Single?	Double	Double?	Single	Single?	Double	Double?	Single	Single?	Double	Double?
000166	3	2	...	...	...	1	...	...	...	...	...	...	...
001461	3	1	...	...	...	1	...	1	...	...	...	...	...
001562	4	1	1	...	...	1	1	...	...	...	...	...	...
003196	6	1	...	...	2	...	...	...	3	...	...	...	...
003651	3	2	...	...	...	1	...	...	...	...	...	...	...
003765	4	1	1	...	...	1	1	...	...	...	...	...	...
004256	2	1	...	...	...	1	...	...	...	...	...	...	...
004628	2	1	...	...	...	1	...	...	...	...	...	...	...
004635	3	2	...	...	...	1	...	...	...	...	...	...	...
004813	1	...	...	...	...	1	...	...	...	...	...	...	...
004915	2	...	...	...	...	2	...	...	...	...	...	...	...
007590	6	2	2	...	...	1	1	...	...	...	...	...	...
007924	2	1	...	...	...	1	...	...	...	...	...	...	...
008997	4	1	1	...	...	2	...	...	...	...	...	...	...
010008	2	...	1	...	...	1	...	...	...	...	...	...	...
010086	2	1	...	...	...	1	...	...	...	...	...	...	...
010476	3	2	...	...	...	1	...	...	...	...	...	...	...
010780	4	2	...	...	...	1	1	...	...	...	...	...	...
012051	4	2	1	...	...	1	...	...	...	...	...	...	...
012846	2	1	...	...	...	1	...	...	...	...	...	...	...
016160	3	2	...	...	...	1	...	...	...	...	...	...	...
016287	2	...	1	1	...	...	...	...	...	...	...	...	...
016673	2	1	...	1	...	...	...	...	...	...	...	...	...
016765	5	3	...	...	...	2	...	...	...	...	...	...	...
017382	4	...	1	...	...	3	...	...	...	...	...	...	...
018143	4	1	1	...	...	1	1	...	...	...	...	...	...
018632	2	...	1	...	...	1	...	...	...	...	...	...	...
018803	2	1	...	...	...	1	...	...	...	...	...	...	...
018757	3	2	...	...	...	1	...	...	...	...	...	...	...
019994	5	4	...	...	...	1	...	...	...	...	...	...	...
020165	2	1	...	...	...	1	...	...	...	...	...	...	...
020619	2	1	...	...	...	1	...	...	...	...	...	...	...
022049	2	2	...	...	...	...	...	...	...	...	...	...	...
022879	3	2	1	...	...	...	...	...	...	...	...	...	...
024496	4	1	2	...	...	1	...	...	...	...	...	...	...
024238	2	...	1	...	...	...	1	...	...	...	...	...	...
024409	3	1	1	...	...	1	...	...	...	...	...	...	...
025457	4	3	...	...	...	1	...	...	...	...	...	...	...
025665	2	...	1	...	...	1	...	...	...	...	...	...	...
026965	...	...	...	...	...	...	...	...	...	...	...	...	...
026913	3	2	...	...	...	1	...	...	...	...	...	...	...
026923	3	2	...	...	...	1	...	...	...	...	...	...	...
029883	2	1	...	...	...	1	...	...	...	...	...	...	...
032850	2	1	...	...	...	1	...	...	...	...	...	...	...
032923	7	6	...	...	...	1	...	...	...	...	...	...	...
035112	2	...	1	...	...	1	...	...	...	...	...	...	...
037008	5	3	...	1	...	1	...	...	...	...	...	...	...
037394	7	3	1	2	...	1	...	...	...	...	...	...	...
038230	4	2	...	1	...	1	...	...	...	...	...	...	...
038858	3	2	...	...	...	1	...	...	...	...	...	...	...
040397	2	...	1	...	...	1	...	...	...	...	...	...	...
041593	3	1	1	...	...	1	...	...	...	...	...	...	...
042618	3	1	1	...	...	1	...	...	...	...	...	...	...
046588	3	2	...	...	...	1	...	...	...	...	...	...	...
051419	3	2	...	...	...	1	...	...	...	...	...	...	...
051866	4	2	1	...	...	1	...	...	...	...	...	...	...
054371	4	2	...	...	...	2	...	...	...	...	...	...	...
055575	5	3	1	...	...	1	...	...	...	...	...	...	...
HIP 36357	...	...	...	...	...	...	...	...	...	...	...	...	...
059747	1	...	...	...	...	1	...	...	...	...	...	...	...

Continued on Next Page...

TABLE 3.3 – Continued

HD Name	Total Obs	S-E Baselines				S-W Baselines				E-W Baselines			
		Single	Single?	Double	Double?	Single	Single?	Double	Double?	Single	Single?	Double	Double?
061606	...	...	...	...	...	...	...	...	...	...	...	...	...
063433	4	1	1	...	...	2	...	...	...	...	...	...	...
064606	...	...	...	...	...	...	...	...	...	...	...	...	...
064468	...	...	...	...	...	...	...	...	...	...	...	...	...
065430	1	...	...	...	...	1	...	...	...	...	...	...	...
065583	2	1	...	...	...	1	...	...	...	...	...	...	...
067228	4	3	1	...	...	...	...	...	...	...	...	...	...
068017	2	1	...	...	...	1	...	...	...	...	...	...	...
068255	2	1	1	...	...	...	...	...	...	...	...	...	...
072760	...	...	...	...	...	...	...	...	...	...	...	...	...
073350	...	...	...	...	...	...	...	...	...	...	...	...	...
073667	...	...	...	...	...	...	...	...	...	...	...	...	...
075767	...	...	...	...	...	...	...	...	...	...	...	...	...
076151	...	...	...	...	...	...	...	...	...	...	...	...	...
079096	12	4	...	1	6	1	...	...	...	...	...	...	...
079969	5	4	...	...	...	1	...	...	...	...	...	...	...
080715	2	1	...	...	...	1	...	...	...	...	...	...	...
082443	5	4	...	...	...	1	...	...	...	...	...	...	...
082885	4	1	1	...	...	2	...	...	...	...	...	...	...
087883	3	...	2	...	...	1	...	...	...	...	...	...	...
089269	2	1	...	...	...	1	...	...	...	...	...	...	...
090343	2	1	...	...	...	1	...	...	...	...	...	...	...
094765	2	1	...	...	...	1	...	...	...	...	...	...	...
096064	2	1	...	...	...	1	...	...	...	...	...	...	...
097334	2	1	...	...	...	1	...	...	...	...	...	...	...
097658	2	2	...	...	...	...	...	...	...	...	...	...	...
098230	15	6	3	...	...	3	2	1	...	...	...	...	...
098281	2	1	...	...	...	1	...	...	...	...	...	...	...
099491	3	1	1	...	...	1	...	...	...	...	...	...	...
099492	2	1	...	...	...	1	...	...	...	...	...	...	...
100180	3	2	...	...	...	1	...	...	...	...	...	...	...
101177	2	1	...	...	...	1	...	...	...	...	...	...	...
101206	2	1	...	...	...	1	...	...	...	...	...	...	...
104304	2	1	...	...	...	1	...	...	...	...	...	...	...
105631	4	1	...	...	...	2	1	...	...	...	...	...	...
108954	3	1	1	...	...	1	...	...	...	...	...	...	...
110833	5	1	1	...	...	2	1	...	...	...	...	...	...
112758	2	1	...	...	...	1	...	...	...	...	...	...	...
113449	2	1	...	...	...	1	...	...	...	...	...	...	...
114783	1	...	...	...	...	1	...	...	...	...	...	...	...
115404	4	2	1	...	...	1	...	...	...	...	...	...	...
116442	2	1	...	...	...	1	...	...	...	...	...	...	...
116443	2	1	...	...	...	1	...	...	...	...	...	...	...
116956	6	3	...	...	...	1	2	...	...	...	...	...	...
119332	3	1	1	...	...	1	...	...	...	...	...	...	...
121560	4	2	1	...	...	1	...	...	...	...	...	...	...
124292	3	2	...	...	...	1	...	...	...	...	...	...	...
124850	7	5	...	...	...	2	...	...	...	...	...	...	...
125455	3	2	...	...	...	1	...	...	...	...	...	...	...
128642	5	2	...	...	...	...	1	2	...	...	...	...	...
127334	4	1	...	...	...	1	1	...	...	1	...	...	...
128165	5	1	2	...	...	1	...	...	...	...	1	...	...
128311	2	...	...	1	...	1	...	...	...	...	...	...	...
130004	5	1	1	1	...	1	1	...	...	...	...	...	...
130307	2	1	...	...	...	1	...	...	...	...	...	...	...
132142	4	1	1	...	...	2	...	...	...	...	...	...	...
132254	3	1	...	...	...	1	...	...	...	1	...	...	...
135204	7	4	...	1	...	2	...	...	...	...	...	...	...
135599	2	1	...	...	...	1	...	...	...	...	...	...	...
136202	6	1	3	...	...	2	...	...	...	...	...	...	...
136713	2	1	...	...	...	1	...	...	...	...	...	...	...
136923	2	1	...	...	...	1	...	...	...	...	...	...	...

Continued on Next Page...

TABLE 3.3 – Continued

HD Name	Total Obs	S-E Baselines Single	S-E Baselines Single?	S-E Baselines Double	S-E Baselines Double?	S-W Baselines Single	S-W Baselines Single?	S-W Baselines Double	S-W Baselines Double?	E-W Baselines Single	E-W Baselines Single?	E-W Baselines Double	E-W Baselines Double?
137763	6	2	...	...	...	3	...	1	...	...	...	...	...
137778	4	...	1	...	...	3	...	...	...	...	...	...	...
139777	4	1	...	...	...	3	...	...	...	...	...	...	...
139813	3	1	...	...	...	2	...	...	...	...	...	...	...
139323	2	1	...	...	...	1	...	...	...	...	...	...	...
139341	4	...	1	...	...	1	1	...	...	1	...	...	...
141272	2	1	...	...	...	1	...	...	...	...	...	...	...
142267	4	2	1	...	...	1	...	...	...	...	...	...	...
144287	2	1	...	...	...	1	...	...	...	...	...	...	...
145675	3	1	...	...	...	...	1	...	...	1	...	...	...
145958	...	...	...	...	...	...	...	...	...	...	...	...	...
146361	30	29	1	...	...	...	...	...	...	...	...	...	...
146233	4	1	2	...	...	1	...	...	...	...	...	...	...
148653	1	1	...	...	...	...	...	...	...	...	...	...	...
149661	2	1	...	...	...	1	...	...	...	...	...	...	...
149806	3	1	...	...	...	2	...	...	...	...	...	...	...
151541	3	1	...	...	...	2	...	...	...	...	...	...	...
153557	4	...	...	...	...	3	1	...	...	...	...	...	...
154345	4	1	...	...	...	2	...	...	...	1	...	...	...
155712	4	1	...	...	...	2	1	...	...	...	...	...	...
157347	3	1	...	...	...	2	...	...	...	...	...	...	...
158633	3	1	...	...	...	2	...	...	...	...	...	...	...
159062	4	1	...	...	...	3	...	...	...	...	...	...	...
158614	3	1	1	...	...	1	...	...	...	...	...	...	...
159222	4	2	...	...	...	2	...	...	...	...	...	...	...
160346	2	1	...	...	...	1	...	...	...	...	...	...	...
161198	5	1	...	...	...	2	2	...	...	...	...	...	...
164922	2	1	...	...	...	1	...	...	...	...	...	...	...
165401	9	6	...	...	...	2	1	...	...	...	...	...	...
166620	4	2	...	...	...	...	1	...	...	1	...	...	...
175742	7	1	2	...	...	3	1	...	...	...	...	...	...
176377	5	2	...	...	...	3	...	...	...	...	...	...	...
178428	3	1	1	...	...	1	...	...	...	...	...	...	...
179957	5	2	...	...	...	2	1	...	...	...	...	...	...
180161	5	3	...	...	...	1	1	...	...	...	...	...	...
182488	4	2	...	...	...	2	...	...	...	...	...	...	...
185144	6	2	1	...	...	2	...	...	...	1	...	...	...
184385	2	1	...	...	...	1	...	...	...	...	...	...	...
185414	2	1	...	...	...	1	...	...	...	...	...	...	...
186858	...	...	...	...	...	...	...	...	...	...	...	...	...
189340	5	3	...	...	...	1	1	...	...	...	...	...	...
189733	3	1	...	...	...	2	...	...	...	...	...	...	...
190067	3	2	...	...	...	1	...	...	...	...	...	...	...
190404	2	1	...	...	...	1	...	...	...	...	...	...	...
190470	5	2	...	...	...	3	...	...	...	...	...	...	...
190771	5	3	...	...	...	2	...	...	...	...	...	...	...
191499	4	2	...	...	...	2	...	...	...	...	...	...	...
191785	3	2	...	...	...	1	...	...	...	...	...	...	...
192263	8	4	1	...	...	2	1	...	...	...	...	...	...
195564	4	1	...	...	...	2	1	...	...	...	...	...	...
197076	4	2	...	...	...	2	...	...	...	...	...	...	...
198425	4	2	...	...	...	1	1	...	...	...	...	...	...
200560	4	2	1	...	...	1	...	...	...	...	...	...	...
202751	3	1	...	...	...	1	1	...	...	...	...	...	...
208038	3	2	...	...	...	1	...	...	...	...	...	...	...
208313	3	2	...	...	...	1	...	...	...	...	...	...	...
210277	6	3	...	...	...	3	...	...	...	...	...	...	...
210667	3	1	1	...	...	1	...	...	...	...	...	...	...
211472	3	1	1	...	...	1	...	...	...	...	...	...	...
215152	3	1	...	...	...	2	...	...	...	...	...	...	...
216520	3	1	1	...	...	1	...	...	...	...	...	...	...
217107	2	1	...	...	...	1	...	...	...	...	...	...	...

Continued on Next Page...

TABLE 3.3 – Continued

HD Name	Total Obs	======= S-E Baselines ======				======= S-W Baselines ======				======= E-W Baselines ======			
		Single	Single?	Double	Double?	Single	Single?	Double	Double?	Single	Single?	Double	Double?
217813	3	1	1	...	...	1	...	...	...	...	...	...	...
218868	4	4	...	...	...	...	...	...	...	...	...	...	...
219134	2	1	...	...	...	1	...	...	...	...	...	...	...
219538	2	1	...	...	...	1	...	...	...	...	...	...	...
219623	3	2	...	...	...	1	...	...	...	...	...	...	...
220140	2	1	...	...	...	1	...	...	...	...	...	...	...
220182	2	1	...	...	...	1	...	...	...	...	...	...	...
220339	2	1	...	...	...	1	...	...	...	...	...	...	...
221354	3	2	...	...	...	1	...	...	...	...	...	...	...
221851	2	1	...	...	...	1	...	...	...	...	...	...	...
222143	4	3	...	...	...	1	...	...	...	...	...	...	...
224465	3	2	...	...	...	1	...	...	...	...	...	...	...

Given the Δmag limit of CHARA of about 2.5 in K-band, it is no surprise that all but one of the systems detected are double-lined spectroscopic binaries. Two additional double-lined binaries escaped detection – HD 158614, the 46.4-year SB2VB whose separation has closed-in from $0\farcs6$ in 1829 to $0\farcs3$ in 2005 (WDS), and HD 189340, the 4.9-year SB2VB with a $0\farcs2$ separation. The former was observed twice along S-E baselines and once along a S-W baseline, and the latter thrice along S-E baselines and twice along S-W baselines, with no evidence of separated fringes. Perhaps the orientation of the binary caused these fringes to be too wide.

Several single-lined spectroscopic binaries, and/or photocentric motion binaries (HD 17382, HD 24409, HD 32850, HD 64468, HD 64606, HD 65430, HD 110833, HD 128642, HD 142267, HD 144287, HD 113449, HD 160346, HD 161198) could have separations in the SFP detection range, but none of these were seen as SFP binaries. This is not surprising because the magnitude difference that causes spectroscopy or visual techniques to only pick up one star is likely too large for detection using CHARA. Finally, five more systems were resolved with speckle or other visual techniques, (HD 32923, HD 100180, HD 135204, HD 145958, HD 217107) but were not seen as SFP binaries. Many of these also have null detections by other observers, so these might be large-contrast pairs or have too-wide a separation for SFP detection.

So why did this study not detect more SFP binaries, filling-in the gap between spectroscopic and visual binaries? This gap is evident from other studies (Bouvier et al. 1997; Mason et al. 1998a), but not seen here. The reason is likely that this study is limited to

nearby stars within 25 pc, for which the angular separations probed by visual techniques translate to smaller linear separations as compared to more distant systems, allowing visual techniques to approach separations studied spectroscopically and thus closing the gap. Additionally, this sample of nearby solar-type stars represents one of the most extensively studied samples. Long-standing campaigns of high-precision radial velocity measurements (e.g., Udry et al. 1998; Marcy et al. 2004) as well as high-resolution visual techniques such as speckle interferometry (e.g., Mason et al. 1998b) have targeted such systems. Planet search teams have now collected radial velocities for many of these stars over some 12 years at a few $\mathrm{m\,s^{-1}}$ precision, and other surveys such as CORALIE and the CfA efforts have almost 30 years of coverage with ~ 0.5 $\mathrm{km\,s^{-1}}$ precision. With such intensive scrutiny, binaries can be detected for periods out to a few tens of years, and several such examples are covered in Chapter 6. As an example, a binary with a 30-year period can easily be identified by such surveys and, for a 1.5 $M_\odot$ total mass, will have a semi-major axis of $11''$. At the median distance of my sample of about 20 pc, this translates to an angular semimajor axis of $0\farcs6$ for a face-on orientation. For a 45° inclination, this separation gets projected down to $0\farcs4$. These limits are well beyond the limits of speckle and of SFP analysis, closing the gap for nearby systems. However, gaps between spectroscopic and visual techniques likely do exist for more distant systems, as the detection limit discussed above shrinks to about 80 mas for systems at a distance of 100 pc. Quist & Lindegren (2000) and references therein show evidence that while gaps may exist for distant systems, they are pretty slim, if at all present, for nearby ones. While limiting the chances for new discoveries, this gives us greater confidence in the

multiplicity statistics derived for such a well-studied nearby sample.

3.1.2 Astrometry from Separated Fringe Packets

For the few instances where separated fringes were seen, C. Farrington helped me derive the projected separations of the two stars in the sky and, where a pair of observations on different baselines was available, did the triangulation to derive actual separations and position angles. The procedure for this is the same as that described in Farrington (2008) but is briefly outlined below. First, the fringe envelope is extracted for each scan and added across all scans of an observation to obtain the summary fringe envelope, as discussed in the previous section. When two fringe peaks are recorded in a scan, an IDL code written by T. ten Brummelaar is used to fit Gaussian profiles to each peak, from which their offset is measured in microns and translated to angular separation in the sky using the projected baseline. This separation corresponds to the projection along the baseline's orientation as interferometry is not sensitive to offsets perpendicular to the baseline. For single-baseline measurements, this would be the final deliverable, i.e. a vector separation between the stars. In instances when multiple observations are available in a time span sufficiently short such that the actual binary motion is negligible, multiple vector projections can be used to triangulate the actual relative positions of the two stars, yielding a separation and position angle at an observational epoch. While the projection vectors rotate over multiple observations over the same baseline due to change in its orientation over time as viewed by the star, the triangulation is most effective if the observations are taken over different, especially roughly orthogonal, baselines.

Of the three stars for which SFP data were recorded (HD 3196, 79096, and 137763),

the first two could be analyzed for astrometry, while the third has only a single observation that clearly shows two fringes, but the data quality was not good enough for measurements. Table 3.4 lists the four vector separations for HD 3196 and six measures for HD 79096 that could be obtained in the manner described here. One of the measures of HD 79096 corresponds to the failure to detect two fringes on 2008 March 10. Based on the observations on the previous and subsequent day, which detected separated packets, I conclude that they were superimposed, and accordingly take this as a measure of zero separation because the orientation of the baseline was nearly perpendicular to the binary separation. As seen below, this fits the data points rather well. Column 1 of the table is the HD number with a component designation of the primary component of the SFP binary. Column 2 is the epoch of mid-exposure in MJD, Column 3 is the projected baseline in meters, and Column 4 is the baseline orientation in degrees measured from North towards East. Column 5 lists the vector separation projected along the baseline, measured from the primary to the secondary along the direction in Column 4. The first two measures of HD 3196 and the last four measures of HD 79096 could be used for triangulation to determine true offsets, as shown in Figure 3.7. The HD 3196 pair has a relative separation of $\rho = 106.9$ mas and $\theta = 335\overset{\circ}{.}3$ at 2007.618. No error bars could be determined because the triangulation was only based on two points. The HD 79096 pair has a relative position of $\rho = 63.70 \pm 0.32$ and $\theta = 285.48 \pm 0.28$ at 2007.187. These new measures are consistent with the known visual orbits for these pairs.

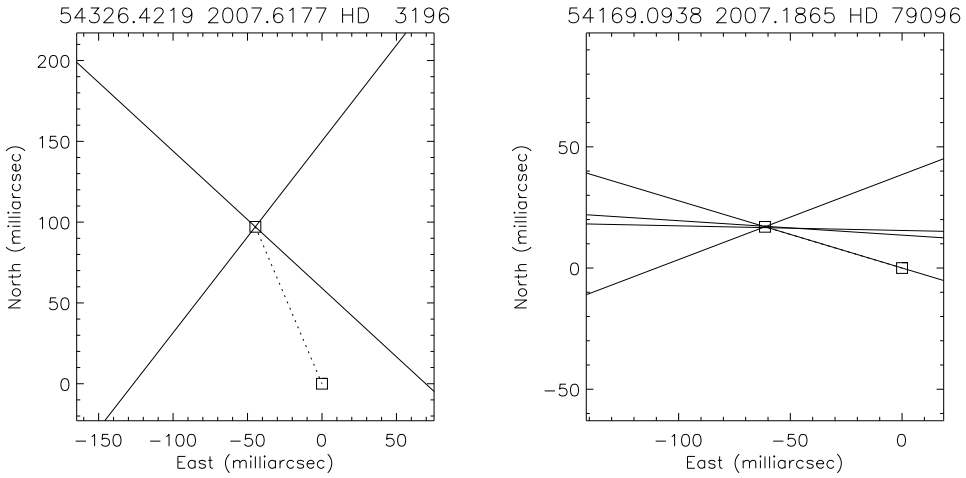

FIGURE 3.7: Triangulation of SFP measures for HD 3196A (left) and HD 79096A (right) corresponding to measures in Table 3.4. The primary is indicated by the square at the origin, and the secondary is the other square connected by the dotted line. The solid lines are perpendicular to the baseline orientation for each measure, and the secondary is at or near their intersections.

TABLE 3.4: Projected Separations for SFP Measurements

HD Name	MJD	Baseline Length (m)	Baseline Angle (deg)	Proj Sep (mas)
003196A	54326.350	321.783	40.32	70.321
003196A	54326.489	258.564	130.13	121.311
003196A	54360.424	244.127	125.50	63.402
003196A	54370.255	230.305	35.33	58.127
079096A	54156.375	297.271	1.18	−37.993
079096A	54156.429	301.887	167.35	57.323
079096A	54168.334	297.568	3.40	−19.573
079096A	54168.424	308.000	160.68	54.324
079096A	54169.283	304.197	15.49	0.000
079096A	54170.337	297.265	1.09	−22.343

3.2 Visual Orbits Derived using the CHARA Array

LBI has been regularly used to resolve short-period binaries and determine their orbits, yielding physical parameters such as mass, radius and luminosity of the component stars (e.g., Hummel et al. 1993; Boden et al. 1999; Torres et al. 2002). However, the shortest period spectroscopic binaries are out of reach of other interferometers, and hence have remained unresolved, yielding only partial orbital solutions and mass functions, but no component masses. An analysis of the targets investigated by this work revealed five double-lined spectroscopic binaries with periods ranging 0.27–10.98 days that had not yet been resolved interferometrically, while longer-period systems had been resolved with other long-baseline interferometers such as the Palomar Testbed Interferometer (PTI) (e.g., Torres et al. 2002) and the Mark III Interferometer (e.g., Hummel et al. 1995), or by other visual techniques (e.g., Hartkopf et al. 1996; Pourbaix 2000). Four of the five systems were studied with CHARA, the results from which are presented in the following subsections.

The shortest-period system (HD 133640B, 0.27-day period) among the five binaries selected as above could not be effectively studied because the spectroscopic binary is the secondary component of a longer period visual binary. The primary, HD 133640 (44 Bootis), is about $4''$ away and about 1.3 magnitudes brighter in the V-band. Despite many attempts, I could not consistently lock the secondary with the CHARA Tip-Tilt system, as it would often lock on the brighter primary. This binary is a W UMa type contact system with an increasing orbital period and has been extensively studied photometrically (Rovithis & Rovithis-Livaniou 1990, and references therein). However, due to observational and modeling

challenges of this system, I was unable to pursue it further.

During the course of this work, five additional systems have been determined to be SB2 without corresponding visual orbits, three of which are suitable candidates for future CHARA observations, while the other two (HD 111312 and HD 148704) are too far south. HD 80715 was reported as a binary but without a full orbital solution (Gliese & Jahreiß 1991; Halbwachs et al. 2003), but the CfA survey efforts have now derived a 3.8-day SB2 solution (see § 6.2.2). HD 101177B is the secondary of a 9″ visual pair and itself a 23.5-day spectroscopic binary with a single-lined solution in DM91 and a double-lined solution (Mazeh et al. 1997) based on three velocity measurements of the secondary. HD 144284 is a 3.1-day SB2 (Mazeh et al. 2002) composed of an F8 primary and an M-dwarf companion. The estimated ΔK of 2.7 for this $q = 0.4$ pair is high, but within the range for which visibility modulations could be seen. Each of these systems is planned to be observed during 2009.

The following sections present the results for the four systems which were observed with CHARA to obtain visual orbits and component masses as described in Raghavan et al. (2009). These results, with the exception of the publication for HD 146361 (Raghavan et al. 2009), are all preliminary and need further analysis and, in some case, more observations.

3.2.1 The Visual Orbit of σ^2 CrB (HD 146361)

The results for this system have been published in the Astrophysical Journal (Raghavan et al. 2009), representing the first visual orbit derived using CHARA visibilities. This work leveraged spectroscopic results from D. Latham and G. Torres at CfA and utilized the longest baselines of the CHARA Array to resolve the 1.1-day spectroscopic binary, the shortest-

period system yet resolved. Because this work was undertaken and completed as part of this thesis effort, the entire text of that publication is reproduced in *Appendix* E.

3.2.2 The Visual Orbit of HD 8997

Forty three calibrated visibility measurements were obtained over five nights for this star using the CHARA Array's E1–E2 baseline in 2008 October and November. For the first two nights, I used HD 10697, a planet host star, as a calibrator. While there is no evidence of this star being a binary, the work done for Baines et al. (2008a) showed a possible pattern in the residuals for its diameter calculation, so I used HD 10477 for the final three nights, which was the calibrator used by Baines et al. and believed to be well-behaved. The data and a preliminary orbital solution are presented below, but this star needs more observations.

TABLE 3.5: Interferometric Visibilities for HD 8997

MJD	**Obs** V	σ_V	**Model** V	$(O-C)_V$	u **(m)**	v **(m)**	**HA (h)**
54769.31961	0.664	0.054	0.809	−0.145	−47.98	−39.24	0.91
54769.32614	0.753	0.081	0.832	−0.079	−46.49	−39.96	1.07
54769.34215	0.771	0.078	0.886	−0.115	−42.50	−41.62	1.45
54769.34819	0.827	0.090	0.905	−0.078	−40.89	−42.21	1.60
54769.35428	0.858	0.074	0.922	−0.064	−39.20	−42.78	1.74
54769.36051	0.872	0.068	0.939	−0.067	−37.40	−43.34	1.89
54769.36796	0.935	0.076	0.956	−0.021	−35.20	−43.96	2.07
54769.37529	0.849	0.083	0.971	−0.122	−32.94	−44.55	2.25
54769.38220	0.861	0.088	0.982	−0.121	−30.75	−45.06	2.42
54769.38929	0.947	0.104	0.990	−0.043	−28.45	−45.55	2.59
54793.19142	0.334	0.058	0.378	−0.044	−57.86	−31.39	−0.60
54793.20114	0.332	0.024	0.367	−0.035	−56.88	−32.70	−0.36
54793.20992	0.340	0.028	0.360	−0.020	−55.82	−33.86	−0.15
54793.21943	0.346	0.044	0.354	−0.008	−54.48	−35.08	0.07
54793.23076	0.344	0.051	0.350	−0.007	−52.65	−36.48	0.35

Continued on Next Page...

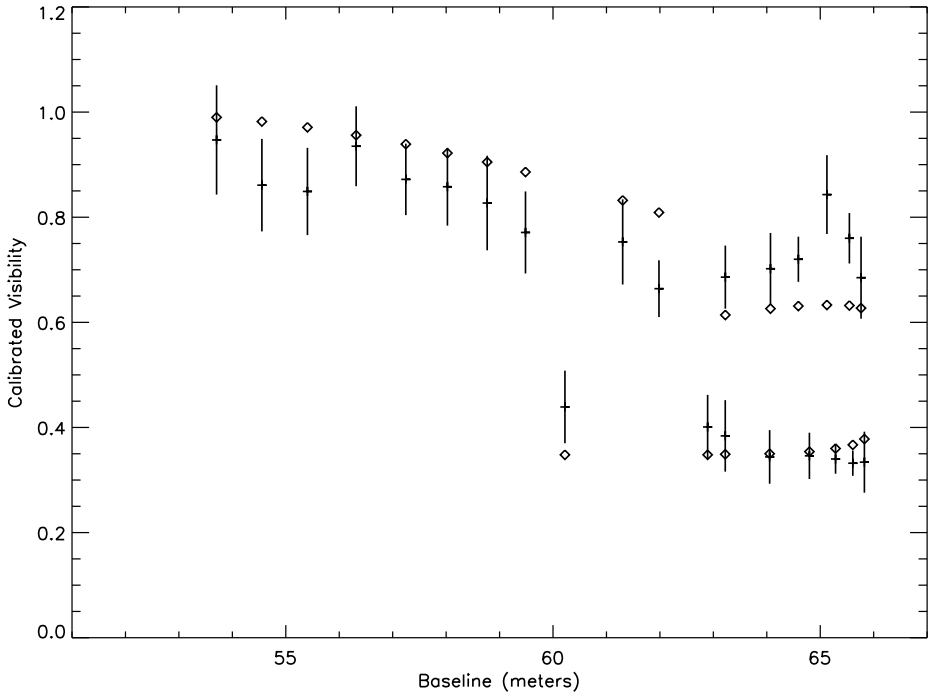

FIGURE 3.8: Calibrated visibility measurements for HD 8997 versus the projected baseline. The plus signs are the calibrated visibilities with vertical error bars, and the diamonds are the calculated visibilities for the best-fit orbit. Table 3.5 lists the numeric values corresponding to this plot.

TABLE 3.5 – Continued

MJD	**Obs** V	σ_V	**Model** V	$(O-C)_V$	u **(m)**	v **(m)**	**HA (h)**
54793.24114	0.384	0.068	0.349	0.036	−50.73	−37.73	0.59
54793.25135	0.401	0.061	0.348	0.053	−48.60	−39.92	0.84
54793.27051	0.439	0.069	0.348	0.091	−44.13	−40.98	1.30
54794.19223	0.685	0.078	0.627	0.058	−57.52	−31.88	−0.51
54794.20040	0.760	0.048	0.632	0.128	−56.65	−32.97	−0.32
54794.21060	0.843	0.075	0.633	0.210	−55.36	−34.30	−0.07
54794.22001	0.720	0.043	0.631	0.089	−53.96	−35.50	0.06
54794.22764	0.702	0.068	0.626	0.076	−52.69	−36.45	0.34
54794.23816	0.686	0.060	0.614	0.071	−50.74	−37.72	0.59

Table 3.5 lists the 24 observed visibilities over the three nights with HD 10477 as calibrator along with the corresponding epoch at mid-exposure, uncertainty of the visibility measurement, model visibility for the best-fit orbit and residuals, baseline projections in meters along East-West (u) and North-South (v) directions, and the hour angle of the target. Similar to the approach in Raghavan et al. (2009), the visual orbit solution uses the spectroscopic elements from the CfA measurements, which are presented in § 6.2.2, propagates their 1σ errors to derive the uncertainty of the visual parameters derived here, namely α, i, Ω, and $\Delta K'$, constraining α and i by the $a \sin i$ from spectroscopy and the FvL07 parallax. Figure 3.8 plots the observed visibilities along with their uncertainties and corresponding model values. There appear to be some systematic patterns in the residuals and the phase coverage of the observations is weak. Table 3.6 lists the visual orbit elements for the above solution, which lead to component mass estimates of 1.446 ± 0.122 and 1.193 ± 0.101, too high for these K dwarfs. More observations are needed to determine the visual orbit for this pair, perhaps with additional calibrators.

TABLE 3.6: Visual Orbit Solution for HD 8997

Orbital Parameter	**Value**	**Source**
Adopted values		
Period (days)	10.98372 ± 0.00026	1
e	0.0368 ± 0.0025	1
T_0 (JD - 2400000)	49085.08 ± 0.16	1
ω (deg)	179.2 ± 5.1	1
$\theta_{\rm p}$ (mas)	0.31 ± 0.03	2
$\theta_{\rm s}$ (mas)	0.26 ± 0.03	2
Visual orbit parameters		
α (mas)	5.63 ± 0.13	3

Continued on Next Page...

TABLE 3.6 – Continued

Orbital Parameter	Value	Source
i (deg)	41.2 ± 1.4	3
Ω (deg)	50 ± 14	3
$\Delta K'$	0.74 ± 0.03	3
Reduced χ^2	0.66	3
Physical parameters		
M_p ($M_\odot$)	1.446 ± 0.122	3
M_s ($M_\odot$)	1.193 ± 0.101	3

NOTES.—Source codes: 1 = From the spectroscopic solution in § 6.2.2; 2 = Estimated using Gray et al. (2003) spectral types and FvL07 parallaxes, with an adopted 10% error; 3 = This work.

3.2.3 The Visual Orbit of HD 45088

Forty calibrated visibility measurements were obtained over four nights for this star using the CHARA Array's E1–E2 baseline in 2008 October and November. The calibrator used for all nights was HD 43947, but, for the last two nights, HD 43042 was also used as an additional calibrator for a total of nine brackets. On final data analysis, the fit to the second calibrator points were not as good, so they were eliminated from the final solution. Table 3.7 lists the 31 observed visibilities used in deriving the visual orbit, in the same format as in Table 3.5. Figure 3.9 plots the observed visibilities along with their uncertainties and corresponding model values for the visual orbit derived as described in § 3.2.2.

TABLE 3.7: Interferometric Visibilities for HD 45088

MJD	**Obs** V	σ_V	**Model** V	$(O-C)_V$	u **(m)**	v **(m)**	**HA (h)**
54767.41212	0.779	0.100	0.788	−0.008	−59.16	−24.51	−1.95
54767.41988	0.865	0.100	0.790	0.075	−59.42	−25.45	−1.76
54767.42666	0.861	0.073	0.794	0.067	−59.53	−26.26	−1.60
54767.43298	0.820	0.104	0.799	0.021	−59.53	−27.02	−1.44
54767.43920	0.914	0.088	0.805	0.110	−59.45	−27.77	−1.30
54767.46480	0.602	0.098	0.839	−0.237	−58.14	−30.83	−0.68
54767.47392	0.857	0.077	0.855	0.002	−57.30	−31.90	−0.46
54767.48083	0.718	0.115	0.868	−0.150	−56.55	−32.69	−0.29
54767.48751	0.826	0.095	0.881	−0.055	−55.71	−33.45	−0.13
54767.49464	0.825	0.094	0.895	−0.070	−54.71	−34.25	0.04
54767.50635	0.852	0.113	0.918	−0.066	−52.82	−35.53	0.32
54767.51346	0.936	0.172	0.932	0.004	−51.54	−36.28	0.49
54767.51978	0.803	0.100	0.944	−0.141	−50.31	−36.93	0.64
54767.52609	0.902	0.113	0.956	−0.053	−49.01	−37.57	0.80
54767.53284	1.119	0.172	0.966	0.153	−47.53	−38.23	0.96
54768.42211	0.245	0.026	0.247	−0.002	−59.51	−26.04	−1.64
54768.43432	0.256	0.029	0.244	0.011	−59.49	−27.51	−1.35
54768.44509	0.228	0.020	0.245	−0.016	−59.18	−28.81	−1.09
54768.45324	0.245	0.021	0.249	−0.004	−58.76	−29.79	−0.89
54768.46295	0.276	0.035	0.260	0.015	−58.06	−30.93	−0.66
54768.47167	0.342	0.059	0.278	0.063	−57.25	−31.95	−0.45
54793.43328	0.595	0.077	0.576	0.019	−53.18	−35.30	0.27
54793.44167	0.566	0.117	0.618	−0.052	−51.69	−36.20	0.47
54793.44837	0.785	0.115	0.652	0.133	−50.40	−36.89	0.63
54793.45545	0.705	0.088	0.689	0.017	−48.93	−37.60	0.80
54793.46250	0.682	0.074	0.725	−0.044	−47.38	−38.29	0.97
54794.48268	0.710	0.079	0.815	−0.105	−41.71	−40.36	1.52
54794.48894	0.866	0.110	0.822	0.044	−39.99	−40.88	1.68
54794.49560	0.825	0.124	0.829	−0.005	−38.11	−40.40	1.84
54794.50473	0.810	0.136	0.839	−0.029	−35.42	−42.08	2.06
54794.51207	0.807	0.121	0.846	−0.038	−33.16	−42.59	2.23

Table 3.8 lists the visual orbit elements for the above solution. To obtain a good fit to the visibility data, I had to vary T_0 wider than the 1σ limits of the spectroscopic solution. The

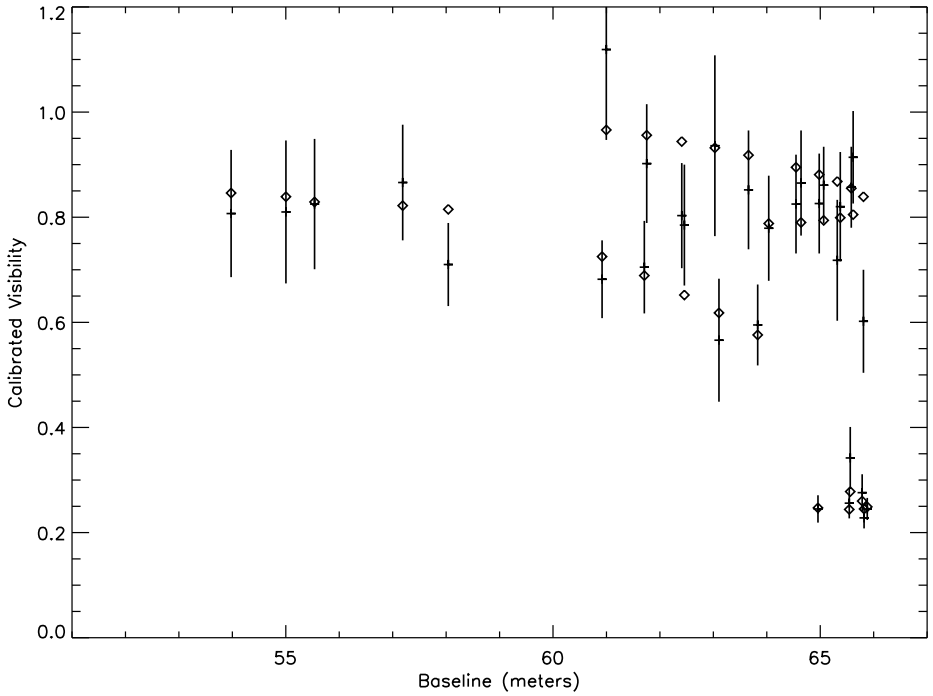

FIGURE 3.9: Calibrated visibility measurements for HD 45088 versus the projected baseline. The plus signs are the calibrated visibilities with vertical error bars, and the diamonds are the calculated visibilities for the best-fit orbit. Table 3.7 lists the numeric values corresponding to this plot.

value of epoch of periastron obtained from the visual orbit is 0.57 days or about 2σ away using the uncertainties from the visual orbit but about 20σ away using the lower uncertainties from the spectroscopic solution. Limiting the epoch to within 1σ of the spectroscopic solution leads to a higher χ^2, but the visual orbit parameters remain well-constrained to the values presented here to within 1σ. While the resulting mass estimates are consistent with the spectral types, the uncertainties are large, due to the relatively large errors for the derived angular semimajor axis (3.4%) as well as for the FvL07 parallax (2.3%).

TABLE 3.8: Visual Orbit Solution for HD 45088

Orbital Parameter	**Value**	**Source**
Adopted values		
Period (days)	6.991888 ± 0.000010	1
e	0.1461 ± 0.0025	1
ω (deg)	78.9 ± 1.0	1
$\theta_{\rm p}$ (mas)	0.49 ± 0.05	2
$\theta_{\rm s}$ (mas)	0.43 ± 0.04	2
Visual orbit parameters		
T_0 (JD - 2400000)	52228.8 ± 0.3	1
α (mas)	5.61 ± 0.19	3
i (deg)	108.5 ± 2.5	3
Ω (deg)	125 ± 4	3
$\Delta K'$	0.53 ± 0.04	3
Reduced χ^2	0.75	3
Physical parameters		
M_p ($M_\odot$)	0.831 ± 0.101	3
M_s ($M_\odot$)	0.709 ± 0.087	3

NOTES.—Source codes: 1 = From the spectroscopic solution in § 6.2.2; 2 = Estimated using Gray et al. (2003) spectral types and FvL07 parallaxes, with an adopted 10% error; 3 = This work.

3.2.4 The Visual Orbit of HD 223778

Forty eight calibrated visibility measurements were obtained over nine nights for this star using the CHARA Array's S1–S2 and E1–E2 baselines in 2008 June–November. The calibrator used for all nights was HD 219485, an apparent single star with an estimated angular diameter of 0.224 ± 0.003 mas, obtained by fitting $BVRIJHK$ photometry to spectral energy distribution (SED) models from R. L. Kurucz, available at `http://cfaku5.cfa.harvard.edu`. Table 3.9 lists the 48 observed visibilities that were used in deriving the visual orbit, in the

same format as in Table 3.5. Figure 3.10 plots the observed visibilities along with their uncertainties and corresponding model values, showing the excellent phase coverage of these data.

TABLE 3.9: Interferometric Visibilities for HD 223778

MJD	**Obs** V	σ_V	**Model** V	$(O-C)_V$	u **(m)**	v **(m)**	**HA (h)**
54639.43052	0.663	0.067	0.639	0.024	10.54	22.61	−3.37
54639.44842	0.646	0.070	0.661	−0.015	8.66	23.65	−2.94
54639.46030	0.659	0.078	0.681	−0.022	7.34	24.24	−2.66
54639.47252	0.710	0.093	0.704	0.005	5.95	24.73	−2.36
54639.48446	0.711	0.068	0.730	−0.019	4.57	25.12	−2.07
54639.49592	0.695	0.060	0.756	−0.062	3.21	25.39	−1.80
54640.42254	0.798	0.068	0.922	−0.124	11.07	22.26	−3.50
54640.43569	0.827	0.066	0.950	−0.123	9.73	23.09	−3.19
54640.44800	0.878	0.084	0.972	−0.094	8.41	23.77	−2.89
54640.46041	0.835	0.107	0.988	−0.153	7.04	24.35	−2.59
54640.47249	0.859	0.106	0.996	−0.137	5.66	24.82	−2.30
54640.48496	0.857	0.075	0.998	−0.141	4.19	25.20	−2.00
54640.49713	0.865	0.095	0.992	−0.126	2.75	25.46	−1.71
54642.48679	0.540	0.038	0.496	0.044	3.32	25.37	−1.82
54653.43650	0.561	0.048	0.610	−0.049	5.61	24.84	−2.29
54653.44289	0.534	0.044	0.583	−0.049	4.86	25.04	−2.13
54653.44951	0.471	0.078	0.556	−0.085	4.09	25.22	−1.98
54653.45650	0.550	0.061	0.528	0.022	3.25	25.38	−1.81
54653.46249	0.510	0.041	0.504	0.006	2.53	25.49	−1.66
54653.46877	0.438	0.048	0.481	−0.044	1.78	25.57	−1.51
54653.47551	0.448	0.060	0.458	−0.010	0.96	25.62	−1.35
54653.48168	0.483	0.044	0.437	0.046	0.21	25.65	−1.20
54653.48768	0.457	0.051	0.418	0.039	−0.52	25.64	−1.06
54653.49392	0.469	0.048	0.400	0.069	−1.27	25.61	−0.51
54654.39421	0.677	0.126	0.574	0.103	9.97	22.95	−3.24
54654.40082	0.590	0.084	0.565	0.024	9.28	23.34	−3.08
54654.40754	0.547	0.043	0.558	−0.011	8.55	23.70	−2.92
54654.41317	0.578	0.058	0.553	0.025	7.94	23.99	−2.78
54654.41906	0.542	0.030	0.549	−0.007	7.28	24.26	−2.64
54674.31861	0.634	0.053	0.651	−0.017	12.05	21.54	−3.75
54674.32518	0.660	0.062	0.655	0.005	11.42	22.01	−3.59

Continued on Next Page...

TABLE 3.9 – Continued

MJD	Obs V	σ_V	Model V	$(O-C)_V$	u (m)	v (m)	HA (h)
54674.33108	0.564	0.045	0.660	−0.097	10.84	22.41	−3.45
54674.33718	0.654	0.049	0.666	−0.012	10.22	22.80	−3.30
54674.34314	0.702	0.042	0.673	0.029	9.60	23.16	−3.16
54674.40283	0.743	0.046	0.783	−0.040	2.81	25.45	−2.72
54674.40866	0.719	0.072	0.796	−0.078	2.11	25.54	−1.58
54674.41447	0.772	0.078	0.810	−0.038	1.41	25.60	−1.44
54792.20403	0.698	0.042	0.614	0.084	−44.68	−45.15	1.25
54792.21701	0.762	0.052	0.806	−0.045	−41.28	−48.59	1.56
54793.14329	1.000	0.102	0.961	0.039	−55.78	−27.22	−0.15
54793.15142	0.973	0.097	0.986	−0.013	−54.64	−29.96	0.05
54793.15817	0.907	0.076	0.986	−0.078	−53.58	−32.19	0.21
54793.16409	0.917	0.075	0.969	−0.052	−52.57	−34.10	0.36
54793.17011	0.932	0.052	0.937	−0.005	−51.48	−36.02	0.50
54794.12873	0.141	0.015	0.147	−0.006	−57.17	−23.14	−0.43
54794.13731	0.295	0.044	0.188	0.107	−56.20	−26.07	−0.23
54794.15074	0.303	0.034	0.308	−0.005	−54.32	−30.64	0.10
54794.16061	0.357	0.032	0.398	−0.041	−52.71	−33.86	0.34

Table 3.10 lists the visual orbit elements for the above solution. If wider excursions are allowed for P, e, and T_0, the visual orbit seems to prefer a smaller period and larger eccentricity, but the visual orbit elements of interest remain very well constrained to the values presented here, which were obtained by limiting the spectroscopic parameters to 1σ variation. The resulting component mass estimates have uncertainties below 2%.

TABLE 3.10: Visual Orbit Solution for HD 223778

Orbital Parameter	Value	Source
Adopted values		
Period (days)	7.75442 ± 0.00052	1
e	0.0162 ± 0.0035	1

Continued on Next Page...

TABLE 3.10 – Continued

Orbital Parameter	**Value**	**Source**
T_0 (JD - 2400000)	52232.28 ± 0.23	1
ω (deg)	279 ± 11	1
$\theta_{\rm p}$ (mas)	0.66 ± 0.06	2
$\theta_{\rm s}$ (mas)	0.62 ± 0.06	2
Visual orbit parameters		
α (mas)	8.12 ± 0.04	3
i (deg)	50.2 ± 0.4	3
Ω (deg)	126.8 ± 1.3	3
$\Delta K'$	0.33 ± 0.03	3
Reduced χ^2	1.12	3
Physical parameters		
M_p ($M_\odot$)	0.786 ± 0.014	3
M_s ($M_\odot$)	0.748 ± 0.014	3

NOTES.—Source codes: 1 = From the spectroscopic solution in § 6.2.2; 2 = Estimated using Gray et al. (2003) spectral types and FvL07 parallaxes, with an adopted 10% error; 3 = This work.

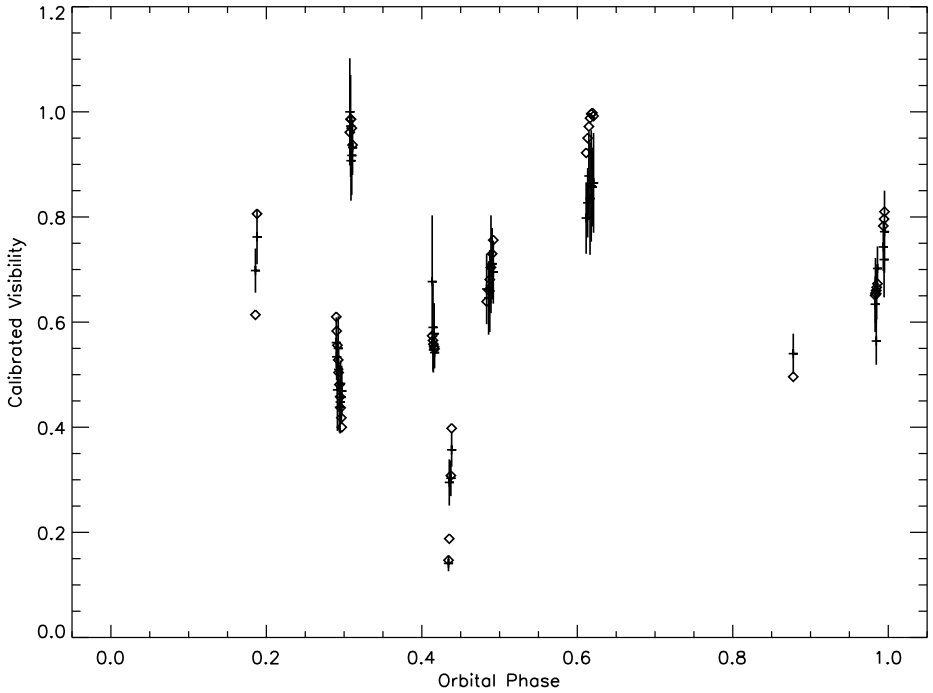

FIGURE 3.10: Calibrated visibility measurements for HD 223778 versus the orbital phase. The plus signs are the calibrated visibilities with vertical error bars, and the diamonds are the calculated visibilities for the best-fit orbit. Table 3.9 lists the numeric values corresponding to this plot.

The true delight is in the finding out rather than in the knowing.

—— *Isaac Asimov*

– 4 –

Common Proper Motion Results

Visual companions span the widest range of separations among binaries, with companions detected within a milli-arcsec by the high resolution techniques covered in the previous chapter and out to several hundred arcseconds by techniques such as common proper motion (CPM) detection. This chapter describes the methods of this effort for observing these wide binaries and presents their results.

4.1 Identification and Confirmation of CPM Companions

Nearby stars, like the ones of the current sample, generally have a larger proper motion than their distant counterparts. This is due to relative motion between the the Sun and the stars, which is visually more pronounced for nearby stars, much like the larger apparent motion of closer trees when riding in a train. This large proper motion becomes a handy tool in identifying widely separated companions, which can be readily identified as stars with similar apparent movement across the sky. The technique involves blinking two digital images, taken many years apart, of the sky around each primary to identify CPM pairs. Candidate companions thus revealed can then be confirmed of refuted by follow-up photometry. This method is not effective for discovering close companions because the bright primaries saturate the images out to several arcseconds. For the wide pairs suited to this technique, orbital

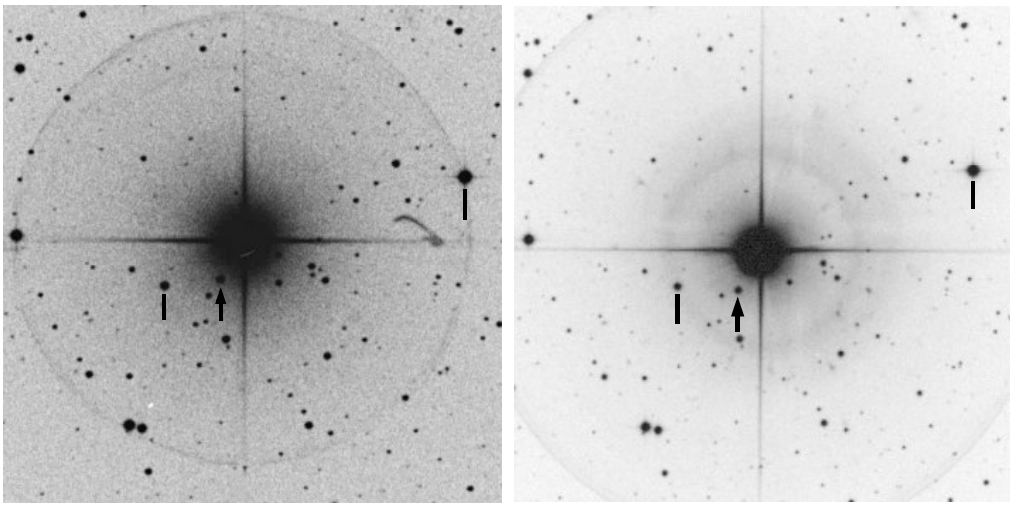

FIGURE 4.1: Example of the images blinked to identify CPM companions. The 10′ square images from the DSS are for HD 9826 (υ And) with north up and east to the left. The epoch of the left image is 1953.71 and for the right image is 1989.77. The arrow marks the CPM companion at a separation of 56″ and the lines identify WDS entries which are field stars. The primary's proper motion is $0\farcs42\,\mathrm{yr}^{-1}$ at 204°.

periods are upwards of several thousand years, and any orbital motion is negligible over the time interval between the two images. Hence, gravitationally bound stars are seen as linked pairs moving in unison across the field of generally more distant and largely stationary stars in the images. Figure 4.1 shows the two images blinked for HD 9826 (υ And), allowing the identification of the CPM companion (marked by the arrow), as well as the detection of two WDS entries as unrelated field stars with minimal proper motion (marked by vertical lines). The effect, while noticeable in these printed images, is readily apparent when they are blinked numerous times in quick succession.

The primary source of the archival images leveraged in this effort is the multi-epoch STScI Digitized Sky Survey[1] (DSS). This resource provides all-sky images for multiple epochs, which

[1] `http://stdatu.stsci.edu/cgi-bin/dss_form`

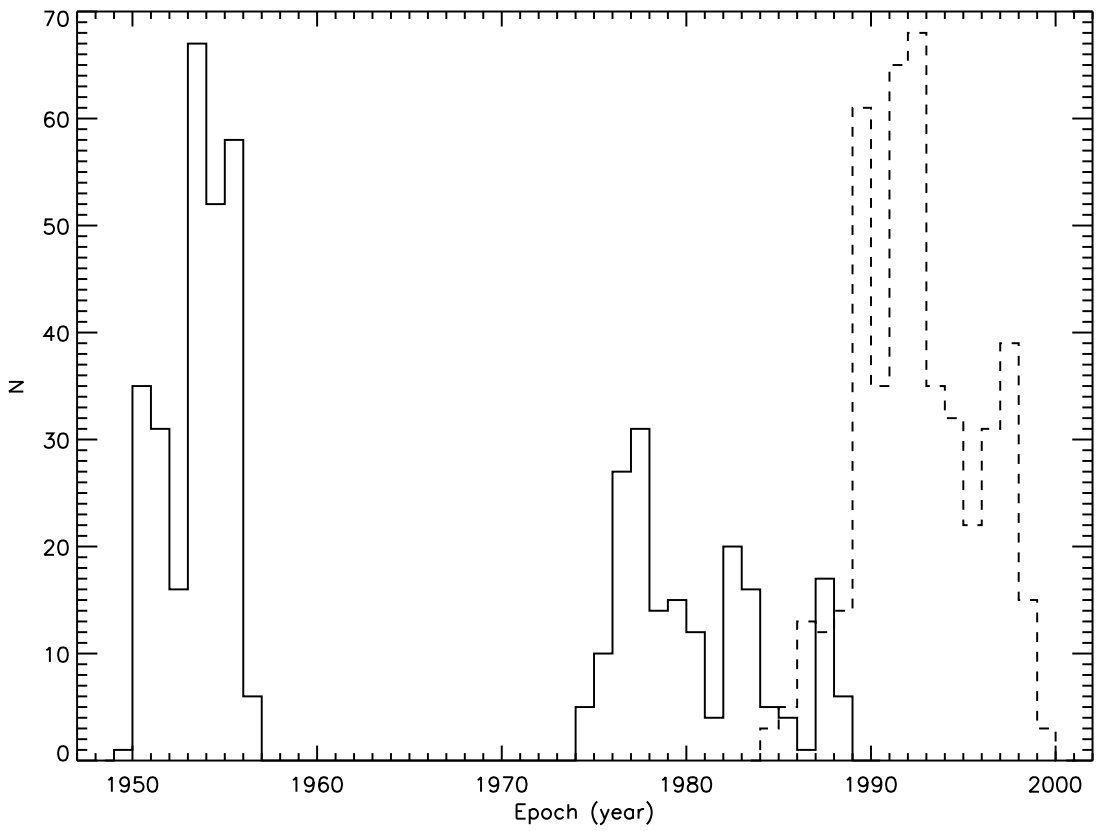

FIGURE 4.2: The epoch distribution of the DSS and SSS images used for blinking to identify CPM companions. A pair of images were blinked for each target, with the earlier epoch identified by the solid line and the later epoch by the dashed line.

can be downloaded in FITS format for a specified central position and size. In some cases, when the time interval between the two DSS images was not sufficient to easily identify the proper motion of the primary star, SuperCOSMOS Sky Survey (Hambly et al. 2001, SSS) images were used for the earlier epoch, significantly increasing the apparent motion seen upon blinking. Figure 4.2 shows the epoch-distribution of the images blinked. The earlier epoch distribution (solid lines) is bimodal, with 266 frames from 1949–1957 with a median of 1953.77 and 187 frames from 1974–1989 with a median of 1979.71. The later epoch (dashed

line) is more tightly constrained, with all 453 frames obtained during 1984–2000 with a median 1992.28.

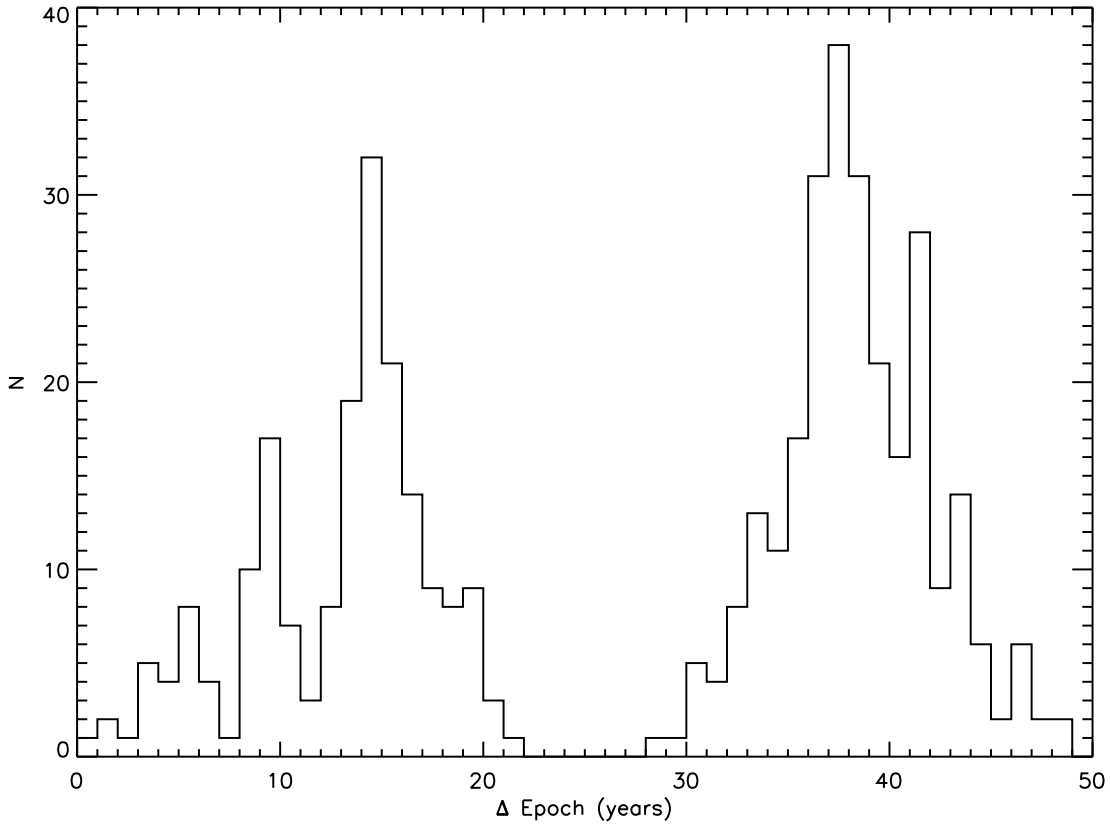

FIGURE 4.3: The distribution of the time interval between the images blinked for each target.

The relevant parameters that determine the effectiveness of this method are the proper motion of the primary star and the time interval between the blinked images for each target, which result in the total motion seen upon blinking. While the characteristics of the individual images such as the relative translation or rotation between the frames and the field of stars available determine the limits of motion detectable upon blinking, experience has shown that total motions under $2''$ are seldom detectable and those under $\sim 4''$ are often

only marginally detectable. Figure 4.3 shows the distribution of the time interval between the images blinked, which again is bimodal. For 187 targets, the images used span a time interval of 1–22 years with a median of 14.1 years, and the remaining 266 targets span of 28–49 years with a median of 38.1 years. Figure 4.4 shows the distribution of the primary's total transverse motion over the duration spanning the images blinked, excluding 12 targets with motions greater than 50″. Forty six targets have transverse motions under 2″ and 97 targets have motions under 4″. As discussed above, detectability of the motion is also affected by individual characteristics of the images used, so these numbers only serve as a rough guide and as a test of the results. When blinking the images, I made individual notes about the detectability of the motion. Of the 453 image-pairs blinked, 44 were flagged as targets whose motion could not be detected and an additional 43 were noted as marginally detectable. These numbers correspond well to the limits identified above. For 366 of the 453 targets investigated, this technique proved to be fully effective in determining CPM companions, and somewhat effective for an additional 43, providing excellent coverage.

This technique is well suited to search for CPM companions wider than $\sim$ 15–30″ from the primary, as companions closer than this are often buried in the saturation around the bright primaries. However, in many instances, bright companions inside the saturation region can be identified by twin, comoving diffraction spikes. Choosing an outer limit is a matter of picking the optimum size of the images blinked. A larger image size will naturally cover a larger search space, but this gain is offset by a diminishing detection capability due to a smaller apparent motion. Additionally, while the reduction code attempts to compensate

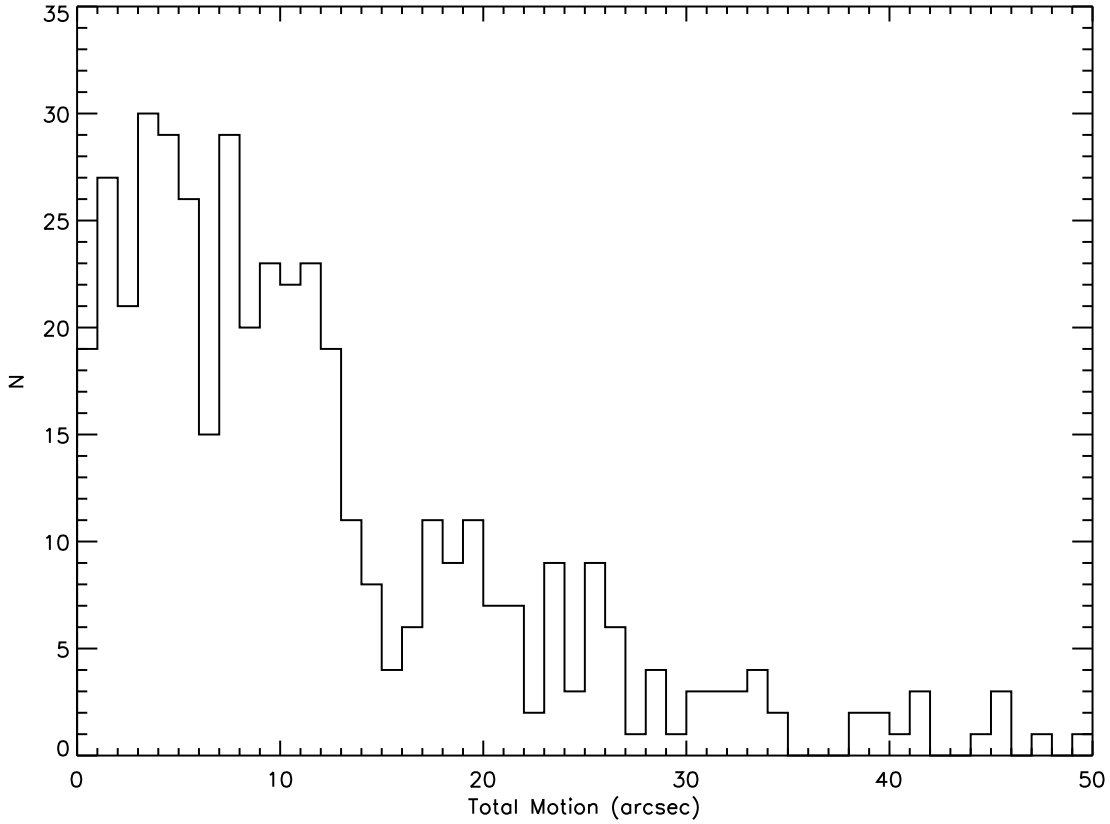

FIGURE 4.4: The distribution of the transverse motion of the primary star seen on blinking the images.

for any translation or rotation between the images blinked, the residual effects could be more pronounced for larger images, causing even the stationary stars to wobble, hindering the detection of CPM candidates. To optimize across these effects, I followed a two-step process as described below. First, I blinked images, 10′ on each side, to thoroughly inspect a search radius of 300″ around each primary. Then, systems closer than 20 pc were blinked again using 22′ square images to expand the search region out to 660″, while systems at a distance of 20–25 pc were blinked using 15′ square images to explore out to 450″. The larger angular size searched for the nearby systems was chosen to enable a similar-sized *linear*

search space for all stars. The subsample of stars within 20 pc contains 238 primaries and has a median distance of 15.6 pc, translating the 660″ angular radius searched to a linear radius of approximately 10,000 AU, while the farther subsample of 215 primaries has a median distance of 22.4 pc, also corresponding to a linear radius of $\sim$ 10,000 AU for the angular radius of 450″. Images larger than 15′ were blinked as four sub-images of 15′ square from each corner of the image, allowing for a closer inspection. Figure 4.5 shows the distribution of the linear projected separation searched around each primary, demonstrating that most systems were effectively searched out to a separation of $\sim$ 10 000 AU. While companions farther than this separation limit have been reported (e.g., Latham et al. 1991; Poveda et al. 1994), the range selected here enables an effective search of the region containing the vast majority of companions. Only 18 of the closest systems were inspected out to less than a 5 000 AU separation from the primary. The blinking was performed with an IDL code that compensated for any relative translation or rotation between the images, scaled them appropriately, displayed a subtracted image and blinked them 15 times with a 0.1 second interval at the user's request to help identify companions. The relative position of the candidate companions thus identified were then captured by clicking first on the primary and then on the companion. The code is included in *Appendix* C.4.

The 366 primaries adequately inspected using this technique revealed 78 candidate companions among 73 primaries, while the remaining 293 primaries revealed no CPM candidates. Fifty three of these were noted as compelling, and the remaining 25 were identified as possibilities deserving follow-up efforts. Table 4.1 summarizes the results of this effort, listing each

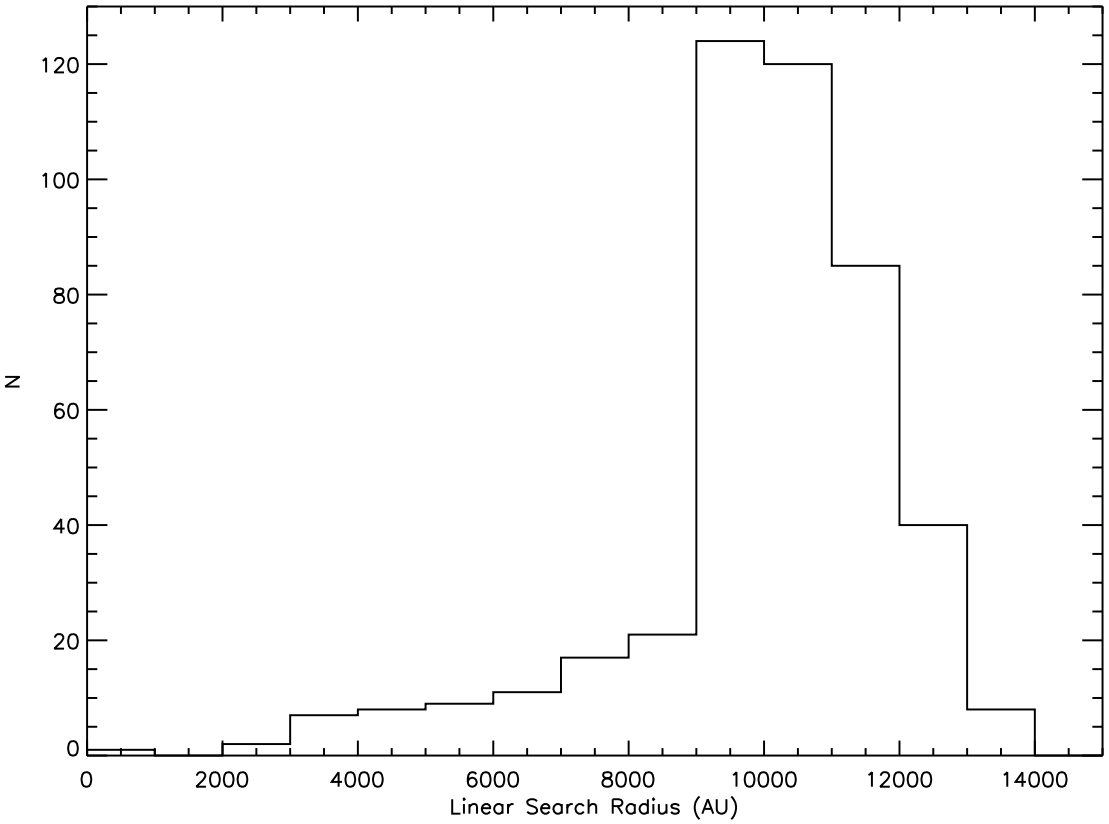

FIGURE 4.5: The distribution of the linear projected separation from the primary searched for CPM companions.

primary (Column 1) along with the epochs of the images used for blinking (Columns 2 and 3), the FvL07 proper motion of the primary (Columns 4 and 5), the total motion between the image-epochs (Column 6), and the blink result (Column 7) identifying whether the motion was detectable and if any candidate companions were identified (see the table footnote for an explanation of the codes used in this column). Column 8 lists the final status of the companion, confirmed companions are flagged as "Yes", and refuted candidates as "No". The methods used to make this determination are described in the following paragraph, and individual footnotes in the table identify the reason for each situation. The last column

identifies the candidate companion either by its HD, HIP, or other name, or by its position relative to the primary. The separation and position angles listed for the companions are measured from the more recent image and are approximate. They are good to within an arcsecond and a degree, respectively for wide companions, but the errors could be larger for close pairs identified by overlapping PSF or twin diffraction spikes. A few pairs, wider than the limits inspected as described above, have nevertheless been published by other efforts, especially in the CNS catalogs. An adequately large image was blinked to check if they exhibit CPM as well, and pairs passing this test are also included in Table 4.1.

TABLE 4.1: Archival Image Blink Results

Name	Image Epochs Epoch 1	Epoch 2	μ_α (mas yr^{-1})	μ_δ (mas yr^{-1})	Total μ	Blink Result	Companion Status	ID
HD 000123	1954.75	1992.73	247.24 ± 0.48	15.68 ± 0.40	9.4	NComp	...	...
HD 000166	1954.83	1989.83	380.98 ± 0.57	−178.68 ± 0.29	14.7	Comp?	No[a]	311″ at 147°
HD 000870	1975.84	1991.85	−118.80 ± 0.48	35.12 ± 0.57	2.0	Marg	...	...
HD 001237	1977.77	1997.58	433.92 ± 0.30	−56.74 ± 0.29	8.7	NComp	...	...
HD 001273	1980.79	1996.84	314.38 ± 0.42	182.44 ± 0.57	5.8	NComp	...	...
HD 001461	1983.77	1996.84	416.87 ± 0.63	−143.83 ± 0.26	5.8	NComp	...	...
HD 001562	1954.76	1989.75	−140.48 ± 0.57	−274.97 ± 0.48	10.9	NComp	...	...
HD 001581	1977.87	1993.64	1707.42 ± 0.15	1164.30 ± 0.16	32.6	Comp?	No[b]	87″ at 343°
HD 001835	1983.77	1996.84	394.45 ± 0.49	61.14 ± 0.29	5.2	NComp	...	...
HD 002025	1977.70	1994.62	665.64 ± 1.03	83.67 ± 0.52	11.4	NComp	...	...
HD 002151	1977.77	1997.58	2219.54 ± 0.11	324.09 ± 0.11	44.4	NComp	...	...
HD 003196	1982.71	1995.90	408.34 ± 0.81	−35.22 ± 0.32	5.4	NComp	...	...
HD 003443	1980.63	1989.74	1450.34 ± 3.77	−19.38 ± 1.77	13.0	NComp	...	...
HD 003651	1953.91	1987.65	−461.32 ± 0.33	−370.02 ± 0.28	20.0	NComp	...	...
HD 003765	1985.96	1989.75	355.07 ± 0.65	−668.18 ± 0.57	2.9	NoPM	...	...
HD 004256	1954.67[c]	1987.73	−49.08 ± 0.60	−573.23 ± 0.47	19.0	NComp	...	...
HD 004308	1977.78	1987.82	157.49 ± 0.27	−742.32 ± 0.31	7.6	NComp	...	...
HD 004391	1975.82	1993.70	183.99 ± 0.34	78.81 ± 0.30	3.6	Comp	Yes[d,e]	49″ at 240°
HD 004614	1952.71	1991.68	1086.59 ± 0.40	−559.43 ± 0.33	47.7	NComp	...	...
HD 004628	1953.83	1994.61	757.11 ± 0.48	−1141.33 ± 0.34	55.9	NComp	...	...
HD 004635	1954.73	1995.59	369.83 ± 0.52	201.35 ± 0.39	17.2	NComp	...	...
HD 004676	1954.00	1990.70	−2.87 ± 0.29	−202.05 ± 0.24	7.4	NComp	...	...
HD 004747	1980.63	1989.74	516.92 ± 0.55	120.05 ± 0.45	4.8	NComp	...	...
HD 004813	1954.68[c]	1989.83	−226.91 ± 0.36	−229.75 ± 0.23	11.2	NComp	...	...
HD 004915	1982.71	1995.90	261.10 ± 0.60	−119.49 ± 0.45	3.8	NComp	...	...

Continued on Next Page...

TABLE 4.1 – Continued

Name	Image Epochs Epoch 1	Epoch 2	μ_α (mas yr^{-1})	μ_δ (mas yr^{-1})	Total μ	Blink Result	Companion Status	ID
HD 005015	1952.71	1991.68	-68.95 ± 0.23	170.15 ± 0.22	7.1	NComp	...	...
HD 005133	1978.82	1988.76	620.35 ± 0.63	30.26 ± 0.48	6.2	NComp	...	...
HD 006582	1954.01	1990.79	3422.23 ± 0.60	-1598.93 ± 0.89	138.9	NComp	...	...
HD 007570	1979.88	1993.70	665.13 ± 0.20	177.63 ± 0.19	9.5	NComp	...	...
HD 007590	1952.81	1989.75	-112.73 ± 0.35	-31.28 ± 0.37	4.3	Marg	...	...
HD 007693	1975.83	1989.73	417.23 ± 0.81	75.32 ± 0.78	5.9	Comp	Yes[f]	HD 7788
HD 007924	1954.72	1995.81	-34.23 ± 0.43	-33.28 ± 0.48	2.0	NoPM	...	...
HD 008997	1954.74	1990.71	456.37 ± 0.86	-183.83 ± 0.57	17.7	NComp	...	...
HD 009407	1953.83	1991.68	-377.76 ± 0.31	113.87 ± 0.34	15.0	NComp	...	...
HD 009540	1983.75	1996.72	271.95 ± 0.52	-158.99 ± 0.32	4.1	Comp?	No[g]	$336''$ at $220°$
HD 009770	1977.92	1996.61	115.48 ± 3.47	115.49 ± 1.97	2.4	Marg	...	...
HD 009826	1953.71	1989.77	-173.33 ± 0.20	-381.80 ± 0.13	15.1	Comp	Yes[h]	$55''$ at $150°$
HD 010008	1982.65	1997.90	171.30 ± 0.67	-98.50 ± 0.53	3.0	Marg	...	...
HD 010086	1953.78	1989.75	217.49 ± 0.48	-228.62 ± 0.56	11.3	NComp	...	...
HD 010307	1953.71	1989.77	791.47 ± 0.48	-180.80 ± 0.36	29.3	NComp	...	...
HD 010360	1977.92	1997.61	282.16 ± 2.16	10.56 ± 1.88	5.6	Comp	Yes[i,j]	$13''$ at $5°$
HD 010476	1954.89	1986.69	-302.42 ± 0.60	-678.88 ± 0.41	23.6	NComp	...	...
HD 010647	1977.92	1997.61	166.32 ± 0.24	-106.52 ± 0.27	3.9	Marg	...	...
HD 010700	1982.73	1991.68	-1721.05 ± 0.18	854.16 ± 0.15	17.2	NComp	...	...
HD 010780	1953.83	1991.70	582.03 ± 0.35	-246.93 ± 0.43	23.9	NComp	...	...
HD 012051	1951.84	1989.92	243.58 ± 0.59	-352.17 ± 0.48	16.3	NComp	...	...
HD 012846	1953.78	1990.87	5.80 ± 0.65	-147.35 ± 0.44	5.5	Comp?	No[g]	$304''$ at $336°$
HD 013445	1975.85	1988.91	2092.86 ± 0.27	653.21 ± 0.30	28.6	NComp	...	...
HD 013974	1951.84	1986.91	1151.83 ± 0.40	-246.89 ± 0.30	41.3	NComp	...	...
HD 014214	1982.66	1995.66	366.69 ± 0.52	370.63 ± 0.36	6.8	NComp	...	...
HD 014412	1976.89	1995.82	-217.55 ± 0.37	444.44 ± 0.28	9.4	NComp	...	...
HD 014802	1976.89	1995.82	196.61 ± 0.81	-4.98 ± 0.58	3.7	Marg	...	...

Continued on Next Page...

TABLE 4.1 – Continued

Name	Image Epochs Epoch 1	Epoch 2	μ_α (mas yr^{-1})	μ_δ (mas yr^{-1})	Total μ	Blink Result	Companion Status	ID
HD 016160	1954.97	1990.73	1807.78 ± 0.89	1444.02 ± 0.40	82.7	Comp	Yes[d]	162″ at 110°
HD 016287	1982.79	1997.74	323.60 ± 1.10	58.00 ± 1.16	4.9	NComp	...	...
HD 016673	1979.72	1993.85	−138.88 ± 0.47	−79.97 ± 0.56	2.3	Marg	...	...
HD 016739	1951.97	1989.67	−17.20 ± 0.43	−183.30 ± 0.43	6.9	NComp	...	...
HD 016765	1982.78	1995.95	216.51 ± 1.23	−129.33 ± 1.09	3.3	Marg	...	...
HD 016895	1953.77	1990.94	334.66 ± 0.17	−89.99 ± 0.17	12.9	NComp	...	...
HD 017051	1977.77	1997.81	332.82 ± 0.19	218.74 ± 0.18	8.0	NComp	...	...
HD 017382	1950.94	1989.98	266.58 ± 1.29	−124.97 ± 0.77	11.5	Comp	Yes[d]	21″ at 27°
HD 017925	1982.71	1995.90	397.41 ± 0.45	−189.32 ± 0.36	5.8	NComp	...	...
HD 018143	1950.94	1989.98	264.78 ± 1.17	−193.91 ± 0.76	12.7	Comp	Yes[f]	NLTT 9303
HD 018632	1955.04	1990.81	327.42 ± 1.59	19.31 ± 1.30	11.8	NComp	...	...
HD 018757	1954.07	1993.94	720.57 ± 0.60	−695.55 ± 0.61	39.9	Comp	Yes[d]	262″ at 68°
HD 018803	1954.89	1989.98	233.13 ± 0.45	−168.88 ± 0.36	10.1	NComp	...	...
HD 019373	1953.77	1989.76	1262.41 ± 0.17	−91.50 ± 0.19	45.6	NComp	...	...
HD 019994	1951.68	1997.85	194.56 ± 0.37	−69.01 ± 0.30	9.5	NComp	...	...
HD 020010	1977.95	1991.93	370.87 ± 0.30	611.33 ± 0.42	10.0	NComp	...	...
HD 020165	1955.87	1991.86	399.63 ± 1.05	−405.51 ± 0.87	20.5	NComp	...	...
HD 020407	1977.78	1995.00	−132.28 ± 0.36	142.00 ± 0.48	3.3	Marg	...	...
HD 020619	1982.73	1998.97	253.64 ± 0.96	−101.49 ± 0.72	4.4	NComp	...	...
HD 020630	1951.68	1990.74	269.30 ± 0.24	93.75 ± 0.22	11.1	NComp	...	...
HD 020794	1977.78	1995.00	3038.34 ± 0.20	726.58 ± 0.21	53.8	NComp	...	...
HD 020807	1977.78	1996.87	1330.74 ± 0.21	647.11 ± 0.19	28.2	Comp	Yes[f]	HD 20766
HD 021175	1976.96	1991.79	40.76 ± 0.61	43.06 ± 0.62	0.9	NoPM	...	...
HD 022049	1982.79	1998.97	−975.17 ± 0.21	19.49 ± 0.20	15.8	NComp	...	...
HD 022484	1954.00[c]	1990.80	−232.60 ± 0.59	−481.92 ± 0.54	19.7	NComp	...	...
HD 022879	1955.88[c]	1987.87	689.15 ± 0.83	−213.18 ± 0.61	23.0	NComp	...	...
HD 023356	1955.88[c]	1991.91	309.90 ± 0.67	157.77 ± 0.66	12.5	NComp	...	...

Continued on Next Page...

TABLE 4.1 – Continued

Name	Image Epochs Epoch 1	Epoch 2	μ_α (mas yr^{-1})	μ_δ (mas yr^{-1})	Total μ	Blink Result	Companion Status	ID
HD 023484	1977.71	1991.91	208.60 ± 0.41	288.38 ± 0.55	5.0	Marg	...	...
HD 024238	1954.01	1992.84	437.05 ± 0.77	−245.46 ± 0.84	19.5	NComp	...	...
HD 024409	1954.01	1992.84	−285.44 ± 0.58	159.82 ± 0.61	12.6	NComp	...	...
HD 024496	1951.91	1992.84	217.60 ± 0.78	−165.28 ± 0.52	11.2	NComp	...	...
HD 025329	1954.97	1993.71	1732.84 ± 1.19	−1365.72 ± 0.90	85.5	NComp	...	...
HD 025457	1951.01[c]	1989.99	149.04 ± 0.42	−253.02 ± 0.43	11.5	NComp	...	...
HD 025665	1953.79	1993.72	72.59 ± 0.38	−298.28 ± 0.64	12.3	Comp?	No[a]	287″ at 134°
HD 025680	1949.97	1989.97	172.47 ± 0.40	−131.27 ± 0.34	8.6	Comp?	No[a]	174″ at 0°
HD 025998	1955.81	1989.76	164.10 ± 0.25	−202.60 ± 0.20	8.9	Comp	Yes[f]	HD 25893
HD 026491	1979.87	1989.98	185.73 ± 0.28	336.98 ± 0.34	3.9	Marg	...	...
HD 026923	1954.97	1986.77	−109.46 ± 0.48	−108.25 ± 0.43	4.9	Comp?	No[g]	223″ at 63°
...	...	...	...	...	...	Comp	Yes[f]	HD 26913
HD 026965	1982.82	1985.96	−2240.12 ± 0.23	−3420.27 ± 0.20	12.8	Comp	Yes[f]	LHS 25
...	...	...	...	...	...	Comp	Yes[i,j]	80″ at 100°
HD 029883	1954.99	1989.90	53.34 ± 0.87	−265.47 ± 0.60	9.5	NComp	...	...
HD 030495	1984.91	1990.90	130.04 ± 0.37	169.27 ± 0.28	1.3	NoPM	...	...
HD 030501	1983.01	1997.02	−446.09 ± 0.46	−336.70 ± 0.52	7.8	NComp	...	...
HD 030876	1977.85	1997.01	−26.13 ± 0.35	−115.26 ± 0.52	2.2	Marg	...	...
HD 032778	1986.97	1989.98	−45.43 ± 0.41	731.74 ± 0.42	2.2	Comp?	Yes[d]	81″ at 145°
HD 032850	1955.96	1989.84	281.27 ± 0.95	−239.00 ± 0.66	12.5	NComp	...	...
HD 032923	1955.88	1992.64	534.73 ± 0.41	17.93 ± 0.18	19.7	NComp	...	...
HD 033262	1980.79	1989.03	−30.97 ± 0.19	117.22 ± 0.19	1.0	NoPM	...	...
HD 033564	1955.04	1998.00	−78.48 ± 0.15	161.95 ± 0.22	7.7	NComp	...	...
HD 034411	1953.12	1988.85	518.99 ± 0.26	−665.06 ± 0.13	30.1	NComp	...	...
HD 034721	1980.94	1997.02	386.13 ± 0.35	61.03 ± 0.36	6.3	NComp	...	...
HD 035112	1953.91	1991.79	56.17 ± 1.29	−139.35 ± 0.77	5.7	NComp	...	...
HD 035296	1953.02	1989.91	251.05 ± 0.38	−7.99 ± 0.21	9.2	Comp	Yes[f]	HD 35171

Continued on Next Page...

TABLE 4.1 – Continued

Name	Image Epochs Epoch 1	Epoch 2	μ_α (mas yr^{-1})	μ_δ (mas yr^{-1})	Total μ	Blink Result	Companion Status	ID
HD 035854	1976.99	1992.00	245.67 ± 0.37	−91.06 ± 0.65	3.9	Marg	...	...
HD 036435	1976.83	1994.10	−148.35 ± 0.53	−93.38 ± 0.60	3.0	Marg	...	...
HD 036705	1987.07	1993.89	33.16 ± 0.39	150.83 ± 0.73	1.1	NoPM	...	...
HD 037008	1953.11	1989.77	−549.16 ± 0.86	106.64 ± 0.62	20.5	NComp	...	...
HD 037394	1953.11	1991.11	1.82 ± 0.48	−523.99 ± 0.31	19.9	Comp	Yes[f]	HD 233153
HD 037572	1976.82	1997.02	25.40 ± 1.65	−3.38 ± 1.45	0.5	Comp?	Yes[f]	HIP 26369
HD 038230	1954.90	1989.76	486.82 ± 0.84	−509.74 ± 0.50	24.6	NComp	...	...
HD 038858	1984.01	1990.97	60.84 ± 0.41	−228.35 ± 0.33	1.7	Marg	...	...
HD 039091	1978.03	1989.99	312.01 ± 0.24	1050.38 ± 0.26	13.1	NComp	...	...
HD 039587	1951.91	1990.81	−162.54 ± 0.28	−99.51 ± 0.16	7.4	NComp	...	...
HD 039855	1982.87	1992.08	93.36 ± 0.72	−27.10 ± 0.77	0.9	NoPM	...	...
HD 040307	1976.83	1994.10	−52.65 ± 0.46	−60.46 ± 0.42	1.4	NoPM	...	...
HD 040397	1983.99	1989.02	70.52 ± 0.69	−203.16 ± 0.37	1.1	NoPM	...	...
HD 041593	1955.90	1990.87	−120.46 ± 0.71	−103.21 ± 0.43	5.6	NComp	...	...
HD 042618	1950.94	1989.85	197.44 ± 0.60	−253.65 ± 0.39	12.5	NComp	...	...
HD 042807	1955.94	1989.85	77.38 ± 0.58	−298.00 ± 0.34	10.4	NComp	...	...
HD 043162	1981.02	1996.04	−47.05 ± 0.28	110.87 ± 0.42	1.8	Comp?	Yes[d,e]	164″ at 171°
HD 043587	1950.94	1990.82	−187.72 ± 0.37	170.69 ± 0.28	10.2	Comp	Yes[d]	102″ at 306°
HD 043834	1977.11	1990.00	121.80 ± 0.14	−212.34 ± 0.16	3.2	NComp	...	...
HD 045088	1955.86	1996.77	−117.60 ± 1.23	−163.48 ± 0.84	8.3	NComp	...	...
HD 045184	1979.00	1992.99	−164.99 ± 0.31	−121.77 ± 0.39	2.9	NComp	...	...
HD 045270	1979.97	1995.07	−11.29 ± 0.35	64.24 ± 0.30	1.0	NoPM	...	...
HD 046588	1954.76	1997.18	−99.16 ± 0.19	−603.76 ± 0.26	25.9	NComp	...	...
HD 048189	1979.97	1995.07	−47.84 ± 1.04	72.73 ± 0.87	1.3	NoPM	...	...
HD 048682	1953.19	1989.90	−1.07 ± 0.36	164.25 ± 0.23	6.1	NComp	...	...
HD 050692	1956.27	1994.03	−35.91 ± 0.47	25.65 ± 0.29	1.7	Marg	...	...
HD 051419	1956.27	1989.84	48.74 ± 0.80	99.14 ± 0.56	3.7	NComp	...	...

Continued on Next Page...

TABLE 4.1 – Continued

Name	Image Epochs Epoch 1	Epoch 2	μ_α (mas yr^{-1})	μ_δ (mas yr^{-1})	Total μ	Blink Result	Companion Status	ID
HD 051866	1953.19	1989.93	544.86 ± 0.92	−430.52 ± 0.65	25.6	NComp	...	...
HD 052698	1979.97	1994.20	206.42 ± 0.36	40.82 ± 0.60	3.0	NComp	...	...
HD 052711	1955.15	1988.13	155.15 ± 0.51	−828.66 ± 0.34	27.9	NComp	...	...
HD 053143	1978.04	1992.17	−161.59 ± 0.35	264.67 ± 0.41	4.4	NComp	...	...
HD 053705	1980.12	1994.93	−104.10 ± 0.91	389.07 ± 1.32	6.0	Comp	Yes[f]	HD 53680
...	...	...	...	...	...	Comp	Yes[f]	HD 53706
HD 053927	1955.15	1988.13	−157.81 ± 1.16	−294.71 ± 0.70	11.0	NComp	...	...
HD 054371	1956.27	1994.03	−122.89 ± 0.56	−174.66 ± 0.40	8.1	NComp	...	...
HD 055575	1953.12	1989.92	29.06 ± 0.36	−186.43 ± 0.23	6.9	Marg	...	...
HD 057095	1978.17	1992.17	−18.24 ± 0.62	584.72 ± 0.63	8.2	NComp	...	...
HD 059468	1978.02	1992.18	−286.36 ± 0.40	−2.50 ± 0.42	4.0	NComp	...	...
HD 059747	1955.12	1990.08	−51.41 ± 1.58	7.65 ± 0.76	1.8	NoPM	...	...
HD 059967	1977.07	1991.88	−87.27 ± 0.27	53.93 ± 0.34	1.5	NoPM	...	...
HD 060491	1984.01	1985.96	−81.17 ± 1.26	−42.66 ± 0.66	0.2	NoPM	...	...
HD 061606	1955.90[c]	1985.96	69.90 ± 0.71	−278.33 ± 0.31	8.6	Comp	Yes[d]	57″ at 112°
HD 062613	1954.90	1998.96	−476.24 ± 0.27	88.83 ± 0.32	21.3	NComp	...	...
HD 063077	1977.07	1991.88	−221.54 ± 0.41	1722.11 ± 0.51	25.7	Comp	Yes[d]	914″ at 6°
HD 063433	1955.20	1999.20	−8.31 ± 0.65	−10.48 ± 0.46	0.7	NoPM	...	...
HD 064096	1955.95[c]	1984.98	−67.75 ± 0.73	−346.66 ± 0.66	10.2	NComp	...	...
HD 064468	1955.94	1998.00	93.00 ± 0.97	−454.43 ± 0.53	19.5	NComp	...	...
HD 064606	1983.04	1988.19	−250.14 ± 2.22	−59.77 ± 1.71	1.3	NoPM	...	...
HD 065430	1950.94	1997.18	181.25 ± 0.63	−544.95 ± 0.34	26.5	NComp	...	...
HD 065583	1955.20	1989.84	−171.26 ± 0.61	−1165.34 ± 0.49	40.8	NComp	...	...
HD 065907	1977.22	1991.21	517.51 ± 0.28	120.02 ± 0.25	7.4	Comp	Yes[d]	61″ at 74°
HD 067199	1976.25	1991.13	−158.06 ± 0.32	−130.33 ± 0.49	3.0	Marg	...	...
HD 067228	1950.94	1997.18	23.00 ± 0.33	−66.42 ± 0.24	3.3	NoPM	...	...
HD 068017	1955.22	1988.95	−462.57 ± 0.72	−644.20 ± 0.38	26.7	NComp	...	...

Continued on Next Page...

TABLE 4.1 – Continued

Name	Image Epochs Epoch 1	Epoch 2	μ_α (mas yr^{-1})	μ_δ (mas yr^{-1})	Total μ	Blink Result	Companion Status	ID
HD 068257	1951.09	1997.18	27.61 ± 1.17	−151.73 ± 0.99	7.1	Comp?	Yes[i,j]	6″ at 90°
...	...	...	...	...	...	Comp?	No[a]	372″ at 107°
HD 069830	1955.88[c]	1986.19	278.99 ± 0.25	−987.59 ± 0.29	31.2	NComp	...	...
HD 071148	1953.12	1989.16	−20.53 ± 0.58	−351.78 ± 0.37	12.7	NComp	...	...
HD 072673	1977.21	1991.26	−1113.37 ± 0.35	761.57 ± 0.32	19.0	NComp	...	...
HD 072760	1954.97	1992.04	−192.18 ± 0.70	24.11 ± 0.58	7.3	NComp	...	...
HD 072905	1954.90	1999.19	−27.44 ± 0.31	88.13 ± 0.26	4.1	Marg	...	...
HD 073350	1954.24[c]	1986.25	−297.10 ± 0.74	43.38 ± 0.50	9.7	NComp	...	...
HD 073667	1951.99	1997.10	−108.92 ± 0.85	−501.23 ± 0.55	23.1	Comp?	No[g]	335″ at 207°
HD 073752	1978.12	1992.09	−267.52 ± 0.61	417.61 ± 0.46	7.0	NComp	...	...
HD 074385	1979.00	1994.18	−269.82 ± 0.52	−86.99 ± 0.57	4.3	Comp?	Yes[d]	46″ at 184°
HD 074576	1977.06	1991.27	−300.84 ± 0.26	339.75 ± 0.29	6.5	NComp	...	...
HD 075732	1953.94	1998.29	−485.80 ± 0.97	−234.05 ± 0.68	23.9	Comp	Yes[d]	84″ at 128°
HD 075767	1955.22	1997.10	153.24 ± 1.02	−234.86 ± 0.62	11.8	Comp?	No[g]	385″ at 41°
HD 076151	1982.14	1992.04	−412.02 ± 0.31	30.00 ± 0.18	4.1	NComp	...	...
HD 076932	1982.01	1992.04	244.14 ± 0.23	213.94 ± 0.15	3.3	NComp	...	...
HD 078366	1955.19	1998.30	−190.31 ± 0.48	−114.96 ± 0.21	9.6	NComp	...	...
HD 079028	1954.90	1996.21	−6.98 ± 0.18	−32.15 ± 0.23	1.4	NoPM	...	...
HD 079096	1950.22	1987.00	−524.40 ± 0.60	245.64 ± 0.29	21.3	NComp	...	...
HD 079969	1955.23	1998.30	49.09 ± 0.86	−507.37 ± 0.46	22.0	NComp	...	...
HD 080715	1953.29	1992.09	−341.40 ± 0.87	−359.04 ± 0.39	19.2	NComp	...	...
HD 082342	1979.00	1992.19	−66.82 ± 0.68	314.76 ± 0.82	4.3	Comp?	Yes[d]	11″ at 204°
HD 082443	1952.08	1998.31	−147.90 ± 0.60	−246.77 ± 0.33	13.3	Comp	Yes[d]	65″ at 68°
HD 082558	1983.20	1987.31	−247.92 ± 0.81	33.43 ± 0.61	1.0	NoPM	...	...
HD 082885	1953.94	1998.29	−728.71 ± 0.34	−259.81 ± 0.18	34.4	Comp?	No[a]	328″ at 333°
HD 084117	1980.06	1995.09	−399.57 ± 0.17	262.92 ± 0.15	7.2	Comp?	No[a]	722″ at 331°
HD 084737	1953.12	1995.24	221.66 ± 0.23	−92.47 ± 0.15	10.1	NComp	...	...

Continued on Next Page...

TABLE 4.1 – Continued

Name	Image Epochs Epoch 1	Epoch 2	μ_α (mas yr^{-1})	μ_δ (mas yr^{-1})	Total μ	Blink Result	Companion Status	ID
HD 086728	1955.29	1989.93	-527.63 ± 0.30	-429.42 ± 0.18	23.6	Comp	Yes[d]	133″ at 278°
HD 087424	1983.11	1986.26	-189.77 ± 1.05	-25.57 ± 0.86	0.6	NoPM	...	...
HD 087883	1955.20	1988.95	-64.04 ± 0.53	-60.51 ± 0.34	3.0	Marg	...	...
HD 088742	1978.03	1992.24	-370.25 ± 0.28	65.35 ± 0.35	5.3	NComp	...	...
HD 089125	1955.22	1990.01	-414.15 ± 0.37	-97.66 ± 0.19	14.8	NComp	...	...
HD 089269	1953.21	1989.92	62.87 ± 0.56	-299.40 ± 0.36	11.2	NComp	...	...
HD 090156	1975.36	1990.10	-38.02 ± 0.46	99.61 ± 0.47	1.6	NoPM	...	...
HD 090343	1953.29	1997.19	17.16 ± 0.63	46.36 ± 0.54	2.3	NoPM	...	...
HD 090508	1955.21	1998.22	80.51 ± 0.32	-880.38 ± 0.27	38.1	NComp	...	...
HD 090839	1955.08	1998.30	-176.71 ± 0.22	-33.21 ± 0.18	7.8	Comp	Yes[f]	HD 237903
HD 091324	1987.19	1996.16	-419.27 ± 0.16	209.18 ± 0.14	4.2	Marg	...	...
HD 091889	1955.96[c]	1986.03	268.46 ± 0.30	-672.57 ± 0.29	21.8	NComp	...	...
HD 092719	1955.96[c]	1986.25	235.35 ± 0.47	-172.56 ± 0.42	8.8	NComp	...	...
HD 092945	1979.38	1993.16	-215.23 ± 0.43	-50.04 ± 0.59	3.0	Marg	...	...
HD 094765	1953.29	1989.94	-258.38 ± 1.12	-77.42 ± 0.81	9.9	NComp	...	...
HD 095128	1955.21	1998.37	-317.01 ± 0.22	54.64 ± 0.20	13.8	NComp	...	...
HD 096064	1984.18	1985.06	-176.60 ± 0.91	-103.81 ± 0.71	0.2	Comp?	Yes[d,j]	13″ at 218°
...	...	...	...	...	...	Comp?	No[g]	296″ at 142°
HD 096612	1955.21	1989.04	-213.59 ± 0.75	40.69 ± 0.63	7.3	NComp	...	...
HD 097334	1953.19	1992.09	-248.91 ± 0.37	-150.98 ± 0.34	11.3	NComp	...	...
HD 097343	1978.20	1990.32	272.41 ± 0.37	-65.72 ± 0.33	3.4	Marg	...	...
HD 097658	1955.22	1992.32	-106.48 ± 0.63	48.82 ± 0.51	4.3	Comp?	No[g]	346″ at 139°
HD 098230	1950.34	1998.38	-453.7 ± 4.4^k	-591.4 ± 4.1^k	35.0	NComp	...	...
HD 098281	1954.24[c]	1986.20	796.04 ± 0.78	-151.07 ± 0.47	25.9	NComp	...	...
HD 099491	1955.29	1996.27	-725.74 ± 0.85	180.67 ± 0.87	30.7	Comp	Yes[f]	HD 99492
HD 100180	1955.31	1993.08	-329.26 ± 1.28	-190.01 ± 0.98	14.3	Comp	Yes[d]	17″ at 332°
HD 100623	1975.19	1991.12	-671.54 ± 0.39	823.85 ± 0.24	16.9	NComp	...	...

Continued on Next Page...

TABLE 4.1 – Continued

Name	Image Epochs Epoch 1	Epoch 2	μ_α (mas yr^{-1})	μ_δ (mas yr^{-1})	Total μ	Blink Result	Companion Status	ID
HD 101177	1953.19	1997.28	-594.65 ± 0.62	15.78 ± 0.38	26.2	Comp	Yes[i,j]	8″ at 270°
HD 101206	1953.28	1997.28	-129.45 ± 0.81	435.83 ± 0.70	20.0	NComp	...	...
HD 101501	1950.37	1999.34	-12.55 ± 0.25	-380.75 ± 0.21	18.6	NComp	...	...
HD 102365	1977.07	1996.22	-1530.99 ± 0.17	403.67 ± 0.18	30.3	NComp	...	...
HD 102438	1979.18	1995.11	-265.17 ± 0.46	-227.79 ± 0.32	5.6	NComp	...	...
HD 102870	1984.39	1998.30	740.23 ± 0.23	-270.43 ± 0.18	11.0	NComp	...	...
HD 103095	1950.37	1997.42	4003.98 ± 0.37	-5813.62 ± 0.23	332.1	NComp	...	...
HD 104067	1983.13	1996.16	143.31 ± 0.80	-423.67 ± 0.48	5.8	NComp	...	...
HD 104304	1954.25[c]	1989.18	141.75 ± 0.29	-483.64 ± 0.19	17.6	NComp	...	...
HD 105631	1955.23	1989.18	-313.55 ± 0.43	-51.62 ± 0.50	10.8	NComp	...	...
HD 108954	1953.29	1996.35	19.78 ± 0.29	182.47 ± 0.29	7.9	NComp	...	...
HD 109200	1987.19	1998.38	-545.97 ± 0.44	-312.32 ± 0.42	7.0	NComp	...	...
HD 109358	1952.64	1990.01	-704.75 ± 0.13	292.74 ± 0.14	28.5	NComp	...	...
HD 110463	1953.29	1996.35	121.51 ± 0.67	-4.90 ± 0.68	5.2	NComp	...	...
HD 110810	1976.48	1998.38	-200.58 ± 0.61	-130.26 ± 0.51	5.3	Marg	...	...
HD 110833	1953.29	1994.34	-379.08 ± 0.52	-183.68 ± 0.46	17.3	NComp	...	...
HD 110897	1952.64	1990.01	-359.87 ± 0.29	140.16 ± 0.24	14.4	NComp	...	...
HD 111312	1982.40	1992.40	82.27 ± 3.01	44.97 ± 2.37	0.9	NoPM	...	...
HD 111395	1955.39	1992.33	-334.58 ± 0.43	-105.52 ± 0.34	13.0	NComp	...	...
HD 112758	1982.30	1991.12	-825.24 ± 0.80	196.16 ± 0.65	7.5	NComp	...	...
HD 112914	1950.43	1990.07	-234.94 ± 0.63	181.12 ± 0.78	11.8	NComp	...	...
HD 113283	1978.33	1993.25	-221.11 ± 0.41	-156.05 ± 0.41	4.0	Marg	...	...
HD 113449	1956.35[c]	1985.16	-191.13 ± 0.86	-218.73 ± 0.68	8.4	NComp	...	...
HD 114613	1979.16	1994.26	-381.72 ± 0.31	45.75 ± 0.20	5.8	NComp	...	...
HD 114710	1955.29	1993.29	-801.44 ± 0.14	882.04 ± 0.10	45.3	NComp	...	...
HD 114783	1956.27	1996.23	-138.66 ± 0.56	10.57 ± 0.57	5.5	Comp	No[g]	240″ at 46°
HD 114853	1985.36	1992.12	-110.14 ± 0.37	-110.75 ± 0.35	1.1	NoPM	...	...

Continued on Next Page...

TABLE 4.1 – Continued

Name	Image Epochs Epoch 1	Epoch 2	μ_α (mas yr^{-1})	μ_δ (mas yr^{-1})	Total μ	Blink Result	Companion Status	ID
HD 115383	1955.37	1997.28	-333.83 ± 0.25	190.24 ± 0.17	16.1	NComp	...	...
HD 115404	1950.29	1997.35	632.60 ± 0.67	-262.21 ± 0.48	32.1	NComp	...	...
HD 115617	1976.49	1993.22	-1070.36 ± 0.22	-1063.69 ± 0.13	25.2	NComp	...	...
HD 116442	1956.19	1997.18	13.54 ± 1.13	196.94 ± 0.74	8.2	Comp	Yes[f]	HD 116443
HD 116956	1953.20	1993.22	-216.61 ± 0.50	11.17 ± 0.46	8.7	NComp	...	...
HD 117043	1953.28	1997.28	-392.35 ± 0.31	220.73 ± 0.27	19.8	NComp	...	...
HD 117176	1955.37	1997.35	-236.02 ± 0.24	-575.73 ± 0.19	26.1	NComp	...	...
HD 118972	1975.27	1991.21	205.63 ± 0.50	-166.77 ± 0.26	4.2	Marg	...	...
HD 119332	1953.20	1993.31	-16.62 ± 0.55	70.21 ± 0.48	2.9	NoPM	...	...
HD 120136	1954.25	1992.19	-479.53 ± 0.16	53.49 ± 0.13	18.3	NComp	...	...
HD 120559	1987.26	1994.19	-360.04 ± 0.85	-412.39 ± 0.67	3.8	NoPM	...	...
HD 120690	1976.48	1991.28	-580.89 ± 0.57	-246.00 ± 0.34	9.3	NComp	...	...
HD 120780	1976.27	1990.45	-583.66 ± 0.58	-61.29 ± 0.39	8.3	NComp	...	...
HD 121370	1954.25	1991.34	-60.95 ± 1.14	-356.29 ± 0.73	13.5	NComp	...	...
HD 121560	1954.34	1996.30	-291.30 ± 0.32	8.92 ± 0.28	12.2	NComp	...	...
HD 122742	1954.34	1989.27	84.41 ± 0.52	-304.40 ± 0.36	11.0	NComp	...	...
HD 124106	1988.15	1992.41	-255.06 ± 1.24	-179.11 ± 0.79	1.3	NoPM	...	...
HD 124292	1955.37[c]	1994.19	-160.88 ± 0.59	-321.90 ± 0.38	14.0	NComp	...	...
HD 124580	1976.33	1993.30	127.85 ± 0.42	-138.05 ± 0.37	3.2	Marg	...	...
HD 124850	1983.50	1994.19	-26.31 ± 0.19	-419.38 ± 0.14	4.5	NComp	...	...
HD 125276	1976.41	1992.25	-356.34 ± 0.90	367.55 ± 0.74	8.1	NComp	...	...
HD 125455	1983.50	1994.19	-632.65 ± 0.90	-121.44 ± 0.64	6.9	Comp?	Yes[l]	$14''$ at $104°$
HD 126053	1979.46	1994.36	223.79 ± 0.39	-477.36 ± 0.36	7.9	NComp	...	...
HD 127334	1950.45	1995.47	161.12 ± 0.29	-219.91 ± 0.29	12.3	NComp	...	...
HD 128165	1953.28	1996.44	-191.79 ± 0.38	248.58 ± 0.37	13.5	NComp	...	...
HD 128311	1950.27	1989.25	204.74 ± 0.74	-249.98 ± 0.61	12.6	NComp	...	...
HD 128400	1976.18	1994.45	119.48 ± 0.36	-18.62 ± 0.38	2.2	Marg	...	...

Continued on Next Page...

TABLE 4.1 – Continued

Name	Image Epochs Epoch 1	Epoch 2	μ_α (mas yr^{-1})	μ_δ (mas yr^{-1})	Total μ	Blink Result	Companion Status	ID
HD 128620	1976.19	1997.19	-3679.25 ± 3.89	473.67 ± 3.24	77.9	Comp	Yes[i,j]	15″ at 213°
...	...	...	...	...	...	Comp	Yes[f]	HIP 70890
HD 128642	1955.22	1994.44	-74.49 ± 0.39	-132.26 ± 0.45	6.0	NComp	...	...
HD 128987	1983.36	1993.25	-111.98 ± 0.50	-64.97 ± 0.35	1.3	NoPM	...	...
HD 130004	1954.42	1993.36	-233.40 ± 0.96	-224.97 ± 0.87	12.6	NComp	...	...
HD 130042	1987.39	1997.19	-107.42 ± 0.51	-320.00 ± 0.69	3.3	Marg	...	...
HD 130307	1955.37	1989.24	-288.02 ± 0.89	-78.88 ± 0.67	10.2	NComp	...	...
HD 130948	1950.35	1994.18	143.91 ± 0.37	32.69 ± 0.34	6.5	NComp	...	...
HD 131156	1950.21	1992.19	154.98 ± 0.40	-66.43 ± 0.45	7.1	NComp	...	...
HD 131511	1950.21	1992.19	-442.23 ± 0.36	217.61 ± 0.43	20.7	NComp	...	...
HD 131582	1950.35	1991.37	-825.30 ± 1.20	3.09 ± 1.06	33.8	NComp	...	...
HD 131923	1988.43	1997.17	-16.82 ± 0.90	-335.04 ± 0.91	2.9	Marg	...	...
HD 132142	1953.28	1991.44	-971.06 ± 0.41	479.89 ± 0.38	41.3	NComp	...	...
HD 132254	1955.23	1996.44	111.37 ± 0.26	-225.83 ± 0.22	10.4	NComp	...	...
HD 133640	1955.23	1996.44	-445.84 ± 1.44	19.86 ± 1.67	18.0	NComp	...	...
HD 134060	1987.65	1997.17	-184.91 ± 0.44	-10.66 ± 0.42	1.8	NoPM	...	...
HD 135204	1955.30	1994.36	-1269.73 ± 0.59	-503.41 ± 0.41	53.3	NComp	...	...
HD 135599	1955.30	1994.36	178.35 ± 0.66	-137.52 ± 0.62	8.8	NComp	...	...
HD 136202	1979.54	1994.36	372.21 ± 0.32	-513.59 ± 0.22	9.4	NComp	...	...
HD 136352	1987.31	1992.56	-1622.61 ± 0.37	-275.62 ± 0.36	8.6	NComp	...	...
HD 136713	1981.34	1991.21	-59.29 ± 1.48	-201.52 ± 1.12	2.1	Marg	...	...
HD 136923	1950.30	1992.49	-230.58 ± 0.63	76.30 ± 0.72	10.3	NComp	...	...
HD 137107	1954.48	1987.30	116.83 ± 0.40	-171.37 ± 0.49	7.1	NComp	...	...
HD 137763	1981.34	1991.21	87.09 ± 1.62	-373.67 ± 1.36	3.7	Comp	Yes[f]	HD 137778
HD 139341	1955.25	1993.29	-481.44 ± 0.52	28.68 ± 0.61	18.4	Comp	Yes[f]	HD 139323
HD 139777	1955.22	1994.44	-224.25 ± 0.40	108.19 ± 0.40	9.8	Comp	Yes[f]	HD 139813
HD 140538	1982.52	1993.25	-43.11 ± 0.79	-143.57 ± 0.56	1.6	Marg	...	...

Continued on Next Page...

TABLE 4.1 – Continued

Name	Image Epochs Epoch 1	Epoch 2	μ_α (mas yr^{-1})	μ_δ (mas yr^{-1})	Total μ	Blink Result	Companion Status	ID
HD 140901	1988.30	1997.29	-414.91 ± 0.39	-215.05 ± 0.33	4.2	Comp	Yes[l]	14″ at 138°
HD 141004	1954.42	1993.25	-224.00 ± 0.29	-70.64 ± 0.27	9.2	Comp	No[g]	235″ at 200°
HD 141272	1982.52	1993.45	-177.08 ± 0.89	-165.63 ± 0.96	2.7	Marg	...	...
HD 142267	1950.44	1994.44	-150.28 ± 0.74	-561.91 ± 0.53	25.6	NComp	...	...
HD 142373	1955.23	1989.19	438.90 ± 0.18	629.70 ± 0.20	26.1	NComp	...	...
HD 143761	1950.28	1992.64	-196.63 ± 0.24	-773.02 ± 0.21	33.8	NComp	...	...
HD 144284	1954.49	1994.42	-319.51 ± 0.11	334.97 ± 0.13	18.5	NComp	...	...
HD 144287	1950.37	1996.53	-489.51 ± 0.48	697.39 ± 0.64	39.3	NComp	...	...
HD 144579	1955.23	1991.27	-571.08 ± 0.29	52.34 ± 0.29	20.7	Comp	Yes[d]	70″ at 280°
HD 144628	1988.43	1991.22	-135.23 ± 0.62	333.37 ± 0.58	1.0	NoPM	...	...
HD 144872	1955.23	1991.27	232.34 ± 0.57	-535.74 ± 0.62	21.1	NComp	...	...
HD 145417	1988.43	1997.32	-853.82 ± 0.61	-1410.71 ± 0.61	14.7	NComp	...	...
HD 145675	1955.23	1991.43	131.83 ± 0.32	-297.54 ± 0.36	11.8	NComp	...	...
HD 145825	1977.52	1992.25	-80.18 ± 0.60	-252.44 ± 0.65	3.9	Marg	...	...
HD 145958	1950.53	1989.27	182.93 ± 0.94	-420.02 ± 0.93	17.7	Comp	Yes[i,j]	3″ at 135°
HD 146233	1983.45	1992.64	230.77 ± 0.51	-495.53 ± 0.33	5.0	NComp	...	...
HD 146361	1954.48	1991.28	-263.39 ± 0.93	-92.67 ± 1.31	10.3	Comp	Yes[i,j]	6″ at 270°
...	...	...	...	...	...	Comp	Yes[f]	HIP 79551
HD 147513	1987.39	1993.25	71.89 ± 0.47	5.26 ± 0.32	0.4	NoPM	...	...
HD 147584	1976.25	1993.30	199.97 ± 0.25	110.97 ± 0.43	3.9	NComp	...	...
HD 147776	1983.50	1995.62	-220.35 ± 1.06	-205.09 ± 0.70	3.7	NComp	...	...
HD 148653	1950.21	1991.43	-353.30 ± 1.01	388.45 ± 0.80	21.4	NComp	...	...
HD 148704	1987.39	1993.25	-431.25 ± 1.89	-331.16 ± 1.81	3.2	Marg	...	...
HD 149612	1987.39	1997.32	-227.00 ± 0.43	-284.80 ± 0.41	3.6	NComp	...	...
HD 149661	1950.45	1988.61	456.04 ± 0.38	-309.63 ± 0.34	21.0	NComp	...	...
HD 149806	1980.59	1994.36	93.69 ± 0.67	76.83 ± 0.55	1.6	NoPM	...	...
HD 151541	1955.31	1992.28	-283.07 ± 0.48	426.91 ± 0.57	18.9	NComp	...	...

Continued on Next Page...

TABLE 4.1 – Continued

Name	Image Epochs Epoch 1	Epoch 2	μ_α (mas yr^{-1})	μ_δ (mas yr^{-1})	Total μ	Blink Result	Companion Status	ID
HD 152391	1950.46	1988.45	-711.70 ± 0.87	-1483.65 ± 0.48	62.5	NComp	...	...
HD 153557	1955.23	1991.30	-147.62 ± 0.58	270.80 ± 0.68	11.2	Comp	Yes[f]	HD 153525
HD 154088	1988.39	1997.33	83.76 ± 0.64	-268.69 ± 0.36	2.5	NoPM	...	...
HD 154345	1955.23	1991.30	123.27 ± 0.35	853.63 ± 0.36	31.1	NComp	...	...
HD 154417	1982.53	1992.41	-17.51 ± 0.50	-335.11 ± 0.28	3.3	NComp	...	...
HD 154577	1976.64	1993.25	70.96 ± 0.55	589.86 ± 0.49	9.9	NComp	...	...
HD 155712	1954.51	1996.45	101.86 ± 0.60	-116.10 ± 0.65	6.5	NComp	...	...
HD 155885	1987.65	1997.33	-465.31 ± 0.55	-1140.97 ± 0.34	12.0	Comp	Yes[i,j]	$3''$ at 180°
...	...	...	...	...	...	Comp	Yes[f]	HD 156026
HD 156274	1987.70	1992.43	1037.56 ± 0.73	108.99 ± 0.32	4.9	Comp?	Yes[i,j]	$15''$ at 231°
HD 157214	1950.46	1993.46	135.55 ± 0.17	-1040.49 ± 0.31	45.1	NComp	...	...
HD 157347	1954.58	1992.35	49.39 ± 0.51	-107.16 ± 0.25	4.5	Comp	Yes[d,e]	$49''$ at 147°
HD 158614	1981.27	1992.35	-127.77 ± 0.87	-168.61 ± 0.48	2.4	Marg	...	...
HD 158633	1953.44	1991.44	-530.81 ± 0.31	4.85 ± 0.38	20.2	NComp	...	...
HD 159062	1953.53	1991.45	174.67 ± 0.62	75.82 ± 0.55	7.2	NComp	...	...
HD 159222	1954.51	1993.61	-239.80 ± 0.26	63.08 ± 0.32	9.7	NComp	...	...
HD 160269	1954.57	1992.36	277.02 ± 0.36	-524.88 ± 0.46	22.5	NComp	...	...
...	...	...	...	...	...	Comp	Yes[f]	HIP 86087
HD 160346	1953.61	1993.62	-179.30 ± 0.44	-96.60 ± 0.32	8.2	NComp	...	...
HD 160691	1987.70	1992.59	-16.85 ± 0.40	-190.60 ± 0.23	0.9	NoPM	...	...
HD 161198	1951.49	1992.57	-123.20 ± 0.85	-619.51 ± 0.86	26.0	NComp	...	...
HD 161797	1952.55	1993.48	-291.66 ± 0.12	-749.60 ± 0.15	32.9	NComp	...	...
HD 162004	1953.67	1993.63	34.89 ± 0.48	-275.94 ± 0.59	11.0	Comp	Yes[f]	HD 162003
HD 164922	1951.49	1991.37	389.41 ± 0.36	-602.03 ± 0.52	28.6	NComp	...	...
HD 165185	1987.71	1996.69	105.05 ± 0.60	7.95 ± 0.32	0.9	NoPM	...	...
HD 165341	1953.53	1988.59	124.16 ± 0.81	-962.82 ± 0.64	34.0	NComp	...	...
HD 165401	1950.52	1991.46	-31.94 ± 0.66	-321.65 ± 0.57	13.2	NComp	...	...

Continued on Next Page...

TABLE 4.1 – Continued

Name	Image Epochs Epoch 1	Epoch 2	μ_α (mas yr^{-1})	μ_δ (mas yr^{-1})	Total μ	Blink Result	Companion Status	ID
HD 165499	1975.66	1995.65	-77.69 ± 0.39	234.43 ± 0.29	4.9	NComp	...	...
HD 165908	1951.52	1989.35	-100.32 ± 0.28	110.08 ± 0.34	5.7	Marg	...	...
HD 166620	1950.60	1992.48	-316.44 ± 0.28	-468.47 ± 0.31	23.7	NComp	...	...
HD 167425	1976.34	1993.61	39.93 ± 0.33	-276.60 ± 0.30	4.8	NComp	...	...
HD 168009	1950.38	1991.60	-76.55 ± 0.33	-114.46 ± 0.29	5.7	NComp	...	...
HD 170657	1987.47	1992.57	-138.73 ± 0.84	-195.99 ± 0.59	1.2	NoPM	...	...
HD 172051	1987.47	1996.69	-74.85 ± 0.77	-152.00 ± 0.47	1.6	NoPM	...	...
HD 175073	1974.56	1989.51	143.53 ± 1.32	-357.50 ± 0.78	5.7	NComp	...	...
HD 175742	1951.53	1992.42	131.31 ± 0.49	-283.72 ± 0.63	12.8	NComp	...	...
HD 176051	1950.46	1992.64	201.96 ± 0.28	-145.46 ± 0.35	10.5	NComp	...	...
HD 176377	1950.46	1989.34	56.74 ± 0.33	194.45 ± 0.50	7.9	NComp	...	...
HD 177474	1977.53	1992.57	96.74 ± 1.05	-281.71 ± 0.58	4.5	NComp	...	...
HD 177565	1974.56	1989.51	-187.45 ± 0.85	-366.74 ± 0.47	6.1	NComp	...	...
HD 178428	1953.62	1990.63	65.56 ± 0.37	-304.79 ± 0.41	11.5	NComp	...	...
HD 179957	1953.69	1992.65	-210.20 ± 0.62	621.79 ± 0.55	25.6	Comp	Yes[i,j]	7″ at 180°
HD 180161	1953.75	1991.66	217.40 ± 0.30	407.79 ± 0.39	17.5	NComp	...	...
HD 181321	1977.53	1992.57	68.54 ± 1.94	-98.78 ± 1.24	2.0	NoPM	...	...
HD 182488	1955.38	1992.44	83.40 ± 0.34	162.32 ± 0.30	6.8	NComp	...	...
HD 182572	1952.40	1992.59	721.02 ± 0.21	642.49 ± 0.17	38.9	NComp	...	...
HD 183870	1987.41	1988.45	234.50 ± 0.65	18.14 ± 0.37	0.2	NoPM	...	...
HD 184385	1950.54	1986.67	-20.39 ± 0.67	-204.32 ± 0.67	7.4	NComp	...	...
HD 184467	1952.62	1991.67	-509.98 ± 0.65	-397.67 ± 0.69	25.3	NComp	...	...
HD 185144	1954.57	1991.60	598.07 ± 0.17	-1738.40 ± 0.19	68.1	NComp	...	...
HD 185414	1953.61	1989.64	0.32 ± 0.34	-200.51 ± 0.33	7.2	NComp	...	...
HD 186408	1951.52	1991.52	-147.82 ± 0.30	-159.01 ± 0.28	8.7	Comp	Yes[f]	HD 186427
HD 186858	1952.54	1992.67	7.34 ± 0.64	-436.03 ± 0.90	17.7	Comp	Yes[f]	HD 187013
...	...	...	...	...	...	Comp	Yes[d]	HD 225732

Continued on Next Page...

TABLE 4.1 – Continued

Name	Image Epochs Epoch 1	Epoch 2	μ_α (mas yr^{-1})	μ_δ (mas yr^{-1})	Total μ	Blink Result	Companion Status	ID
HD 187691	1953.62	1991.53	242.28 ± 0.27	−136.48 ± 0.23	10.4	Comp	Yes[d]	23″ at 221°
HD 189340	1951.72[c]	1984.65	−251.27 ± 1.14	−398.65 ± 1.01	15.2	NComp	...	...
HD 189567	1979.71	1995.65	844.50 ± 0.25	−673.62 ± 0.29	17.2	NComp	...	...
HD 189733	1951.53	1996.53	−2.14 ± 0.53	−251.40 ± 0.40	11.3	NComp	...	...
HD 190067	1951.72	1992.74	−159.88 ± 0.54	−582.87 ± 0.62	24.8	NComp	...	...
HD 190248	1979.71	1995.65	1211.03 ± 0.13	−1130.05 ± 0.13	26.4	NComp	...	...
HD 190360	1953.53	1992.49	683.94 ± 0.22	−524.70 ± 0.27	33.6	Comp	Yes[f]	LHS 3509
HD 190404	1951.53	1992.72	−1002.97 ± 0.42	−913.19 ± 0.35	55.8	NComp	...	...
HD 190406	1951.72	1992.74	−394.57 ± 0.27	−407.82 ± 0.33	23.2	NComp	...	...
HD 190422	1976.50	1991.66	18.30 ± 0.45	35.88 ± 0.44	0.6	NoPM	...	...
HD 190470	1951.53	1992.72	−75.76 ± 0.65	−39.75 ± 0.53	3.5	Marg	...	...
HD 190771	1950.61	1991.60	262.77 ± 0.29	111.84 ± 0.33	11.7	NComp	...	...
HD 191408	1976.57	1990.72	456.99 ± 0.33	−1574.64 ± 0.22	23.2	NComp	...	...
HD 191499	1951.72	1992.74	4.65 ± 0.78	174.51 ± 0.85	7.2	NComp	...	...
HD 191785	1951.72	1992.74	−414.75 ± 0.50	398.26 ± 0.56	23.6	Comp	Yes[d]	102″ at 95°
HD 192263	1951.58	1988.67	−61.13 ± 1.21	261.37 ± 0.50	10.0	NComp	...	...
HD 192310	1977.55	1992.43	1241.85 ± 0.34	−180.96 ± 0.21	18.7	NComp	...	...
HD 193664	1953.61	1991.67	468.58 ± 0.26	296.61 ± 0.22	21.1	NComp	...	...
HD 194640	1977.60	1991.74	−14.62 ± 0.51	−521.82 ± 0.36	7.4	NComp	...	...
HD 195564	1953.77[c]	1986.65	307.35 ± 0.42	106.94 ± 0.33	10.7	NComp	...	...
HD 195987	1953.45	1992.49	−156.76 ± 0.34	452.84 ± 0.34	18.7	NComp	...	...
HD 196378	1976.50	1991.68	313.48 ± 0.21	−569.91 ± 0.24	9.9	NComp	...	...
HD 196761	1974.54	1992.43	501.45 ± 0.56	461.36 ± 0.39	12.2	NComp	...	...
HD 197076	1951.51	1992.67	118.14 ± 0.30	312.63 ± 0.26	13.8	Comp	Yes[d]	125″ at 184°
HD 197214	1974.47	1990.73	−42.69 ± 1.09	−208.55 ± 0.82	3.4	NComp	...	...
HD 198425	1953.45	1992.56	−161.13 ± 0.49	−266.74 ± 0.56	12.2	Comp	Yes[d]	33″ at 247°
HD 199260	1976.41	1994.50	93.79 ± 0.43	−64.78 ± 0.37	2.0	NoPM	...	...

Continued on Next Page...

TABLE 4.1 – Continued

Name	Image Epochs Epoch 1	Epoch 2	μ_α (mas yr^{-1})	μ_δ (mas yr^{-1})	Total μ	Blink Result	Companion Status	ID
HD 199288	1976.71	1990.78	-515.34 ± 0.42	-975.52 ± 0.22	15.5	NComp	...	...
HD 199509	1976.66	1992.64	264.65 ± 0.42	-49.01 ± 0.33	4.3	Marg	...	...
HD 200525	1975.68	1992.43	460.33 ± 1.46	-285.96 ± 1.39	9.1	NComp	...	...
HD 200968	1953.62[c]	1984.59	382.85 ± 0.72	-46.70 ± 0.29	11.9	NComp	...	...
HD 200560	1952.55	1990.70	403.83 ± 0.58	140.93 ± 0.53	16.3	NComp	...	...
HD 202275	1951.58	1987.74	42.39 ± 0.68	-304.19 ± 0.42	11.1	NComp	...	...
HD 202628	1980.61	1993.61	240.89 ± 0.34	21.00 ± 0.29	3.2	Marg	...	...
HD 202751	1952.65	1991.54	468.58 ± 1.02	-187.74 ± 0.91	19.6	NComp	...	...
HD 202940	1979.77	1994.65	-582.58 ± 0.78	-358.93 ± 0.52	10.2	NComp	...	...
HD 203244	1985.44	1990.79	141.93 ± 0.54	168.40 ± 0.55	1.2	Marg	...	...
HD 203850	1975.45	1991.68	661.43 ± 1.05	139.55 ± 0.71	11.0	NComp	...	...
HD 203985	1980.61	1993.61	258.62 ± 0.97	187.57 ± 0.74	4.2	Comp	Yes[d]	$88''$ at $259°$
HD 205390	1976.48	1992.64	424.24 ± 0.57	-199.70 ± 0.35	7.6	NComp	...	...
HD 205536	1977.78	1996.78	-139.36 ± 0.51	212.55 ± 0.45	4.8	NComp	...	...
HD 206826	1954.72	1987.65	260.72 ± 0.36	-243.21 ± 0.31	11.7	NComp	...	...
HD 206860	1953.63	1990.80	229.93 ± 0.55	-113.46 ± 0.32	9.6	Comp?	No[g]	$591''$ at $16°$
HD 207129	1978.81	1996.69	164.43 ± 0.30	-295.37 ± 0.22	6.0	NComp	...	...
HD 207144	1974.64	1990.72	107.69 ± 0.93	-352.31 ± 0.53	5.9	NComp	...	...
HD 208038	1951.73	1994.52	-5.96 ± 0.64	-101.58 ± 0.76	4.4	NComp	...	...
HD 208313	1954.72	1987.65	211.06 ± 0.67	-233.89 ± 0.79	10.4	NComp	...	...
HD 210277	1951.60[c]	1987.79	85.07 ± 0.46	-449.74 ± 0.30	16.6	NComp	...	...
HD 210667	1953.69	1992.67	25.52 ± 0.48	-251.98 ± 0.47	9.8	NComp	...	...
HD 210918	1980.55	1995.63	571.11 ± 0.36	-789.84 ± 0.32	14.7	NComp	...	...
HD 211415	1978.80	1993.69	438.75 ± 0.29	-632.46 ± 0.22	11.5	NComp	...	...
HD 211472	1952.70	1991.60	213.52 ± 0.44	69.87 ± 0.43	8.7	Comp	Yes[d]	$76''$ at $105°$
HD 212168	1977.78	1996.78	57.79 ± 0.50	12.25 ± 0.39	1.1	Comp?	Yes[d]	$20''$ at $93°$
HD 212330	1980.60	1995.51	180.06 ± 0.23	-331.66 ± 0.20	5.6	NComp	...	...

Continued on Next Page...

TABLE 4.1 – Continued

Name	Image Epochs Epoch 1	Epoch 2	μ_α (mas yr^{-1})	μ_δ (mas yr^{-1})	Total μ	Blink Result	Companion Status	ID
HD 214683	1954.58	1991.77	176.80 ± 0.82	107.79 ± 0.71	7.8	NComp	...	...
HD 214953	1976.74	1995.65	6.24 ± 0.37	−331.18 ± 0.29	6.3	NComp	...	...
HD 215152	1954.52[c]	1989.80	−155.75 ± 1.20	−290.81 ± 0.97	11.6	NComp	...	...
HD 215648	1953.63	1990.64	234.18 ± 0.21	−493.29 ± 0.17	20.1	NComp	...	...
HD 216259	1953.63	1991.70	405.69 ± 1.02	202.72 ± 0.97	17.2	NComp	...	...
HD 216520	1954.73	1996.64	−150.23 ± 0.56	116.22 ± 0.40	8.0	NComp	...	...
HD 217014	1954.58	1990.79	207.25 ± 0.31	60.34 ± 0.30	7.8	NComp	...	...
HD 217107	1982.80	1991.68	−6.35 ± 0.46	−15.80 ± 0.31	0.2	NoPM	...	...
HD 217813	1954.58	1991.75	−117.70 ± 0.59	−27.66 ± 0.49	4.4	Marg	...	...
HD 218868	1953.83	1989.68	−86.52 ± 0.29	−287.42 ± 0.36	10.7	Comp	Yes[d,e]	50″ at 90°
HD 219134	1952.71	1990.79	2075.07 ± 0.33	295.45 ± 0.25	79.8	NComp	...	...
HD 219482	1979.51	1994.51	175.24 ± 0.30	−27.24 ± 0.25	2.7	NoPM	...	...
HD 219538	1954.66	1991.76	359.78 ± 0.57	89.75 ± 0.42	13.7	NComp	...	...
HD 219623	1952.71	1990.79	111.87 ± 0.22	−236.51 ± 0.21	10.0	NComp	...	...
HD 220140	1954.72	1996.64	201.56 ± 0.50	71.59 ± 0.41	9.0	NComp	...	...
HD 220182	1953.83	1989.68	636.54 ± 0.38	219.49 ± 0.38	24.1	NComp	...	...
HD 220339	1983.82	1991.76	453.40 ± 1.09	260.15 ± 0.79	4.1	NComp	...	...
HD 221354	1954.60	1991.60	1105.17 ± 0.46	113.28 ± 0.51	41.1	NComp	...	...
HD 221851	1953.93	1991.76	−197.70 ± 0.72	−281.07 ± 0.40	13.0	NComp	...	...
HD 222143	1951.69	1990.64	357.60 ± 0.33	−12.14 ± 0.30	13.9	NComp	...	...
HD 222237	1977.78	1987.71	141.94 ± 0.42	−736.82 ± 0.42	7.4	NComp	...	...
HD 222335	1985.55	1997.66	133.37 ± 0.58	−304.64 ± 0.54	4.0	Marg	...	...
HD 222368	1953.62	1986.77	377.15 ± 0.19	−437.43 ± 0.15	19.1	NComp	...	...
HD 223778	1952.64	1992.76	341.01 ± 0.32	41.50 ± 0.29	13.8	NComp	...	...
HD 224228	1977.71	1996.72	206.72 ± 0.51	−185.07 ± 0.54	5.3	NComp	...	...
HD 224465	1953.75	1991.68	−45.02 ± 0.40	244.82 ± 0.39	9.5	NComp	...	...
HD 224930	1950.61	1991.77	780.22 ± 2.01	−917.75 ± 1.20	49.6	NComp	...	...

Continued on Next Page...

TABLE 4.1 – Continued

Name	Image Epochs Epoch 1	Epoch 2	μ_α (mas yr^{-1})	μ_δ (mas yr^{-1})	Total μ	Blink Result	Companion Status	ID
HD 232781	1954.74	1989.77	-311.48 ± 1.08	-266.47 ± 0.97	14.4	NComp	...	...
HD 263175	1953.93	1989.84	-452.64 ± 1.41	99.28 ± 0.81	16.7	Comp	Yes[d]	$30''$ at 101°
HIP 036357	1953.13	1988.93	157.85 ± 1.28	175.95 ± 0.73	8.5	Comp	Yes[f]	HD 58946
HIP 040774	1983.04	1987.02	-164.53 ± 1.35	-52.64 ± 0.85	0.7	NoPM	...	...
HIP 087579	1951.49	1992.57	-73.12 ± 0.85	56.21 ± 0.88	3.8	NComp	...	...
HIP 091605	1951.51	1989.34	86.87 ± 0.85	-837.41 ± 1.16	31.9	Comp	Yes[j,l]	$9''$ at 150°

NOTES.—Column 7 values: NoPM = Primary's proper motion undetectable, Marg = Primary's proper motion marginal, NComp = No CPM candidates identified, Comp = Candidate with visually compelling CPM identified, Comp? = Candidate with possible CPM identified

[a] Primary and candidate companion have significantly different proper motions from the literature (see § 7.4). [b] The candidate companion is a non-stellar artifact such as a plate defect. [c] Epoch-1 image is from SuperCOSMOS Sky Survey in order to increase the time interval between the two images. [d] Photometric distance to the CPM candidate matches the *Hipparcos* distance to the primary (see Table 4.2). [e] New (candidate) companion discovered. [f] Parallax and proper motion for the CPM candidate from literature match the corresponding primary's values from *Hipparcos*. [g] Photometric distance to the CPM candidate is significantly different than primary's *Hipparcos* distance (see Table 4.2). [h] Spectroscopic distance to the CPM candidate matches the *Hipparcos* distance to the primary. [i] Known companion with a published orbit. [j] Identified as twin, comoving diffraction spikes. [k] This star

is not in *Hipparcos* or FvL07 catalogs. It was selected based on Söderhjelm (1999) parallax. Proper motion is from Høg et al. (2000). [1] Companionship confirmed based on matching proper motion and proximity to the primary.

While CPM is necessary for physical association, it is by no means sufficient. In addition to exhibiting CPM, a physically bound companion must pass additional criteria. The attributes I used to make this determination are the magnitude of the proper motion and the proximity to the primary, or a comparison of the estimated distance to the companion with that of the primary from *Hipparcos*. For example, a candidate companion at a small angular separation and sharing a high proper motion with the primary is likely to be physically bound, simply based on the laws of probability. Similarly, if an independent distance estimate to the candidate matches the *Hipparcos* distance to the primary, one can be quite certain that the stars are bound by gravity. Accordingly, candidates were confirmed as true companions if they passed one or more of the following tests.

1. The candidate has independent published measures of trigonometric parallaxes *and* proper motions matching the corresponding *Hipparcos* values of the primary. Each of these companions is identified by its HD, HIP, or other identifier in the last column. Twenty four of the 28 companions confirmed by this method are *Hipparcos* stars themselves, allowing for a check of independent measures of the astrometry by the same instrument and technique. The remaining four non-*Hipparcos* stars, NLTT 9303, LHS 25, HD 237903, and LHS 3509, companions to HD 18143, 26965, 90839, and 190360, respectively, have proper motion measurements from Lépine & Shara (2005) or Salim & Gould (2003) and parallax measures from ground-based efforts (Harrington & Dahn 1980; van Altena et al. 1995; Oppenheimer et al. 2001) that match the corresponding *Hipparcos* values for the primaries within the uncertainties.

2. The candidate has published orbits based on many resolved measures listed in the WDS. All 10 companions confirmed by this method were well-within the saturation region around the primary and identified by twin, comoving diffraction spikes, seen due to the low magnitude-difference between the components. While some of the orbital solutions may be preliminary, they are all good enough to confirm that the measures represent a gravitationally-bound pair.

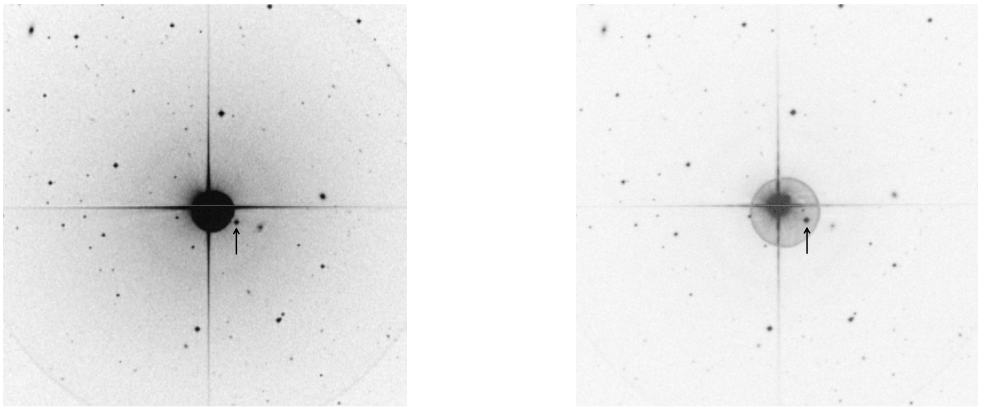

FIGURE 4.6: A new CPM companion to HD 4391 was discovered by blinking the above images and confirmed with photometric distance estimates (see Table 4.2). The companion is marked by the arrows and the primary is the bright star at the center of the images, which are $10'$ on each side and oriented with North up and East to the left. The image on the left is the earlier epoch and on the right is the later epoch of DSS images as listed in Table 4.1.

3. The candidate has photometric distance estimates and published proper motions that match the primary's *Hipparcos* values. The distance estimates were derived using the candidates' $VRIJHK_S$ photometry and fitting various colors to the M_{K_S}–color relations from Henry et al. (2004) for red dwarfs and M_V to $V-I$ relation from Salim et al. (2004) for white dwarfs. The VRI photometry were obtained at the Cerro Tololo Inter-American Observatory's (CTIO) 0.9-m telescope, a facility of the Small and Moderate Aperture Re-

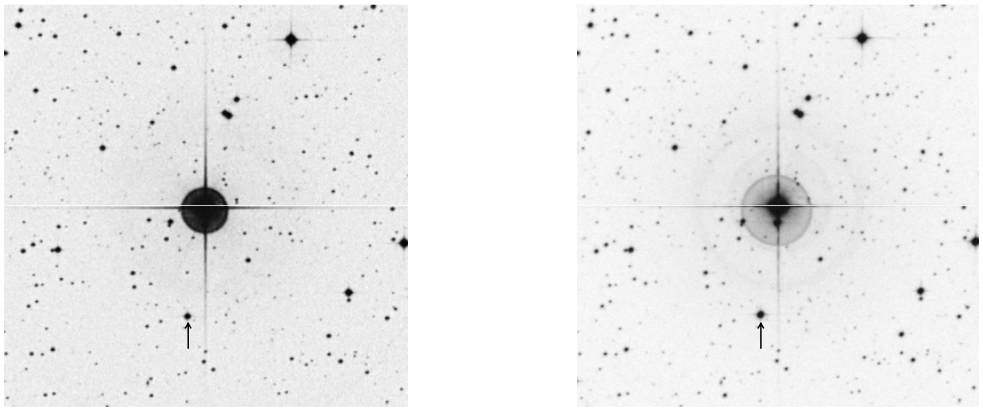

FIGURE 4.7: A new CPM companion to HD 43162 was discovered by blinking the above images. See the caption for Figure 4.6 for further details.

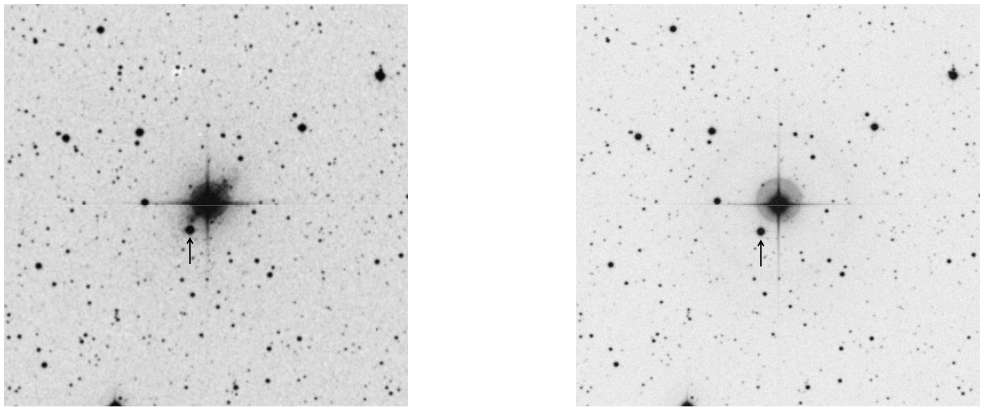

FIGURE 4.8: A new CPM companion to HD 157347 was discovered by blinking the above images. See the caption for Figure 4.6 for further details.

search Telescope System (SMARTS) Consortium, or from publications accessed via VizieR on SIMBAD, and the JHK_S magnitudes were extracted from the Two Micron All Sky Survey Catalog (2MASS). This method enabled the confirmation of 28 candidates. An additional candidate (υ And B) was confirmed based on its infrared magnitudes and spectral type. These candidates are listed in Table 4.2 along with their spectral types, proper motions, and photometry along with their references, and distance estimates. The #1 or #2 notation after

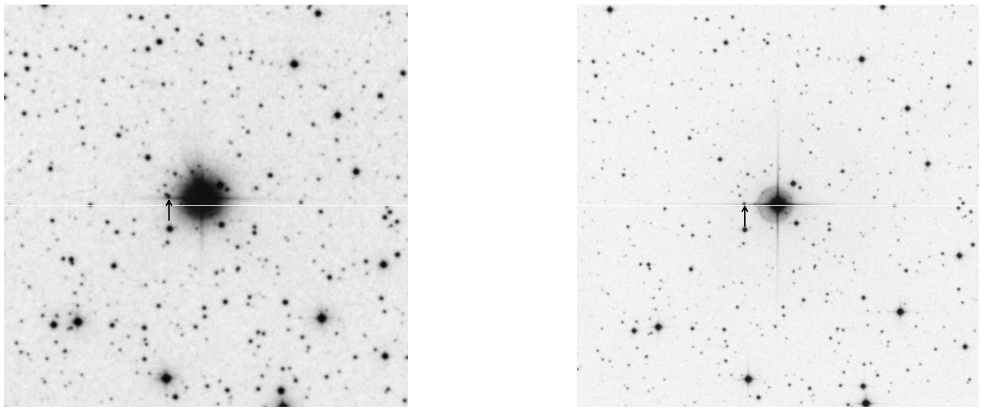

FIGURE 4.9: A new CPM companion to HD 218868 was discovered by blinking the above images. See the caption for Figure 4.6 for further details.

the HD or HIP name in Column 1 denotes the sequence of the companion's listing for the corresponding primary in Table 4.1. While many of these companions have been recognized as companions in publications, several of them are confirmed indisputably for the first time here by matching not only proper motions, but also distances. These results also contain four new companion discoveries, for HD 4391, 43162, and 157347, and HD 218868, which are shown in Figures 4.6–4.9.

TABLE 4.2: Spectral Type, Proper Motion, and Photometry of CPM Candidates

Name	Spectral Type	R	μ_α (mas yr^{-1})	μ_δ (mas yr^{-1})	R	==== CCD Magnitudes ==== V	R	R	R	I	R	Nbr Obs	Infrared Magnitudes J	H	K	D (pc)	Error (pc)
						Confirmed Companions											
HD 004391#1	...	...	...	...	...	14.36	1	13.14	1	11.46	1	3	9.88	9.34	9.03	19.3	3.1
HD 016160#1	...	...	...	...	...	11.68	1	10.47	1	8.87	1	1	7.33	6.79	6.57	6.9	1.1
HD 017382#1	...	...	275	−123	2	16.5	3	13.89	4	...	...	...	10.73	10.17	9.87	22.1	9.0
HD 018757#1	...	...	717	−697	2	12.65	5	...	...	10.07	6	...	8.88	8.33	8.10	22.6	5.2
HD 032778#1	...	...	...	...	...	10.49	1	9.64	1	8.85	1	1	7.86	7.32	7.06	23.9	3.9
HD 043162#1	...	...	...	...	...	12.96	1	11.78	1	10.21	1	1	8.72	8.16	7.87	13.2	2.0
HD 043587#1	...	...	...	...	...	13.29	1	12.11	1	10.58	1	1	9.09	8.56	8.27	16.5	2.5
HD 061606#1	...	...	67	−286	7	8.93	8	8.09	8	7.34	8	...	6.38	5.70	5.57	12.5	2.1
HD 063077#1	DC	15	−246	...1654	6	16.60	1	15.97	1	15.39	1	1	14.78	14.55	14.40	15.3	1.1
HD 065907#1	...	...	521	103	9	9.33	9	...	...	7.47	6	...	6.91	6.28	6.06	17.5	4.8
HD 074385#1	...	...	−294	−84	10	12.68	11	...	...	...	...	...	9.00	8.42	8.17	22.0	3.4
HD 075732#1	...	...	...	...	...	13.26	1	11.91	1	10.24	1	2	8.56	7.93	7.67	8.7	1.4
HD 082342#1	...	...	−75	386	10	13.14	1	12.03	1	10.58	1	1	9.27	8.77	8.50	23.7	4.2
HD 082443#1	...	...	−134	−242	2	16.8	3	14.39	4	12.07	6	...	10.36	9.86	9.47	12.6	5.1
HD 086728#1	M6.5V	12	−408	−327	...	...	...	...	...	...	...	...	10.26	9.64	9.27	...	...
HD 096064#1	...	...	...	...	...	10.0	3	...	...	...	...	...	7.27	6.62	6.42	17.0[a]	2.6
HD 100180#1	...	...	−328	−189	2	9.24	13	7.75	6	...	...	...	7.04	6.52	6.37	23.5	4.3
HD 144579#1	...	...	−547	55	2	14.23	17	12.75	17	11.47	17	...	9.90	9.45	9.16	25.4[b]	7.3
HD 157347#1	M3.0V	1	...	...	...	12.18	1	11.06	1	9.64	1	3	8.26	7.68	7.44	13.4	2.1
HD 187691#1	...	...	...	...	...	12.67	1	11.55	1	10.04	1	1	8.89	8.30	8.01	20.0	4.8
HD 191785#1	M3.5V	1	...	...	...	13.93	1	12.73	1	11.14	1	1	9.63	9.11	8.88	20.9	3.4
HD 197076#1	...	...	...	...	...	11.88	1	10.80	1	9.47	1	1	8.16	7.65	7.42	15.8	2.5
HD 198425#1	...	...	−158	−278	2	18.6	3	15.47	6	13.68	6	...	11.78	11.18	10.86	25.7	7.3
HD 203985#1	M3.5V	1	...	...	...	13.49	1	12.29	1	10.71	1	1	9.22	8.62	8.35	15.9	2.4
HD 211472#1	...	...	205	66	2	13.93	14	...	...	...	...	...	9.72	9.19	8.93	22.3	3.5
HD 212168#1	...	...	...	...	...	8.80	1	8.09	1	7.43	1	1	6.56	5.94	5.81	16.9	2.8
HD 218868#1	...	...	−50	−322	6	15.32	14	...	...	12.57	6	...	10.84	10.23	9.90	25.9	6.0
HD 263175#1	M0.5V	8	...	...	...	12.15	8	11.18	8	10.11	8	...	8.99	8.43	8.18	30.6	4.8
						Refuted Candidate Companions											
HD 009540#1	...	...	...	...	...	12.75	1	11.94	1	11.12	1	1	10.10	9.47	9.35	69.1	11.7
HD 012846#1	...	...	−32	−102	6	11.48	18	10.62	18	9.84	6	...	10.18	9.80	9.66	81.7	13.2
HD 026923#1	...	...	−15	−131	...	9.99	1	9.50	1	9.06	1	1	8.43	8.04	7.88	55.6	8.9
HD 073667#1	...	...	...	...	...	15.35	1	14.27	1	12.96	1	1	11.70	11.18	10.92	82.4	13.4
HD 075767#1	...	...	58	−178	2	13.77	1	12.74	1	11.51	1	1	10.22	9.57	9.30	38.1[b]	6.8
HD 096064#2	...	...	...	...	...	16.20	1	15.36	1	14.60	1	1	13.63	13.06	12.85	355.8	58.7
HD 097658#1	...	...	...	...	...	15.94	1	14.95	1	13.61	1	1	12.32	11.74	11.56	109.4	18.3
HD 114783#1	...	...	...	...	...	9.78	1	9.31	1	8.90	1	2	8.32	7.90	7.79	54.0	9.3
HD 141004#1	...	...	...	...	...	18.35	1	16.92	1	15.11	1	2	13.40	12.85	12.59	76.9	13.2
HD 206860#1	...	...	111	−89	19	15.04	18	14.07	6	13.63	6	...	12.77	12.15	12.06	300.0	83.9
...																	

NOTES.—Reference codes for columns 3, 6, 8, 10, and 12: 1 = CTIO observations obtained for this work, 2 = The LSPM North catalog (Lépine & Shara 2005), 3 = Visual Double Stars in *Hipparcos* (Dommanget & Nys 2000), 4 = The Guide Star Catalog, Version 2.2.01 (I/271), 5 = Catalog of stars with high proper motions (I/306A), 6 = The USNO B 1.0 Catalog (Monet et al. 2003), 7 = The Revised NLTT Catalog (Salim & Gould 2003), 8 = Reid et al. (2004), 9 = All-sky Compiled Catalog (Kharchenko 2001), 10 = NLTT Catalog (Luyten 1979), 11 = The Catalog of Nearby Stars (Gliese & Jahreiß 1991), 12 = Gizis et al. (2000), 13 = An Astrometric Catalog (Rapaport et al. 2001), 14 = The Guide Star Catalog, Version 2.3.2 (Lasker et al. 2008), 15 = Kunkel et al. (1984), 16 = The Tycho-2 Catalog (Høg et al. 2000), 17 = Weis (1996), 18 = The NOMAD Catalog (Zacharias et al. 2004), 19 = The DENIS Consortium (The 2005).

[a] While this distance is too low compared to the primary's *Hipparcos* distance of 24.6 pc, the companion is a tight, roughly equal-brightness binary. Adjusting the *Hipparcos* and 2MASS magnitudes accordingly changes the distance estimate to 24.0 ± 3.7, a much better match with the distance to the primary. [b] See § 7.4.

4. The candidate has a large, matching proper motion with the primary. Three candidates (LHS 2995, NLTT 41169, and LHS 3402, companions to HD 125455, HD 140901, and HIP 91605, respectively) were confirmed by matching proper motions with the primary in the $0\farcs5\,\mathrm{yr}^{-1}$ – $0\farcs8\,\mathrm{yr}^{-1}$ range and proximity within $15''$. One additional candidate (LHS 25, companion to HD 26965) was confirmed despite a large separation of $83''$ because of the unusually large proper motion of $4\farcs1\,\mathrm{yr}^{-1}$ which matches the primary's *Hipparcos* measure. As an additional support, these pairs have been recognized as gravitationally bound in many publications.

Several candidates were also refuted as physical associations upon a closer inspection. Six candidates were refuted because, despite an apparently matching proper motion with the primary seen on blinking, published proper motion values for the candidates were significantly different than the primary's *Hipparcos* value. One candidate was identified as a non-stellar plate defect because no star was found at the telescope at the expected position, and 10 more were refuted after the photometry obtained indicated a significantly different distance than the primary's *Hipparcos* value. In summary, this method revealed 78 candidate CPM companions, 61 of which were confirmed and 17 refuted.

4.2 Linear Motion of Field Stars

In addition to identifying CPM companions, blinking archival images is an effective method for verifying the status of double star measures in catalogs such as the WDS. The WDS is a *double* star catalog, not a *binary* star catalog, and as such explicitly contains many entries of

unrelated pairs with relative separation measures. The blinking of archival images affords a simple way of identifying these pairs as potential companions with matching proper motions or unrelated field stars with differing motions. For distant field stars that have many WDS measures over an extended period, the relative separations will change in a linear fashion, reflecting the high proper motion of the primary. Figure 4.10 shows such an example of two WDS entries for HD 146361 (σ^2 CrB) that are clearly unrelated field stars, and Table 4.3 lists all the WDS entries for the stars of this study that were identified as field stars with a chance alignment but a differing transverse motion.

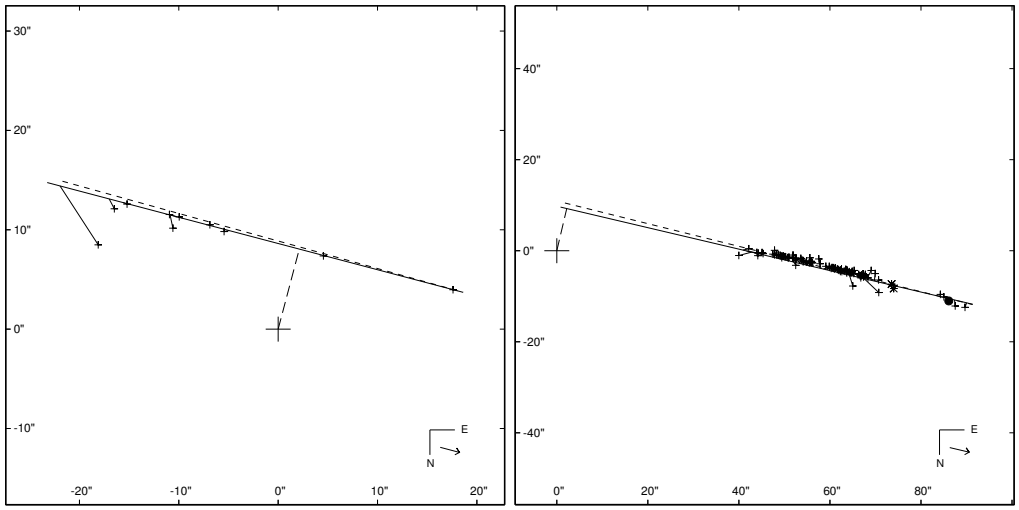

FIGURE 4.10: Examples of the linear motion of unrelated field stars that are listed in the WDS catalog as double star entries for HD 146361. The left panel is for WDS component C (ADS 9979C) and the right panel is for WDS component D (ADS 9979D). Plus signs indicate micrometric observations, asterisks indicate photographic measures, and filled circles represent Tycho measures. $O-C$ lines connect each measure to its predicted position along the linear fit (thick solid line). The thick dashed line is the predicted movement based on the differential proper motions. The long dashed line connected to the origin indicates the predicted closest apparent position. The scale is in seconds of arc. An arrow in the lower right corner by the north and east direction indicators shows the direction of motion of the star.

TABLE 4.3: Optical WDS entries

WDS ID	Disc Desig	Comp ID	Primary Name	Nbr Obs	θ (deg)	ρ ($''$)	Epoch
00022+2705	BU 733	AC	HD 224930	64	325	161.7	2000
00022+2705	BU 733	AD	HD 224930	15	296	109.9	1921
00022+2705	HSW 1	AE	HD 224930	2	309	100.9	1998
00066+2901	ENG 1	A-CD	HD 000166	9	196	142.4	1991
00066+2901	STT 549	AB	HD 000166	15	259	186.7	2002
00066+2901	BU 1338	CD	HD 000166	8	210	3.2	1999
00200+3814	S 384	AB	HD 001562	43	22	100.7	2003
00200+3814	S 384	AC	HD 001562	4	260	22.6	1998
00229−1213	BUP 6	...	HD 001835	5	294	213.9	1998
00352−0336	BU 490	AB-C	HD 003196	15	324	24.4	1998
00394+2115	STT 550	AB	HD 003651	9	80	167.6	1997
00484+0517	BUP 10	Aa-B	HD 004628	4	241	158.5	2000
00490+1656	BUP 12	AB	HD 004676	4	330	82.9	1998
00490+1656	BUP 12	AC	HD 004676	4	162	64.2	1998
00491+5749	STF 60	AC	HD 004614	4	258	216.0	1991
00491+5749	STF 60	AD	HD 004614	5	1	177.0	1991
00491+5749	STF 60	AE	HD 004614	12	127	91.8	2002
00491+5749	STF 60	AF	HD 004614	2	275	369.3	1991
00491+5749	STF 60	AG	HD 004614	15	256	409.8	2002
00491+5749	STF 60	AH	HD 004614	2	355	689.2	1991
00491+5749	STF 60	BC	HD 004614	3	237	152.0	1921
00491+5749	STF 60	BE	HD 004614	3	121	220.8	1991
00491+5749	STF 60	BH	HD 004614	3	356	679.9	1991
00491+5749	STF 60	FG	HD 004614	5	188	142.3	2000
00498+7027	ENG 2	...	HD 004635	9	277	90.9	1999
00531+6107	BU 497	AB	HD 005015	22	172	145.0	2003
00531+6107	BU 497	AD	HD 005015	3	145	105.6	1991
00531+6107	BU 497	AE	HD 005015	2	42	127.4	1959
00531+6107	BU 497	BC	HD 005015	7	162	0.9	1946
01083+5455	STT 551	Aa-B	HD 006582	14	270	428.9	1998
01083+5455	BUP 14	Aa-C	HD 006582	2	258	175.6	1991
01083+5455	BUP 14	Aa-E	HD 006582	1	145	87.7	1907
01083+5455	STT 551	Aa-F	HD 006582	2	328	53.2	1854
01083+5455	BUP 14	CD	HD 006582	2	115	4.3	1998
01291+2143	HO 9	AB	HD 008997	24	47	55.7	2003

Continued on Next Page...

TABLE 4.3 – Continued

WDS ID	Disc Desig	Comp ID	Primary Name	Nbr Obs	(θ (deg)	ρ ($''$)	Epoch
01291+2143	HO 9	AD	HD 008997	11	217	81.8	1999
01291+2143	HO 9	BC	HD 008997	23	91	2.7	2001
01350−2955	BU 1000	AB-D	HD 009770	12	19	132.2	1998
01368+4124	BUP 23	AB	HD 009826	1	128	114.0	1909
01368+4124	STT 554	AC	HD 009826	9	291	271.6	2006
01425+2016	HJ 2071	AB	HD 010476	6	10	53.2	1998
01425+2016	HJ 2071	AC	HD 010476	13	4	154.0	1998
01441−1556	BUP 25	...	HD 010700	5	157	137.0	2000
01477+6351	ENG 7	...	HD 010780	10	176	45.9	2003
01591+3313	ENG 9	AB	HD 012051	11	137	92.8	2002
01591+3313	BUP 28	AC	HD 012051	3	26	91.2	1934
02171+3413	DOR 66	AB	HD 013974	2	337	65.4	1907
02442+4914	STF 296	AC	HD 016895	18	229	77.2	1924
02442+4914	STF 296	BC	HD 016895	13	215	73.5	1924
03042+6142	KUI 11	AB	HD 018757	1	132	12.7	1931
03091+4937	BUP 38	...	HD 019373	1	132	146.2	1911
03194+0322	STT 557	AB	HD 020630	16	166	266.6	2002
03194+0322	BUP 42	BC	HD 020630	6	272	214.2	2000
03329−0927	MBA 1	AB	HD 022049	1	326	17.1	2001
03329−0927	MBA 1	AC	HD 022049	1	15	17.6	2001
03329−0927	MBA 1	AD	HD 022049	1	355	44.3	2001
03329−0927	MBA 1	AE	HD 022049	1	69	28.7	2001
03329−0927	MBA 1	AF	HD 022049	1	70	41.3	2001
03329−0927	MBA 1	AG	HD 022049	1	119	41.1	2001
03329−0927	MBA 1	AH	HD 022049	1	321	21.0	2001
03329−0927	MBA 1	AI	HD 022049	1	294	34.0	2001
03329−0927	MBA 1	AJ	HD 022049	1	145	27.9	2001
03329−0927	MBA 1	AK	HD 022049	1	208	38.5	2001
03562+5939	ENG 16	AB	HD 024409	10	7	134.7	1999
03562+5939	ENG 16	AC	HD 024409	7	50	193.4	1999
03562+5939	BUP 48	AF	HD 024409	2	75	37.6	1925
04033+3516	OSO 16	...	HD 025329	3	240	16.0	1994
04053+2201	STT 559	Aa-B[a]	HD 025680	20	359	176.8	2003
04053+2201	STT 559	Aa-C	HD 025680	5	17	149.2	1997
04053+2201	STT 559	BC	HD 025680	8	124	58.2	1997
04076+3804	STT 531	AC	HD 025998	15	218	225.2	2002
04076+3804	BU 545	CD	HD 025998	15	305	1.3	1991

Continued on Next Page...

TABLE 4.3 – Continued

WDS ID	Disc Desig	Comp ID	Primary Name	Nbr Obs	(θ (deg)	ρ ($''$)	Epoch
04153−0739	STF 518	AD	HD 026965	18	97	77.9	1992
04153−0739	STF 518	AE	HD 026965	10	8	211.0	1907
04153−0739	STF 518	BD	HD 026965	1	196	147.0	1922
04153−0739	STF 518	BE	HD 026965	1	356	279.5	1922
04155+0611	H 4 98	AC	HD 026923	8	48	230.1	2003
04155+0611	H 4 98	CD	HD 026923	7	316	54.3	1987
05188−1808	SEE 50	AB	HD 034721	4	234	45.5	1951
05188−1808	SEE 50	BC	HD 034721	2	101	15.8	1951
05191+4006	STFB 3	AB	HD 034411	1	274	29.1	1900
05191+4006	STFB 3	AC	HD 034411	6	268	41.7	1934
05191+4006	STFB 3	AD	HD 034411	29	349	203.4	2003
05191+4006	DOB 4	AE	HD 034411	5	34	174.8	2003
05191+4006	KUI 20	CB	HD 034411	2	351	27.2	1934
05191+4006	DOB 4	DE	HD 034411	10	112	147.7	2003
05226+7914	STF 634	AB	HD 033564	86	135	25.8	2001
05226+7914	STF 634	AC	HD 033564	3	333	173.1	1999
05244+1723	S 478	AB	HD 035296	35	271	102.7	2002
05413+5329	BUP 82	AC	HD 037394	3	307	87.1	1925
05413+5329	BUP 82	AD	HD 037394	2	262	688.0	1909
05413+5329	BUP 82	BE	HD 037394	2	159	129.7	1910
05460+3717	BLL 16	...	HD 038230	3	104	104.0	1954
05584−0439	A 322	AC	HD 040397	13	304	195.5	2002
06173+0506	ENG 26	AB	HD 043587	8	241	179.7	2002
06173+0506	BUP 87	AC	HD 043587	1	265	58.5	1911
06173+0506	BUP 87	AD	HD 043587	1	231	69.3	1911
06467+4335	SHJ 75	AB	HD 048682	47	40	30.1	2007
06467+4335	WAL 47	AC	HD 048682	1	330	80.0	1944
07040−4337	WRH 38	AD	HD 053705	2	268	33.3	1999
07096+2544	HO 519	AB	HD 054371	6	103	22.2	1927
07096+2544	STTA 83	AC	HD 054371	32	80	120.5	2002
07291+3147	A 2124	AC	HIP 036357	14	285	221.7	1998
07291+3147	A 2124	CD	HIP 036357	3	270	102.3	1998
07549+1914	ENG 33	AB	HD 064468	12	285	96.8	2007
07549+1914	ENG 33	AC	HD 064468	10	65	125.4	2007
07549+1914	BUP 109	AD	HD 064468	3	28	43.1	1925
08116+3227	STT 564	AB	HD 068017	6	327	55.0	1915
08116+3227	STT 564	AC	HD 068017	10	66	289.3	2007

Continued on Next Page...

TABLE 4.3 – Continued

WDS ID	Disc Desig	Comp ID	Primary Name	Nbr Obs	(θ (deg)	ρ ($''$)	Epoch
08122+1739	STF1196	AB-D	HD 068257	12	107	275.2	2007
08122+1739	ENH 1	AB-E	HD 068257	3	26	557.7	1991
08122+1739	ENH 1	AB-F	HD 068257	2	47	629.2	1894
08122+1739	ENH 1	AB-G	HD 068257	3	332	664.4	1991
08122+1739	STF1196	CD	HD 068257	5	107	274.8	1991
08122+1739	ENH 1	EF	HD 068257	6	106	218.7	1997
08379−0648	HJ 99	AB	HD 073350	15	181	60.2	2002
08379−0648	HJ 99	BC	HD 073350	3	215	9.8	1999
08391−2240	BU 208	AC	HD 073752	6	186	113.7	1999
08398+1131	ENG 36	AB	HD 073667	9	337	142.3	2002
08398+1131	BUP 119	BC	HD 073667	10	13	30.6	2002
09123+1500	BUP 125	Aa-B[b]	HD 079096	1	118	35.4	1907
09123+1500	STT 569	Aa-C	HD 079096	11	217	204.4	2007
09123+1500	SLE 478	Aa-D[b]	HD 079096	1	118	80.1	1984
09179+2834	ABT 6	AB-C	HD 079969	1	56	152.4	1921
09179+2834	ABT 6	AB-D	HD 079969	3	133	166.4	1999
10189+4403	ENG 43	...	HD 089269	14	97	145.2	2002
10306+5559	ARN 4	AC	HD 090839	3	294	233.1	2002
10314−5343	HJ 4329	...	HD 091324	28	103	73.9	2000
10365−1214	KUI 51	...	HD 091889	6	0	37.5	2007
11125+3549	STTA108	AB	HD 097334	23	67	156.5	2004
11125+3549	STTA108	AC	HD 097334	4	144	86.5	1998
11125+3549	STTA108	BD	HD 097334	2	88	34.9	1910
11182+3132	POP1219	AC	HD 098230	3	324	56.4	2007
11268+0301	STF1540	AC	HD 099491	3	187	90.5	1937
11387+4507	STF1561	AC	HD 101177	22	90	164.9	2006
11387+4507	STF1561	AD	HD 101177	2	76	704.2	1991
11387+4507	STF1561	AE	HD 101177	6	331	64.5	2001
11387+4507	STF1561	BC	HD 101177	17	89	173.3	2002
11387+4507	STF1561	BE	HD 101177	5	340	64.0	2000
11387+4507	STF1561	CD	HD 101177	3	72	552.9	1991
11411+3412	STT 574	...	HD 101501	11	88	158.4	1998
11507+0146	STT 576	AB	HD 102870	11	285	305.3	1984
11507+0146	STT 576	AC	HD 102870	4	80	421.7	2002
12337+4121	BU 1433	Aa-B	HD 109358	6	200	264.7	2007
13119+2753	STT 578	...	HD 114710	11	238	85.8	1924
13168+0925	KUI 62	...	HD 115383	1	89	34.3	1958

Continued on Next Page...

TABLE 4.3 – Continued

WDS ID	Disc Desig	Comp ID	Primary Name	Nbr Obs	(θ (deg)	ρ ($''$)	Epoch
13169+1701	BU 800	AC	HD 115404	7	339	120.6	1999
13169+1701	BU 800	AD	HD 115404	1	88	50.8	1990
13184−1819	H 6 90	...	HD 115617	13	37	376.2	2007
13284+1347	STT 579	AB	HD 117176	14	127	268.6	2002
13284+1347	DIC 3	AC	HD 117176	1	263	325.5	1923
13547+1824	SHJ 169	...	HD 121370	27	87	113.3	2007
14190−2549	BU 1246	AB	HD 125276	4	217	8.0	1936
14190−2549	BU 1246	AC	HD 125276	9	117	82.6	1999
14514+1906	STF1888	AC	HD 131156	8	342	68.6	2000
14514+1906	STF1888	AD	HD 131156	7	286	159.6	2007
14514+1906	ARN 11	AE	HD 131156	6	99	269.2	2007
14514+1906	ARN 12	AF	HD 131156	5	38	333.7	2007
14514+1906	STF1888	BC	HD 131156	6	347	60.3	1953
14514+1906	STF1888	BE	HD 131156	10	99	274.5	2007
14537+2321	COU 101	...	HD 131582	3	68	51.0	2000
15193+0146	STF1930	AC	HD 136202	5	40	127.2	1924
15193+0146	STF1930	AD	HD 136202	4	268	674.7	1911
15232+3017	STF1937	AB-C	HD 137107	8	0	69.2	1984
15232+3017	STF1937	AB-D	HD 137107	6	41	217.5	2000
15282−0921	SHJ 202	BC	HD 137763	4	99	152.8	1999
15292+8027	STF1972	AC	HD 139777	3	102	153.8	1983
15360+3948	STT 298	AB-D	HD 139341	4	232	189.3	1934
15360+3948	STT 298	AB-E	HD 139341	4	335	456.4	1999
15360+3948	STT 298	CE	HD 139341	4	337	335.8	1999
15440+0231	A 2230	AC	HD 140538	9	208	195.5	2002
15440+0231	A 2230	AD	HD 140538	17	285	172.8	2002
15440+0231	A 2230	CE	HD 140538	14	235	171.0	2002
15475−3755	SEE 249	AC	HD 140901	6	125	8.4	1956
15532+1312	STT 583	...	HD 142267	9	86	102.4	1998
16010+3318	S 676	...	HD 143761	23	49	135.3	2002
16133+1332	STF2021	Aa-C	HD 145958	12	118	206.7	1998
16147+3352	STF2032	AC	HD 146361	11	93	24.2	2007
16147+3352	STF2032	AD	HD 146361	107	82	90.5	2006
16147+3352	STF2032	BD	HD 146361	66	81	95.0	1998
16156−0822	BUP 165	...	HD 146233	2	280	25.8	1958
16243−1338	BUP 169	AB	HD 147776	3	281	103.0	1909
16289+1825	STF2052	AC	HD 148653	2	29	143.3	1925

Continued on Next Page...

TABLE 4.3 – Continued

WDS ID	Disc Desig	Comp ID	Primary Name	Nbr Obs	(θ (deg)	ρ ($''$)	Epoch
16315−3901	HDS2335	...	HD 148704	2	221	4.1	1991
16364−0219	BUP 171	...	HD 149661	1	245	100.3	1910
17153−2636	SHJ 243	AD	HD 155885	11	338	276.6	1998
17153−2636	SHJ 243	AE	HD 155885	3	312	38.4	1998
17153−2636	SHJ 243	BD	HD 155885	6	339	284.9	1987
17191−4638	BSO 13	AC	HD 156274	2	279	41.8	1900
17191−4638	BSO 13	AD	HD 156274	1	30	47.0	1900
17207+3228	DOR 1	AB	HD 157214	12	340	308.1	2002
17207+3228	ARN 14	AD	HD 157214	1	59	395.0	2002
17207+3228	ARN 14	AE	HD 157214	3	51	302.2	2002
17207+3228	ARN 14	AF	HD 157214	3	104	383.2	2002
17207+3228	DOR 1	BC	HD 157214	2	216	8.8	1911
17350+6153	SDR 1	AB-D	HD 160269	2	245	23.9	1999
17419+7209	STF2241	AC	HD 162004	12	108	79.2	1999
17419+7209	STF2241	AD	HD 162004	1	84	100.5	1905
17419+7209	STF2241	CD	HD 162004	1	19	67.6	1908
17465+2743	ABT 14	Aa-D	HD 161797	1	0	256.1	1921
17465+2743	ABT 14	BC-D	HD 161797	1	7	272.6	1921
18025+2619	HO 564	AB	HD 164922	6	326	96.1	1999
18025+2619	HO 564	AC	HD 164922	2	57	80.3	1924
18055+0230	STF2272	AC	HD 165341	53	282	34.9	1947
18055+0230	STF2272	AD	HD 165341	18	324	88.1	2007
18055+0230	STF2272	AR	HD 165341	24	29	155.0	2000
18055+0230	STF2272	AS	HD 165341	35	11	193.2	2000
18055+0230	STF2272	AT	HD 165341	23	48	125.9	2007
18055+0230	STF2272	AU	HD 165341	15	334	184.5	1945
18055+0230	STF2272	AV	HD 165341	37	246	138.6	1946
18055+0230	STF2272	AY	HD 165341	2	354	231.9	2000
18055+0230	STF2272	BC	HD 165341	4	252	32.4	1932
18055+0230	STF2272	BD	HD 165341	1	247	69.3	1900
18055+0230	STF2272	BR	HD 165341	22	50	121.1	2000
18055+0230	STF2272	BZ	HD 165341	2	163	68.3	2000
18055+0230	STF2272	VT	HD 165341	21	72	247.3	1946
18055+0230	STF2272	VW	HD 165341	4	270	180.9	1910
18055+0230	STF2272	VX	HD 165341	2	254	17.4	2002
18070+3034	AC 15	AC	HD 165908	6	59	96.2	1998
18070+3034	AC 15	AD	HD 165908	4	103	140.0	1998

Continued on Next Page...

TABLE 4.3 – Continued

WDS ID	Disc Desig	Comp ID	Primary Name	Nbr Obs	(θ (deg)	ρ ($''$)	Epoch
18070+3034	AC 15	AE	HD 165908	4	78	168.8	1998
18070+3034	AC 15	AF	HD 165908	2	165	162.5	1998
18070+3034	AC 15	AG	HD 165908	5	360	177.0	1998
18570+3254	BU 648	AB-C	HD 176051	7	289	64.7	1960
18570+3254	BU 648	AB-D	HD 176051	4	198	85.0	1998
18570+3254	BU 648	AE	HD 176051	3	320	105.3	1934
18570+3254	BU 648	AF	HD 176051	3	87	100.3	1934
19080+1651	ENG 66	Aa-B	HD 178428	10	288	132.3	2007
19121+4951	STF2486	AC	HD 179957	4	101	26.8	2005
19121+4951	STF2486	AD	HD 179957	6	102	192.9	2000
19250+1157	STT 588	AB	HD 182572	29	286	101.7	2006
19250+1157	STT 588	AC	HD 182572	7	282	140.6	2000
19250+1157	COM 7	AD	HD 182572	3	140	78.8	1914
19250+1157	STT 588	BC	HD 182572	24	266	44.2	2006
19324+6940	STT 590	...	HD 185144	6	339	492.8	1999
19456+3337	STF2576	AC	HD 186858	3	348	51.8	1998
19456+3337	STF2576	AD	HD 186858	7	333	35.1	1998
19456+3337	TKA 1	AE	HD 186858	2	249	25.9	2006
19456+3337	STF2576	BD	HD 186858	2	257	15.9	1919
19464+3344	STF2580	FH	HD 186858	32	125	110.5	2005
19464+3344	KPR 4	FI	HD 186858	4	63	105.6	2005
19464+3344	KPR 4	FJ	HD 186858	1	61	40.9	1960
19464+3344	STF2580	GH	HD 186858	21	139	101.3	1999
19510+1025	J 124	AB	HD 187691	4	203	14.4	1958
19510+1025	POP1228	AD	HD 187691	3	121	53.5	2002
19510+1025	POP1228	AE	HD 187691	3	147	84.6	2002
20041+1704	STT 592	AB	HD 190406	20	289	166.9	2002
20041+1704	STT 592	AC	HD 190406	22	333	213.9	2001
20041+1704	BUP 202	AD	HD 190406	6	360	83.7	2002
20041+1704	BUP 202	AE	HD 190406	3	51	169.0	2000
20041+1704	BUP 202	AF	HD 190406	2	312	142.3	2000
20041+1704	ENG 69	BC	HD 190406	19	204	151.5	2000
20041+1704	STTA202	BG	HD 190406	15	232	182.7	2002
20041+1704	BUP 202	CH	HD 190406	3	185	95.4	2000
20052+3829	BU 1481	AB	HD 190771	1	230	12.4	1906
20052+3829	WAL 126	AC	HD 190771	3	180	40.0	1944
20096+1648	STF2634	AC	HD 191499	2	312	74.8	1924

Continued on Next Page...

TABLE 4.3 – Continued

WDS ID	Disc Desig	Comp ID	Primary Name	Nbr Obs	(θ (deg)	ρ ($''$)	Epoch
20111+1611	ENG 71	AB	HD 191785	9	148	205.4	2002
20111+1611	HZG 15	AD	HD 191785	7	267	40.8	1998
20111+1611	BUP 205	BC	HD 191785	4	273	61.7	2002
20140−0052	BU 1485	A-BC	HD 192263	19	102	73.1	2003
20140−0052	ABT 15	AD	HD 192263	1	244	71.3	1921
20140−0052	J 551	BC	HD 192263	4	265	0.2	1949
20140−0052	BU 1485	BC-D	HD 192263	8	65	23.5	1998
20324−0951	BU 668	AC	HD 195564	6	200	103.2	1921
20408+1956	BUP 215	AB	HD 197076	2	25	93.7	1924
21028+4551	BU 1138	AB	HD 200560	54	170	0.1	1985
21028+4551	BU 1138	CA	HD 200560	19	150	153.1	2002
21028+4551	BU 1138	CE	HD 200560	6	250	5.6	1962
21072−1355	BU 157	AC	HD 200968	15	287	26.2	1999
21072−1355	KPR 5	AD	HD 200968	1	78	276.2	1950
21145+1000	STF2777	AB-C	HD 202275	80	6	72.5	2005
21180+0010	ENG 82	AB	HD 202751	10	44	157.0	2003
21180+0010	TOB 317	AD	HD 202751	2	56	129.1	2000
21180+0010	BUP 228	BC	HD 202751	3	117	12.3	2000
21180+0010	LYS 44	BD	HD 202751	2	182	41.8	2000
21198−2621	BU 271	AC	HD 202940	3	72	81.7	1909
21198−2621	BU 271	AD	HD 202940	1	62	247.2	1917
21198−2621	BU 271	AE	HD 202940	2	32	180.6	1999
21441+2845	STF2822	AC	HD 206826	14	290	72.6	1999
21441+2845	STF2822	AD	HD 206826	46	45	197.5	2001
21441+2845	STF2822	BD	HD 206826	23	46	198.7	1991
21441+2845	ES 521	DE	HD 206826	3	284	16.9	1999
21483−4718	BSO 15	...	HD 207129	29	351	75.2	1999
22159+5440	BU 377	AB	HD 211472	17	62	38.0	2006
22159+5440	BU 377	AC	HD 211472	6	52	35.2	2006
22159+5440	BU 377	AD	HD 211472	5	158	22.2	2006
22159+5440	BU 377	AQ	HD 211472	3	259	56.6	1999
22159+5440	BU 377	AR	HD 211472	2	256	62.7	1999
22159+5440	BU 377	AS	HD 211472	3	336	55.4	2006
22159+5440	BU 377	BC	HD 211472	11	303	6.7	2007
22159+5440	BU 377	QR	HD 211472	2	233	6.6	1999
22249−5748	I 383	...	HD 212330	2	237	81.2	1914
22467+1210	HJ 301	AC	HD 215648	5	15	145.0	1924

Continued on Next Page...

TABLE 4.3 – Continued

WDS ID	Disc Desig	Comp ID	Primary Name	Nbr Obs	(θ (deg)	ρ ($''$)	Epoch
22514+1358	STT 597	AB	HD 216259	12	329	201.2	1998
22514+1358	BUP 233	BC	HD 216259	3	194	114.1	1998
23108+4531	HJ 1853	...	HD 218868	2	281	31.4	1905
23133+5710	STT 599	...	HD 219134	12	244	271.6	2002
23167+5313	BUP 235	...	HD 219623	2	320	129.3	1930
23399+0538	BUP 240	AB	HD 222368	4	305	119.2	2002
23399+0538	BUP 240	AC	HD 222368	3	21	307.3	2002
23524+7533	BU 996	AC	HD 223778	11	141	145.7	2000

[a] Candidate companion is HIP 19075 which is a G-dwarf with a *Hipparcos* parallax indicating a distance of 220 pc, clearly unrelated to the primary as also seen upon blinking the DSS images. [b] The pairs Aa-B and Aa-D are in fact measures of the same pair, 74 years apart.

The large-scale homogeneity of the universe makes it very difficult to believe that the structure of the universe is determined by anything so peripheral as some complicated molecular structure on a minor planet orbiting a very average star in the outer suburbs of a fairly typical galaxy.

—— Stephen W. Hawking

– 5 –

Other Astrometric Results

5.1 The *Hipparcos* Double Stars

The *Hipparcos* mission obtained accurate astrometry of over 100,000 stars from space, and the cataloged results have revolutionized the understanding of all types of stars. The current effort has greatly benefited from this catalog, not only in defining a more accurate and complete sample as discussed in Chapter 2, but also in a more thorough investigation of companions. While astrometric companions were historically limited to wide CPM pairs as discussed in Chapter 4, the precise measurements of *Hipparcos* enabled one to probe significantly closer to the primary stars by, for example, deriving orbits from the observed photocentric motion around an implied center-of-mass or identifying unseen companions by the deviation of proper motion from a linear path. This section covers the analysis of the *Hipparcos* double stars and their evaluation for the multiplicity statistics derived.

The primary identification of companion stars in the *Hipparcos* catalog is done via field H59, with further details in the *Double and Multiple Systems Annex*. Potential companions are identified as one of five types by this multiplicity flag: C (component solutions) where a nearby source is resolved, G (acceleration observed in the proper motion implying an unseen companion), O (orbital solutions obtained using *Hipparcos* data), V (movement detected in the photocenter based on the variability of one or more components), or X (stochastic solutions, implying that an acceptable astrometric solution was not obtained as either a single

or a double star). None of the targets of this work are flagged as 'V' in field H59, and hence this indicator is not discussed further. In addition to this multiplicity flag, field H61 of the main catalog lists an 'S' for suspected non-single stars, based on the astrometric fit obtained, although a satisfactory double star solution could not be obtained. Some of these correspond to the 'X' entries of field H59. Also, field H52 contains a 'D' (duplicity-induced variability) identifying photometric variability presumably caused by a companion. While these two indicators contribute 16 possible companions that are not identified by field H59, I do not consider them reliable companion detection indicators for this work without an independent confirmation. There are several additional flags in the catalog that can imply a companion, such as H10, which contains a reference flag for components of double or multiple systems, and H62, which is a component designation for double or multiple systems. However, these indicators overlap with the flags discussed above in all cases, and are not discussed further because they do not contribute any new companions. The following subsections treat each of the companion indicators considered and describe the methods of this survey in evaluating their verity.

While the *Hipparcos* identification of companions is a very useful source, it is neither definite nor complete. Quist & Lindegren (2000) modeled a binary distribution based on the DM91 statistics and found that the number of orbits presented in the *Hipparcos* catalog is deficient by a factor of about three. On the other hand, the description of the catalog points out that several of the companion identification flags may correspond to optical pairs (more on this in the subsections below), and follow-up efforts have had limited success in

resolving suspected companions. Mason et al. (1999) studied a majority of the unresolved *Hipparcos* double stars via speckle interferometry and were able to resolve components for only 13% of the binaries flagged as 'G' in field H59. Mason et al. (2001) confirm this low detection fraction, pointing out that the multiplicity fraction observed among *Hipparcos* double stars is far less than that of a random selection of bright field stars, and speculate that speckle interferometry may not adequately address the separation–Δmag space occupied by the *Hipparcos* double stars. Falin & Mignard (1999) reanalyzed the *Hipparcos* raw data with a specific view to improving the double or multiple star information presented and found that many well-observed systems retain poor solutions. They speculated that this could be due to one of three reasons – they are binaries with periods of 1–10 years, or they are components of multiple systems of weak hierarchy with motions too complicated to model with *Hipparcos* data, or that some of the data relates to poor pointing. Finally, one notable example involving Arcturus has been published, concluding that instrumental and random errors resulted in the mimicking of a spurious binary (Soderhjelm & Mignard 1998). Due to these factors, I have not taken every *Hipparcos* companion designation as real, but rather evaluated them individually depending on their type, as described below.

5.1.1 Component Solutions

These companions, identified by a 'C' in field H59, represent double stars resolved by *Hipparcos* as separated components which could be modeled as single stars, usually with an assumed common parallax. For these systems, field H61 gives an indication of the reliability of the double or multiple star solution with a quality of A (good), B (fair), C (poor), and D

(uncertain). Among the sample studied here, 62 stars were flagged as *Hipparcos* component solutions, and 59 of these have independent supporting evidence and are hence considered real. Of the remaining three, two are flagged as quality 'C', or poor solution, in field H61 (HD 64606 and 111312) and are retained as candidate companions, and an additional one (HD 148704) has been refuted by this work despite its quality 'A' designation in *Hipparcos* based on evidence of differential proper motion (see § 7.4 for more information). Table 5.1 lists all entries of this type identified by the HD and HIP names and the companion ID as in the Annex, along with the quality flag (field H61), the final status used in the multiplicity statistics derived here, and the reason for this conclusion.

TABLE 5.1: *Hipparcos* Component Solutions

HD Name	**HIP Name**	**Companion ID**	**Solution Quality**	**Companion Status**	**Reason**
000123	000518	B	A	YES	1
003196	002762	B	A	YES	2
003443	002941	B	A	YES	2
004614	003821	B	A	YES	1
007693	005842	D	A	YES	1
009770	007372	B	C	YES	1
010360	007751	A	D	YES	1
016765	012530	B	B	YES	3
018143	013642	B	A	YES	1
020010	014879	B	A	YES	1
024409	018413	D	A	YES	4
025893	019255	B	A	YES	1
035112	025119	B	A	YES	1
037572	026373	B	B	YES	6
039855	027922	B	A	YES	6
048189	031711	B	A	YES	7
053705	034065	B	A	YES	6

Continued on Next Page...

TABLE 5.1 – Continued

HD Name	HIP Name	Companion ID	Solution Quality	Companion Status	Reason
057095	035296	B	A	YES	1
064096	038382	B	A	YES	2
064606	038625	B	C	MAY	4
068255	040167	B	B	YES	1
068255	040167	C	B	YES	1
073752	042430	B	A	YES	1
096064	054155	B	C	YES	1
096064	054155	C	C	YES	6
099491	055846	B	D	YES	6
100180	056242	B	A	YES	6
101177	056809	B	A	YES	1
111312	062505	B	C	MAY	10
115404	064797	B	A	YES	1
116442	065352	B	A	YES	6
128620	071683	B	D	YES	2
130042	072493	B	A	YES	7
131156	072659	B	A	YES	1
133640	073695	B	B	YES	1
137107	075312	B	A	YES	2
139341	076382	B	A	YES	1
145958	079492	B	A	YES	1
146361	079607	B	B	YES	2
148653	080725	B	A	YES	1
148704	080925	C	A	NO	8
153557	083020	B	B	YES	7
155885	084405	A	A	YES	1
156274	084720	B	A	YES	9
158614	085667	B	A	YES	2
160269	086036	B	A	YES	9
162004	086620	B	D	YES	6
165341	088601	B	D	YES	2
165908	088745	B	A	YES	1
...	091605	B	B	YES	6
176051	093017	B	A	YES	9
177474	093825	B	A	YES	1
179957	094336	B	A	YES	1
184467	095995	S	B	YES	2

Continued on Next Page...

TABLE 5.1 – Continued

HD Name	HIP Name	Companion ID	Solution Quality	Companion Status	Reason
186858	097222	B	A	YES	1
189340	098416	B	A	YES	2
191499	099316	B	A	YES	10
200968	104239	B	A	YES	3
202275	104858	B	A	YES	2
202940	105312	B	A	YES	9
206826	107310	B	A	YES	1
212168	110712	B	A	YES	11

NOTES.—Column 6 notes: (1) = Visual orbit exists (see § 5.2); (2) = Double-lined spectroscopic and visual orbits exist (see § 5.2 and § 6.2); (3) = Measurements in the WDS confirm orbital motion; (4 = Single-lined spectroscopic orbit exists (see § 6.2); (5) = Radial velocity variations observed (see § 6.2); (6) = Companion has matching independent parallax and proper motion with primary (see § 4.1); (7) = Matching proper motion and proximity to primary confirm companionship; (8) = Proper motions do not match (see § 7.4); (9) = Single-lined spectroscopic and visual orbits exist (see § 5.2 and § 6.2); (10) = See individual system notes in § 7.4; (11) = Companion has matching proper motion and distances with the primary (see § 4.1).

5.1.2 Accelerating Proper Motions

Due to the high precision of the *Hipparcos* astrometry, deviations of proper motion from a linear path can be detected during the approximately three years of observations, indicating orbital motion around a center of mass with an unseen companion with orbital periods larger than some 10 years. Such companions, identified as ones requiring higher-order terms

of proper motion to obtain an acceptable fit with the observations, are identified with a value of 'G' in field H59. As noted above, follow-up efforts with speckle interferometry (Mason et al. 1999, 2001) have failed to resolve the majority of these companions. In a complementary approach, several studies (e.g., Makarov & Kaplan 2005; Frankowski et al. 2007, and references therein) have compared the *Hipparcos* proper motions with compilations of ground-based measurements over a much longer period, such as the Tycho-2 catalog (Høg et al. 2000). Proper motions in the Tycho-2 catalog are the average of measurements over many decades, and typically over 100 years, so these values should average out any curvilinear motion from orbits of a few decades and represent the transverse space motion. In comparison, the *Hipparcos* data obtained over some three years should be significantly influenced by such orbits. On the other hand, orbits of many decades to a few centuries will affect the Tycho-2 measurements, but hardly influence the *Hipparcos* data. So, differences in the proper motions listed in these two catalogs can contain clues about companions, some of which might already be known via spectroscopic or visual techniques. Makarov & Kaplan (2005) followed this approach in identifying companions based on a 3.5-σ difference between the proper motion in either coordinate from these two catalogs and estimated a minimum companion mass. Frankowski et al. (2007) developed a χ^2 test to minimize false identification of companions, and identified 3 565 proper-motion binaries with a greater than 99.99% confidence level, which they estimate to be an order of magnitude better than that of Makarov & Kaplan (2005).

Table 5.2 lists all stars from the sample studied here which either have a 'G' designation in

Hipparcos field H59, or have a greater than 3-σ difference between the *Hipparcos* and Tycho-2 proper motions. Taking a conservative approach, I divide the absolute difference between the proper motion from the two catalogs in each coordinate by the larger of the corresponding uncertainties, representing the x-σ difference in each coordinate. The root-sum-square of these two values is then used to test for the 3-σ difference and this value is also listed in column 8 of the table. For the purposes of the multiplicity statistics derived here, companions which are flagged as 'G' in field H59 are only considered real if they are confirmed by a 3-σ difference between *Hipparcos* and Tycho-2 proper motions or by other factors such as the existence of spectroscopic or visual orbits of a few decades. Entries lacking definite supporting evidence, but passing the Frankowski et al. (2007) χ^2 test are retained as candidates for further investigation, and *Hipparcos* entries without any supporting evidence are refuted as false detections. On the other hand, companions not flagged as 'G' in *Hipparcos* field H59, but with a 3-σ difference in the *Hipparcos* and Tycho-2 proper motions are also evaluated and considered real if they passed the χ^2 test developed by Frankowski et al. (2007) or are supported by other evidence of the companion such as a visual or spectroscopic orbit, or the presence of a nearby companion which could induce curvilinear motion over a hundred years such that it would have been picked up by the Tycho-2 values. The remaining such detections are left as candidates for further investigations.

In addition to the HD and HIP designation of the primaries, Table 5.2 lists the H59 value, the *Hipparcos* and Tycho-2 proper motions, an indicator if the star was identified as a proper-motion binary in Makarov & Kaplan (2005) or Frankowski et al. (2007), a final

companion status of YES (confirmed) or MAY (candidate), and a reason for this status. Among the stars of the current sample, 18 are flagged as 'G' in field H59, all but two of which are supported by a greater than 3-σ difference between the proper motions. One of the remaining two (HIP 36357) is supported by other evidence of companionship, while the other (HD 25998) is retained as a candidate. Most of the entries in the table have supporting visual or spectroscopic evidence and were independently detected by these methods, but nine companions were identified solely by the 'G' flag and supported by proper motion differences of 3.5–58.4 σ. An additional 11 systems were identified solely based on proper motion differences without the *Hipparcos* 'G' flag designation. Five of these are supported by the Frankowski et al. (2007) χ^2 test and have differences of 5.3–30.0 σ. The remaining six are identified as candidates for follow-up work and have proper motion differences of 3.1–4.4 σ.

TABLE 5.2: Accelerating Proper Motion Solutions

HD	HIP		===== *Hipparcos* =====		====== Tycho-2 ======		μ difference			Companion	
Name	Name	H59	μ_α (mas yr^{-1})	μ_δ (mas yr^{-1})	μ_α (mas yr^{-1})	μ_δ (mas yr^{-1})	(σ)	MK05[a]	F07[b]	Status	Reason
000123	000518	C	247.36 ± 0.81	17.77 ± 0.70	270.6 ± 1.6	30.1 ± 1.7	16.2	...	...	YES	1
003196	002762	C	407.68 ± 1.31	−36.47 ± 0.61	415.9 ± 0.5	−23.2 ± 0.5	22.6	...	...	YES	2
003443	002941	C	1422.09 ± 2.84	−17.15 ± 1.23	1391.0 ± 2.3	−13.0 ± 2.3	11.1	...	...	YES	2
004747	003850	...	516.74 ± 1.04	119.52 ± 0.72	518.8 ± 1.4	124.7 ± 1.4	4.0	...	...	YES	3
007788[c]	005896	C	411.11 ± 0.50	127.43 ± 0.48	404.9 ± 3.3	108.3 ± 3.0	6.6	...	...	YES	1
010307	007918	G	791.35 ± 0.65	−180.16 ± 0.47	806.6 ± 1.0	−152.2 ± 1.0	31.8	Y	Y	YES	4
010360	007751	C	286.10 ± 1.01	16.66 ± 1.41	302.6 ± 1.4	−14.1 ± 1.3	24.8	...	...	YES	1
013445	010138	...	2092.84 ± 0.50	654.32 ± 0.55	2150.3 ± 2.5	673.2 ± 2.4	24.3	Y	Y	YES	5
014802	011072	G	197.34 ± 0.77	−4.39 ± 0.51	...	...	...	...	...	YES	12
017382	013081	G	264.17 ± 1.24	−127.75 ± 0.81	274.5 ± 1.1	−122.6 ± 1.1	9.6	Y	Y	YES	4
018143	013642	C	262.72 ± 1.86	−191.44 ± 1.15	274.0 ± 1.7	−185.4 ± 1.6	7.1	...	...	YES	1
024409	018413	C	−284.06 ± 0.90	159.32 ± 0.96	−265.1 ± 0.9	169.7 ± 1.0	23.5	...	...	YES	3
025998	019335	G	163.93 ± 0.65	−203.52 ± 0.55	166.8 ± 1.2	−203.1 ± 1.3	2.4	...	Y	MAY	6
026491	019233	...	185.91 ± 0.46	336.76 ± 0.51	196.7 ± 1.1	333.7 ± 1.2	10.1	Y	Y	YES	3
035112	025119	C	54.20 ± 1.44	−139.41 ± 0.94	69.7 ± 1.3	−152.1 ± 1.3	14.5	...	...	YES	1
036705	025647	G	32.14 ± 0.53	150.97 ± 0.73	48.9 ± 1.3	137.6 ± 1.2	17.0	Y	Y	YES	5
039587	027913	...	−163.17 ± 1.06	−98.92 ± 0.60	−174.6 ± 0.7	−89.9 ± 0.7	16.8	Y	Y	YES	4
040397	028267	...	71.23 ± 0.93	−203.34 ± 0.66	73.6 ± 1.0	−206.5 ± 1.1	3.7	...	...	YES	5
043587	029860	...	−189.37 ± 0.71	171.18 ± 0.50	−195.4 ± 1.0	164.6 ± 1.0	8.9	Y	Y	YES	3
045088	030630	...	−119.32 ± 1.06	−164.06 ± 0.76	−115.3 ± 0.8	−167.8 ± 0.8	6.0	...	Y	YES	2
048189	031711	C	−50.08 ± 0.73	72.69 ± 0.66	−26.0 ± 3.8	72.4 ± 3.4	6.3	...	...	YES	5
052698	033817	G	206.58 ± 0.48	40.89 ± 0.72	203.3 ± 1.4	37.5 ± 1.3	3.5	...	Y	YES	7
053680[d]	034052	G	−75.43 ± 0.75	401.32 ± 2.10	−93.0 ± 1.2	395.3 ± 1.1	14.9	...	Y	YES	7
058946[e]	036366	...	159.33 ± 1.26	193.82 ± 0.46	157.2 ± 0.6	186.9 ± 0.6	11.7	...	...	YES	5
063077	037853	G	−220.83 ± 0.46	1722.89 ± 0.55	−274.1 ± 1.1	1687.0 ± 1.1	58.4	Y	Y	YES	8
064096	038382	C	−68.46 ± 1.11	−344.83 ± 1.03	−60.0 ± 0.7	−338.9 ± 0.7	9.6	...	...	YES	2
064606	038625	C	−251.57 ± 2.07	−62.07 ± 1.48	−259.1 ± 1.5	−47.7 ± 1.4	10.4	...	...	YES	3
065430	039064	...	180.46 ± 0.91	−544.36 ± 0.50	180.1 ± 1.1	−550.8 ± 1.0	6.4	Y	Y	YES	3
067199	039342	...	−157.34 ± 0.47	−130.52 ± 0.66	−155.9 ± 1.4	−126.7 ± 1.3	3.1	...	...	MAY	9
068017	040118	...	−460.69 ± 1.17	−644.64 ± 0.61	−464.7 ± 0.8	−646.5 ± 0.8	4.1	...	...	MAY	9
068255	040167	C	28.29 ± 2.00	−150.94 ± 1.15	79.8 ± 1.7	−129.4 ± 1.7	28.7	...	...	YES	10
072760	042074	...	−194.28 ± 1.05	23.42 ± 0.82	−197.5 ± 1.0	18.9 ± 0.9	5.9	Y	Y	YES	5
079969	045617	...	49.78 ± 1.15	−507.62 ± 0.51	52.8 ± 1.2	−510.5 ± 1.1	3.6	...	...	YES	1
082885	047080	...	−730.05 ± 0.71	−260.62 ± 0.46	−723.0 ± 1.3	−247.8 ± 1.4	10.6	Y	Y	YES	1
101177	056809	C	−593.87 ± 0.68	14.80 ± 0.52	−577.3 ± 1.0	1.5 ± 1.0	21.2	...	...	YES	1
110833	062145	O	−378.76 ± 0.59	−183.86 ± 0.60	−389.8 ± 1.1	−176.9 ± 1.2	11.6	...	...	YES	4
111312	062505	C	79.70 ± 1.90	44.66 ± 1.46	59.9 ± 1.9	39.2 ± 1.7	10.9	...	...	YES	11
113283	064690	...	−221.35 ± 0.55	−155.49 ± 0.57	−226.1 ± 2.2	−160.4 ± 2.0	3.3	...	...	MAY	9
113449	063742	O	−189.79 ± 1.16	−219.55 ± 1.10	−189.6 ± 0.7	−223.2 ± 0.8	3.3	...	...	YES	13
115404	064797	C	631.21 ± 0.90	−260.84 ± 0.63	623.9 ± 1.2	−259.0 ± 1.1	6.3	...	...	YES	1
120136	067275	...	−480.33 ± 0.61	54.18 ± 0.47	−480.8 ± 0.4	50.4 ± 0.4	8.1	Y	Y	YES	1
120690	067620	...	−580.93 ± 0.95	−244.87 ± 0.71	−584.2 ± 3.0	−290.9 ± 3.0	15.4	Y	Y	YES	3
120780	067742	G	−583.27 ± 0.91	−60.27 ± 0.59	−596.4 ± 1.1	−45.9 ± 1.0	18.7	...	...	YES	7
122742	068682	O	85.26 ± 0.64	−304.04 ± 0.47	91.1 ± 1.2	−307.5 ± 1.2	5.7	...	...	YES	4
125276	069965	...	−356.39 ± 0.81	366.76 ± 0.78	−351.9 ± 1.1	365.3 ± 1.1	4.3	...	...	MAY	9
128642	070857	O	−73.73 ± 0.65	−132.93 ± 0.59	−72.0 ± 0.8	−129.6 ± 0.9	4.3	...	...	YES	4
130042	072493	C	−107.28 ± 0.70	−320.91 ± 0.95	−109.4 ± 1.7	−330.8 ± 1.7	5.9	...	...	YES	5
131582	072875	G	−824.15 ± 1.27	2.29 ± 1.07	−824.4 ± 0.8	11.0 ± 0.8	8.1	Y	Y	YES	7
131923	073241	G	−15.47 ± 0.89	−337.07 ± 0.88	−15.5 ± 1.0	−327.8 ± 1.2	7.7	Y	Y	YES	3
133640	073695	C	−436.24 ± 1.20	18.94 ± 1.17	−443.7 ± 1.2	9.9 ± 1.2	9.8	...	Y	YES	1
137763	075718	G	72.69 ± 1.09	−363.37 ± 0.79	76.4 ± 1.0	−359.0 ± 1.0	5.5	...	...	YES	2
139341	076382	C	−482.47 ± 2.25	27.52 ± 1.47	−455.2 ± 0.8	51.0 ± 0.9	20.1	...	...	YES	1
140538	077052	...	−44.96 ± 0.95	−144.73 ± 0.78	−48.0 ± 0.8	−147.2 ± 0.8	4.4	...	...	YES	5
144287	078709	G	−488.79 ± 0.58	696.64 ± 0.73	−532.9 ± 1.0	683.0 ± 1.1	45.8	Y	Y	YES	3
145825	079578	...	−81.41 ± 0.89	−252.61 ± 1.04	−78.4 ± 1.2	−256.9 ± 1.2	4.4	...	...	YES	3
146361	079607	C	−266.47 ± 0.86	−86.88 ± 1.12	−289.0 ± 3.0	−85.1 ± 2.8	7.5	...	...	YES	2
147584	080686	...	199.89 ± 0.31	110.77 ± 0.51	197.8 ± 0.7	111.5 ± 0.7	3.2	...	...	YES	4
148653	080725	C	−345.93 ± 1.56	385.98 ± 1.36	−339.9 ± 1.2	383.3 ± 1.3	4.3	...	...	YES	1
148704	080925	C	−428.05 ± 1.47	−333.41 ± 1.43	−427.6 ± 1.1	−326.2 ± 1.2	5.1	...	...	YES	11

Continued on Next Page...

TABLE 5.2 – Continued

HD	HIP		===== *Hipparcos* =====		====== Tycho-2 ======		μ difference			Companion	
Name	Name	H59	μ_α (mas yr^{-1})	μ_δ (mas yr^{-1})	μ_α (mas yr^{-1})	μ_δ (mas yr^{-1})	(σ)	MK05[a]	F07[b]	Status	Reason
153557	083020	C	-146.90 ± 1.15	272.21 ± 1.35	-153.9 ± 1.3	267.8 ± 1.4	6.2	...	...	YES	5
156274	084720	C	1035.25 ± 1.38	109.22 ± 0.65	1053.5 ± 2.1	144.0 ± 2.0	19.4	...	...	YES	3
158614	085667	C	-126.64 ± 1.72	-172.00 ± 0.91	-126.7 ± 1.1	-179.6 ± 1.1	6.9	...	...	YES	2
160269	086036	C	277.38 ± 0.54	-525.62 ± 0.60	265.4 ± 3.3	-520.9 ± 3.2	3.9	...	...	YES	4
161198	086722	G	-123.15 ± 1.00	-619.84 ± 0.88	-123.1 ± 1.1	-628.0 ± 1.0	8.2	Y	Y	YES	4
161797	086974	...	-291.42 ± 0.49	-750.00 ± 0.53	-310.3 ± 0.4	-750.3 ± 0.4	38.5	Y	Y	YES	1
165341	088601	C	124.56 ± 1.15	-962.66 ± 0.91	276.3 ± 2.3	-1091.8 ± 2.3	86.6	...	...	YES	2
165401	088622	...	-30.66 ± 0.88	-322.06 ± 0.75	-26.0 ± 1.1	-316.7 ± 1.1	6.5	Y	Y	YES	9
165499	089042	G	-77.60 ± 0.59	234.68 ± 0.44	-81.5 ± 0.9	221.2 ± 0.9	15.6	Y	Y	YES	7
167425	089805	...	38.89 ± 0.57	-276.16 ± 0.51	37.9 ± 1.4	-280.4 ± 1.4	3.1	...	...	YES	5
177474	093825	C	96.93 ± 2.44	-279.67 ± 1.34	87.7 ± 1.2	-283.9 ± 1.2	4.9	...	...	YES	1
179957	094336	C	-205.02 ± 0.97	624.33 ± 0.89	-209.5 ± 1.3	622.2 ± 1.4	3.8	...	...	YES	1
181321	095149	G	78.88 ± 4.08	-108.93 ± 2.50	87.6 ± 1.2	-86.4 ± 1.3	9.3	Y	Y	YES	7
186858	097222	C	13.30 ± 1.07	-440.57 ± 1.35	18.9 ± 2.6	-445.8 ± 2.4	3.1	...	...	YES	1
189340	098416	C	-246.73 ± 2.31	-392.36 ± 1.63	-282.0 ± 1.0	-399.7 ± 1.0	15.9	...	...	YES	2
190771	098921	...	263.35 ± 0.46	111.57 ± 0.46	259.2 ± 1.1	115.7 ± 1.1	5.3	Y	Y	YES	9
191408	099461	...	456.89 ± 0.89	-1574.91 ± 0.61	458.4 ± 1.1	-1569.3 ± 1.1	5.3	Y	Y	YES	5
191499	099316	C	3.79 ± 1.00	175.79 ± 1.02	3.9 ± 1.4	167.9 ± 1.4	5.6	...	...	YES	5
193664	100017	...	468.52 ± 0.55	296.81 ± 0.41	472.5 ± 1.1	296.1 ± 1.2	3.7	...	...	MAY	9
195564	101345	...	307.59 ± 0.88	106.07 ± 0.66	307.2 ± 0.7	103.7 ± 0.7	3.4	...	...	YES	5
195987	101382	O	-156.89 ± 0.53	452.80 ± 0.47	-154.3 ± 0.9	454.5 ± 0.9	3.4	...	...	YES	2
200560	103859	...	402.30 ± 0.66	141.72 ± 0.57	396.1 ± 0.8	141.0 ± 0.8	7.8	Y	Y	YES	5
200968	104239	C	382.32 ± 1.31	-46.55 ± 0.60	382.3 ± 0.9	-39.9 ± 0.8	8.3	...	...	YES	5
202940	105312	C	-582.35 ± 1.11	-357.67 ± 0.62	-568.3 ± 1.5	-353.7 ± 1.5	9.7	...	...	YES	4
203985	105911	G	264.07 ± 1.28	184.71 ± 0.97	253.2 ± 1.1	179.6 ± 1.2	9.5	Y	Y	YES	7
206826	107310	C	260.33 ± 0.61	-242.73 ± 0.57	277.4 ± 2.7	-251.1 ± 2.6	7.1	...	...	YES	1
211415	110109	...	439.86 ± 0.53	-632.60 ± 0.43	436.8 ± 0.9	-632.8 ± 0.9	3.4	...	...	YES	5
212330	110649	...	180.71 ± 0.41	-331.27 ± 0.38	150.6 ± 1.1	-344.9 ± 1.1	30.0	Y	Y	YES	9
214953	112117	...	6.15 ± 0.63	-331.43 ± 0.51	3.1 ± 1.1	-326.9 ± 1.0	5.3	Y	Y	YES	5
223778	117712	...	341.82 ± 0.53	41.88 ± 0.47	325.8 ± 1.0	45.6 ± 1.1	16.4	Y	Y	YES	2
224930	000171	X	778.59 ± 2.81	-918.72 ± 1.81	829.9 ± 1.2	-989.4 ± 1.1	43.1	Y	Y	YES	4
.....	036357	G	160.40 ± 1.56	174.68 ± 1.02	159.7 ± 1.0	175.8 ± 1.1	1.1	...	...	YES	5

NOTES.—Column 12 notes: (1) = Visual orbit exists (see § 5.2); (2) = Double-lined spectroscopic and visual orbits exist (see § 5.2 and § 6.2); (3) = Single-lined spectroscopic orbit exists (see § 6.2); (4) = Single-lined spectroscopic and visual orbits exist (see § 5.2 and § 6.2); (5) = Nearby resolved companion exists, likely causing detectable proper motion deviation over several decades; (6) = *Hipparcos* G flag and the χ^2 test in Frankowski et al. (2007) suggest an unseen companion, but because the *Hipparcos* and Tycho-2 proper motions differ by less than 3σ, this is retained as a candidate for further investigations. (7) = Companionship is confirmed based on *Hipparcos* 'G' flag and a greater than 3σ difference in proper motion; (8) = Radial velocity variations indicate a spectroscopic binary, but not enough observations exist to derive an orbit. (9) = Greater than 3σ difference in proper motion is the only evidence of a companion. Companion is considered confirmed if it also passed the χ^2 test in Frankowski et al. (2007), otherwise is retained as a candidate; (10) = Thesis primary star is HD 68257. At least a quintuple system with two visual and spectroscopic orbits; (11) = Double-lined spectroscopic orbit exists (see § 6.2); (12) = Tycho-2 does not have a proper motion for this star, but Gontcharov et al. (2000) show that the *Hipparcos* motion is significantly different from that of the Fifth Fundamental Catalog (Fricke et al. 1988,FK5) and present a convincing photocentric orbit; (13) = See Table 5.3.

[a] 'Y' in this column indicates that this was identified as a proper-motion binary in Makarov & Kaplan (2005) [b] 'Y' in this column indicates that this was identified as a proper-motion binary in Frankowski et al. (2007) [c] Wide companion, 319″ away from to HD 7693. [d] Wide companion, 185″ away from to HD 53705. [e] Wide companion, 756″ away from to HD 36357.

5.1.3 Orbital Solutions

Nineteen of the targets studied in this work have orbital solutions in the *Hipparcos* catalog, for which the *Hipparcos* data enabled the determination of at least one of the orbital parameters. Table 5.3 lists these stars along with their orbital period from *Hipparcos*, the final status for the multiplicity statistics derived, and a corresponding reason for this conclusion. As seen in the table, 15 of the 19 are confirmed companions, three are refuted, and one is still a candidate.

TABLE 5.3: *Hipparcos* Orbital Solutions

HD Name	HIP Name	Period (days)	Companion Status	Reason
001273	001349	411.4	YES	1
006582	005336	7816.0	YES	1
010476	007981	207.3	NO	2
013974	010644	10.0	YES	3
014214	010723	93.5	YES	1
016739	012623	331.0	YES	3
032850	023786	204.4	YES	1
110833	062145	270.2	YES	1
112914	063406	736.8	YES	1
113449	063742	231.2	YES	4
121370	067927	494.2	YES	1
122742	068682	3614.9	YES	1
128642	070857	179.7	YES	1
131511	072848	125.4	YES	1
142373	077760	51.3	NO	5
143761	078459	78.0	NO	4
160346	086400	83.9	YES	1
195987	101382	57.3	YES	3
203244	105712	1060.6	MAY	4

NOTES.—Column 5 notes: (1) = Single-lined spectroscopic and visual orbits exist (see § 5.2 and § 6.2); (2) = *Hipparcos* orbital solution has $i = 89° \pm 23°$, but the radial velocity variations of less than 0.1 $\mathrm{km\,s^{-1}}$ over 3.8 years or 6.7 orbital periods (Nidever et al. 2002) raise substantial doubts about the *Hipparcos* orbit; (3) = Double-lined spectroscopic and visual orbits exist (see § 5.2 and § 6.2); (4) = See individual system notes in § 7.4; (5) = *Hipparcos* orbital solution has $i = 132° \pm 28°$, but radial velocity variations of less than 0.1 $\mathrm{km\,s^{-1}}$ over 9.7 years or 69.4 orbital periods (Nidever et al. 2002) raise substantial doubts about the *Hipparcos* orbit.

5.1.4 Stochastic Solutions

Three of the sample stars have a stochastic solution designation in *Hipparcos*, implying that they had neither a satisfactory single or double-star solution. The three stars are HD 21175, 200525, and 224930, and all three also have the suspected non-single flag set in field H61. HD 21175 and 224930 have published visual and/or spectroscopic orbits (see § 5.2 and § 6.2) and are hence confirmed as true companions. For HD 200525, Goldin & Makarov (2006) present a photocentric orbit, confirming companionship (see § 7.4).

5.2 Visual Orbits

The Sixth Catalog of Orbits of Visual Binary Stars[1] (Hartkopf et al. 2001, hereafter VB6) is maintained by the United States Naval Observatory (USNO) and is a frequently updated online resource containing over 2,000 visual orbits. Table 5.4 contains 98 orbits from this

[1] *http://ad.usno.navy.mil/wds/orb6.html*

source for the current sample, selected from the catalog as of July 8, 2008. Each orbit is listed on two lines. The first line contains the fields described below and the second line lists the corresponding uncertainties. The first column lists the WDS coordinates of the pair, and the next two columns identify the star's HD and *Hipparcos* identifiers, respectively. Some of these are the primaries listed in Table 2.1 while others are their companions with visual orbits of their own. Column 4 lists the WDS discovery designation or other catalog designations as listed in the catalog along with an identifier of the specific pair for which the orbit is listed. The next five columns list the orbital elements from the catalog. The orbital period (P) is listed in days (d) or years (y). The semi-major axis (a) is the orbital semimajor axis for all grades except 9, for which it is the photocentric-motion semi-major axis, and is listed in arcsec (a) or mill-arcsec (m). The epoch of periastron passage (T_0) is listed in modified Julian date (d) or fractional Besselian year (y). These units immediately follow their corresponding values. The next two columns list the grade of the orbit and the reference code as in the catalog. The catalog's website provides a link identifying these references, so they have not been reproduced in the bibliography of this work. Column 14 contains a code identifying whether the orbit also has a published single-lined (1) or double-lined (2) spectroscopic orbit, if it is refuted (R) by other evidence, or if it is an unconfirmed candidate (M) for the multiplicity statistics derived here. Finally, the last two columns list the number of observations and the time range of these observations, in years, from the WDS catalog as of July 8, 2008. For some pairs, the VB6 catalog lists multiple, presumably equally possible, orbital solutions. I have evaluated these and only included one per pair, selecting the more

robust solution when that determination could be made, otherwise selecting the more recent one.

The VB6 contains orbits of resolved pairs based on measurements of their separation and position angle (grades 1–5 as described below), pairs resolved using LBI by measuring their interferometric visibility ("grade" 8), and photocentric orbits of unresolved pairs ("grade" 9). The description of grades 1–5 are reproduced below from the catalog's web site.

1 = Definitive. Well-distributed coverage exceeding one revolution; no revisions expected except for minor adjustments.

2 = Good. Most of a revolution, well observed, with sufficient curvature to give considerable confidence in the derived elements. No major changes in the elements likely.

3 = Reliable. At least half of the orbit defined, but the lesser coverage (in number or distribution) or data consistency leaves the possibility of larger errors than in grade 2.

4 = Preliminary. Individual elements entitled to little weight, and may be subject to substantial revisions. The quantity 3 log(a) - 2 log(P) should not be grossly erroneous. This class contains: orbits with less than half the ellipse defined; orbits with weak or inconsistent data; and orbits showing deteriorating representations of recent data.

5 = Indeterminate. The elements may not even be approximately correct. The observed arc is usually too short, with little curvature, and frequently there are large residuals associated with the computations.

The orbits listed in Table 5.4 are separated into three groups by their orbit classification. Orbits with grades 1–4 and grade 8 are listed in the first group, and represent orbital

solutions of excellent (grade 1 and 8) to preliminary (grade 4) quality. Each of these pairs, with one notable exception (HD 32923, see § 7.4), is a reliable physical association for the multiplicity statistics derived here, supported, in most cases, by many tens to over a thousand observations measured over tens to a few hundred years, as listed in the WDS. The few exceptions with less than 10 measures are each supported by a matching spectroscopic orbits, as identified in Column 14. HD 4676 (64 Psc) does not have any measures because the orbit was derived based on interferometric visibility (Boden et al. 1999), similar to the results presented in § 3.2. While these observations do not directly measure the pair's separation and position angles, which is the criteria for a pair to be listed in the WDS, they are nevertheless very robust solutions, as mentioned in the online description of the orbit catalog. The two remaining grade 8 orbits (HD 16739 and 195987) have independent measurement(s) listed in the WDS, but the orbital solutions are from LBI observations (Torres et al. 2002; Bagnuolo et al. 2006). Not surprisingly, there is a strong correlation between an orbit's grade and its period. Grade 8 orbits represent the shortest-period orbits, with periods ranging from 13–57 days for orbits from visibility measurements, and 331 days for HD 16739 (12 Per), whose orbit was derived from astrometry obtained by studying spatially resolved, separated fringe packets (Bagnuolo et al. 2006). An additional orbit based on LBI visibility measurements is listed for HD 13974 in the table, but this is listed as grade 1 because Hummel et al. (1995), when presenting the orbital solution, also gave the separations and position angles derived from their visibility measurements. For grades 1–4 excluding these LBI pairs, orbital period increases with increasing grade because shorter-period systems can

be more comprehensively studied with the measurements recorded over some 200 years since the days of William Herschel. Grade 1 orbits range from 1–88 years, grade 2 orbits from 5–232 years, grade 3 orbits from 76–480 years excluding one orbit of 1.2 years, and grade 4 orbits range from 20–3100 years. The one short-period orbit for grade 3 (HD 32923 with an orbital period of 1.2 years) is poorly sampled. While the WDS lists 19 observations for this similar-brightness pair separated by $0\farcs1$, the 4th interferometry catalog (see § 5.4) also lists over 20 null-results with speckle interferometry.

Orbits of grade 5 are listed in the second group because their orbital elements are extremely preliminary and subject to significant modifications. In fact, a few of these orbits may even be solutions fitted to the linear motions of unrelated stars, and hence each of these is individually evaluated to confirm a physical association. Most of the entries in this group in Table 5.4 are again supported by more than, and in many cases, much more than 10 measurements over many decades to a few centuries, and are confirmed as physical based on evidence of curved orbital motion or, in the case of very long-period systems, as linear motions consistent with a small arc of a large orbit, but definitely inconsistent with that of unrelated field stars as discussed in § 4.2. This method confirms all but five systems of this group, and three of these exceptions (HD 43587, 68256, and 161198) are confirmed by matching spectroscopic orbits. The two remaining exceptions (HD 13445 and 21175) are confirmed by published results (see § 7.4). Only five of these orbits have periods less than 200 years, and each of these is poorly sampled. The periods of the rest range from 201 years to 320 centuries.

Grade 9 orbits, listed in the last group of Table 5.4, are binaries for which the photocentric motion of an unresolved point of light is modeled as an orbit. Seventeen of the 26 orbits of this type have supporting spectroscopic orbits, as indicated by a 1 (single-lined) or 2 (double-lined) in Column 14. Three, flagged with an 'R' in Column 14 were refuted using proper motion and/or radial velocity data (see § 7.4) and one, flagged with an 'M' is still a candidate (see § 7.4). The remaining five entries with a blank in Column 14 are all physical associations, as confirmed by evidence presented in the indicated references.

TABLE 5.4: Visual Orbit Solutions

WDS Coord	HD Name	HIP Name	WDS DD	P	a	i (deg)	Ω (deg)	T_0	e	ω (deg)	G	Ref	SB	N	ΔT (years)
Visual orbit solutions for grades 1–4															
00022+2705	224930	000171	BU 733AB	26.28 y	0.83 a	49	290	1989.4 y	0.38	96	2	Sod1999	1	178	127
...	...	...	...	...	...	...	...	...	...	...	...	...	...	...	...
00063+5826	000123	000518	STF3062	106.7 y	1.44 a	45	221	1943.1 y	0.45	277	2	Sod1999	...	582	183
...	...	...	...	...	...	...	...	...	...	...	...	...	...	...	...
00352−0336	003196	002762	HO 212AB	6.89 y	0.24 a	49.4	149.0	2000.98 y	0.77	283.8	1	Msn2005	2	201	121
...	...	...	...	...	...	...	...	...	...	...	...	...	...	...	...
00373−2446	003443	002941	BU 395	25.09 y	0.67 a	77.6	291.8	1898.5 y	0.24	317	1	Pbx2000b	2	163	132
...	...	...	...	0.03	0.01	0.3	0.5	0.17	0.01	2.8	...	...	...	...	...
00490+1656	004676	003810	64 PscAa	13.82 d	6.53 m	73.8	63.6	50905.98 d	0.24	203.6	8	Bod1999b	2	...	...
...	...	...	...	0.00	0.06	0.9	0.8	0.02	0.00	0.4	...	...	...	...	...
00491+5749	004614	003821	STF 60AB	480 y	11.99 a	34.8	278.4	1889.6 y	0.50	268.6	3	Str1969a	...	1029	228
...	...	...	...	...	...	...	...	...	...	...	...	...	...	...	...
01083+5455	006582	005336	WCK 1Aa	21.75 y	1.01 a	106.8	47.3	1975.74 y	0.56	152.7	4	Dru1995	1	14	31
...	...	...	...	0.07	0.02	0.9	1.0	0.15	0.02	3.1	...	...	...	...	...
01158−6853	007693	005842	I 27CD	85.2 y	1.14 a	35	142	1919 y	0.04	141	3	Sod1999	...	69	106
...	...	...	...	...	...	...	...	...	...	...	...	...	...	...	...
01350−2955	009770	007372	DAW 31AB	4.56 y	0.18 a	21.8	57.4	1932.59 y	0.30	51.3	1	Msn1999c	...	88	79
...	...	...	...	...	...	...	...	...	...	0.0	...	...	...	...	...
01350−2955	009770	007372	BU 1000AB-C	111.8 y	1.42 a	29.3	141.8	1960.06 y	0.21	64.6	4	Nwb1969a	...	44	120
...	...	...	...	...	...	...	...	...	...	...	...	...	...	...	...
01418+4237	010307	007918	MCY 2	19.5 y	0.58 a	105	33	1997.1 y	0.43	22	4	Sod1999	1	6	13
...	...	...	...	...	...	...	...	...	...	...	...	...	...	...	...
02171+3413	013974	010644	MKT 5Aa	10.02 d	9.80 m	167	15	48117.0 d	0.02	121	1	MkT1995	2	21	2
...	...	...	...	0.00	0.06	3	9	0.2	0.01	11	...	...	...	...	...
02422+4012	016739	012623	MCA 8	330.98 d	53.18 m	128.2	269.3	1993.34 y	0.66	49.3	8	Bgn2006	2	41	23
...	...	...	...	...	0.15	0.1	...	...	...	...	...	...	...	...	...
03121−2859	020010	014879	HJ 3555	269 y	4.0 a	81	117	1947 y	0.73	43	4	Sod1999	...	94	167
...	...	...	...	...	...	...	...	...	...	...	...	...	...	...	...
04153−0739	026976	000000	STF 518BC	252.1 y	6.94 a	108.9	150.9	1849.6 y	0.41	327.8	4	Hei1974c	...	173	149
...	...	...	...	...	...	...	...	...	...	...	...	...	...	...	...
05074+1839	032923	023835	A 3010	1.19 y	0.18 a	73	122.3	1911.37 y	0.90	90.3	3	Egg1956	R	19	76
...	...	...	...	...	...	...	...	...	...	...	...	...	...	...	...
05226+0236	035112	025119	A 2641	93 y	1.1 a	114	164	1950 y	0.13	153	4	Sod1999	...	21	88
...	...	...	...	...	...	...	...	...	...	...	...	...	...	...	...
07175−4659	057095	035296	I 7	94.0 y	0.75 a	107.7	51.8	1958.0 y	0.94	55.0	4	Hei1995	...	60	107
...	...	...	...	...	...	...	...	...	...	...	...	...	...	...	...
07518−1354	064096	038382	BU 101	22.70 y	0.60 a	80.4	102.9	1985.92 y	0.74	73.1	2	Pbx2000b	2	229	132
...	...	...	...	0.03	0.01	0.2	0.3	0.02	0.01	0.4	...	...	...	...	...
08122+1739	068257	040167	STF1196AB	59.58 y	0.86 a	173.9	157.6	1989.09 y	0.32	330.2	1	WSI2006b	...	1133	182
...	...	...	...	0.03	0.00	0.8	6.7	0.01	0.00	6.7	...	...	...	...	...
08122+1739	068257	040167	STF1196AB-C	1115 y	7.70 a	146	74.2	1970 y	0.24	345.5	4	Hei1996b	...	515	207
...	...	...	...	...	...	...	...	...	...	...	...	...	...	...	...
08391−2240	073752	042430	BU 208AB	123.0 y	1.71 a	82.9	31.8	1986.6 y	0.33	309.2	3	Hei1990c	...	126	124
...	...	...	...	...	...	...	...	...	...	...	...	...	...	...	...
09123+1500	079096	045170	FIN 347Aa	2.71 y	0.12 a	124.3	317.8	1979.99 y	0.43	351.0	1	Msn1996a	2	99	40
...	...	...	...	...	0.00	...	...	...	...	...	...	...	...	...	...
09179+2834	079969	045617	STF3121AB	34.17 y	0.68 a	76	24	1981.0 y	0.32	311	1	Sod1999	...	388	173
...	...	...	...	...	...	...	...	...	...	...	...	...	...	...	...
11047−0413	096064	054155	A 676BC	23.23 y	0.34 a	62.6	71.7	1995.22 y	0.12	111.2	2	Doc2001e	...	53	95
...	...	...	...	...	...	...	...	...	...	...	...	...	...	...	...
11182+3132	098231	055203	STF1523AB	59.88 y	2.54 a	122.1	101.9	1935.20 y	0.40	127.9	1	Msn1995	...	1560	227
...	...	...	...	...	...	...	...	...	...	...	...	...	...	...	...
13169+1701	115404	064797	BU 800AB	770.0 y	8.06 a	93.4	104.7	1875.0 y	0.12	277.0	4	Hle1994	...	194	123
...	...	...	...	...	...	...	...	...	...	...	...	...	...	...	...
14396−6050	128620	071683	RHD 1AB	79.91 y	17.57 a	79.2	204.9	1875.66 y	0.52	231.7	2	Pbx2002	2	438	255
...	...	...	...	0.01	0.02	0.0	0.1	0.01	0.00	0.1	...	...	...	...	...
14514+1906	131156	072659	STF1888AB	151.6 y	4.94 a	139	347	1909.3 y	0.51	203	2	Sod1999	...	1358	227

Continued on Next Page...

TABLE 5.4 – Continued

WDS Coord	HD Name	HIP Name	WDS DD	P	a	i (deg)	Ω (deg)	T_0	e	ω (deg)	G	Ref	SB	N	ΔT (years)
...	...	...	...	...	...	...	...	...	...	...	...	...	...	...	...
15038+4739	133640	073695	STF1909	206 y	3.8 a	84	57	2013 y	0.55	45	2	Sod1999	...	769	226
...	...	...	...	...	...	...	...	...	...	...	...	...	...	...	...
15232+3017	137107	075312	STF1937AB	41.56 y	0.87 a	58.0	203.2	1975.46 y	0.27	38.8	1	WSI2006b	2	1002	225
...	...	...	...	0.01	0.00	0.1	0.1	0.03	0.00	0.3	...	...	...	...	...
15360+3948	139341	076382	STT 298AB	55.6 y	0.79 a	63	0	1993.99 y	0.59	23	1	Sod1999	...	515	164
...	...	...	...	...	...	...	...	...	...	...	...	...	...	...	...
16133+1332	145958	079492	STF2021Aa-B	1354 y	5.09 a	58.7	148.5	1754 y	0.39	111.4	4	Hop1964b	...	395	224
...	...	...	...	...	...	...	...	...	...	...	...	...	...	...	...
16147+3352	146361	079607	STF2032AB	888.99 y	5.93 a	31.8	16.9	1826.95 y	0.76	72.2	4	Sca1979	...	1041	226
...	...	...	...	...	...	...	...	...	...	...	...	...	...	...	...
16289+1825	148653	080725	STF2052AB	224 y	2.21 a	108	94	1921.1 y	0.75	130	2	Sod1999	...	528	185
...	...	...	...	...	...	...	...	...	...	...	...	...	...	...	...
17153−2636	155885	084405	SHJ 243AB	470.9 y	13.0 a	99.8	94.2	1677.86 y	0.92	89.8	4	Irw1996	...	264	230
...	...	...	...	...	...	...	...	...	...	...	...	...	...	...	...
17304−0104	158614	085667	STF2173	46.40 y	0.98 a	99.1	152.1	1962.46 y	0.18	327.5	1	Hei1994a	2	692	176
...	...	...	...	...	...	...	...	...	...	...	...	...	...	...	...
17350+6153	160269	086036	BU 962AB	76.1 y	1.53 a	104	151	1947 y	0.18	307	3	Sod1999	1	129	125
...	...	...	...	...	...	...	...	...	...	...	...	...	...	...	...
17465+2743	161797	086794	AC 7BC	43.20 y	1.36 a	66.2	60.7	1965.40 y	0.18	174.0	2	Cou1960b	...	343	153
...	...	...	...	...	...	...	...	...	...	...	...	...	...	...	...
18055+0230	165341	088601	STF2272AB	88.38 y	4.55 a	121.2	302.1	1895.94 y	0.50	14.0	1	Pbx2000b	2	1678	230
...	...	...	...	0.02	0.01	0.1	0.1	0.02	0.00	0.1	...	...	...	...	...
18070+3034	165908	088745	AC 15AB	56.4 y	1.0 a	34	216	1998 y	0.75	301	2	Sod1999	...	205	146
...	...	...	...	...	...	...	...	...	...	...	...	...	...	...	...
18570+3254	176051	093017	BU 648AB	61.18 y	1.24 a	115.1	49.0	1971.82 y	0.25	280.3	2	Doc2008f	1	332	127
...	...	...	...	...	...	...	...	...	...	...	...	...	...	...	...
19064−3704	177474	093825	HJ 5084	121.76 y	1.90 a	149.6	50.3	2000.64 y	0.32	349.0	2	Hei1986b	...	260	165
...	...	...	...	...	...	...	...	...	...	...	...	...	...	...	...
19121+4951	179958	094336	STF2486AB	3100 y	12.75 a	119.1	255.2	2520 y	0.50	186.1	4	Hle1994	...	258	188
...	...	...	...	...	...	...	...	...	...	...	...	...	...	...	...
19311+5835	184467	095995	MCA 56	1.35 y	86 m	144	243	1985.27 y	0.36	356	1	Pbx2000b	2	28	21
...	...	...	...	0.00	1.40	2.4	1.5	0.00	0.01	2.1	...	...	...	...	...
19418+5032	186408	096895	STFA 46Aa,B	18212 y	40.79 a	135.4	313.4	43.64 y	0.86	31.7	4	Mrc1999	...	534	206
...	...	...	...	...	...	...	...	...	...	...	...	...	...	...	...
19456+3337	186858	097222	STF2576AB	232 y	2.07 a	156	91	1945.3 y	0.77	128	2	Sod1999	...	426	179
...	...	...	...	...	...	...	...	...	...	...	...	...	...	...	...
19598−0957	189340	098416	HO 276	4.90 y	0.15 a	6	147	1982.81 y	0.59	142	2	Pbx2000b	2	36	39
...	...	...	...	0.00	0.00	20	3	0.03	0.01	4.3	...	...	...	...	...
20329+4154	195987	101382	BLA 8	57.32 d	15.38 m	99.4	335.0	51353.81 d	0.31	357.4	8	Trr2002	2	1	0
...	...	...	...	0.00	0.03	0.1	0.1	0.04	0.00	0.3	...	...	...	...	...
21145+1000	202275	104858	STT 535AB	2084.03 d	231.97 m	99.4	23.4	53112.07 d	0.44	7.7	1	Mut2008	2	486	155
...	...	...	...	0.10	0.01	0.0	0.0	0.05	0.00	0.0	...	...	...	...	...
21441+2845	206826	107310	STF2822AB	789 y	5.32 a	75.5	110.1	1958.0 y	0.66	145.7	4	Hei1995	...	693	229
...	...	...	...	...	...	...	...	...	...	...	...	...	...	...	...
							Grade 5 visual orbit solutions								
01158−6853	007788	005896	HJ 3423AB	857.0 y	5.96 a	127.1	10.3	1763.50 y	0.38	284.9	5	Sca2005b	...	70	165
...	...	...	...	...	0.00	0.0	0.0	...	0.00	0.0	...	...	...	...	...
01398−5612	010361	007751	DUN 5	483.66 y	7.82 a	142.8	13.1	1813.49 y	0.53	18.4	5	vAb1957	...	159	177
...	...	...	...	...	...	...	...	...	...	...	...	...	...	...	...
02104−5049	013445	010138	ESG 1	69.7 y	1.69 a	150	335	1983 y	0.40	342.0	5	Lgr2006	...	4	5
...	...	...	...	...	...	...	...	...	...	...	...	...	...	...	...
02442+4914	016895	012777	STF 296AB	2720 y	22.29 a	75.4	128.0	1613 y	0.13	100.6	5	Hop1958	...	71	224
...	...	...	...	...	...	...	...	...	...	...	...	...	...	...	...
02556+2652	018143	013642	STF 326AB	...	...	81.5	34.5	2248.0 y	1.0	308.2	5	Hop1967	...	76	175
...	...	...	...	...	...	...	...	...	...	...	...	...	...	...	...
03128−0112	019994	014954	HJ 663	1420 y	6.77 a	114.1	84.1	1982 y	0.26	247.7	5	Hle1994	...	15	154
...	...	...	...	...	...	...	...	...	...	...	...	...	...	...	...
03236−4005	021175	015799	I 468	111 y	1.8 a	32	49	1982 y	0.20	348	5	Sod1999	...	3	56
...	...	...	...	...	...	...	...	...	...	...	...	...	...	...	...

Continued on Next Page...

TABLE 5.4 – Continued

WDS Coord	HD Name	HIP Name	WDS DD	P	a	i (deg)	Ω (deg)	T_0	e	ω (deg)	G	Ref	SB	N	ΔT (years)
04076+3804	025893	019255	STT 531AB	590 y	3.87 a	104.0	160.3	2070 y	0.25	195.0	5	Hei1986b	...	171	153
...	...	...	...	...	...	...	...	...	...	...	...	...	...	...	...
06173+0506	043587	029860	CAT 1Aa	28.8 y	0.62 a	35.4	166.8	1998.05 y	0.78	75.0	5	Cat2006	1	4	3
...	...	...	...	1.1	0.02	2.5	1.3	0.00	0.01	0.3	...	...	...	...	...
06262+1845	045088	030630	BU 1191	600 y	3.23 a	76.0	139.8	1896 y	0.25	64.7	5	Hle1994	...	14	106
...	...	...	...	...	...	...	...	...	...	...	...	...	...	...	...
08122+1739	068256	040167	HUT 1Ca	17.32 y	0.18 a	142	77	1984.06 y	0.08	193	5	Hei1996b	1	5	19
...	...	...	...	...	...	...	...	...	...	...	...	...	...	...	...
09357+3549	082885	047080	HU 1128	201 y	3.84 a	117.0	41.3	1948.0 y	0.88	170.0	5	Hei1988d	...	19	101
...	...	...	...	...	...	...	...	...	...	...	...	...	...	...	...
10281+4847	090508	051248	KUI 50	765 y	7.08 a	72.0	18.9	1997 y	0.53	67.7	5	Hle1994	...	11	67
...	...	...	...	...	...	...	...	...	...	...	...	...	...	...	...
11268+0301	099491	055846	STF1540AB	32000 y	40.76 a	126.6	164.3	5200 y	0.46	112.9	5	Hop1960a	...	120	227
...	...	...	...	...	...	...	...	...	...	...	...	...	...	...	...
11387+4507	101177	056809	STF1561AB	2050 y	10.33 a	125.9	271.2	2500 y	0.05	129.6	5	Hle1994	...	110	224
...	...	...	...	...	...	...	...	...	...	...	...	...	...	...	...
13473+1727	120136	067275	STT 270	2000 y	14.39 a	50.7	28.4	2017 y	0.91	99.3	5	Hle1994	...	56	169
...	...	...	...	...	...	...	...	...	...	...	...	...	...	...	...
17191−4638	156274	084720	BSO 13AB	693.24 y	10.42 a	35.6	131.8	1907.18 y	0.78	333.4	5	Wie1957	...	127	127
...	...	...	...	...	...	...	...	...	0.00	0.0	...	...	...	...	...
17419+7209	162003	086614	STF2241AB	12500 y	55.2 a	72	1	942 y	0.54	312	5	Rmn1994	...	141	207
...	...	...	...	...	...	...	...	...	...	...	...	...	...	...	...
17433+2137	161198	086722	DUQ 1	2558.4 d	0.17 a	42.8	309.2	49422.53 d	0.94	129.6	5	Duq1996	1	6	5
...	...	...	...	10.4	0.01	3.7	1.5	0.10	0.00	0.6	...	...	...	...	...
21198−2621	202940	105312	BU 271AB	261.62 y	3.01 a	74.1	59.1	1845.99 y	0.42	57.6	5	Jas1997	...	49	117
...	...	...	...	...	...	...	...	...	...	...	...	...	...	...	...
23524+7533	223778	117712	BU 996AB	290.0 y	4.14 a	49.6	93.9	2015.0 y	0.55	134.1	5	Hle1994	...	15	103
...	...	...	...	...	...	...	...	...	...	...	...	...	...	...	...
						Photocentric-motion orbits (grade 9)									
00169−5239	001273	001349	GJ 13	411.4 d	20.98 m	74.7	352.3	34233.3 d	0.57	4.7	9	Jnc2005	1	...	...
...	...	...	...	...	0.56	2.1	3.3	...	...	...	...	...	...	...	...
01425+2016	010476	007981	107 Psc	207.27 d	4.55 m	89.0	12.7	48213.79 d	0.00	0.0	9	HIP1997d	R	...	...
...	...	...	...	6.18	2.10	23.0	23.8	11.96	...	...	...	...	...	...	...
02180+0145	014214	010723	GC 2770	93.29 d	6.07 m	110.0	172	53338.33 d	0.52	104.0	9	Fek2007	1	...	...
...	...	...	...	0.00	0.38	8.4	14	0.01	0.00	0.1	...	...	...	...	...
02225−2349	014802	011072	κ For	26.5 y	0.54 a	56	133	1983.6 y	0.2	22	9	Gon2000	...	...	...
...	...	...	...	...	...	...	...	...	...	...	...	...	...	...	...
02361+0653	016160	012114	PLQ 32Aa,P	61 y	0.17 a	49	13	1940 y	0.67	249	9	Hei1994b	...	6	5
...	...	...	...	...	...	...	...	...	...	...	...	...	...	...	...
02481+2704	017382	013081	GC 3359	15.5 y	0.04 a	84	54	1986.5 y	0.00	0	9	Hei1990d	1	...	...
...	...	...	...	...	...	...	...	...	...	...	...	...	...	...	...
05067+1427	032850	023786	GJ 3330	204.38 d	10.14 m	29.4	153.0	48444.84 d	0.14	293.1	9	HIP1997d	1	...	...
...	...	...	...	2.44	1.29	35.8	63.0	41.29	0.24	81.1	...	...	...	...	...
05544+2017	039587	027913	χ^1 Ori	5156.29 d	89.66 m	95.9	126.4	51468.2 d	0.45	111.5	9	HaI2002	1	...	...
...	...	...	...	2.51	0.88	0.8	0.6	3.08	0.00	0.2	...	...	...	...	...
11182+3132	098231	055203	ξ UMa Aa	1.83 y	0.05 a	91	318	1992.29 y	0.61	324	9	Hei1996b	1	...	...
...	...	...	...	...	...	...	...	...	0.00	...	...	...	...	...	...
12442+5146	110833	062145	GC 17326	270.21 d	7.19 m	48.9	154.9	48401.43 d	0.00	0.0	9	HIP1997d	1	...	...
...	...	...	...	3.31	0.71	10.2	13.0	8.95	...	...	...	...	...	...	...
12595+4159	112914	063406	LTT 13738	710.6 d	14.12 m	81.8	101.3	49220.0 d	0.33	65.0	9	Jnc2005	1	...	...
...	...	...	...	...	0.47	5.0	4.9	...	...	...	...	...	...	...	...
13038−0510	113449	063742	GC 17714	231.23 d	11.21 m	126.5	33.3	48369.75 d	0.51	42.0	9	HIP1997d	...	...	...
...	...	...	...	1.96	1.57	10.8	14.5	10.27	0.21	21.8	...	...	...	...	...
13546+1825	121370	067927	η Boo	494.2 d	36.02 m	115.7	75.2	28136.2 d	0.26	326.3	9	Jnc2005	1	...	...
...	...	...	...	...	0.56	1.6	1.4	...	...	...	...	...	...	...	...
14035+1047	122742	068682	GJ 538	3614.89 d	105.28 m	93.5	252.3	33998.20 d	0.55	189.0	9	HIP1997d	1	...	...
...	...	...	...	...	2.02	...	...	...	...	...	...	...	...	...	...
14160−0600	124850	069701	ι Vir	55 y	0.87 a	60	3	1950.7 y	0.1	336	9	Gon2003	M	...	...
...	...	...	...	...	...	...	...	...	...	...	...	...	...	...	...
14294+8049	128642	070857	GC 19630	179.73 d	13.07 m	54.8	80.4	48361.86 d	0.15	158.6	9	HIP1997d	1	...	...

Continued on Next Page...

TABLE 5.4 – Continued

WDS Coord	HD Name	HIP Name	WDS DD	P	a	i (deg)	Ω (deg)	T_0	e	ω (deg)	G	Ref	SB	N	ΔT (years)
...	...	...	...	0.76	0.78	5.2	6.3	35.04	0.12	69.5	...	...	...	...	...
14534+1909	131511	072848	DE Boo	125.4 d	16.54 m	93.4	248.3	50203.4 d	0.51	219	9	Jnc2005	1	...	...
...	...	...	...	...	0.18	4.2	3.6	...	...	...	...	...	...	...	...
15282−0921	137763	075718	BAG 25Aa,Ab	889.6 d	38.6 m	60.3	95.8	47967.5 d	0.97	253.9	9	Jnc2005	2	1	0
...	...	...	...	...	1.0	1.8	3.5	...	...	...	...	...	...	...	...
15527+4227	142373	077760	χ Her	51.29 d	0.96 m	131.7	51.7	48349.00 d	0.00	0.0	9	HIP1997d	R	...	...
...	...	...	...	0.41	0.58	27.6	38.0	4.44	...	...	...	...	...	...	...
16010+3318	143761	078459	ρ CrB	0.11 y	1.66 m	0.5	30.5	1997.57 y	0.13	30	9	Gat2001a	...	...	...
...	...	...	...	...	0.35	...	12.3	...	...	...	...	...	...	...	...
16147+3352	146361	079607	σ CrB C	52 y	0.11 a	59	30	1963.0 y	0.36	127	9	Hei1990d	...	...	...
...	...	...	...	...	...	...	...	...	...	...	...	...	...	...	...
16285−7005	147584	080686	ζ TrA	12.9 d	2.71 m	16.0	2.1	18103.6 d	0.06	274.5	9	Jnc2005	1	...	...
...	...	...	...	...	0.44	2.5	6.8	...	...	...	...	...	...	...	...
17393+0333	160346	086400	GJ 688	83.70 d	12.71 m	18.4	274.2	47724.9 d	0.23	140.5	9	Jnc2005	1	...	...
...	...	...	...	...	0.78	1.1	2.7	...	...	...	...	...	...	...	...
17465+2743	161797	086974	TRN 2Aa	65 y	0.27 a	68	81.8	1951.0 y	0.32	92	9	Hei1994a	...	2	0
...	...	...	...	...	...	...	...	...	...	...	...	...	...	...	...
21094−7310	200525	104440	I 379A	2145 d	68 m	90	13	49422 d	0.70	148	9	Gln2006	...	4	34
...	...	...	...	1975	54	2	92	1513	0.09	84	...	...	...	...	...
21247−6814	203244	105712	GC 29928	1060.61 d	31.78 m	110.3	70.7	48167.89 d	0.29	11.9	9	HIP1997d	R	...	...
...	...	...	...	54.98	2.28	2.5	2.2	28.32	0.04	13.2	...	...	...	...	...

5.3 The Washington Double Star Catalog

The WDS is a frequently updated online[2] catalog maintained by the USNO. It contains measurements of double stars spanning the entire history of their observations. The online catalog contains summary information for each pair giving the earliest and latest separation and position angle measures along with their epochs, and the full catalog contains detailed information on each published measure. While the catalog contains measures of unrelated field stars as discussed in § 4.2, it is a very useful source in identifying and examining candidate companions. Cross-referencing the catalog as of July 8, 2008 with the stars of this work, I extracted measures for 503 pairs for 210 distinct primaries. In § 4.2, I described the method of blinking archival images, which identified 302 of these pairs as optical, and hence not gravitational bound. This section analyzes the remaining 201 pairs and utilizes the WDS to identify, confirm, or refute the candidate companions.

Seventy eight of the WDS pairs have supporting spectroscopic or visual orbits, or both, and these are included in the discussions in § 5.1.3 or § 6.2. An additional 35 pairs were confirmed by the matching proper motions and photometric distance estimates of the companions to the corresponding *Hipparcos* values of their primaries. Twenty two of these were also independently identified by blinking the archival images and are hence included in Table 4.2, and the remaining 13 are listed in Table 5.5. The first column identifies the primary star and the next three columns identify the companion by the separation, position angle, and epoch of the most recent observation listed in the WDS. Columns 5 and 6 list the

[2] *http* : *//ad.usno.navy.mil/wds/*

number of measurements of the pair listed in the WDS and the number of years they span. The next three columns list the proper motion of the companion, if available, along with its reference. This is followed by VRI photometry from the literature if available, again with the reference identified, and then the JHK_S magnitudes from 2MASS. The last two columns list the photometric distance estimate indicated by these magnitudes and its corresponding uncertainty. As in § 4.1, the distance estimates were derived by fitting various colors to the M_{K_S}–color relations from Henry et al. (2004).

TABLE 5.5: WDS companions confirmed by photometry

HD Name	Sep (arcsec)	PA (deg)	Epoch (year)	N	Δ T (years)	μ_α (mas yr^{-1})	μ_δ (mas yr^{-1})	R	==== CCD Magnitudes ==== V	R	R	R	I	R	Infrared Magnitudes J	H	K	D (pc)	Error (pc)
004391	16.6	307	1993	3	98	...	...		12.7	5	...		...		8.44	7.95	7.64	12.0	1.9
024409	8.9	228	1999	3	92	...	...		12.9	2	...		...		9.22	8.66	8.50	26.3	4.1
036705	9.2	345	1998	3	69	...	...		13.0	2	...		...		8.17	7.66	7.34	7.2[a]	1.1
039855	10.6	20	2003	12	127	...	...		...		...		9.13	3	7.99	7.40	7.22	19.0	2.9
040397	89.3	313	2000	2	40	78	−216	3	...		15.15	4	13.28	3	11.11	10.64	10.31	19.0	3.6
089125	7.7	299	2005	30	154	...	...		11.4	2	...		...		8.36	7.79	7.59	24.9	3.9
136202	11.4	35	2000	45	175	376	−517	1	10.2	2	...		...		7.49	6.91	6.75	20.6	3.5
149806	6.3	19	2000	3	54	...	...		13.0	2	...		...		8.09	7.57	7.28	6.7[a]	1.0
161797	34.9	248	2007	108	226	−333	−753	1	10.4	2	...		...		6.52[b]	5.92[b]	5.70[b]	6.2	0.9
167425	7.8	352	2000	6	103	...	...		10.8	2	...		...		8.00	7.42	7.19	23.7	3.7
186858	26.0	68	2006	117	184	19	−447	1	9.2	2	...		...		6.64	6.12	6.00	15.9	3.3
191499	4.0	14	2003	51	221	...	...		9.4	2	...		...		6.21	5.88	5.95	12.9[a]	3.5
214953	7.5	125	1998	15	104	...	...		10.3	2	...		...		7.44	6.86	6.63	17.8	2.8

NOTES.—Reference codes for columns 9, 11, 13, 15: 1 = The LSPM North catalog (Lépine & Shara 2005), 2 = Visual Double Stars in *Hipparcos* (Dommanget & Nys 2000), 3 = The USNO B 1.0 Catalog (Monet et al. 2003), 4 = The NOMAD Catalog (Zacharias et al. 2004), 5 = Differential photometry with CTIO 0.9m V-band image

[a] See § 7.4. [b] The companion is a visual binary. The *Hipparcos* input catalog lists individual V magnitudes of 10.2 and 10.7 for the components. 2MASS lists combined magnitudes for the two stars. The 2MASS magnitudes have been accordingly adjusted for one component.

Twenty seven pairs from the WDS contain bright companions with independent measures of parallaxes and proper motions that were compared with the primaries' *Hipparcos* measures to confirm a physical association and are accordingly listed in Table 4.1. Twenty additional pairs were confirmed based on proximity to the primary and matching proper motions. While an independent confirmation of distance could not be obtained for these pairs, mainly because obtaining reliable photometry is difficult for tight binaries, the proximity and CPM imply a physical association. Two of these 20 were also identified by blinking archival images as twin diffraction spikes (HIP 91605) or overlapping PSF (HD 125455), and were discussed in § 4.1. The remaining 18 could not be seen in the archival images because the companion was lost in the saturation around the primary due to the proximity and magnitude difference. All of these companions are within 23″ of the primary, and all but four are within 7″. Each companion has a matching proper motion with its primary in the range of $0\farcs1\,\mathrm{yr}^{-1}$ to $1\farcs6\,\mathrm{yr}^{-1}$. Further details for each of these stars, as well as 13 additional pairs which were confirmed based on published evidence, are included in § 7.4. Finally, 10 pairs listed in the WDS were confirmed as physical associations because the measures clearly demonstrate not only CPM, but also orbital motion, although they lack sufficient observations to derive an orbit. Table 5.6 lists these 10 pairs with their summary information from the WDS.

TABLE 5.6: WDS pairs demonstrating orbital motion

				First			Last			
Name	**Coord**	**DD**	**Pair ID**	**Sep (″)**	**PA (deg)**	**Epoch**	**Sep (″)**	**PA (deg)**	**Epoch**	**N**
HD 016765	02412−0042	STF 295	...	4.6	335	1829	3.3	306	2006	115
HD 130042	14494−6714	DON 680	...	1.0	64	1929	1.5	248	1991	7
HD 135204	15138−0121	A 691	...	0.1	226	1904	0.1	39	1986	17
HD 140538	15440+0231	A 2230	AB	3.6	103	1910	4.4	47	1974	15
HD 191408	20112−3606	HJ 5173	...	15.0	119	1834	5.3	126	1987	22
HD 200968	21072−1355	STF2752	AB	5.2	145	1827	3.7	177	1999	29
HD 211415	22183−5338	HDO 298	...	2.5	10	1894	5.0	39	1988	20
HD 215648	22467+1210	HJ 301	AB	15.0	123	1828	11.1	95	2007	23
HIP 036357	07291+3147	A 2124	AB	2.8	11	1910	3.4	8	1935	5
HIP 091605	18409+3132	HJ 1337	...	6.0	175	1828	9.3	154	2005	15

In addition to the 302 WDS pairs discussed in § 4.2 that were refuted as physical associations by demonstrating that the companions are field stars, 11 additional pairs were refuted based on a closer inspection. Two of these (HD 9540 and HD 26923 CD) had photometric distance estimates that were significantly different from the primary's *Hipparcos* distance and are included in Table 4.2. The other nine pairs (HD 20807 Aa, HD 22049 Aa-Ab, HD 64606 AB, HD 109358 Aa, HD 128620 Ca, HD 145958 Aa, HD 147776 AE, HD 178428Aa, and HD 186408 BC) were refuted based on published evidence and/or observations and are detailed in § 7.4. Finally, seven WDS pairs do not have sufficient evidence to be confirmed or refuted, and hence remain candidates. These are HD 4628 Aa, HD 45270, HD 100180 Aa, HD 111312 Aa-B, HD 147776 AC, HD 165908 Aa-Ab, and HD 217107, individual notes for which are included in § 7.4. The candidate companion for HD 217107 may in fact be the "exoplanet" reported by radial velocity surveys, but in order to be resolved by speckle, must be at least as massive as an early M-dwarf.

5.4 The Fourth Interferometric Catalog

While the WDS contains all measurements of pairs with separation and position angle measurements, the Fourth Catalog of Interferometric Measurements of Binary Stars[3] (FIC), maintained by the USNO as an online database, contains the results of observations using high-resolution techniques such as speckle interferometry, CCD imaging, adaptive optics, and long-baseline interferometry. This online catalog lists the details of every observation of

[3] *http : //ad.usno.navy.mil/wds/int4.html*

a pair including information such as the epoch of observation, the separation and position angle measured when available, and the reference. A feature of this catalog is that it also lists null results identifying the detection limits of the technique used. This source was very useful in deciding the status of many pairs, especially based on the null results published. Rather than list the information for individual pairs in this section, I mention this source in discussing the status of pairs when they are being evaluated, and the bulk of these references are in the notes to individual systems (§ 7.4).

5.5 The Catalog of Nearby Stars

The Catalog of Nearby Stars (Gliese 1969; Gliese & Jahreiß 1979, 1991, hereafter CNS) contains valuable information on stars within 25 pc. While it is dated and its astrometry has been superseded by *Hipparcos*, the information it contains about suspected or confirmed stellar companions was evaluated and included in this effort. Wide pairs are identified with measurement details and often confirmed via CPM. These pairs are typically also found in other sources such as the WDS, although a few really wide pairs (separations greater than some 10′) are listed only in the CNS. The catalog also identifies several stars as "SB", "SB?", "RV-Var", or "RV-Var?", but additional supporting information is often not included. Each of these was evaluated based on independent information that would allow their confirmation or rejection as physically bound.

For the targets studied here, the CNS indicates 198 possible companions. Most of these entries are also listed in one or more of the other sources checked and a majority of the

companions listed solely in the CNS have been found to be spurious. However, two wide companions (15′ from HD 63077 and 20′ from 137763) were identified solely based on their CNS entries, both of which were subsequently verified by blinking large enough images and confirmed by matching proper motions and parallaxes. Ninety one companions listed in the CNS have supporting spectroscopic and/or visual orbits, 51 were confirmed based on CPM and matching trigonometric or photometric parallaxes, and 22 were confirmed based on evidence of orbital motion or CPM and proximity. Twenty three of the CNS companions were refuted based on results of modern radial velocity surveys that negate claims of velocity variation or spectroscopic companions, and an additional eight were refuted by other methods utilized here. Finally, three companions (HD 20010, 23484, and 90839) have "RV-Var" or "RV-Var?" designations in the CNS for which I could not find any evidence to confirm or refute, and hence are retained as candidates. In summary, this catalog was found to be very reliable for CPM companions, with only six (4%) of the 148 CPM companions refuted, but less so for pairs identified as spectroscopic binaries, 23 (46%) of which were refuted.

Science is spectral analysis. Art is light synthesis.

—— *Karl Kraus*

– 6 –

Spectroscopic and Photometric Results

Spectroscopic techniques have been very useful in discovering and characterizing many stellar and most planetary companions. Photometric techniques have also been productive in detecting close pairs and estimating the components' physical parameters. This chapter presents the results from these techniques. With all my observing programs focused on astrometric techniques, I leveraged catalogs, publications, and collaborations to include the results from these methods.

To address spectroscopic companions, I first extracted information on known pairs from the 9$^{\text{th}}$ Catalogue of Spectroscopic Binary Orbits[1] (SB9), the exoplanet catalogs discussed in § 6.3, and publications. However, in order to present a credible update to the DM91 results, I needed to include the results of a more comprehensive effort. I have been able to achieve this goal with tremendous support from David W. Latham at the Harvard-Smithsonian Center for Astrophysics (CfA), Geoffrey W. Marcy at the University of California, Berkeley, Artie P. Hatzes at Thüringer Landessternwarte in Tautenburg, Germany, and William D. Cochran at the McDonald Observatory. Dr. Hatzes sent me the measured radial velocities on 51 stars of this work that were observed as part of his planet search program so that I could look for signatures of possible new stellar companions. Dr. Cochran looked at his planet search database and sent comments on 13 of my stars, confirming that they did not contain evidence for new stellar companions. Information from these surveys is presented in § 6.1.

[1] $http://sb9.astro.ulb.ac.be/$

Dr. Marcy sent me radial velocity measurements on 255 overlapping stars, obtained as part of planet-search efforts of the California and Carnegie Planet Search (CCPS) program, for the purpose of statistical analyses of companions. The results from these data are discussed in the statistical and incompleteness analyses in Chapter 8. I am grateful to each of these collaborators for enabling a much more comprehensive multiplicity survey. I am particularly indebted to Dr. Latham for sharing with me the spectroscopic results on over 300 overlapping stars based on over 20 years of radial-velocity measurements at the CfA for various surveys (Carney & Latham 1987; Udry et al. 1998). Sections 6.1 & 6.2 present these results for constant velocity stars as well as spectroscopic binaries.

This chapter also includes results from photometric techniques in § 6.4. While this method has been very useful in identifying and characterizing eclipsing stellar and sub-stellar components, most photometric discoveries are for distant systems with very short periods, and the overlap with this study is small.

6.1 Constant Radial Velocity Stars

Table 6.1 lists 269 stars that do not show evidence of radial velocity variations. The results are primarily from the CfA surveys but also include information from the high-precision surveys of A. Hatzes, W. Cochran, and Nidever et al. (2002). Stars with zero or one CfA observation have been excluded unless they have evidence of stable radial velocities from the high-precision measures, resulting in the inclusion of five with no observations and 11 with one observation. All but 23 of the stars in the table have at least four CfA observations ob-

tained over at least five years, or have stable velocities from the the high-precision searches. The first column identifies the star by its HD or HIP identification and a component designation when required. Columns 2–7 pertain to the CfA observations. Column 2 lists the number of velocity measurements and Column 3 the number of years (y) or days (d) spanned by these measurements. The next column lists the mean radial velocity in $\mathrm{km\,s^{-1}}$, followed by the external error, a measure of the rms scatter around the mean. Column 6 lists the $P(\chi^2)$ value of these measures, indicating the probability that the scatter around the mean is solely due to measurement errors. Column 7 lists the ratio of external to internal error, serving as another diagnostic for variability. All stars listed in this table are considered as constant velocity stars for this work. Column 8 lists a "C" if this star was identified as a constant velocity star in the Hatzes or Cochran surveys, "F" if the survey had too-few observations to tell, "L" if the data showed a linear trend, and "V" if the data showed variations. These surveys typically have a few dozen observations for each star, measured over a few (1–4) years. The last column lists these same flags from Nidever et al. (2002), where a "C" designation is assigned to stars listed in Table 1, i.e. those with a velocity scatter of less than 0.1 $\mathrm{km\,s^{-1}}$ and "V" to stars listed in Table 2, i.e. stars with a scatter greater than 0.1 $\mathrm{km\,s^{-1}}$. Any "L" or "V" values are individually footnoted and these variations relate to known planet(s) or to visual companions for which the high-precision data show a slow linear drift. Note that some of these stars may be planet hosts, and in that sense show periodic variations in their velocities, but for the purposes of this section, we are concerned about stellar companions and include planet hosts that do not show any evidence of longterm

trends.

TABLE 6.1: Stars with no Evidence of Radial Velocity Variations

Name	N	ΔT	$\langle$**RV**$\rangle$ (**km s**$^{-1}$)	**Ext Err** (**km s**$^{-1}$)	$P(\chi^2)$	**E/I**	**H,C**	**Nid02**
HD 000166	75	15.05 y	−6.71	0.46	0.00310	1.2	C	C
HD 001461	49	13.08 y	−10.15	0.58	0.00001	1.4	C	C
HD 001562	10	11.29 y	15.06	0.21	0.95538	0.5	...	...
HD 001835	51	15.05 y	−2.51	0.40	0.55195	0.9	...	C
HD 002025	...	...	...	...	...	...	...	C
HD 003651	23	25.45 y	−33.13	0.77	0.00000	2.3	...	C
HD 003765	180	26.78 y	−63.37	0.53	0.00000	1.4	...	C
HD 004256	4	2.11 y	9.39	0.28	0.75400	0.6	...	C
HD 004614A	4	6.96 y	7.61	0.35	0.30936	1.0	...	C
HD 004614B	89	18.74 y	10.71	0.55	0.00254	1.2	...	C
HD 004628	23	12.41 y	−10.08	0.56	0.00337	1.5	...	C
HD 004635	18	8.46 y	−31.83	0.44	0.17025	1.2	...	...
HD 004813	4	11.16 y	7.98	0.48	0.04838	1.7	...	...
HD 004915	10	8.36 y	−3.77	0.26	0.92060	0.6	...	C
HD 005015	4	7.90 y	20.23	0.40	0.24600	1.1	...	...
HD 005133	...	...	...	...	...	...	...	C
HD 007590	10	11.25 y	−13.30	0.48	0.43457	1.0	C	C
HD 007924	4	8.49 y	−22.56	0.62	0.05050	1.7	...	...
HD 009407	12	8.50 y	−33.26	0.30	0.67109	0.9	F	C
HD 009540	3	12.04 y	2.72	0.16	0.91613	0.3	...	...
HD 009826	14	21.20 y	−28.64	0.87	0.00107	2.0	...	C
HD 010008	7	5.99 y	11.42	0.77	0.00188	1.7	...	...
HD 010086	3	1.08 y	1.76	0.34	0.35239	0.9	...	C
HD 010476	20	25.45 y	−33.67	0.66	0.00000	1.9	...	C
HD 010700	29	18.32 y	−16.66	0.50	0.01893	1.3	...	C
HD 010780	72	22.40 y	2.73	0.49	0.00000	1.4	C	C
HD 012051	11	8.33 y	−35.08	0.49	0.41728	1.0	...	C
HD 012846	11	11.37 y	−4.53	0.56	0.40119	1.2	...	C
HD 014412	4	3.94 y	7.34	0.40	0.19585	1.1	...	C
HD 016160	19	12.61 y	26.03	0.42	0.07031	1.2	...	C
HD 016895A	37	17.47 y	24.12	0.36	0.37098	1.0	...	C
HD 016895B	34	14.25 y	25.81	0.93	0.33501	0.7	...	C
HD 017925	41	10.36 y	18.04	0.43	0.57961	1.0	C	C
HD 018143	11	8.34 y	31.96	0.56	0.12744	1.3	...	C

Continued on Next Page...

TABLE 6.1 – Continued

Name	N	ΔT	$\langle$RV$\rangle$ (km s^{-1})	Ext Err (km s^{-1})	$P(\chi^2)$	E/I	H,C	Nid02
HD 018632	8	17.45 y	28.79	0.31	0.79244	0.7	...	C
HD 018757	7	11.40 y	−2.55	0.24	0.87338	0.6	...	...
HD 018803	6	1.59 y	9.82	0.38	0.30351	1.1	...	C
HD 019373	29	13.16 y	49.42	0.62	0.00000	1.7	...	C
HD 019994	3	3.61 y	19.47	0.44	0.26507	1.2	...	C
HD 020165	10	14.49 y	−16.82	0.39	0.79352	0.7	...	C
HD 020619	3	3.85 y	23.03	0.75	0.03899	1.7	...	C
HD 020630	79	13.03 y	19.00	0.46	0.00049	1.3	C	C
HD 022049	32	17.14 y	16.33	0.57	0.00017	1.5	...	C
HD 022484	183	23.44 y	28.01	0.40	0.00031	1.1	...	C
HD 022879	70	16.85 y	120.15	0.55	0.17919	1.0	...	C
HD 023356	1	...	25.24	...	1.00000	...	...	C
HD 024238	10	8.42 y	38.49	0.43	0.72252	0.9	...	C
HD 024496	8	11.99 y	18.65	0.30	0.78679	0.7	...	C
HD 025329	35	14.08 y	−25.76	0.68	0.78191	0.9	...	V[a]
HD 025665	...	...	...	...	...	...	...	C
HD 025680	9	10.93 y	23.98	0.35	0.52202	1.0	...	C
HD 025998	12	1.87 y	25.35	0.42	0.94963	0.7	...	...
HD 026913	25	16.23 y	−8.02	0.50	0.02160	1.2	C	...
HD 026923	9	11.96 y	−7.28	0.21	0.95513	0.5	C	...
HD 026965	49	17.90 y	−42.24	0.51	0.00011	1.4	...	C
HD 029883	4	2.12 y	17.20	0.63	0.06590	1.6	...	C
HD 030495	4	2.41 y	21.70	0.29	0.54368	0.8	...	...
HD 030876	3	7.11 y	20.59	0.34	0.37180	1.0	...	...
HD 032923	94	16.96 y	20.49	0.52	0.00000	1.4	...	C
HD 034411	4	11.15 y	66.23	0.23	0.64464	0.7	C	C
HD 034721	4	3.82 y	40.34	0.20	0.79302	0.6	...	C
HD 035112A	10	13.25 y	36.31	0.63	0.05785	1.4	...	...
HD 035296	61	13.03 y	37.59	0.53	0.03684	1.1	C	...
HD 037008	3	1.94 y	−45.88	0.23	0.74151	0.6	...	...
HD 037394	20	11.91 y	1.11	0.38	0.85286	0.8	C	C
HD 038230	10	11.87 y	−29.53	0.44	0.60342	1.0	C	C
HD 038858	5	2.96 y	31.25	0.49	0.09018	1.3	...	C
HD 039855	5	5.01 y	42.58	0.71	0.07564	1.3	...	...
HD 040397AB	6	7.06 y	143.48	0.31	0.85357	0.7	C	C
HD 041593	14	10.47 y	−9.83	0.40	0.67405	0.9	C	...
HD 042618	10	12.39 y	−53.95	0.58	0.44411	1.1	...	C

Continued on Next Page...

TABLE 6.1 – Continued

Name	N	ΔT	$\langle$RV$\rangle$ (km s^{-1})	Ext Err (km s^{-1})	$P(\chi^2)$	E/I	H,C	Nid02
HD 042807	14	6.86 y	5.86	0.31	0.83090	0.8	...	...
HD 043162	7	7.23 y	21.86	0.23	0.97369	0.5	...	...
HD 045184	3	3.13 y	−4.27	0.45	0.09803	1.5	...	C
HD 046588	2	16.65 y	15.21	0.03	0.97903	0.1	...	...
HD 048682	5	2.81 y	−23.83	0.68	0.01704	1.8	C	C
HD 050692	7	11.05 y	−15.11	0.37	0.36320	1.0	...	C
HD 051419	9	12.44 y	−27.16	0.46	0.19319	1.1	C	...
HD 051866	4	2.83 y	−21.75	0.27	0.77038	0.6	...	C
HD 052711	11	4.26 y	24.43	0.24	0.99114	0.6	...	C
HD 055575	9	14.90 y	84.29	0.27	0.77500	0.7	...	C
HD 059747	5	3.25 y	−15.97	0.29	0.70835	0.7	...	C
HD 059967	6	5.89 y	9.15	0.65	0.00303	1.7	...	...
HD 060491	4	1.96 y	−9.96	0.35	0.74222	0.5	...	C
HD 061606	4	11.70 y	−18.23	0.65	0.07653	1.5	...	C
HD 063433	9	11.35 y	−16.05	0.44	0.48748	0.9	C	C
HD 065583	328	26.80 y	14.71	0.58	0.00000	1.3	...	C
HD 067228	3	2.18 y	−36.27	0.33	0.31834	1.0	...	C
HD 068017	12	11.96 y	29.68	0.45	0.37359	1.0	...	C
HD 068255	23	11.14 y	−6.50	0.90	0.00000	2.8	...	...
HD 068257	21	11.14 y	−4.88	1.05	0.00000	3.1	...	...
HD 069830	4	3.72 y	30.04	0.61	0.14309	1.5	...	...
HD 071148	7	2.41 y	−32.39	0.46	0.19645	1.3	...	C
HD 072673	3	2.98 y	14.51	0.38	0.31705	1.1	...	C
HD 072760	8	9.20 y	35.05	0.24	0.96311	0.5	...	C
HD 072905	40	18.02 y	−12.86	0.67	0.00000	1.9	C	...
HD 073350	4	14.81 y	35.52	0.55	0.02966	1.4	...	C
HD 073667	13	15.02 y	−12.11	0.64	0.00346	1.4	...	C
HD 074576	2	5.91 y	12.26	0.29	0.40422	0.8	...	...
HD 075732	6	3.98 y	27.52	0.45	0.19116	1.1	...	C
HD 076151	5	7.09 y	32.26	0.31	0.66501	0.8	...	C
HD 076932	6	11.67 y	119.32	0.55	0.51166	1.0	...	...
HD 078366	3	90.00 d	25.84	0.63	0.15253	1.3	...	C
HD 079969	6	16.76 y	−20.41	0.26	0.85587	0.7	...	...
HD 082443	77	14.44 y	8.31	0.45	0.27239	1.0	...	...
HD 082558	...	...	...	...	...	...	C[b]	...
HD 082885	9	16.18 y	14.47	0.29	0.72885	0.8	...	...
HD 084737	1	...	4.62	...	1.00000	...	...	C

Continued on Next Page...

TABLE 6.1 – Continued

Name	N	ΔT	$\langle$RV$\rangle$ (km s^{-1})	Ext Err (km s^{-1})	$P(\chi^2)$	E/I	H,C	Nid02
HD 086728	7	6.03 y	56.10	0.35	0.29604	1.0	...	C
HD 087424	1	...	−12.22	...	1.00000	...	...	C
HD 087883	5	3.06 y	9.44	0.31	0.70012	0.7	...	C
HD 089125A	7	5.91 y	36.79	0.30	0.58788	0.8	...	...
HD 089269	15	16.34 y	−7.62	0.34	0.73340	0.9	C	C
HD 090156	5	5.03 y	26.50	0.45	0.09886	1.4	...	C
HD 090508	7	2.40 y	−7.64	0.22	0.90382	0.6	...	...
HD 090839A	44	13.24 y	8.40	0.47	0.00016	1.4	...	C
HD 091889	16	13.74 y	−6.30	0.65	0.00040	1.7	...	...
HD 092719	3	12.76 y	−18.25	0.06	0.97882	0.1	...	...
HD 092945	...	...	...	...	...	...	...	C
HD 094765	6	7.68 y	5.57	0.68	0.05949	1.4	...	C
HD 095128	6	5.58 y	11.47	0.42	0.21593	1.2	...	C
HD 096064A	22	7.75 y	18.56	0.55	0.02311	1.3	...	...
HD 096612	3	5.78 y	−36.37	0.35	0.53940	0.8	...	...
HD 097334	50	3.21 y	−3.72	0.37	0.90191	0.9	C	C
HD 097343	6	3.23 y	39.25	0.42	0.07846	1.3	...	C
HD 097658	4	2.12 y	−1.34	0.84	0.05214	1.5	...	C
HD 098281	3	1.07 y	13.36	0.36	0.49961	0.8	...	C
HD 099491	11	11.25 y	4.20	0.34	0.78680	0.8	...	C
HD 099492	6	2.82 y	3.95	0.42	0.65762	0.9	...	C
HD 100180A	11	12.05 y	−4.52	0.53	0.04321	1.4	...	C
HD 100180B	9	11.21 y	−4.45	0.47	0.29165	1.0	...	...
HD 100623	4	3.15 y	−22.44	0.29	0.47680	0.9	...	C
HD 101177	3	361 d	−16.86	0.32	0.40733	1.8	...	C
HD 101501	23	12.86 y	−5.82	0.52	0.00007	1.6	...	C
HD 102870	96	16.20 y	4.52	0.58	0.00000	1.6	C	C
HD 103095	348	27.17 y	−98.49	0.48	0.99717	0.9	C	C
HD 104067	1	...	14.73	...	1.00000	...	...	C
HD 104304	6	6.02 y	0.49	0.61	0.01160	1.6	...	...
HD 105631	6	9.06 y	−2.43	0.40	0.72285	0.8	...	C
HD 108954	10	11.02 y	−21.66	0.48	0.16086	1.3	...	...
HD 109358	9	16.10 y	6.02	0.45	0.06352	1.4	...	C
HD 110897	17	10.67 y	80.13	0.39	0.54730	0.9	...	...
HD 111395	126	16.11 y	−9.12	0.53	0.00000	1.4	...	...
HD 114710	138	25.87 y	5.22	0.54	0.00000	1.5	...	C
HD 114783	11	4.22 y	−11.54	0.81	0.00389	1.8	...	C

Continued on Next Page...

TABLE 6.1 – Continued

Name	N	ΔT	$\langle$RV$\rangle$ (km s^{-1})	Ext Err (km s^{-1})	$P(\chi^2)$	E/I	H,C	Nid02
HD 115383	24	10.87 y	−27.23	0.76	0.00000	2.0	C	C
HD 115404A	24	10.87 y	7.57	0.54	0.00449	1.4	...	...
HD 115404B	3	8.06 y	6.80	0.47	0.48180	0.8	...	...
HD 115617	33	13.06 y	−7.77	0.53	0.00001	1.5	...	C
HD 116442	18	11.25 y	27.99	0.53	0.01646	1.3	...	C
HD 116443	9	11.25 y	27.59	0.36	0.49441	0.9	...	C
HD 116956	9	10.91 y	−12.15	0.39	0.55529	0.9	C	...
HD 117043	3	16.58 y	−30.89	0.28	0.58756	0.7	...	...
HD 117176	6	5.70 y	4.83	0.36	0.30112	1.0	...	V[c]
HD 118972	5	4.72 y	−7.83	0.34	0.70987	0.8	...	...
HD 119332	6	9.78 y	−8.50	0.29	0.76803	0.7	...	...
HD 121560	1	...	−11.44	...	1.00000	...	...	C
HD 124106	1	...	1.95	...	1.00000	...	...	C
HD 124292	8	8.71 y	37.58	0.37	0.38476	0.9	...	C
HD 125455	9	14.81 y	−10.32	0.91	0.00039	2.2	...	C
HD 126053	131	27.40 y	−19.44	0.54	0.00017	1.2	...	C
HD 127334	5	2.19 y	−0.65	0.44	0.42005	1.0	...	C
HD 128311	1	...	−10.00	...	1.00000	...	...	C
HD 128987	4	1.83 y	−22.71	0.44	0.55664	0.8	...	...
HD 130307	5	3.52 y	13.15	0.47	0.31642	1.1	...	C
HD 130948	135	16.30 y	−2.70	0.53	0.00000	1.2	C	C
HD 131156	120	13.48 y	1.37	0.48	0.00000	1.4	L[d]	C
HD 131582	3	7.95 y	−31.95	0.07	0.97192	0.1	...	...
HD 132142	14	21.69 y	−14.90	0.46	0.24205	1.0	...	C
HD 132254	5	2.76 y	−15.59	0.34	0.46292	1.0	...	...
HD 135204	5	12.85 y	−69.25	0.60	0.05294	1.4	C	...
HD 135599	4	2.21 y	−3.30	0.84	0.00614	2.0	C	C
HD 136202A	272	22.98 y	54.49	0.47	0.00000	1.4	...	...
HD 136202B	37	16.64 y	55.08	0.60	0.55414	1.0	...	...
HD 136713	2	54.00 d	−6.12	0.39	0.43150	0.8	C	C
HD 136923	11	8.67 y	−7.25	0.52	0.09426	1.2	...	C
HD 137778	3	76.00 d	7.98	0.51	0.52087	0.9	...	C
HD 139323	7	2.87 y	−66.84	0.69	0.15562	1.5	...	...
HD 139777	13	14.30 y	−16.71	0.78	0.00000	1.9	...	...
HD 139813	9	12.05 y	−15.97	0.67	0.27068	1.4	...	...
HD 140538A	85	13.17 y	19.10	0.48	0.00004	1.3	...	...
HD 140538B	4	7.00 d	20.10	0.46	0.84604	0.5	...	...

Continued on Next Page...

TABLE 6.1 – Continued

Name	N	ΔT	$\langle$RV$\rangle$ (km s^{-1})	Ext Err (km s^{-1})	$P(\chi^2)$	E/I	H,C	Nid02
HD 141004	9	14.87 y	−66.43	0.45	0.04026	1.3	...	C
HD 141272	13	15.00 y	−26.56	0.52	0.33443	1.1	...	...
HD 142373	8	18.78 y	−56.44	0.55	0.19632	1.4	...	C
HD 143761	9	13.01 y	18.00	0.35	0.41648	1.0	...	C
HD 144579	132	25.13 y	−59.63	0.48	0.04102	1.0	...	C
HD 144872	6	8.88 y	23.63	0.51	0.25412	1.2	...	...
HD 145675	11	5.95 y	−14.07	0.49	0.08689	1.3	L[e]	C
HD 145958A	9	2.88 y	18.53	0.37	0.53610	1.0	...	C
HD 145958B	10	2.88 y	18.26	0.39	0.51763	1.3	...	C
HD 146233	60	13.56 y	11.68	0.34	0.92058	0.9	...	C
HD 146362	18	8.17 y	−14.72	0.46	0.00770	1.3	...	C
HD 147776	2	69.00 d	6.84	0.41	0.33917	0.9	...	C
HD 148653	41	12.27 y	−31.26	0.39	0.90813	0.9	...	...
HD 149661	6	12.88 y	−12.65	0.46	0.34464	1.1	...	C
HD 149806	4	3.51 y	10.46	0.18	0.90865	0.4	...	C
HD 151541	10	22.48 y	9.16	0.33	0.47753	0.9	...	C
HD 152391	23	17.97 y	45.06	0.45	0.05422	1.2	C	C
HD 153525	5	8.73 y	−7.19	0.42	0.36486	1.1	...	...
HD 153557	5	8.73 y	−7.07	0.37	0.54220	0.9	...	...
HD 154345	5	12.85 y	−47.29	0.48	0.26233	1.0	...	C
HD 154417	183	26.23 y	−16.89	0.49	0.00000	1.2	...	C
HD 155885A	18	12.97 y	0.20	0.71	0.00000	2.0	...	...
HD 155885B	19	12.97 y	0.17	0.72	0.00000	2.0	...	...
HD 156026	3	11.96 y	−0.96	0.60	0.04082	1.8	...	C
HD 157214	7	12.88 y	−78.81	0.38	0.20595	1.1	...	C
HD 157347	5	3.79 y	−35.70	0.26	0.79978	0.7	...	C
HD 158633	12	12.77 y	−38.92	0.58	0.00186	1.7	...	...
HD 159062	11	12.51 y	−84.18	0.43	0.67373	0.9	...	...
HD 159222	5	12.88 y	−51.49	0.41	0.62860	0.9	...	C
HD 162004	3	5.26 y	−10.65	1.28	0.00000	3.5	...	...
HD 164922	6	8.64 y	20.34	0.39	0.36942	1.0	...	C
HD 166620	7	11.00 y	−19.38	0.26	0.70265	0.7	...	C
HD 168009	10	16.10 y	−64.82	0.53	0.08996	1.3	...	C
HD 170657	4	8.94 y	−42.95	0.37	0.73030	0.7	...	C
HD 172051	5	12.15 y	37.05	0.10	0.99095	0.2	...	C
HD 176377	15	12.67 y	−40.78	0.65	0.00634	1.5	...	C
HD 179957A	5	2.66 y	−41.13	0.22	0.80528	0.6	...	C

Continued on Next Page...

TABLE 6.1 – Continued

Name	N	ΔT	$\langle$RV$\rangle$ (km s^{-1})	Ext Err (km s^{-1})	$P(\chi^2)$	E/I	H,C	Nid02
HD 179957B	5	2.66 y	−41.73	0.29	0.59761	0.7	...	C
HD 182488	10	12.52 y	−21.82	0.32	0.76760	0.8	...	C
HD 182572	357	23.53 y	−100.33	0.43	0.00000	1.2	C	...
HD 183870	1	...	−49.74	...	1.00000	...	...	C
HD 184385	2	182.00 d	11.29	0.49	0.15298	1.4	...	C
HD 185144	6	8.17 y	26.05	0.47	0.11850	1.3	...	C
HD 186427	8	24.90 y	−28.18	0.87	0.00000	2.4	...	C
HD 187691	211	23.93 y	0.06	0.43	0.00000	1.2	C	...
HD 190067	8	5.51 y	19.98	0.39	0.68373	0.9	...	C
HD 190360	128	16.02 y	−45.38	0.53	0.00000	1.4	...	C
HD 190404	15	21.21 y	−2.80	0.59	0.15044	1.3	...	...
HD 190406	146	11.97 y	4.89	0.37	0.15516	1.0	...	L[f]
HD 190470	5	21.31 y	−7.56	0.20	0.86806	0.5	...	...
HD 191785	6	2.52 y	−49.12	0.68	0.01536	1.5	...	C
HD 192263	1	...	−10.71	...	1.00000	...	...	C
HD 193664	3	352.00 d	−5.40	0.77	0.00192	2.5	...	...
HD 194640	4	12.30 y	−0.45	0.38	0.33068	1.0	...	...
HD 195564	3	3.12 y	9.23	0.16	0.70966	0.7	...	C
HD 196761	4	12.02 y	−41.77	0.18	0.94571	0.3	...	C
HD 197076	159	17.14 y	−35.51	0.45	0.00000	1.2	...	C
HD 199260	2	84.00 d	−16.55	0.34	0.33843	1.0	...	...
HD 202751	4	2.84 y	−27.49	0.32	0.66950	0.8	...	C
HD 206860	28	21.17 y	−16.92	0.48	0.04936	1.1	C	C
HD 208038	9	9.62 y	13.63	0.65	0.03537	1.4	...	...
HD 208313	5	2.51 y	−13.45	0.69	0.05007	1.4	...	C
HD 210277	1	...	−19.68	...	1.00000	...	...	C
HD 210667	6	2.50 y	−19.44	0.22	0.94965	0.5	...	C
HD 211472	11	12.03 y	−7.55	0.66	0.05574	1.5	...	...
HD 214683	5	6.52 y	22.24	0.90	0.00182	2.0	...	...
HD 215152	1	...	19.18	...	1.00000	...	...	C
HD 215648	5	11.25 y	−5.62	0.48	0.11565	1.4	...	C
HD 216259	11	2.11 y	1.44	1.05	0.00782	1.8	...	C
HD 217014	130	16.27 y	−33.17	0.49	0.00000	1.3	...	C
HD 217107	3	2.99 y	−12.95	0.48	0.36033	1.1	V[g]	C
HD 217813	11	12.13 y	1.95	0.55	0.00681	1.5	C	C
HD 218868	5	2.21 y	−30.62	0.47	0.36929	1.1	...	...
HD 219134	31	14.95 y	−18.57	0.56	0.00000	1.6	...	...

Continued on Next Page...

TABLE 6.1 – Continued

Name	N	ΔT	$\langle$RV$\rangle$ (km s^{-1})	Ext Err (km s^{-1})	$P(\chi^2)$	E/I	H,C	Nid02
HD 219538	5	2.10 y	9.85	0.57	0.18438	1.2	...	C
HD 219623	10	12.51 y	−27.29	0.49	0.09274	1.3	...	...
HD 220182	25	18.84 y	3.43	0.46	0.08394	1.1	...	...
HD 220339	2	30 d	33.62	1.05	0.03781	2.0	...	C
HD 221354	12	8.73 y	−25.37	0.40	0.32416	0.9	...	C
HD 221851	13	9.20 y	−21.13	0.33	0.88510	0.8	...	...
HD 222143	12	8.45 y	−0.01	0.50	0.17576	1.2	...	C
HD 222368	142	23.45 y	5.56	0.46	0.01885	1.2	...	...
HD 232781	5	9.11 y	−40.17	0.42	0.43936	0.9	...	...
HD 263175	5	16.69 y	−31.93	0.57	0.16046	1.2	...	...
HIP 036357	20	18.84 y	−4.14	0.58	0.01862	1.4	...	...
HIP 040774	4	8.02 y	27.28	0.64	0.24353	1.3	...	...
HIP 087579	21	16.57 y	−13.10	0.49	0.27335	1.0	...	C

[a] Identified in Nidever et al. (2002) as $\sigma_{\rm RV} > 0.1$ km s^{-1} based on three observations, but the 35 CfA measures over 14 years do not show any periodic variation consistent with a stellar companion. [b] While this star shows an increased scatter in 19 high-precision observations over 5 years, there is no periodic signature and the scatter is believed to be due to spots (A. Hatzes 2008, private communication) [c] The $\sigma_{\rm RV} > 0.1$ km s^{-1} variations noted in Nidever et al. (2002) are consistent with a published 7.5 M_J planet. [d] A linear trend with $\sigma_{\rm RV} < 0.1$ km s^{-1} is seen in 54 observations over 4.2 years in the high-precision data from A. Hatzes, but is likely due to the known 150-year VB. [e] A linear trend with $\sigma_{\rm RV} < 0.1$ km s^{-1}, consistent with the known 5 M_J planet, is seen in 25 measures over 1.3 years by A. Hatzes. [f] A linear trend with a slope of -0.066 m s^{-1} day^{-1} over 58 observations is mentioned in Nidever et al. (2002), and these variations are consistent with a

brown dwarf discovered 0.″8 away by Liu et al. (2002). [g] A. Hatzes measured variations with $\sigma_{\rm RV} < 0.1$ km s^{-1}, consistent with the published planets of 1.4 M_J and 2.5 M_J.

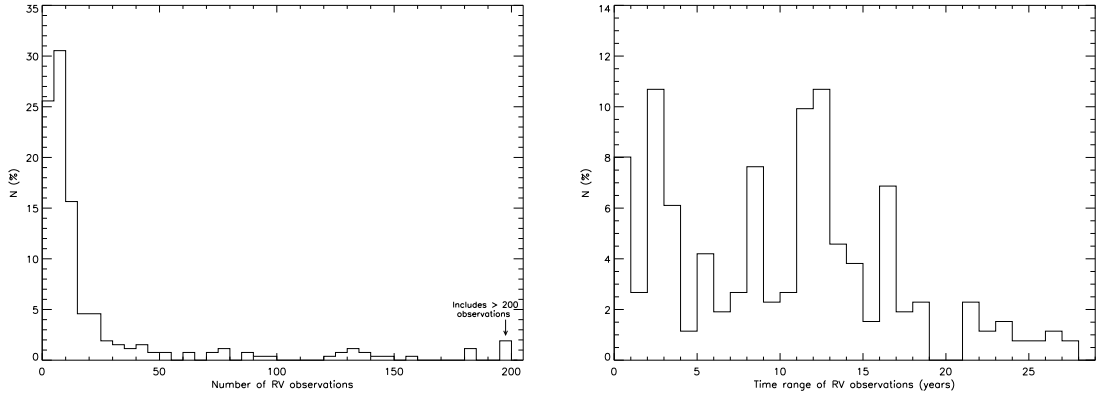

FIGURE 6.1: The distributions of the number of radial velocity measurements per star (left) and their time span (right) in the CfA survey.

Figure 6.1 shows the extensive radial velocity coverage of these stable velocity stars. Thirty-nine percent of the systems listed have over 10 observations and 23% have over 20 observations. As seen in right panel of the figure, a majority of the stars have radial velocity measurements gathered over more than 10 years, and almost 10% of the systems observed have over 20 years of coverage. The left panel of Figure 6.2 shows that the distribution of the external error is roughly normal around a strong peak at 0.4–0.5 km s^{-1}, the typical measurement errors of the CfA observations, as expected for constant velocity stars. Only five stars (HD 68255, 68257, 162004, 216259, and 220339) have external errors larger than 1 km s^{-1}. The first two stars are separated by 1″ and belong to a system with the largest number of stellar components (five, maybe six, see § 7.4) for the sample studied here. The large error for these stars could be due to contamination from nearby sources (D. Latham 2008, private communication). HD 162004 appears to vary in a linear fashion in the 3 CfA

observations over 5.3 years, but the first observation is 2 $\mathrm{km\,s^{-1}}$away from the other two. Moreover, eight early observations from Duquennoy et al. (1991) and 9 later measures from Abt & Willmarth (2006) are all consistent with the two latter CfA measures. While it is possible that this star is a highly eccentric binary, it appears to be a constant velocity star if the first CfA observation is excluded. HD 216529 has 11 observations over two years, the first of which is about 3 $\mathrm{km\,s^{-1}}$ away from the other observations, causing the large error. However, Nidever et al. (2002) reports this star with a scatter of less than 0.1 $\mathrm{km\,s^{-1}}$ based on 4 years of measurements at an earlier epoch, and their reported velocity agrees well with the CfA mean. It appears that the outlier point is erroneous and not indicative of variability. Finally, the two CfA measures for HD 220339, 30 days apart, vary by 1.5 $\mathrm{km\,s^{-1}}$, but Nidever et al. (2002) show it to be of stable velocity in observations over almost 4 years. The right panel of Figure 6.2 shows that the distribution of the ratio of external to internal error has a broad peak at 1.0–1.5 $\mathrm{km\,s^{-1}}$, again as expected for constant velocity stars. Fourteen stars have a ratio ≥ 2, and an inspection of these reveals that it is due to one or two outliers and/or possible contamination from close sources. Some of these are exoplanet hosts exhibiting an increased scatter in the CfA data which is not supported by the higher precision measures from the planet search efforts.

For a fit with a given χ^2 value, the probability that the scatter around the fit is solely due to observational effects is given by $P(\chi^2)$, defined by Equation (6.1) (Barlow 1999). This metric has been used as an indicator of radial velocity variability in prior studies (DM91,

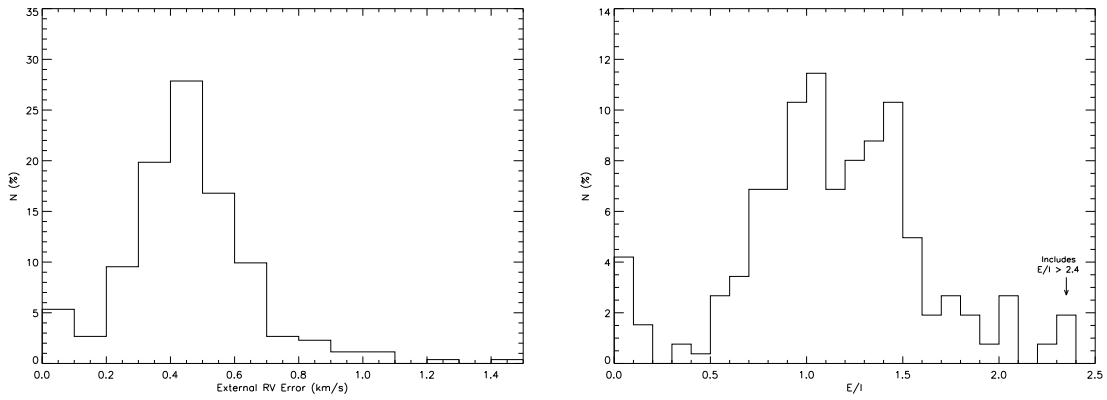

FIGURE 6.2: The distributions of the external errors (left) and the ratio of external to internal errors (right) for the CfA measurements.

Nordström et al. 2004).

$$P(\chi^2; N) = \int_{\chi^2}^{\infty} p(\chi'^2; N) d\chi'^2, \tag{6.1}$$

where N is the degrees of freedom of the fit, and $p(\chi'^2; N)$ is the probability for a specific χ'^2 value, given by Equation (6.2).

$$p(\chi^2; N) = \frac{2^{-N/2}}{\Gamma(N/2)} \chi^{N-2} e^{-\chi^2/2} \tag{6.2}$$

Figure 6.3 shows the $P(\chi^2)$ distribution, which is similar to that in DM91, with a clear discontinuity at $P(\chi^2) = 0.01$, to the left of which is a strong peak followed by a fairly flat distribution to the right. However, there is one key difference. While DM91 included all stars studied in their plot, I have only plotted stars that I believe are of constant velocity based on an examination of the individual velocity plots and consistent evidence from the high-precision measures. Moreover, the distribution of other metrics such as the external error and the external-to-internal error ratio are fully consistent with what would be expected for a set of single stars, as discussed in the paragraph above. Hence, it appears that a low

$P(\chi^2)$ value does not, by itself, indicate variability due to binary orbital motion. Duquennoy et al. (1991) state that the $P(\chi^2)$ distribution is expected to be flat from 0 to 1 for single stars, while for variable radial velocity stars, it should be strongly peaked towards lower values. DM91 then use the discontinuity at 0.01 to argue that values smaller than this limit imply variability which, at least in some cases, is due to an unseen companion. Nordström et al. (2004) also use the same criteria of $P(\chi^2) < 0.01$ for "certain velocity variability – mostly due to binary orbital motion." However, given the similar appearance of Figure 6.3 for constant velocity stars to the DM91 plot of all stars, $P(\chi^2)$ does not appear to be a good indicator of variability. For instance, stars HD 3651 (a planet host), 4628, 90839, 126053, and 130948 have $P(\chi^2) < 0.01$, but a visual inspection of the velocity plots indicates either random scatter over many observations, or a couple of outlier points, but no evidence of periodic variation. Furthermore, each of these stars has a scatter of less than 0.1 $\mathrm{km\,s^{-1}}$ in Nidever et al. (2002) across observations spanning at least 3000 days, increasing confidence in the conclusion that these are indeed stable radial velocity stars.

DM91 discuss the example of one star (HD 102870), an IAU velocity standard, which has $P(\chi^2) < 0.01$, and they point out that this low value is due to the large number of observations rather than due to variability, which they believe is clearly ruled out by a low $\sigma_{\mathrm{RV}} = 0.32$ $\mathrm{km\,s^{-1}}$. However, they also point out three other examples where a low $P(\chi^2)$ led to the suspicion of a companion, and they note that in each case companions were later reported in the sub-stellar regime. However, their study could not benefit from the high-precision measurements of the current planet search programs, which yield results accurate

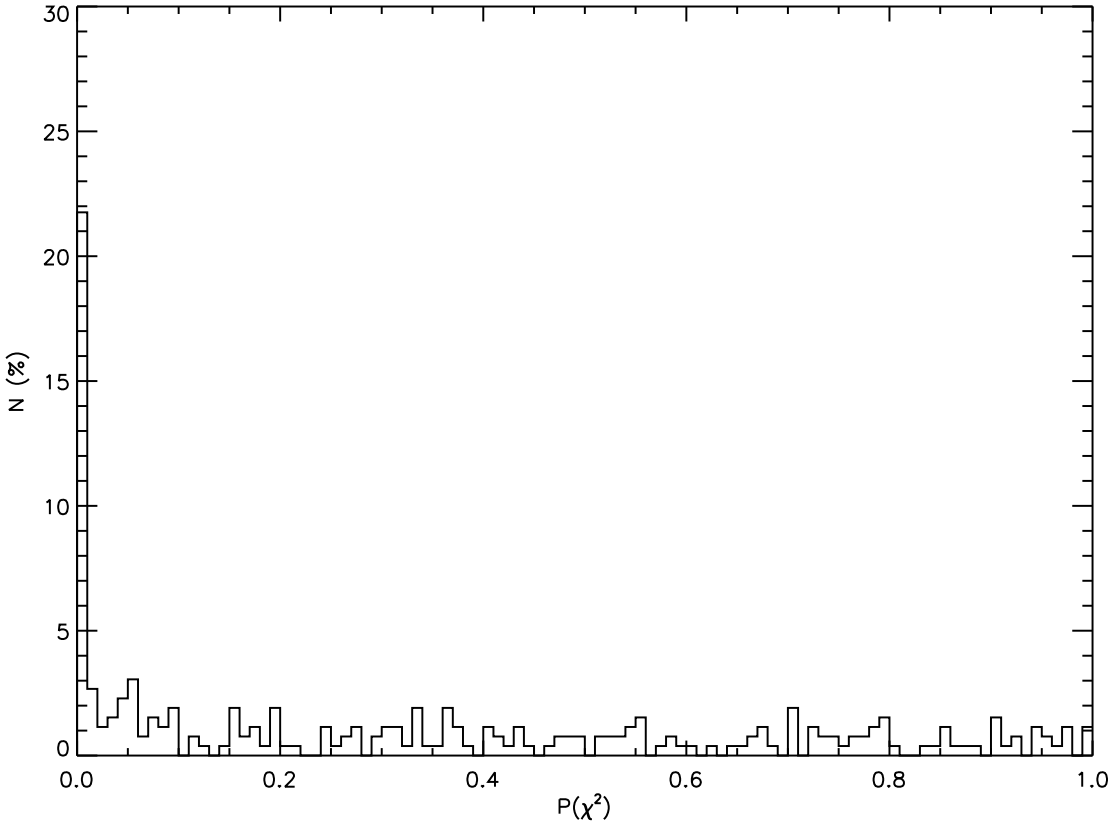

FIGURE 6.3: $P(\chi^2)$ distribution for constant radial velocity stars from CfA measurements.

to within a few $\mathrm{m\,s^{-1}}$ and clearly show many of the low $P(\chi^2)$ stars to be of stable velocities. Figure 6.4 clearly shows the correlation between $P(\chi^2)$ and the number of observations. While only 4% of stars with fewer than 10 observations have $P(\chi^2) < 0.01$, 50% of the stars with greater than 10 observations and almost 80% of the stars with greater than 100 observations satisfy this criterion. To explore this further, let's look at the set of stars with greater than 10 observations and see if the subset with $P(\chi^2) < 0.01$ and $P(\chi^2) > 0.01$ differ in their external or internal error distributions as shown in Figure 6.5. First, note that the 11 points with the lowest values of external error belong exclusively to the high $P(\chi^2)$

subset, which follows from the fact that a low external error implies a low χ^2 and hence a high $P(\chi^2)$. In fact each of these has $P(\chi^2) > 0.15$. More importantly, the figure clearly shows that the low $P(\chi^2)$ subset has internal errors fairly well constrained between 0.3 and 0.5 $\mathrm{km\,s^{-1}}$, while the high $P(\chi^2)$ subset shows a greater excursion in internal errors. If one were to fit lines to the two distributions, the circles will be best fit by a flat line while the triangles will be fit with a line that has a significant positive slope. This is a direct result of the the fact that when internal and external errors are both high, the χ^2 value is reduced and hence the P(χ^2) value increases. This emphasizes that an accurate estimate of the floor error and a Gaussian distribution of the internal errors are essential in arriving at a reliable $P(\chi^2)$ value (D. Latham 2009, private communication), which apparently gets trickier as the number of observations increases. In any case, the large overlap between the two subsets for external error under 0.7 $\mathrm{km\,s^{-1}}$ illustrates the point that the cutoff of $P(\chi^2) < 0.01$ does not necessarily imply velocity variability. So, it does appear that $P(\chi^2)$ is not a good measure when the number of observations is large. A visual inspection of the velocity and power spectrum plots as followed in this work, is a better approach in these cases. This has implications on the incompleteness analysis of DM91, and I will return to this issue in § 8.2.

For stars with few observations, a $P(\chi^2) < 0.001$ can indicate evidence of variability, suggesting follow-up observations (D. Latham 2009, private communication). Three stars in Figure 6.4 satisfy these criteria – HD 125455, 162004, and 186427, each of which has one outlying measure by about 2 $\mathrm{km\,s^{-1}}$ that seems to be responsible for the low $P(\chi^2)$. HD 125455 has one outlier among 9 CfA observations, but Nidever et al. (2002) shows it to

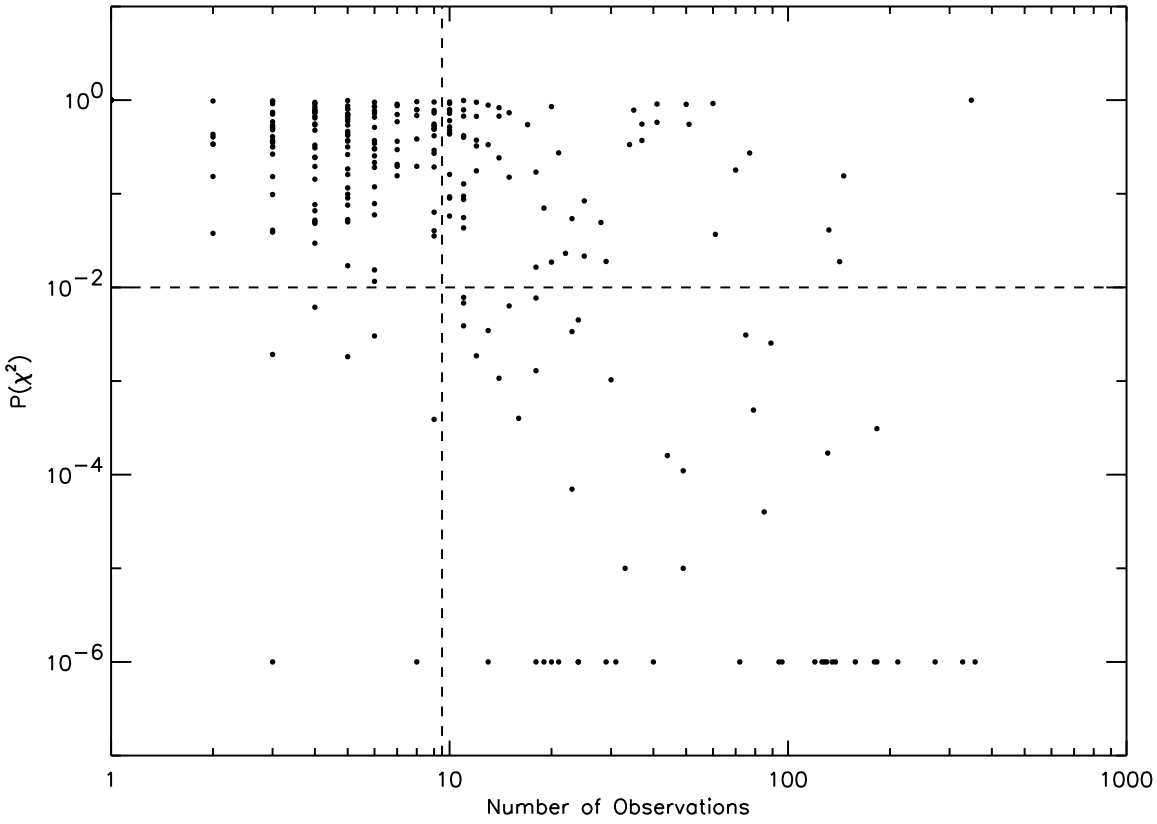

FIGURE 6.4: $P(\chi^2)$ distribution for constant velocity stars from the CfA measurements as a function of the number of observations. Stars with zero $P(\chi^2)$ values down to the precision limit of the calculations are plotted one order of magnitude below that precision limit, i.e. 0.000001. The horizontal dashed line marks the $P(\chi^2)$ value of 0.01, and the vertical dashed line delineates stars with 10 or more observations from stars with fewer observations.

be of stable radial velocity over almost 4 years with a velocity that is consistent with the remaining CfA measures. HD 162044 is discussed above in this section and is also likely of stable radial velocity. HD 186427 is the planet host 16 Cyg B, and shows no evidence of longterm variability beyond the reported planet, and is reported in Nidever et al. (2002) as a scatter less than 0.1 $\mathrm{km\,s^{-1}}$ over 7 years of coverage. So, upon a closer inspection, these three candidates with low $P(\chi^2)$ and few observations also appear to be constant velocity

stars.

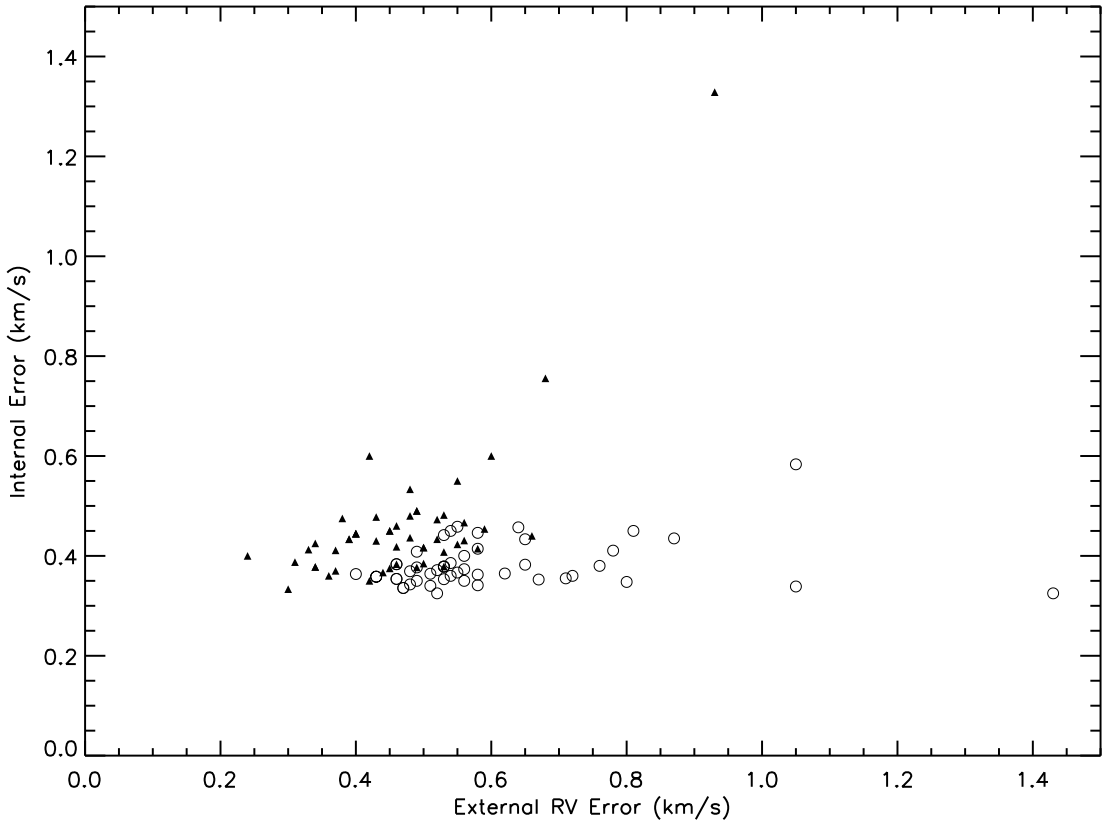

FIGURE 6.5: External and internal error distributions for constant velocity stars with more than. Open circles are for stars with $P(\chi^2) < 0.01$ and filled triangles are for stars with $P(\chi^2) \geq 0.01$.

6.2 Stellar Companions

6.2.1 Single-lined Spectroscopic Binaries

Table 6.2 lists the 48 stars of the sample that have a single-lined spectroscopic orbit. Each star is listed on two lines with the first line specifying the orbital parameters, below which are listed their corresponding errors. The first column lists the HD name, with a suffix when

needed, of the primary of the orbit. The next eight columns specify the parameters from the spectroscopic orbital solution, namely the period in days, the systemic radial velocity in $\mathrm{km\,s^{-1}}$, the velocity semiamplitude of the primary in $\mathrm{km\,s^{-1}}$, the eccentricity, angle of periastron in degrees, the epoch of periastron as HJD-2400000, the $a \sin i$ of the primary in gigameters, and the mass function in solar-mass units. Columns 10–12 specify the number of observations, their time-span in days, and the rms of the fit in $\mathrm{km\,s^{-1}}$. Listed below the time span is the number of orbital cycles it represents. Column 13 lists the grade of the corresponding visual orbit, if one exists, as described in § 5.2. Columns 14–16 list the orbital inclination in degrees and the primary and secondary stars' masses, in solar units, if available. Column 17 lists the reference for the spectroscopic orbit on the first line and the reference for the visual orbit, if available and different from the spectroscopic orbit, on the second line. Reference codes are expanded at the bottom of the table, except for visual orbit references, which are the same as in Table 5.4.

The table includes two new companion discoveries by the CfA surveys corresponding to the orbits of HD 185414 and 224465, two new spectroscopic orbits from the CfA surveys for *Hipparcos* photocentric motion orbits (HD 32850 and 128642) and one new preliminary spectroscopic orbit for HD 22409 that likely corresponds to a *Hipparcos* double star resolution (H59 flag = 'C'). An additional eight systems have the reference listed as "CfA", and for these the orbital solutions presented here from the CfA measurements are improvements over published solutions. The radial velocities and orbital solutions for these 13 binaries are presented in Figures 6.6–6.12. Because accurate parallaxes are available from FvL07 for all

stars of this study, component masses can be estimated when the spectroscopic orbit has a corresponding visual orbit for resolved components. This is done by using the parallax and the visual orbit's angular semi-major axis to estimate the linear semimajor axis, then using the period from either solution and Newton's generalization of Kepler's Third Law to estimate the mass-sum. Then, the spectroscopic orbit's mass function along with inclination of the visual orbit lead to the component masses. Masses were determined in this manner only for HD 6582 and 10307, and these values are included in the table along with corresponding uncertainties. The other visual orbits were either for photocentric motions or were so poorly constrained that meaningful masses could not be estimated.

TABLE 6.2: Single-lined Spectroscopic Binary Orbits

HD Name	P (d)	γ (km s^{-1})	K (km s^{-1})	e	ω (deg)	T_0 HJD-2400000	$a_A \sin i$ (Gm)	f(M)	N	ΔT(d) cycl	rms (km s^{-1})	V	i (deg)	M_1 ($M_\odot$)	M_2 ($M_\odot$)	Ref
000123B	47.685	−11.70	10.2	0.610	290	49891.50	5.31	0.0026	71	29328.8	0.57	...	...	...	...	Gri1999
	0.003	0.19	0.5	0.024	4	0.22	0.27	0.0004	...	615.1	...	...	...	...	...	...
001273	411.449	−14.32	13.88	0.567	4.68	34233.31	64.7	0.0639	28	4505.8	1.83	9	74.7	...	...	Bop1970
	0.076	0.08	0.10	0.004	0.79	0.77	...	...	...	11.0	...	...	2.1	...	...	Jnc2005
003196A	2.082	11.23	43.98	0.0	0.0	43400.45	1.26	0.01844	46	3732.9	2.65	...	...	...	...	Duq1991b
	0.000	...	0.39	fixed	fixed	0.00	0.01	0.00046	...	1792.9	...	...	...	...	...	...
004747	6832	9.97	0.65	0.64	257	50453	1000[a]	0.00009	21	1731.2	0.00	...	...	0.83	0.04[b]	Nid2002
	653	0.3	0.1	0.06	5	473	...	...	...	0.3	...	...	...	...	...	...
006582A	7827	−98.10	2.68	0.61	147.9	42694	228	0.0078	31	4379.0	0.44	4	106.8	0.74	0.20	Duq1991b
	fixed	0.09	0.18	fixed	4.8	fixed	15	0.0015	...	0.5	...	...	0.9	0.06	0.02	Dru1995
010307	7383	3.34	2.58	0.441	214.77	58037	234.9	0.00947	56	8157.9	0.51	4	105	0.81	0.25	CfA
	653	0.13	0.13	0.053	5.92	667	13.4	0.00169	...	1.1	...	...	...	0.40	0.07	Sod1999
014214	93.290	25.72	19.28	0.543	104.04	53338.33	21.05	0.04279	281	1094.8	0.08	9	110.0	1.15	0.53	Fek2007
	0.001	0.01	0.01	0.000	0.05	0.01	0.01	0.00006	...	11.7	...	...	8.4	...	...	...
016287	14.838	22.10	10.53	0.216	11.3	47103.16	2.10	0.00168	36	5427.2	...	...	...	...	...	Imb2006
	0.000	0.06	0.10	0.009	2.2	0.09	0.02	0.00005	...	365.8	...	...	...	...	...	...
017382A	5575.8	9.14	2.89	0.688	114.4	48041.6	161.0	0.00535	92	7153.7	0.58	9	84	...	...	CfA
	61.1	0.07	0.17	0.034	4.6	67.1	11.6	0.00100	...	1.3	...	...	...	...	...	Hei1990d
024409	12625	−18.05	4.19	0.554	258.5	53916.9	605.5	0.0555	40	5396.1	0.44	...	...	...	...	CfA
	5700	1.27	0.68	0.067	15.1	123.9	103.8	0.0373	...	0.5	...	...	...	...	...	...
026491	7008	...	2.67	0.51	215	50475	1143	...	8	1879.8	0.00	...	...	...	...	Jon2008
	798	...	0.30	0.02	5	54	283	...	...	0.3	...	...	...	...	...	...
032850	205.684	23.70	10.42	0.324	256.27	49985.20	27.89	0.0204	17	4334.1	0.41	9	29.4	...	...	CfA
	0.084	0.12	0.19	0.018	3.10	1.49	0.54	0.0011	...	21.1	...	...	35.8	...	...	*Hipparcos*
039587	5136	−13.47	1.85	0.45	111	51463	883[a]	0.0024	38	4579.7	0.03	9	95.9	0.89	0.14[b]	Nid2002
	12	0.3	0.02	0.01	1	17	...	...	...	0.9	...	...	0.8	...	...	HaI2002
043587A	12325	...	4.32	0.80	75	50832	1735[a]	...	14	1637.6	0.01	...	...	1.0	0.34[b]	Vog2002
	500	...	0.01	0.01	1	1	...	...	...	0.1	...	...	...	...	...	...
054371	32.807	19.65	25.05	0.054	48.62	51151.93	11.28	0.0532	11	5909.1	0.24	...	...	...	...	CfA
	0.000	0.14	0.20	0.007	4.61	0.43	0.09	0.0013	...	180.1	...	...	...	...	...	...
064468	161.2	...	5.73	0.262	328.1	50457.0	11.2[a]	...	13	1540.9	0.02	...	...	0.78	0.13[b]	Vog2002
	0.1	...	0.01	0.002	0.2	0.2	...	...	...	9.6	...	...	...	...	...	...
064606	450.4	102.22	5.91	0.344	220.8	47029.9	34.4	0.00798	26	5025.3	0.57	...	...	...	...	Lat2002
	4.3	0.18	0.24	0.031	5.7	8.8	1.4	0.00097	...	11.2	...	...	...	...	...	...
065430	3138	−28.43	1.11	0.32	77	3267	598[a]	0.00038	26	1846.0	0.01	...	...	0.78	0.07[b]	Nid2002
	342	0.3	0.2	0.02	1	302	...	...	...	0.6	...	...	...	...	...	...
068257C	6302	−7.93	4.28	0.119	307	44696	368	0.050	103	7810	0.40	5	142	...	...	Gri2000
	59	0.08	0.12	0.018	8	135	13	0.005	...	1.2	...	...	...	...	...	Hei1996b
075767A	10.248	5.96	23.59	0.0	...	47212.16	3.32	0.01396	97	24448.6	...	...	...	...	...	Gri1991
	0.000	0.07	0.09	...	...	0.01	0.01	0.00017	...	2387.6	...	...	...	...	...	...
079028	16.239	−14.91	35.31	0.102	137.7	53010.32	7.844	0.0729	13	1431.1	0.41	...	...	...	...	CfA
	0.000	0.15	0.19	0.006	3.4	0.16	0.043	0.0012	...	88.1	...	...	...	...	...	...
098230A	670.24	...	8.95	0.532	314.1	47389.1	69.8	0.0303	46	3812.7	0.43	9	91	...	...	Gri1998
	0.09	...	0.12	0.008	2.1	2.2	1.0	0.0013	...	5.7	...	...	...	...	...	Hei1996b
098230B	3.981	...	4.83	0.0	...	42441.42	0.26	0.00005	45	3812.7	0.62	...	...	...	...	Gri1998
	0.000	...	0.14	...	...	0.02	0.01	0.00000	...	958.0	...	...	...	...	...	...
101206	12.920	12.67	27.75	0.010	315.5	49159.98	4.93	0.0286	43	633.2	0.42	...	...	...	...	CfA
	0.001	0.07	0.09	0.003	19.4	0.70	0.02	0.0003	...	49.0	...	...	...	...	...	...
110833	271.165	...	...	0.784	264.43	50607.41	2.48	...	...	...	...	9	48.9	0.72	0.14	Hal2000
	0.472	...	...	0.010	1.31	1.26	0.07	...	...	...	...	...	10.2	...	0.01	*Hipparcos*
112758A[c]	103.171	4.20	1.92	0.116	59.3	51142.35	2.70	0.00007	7	4429.8	0.05	...	...	0.79	0.20	CfA
	0.026	0.03	0.04	0.032	29.5	7.83	0.05	0.00000	...	42.9	...	...	...	...	...	Hal2003
112914	710.6	27.51	5.61	0.326	65.0	49220	51.91	0.0110	88	11785.8	0.39	9	81.8	...	...	Gri2002b
	0.4	0.05	0.08	0.013	2.5	4	0.75	0.0005	...	16.6	...	...	5.0	...	...	Jnc2005
120690	3762	5.93	4.15	0.20	161	55176	210.3	0.02626	21	1187	...	...	...	...	...	Abt2006
	12	0.15	0.39	0.05	8	84	...	...	...	0.3	...	...	...	...	...	...
121370	489.74	−0.62	7.87	0.327	323.22	52350.0	50.08	0.0209	12	1387.1	0.48	9	115.7	...	...	CfA
	3.30	0.15	0.22	0.023	5.08	5.6	1.46	0.0018	...	2.8	...	...	1.6	...	...	Jnc2005
122742	3617	−11.20	6.41	0.480	183.0	52030	792.9[a]	0.0670	24	3545.2	0.02	9	93.5	0.96	0.52[b]	Nid2002

Continued on Next Page...

TABLE 6.2 – Continued

HD Name	P (d)	γ (km s^{-1})	K (km s^{-1})	e	ω (deg)	T_0 HJD-2400000	$a_A \sin i$ (Gm)	f(M)	N	ΔT(d) cycl	rms (km s^{-1})	V	i (deg)	M_1 ($M_\odot$)	M_2 ($M_\odot$)	Ref
	7	0.3	0.01	0.001	0.1	3	...	...	...	1.0	...	...	...	...	...	*Hipparcos*
128642	178.780	−39.12	13.46	0.171	91.74	51366.54	32.60	0.0432	23	4491.8	0.58	9	54.8	...	...	CfA
	0.031	0.13	0.21	0.016	4.07	1.86	0.51	0.0020	...	25.1	...	...	5.2	...	...	*Hipparcos*
131511	125.396	−31.27	19.10	0.510	219.0	50203.41	77.79[a]	0.0580	20	2866.1	0.03	9	93.4	0.78	0.43[b]	Nid2002
	0.001	0.3	0.01	0.001	0.1	0.00	...	...	...	22.9	...	...	4.2	...	...	Jnc2005
131923	5431	...	4.91	0.64	304	50512	1028	...	9	1917	...	...	...	...	...	Jon2008
	1025	...	0.67	0.06	7	38	387	...	...	0.4	...	...	...	...	...	...
142267	138.562	34.89	6.86	0.561	264.86	51782.99	10.81	0.00262	14	4791.0	0.40	...	...	...	...	CfA
	0.068	0.14	0.31	0.034	4.19	1.28	0.58	0.00038	...	34.6	...	...	...	...	...	...
144287	4450.8	−48.17	5.30	0.683	18.8	47679.7	237.1	0.0269	68	4602.6	0.30	...	...	...	0.32[d]	Duq1991b
	6.8	0.04	0.07	0.007	1.0	5.4	5.8	0.0019	...	1.0	...	...	...	...	...	...
145825	2609	...	0.58	0.21	86	50718	568	...	12	1796	...	...	...	...	...	Jon2008
	379	...	0.04	0.04	16	36	145	...	...	0.7	...	...	...	...	...	...
147584	12.977	6.39	7.50	0.014	252.98	52752.32	...	...	228	156.1	...	9	16.0	1.12	0.09-0.45	Sku2004
	0.000	0.01	0.00	0.000	0.80	0.00	...	...	...	12.0	...	...	2.5	...	...	Jnc2005
156274	88.033	...	16.26	0.81	306.9	51628.33	58.34	...	11	496.7	...	...	...	...	...	Jon2008
	0.001	...	0.01	0.00	0.1	0.00	4.49	...	...	5.6	...	...	...	...	...	...
160269A	27087	−16.30	3.84	0.019	126.4	33184	1405	0.151	12	2813.6	0.27	3	104	1.00	0.82	Duq1991b
	fixed	fixed	0.41	fixed	4.2	fixed	150	0.048	...	0.1	...	...	...	...	...	Sod1999
160346	83.728	21.19	5.7	0.226	140.5	47724.9	...	0.00135	35	4535.3	0.42	9	...	...	0.09[d]	Tok1991
	0.037	0.08	0.1	0.021	4.9	1.2	...	0.00011	...	54.2	...	...	...	...	...	...
161198	2558.4	23.88	9.09	0.936	129.6	49422.53	...	0.00867	138	3196.3	0.33	5	42.8	0.78	0.32	Duq1996
	10.4	0.04	0.05	0.001	0.6	0.10	...	0.00012	...	1.2	...	...	3.7	...	...	...
175742	2.879	10.31	49.46	0.003	266.7	43675.58	1.96	0.0362	76	12826.7	...	...	...	...	...	Imb1979
	0.000	0.06	0.09	0.002	31.4	0.25	0.00	0.0002	...	4455.3	...	...	...	...	...	...
176051	22423	−45.82	3.51	0.25	102	41398	1047	0.091	16	...	0.36	2	115.1	1.00	0.71	Duq1991b
	fixed	0.69	0.74	fixed	fixed	fixed	222	0.058	...	...	...	...	...	...	...	Doc2008f
178428A	21.955	14.36	13.42	0.08	57.4	45592.23	4.04	0.00546	17	2256.8	0.28	...	...	...	...	Duq1991b
	0.001	0.08	0.12	0.01	4.9	0.29	0.04	0.00016	...	102.8	...	...	...	...	...	...
185414	4778.0	−16.70	1.65	0.670	136.84	55462.6	80.31	0.00090	47	5698.4	0.47	...	...	...	...	CfA
	1119.1	0.18	0.14	0.070	9.77	1133.6	9.73	0.00034	...	1.2	...	...	...	...	...	...
202940A	21.346	−17.19	23.98	0.251	89.48	19224.11	6.81	0.0277	22	19373.6	2.98	...	...	...	...	Bop1970
	0.001	0.11	0.15	0.007	1.34	0.12	...	...	...	907.6	...	...	...	...	...	...
224465	52.413	1.60	11.10	0.143	164.83	50600.64	7.92	0.00720	19	4136.0	0.47	...	...	...	...	CfA
	0.004	0.11	0.17	0.016	5.64	0.80	0.12	0.00033	...	78.9	...	...	...	...	...	...
224930	9610	−36.22	4.49	0.372	285.0	47738	551	0.0722	126	12519.8	0.25	2	49	...	...	Gri2004
	fixed	0.03	0.05	0.009	1.6	32	6	0.0024	...	1.3	...	...	...	...	...	Sod1999

[a] Estimated assuming a low-mass companion according to equation (2) in Butler et al. (2006). [b] $M \sin i$ estimated using equation (1) in Butler et al. (2006). [c] Halbwachs et al. (2003) reported an orbit for this star with some parameters, but the reference cited (Udry et al. 2002) was not found. The orbit presented here is a preliminary solution based on only seven CfA observations. [d] Minimum-mass estimates in the cited references.

REFERENCES.— Abt2006 = Abt & Willmarth (2006); Bop1970 = Bopp et al. (1970); CfA = D. Latham 2008 (private communication); Duq1991b = DM91; Duq1996 = Duquennoy et al. (1996); Fek2007 = Fekel et al. (2007); Gri1991 = Griffin (1991); Gri1998 = Griffin (1998); Gri1999 = Griffin (1999); Gri2000 = Griffin (2000); Gri2002b = Griffin (2002); Gri2004 = Griffin (2004); Hal2000 = Halbwachs et al. (2000); Hal2003 = Halbwachs et al. (2003); Imb1979 = Imbert (1979); Imb2006 = Imbert (2006); Lat2002 = Latham et al. (2002); Jon2008 = H. Jones 2008, (private communication); Nid2002 = Nidever et al. (2002); Sku2004 = Skuljan et al. (2004); Tok1991 = Tokovinin (1991); Vog2002 = Vogt et al. (2002).

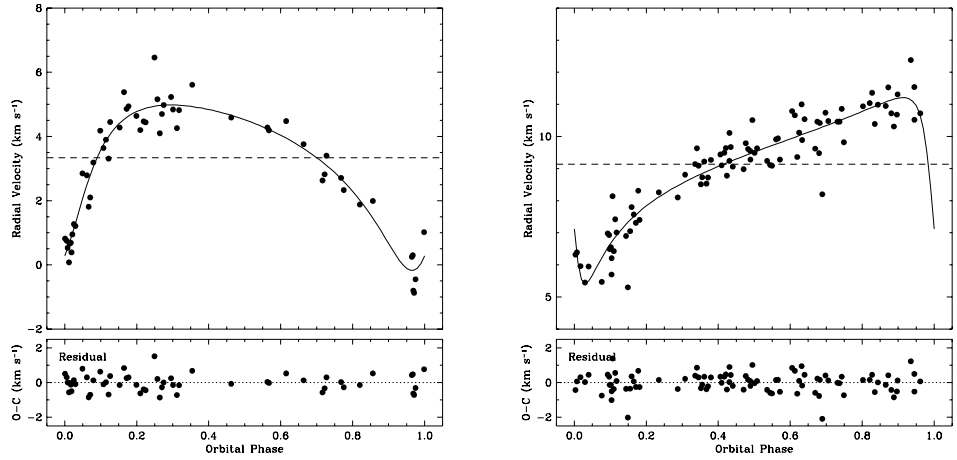

FIGURE 6.6: Single-lined spectroscopic orbits of HD 10307 (left) and HD 17382 (right)

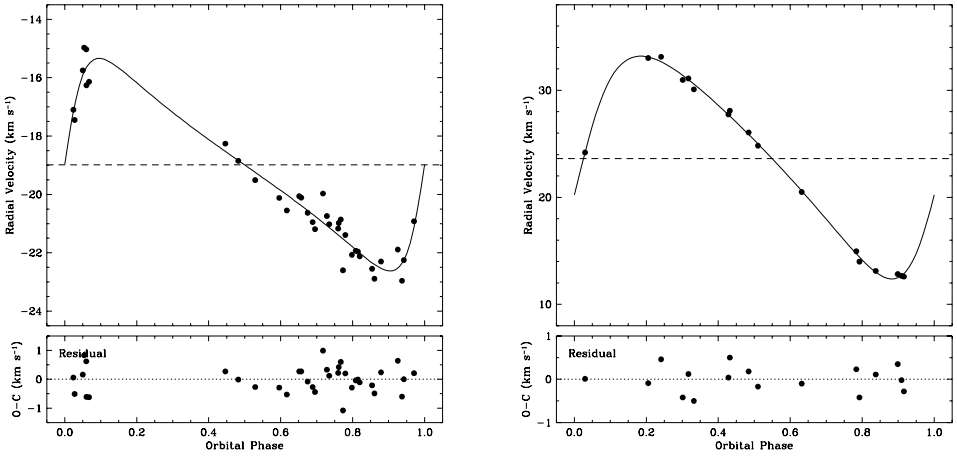

FIGURE 6.7: Single-lined spectroscopic orbits of HD 24409 (left) and HD 32850 (right)

6.2.2 Double-lined Spectroscopic Binaries

Table 6.3 lists the 26 double-lined spectroscopic binary solutions for the stars of this sample. Additionally, Fuhrmann et al. (2005) identified HD 75767B itself as a double-lined binary by resolving pairs of lines in their spectra (see§ 7.4), but they do not have enough observations or

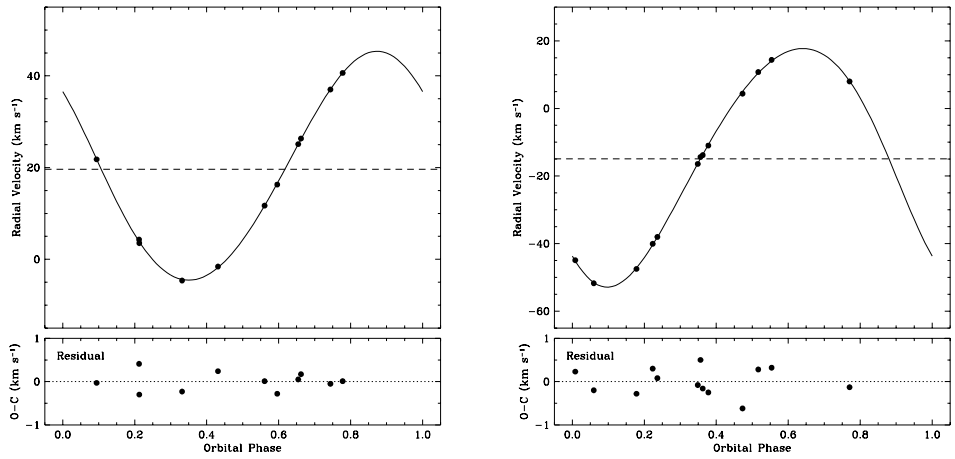

FIGURE 6.8: Single-lined spectroscopic orbits of HD 54371 (left) and HD 79028 (right)

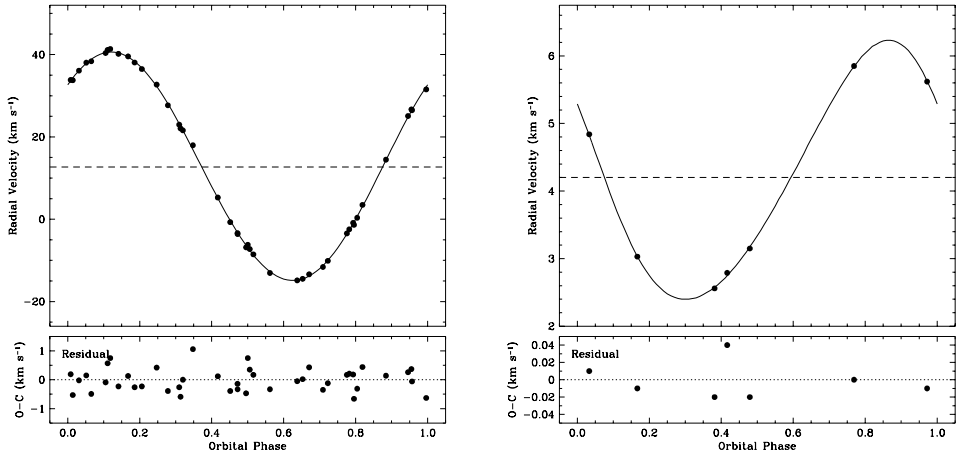

FIGURE 6.9: Single-lined spectroscopic orbits of HD 101206 (left) and HD 112758A (right)

radial velocity measurements to derive an orbit, so it is not listed in the table. The table lists each star on two lines, the first line contains orbital and physical parameters, and the second line lists the corresponding uncertainties. The first column identifies the spectroscopic pair by its HD number and, when required, its component designation. Columns 2–10 list the spectroscopic parameters, namely, period in years (y) or days (d), systemic velocity in $\mathrm{km\,s^{-1}}$,

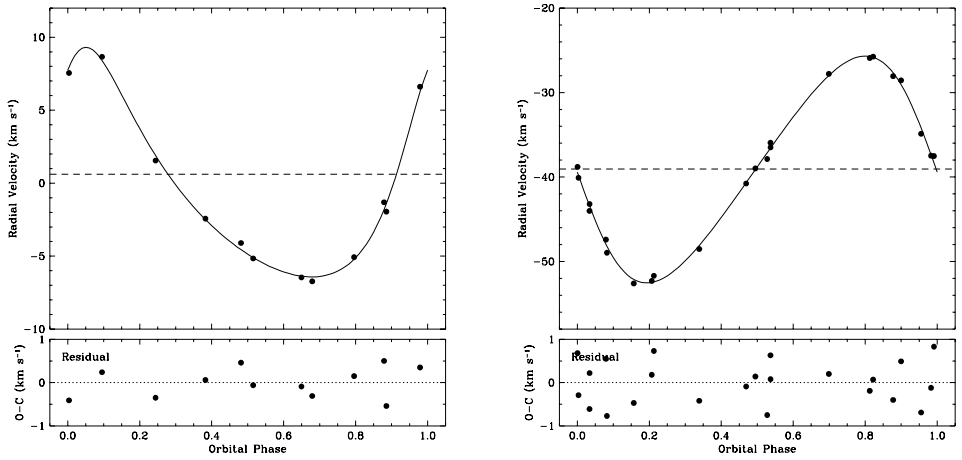

FIGURE 6.10: Single-lined spectroscopic orbits of HD 121370 (left) and HD 128642 (right)

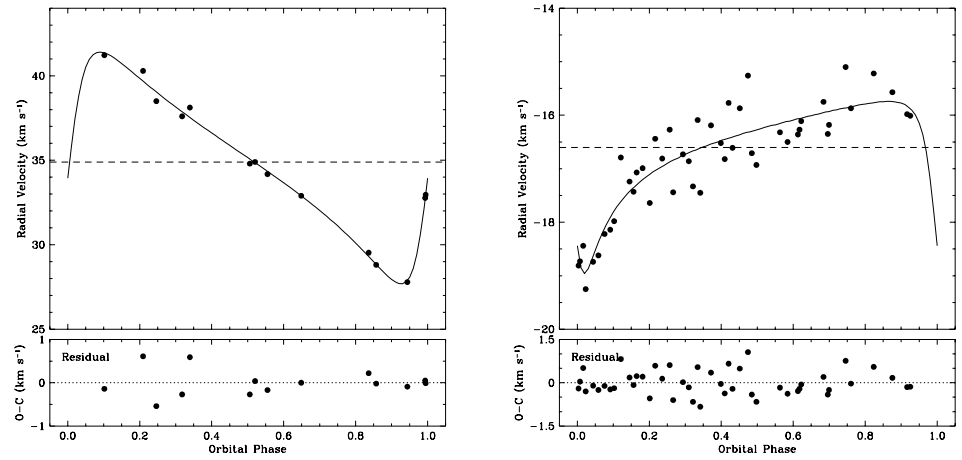

FIGURE 6.11: Single-lined spectroscopic orbits of HD 142267 (left) and HD 185414 (right)

the primary and secondary semiamplitudes in $\mathrm{km\,s^{-1}}$, mass ratio, eccentricity, angle and epoch of periastron in degrees and HJD-2400000 respectively, and $a \sin i = (a_1 + a_2) \sin i$ in gigameters. Column 11 lists the number of velocity measures for the primary and secondary on the first line, and their time span in days below it. The next column lists the residuals for the primary and secondary from the orbital fit in $\mathrm{km\,s^{-1}}$. Column 13 lists the grade of

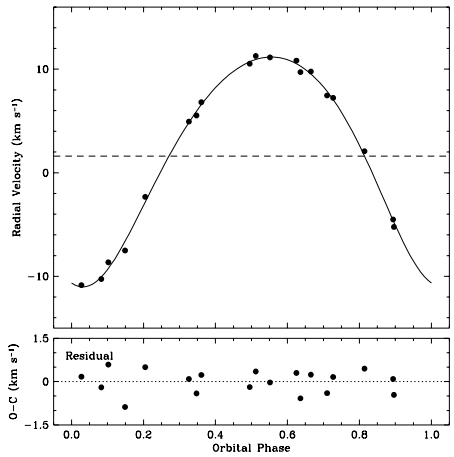

FIGURE 6.12: Single-lined spectroscopic orbits of HD 224465

the visual orbit, if one exists, as described in § 5.2, following which appear the inclination in degrees and the longitude of the ascending node in degrees, from the visual-orbit solution or a joint spectroscopic-visual solution. The next two columns list the component masses, again from a joint or the visual orbit solution. The last column lists the reference for the spectroscopic or joint solution on the first line, and the reference for the visual orbit below it, if different. Reference codes are expanded at the bottom of the table, except for visual orbit references, which are the same as in Table 5.4. Parameters are preferentially listed from joint solutions over isolated spectroscopic and visual results.

TABLE 6.3: Double-lined Spectroscopic Binary Orbits

HD Name	P (d)	γ	K_1 (km s^{-1})	K_2	q	e	ω (deg)	T_0 HJD-24e5	asin i (Gm)	N_1/N_2 ΔT (d)	σ_1 σ_2 (km s^{-1})	V	i (deg)	Ω (deg)	M_1 ($M_\odot$)	M_2 ($M_\odot$)	Ref
003196AB	2527.165	8.83	10.90	16.44	0.66	0.77	109.0	46864.8	606.4	46/46	0.7	1	49.4	149.	1.53	1.00	Duq1991b
	fixed	0.22	0.59	0.43	0.04	fixed	3.1	3.9	16.1	3733	...	...	...	...	...	...	Msn2005
003443	9164.123	18.4	5.13	6.93	0.72	0.235	317	14482.7	1511.9	25/25	1.0	1	77.6	291.8	0.94	0.70	Pou2000
	10.958	0.1	0.29	0.22	0.05	0.010	3	60.2	52.8	7019	0.8	...	0.3	0.5	0.09	0.08	...
004676	13.825	...	57.35	59.95	...	0.238	203.6	50906.4	22.6	...	...	8	73.8	63.6	1.22	1.17	Bod1999
	0.000	...	0.31	0.32	...	0.001	0.4	0.0	0.3	...	...	...	0.9	0.8	0.02	0.02	...
008997	10.984	21.26	39.08	47.35	0.825	0.037	179.2	49085.1	13.1	25/25	0.4	...	...	...	...	...	CfA
	0.000	0.08	0.12	0.45	0.009	0.003	5.1	0.2	0.1	744	1.4	...	...	...	...	...	...
013974	10.020	−6.42	9.99	14.89	0.671	0.034	336	50772.8	3.4	29/29	0.6	1	167.	15.	...	...	CfA
	0.000	0.11	0.17	0.34	0.020	0.014	23	0.6	0.1	2985	1.3	...	3.	9.	...	...	MkT1999
016739	330.991	−23.03	20.91	23.73	0.881	0.663	89.9	52765.1	152.1	89/87	1.2	8	128.2	269.3	1.38	1.24	Pou2000
	0.004	0.04	0.09	0.09	0.005	0.002	0.3	0.1	0.5	35142	1.9	...	0.1	...	0.02	0.02	Bag2006
045088	6.992	−8.50	56.76	66.48	0.854	0.146	78.9	52480.9	11.7	20/20	0.5	8	108.0	125.0	0.83	0.71	CfA
	0.000	0.10	0.20	0.27	0.005	0.003	1.0	0.0	0.0	6159	0.8	...	3.0	4.0	0.10	0.08	§ 3.2.3
064096	8291.175	−21.3	9.12	9.69	0.92	0.741	73.1	46400.1	1452.6	26/18	2.3	2	80.4	102.9	0.93	0.9	Pou2000
	10.958	0.2	0.63	0.26	0.04	0.007	0.4	7.4	63.3	25282	0.7	...	0.2	0.3	0.08	0.1	...
079096A	988.001	49.82	11.49	12.13	0.96	0.433	350.7	45222.0	349.5	104/103	0.8	1	124.1	317.6	0.89	0.85	Pou2000
	0.365	0.08	0.11	0.14	0.02	0.003	0.8	1.5	4.8	5412	1.1	...	0.6	0.5	0.03	0.03	...
080715	3.804	−4.23	71.04	71.31	0.996	0.000	339	49191	7.5	36/36	0.7	...	...	...	...	...	CfA
	0.000	0.08	0.16	0.15	0.003	0.002	339	93	0.0	688	0.6	...	...	...	...	...	...
101177B	23.542	−18.71	24.41	50.5	0.48	0.402	354.0	46998.2	...	32/3	2.2	...	...	...	...	...	Maz1997
	0.001	0.18	0.15	2.7	0.03	0.007	0.8	0.1	...	...	2.3	...	...	...	...	...	...
111312	978.5	−2.88	10.60	13.28	0.798	0.502	148.5	52687.8	277.9	23/23	0.5	...	...	...	...	...	CfA
	2.0	0.10	0.18	0.63	0.042	0.011	1.7	2.6	8.0	2511	2.0	...	...	...	...	...	...
128620AB	29183.48	−21.87	4.6	5.5	0.82	0.519	231.8	35330.0	3570.5	283/152	1.1	2	79.2	204.8	1.16	0.97	Pou1999
	3.65	0.05	0.1	0.1	0.04	0.001	0.2	6.9	13.8	31946	1.2	...	0.1	0.1	0.03	0.03	...
133640B	0.27	−17.89	231.31	112.70	0.49	0.0	...	50944.7	...	65/63	5.5	...	...	...	0.37	0.76	Lu2001
	...	0.40	0.65	0.46	0.01	...	...	0.0	...	10	3.3	...	...	...	0.00	0.01	...
137763	889.62	6.82	37.14	55.50	0.669	0.975	253.9	47967.5	251.8	97/10	0.3	...	...	...	...	...	Duq1992
	0.12	0.04	0.12	0.43	0.006	0.000	0.3	0.0	1.2	4402	2.0	...	...	...	...	...	...
137107AB	15190.75	−7.41	4.71	5.28	0.89	0.277	219.2	12214.2	2343.5	31/31	0.3	1	58.7	22.9	1.19	1.05	Pou2000
	3.65	0.05	0.10	0.14	0.03	0.001	0.4	11.0	42.4	7614	0.6	...	0.2	0.2	0.07	0.05	...
144284	3.071	−8.23	25.10	66.0	0.380	0.039	63	45972.0	...	4/4	1.7	...	...	...	1.2	0.46	Maz2002
	0.000	0.20	0.31	2.2	0.013	0.012	15	0.1	...	...	2.7	...	...	...	0.1	0.04	...
146361A	1.140	−13.03	61.25	63.89	0.959	0.0	...	50127.6	4.2	46/46	1.0	8	28.1	207.9	1.14	1.09	Rag2009
	0.000	0.11	0.21	0.22	0.005	...	...	0.0	0.0	2610	1.1	...	0.3	0.7	0.04	0.04	...
148704	31.865	−50.94	31.28	32.95	0.949	0.165	167.1	53644.2	27.8	11/11	0.3	...	...	...	...	...	CfA
	0.003	0.12	0.15	0.24	0.010	0.006	1.4	0.1	0.2	980	0.6	...	...	...	...	...	...
158614	16925.69	−77.18	4.93	5.32	0.93	0.168	148	37898.0	2396.1	29/29	0.4	1	99.1	332.3	0.98	0.90	Pou2000
	7.31	0.07	0.11	0.12	0.03	0.003	1	56.7	40.1	9146	0.6	...	0.1	0.1	0.05	0.05	...
165341	44253.69	−6.87	3.66	4.19	0.85	0.499	14.0	13539.3	3529.9	91/5	0.6	1	121.2	302.1	0.90	0.78	Pou2000
	29.22	0.08	0.08	0.16	0.04	0.000	0.1	6.0	76.9	34050	0.5	...	0.1	0.1	0.07	0.04	...
184467	494.183	11.31	9.56	10.27	0.93	0.360	356	46164.9	218.1	36/36	0.6	1	144	243	0.8	0.8	Pou2000
	0.365	0.10	0.14	0.15	0.02	0.008	2	1.7	15.6	4016	0.7	...	2	2	0.2	0.1	...
189340[a]	1787.899	30.02	4.69	4.64	0.99	0.592	142	45265	184.5	25/25	0.4	2	...	147	...	...	Pou2000
	1.826	0.09	0.13	0.28	0.07	0.009	4	11	6.2	5136	0.9	...	...	3	...	...	...
195987	57.322	−5.87	28.94	36.73	0.79	0.306	357.4	49404.8	49.9	73/73	0.3	8	99.4	335.0	0.84	0.67	Tor2002
	0.000	0.04	0.05	0.21	0.01	0.001	0.3	0.0	0.3	6458	1.3	...	0.1	0.1	0.02	0.01	...
202275	2083.021	−15.85	11.73	12.52	0.94	0.440	8	44778	631.0	46/46	0.7	1	99.0	203.8	1.19	1.12	Pou2000
	2.557	0.07	0.15	0.15	0.02	0.005	1	4	9.1	5562	0.7	...	0.4	0.3	0.03	0.03	...
223778	7.754	4.80	46.54	48.91	0.951	0.016	279	52232.3	10.2	18/18	0.5	8	50.2	126.8	0.79	0.75	CfA
	0.001	0.10	0.18	0.24	0.006	0.004	11	0.2	0.0	198	0.7	...	0.4	1.3	0.01	0.01	§ 3.2.4

[a] Pourbaix (2000) notes that a meaningful inclination or component masses could not be derived because of the very large correlation between inclination and parallax. At my request, he took another look at this system adopting FvL07parallaxes, but still could not constrain the mass estimates to be useful (D. Pourbaix, 2008, private communication). Apparently this system needs more observations to derive useful physical parameters.

REFERENCES.— Bag2006 = Bagnuolo et al. (2006); Bod1999 = Boden et al. (1999); CfA = D. Latham 2008 (private communication); Duq1991b = Duquennoy & Mayor (1991); Duq1992 = Duquennoy et al. (1992); Lu2001 = Lu et al. (2001); Maz1997 = Mazeh et al. (1997); Maz2002 = Mazeh et al. (2002); Pou1999 = Pourbaix et al. (1999); Pou2000 = Pourbaix (2000); Rag2009 = Raghavan et al. (2009); Tor2002 = Torres et al. (2002).

The table includes seven orbital solutions from the CfA results presented here, including five improved solutions, one new orbit for a new companion detection (HD 111312), and one double-lined solution for a previous SB1 pair (HD 148704). The velocities along with the orbital fit and residuals for each of these are shown in Figures 6.13–6.16. Most entries in Table 6.3 have mass estimates from the references. In cases where mass estimates do not exist, one can determine them using the separate spectroscopic and visual solutions, specifically, $M_{1,2} \sin i^3$ from spectroscopy and the inclination from the visual solution. However, this method resulted in uncertainties too large to be astrophysically useful. A better estimate of the companion's mass can be derived using the mass ratio and primary's mass estimates from other sources, and this will be the approach used in Chapter 8.

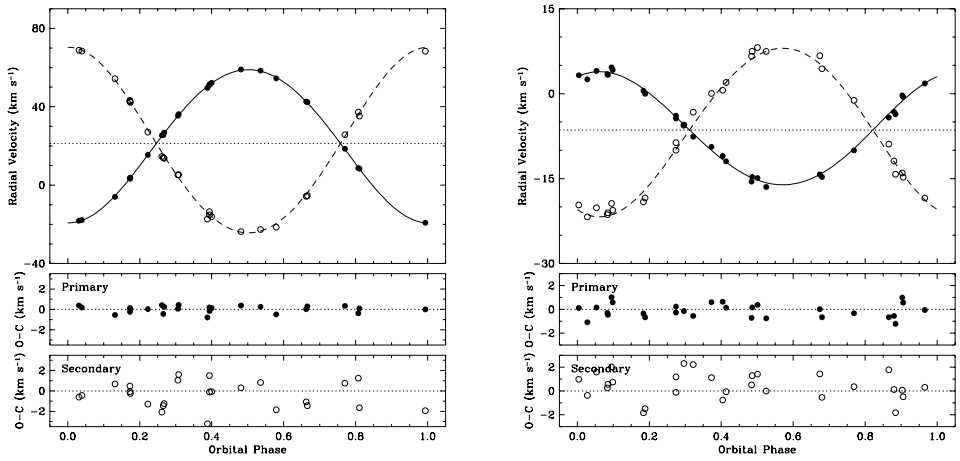

FIGURE 6.13: Double-lined spectroscopic orbits of HD 8997 (left) and HD 13974 (right)

In addition to radial velocity measurements, double-lined binaries can be identified by even a single observation if their spectrum shows the signatures of two stars. Hynek (1938) reported on the results of a comprehensive survey, presenting 566 such composite-spectrum

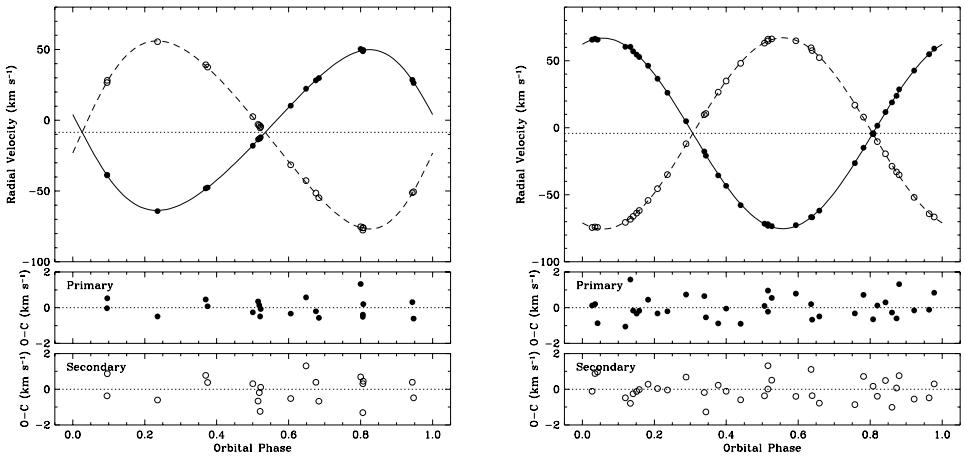

FIGURE 6.14: Double-lined spectroscopic orbits of HD 45088 (left) and HD 80715 (right)

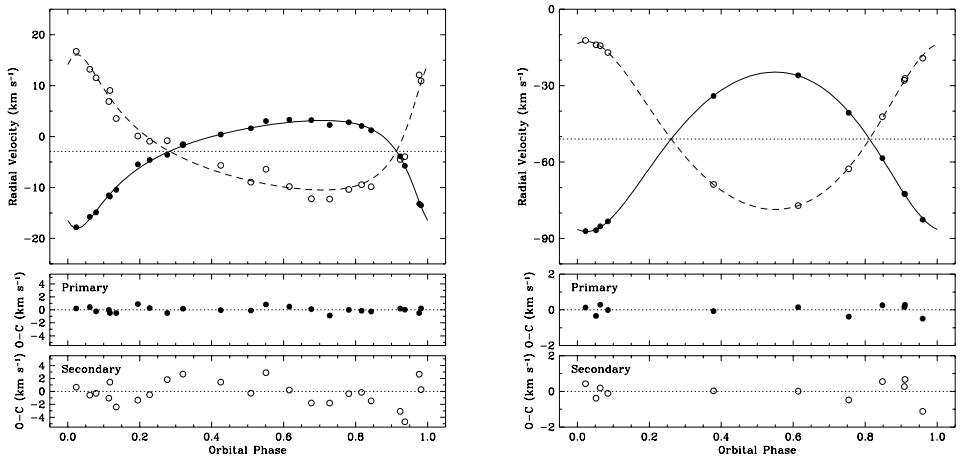

FIGURE 6.15: Double-lined spectroscopic orbits of HD 111312 (left) and HD 148704 (right)

binaries. While this compilation has proved to be a happy hunting ground for visually resolving the component stars through speckle interferometry (e.g., McAlister 1978b, 1979), only one star from the list belongs to the sample of this study. The overlapping star, HD 109358, is now recognized as one that does not show any evidence of binarity (see § 7.4).

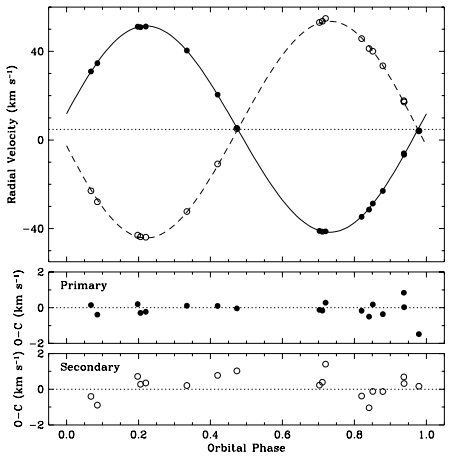

FIGURE 6.16: Double-lined spectroscopic orbits of HD 223778

6.2.3 Radial Velocity Variations Without Orbits

In some instances, radial velocities show a clear or suggestive variation consistent with a spectroscopic binary, but there are insufficient observations to develop even a preliminary orbit. Table 6.4 lists 16 such stars, eight of which, listed in the first section, show velocity variations consistent with companions known by other means as discussed in previous chapters, such as visual resolutions with evidence of orbital motion or a variation in proper motion, suggesting an unseen companion. The second section lists one star that shows convincing variations in the CfA measures indicative of a new companion, and the final section includes seven additional candidate companions, four of which suggest a linear trend over a few CfA observations, and three of which were identified in the CNS catalogs as radial velocity variables with no additional information and no independent confirmation or refutation.

TABLE 6.4: Stars with Possible RV Variations

HD Name	N	ΔT **(y)**	$\langle$**RV**$\rangle$ **(km s^{-1})**	**Ext Err (km s^{-1})**	$P(\chi^2)$	**E/I**	**Ref**
Variations corresponding to known companions							
016765	3	7.87	8.10	1.19	0.14208	1.5	CfA
043834	...	...	...	...	...	...	Egg2007
052698	6	7.12	12.03	0.75	0.00018	2.1	CfA
063077	4	3.95	102.54	1.97	0.00000	4.6	CfA
096064BC	19	4.98	16.91	1.67	0.00000	2.3	CfA
161797	134	16.92	−16.67	0.57	0.00000	1.6	CfA
186408	4	24.90	−27.15	0.85	0.00151	2.2	CfA
190771	13	27.48	−25.65	0.78	0.00000	2.1	CfA
Variations implying a new companion							
016673	6	11.23	−7.06	7.44	0.00000	18.6	CfA
Variations suggesting a possible new companion							
020010B	...	...	...	...	...	...	CNS
023484	...	...	...	...	...	...	CNS
090839B	...	...	...	...	...	...	CNS
102438	8	19.14	13.64	0.44	0.13325	1.3	CfA
110463	3	4.83	−9.43	0.73	0.06480	1.7	CfA
186858	3	16.56	4.75	0.70	0.05576	1.7	CfA
198425	4	8.08	10.46	0.78	0.07981	1.6	CfA

REFERENCES.— CfA = D. Latham 2008 (private communication); CNS = Gliese (1969); Gliese & Jahreiß (1979, 1991); Egg2007 = Eggenberger et al. (2007).

Column 1 of the table lists the HD number and component designation, when required. Columns 2 and 3 list the number of observations and their time span in years, if available.

The next two columns list the mean radial velocity and its external error in $\mathrm{km\,s^{-1}}$followed by the $P(\chi^2)$ and the external to internal error ratio from the CfA results. The last column identifies the source of the velocity variation.

6.3 Planetary Companions

In addition to the stellar companions discussed in the previous section, the spectroscopic technique is responsible for identifying a majority of the planetary companions discovered to-date. As one of the objectives of this effort is studying the correlation between stellar and planetary companions, it is essential to include a current list of planets around the stars of this study. The two online sources which maintain frequently updated results on planetary companions, the Extrasolar Planets Encyclopedia[2] and the CCPS program's website[3] aided this piece of the effort. While the former source is updated much more regularly, almost on a daily basis, it does not list the uncertainties of the parameters. I have listed the 50 planetary companions in 33 systems from the latter source in Table 6.5, downloaded on December 8, 2008, but with a last update date of January 26, 2008. I also cross-checked against the Extrasolar Planets Encyclopedia to ensure completeness. Given the large volume of work focused in this field, the list presented in this table is certain to be obsolete before it is printed, but provides enough information to enable the statistical analysis in later chapters.

The first column of the table lists the HD number of the planet host and the next column gives the planet's designation. Columns 3–7 list the orbital elements, namely the period

[2] *http://exoplanet.eu/*
[3] *http://exoplanets.org/*

in days, velocity semiamplitude in $\mathrm{m\,s^{-1}}$, eccentricity, and the argument and epoch of the periastron in degrees and JD-2440000 respectively. The second line for each planet lists the corresponding uncertainties. Columns 8 and 9 list the minimum companion mass and semimajor axis, as described in Butler et al. (2006). The last two columns list the number of velocity measurements used to determine the orbit, and the reference as listed in the website.

6.4 Eclipsing Binaries

A search of the All Sky Automated Survey[4] for variable stars and Malkov et al. (2006), who cataloged 6330 stars from the General Catalog of Variable Stars, revealed only three potential eclipsing stellar companions to the stars of this study: HD 123, 9770, and 133640, the first of which was later refuted while the other two are real. HD 123 is listed in the catalogs without a period, but the entry likely corresponds to a suspected brightness variability with a 1-day period, which was refuted by Griffin (1999) (see § 7.4). For HD 9770, Cutispoto et al. (1997) present an eclipsing light curve and a corresponding orbit with a period of 11.4 hours. HD 133640 is listed in Malkov et al. (2006) with a period of 6.4 hours, which matches that of the double-lined spectroscopic orbit. Only one of the extrasolar planets of this sample, HD 189733b, also has a transiting light-curve solution.

[4] *http : //archive.princeton.edu/ asas/*

TABLE 6.5: Planetary Companions

HD Name	Planet Name	P (d)	K_1 ($m\,s^{-1}$)	e	ω (deg)	T_0 (JD-2440000)	$M \sin i$ ($M_\odot$)	a_{min} (AU)	rms ($m\,s^{-1}$)	N	Ref
001237	HD 1237 b	133.71	167.0	0.511	291	11545.9	3.37	0.495	19	61	Naef 2001
		0.20	4.0	0.017	3	0.6	...	...	...	...	...
003651	HD 3651 b	62.241	16.1	0.590	238	12190.7	0.235	0.296	5.7	118	Butler 2006
		0.026	1.2	0.051	7	0.7	...	...	...	...	...
004308	HD 4308 b	15.560	4.1	0.0	...	...	0.047	0.118	1.3	41	Udry 2005
		0.020	0.2	fixed	...	...	...	...	...	...	...
009826	υ And b	1296	63.7	0.267	280	10125	3.97	2.55	12	251	Butler 2006
		12	1.5	0.041	170	21	...	...	...	...	...
009826	υ And c	241.31	55.5	0.258	250	10158.5	1.98	0.832	12	251	Butler 2006
		0.24	1.4	0.022	180	3.1	...	...	...	...	...
009826	υ And d	4.617	69.7	0.022	58	11807.2	0.686	0.060	12	251	Butler 2006
		0.000	1.1	0.016	...	0.6	...	...	...	...	...
010647	HD 10647 b	1003	17.9	0.16	336	10960	0.929	2.03	9.4	28	Butler 2006
		56	4.6	0.22	...	160	...	...	...	...	...
013445	HD 13445 b	15.765	376.7	0.042	269	11903.4	3.91	0.113	12	42	Butler 2006
		0.000	2.9	0.007	16	0.6	...	...	...	...	...
017051	ι Hor b	302.8	57.1	0.14	346	11227	2.08	0.93	19	25	Butler 2006
		2.3	5.2	0.13	...	46	...	...	...	...	...
019994	HD 19994 b	535.7	36.2	0.300	41	10944	1.69	1.43	8.1	48	Mayor 2004
		3.1	1.9	0.040	8	12	...	...	...	...	...
022049	ϵ Eri b	2630	10.8	0.35	148	9780	0.603	3.5	8.6	107	Butler 2006
		260	3.7	0.20	...	340	...	...	...	...	...
033564	HD 33564 b	388.0	232.0	0.340	205	12603.0	9.13	1.12	6.7	15	Galland 2005
		3.0	5.0	.020	4	8.0	...	...	...	...	...
039091	HD 39091 b	2151	196.4	0.641	330	7820	10.3	3.38	5.5	42	Butler 2006
		85	1.3	0.007	1	170	...	...	...	...	...
040307	HD 40307b	4.312	2.0	0.0	0	14562.8	0.013	0.047	0.9	135	Mayor 2008
		0.001	0.1	fixed	fixed	0.1	...	...	...	...	...
040307	HD 40307c	9.620	2.5	0.0	0	14551.5	0.021	0.081	0.9	135	Mayor 2008
		0.002	0.1	fixed	fixed	0.2	...	...	...	...	...
040307	HD 40307d	20.46	4.6	0.0	0	14532.4	0.029	0.134	0.9	135	Mayor 2008
		0.01	0.1	fixed	fixed	0.3	...	...	...	...	...
069830	HD 69830 b	8.667	3.5	0.100	340	13496.8	0.032	0.079	0.8	74	Lovis 2006
		0.003	0.2	0.040	26	0.1	...	...	...	...	...
069830	HD 69830 c	31.560	2.7	0.130	221	13469.6	0.037	0.187	0.8	74	Lovis 2006
		0.040	0.2	0.060	35	2.8	...	...	...	...	...
069830	HD 69830 d	197.0	2.2	0.070	224	13358	0.057	0.633	0.8	74	Lovis 2006
		3.0	0.2	0.070	61	34	...	...	...	...	...
075732	55 Cnc b	14.651	71.8	0.016	164	7572.0	0.816	0.114	6.7	636	Fischer 2007b
		0.001	0.4	0.008	30	1.2	...	...	...	...	...
075732	55 Cnc c	44.379	10.1	0.053	57	7547.5	0.165	0.238	6.7	636	Fischer 2007b
		0.007	0.4	0.052	29	3.3	...	...	...	...	...
075732	55 Cnc d	5370	47.2	0.063	163	6860	3.84	5.84	6.7	636	Fischer 2007b
		230	1.8	0.030	32	230	...	...	...	...	...
075732	55 Cnc e	2.797	3.7	0.264	157	7578.2	0.024	0.038	6.7	636	Fischer 2007b
		0.000	0.5	0.060	38	0.0	...	...	...	...	...
075732	55 Cnc f	260.7	4.8	0.00	206	7488.0	0.141	0.775	6.7	636	Fischer 2007b
		1.1	0.6	0.20	60	1.1	...	...	...	...	...
095128	47 UMa b	1095.0	49.0	0.0	...	...	2.62	2.14	7.4	182	Fischer 2002
		2.9	0.9	fixed	...	...	...	...	...	...	...
095128	47 UMa c	2190	7.0	0.220	180	11581	0.46	3.39	7.4	182	Fischer 2002
		460	2.3	0.068	170	40	...	...	...	...	...
099492	HD 99492 b	17.043	9.8	0.254	219	10468.7	0.109	0.123	3.6	51	Butler 2006
		0.005	1.0	0.092	22	1.4	...	...	...	...	...
114783	HD 114783 b	494.3	30.2	0.122	95	10850	1.06	1.17	4.1	57	Butler 2006
		1.7	0.8	0.033	25	16	...	...	...	...	...
117176	70 Vir b	116.688	316.3	0.401	358	7239.8	7.49	0.484	7.4	74	Butler 2006
		0.004	1.7	0.004	1	0.2	...	...	...	...	...
120136	τ Boo b	3.312	461.1	0.023	188	6957.8	4.13	0.048	62	98	Butler 2006
		0.000	7.6	0.015	...	0.5	...	...	...	...	...

Continued on Next Page...

TABLE 6.5 – Continued

HD Name	Planet Name	P (d)	K_1 ($m\,s^{-1}$)	e	ω (deg)	T_0 (JD-2440000)	$M \sin i$ ($M_\odot$)	a_{min} (AU)	rms ($m\,s^{-1}$)	N	Ref
128311	HD 128311 b	456.7	71.7	0.217	110	10218	2.37	1.1	17	86	Vogt 2005
		1.5	8.8	0.081	160	17	...	...	...	...	...
128311	HD 128311 c	912.9	77.9	0.24	198	10060	3.23	1.74	17	86	Vogt 2005
		6.8	4.3	0.13	...	160	...	...	...	...	...
143761	ρ CrB b[a]	39.845	64.9	0.057	303	10563.2	1.09	0.229	6.9	26	Butler 2006
		0.006	2.4	0.028	...	4.1	...	...	...	...	...
145675	14 Her b	1755.3	91.8	0.373	19	11368.1	5.07	2.85	7.6	51	Butler 2006
		3.2	1.0	0.009	2	5.9	...	...	...	...	...
147513	HD 147513 b	528.4	29.3	0.260	282	11123	1.18	1.31	5.7	30	Mayor 2004
		6.3	1.8	0.050	9	20	...	...	...	...	...
154345	HD 154345 b	3322	14.3	0.036	113	13230	0.963	4.18	2.7	41	Butler 2006
		93	0.8	0.046	...	330	...	...	...	...	...
160691	μ Ara b	630.0	37.4	0.271	260	10881	1.67	1.51	4.7	108	Butler 2006
		6.2	1.6	0.040	7	28	...	...	...	...	...
160691	μ Ara c	2490	18.1	0.463	184	11030	1.18	3.78	4.7	108	Butler 2006
		100	1.1	0.053	8	110	...	...	...	...	...
160691	μ Ara d	9.550	4.1	0.0	...	...	0.047	0.092	0.9	24	Santos 2004b
		0.030	0.2	fixed	...	...	...	...	...	...	...
160691	μ Ara e	310.55	14.9	0.067	9	12708.7	0.546	0.942	0.9	24	Santos 2004b
		0.83	0.6	0.012	2	8.3	...	...	...	...	...
164922	HD 164922 b	1155	7.3	0.05	195	11100	0.36	2.11	3.7	64	Butler 2006
		23	1.2	0.14	...	280	...	...	...	...	...
186427	16 Cyg B b	798.5	50.5	0.681	86	6549.1	1.68	1.68	7.3	95	Butler 2006
		1.0	1.6	0.017	2	6.6	...	...	...	...	...
189733	HD 189733 b	2.219	205.0	0.0	...	...	1.14	0.031	15	...	Knutson 2007
		0.001	6.0	fixed	...	...	...	...	...	...	...
190360	HD 190360 b	2925	23.2	0.307	10	10632	1.56	4.02	3.1	105	Vogt 2005
		28	0.5	0.021	80	32	...	...	...	...	...
190360	HD 190360 c	17.112	4.6	0.004	168	9999.8	0.058	0.13	3.1	105	Vogt 2005
		0.008	0.4	0.004	...	0.1	...	...	...	...	...
192263	HD 192263 b	24.356	51.9	0.055	200	10994.3	0.641	0.153	7.7	31	Butler 2006
		0.005	2.6	0.039	...	3.9	...	...	...	...	...
210277	HD 210277 b	442.19	38.9	0.476	119	10104.3	1.29	1.14	3.8	69	Butler 2006
		0.50	0.8	0.017	3	2.6	...	...	...	...	...
217014	51 Peg b	4.231	55.9	0.013	58	10001.5	0.472	0.053	7	256	Butler 2006
		0.000	0.7	0.012	...	0.6	...	...	...	...	...
217107	HD 217107 b	7.127	139.7	0.129	20	...	1.4	0.075	13	297	Vogt 2005
		0.000	1.0	0.006	60	...	...	...	...	...	...
217107	HD 217107 c[a]	4070	34.7	0.529	200	11133	2.46	5.15	13	297	Vogt 2005
		140	1.0	0.024	180	28	...	...	...	...	...

[a] This "planet" may in fact be a stellar companion. See § 7.4 for further details.

A kind of synthesis, but with some elements that perhaps you wouldn't have expected in advance. I always like that when that happens, when something comes that is more than the sum of the parts.

—— *Evan Parker*

– 7 –

Synthesis of Results

Having explored the many techniques for identifying stellar and substellar companions in the previous chapters, it is now time to consolidate the results and present the observed multiplicity of each system, which is the main content of this chapter. After presenting the results, I discuss specific notes for certain systems which need an explanation about confirmed, candidate, or refuted companions.

7.1 Nomenclature

The stars of the current sample have been the subjects of extensive monitoring with many observational techniques, resulting in a comprehensive assessment of stellar, brown dwarf, and planetary companions. These components are named by their discoverers using historical and evolving standards, and as such, there is some confusion when it comes to the names of components in specific systems. Much effort has gone into standardizing the nomenclature, culminating in the adoption of the Washington Multiplicity Catalog[1] (WMC) standards by the IAU via a resolution of C Type for Commissions 5 and 26 in Special Session 3 of the XXV$^{\text{th}}$ General Assembly in Sydney, Australia, in 2003. In this work, I follow the WMC standards for stellar and brown dwarf companions as prescribed in Hartkopf & Mason (2004), my adaptation of which is described in the following paragraph. While the IAU

[1] *http : //ad.usno.navy.mil/wds/wmc.html*

pronouncement applied to companions of all types, a separate de-facto standard has evolved for naming planetary companions, including some brown dwarf companions discovered by the planet search teams. This method attaches a lowercase alphabetic suffix, separated by a blank, to the host star's name for each substellar companion, starting with "b" for the first discovery and incremented alphabetically for each subsequent discovery. It is this standard that is used in the two primary online catalogs mentioned in § 6.3, and followed in the the large volume of work ongoing in this field, thus becoming the widely-accepted standard. Reassigning names to planets according to the WMC prescription at this stage will cause too much confusion, so I follow the lowercase letters as described above for the planetary companions.

The WMC standard uses a hierarchical approach to naming the components of multiple systems, using a combination of uppercase and lowercase alphabets, and in the case of exceptionally complex systems, numbers as well. It is best understood by following the illustration of a fictitious example in Figure 7.1, which is adapted from a similar example in Hartkopf & Mason (2004) and described in the figure's caption. When reviewing the example, it will help to keep one point in mind. The study of binary stars, like all scientific endeavors, is an evolving process. We will hence encounter components discovered and assigned to systems that were later realized to be unrelated stars. As seen in § 4.2, the WDS, which is the current comprehensive catalog of visual double stars and the predecessor to the WMC still under construction, lists many double star entries which are optical rather than physical. When a component is understood to not belong to a system, what should

one do about the name it has already been assigned? For example, if component B of a three-component system ABC is found to be optical and component C is determined to be physically associated to A, should C be renamed B? No, because this would cause too much confusion with ever-changing component names. Therefore, we will have situations where, as in the above example, AC represents a binary system, while component B is only optically associated. The designations used here follow the WMC standards, but inherit the actual WDS designations, when available, with only minor cosmetic tweaks to conform to the WMC standards. For systems which have only two components in the WDS, the pair ID is left blank as there is only one, which is meant to imply AB (W. Hartkopf 2009, private communication), and used as such here. It is also relevant to note that the WDS is not a comprehensive multiplicity catalog and only includes pairs with at least one visual measure with separation and position angle measures, but the WMC catalog will contain companions of all kind. The results presented here follow the WMC standards for all stellar and brown dwarf companions, and the nomenclature described in the previous paragraph for planetary components.

7.2 Results for Each of the 454 Systems

Table 7.1 summarizes the stellar and planetary companions to each star in the sample studied in this work. Note that this table only includes confirmed or candidate companions, leaving out components that are now known to be physically unassociated with these systems. Such components are discussed in the preceding chapters and in § 7.4. The stars of the current

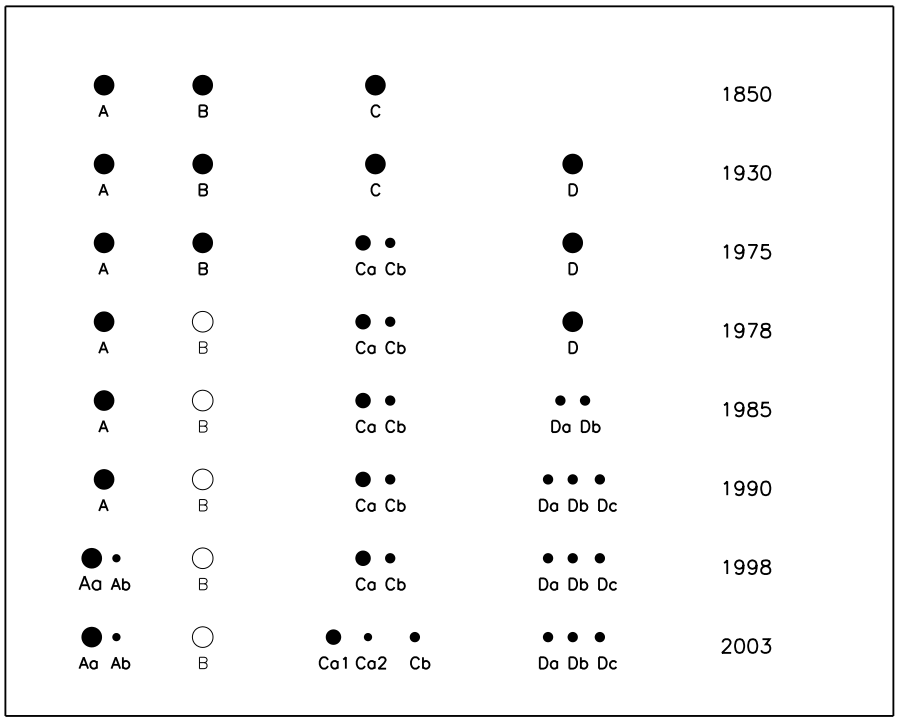

FIGURE 7.1: Illustration of companion nomenclature according to the WMC standards for a fictitious system that grows more complex over time. The following hypothetical events took place as components of this system were discovered. 1850: A telescopic inspection of this star reveals three visual components. The companions are resolved 3″ and 12″ away, and labeled B and C, respectively, while the primary is designated as A. 1930: A wide CPM companion is discovered and labeled D. 1975: Component C is discovered to be a spectroscopic binary and the original designation is split into Ca and Cb for the new components, while C refers to the pair. 1978: A new measure of the AB pair shows that it is optical rather than physical, but the components names previously assigned are retained. 1985: Component D is split by speckle interferometry, and the components are named Da and Db. 1990: An additional speckle component is found in D and named Dc; 1998: AO reveals a faint source near A, which is identified as a brown dwarf companion by follow-up spectroscopy, splitting A into Aa, referring to the stellar primary, and Ab, identifying the brown dwarf. 2003: Another brown dwarf is discovered near Ca, so the star and brown dwarf are named Ca1 and Ca2 respectively.

sample are listed in order of right ascension, immediately followed in subsequent lines by the stellar and planetary companions of that system. Note that a few stars in this sample

are actually not the primary component of their system, but are still listed first within their group. Stellar companions are listed in order of proximity and planetary companions are listed directly under the star they orbit, also sequenced by proximity to the star. For ease of readability, the right ascension (Column 1) and declination (Column 2) are only listed at the beginning of each group and correspond to the sample star. Column 3 lists the HD number of the star, when available, and Column 4 lists an alternate name of the star or the name of the planet. For the first line of each group, Column 5 identifies the component designation of the sample star according to the nomenclature described above, unless it has no companions, in which case the column is empty. For stellar companions, this column identifies the pair whose period and separation are listed in Columns 6 and 7 respectively, again according to the WMC standards. The components are separated by a comma, which is suppressed when two components are each an uppercase alphabet (e.g., AB, AB,C, and Aa,Ab are valid pair designations). For planetary companions, this column is left empty. The period is listed from the spectroscopic orbit, if one exists, otherwise from a visual orbit, if available, along with its unit – h for hours, d for days, and y for years. The separation is listed typically from the latest measure in the WDS, and in cases of no WDS measurements, from other published references, or is my approximate measure from the archival images for new CPM companions, and is listed in milli-arcseconds (m) or arcseconds (a) for angular measures, or AU (A) for linear separations. Column 8 lists the status of companionship used for the multiplicity statistics derived here – "Y" indicates a confirmed companion and "M" implies an unconfirmed candidate. The next five columns list additional information about

the techniques used to identify each companion and are described below.

Column 9 corresponds to visual orbits and contains an "O" for robust orbits of grade 1, 2, 3, or 8, "P" for preliminary orbits of grade 4 or 5, and "U" for unresolved photocentric-motion orbits (see § 5.2 for details). Additionally, two of the LBI visual orbits from § 3.2 (HD 146361 and 223778) are counted as robust orbits, one (HD 45088) is included as preliminary, and the trial orbit for HD 8997 is not included due to its low quality. Column 10 identifies spectroscopic companions as a "1" for single-lined orbits, "2" for double-lined orbits, and "V" for radial velocity variations indicating a companion, but without an orbital solution (see Chapter 6). Column 11 identifies CPM companions as close pairs with matching proper motions ("M", see § 5.3), pairs with evidence of orbital motion ("O", see § 5.3), companions with matching proper motions and photometric distances ("P", see Tables 4.2 and 5.5), close pairs with published evidence of companionship ("R", see § 7.4), companions with matching proper motions and spectral type identifications that are consistent with the primary's distance ("S", see § 7.4), or pairs with independently-measured matching proper motions and trigonometric parallaxes ("T", see § 5.3). Column 12 identifies unresolved companions other than spectroscopic or visual ones which were covered in Columns 9 and 10 as eclipsing binaries ("E", see § 6.4), companions indicated by an overluminous star ("L", see § 7.4), or implied by proper motion accelerations ("M", see § 5.1.2). Finally, Column 13 identifies companions seen by CHARA LBI as SFP ("S", see § 3.1), or as visibility-modulation binaries ("V", see § 3.2).

TABLE 7.1: Stellar and Planetary Companions

R.A. (J2000.0) (1)	Decl. (J2000.0) (2)	HD Name (3)	Other Name (4)	Comp ID (5)	Period (6)	Sep (7)	Sts (8)	VB (9)	SB (10)	CP (11)	UR (12)	CH (13)
...	...	...	Sun	A	...	...	...	...	...	...	...	...
...	...	...	Mercury	...	0.24 y	0.39 A	Y	...	...	...	...	...
...	...	...	Venus	...	0.62 y	0.72 A	Y	...	...	...	...	...
...	...	...	Earth	...	1.00 y	1.00 A	Y	...	...	...	...	...
...	...	...	Mars	...	1.88 y	1.52 A	Y	...	...	...	...	...
...	...	...	Jupiter	...	11.86 y	5.20 A	Y	...	...	...	...	...
...	...	...	Saturn	...	29.42 y	9.54 A	Y	...	...	...	...	...
...	...	...	Uranus	...	84.01 y	19.19 A	Y	...	...	...	...	...
...	...	...	Neptune	...	164.8 y	30.06 A	Y	...	...	...	...	...
00 02 10.16	+27 04 56.1	224930	85 Peg	A	...	...	...	...	...	...	...	...
...	...	...	...	AB	26.31 y	0.8 a	Y	O	1	...	M	...
00 06 15.81	+58 26 12.2	000123	HIP 000518	A	...	...	...	...	...	...	...	...
...	...	...	...	AB	106.7 y	1.46 a	Y	O	...	...	M	...
...	...	...	...	Ba,Bb	47.69 d	...	Y	...	1	...	...	...
00 06 36.78	+29 01 17.4	000166	HIP 000544	...	...	...	...	...	...	...	...	...
00 12 50.25	−57 54 45.4	000870	HIP 001031	...	...	...	...	...	...	...	...	...
00 16 12.68	−79 51 04.3	001237	HIP 001292	A	...	...	...	...	...	...	...	...
...	...	...	GJ 3021 b	...	133.82 d	0.49 A	Y	...	1	...	...	...
...	...	...	HD 1237B	AB	...	3.87 a	Y	...	...	S	...	...
00 16 53.89	−52 39 04.1	001273	HIP 001349	A	...	...	...	...	...	...	...	...
...	...	...	...	Aa,Ab	1.13 y	...	Y	U	1	...	...	...
00 18 41.87	−08 03 10.8	001461	HIP 001499	...	...	...	...	...	...	...	...	...
00 20 00.41	+38 13 38.6	001562	HIP 001598	...	...	...	...	...	...	...	...	...
00 20 04.26	−64 52 29.2	001581	ζ Tuc	...	...	...	...	...	...	...	...	...
00 22 51.79	−12 12 34.0	001835	HIP 001803	...	...	...	...	...	...	...	...	...
00 24 25.93	−27 01 36.4	002025	HIP 001936	...	...	...	...	...	...	...	...	...
00 25 45.07	−77 15 15.3	002151	β Hyi	...	...	...	...	...	...	...	...	...
00 35 14.88	−03 35 34.2	003196	13 Cet	A	...	...	...	...	...	...	...	...
...	...	...	...	Aa,Ab	2.08 d	...	Y	...	1	...	...	...
...	...	...	...	AB	6.92 y	0.28 a	Y	O	2	...	M	S
00 37 20.70	−24 46 02.2	003443	HIP 002941	A	...	...	...	...	...	...	...	...
...	...	...	GJ 25 B	AB	25.09 y	0.74 a	Y	O	2	...	M	...
00 39 21.81	+21 15 01.7	003651	54 Psc	A	...	...	...	...	...	...	...	...
...	...	...	HD 003651 b	...	62.23 d	0.28 A	Y	...	1	...	...	...
...	...	...	HD 3651B	AB	...	43.07 a	Y	...	...	S	...	...
00 40 49.27	+40 11 13.8	003765	HIP 003206	...	...	...	...	...	...	...	...	...
00 44 39.27	−65 38 58.3	004308	HIP 003497	A	...	...	...	...	...	...	...	...
...	...	...	HD 004308 b	...	15.56 d	0.11 A	Y	...	1	...	...	...
00 45 04.89	+01 47 07.9	004256	HIP 003535	...	...	...	...	...	...	...	...	...
00 45 45.59	−47 33 07.2	004391	HIP 003583	A	...	...	...	...	...	...	...	...
...	...	...	...	AB	...	16.6 a	Y	...	...	P	...	...
...	...	...	...	AC	...	49.0 a	Y	...	...	P	...	...
00 48 22.98	+05 16 50.2	004628	HIP 003765	A	...	...	...	...	...	...	...	...
...	...	...	...	Aa,Ab	...	2.7 a	M	...	...	R	...	...
00 48 58.71	+16 56 26.3	004676	64 Psc	A	...	...	...	...	...	...	...	...
...	...	...	...	Aa,Ab	13.82 d	6.53 m	Y	O	2	...	...	S
00 49 06.29	+57 48 54.7	004614	η Cas	A	...	...	...	...	...	...	...	...
...	...	...	LHS 122	AB	480 y	12.49 a	Y	O	...	...	...	...
00 49 26.77	−23 12 44.9	004747	HIP 003850	A	...	...	...	...	...	...	...	...
...	...	...	...	Aa,Ab	18.7 y	...	Y	...	1	...	M	...
00 49 46.48	+70 26 58.1	004635	HIP 003876	...	...	...	...	...	...	...	...	...
00 50 07.59	−10 38 39.6	004813	HIP 003909	...	...	...	...	...	...	...	...	...
00 51 10.85	−05 02 21.4	004915	HIP 003979	...	...	...	...	...	...	...	...	...
00 53 01.13	−30 21 24.9	005133	HIP 004148	...	...	...	...	...	...	...	...	...
00 53 04.20	+61 07 26.3	005015	HIP 004151	...	...	...	...	...	...	...	...	...
01 08 16.39	+54 55 13.2	006582	μ Cas	A	...	...	...	...	...	...	...	...
...	...	...	μ Cas B	Aa,Ab	21.43 y	0.8 a	Y	P	1	...	...	...
01 15 00.99	−68 49 08.1	007693	HIP 005842	C[a]	...	...	...	...	...	...	...	...
...	...	...	GJ 55.1B	CD	85.2 y	0.91 a	Y	O	...	...	M	...
...	...	...	HD 7788	A,CD	...	318 a	Y	...	...	T	...	...
...	...	...	GJ 55.3B	AB	857 y	5 a	Y	P	...	...	...	...
01 15 11.12	−45 31 54.0	007570	ν Phe	...	...	...	...	...	...	...	...	...
01 16 29.25	+42 56 21.9	007590	HIP 005944	...	...	...	...	...	...	...	...	...
01 21 59.12	+76 42 37.0	007924	HIP 006379	...	...	...	...	...	...	...	...	...
01 29 04.90	+21 43 23.4	008997	HIP 006917	A	...	...	...	...	...	...	...	...
...	...	...	...	Aa,Ab	10.98 d	...	Y	...	2	...	...	V
01 33 15.81	−24 10 40.7	009540	HIP 007235	...	...	...	...	...	...	...	...	...
01 34 33.26	+68 56 53.3	009407	HIP 007339	...	...	...	...	...	...	...	...	...
01 35 01.01	−29 54 37.2	009770	HIP 007372	A	...	...	...	...	...	...	...	...
...	...	...	...	AB	4.56 y	0.18 a	Y	O	...	...	...	...
...	...	...	...	Ba,Bb	11.50 h	0.01 A	Y	...	...	...	E	...
...	...	...	...	AB,C	111.8 y	1.7 a	Y	P	...	...	...	...
01 36 47.84	+41 24 19.7	009826	υ And	A	...	...	...	...	...	...	...	...
...	...	...	υ And b	...	4.62 d	0.06 A	Y	...	1	...	...	...
...	...	...	υ And c	...	241.52 d	0.83 A	Y	...	1	...	...	...
...	...	...	υ And d	...	3.49 y	2.51 A	Y	...	1	...	...	...
...	...	...	υ And B	AD	...	55 a	Y	...	...	S	...	...
01 37 35.47	−06 45 37.5	010008	HIP 007576	...	...	...	...	...	...	...	...	...
01 39 36.02	+45 52 40.0	010086	HIP 007734	...	...	...	...	...	...	...	...	...

Continued on Next Page...

TABLE 7.1 – Continued

R.A. (J2000.0) (1)	Decl. (J2000.0) (2)	HD Name (3)	Other Name (4)	Comp ID (5)	Period (6)	Sep (7)	Sts (8)	VB (9)	SB (10)	CP (11)	UR (12)	CH (13)
01 39 47.54	−56 11 47.0	010360	HIP 007751	B[a]	...	...	...	...	...	...	...	...
...	...	...	HD 10361	AB	483.66 y	11.4 a	Y	P	...	...	M	...
01 41 47.14	+42 36 48.1	010307	HIP 007918	A	...	...	...	...	...	...	...	...
...	...	...	...	Aa,Ab	20.21 y	0.3 a	Y	P	1	...	M	...
01 42 29.32	−53 44 27.0	010647	q[1] Eri	A	...	...	...	...	...	...	...	...
...	...	...	HD 010647 b	...	2.85 y	2.1 a	Y	...	1	...	...	...
01 42 29.76	+20 16 06.6	010476	107 Psc	...	...	...	...	...	...	...	...	...
01 44 04.08	−15 56 14.9	010700	τ Cet	...	...	...	...	...	...	...	...	...
01 47 44.83	+63 51 09.0	010780	HIP 008362	...	...	...	...	...	...	...	...	...
01 59 06.63	+33 12 34.9	012051	HIP 009269	...	...	...	...	...	...	...	...	...
02 06 30.24	+24 20 02.4	012846	HIP 009829	...	...	...	...	...	...	...	...	...
02 10 25.93	−50 49 25.4	013445	HIP 010138	A	...	...	...	...	...	...	...	...
...	...	...	Gl 86 b	...	15.77 d	0.11 A	Y	...	1	...	...	...
...	...	...	GJ 86 B	AB	69.7 y	1.97 a	Y	P	...	...	M	...
02 17 03.23	+34 13 27.2	013974	δ Tri	A	...	...	...	...	...	...	...	...
...	...	...	...	Aa,Ab	10.02 d	...	Y	O	2	...	...	...
02 18 01.44	+01 45 28.1	014214	HIP 010723	A	...	...	...	...	...	...	...	...
...	...	...	...	Aa,Ab	93.29 d	...	Y	U	1	...	...	...
02 18 58.50	−25 56 44.5	014412	HIP 010798	...	...	...	...	...	...	...	...	...
02 22 32.55	−23 48 58.8	014802	κ For	A	...	...	...	...	...	...	...	...
...	...	...	...	AB	26.5 y	0.5 a	Y	U	...	R	M	...
02 36 04.89	+06 53 12.7	016160	HIP 012114	A	...	...	...	...	...	...	...	...
...	...	...	...	Aa,Ab	61 y	3.2 a	Y	U	...	R	...	...
...	...	...	NLTT 8455	Aa,B	...	164 a	Y	...	...	P	...	...
02 36 41.76	−03 09 22.1	016287	HIP 012158	A	...	...	...	...	...	...	...	...
...	...	...	...	Aa,Ab	14.84 d	0.01 a	Y	...	1	...	...	...
02 40 12.42	−09 27 10.3	016673	HIP 012444	A	...	...	...	...	...	...	...	...
...	...	...	...	Aa,Ab	...	...	Y	...	V	...	...	...
02 41 14.00	−00 41 44.4	016765	HIP 012530	A	...	...	...	...	...	...	...	...
...	...	...	...	AB	...	3.3 a	Y	...	V	O	...	...
02 42 14.92	+40 11 38.2	016739	12 Per	A	...	...	...	...	...	...	...	...
...	...	...	...	Aa,Ab	330.99 d	0.1 a	Y	O	2	...	...	S
02 42 33.47	−50 48 01.1	017051	ι Hor	A	...	...	...	...	...	...	...	...
...	...	...	HR 810 b	...	311.29 d	0.91 A	Y	...	1	...	...	...
02 44 11.99	+49 13 42.4	016895	θ Per	A	...	...	...	...	...	...	...	...
...	...	...	NLTT 8787	AB	2720 y	19.6 a	Y	P	...	...	...	...
02 48 09.14	+27 04 07.1	017382	HIP 013081	A	...	...	...	...	...	...	...	...
...	...	...	...	Aa,Ab	15.27 y	...	Y	U	1	...	M	...
...	...	...	NLTT 8996	AB	...	20.7 a	Y	...	...	P	...	...
02 52 32.13	−12 46 11.0	017925	HIP 013402	...	...	...	...	...	...	...	...	...
02 55 39.06	+26 52 23.6	018143	HIP 013642	A	...	...	...	...	...	...	...	...
...	...	...	HD 18143 B	AB	...	5 a	Y	P	...	...	M	...
...	...	...	NLTT 9303	AC	...	44 a	Y	...	...	T	...	...
03 00 02.81	+07 44 59.1	018632	HIP 013976	...	...	...	...	...	...	...	...	...
03 02 26.03	+26 36 33.3	018803	51 Ari	...	...	...	...	...	...	...	...	...
03 04 09.64	+61 42 21.0	018757	HIP 014286	A	...	...	...	...	...	...	...	...
...	...	...	NLTT 9726	AC	...	263.2 a	Y	...	...	P	...	...
03 09 04.02	+49 36 47.8	019373	ι Per	...	...	...	...	...	...	...	...	...
03 12 04.53	−28 59 15.4	020010	12 Eri	A	...	...	...	...	...	...	...	...
...	...	...	GJ 127 B	AB	269 y	4.8 a	Y	P	...	...	...	...
...	...	...	...	Ba,Bb	...	...	M	...	V	...	...	...
03 12 46.44	−01 11 46.0	019994	94 Cet	A	...	...	...	...	...	...	...	...
...	...	...	HD 019994 b	...	1.2 y	1.3 a	Y	...	1	...	...	...
...	...	...	...	AB	1420 y	2.5 a	Y	P	...	...	...	...
03 14 47.23	+08 58 50.9	020165	HIP 015099	...	...	...	...	...	...	...	...	...
03 15 06.39	−45 39 53.4	020407	HIP 015131	...	...	...	...	...	...	...	...	...
03 18 12.82	−62 30 22.9	020807	ζ^2 Ret	A	...	...	...	...	...	...	...	...
...	...	...	HD 20766	AB	...	309.2 a	Y	...	...	T	...	...
03 19 01.89	−02 50 35.5	020619	HIP 015442	...	...	...	...	...	...	...	...	...
03 19 21.70	+03 22 12.7	020630	κ Cet	...	...	...	...	...	...	...	...	...
03 19 55.65	−43 04 11.2	020794	HIP 015510	...	...	...	...	...	...	...	...	...
03 21 54.76	+52 19 53.4	232781	HIP 015673	...	...	...	...	...	...	...	...	...
03 23 35.26	−40 04 35.0	021175	HIP 015799	A	...	...	...	...	...	...	...	...
...	...	...	...	AB	111 y	1.3 a	Y	P	...	...	...	...
03 32 55.84	−09 27 29.7	022049	ϵ Eri	A	...	...	...	...	...	...	...	...
...	...	...	ϵ Eri b	...	6.85 y	3.39 A	Y	...	1	...	...	...
03 36 52.38	+00 24 06.0	022484	10 Tau	...	...	...	...	...	...	...	...	...
03 40 22.06	−03 13 01.1	022879	HIP 017147	...	...	...	...	...	...	...	...	...
03 43 55.34	−19 06 39.2	023356	HIP 017420	...	...	...	...	...	...	...	...	...
03 44 09.17	−38 16 54.4	023484	HIP 017439	A	...	...	...	...	...	...	...	...
...	...	...	...	Aa,Ab	...	...	M	...	V	...	...	...
03 54 28.03	+16 36 57.8	024496	HIP 018267	A	...	...	...	...	...	...	...	...
...	...	...	...	AB	...	2.7 a	Y	...	...	M	...	...
03 55 03.84	+61 10 00.5	024238	HIP 018324	...	...	...	...	...	...	...	...	...
03 56 11.52	+59 38 30.8	024409	HIP 018413	A	...	...	...	...	...	...	...	...
...	...	...	...	AD	34.57 y	0.4 a	Y	...	1	...	M	...
...	...	...	...	AE	...	8.9 a	Y	...	...	P	...	...
04 02 36.74	−00 16 08.1	025457	HIP 018859	...	...	...	...	...	...	...	...	...
04 03 15.00	+35 16 23.8	025329	HIP 018915	...	...	...	...	...	...	...	...	...
04 05 20.26	+22 00 32.1	025680	39 Tau	A	...	...	...	...	...	...	...	...
...	...	...	...	Aa,Ab	...	0.4 a	Y	...	...	M	...	...

Continued on Next Page...

TABLE 7.1 – Continued

R.A. (J2000.0) (1)	Decl. (J2000.0) (2)	HD Name (3)	Other Name (4)	Comp ID (5)	Period (6)	Sep (7)	Sts (8)	VB (9)	SB (10)	CP (11)	UR (12)	CH (13)
04 07 21.54	−64 13 20.2	026491	HIP 019233	A	...	...	...	...	...	...	...	...
...	...	...	...	Aa,Ab	19.19 y	...	Y	...	1	...	M	...
04 08 36.62	+38 02 23.0	025998	HIP 019335	E[b]	...	...	...	...	...	...	...	...
...	...	...	...	Ea,Eb	...	...	M	...	...	...	M	...
...	...	...	HD 25893	AE	...	746 a	Y	...	...	T	...	...
...	...	...	...	AB	590 y	2.4 a	Y	P	...	...	...	...
04 09 35.04	+69 32 29.0	025665	HIP 019422	...	...	...	...	...	...	...	...	...
04 15 16.32	−07 39 10.3	026965	HIP 019849	A	...	...	...	...	...	...	...	...
...	...	...	LHS 25	A,BC	...	83 a	Y	...	...	T	...	...
...	...	...	HD 26976	BC	252.1 y	6.9 a	Y	P	...	...	...	...
04 15 28.80	+06 11 12.7	026923	HIP 019859	A	...	...	...	...	...	...	...	...
...	...	...	HD 26913	AB	...	64.5 a	Y	...	...	T	...	...
04 43 35.44	+27 41 14.6	029883	HIP 021988	...	...	...	...	...	...	...	...	...
04 45 38.58	−50 04 27.2	030501	HIP 022122	...	...	...	...	...	...	...	...	...
04 47 36.29	−16 56 04.0	030495	HIP 022263	...	...	...	...	...	...	...	...	...
04 49 52.33	−35 06 27.5	030876	HIP 022451	...	...	...	...	...	...	...	...	...
05 02 17.06	−56 04 49.9	032778	HIP 023437	A	...	...	...	...	...	...	...	...
...	...	...	NLTT 14447	AB	...	79.1 a	Y	...	...	P	...	...
05 05 30.66	−57 28 21.7	033262	ζ Dor	...	...	...	...	...	...	...	...	...
05 06 42.22	+14 26 46.4	032850	HIP 023786	A	...	...	...	...	...	...	...	...
...	...	...	...	Aa,Ab	205.68 d	...	Y	U	1	...	...	...
05 07 27.01	+18 38 42.2	032923	104 Tau	...	...	...	...	...	...	...	...	...
05 18 50.47	−18 07 48.2	034721	HIP 024786	...	...	...	...	...	...	...	...	...
05 19 08.47	+40 05 56.6	034411	HIP 024813	...	...	...	...	...	...	...	...	...
05 22 33.53	+79 13 52.1	033564	HIP 025110	A	...	...	...	...	...	...	...	...
...	...	...	HD 033564 b	...	1.06 y	1.1 a	Y	...	1	...	...	...
05 22 37.49	+02 36 11.5	035112	HIP 025119	A	...	...	...	...	...	...	...	...
...	...	...	...	AB	93 y	1.2 a	Y	P	...	...	M	...
05 24 25.46	+17 23 00.7	035296	HIP 025278	A	...	...	...	...	...	...	...	...
...	...	...	HD 35171	AC	...	707.2 a	Y	...	...	T	...	...
05 26 14.74	−32 30 17.2	035854	HIP 025421	...	...	...	...	...	...	...	...	...
05 27 39.35	−60 24 57.6	036435	HIP 025544	...	...	...	...	...	...	...	...	...
05 28 44.83	−65 26 54.9	036705	AB Dor	A	...	...	...	...	...	...	...	...
...	...	...	...	Aa,Ab	...	0.16 a	Y	...	...	S	M	...
...	...	...	...	AB	...	9.2 a	Y	...	...	P	...	...
...	...	...	...	Ba,Bb	...	0.07 a	Y	...	...	R	...	...
05 36 56.85	−47 57 52.9	037572	UY Pic	A	...	...	...	...	...	...	...	...
...	...	...	HIP 26369	AB	...	18.3 a	Y	...	...	T	...	...
05 37 09.89	−80 28 08.8	039091	π Men	A	...	...	...	...	...	...	...	...
...	...	...	HD 039091 b	...	5.65 y	3.29 A	Y	...	1	...	...	...
05 38 11.86	+51 26 44.7	037008	HIP 026505	...	...	...	...	...	...	...	...	...
05 41 20.34	+53 28 51.8	037394	HIP 026779	A	...	...	...	...	...	...	...	...
...	...	...	HD 233153	AB	...	98.8 a	Y	...	...	T	...	...
05 46 01.89	+37 17 04.7	038230	HIP 027207	...	...	...	...	...	...	...	...	...
05 48 34.94	−04 05 40.7	038858	HIP 027435	...	...	...	...	...	...	...	...	...
05 54 04.24	−60 01 24.5	040307	HIP 027887	A	...	...	...	...	...	...	...	...
...	...	...	HD 040307 b	...	4.31 d	0.05 A	Y	...	1	...	...	...
...	...	...	HD 040307 c	...	9.62 d	0.08 A	Y	...	1	...	...	...
...	...	...	HD 040307 d	...	20.46 d	0.13 A	Y	...	1	...	...	...
05 54 22.98	+20 16 34.2	039587	χ^1 Ori	A	...	...	...	...	...	...	...	...
...	...	...	...	Aa,Ab	14.06 y	0.5 a	Y	U	1	R	M	...
05 54 30.16	−19 42 15.7	039855	HIP 027922	A	...	...	...	...	...	...	...	...
...	...	...	BD-19 1297B	AB	...	10.6 a	Y	...	...	P	...	...
05 58 21.54	−04 39 02.4	040397	HIP 028267	A	...	...	...	...	...	...	...	...
...	...	...	...	AB	...	3.9 a	Y	...	...	M	M	...
...	...	...	NLTT 15867	AD	...	89.3 a	Y	...	...	P	...	...
06 06 40.48	+15 32 31.6	041593	HIP 028954	...	...	...	...	...	...	...	...	...
06 10 14.47	−74 45 11.0	043834	α Men	A	...	...	...	...	...	...	...	...
...	...	...	...	Aa,Ab	...	3.05 a	Y	...	V	M	...	...
06 12 00.57	+06 46 59.1	042618	HIP 029432	...	...	...	...	...	...	...	...	...
06 13 12.50	+10 37 37.7	042807	HIP 029525	...	...	...	...	...	...	...	...	...
06 13 45.30	−23 51 43.0	043162	HIP 029568	A	...	...	...	...	...	...	...	...
...	...	...	...	AB	...	164 a	Y	...	...	P	...	...
06 17 16.14	+05 06 00.4	043587	HIP 029860	A	...	...	...	...	...	...	...	...
...	...	...	...	Aa,Ab	33.74 y	0.7 a	Y	...	1	...	M	...
...	...	...	NLTT 16333	AE	...	103.1 a	Y	...	...	P	...	...
06 22 30.94	−60 13 07.2	045270	HIP 030314	A	...	...	...	...	...	...	...	...
...	...	...	...	AB	...	16.2 a	M	...	...	R	...	...
06 24 43.88	−28 46 48.4	045184	HIP 030503	...	...	...	...	...	...	...	...	...
06 26 10.25	+18 45 24.8	045088	OU Gem	A	...	...	...	...	...	...	...	...
...	...	...	...	Aa,Ab	6.99 d	...	Y	P	2	...	...	V
...	...	...	...	AB	600 y	2.4 a	Y	P	...	...	M	...
06 38 00.36	−61 32 00.2	048189	HIP 031711	A	...	...	...	...	...	...	...	...
...	...	...	...	AB	...	0.3 a	Y	...	...	M	M	...
06 46 05.05	+32 33 20.4	263175	HIP 032423	A	...	...	...	...	...	...	...	...
...	...	...	HD 263175B	AB	...	30 a	Y	...	...	P	...	...
06 46 14.15	+79 33 53.3	046588	HIP 032439	...	...	...	...	...	...	...	...	...
06 46 44.34	+43 34 38.7	048682	ψ^5 Aur	...	...	...	...	...	...	...	...	...
06 55 18.67	+25 22 32.5	050692	HIP 033277	...	...	...	...	...	...	...	...	...
06 58 11.75	+22 28 33.2	051419	HIP 033537	...	...	...	...	...	...	...	...	...
06 59 59.66	−61 20 10.3	053143	HIP 033690	...	...	...	...	...	...	...	...	...

Continued on Next Page...

TABLE 7.1 – Continued

R.A. (J2000.0) (1)	Decl. (J2000.0) (2)	HD Name (3)	Other Name (4)	Comp ID (5)	Period (6)	Sep (7)	Sts (8)	VB (9)	SB (10)	CP (11)	UR (12)	CH (13)
07 01 13.74	−25 56 55.4	052698	HIP 033817	A	...	...	...	...	...	...	...	...
...	...	...	...	Aa,Ab	...	...	Y	...	V	...	M	...
07 01 38.59	+48 22 43.2	051866	HIP 033852	...	...	...	...	...	...	...	...	...
07 03 30.46	+29 20 13.5	052711	HIP 034017	...	...	...	...	...	...	...	...	...
07 03 57.32	−43 36 28.9	053705	HIP 034065	A	...	...	...	...	...	...	...	...
...	...	...	HD 53706	AB	...	20.9 a	Y	...	...	T	...	...
...	...	...	HD 53680	AC	...	184.9 a	Y	...	...	T	...	...
...	...	...	...	Ca,Cb	...	...	Y	...	...	...	M	...
07 08 04.24	+29 50 04.2	053927	HIP 034414	...	...	...	...	...	...	...	...	...
07 09 35.39	+25 43 43.1	054371	HIP 034567	A	...	...	...	...	...	...	...	...
...	...	...	...	Aa,Ab	32.81 d	...	Y	...	1	...	...	...
07 15 50.14	+47 14 23.9	055575	HIP 035136	...	...	...	...	...	...	...	...	...
07 17 29.56	−46 58 45.3	057095	HIP 035296	A	...	...	...	...	...	...	...	...
...	...	...	...	AB	94 y	0.8 a	Y	P	...	...	...	...
07 27 25.47	−51 24 09.4	059468	HIP 036210	...	...	...	...	...	...	...	...	...
07 29 01.77	+31 59 37.8	...	HIP 036357	E[a]	...	...	...	...	...	...	...	...
...	...	...	HD 58946	AE	...	756.1 a	Y	...	...	T	...	...
...	...	...	GJ 274B	AB	...	3.4 a	Y	...	...	O	M	...
07 30 42.51	−37 20 21.7	059967	HIP 036515	...	...	...	...	...	...	...	...	...
07 33 00.58	+37 01 47.4	059747	HIP 036704	...	...	...	...	...	...	...	...	...
07 34 26.17	−06 53 48.0	060491	HIP 036827	...	...	...	...	...	...	...	...	...
07 39 59.33	−03 35 51.0	061606	HIP 037349	A	...	...	...	...	...	...	...	...
...	...	...	NLTT 18260	AB	...	58.3 a	Y	...	...	P	...	...
07 45 35.02	−34 10 20.5	063077	HIP 037853	A	...	...	...	...	...	...	...	...
...	...	...	...	Aa,Ab	...	...	Y	...	V	...	M	...
...	...	...	NLTT 18414	AB	...	914 a	Y	...	...	P	...	...
07 49 55.06	+27 21 47.4	063433	HIP 038228	...	...	...	...	...	...	...	...	...
07 51 46.30	−13 53 52.9	064096	9 Pup	A	...	...	...	...	...	...	...	...
...	...	...	...	AB	22.7 y	0.3 a	Y	O	2	...	M	...
07 54 34.18	−01 24 44.1	064606	HIP 038625	A	...	...	...	...	...	...	...	...
...	...	...	...	Aa,Ab	1.23 y	...	Y	...	1	...	M	...
07 54 54.07	+19 14 10.8	064468	HIP 038657	A	...	...	...	...	...	...	...	...
...	...	...	...	Aa,Ab	161.2 d	...	Y	...	1	...	...	...
07 56 17.23	+80 15 55.9	062613	HIP 038784	...	...	...	...	...	...	...	...	...
07 57 46.91	−60 18 11.1	065907	HIP 038908	A	...	...	...	...	...	...	...	...
...	...	...	LHS 1960	AB	...	60.3 a	Y	...	...	P	...	...
...	...	...	...	BC	...	3 a	Y	...	...	M	...	...
07 59 33.93	+20 50 38.0	065430	HIP 039064	A	...	...	...	...	...	...	...	...
...	...	...	...	Aa,Ab	8.59 y	...	Y	...	1	...	M	...
08 00 32.13	+29 12 44.5	065583	HIP 039157	...	...	...	...	...	...	...	...	...
08 02 31.19	−66 01 15.4	067199	HIP 039342	A	...	...	...	...	...	...	...	...
...	...	...	...	Aa,Ab	...	...	M	...	...	...	M	...
08 07 45.86	+21 34 54.5	067228	μ Cnc	...	...	...	...	...	...	...	...	...
08 11 38.64	+32 27 25.7	068017	HIP 040118	A	...	...	...	...	...	...	...	...
...	...	...	...	Aa,Ab	...	...	M	...	...	...	M	...
08 12 12.73	+17 38 52.0	068257	ζ Cnc C	A	...	...	...	...	...	...	...	...
...	...	...	HD 68255	AB	59.58 y	1 a	Y	O	...	...	M	...
...	...	...	HD 68256	AB,C	1115 y	6.2 a	Y	P	...	...	M	...
...	...	...	...	Ca,Cb	17.25 y	0.3 a	Y	P	1	...	...	...
...	...	...	...	Cb1,Cb2	...	...	Y	...	...	...	L	...
...	...	...	...	Cb1,Cb3	...	...	M	...	...	R	...	...
08 18 23.95	−12 37 55.8	069830	HIP 040693	A	...	...	...	...	...	...	...	...
...	...	...	HD 069830 b	...	8.67 d	0.08 A	Y	...	1	...	...	...
...	...	...	HD 069830 c	...	31.56 d	0.19 A	Y	...	1	...	...	...
...	...	...	HD 069830 d	...	197 d	0.63 A	Y	...	1	...	...	...
08 19 19.05	+01 20 19.9	...	HIP 040774	...	...	...	...	...	...	...	...	...
08 27 36.79	+45 39 10.8	071148	HIP 041484	...	...	...	...	...	...	...	...	...
08 32 51.50	−31 30 03.1	072673	HIP 041926	...	...	...	...	...	...	...	...	...
08 34 31.65	−00 43 33.8	072760	HIP 042074	A	...	...	...	...	...	...	...	...
...	...	...	...	Aa,Ab	...	0.96 a	Y	...	...	R	M	...
08 37 50.29	−06 48 24.8	073350	HIP 042333	...	...	...	...	...	...	...	...	...
08 39 07.90	−22 39 42.8	073752	HIP 042430	A	...	...	...	...	...	...	...	...
...	...	...	...	AB	123 y	1.3 a	Y	O	...	...	...	...
08 39 11.70	+65 01 15.3	072905	π^1 UMa	...	...	...	...	...	...	...	...	...
08 39 50.79	+11 31 21.6	073667	HIP 042499	...	...	...	...	...	...	...	...	...
08 42 07.52	−42 55 46.0	074385	HIP 042697	A	...	...	...	...	...	...	...	...
...	...	...	NLTT 20102	AB	...	45 a	Y	...	...	P	...	...
08 43 18.03	−38 52 56.6	074576	HIP 042808	...	...	...	...	...	...	...	...	...
08 52 16.39	+08 03 46.5	075767	HIP 043557	A	...	...	...	...	...	...	...	...
...	...	...	...	Aa,Ab	10.25 d	...	Y	...	1	...	...	...
...	...	...	...	AB	...	3.4 a	Y	...	...	M	...	...
...	...	...	...	Ba,Bb	...	...	Y	...	2	...	...	...
08 52 35.81	+28 19 50.9	075732	55 Cnc	A	...	...	...	...	...	...	...	...
...	...	...	55 Cnc b	...	14.65 d	0.12 A	Y	...	1	...	...	...
...	...	...	55 Cnc c	...	44.34 d	0.24 A	Y	...	1	...	...	...
...	...	...	55 Cnc d	...	14.29 y	5.77 A	Y	...	1	...	...	...
...	...	...	55 Cnc e	...	2.82 d	0.04 A	Y	...	1	...	...	...
...	...	...	55 Cnc f	...	260 d	0.78 A	Y	...	1	...	...	...
...	...	...	LHS 2063	AB	...	84.7 a	Y	...	...	P	...	...
08 54 17.95	−05 26 04.1	076151	HIP 043726	...	...	...	...	...	...	...	...	...
08 58 43.93	−16 07 57.8	076932	HIP 044075	...	...	...	...	...	...	...	...	...

Continued on Next Page...

TABLE 7.1 – Continued

R.A. (J2000.0) (1)	Decl. (J2000.0) (2)	HD Name (3)	Other Name (4)	Comp ID (5)	Period (6)	Sep (7)	Sts (8)	VB (9)	SB (10)	CP (11)	UR (12)	CH (13)
09 08 51.07	+33 52 56.0	078366	HIP 044897	...	...	...	...	...	...	...	...	...
09 12 17.55	+14 59 45.7	079096	81 Cnc	A	...	...	...	...	...	...	...	...
...	...	...	...	Aa,Ab	2.7 y	0.1 a	Y	O	2	...	...	S
...	...	...	Gl 337C	AE	...	43 a	Y	...	...	P	...	...
...	...	...	...	Ea,Eb	...	0.53 a	Y	...	...	M	...	...
09 14 20.54	+61 25 23.9	079028	HIP 045333	A	...	...	...	...	...	...	...	...
...	...	...	...	Aa,Ab	16.24 d	...	Y	...	1	...	...	...
09 17 53.46	+28 33 37.9	079969	HIP 045617	A	...	...	...	...	...	...	...	...
...	...	...	...	AB	34.17 y	0.8 a	Y	O	...	...	M	...
09 22 25.95	+40 12 03.8	080715	HIP 045963	A	...	...	...	...	...	...	...	...
...	...	...	...	Aa,Ab	3.8 d	...	Y	...	2	...	...	...
09 30 28.09	−32 06 12.2	082342	HIP 046626	A	...	...	...	...	...	...	...	...
...	...	...	...	AB	...	12 a	Y	...	...	P	...	...
09 32 25.57	−11 11 04.7	082558	HIP 046816	...	...	...	...	...	...	...	...	...
09 32 43.76	+26 59 18.7	082443	HIP 046843	A	...	...	...	...	...	...	...	...
...	...	...	NLTT 22015	AB	...	65.2 a	Y	...	...	P	...	...
09 35 39.50	+35 48 36.5	082885	HIP 047080	A	...	...	...	...	...	...	...	...
...	...	...	...	AB	201 y	5.8 a	Y	P	...	...	M	...
09 42 14.42	−23 54 56.1	084117	HIP 047592	...	...	...	...	...	...	...	...	...
09 48 35.37	+46 01 15.6	084737	HIP 048113	...	...	...	...	...	...	...	...	...
10 01 00.66	+31 55 25.2	086728	HIP 049081	A	...	...	...	...	...	...	...	...
...	...	...	GJ 376 B	AB	...	133 a	Y	...	...	P	...	...
...	...	...	...	Ba,Bb	...	...	M	...	...	...	L	...
10 04 37.66	−11 43 46.9	087424	HIP 049366	...	...	...	...	...	...	...	...	...
10 08 43.14	+34 14 32.1	087883	HIP 049699	...	...	...	...	...	...	...	...	...
10 13 24.73	−33 01 54.2	088742	HIP 050075	...	...	...	...	...	...	...	...	...
10 17 14.54	+23 06 22.4	089125	HIP 050384	A	...	...	...	...	...	...	...	...
...	...	...	GJ 387 B	AB	...	7.7 a	Y	...	...	P	...	...
10 18 51.95	+44 02 54.0	089269	HIP 050505	...	...	...	...	...	...	...	...	...
10 23 55.27	−29 38 43.9	090156	HIP 050921	...	...	...	...	...	...	...	...	...
10 28 03.88	+48 47 05.6	090508	HIP 051248	A	...	...	...	...	...	...	...	...
...	...	...	LHS 2266	AB	765 y	4.7 a	Y	P	...	...	...	...
10 30 37.58	+55 58 49.9	090839	HIP 051459	A	...	...	...	...	...	...	...	...
...	...	...	HD 237903	AB	...	122.5 a	Y	...	...	T	...	...
...	...	...	...	Ba,Bb	...	...	M	...	V	...	...	...
10 31 21.82	−53 42 55.7	091324	HIP 051523	...	...	...	...	...	...	...	...	...
10 35 11.27	+84 23 57.6	090343	HIP 051819	...	...	...	...	...	...	...	...	...
10 36 32.38	−12 13 48.4	091889	HIP 051933	...	...	...	...	...	...	...	...	...
10 42 13.32	−13 47 15.8	092719	HIP 052369	...	...	...	...	...	...	...	...	...
10 43 28.27	−29 03 51.4	092945	HIP 052462	...	...	...	...	...	...	...	...	...
10 56 30.80	+07 23 18.5	094765	HIP 053486	...	...	...	...	...	...	...	...	...
10 59 27.97	+40 25 48.9	095128	47 UMa	A	...	...	...	...	...	...	...	...
...	...	...	47 UMa b	...	2.97 y	2.11 A	Y	...	1	...	...	...
...	...	...	47 UMa c	...	6.00 y	3.39 A	Y	...	1	...	...	...
11 04 41.47	−04 13 15.9	096064	HIP 054155	A	...	...	...	...	...	...	...	...
...	...	...	NLTT 26194	A,BC	...	11.8 a	Y	...	...	P	...	...
...	...	...	BD-033040C	BC	23.23 y	0.3 a	Y	O	V	...	...	...
11 08 14.01	+38 25 35.9	096612	HIP 054426	...	...	...	...	...	...	...	...	...
11 12 01.19	−26 08 12.0	097343	HIP 054704	...	...	...	...	...	...	...	...	...
11 12 32.35	+35 48 50.7	097334	HIP 054745	A	...	...	...	...	...	...	...	...
...	...	...	Gl 417B	AE	...	89.7 a	Y	...	...	R	...	...
...	...	...	...	Ea,Eb	...	0.1 a	Y	...	...	M	...	...
11 14 33.16	+25 42 37.4	097658	HIP 054906	...	...	...	...	...	...	...	...	...
11 18 10.95	+31 31 45.7	098230	ξ UMa B	B[a]	...	...	...	...	...	...	...	...
...	...	...	...	Ba,Bb	3.98 d	26 m	Y	...	1	...	...	...
...	...	...	HD 98231	AB	59.88 y	1.6 a	Y	O	...	...	...	S
...	...	...	...	Aa,Ab	1.84 y	...	Y	U	1	...	...	...
11 18 22.01	−05 04 02.3	098281	HIP 055210	...	...	...	...	...	...	...	...	...
11 26 45.32	+03 00 47.2	099491	83 Leo	A	...	...	...	...	...	...	...	...
...	...	...	HD 99492	AB	32000 y	28 a	Y	...	...	T	...	...
...	...	...	HD 099492 b	...	17.04 d	0.12 A	Y	...	1	...	...	...
11 31 44.95	+14 21 52.2	100180	88 Leo	A	...	...	...	...	...	...	...	...
...	...	...	...	Aa,Ab	...	0.1 a	M	...	...	R	...	...
...	...	...	NLTT 27656	AB	...	15.3 a	Y	...	...	P	...	...
11 34 29.49	−32 49 52.8	100623	HIP 056452	A	...	...	...	...	...	...	...	...
...	...	...	LHS 309	AB	...	17 a	Y	...	...	M	...	...
11 38 44.90	+45 06 30.3	101177	HIP 056809	A	...	...	...	...	...	...	...	...
...	...	...	LHS 2436	AB	2050 y	9.3 a	Y	P	...	...	M	...
...	...	...	...	Ba,Bb	23.54 d	...	Y	...	2	...	...	...
11 38 59.72	+42 19 43.7	101206	HIP 056829	A	...	...	...	...	...	...	...	...
...	...	...	...	Aa,Ab	12.92 d	...	Y	...	1	...	...	...
11 41 03.02	+34 12 05.9	101501	61 UMa	...	...	...	...	...	...	...	...	...
11 46 31.07	−40 30 01.3	102365	HIP 057443	A	...	...	...	...	...	...	...	...
...	...	...	LHS 313	AB	...	22.9 a	Y	...	...	M	...	...
11 47 15.81	−30 17 11.4	102438	HIP 057507	...	...	...	...	...	...	...	...	...
...	...	...	...	Aa,Ab	...	...	M	...	V	...	...	...
11 50 41.72	+01 45 53.0	102870	β Vir	...	...	...	...	...	...	...	...	...
11 52 58.77	+37 43 07.2	103095	HIP 057939	...	...	...	...	...	...	...	...	...
11 59 10.01	−20 21 13.6	104067	HIP 058451	...	...	...	...	...	...	...	...	...
12 00 44.45	−10 26 45.6	104304	HIP 058576	...	...	...	...	...	...	...	...	...
12 09 37.26	+40 15 07.4	105631	HIP 059280	...	...	...	...	...	...	...	...	...

Continued on Next Page...

TABLE 7.1 – Continued

R.A. (J2000.0) (1)	Decl. (J2000.0) (2)	HD Name (3)	Other Name (4)	Comp ID (5)	Period (6)	Sep (7)	Sts (8)	VB (9)	SB (10)	CP (11)	UR (12)	CH (13)
12 30 50.14	+53 04 35.8	108954	HIP 061053	...	...	...	...	...	...	...	...	...
12 33 31.38	−68 45 20.9	109200	HIP 061291	...	...	...	...	...	...	...	...	...
12 33 44.54	+41 21 26.9	109358	HIP 061317	...	...	...	...	...	...	...	...	...
12 41 44.52	+55 43 28.8	110463	HIP 061946	A	...	...	...	...	...	...	...	...
...	...	...	...	Aa,Ab	...	...	M	...	V	...	...	...
12 44 14.55	+51 45 33.5	110833	HIP 062145	A	...	...	...	...	...	...	...	...
...	...	...	...	Aa,Ab	271.17 d	...	Y	U	1	...	M	...
12 44 59.41	+39 16 44.1	110897	HIP 062207	...	...	...	...	...	...	...	...	...
12 45 14.41	−57 21 28.8	110810	HIP 062229	...	...	...	...	...	...	...	...	...
12 48 32.31	−15 43 10.1	111312	HIP 062505	A	...	...	...	...	...	...	...	...
...	...	...	...	Aa,Ab	2.68 y	0.1 a	Y	...	2	...	M	...
...	...	...	...	Aa,B	...	2.7 a	M	...	...	R	M	...
12 48 47.05	+24 50 24.8	111395	HIP 062523	...	...	...	...	...	...	...	...	...
12 59 01.56	−09 50 02.7	112758	HIP 063366	A	...	...	...	...	...	...	...	...
...	...	...	...	Aa,Ab	103.17 d	...	Y	...	1	...	...	...
...	...	...	...	AB	...	0.8 a	Y	...	...	M	...	...
12 59 32.78	+41 59 12.4	112914	HIP 063406	A	...	...	...	...	...	...	...	...
...	...	...	...	Aa,Ab	1.95 y	...	Y	U	1	...	...	...
13 03 49.66	−05 09 42.5	113449	HIP 063742	A	...	...	...	...	...	...	...	...
...	...	...	...	Aa,Ab	231.23 d	...	Y	U	...	R	M	...
13 11 52.39	+27 52 41.5	114710	β Com	...	...	...	...	...	...	...	...	...
13 12 03.18	−37 48 10.9	114613	HIP 064408	...	...	...	...	...	...	...	...	...
13 12 43.79	−02 15 54.1	114783	HIP 064457	A	...	...	...	...	...	...	...	...
...	...	...	HD 114783 b	...	1.37 y	1.2 a	Y	...	1	...	...	...
13 13 52.23	−45 11 08.9	114853	HIP 064550	...	...	...	...	...	...	...	...	...
13 15 26.45	−87 33 38.5	113283	HIP 064690	A	...	...	...	...	...	...	...	...
...	...	...	...	Aa,Ab	...	...	M	...	...	...	M	...
13 16 46.52	+09 25 27.0	115383	59 Vir	...	...	...	...	...	...	...	...	...
13 16 51.05	+17 01 01.9	115404	HIP 064797	A	...	...	...	...	...	...	...	...
...	...	...	LHS 2714	AB	770 y	7.5 a	Y	P	...	...	M	...
13 18 24.31	−18 18 40.3	115617	61 Vir	...	...	...	...	...	...	...	...	...
13 23 39.15	+02 43 24.0	116442	HIP 065352	A	...	...	...	...	...	...	...	...
...	...	...	HD 116443	AB	...	26.2 a	Y	...	...	T	...	...
13 25 45.53	+56 58 13.8	116956	HIP 065515	...	...	...	...	...	...	...	...	...
13 25 59.86	+63 15 40.6	117043	HIP 065530	...	...	...	...	...	...	...	...	...
13 28 25.81	+13 46 43.6	117176	70 Vir	A	...	...	...	...	...	...	...	...
...	...	...	70 Vir b	...	116.69 d	0.48 A	Y	...	1	...	...	...
13 41 04.17	−34 27 51.0	118972	HIP 066765	...	...	...	...	...	...	...	...	...
13 41 13.40	+56 43 37.8	119332	HIP 066781	...	...	...	...	...	...	...	...	...
13 47 15.74	+17 27 24.9	120136	τ Boo	A	...	...	...	...	...	...	...	...
...	...	...	τ Boo b	...	3.31 d	0.05 A	Y	...	1	...	...	...
...	...	...	HD 120136B	AB	2000 y	2.8 a	Y	P	...	...	M	...
13 51 20.33	−24 23 25.3	120690	HIP 067620	A	...	...	...	...	...	...	...	...
...	...	...	...	Aa,Ab	10.3 y	...	Y	...	1	...	M	...
13 51 40.40	−57 26 08.4	120559	HIP 067655	...	...	...	...	...	...	...	...	...
13 52 35.87	−50 55 18.3	120780	HIP 067742	A	...	...	...	...	...	...	...	...
...	...	...	...	Aa,Ab	...	...	Y	...	...	...	M	...
...	...	...	...	AB	...	5.8 a	Y	...	...	M	...	...
13 54 41.08	+18 23 51.8	121370	η Boo	A	...	...	...	...	...	...	...	...
...	...	...	...	Aa,Ab	1.34 y	...	Y	U	1	...	...	...
13 55 49.99	+14 03 23.4	121560	HIP 068030	...	...	...	...	...	...	...	...	...
14 03 32.35	+10 47 12.4	122742	HIP 068682	A	...	...	...	...	...	...	...	...
...	...	...	...	Aa,Ab	9.9 y	...	Y	U	1	...	M	...
14 11 46.17	−12 36 42.4	124106	HIP 069357	...	...	...	...	...	...	...	...	...
14 12 45.24	−03 19 12.3	124292	HIP 069414	...	...	...	...	...	...	...	...	...
14 15 38.68	−45 00 02.7	124580	HIP 069671	...	...	...	...	...	...	...	...	...
14 16 00.87	−06 00 02.0	124850	ι Vir	A	...	...	...	...	...	...	...	...
...	...	...	...	Aa,Ab	55 y	...	M	U	...	...	...	...
14 19 00.90	−25 48 55.5	125276	HIP 069965	A	...	...	...	...	...	...	...	...
...	...	...	...	Aa,Ab	...	...	M	...	...	...	M	...
14 19 34.86	−05 09 04.3	125455	HIP 070016	A	...	...	...	...	...	...	...	...
...	...	...	LHS 2895	AB	...	8.1 a	Y	...	...	M	...	...
14 23 15.28	+01 14 29.6	126053	HIP 070319	...	...	...	...	...	...	...	...	...
14 29 22.30	+80 48 35.5	128642	HIP 070857	A	...	...	...	...	...	...	...	...
...	...	...	...	Aa,Ab	178.78 d	...	Y	U	1	...	M	...
14 29 36.81	+41 47 45.3	127334	HIP 070873	...	...	...	...	...	...	...	...	...
14 33 28.87	+52 54 31.6	128165	HIP 071181	...	...	...	...	...	...	...	...	...
14 36 00.56	+09 44 47.5	128311	HIP 071395	A	...	...	...	...	...	...	...	...
...	...	...	HD 128311 b	...	1.23 y	1.1 a	Y	...	1	...	...	...
...	...	...	HD 128311 c	...	2.52 y	1.76 A	Y	...	1	...	...	...
14 39 36.50	−60 50 02.3	128620	α Cen	A	...	...	...	...	...	...	...	...
...	...	...	HD 128621	AB	79.9 y	8.8 a	Y	O	2	...	...	...
...	...	...	Proxima Cen	AC	...	7867 a	Y	...	...	T	...	...
14 40 31.11	−16 12 33.4	128987	HIP 071743	...	...	...	...	...	...	...	...	...
14 41 52.46	−75 08 22.1	128400	HIP 071855	...	...	...	...	...	...	...	...	...
14 45 24.18	+13 50 46.7	130004	HIP 072146	...	...	...	...	...	...	...	...	...
14 47 16.10	+02 42 11.6	130307	HIP 072312	...	...	...	...	...	...	...	...	...
14 49 23.72	−67 14 09.5	130042	HIP 072493	A	...	...	...	...	...	...	...	...
...	...	...	...	AB	...	1.5 a	Y	...	...	O	M	...
14 50 15.81	+23 54 42.6	130948	HIP 072567	A	...	...	...	...	...	...	...	...
...	...	...	HD 130948 B	AB	...	2.6 a	Y	...	...	M	...	...

Continued on Next Page...

TABLE 7.1 – Continued

R.A. (J2000.0) (1)	Decl. (J2000.0) (2)	HD Name (3)	Other Name (4)	Comp ID (5)	Period (6)	Sep (7)	Sts (8)	VB (9)	SB (10)	CP (11)	UR (12)	CH (13)
...	...	...	HD 130948 C	BC	...	0.1 a	Y	...	...	M	...	...
14 51 23.38	+19 06 01.7	131156	ξ Boo	A	...	...	...	...	...	...	...	...
...	...	...	HD 131156B	AB	151.6 y	6.3 a	Y	O	...	...	...	...
14 53 23.77	+19 09 10.1	131511	HIP 072848	A	...	...	...	...	...	...	...	...
...	...	...	...	Aa,Ab	125.4 d	...	Y	U	1	...	...	S
14 53 41.57	+23 20 42.6	131582	HIP 072875	A	...	...	...	...	...	...	...	...
...	...	...	...	Aa,Ab	...	...	Y	...	...	...	M	...
14 55 11.04	+53 40 49.2	132142	HIP 073005	...	...	...	...	...	...	...	...	...
14 56 23.04	+49 37 42.4	132254	HIP 073100	...	...	...	...	...	...	...	...	...
14 58 08.80	−48 51 46.8	131923	HIP 073241	A	...	...	...	...	...	...	...	...
...	...	...	...	Aa,Ab	14.87 y	...	Y	...	1	...	M	...
15 03 47.30	+47 39 14.6	133640	44 Boo	A	...	...	...	...	...	...	...	...
...	...	...	NLTT 39210	AB	206 y	1.8 a	Y	O	...	...	M	...
...	...	...	...	Ba,Bb	6.43 h	...	Y	...	2	...	E	...
15 10 44.74	−61 25 20.3	134060	HIP 074273	...	...	...	...	...	...	...	...	...
15 13 50.89	−01 21 05.0	135204	HIP 074537	A	...	...	...	...	...	...	...	...
...	...	...	...	AB	...	0.1 a	Y	...	...	O	...	...
15 15 59.17	+00 47 46.9	135599	HIP 074702	...	...	...	...	...	...	...	...	...
15 19 18.80	+01 45 55.5	136202	HIP 074975	A	...	...	...	...	...	...	...	...
...	...	...	LHS 3060	AB	...	11.4 a	Y	...	...	P	...	...
15 21 48.15	−48 19 03.5	136352	HIP 075181	...	...	...	...	...	...	...	...	...
15 22 36.69	−10 39 40.0	136713	HIP 075253	...	...	...	...	...	...	...	...	...
15 22 46.83	+18 55 08.3	136923	HIP 075277	...	...	...	...	...	...	...	...	...
15 23 12.31	+30 17 16.1	137107	η CrB	A	...	...	...	...	...	...	...	...
...	...	...	HD 137108	AB	41.59 y	0.6 a	Y	O	2	...	...	...
...	...	...	GJ 584 C	AB,E	...	193.5 a	Y	...	...	S	...	...
15 28 09.61	−09 20 53.1	137763	HIP 075718	A	...	...	...	...	...	...	...	...
...	...	...	...	Aa,Ab	2.44 y	0.1 a	Y	U	2	R	M	S
...	...	...	HD 137778	AB	...	52.3 a	Y	...	...	T	...	...
...	...	...	GJ 586C	AC	...	1212 a	Y	...	...	T	...	...
15 29 11.18	+80 26 55.0	139777	HIP 075809	A	...	...	...	...	...	...	...	...
...	...	...	HD 139813	AB	...	31.3 a	Y	...	...	T	...	...
15 36 02.22	+39 48 08.9	139341	HIP 076382	A	...	...	...	...	...	...	...	...
...	...	...	...	AB	55.6 y	0.9 a	Y	O	...	...	M	...
...	...	...	HD 139323	AB,C	...	121.5 a	Y	...	...	T	...	...
15 44 01.82	+02 30 54.6	140538	ψ Ser	A	...	...	...	...	...	...	...	...
...	...	...	...	AB	...	4.4 a	Y	...	...	O	M	...
15 46 26.61	+07 21 11.1	141004	HIP 077257	...	...	...	...	...	...	...	...	...
15 47 29.10	−37 54 58.7	140901	HIP 077358	A	...	...	...	...	...	...	...	...
...	...	...	NLTT 41169	AB	...	15 a	Y	...	...	M	...	...
15 48 09.46	+01 34 18.3	141272	HIP 077408	A	...	...	...	...	...	...	...	...
...	...	...	...	AB	...	17.9 a	Y	...	...	S	...	...
15 52 40.54	+42 27 05.5	142373	χ Her	...	...	...	...	...	...	...	...	...
15 53 12.10	+13 11 47.8	142267	39 Ser	A	...	...	...	...	...	...	...	...
...	...	...	...	Aa,Ab	138.56 d	...	Y	...	1	...	...	...
16 01 02.66	+33 18 12.6	143761	ρ CrB	A	...	...	...	...	...	...	...	...
...	...	...	ρ CrB b	...	39.85 d	0.22 A	M	...	1	...	...	...
...	...	...	...	Aa,Ab	40.18 d	...	M	U	...	...	...	...
16 01 53.35	+58 33 54.9	144284	θ Dra	A	...	...	...	...	...	...	...	...
...	...	...	...	Aa,Ab	3.07 d	...	Y	...	2	...	...	...
16 04 03.71	+25 15 17.4	144287	HIP 078709	A	...	...	...	...	...	...	...	...
...	...	...	...	Aa,Ab	12.19 y	0.2 a	Y	...	1	...	M	...
16 04 56.79	+39 09 23.4	144579	HIP 078775	A	...	...	...	...	...	...	...	...
...	...	...	LHS 3150	AB	...	70.3 a	Y	...	...	P	...	...
16 06 29.60	+38 37 56.1	144872	HIP 078913	...	...	...	...	...	...	...	...	...
16 09 42.79	−56 26 42.5	144628	HIP 079190	...	...	...	...	...	...	...	...	...
16 10 24.31	+43 49 03.5	145675	14 Her	A	...	...	...	...	...	...	...	...
...	...	...	14 Her b	...	4.86 y	2.77 A	Y	...	1	...	...	...
16 13 18.45	+13 31 36.9	145958	HIP 079492	A	...	...	...	...	...	...	...	...
...	...	...	NLTT 42272	AB	1354 y	4.1 a	Y	P	...	...	...	...
...	...	...	...	AD	...	1623.26 a	M	...	...	S	...	...
16 13 48.56	−57 34 13.8	145417	HIP 079537	...	...	...	...	...	...	...	...	...
16 14 11.93	−31 39 49.1	145825	HIP 079578	A	...	...	...	...	...	...	...	...
...	...	...	...	Aa,Ab	7.14 y	...	Y	...	1	...	M	...
16 14 40.85	+33 51 31.0	146361	σ^2 CrB	A	...	...	...	...	...	...	...	...
...	...	...	...	Aa,Ab	1.14 d	...	Y	O	2	...	...	V
...	...	...	HD 146362	AB	889 y	7.1 a	Y	P	...	...	M	...
...	...	...	HIP 79551	AE	...	633.7 a	Y	...	...	T	...	...
...	...	...	σ CrB D	Ea,Eb	52 y	...	Y	U	...	...	...	...
16 15 37.27	−08 22 10.0	146233	18 Sco	...	...	...	...	...	...	...	...	...
16 24 01.29	−39 11 34.7	147513	HIP 080337	A	...	...	...	...	...	...	...	...
...	...	...	HD 147513 b	...	1.48 y	1.26 A	Y	...	1	...	...	...
...	...	...	...	AB	...	345 a	Y	...	...	T	...	...
16 24 19.81	−13 38 30.0	147776	HIP 080366	A	...	...	...	...	...	...	...	...
...	...	...	...	AC	...	6.4 a	M	...	...	R	...	...
...	...	...	...	AD	...	9.7 a	Y	...	...	M	...	...
16 28 28.14	−70 05 03.8	147584	ζ TrA	A	...	...	...	...	...	...	...	...
...	...	...	...	Aa,Ab	12.98 d	...	Y	U	1	...	M	...
16 28 52.67	+18 24 50.6	148653	HIP 080725	A	...	...	...	...	...	...	...	...
...	...	...	LHS 3204	AB	224 y	2.2 a	Y	O	...	...	M	...
16 31 30.03	−39 00 44.2	148704	HIP 080925	A	...	...	...	...	...	...	...	...

Continued on Next Page...

TABLE 7.1 – Continued

R.A. (J2000.0) (1)	Decl. (J2000.0) (2)	HD Name (3)	Other Name (4)	Comp ID (5)	Period (6)	Sep (7)	Sts (8)	VB (9)	SB (10)	CP (11)	UR (12)	CH (13)
...	...	...	...	Aa,Ab	31.86 d	...	Y	...	2	...	M	...
16 36 21.45	−02 19 28.5	149661	HIP 081300	...	...	...	...	...	...	...	...	...
16 37 08.43	+00 15 15.6	149806	HIP 081375	A	...	...	...	...	...	...	...	...
...	...	...	...	AB	...	6.3 a	Y	...	...	P	...	...
16 39 04.14	−58 15 29.5	149612	HIP 081520	...	...	...	...	...	...	...	...	...
16 42 38.58	+68 06 07.8	151541	HIP 081813	...	...	...	...	...	...	...	...	...
16 52 58.80	−00 01 35.1	152391	HIP 082588	...	...	...	...	...	...	...	...	...
16 57 53.18	+47 22 00.1	153557	HIP 083020	A	...	...	...	...	...	...	...	...
...	...	...	...	AB	...	4.9 a	Y	...	...	M	M	...
...	...	...	HD 153525	AC	...	112.1 a	Y	...	...	T	...	...
17 02 36.40	+47 04 54.8	154345	HIP 083389	A	...	...	...	...	...	...	...	...
...	...	...	HD 154345 b	...	9.14 y	4.19 A	Y	...	1	...	...	...
17 04 27.84	−28 34 57.6	154088	HIP 083541	...	...	...	...	...	...	...	...	...
17 05 16.82	+00 42 09.2	154417	HIP 083601	...	...	...	...	...	...	...	...	...
17 10 10.35	−60 43 43.6	154577	HIP 083990	...	...	...	...	...	...	...	...	...
17 12 37.62	+18 21 04.3	155712	HIP 084195	...	...	...	...	...	...	...	...	...
17 15 20.98	−26 36 10.2	155885	36 Oph	A	...	...	...	...	...	...	...	...
...	...	...	...	AB	470.9 y	5.1 a	Y	P	...	...	...	...
...	...	...	HD 156026	AC	...	731.6 a	Y	...	...	T	...	...
17 19 03.83	−46 38 10.4	156274	41 Ara	A	...	...	...	...	...	...	...	...
...	...	...	...	Aa,Ab	88.03 d	...	Y	...	1	...	M	...
...	...	...	NLTT 44525	AB	693.24 y	15 a	Y	P	...	...	...	...
17 20 39.57	+32 28 03.9	157214	72 Her	...	...	...	...	...	...	...	...	...
17 22 51.29	−02 23 17.4	157347	HIP 085042	A	...	...	...	...	...	...	...	...
...	...	...	HR 6465	AB	...	49 a	Y	...	...	P	...	...
17 25 00.10	+67 18 24.1	158633	HIP 085235	...	...	...	...	...	...	...	...	...
17 30 16.43	+47 24 07.9	159062	HIP 085653	...	...	...	...	...	...	...	...	...
17 30 23.80	−01 03 46.5	158614	HIP 085667	A	...	...	...	...	...	...	...	...
...	...	...	...	AB	46.34 y	0.3 a	Y	O	2	...	M	...
17 32 00.99	+34 16 16.1	159222	HIP 085810	...	...	...	...	...	...	...	...	...
17 34 59.59	+61 52 28.4	160269	26 Dra	A	...	...	...	...	...	...	...	...
...	...	...	...	AB	74.16 y	1.55 a	Y	O	1	...	M	...
...	...	...	HIP 86087	AB,C	...	737.6 a	Y	...	...	T	...	...
17 39 16.92	+03 33 18.9	160346	HIP 086400	A	...	...	...	...	...	...	...	...
...	...	...	...	Aa,Ab	83.73 d	...	Y	U	1	...	...	...
17 41 58.10	+72 09 24.9	162004	31 Dra B	B[a]	...	...	...	...	...	...	...	...
...	...	...	HD 162003	AB	12500 y	31 a	Y	P	...	T	...	...
17 43 15.64	+21 36 33.1	161198	HIP 086722	A	...	...	...	...	...	...	...	...
...	...	...	...	Aa,Ab	7.0 y	0.1 a	Y	P	1	...	M	...
17 44 08.70	−51 50 02.6	160691	μ Ara	A	...	...	...	...	...	...	...	...
...	...	...	HD 160691 b	...	1.79 y	1.5 a	Y	...	1	...	...	...
...	...	...	HD 160691 c	...	8.18 y	4.17 A	Y	...	1	...	...	...
...	...	...	HD 160691 d	...	9.55 d	0.09 A	Y	...	1	...	...	...
...	...	...	HD 160691 e	...	310.55 d	0.92 A	Y	...	1	...	...	...
17 46 27.53	+27 43 14.4	161797	μ Her A	A	...	...	...	...	...	...	...	...
...	...	...	...	Aa,Ab	65.0 y	1.43 a	Y	U	V	R	M	...
...	...	...	NLTT 45430	Aa,BC	...	34 a	Y	...	...	P	...	...
...	...	...	...	BC	43.2 y	1.1 a	Y	O	...	...	...	...
17 53 29.94	+21 19 31.1	...	HIP 087579	...	...	...	...	...	...	...	...	...
18 02 30.86	+26 18 46.8	164922	HIP 088348	A	...	...	...	...	...	...	...	...
...	...	...	HD 164922 b	...	3.16 y	2.11 A	Y	...	1	...	...	...
18 05 27.29	+02 30 00.4	165341	70 Oph	A	...	...	...	...	...	...	...	...
...	...	...	NLTT 45900	AB	121.2 y	1.59 a	Y	O	2	...	M	...
18 05 37.46	+04 39 25.8	165401	HIP 088622	A	...	...	...	...	...	...	...	...
...	...	...	...	Aa,Ab	...	...	Y	...	...	...	M	...
18 06 23.72	−36 01 11.2	165185	HIP 088694	...	...	...	...	...	...	...	...	...
18 07 01.54	+30 33 43.7	165908	HIP 088745	A	...	...	...	...	...	...	...	...
...	...	...	...	Aa,Ab	...	0.2 a	M	...	...	R	...	...
...	...	...	...	AB	56.4 y	0.97 a	Y	O	...	...	...	...
18 09 37.42	+38 27 28.0	166620	HIP 088972	...	...	...	...	...	...	...	...	...
18 10 26.16	−62 00 07.9	165499	ι Pav	A	...	...	...	...	...	...	...	...
...	...	...	...	Aa,Ab	...	...	Y	...	...	...	M	...
18 15 32.46	+45 12 33.5	168009	HIP 089474	...	...	...	...	...	...	...	...	...
18 19 40.13	−63 53 11.6	167425	HIP 089805	A	...	...	...	...	...	...	...	...
...	...	...	...	AB	...	7.8 a	Y	...	...	P	M	...
18 31 18.96	−18 54 31.7	170657	HIP 090790	...	...	...	...	...	...	...	...	...
18 38 53.40	−21 03 06.7	172051	HIP 091438	...	...	...	...	...	...	...	...	...
18 40 54.88	+31 31 59.1	...	HIP 091605	A	...	...	...	...	...	...	...	...
...	...	...	LHS 3402	AB	...	9.3 a	Y	...	...	O	...	...
18 55 18.80	−37 29 54.1	175073	HIP 092858	...	...	...	...	...	...	...	...	...
18 55 53.22	+23 33 23.9	175742	HIP 092919	A	...	...	...	...	...	...	...	...
...	...	...	...	Aa,Ab	2.88 d	...	Y	...	1	...	...	...
18 57 01.61	+32 54 04.6	176051	HIP 093017	A	...	...	...	...	...	...	...	...
...	...	...	...	AB	61.39 y	0.8 a	Y	O	1	...	...	...
18 58 51.00	+30 10 50.3	176377	HIP 093185	...	...	...	...	...	...	...	...	...
19 06 25.11	−37 03 48.4	177474	γ CrA A	A	...	...	...	...	...	...	...	...
...	...	...	...	AB	121.8 y	1.21 a	Y	O	...	...	M	...
19 06 52.46	−37 48 38.4	177565	HIP 093858	...	...	...	...	...	...	...	...	...
19 07 57.32	+16 51 12.2	178428	HIP 093966	A	...	...	...	...	...	...	...	...
...	...	...	...	Aa,Ab	21.96 d	...	Y	...	1	...	...	...
19 12 05.03	+49 51 20.7	179957	HIP 094336	A	...	...	...	...	...	...	...	...

Continued on Next Page...

TABLE 7.1 – Continued

R.A. (J2000.0) (1)	Decl. (J2000.0) (2)	HD Name (3)	Other Name (4)	Comp ID (5)	Period (6)	Sep (7)	Sts (8)	VB (9)	SB (10)	CP (11)	UR (12)	CH (13)
...	...	...	HD 179958	AB	3100 y	7.65 a	Y	P	...	...	M	...
19 12 11.36	+57 40 19.1	180161	HIP 094346	...	...	...	...	...	...	...	...	...
19 21 29.76	−34 59 00.6	181321	HIP 095149	A	...	...	...	...	...	...	...	...
...	...	...	...	Aa,Ab	...	...	Y	...	...	...	M	...
19 23 34.01	+33 13 19.1	182488	HIP 095319	...	...	...	...	...	...	...	...	...
19 24 58.20	+11 56 39.9	182572	31 Aql	...	...	...	...	...	...	...	...	...
19 31 07.97	+58 35 09.6	184467	HIP 095995	A	...	...	...	...	...	...	...	...
...	...	...	...	AB	1.35 y	0.1 a	Y	O	2	...	...	...
19 32 06.70	−11 16 29.8	183870	HIP 096085	...	...	...	...	...	...	...	...	...
19 32 21.59	+69 39 40.2	185144	σ Dra	...	...	...	...	...	...	...	...	...
19 33 25.55	+21 50 25.2	184385	HIP 096183	...	...	...	...	...	...	...	...	...
19 35 55.61	+56 59 02.0	185414	HIP 096395	A	...	...	...	...	...	...	...	...
...	...	...	...	Aa,Ab	13.08 y	...	Y	...	1	...	...	...
19 41 48.95	+50 31 30.2	186408	16 Cyg A	A	...	...	...	...	...	...	...	...
...	...	...	...	Aa,Ab	...	3.4 a	Y	...	V	R	...	...
...	...	...	HD 186427	Aa,B	18212 y	40.0 a	Y	...	...	T	...	...
...	...	...	16 Cyg B b	...	2.19 y	1.68 A	Y	...	1	...	...	...
19 45 33.53	+33 36 07.2	186858	HIP 097222	F[a]	...	...	...	...	...	...	...	...
...	...	...	...	Fa,Fb	...	...	M	...	V	...	...	...
...	...	...	HD 225732	FG	...	26 a	Y	...	...	P	...	...
...	...	...	HD 187013	AF	...	780 a	Y	...	...	T	...	...
...	...	...	...	AB	232 y	2.46 a	Y	O	...	...	M	...
19 51 01.64	+10 24 56.6	187691	HIP 097675	A	...	...	...	...	...	...	...	...
...	...	...	...	AC	...	22.5 a	Y	...	...	P	...	...
19 59 47.34	−09 57 29.7	189340	HIP 098416	A	...	...	...	...	...	...	...	...
...	...	...	...	AB	4.90 y	0.2 a	Y	O	2	...	M	...
20 00 43.71	+22 42 39.1	189733	HIP 098505	A	...	...	...	...	...	...	...	...
...	...	...	HD 189733 b	...	2.22 d	0.03 A	Y	...	1	...	E	...
20 02 34.16	+15 35 31.5	190067	HIP 098677	A	...	...	...	...	...	...	...	...
...	...	...	...	AB	...	2.9 a	Y	...	...	M	...	...
20 03 37.41	+29 53 48.5	190360	HIP 098767	A	...	...	...	...	...	...	...	...
...	...	...	HD 190360 b	...	7.92 y	3.92 A	Y	...	1	...	...	...
...	...	...	HD 190360 c	...	17.10 d	0.13 A	Y	...	1	...	...	...
...	...	...	LHS 3509	AB	...	178.2 a	Y	...	...	T	...	...
20 03 52.13	+23 20 26.5	190404	HIP 098792	...	...	...	...	...	...	...	...	...
20 04 06.22	+17 04 12.6	190406	HIP 098819	A	...	...	...	...	...	...	...	...
...	...	...	HD 354613	Aa,Ab	...	0.79 a	Y	...	...	M	...	...
20 04 10.05	+25 47 24.8	190470	HIP 098828	...	...	...	...	...	...	...	...	...
20 05 09.78	+38 28 42.4	190771	HIP 098921	A	...	...	...	...	...	...	...	...
...	...	...	...	Aa,Ab	...	...	Y	...	V	...	M	...
20 05 32.76	−67 19 15.2	189567	HIP 098959	...	...	...	...	...	...	...	...	...
20 07 35.09	−55 00 57.6	190422	HIP 099137	...	...	...	...	...	...	...	...	...
20 08 43.61	−66 10 55.4	190248	δ Pav	...	...	...	...	...	...	...	...	...
20 09 34.30	+16 48 20.8	191499	HIP 099316	A	...	...	...	...	...	...	...	...
...	...	...	ADS 13434B	AB	...	4.45 a	Y	...	...	P	M	...
20 11 06.07	+16 11 16.8	191785	HIP 099452	A	...	...	...	...	...	...	...	...
...	...	...	...	AE	...	103.8 a	Y	...	...	P	...	...
20 11 11.94	−36 06 04.4	191408	HIP 099461	A	...	...	...	...	...	...	...	...
...	...	...	LHS 487	AB	...	7.1 a	Y	...	...	O	M	...
20 13 59.85	−00 52 00.8	192263	HIP 099711	A	...	...	...	...	...	...	...	...
...	...	...	HD 192263 b	...	24.35 d	0.15 A	Y	...	1	...	...	...
20 15 17.39	−27 01 58.7	192310	HIP 099825	...	...	...	...	...	...	...	...	...
20 17 31.33	+66 51 13.3	193664	HIP 100017	A	...	...	...	...	...	...	...	...
...	...	...	...	Aa,Ab	...	...	M	...	...	...	M	...
20 27 44.24	−30 52 04.2	194640	HIP 100925	...	...	...	...	...	...	...	...	...
20 32 23.70	−09 51 12.2	195564	HIP 101345	A	...	...	...	...	...	...	...	...
...	...	...	LTT 8128	AB	...	4.4 a	Y	...	...	M	M	...
20 32 51.64	+41 53 54.5	195987	HIP 101382	A	...	...	...	...	...	...	...	...
...	...	...	...	Aa,Ab	57.32 d	...	Y	O	2	...	M	...
20 40 02.64	−60 32 56.0	196378	ϕ^2 Pav	...	...	...	...	...	...	...	...	...
20 40 11.76	−23 46 25.9	196761	HIP 101997	...	...	...	...	...	...	...	...	...
20 40 45.14	+19 56 07.9	197076	HIP 102040	A	...	...	...	...	...	...	...	...
...	...	...	NLTT 49681	AC	...	125.1 a	Y	...	...	P	...	...
20 43 16.00	−29 25 26.1	197214	HIP 102264	...	...	...	...	...	...	...	...	...
20 49 16.23	+32 17 05.2	198425	HIP 102766	A	...	...	...	...	...	...	...	...
...	...	...	...	Aa,Ab	...	...	M	...	V	...	...	...
...	...	...	NLTT 49961	AB	...	33.0 a	Y	...	...	P	...	...
20 56 47.33	−26 17 47.0	199260	HIP 103389	...	...	...	...	...	...	...	...	...
20 57 40.07	−44 07 45.7	199288	HIP 103458	...	...	...	...	...	...	...	...	...
21 02 40.76	+45 53 05.2	200560	HIP 103859	C	...	...	...	...	...	...	...	...
...	...	...	GJ 816.1B	CD[c]	...	3.3 a	Y	...	...	M	M	...
21 07 10.38	−13 55 22.6	200968	HIP 104239	A	...	...	...	...	...	...	...	...
...	...	...	GJ 819B	AB	...	4.31 a	Y	...	...	O	M	...
21 09 20.74	−82 01 38.1	199509	HIP 104436	...	...	...	...	...	...	...	...	...
21 09 22.45	−73 10 22.7	200525	HIP 104440	A	...	...	...	...	...	...	...	...
...	...	...	...	AB	5.87 y	0.2 a	Y	U	...	R	...	...
...	...	...	NLTT 50542	AB,C	...	7.2 a	Y	...	...	M	...	...
21 14 28.82	+10 00 25.1	202275	δ Equ	A	...	...	...	...	...	...	...	...
...	...	...	...	AB	5.70 y	0.3 a	Y	O	2	...	...	S
21 18 02.97	+00 09 41.7	202751	HIP 105152	...	...	...	...	...	...	...	...	...
21 18 27.27	−43 20 04.7	202628	HIP 105184	...	...	...	...	...	...	...	...	...

Continued on Next Page...

TABLE 7.1 – Continued

R.A. (J2000.0) (1)	Decl. (J2000.0) (2)	HD Name (3)	Other Name (4)	Comp ID (5)	Period (6)	Sep (7)	Sts (8)	VB (9)	SB (10)	CP (11)	UR (12)	CH (13)
21 19 45.62	−26 21 10.4	202940	HIP 105312	A	...	...	...	...	...	...	...	...
...	...	...	...	Aa,Ab	21.35 d	...	Y	...	1	...	...	...
...	...	...	LHS 3656	AB	261.62 y	3.2 a	Y	P	...	...	M	...
21 24 40.64	−68 13 40.2	203244	HIP 105712	...	...	...	...	...	...	...	...	...
21 26 58.45	−56 07 30.9	203850	HIP 105905	...	...	...	...	...	...	...	...	...
21 27 01.33	−44 48 30.9	203985	HIP 105911	A	...	...	...	...	...	...	...	...
...	...	...	...	Aa,Ab	...	...	Y	...	...	...	M	...
...	...	...	LTT 8515	AB	...	88.0 a	Y	...	...	P	...	...
21 36 41.24	−50 50 43.4	205390	HIP 106696	...	...	...	...	...	...	...	...	...
21 40 29.77	−74 04 27.4	205536	HIP 107022	...	...	...	...	...	...	...	...	...
21 44 08.58	+28 44 33.5	206826	μ Cyg A	A	...	...	...	...	...	...	...	...
...	...	...	HD 206827	AB	789 y	1.9 a	Y	P	...	...	M	...
21 44 31.33	+14 46 19.0	206860	HIP 107350	A	...	...	...	...	...	...	...	...
...	...	...	HN Peg B	AB	...	43.2 a	Y	...	...	M	...	...
21 48 00.05	−40 15 21.9	207144	HIP 107625	...	...	...	...	...	...	...	...	...
21 48 15.75	−47 18 13.0	207129	HIP 107649	...	...	...	...	...	...	...	...	...
21 53 05.35	+20 55 49.9	208038	HIP 108028	...	...	...	...	...	...	...	...	...
21 54 45.04	+32 19 42.9	208313	HIP 108156	...	...	...	...	...	...	...	...	...
22 09 29.87	−07 32 55.1	210277	HIP 109378	A	...	...	...	...	...	...	...	...
...	...	...	HD 210277 b	...	1.21 y	1.1 a	Y	...	1	...	...	...
22 11 11.91	+36 15 22.8	210667	HIP 109527	...	...	...	...	...	...	...	...	...
22 14 38.65	−41 22 54.0	210918	HIP 109821	...	...	...	...	...	...	...	...	...
22 15 54.14	+54 40 22.4	211472	HIP 109926	A	...	...	...	...	...	...	...	...
...	...	...	GJ 4269	AT	...	77.2 a	Y	...	...	P	...	...
22 18 15.62	−53 37 37.5	211415	HIP 110109	A	...	...	...	...	...	...	...	...
...	...	...	...	AB	...	3.4 a	Y	...	...	O	M	...
22 24 56.39	−57 47 50.7	212330	HIP 110649	A	...	...	...	...	...	...	...	...
...	...	...	...	Aa,Ab	...	...	Y	...	...	...	M	...
22 25 51.16	−75 00 56.5	212168	HIP 110712	A	...	...	...	...	...	...	...	...
...	...	...	HIP 110719	AB	...	20.8 a	Y	...	...	P	...	...
22 39 50.77	+04 06 58.0	214683	HIP 111888	A	...	...	...	...	...	...	...	...
22 42 36.88	−47 12 38.9	214953	HIP 112117	A	...	...	...	...	...	...	...	...
...	...	...	NLTT 54607	AB	...	7.8 a	Y	...	...	P	M	...
22 43 21.30	−06 24 03.0	215152	HIP 112190	...	...	...	...	...	...	...	...	...
22 46 41.58	+12 10 22.4	215648	ξ Peg	A	...	...	...	...	...	...	...	...
...	...	...	...	AB	...	11.1 a	Y	...	...	O	...	...
22 47 31.87	+83 41 49.3	216520	HIP 112527	...	...	...	...	...	...	...	...	...
22 51 26.36	+13 58 11.9	216259	HIP 112870	...	...	...	...	...	...	...	...	...
22 57 27.98	+20 46 07.8	217014	51 Peg	A	...	...	...	...	...	...	...	...
...	...	...	51 Peg b	...	4.23 d	0.05 A	Y	...	1	...	...	...
22 58 15.54	−02 23 43.4	217107	HIP 113421	A	...	...	...	...	...	...	...	...
...	...	...	HD 217107 b	...	7.13 d	0.07 A	Y	...	1	...	...	...
...	...	...	HD 217107 c	...	9.18 y	4.41 A	M	...	1	...	...	...
...	...	...	...	AB	...	0.3 a	M	...	...	R	...	...
23 03 04.98	+20 55 06.9	217813	HIP 113829	...	...	...	...	...	...	...	...	...
23 10 50.08	+45 30 44.2	218868	HIP 114456	A	...	...	...	...	...	...	...	...
...	...	...	...	AB	...	50 a	Y	...	...	P	...	...
23 13 16.98	+57 10 06.1	219134	HIP 114622	...	...	...	...	...	...	...	...	...
23 16 18.16	+30 40 12.8	219538	HIP 114886	...	...	...	...	...	...	...	...	...
23 16 42.30	+53 12 48.5	219623	HIP 114924	...	...	...	...	...	...	...	...	...
23 16 57.69	−62 00 04.3	219482	HIP 114948	...	...	...	...	...	...	...	...	...
23 19 26.63	+79 00 12.7	220140	HIP 115147	A	...	...	...	...	...	...	...	...
...	...	...	NLTT 56532	AB	...	10.8 a	Y	...	...	M	...	...
...	...	...	...	AC	...	962.6 a	Y	...	...	T	...	...
23 21 36.51	+44 05 52.4	220182	HIP 115331	...	...	...	...	...	...	...	...	...
23 23 04.89	−10 45 51.3	220339	HIP 115445	...	...	...	...	...	...	...	...	...
23 31 22.21	+59 09 55.9	221354	HIP 116085	...	...	...	...	...	...	...	...	...
23 35 25.61	+31 09 40.7	221851	HIP 116416	...	...	...	...	...	...	...	...	...
23 37 58.49	+46 11 58.0	222143	HIP 116613	...	...	...	...	...	...	...	...	...
23 39 37.39	−72 43 19.8	222237	HIP 116745	...	...	...	...	...	...	...	...	...
23 39 51.31	−32 44 36.3	222335	HIP 116763	...	...	...	...	...	...	...	...	...
23 39 57.04	+05 37 34.6	222368	ι Psc	...	...	...	...	...	...	...	...	...
23 52 25.32	+75 32 40.5	223778	HIP 117712	A	...	...	...	...	...	...	...	...
...	...	...	...	Aa,Ab	7.75 d	...	Y	O	2	...	...	V
...	...	...	...	AB	290 y	4.6 a	Y	P	...	...	M	...
23 56 10.67	−39 03 08.4	224228	HIP 118008	...	...	...	...	...	...	...	...	...
23 58 06.82	+50 26 51.6	224465	HIP 118162	A	...	...	...	...	...	...	...	...
...	...	...	...	Aa,Ab	52.41 d	...	Y	...	1	...	...	...

[a] The sample star is not the system's primary, which is identified as component A below. [b] The brightest component of the system is HD 25998, but is designated as component E in the WDS. The A component is the wide CPM companion, HD 25893, which is about 2 magnitudes fainter and itself a visual binary. I have retained the component designations of the WDS, so the fainter visual pair is AB and the wide CPM companion is E. WDS components C and D are optical, and E itself might have a close companion, as evidenced by its accelerating proper motion (see Table 5.2). [c] WDS lists these entries for HD 200595, a bright binary 153″ away from the sample star HD 200560, but one that is not physically associated to it. HD 200560 is itself is a close CPM pair and listed in the WDS as CD. I have retained the WDS designations, which makes C and D the only physically associated components of this system.

7.3 Observed Stellar Multiplicity

The multiplicity of the 454 solar-type stars studied here is summarized in Table 7.2 below. Column 1 identifies the multiplicity order and Column 2 lists the corresponding number of stars from observations. Column 3 contains the implied percentage of stars along with its uncertainty, obtained by bootstrap analysis as described below. Columns 4 and 5 contain the number and percentages when all candidate companions are considered to be real.

The uncertainties were estimated by performing a bootstrap analysis on the data over 10,000 iterations. This analysis involves a resampling of the observed statistics. For each iteration, a new sample of 454 stars is created by randomly selecting stars from the observed sample of 454 stars. Every such sample may include the same star more than once and leave out other stars altogether. The multiplicity frequencies are then computed for each iteration. The distribution shown in Figure 7.2 is the result for the 10,000 iterations. The mean and uncertainty of the resulting statistic are the the mean and standard deviation of the fitted Gaussian curves.

TABLE 7.2: Observed Multiplicity Statistics

Stellar	**Confirmed**		**Including Candidates**	
Multiplicity	**Number**	**Percent**	**Number**	**Percent**
Single	257	56.6 ± 2.4	244	53.7 ± 2.4
Binary	150	33.0 ± 2.2	154	33.9 ± 2.2
Triple	35	7.7 ± 1.3	43	9.5 ± 1.4
Quadruple	10	2.0 ± 0.8	10	2.0 ± 0.8
Quintuple	2	0.7 ± 0.3	2	0.7 ± 0.3
Sextuple	...	...	1	0.6 ± 0.3

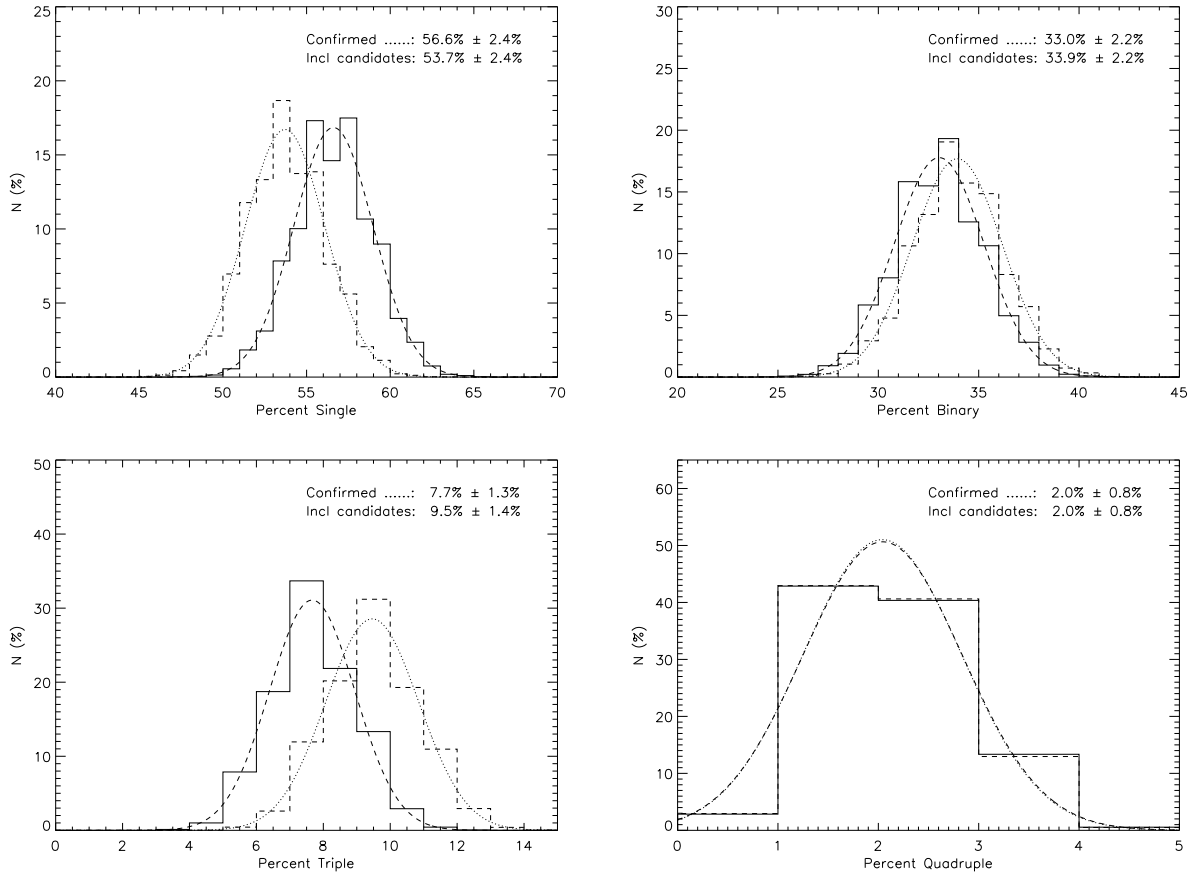

FIGURE 7.2: The observed frequency of single, binary, triple, and quadruple systems. These results were obtained by a bootstrap analysis with 10,000 iterations. The solid line and dashed curve represents confirmed systems and the dashed line and dotted curve includes candidate companions. The uncertainties are estimated as the standard deviation corresponding to the fitted Gaussian curve.

Table 7.3 lists the numbers of pairs detected and confirmed as physical associations by the various techniques studied here. The information is presented in a matrix form showing the overlap between various techniques. Column 1 contains a code identifying the method which confirms a physical association and is composed of a prefix corresponding to the column headings for columns 8–13 in Table 7.1 and a suffix which is the value listed for the pairs in the column in Table 7.1. The values for CPM companions are listed in order of priority

in confirming the companion. For example, the first row lists CPM pairs with matching independent measures of proper motion and trigonometric parallax, followed by matching proper motion and photometric parallax, and so on. Column 2 contains a short description of this code. Column 3 identifies the number of pairs uniquely confirmed by this method alone. The remaining columns make up a symmetric matrix whose diagonal lists the total number of pairs identified by this method and other cells show the number of pairs overlapping with other techniques. For example, The SB-1 row indicates that 48 pairs were confirmed based on evidence of a single-lined spectroscopic orbit, of which three have corresponding good-quality visuals orbits, four have preliminary visual orbits, 14 have photocentric-motion orbits, 21 show evidence of proper motion acceleration, and two were detected as SFP binaries. Sixteen of the 48 SB1 pairs have no other evidence of companionship. Table 7.4 shows similar statistics when all candidate companions are also included.

TABLE 7.3: Classification of 258 Confirmed Companions in the sample of 454 Solar-Type Stars

Code	Description	U	VBO	VBP	VBU	SB1	SB2	SBV	CPT	CPP	CPS	CPO	CPM	CPR	URE	URL	URM	CHS	CHV
VB-O	VBO: Definitive	7	38	...	...	3	18	1	...	...	...	...	...	...	...	...	17	6	3
VB-P	VBO: Preliminary	12	...	33	...	4	...	...	1	...	...	...	...	...	...	...	18	...	...
VB-U	VBO: Photocentric Motion	1	...	...	21	14	1	1	...	...	...	...	...	7	...	...	10	2	...
SB-1	SB1: Orbital Solution	16	3	4	14	48	...	...	...	...	...	...	...	1	...	...	21	1	...
SB-2	SB2: Orbital Solution	4	18	...	1	...	27	...	...	...	...	...	...	1	1	...	10	6	4
SB-V	RVV: RV Variations	1	1	...	1	...	...	9	...	...	...	1	1	2	...	...	4	...	...
CP-T	CPM: Matching $\pi_{\rm trig}$	29	...	1	...	...	...	...	30	...	...	...	...	...	...	...	...	...	...
CP-P	CPM: Matching $\pi_{\rm phot}$	39	...	...	...	...	...	...	...	42	...	...	...	...	...	...	3	...	...
CP-S	CPM: Matching $\pi_{\rm spec}$	5	...	...	...	...	...	...	...	...	6	...	...	...	...	...	1	...	...
CP-O	CPM: Orbital Motion	3	...	...	...	...	...	1	...	...	...	10	...	...	...	...	6	...	...
CP-M	CPM: Matching μ	20	...	...	...	...	...	1	...	...	...	...	26	...	...	...	5	...	...
CP-R	CPM: Other (Published)	2	...	...	7	1	1	2	...	...	...	...	...	11	...	...	6	1	...
UR-E	Unres: Eclipsing Binary	1	...	...	...	...	1	...	...	...	...	...	...	...	2	...	...	...	...
UR-L	Unres: Over-luminous	1	...	...	...	...	...	...	...	...	...	...	...	...	...	1	...	...	...
UR-M	Unres: Accelerating μ	8	17	18	10	21	10	4	...	3	1	6	5	6	...	...	85	2	...
CH-S	CHARA: SFP	...	6	...	2	1	6	...	...	...	...	...	...	1	...	...	2	8	...
CH-V	CHARA: Visibility	...	3	...	...	...	4	...	...	...	...	...	...	...	...	...	...	...	4

TABLE 7.4: Classification of 258 Confirmed and 25 Candidate Companions in the sample of 454 Solar-Type Stars

Code	Description	U	VBO	VBP	VBU	SB1	SB2	SBV	CPT	CPP	CPS	CPO	CPM	CPR	URE	URL	URM	CHS	CHV
VB-O	VBO: Definitive	7	38	...	...	3	18	1	...	...	...	...	...	...	...	...	17	6	3
VB-P	VBO: Preliminary	12	...	33	...	4	...	...	1	...	...	...	...	...	...	...	18	...	...
VB-U	VBO: Photocentric Motion	3	...	...	23	14	1	1	...	...	...	...	...	7	...	...	10	2	...
SB-1	SB1: Orbital Solution	16	3	4	14	48	...	...	...	...	...	...	...	1	...	...	21	1	...
SB-2	SB2: Orbital Solution	4	18	...	1	...	27	...	...	...	...	...	...	1	1	...	10	6	4
SB-V	RVV: RV Variations	8	1	...	1	...	...	16	...	...	...	1	1	2	...	...	4	...	...
CP-T	CPM: Matching $\pi_{\rm trig}$	29	...	1	...	...	...	...	30	...	...	...	...	...	...	...	...	...	...
CP-P	CPM: Matching $\pi_{\rm phot}$	39	...	...	...	...	...	...	...	42	...	...	...	...	...	...	3	...	...
CP-S	CPM: Matching $\pi_{\rm spec}$	6	...	...	...	...	...	...	...	...	7	...	...	...	...	...	1	...	...
CP-O	CPM: Orbital Motion	3	...	...	...	...	...	1	...	...	...	10	...	...	...	...	6	...	...
CP-M	CPM: Matching μ	20	...	...	...	...	...	1	...	...	...	...	26	...	...	...	5	...	...
CP-R	CPM: Other (Published)	9	...	...	7	1	1	2	...	...	...	...	...	19	...	...	7	1	...
UR-E	Unres: Eclipsing Binary	1	...	...	...	...	1	...	...	...	...	...	...	...	2	...	...	...	...
UR-L	Unres: Over-luminous	2	...	...	...	...	...	...	...	...	...	...	...	...	...	2	...	...	...
UR-M	Unres: Accelerating μ	14	17	18	10	21	10	4	...	3	1	6	5	7	...	...	92	2	...
CH-S	CHARA: SFP	...	6	...	2	1	6	...	...	...	...	...	...	1	...	...	2	8	...
CH-V	CHARA: Visibility	...	3	...	...	...	4	...	...	...	...	...	...	...	...	...	...	...	4

7.4 Notes on Individual Systems

Following are the notes on individual systems that require an explanation for confirmed, candidate, and refuted companions.

HD 123: *Triple.* This system is composed of a 106-year visual-orbit pair, the secondary of which was shown to be the more massive component from the absolute astrometry (see Griffin 1999, for a full description of the history of this system), suggesting that it itself was an unresolved binary. Brettman et al. (1983) reported a periodic variation in the component's brightness over roughly a 1-day period, which Griffin (1999) later disproved based on *Hipparcos* photometry and instead showed it to be a spectroscopic binary with a 47.7-day period, estimating component masses of 0.98, 0.95, and 0.22 $M_{\odot}$ for the three components.

HD 166: *Single.* A possible companion, 311″ away at 147° was identified by blinking archival images. The proper motion of the candidate companion from Høg et al. (1998) is $\mu_{\alpha} = 0\farcs104\,\mathrm{yr}^{-1}$ and $\mu_{\delta} = -0\farcs080\,\mathrm{yr}^{-1}$, directionally similar to, but significantly smaller than the primary's *Hipparcos* values of $\mu_{\alpha} = 0\farcs380\,\mathrm{yr}^{-1}$ and $\mu_{\delta} = -0\farcs178\,\mathrm{yr}^{-1}$, refuting a physical association.

HD 1237: *Binary, one planet.* In a systematic search for faint companions to planet hosts, Chauvin et al. (2006) discovered a CPM companion to this star using VLT NACO adaptive optics and demonstrated orbital motion. Chauvin et al. (2007) characterized the companion as M4±1V.

HD 3651: *Binary, one planet.* Luhman et al. (2007) reported the discovery of a T-dwarf companion 43″ away from this planet-host star using Spitzer IRAC images, and confirmed

CPM using 2MASS images. The brown dwarf's infrared colors are consistent with the distance to the primary, confirming companionship. They estimate the companion's mass as 0.051 ± 0.014 $M_\odot$ and age as 7 ± 3 Gyr by comparing luminosity with evolutionary tracks. This was the first substellar object imaged around an exoplanet host.

HD 4391: *Triple.* The WDS lists three detections of a pair with separations ranging 10.″0–16.″6 over 98 years. Bailey might have under-estimated the separation as 10″ in 1895, but the 1901 measure of 14.″1 at 306.°6 and the 1993 measure of 16.″6 at 307.°0 are consistent with a bound pair. In addition to this candidate, I discovered another possible companion, 49″ away by blinking archival images (see § 4.1). With the help of the SMARTS Consortium, I obtained VRI images in 2007 July and October to investigate these two candidates. The images clearly revealed the closer companion 16.″2 away at 307.°6, confirming CPM. The candidate was saturated in all but one V-band image, but the single unsaturated image allowed me to extract its V magnitude via differential photometry, and enabled confirmation as a companion (see Table 5.5). Absolute photometry for the wider candidate was also extracted from these images and the resulting VRI magnitudes along with 2MASS JHK_S magnitudes enabled confirmation of this newly discovered companion as well (see Table 4.2).

HD 4628: *Single,* maybe *Binary.* Heintz & Borgman (1984) resolved a pair, separated by 2.″7, on 11 exposures over two nights, but did not see the companion on 164 other plates or on multiple visual checks with a micrometer. Their two observations about 25 days apart show evidence of variation in the companion's brightness of about 1 magnitude. Heintz (1994) notes an acceleration in proper motion for the primary and speculates that this

might be caused by the companion reported earlier. Roberts et al. (2005) did not detect a companion using AO down to $\Delta I \lesssim 10$ and note that only a white dwarf companion could have escaped detection, while the flaring companion as seen by Heintz should have been detected. Moreover, the *Hipparcos* and Tycho-2 proper motions of HD 4628 match to within 2σ, and the FIC lists several null results with speckle interferometry and adaptive optics. B. Mason and I observed this target using the KPNO 4-m telescope in 2008 June, and while the separation was too wide and the Δm too large for speckle observations, the finder TV showed a faint source about $5''$ away at about 230°. Could this be the companion seen by Heintz after about 30 years of orbital motion? While a possibility, follow-up observations by Elliott Horch two days later with the WIYN 3.6m telescope on KPNO failed to identify the source seen by us. Additionally, 5-second exposures in VRI taken by T. Henry at the CTIO 0.9-m telescope in 2008 June also failed to identify any companion, although saturation around the primary could hide the companion in these images. Nidever et al. (2002) report that the primary shows no variation in radial-velocity. At this time, I do not feel that I have sufficient information to confirm or refute this pair, although, chances of a physical companion appear slim.

HD 4676: *Binary.* Boden et al. (1999) presented a visual orbit based on LBI observations for this 14-day SB2 and derived component masses of 1.223±0.021 $M_\odot$ and 1.170±0.018 $M_\odot$. Earlier, Nadal et al. (1979) had speculated on the presence of a third companion based on temporal changes in the spectroscopic orbital elements. While this suspected companion has been mentioned in subsequent literature (Fekel 1981; Tokovinin et al. 2006), Boden et al.

(1999) refute it based on imaging and spectroscopic evidence.

HD 4813: *Single.* The CNS (Gliese & Jahreiß 1991) and DM91 list this star as "SB?". Duquennoy et al. (1991) list 12 velocities measured over nine years, and while there is a hint of a trend, the measured velocity of 8.17 ± 0.44 km s^{-1} is constant within their measurement errors. Abt & Willmarth (2006) present 23 observations over three years with a radial velocity of 8.07 ± 0.14 km s^{-1}, consistent with the Duquennoy et al. measures 10 years earlier. There seems to be enough evidence to refute the earlier claim of binarity.

HD 5133: *Single.* Abt & Biggs (1972) and CNS list this star as SB, based on a 34 km s^{-1} variation over three observations presented by Joy (1947). More recent observations do not support this conclusion (Abt 1970; Nidever et al. 2002; Gontcharov 2006), refuting the earlier claim of a spectroscopic companion.

HD 9770: *Quadruple.* This system consists of a 4.6-year visual binary, whose secondary is a 11.5-hour eclipsing binary (Cutispoto et al. 1997). The fourth component is in a 112-year visual orbit.

HD 9826: *Binary, three planets.* Lowrance et al. (2002) discovered an M4.5V companion, 55″ away from planet host υ And, and confirmed its physical association by demonstrating CPM and showing that its spectral type is consistent with its magnitudes at the primary's distance. They estimate a mass of ~ 1.2 M$_\odot$ for the primary and 0.2 M$_\odot$ for the secondary using on spectral-type mass relations from Cox (2000) and Henry & McCarthy (1993).

HD 10476: *Single. Hipparcos* lists a photocentric orbit for this star with a period of

207 days and an inclination of 89° ± 23°. This is not consistent with the constant radial velocities observed by Nidever et al. (2002) and CfA (see § 6.1). Several studies have used this as a single star (Mazeh et al. 2002; Frasca et al. 2006), and there is no other published evidence of binarity. The WDS lists two additional pairs for this star, both of which are optical pairs (see § 4.2).

HD 13445: *Binary, one planet.* This planet-host star with a 4 M_J planet exhibits a longterm trend in radial velocity, consistent with a stellar companion beyond 20 AU (Queloz et al. 2000). Later work has resolved this companion and demonstrated orbital motion (Lagrange et al. 2006). The companion was initially misidentified as a T dwarf (Els et al. 2001) and later shown to be a white dwarf based on spectroscopy (Mugrauer & Neuhäuser 2005) and a dynamical analysis of astrometry and radial velocities (Lagrange et al. 2006).

HD 17925: *Single.* Listed as "RV-Var" in the CNS (Gliese 1969; Gliese & Jahreiß 1991), but Nidever et al. (2002) show that RMS scatter is less than 0.1 $\mathrm{km\,s^{-1}}$ in observations over 10 years, a conclusion supported by the CfA velocities (see § 6.1).

HD 20010: *Binary,* maybe *Triple.* This 5″ CPM pair has a preliminary visual orbit. The secondary is listed in the CNS (Gliese 1969) as "RV-Var?". Eggen (1956) mentions that there is a strong evidence of variability of the faint companion, but the quoted reference (van den Bos 1928) could not be found. With insufficient evidence to confirm or refute a physical association, the additional companion to the secondary remains a possibility.

HD 20630: *Single.* Listed as "SB?" in the CNS (Gliese & Jahreiß 1991), but Nidever et al. (2002) show that the RMS scatter is less than 0.1 $\mathrm{km\,s^{-1}}$ in observations over five

years, a conclusion supported by the CfA velocities (see § 6.1).

HD 20794: *Single.* CNS (Gliese & Jahreiß 1991) lists this star as "SB", but radial velocity data from various catalogs (Abt & Biggs 1972; Duflot et al. 1995; Gontcharov 2006) show a fairly stable velocities with no mention of variability or binarity.

HD 20807: *Binary.* The wide CPM companion HD 20766 lies 309″ away and is confirmed by matching proper motions and parallax. Additionally, the WDS lists a single speckle interferometry measure of a companion in 1978, 0.″046 away at 11°(Bonneau et al. 1980). However, Bonneau et al. failed to resolve the companion in 1979 and da Silva & Foy (1987) mention that the 1978 measure was in fact an artifact in the diffraction pattern of the telescope spider.

HD 21175: *Binary.* While this pair only has three ground-based measurements, they span over 50 years and are consistent with a bound pair. Söderhjelm (1999) presents a visual orbit combining *Hipparcos* and ground-based measures, confirming a physical association.

HD 22049: *Single, one planet.* This is ϵ Eri, the well-studied exoplanet host. The single measure listed in WDS is from speckle observation by Blazit et al. (1977). This system has subsequently been observed 13 other times by speckle and AO, and no companion was identified (e.g., McAlister 1978a; Hartkopf & McAlister 1984; Oppenheimer et al. 2001). Presumably, the Blazit measure is spurious. The WDS lists 10 additional pairs, all of which were confirmed as optical by blinking archival images (see § 4.2).

HD 22484: *Single.* Listed as "SB?" in the CNS (Gliese & Jahreiß 1991), but Nidever et al. (2002) show that the RMS scatter is less than 0.1 $\mathrm{km\,s^{-1}}$ in observations over seven

years, a conclusion supported by the CfA velocities (see § 6.1).

HD 23484: *Single,* maybe *Binary.* The CNS (Gliese 1969; Gliese & Jahreiß 1991) list this as "RV-Var", but no radial velocity data could be found in modern surveys. Catalogs (Abt & Biggs 1972; Duflot et al. 1995; Gontcharov 2006) list velocities with RMS scatter of about 3 $\mathrm{km\,s^{-1}}$, but this could be due to measurement errors or zero-point variances.

HD 24496: *Binary.* The two measurements with $\rho = 2\farcs6$–$2\farcs7$ and $\theta = 254°$–$256°$ listed in the WDS are by Wulff Heintz, nine years apart and consistent with a bound pair. The first measure is based on observations over three nights and the second on observations over two additional nights. Given the observer, the quality of observations (Δm = 4–5 measured) and the reasonably high proper motion of the primary, this is likely a physical pair, but one that could use new measurements.

HD 25457: *Single.* The CNS (Gliese & Jahreiß 1991) lists this star as "RV Var", but several catalogs (Abt & Biggs 1972; Duflot et al. 1995; Gontcharov 2006) show a fairly stable radial velocity over many decades.

HD 25665: *Single.* A possible companion, 287″ away at 134° was identified by blinking archival images but refuted based on proper motion differences between the components. The candidate companion has $\mu_\alpha = 0\farcs093\,\mathrm{yr^{-1}}$ and $\mu_\delta = -0\farcs138\,\mathrm{yr^{-1}}$ (Lépine & Shara 2005), which is directionally similar to but significantly different from the corresponding values for the primary of $\mu_\alpha = 0\farcs074\,\mathrm{yr^{-1}}$ and $\mu_\delta = -0\farcs299\,\mathrm{yr^{-1}}$.

HD 25680: *Binary.* A companion $0\farcs2$ away was discovered by McAlister et al. (1993) with speckle interferometry and confirmed by the same technique by Hartkopf et al. (2008).

These measures show evidence of orbital motion, and given the $0\farcs2\,\mathrm{yr}^{-1}$ proper motion of the primary and an elapsed time of 15 years between them, this pair can be confirmed as physical. Given the constant radial velocity of the primary (see § 6.1), this might be close to a face-on orbit. The WDS also lists a potential companion 177″away, which I also identified by blinking archival images. This candidate (HIP 19075) was however refuted based on its significantly different proper motion in *Hipparcos* from the corresponding value of the primary. The two additional WDS entries are clearly optical.

HD 26491: *Binary.* Astrometric and spectroscopic evidence indicate an unresolved companion. A comparison of *Hipparcos* and Tycho-2 proper motions shows a significant difference suggesting a companion (see § 5.1.2), which was confirmed by radial velocity measurements (Jones et al. 2002). Preliminary orbital elements are presented in Table 6.2 (H. Jones 2008, private communication).

HD 32923: *Single.* The WDS lists 19 measurements at roughly 0″.1 separation over 76 years, and Eggen (1956) even derived two preliminary visual orbits from these measures. However, Heintz & Borgman (1984) suggest that this is likely spurious and show that the observations are not consistent with orbital motion of any period. Three additional speckle observations exist since the Heintz & Borgman publication, from 1984–1987 (Tokovinin 1985; Tokovinin & Ismailov 1988; McAlister et al. 1993), but there are 17 null detections listed in the FIC by speckle interferometry as well as by AO. This star has a stable radial velocity based on CfA and Nidever et al. (2002) observations (see § 6.1). It appears that these multiple, but sporadic, measures are spurious.

HD 34721: *Single.* The CNS (Gliese 1969) lists this as "SB", but this is not consistent with constant radial velocities observed by Nidever et al. (2002) to within 0.1 $\mathrm{km\,s^{-1}}$ and CfA (see § 6.1).

HD 35296: *Binary.* DM91 noted the primary of a 12′ CPM pair as "SB", but one that was not confirmed by their work. Nidever et al. (2002) show that this star has a stable radial velocity, and the CfA measures support this conclusion (see § 6.1), refuting the earlier claim.

HD 36705: *Quadruple.* The WDS lists two measurements of this 10″ pair (AB Dor AB), separated by 69 years and consistent with a bound pair. The first measurement by Rossiter (1955) measured a Δm $\sim$ 6, explaining the lack of many more measures. Close et al. (2005) recovered this pair with AO at the VLT and it is also seen in VRI images obtained by T. Henry in 2008 September at the CTIO 0.9-m telescope using VRI filters. While the photometric distance estimate is a match within only 7σ (see Table 5.5), the V magnitude from Rossiter (1955) is likely approximate. Given the high proper motion of the primary, the consistent measures over 79 years indicate a physical association. The 2MASS colors indicate an M-dwarf with a V magnitude estimate of about 12.0, in good agreement with the measure of Rossiter (1955) and consistent with the primary's *Hipparcos* distance. High-contrast AO efforts have split each of these components into binaries themselves. The primary was identified by *Hipparcos* as showing accelerating proper motion, indicating an unseen companion, and this is supported by the significant difference between *Hipparcos* and Tycho-2 proper motions (see § 5.1.2). The suspected companion has since been revealed by LBI (Guirado et al. 1997), resolved by AO (Close et al. 2005), and confirmed as a physical

association by photometry and spectroscopy (Close et al. 2005, 2007; Boccaletti et al. 2008, and references therein). Close et al. (2005) also split the secondary into a $0\farcs070$ pair, which was later confirmed by Janson et al. (2007) who measured it at a separation of 66.1 mas at $238\fdg5$.

HD 40397: *Triple.* The five measures in the WDS for AB between 1902 & 1932 are consistent with a bound pair and include observations by Aitken and Burnham. The measured $\Delta m \sim 7$ makes this a difficult target for classical techniques and out of the reach of speckle interferometry. Given that more than 70 years have passed since the latest measure, this is a a good candidate for follow-up AO observations. This pair also has a wide CPM companion, NLTT 15867, which was confirmed by photometric distance estimates (see Table 5.5).

HD 42807: *Single.* The CNS (Gliese & Jahreiß 1991) list this as "SB?", but this is not consistent with constant radial velocities observed by CfA (see § 6.1).

HD 43834: *Binary.* Eggenberger et al. (2007) resolved this $3''$ pair three times over three years with AO at the VLT, demonstrating CPM and showing a hint of orbital motion. They also mention a linear trend in CORALIE radial velocities consistent with this companion, confirming a physical association, and estimate the companion to be M3.5–M6.5 with a mass of 0.14 ± 0.01 $M_\odot$.

HD 45270: *Single,* maybe *Binary.* The WDS lists three measurements spanning 43 years of a $\Delta m \sim 4$ pair separated by about $16''$, which are consistent with a bound pair. Curiously, no additional measurements exist. This pair was listed in the *Hipparcos* input catalog, but not resolved by *Hipparcos.* 2MASS lists a source near this candidate companion,

but it is clearly not the same star because its infrared colors are more than three magnitudes fainter than the visual magnitude of 10.6 from the *Hipparcos* input catalog. No additional information was found on this pair and hence it is retained as a candidate.

HD 46588: *Single.* The CNS (Gliese & Jahreiß 1991) lists this as "SB?" but this star was not included in the Nidever et al. (2002) or CfA surveys. Abt & Biggs (1972) lists two velocity measures, 55 years apart and roughly consistent. In a follow-up search, McAlister (1978a) did not resolve any companions via speckle interferometry. Batten's Seventh Catalog of Spectroscopic Binary Orbits lists this as SB with a 60-day period from Abt & Levy (1976), but the orbit is flagged as "very poor". Gomez & Abt (1982) lists this star as a possible negative result. The SB9 catalog does not have an orbit for this star.

HD 48189: *Binary.* The WDS lists 19 measurements over 105 years that are consistent with a bound pair. During this time, the separation has closed in from about 3″ to about 0.″3 and the position angle has changed by about 15°. Given the small projected separation of 6–40 AU, one might expect a greater change in position angle as evidence of orbital motion. The change of only 15° indicates that the semimajor axis is larger than the observed separations, perhaps due to a high inclination. While a more robust confirmation is not available, the primary has moved about 9″ during the measures, and the companion seems to be moving along with it, indicating a physical association.

HD 64606: *Binary.* For the primary of an SB1 pair, the WDS lists two measures of another Δm $\sim$ 4 pair separated by 4.″9, one each from *Hipparcos* and Tycho. The *Hipparcos* solution is flagged as "poor" quality, and there is no independent confirmation of this

pair. T. Henry observed this star using the CTIO 0.9-m telescope in 2008 September and obtained 1-second exposure images in VRI. No source was found at the expected position in these images, whereas a companion of Δm $\sim$ 4 should easily have been seen above the background. While the SB1 pair is real, this astrometric detection is refuted.

HD 65907: *Triple.* LHS 1960 is a companion to this star, separated by about 60″, and confirmed by photometric distance estimates (see Table 4.2). The WDS lists four measures of an additional companion to LHS 1960, observed 1930–1983, indicating that this component itself is a 3″ CPM binary. No further evidence of companionship could be found, but given the high proper motion of the primary and the four consistent measurements on four different telescopes over 53 years, this system can be confirmed as a triple.

HD 67199: *Single,* maybe *Binary.* The *Hipparcos* and Tycho-2 proper motions differ by greater than a 3σ significance indicating an unseen companion (see § 5.1.2), but in the absence of other conclusive evidence, this companion is retained as a candidate.

HD 68017: *Single,* maybe *Binary.* The *Hipparcos* and Tycho-2 proper motions differ by greater than a 3σ significance indicating an unseen companion (see § 5.1.2), but in the absence of other conclusive evidence, this companion is retained as a candidate. Two other WDS components are clearly optical.

HD 68257: *Quintuple,* maybe *Sextuple.* The three brightest roughly solar-type components (ζ Cancri A, B, and C) are supported by over 1000 visual measurements each, corresponding to two visual orbits. Component C has been noted to have an irregular motion for most of its history and was identified as an SB1 with an orbit of 6302 ± 59 days

(Griffin 2000), consistent with earlier astrometric orbits. However, earlier efforts (Heintz 1996) had noted a mass ratio for the C component binary of about 1, and with C being a G0 star, the non-detection was puzzling and attributed to the companion being a white dwarf or itself a binary. Hutchings et al. (2000) finally resolved this pair (Ca,Cb) via AO observations at infrared wavelengths, designated it (Cb) as an M2 dwarf based on its infrared colors, and argued on the basis of prior mass-ratio estimates that it itself is an unresolved binary (Cb1,Cb2). Richichi (2000) confirmed the presence of Cb via lunar occultation measures. While she could not confirm its binary nature, her K-band photometry supported the binary M-dwarf hypothesis, for which she determined an upper-limit for projected separation of 20-30 mas. Further, Richichi reports the potential discovery of a sixth component in this system. While seen just above her detection limit and hence retained as a candidate for this work, she nonetheless confirmed its presence by three independent data analysis methods and excluded it from being the unresolved companion Cb2 noted above. This exclusion is primarily due to its larger separation of about at least 1.6 AU from the lunar occultations, and tentatively identified it as an M2–M4 dwarf. In addition to all this, I identified a potential wide companion, 372″ away at 107°, but a physical association could be ruled out based on a significantly different proper motion of the companion of $\mu_\alpha = 0\farcs084\,\mathrm{yr}^{-1}$ and μ_δ = -0″.091 yr^{-1} from UCAC2, compared to the primary's values of $\mu_\alpha = 0\farcs283\,\mathrm{yr}^{-1}$ and μ_δ = -0″.150 yr^{-1} from *Hipparcos*.

HD 72760: *Binary.* This companion was identified based on a significant difference in *Hipparcos* and Tycho-2 proper motions. Recently, Metchev & Hillenbrand (2008) resolved

the companion in a Palomar/Keck AO survey, confirmed companionship based on color and magnitude measurements, and estimated the companion's mass as 0.13 $M_{\odot}$.

HD 73350: *Single.* The WDS lists a B component 60″ away with a C component about 10″ from B. While the DSS images were taken over just a two-year interval, the SSS image provides a longer time baseline and helps confirm component B (HD 73351) as a field star. Component C is a CPM companion of B based on three consistent measures separated by over 100 years, and hence also physically unassociated with HD 73350.

HD 73667: *Single.* While the blinking of archival images allow confirmation of the two WDS entries as field stars, it revealed a possible CPM companion 335″ away at 207°. However, its photometric distance estimate refuted this candidate as well (see § 4.1).

HD 73752: *Binary.* The CNS (Gliese 1969) lists the primary of the 1.″3 visual binary as "SB" and notes that there are suspected perturbations in its proper motion. The reference detailing the perturbations (Hirst 1943) presents a 35-year inner orbit, which is noted as very preliminary with several different orbits equally permissible. The author also states that systematic effects alone may explain the residuals. His outer 214-year visual orbit was later revised to 145 years by Heintz (1968) with no mention of a third component. In fact Heintz pointed out that that the observed range of radial velocities could be ascribed to scatter. Adopting a parallax of 0.″058, he derived a mass-sum of 1.1 $M_{\odot}$, and noted that at least one component must be over-luminous. If we adopt the HIP parallax of 50.2 mas, we get a mass-sum of 1.9, so the components are likely not over-luminous. Radial velocity catalogs (Abt & Biggs 1972; Gontcharov 2006) lists velocities in the range 40–48 $\mathrm{km\,s^{-1}}$,

but the differences could be due to zero-point offsets between observers. The early claim of a possible companion is not supported by subsequent observations, which in fact question it. While the visual binary is real, the third component is refuted. An additional wide component listed in the WDS and measured 113.″7 away in 1999 is clearly optical.

HD 75767: *Quadruple.* Tokovinin et al. (2006) reported the discovery of a wide Δm=4.3 companion to a 10.3-day SB1 binary with NACO adaptive optics and confirmed CPM using a partial resolution in 2MASS images. This companion was independently discovered by Fuhrmann et al. (2005), who obtained two observations four years apart, demonstrating CPM, and confirmed companionship by showing consistent radial velocity with the primary. Their spectra also enabled them to identify the companion itself as a double-lined binary, as evidenced by its H-alpha emission and near-infrared absorption lines appearing as pairs with an offset of about 21 $\mathrm{km\,s^{-1}}$. Using composite-spectrum analysis, they derived spectral types of M3 and M4. Blinking archival images revealed a possible fifth companion 385″ away, and its photometric distance estimate matches the primary's *Hipparcos* value within 2σ. However, the Lépine & Shara (2005) proper motions of the two stars are significantly different, indicating that this might be a comoving star perhaps born out of the same cloud as HD 75767, but one that is not gravitationally bound to it.

HD 79096: *Quadruple.* Wilson et al. (2001) discovered a L8V comp (Gl 337C) 43″ from the SB2VB pair from 2MASS images. The two images, separated by 2.5 years, allowed confirmation of CPM. They also showed that the magnitudes are consistent with the primary's distance to within 1σ, confirming companionship. Burgasser et al. (2005) resolved Gl

337C as a nearly equal-magnitude binary (separated by $0\farcs53 \pm 0\farcs03$ at $291° \pm 8°$) using Lick natural guide star AO. Companionship was confirmed based on proximity and CPM, which was demonstrated by the absence of a source in 2MASS images at the expected position of a background star.

HD 82885: *Binary.* This is a visual binary with a period of some 200 years. A potential wide companion (NLTT 22106), $328''$ away at 333° was identified by blinking archival images but refuted based on significantly different proper motions.

HD 84117: *Single.* A potential wide companion (NLTT 22384), $722''$ away at 331° was identified by blinking archival images but refuted based on significantly different proper motions.

HD 86728: *Binary,* maybe *Triple.* Gizis et al. (2000) identified a wide CPM companion from 2MASS and confirm it via a spectral type of identification M6.5. However, based on it being over-luminous ($M_K = 8.19$ using 2MASS magnitudes and *Hipparcos* parallax versus $M_K = 9.60$ for an M6.5 dwarf) and having high activity (emission observed twice), they argued that it is an unresolved equal-mass binary, or even possibly a triple. I could not find any follow-up work confirming or refuting this claim, so while this system is confirmed as a binary, I retain a third component as a candidate.

HD 90839: *Binary,* maybe *Triple.* The primary of a wide CPM pair is listed in the CNS (Gliese & Jahreiß 1991) as "SB?" and the secondary (HD 237903, GJ 394) is listed in an earlier version of the catalog (Gliese 1969) as "RV-Var". The primary is a constant velocity star, as evidenced by Nidever et al. (2002) and the CfA survey (see § 6.1). These modern

surveys did not observe the secondary. DM91 listed this companion with a constant velocity of 8.24–8.62 $\mathrm{km\,s^{-1}}$ over 700 days. Heintz (1981) listed velocities of 7.7–8.4 $\mathrm{km\,s^{-1}}$ over four days and noted that coverage is too weak to show whether the velocity varies. He also noted that the spectrum had emission features. Wilson (1967) listed a velocity of 7.8 $\mathrm{km\,s^{-1}}$ over three plates with a range of 7.7 $\mathrm{km\,s^{-1}}$ and standard deviation of 3.1 $\mathrm{km\,s^{-1}}$. Radial velocity catalogs (Abt & Biggs 1972; Duflot et al. 1995) list values that range over many $\mathrm{km\,s^{-1}}$, but this could be due to zero-point differences between observers, and these catalogs do not note any variation. While the wide binary is confirmed based on matching parallax and proper motion and the primary's SB claim is refuted, the possible radial velocity variation of the secondary is inconclusive and hence retained as a candidate.

HD 96064: *Triple.* This system is composed of a CPM pair separated by $11\farcs8$, the secondary of which is a 23-year visual binary. Additionally, the blinking of archival images revealed a possible wide companion about $5'$ away, but this was refuted based on photometric distance estimates (see § 4.1).

HD 97334: *Triple.* Kirkpatrick et al. (2001) discovered an L4.5V CPM companion (Gl 417B) $90''$ away at 245° from the primary using 2MASS images and confirmed a physical association by demonstrating CPM and consistent parallaxes. Bouy et al. (2003) resolved this brown dwarf into a binary ($0\farcs070 \pm 0\farcs0028$ at $79\fdg6 \pm 1\fdg2$) using HST WFPC2. While companionship of this pair has not been established conclusively, proximity argues for a physical association.

HD 97658: *Single.* A possible CPM companion was discovered by blinking archival images but refuted based on inconsistent photometric distance estimates (see § 4.1).

HD 98230: *Quadruple.* ξ UMa is a quadruple system composed of a 60-year visual binary, the primary of which is a SB1VB and the secondary is an SB1. Mason et al. (1995) reported a possible fifth companion detected via speckle interferometry near the secondary. While the single detection reported is quite convincing, this companion has never again been seen, despite multiple attempts. My efforts with CHARA, while limited to $\Delta K \lesssim 2.5$, also failed to resolve any additional components. Given only one measure and about a dozen null results with the same technique, this new companion is probably spurious. For the purposes of this survey, I retain ξ UMa as a quadruple system.

HD 100180: *Binary,* maybe *Triple.* The primary of the 15″ CPM binary has two speckle interferometry measurements of a close companion, observed 0.″035 away at 6.°8 in 2001 and 0.″122 at 355.°8 in 2004. One of the two attempts by B. Mason and me at the KPNO 4-m telescope in 2008 June resulted in an "uncertain" measure of 0.″218 at 14.°6. Given the $0.''378\,\mathrm{yr}^{-1}$ proper motion of the primary, these measures are consistent with a bound pair, but further observations are warranted to obtain a definitive confirmation, especially given the constant radial velocity reported by Nidever et al. (2002). While the wide binary is confirmed by photometric distance estimates, the third component is retained as a candidate.

HD 100623: *Binary.* The WDS lists only a single measure of this large Δm pair discovered by Luyten in 1960. While the proximity and large magnitude difference make follow-up observations difficult, Henry et al. (2002) obtained spectra of this 15th magnitude

companion and showed that it is a DC or DQ white-dwarf, not an M-dwarf as reported in the CNS (Gliese & Jahreiß 1991). The second observation confirms CPM, and the spectral type and photometry are consistent with a physical association.

HD 102365: *Binary.* Luyten first resolved this pair in 1960. The companion is LHS 313 with a proper motion that matches the primary's $1\farcs6\,\mathrm{yr}^{-1}$. Hawley et al. (1996) identified the companion as a M4V, which was recovered by 2MASS at a similar position angle and separation as Luyten and its infrared colors are consistent with an M4 dwarf at the primary's distance.

HD 102870: *Single.* The CNS (Gliese & Jahreiß 1991) lists this as "SB?", but Nidever et al. (2002) and the CfA survey show it to be a constant velocity star (see § 6.1). The WDS lists two additional components, B and C, which are clearly optical.

HD 103095: *Single.* The CNS (Gliese 1969) and DM91 listed a companion with separation $2''$ at 175°. DM91 mentioned that the companion was flaring with magnitudes of 8.5–12 and also mention that it is normally not seen. The FIC lists four null measurements with speckle interferometry and as shown in Table 6.1, there are no radial velocity variations. Three attempts by B. Mason and me in 2008 June at the KPNO 4-m telescope failed to identify a companion. Recently, Schaefer et al. (2000) have shown that the brightness enhancements observed are likely due to superflares on the stellar surface rather than due to a companion.

HD 109358: *Single.* The WDS lists a single speckle measure (Bonneau & Foy 1980) of a $0\farcs1$ pair, but the FIC has over 20 null speckle detections. B. Mason and I observed this star

with the KPNO 4-m telescope in 2008 June and failed to resolve the suspected companion. Given the mention of telescope artifacts as being responsible for some detections by this observer (da Silva & Foy 1987), I side with the many null detections, including one by the same observer. Additionally, the CNS (Gliese & Jahreiß 1991) listed this star as "SB", and Abt & Levy (1976) presented a preliminary orbital solution, but that was later shown to be spurious (Morbey & Griffin 1987). CfA radial velocity coverage of 16 years, and the high precision measurements of Nidever et al. (2002) confirm this star as a stable radial velocity star. The AB pair in the WDS is clearly optical. This star appears to be single.

HD 111312: *Binary,* maybe *Triple*. This is a 2.7-year SB2, for which a new orbital solution is presented here based on CfA velocities. The WDS lists a single speckle measure with a separation of $0\farcs089$ at 91° in 2001, and the pair was seen again in 2006 with a separation of $0\farcs050$ at $44\fdg6$ (B. Mason 2008, private communication). These measurements are consistent with the spectroscopic binary and more observations are needed to develop a visual orbit. The WDS lists an additional companion, $2\farcs7$ away with Δm $\sim$ 4 pair based on *Hipparcos* and Tycho measures. The *Hipparcos* solution is flagged as "poor" quality, and there is no independent confirmation of this pair. Its orbital period, if real, would be too long to affect the velocities obtained over some 7 years. With no conclusive evidence to confirm or refute this companion, it is retained as a candidate requiring further observations.

HD 112758: *Triple*. This is triple system with an inner SB1 pair and a wider visual component which was first resolved by van den Bos in 1945 and then again in 1960 with Δm $\sim$ 5. McAlister et al. (1987) recovered this pair in 1983, and the three observations show

evidence of orbital motion. The McAlister et al. measurement with speckle interferometry implies $\Delta m \lesssim 3$, suggesting that the companion may be variable. B. Mason and I attempted to resolve this pair at the KPNO 4-m telescope on 2008-06-13, but could not see it, perhaps because of the large magnitude difference.

HD 113283: *Single,* maybe *Binary.* The *Hipparcos* and Tycho-2 proper motions differ to greater than a 3σ significance indicating an unseen companion (see § 5.1.2), but in the absence of other conclusive evidence, this companion is retained as a candidate.

HD 113449: *Binary. Hipparcos* presents a photocentric orbit for this star with a period of about 231 days. Moore & Paddock (1950) noted this star as a radial velocity variable and Gaidos et al. (2000) mentioned that the velocity changed by 20 $\mathrm{km\,s^{-1}}$ over 10 months, but no definitive orbit exists. The companion was resolved at the Palomar 200-inch telescope with aperture masking in 2007 January, 35.65 ± 0.6 mas away at $225\overset{\circ}{.}2 \pm 0\overset{\circ}{.}5$ with $\Delta H \sim 1.6$, and confirmed at the Keck telescope more than a year later (M. Ireland 2008, private communication). With consistent astrometric and spectroscopic evidence, this is a bound pair.

HD 114613: *Single.* The CNS (Gliese & Jahreiß 1991) list this star as "RV-Var", but Murdoch et al. (1993) show it to be a constant velocity with a scatter less than 0.1 $\mathrm{km\,s^{-1}}$ over almost three years. Radial velocity catalogs also list stable velocities with no mention of variability.

HD 114783: *Single, one planet.* A potential CPM companion was identified $240''$ away at 46° by blinking archival images but subsequently refuted based on photometric distance

estimates (see § 4.1).

HD 120136: *Binary, one planet.* τ Boo hosts a 4.13 M_J minimum-mass planet in a 3-day orbit and has a visual orbit stellar companion, measured $2\farcs8$ away at 33° in 2000. While the visual orbit is very preliminary, physical association is confirmed by 56 observations in the WDS over 170 years which demonstrate not only CPM, but also orbital motion. Furthermore, Wright et al. (2007) and references therein mention a longterm drift in radial velocity which is likely consistent with this visual companion.

HD 120780: *Triple.* The WDS lists two measures of a $6''$ pair. The measurements are 51 years apart and consistent with a bound pair, but follow-up observations have been difficult due to a magnitude difference of ~ 5.5. With the help of the SMARTS Consortium, I obtained I-band images in 2006 July and 2007 June. The companion was seen at both epochs about $5\farcs6$ away at 89° with $\Delta I \sim 3.3$. These three observations demonstrate CPM with a fast-moving primary ($0\farcs6\,\mathrm{yr}^{-1}$), and, in fact, hint at orbital motion, confirming companionship. Additionally, *Hipparcos* identifies this star as an accelerating proper-motion binary, and the Tycho-2 proper motion differs from the *Hipparcos* value to a 19σ significance. While the Tycho-2 proper motion, averaged over about 100 years, is no doubt affected by the wide pair mentioned above, whose orbital period could be about 1000 years, the *Hipparcos* observations are over some three years and indicate a closer companion. I conclude that this is a triple star system.

HD 124850: *Single,* maybe *Binary.* The VB6 catalog lists a photocentric orbit for this star with a period of 55 years and an inclination of 60° from Gontcharov et al. (2003, A&A

in press), but this reference could not be found. This star was not included in the Nidever et al. (2002) or CfA radial velocity surveys, and radial velocity catalogs (Abt & Biggs 1972; Duflot et al. 1995; de Medeiros & Mayor 1999; Gontcharov 2006) do not indicate variation. B. Mason and I could not resolve any companion via speckle interferometry on the KPNO 4-m telescope in 2008 June. Retained as a candidate.

HD 125276: *Single,* maybe *Binary.* The *Hipparcos* and Tycho-2 proper motions differ to greater than a 3σ significance indicating an unseen companion (see § 5.1.2), but in the absence of other conclusive evidence, this companion is retained as a candidate. The WDS lists two companions for this star, the wider one of which, 83″ away in 1999, is clearly a background star as seen by blinking archival images. The closer pair is separated by 3″–8″ over four measures listed in the WDS between 1891 and 1936. Some of these measures indicate a Δm $\sim$ 8, which might explain the several non-detections also included in the WDS. B. Mason and I observed this star at the KPNO 4-m telescope in 2008 June. While the pair is too wide and too high in contrast for detection via speckle, the finder TV at the telescope revealed a faint stellar source about 60″ away at 130°. No other source was found 6″–80″ away from the primary.

HD 125455: *Binary.* This pair was discovered by Kuiper in 1937 and has measurements in 1960 and 1987 that are consistent with as bound pair. The companion is LHS 2895 with a proper motion that matches the primary's, and its 2MASS colors indicate a late M-dwarf at approximately the primary's distance.

HD 128620: *Triple.* This is the closest star system, α Centauri, which is composed of a

an SB2VB pair and a wide companion, Proxima Centauri, about 2° away. While the angular separation is extreme for bound systems, it translates to a linear projected separation of 10,000 AU, which is well within the limits of gravitationally bound pairs. Wertheimer & Laughlin (2006) used kinematic and radial velocity data to show that Proxima Centauri is bound to α Centauri. A possible new companion to Proxima Centauri was reported by Schultz et al. (1998) 0.″34 away using the HST FOS as a coronagraphic camera. In a follow-up effort, Golimowski & Schroeder (1998) use HST WFPC2 to show that the FOS feature seen was likely not a substellar companion to Proxima Centauri, but rather an instrumental effect of the FOS, noting that if the prior observation was real, it would have easily been identified by WFPC2, given its expected separation and contrast. They exclude any stellar or substellar companion within 0.″09–0.″85 of Proxima Centauri.

HD 130948: *Triple.* Potter et al. (2002) discovered a pair of brown dwarf companions using AO on the Gemini North 8-m telescope. They demonstrated CPM with observations over seven months and confirmed companionship based on their infrared colors, spectral-type of dL2 $\pm$ 2 and a consistent age with the primary of less than 0.8 Gyr derived by placing these stars on an HR diagram and comparing with theoretical models. They also noted that the young age is consistent with the high X-ray activity, Li abundance, and fast rotation. Additionally, this star is listed as SB in the CNS (Gliese 1969), but clearly seen as a constant velocity star in Nidever et al. (2002) and the CfA survey (see § 6.1). This system apparently has one star and two brown dwarfs.

HD 137107: *Triple.* Kirkpatrick et al. (2001) discovered this wide L8V companion (Gl

584C) to the SB2VB binary using 2MASS images, and confirmed as a physical association with additional measures and spectroscopy.

HD 137763: *Quadruple.* The primary of a 52″ CPM binary is itself SB2, and also has a wide companion about 20′ away that was first mentioned by CNS and confirmed based on a spectral type of M4.5 and a distance estimate of 21.6 ± 1.9 pc (Reid et al. 1995).

HD 140901: *Binary.* The WDS lists seven measures for this pair from 1897 to 1960 which are consistent with a bound pair. With the help of the SMARTS Consortium, I obtained VRI images from the CTIO 0.9-m telescope in 2006 July and 2007 July, which reveal the companion at the expected position, confirming CPM. The magnitude difference of over six makes photometry difficult, but given the large matching proper motion and proximity, this pair can be confirmed as physical. The WDS C component is clearly optical.

HD 141004: *Single.* Two candidate companions were refuted for this star. A CPM companion identified 235″ away by blinking archival images was refuted by photometric distance estimates (see § 4.1). Additionally, the CNS (Gliese & Jahreiß 1991) designates this star as "SB1", which is spurious as indicated on the CNS website and by constant velocities observed by Nidever et al. (2002) and the CfA survey. This star appears to be single.

HD 141272: *Binary.* The WDS lists four micrometer observations of this pair over 56 years that are consistent with a bound pair. Eisenbeiss et al. (2007) confirm companionship based on photometry and spectroscopy and derive an estimated mass for the dM3 ± 0.5 companion of $0.26^{+0.07}_{-0.06}$ $M_{\odot}$.

HD 142373: *Single. Hipparcos* lists a photocentric orbit for this star with a period of 51

days and an inclination of 132°± 28°. This is not consistent with constant radial velocities observed by Nidever et al. (2002) to within 0.1 $\mathrm{km\,s^{-1}}$ and CfA (see § 6.1). There is no other published evidence of a companion to this star.

HD 143761: *Single planet-host or binary with no known planets.* ρ CrB definitely has a companion, but it is not clear if it is planetary or stellar in nature. *Hipparcos* identified a photocentric orbit with a period of 78 days, exactly twice that of the planetary companion reported by Noyes et al. (1997). Gatewood et al. (2001) used *Hipparcos* and ground-based observations to conclude that the photocentric orbit is of the same period as the planet, and in fact the "planet" is an M-dwarf companion with a mass estimate of 0.14 $\mathrm{M_\odot}$ in a nearly face-on orbit. Bender et al. (2005) failed to identify such a companion using high-resolution infrared spectroscopy, and placed an upper limit on the companion's mass of 0.11–0.15 $\mathrm{M_\odot}$. Baines et al. (2008b) attempted to resolve this question with LBI observations at the CHARA Array, and could not settle the issue once again. While interferometric visibilities did not perfectly fit a single-star solution, they indicate that additional data is required for a definitive conclusion. This system has a stellar or planetary companion, but not both. Further observations are warranted.

HD 144284: *Binary.* Mazeh et al. (2002) presented a 3-day SB2 orbit for this star using infrared spectroscopy to measure the faint companion, deriving a mass ratio of 0.380 ± 0.013. Mayor & Mazeh (1987) had identified this system as a possible triple based on a 1.7 $\mathrm{km\,s^{-1}}$ variation in the velocity semiamplitude between their solution and that of Luyten (1936). While the velocity semiamplitude does seem to vary for the different orbital

solutions presented for this pair (Luyten 1936; Mazeh et al. 2002, DM91) and the CfA SB1 orbital solution has residuals of up to 2 $\mathrm{km\,s^{-1}}$ on each side, there is no obvious periodic pattern or longterm drift over the 4.8 years of velocity coverage (D. Latham 2008, private communication). The most recent CfA velocity measure of this star is from 1990, and additional observations are warranted.

HD 144579: *Binary.* The proper motion of the candidate from LSPM is quite different from the primary's *Hipparcos* or LSPM value. Further, the distance estimate has a large error and matches the primary's at a greater than 1σ significance (see Table 4.2). However, given the proximity of these two stars in the sky, the very large and similar proper motions and similar distances, this appears to be a physical companion, as it has been previously recognized (DM91, Gliese & Jahreiß 1991). The differences in the proper motions might indicate that the companion (or primary) has a close unresolved companion and warrants further observations. For this work, I will consider this a binary.

HD 145958: *Binary,* maybe *Triple.* The primary of a $4''$ visual binary has two additional possible companions, one of which was refuted by this effort and the other remains a candidate. The WDS lists a nearby companion, $0\farcs2$ away, detected by H. McAlister in 1983. The FIC catalog lists this as a weak detection and possibly spurious, and includes a null detection using the same technique. B. Mason and I failed to resolve a companion at the KPNO 4-m telescope in 2008 June. Nidever et al. (2002) identifies this as a constant velocity star. Evidence seems to be mounting against this candidate companion, which is considered refuted for this work. Separately, the Dwarf Archives[2] includes a T6 object about

[2] $http://spider.ipac.caltech.edu/staff/davy/ARCHIVE/index.shtml$

27′ away from this star. Looper et al. (2007) discovered this T dwarf in the 2MASS survey, obtained spectra, typing it as T6, and estimated its proper motion and distance. Their proper motion of $0\farcs48 \pm 0\farcs05\,\mathrm{yr}^{-1}$ at $139\fdg0 \pm 0\fdg2$ is similar to the primary's FvL07 value of $0\farcs46\,\mathrm{yr}^{-1}$ at 156°. Additionally, their distance estimate of 29.0 ± 2.3 pc is within 3σ of the primary's FvL07 distance of 23.6 pc. While the projected linear separation is very large at about 40,000 AU, this could be a loosely bound companion to HD 145958, and is retained as a candidate.

HD 146361: *Quintuple.* As part of this effort, I derived a visual orbit for the central 1.14-day binary of this quintuple system. For a comprehensive treatment of all components, see *Appendix* E.

HD 147776: *Binary,* maybe *Triple.* The WDS lists three candidate companions, but the details actually correspond to four stars. The Δm $\sim$ 4 pair 103″ away at 281° is clearly a field star, as seen by blinking the archival images (see § 4.2). Three additional pairs were reported by Sinachopoulos (1988) – 6.″4 separation at 173° with Δm $\sim$ 3, 9.″7 separation at 14°, and 71.″9 separation at 28°. The latter two pairs do not have a magnitude difference measurement. Sinachopoulos measured these pairs using a 1.5-m telescope by combining 4–16 exposures of a few seconds each. The wide companion 72″ away should have been seen in the DSS images, but no stellar source was seen at the expected position. The closest star to this position in the 1995 DSS image is 83″ away at 15° and is clearly a field star. The other two sources seen by them would be buried in the saturation around the primary in the DSS images, so I obtained VRI frames in 2008 May and August from the CTIO 0.9-m

telescope which is operated by the SMARTS consortium. The images clearly show a faint companion about 9″ away at 19°. This is likely the 9.″7 companion seen by Sinachopoulos (1988), exhibiting CPM, and given the proximity, is likely physical. The closest source seen by Sinachopoulos is not detected in the CTIO images and remains a candidate. Additionally, the CNS (Gliese 1969) lists a companion for this star 3″ away at 281°in 1909. This is likely the same as the pair measured by Burnham as listed in the WDS, which was seen 103″ away at 281° in 1909 and as discussed above, is clearly optical.

HD 148704: *Binary.* This is a 32-day SB2 binary for which *Hipparcos* and Tycho identified another companion 4.″1 away at 221°. I obtained VRI images from the CTIO 0.9-m telescope in 2008 October with the help of the SMARTS Consortium. No companion was seen at the expected position, while a Δm $\sim$ 3 companion as indicated by *Hipparcos* should have been seen above the tail of the primary's PSF. However, given the proper motion of the primary, a field star would have moved closer and possibly could be buried within the primary's PSF. Gray et al. (2006) list the spectral type of the companion as G9V and its coordinates imply a separation of 2.″4 at 55°, the exact position where a field star would be fifteen years since the *Hipparcos* measure. The Gray et al. spectral type, along with the Tycho-2 V-magnitude of 10.5 imply a significantly larger distance to this star compared to the primary, enabling me to refute this candidate.

HD 149806: *Binary.* This pair was first reported by Rossiter (1955) 5.″9 away at 22°and has two additional measurements in the WDS over the next 54 years, which are consistent with a bound pair. While the photometric distance estimate is not a good match

(see Table 4.2), the R magnitude listed is likely approximate. Given the moderate proper motion of the primary, the consistent measures over 54 years indicate a physical association. The 2MASS colors indicate an M-dwarf with a V magnitude estimate of about 12, in fair agreement with the measure of Rossiter (1955). On In 2008 June, B. Mason and I attempted to observe this pair at the KPNO 4-m telescope. While the separation and Δm are too large to be resolved using speckle, the finder image at the telescope showed a source at the expected position with a Δm similar to those of prior observations.

HD 153557: *Triple*. The WDS lists 17 measurements over 95 years with separations ranging from $1\farcs9$–$4\farcs9$, which are consistent with a bound pair, and given the $0\farcs3\,\mathrm{yr}^{-1}$ proper motion of the primary, imply a physical association. This pair also has a wider companion, HD 153525, about $2'$ away, which is confirmed by matching proper motion and parallax.

HD 155885: *Triple*. This system comprises a 470-year VB and a wide companion (HD 156026) about $12'$ away. Additionally, the CNS (Gliese 1969) list this star as "RV-Var", but the CfA survey shows that this is a constant velocity star (see § 6.1), allowing me to refute this component. WDS components D and E are optical.

HD 158633: *Single*. The CNS (Gliese 1969; Gliese & Jahreiß 1991) list this as "SB" and note a radial velocity range of 28 $\mathrm{km\,s^{-1}}$. CfA observations span 28 years and indicate a constant velocity star with an RMS scatter of 0.46 $\mathrm{km\,s^{-1}}$, in line with typical measurement errors.

HD 165341: *Binary*. CNS lists the component A of a 88-year SB2VB as a possible binary with a period of about 17 years. Radial velocity data from CfA do not show any

evidence of variation in 26 observations over 13 years. Heintz (1988) presents a revised orbit of the SB2 and points out that previous efforts to explain the residuals by a third unseen companion have led to contradictory results on the nature of the companion. He excludes the possibility of any period with $P < 55$ years and states that the once suspected velocity variation of A is disallowed by the more precise recent measurements.

HD 165908: *Binary,* maybe *Triple.* This is a 56-year VBO. Additionally, the WDS lists one speckle measure of a pair with a separation of $0\farcs228$ at $50\fdg2$ from Scardia et al. (2008), who list this new discovery as "faint". They also resolved the known VB companion about $1''$ away, and noted it as "very faint". In the absence of additional measures that can help confirm CPM, this close pair is retained as a candidate.

HD 178428: *Binary.* The primary of a 22-day SB1 has a single 1987 measure listed in the WDS with a separation of $0\farcs2$. Repeated attempts by speckle interferometry have failed to confirm this pair. The FIC lists six null results and attempts by B. Mason and I at the KPNO 4-m telescope in 2008 June once again failed to reveal any companion.

HD 182572: *Single.* The CNS (Gliese 1969; Gliese & Jahreiß 1991) lists this is as "SB?" and "RV-Var?" in the two versions of the catalog. Nidever et al. (2002) show this to a constant velocity star with a scatter less than 0.1 $\mathrm{km\,s^{-1}}$ in observations over four years, which is confirmed by other high-precision radial-velocity campaigns (A. Hatzes 2008, private communication).

HD 184385: *Single.* The CNS (Gliese 1969) list this as "RV-Var", but Nidever et al. (2002) and the CfA survey show this to be a constant velocity star (see § 6.1).

HD 186408: *Triple, one planet.* This close companion to 16 Cyg A was first resolved 3″ away by Turner et al. (2001) with AO at the Mount Wilson Observatory and confirmed by Patience et al. (2002b), who demonstrated CPM and measured infrared magnitudes consistent with the primary's distance. Four CfA velocity measures over 25 years show a slow downward drift, consistent with this companion. This system also has a wide companion, 16 Cyg B, which is a planet host. The WDS lists an additional source, 16″ away from 16 Cyg B, but Patience et al. (2002b) measured the infrared magnitudes of this candidates, demonstrating that it is a background star. This is the only planetary system in this study with more than two stars.

HD 190067: *Binary.* This pair was discovered by Turner et al. (2001) with AO at the Mount Wilson Observatory, but the single-epoch measure with no color information does not allow confirmation of a physical association. B. Mason and I observed this pair at the KPNO 4-m telescope in 2008 June. While the separation and Δm are too large for speckle observations, a stellar source was seen at the expected position, confirming CPM, and given the proximity to a large proper motion ($0\farcs6\,\mathrm{yr}^{-1}$) primary, the physical association of this pair is very likely.

HD 190406: *Binary.* Liu et al. (2002) discovered a faint companion 0.″8 from this star with AO at the Gemini North and Keck II telescopes and confirmed a physical association by demonstrating CPM, consistent spectroscopy, and longterm radial-velocity trend. They determined a spectral type for the companion of L4.5 $\pm$ 1.5, estimated its mass to be 55–78 M_J and age as 1–3 Gyr. This is the first substellar object imaged so close to a solar-type

star and indicates that brown dwarfs can exist in extrasolar systems at positions comparable to the gas giants in our solar system.

HD 191499: *Binary.* The WDS lists 51 measurements of this pair between 1782 and 2003, which are all consistent with a bound pair. There is little evidence of orbital motion during the roughly 200 years of observations, possibly because the companion is near apastron or the orbit is highly inclined. *Hipparcos* and Tycho-2 proper motions differ by 5.6σ, indicating some orbital motion (see Table 5.2). The photometric distance estimate is not a very good match (see Table 4.2), but photometry would be tricky for this close pair as indicated by the large uncertainties of the 2MASS magnitudes. Given the evidence of consistent WDS measures, proper motion differences between *Hipparcos* and Tycho-2, and similar distance estimates, this pair likely has a physical association.

HD 192310: *Single.* The CNS (Gliese 1969) designates this star as "SB?", but there is no independent confirmation. On the contrary, published velocities show little variation over a long period of time (Kennedy & Przybylski 1963; Abt & Biggs 1972; Beavers & Eitter 1986; Duflot et al. 1995; Gontcharov 2006).

HD 193664: *Single,* maybe *Binary.* The *Hipparcos* and Tycho-2 proper motions differ to greater than a 3σ significance indicating an unseen companion (see § 5.1.2), but in the absence of other conclusive evidence, this companion is retained as a candidate.

HD 195564: *Binary.* The WDS lists 16 measures over 110 years that are consistent with a bound pair. While proximity to the primary and Δm $\sim$ 5 (from WDS) make photometry of the companion difficult, the proximity and CPM implied by the measures argue for a

physical association.

HD 200525: *Triple.* The CNS (Gliese 1969) and *Hipparcos* identified the closer pair as a possible binary (stochastic solution) and Goldin & Makarov (2006) derived a photocentric orbit using the *Hipparcos* intermediate astrometry data. Their orbital solutions using data from the two independent *Hipparcos* reduction methods, Fundamental Astronomy by Space Techniques (FAST) and the Northern Data Analysis Consortium (NDAC), are consistent. The FAST data yielded $a_0 = 68^{+82}_{-27}$ mas, $P = 2145^{+3036}_{-914}$ days, $e = 0.70^{+0.10}_{-0.08}$, $\Omega = 13^{+180\circ}_{-4}$, $\omega = 148^{+32}_{-135}{}^\circ$, $i = 90^\circ \pm 2^\circ$, and $\pi = 51 \pm 1$ mas, and the NDAC orbit resulted in $a_0 = 88^{+106}_{-41}$ mas, $P = 2429^{+3089}_{-1104}$ days, $e = 0.65^{+0.11}_{-0.07}$, $\Omega = 17^{+180\circ}_{-3}$, $\omega = 147^{+32}_{-136}{}^\circ$, $i = 91^\circ \pm 1^\circ$, and $\pi = 51 \pm 1$ mas. They tested their orbit determination method satisfactorily against 235 known binaries and derived a better than 99% confidence level based on simulations. The WDS lists four measurements from 1898 to 1932 during which time the separation reduced from about $1''$ to $0''.16$. The respective position angles of the measurements fall in the first, second, and third quadrants, and are consistent with a high-inclination orbit. Given these independent measurements leading to similar results, I conclude that while the orbital elements may be preliminary, this pair is physically bound. For the wider pair, the WDS has five measures over 88 years that are also consistent with a bound pair. The companion is NLTT 50542 with a proper motion that matches the primary's, and the notes in the catalog recognize this pair as gravitationally bound. 2MASS magnitudes have a large error, but, within 1σ, are consistent with a mid-K dwarf companion at approximately the primary's distance.

HD 200560: *Binary.* The WDS has seven measurements of a pair with separations ranging from 2.″8–3.″3 over 28 years and are consistent with a bound pair. This is especially significant given the primary's large proper motion of $0.''4\,\mathrm{yr}^{-1}$. The companion, GJ 816.1B, is recognized in the CNS as bound, although no conclusive evidence is presented. The 2MASS photometry has large errors, and hence is not very useful. The *Hipparcos* and Tycho-2 proper motions are different to about 8σ, providing evidence of orbital motion and lending credibility to a physical association. The WDS lists this pair as the CD component of the B3V binary HD 200595 AB, but there is clearly no physical association between HD 200560 and HD 200595 as seen by blinking archival images.

HD 202275: *Binary.* This is a 5.7-year SB2VB. Tokovinin et al. (2006) gives an additional orbit with a period of 5.7 days, which is in fact the former orbit listed with an incorrect unit (A. Tokovinin 2007, private communication). This system is a binary with mass estimates of 1.2 $M_\odot$ and 1.1 $M_\odot$ by Pourbaix (2000).

HD 203244: *Single.* *Hipparcos* lists a photocentric orbit for this star with a period of 2.9 years and an inclination of 110°± 3°. *Hipparcos* and Tycho-2 proper motions match to within 1σ. Radial velocities in Abt & Biggs (1972) and Gontcharov (2006) indicate a constant velocity star.

HD 206860: *Binary.* Luhman et al. (2007) report the discovery of a T2.5 ± 0.5 companion using Spitzer IRAC images and confirm CPM using 2MASS images. The infrared colors are consistent with the distance to the primary, confirming companionship. By comparing the luminosity with evolutionary tracks, they estimate the companion's mass as 0.021 ±

0.009 $M_\odot$ and age as 0.3 ± 0.2 Gyr. Additionally, a potential wide companion, 591″ away at 16°, was identified by blinking archival images but refuted because its proper motion of $\mu_\alpha = 0\farcs111\,\mathrm{yr}^{-1}$ and $\mu_\delta = -0\farcs089\,\mathrm{yr}^{-1}$ from Ducourant et al. (2006) is significantly different from the primary's *Hipparcos* value of $\mu_\alpha = 0\farcs231\,\mathrm{yr}^{-1}$ and $\mu_\delta = -0\farcs114\,\mathrm{yr}^{-1}$. Photometric distance estimates to the candidate companion show it to be a distant field star.

HD 217107: *Single star with two planets or a binary with one planet.* The WDS lists two measurements, fifteen years apart, of a companion 0.″3 away from this star, which also hosts two planets. These speckle interferometry detections could however not be confirmed by the same technique on at least three other occasions, indicating that this pair might have a large or varying Δm. Interestingly, the farther planet is one of the most widely separated planets reported, lying at least 5 AU from the star. Vogt et al. (2005) present orbital solutions with periods of 7–9 years, but mention that it could be three times larger. Wright et al. (2008) present an updated orbit with $P = 11.5 \pm 0.5$ years and $a = 5.27 \pm 0.36$ AU. At the 20-pc distance to the star, these separations are consistent with the speckle observations. Given the inconsistent measures, if we assume a ΔV near the speckle limit of about 3, the companion to the G8 IV-V primary (Gray et al. 2003) could be an early M-dwarf. The mass-sum of such a binary is consistent with the Wright et al. (2008) orbital elements. Vogt et al. (2005) note that an AO image obtained with the Keck telescope did not reveal any stars beyond 0.″1 from the primary, and Chauvin et al. (2006) confirm this null result with VLT and CFHT AO observations. The M-dwarf companion would also imply a significantly larger velocity semi-amplitude for the primary, but that possibility is

not convincingly excluded by the orbital plot in Wright et al. (2008). While it appears that this "planetary" companion could be a star, further observations are warranted.

HD 220140: *Triple.* The WDS has five measurements over 100 years for the closer visual companion at separations of about 10″that are consistent with a bound pair. The companion is NLTT 56532 with a proper motion matching that of the primary. 2MASS colors of the companion indicate an early M-dwarf at approximately the primary's distance. The wide CPM companion, 16′ away, was first identified by Lépine & Shara (2005). Makarov et al. (2007) confirm companionship by obtaining a trigonometric parallax of 51.6 ± 0.8 mas for the companion, which agrees well with the primary's *Hipparcos* parallax of 50.7 ± 0.6 mas. Their BVRI photometry along with 2MASS near-infrared magnitudes show that this star is over-luminous in the K_s band, confirming its suspected pre-main-sequence status, and enabling an age estimate of 12–20 Myr.

HD 222368: *Single.* The CNS (Gliese & Jahreiß 1991) lists this as "SB?", but Nidever et al. (2002) confirms it as a constant velocity star.

Astronomy compels the soul to look upwards and leads us from this world to another.

—— *Plato*

– 8 –

Discussion and Analysis

8.1 Comparison with DM91 Multiplicity Statistics

DM91 studied 164 solar-type stars in the solar neighborhood and derived observed multiplicity percentages for Single:Double:Triple:Quadruple systems of 57:38:4:1. They also identified candidate companions for stars with $P(\chi^2) < 0.01$, and when these are also included, the percentages change to 50:41:7:2. The current study with a sample of 454 primaries yields corresponding numbers of 57:33:8:3 for confirmed systems and 54:34:10:3 when candidates are included. To compare these results meaningfully, I first estimated the uncertainties for each of these numbers using bootstrap analysis with 10,000 iterations, as explained in § 7.2. The results of the current study are listed in Table 7.2, and the corresponding fractions for the DM91 confirmed pairs are $57 \pm 4 : 38 \pm 4 : 4 \pm 1 : 1 \pm 1$, for which Figure 8.1 shows the distribution of the multiplicity frequencies. The uncertainties are larger for the DM91 results because their sample is about a third the size of the current work.

These results reveal the following interesting points:

(i) The percentage of triple and quadruple systems in the current study is double that of the DM91 results. Additionally, the current study includes two quintuple systems while DM91 had none. These differences are significant to 3σ for triple systems and 2σ for quadruples. The current results show that 24% of non-single stars are higher-order than binaries, compared to 13% in DM91, confirming their prediction that additional multiple systems were

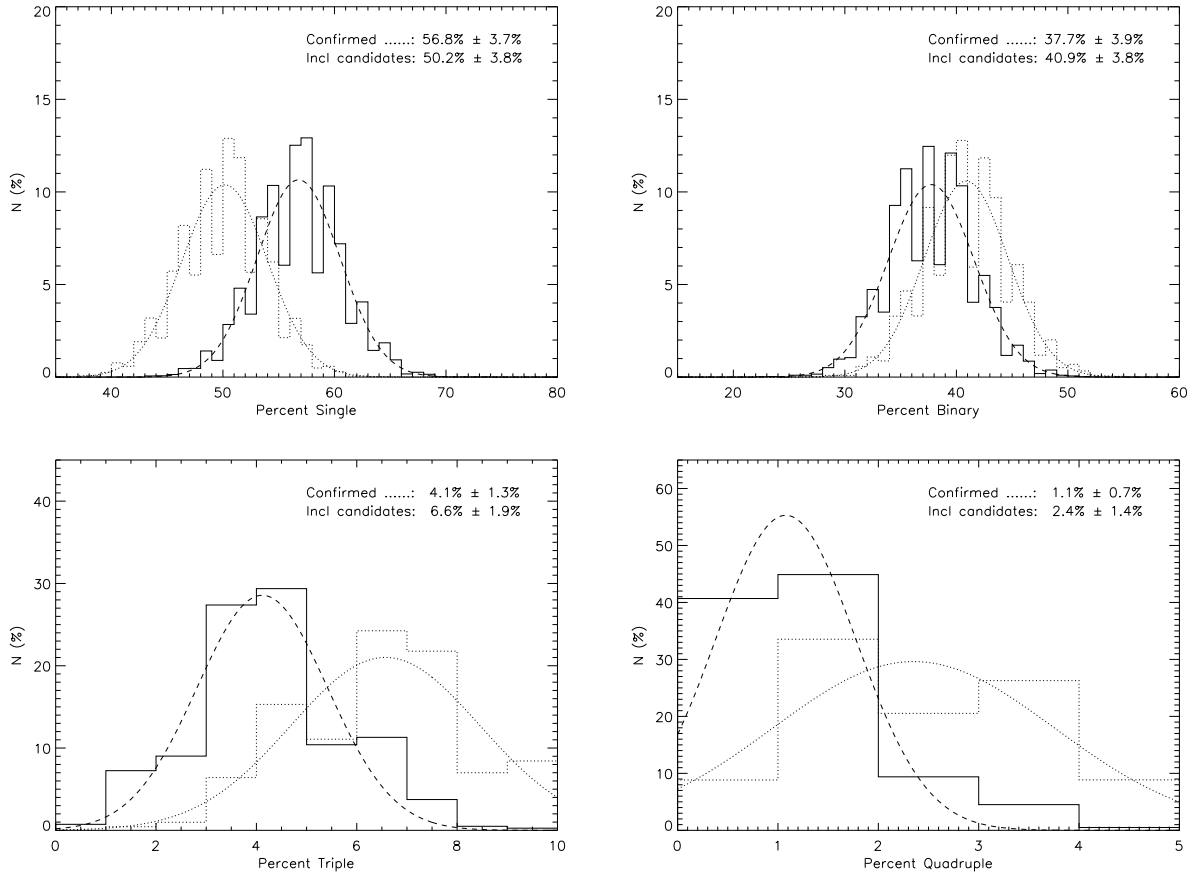

FIGURE 8.1: The DM91 frequency of single, binary, triple, and quadruple systems. Symbols and methods are same as Figure 7.2

likely to be detected among nearby solar-type stars. Apparently, the attention garnered by this sample of stars has indeed revealed these multiple systems missing in the earlier study. Could the present work still underestimate the percentage of higher-order multiples? That is certainly a possibility, especially given my approach of matching suspected or confirmed companions by different methods. Whenever companions revealed by different methods were consistent with indicating the same physical companion, I assumed that they did. Sometimes this could be confirmed, as in the case of spectroscopic and visual orbits with the same

orbital period, but often all I had was a consistency check. For example, does a slow linear drift in radial velocities over, say, 20 years indicate a new companion or is it measuring the known 250-year visual pair? The nature of hierarchical systems indicates that these two measurements relate to the same companion, and this is the assumption I make. Similarly, proper motion acceleration seen for a component of a visual orbit pair is assumed to not indicate an additional component. It is important to note that even if this approach misidentifies two different companions as one, a later rectification can only enhance the multiplicity order of binaries or higher-order systems, but will not change the estimated percentage of single stars.

(ii) While the percentage of multiple systems has doubled, it has come solely at the expense of binary systems. It is indeed remarkable that despite almost twenty years of monitoring since DM91, the observed percentage of single stars remains steadfastly fixed at 57%. This, despite not only a great deal of additional monitoring with techniques available at the time of DM91, but also with far improved sensitivity levels and entirely new methods. This could either be because the current study has missed many companions to presumed single stars or because the majority of Sun-like stars are indeed single. One way to answer this question is to see if binary systems have received greater attention in finding additional companions while single stars have been neglected. While it is true that some studies focus on higher-order multiplicity (e.g. Tokovinin et al. 2006), single stars have also received a lot of attention, and perhaps a lot more attention, given that the high-precision radial velocity search efforts avoid close binaries. I will return to this in the next section on incompleteness

analysis, but the data seem to indicate that the fraction of single Sun-like stars estimated from observations may be coming close to the real answer.

(iii) The reduction in the percentage of single stars when candidates are included is smaller in the current study (3%) when compared to DM91 (7%). This is also a consequence of the varied efforts in monitoring these Sun-like stars and the comprehensive nature of this study. The DM91 candidate list was mostly comprised of suspected spectroscopic binaries based on $P(\chi^2) < 0.01$, which I have shown to be an unreliable metric in Chapter 6. In contrast, the candidate list of this study is what remains so after inspecting every suspected companion revealed from many different methods, by using other means to decide their ultimate fate. A majority of the initial candidates were thus confirmed or refuted during the course of this effort. The details of this process have been covered in preceding chapters, but I mention a couple of examples here. Most suspected radial-velocity variables in DM91 or in the CNS were identified as either bonafide binaries or spurious entries using the results from modern monitoring surveys. On the other hand, ongoing measurement of visual pairs and the blinking of digitized images helped refute many suspected companions as they clearly did not exhibit CPM or helped confirm suspected pairs through observed orbital motion. Section 7.4 describes the rationale for making a lot of these decisions, which have led to a shorter, more qualified list of candidates.

To further check my results with the DM91 study, I investigated the 106 systems common to the two surveys. Results of bootstrap analysis with 10,000 iterations for confirmed companions, as explained in § 7.2, are listed in Table 8.1. The first row lists the DM91 results for

their entire sample of 164 stars, and the second row only includes their multiplicity results for the 106 stars in common with this work. As expected, these results are fairly consistent. The third row lists the overall ratios of this work for the sample of 454 stars, and the fourth row lists the statistics for the same set of 106 stars as in the second row, but using the multiplicity results of this work. While the results for triples and quadruples are consistent with the full sample, the single star percentage drops by 8% and the binaries increase by 7%. At first glance this appears to be significant as the deviations are significant to about 1.5σ. Why did this work result in a noticeable change in the fraction of single stars for these 106 stars compared to DM91, while such a result was not seen in the overall sample? An investigation of the individual systems revealed that three of the DM91 companions are now refuted, two by blinking archival images to show that suspected companions are field stars and one (HD 103095) by leveraging recent work which showed that superflares intrinsic to the star were incorrectly interpreted as a varying companion (see § 7.4). On the other hand, new companions have been confirmed in 16 of these systems, three by identifying CPM companions by blinking multi-epoch images, two SB1 with $K_1 = 4 - 10$ km s^{-1}, two by speckle interferometry, two more by visual orbits, six faint companions by AO or infrared imaging, and one by accelerating proper motion. I will return to this discussion in the next section on incompleteness analysis as it appears that many companions suspected by DM91 as missed have indeed been found. The puzzle being considered here is why these 106 stars are rich in companions compared to the overall sample. Is the difference merely statistical scatter or indicative of something more significant? To test this, I selected 10,000 random subsets

of 106 stars from the sample for which the results are listed on the fifth row of Table 8.1. These results are very consistent with the overall results suggesting that the particular set of 106 stars overlapping with DM91 is simply statistical wander.

TABLE 8.1: Comparison of Multiplicity Statistics with DM91

Sample	**N**	**Single**	**Binary**	**Triple**	**Quadruple+**
DM91, overall.....	164	57 ± 4	38 ± 4	4 ± 1	1 ± 1
DM91, common.....	106	55 ± 5	38 ± 5	3 ± 2	1 ± 1
This work, overall.....	454	57 ± 2	33 ± 2	8 ± 1	2 ± 1
This work, common....	106	49 ± 5	40 ± 5	9 ± 3	2 ± 1
This work, subset.....	106	55 ± 5	34 ± 4	8 ± 3	3 ± 2
This work, dec $> -15°$	307	54 ± 3	35 ± 3	8 ± 2	3 ± 1

Are there other factors that could explain the richness of companions in stars common to DM91? I explored two other avenues and did not find anything significant. First, the current sample is all-sky, but DM91 was limited to declination north of -15°. Could it be that the southern hemisphere stars included in this study are less studied and hence missing companions? The last row of Table 8.1 shows the multiplicity fractions for the 307 stars of this study with declination $> -15°$. Indeed, the percentage of single stars drops by 3%, a 1σ departure, but not enough account for the 8% difference seen for overlapping stars. Moreover, the correction for missed systems that is handled in the next section addresses this gap in deriving the true multiplicity fractions. The second factor I consider is the difference in color range between the samples of this effort and that of DM91. This is covered in § 8.3.1 and again seen to not explain the difference seen for the overlapping stars.

Finally, I considered if the DM91 sample was perhaps biased to a selection of binaries? While their work specifically selected a volume-limited sample to avoid such effects, we now know that their source for parallax, the CNS catalog (Gliese 1969), has significant errors as seen in Figure 2.5. While there is no reason to believe that the Gliese catalog would systematically overestimate the parallax of brighter stars, Figure 8.2 shows that almost all stars significantly above the main sequence are ones now known to lie outside their criteria, illustrating that the distributions around the main sequence for stars selected from *Hipparcos* and Gliese (1969) are substantially different, in contrast to the results presented in Halbwachs et al. (2003). However, most of these outliers appear to be evolved stars which are expected to have fewer detected companions because older stars have a greater chance of losing companions through dynamical interactions and the increasing Δm as one component evolves makes it harder to find companions. The percentage of binaries among these outliers is under 35%, so confirming the above suspicion. Hence, the extraneous stars in the DM91 sample do not introduce a bias in their multiplicity results.

So, we are left with two possibilities. Either the thoroughness with which the 106 overlapping stars have been studied is higher than the rest of the stars in the sample, causing us to underestimate the binary fraction, or the difference seen is strictly statistical scatter. The coverage of the stars presented in the previous chapters does not suggest any bias towards a better analysis of any particular subset of stars, which is also supported by the data on the fifth row of Table 8.1, leading me to conclude that the difference in the fourth row of the table is simply within the expected distribution.

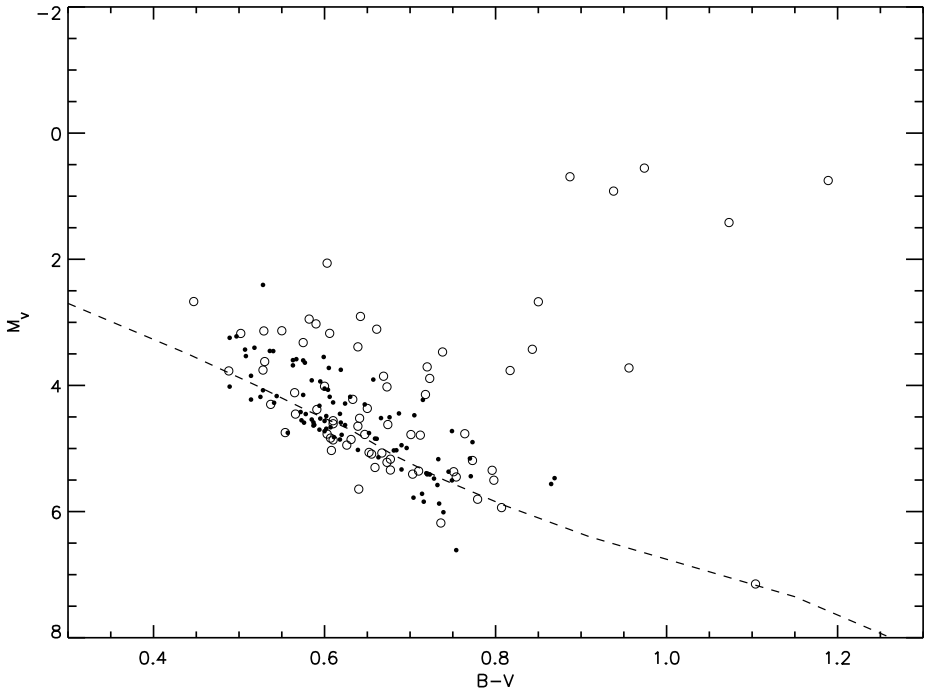

FIGURE 8.2: HR diagram for the DM91 sample using magnitudes and parallax from *Hipparcos*. Small filled circles represent stars in the DM91 sample that are still consistent with their criteria using *Hipparcos* data while large open circles are now known to fall outside the DM91 selection criteria. The dashed line is the main sequence from Cox (2000).

8.2 Incompleteness Analysis & True Stellar Multiplicity

This survey of nearby solar-type stars benefits from the tremendous attention these stars have garnered over the years from observers using many different techniques. Various published results from many surveys have augmented the observations of this survey, resulting in excellent coverage for spectroscopic and high-resolution astrometric techniques suited for short-period systems, to systematic searches for the widest companions out to the limits of gravitational binding. A usual deterrent in collecting comprehensive information from

prior efforts is that while positive results are generally published promptly, null results often remain unpublished, keeping the rest of us guessing as to the true nature of unreported systems. The unpublished radial velocity data obtained from D. Latham, A. Hatzes, and W. Cochran and treated in Chapter 6, along with the published list of stable velocity stars in Nidever et al. (2002), significantly address this gap and permit reliably estimating the population of stable velocity stars. The high-precision radial velocity data of the CCPS efforts obtained from G. Marcy for statistical analyses and discussed below in § 8.2.1 help further constrain the number of spectroscopic companions missed. Given the high precision of these velocity measures and the systematic monitoring over the past 13 years, the resulting estimates include not only the lowest-mass stellar companions but also brown dwarfs.

Since DM91, significant progress has also been made in the observations of visual pairs with various techniques. Almost every star of the sample has been observed with speckle interferometry, probing for the closest visual companions, and AO surveys have unearthed close high-contrast pairs. The *Hipparcos* mission identified nearby companions out to a few-arcsecond separations, and the blinking of archival images as described in Chapter 4 identifies companions out to about 10,000 AU. I have also included published and unpublished results of AO surveys and the results of various searches for wide and close brown dwarf companions (see § 8.2.3). Much progress has also been made in searches for nearby field white dwarfs (Holberg et al. 2008; Gatewood & Coban 2009; Lepine et al. 2009; Subasavage et al. 2009), which preferentially select high proper motion targets, and hence improve the chances of finding companions to the sample stars, which also have high transverse motions. These

results have augmented early efforts in identifying five white dwarf companions to the stars of this study (HD 13445, 26965, 63077, 100623, and 147513), while DM91 had none, and estimated eight undetected white dwarfs. Given all these observations covering a wide range of methods, the survey results presented here are relatively complete, allowing a more simple extrapolation approach to reliably estimate the number of companions missed. The following sections carries out this analysis for spectroscopic and visual pairs.

8.2.1 Missing Spectroscopic Companions

DM91 performed a simulation based on the criteria for missed spectroscopic binaries outlined in Abt & Levy (1976), which specified that no SB1 with $K_1 < 2$ km s^{-1} and no SB2 with $K_1 < 20$ km s^{-1} could be detected by their surveys. They generated a large sample of fictitious binaries for various trial values of M_2 and P with randomly distributed T, ω, and i, and an eccentricity distribution which assumed circularization for period below 10 days, the Hyades dwarf distribution for intermediate periods, and $f(e) = 2e$ for for periods larger than 1000 days. Their basis for this eccentricity distribution for long-period systems was a theoretical study by Ambartsumian (1937), but our data, presented in the following section, seems to indicate a more random distribution of eccentricities. For each fictitious binary, they estimated the radial velocities at the epochs of actual observations of their stars, and computed a $P(\chi^2)$. The resulting detection probability curves for various periods and mass ratios led them to conclude that the average detection probability for $-1 < \log(P) < 4$ was 0.75, yielding an incompleteness factor of 1.33.

Ongoing efforts with increased sensitivity have effectively plugged the detection gaps

mentioned above. Six of the 48 single-lined solutions listed in Table 6.2 have $K_1 < 2$ km s^{-1}, two of which have $K_1 < 1$ km s^{-1}. All 50 of the exoplanets reported in Table 6.5 have $K_1 < 0.5$ km s^{-1}, 42 of which have $K_2 < 0.1$ km s^{-1}, and many less than 10 m s^{-1}. Nearly half of the double-lined solutions listed in Table 6.3 have $K_1 < 20$ km s^{-1}, two thirds of which are below 10 km s^{-1}. These results show that we can now reliably detect companions to a much higher sensitivity than was available to DM91. Further, as shown in § 6.1, I do not believe that the $P(\chi^2)$ test provides reliable results and likely contributes many false positives. In fact, of the 26 entries in their Table 1 flagged as "SB?", i.e. candidate companions, 15 overlap with this study and 14 of them appear to be constant velocity stars based on the analyses in § 6.1. The one exception is HD 165908 for which DM91 might have detected the reflex motion of the 56-year VBO in their 14 measures over 10 years. In addition to an individual inspection of the velocity and power spectrum plots conducted by this work, I have greatly benefited from analysis of the high-precision velocities from Geoff Marcy obtained as part of the CCPS program and made available to this effort for statistical analyses. Figure 8.3 shows the excellent coverage in terms of both the number of velocity measures and their time span for the 255 common stars of the CCPS with this effort. Having access to these unpublished data extended the time horizon on the Nidever et al. (2002) results greatly, enabling a thorough search for hidden stellar companions.

Contrary to my expectations, this search resulted in detecting few new binaries. Thirteen of the 255 stars have either too few observations or too brief a time coverage to say anything meaningful. Of the remaining 242 stars, 168 (69%) appear to be of stable radial velocities

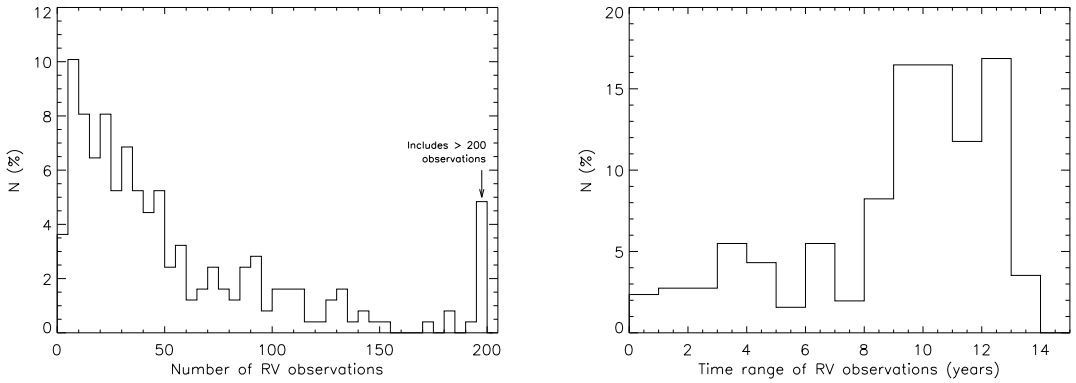

FIGURE 8.3: The distributions of the number of radial velocity measurements per star (left) and their time span (right) in the CCPS survey.

with external errors well below the 0.1 $\mathrm{km\,s^{-1}}$ threshold used by Nidever et al. (2002) and this effort as signaling stellar companions. As expected, this percentage is higher than the frequency of single stars in the entire sample because the CCPS effort avoids known close binaries. Figure 8.4 shows the external error distribution of these stars from the CCPS observations. Of the 25 stars exhibiting rms scatter greater than 0.1 $\mathrm{km\,s^{-1}}$, three have published planets (Butler et al. 2006) and seven have published stellar companions (Nidever et al. 2002; Vogt et al. 2002), six of which also have corresponding orbits from the CfA data. Fourteen of the remaining 15 show variations consistent with known visual companions, yielding only two new companions from this effort that were not detected by any of the other methods.

This information is very useful in constraining the incompleteness of this work as it relates to spectroscopic companions. With two new companions revealed in 242 stars, more than half the size of the overall sample of 454, we could perhaps be missing a total of four new spectroscopic stellar companions. However, as the published solution for HD 4747 is included

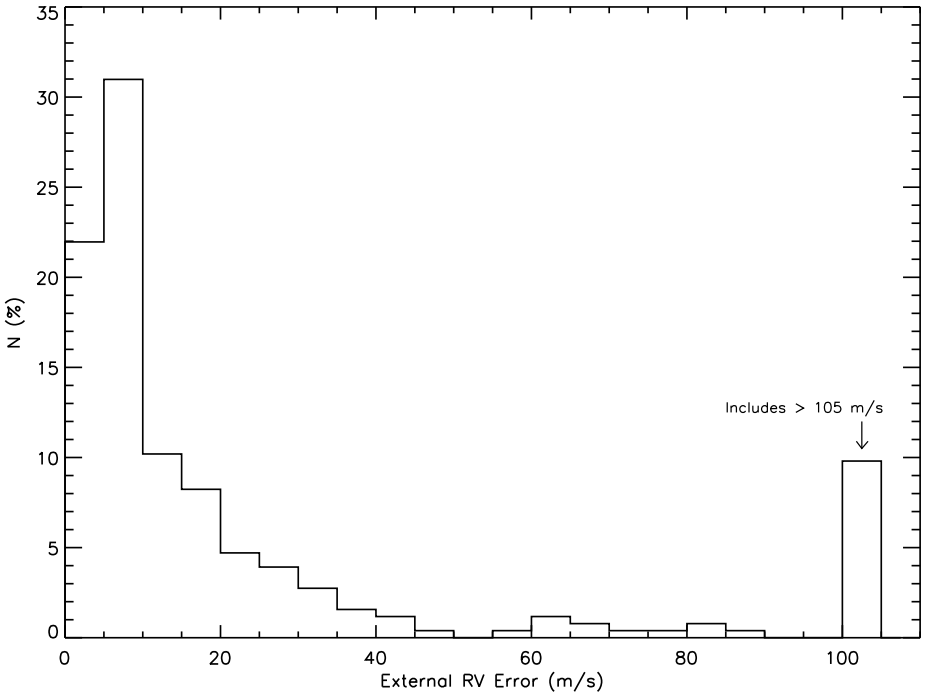

FIGURE 8.4: External error distribution in the CCPS RV measurements.

in this study, the net additional contribution is three new companions. In addition to this, the results presented in Chapter 6 include five new SB1, two new SB2, and one new RV-variable solutions. Two of the new SB1 orbits correspond to known *Hipparcos* photocentric motion orbits and an additional one corresponds to a *Hipparcos* double star. One new SB2 solution is a promotion of an SB1 binary. So, this effort yielded four new binaries that were not known before. These new detections were obtained from the larger than 70% overlap of the sample stars with CfA data, implying possibly two additional undetected companions among the stars not studied by CfA. These two resources of radial velocities are limited by declination constraints and cannot reach close to the south pole, but the extrapolation above should adequately address this gap, implying that a total of only five spectroscopic binaries

are missing from these observed results.

8.2.2 Missing Visual Companions

As seen for the spectroscopic companions above, this work is relatively complete in the visual regime as well. DM91 assumed that their work could not detect any visual companions with $a < 0\farcs3$ and $\Delta V > 0.4$ mag, half the VBs with $0\farcs3 < a < 1\farcs0$ and $2.0 < \Delta V < 3.5$, and essentially all of those with $\Delta V > 3.5$. Significant progress with speckle interferometry and AO have filled these gaps. Comprehensive speckle interferometry programs (McAlister 1978a; McAlister et al. 1993; Mason et al. 2001; Hartkopf et al. 2008; Horch et al. 2008) on telescopes with apertures up to 4 meters can reliably detect sources with $\Delta V < 3$ down to the diffraction limit of the telescopes, and such efforts have studied all but three (HD 2151, 16765, 219538) of the 454 stars of this sample. Coronagraphic and AO efforts on telescopes with apertures up to 10 meters can detect close companions with magnitude differences as large as 10 (Liu et al. 2002; Luhman & Jayawardhana 2002; Potter et al. 2002; Roberts et al. 2005; Turner et al. 2001; Chauvin et al. 2006; Lagrange et al. 2006). An added aspect of completion of these close companions comes from the spectroscopic studies mentioned in the previous section, which reliably detect velocity variations from close low-mass companions.

DM91 pointed out that their effort was likely missing faint, wide companions in the largest numbers. Their incompleteness study estimates that they missed 22 systems with $q > 0.1$, mainly with long orbital periods. As discussed in § 8.1, this work adds two spectroscopic and 14 visual companions to the 106 common stars between DM91 and this effort. Four of these are brown dwarfs discovered by AO and two more are wide brown dwarfs discovered by

infrared imaging. So, we have added eight new companions with $q > 0.1$, which extrapolates to 12 new detections in their full sample of 164 stars. Including brown dwarfs, we have added a total of 25 new companions, confirming DM91's incompleteness analysis and effectively addressing it.

The SFP survey (§ 3.1) revealed no new companions, confirming that the presumed gap between spectroscopic and visual efforts for the stars of this sample is nonexistent, at least for modest Δm pairs. At wider separations, this effort has revealed four previously unknown companions, identified as CPM candidates by blinking the archival images and confirmed by follow-up photometry (see § 4.1). While every star of the sample was blinked, 44 of them did not reveal any motion of the primary between the images blinked, thwarting an attempt to identify CPM candidates, and an additional 43 had marginal movement. Conservatively assuming that only half of the marginal frames were adequately examined results in about 85% completion with this technique, yielding one possible companion missed. This technique is quite effective in detecting companions down to $R = 17$ mag, as evidenced by the refuted candidate to HD 141004 which was measured as $R = 16.9$ and stands well above the background in the images. Assuming an R limit of 17, we can detect down to late M dwarfs at our distance limit of 25 pc. Confirmed companions include a white dwarf companion to HD 63077 and an M6.5 companion to HD 86728, supporting these detection limit estimates. Hence, this technique is well suited for wide companions down to late M dwarf companions. However, it fails for nearby sources which fall within the primary's saturation, which typically is about $15''$, but can be as large as $30''$. Fortunately, the other techniques mentioned above

including traditional visual techniques and the *Hipparcos* mission addressed that parameter space.

8.2.3 Very Low-Mass Companions

The brown dwarf desert at close separations of under $\sim$ 5 AU has now been firmly established by the high-precision radial velocity surveys, which have revealed many planets but few brown dwarfs, even though they are more sensitive to detecting the more massive companions. Based on the discovery of three brown dwarf companions, Gizis et al. (2001) suggested that the brown dwarf desert applicable to radial velocity regimes may not extend out to wider separations, for which they ruled out the low 0.5% brown dwarf frequency seen in radial velocity studies. Many systematic searches for wider brown dwarf companions have been carried out using high-resolution techniques such as coronagraphy, AO, and space-based observations, yielding a few companions to the stars of this sample (e.g. Potter et al. 2002; Bouy et al. 2003; Burgasser et al. 2005; Luhman et al. 2007), which are included in the results presented in the previous chapter. McCarthy & Zuckerman (2004) conducted a comprehensive infrared coronagraphic search for substellar companions in a sample of 280 GKM stars, looking for companions with mass greater than 30 M_J and separations in the range 75–1200 AU. They found only one brown dwarf companion. Grether & Lineweaver (2006) studied the nature of close companions ($P < 5$ years) to Sun-like stars and concluded that while 16% of the primaries have companions more massive than Jupiter, 11 ± 3% are stellar, 5 ± 2% are planets, and less than 1% are brown dwarfs. Other studies have suggested a somewhat higher percentage of wide brown dwarf companions, albeit with large uncertain-

ties. Neuhäuser & Guenther (2004) searched for brown dwarfs wider than 50 AU around 79 stars in three stellar associations using high-resolution imaging techniques, and reported only a single brown dwarf in each group, concluding that $6\% \pm 4\%$ of stars may have wide brown dwarf companions, consistent with the Gizis et al. (2001) conclusion assuming that binaries have the same mass function as field stars. Metchev & Hillenbrand (2008) discovered only two brown dwarf companions in an AO search around 266 F5–K5 stars, and based on an incompleteness analysis, estimated a most-likely brown dwarf companion frequency of 3.2%. Their 1σ confidence interval confines brown dwarf frequencies to $1.5 - 6.3\%$ for separations of 28–1590 AU and mass range of 12–72 M_J. They note that this is a factor of eight smaller than stellar companions, and present a universal companion mass function consistent with their results.

What about the widest of brown dwarf companions at separations of many thousand AU? While the blinking of archival images discussed in the previous section is sensitive to late M dwarfs, it cannot detect brown dwarfs, but this work benefits from other systematic searches for wide brown dwarfs to nearby stars (e.g. Kirkpatrick et al. 2001; Lowrance et al. 2002; Looper et al. 2007). Taking advantage of the steep $V - K$ gradient of substellar sources, these efforts looked for sources around Sun-like stars in 2MASS images with no corresponding source in USNO-A visible images. Candidates thus revealed were followed up to determine if they were low-mass stellar or substellar sources at the distance to the primary. While a number of detections are published, confirming the viability of the technique, these efforts have primarily yielded null results (D. Kirkpatrick 2009, private communication). A

specific search for low-mass companions out to separations of 10,000 AU around solar-type stars within 10 pc resulted in no new detections (D. Looper 2009, private communication). Allen et al. (2007) searched for wide companions in a sample of 132 M7–L8 primaries and detected none, indicating that less than 3% of these low-mass primaries have wide companions. Burgasser et al. (2003) conducted an HST search for brown dwarf binaries, finding a binary fraction of 9^{+15}_{-4}%, most of which were tight binaries with separations $\lesssim$ 10 AU. These conclusions were reaffirmed by Kraus et al. (2006). Dieterich et al. (2009) conducted an HST/NICMOS search for companions to 233 stars within 10 pc. Their search, sensitive to early L dwarf companions at separations of 0.″5 – 10″ and T dwarfs at separations of 1″– 10″, recovered two known brown dwarfs and split an additional one into a nearly equal-mass binary, but found no other brown dwarf companions. The published and unpublished results discussed above indicate a true paucity of brown dwarf companions rather than an incompleteness of search efforts.

This work includes 12 brown dwarf companions in 9 systems (HD 3651, 72760, 79096, 97334, 130948, 137107, 145958, 190406, and 206860). Three of these systems have projected separations of less than 100 AU, and three more have projected separations less than 1000 AU. The implied fractions of stars with brown dwarf companions are consistent with prior studies (McCarthy & Zuckerman 2004; Metchev & Hillenbrand 2008). In contrast, none of the radial-velocity-detected companions to stars in this sample has a minimum mass of over 13 M_J, and only two have a minimum mass of greater than 8 M_J (see Table 6.5), consistent with the expectations of the brown dwarf desert. The widest separation of a confirmed

brown dwarf is 3800 AU (HD 137107E), while the brown dwarf with the extreme separation of 40,000 AU from HD 145958 is retained as a candidate (see § 7.4). Interestingly, three of the nine systems with brown dwarf companions have a pair of closely orbiting brown dwarfs separated relatively widely from the primary. This shows that brown dwarf binaries are overabundant as companions to main sequence stars than for field brown dwarfs, as pointed out by Burgasser et al. (2005) who speculate on the possibility that a pair of brown dwarfs are better able to withstand the dynamical ejection that may be responsible for the formation of these wide pairs.

The above analysis suggests that this work is missing few, if any, brown dwarf companions, and that the true percentage of very low mass companions to solar-type stars is close to the lower limit of 1.9% estimated by DM91 and certainly much less than their upper limit of 14% or the 20% they estimate from the null results of Campbell et al. (1988).

8.2.4 Results from DM91 Incompleteness Analysis

DM91 made two levels of corrections to the fraction of single stars. The adjustment from their observed 57% single stars to 43% single stars was largely based on wide faint companions missed. This works lends credibility to this estimate, identifying 14 visual companions to the subsample of overlapping stars against their estimate of a total of 22 missed, but the current observed fraction of single stars, including these companions, stands at 57% – exactly what DM91 observed! The second adjustment they made was based on the mass-ratio distribution analysis combined with the $P(\chi^2)$ simulations, and this led them to conclude that only one-third of solar-type stars may be truly single, i.e. without stellar or brown dwarf companions.

The current effort shows that this adjustment, although consistent with their analysis and prevailing expectations, was a significant overestimate. There have been other efforts which claimed that DM91 significantly under-estimated the binary frequency of solar-type stars (Söderhjelm 2000; Quist & Lindegren 2000; Kouwenhoven 2006), but the current results were unable to confirm these predictions. Apparently, a majority of solar-type stars are, in fact, single like our Sun.

8.2.5 Missed Companions and True Multiplicity

The above discussion strongly suggests that the results of this survey are relatively complete, and likely represent the most complete survey yet of the sample of nearby solar-type stars. The estimates of five missed spectroscopic and one missed visual companion only suggest a total of six companions missed, representing 1.3% of the stars studied. If we assume that these missed detections are distributed according to the ratio of single to non-single stars presented in § 7.2, the percent of single stars would decrease from 56.7% to 56.0%, a shift well within the 1σ uncertainties, but one that is used to present the final numbers below. In § 8.1, I discussed a possible bias in my results because of an all-sky sample, which may include historically less studied southern-hemisphere systems. The difference in the percentage of single stars between the overall study of 454 stars and the 307 stars with declination above $-15°$ was 2.4%, and the incompleteness analysis performed here, which, given my extrapolation approach, mostly addresses the southern hemisphere stars, accounts for over half this difference, raising the confidence in these numbers. The remaining difference is well within any expected statistical margin of error.

Finally, let us evaluate the candidate companions identified by this effort. Of the 25 candidates, 7 are RV variables, 4 from CfA and 3 from CNS. The four candidates from CfA all show a possible linear trend over a few observations, but the variations are small and well within measurement errors. While more observations are warranted, each of these has a $P(\chi^2)$ larger than 0.01, suggesting that they may have stable velocities. The three candidates from CNS are also questionable. While no independent observations are available to definitively refute them, no confirmation exists either. As discussed in § 5.5, over 50% of the spectroscopic binaries identified in the CNS have later been refuted. So, perhaps one or two of these seven candidates may prove to be real. The remaining candidates include seven close visual pairs, six proper motion accelerations, one *Hipparcos* photocentric orbit, one over-luminous companion, and one (HD 145958) wide brown dwarf companion at 40,000 AU separation with similar proper motion, but perhaps too wide to be bound (see § 7.4). It is hard to say which of these will be confirmed and which refuted, but assuming that half of them are real, the percentage of single:double:triple:quadruple, taking the mid-point of the confirmed and possible fractions in Table 7.2 and including the incompleteness analysis is $55 \pm 3 : 34 \pm 2 : 9 \pm 2 : 2 \pm 1$.

Additionally, the CCPS data revealed 33 radial-velocity variables with rms scatter less than the threshold of 0.1 $\mathrm{km\,s^{-1}}$ used in § 8.2.1. Seventeen of these can be explained by known stellar companions within a few arcseconds, leaving 16 possible new discoveries in these data. These could be long-period planets or yet undiscovered low-mass stellar or brown dwarf companions at a separation of a few arcseconds. Given the extensive monitoring of

these stars with various visual techniques, an estimate that at most half of these turn out to be stellar or brown dwarf companions appears reasonable. Assuming that the implied eight companions missed are distributed across single stars and those with companions in their respective ratios, an additional 1% of the presumed single stars may have companions. Hence, $54\% \pm 3\%$ of Sun-like stars are expected to be single, i.e. with no stellar or brown dwarf-companions.

8.3 Multiplicity Dependency on Physical Parameters

Let us now see if and how the stellar multiplicity is effected by physical parameters such as temperature, age, and elemental abundance. As dynamical masses have only been obtained for a small fraction of the stars, a direct study of the relation of multiplicity to mass is difficult. However, because all stars of the sample fit in a band around the main sequence, the temperature analysis can be interpreted as a dependence of multiplicity on stellar mass. Unless otherwise specified, the following sections limit analyses to confirmed companions. With the large sample studied here, and the proportionally few candidate systems, the patterns seen and conclusions drawn are not expected to materially change by focusing on the confirmed systems.

Before looking at the specific results, let us review the sources of the various physical parameters, which are listed in *Appendix* A along with their references. For the primary stars, spectral types were obtained from Gray et al. (2003, 2006) or *Hipparcos*. Primary star masses, for the few with dynamical estimates, were extracted from the relevant sources.

For the remaining stars, the table in *Appendix* A lists estimates extracted from Valenti & Fischer (2005) or Nordström et al. (2004), in that order of preference. However, the analyses below use dynamical mass estimates, when available, and interpolated masses from spectral types using the relations in Cox (2000) when not, in order to follow a consistent approach. Metallicity, as measured by [Fe/H], was extracted from Valenti & Fischer (2005), Nordström et al. (2004), Gray et al. (2003), and Gray et al. (2006), and the chromospheric activity index, $\log(R'_{HK})$, from Wright et al. (2004), Gray et al. (2003), Gray et al. (2006), or from B. Mason (2008, private communication). For the companions, mass estimates were extracted from the various discovery or characterization publications, when available. Otherwise, spectral types were extracted when available in these publications. For double-lined spectroscopic systems, the measured mass ratio led to an estimate of the companion's mass and spectral type. As a next step, multi-color photometry of the companion was used to estimate its spectral type, otherwise Δm information and the primary's spectral type led to an estimate of the companion's spectral type, and thereby to its mass, using the relations from Cox (2000).

8.3.1 Multiplicity by Spectral Type and Color

It is now well established that a greater percentage of bluer, more massive stars have companions when compared to their redder, less massive counterparts (Burgasser et al. 2003; Mason et al. 2009a, DM91). Let us now test this dependence on the sample studied here and review these results in the overall context across the entire spectral sequence. The reasonably wide color range of $0.5 \leq B-V \leq 1.0$ for the sample of stars studied here enables a

check for the dependence of multiplicity on spectral type or color, and hence indirectly, on mass. Indeed, the bluer stars of this study seem to favor binaries to a 2σ significance when compared to the redder stars, consistent with the overall trend seen for O–M stars. The data seem to suggest a relatively steep drop in the multiplicity fraction at $B-V$ of about 0.63, corresponding to a ZAMS star with the Sun's spectral type. Table 8.2 summarizes the multiplicity fractions by color and spectral type, and Figure 8.5 shows the distribution for four equal color bins.

TABLE 8.2: Multiplicity Statistics by Spectral Type and Color

Sample	**N**	**Single**	**Binary**	**Triple**	**Quadruple+**
F6 $\leq$ SpT $<$ G5	179	52 ± 4	37 ± 4	8 ± 2	3 ± 2
G5 $\leq$ SpT $\leq$ K3	275	60 ± 3	31 ± 3	7 ± 2	2 ± 1
$0.500 \leq B-V \leq 0.625$	131	50 ± 4	38 ± 4	8 ± 2	3 ± 2
$0.625 < B-V \leq 1.000$	323	59 ± 3	31 ± 3	7 ± 2	3 ± 1
F7 $\leq$ SpT $\leq$ G9	281	56 ± 3	34 ± 3	7 ± 2	3 ± 2

The dependence of multiplicity on color raises the question about directly comparing the results of this effort with those of DM91. The color range of $0.5 \leq B-V \leq 1.0$ used for this study selects stars from F6–K3 types. In contrast, the DM91 study was limited to F7–G9. As 167 (37%) of the stars in the current sample have a K spectral type, could they influence the higher percentage of single stars derived here? As the last line in Table 8.2 shows, a selection of F7–G9 stars from this study includes 281 stars, and yields observed multiplicity frequencies consistent with my entire sample, showing that the color-range difference between the two samples does not bias the results presented here.

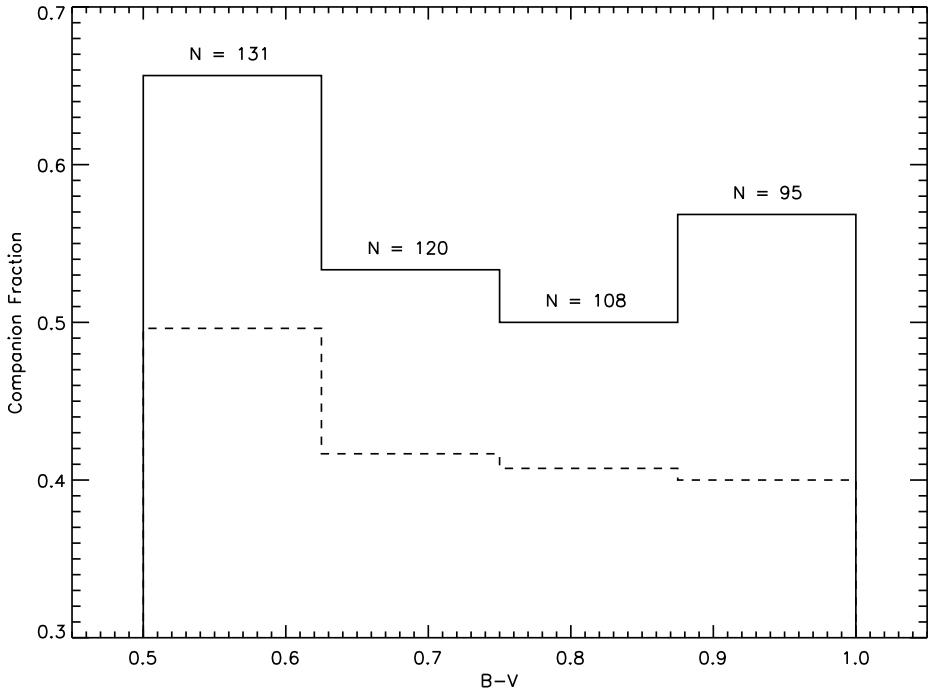

FIGURE 8.5: Multiplicity Statistics by $B - V$ Color.

Let's now look at these results in the context of multiplicity fractions across the entire range of O stars to T brown dwarfs. Most O-type stars seem to form in binary or multiple systems, with an estimated lower limit of 75% in clusters and associations having companions (Mason et al. 1998a, 2009a). Studies of OB-associations show that these high percentages (over 70%) of companionship also apply to B and A type stars (Shatsky & Tokovinin 2002; Kobulnicky & Fryer 2007; Kouwenhoven et al. 2007). M-dwarfs have companions in significantly fewer numbers, with estimates of 30–40% with companions (Henry & McCarthy 1990; Fischer & Marcy 1992; Reid & Gizis 1997). Finally, estimates for late M-dwarfs and brown dwarfs show that only 10–30% of them have companions (Burgasser et al. 2003; Siegler et al. 2005; Allen et al. 2007; Maxted et al. 2008; Joergens 2008). Including the results of this

effort, Figure 8.6 shows the dependence of multiplicity on spectral type for the entire range of stars and brown dwarfs. While the revised results are consistent with the overall trend that multiplicity reduces with reducing mass, they indicate a sharper drop-off at solar-type stars than previously believed.

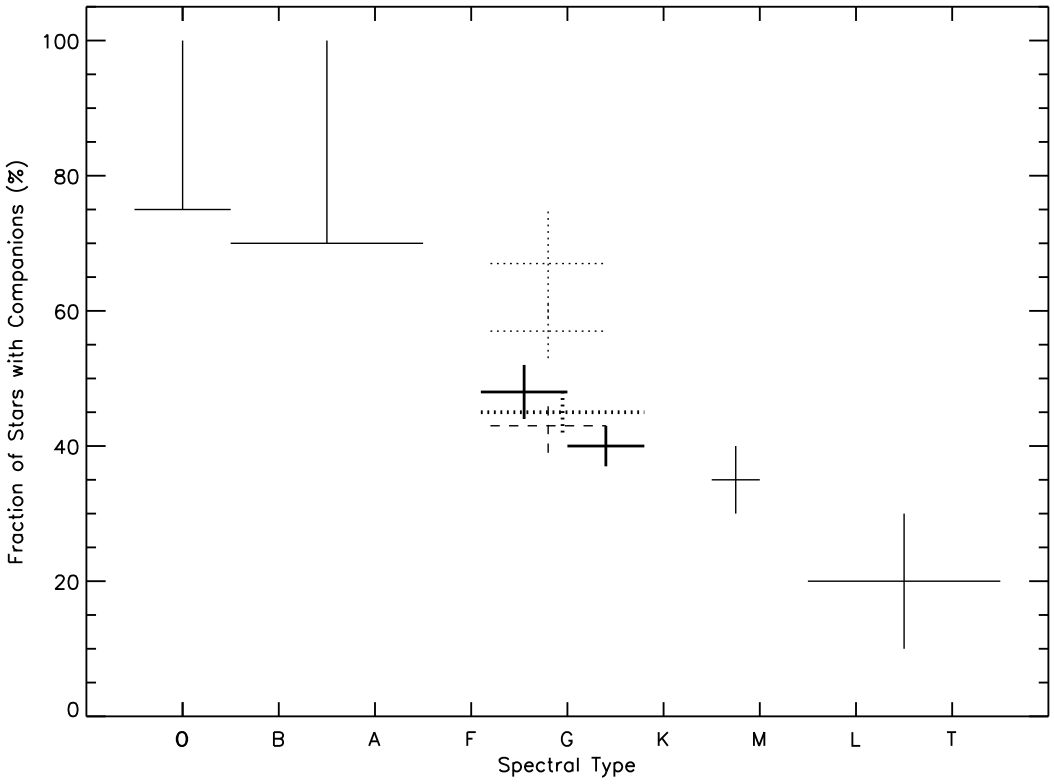

FIGURE 8.6: Multiplicity Statistics by Spectral Type. The thin solid lines represent stars and brown dwarfs beyond the spectral range of this study, and their sources are listed in the text. The OBA stars have only lower limits for the fraction of stars with companions. For the FGK stars studied here, the thick solid lines show the observed results of this work for spectral types F6–G5 and G5–K3, and the thick dotted lines show the corresponding incompleteness adjusted numbers for the F6–K3 range. The uncertainties are estimated by bootstrap analysis as explained in § 7.3. The thin dashed lines show the observed statistics from DM91 with uncertainties estimated here, and the dotted lines show the revised DM91 statistics for incompleteness including only companions more massive than 0.1 $M_\odot$ (lower line) and all companions more massive than 10 M_J (higher line). The observed and corrected results of this study include all stellar and brown dwarf companions.

8.3.2 Multiplicity by Chromospheric Activity

Multiplicity studies of young stars (Ghez et al. 1997; Kouwenhoven et al. 2007), of nearby solar-type stars (Mason et al. 1998b), and of aging stars in globular clusters (Sollima et al. 2007) suggest that binaries and multiple systems tend to get disrupted with age, presumably due to dynamical interactions. The selection of this current sample of solar-type stars is limited to a band around the main sequence to focus on spectral classes IV, V, and VI. This sample contains stars over a wide age range, from stars such as HD 146361, which is believed to be a few 100 Myr old, to stars like the Sun, which are about 5 Gyr old, enabling such a check, but age estimates are tricky. The prolonged evolutionary process of solar-type stars as well as the diversity of abundances in the sample result in a considerable width for the main sequence, preventing the departure from the main sequence as a reliable age indicator. Fortunately, chromospheric emission, as measured by $\log(R'_{\rm HK})$, the ratio of the flux in the cores of a star's Ca [II] H and K lines relative to the star's bolometric flux, is a good age indicator for solar-type stars (Henry et al. 1996), and has been used in prior multiplicity studies (Mason et al. 1998b). This index was extracted for the current sample from Wright et al. (2004); Gray et al. (2003, 2006, and B. Mason 2008, private communication), leaving out only 12 stars without a measurement.

Figure 8.7 shows that the current sample seems to be divided into two subsets, 156 active (younger) stars with $\log(R'_{\rm HK}) \geq -4.75$, and 286 inactive (older) stars with $\log(R'_{\rm HK}) < -4.75$. The figure also helps confirm that the metric used here does not correlate with color, i.e. mass, and seems to be an effective age indicator (Mason et al. 2009b). As seen in

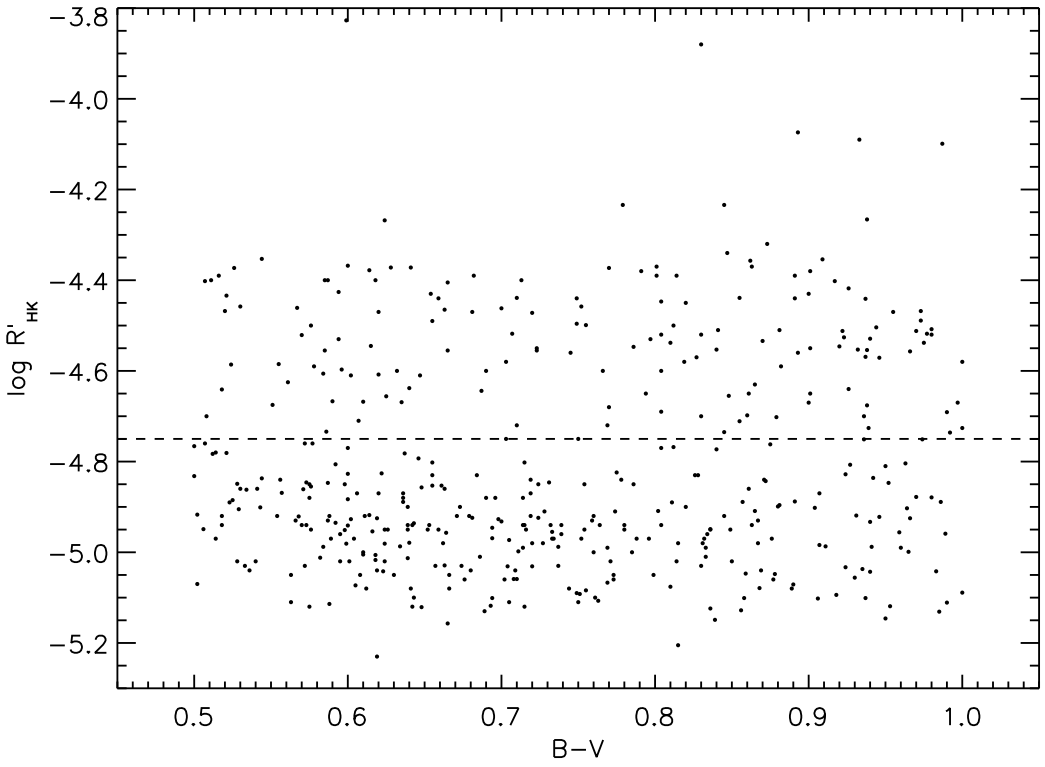

FIGURE 8.7: The distribution of chromospheric activity by $B - V$ color. The dashed horizontal line separates the active subset of stars above the line from the inactive subset below it.

Figure 8.8, the more active stars do have a higher binarity fraction to a 2σ significance.

8.3.3 Multiplicity by Metallicity

Fischer & Valenti (2005) showed that stars with planets preferentially have higher metallicity than those without planets, and concluded that this is because planets are more likely to condense in the circumstellar disks around stars that form out of metal-rich clouds (the "nature" alternative), rather than a result of stars accreting metal-rich planets during the formation process (the "nurture" alternative). The current results allow us to verify the

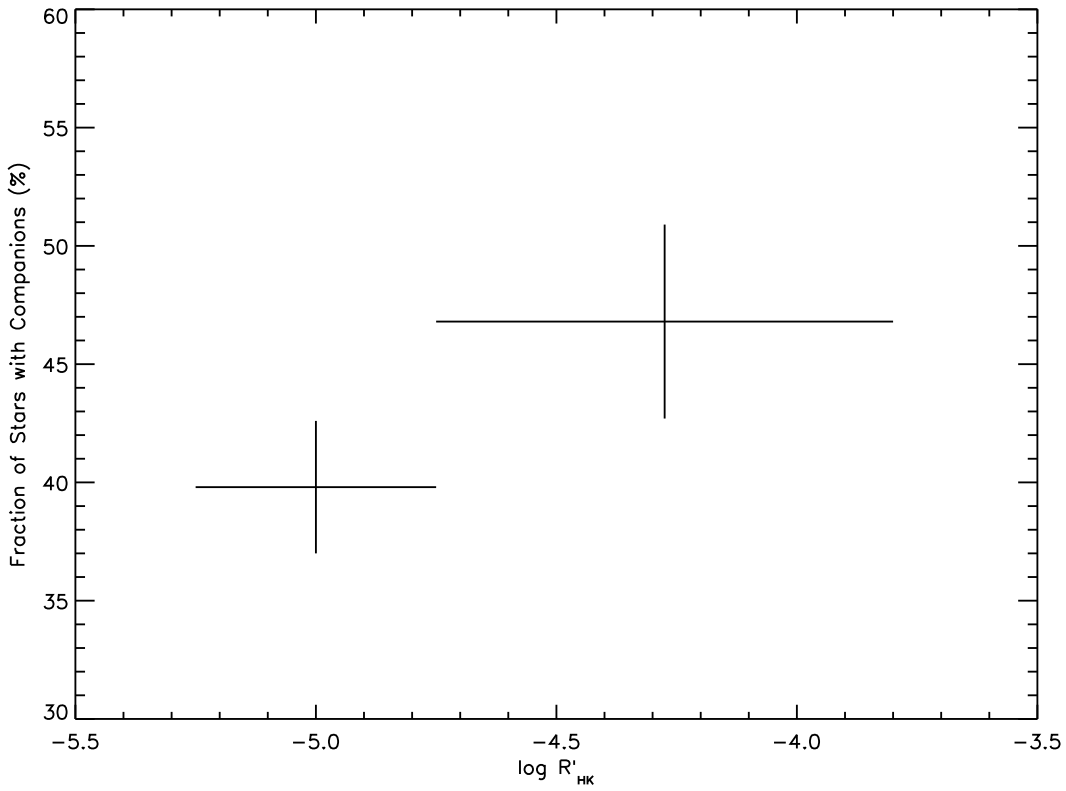

FIGURE 8.8: Multiplicity Statistics by Chromospheric Activity. The percentage of stars with companions among the 156 active (young) and 286 inactive (old) subsets of the sample for the 442 stars with chromospheric activity data. The percentages are for confirmed companions and the uncertainties are estimated from bootstrap analysis as explained in § 7.3.

planet-metallicity correlation and see if they apply to more massive companions such as brown dwarfs and stars.

Figure 8.9 shows the metallicity distribution for stars with and without stellar and substellar companions. Metallicity values for 416 stars of this sample were extracted from Valenti & Fischer (2005), Nordström et al. (2004), and Gray et al. (2003, 2006) in that order of preference. Metallicity is plotted against the $B - V$ colors, showing that there is no correlation between these parameters, and allowing us to focus on multiplicity as it relates to

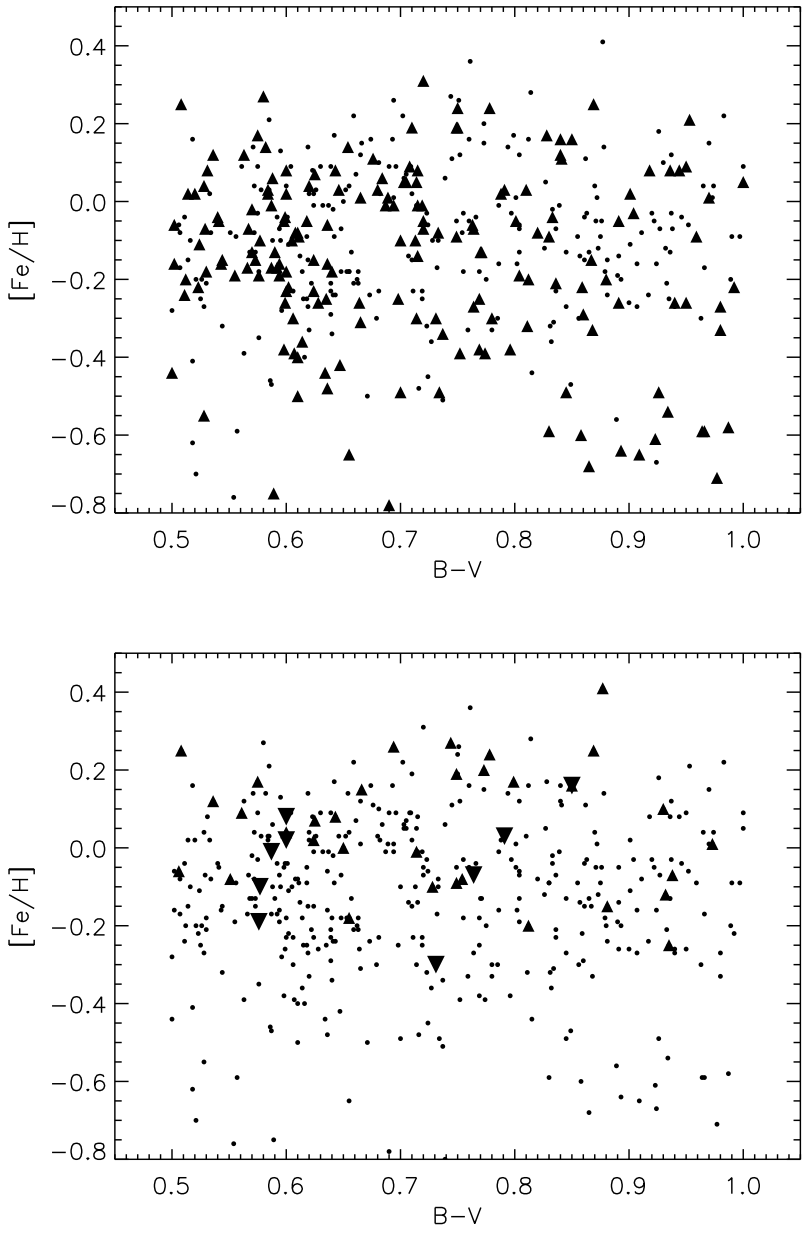

FIGURE 8.9: Multiplicity Statistics by Metallicity. The plot on the top shows stars with (filled triangles) and without (small filled circles) stellar companions plotted with respect to their metallicity and $B - V$ color. The bottom plot shows stars with planetary (filled upward triangles), brown dwarf (large, filled downward triangles) and no substellar (small filled circles) companions.

metallicity. The top panel shows stars with (filled triangles) and without (small filled circles) stellar companions, clearly demonstrating that there is no relationship between metallicity and the tendency of a star to have stellar companions. This is not surprising because while planets may require the presence of higher elements to trigger the condensation process by which they form, the primordial matter that can form one star should be equally likely to form others as well (i.e. this merely illustrates that stars form like stars). But perhaps this clear difference between stars and planets allows one to check if brown dwarfs are more like stars or planets.

The bottom panel clearly demonstrates that planets preferentially form around higher-metallicity stars, as shown by Fischer & Valenti (2005) and confirmed by Figure 8.10. Data on brown dwarf companions is sparse, but the nine systems with such companions are plotted on the bottom panel as the large, downward filled triangles. The lowest metallicity star with a brown dwarf companion is only slightly below that with a planetary companion, and no stars with [Fe/H] below -0.3 dex have either planetary or brown dwarf companions, while many of them have stellar companions. While more data are required to make a definitive conclusion, these preliminary results suggest that brown dwarfs, at least when they are companions to stars, form like planets rather than like stars.

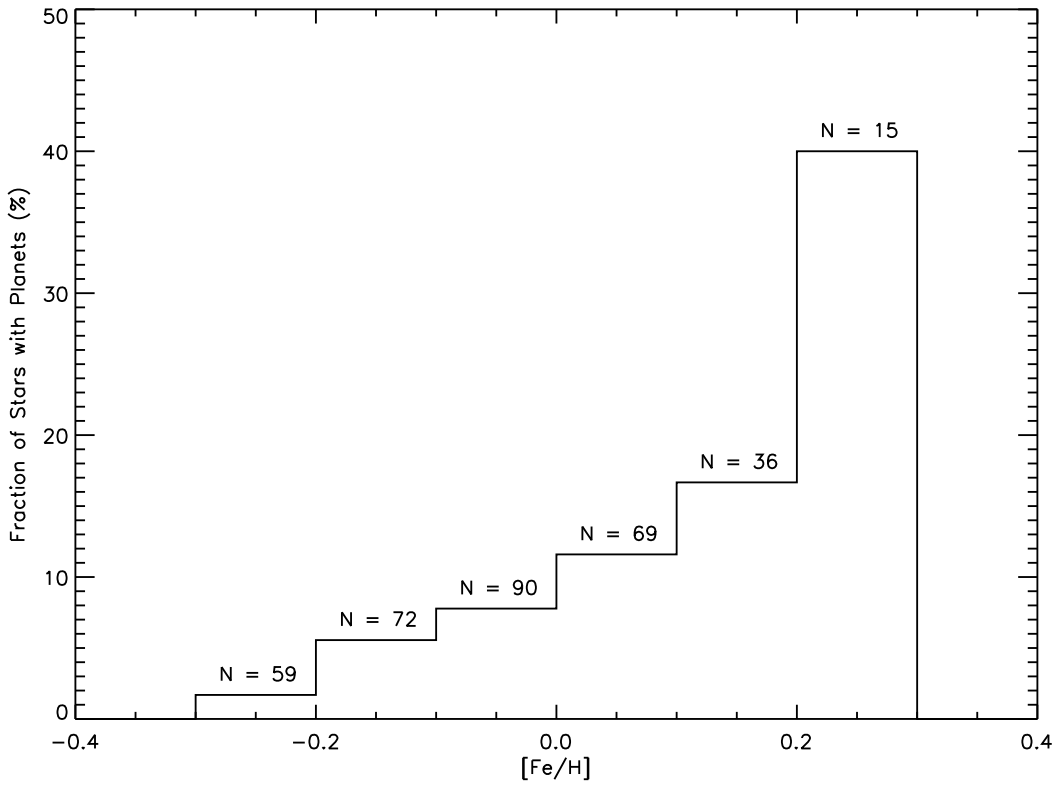

FIGURE 8.10: Planet metallicity correlation for the well-populated [Fe/H] bins of −0.3 to +0.3 dex, containing a total of 341 stars. The histogram shows the percentage of stars with planets, and "N" values are the total number of stars in each bin.

8.4 The Distribution of Orbital Elements

8.4.1 Period Distribution

For some binaries, such as those with spectroscopic, visual, or combined orbital solutions, we have a reliable period estimate. For others, such as radial-velocity variations, proper motion accelerations, or wide CPM companions, the period was estimated as described below. For CPM companions with good measurements of separations, I used the statistical relation $\log(a'') = \log(\rho'') + 0.13$ from DM91 to estimate the semimajor axis. Then, using the

FvL07 parallax, I converted this to a linear semimajor axis in AU and used Newton's generalization of Kepler's Third Law to estimate the period. Mass estimates for the components were obtained as described in § 8.3, taking into account the hierarchical nature of multiple systems. For only two confirmed pairs (HD 25680 AB and HD 147776 AD), companion mass estimates were not available as described above, and they were estimated assuming a mass-ratio of 0.2. For 14 confirmed pairs with unresolved companions, mostly radial velocity variables or proper motion accelerations, no period or separation information was available. For the radial velocity variables, I assumed periods in the range of 30-200 years, reasonable because a shorter period would likely have an orbital solution due to the extensive radial velocity coverage for stars of this sample and periods longer than 200 years are unlikely to be detected with the few decades of velocity measurements to a precision of $\sim 0.5 \mathrm{km\,s^{-1}}$. The accelerating proper motion pairs indicate an observed curvature in proper motions with observations over a few decades, so I assumed periods between 10 and 25 years for these unresolved pairs. The specific value of the assumed period within the above ranges does not impact the following analysis because the entire range fits within one bin in each case.

Figure 8.11 shows the period distribution of all 258 confirmed companions to the sample of solar-type stars, with an identification of the technique used to discover and/or characterize the pair. To provide better context, the axis at the top shows the semimajor axis corresponding to the period below assuming a mass sum of 1.47 $\mathrm{M_\odot}$, which is the average value of all the confirmed pairs. The period distribution seems to follow a roughly Gaussian profile with a peak at $\log(P) = 5.03$, corresponding to a period of 293 years, slightly larger

than that of Pluto around the Sun. The median of the period distribution is 261 years, similar to the Gaussian peak. This compares with a corrected peak and median of 180 years from DM91. The larger value of the current survey is a result of more robust companion information for wide CPM companions. The overall profile of the curve is quite similar to the corrected plot in DM91, suggesting that the companions they estimated as missed have now been found.

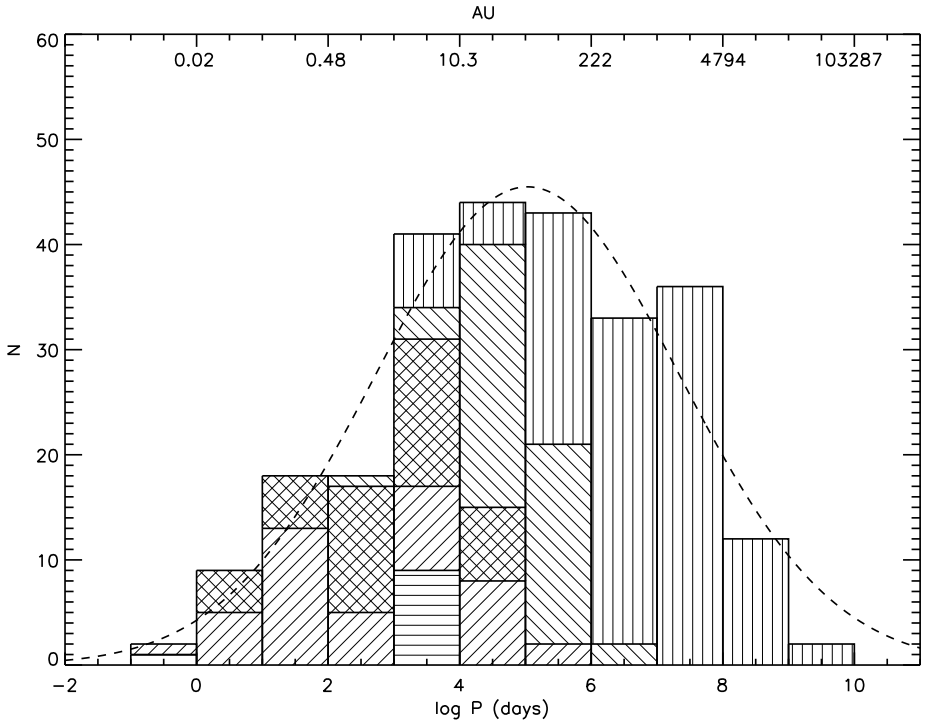

FIGURE 8.11: Period distribution for the 258 confirmed companions plotted by the companion detection method. Unresolved companions such as proper motion accelerations are identified by horizontal line shading, spectroscopic binaries by positively sloped lines, visual binaries by negatively sloped lines, companions found by both spectroscopic and visual techniques by crosshatching, and CPM pairs by vertical lines. The AU separations shown at the top correspond to the periods below for a system with a mass-sum of 1.47 $M_{\odot}$, the average value for all the pairs. The dashed curve shows a Gaussian fit to the distribution. The overlap of multiple techniques for all but the longest-period bins suggests that the coverage is complete. The fall-off of the long-period systems is consistent with canonical limits for gravitational binding.

The overlap of the various detection methods for each period bin, except for the longest bins which, as expected are dominated by CPM companions alone, indicates that there is no gap in the parameter space between the complementary approaches used for detecting companions. The robust overlap between spectroscopic and visual techniques out to periods longer than 20 years shows why the CHARA SFP survey produced null results. While the overall distribution of the various techniques follows the expected pattern, a few notes are warranted. The single unresolved companion of period under 1 day is the 11.5-hour eclipsing binary secondary in the quadruple HD 9770 system, and the only other orbit with less than a one day period is the 6.4-hour SB2 secondary to HD 133640. The shortest-period visual orbit that is not known spectroscopically is the 231-day photocentric motion orbit of HD 113449 mapped by *Hipparcos* which has also been resolved with aperture masking on large-aperture telescopes (see § 7.4). All the nine visual orbits with $P < 100$ days also have spectroscopic solutions, and are probably follow-on visual efforts after the binaries were detected by radial velocity. Three of these (HD 14241, 147584, and 160346) are photocentric-motion orbits with corresponding spectroscopic solutions, and the remaining are all LBI resolutions of double-lined spectroscopic binaries. The three such systems with the shortest periods were all resolved by this work with the CHARA array.

The two spectroscopic binaries (HD 16765 and 186408) with $\log(P) > 5$ are both radial-velocity variations seen in the CfA data consistent with a $3 - 4''$ visual pair. The longest-period spectroscopic orbital solutions are for HD 24409 and HD 43587, both of which have preliminary solutions from partial orbital coverage. The other five counts of spectroscopic

solutions in this bin are all radial velocity variations with the assumed period as described in the first paragraph of this section. The joint spectroscopic and visual solutions in this bin have radial-velocity-based solutions that rely on orbital parameters, such as period, from the visual orbits to present preliminary solutions. The nine unresolved pairs listed in the $3 < \log(P) < 4$ bin all have assumed periods as explained in the first paragraph of this section. Overall, the plot supports earlier conclusions that the results of this work are relatively comprehensive and complete.

8.4.2 Period-Eccentricity Relationship

Figure 8.12 shows the period-eccentricity relationship for the 129 pairs with estimates of these parameters from visual and/or spectroscopic orbital solutions. Pairs with periods below 12 days seem to be well circularized with eccentricities close to zero, with one notable exception. The 7-day SB2 pair in HD 45088 seems to have an unusually high eccentricity of 0.1471 ± 0.0034 for its short period, and the longer 600-year orbit has an eccentricity of 0.25. A likely explanation is that this system is relatively young and hence not yet circularized. The $\log(R'_{HK})$ of the primary of -4.266 (Gray et al. 2003) is among the highest for the stars plotted in Figure 8.7, indicating relative youth, which is confirmed by a high rotational-velocity and emission features in its spectra (Mishenina et al. 2008).

The figure does show a general trend that was pointed out by DM91, namely, components of multiple systems have generally higher eccentricity. While the overall results of this survey show a 60–40 split between pairs in binary versus multiple systems, 9 of the 14 highest-eccentricity pairs are components of higher order multiples, yielding a corresponding ratio

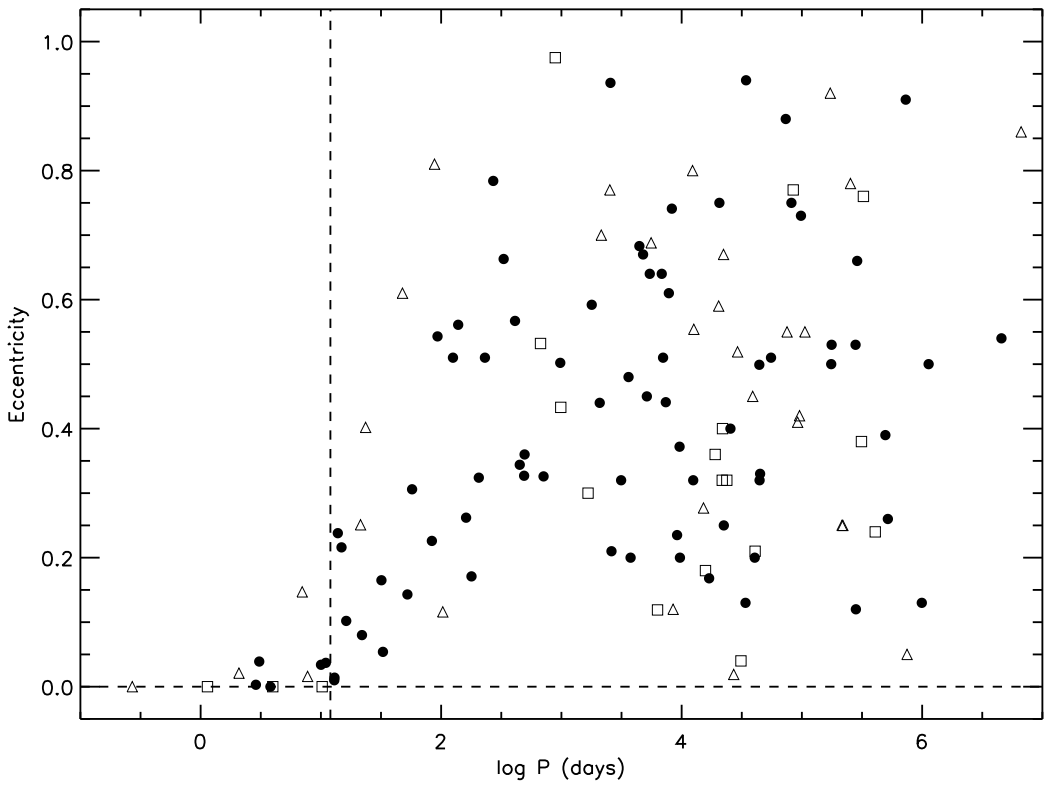

FIGURE 8.12: Planet-eccentricity relationship for the 129 pairs with estimates of those parameters from visual and/or spectroscopic orbital solutions. Components of binaries are plotted as filled circles, of triples as open triangles, and of quadruple systems as open squares. The horizontal dashed line marks a zero-eccentricity limit and the vertical dashed line marks the 12 day period, which roughly corresponds to the circularization period for this population of stars. The exceptions with notable eccentricities to the left of this line are discussed in the text.

of 35–65. The four binary systems with high eccentricity (HD 57095, 82885, 120136, and 161198) may contain the telltale signs of an interesting dynamical past or harbor yet unseen companions. With the exception of HD 161198, the others are all preliminary visual orbits with periods of 93–2000 years, indicating either that the eccentricity estimate is preliminary and approximate, or that they have perhaps endured dynamical ejection of other components. The shortest period among these is the 7-year SB1VB, HD 161198.

Figure 8.13 shows the eccentricity distribution for the 117 systems with periods greater than the circularization limit of 12 days. The dotted line shows the distribution for the 35 systems with periods below 1000 days, and the dashed line for the 82 systems with periods longer than 1000 days. The two distributions look fairly similar, in contrast to the results in DM91, which claimed a "bell shaped" distribution for the shorter period and a $f(e) = 2e$ pattern when corrected for missing systems. They also point out that the $f(e) = 2e$ relation is expected from theoretical considerations from Ambartsumian (1937). Looking at Figure 6b of DM91, I do not see the conformity to the above relation in their plot, even after adding in their estimated missed systems of high eccentricity based on the simulations of Harrington & Miranian (1977). While the current effort shows that many systems missed by DM91 have now been found, eccentricity measurements are not available for the wide CPM companions, and hence, a similar correction may be warranted for the data analyzed here. Figure 8.13 shows a roughly uniform distribution for eccentricities below 0.6, followed by a drop-off for larger eccentricities. Compensating for missed systems at high eccentricities as done by DM91, the distribution appears flat for all eccentricities. It certainly does not follow the $f(e) = 2e$ distribution, confirming the conclusion reached by Shatsky (2001) based on 174 objects in the Multiple Star Catalog (Tokovinin 1997).

8.4.3 Mass-Ratio Distribution

Figure 8.14 shows the mass-ratio distribution for the 204 confirmed pairs with primary and secondary mass estimates, obtained as described in § 8.3. For hierarchical systems, appropriate mass sums were considered for the successive "pairs". For example, a triple

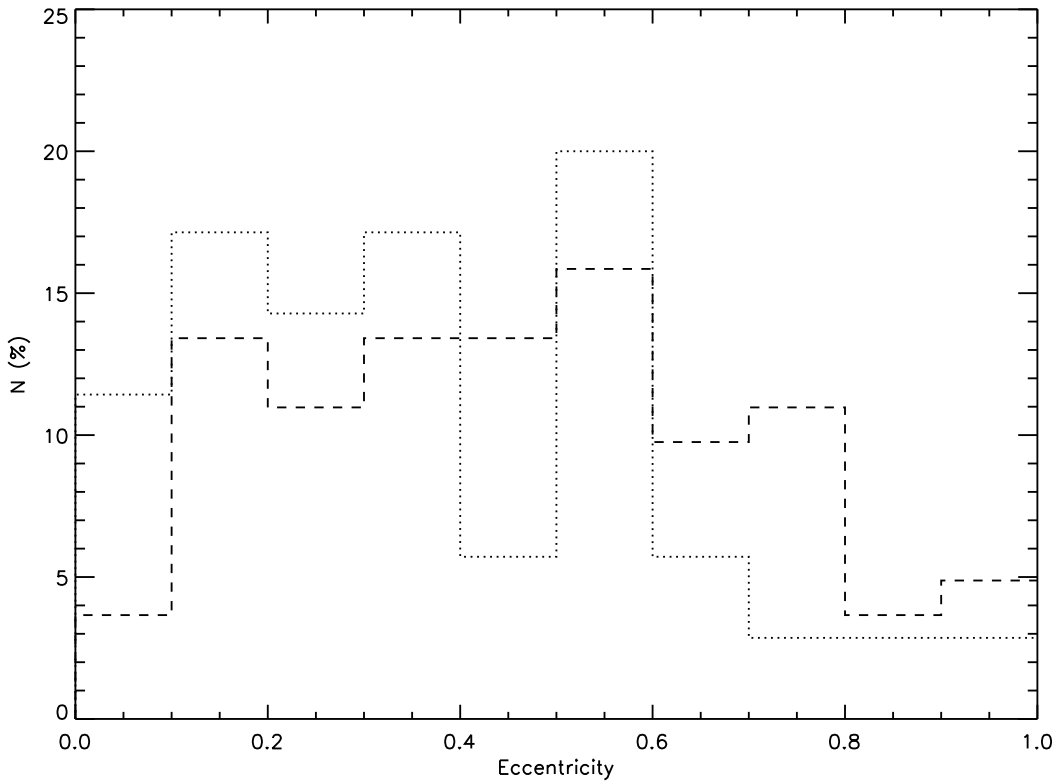

FIGURE 8.13: Eccentricity distribution for the 117 systems with periods longer than the 12-day circularization limit with estimated eccentricities from visual or spectroscopic solutions. The dotted line represents the 35 systems with periods below 1000 days, and the dashed line for the 82 systems with periods longer than 1000 days.

with Aa, Ab, and B has two pairs. For the AB pair, the masses used were that of Aa + Ab for the primary, and B for the secondary. For the Aa,Ab pair, the masses used were for the individual components. Also, for the purposes of the figures in this section, M_1 was always taken to be the larger mass. So, in a A,BC triple, if the mass of B and C added up to more than that of A, the larger mass of BC was considered as M_1 and that of A was considered as M_2 for these plots.

The fall-off of the number of systems at mass-ratios below 0.2 is consistent with the

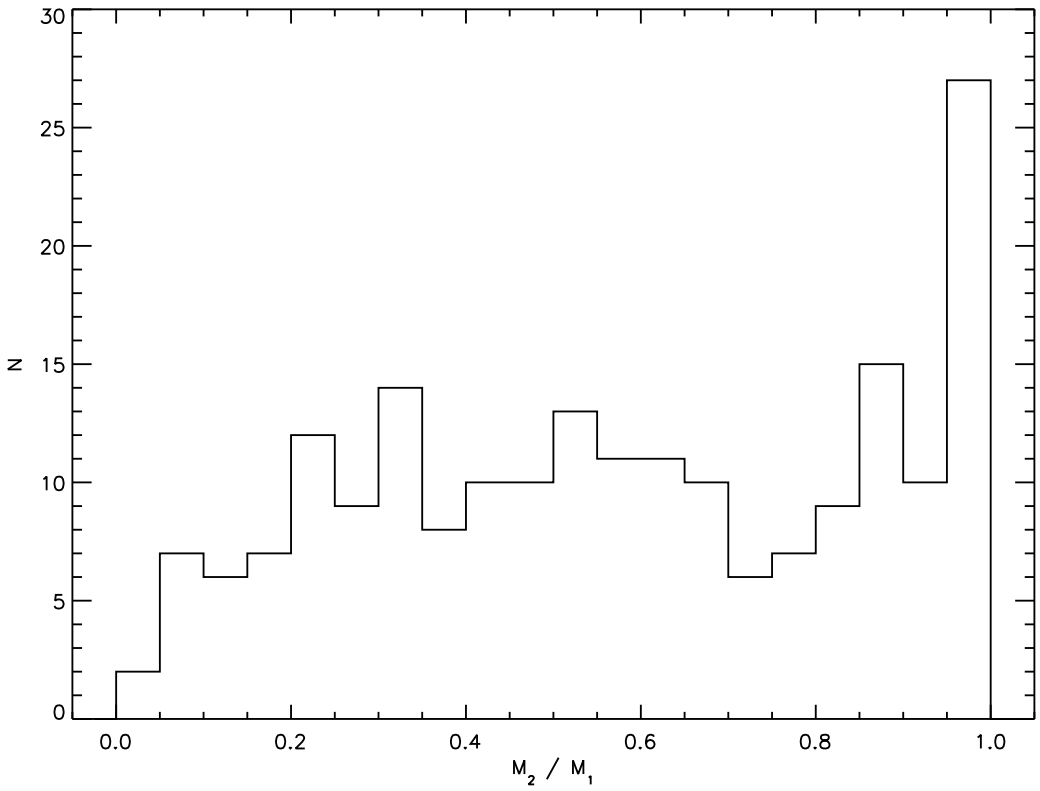

FIGURE 8.14: Mass-ratio distribution for the 204 confirmed pairs with primary and secondary mass estimates.

observed results of DM91 and probably close to the true distribution, as discussed in § 8.2.3. There is a definite and pronounced peak at a mass-ratio of 1, which was not seen in DM91, but has been observed for *Hipparcos* doubles (Söderhjelm 2007). While Abt & Levy (1976) suggested different distributions for orbital periods shorter and longer than 100 years, I do not see that trend in the data. DM91 concluded that no peak was observed at a unit mass-ratio, and suggested as a result that binaries can form by random associations of stars from the IMF. The current results lead me to a different conclusion.

The peak for equal-mass binaries appears real upon closer inspection. Of the 27 systems

at that peak, only two are triples where the mass of the primary is nearly equal to the sum of the other two components. Three more are the wide brown-dwarf pairs mentioned in § 8.2.3. The remaining 22 are two-star pairs, some in hierarchical multiple systems, that are made of nearly equal-mass components. Let us also consider how the companion masses for these were obtained. Five of these have dynamical SB2VB mass estimates for each component, two more have SB2 mass ratios of nearly one, five are wide pairs with independent measurements of similar spectral types, and ten more have multiple resolutions in the WDS with a nearly zero magnitude difference. So, binaries do seem to disproportionately favor equal-mass components.

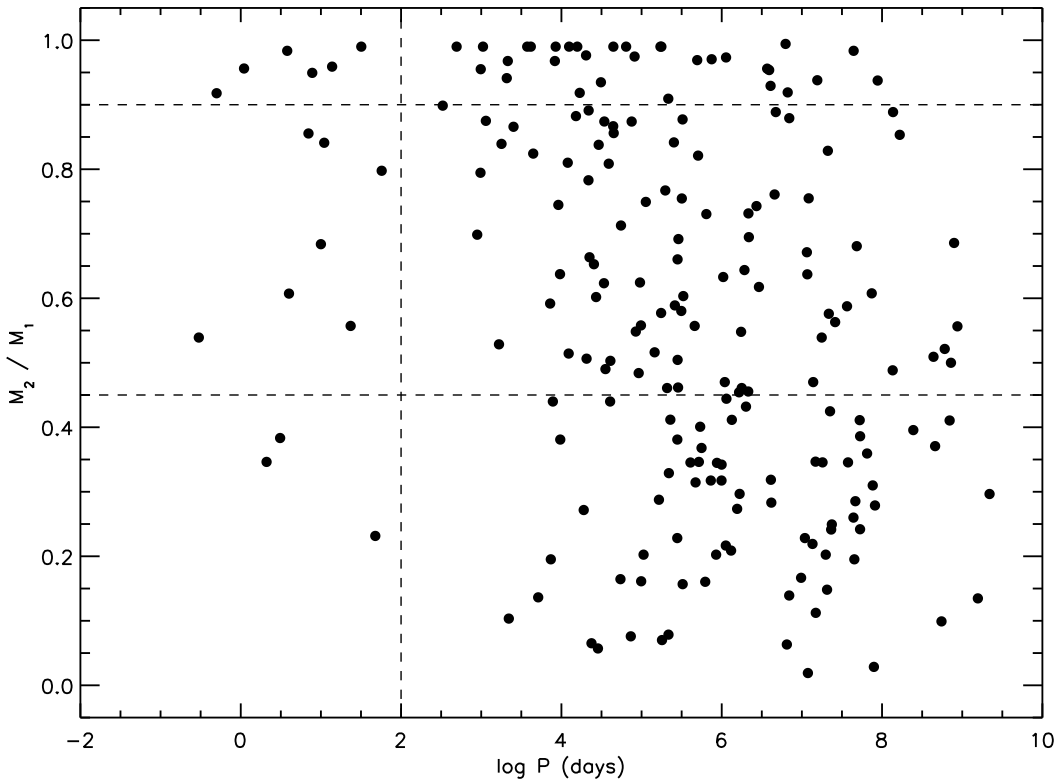

FIGURE 8.15: Mass-ratio distribution as a function of orbital period.

Figure 8.15 shows the mass-ratios plotted by $\log(P)$ to see if there is a period dependence, illustrating two points. First, there is an overall trend that systems with high mass ratios prefer shorter periods. Only 4% of the systems with mass ratios below 0.45 have periods shorter than 100 days, but this percentage doubles to 8% for mass ratios between 0.45 and 0.9, and doubles again to 16% for mass ratios above 0.9. These results have a greater than 1σ significance using Poisson statistics, indicating that nearly equal-mass pairs prefer shorter periods, perhaps suggesting a fission formation process for some systems. Second, only four of the 27 systems with mass ratios above 0.95 have periods less than 100 days and twins are seen to have periods as large as $\log(P) = 5.5$ (900 years). This indicates that while twins may form preferentially due to fission when compared to pairs of disparate stars, the vast majority of them (85%) still have long periods. This suggests that there are multiple processes responsible for the formation of binaries – fission, that accounts for as many as 16% for similar-mass pairs, and fragmentation or random associations, which account for the majority of binaries which prefer longer periods.

Figure 8.16 shows the distribution of the secondary mass on the left, and as a function of the primary mass on the right. The patterns seem to match expectations, with a drop-off at the very low mass end. The drop-off at masses above 0.8 $M_\odot$ are more a function of the sample selection, with primary masses in the 0.7–1.4 $M_\odot$ range, and the definition above that M_2 is always the smaller mass. The right panel shows that systems with the lowest total mass tend to be equal-mass pairs, which likely is because primaries of small mass have only a small mass-range left over for secondaries.

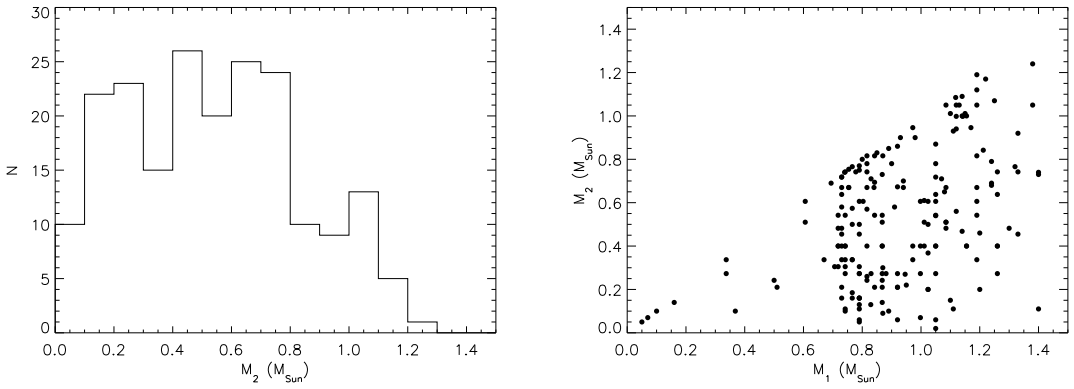

FIGURE 8.16: Secondary mass distribution (left) and as a function of the primary mass (right).

These results, especially the distribution in Figure 8.14, suggest that binaries may form by different mechanisms, at least some of which favor the formation of "twins", and that the brown dwarf desert extends to wide separations and perhaps even to the very low-mass stars, when considered as companions to Sun-like stars.

8.5 Multiplicity in Exoplanetary Systems

Multiplicity among exoplanet systems can tell us a great deal about the formation and stability of solar systems, but unfortunately is thwarted by selection effects. Most planet-search efforts avoid known close binaries, and recent efforts to discover planets around binaries (e.g., Konacki 2005) have not yet yielded any positive results. However, searches for stellar companions to exoplanet systems have yielded surprising results. Contrary to earlier expectations, Raghavan et al. (2006) showed that almost 23% of the 131 exoplanet systems studied contained stellar companions at wide-enough separations to leave the solar system intact around one star. A recent report by Mugrauer & Neuhäuser (2009) states that 43

of the 250 exoplanet hosts (17%) are members of binary or multiple systems, implying that while the number of stellar companions to exoplanet hosts has been growing, the number of exoplanet systems detected is growing proportionally faster. The 34 exoplanet systems of this study are composed of 23 (67.6%) single stars, 10 (29.4%) binaries, and 1 (2.9%) triple systems. The higher percentage of binaries or multiples among exoplanet-hosts obtained here is likely because the current volume-limited sample is probably better-studied for stellar companions as compared to the exoplanet sample, which covers a larger volume of space, and hence, less-studied stars.

Do these results suggest that stellar companions are more common in stars without planets? They do not, because the likely explanation for the relative paucity of stellar companions to stars with planets is likely due to the selection effect outlined above. The non-correlation between metallicity and stellar companionship discussed in § 8.3.3 also supports the possibility that planetary systems are as likely to form around single stars as they are around components of binary or multiple star systems. We can test the dependence of planetary and stellar companions with the current results. Twenty one of the 257 single stars, 10 of the 150 binaries, and 1 of the 34 triple systems of this study have planets. Using Poisson statistics, the frequency of planet-hosts is $8.2\% \pm 1.8\%$ for singles, $6.7\% \pm 2.1\%$ for binaries, and $2.9\% \pm 2.9\%$ for triples. These frequencies are statistically indistinguishable, suggesting that the presence of stellar companions does not affect planet formation or stability, as has been seen in other studies (Bonavita & Desidera 2007). In fact, Boss (2006) presents the results of a modeling effort, showing that binary stars are quite capable of forming solar

systems like ours, and that the presence of a nearby ($\sim$ 50 AU) star might in fact help trigger planet formation.

However, sufficiently shot-period binaries will disrupt the protoplanetary disk, hampering planet formation about either star(e.g., see Desidera & Barbieri 2007). The evolution of our own solar system would have undoubtedly taken a different course, although one that might still foster life, if the Sun had a stellar companion within 50 AU. We can see from Figure 8.11 that 132 orbits have separations under 100 AU, assuming a mass-sum of 1.47 $M_{\odot}$. These pairs represent 125 systems, some of which are tight pairs in a wide triple, still leaving room for a solar system to form around the third star. I adopt a conservative estimate of 100 (22%) stars in this study that may not provide suitable environments for the formation of a solar system like ours. More importantly, as seen in Figure 8.11, stellar companions seem to prefer a relatively wide separation between them, leaving the regions around their respective habitable zones intact for planets, and perhaps life. In this context, binary star systems may provide more real-estate conducive to the formation of life, not less, as has been previously thought.

8.6 Hierarchy of Multiple Systems

This section presents the hierarchical or "mobile diagram" for each system with three or more stellar and brown dwarf components. Figures 8.17–8.19 show the hierarchy of triple systems, and Figures 8.20–8.21 shows the hierarchy of higher order systems.

8.7 Conclusions

In this effort, I have attempted a comprehensive evaluation of the multiplicity of solar-type stars. The sample studied consists of 454 stars, including the Sun, which serve as representatives of the tens of billions of such stars in the Galaxy. All the sample stars are within 25 pc of the Sun, selected from the *Hipparcos* catalog based on the following criteria: $\pi_{\rm trig} > 40$ mas with an uncertainty of less than 5%, $0.5 \leq B - V \leq 1.0$, and positioned on an HR diagram within a band extending 1.5 magnitudes below and 2 magnitudes above an iterative best-fit main sequence (Chapter 2). The resulting sample is an exhaustive set of stars with a V-band flux of one-tenth to ten times that of the Sun, providing a physical basis for the term "solar-type".

This work is an update to the seminal effort of DM91, utilizing a larger and more accurate sample and targeting new observations to augment the vast amount of data available from extensive multiplicity studies of these stars by many different techniques. In fact, a key motivator of this effort was the chance to present results from the first nearly-complete survey of these stars. I believe that the robust monitoring of these stars over the past several decades with virtually every available method for finding and characterizing companions, and the comprehensive synthesis effort of this study, have enabled such a result. The primary observational efforts of this work include a survey for SFP companions using the CHARA Array (§ 3.1), a search for wide companions using archival images (Chapter 4), and improving the completeness of speckle interferometry coverage. The null results of the SFP survey (§ 3.1.1) show that the expected gap between short-period spectroscopic companions and

longer-period visual companions is effectively closed for nearby solar-type stars. The long baselines of the CHARA Array were also used to monitor four known short-period binaries of this sample and develop visual orbits (§ 3.2), leading to component mass estimates for HD 8997, 45088, 146361, and 223778. The search for wide companions by blinking multi-epoch archival images yielded four new CPM companion discoveries (around HD 4391, 43162, 157347, and 218868), which were confirmed as physical associations based on follow-up photometry yielding distance estimates consistent with the primary's *Hipparcos* parallax. The blinking method also helped identify many WDS pairs as optical because they clearly were field stars that did not share the primary's proper motion (§ 4.2). The photometric follow-up also confirmed several previously suspected CPM companions as physical associations and helped refute other candidates. Finally, targeted speckle interferometry observations have ensured that all but three of the sample stars have been observed with this technique at least once.

The observational efforts of this work have been tremendously augmented by synthesizing previous results, enabling more robust multiplicity statistics. Visual companions unearthed by the *Hipparcos* mission were individually investigated using other data to determine if they were physical (§ 5.1). The photocentric-motion and resolved-pair visual orbits in the VB6 catalog were analyzed and included (§ 5.2). While all visual orbits of resolved pairs, excluding one exception (HD 32923), are physical, several of the photocentric motion pairs were deemed spurious based on the availability of high-precision radial velocities. The WDS (§ 5.3), FIC (§ 5.4), and MSC catalog entries for all overlapping stars were investigated and

included. The CNS catalog entries for common stars were also individually checked and found to be very reliable for CPM pairs, but not so for entries flagged as spectroscopic pairs (§ 5.5). Faint companions found by high-contrast coronagraphic and AO techniques have also been included from the WDS or by searching publications. Unpublished null results of the many searches looking for low-mass stellar and brown dwarf companions have been included in the incompleteness analysis (§ 8.2.3). Known spectroscopic companions listed in the SB9 catalog or in publications have also been included (Chapter 6). Publications of high-precision velocity measurements (Nidever et al. 2002) were very useful not only in improving the statistics of physical companions, but also in helping test the veracity of claims in other sources like the CNS and *Hipparcos* catalogs.

While the above efforts provide a fairly complete coverage, this work would not have been nearly as comprehensive without the results from modern radial-velocity surveys. I obtained and included unpublished results from D. Latham for over 300 of the sample stars from the systematic monitoring of radial velocities at the CfA over more than 20 years. These data include five new SB1 orbits (§ 6.2.1), two new SB2 orbits (§ 6.2.2), and one new binary identified by radial-velocity variations. Two of the SB1 orbits (HD 185414 and HD 224465) are new binary detections, while the remaining three (HD 24409, 32850, and 128642) are the first spectroscopic orbits for known *Hipparcos* doubles. One SB2 solution represents a new companion detection (HD 111312) while the other was previously known as a single-lined system (HD 148704). These results also include improved orbital solutions for 16 SB1 orbits and 7 SB2 orbits. Radial velocity variations for HD 16673 indicate a previously unknown

companion, and four more candidates have been identified for future observations (§ 6.2.3). A. Hatzes and W. Cochran also helped me check for stellar companions in their planet-search data (§ 6.1). Finally, I obtained data from the systematic monitoring of high-precision radial velocities for 255 of the sample stars from G. Marcy for statistical analyses. These data included only two stellar companions not detected by any other means, and this unexpected results greatly enhances the robustness of my incompleteness analysis (§ 8.2.1).

This effort finds that the majority of solar-type stars are in fact even more Sun-like, for they are single. This revises prior expectations from DM91, who predict that only 43% of solar-type stars lack companions with masses greater than 0.1 $M_\odot$ and only 33% are without companions more massive than 10 M_J. My results include all stellar and brown dwarf companions, yielding the observed percentage of single, double, triple, and quadruple or higher order systems as $57\% \pm 3\%$, $33\% \pm 2\%$, $8\% \pm 1\%$, and $3\% \pm 1\%$, respectively (§ 7.3). As predicted by DM91, these results double the percentage of triple and higher order systems compared to their fractions. Remarkably, however, the observed percentage of single stars of this effort is identical to that of DM91, and given all the observational effort since their work, suggest that most of them may indeed be single. If all of the candidates revealed by this work are found to be real, the corresponding percentages would change to $54\% \pm 2\%$, $34\% \pm 2\%$, $9\% \pm 2\%$, and $3\% \pm 1\%$. The incompleteness analysis (§ 8.2) shows that only a few companions are likely missed by this effort, resulting in only about a 1% reduction in the percentage of single stars. The current sample has a more extended coverage when compared to the sample of DM91 in two areas – it includes stars out to K3 spectral type

while DM91 stopped at G9, and it extends the declination coverage to all-sky from their limit of $> -15°$. However, checks of subsamples from this work matching their criteria yield statistically indistinguishable results with the overall sample, showing that these do not introduce an undue bias (§ 8.3.1 and § 8.2.5). Including incompleteness analysis and estimating the fraction of candidate companions that are real, the probable percentages of single, double, triple, and quadruple or higher-order systems derived here are $55\% \pm 3\%$, $34\% \pm 2\%$, $9\% \pm 2\%$, and $2\% \pm 1\%$, and the percentage of single stars could drop by another percent if we account for possible new companions in the CCPS radial-velocity data (§ 8.2.5).

The large sample of this study enables the creation of subsamples to check the dependence of multiplicity ratios on physical parameters such as temperature (or mass, as checked using colors and spectral types), age, and metallicity. The recognized trend that more massive stars have a higher percentage of binaries is seen to hold even within the stars of this sample. The $B - V$ color as well as spectral type analyses show a clear divide at around $B - V = 0.63$ and spectral type of G5 (§ 8.3.1). Roughly 50% of the stars bluer than this limit, but only about 40% of stars redder than this limit, have stellar companions. Figure 8.6 shows how the stars of this sample fit the overall trend of multiplicity from O stars to T brown dwarfs, but a steeper drop-off than previously thought is observed at solar-type stars. In terms of age, represented by chromospheric emission and measured as $\log(R'_{\rm HK})$, the current sample divides into a relatively young, more active subgroup, 47% of which have companions, and a relatively old, less active subgroup, only 40% of which have companions (§ 8.3.2). Finally, while it has been shown that stars with higher metallicity are more likely to have planets,

the same is not true for stellar companions (§ 8.3.3). This is not surprising because, while planets may require the presence of heavier elements to trigger the condensation process by which they form, the primordial matter that can form one star should be equally likely to form others as well. But this clear difference between stars and planets allows one to check which of them brown dwarfs resemble. While there are only a few data points and more work is needed before drawing definitive conclusions, these results tend to show that brown dwarfs, like planets, are more likely to form around stars with higher metallicity. This leads us to a preliminary conclusion that brown dwarfs, at least when they are companions to stars, form like planets rather than like stars (Figure 8.9).

Looking at orbital elements, binaries among solar-type stars have a period range from a few hours to millions of years. The period distribution seems to follow a roughly Gaussian pattern (Figure 8.11) with a peak and median period of about 300 years, slightly larger than that of Pluto around the Sun. This is significantly larger than the 180-year incompleteness-corrected value in DM91, showing that the current effort is more complete with respect to wide companions. The significant overlap of the various techniques in each period bin (Figure 8.11) shows that there are no major gaps in parameter space that are not adequately addressed by current techniques, a testament to the exacting methods developed over the years. The period-eccentricity relation derived here shows that beyond the expected circularization for short-period systems with periods below 12 days, the distribution is largely flat out to $e = 0.6$, followed by a fall-off for large eccentricities. I was not able to confirm either the roughly Gaussian distribution seen by DM91 for periods below 1000 days, or the

$f(e) = 2e$ distribution they claim for the longer-period systems. Finally, the companion mass-ratio distribution shows a clear preference for nearly-equal-mass pairs (Figure 8.14), suggesting that there is likely some formation mechanism that favors twins. This result is consistent with the results of Abt & Levy (1976), but another departure from the conclusion of DM91, who saw no such peak. A closer look at the mass-ratio-period relationship (Figure 8.15) reveals that higher-mass ratio pairs are more likely to have shorter periods, suggesting that they may preferentially form by fission. However, the vast majority of the pairs have long periods, even in the highest-mass-ratio bins, demonstrating that binaries form by multiple mechanisms – fission, which may be confined to like pairs, and fragmentation or random associations, which prefer longer periods and apply to the majority of stellar systems The mass-ratio distribution also shows a deficiency of low-mass companions, in contrast with some earlier results (Scarfe 1986; Trimble 1987, 1990), but consistent with the DM91 observations. However, DM91 presumed that the deficiency of lower-mass companions was due to missed pairs. We now have enough evidence that the paucity of low-mass companions is not a detection gap, but rather physical, showing that the brown dwarf desert extends to wide separations (§ 8.2.3).

Two-thirds of the 34 exoplanet hosts of this sample are single stars, significantly lower than those in prior studies (Raghavan et al. 2006; Mugrauer & Neuhäuser 2009), and approaching the overall statistics of the volume-limited sample. This is surprising, because planet search efforts avoid known binaries, yielding a higher percentage of single stars among planet hosts, and suggests that the assessment of stellar companions of this study is compre-

hensive. The fraction of planet hosts among single, binary, and triple systems are statistically indistinguishable, indicating that planets are as likely to form around single stars as they are around components of binary or multiple systems. The period distribution in Figure 8.11 also shows that stellar companions prefer a wide separation. Only 34% of the pairs have periods below 27 years, which corresponds to a separation of 10 AU for an mass-sum of 1.47, the average values for all pairs of this study. This could be interpreted as good news for planets and life, as only a few stellar companions are close enough to disrupt objects in the habitable zones around these stars. So, binary systems may offer more places for planets, and perhaps life, not less as has been thought.

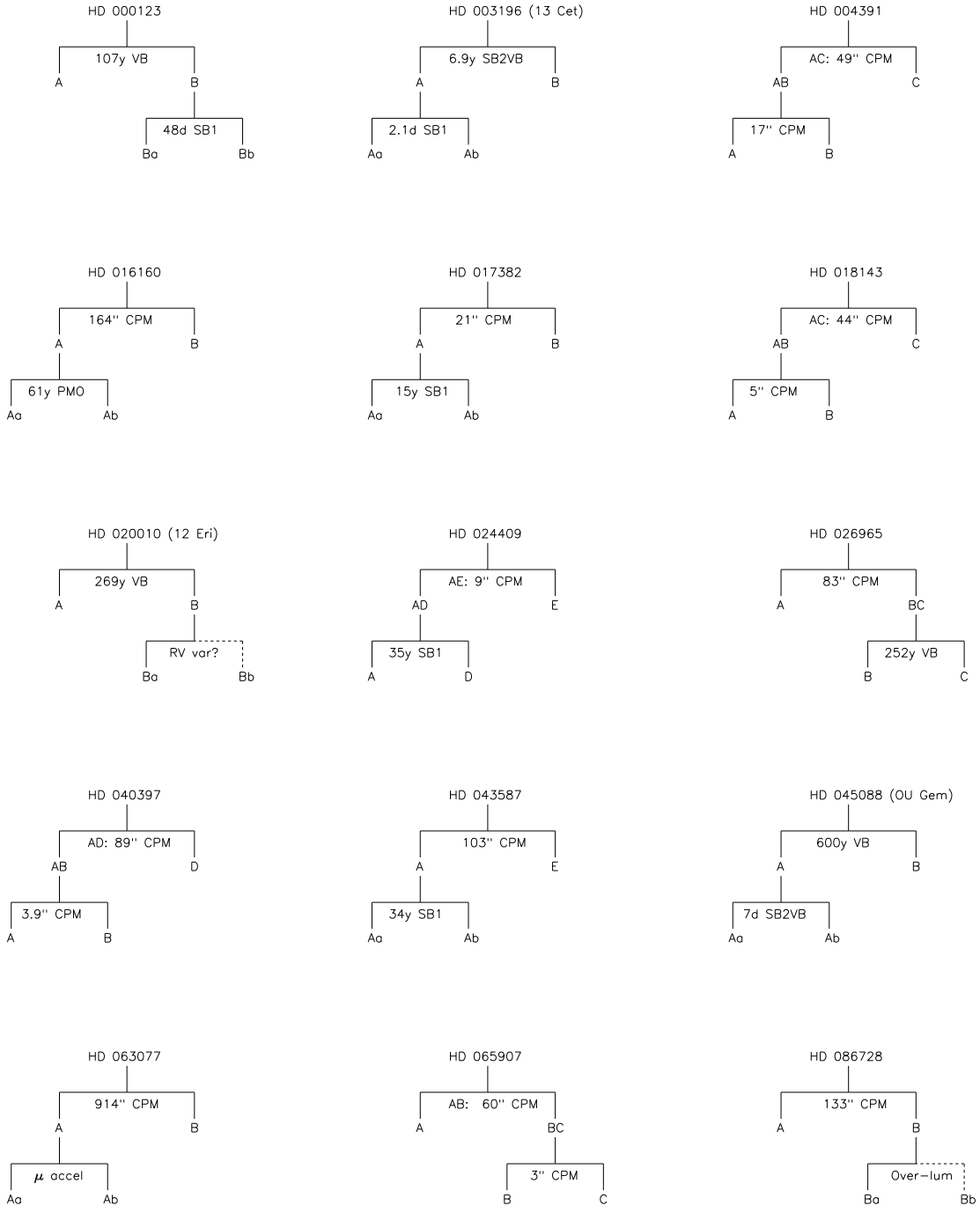

FIGURE 8.17: Mobile diagrams of triple systems (1 of 3). Solid lines connect confirmed companions and dashed lines connect candidate companions.

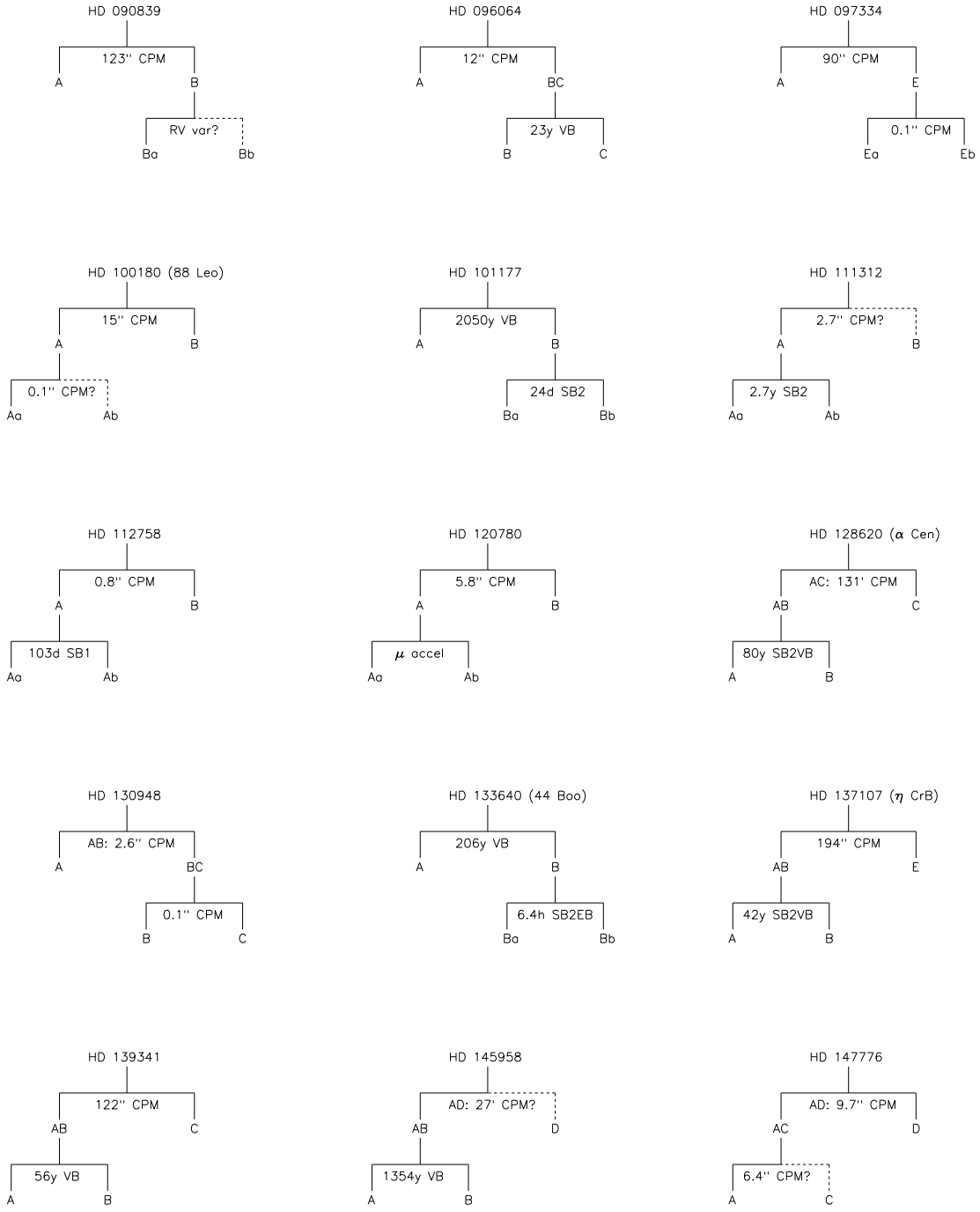

FIGURE 8.18: Mobile diagrams of triple systems (2 of 3). Solid lines connect confirmed companions and dashed lines connect candidate companions.

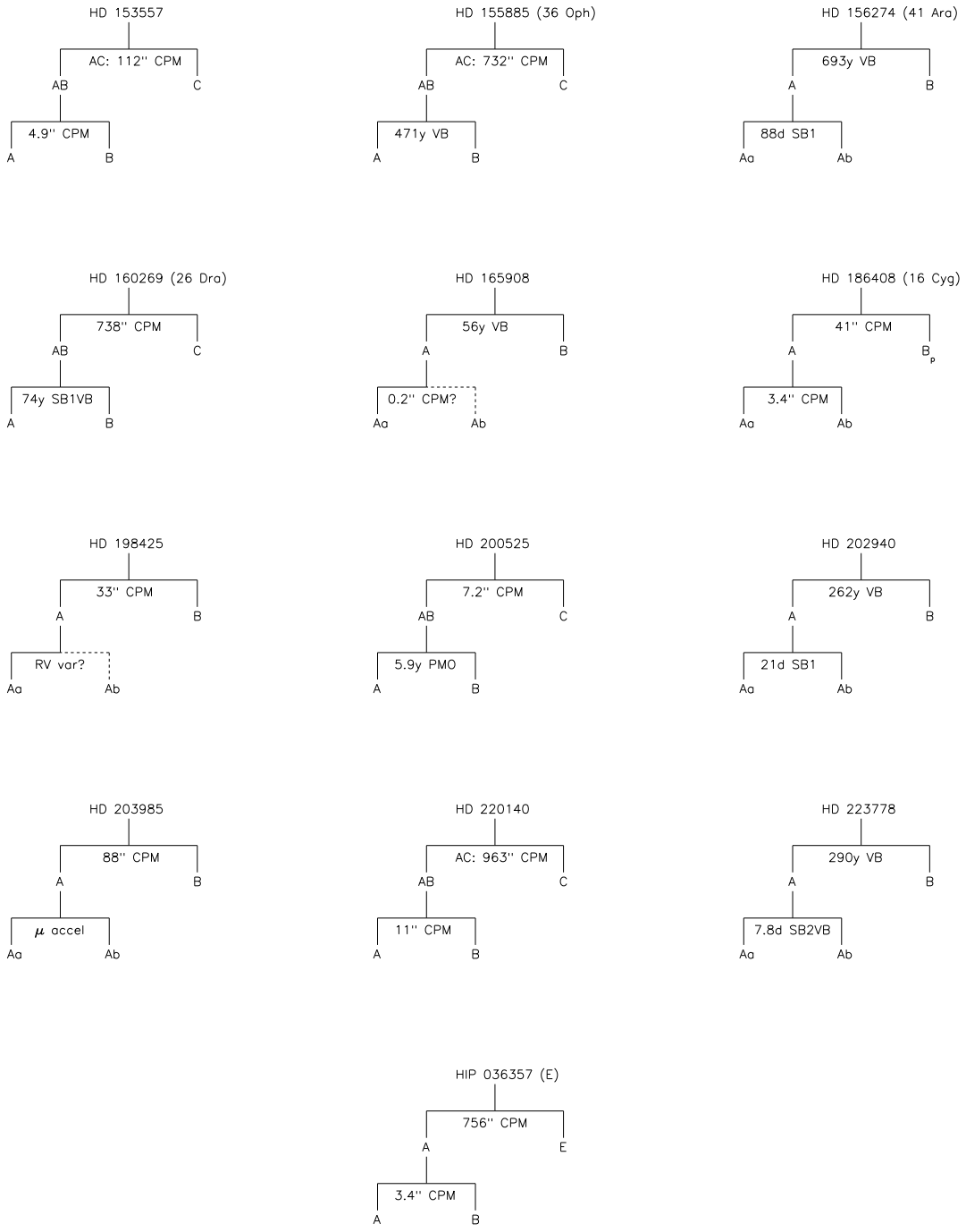

FIGURE 8.19: Mobile diagrams of triple systems (3 of 3). Solid lines connect confirmed companions and dashed lines connect candidate companions. The "p" subscript for HD 186408 B indicates that it is a planet-host star.

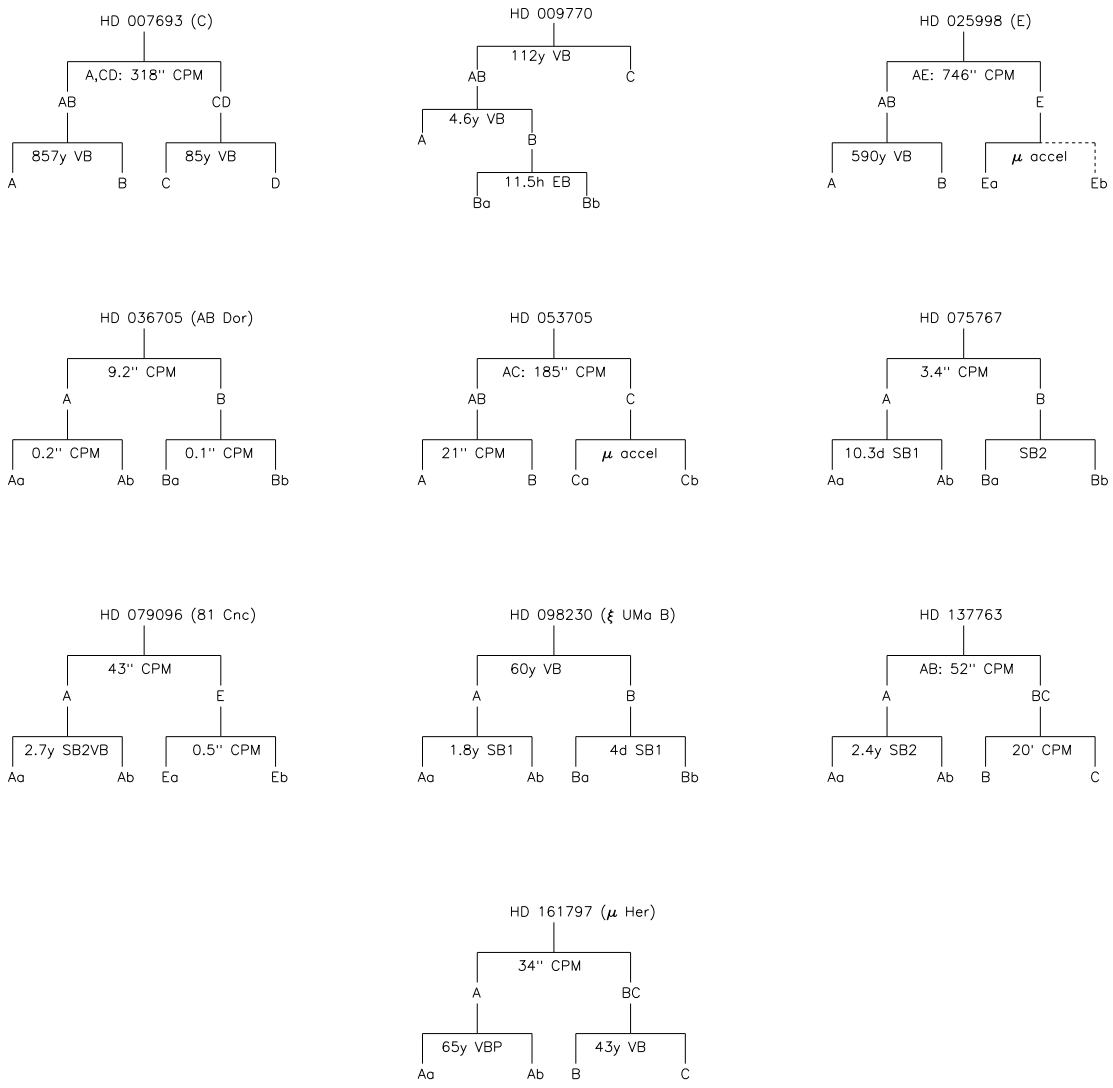

FIGURE 8.20: Mobile diagrams of quadruple systems. Solid lines connect confirmed companions and dashed lines connect candidate companions.

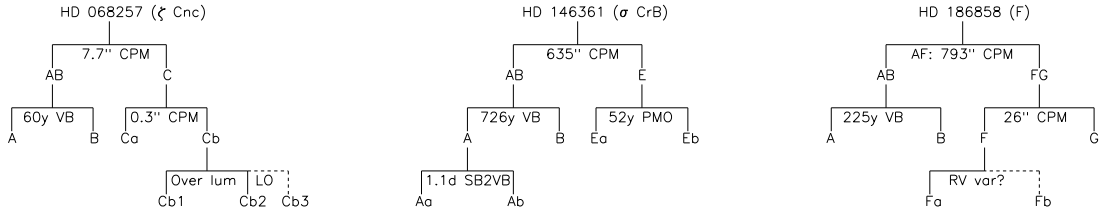

FIGURE 8.21: Mobile diagrams of quintuple and higher order systems. Solid lines connect confirmed companions and dashed lines connect candidate companions.

If I have seen farther than others, it is because I was standing on the shoulder of giants.

—— Sir Isaac Newton

References

Abt, H. A. 1970, ApJS, 19, 387

Abt, H. A., & Biggs, E. S. 1972, Bibliography of stellar radial velocities (New York: Latham Process Corp.)

Abt, H. A., & Levy, S. G. 1976, ApJS, 30, 273

Abt, H. A., & Willmarth, D. 2006, ApJS, 162, 207

Aitken, R. G. 1964, The Binary Stars (New York: Dover Publication)

Aitken, R. G., & Doolittle, E. 1932, New general catalogue of double stars within 120 of the North pole ... (Washington, D.C.: Carnegie institution of Washington)

Albrow, M. D., Gilliland, R. L., Brown, T. M., Edmonds, P. D., Guhathakurta, P., & Sarajedini, A. 2001, ApJ, 559, 1060

Allen, P. R., Koerner, D. W., McElwain, M. W., Cruz, K. L., & Reid, I. N. 2007, AJ, 133, 971

Ambartsumian, V. A. 1937, Astron. Zh., 14, 207

Bagnuolo, Jr., W. G. et al. 2006, AJ, 131, 2695

Baines, E. K., McAlister, H. A., ten Brummelaar, T. A., Turner, N. H., Sturmann, J., Sturmann, L., Goldfinger, P. J., & Ridgway, S. T. 2008a, ApJ, 680, 728

Baines, E. K., McAlister, H. A., ten Brummelaar, T. A., Turner, N. H., Sturmann, J., Sturmann, L., & Ridgway, S. T. 2008b, ApJ, 682, 577

Bakos, G. Á., Lázár, J., Papp, I., Sári, P., & Green, E. M. 2002, PASP, 114, 974

Ball, B., Drake, J. J., Lin, L., Kashyap, V., Laming, J. M., & García-Alvarez, D. 2005, ApJ, 634, 1336

Baranne, A., Mayor, M., & Poncet, J. L. 1979, Vistas in Astronomy, 23, 279

Baranne, A. et al. 1996, A&AS, 119, 373

Barlow, R. J. 1999, Statistics: A Guide to the Use of Statistical Methods in the Physical Sciences (Chichester: John Wiley & Sons Ltd.)

Batten, A. H., Fletcher, J. M., & MacCarthy, D. G. 1989, Publications of the Dominion Astrophysical Observatory Victoria, 17, 1

Batten, A. H., Fletcher, J. M., & Mann, P. J. 1978, Publications of the Dominion Astrophysical Observatory Victoria, 15, 121

Beavers, W. I., & Eitter, J. J. 1986, ApJS, 62, 147

Bender, C., Simon, M., Prato, L., Mazeh, T., & Zucker, S. 2005, AJ, 129, 402

Blazit, A., Bonneau, D., Koechlin, L., & Labeyrie, A. 1977, ApJ, 214, L79

Boccaletti, A., Chauvin, G., Baudoz, P., & Beuzit, J.-L. 2008, A&A, 482, 939

Boden, A. F. et al. 1999, ApJ, 527, 360

Bonavita, M., & Desidera, S. 2007, A&A, 468, 721

Bonneau, D., Blazit, A., Foy, R., & Labeyrie, A. 1980, A&AS, 42, 185

Bonneau, D., & Foy, R. 1980, A&A, 86, 295

Bopp, B. W., Evans, D. S., Laing, J. D., & Deeming, T. J. 1970, MNRAS, 147, 355

Boss, A. P. 2006, ApJ, 641, 1148

Bouvier, J., Rigaut, F., & Nadeau, D. 1997, A&A, 323, 139

Bouy, H., Brandner, W., Martín, E. L., Delfosse, X., Allard, F., & Basri, G. 2003, AJ, 126, 1526

Branch, D. 1976, ApJ, 210, 392

Brandner, W., & Koehler, R. 1998, ApJ, 499, L79

Brettman, O. H., Fried, R. E., Duvall, W. M., Hall, D. S., Poe, C. H., & Shaw, J. S. 1983, Information Bulletin on Variable Stars, 2389, 1

Burgasser, A. J., Kirkpatrick, J. D., & Lowrance, P. J. 2005, AJ, 129, 2849

Burgasser, A. J., Kirkpatrick, J. D., Reid, I. N., Brown, M. E., Miskey, C. L., & Gizis, J. E. 2003, ApJ, 586, 512

Butler, R. P., Marcy, G. W., Williams, E., McCarthy, C., Dosanjh, P., & Vogt, S. S. 1996, PASP, 108, 500

Butler, R. P. et al. 2006, ApJ, 646, 505

Campbell, B., Walker, G. A. H., & Yang, S. 1988, ApJ, 331, 902

Carney, B. W., & Latham, D. W. 1987, AJ, 93, 116

Catala, C., Forveille, T., & Lai, O. 2006, AJ, 132, 2318

Charbonneau, D., Brown, T. M., Latham, D. W., & Mayor, M. 2000, ApJ, 529, L45

Chauvin, G., Lagrange, A.-M., Udry, S., Fusco, T., Galland, F., Naef, D., Beuzit, J.-L., & Mayor, M. 2006, A&A, 456, 1165

Chauvin, G., Lagrange, A.-M., Udry, S., & Mayor, M. 2007, A&A, 475, 723

Close, L. M. et al. 2005, Nature, 433, 286

Close, L. M., Thatte, N., Nielsen, E. L., Abuter, R., Clarke, F., & Tecza, M. 2007, ApJ, 665, 736

Cox, A. N. 2000, Allen's astrophysical quantities (New York:Springer-Verlag)

Cutispoto, G., Kuerster, M., Messina, S., Rodono, M., & Tagliaferri, G. 1997, A&A, 320, 586

da Silva, L., & Foy, R. 1987, A&A, 177, 204

de Medeiros, J. R., & Mayor, M. 1999, A&AS, 139, 433

Desidera, S., & Barbieri, M. 2007, A&A, 462, 345

Dieterich, S. B., Henry, T. J., Golimowski, D. A., Krist, J. E., & Raghavan, D. 2009, AJ, in preparation

Dommanget, J., & Nys, O. 2000, A&A, 363, 991

Ducourant, C. et al. 2006, A&A, 448, 1235

Duflot, M., Figon, P., & Meyssonnier, N. 1995, A&AS, 114, 269

Duquennoy, A., & Mayor, M. 1991, A&A, 248, 485 (DM91)

Duquennoy, A., Mayor, M., Andersen, J., Carquillat, J. M., & North, P. 1992, A&A, 254, L13+

Duquennoy, A., Mayor, M., & Halbwachs, J.-L. 1991, A&AS, 88, 281

Duquennoy, A., Tokovinin, A. A., Leinert, C., Glindemann, A., Halbwachs, J.-L., & Mayor, M. 1996, A&A, 314, 846

Dyck, H. M., Benson, J. A., & Schloerb, F. P. 1995, AJ, 110, 1433

Edwards, D. A., Evans, D. S., Fekel, F. C., & Smith, B. W. 1980, AJ, 85, 478

Eggen, O. J. 1956, AJ, 61, 405

Eggenberger, A., Udry, S., Chauvin, G., Beuzit, J.-L., Lagrange, A.-M., Ségransan, D., & Mayor, M. 2007, A&A, 474, 273

Eggenberger, A., Udry, S., & Mayor, M. 2004, A&A, 417, 353

Eisenbeiss, T., Seifahrt, A., Mugrauer, M., Schmidt, T. O. B., Neuhäuser, R., & Roell, T. 2007, Astronomische Nachrichten, 328, 521

Els, S. G., Sterzik, M. F., Marchis, F., Pantin, E., Endl, M., & Kürster, M. 2001, A&A, 370, L1

Evans, D. S. 1950, Monthly Notes of the Astronomical Society of South Africa, 9, 69

——. 1952, Monthly Notes of the Astronomical Society of South Africa, 11, 71

Fabrycky, D., & Tremaine, S. 2007, ApJ, 669, 1298

Falin, J. L., & Mignard, F. 1999, A&AS, 135, 231

Farrington, C. D. 2008, PhD thesis, Georgia State University

Fekel, F. C., Williamson, M., & Pourbaix, D. 2007, AJ, 133, 2431

Fekel, Jr., F. C. 1981, ApJ, 246, 879

Fischer, D. A., & Marcy, G. W. 1992, ApJ, 396, 178

Fischer, D. A., & Valenti, J. 2005, ApJ, 622, 1102

Frankowski, A., Jancart, S., & Jorissen, A. 2007, A&A, 464, 377

Frasca, A., Guillout, P., Marilli, E., Freire Ferrero, R., Biazzo, K., & Klutsch, A. 2006, A&A, 454, 301

Fricke, W. et al. 1988, Veroeffentlichungen des Astronomischen Rechen-Instituts Heidelberg, 32, 1

Fuhrmann, K., Guenther, E., König, B., & Bernkopf, J. 2005, MNRAS, 361, 803

Gaidos, E. J., Henry, G. W., & Henry, S. M. 2000, AJ, 120, 1006

Gatewood, G., & Coban, L. 2009, AJ, 137, 402

Gatewood, G., Han, I., & Black, D. C. 2001, ApJ, 548, L61

Ghez, A. M., McCarthy, D. W., Patience, J. L., & Beck, T. L. 1997, ApJ, 481, 378

Ghez, A. M., Neugebauer, G., & Matthews, K. 1993, AJ, 106, 2005

Gizis, J. E., Kirkpatrick, J. D., Burgasser, A., Reid, I. N., Monet, D. G., Liebert, J., & Wilson, J. C. 2001, ApJ, 551, L163

Gizis, J. E., Monet, D. G., Reid, I. N., Kirkpatrick, J. D., & Burgasser, A. J. 2000, MNRAS, 311, 385

Gliese, W. 1969, Veroeffentlichungen des Astronomischen Rechen-Instituts Heidelberg, 22, 1

Gliese, W., & Jahreiß, H. 1979, Bulletin d'Information du Centre de Donnees Stellaires, 16, 92

——. 1991, Preliminary Version of the Third Catalogue of Nearby Stars, Tech. rep.

Goldberg, D., Mazeh, T., & Latham, D. W. 2003, ApJ, 591, 397

Goldberg, D., Mazeh, T., Latham, D. W., Stefanik, R. P., Carney, B. W., & Laird, J. B. 2002, AJ, 124, 1132

Goldin, A., & Makarov, V. V. 2006, ApJS, 166, 341

Golimowski, D. A., & Schroeder, D. J. 1998, AJ, 116, 440

Gomez, A. E., & Abt, H. A. 1982, PASP, 94, 650

Gontcharov, G. A. 2006, Astronomy Letters, 32, 759

Gontcharov, G. A., Andronova, A. A., & Titov, O. A. 2000, A&A, 355, 1164

Gray, R. O., Corbally, C. J., Garrison, R. F., McFadden, M. T., Bubar, E. J., McGahee, C. E., O'Donoghue, A. A., & Knox, E. R. 2006, AJ, 132, 161

Gray, R. O., Corbally, C. J., Garrison, R. F., McFadden, M. T., & Robinson, P. E. 2003, AJ, 126, 2048

Grether, D., & Lineweaver, C. H. 2006, ApJ, 640, 1051

Griffin, R. F. 1967, ApJ, 148, 465

——. 1991, Bulletin of the Astronomical Society of India, 19, 183

——. 1998, The Observatory, 118, 273

——. 1999, The Observatory, 119, 27

——. 2000, The Observatory, 120, 1

——. 2002, The Observatory, 122, 329

——. 2004, The Observatory, 124, 258

——. 2008, The Observatory, 128, 176

Guirado, J. C. et al. 1997, ApJ, 490, 835

Halbwachs, J. L. 1986, A&A, 168, 161

——. 1987, A&A, 183, 234

Halbwachs, J. L., Arenou, F., Mayor, M., Udry, S., & Queloz, D. 2000, A&A, 355, 581

Halbwachs, J. L., Mayor, M., Udry, S., & Arenou, F. 2003, A&A, 397, 159

Hambly, N. C., Irwin, M. J., & MacGillivray, H. T. 2001, MNRAS, 326, 1295

Harrington, R. S. 1977, AJ, 82, 753

Harrington, R. S., & Dahn, C. C. 1980, AJ, 85, 454

Harrington, R. S., & Miranian, M. 1977, PASP, 89, 400

Hartkopf, W. I., & Mason, B. D. 2004, in Revista Mexicana de Astronomia y Astrofisica, vol. 27, Vol. 21, Revista Mexicana de Astronomia y Astrofisica Conference Series, ed. C. Allen & C. Scarfe, 83–90

Hartkopf, W. I., Mason, B. D., & McAlister, H. A. 1996, AJ, 111, 370

Hartkopf, W. I., Mason, B. D., & Rafferty, T. J. 2008, AJ, 135, 1334

Hartkopf, W. I., Mason, B. D., & Worley, C. E. 2001, AJ, 122, 3472

Hartkopf, W. I., & McAlister, H. A. 1984, PASP, 96, 105

Hawley, S. L., Gizis, J. E., & Reid, I. N. 1996, AJ, 112, 2799

Heacox, W. D. 1995, AJ, 109, 2670

——. 1998, AJ, 115, 325

Heintz, W. D. 1968, AJ, 73, 512

——. 1969, JRASC, 63, 275

——. 1978

——. 1981, ApJS, 46, 247

——. 1988, JRASC, 82, 140

——. 1990, AJ, 99, 420

——. 1994, AJ, 108, 2338

——. 1996, AJ, 111, 408

Heintz, W. D., & Borgman, E. R. 1984, AJ, 89, 1068

Henry, T. J., & McCarthy, Jr., D. W. 1990, ApJ, 350, 334

——. 1993, AJ, 106, 773

Henry, T. J., Soderblom, D. R., Donahue, R. A., & Baliunas, S. L. 1996, AJ, 111, 439

Henry, T. J., Subasavage, J. P., Brown, M. A., Beaulieu, T. D., Jao, W.-C., & Hambly, N. C. 2004, AJ, 128, 2460

Henry, T. J., Walkowicz, L. M., Barto, T. C., & Golimowski, D. A. 2002, AJ, 123, 2002

Hertzsprung, E. 1922, Bull. Astron. Inst. Netherlands, 1, 149

Hirst, W. P. 1943, Monthly Notes of the Astronomical Society of South Africa, 2, 100

Hoffleit, D., & Jaschek, C. 1982, The Bright Star Catalogue 4th Ed. (New Haven: Yale University Observatory)

Hoffleit, D., Saladyga, M., & Wlasuk, P. 1983, Bright star catalogue. Supplement (New Haven: Yale University Observatory, 1983)

Høg, E. et al. 2000, A&A, 355, L27

Høg, E., Kuzmin, A., Bastian, U., Fabricius, C., Kuimov, K., Lindegren, L., Makarov, V. V., & Roeser, S. 1998, A&A, 335, L65

Holberg, J. B., Oswalt, T. D., & Sion, E. M. 2002, ApJ, 571, 512

Holberg, J. B., Sion, E. M., Oswalt, T., McCook, G. P., Foran, S., & Subasavage, J. P. 2008, AJ, 135, 1225

Holman, M. J., & Wiegert, P. A. 1999, AJ, 117, 621

Horch, E. P., van Altena, W. F., Cyr, W. M., Kinsman-Smith, L., Srivastava, A., & Zhou, J. 2008, AJ, 136, 312

Hummel, C. A., Armstrong, J. T., Buscher, D. F., Mozurkewich, D., Quirrenbach, A., & Vivekanand, M. 1995, AJ, 110, 376

Hummel, C. A., Armstrong, J. T., Quirrenbach, A., Buscher, D. F., Mozurkewich, D., Simon, R. S., & Johnston, K. J. 1993, AJ, 106, 2486

Hutchings, J. B., Griffin, R. F., & Ménard, F. 2000, PASP, 112, 833

Hynek, J. A. 1938, Contributions of Perkins Observatory, 1, 10

Imbert, M. 1979, A&AS, 38, 401

——. 2006, Romanian Astronomical Journal, 16, 3

Innes, R. T. A. 1901, MNRAS, 61, 414

Ivanova, N., Belczynski, K., Fregeau, J. M., & Rasio, F. A. 2005, MNRAS, 358, 572

Janson, M., Brandner, W., Lenzen, R., Close, L., Nielsen, E., Hartung, M., Henning, T., & Bouy, H. 2007, A&A, 462, 615

Jaschek, C., & Gómez, A. E. 1970, PASP, 82, 809

Jaschek, C., & Jaschek, M. 1957, PASP, 69, 546

Joergens, V. 2008, A&A, 492, 545

Jones, H. R. A., Paul Butler, R., Marcy, G. W., Tinney, C. G., Penny, A. J., McCarthy, C., & Carter, B. D. 2002, MNRAS, 337, 1170

Joy, A. H. 1947, ApJ, 105, 96

Kähler, H. 1999, A&A, 346, 67

Kennedy, P. M., & Przybylski, A. 1963, MNRAS, 126, 381

Kharchenko, N. V. 2001, Kinematika i Fizika Nebesnykh Tel, 17, 409

Kirillova, T. S., & Pavlovskaya, E. D. 1963, Soviet Astronomy, 7, 99

Kirkpatrick, J. D., Dahn, C. C., Monet, D. G., Reid, I. N., Gizis, J. E., Liebert, J., & Burgasser, A. J. 2001, AJ, 121, 3235

Kobulnicky, H. A., & Fryer, C. L. 2007, ApJ, 670, 747

Konacki, M. 2005, ApJ, 626, 431

König, B., Fuhrmann, K., Neuhäuser, R., Charbonneau, D., & Jayawardhana, R. 2002, A&A, 394, L43

Kouwenhoven, M. B. N. 2006, PhD thesis, University of Amsterdam, The Netherlands

Kouwenhoven, M. B. N., Brown, A. G. A., Portegies Zwart, S. F., & Kaper, L. 2007, A&A, 474, 77

Kraus, A. L., White, R. J., & Hillenbrand, L. A. 2006, ApJ, 649, 306

Kuiper, G. P. 1935a, PASP, 47, 15

——. 1935b, PASP, 47, 121

——. 1942, ApJ, 95, 201

Kunkel, W. E., Liebert, J., & Boroson, T. A. 1984, PASP, 96, 891

Lagrange, A.-M., Beust, H., Udry, S., Chauvin, G., & Mayor, M. 2006, A&A, 459, 955

Lasker, B. M. et al. 2008, AJ, 136, 735

Latham, D. W., Davis, R. J., Stefanik, R. P., Mazeh, T., & Abt, H. A. 1991, AJ, 101, 625

Latham, D. W., Stefanik, R. P., Torres, G., Davis, R. J., Mazeh, T., Carney, B. W., Laird, J. B., & Morse, J. A. 2002, AJ, 124, 1144

Lawson, P. R., ed. 2000, Principles of Long Baseline Stellar Interferometry (Pasadena, Jet Propulsion Laboratory)

Leinert, C., Zinnecker, H., Weitzel, N., Christou, J., Ridgway, S. T., Jameson, R., Haas, M., & Lenzen, R. 1993, A&A, 278, 129

Lépine, S., & Shara, M. M. 2005, AJ, 129, 1483

Lepine, S., Thorstensen, J. R., Shara, M. M., & Rich, R. M. 2009, ArXiv e-prints

Liu, M. C., Fischer, D. A., Graham, J. R., Lloyd, J. P., Marcy, G. W., & Butler, R. P. 2002, ApJ, 571, 519

Looper, D. L., Kirkpatrick, J. D., & Burgasser, A. J. 2007, AJ, 134, 1162

Lowrance, P. J., Kirkpatrick, J. D., & Beichman, C. A. 2002, ApJ, 572, L79

Lu, W., Rucinski, S. M., & Ogłoza, W. 2001, AJ, 122, 402

Luhman, K. L., & Jayawardhana, R. 2002, ApJ, 566, 1132

Luhman, K. L. et al. 2007, ApJ, 654, 570

Luyten, W. J. 1927, Harvard College Observatory Bulletin, 852, 14

——. 1930a, Proceedings of the National Academy of Science, 16, 252

——. 1930b, Proceedings of the National Academy of Science, 16, 257

——. 1936, ApJ, 84, 85

Luyten, W. J. 1979, in New Luyten Catalogue of stars with proper motions larger than two tenths of an arcsecond, 2, 0 (1979), 0

Luyten, W. J., & Shapley, H. 1930, Annals of Harvard College Observatory, 85, 73

Makarov, V. V., & Kaplan, G. H. 2005, AJ, 129, 2420

Makarov, V. V., Zacharias, N., Hennessy, G. S., Harris, H. C., & Monet, A. K. B. 2007, ApJ, 668, L155

Malkov, O. Y., Oblak, E., Snegireva, E. A., & Torra, J. 2006, A&A, 446, 785

Marcy, G., Butler, R. P., Fischer, D., Vogt, S., Wright, J. T., Tinney, C. G., & Jones, H. R. A. 2005, Progress of Theoretical Physics Supplement, 158, 24

Marcy, G. W., & Butler, R. P. 1996, ApJ, 464, L147

Marcy, G. W., Butler, R. P., Fischer, D. A., & Vogt, S. S. 2004, in Astronomical Society of the Pacific Conference Series, Vol. 321, Extrasolar Planets: Today and Tomorrow, ed. J. Beaulieu, A. Lecavelier Des Etangs, & C. Terquem, 3

Mason, B. D., Gies, D. R., Hartkopf, W. I., Bagnuolo, Jr., W. G., ten Brummelaar, T., & McAlister, H. A. 1998a, AJ, 115, 821

Mason, B. D., Hartkopf, W. I., Gies, D. R., Henry, T. J., & Helsel, J. W. 2009a, AJ, 137, 3358

Mason, B. D., Hartkopf, W. I., Holdenried, E. R., & Rafferty, T. J. 2001, AJ, 121, 3224

Mason, B. D., Henry, T. J., Hartkopf, W. I., Ten Brummelaar, T., & Soderblom, D. R. 1998b, AJ, 116, 2975

Mason, B. D., Henry, T. J., & Soderblom, D. R. 2009b, AJ, in preparation

Mason, B. D. et al. 1999, AJ, 117, 1890

Mason, B. D., McAlister, H. A., Hartkopf, W. I., & Shara, M. M. 1995, AJ, 109, 332

Maxted, P. F. L., Jeffries, R. D., Oliveira, J. M., Naylor, T., & Jackson, R. J. 2008, MNRAS, 385, 2210

Mayor, M., & Mazeh, T. 1987, A&A, 171, 157

Mazeh, T. 1990, AJ, 99, 675

Mazeh, T., Goldberg, D., Duquennoy, A., & Mayor, M. 1992, ApJ, 401, 265

Mazeh, T., Martin, E. L., Goldberg, D., & Smith, H. A. 1997, MNRAS, 284, 341

Mazeh, T., Prato, L., Simon, M., Goldberg, E., Norman, D., & Zucker, S. 2002, ApJ, 564, 1007

Mazeh, T., Simon, M., Prato, L., Markus, B., & Zucker, S. 2003, ApJ, 599, 1344

McAlister, H. A. 1978a, PASP, 90, 288

——. 1978b, ApJ, 225, 932

——. 1979, ApJ, 230, 497

McAlister, H. A., Hartkopf, W. I., Hutter, D. J., & Franz, O. G. 1987, AJ, 93, 688

McAlister, H. A., Mason, B. D., Hartkopf, W. I., & Shara, M. M. 1993, AJ, 106, 1639

McCarthy, C., & Zuckerman, B. 2004, AJ, 127, 2871

Melo, C. H. F. 2003, A&A, 410, 269

Metchev, S., & Hillenbrand, L. 2008, ArXiv e-prints

Michelson, A. A. 1890, Phil.Mag., 30, 1

——. 1920, ApJ, 51, 257

Mishenina, T. V., Soubiran, C., Bienaymé, O., Korotin, S. A., Belik, S. I., Usenko, I. A., & Kovtyukh, V. V. 2008, A&A, 489, 923

Monet, D. G. et al. 2003, AJ, 125, 984

Moore, J. H., & Paddock, G. F. 1950, ApJ, 112, 48

Morbey, C. L., & Griffin, R. F. 1987, ApJ, 317, 343

Moutou, C. et al. 2008, A&A, 488, L47

Mugrauer, M., & Neuhäuser, R. 2005, MNRAS, 361, L15

——. 2009, A&A, 494, 373

Mugrauer, M., Neuhäuser, R., Seifahrt, A., Mazeh, T., & Guenther, E. 2005, A&A, 440, 1051

Murdoch, K. A., Hearnshaw, J. B., & Clark, M. 1993, ApJ, 413, 349

Musielak, Z. E., Cuntz, M., Marshall, E. A., & Stuit, T. D. 2005, A&A, 434, 355

Muterspaugh, M. W. 2005, PhD thesis, Massachusetts Institute of Technology

Nadal, R., Ginestet, N., Carquillat, J.-M., & Pedoussaut, A. 1979, A&AS, 35, 203

Nather, R. E., & Evans, D. S. 1970, AJ, 75, 575

Neuhäuser, R., & Guenther, E. W. 2004, A&A, 420, 647

Nidever, D. L., Marcy, G. W., Butler, R. P., Fischer, D. A., & Vogt, S. S. 2002, ApJS, 141, 503

Nordström, B. et al. 2004, A&A, 418, 989

Noyes, R. W., Jha, S., Korzennik, S. G., Krockenberger, M., Nisenson, P., Brown, T. M., Kennelly, E. J., & Horner, S. D. 1997, ApJ, 487, L195

Oppenheimer, B. R., Golimowski, D. A., Kulkarni, S. R., Matthews, K., Nakajima, T., Creech-Eakman, M., & Durrance, S. T. 2001, AJ, 121, 2189

Patience, J., Ghez, A. M., Reid, I. N., & Matthews, K. 2002a, AJ, 123, 1570

Patience, J. et al. 2002b, ApJ, 581, 654

Perryman, M. A. C., & ESA, eds. 1997, ESA Special Publication, Vol. 1200, The HIPPARCOS and TYCHO catalogues. Astrometric and photometric star catalogues derived from the ESA HIPPARCOS Space Astrometry Mission

Petrie, R. M. 1960, Annales d'Astrophysique, 23, 744

Pilat-Lohinger, E., Funk, B., & Dvorak, R. 2003, A&A, 400, 1085

Pollacco, D. L. et al. 2006, PASP, 118, 1407

Potter, D., Martín, E. L., Cushing, M. C., Baudoz, P., Brandner, W., Guyon, O., & Neuhäuser, R. 2002, ApJ, 567, L133

Pourbaix, D. 2000, A&AS, 145, 215

Pourbaix, D., Neuforge-Verheecke, C., & Noels, A. 1999, A&A, 344, 172

Pourbaix, D. et al. 2002, A&A, 386, 280

Poveda, A., Herrera, M. A., Allen, C., Cordero, G., & Lavalley, C. 1994, Revista Mexicana de Astronomia y Astrofisica, 28, 43

Queloz, D. et al. 2000, A&A, 354, 99

Quist, C. F., & Lindegren, L. 2000, A&A, 361, 770

Raghavan, D., Henry, T. J., Mason, B. D., Subasavage, J. P., Jao, W.-C., Beaulieu, T. D., & Hambly, N. C. 2006, ApJ, 646, 523

Raghavan, D. et al. 2009, ApJ, 690, 394

Rapaport, M. et al. 2001, A&A, 376, 325

Reid, I. N. et al. 2004, AJ, 128, 463

Reid, I. N., & Gizis, J. E. 1997, AJ, 114, 1992

Reid, I. N., Hawley, S. L., & Gizis, J. E. 1995, AJ, 110, 1838

Richichi, A. 2000, A&A, 364, 225

Roberts, Jr., L. C. et al. 2005, AJ, 130, 2262

Rossiter, R. A. 1955, Publications of Michigan Observatory, 11, 1

Rovithis, P., & Rovithis-Livaniou, H. 1990, A&AS, 86, 523

Salim, S., & Gould, A. 2003, ApJ, 582, 1011

Salim, S., Rich, R. M., Hansen, B. M., Koopmans, L. V. E., Oppenheimer, B. R., & Blandford, R. D. 2004, ApJ, 601, 1075

Scardia, M. et al. 2008, Astronomische Nachrichten, 329, 54

Scarfe, C. D. 1986, JRASC, 80, 257

Schaefer, B. E., King, J. R., & Deliyannis, C. P. 2000, ApJ, 529, 1026

Schultz, A. B. et al. 1998, AJ, 115, 345

Shatsky, N. 2001, A&A, 380, 238

Shatsky, N., & Tokovinin, A. 2002, A&A, 382, 92

Siegler, N., Close, L. M., Cruz, K. L., Martín, E. L., & Reid, I. N. 2005, ApJ, 621, 1023

Sinachopoulos, D. 1988, A&AS, 76, 189

Skuljan, J., Ramm, D. J., & Hearnshaw, J. B. 2004, MNRAS, 352, 975

Söderhjelm, S. 1999, A&A, 341, 121

——. 2000, Astronomische Nachrichten, 321, 165

——. 2007, A&A, 463, 683

Soderhjelm, S., & Mignard, F. 1998, The Observatory, 118, 365

Sollima, A., Beccari, G., Ferraro, F. R., Fusi Pecci, F., & Sarajedini, A. 2007, MNRAS, 380, 781

Subasavage, J. P., Jao, W.-C., Henry, T. J., Bergeron, P., Dufour, P., Ianna, P. A., Costa, E., & Mendez, R. A. 2009, ArXiv e-prints

Takeda, G., Kita, R., & Rasio, F. A. 2008, ApJ, 683, 1063

ten Brummelaar, T., Mason, B. D., McAlister, H. A., Roberts, Jr., L. C., Turner, N. H., Hartkopf, W. I., & Bagnuolo, Jr., W. G. 2000, AJ, 119, 2403

ten Brummelaar, T. A. et al. 2005, ApJ, 628, 453

The, C. D. 2005, VizieR Online Data Catalog, 2263, 0

Tokovinin, A. 2008, MNRAS, 389, 925

Tokovinin, A., Thomas, S., Sterzik, M., & Udry, S. 2006, A&A, 450, 681

Tokovinin, A. A. 1985, A&AS, 61, 483

——. 1991, A&AS, 91, 497

——. 1997, A&AS, 124, 75

——. 2000, A&A, 360, 997

Tokovinin, A. A., & Ismailov, R. M. 1988, A&AS, 72, 563

Torres, G., Boden, A. F., Latham, D. W., Pan, M., & Stefanik, R. P. 2002, AJ, 124, 1716

Trimble, V. 1987, Astronomische Nachrichten, 308, 343

——. 1990, MNRAS, 242, 79

Turner, N. H., ten Brummelaar, T. A., McAlister, H. A., Mason, B. D., Hartkopf, W. I., & Roberts, Jr., L. C. 2001, AJ, 121, 3254

Turner, N. H., ten Brummelaar, T. A., Roberts, L. C., Mason, B. D., Hartkopf, W. I., & Gies, D. R. 2008, AJ, 136, 554

Udalski, A. et al. 2002, Acta Astronomica, 52, 1

Udry, S., Eggenberger, A., Mayor, M., Mazeh, T., & Zucker, S. 2004, in Revista Mexicana de Astronomia y Astrofisica, vol. 27, Vol. 21, Revista Mexicana de Astronomia y Astrofisica Conference Series, ed. C. Allen & C. Scarfe, 207–214

Udry, S. et al. 1998, in Astronomical Society of the Pacific Conference Series, Vol. 154, Cool Stars, Stellar Systems, and the Sun, ed. R. A. Donahue & J. A. Bookbinder, 2148–+

Udry, S., & Santos, N. C. 2007, ARA&A, 45, 397

Valenti, J. A., & Fischer, D. A. 2005, ApJS, 159, 141

van Altena, W. F., Lee, J. T., & Hoffleit, E. D. 1995, The general catalogue of trigonometric stellar parallaxes 4th Ed. (New Haven, CT: Yale University Observatory)

van Leeuwen, F., ed. 2007a, Astrophysics and Space Science Library, Vol. 250, Hipparcos, the New Reduction of the Raw Data

van Leeuwen, F. 2007b, A&A, 474, 653 (FvL07)

Verrier, P. E., & Evans, N. W. 2007, MNRAS, 382, 1432

Vogt, S. S., Butler, R. P., Marcy, G. W., Fischer, D. A., Henry, G. W., Laughlin, G., Wright, J. T., & Johnson, J. A. 2005, ApJ, 632, 638

Vogt, S. S., Butler, R. P., Marcy, G. W., Fischer, D. A., Pourbaix, D., Apps, K., & Laughlin, G. 2002, ApJ, 568, 352

Weis, E. W. 1996, AJ, 112, 2300

Wertheimer, J. G., & Laughlin, G. 2006, AJ, 132, 1995

Wilson, J. C., Kirkpatrick, J. D., Gizis, J. E., Skrutskie, M. F., Monet, D. G., & Houck, J. R. 2001, AJ, 122, 1989

Wilson, O. C. 1967, AJ, 72, 905

Woitas, J., Leinert, C., & Köhler, R. 2001, A&A, 376, 982

Wright, J. T., Marcy, G. W., Butler, R. P., & Vogt, S. S. 2004, ApJS, 152, 261

Wright, J. T. et al. 2007, ApJ, 657, 533

Wright, J. T., Upadhyay, S., Marcy, G. W., Fischer, D. A., Ford, E. B., & Johnson, J. A. 2008, ArXiv e-prints

Zacharias, N., Monet, D. G., Levine, S. E., Urban, S. E., Gaume, R., & Wycoff, G. L. 2004, in Bulletin of the American Astronomical Society, Vol. 36, Bulletin of the American Astronomical Society, 1418–+

Zinnecker, H. 1984, Ap&SS, 99, 41

Appendices

– A –

Physical Parameters for Primaries and Companions

This appendix lists the physical parameters extracted for the primary stars and extracted or estimated values for many companions. These data are used in the analyses presented in Chapter 8 (see the discussion in § 8.3 for more information).

TABLE A.1: Physical parameters and mass of the sample stars

HD Name	**HIP Name**	**Spec Type**	**Ref**	**Mass ($M_\odot$)**	**Ref**	**[Fe/H]**	**Ref**	$\log(R'_{HK})$	**Ref**
Sun	...	G2V	...	1.00	...	0.00	...	...	...
000123	000518	G4V	Gra2003	0.98	Nor2004	−0.01	Nor2004	−4.644	Gra2003
000166	000544	G8V	Gra2003	0.96	Val2005	0.12	Val2005	−4.458	Gra2003
000870	001031	K0V	Gra2006	0.81	Nor2004	−0.20	Nor2004	−4.824	Gra2006
001237	001292	G8.5V	Gra2006	0.85	Nor2004	−0.09	Nor2004	−4.496	Gra2006
001273	001349	G5V	Gra2006	0.80	Nor2004	−0.65	Nor2004	−4.802	Gra2006
001461	001499	G3V	Gra2003	1.14	Val2005	0.16	Val2005	−5.030	Wri2004
001562	001598	G1V	Gra2003	0.85	Nor2004	−0.34	Nor2004	−4.979	Gra2003
001581	001599	F9.5V	Gra2006	1.17	Val2005	−0.18	Val2005	−4.855	Gra2006
001835	001803	G5V	Gra2006	0.98	Val2005	0.22	Val2005	−4.440	Wri2004
002025	001936	K3V	Gra2006	0.70	Val2005	−0.27	Val2005	−4.933	Gra2006
002151	002021	G0V	Gra2006	1.43	Val2005	−0.09	Val2005	−5.006	Gra2006
003196	002762	F8.5V	Gra2003	1.13	Nor2004	−0.07	Nor2004	−4.461	Gra2003
003443	002941	G7V	Gra2006	0.94	Pou2000	−0.14	Nor2004	−4.940	Wri2004
003651	003093	K0V	Gra2003	0.79	Val2005	0.16	Val2005	−5.020	Wri2004
003765	003206	K2.5V	Gra2003	0.84	Val2005	0.12	Val2005	−5.101	Gra2003
004256	003535	K3IV-V	Gra2003	1.36	Val2005	0.22	Val2005	−5.042	Gra2003
004308	003497	G6V	Gra2006	1.47	Val2005	−0.18	Val2005	−4.853	Gra2006
004391	003583	G5V	Gra2006	0.88	Nor2004	−0.25	Nor2004	−4.669	Gra2006
004614	003821	G0V	HIP	1.10	Val2005	−0.17	Val2005	−4.930	Wri2004
004628	003765	K2V	Gra2003	0.63	Val2005	−0.19	Val2005	−5.071	Gra2003
004635	003876	K2.5V+	Gra2003	...	...	...	...	−4.670	Wri2004
004676	003810	F8V	Gra2003	1.22	Bod1999	−0.06	Nor2004	−4.917	Gra2003
004747	003850	G9V	Gra2006	0.99	Val2005	−0.25	Val2005	−4.720	Wri2004
004813	003909	F7V	Gra2003	1.10	Nor2004	−0.15	Nor2004	−4.780	Gra2003

Continued on Next Page...

TABLE A.1 – Continued

HD Name	HIP Name	Spec Type	Ref	Mass ($M_\odot$)	Ref	[Fe/H]	Ref	$\log(R'_{HK})$	Ref
004915	003979	G6V	Gra2003	1.02	Val2005	−0.18	Val2005	−4.860	Wri2004
005015	004151	F8V	HIP	1.25	Nor2004	...	...	−5.02	MAs2009b
005133	004148	K2.5V	Gra2006	1.19	Val2005	−0.13	Val2005	−4.751	Gra2006
006582	005336	K1V	Gra2003	0.75	Nor2004	−0.83	Nor2004	−5.031	Gra2003
007570	005862	F9V	Gra2006	1.16	Val2005	0.14	Val2005	−4.861	Gra2006
007590	005944	G0-V	Gra2003	1.12	Val2005	−0.07	Val2005	−4.530	Wri2004
007693	005842	K2+V	Gra2006	0.92	Sod1999	0.05	Val2005	−4.580	Gra2006
007924	006379	K0	HIP	0.80	Val2005	−0.12	Val2005	−4.830	Wri2004
008997	006917	K2.5V	Gra2003	...	...	−0.59	Nor2004	−4.557	Gra2003
009407	007339	G6.5V	Gra2003	1.13	Val2005	...	...	−5.010	Wri2004
009540	007235	G8.5V	Gra2006	0.91	Val2005	−0.04	Val2005	−4.600	Wri2004
009770	007372	K2V	Gra2006	0.74	Sod1999	−0.65	Nor2004	−4.354	Gra2006
009826	007513	F8V	HIP	1.2	Low2002	0.12	Val2005	−5.040	Wri2004
010008	007576	G9V	Gra2003	0.86	Nor2004	−0.03	Gra2003	−4.530	Gra2003
010086	007734	G5V	Gra2003	0.98	Val2005	0.09	Val2005	−4.600	Wri2004
010307	007918	G1V	Gra2003	1.01	Nor2004	−0.05	Nor2004	−5.017	Gra2003
010360	007751	K2V	Gra2006	0.44	Val2005	−0.20	Val2005	−4.899	Gra2006
010476	007981	K0V	Gra2003	0.81	Val2005	−0.07	Val2005	−4.950	Wri2004
010647	007978	F9V	Gra2006	0.98	Val2005	−0.08	Val2005	−4.675	Gra2006
010700	008102	G8.5V	Gra2006	0.99	Val2005	−0.36	Val2005	−4.980	Wri2004
010780	008362	G9V	Gra2003	0.88	Val2005	−0.06	Val2005	−4.690	Wri2004
012051	009269	G9V	Gra2003	1.37	Val2005	0.15	Val2005	−5.050	Wri2004
012846	009829	G2V-	Gra2003	0.87	Val2005	−0.20	Val2005	−4.980	Wri2004
013445	010138	K1V	Gra2006	0.92	Val2005	−0.20	Val2005	−4.768	Gra2006
013974	010644	G0V	HIP	0.85	Nor2004	−0.39	Nor2004	−4.710	Wri2004
014214	010723	G0IV-	Gra2003	1.14	Nor2004	0.06	Nor2004	−5.114	Gra2003
014412	010798	G8V	Gra2006	1.03	Val2005	−0.45	Val2005	−4.850	Wri2004

Continued on Next Page...

TABLE A.1 – Continued

HD Name	HIP Name	Spec Type	Ref	Mass ($M_\odot$)	Ref	[Fe/H]	Ref	$\log(R'_{HK})$	Ref
014802	011072	G0V	Gra2006	1.15	Nor2004	−0.08	Nor2004	−5.050	Wri2004
016160	012114	K3V	Gra2003	0.90	Val2005	0.08	Nor2004	−5.094	Gra2003
016287	012158	K2.5V	Gra2003	0.97	Val2005	0.08	Val2005	−4.504	Gra2003
016673	012444	F8V	Gra2003	1.12	Nor2004	−0.11	Nor2004	−4.586	Gra2003
016739	012623	F9IV-V	Gra2003	1.38	Bag2006	0.14	Nor2004	−5.012	Gra2003
016765	012530	F7V	Gra2003	1.06	Nor2004	−0.24	Nor2004	−4.400	Gra2003
016895	012777	F7V	HIP	1.37	Val2005	0.02	Val2005	−4.970	Wri2004
017051	012653	F9V	Gra2006	1.07	Val2005	0.09	Val2005	−4.625	Gra2006
017382	013081	K0V	Gra2003	...	...	...	...	−4.450	Wri2004
017925	013402	K1.5V	Gra2006	0.81	Val2005	0.11	Val2005	−4.357	Gra2006
018143	013642	K2IV	Gra2003	1.05	Val2005	0.21	Val2005	−5.119	Gra2003
018632	013976	K2.5V	Gra2003	0.55	Val2005	0.18	Val2005	−4.418	Gra2003
018757	014286	G1.5V	Gra2003	0.84	Nor2004	−0.44	Nor2004	−4.987	Gra2003
018803	014150	G6V	Gra2003	0.97	Val2005	0.09	Val2005	−4.880	Wri2004
019373	014632	F9.5V	Gra2003	1.35	Val2005	0.13	Val2005	−5.020	Wri2004
019994	014954	F8.5V	Gra2003	1.81	Val2005	0.17	Val2005	−4.880	Wri2004
020010	014879	F6V	Gra2006	1.30	Nor2004	−0.16	Nor2004	−4.901	Gra2006
020165	015099	K1V	Gra2003	0.66	Val2005	−0.04	Val2005	−4.860	Wri2004
020407	015131	G5V	Gra2006	0.90	Nor2004	−0.46	Nor2004	−4.734	Gra2006
020619	015442	G2V	Gra2003	1.06	Val2005	−0.18	Val2005	−4.830	Wri2004
020630	015457	G5Vvar	HIP	0.94	Val2005	0.10	Val2005	−4.47	MAs2009b
020794	015510	G8V	Gra2006	1.30	Val2005	−0.23	Val2005	−4.998	Gra2006
020807	015371	G0V	Gra2006	1.19	Val2005	−0.23	Val2005	−4.827	Gra2006
021175	015799	K1V	Gra2006	0.85	Nor2004	0.12	Nor2004	−4.773	Gra2006
022049	016537	K2V	Gra2006	0.70	Val2005	−0.15	Gra2006	−4.510	Wri2004
022484	016852	F9V	HIP	1.46	Val2005	−0.03	Val2005	−5.120	Wri2004
022879	017147	F9V	HIP	1.12	Val2005	−0.76	Val2005	−4.920	Wri2004

Continued on Next Page...

TABLE A.1 – Continued

HD Name	HIP Name	Spec Type	Ref	Mass ($M_\odot$)	Ref	[Fe/H]	Ref	$\log(R'_{HK})$	Ref
023356	017420	K2.5V	Gra2006	0.74	Val2005	−0.07	Val2005	−4.807	Gra2006
023484	017439	K2V	Gra2006	0.66	Val2005	0.04	Val2005	−4.534	Gra2006
024238	018324	K2V	Gra2003	0.87	Val2005	−0.32	Val2005	−4.980	Wri2004
024409	018413	G3V	Gra2003	0.87	Nor2004	−0.25	Nor2004	−4.927	Gra2003
024496	018267	G7V	Gra2003	1.08	Val2005	−0.01	Val2005	−4.870	Wri2004
025329	018915	K3Vp	Gra2003	0.58	Nor2004	−1.69	Nor2004	−4.940	Wri2004
025457	018859	F7V	Gra2003	1.15	Nor2004	−0.10	Nor2004	−4.390	Wri2004
025665	019422	K2.5V	Gra2003	0.66	Val2005	−0.06	Val2005	−4.847	Gra2003
025680	019076	G1V	Gra2003	1.15	Val2005	0.04	Val2005	−4.608	Gra2003
025998	019335	F8V	Gra2003	1.22	Nor2004	0.02	Nor2004	−4.468	Gra2003
026491	019233	G1V	Gra2006	1.06	Val2005	−0.06	Val2005	−4.889	Gra2006
026923	019859	G0V	Gra2006	1.01	Nor2004	−0.13	Nor2004	−4.521	Gra2006
026965	019849	K0.5V	Gra2006	0.89	Val2005	−0.08	Val2005	−4.900	Wri2004
029883	021988	K5III	HIP	0.89	Val2005	−0.16	Val2005	−4.87	MAs2009b
030495	022263	G1.5V	Gra2006	0.86	Val2005	−0.01	Val2005	−4.600	Wri2004
030501	022122	K2V	Gra2006	0.82	Nor2004	−0.09	Gra2006	−4.762	Gra2006
030876	022451	K2V	HIP	0.85	Val2005	−0.11	Val2005	−4.55	MAs2009b
032778	023437	G7V	Gra2006	0.95	Val2005	−0.48	Val2005	−4.870	Gra2006
032850	023786	G9V	Gra2003	0.80	Nor2004	−0.19	Nor2004	−4.600	Wri2004
032923	023835	G1V	Gra2003	1.44	Val2005	−0.13	Val2005	−5.030	Wri2004
033262	023693	F9V	Gra2006	1.07	Nor2004	−0.20	Nor2004	−4.373	Gra2006
033564	025110	F7V	Gra2003	1.25	Nor2004	−0.06	Nor2004	−4.949	Gra2003
034411	024813	G1V	Gra2003	1.36	Val2005	0.09	Val2005	−5.050	Wri2004
034721	024786	F9-V	Gra2006	1.17	Val2005	−0.08	Val2005	−5.030	Wri2004
035112	025119	K2.5V	Gra2003	...	...	−0.27	Nor2004	−4.879	Gra2003
035296	025278	F8V	Gra2003	1.06	Nor2004	−0.15	Nor2004	−4.353	Gra2003
035854	025421	K3-V	Gra2006	0.77	Val2005	−0.04	Val2005	−4.922	Gra2006

Continued on Next Page...

TABLE A.1 – Continued

HD Name	HIP Name	Spec Type	Ref	Mass ($M_\odot$)	Ref	[Fe/H]	Ref	$\log(R'_{HK})$	Ref
036435	025544	G9V	Gra2006	0.83	Nor2004	−0.18	Nor2004	−4.499	Gra2006
036705	025647	K2V	Gra2006	0.87	Clo2005	−0.59	Nor2004	−3.880	Gra2006
037008	026505	K1V	Gra2003	0.80	Val2005	−0.31	Val2005	−4.960	Wri2004
037394	026779	K0V	Gra2003	0.88	Val2005	0.16	Val2005	−4.553	Gra2003
037572	026373	K1.5V	Gra2006	0.76	Nor2004	−0.49	Nor2004	−4.234	Gra2006
038230	027207	K0V	Gra2003	0.90	Val2005	−0.02	Val2005	−4.990	Wri2004
038858	027435	G2V	Gra2003	1.05	Val2005	−0.21	Val2005	−4.950	Wri2004
039091	026394	G0V	Gra2006	1.11	Val2005	0.04	Val2005	−4.941	Gra2006
039587	027913	G0V	Gra2006	1.10	Cat2006	−0.16	Nor2004	−4.426	Gra2006
039855	027922	G8V	Gra2006	0.80	Nor2004	−0.49	Nor2004	−4.932	Gra2006
040307	027887	K2.5V	Gra2006	0.77	Val2005	−0.25	Val2005	−5.037	Gra2006
040397	028267	G7V	Gra2003	1.50	Val2005	−0.05	Val2005	−4.980	Wri2004
041593	028954	G9V	Gra2003	...	...	...	...	−4.390	Wri2004
042618	029432	G3V	Gra2003	0.84	Val2005	−0.09	Val2005	−4.940	Wri2004
042807	029525	G5V	Gra2003	0.87	Nor2004	−0.21	Nor2004	−4.465	Gra2003
043162	029568	G6.5V	Gra2006	0.88	Nor2004	−0.10	Nor2004	−4.400	Wri2004
043587	029860	G0V	Gra2006	1.17	Val2005	−0.08	Val2005	−5.000	Wri2004
043834	029271	G7V	Gra2006	1.10	Val2005	0.05	Val2005	−4.940	Gra2006
045088	030630	K3V	Gra2003	0.83	This work	−0.85	Nor2004	−4.266	Gra2003
045184	030503	G1.5V	Gra2006	0.97	Val2005	0.03	Val2005	−4.950	Wri2004
045270	030314	G0Vp	Gra2006	0.96	Nor2004	−0.18	Nor2004	−4.378	Gra2006
046588	032439	F8V	Gra2003	1.03	Nor2004	−0.25	Nor2004	−4.885	Gra2003
048189	031711	G1V	Gra2006	0.94	Nor2004	−0.23	Nor2004	−4.268	Gra2006
048682	032480	F9V	Gra2003	1.12	Val2005	0.09	Val2005	−4.850	Wri2004
050692	033277	G0V	Gra2003	0.98	Val2005	−0.13	Val2005	−4.940	Wri2004
051419	033537	G5V	Gra2003	1.00	Val2005	−0.33	Val2005	−4.870	Wri2004
051866	033852	K3V	Gra2003	...	...	...	...	−4.889	Gra2003

Continued on Next Page...

TABLE A.1 – Continued

HD Name	HIP Name	Spec Type	Ref	Mass ($M_\odot$)	Ref	[Fe/H]	Ref	$\log(R'_{HK})$	Ref
052698	033817	K1V	Gra2006	...	...	...	...	−4.590	Wri2004
052711	034017	G0V	Gra2003	1.13	Val2005	−0.10	Val2005	−4.960	Wri2004
053143	033690	K0IV-V	Gra2006	0.85	Nor2004	−0.01	Nor2004	−4.547	Gra2006
053705	034065	G0V	Gra2006	1.31	Val2005	−0.15	Val2005	−4.981	Gra2006
053927	034414	K2.5V	Gra2003	0.74	Nor2004	−0.27	Nor2004	−4.984	Gra2003
054371	034567	G6V	Gra2003	0.88	Nor2004	−0.10	Nor2004	−4.462	Gra2003
055575	035136	F9V	Gra2003	0.95	Nor2004	−0.35	Nor2004	−4.950	Wri2004
057095	035296	K2.5V	Gra2006	...	...	...	...	−4.538	Gra2006
059468	036210	G6.5V	Gra2006	1.04	Val2005	0.01	Val2005	−4.946	Gra2006
059747	036704	K1V	Gra2003	0.74	Val2005	−0.03	Val2005	−4.370	Wri2004
059967	036515	G2V	Gra2006	0.88	Nor2004	−0.24	Nor2004	−4.372	Gra2006
060491	036827	K2.5V	Gra2003	0.86	Val2005	−0.26	Val2005	−4.430	Wri2004
061606	037349	K3-V	Gra2003	0.97	Val2005	−0.05	Val2005	−4.390	Wri2004
062613	038784	G8V	HIP	0.83	Nor2004	−0.23	Nor2004	−4.840	Wri2004
063077	037853	F9V	Gra2006	0.84	Nor2004	−0.75	Nor2004	−4.970	Wri2004
063433	038228	G5V	Gra2003	0.95	Val2005	0.02	Val2005	−4.390	Wri2004
064096	038382	G0V	Gra2006	0.93	Pou2000	−0.18	Nor2004	−4.883	Gra2006
064468	038657	K2.5V	Gra2003	0.66	Val2005	0.09	Val2005	−5.146	Gra2003
064606	038625	K0V	Gra2003	0.74	Nor2004	−0.80	Nor2004	−4.940	Wri2004
065430	039064	K0V	Gra2003	0.87	Val2005	−0.04	Val2005	−5.010	Wri2004
065583	039157	K0V	Gra2003	1.29	Val2005	−0.48	Val2005	−4.950	Wri2004
065907	038908	F9.5V	Gra2006	1.77	Val2005	−0.15	Val2005	−4.846	Gra2006
067199	039342	K2V	Gra2006	0.77	Val2005	0.01	Nor2004	−4.843	Gra2006
067228	039780	G2IV	Gra2003	1.22	Val2005	0.17	Val2005	−5.120	Wri2004
068017	040118	G3V	Gra2003	1.55	Val2005	−0.30	Val2005	−4.920	Wri2004
068257	040167	F8V	Gra2003	1.52	Nor2004	0.08	Nor2004	...	...
069830	040693	G8+V	Gra2006	0.86	Val2005	−0.08	Val2005	−4.950	Wri2004

Continued on Next Page...

TABLE A.1 – Continued

HD Name	HIP Name	Spec Type	Ref	Mass ($M_\odot$)	Ref	[Fe/H]	Ref	$\log(R'_{HK})$	Ref
071148	041484	G1V	Gra2003	1.03	Val2005	−0.01	Val2005	−4.950	Wri2004
072673	041926	G9V	Gra2006	0.98	Val2005	−0.33	Val2005	−4.950	Wri2004
072760	042074	K0-V	Gra2003	0.92	Val2005	0.03	Val2005	−4.380	Wri2004
072905	042438	G1.5Vb	HIP	0.90	Nor2004	−0.25	Nor2004	−4.400	Wri2004
073350	042333	G5V	Gra2003	1.01	Val2005	0.04	Val2005	−4.490	Wri2004
073667	042499	K2V	Gra2003	0.91	Val2005	−0.36	Val2005	−4.970	Wri2004
073752	042430	G5IV	Gra2006	1.25	Sod1999	0.31	Nor2004	−5.031	Gra2006
074385	042697	K2+V	Gra2006	0.79	Nor2004	−0.03	Nor2004	−4.902	Gra2006
074576	042808	K2.5V	Gra2006	0.77	Nor2004	−0.24	Nor2004	−4.402	Gra2006
075732	043587	K0IV-V	Gra2003	0.92	Val2005	0.25	Val2005	−5.040	Wri2004
075767	043557	G1.5V	Gra2003	0.91	Nor2004	−0.18	Nor2004	−4.638	Gra2003
076151	043726	G3V	Gra2006	1.24	Val2005	0.07	Val2005	−4.853	Gra2006
076932	044075	G2V	Gra2006	0.89	Nor2004	−0.70	Nor2004	−4.781	Gra2006
078366	044897	G0IV-V	Gra2003	1.34	Val2005	0.03	Val2005	−4.555	Gra2003
079028	045333	G0IV-V	Gra2003	1.08	Nor2004	−0.10	Nor2004	−5.073	Gra2003
079096	045170	G9V	Gra2003	0.89	Pou2000	−0.30	Nor2004	−4.846	Gra2003
079969	045617	K3V	Gra2003	0.74	Sod1999	−0.22	Nor2004	−4.736	Gra2003
080715	045963	K2.5V	Gra2003	...	...	−0.58	Gra2003	−4.099	Gra2003
082342	046626	K3.5V	Gra2006	...	...	...	...	−5.131	Gra2006
082443	046843	K1V	Gra2006	...	...	...	...	−4.234	Gra2006
082558	046816	K0	HIP	2.05	Val2005	−0.21	Val2005	−4.09	MAs2009b
082885	047080	K0V	VJHK	...	...	...	...	−4.68	MAs2009b
084117	047592	F8V	Gra2006	1.11	Val2005	−0.08	Val2005	−4.862	Gra2006
084737	048113	G0IV-V	Gra2003	1.42	Val2005	0.14	Val2005	−5.230	Wri2004
086728	049081	G4V	Gra2003	0.73	Val2005	0.11	Val2005	−5.060	Wri2004
087424	049366	K2V	Gra2006	0.78	Val2005	−0.14	Val2005	−4.440	Wri2004
087883	049699	K2.5V	Gra2003	0.78	Val2005	0.04	Val2005	−4.999	Gra2003

Continued on Next Page...

TABLE A.1 – Continued

HD Name	HIP Name	Spec Type	Ref	Mass ($M_\odot$)	Ref	[Fe/H]	Ref	$\log(R'_{HK})$	Ref
088742	050075	G0V	Gra2006	0.99	Val2005	−0.04	Val2005	−4.806	Gra2006
089125	050384	F6V	Gra2003	1.01	Nor2004	−0.44	Nor2004	−4.832	Gra2003
089269	050505	G4V	Gra2003	0.94	Val2005	−0.18	Val2005	−4.940	Wri2004
090156	050921	G5V	Gra2006	1.25	Val2005	−0.21	Val2005	−4.950	Wri2004
090343	051819	K0	HIP	...	...	...	...	−4.58	MAs2009b
090508	051248	G0V	Gra2003	0.85	Nor2004	−0.40	Nor2004	−5.005	Gra2003
090839	051459	F8V	Gra2003	0.99	Val2005	−0.05	Val2005	−4.860	Wri2004
091324	051523	F9V	Gra2006	1.16	Nor2004	−0.28	Nor2004	−4.766	Gra2006
091889	051933	F8V	Gra2006	1.04	Nor2004	−0.27	Nor2004	−4.849	Gra2006
092719	052369	G1.5V	Gra2006	0.91	Nor2004	−0.21	Nor2004	−4.826	Gra2006
092945	052462	K1.5V	Gra2006	1.18	Val2005	−0.12	Val2005	−4.320	Wri2004
094765	053486	K2.5V	Gra2003	1.19	Val2005	−0.03	Val2005	−4.546	Gra2003
095128	053721	G0V	HIP	1.29	Val2005	0.02	Val2005	−5.020	Wri2004
096064	054155	G8+V	Gra2003	0.83	Nor2004	−0.13	Nor2004	−4.373	Gra2003
096612	054426	K3-V	Gra2003	...	...	...	...	−4.836	Gra2003
097334	054745	G1V	Gra2003	0.93	Val2005	0.08	Val2005	−4.368	Gra2003
097343	054704	G8.5V	Gra2006	1.11	Val2005	−0.05	Val2005	−5.000	Wri2004
097658	054906	K1V	Gra2003	0.90	Val2005	−0.27	Val2005	−4.920	Wri2004
098230	055203	G2V	Bal2005	0.96	Nor2004	−0.30	Nor2004	...	...
098281	055210	G8V	HIP	1.00	Val2005	−0.17	Val2005	−4.940	Wri2004
099491	055846	K0IV	HIP	1.15	Val2005	0.24	Val2005	−4.840	Wri2004
100180	056242	F9.5V	Gra2003	1.01	Val2005	−0.02	Val2005	−4.940	Wri2004
100623	056452	K0-V	Gra2006	0.96	Val2005	−0.32	Val2005	−4.890	Wri2004
101177	056809	F9.5V	Gra2003	0.99	Val2005	−0.17	Val2005	−4.930	Wri2004
101206	056829	K5V	HIP	...	...	...	...	−4.52	MAs2009b
101501	056997	G8V	Gra2003	0.73	Val2005	−0.03	Val2005	−4.550	Wri2004
102365	057443	G2V	Gra2006	1.22	Val2005	−0.26	Val2005	−4.957	Gra2006

Continued on Next Page...

TABLE A.1 – Continued

HD Name	HIP Name	Spec Type	Ref	Mass ($M_\odot$)	Ref	[Fe/H]	Ref	$\log(R'_{HK})$	Ref
102438	057507	G6V	Gra2006	1.01	Val2005	−0.23	Val2005	−4.924	Gra2006
102870	057757	F8V	HIP	1.61	Val2005	0.16	Val2005	−4.940	Wri2004
103095	057939	K1V	Gra2003	0.71	Val2005	−1.16	Val2005	−4.850	Wri2004
104067	058451	K3-V	Gra2006	0.91	Val2005	0.04	Val2005	−4.751	Gra2006
104304	058576	G8IV	Gra2006	1.34	Val2005	0.16	Val2005	−4.920	Wri2004
105631	059280	G9V	Gra2003	0.91	Val2005	0.14	Val2005	−4.650	Wri2004
108954	061053	F9V	Gra2003	1.04	Nor2004	−0.13	Nor2004	−4.921	Gra2003
109200	061291	K1V	Gra2006	0.79	Val2005	−0.23	Val2005	−5.124	Gra2006
109358	061317	G0V	Gra2003	1.05	Val2005	−0.10	Val2005	−4.920	Wri2004
110463	061946	K3V	HIP	...	...	...	...	−4.47	MAs2009b
110810	062229	K2+V	Gra2006	0.76	Val2005	−0.03	Val2005	−4.441	Gra2006
110833	062145	K3V	HIP	0.84	Nor2004	0.08	Nor2004	−4.70	MAs2009b
110897	062207	F9V	Gra2003	0.83	Nor2004	−0.59	Nor2004	−4.869	Gra2003
111312	062505	K2.5V	Gra2006	...	...	...	...	−4.571	Gra2006
111395	062523	G7V	Gra2003	1.08	Val2005	0.06	Val2005	−4.580	Wri2004
112758	063366	G9V	Gra2006	0.76	Nor2004	−0.38	Nor2004	−5.067	Gra2006
112914	063406	K3-V	Gra2003	0.70	Val2005	−0.26	Val2005	−5.043	Gra2003
113283	064690	G5V	Gra2006	0.87	Nor2004	−0.15	Nor2004	−4.720	Gra2006
113449	063742	K1V	Gra2003	...	...	...	...	−4.340	Gra2003
114613	064408	G4IV	Gra2006	1.80	Val2005	0.16	Val2005	−5.118	Gra2006
114710	064394	G0V	HIP	1.54	Val2005	0.04	Val2005	−4.760	Wri2004
114783	064457	K1V	Gra2003	0.75	Val2005	0.10	Val2005	−5.056	Gra2003
114853	064550	G1.5V	Gra2006	1.04	Val2005	−0.24	Val2005	−4.936	Gra2006
115383	064792	G0Vs	HIP	2.31	Val2005	0.21	Val2005	−4.400	Wri2004
115404	064797	K2.5V	Gra2003	...	...	−0.49	Gra2003	−4.640	Gra2003
115617	064924	G7V	Gra2006	0.99	Val2005	0.09	Val2005	−5.040	Wri2004
116442	065352	G9V	Gra2003	0.75	Val2005	−0.30	Val2005	−4.940	Wri2004

Continued on Next Page...

TABLE A.1 – Continued

HD Name	HIP Name	Spec Type	Ref	Mass ($M_\odot$)	Ref	[Fe/H]	Ref	$\log(R'_{HK})$	Ref
116956	065515	G9V	Gra2003	...	...	−0.13	Nor2004	−4.447	Gra2003
117043	065530	G6V	HIP	0.89	Nor2004	0.06	Nor2004	−4.96	MAs2009b
117176	065721	G5V	HIP	1.48	Val2005	−0.01	Val2005	−4.990	Wri2004
118972	066765	K0V	Gra2006	0.77	Val2005	−0.09	Val2005	−4.439	Gra2006
119332	066781	K0IV-V	HIP	...	...	...	...	−4.70	MAs2009b
120136	067275	F7V	HIP	1.33	Val2005	0.25	Val2005	−4.700	Wri2004
120559	067655	G7V	Gra2006	...	...	−0.95	Nor2004	−5.029	Gra2006
120690	067620	G5+V	Gra2006	1.11	Val2005	0.05	Val2005	−4.750	Wri2004
120780	067742	K2V	Gra2006	0.59	Val2005	−0.26	Val2005	−4.888	Gra2006
121370	067927	G0IV	HIP	1.62	Nor2004	0.27	Nor2004	...	...
121560	068030	F6V	HIP	0.96	Val2005	−0.41	Val2005	−4.920	Wri2004
122742	068682	G6V	Gra2003	1.01	Val2005	−0.08	Nor2004	−4.955	Gra2003
124106	069357	K1V	Gra2006	0.79	Val2005	−0.13	Val2005	−4.630	Wri2004
124292	069414	G8+V	Gra2003	1.30	Val2005	−0.10	Val2005	−4.970	Wri2004
124580	069671	G0V	Gra2006	0.92	Nor2004	−0.28	Nor2004	−4.597	Gra2006
124850	069701	F7V	HIP	1.52	Nor2004	−0.04	Nor2004	...	...
125276	069965	F9V	Gra2006	0.97	Nor2004	−0.62	Nor2004	−4.641	Gra2006
125455	070016	K1V	HIP	0.78	Val2005	−0.15	Val2005	−4.930	Wri2004
126053	070319	G1.5V	Gra2003	1.14	Val2005	−0.29	Val2005	−4.940	Wri2004
127334	070873	G5V	Gra2003	1.17	Val2005	0.22	Val2005	−5.060	Wri2004
128165	071181	K3V	HIP	0.91	Val2005	−0.09	Val2005	−4.67	MAs2009b
128311	071395	K3-V	Gra2003	1.32	Val2005	0.01	Val2005	−4.489	Gra2003
128400	071855	G5V	Gra2006	0.86	Nor2004	−0.14	Nor2004	−4.518	Gra2006
128620	071683	G2V	Gra2006	1.11	Pou2002	0.19	Val2005	−5.059	Gra2006
128642	070857	G5	HIP	...	...	−0.39	Nor2004	−4.910	Wri2004
128987	071743	G8V	Gra2006	0.92	Nor2004	0.02	Nor2004	−4.439	Gra2006
130004	072146	K2.5V	Gra2003	...	...	...	...	−4.919	Gra2003

Continued on Next Page...

TABLE A.1 – Continued

HD Name	HIP Name	Spec Type	Ref	Mass ($M_\odot$)	Ref	[Fe/H]	Ref	$\log(R'_{HK})$	Ref
130042	072493	K1V	Gra2006	...	...	−0.21	Nor2004	−4.949	Gra2006
130307	072312	K2.5V	Gra2003	0.81	Val2005	−0.20	Val2005	−4.560	Wri2004
130948	072567	G2V	HIP	1.35	Val2005	−0.19	Nor2004	−4.500	Wri2004
131156	072659	G7V	Gra2003	0.94	Sod1999	−0.07	Val2005	−4.472	Gra2003
131511	072848	K0V	Gra2003	0.97	Val2005	0.11	Val2005	−4.510	Gra2003
131582	072875	K3V	HIP	0.69	Nor2004	−0.54	Nor2004	...	...
131923	073241	G4V	Gra2006	1.56	Val2005	0.09	Val2005	−5.059	Gra2006
132142	073005	K1V	HIP	1.03	Val2005	−0.30	Val2005	−5.000	Wri2004
132254	073100	F8-V	Gra2003	1.23	Nor2004	0.02	Nor2004	−5.030	Gra2003
133640	073695	G2V	HIP	0.85	Nor2004	−0.42	Nor2004	−4.61	MAs2009b
134060	074273	G0V	Gra2006	1.14	Val2005	0.08	Val2005	−5.042	Gra2006
135204	074537	G9V	Gra2003	0.85	Nor2004	−0.06	Nor2004	−5.107	Gra2003
135599	074702	K0V	Gra2003	0.61	Val2005	−0.09	Val2005	−4.520	Wri2004
136202	074975	F8III-IV	HIP	1.34	Nor2004	−0.04	Nor2004	...	...
136352	075181	G2-V	Gra2006	1.51	Val2005	−0.23	Val2005	−5.013	Gra2006
136713	075253	K3IV-V	Gra2003	0.86	Val2005	0.15	Val2005	−4.878	Gra2003
136923	075277	G9V	Gra2003	0.93	Val2005	−0.07	Val2005	−4.770	Wri2004
137107	075312	G2V	HIP	1.19	Pou2000	−0.10	Nor2004	−4.76	MAs2009b
137763	075718	G9V	Gra2003	0.85	Nor2004	0.02	Nor2004	−4.970	Wri2004
139341	076382	K1V	Gra2003	0.85	Sod1999	...	...	−5.102	Gra2003
139777	075809	G1.5V(n)	Gra2003	0.86	Nor2004	−0.31	Nor2004	−4.405	Gra2003
140538	077052	G5V	HIP	0.98	Val2005	0.06	Val2005	−4.830	Wri2004
140901	077358	G7IV-V	Gra2006	1.07	Val2005	0.08	Val2005	−4.802	Gra2006
141004	077257	G0IV-V	Gra2003	1.27	Val2005	0.09	Val2005	−4.970	Wri2004
141272	077408	G9V	Gra2003	0.83	Nor2004	−0.05	Nor2004	−4.390	Wri2004
142267	077801	G0IV	HIP	1.09	Val2005	−0.38	Val2005	−4.850	Wri2004
142373	077760	G0V	Gra2003	1.46	Val2005	−0.39	Val2005	−5.110	Wri2004

Continued on Next Page...

TABLE A.1 – Continued

HD Name	HIP Name	Spec Type	Ref	Mass ($M_\odot$)	Ref	[Fe/H]	Ref	$\log(R'_{HK})$	Ref
143761	078459	G0V	Gra2003	1.04	Gat2001	−0.14	Val2005	−5.080	Wri2004
144284	078527	F8IV-V	HIP	1.2	Maz2002	0.04	Nor2004	...	...
144287	078709	G8+V	Gra2003	0.84	Nor2004	−0.13	Nor2004	−5.020	Wri2004
144579	078775	K0V	Gra2003	1.20	Val2005	−0.49	Val2005	−4.970	Wri2004
144628	079190	K1V	Gra2006	0.66	Val2005	−0.30	Val2005	−5.128	Gra2006
144872	078913	K3V	Gra2003	0.72	Nor2004	−0.30	Nor2004	−4.804	Gra2003
145417	079537	K3V	Gra2006	0.63	Nor2004	−1.37	Nor2004	−5.205	Gra2006
145675	079248	K0IV-V	Gra2003	1.07	Val2005	0.41	Val2005	−5.060	Wri2004
145825	079578	G2V	Gra2006	1.07	Val2005	0.03	Val2005	−4.793	Gra2006
145958	079492	G8V	Gra2003	0.88	Val2005	−0.07	Val2005	−4.940	Wri2004
146233	079672	G2V	Gra2003	0.98	Val2005	0.03	Val2005	−4.950	Wri2004
146361	079607	G1IV-V	Gra2003	1.14	Rag2009	−0.26	Nor2004	−3.827	Gra2003
147513	080337	G1V	Gra2006	1.30	Val2005	0.07	Val2005	−4.656	Gra2006
147584	080686	F9V	Gra2006	1.06	Nor2004	−0.19	Nor2004	−4.585	Gra2006
147776	080366	K3-V	Gra2006	0.82	Val2005	−0.26	Val2005	−4.810	Gra2006
148653	080725	K2V	Gra2003	0.79	Sod1999	...	...	−4.655	Gra2003
148704	080925	K1V	Gra2006	...	...	−0.60	Nor2004	−5.101	Gra2006
149612	081520	G5V	Gra2006	1.02	Val2005	−0.40	Val2005	−4.954	Gra2006
149661	081300	K0V	Gra2006	0.85	Val2005	0.05	Val2005	−4.570	Wri2004
149806	081375	K0V	Gra2003	1.00	Val2005	0.17	Val2005	−4.830	Wri2004
151541	081813	K1V	HIP	0.96	Val2005	−0.18	Val2005	−4.990	Wri2004
152391	082588	G8.5V	Gra2006	0.92	Val2005	−0.05	Val2005	−4.440	Wri2004
153557	083020	K3V	Gra2003	...	...	−0.33	Nor2004	−4.508	Gra2003
154088	083541	K0IV-V	Gra2006	0.93	Val2005	0.28	Val2005	−5.020	Wri2004
154345	083389	G8V	HIP	0.90	Val2005	−0.10	Val2005	−4.910	Wri2004
154417	083601	F9V	Gra2003	0.84	Val2005	0.03	Val2005	−4.590	Wri2004
154577	083990	K2.5V	Gra2006	0.65	Val2005	−0.56	Val2005	−5.080	Gra2006

Continued on Next Page...

TABLE A.1 – Continued

HD Name	HIP Name	Spec Type	Ref	Mass ($M_\odot$)	Ref	[Fe/H]	Ref	$\log(R'_{HK})$	Ref
155712	084195	K2.5V	Gra2003	...	...	...	...	−4.988	Gra2003
155885	084405	K1.5V	Gra2006	...	...	...	...	−4.711	Gra2006
156274	084720	M0V	HIP	0.90	Val2005	−0.27	Val2005	...	...
157214	084862	G0V	HIP	1.54	Val2005	−0.15	Val2005	−5.040	Wri2004
157347	085042	G3V	Gra2003	1.19	Val2005	0.03	Val2005	−5.040	Wri2004
158614	085667	G8IV-V	HIP	0.98	Pou2000	−0.01	Nor2004	−5.12	MAs2009b
158633	085235	K0V	HIP	0.94	Val2005	−0.33	Val2005	−4.930	Wri2004
159062	085653	G9V	Gra2003	...	...	−0.51	Nor2004	−5.030	Wri2004
159222	085810	G1V	Gra2003	0.80	Val2005	0.09	Val2005	−4.900	Wri2004
160269	086036	G0V	HIP	1.08	Sod1999	−0.22	Nor2004	−4.61	MAs2009b
160346	086400	K2.5V	Gra2003	0.78	Nor2004	−0.09	Nor2004	−4.956	Gra2003
160691	086796	G3IV-V	Gra2006	1.25	Val2005	0.26	Val2005	−5.101	Gra2006
161198	086722	G9V	Gra2003	0.78	Nor2004	−0.39	Nor2004	−4.970	Wri2004
161797	086974	G5IV	HIP	1.34	Val2005	0.24	Val2005	−5.110	Wri2004
162004	086620	G0V	HIP	1.05	Nor2004	−0.18	Nor2004	−4.86	MAs2009b
164922	088348	G9V	Gra2003	1.05	Val2005	0.17	Val2005	−5.050	Wri2004
165185	088694	G0V	Gra2006	0.93	Nor2004	−0.25	Nor2004	−4.545	Gra2006
165341	088601	K0-V	Gra2003	0.90	Pou2000	−0.29	Nor2004	−4.698	Gra2003
165401	088622	G0V	Gra2003	0.83	Nor2004	−0.50	Nor2004	−4.668	Gra2003
165499	089042	G0V	Gra2006	1.00	Nor2004	−0.17	Nor2004	−4.935	Gra2006
165908	088745	F7V	HIP	0.91	Nor2004	−0.55	Nor2004	−5.020	Wri2004
166620	088972	K2V	Gra2003	0.66	Val2005	−0.05	Val2005	−4.970	Wri2004
167425	089805	F9.5V	Gra2006	1.11	Nor2004	0.02	Nor2004	−4.606	Gra2006
168009	089474	G1V	Gra2003	0.98	Val2005	−0.02	Val2005	−5.080	Wri2004
170657	090790	K2V	Gra2006	0.79	Val2005	−0.15	Val2005	−4.650	Wri2004
172051	091438	G6V	Gra2006	0.91	Val2005	−0.24	Val2005	−4.900	Wri2004
175073	092858	K1V	Gra2006	0.80	Nor2004	−0.14	Nor2004	−4.889	Gra2006

Continued on Next Page...

TABLE A.1 – Continued

HD Name	HIP Name	Spec Type	Ref	Mass ($M_\odot$)	Ref	[Fe/H]	Ref	$\log(R'_{HK})$	Ref
175742	092919	K0V	HIP	...	...	...	...	...	...
176051	093017	G0V	HIP	1.07	Sod1999	−0.19	Nor2004	...	...
176377	093185	G1V	Gra2003	0.81	Val2005	−0.23	Val2005	−4.870	Wri2004
177474	093825	F8V	Gra2006	1.29	Nor2004	−0.22	Nor2004	−4.890	Gra2006
177565	093858	G6V	Gra2006	1.08	Val2005	0.07	Val2005	−4.973	Gra2006
178428	093966	G4V	Gra2006	0.97	Nor2004	0.05	Nor2004	−5.110	Gra2006
179957	094336	G3V	Gra2003	0.73	Val2005	...	...	−5.050	Wri2004
180161	094346	G8V	HIP	...	...	...	...	−4.520	Wri2004
181321	095149	G1V	Gra2006	0.89	Nor2004	−0.26	Nor2004	−4.372	Gra2006
182488	095319	G9+V	Gra2003	1.28	Val2005	0.12	Val2005	−4.940	Wri2004
182572	095447	G8IVvar	HIP	1.38	Val2005	0.36	Val2005	−5.100	Wri2004
183870	096085	K2.5V	Gra2006	0.96	Val2005	−0.05	Val2005	−4.512	Gra2006
184385	096183	G8V	Gra2003	0.88	Val2005	0.11	Val2005	−4.560	Wri2004
184467	095995	K2V	Gra2003	0.8	Pou2000	−0.22	Nor2004	−5.047	Gra2003
185144	096100	G9V	Gra2003	0.75	Val2005	−0.16	Val2005	−4.850	Wri2004
185414	096395	G0	HIP	0.95	Nor2004	−0.16	Nor2004	−4.88	MAs2009b
186408	096895	G1.5V	Gra2003	1.25	Val2005	0.08	Val2005	−5.100	Wri2004
186858	097222	K3+V	Gra2003	0.69	Sod1999	...	...	−4.726	Gra2003
187691	097675	F8V	HIP	1.37	Val2005	0.12	Val2005	−5.050	Wri2004
189340	098416	F9V	Gra2003	1.12	Sod1999	−0.05	Nor2004	−4.951	Gra2003
189567	098959	G2V	Gra2006	1.08	Val2005	−0.18	Val2005	−4.857	Gra2006
189733	098505	K2V	Gra2003	0.78	Nor2004	−0.12	Nor2004	−4.553	Gra2003
190067	098677	K0V	Gra2003	0.95	Val2005	−0.30	Val2005	−4.880	Wri2004
190248	099240	G8IV	Gra2006	1.04	Val2005	0.26	Val2005	−5.092	Gra2006
190360	098767	G7IV-V	Gra2006	1.16	Val2005	0.19	Val2005	−5.090	Wri2004
190404	098792	K1V	Gra2003	0.89	Val2005	−0.44	Val2005	−4.980	Wri2004
190406	098819	G0V	Gra2006	1.13	Val2005	0.02	Val2005	−4.770	Wri2004

Continued on Next Page...

TABLE A.1 – Continued

HD Name	HIP Name	Spec Type	Ref	Mass ($M_\odot$)	Ref	[Fe/H]	Ref	$\log(R'_{HK})$	Ref
190422	099137	F9V	Gra2006	1.04	Nor2004	−0.21	Nor2004	−4.458	Gra2006
190470	098828	K2.5V	Gra2003	...	...	−0.16	Gra2003	−4.828	Gra2003
190771	098921	G2V	Gra2003	0.96	Val2005	0.14	Val2005	−4.430	Wri2004
191408	099461	K2.5V	Gra2006	0.76	Val2005	−0.33	Val2005	−5.079	Gra2006
191499	099316	G9V	Gra2003	...	...	...	...	−5.076	Gra2003
191785	099452	K0V	Gra2003	1.08	Val2005	−0.09	Val2005	−5.030	Wri2004
192263	099711	K2.5V	Gra2003	0.83	Val2005	−0.07	Val2005	−4.676	Gra2003
192310	099825	K2+V	Gra2006	0.84	Val2005	0.14	Nor2004	−5.048	Gra2006
193664	100017	G0V	Gra2003	1.13	Val2005	−0.11	Val2005	−4.927	Gra2003
194640	100925	G8V	Gra2006	1.01	Val2005	−0.06	Val2005	−4.924	Gra2006
195564	101345	G2V	Gra2003	1.34	Val2005	0.01	Val2005	−5.130	Wri2004
195987	101382	G9V	Gra2003	0.84	Tor2002	−0.38	Nor2004	−4.970	Wri2004
196378	101983	G0V	Gra2006	1.41	Val2005	−0.32	Val2005	−4.837	Gra2006
196761	101997	G8V	Gra2006	0.90	Val2005	−0.25	Val2005	−4.920	Wri2004
197076	102040	G1V	Gra2003	1.03	Val2005	−0.09	Val2005	−4.920	Wri2004
197214	102264	G6V	Gra2006	0.81	Nor2004	−0.50	Nor2004	−4.920	Wri2004
198425	102766	K2.5V	Gra2003	...	...	...	...	−4.726	Gra2003
199260	103389	F6V	Gra2006	1.12	Nor2004	−0.17	Nor2004	−4.402	Gra2006
199288	103458	G2V	Gra2006	1.51	Val2005	−0.47	Val2005	−4.847	Gra2006
199509	104436	G1V	Gra2006	1.05	Val2005	−0.27	Val2005	−4.925	Gra2006
200525	104440	F9.5V	Gra2006	1.01	Nor2004	−0.13	Nor2004	−4.667	Gra2006
200560	103859	K2.5V	Gra2003	...	...	0.01	Nor2004	−4.512	Gra2003
200968	104239	G9.5V	Gra2006	0.86	Val2005	0.02	Val2005	−4.650	Gra2006
202275	104858	F7V	Gra2003	1.19	Pou2000	−0.07	Nor2004	−4.905	Gra2003
202628	105184	G1.5V	Gra2006	1.04	Val2005	−0.01	Val2005	−4.782	Gra2006
202751	105152	K3V	Gra2003	0.88	Val2005	−0.09	Val2005	−5.111	Gra2003
202940	105312	G7V	Gra2006	...	...	−0.34	Nor2004	−4.988	Gra2006

Continued on Next Page...

TABLE A.1 – Continued

HD Name	HIP Name	Spec Type	Ref	Mass ($M_\odot$)	Ref	[Fe/H]	Ref	$\log(R'_{HK})$	Ref
203244	105712	G8V	Gra2006	0.82	Nor2004	−0.32	Nor2004	−4.555	Gra2006
203850	105905	K2.5V	Gra2006	0.68	Nor2004	−0.67	Nor2004	−5.033	Gra2006
203985	105911	K2III-IV	Gra2006	...	...	...	...	...	...
205390	106696	K1.5V	Gra2006	0.78	Val2005	−0.18	Val2005	−4.702	Gra2006
205536	107022	G9V	Gra2006	0.98	Val2005	−0.03	Val2005	−5.084	Gra2006
206826	107310	F6V	Gra2003	1.39	Nor2004	−0.20	Nor2004	−4.783	Gra2003
206860	107350	G0V	Gra2006	1.08	Val2005	−0.01	Val2005	−4.400	Gra2006
207129	107649	G0V	Gra2006	1.06	Val2005	−0.04	Val2005	−5.020	Gra2006
207144	107625	K3V	Gra2006	...	...	...	...	−4.990	Gra2006
208038	108028	K2.5V	Gra2003	...	...	...	...	−4.569	Gra2003
208313	108156	K2V	Gra2003	0.74	Val2005	−0.08	Val2005	−4.987	Gra2003
210277	109378	G8V	Gra2003	1.27	Val2005	0.20	Val2005	−5.060	Wri2004
210667	109527	G9V	Gra2003	0.95	Val2005	0.16	Val2005	−4.500	Wri2004
210918	109821	G2V	Gra2006	1.20	Val2005	−0.07	Val2005	−5.121	Gra2006
211415	110109	G0V	Gra2006	0.85	Nor2004	−0.36	Nor2004	−4.918	Gra2006
211472	109926	K0V	Gra2003	0.87	Nor2004	0.03	Nor2004	−4.538	Gra2003
212168	110712	G0V	Gra2006	1.13	Val2005	−0.04	Val2005	−4.981	Gra2006
212330	110649	G2IV-V	Gra2006	1.40	Val2005	0.01	Val2005	−5.157	Gra2006
214683	111888	K3V	Gra2003	...	...	...	...	−4.554	Gra2003
214953	112117	F9.5V	Gra2006	0.81	Val2005	0.03	Val2005	−4.988	Gra2006
215152	112190	K3V	Gra2003	...	...	−0.17	Gra2003	−4.925	Gra2003
215648	112447	F7V	HIP	1.24	Val2005	−0.16	Val2005	−5.070	Wri2004
216259	112870	K2.5V	Gra2003	0.94	Val2005	−0.47	Val2005	−4.950	Wri2004
216520	112527	K0V	Gra2003	...	...	...	...	−4.980	Wri2004
217014	113357	G2V+	Gra2006	1.33	Val2005	0.15	Val2005	−5.080	Wri2004
217107	113421	G8IV-V	Gra2003	1.49	Val2005	0.27	Val2005	−5.080	Wri2004
217813	113829	G1V	Gra2003	1.15	Val2005	0.02	Val2005	−4.470	Wri2004

Continued on Next Page...

TABLE A.1 – Continued

HD Name	HIP Name	Spec Type	Ref	Mass ($M_\odot$)	Ref	[Fe/H]	Ref	$\log(R'_{HK})$	Ref
218868	114456	G8V	Gra2003	0.93	Val2005	0.19	Val2005	−4.750	Wri2004
219134	114622	K3V	Gra2003	0.74	Val2005	0.09	Val2005	−5.089	Gra2003
219482	114948	F6V	Gra2006	1.07	Nor2004	−0.20	Nor2004	−4.434	Gra2006
219538	114886	K2V	Gra2003	0.66	Val2005	−0.05	Val2005	−4.840	Wri2004
219623	114924	F7V	HIP	1.07	Nor2004	−0.09	Nor2004	−4.84	MAs2009b
220140	115147	K2V	Gra2003	...	...	−0.64	Nor2004	−4.074	Gra2003
220182	115331	G9V	Gra2003	0.85	Nor2004	0.01	Nor2004	−4.370	Wri2004
220339	115445	K2.5V	Gra2003	0.65	Val2005	−0.24	Val2005	−4.896	Gra2003
221354	116085	K0V	Gra2003	0.75	Val2005	−0.01	Val2005	−5.149	Gra2003
221851	116416	K1V	Gra2003	0.80	Nor2004	−0.13	Nor2004	−4.735	Gra2003
222143	116613	G3V	Gra2003	0.98	Val2005	0.12	Val2005	−4.555	Gra2003
222237	116745	K3+V	Gra2006	0.88	Val2005	−0.20	Val2005	−4.959	Gra2006
222335	116763	G9.5V	Gra2006	0.81	Val2005	−0.16	Val2005	−4.909	Gra2006
222368	116771	F7V	HIP	1.42	Val2005	−0.08	Val2005	−4.76	MAs2009b
223778	117712	K3V	Gra2003	0.79	This work	−0.71	Nor2004	−4.518	Gra2003
224228	118008	K2.5V	Gra2006	...	...	...	...	−4.468	Gra2006
224465	118162	G4V	Gra2003	0.95	Nor2004	−0.01	Nor2004	−4.969	Gra2003
224930	000171	G5V	Gra2003	0.91	Sod1999	−0.78	Nor2004	−4.880	Gra2003
232781	015673	K3.5V	Gra2003	...	...	...	...	−4.691	Gra2003
263175	032423	K3V	Gra2003	...	...	−0.59	Gra2003	−4.903	Gra2003
...	036357	K2.5V	Gra2003	...	...	−0.61	Gra2003	−4.526	Gra2003
...	040774	G5	HIP	...	...	...	...	−4.38	MAs2009b
...	087579	K2.5V	Gra2003	...	...	...	...	−4.529	Gra2003
...	091605	K2.5V	Gra2003	...	...	−0.68	Gra2003	−4.909	Gra2003

NOTES.—Reference codes for columns 4 and 6 are as follows: Bod1999 = Boden et al. (1999); Clo2005 = Close et al. (2005); Gra2003 = Gray et al. (2003); Gra2006 = Gray et al. (2006); HIP = *Hipparcos*; Low2002 = Lowrance et al. (2002); MAs2009b = Mason et al. (2009b); Nor2004 = Nordström et al. (2004); Pou2000 = Pourbaix (2000); Pou2002 = Pourbaix et al. (2002); Rag2009 = Raghavan et al. (2009); Sod1999 = Söderhjelm (1999); Tor2002 - Torres et al. (2002); Val2005 = Valenti & Fischer (2005); Wri2004 = Wright et al. (2004).

TABLE A.2: Spectral type and mass of the companions

Comp Name	Alt Name	Spec Type	Ref	Mass ($M_\odot$)	Ref
HD 000123 Ba	...	...	...	0.95	Gri1999
HD 000123 Bb	...	...	...	0.22	Gri1999
HD 001237 B	HD 1237B	M4±1V	Cha2007	0.13	Cha2006
HD 001273 Ab	...	...	...	...	...
HD 003196 Ab	...	...	...	0.40[a]	DM91
HD 003196 B	...	G2V	ΔV	1.00	DM91
HD 003443 B	GJ 25 B	...	...	0.70	Pou2000
HD 003651 B	HD 3651B	T7.5 ± 0.5	Luh2007	0.05	Luh2007
HD 004391 B	...	M4V	$VJHK$	...	...
HD 004391 C	...	M5V	$VJHK$	...	...
HD 004614 B	LHS 122	K7V	$VJHK$	...	...
HD 004628 Ab	...	...	...	...	...
HD 004676 Ab	...	...	...	1.17	Bod1999
HD 004747 Ab	...	...	...	...	...
HD 006582 Ab	mu Cas B	M3V	ΔV	...	...
HD 007693 A	HD 7788	F5V	Gra2006	1.32	Nor2004
HD 007693 B	GJ 55.3B	K1V	Gra2006	...	...
HD 007693 D	GJ 55.1B	...	...	0.86	Sod1999
HD 008997 Ab	...	G7V	SB2q	...	...
HD 009770 Ba	...	...	...	0.73	Cut1997
HD 009770 Bb	...	...	...	0.67	Cut1997
HD 009770 C	...	M3V	ΔV	...	...
HD 009826 D	ups And B	M4.5V	Low2002	0.2	Low2002
HD 010307 Ab	...	...	...	0.2	Sod1999
HD 010360 A	HD 10361	K2V	Gra2006	...	...
HD 013445 B	GJ 86 B	WD	Mug2005a	0.5	Lag2006
HD 013974 Ab	...	K3V	SB2q	...	...
HD 014214 Ab	...	...	...	...	...
HD 014802 B	...	M2V	ΔV	...	...
HD 016160 Ab	...	...	...	...	...
HD 016160 B	NLTT 8455	M3.5V	Hen2002	...	...
HD 016287 Ab	...	...	...	...	...
HD 016739 Ab	...	...	...	1.24	Bag2006
HD 016765 B	...	K2V	ΔV	...	...
HD 016895 B	NLTT 8787	M2V	$BRJHK$	...	...

Continued on Next Page...

TABLE A.2 – Continued

Comp Name	Alt Name	Spec Type	Ref	Mass ($M_\odot$)	Ref
HD 017382 Ab	...	...	...	...	...
HD 017382 B	NLTT 8996	M7V	$VRJHK$	...	...
HD 018143 B	HD 18143 B	K9V	ΔV	...	...
HD 018143 C	NLTT 9303	M7V	$VRJHK$	...	...
HD 018757 C	NLTT 9726	M2V	$VIJHK$	...	...
HD 019994 B	...	M2V	ΔV	...	...
HD 020010 Bb	...	...	...	...	...
HD 020010 B	GJ 127 B	K2V	ΔV	...	...
HD 020807 B	HD 020766	G2V	Gra2006	1.12	Val2005
HD 021175 B	...	M3V	ΔV	...	...
HD 023484 Ab	...	...	...	...	...
HD 024409 D	...	...	...	...	...
HD 024409 E	...	M2V	$VJHK$	...	...
HD 024496 B	...	M2V	ΔV	...	...
HD 025680 Ab	...	...	...	...	...
HD 025998 A	HD 25893	G9V	Gra2003	...	...
HD 025998 B	...	K2V	ΔV	...	...
HD 025998 Eb	...	...	...	...	...
HD 026491 Ab	...	...	...	...	...
HD 026923 B	HD 26913	G6V	Gra2003	0.87	Nor2004
HD 026965 B	LHS 25	M4.5	Rei2004	...	...
HD 026965 C	HD 26976	DA3	Hol2002	...	...
HD 032778 B	NLTT 14447	M0V	$VRIJHK$	...	...
HD 032850 Ab	...	...	...	...	...
HD 032923 B	...	G1V	ΔV	...	...
HD 035112 B	...	M1V	ΔV	...	...
HD 035296 C	HD 35171	K7V	$VJHK$	...	...
HD 036705 Ab	...	M8V	Boc2008	0.09	Clo2007
HD 036705 Ba	...	M5V	Jan2007	0.16	Jan2007
HD 036705 Bb	...	M4V $\pm$ 1	Jan2007	0.14	Jan2007
HD 037394 B	HD 233153	M1V	$VJHK$	...	...
HD 037572 B	HIP 26369	K5V	Gra2006	...	...
HD 039587 Ab	...	...	...	0.15	Kon2002
HD 039855 B	BD-19 1297B	K9V	$VIJHK$	...	...
HD 040397 B	...	M4V	ΔV	...	...
HD 040397 D	NLTT 15867	M5V	$RJHK$	...	...
HD 043162 B	...	M4V	$VRIJHK$	...	...

Continued on Next Page...

TABLE A.2 – Continued

Comp Name	Alt Name	Spec Type	Ref	Mass ($M_\odot$)	Ref
HD 043587 Ab	...	...	...	0.54	Cat2006
HD 043587 E	NLTT 16333	M4V	$VRIJHK$	...	...
HD 043834 Ab	...	M5V ± 1.5	Egg2007	0.14	Egg2007
HD 045088 Ab	...	...	...	0.71	This work
HD 045088 B	...	M4V	ΔV	...	...
HD 045270 B	...	M0V	ΔV	...	...
HD 048189 B	...	K7V	ΔV	...	...
HD 052698 Ab	...	...	...	...	...
HD 053705 B	HD 053706	K0.5V	Gra2006	0.78	Val2005
HD 053705 Ca	HD 053680	K6V	Gra2006	...	...
HD 053705 Cb	...	...	...	...	...
HD 054371 Ab	...	...	...	...	...
HD 057095 B	...	K6V	ΔV	...	...
HD 061606 B	NLTT 18260	K9V	$VRIJHK$	...	...
HD 063077 Ab	...	...	...	...	...
HD 063077 B	NLTT 18414	DC	Kun1984	0.56	Hol2008
HD 064096 B	...	...	...	0.9	Pou2000
HD 064468 Ab	...	...	...	...	...
HD 064606 Ab	...	...	...	...	...
HD 065430 Ab	...	...	...	...	...
HD 065907 B	LHS 1960	M0V	$IJHK$	...	...
HD 065907 C	...	M5V	ΔV	...	...
HD 067199 Ab	...	...	...	...	...
HD 068017 Ab	...	...	...	...	...
HD 068257 B	HD 068255	F8V	Gra2003	1.52	Nor2004
HD 068257 Ca	HD 068256	G0 IV-V	Gra2003	...	...
HD 068257 Cb1	...	M2V	...	...	...
HD 068257 Cb2	...	M2V	...	...	...
HD 068257 Cb3	...	M2V–M4V	...	...	...
HD 072760 Ab	...	...	...	0.13	Met2008
HD 073752 B	...	K2V	ΔV	1.07	Sod1999
HD 074385 B	NLTT 20102	M2V	$VRIJHK$	...	...
HD 075732 B	LHS 2063	M6V	$VRIJHK$	...	...
HD 075767 Ab	...	...	...	...	...
HD 075767 Ba	...	M3V	Fuh2005	...	...
HD 075767 Bb	...	M4V	Fuh2005	...	...
HD 079028 Ab	...	...	...	...	...

Continued on Next Page...

TABLE A.2 – Continued

Comp Name	Alt Name	Spec Type	Ref	Mass ($M_\odot$)	Ref
HD 079096 Ab	...	...	...	0.85	Pou2000
HD 079096 Ea	Gl 337C	L8	Wil2001	...	...
HD 079096 Eb	...	L8	Bur2005	...	...
HD 079969 B	...	K4V	ΔV	0.74	Sod1999
HD 080715 Ab	...	K3V	SB2q	...	...
HD 082342 B	...	M3.5V	Haw1996	...	...
HD 082443 B	NLTT 22015	M5.5V	Haw1996	...	...
HD 082885 B	...	M8V	ΔV	...	...
HD 086728 Ba	GJ 376 B	M6.5V	Giz2000	...	...
HD 086728 Bb	...	M6.5V	Giz2000	...	...
HD 089125 B	GJ 387 B	M1V	$VJHK$	...	...
HD 090508 B	LHS 2266	M2V	ΔV	...	...
HD 090839 Ba	HD 237903	K5	$RJHK$	...	...
HD 090839 Bb	...	...	...	...	...
HD 096064 B	NLTT 26194	K7	ΔV	...	...
HD 096064 C	BD-033040C	K7	ΔV	...	...
HD 097334 Ea	Gl 417B	L4.5V	Kir2001	0.1	Bou2003
HD 097334 Eb	...	L4.5V	Bou2003	0.1	Bou2003
HD 098230 Ab	...	M3V	Bal2005	...	...
HD 098230 A	HD 98231	F9V	ten2000	...	...
HD 098230 Bb	...	K7V	ΔV	...	...
HD 099491 B	HD 099492	K2V	*Hipparcos*	1.24	Val2005
HD 100180 Ab	...	...	...	...	...
HD 100180 B	NLTT 27656	K5V	$RIJHK$	...	...
HD 100623 B	LHS 309	DC	Hen2002	...	...
HD 101177 Ba	LHS 2436	K3V	$VRJHK$	...	...
HD 101177 Bb	...	M2V	SB2q	...	...
HD 101206 Ab	...	...	...	...	...
HD 102365 B	LHS 313	M4V	Haw1996	...	...
HD 102438 Ab	...	...	...	...	...
HD 110463 Ab	...	...	...	...	...
HD 110833 Ab	...	...	...	...	...
HD 111312 Ab	...	M2V	ΔV	0.58	sb2q
HD 111312 B	...	K8V	SB2q	...	...
HD 112758 Ab	...	...	...	...	...
HD 112758 B	...	M2V	ΔV	...	...
HD 112914 Ab	...	...	...	...	...

Continued on Next Page...

TABLE A.2 – Continued

Comp Name	Alt Name	Spec Type	Ref	Mass ($M_\odot$)	Ref
HD 113283 Ab	...	...	...	...	...
HD 113449 Ab	...	...	...	...	...
HD 115404 B	LHS 2714	M0.5V	Haw1996	...	...
HD 116442 B	HD 116443	K2V	Gra2003	0.78	Val2005
HD 120136 B	HD 120136B	M2V	ΔV	...	...
HD 120690 Ab	...	...	...	...	...
HD 120780 Ab	...	...	...	...	...
HD 120780 B	...	M4V	ΔV	...	...
HD 121370 Ab	...	...	...	...	...
HD 122742 Ab	...	...	...	...	...
HD 124850 Ab	...	...	...	...	...
HD 125276 Ab	...	...	...	...	...
HD 125455 B	LHS 2895	M6	$VJHK$	...	...
HD 128620 B	HD 128621	K2IV	Gra2006	0.93	Pou2002
HD 128620 C	HIP 070890	...	...	0.11	Wer2006
HD 128642 Ab	...	...	...	...	...
HD 130042 B	...	K8V	ΔV	...	...
HD 130948 B	HD 130948 B	L2 $\pm$ 2	Pot2002	0.07	Pot2002
HD 130948 C	HD 130948 C	L2 $\pm$ 2	Pot2002	0.07	Pot2002
HD 131156 B	HD 131156B	...	...	0.67	Sod1999
HD 131511 Ab	...	...	...	...	...
HD 131582 Ab	...	...	...	...	...
HD 131923 Ab	...	...	...	...	...
HD 133640 Ba	NLTT 39210	K2V	Lu2001	...	...
HD 133640 Bb	...	M2V	SB2q	...	...
HD 135204 B	...	G9V	ΔV	...	...
HD 136202 B	LHS 3060	K9V	$VJHK$	...	...
HD 137107 B	HD 137108	...	...	1.05	Pou2000
HD 137107 E	GJ 584 C	L8V	Kir2001	0.06	Kir2001
HD 137763 Ab	K9	SB2q	...	0.57	SB2
HD 137763 B	HD 137778	K2V	Gra2003	0.87	Val2005
HD 137763 C	GJ 586C	M4.5V	Rei1995	...	...
HD 139341 B	...	K1V	ΔV	0.83	Sod1999
HD 139341 C	HD 139323	K2IV-V	Gra2003	1.13	Val2005
HD 139777 B	HD 139813	K2V	$RJHK$	1.15	Val2005
HD 140538 B	...	M5V	ΔV	...	...
HD 140901 B	NLTT 41169	M2	ΔV	...	...

Continued on Next Page...

TABLE A.2 – Continued

Comp Name	Alt Name	Spec Type	Ref	Mass ($M_\odot$)	Ref
HD 141272 B	...	M3V ± 0.5	Eis2007	0.26	Eis2007
HD 142267 Ab	...	...	...	...	...
HD 143761 Ab	...	...	...	0.14	Gat2001
HD 144284 Ab	...	...	...	0.46	Maz2002
HD 144287 Ab	...	K4V	ΔV	...	...
HD 144579 B	LHS 3150	M4V	$VRIJHK$	...	...
HD 145825 Ab	...	...	...	...	...
HD 145958 B	NLTT 42272	G9V	Gra2003	...	...
HD 145958 D	...	T6	Loo2007	...	...
HD 146361 Ab	...	...	...	1.09	Rag2009
HD 146361 B	HD 146362	...	...	1.0	Rag2009
HD 146361 Ea	HIP 079551	M2.5V	Rei1995	...	...
HD 146361 Eb	sig CrB D	...	...	0.1	Hei1990
HD 147513 B	...	DA2	Hol2002	...	...
HD 147584 Ab	...	...	...	...	...
HD 147776 C	...	...	...	...	...
HD 147776 D	...	...	...	...	...
HD 148653 B	LHS 3204	...	...	0.77	Sod1999
HD 148704 Ab	...	K1V	SB2q	...	...
HD 149806 B	...	M6V	$RJHK$	...	...
HD 153557 B	...	M2V	ΔV	...	...
HD 153557 C	HD 153525	...	...	0.73	Nor2004
HD 155885 B	...	K1.5V	ΔV	...	...
HD 155885 C	HD 156026	K5V	Gra2006	...	...
HD 156274 Ab	...	...	...	...	...
HD 156274 B	NLTT 44525	K7V	Haw1996	...	...
HD 157347 B	HR 6465	M3V	This work	...	...
HD 158614 B	...	...	...	0.90	Pou2000
HD 160269 B	...	...	...	0.65	Sod1999
HD 160269 C	HIP 86087	M0.5V	Rei2004	...	...
HD 160346 Ab	...	...	...	...	...
HD 161198 Ab	...	...	...	...	...
HD 161797 Ab	...	M8V	ΔV	...	...
HD 161797 B	NLTT 45430	M3V	ΔV	...	...
HD 161797 C	...	M3V	ΔV	...	...
HD 162004 A	HD 162003	F5V	$RJHK$	1.38	Nor2004
HD 165341 B	NLTT 45900	...	...	0.78	Pou2000

Continued on Next Page...

TABLE A.2 – Continued

Comp Name	Alt Name	Spec Type	Ref	Mass ($M_\odot$)	Ref
HD 165401 Ab	...	...	...	...	...
HD 165499 Ab	...	...	...	...	...
HD 165908 Ab	...	...	...	...	...
HD 165908 B	...	K6V	ΔV	...	...
HD 167425 B	...	M0V	$VJHK$	...	...
HD 175742 Ab	...	...	...	...	...
HD 176051 B	...	K3V	ΔV	0.71	Sod1999
HD 177474 B	...	F8V	ΔV	...	...
HD 178428 Ab	...	...	...	...	...
HD 179957 B	HD 179958	G4V	ΔV	...	...
HD 181321 Ab	...	...	...	...	...
HD 184467 B	...	...	...	0.8	Pou2000
HD 185414 Ab	...	...	...	...	...
HD 186408 Ab	...	M0V	ΔV	...	...
HD 186408 B	HD 186427	G3V	Gra2006	1.10	Val2005
HD 186858 A	HD 187013	F5.5IV-V	Gra2003	1.24	Nor2004
HD 186858 B	...	K3V	ΔV	0.68	Sod1999
HD 186858 G	HD 225732	K4V	ΔV	...	...
HD 187691 C	...	M3V	$VRIJHK$	...	...
HD 189340 B	...	...	...	0.94	Sod1999
HD 190067 B	...	K7V	ΔV	...	...
HD 190360 B	LHS 3509	M4.5V	Rei2004	...	...
HD 190406 Ab	HD 354613	L4.5 $\pm$ 1.5	Liu2002	0.06	Liu2002
HD 190771 Ab	...	...	...	...	...
HD 191408 B	LHS 487	M5V	ΔV	...	...
HD 191499 B	ADS 13434B	K5V	ΔV	...	...
HD 191785 E	...	M3.5V	This work	...	...
HD 193664 Ab	...	...	...	...	...
HD 195564 B	LTT 8128	M2V	ΔV	...	...
HD 195987 Ab	...	...	...	0.67	Tor2002
HD 197076 C	NLTT 49681	M2.5V	Rei2004	...	...
HD 198425 Ab	...	...	...	...	...
HD 198425 B	NLTT 49961	M6V	$VJHK$	...	...
HD 200525 B	...	G0V	ΔV	...	...
HD 200525 C	NLTT 50542	M3V	ΔV	...	...
HD 200560 D	GJ 816.1B	M3V	ΔV	...	...
HD 200968 B	GJ 819B	K7V	Haw1996	...	...

Continued on Next Page...

TABLE A.2 – Continued

Comp Name	Alt Name	Spec Type	Ref	Mass ($M_\odot$)	Ref
HD 202275 B	...	...	...	1.12	Pou2000
HD 202940 Ab	...	...	...	...	...
HD 202940 B	LHS 3656	K9V	ΔV	...	...
HD 203985 Ab	...	...	...	...	...
HD 203985 B	LTT 8515	M3.5V	This work	...	...
HD 206826 B	HD 206827	G5V	ΔV	...	...
HD 206860 B	HN Peg B	T2.5 ± 0.5	Luh2007	0.02	Luh2007
HD 211415 B	...	K9V	ΔV	...	...
HD 211472 T	GJ 4269	M4V	$VJHK$	...	...
HD 212168 B	HIP 110719	G0V	Gra2006	1.13	Val2005
HD 212330 Ab	...	...	...	...	...
HD 214953 B	NLTT 54607	M0.5V	Haw1996	...	...
HD 215648 B	...	M4V	ΔV	...	...
HD 217107 B	...	...	...	...	...
HD 218868 B	...	M5V	$VJHK$	...	...
HD 220140 B	NLTT 56532	M3V	$VRIJHK$	...	...
HD 220140 C	...	M7V	$VRIJHK$	0.1	Mak2007
HD 223778 Ab	...	...	...	0.75	This work
HD 223778 B	...	M6V	ΔV	...	...
HD 224465 Ab	...	...	...	...	...
HD 224930 B	...	K5±1 V	ten2000	0.58	Sod1999
HD 263175 B	HD 263175B	M0.5V	Rei2004	...	...
HIP 036357 A	HD 58946	F1V	Gra2003	1.40	Nor2004
HIP 036357 B	GJ 274B	M7V	ΔV	...	...
HIP 091605 B	LHS 3402	M2V	$VJHK$	...	...

NOTES.—Reference codes for columns 4 and 6 are as follows: Bag2006 = Bagnuolo et al. (2006); Bal2005 = Ball et al. (2005); Boc2008 = Boccaletti et al. (2008); Bod1999 = Boden et al. (1999); Bou2003 = Bouy et al. (2003); Bur2005 = Burgasser et al. (2005); Cat2006 = Catala et al. (2006); Cha2006 = Chauvin et al. (2006); Cha2007 = Chauvin et al. (2007); Cut1997 = Cutispoto et al. (1997); Egg2007 = Eggenberger et al. (2007); Eis2007 = Eisenbeiss et al. (2007); Fuh2005 = Fuhrmann et al. (2005); Gat2001 = Gatewood et al.

(2001); Giz2000 = Gizis et al. (2000); Gra2003 = Gray et al. (2003); Gra2006 = Gray et al. (2006); Gri1999 = Griffin (1999); Haw1996 = Hawley et al. (1996); Hei1990 = Heintz (1990); Hen2002 = Henry et al. (2002); Hol2002 = Holberg et al. (2002); Hol2008 = Holberg et al. (2008); Jan2007 = Janson et al. (2007); Kir2001 = Kirkpatrick et al. (2001); Kon2002 = König et al. (2002); Kun1984 = Kunkel et al. (1984); Lag2006 = Lagrange et al. (2006); Liu2002 = Liu et al. (2002); Loo2007 = Looper et al. (2007); Low2002 = Lowrance et al. (2002); Lu2001 = Lu et al. (2001); Luh2007 = Luhman et al. (2007); Mak2007 = Makarov et al. (2007); Maz2002 = Mazeh et al. (2002); Met2008 = Metchev & Hillenbrand (2008); Mug2005a = Mugrauer & Neuhäuser (2005); Nor2004 = Nordström et al. (2004); Pot2002 = Potter et al. (2002); Pou2000 = Pourbaix (2000); Rag2009 = Raghavan et al. (2009); Rei1995 = Reid et al. (1995); Rei2004 = Reid et al. (2004); Sod1999 = Söderhjelm (1999); ten2000 = ten Brummelaar et al. (2000); Tor2002 = Torres et al. (2002); Val2005 = Valenti & Fischer (2005); Wer2006 = Wertheimer & Laughlin (2006); Wil2001 = Wilson et al. (2001); ΔV = estimated using primary's spectral type and measured ΔV; SB2q = estimated using primary's mass or spectral type and mass-ratio from SB2 solution; $VRIJHK$ etc. colors = estimated from colors.

[a] Estimated using mass-sum of Aa+Ab from DM91 and mass of Aa from Nor2004

– B –

SFP Investigation Plots for Individual Systems

This appendix includes the plots used to inspect individual observations for separted fringe packets as described in § 3.1.1. The figures are listed in order of HD number, baseline, UT observing date, and sequence number. The sequence number identifies multiple observations for the same star on a given night. The captions of the figures specify the above parameters, and their format of is the same as that of Figures 3.5 and 3.6.

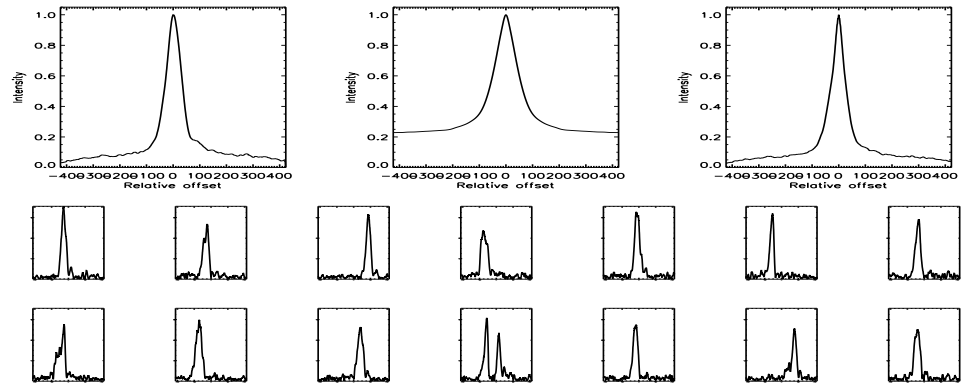

Figure B.1: SFP inspection for HD 000166 with S1-E1 on UT 2007/07/29, seq 001

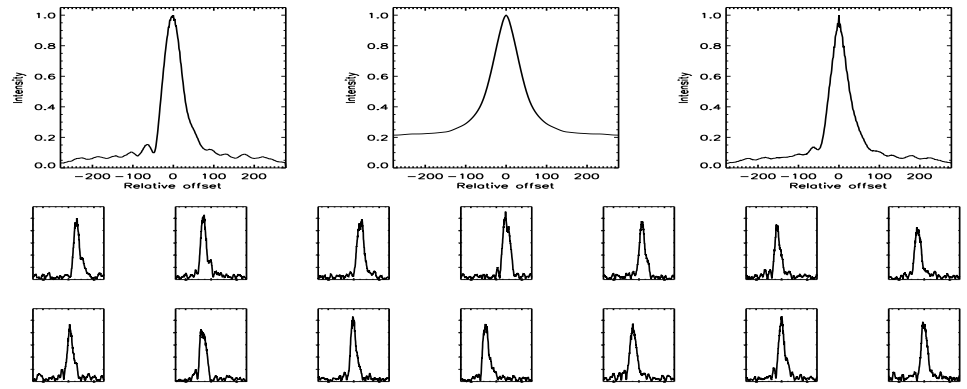

FIGURE B.2: SFP inspection for HD 000166 with S1-E1 on UT 2007/08/14, seq 001

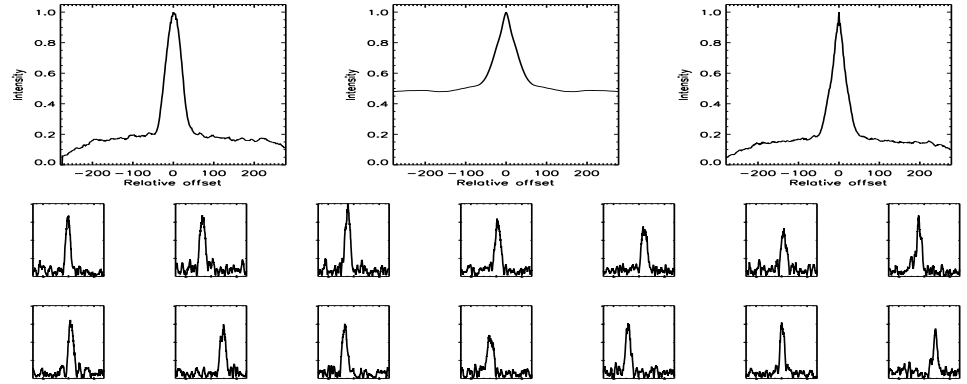

FIGURE B.3: SFP inspection for HD 000166 with S1-W1 on UT 2007/08/14, seq 002

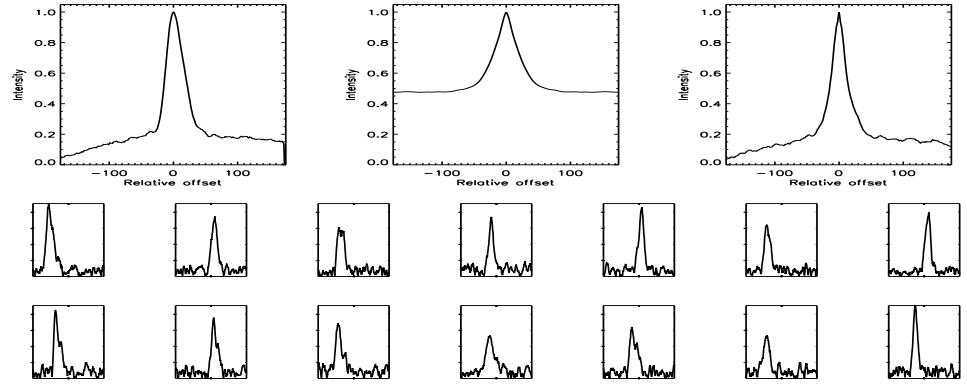

FIGURE B.4: SFP inspection for HD 001461 with S1-E1 on UT 2008/07/22, seq 001

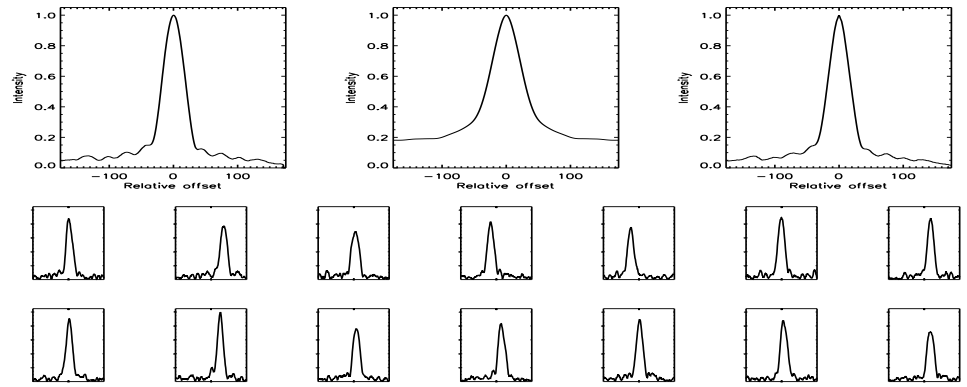

FIGURE B.5: SFP inspection for HD 001461 with S1-W1 on UT 2008/07/27, seq 001

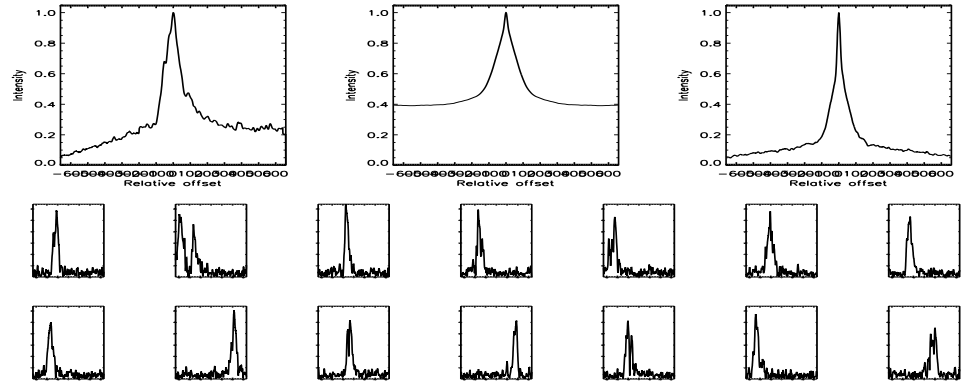

FIGURE B.6: SFP inspection for HD 001461 with S2-W1 on UT 2007/09/17, seq 001

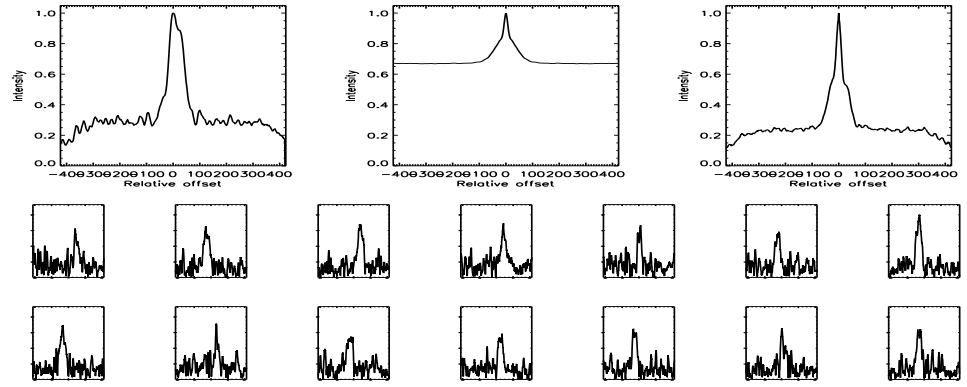

FIGURE B.7: SFP inspection for HD 001562 with S1-E1 on UT 2007/08/16, seq 002

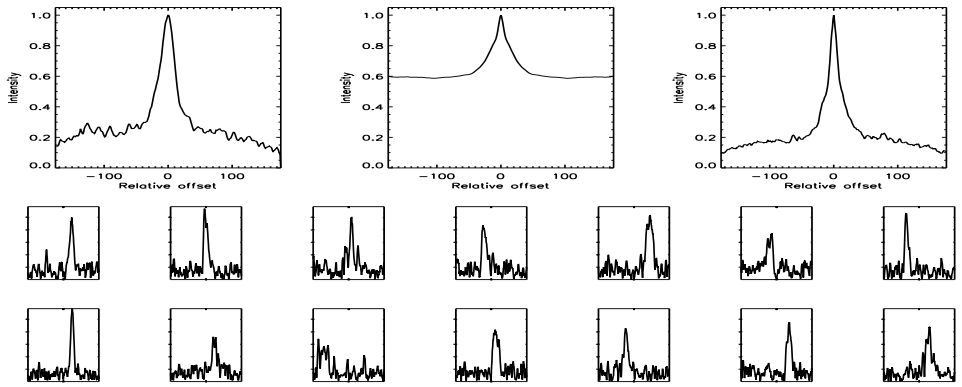

FIGURE B.8: SFP inspection for HD 001562 with S1-E1 on UT 2008/07/09, seq 001

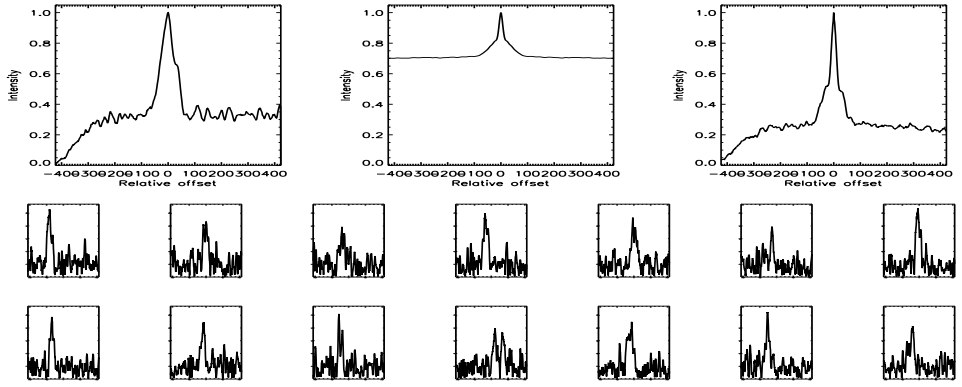

FIGURE B.9: SFP inspection for HD 001562 with S1-W1 on UT 2007/08/16, seq 001

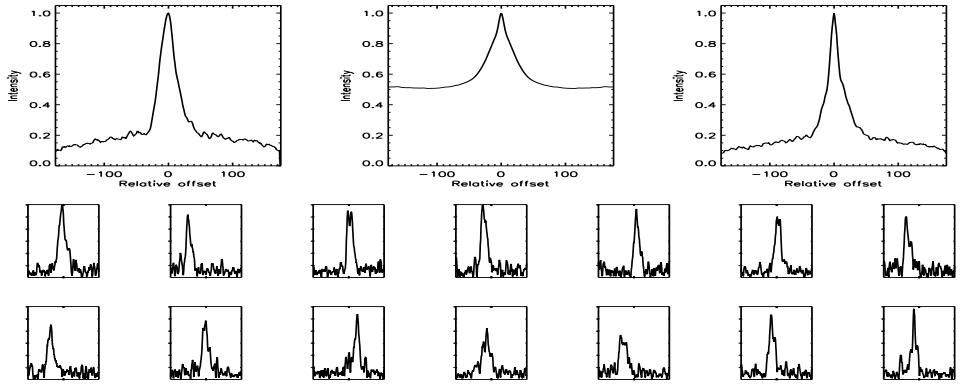

FIGURE B.10: SFP inspection for HD 001562 with S1-W1 on UT 2008/07/08, seq 001

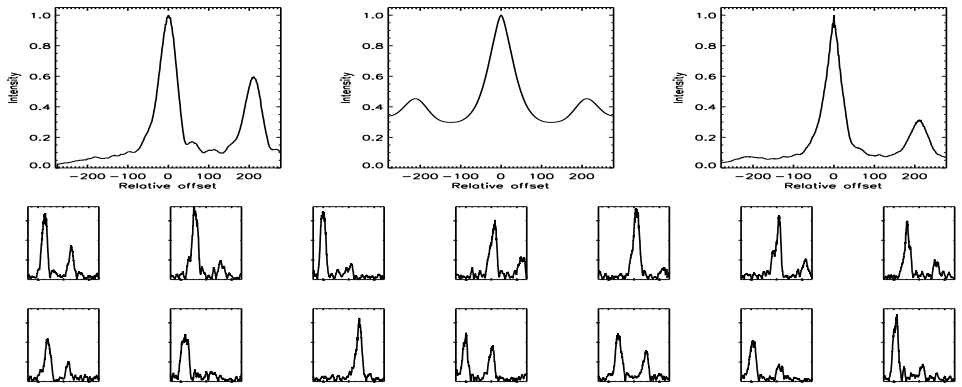

FIGURE B.11: SFP inspection for HD 003196 with S1-E1 on UT 2007/08/14, seq 003

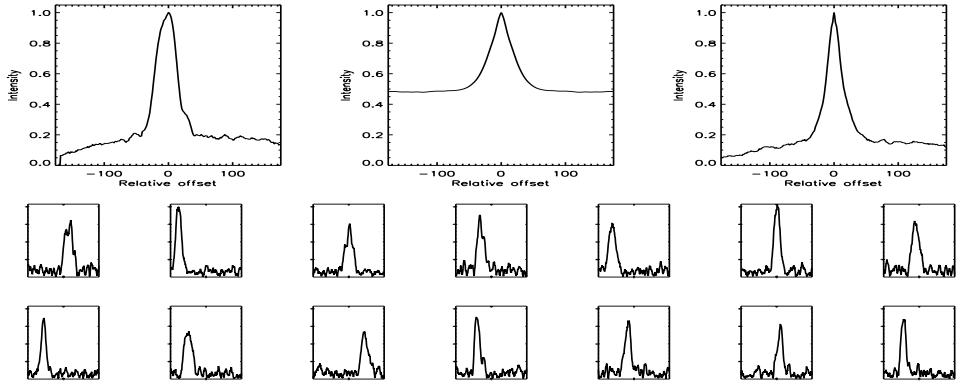

FIGURE B.12: SFP inspection for HD 003196 with S1-E1 on UT 2008/07/22, seq 001

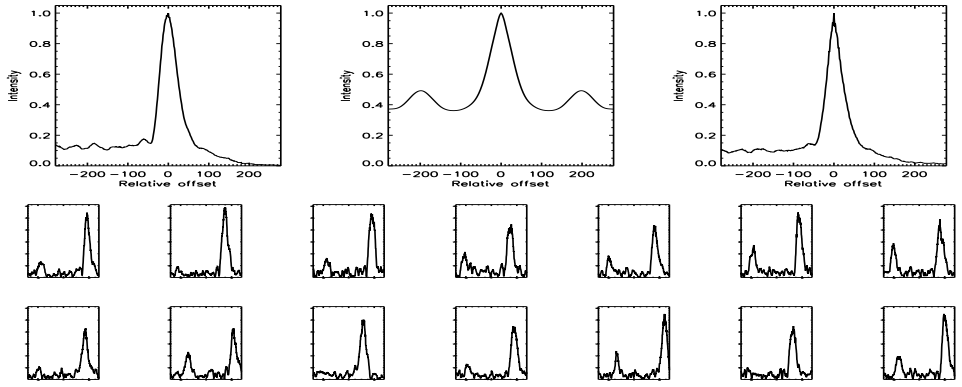

FIGURE B.13: SFP inspection for HD 003196 with S1-W1 on UT 2007/08/14, seq 004

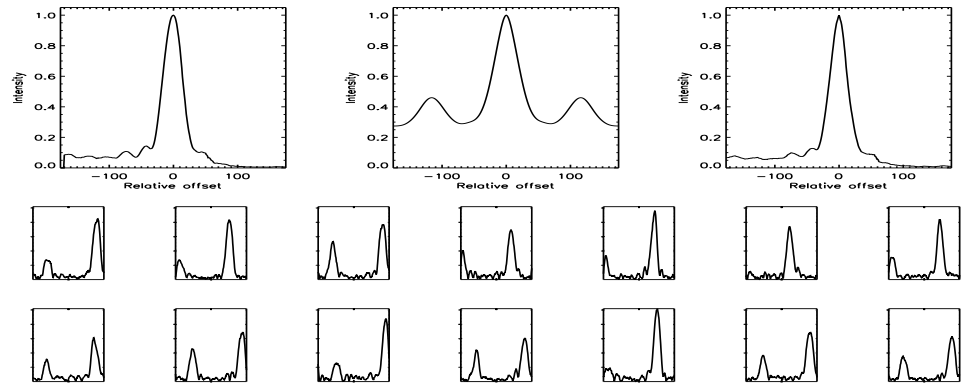

FIGURE B.14: SFP inspection for HD 003196 with S1-W1 on UT 2008/07/07, seq 001

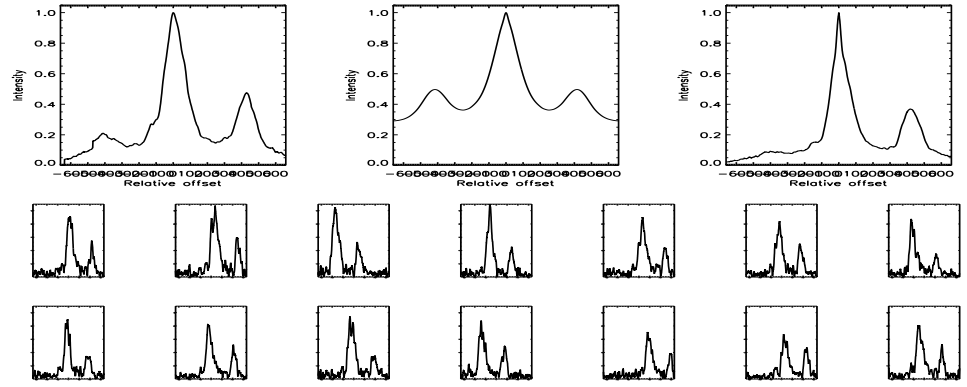

FIGURE B.15: SFP inspection for HD 003196 with S2-E2 on UT 2007/09/27, seq 001

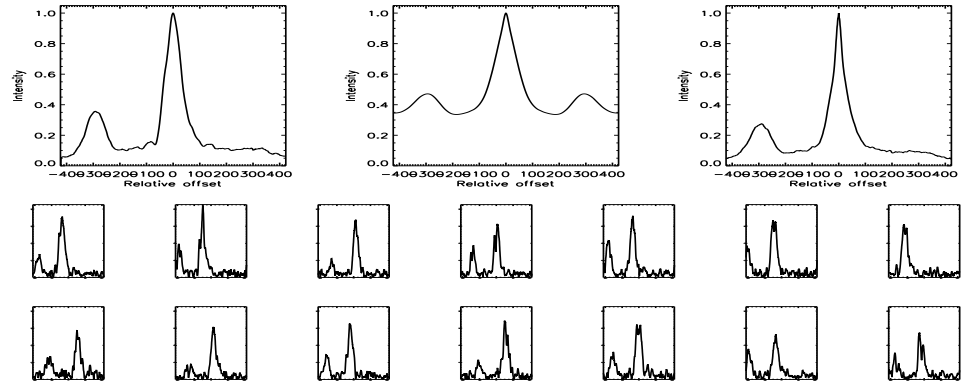

FIGURE B.16: SFP inspection for HD 003196 with S2-W1 on UT 2007/09/17, seq 001

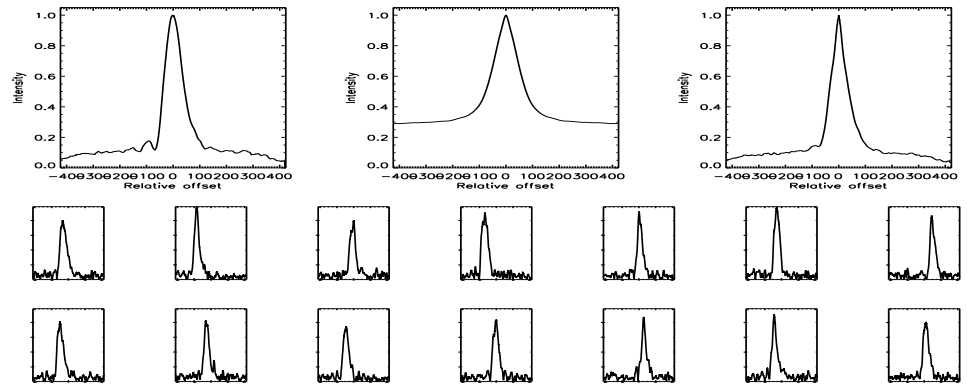

FIGURE B.17: SFP inspection for HD 003651 with S1-E1 on UT 2007/07/29, seq 001

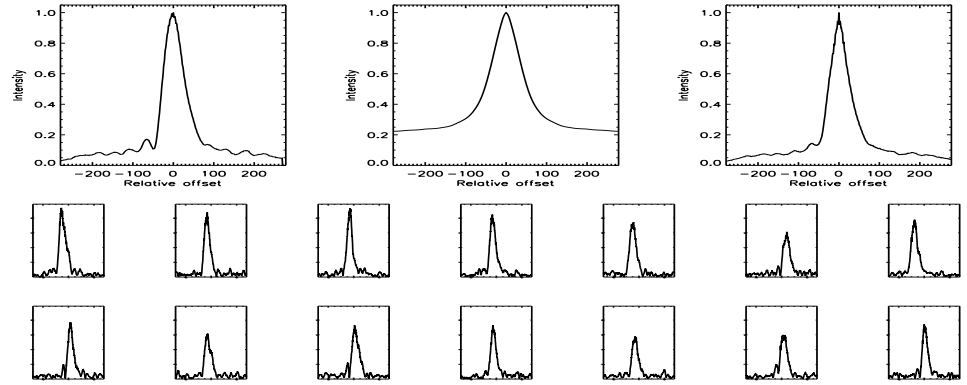

FIGURE B.18: SFP inspection for HD 003651 with S1-E1 on UT 2007/08/14, seq 001

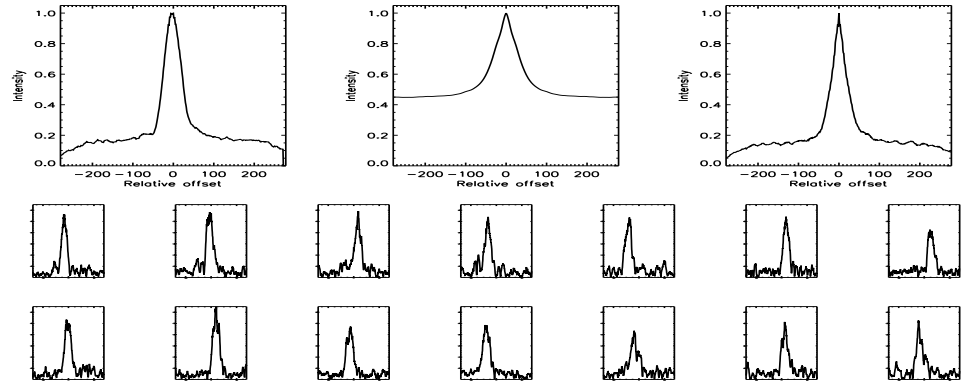

FIGURE B.19: SFP inspection for HD 003651 with S1-W1 on UT 2007/08/14, seq 002

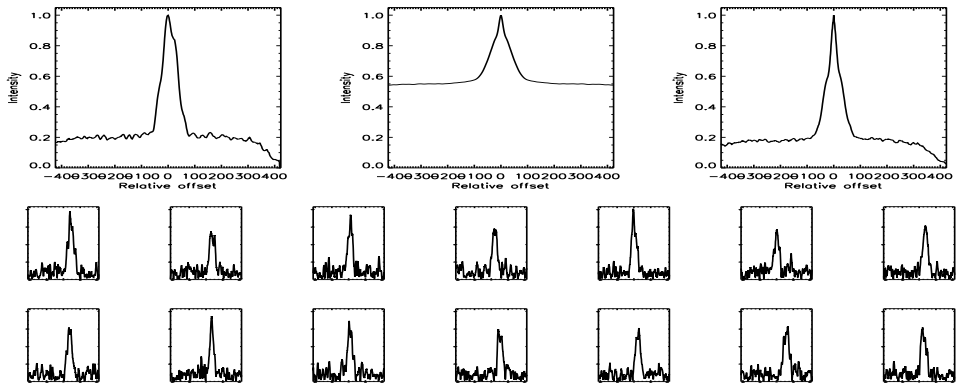

FIGURE B.20: SFP inspection for HD 003765 with S1-E1 on UT 2007/08/16, seq 002

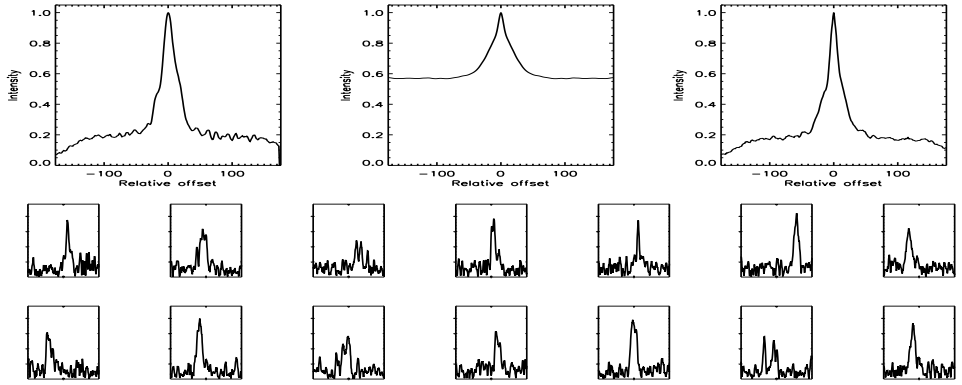

FIGURE B.21: SFP inspection for HD 003765 with S1-E1 on UT 2008/07/09, seq 001

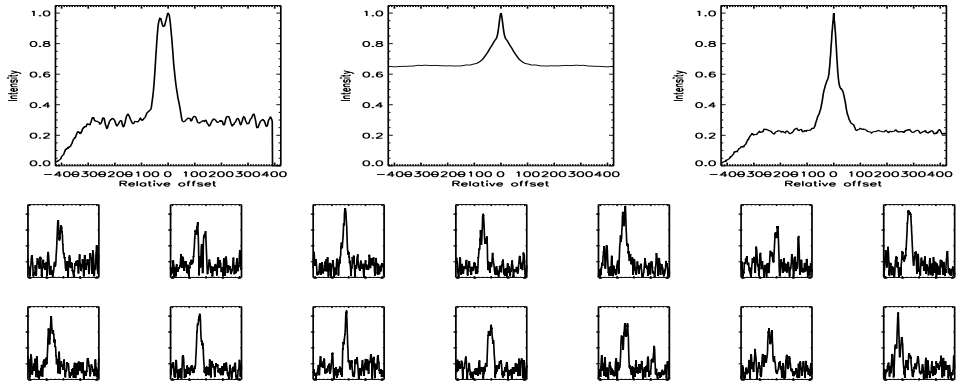

FIGURE B.22: SFP inspection for HD 003765 with S1-W1 on UT 2007/08/16, seq 001

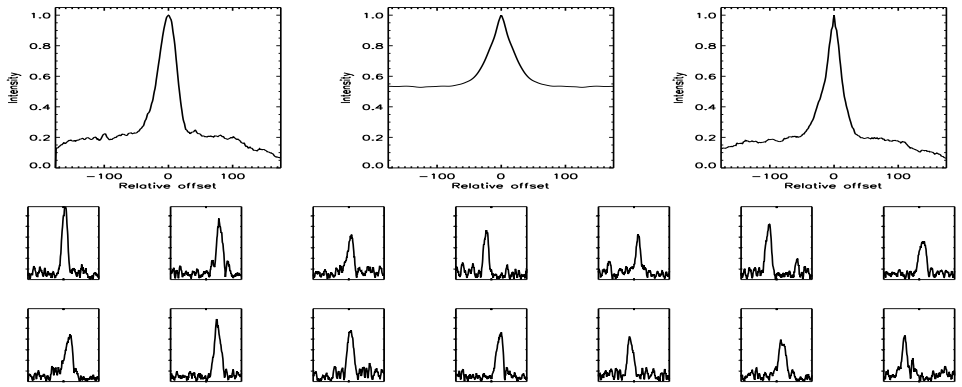

FIGURE B.23: SFP inspection for HD 003765 with S1-W1 on UT 2008/07/08, seq 001

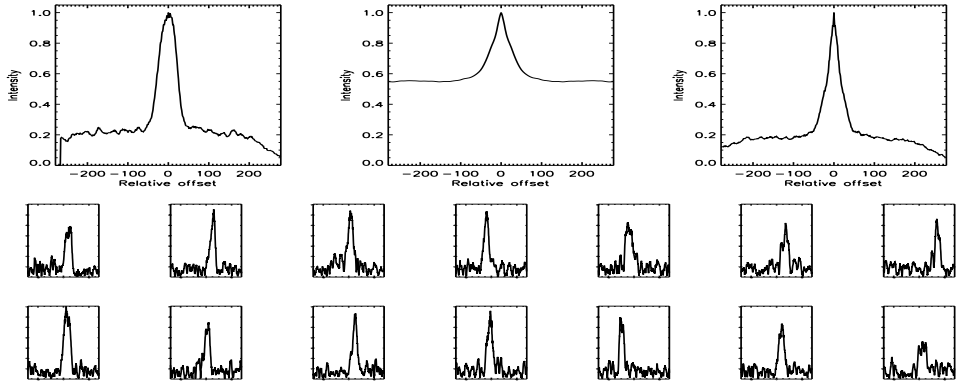

FIGURE B.24: SFP inspection for HD 004256 with S1-E1 on UT 2007/08/14, seq 001

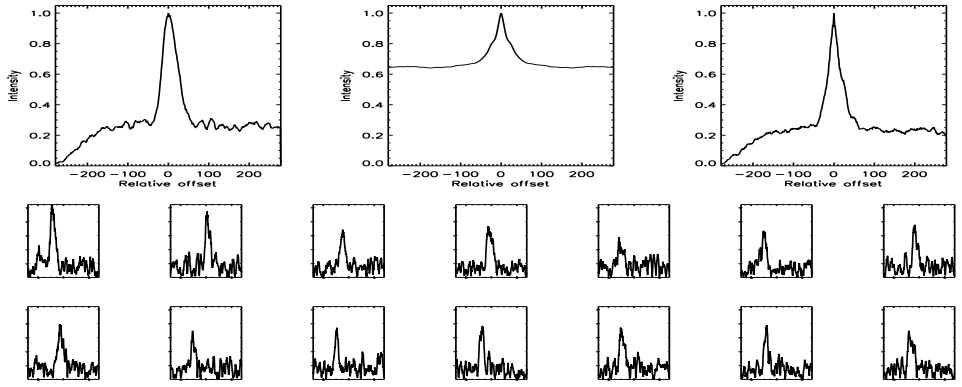

FIGURE B.25: SFP inspection for HD 004256 with S1-W1 on UT 2007/08/14, seq 002

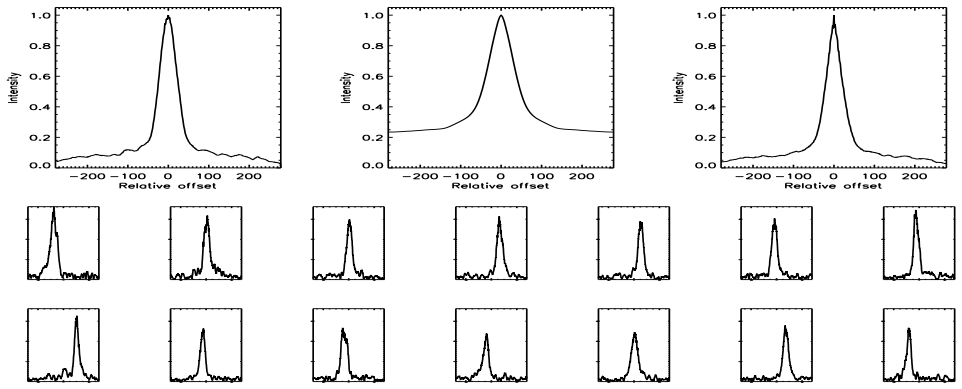

FIGURE B.26: SFP inspection for HD 004628 with S1-E1 on UT 2007/08/14, seq 001

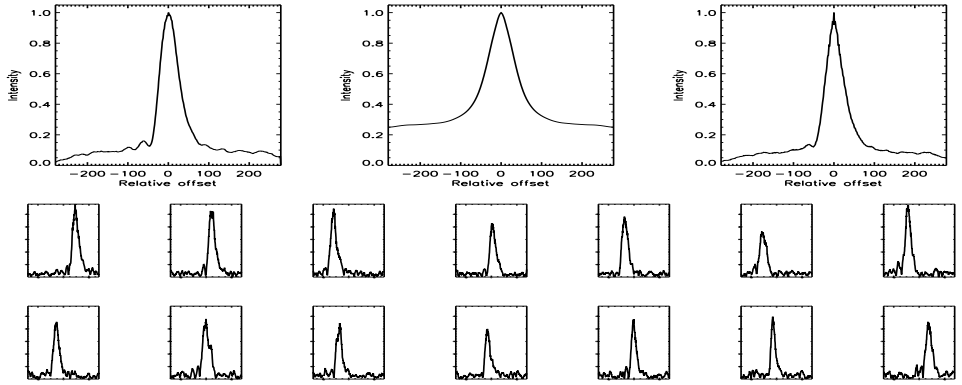

FIGURE B.27: SFP inspection for HD 004628 with S1-W1 on UT 2007/08/14, seq 002

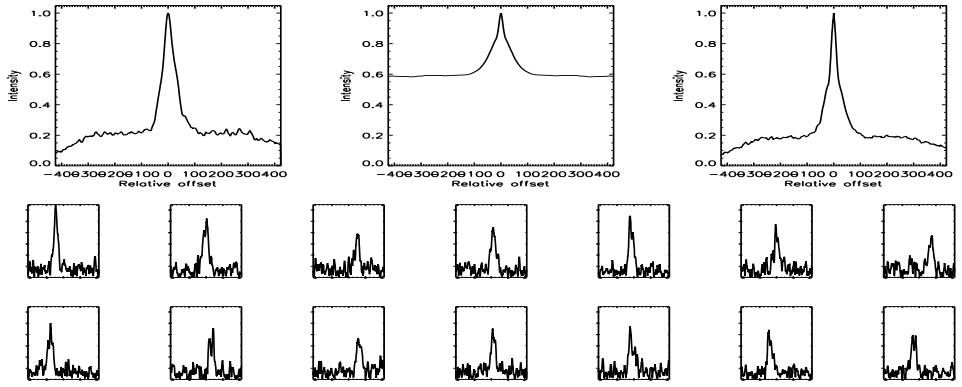

FIGURE B.28: SFP inspection for HD 004635 with S1-E1 on UT 2007/09/16, seq 002

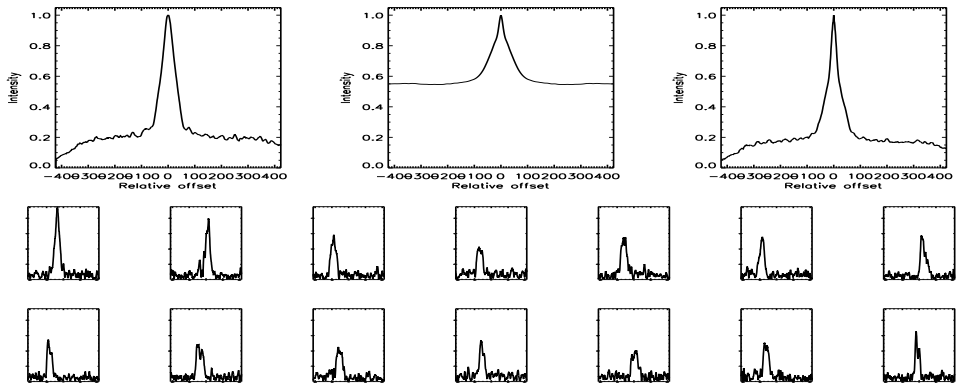

FIGURE B.29: SFP inspection for HD 004635 with S1-W1 on UT 2007/09/16, seq 001

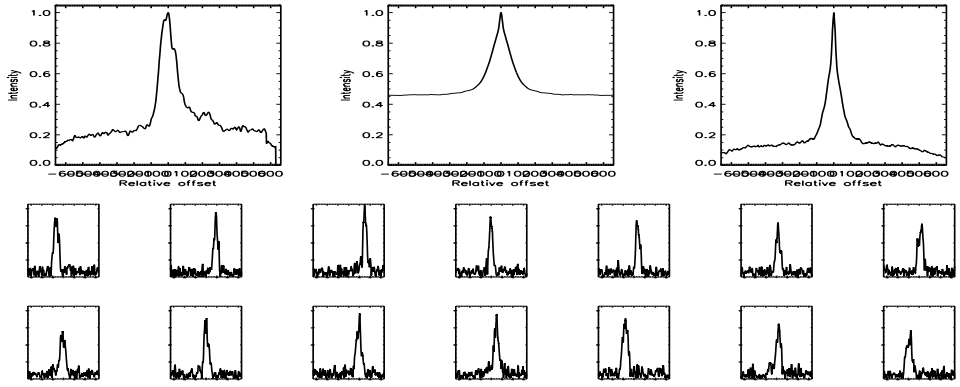

FIGURE B.30: SFP inspection for HD 004635 with S2-E1 on UT 2007/08/20, seq 001

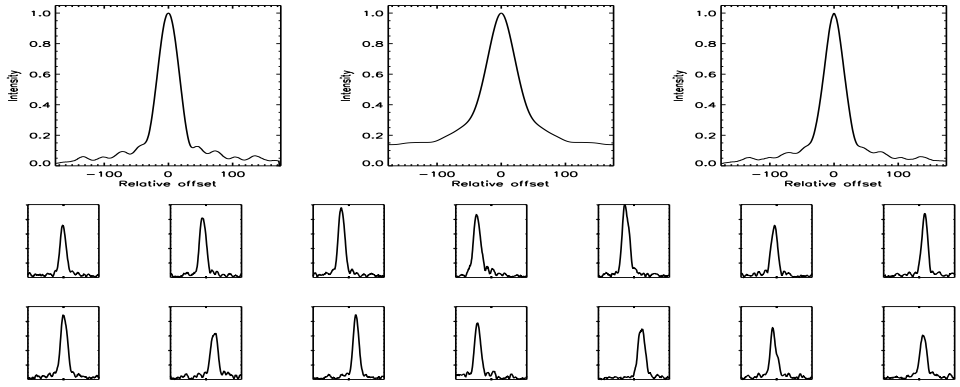

FIGURE B.31: SFP inspection for HD 004813 with S1-W1 on UT 2008/07/27, seq 001

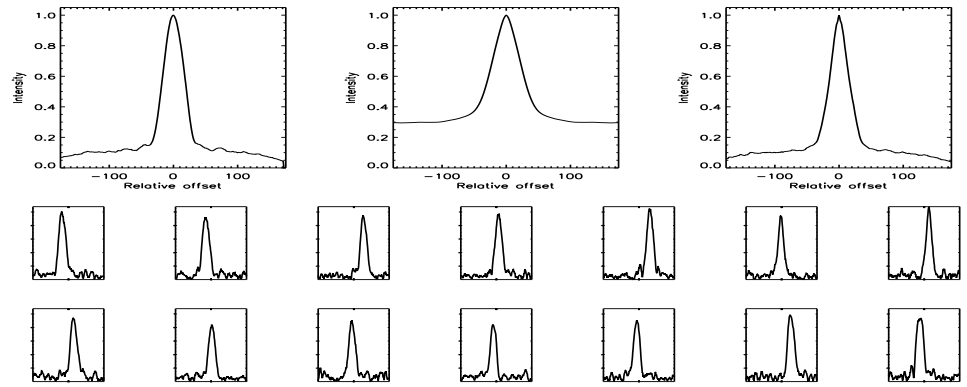

FIGURE B.32: SFP inspection for HD 004915 with S1-W1 on UT 2008/07/27, seq 001

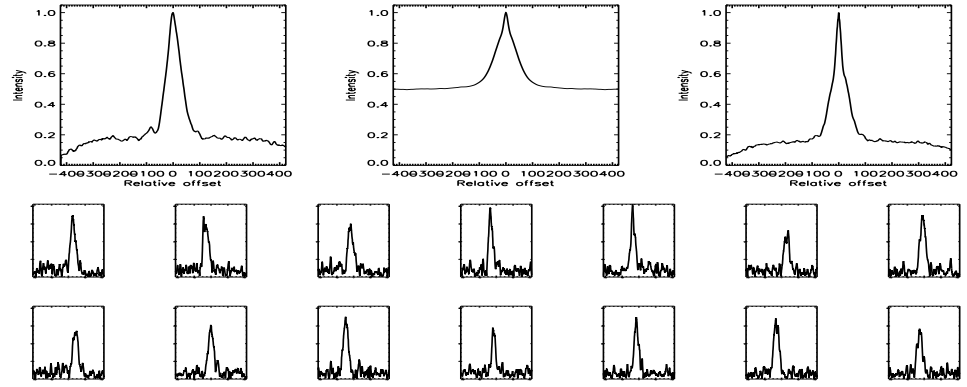

FIGURE B.33: SFP inspection for HD 004915 with S2-W1 on UT 2007/09/17, seq 001

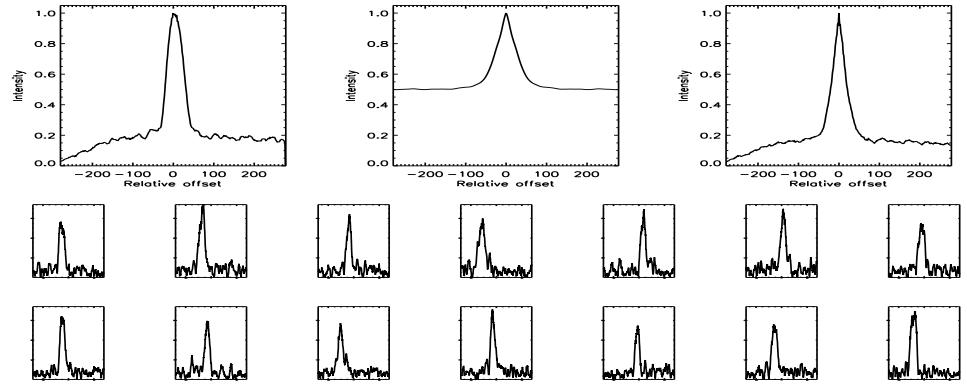

FIGURE B.34: SFP inspection for HD 007590 with S1-E1 on UT 2007/02/04, seq 001

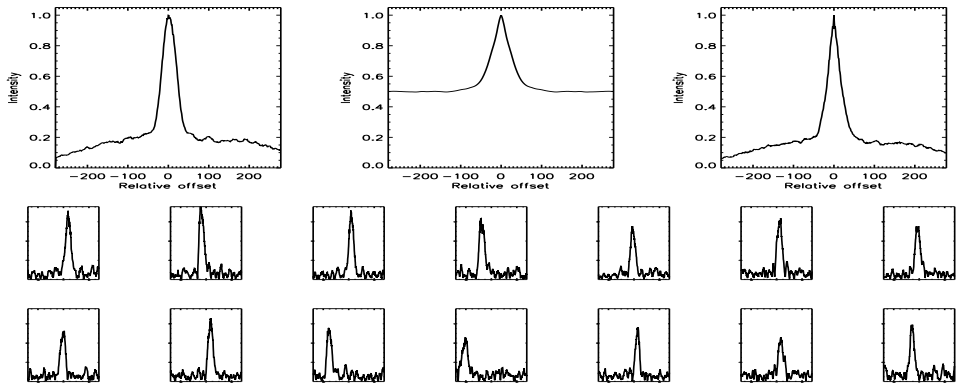

FIGURE B.35: SFP inspection for HD 007590 with S1-E1 on UT 2007/02/04, seq 002

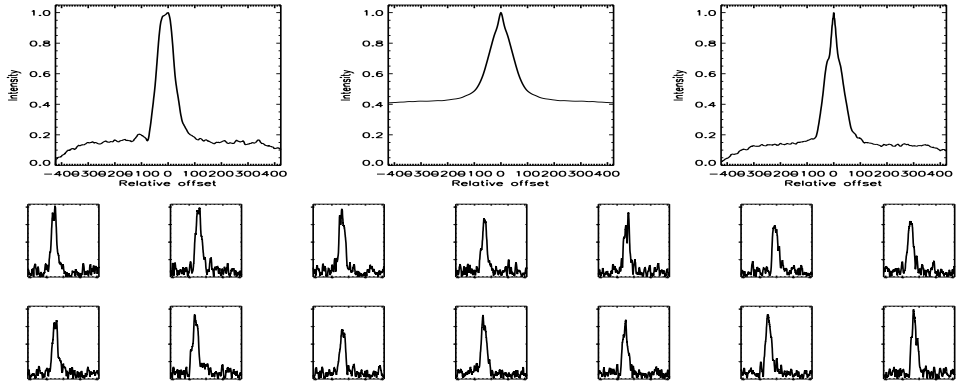

FIGURE B.36: SFP inspection for HD 007590 with S1-E1 on UT 2007/08/16, seq 002

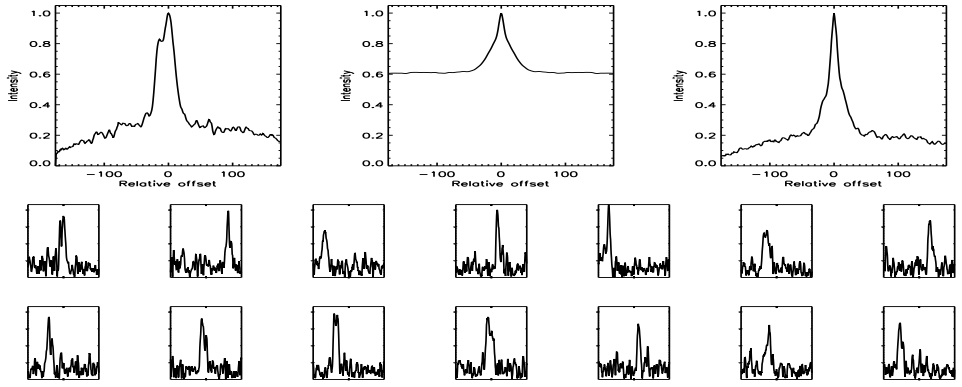

FIGURE B.37: SFP inspection for HD 007590 with S1-E1 on UT 2008/07/09, seq 001

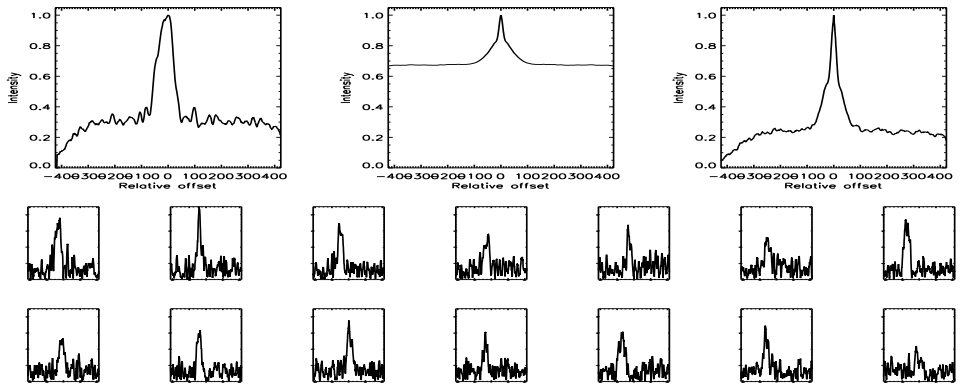

FIGURE B.38: SFP inspection for HD 007590 with S1-W1 on UT 2007/08/16, seq 001

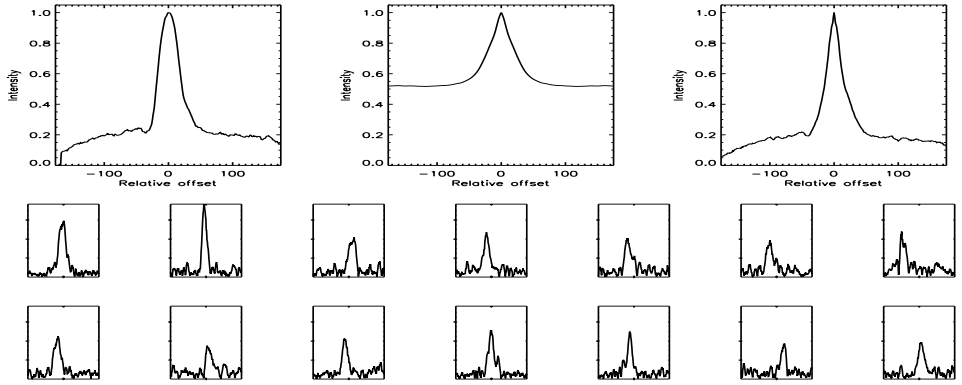

FIGURE B.39: SFP inspection for HD 007590 with S1-W1 on UT 2008/07/08, seq 001

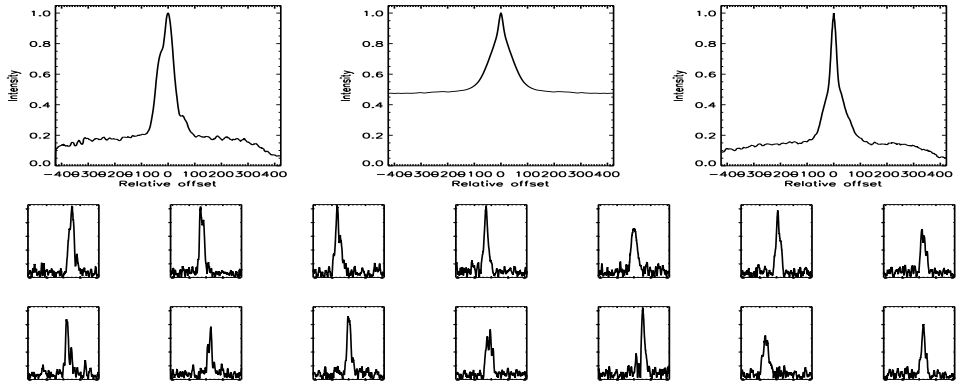

FIGURE B.40: SFP inspection for HD 007924 with S1-E1 on UT 2007/09/16, seq 002

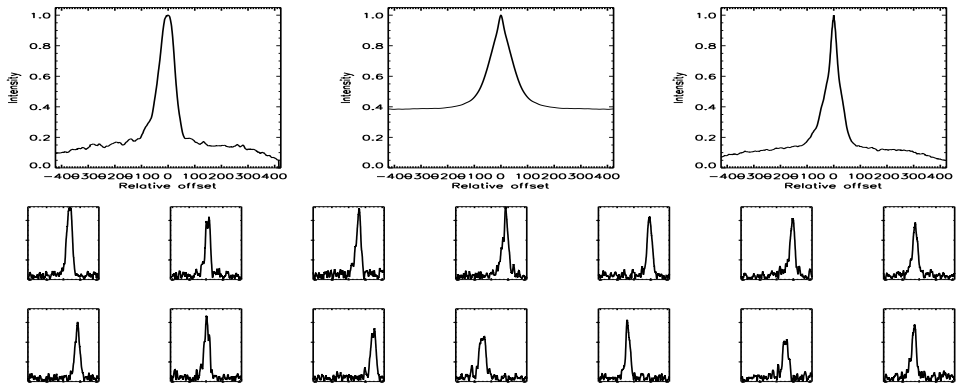

FIGURE B.41: SFP inspection for HD 007924 with S1-W1 on UT 2007/09/16, seq 001

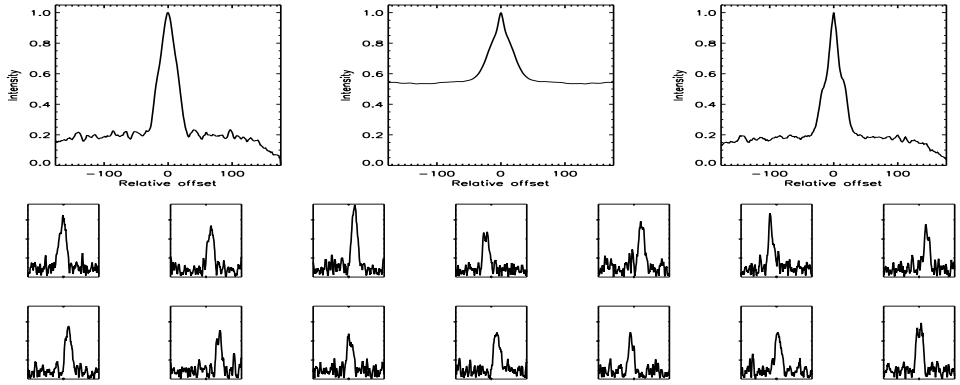

FIGURE B.42: SFP inspection for HD 008997 with S1-E1 on UT 2008/07/23, seq 001

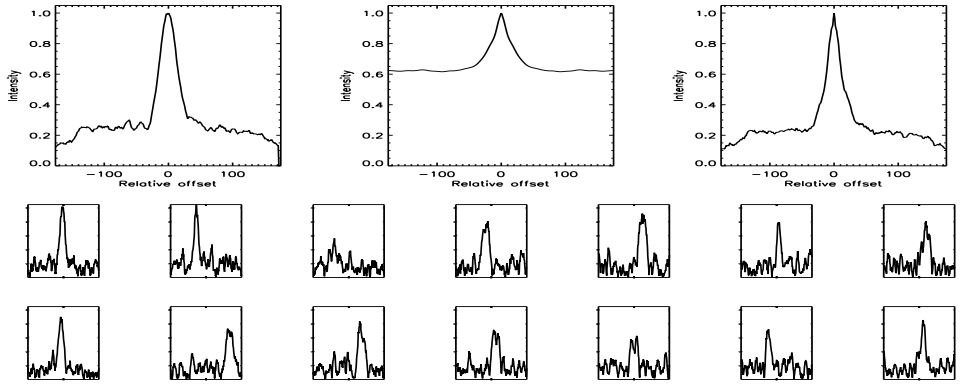

FIGURE B.43: SFP inspection for HD 008997 with S1-W1 on UT 2008/07/07, seq 001

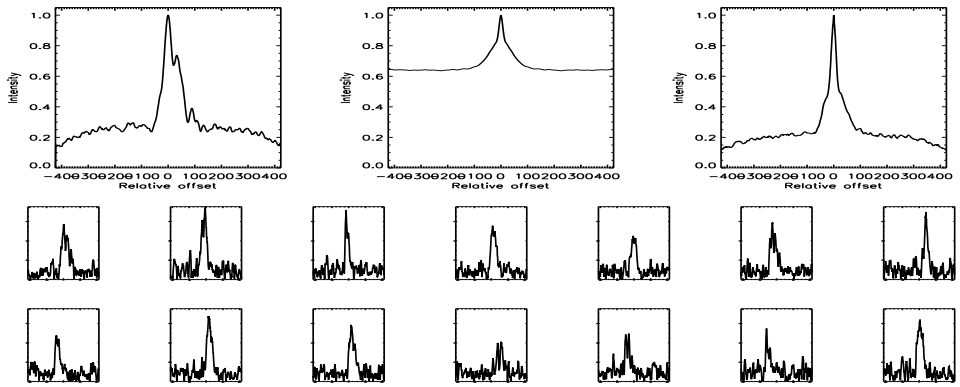

FIGURE B.44: SFP inspection for HD 008997 with S2-E2 on UT 2007/09/18, seq 001

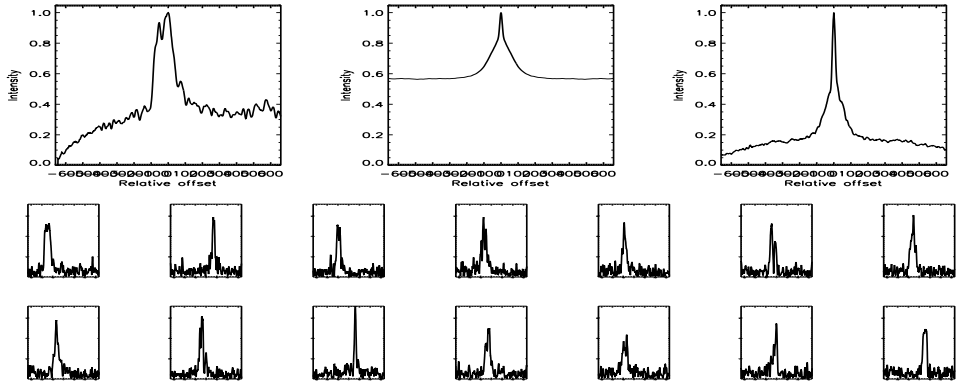

FIGURE B.45: SFP inspection for HD 008997 with S2-W1 on UT 2007/09/17, seq 001

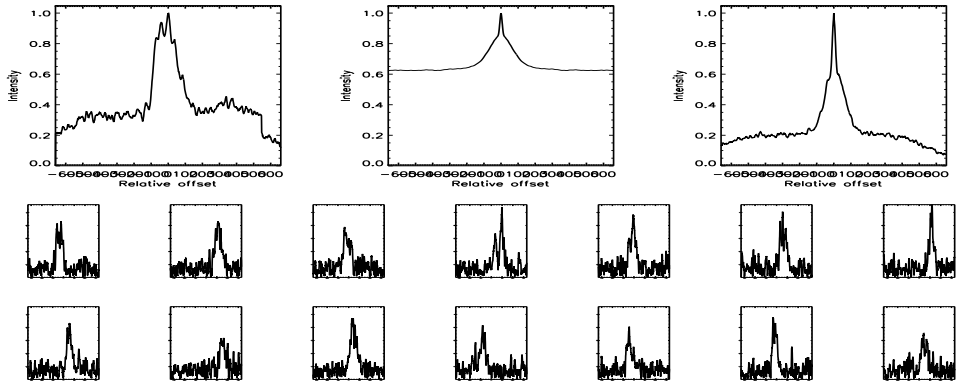

FIGURE B.46: SFP inspection for HD 010008 with S2-E2 on UT 2007/09/27, seq 001

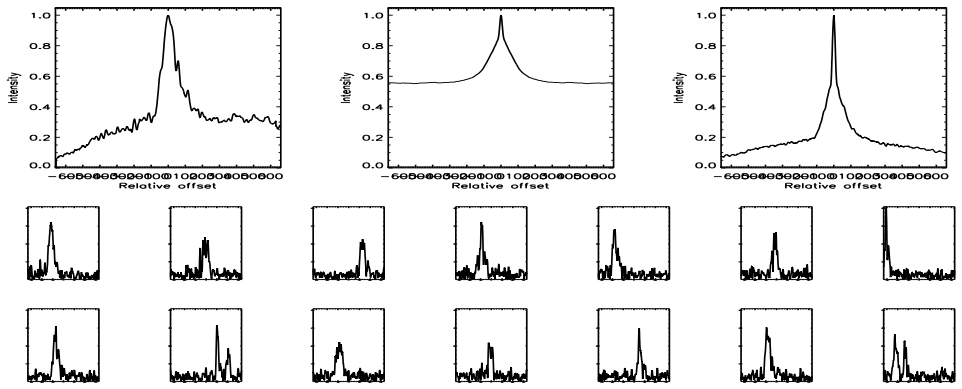

FIGURE B.47: SFP inspection for HD 010008 with S2-W1 on UT 2007/09/17, seq 001

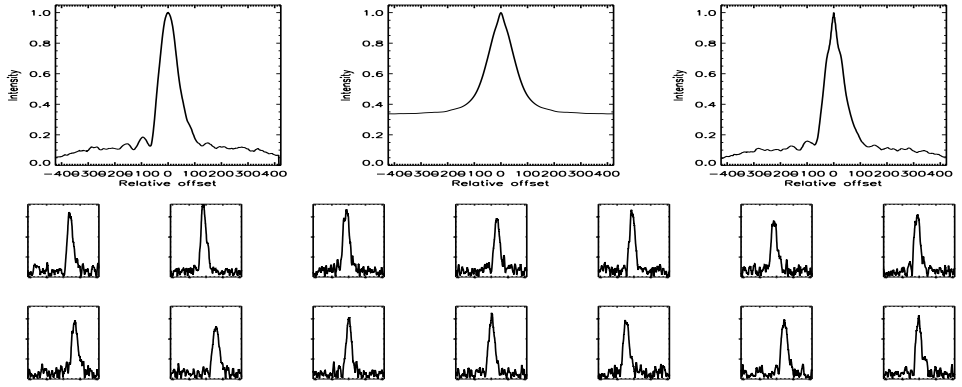

FIGURE B.48: SFP inspection for HD 010086 with S1-E1 on UT 2007/08/16, seq 002

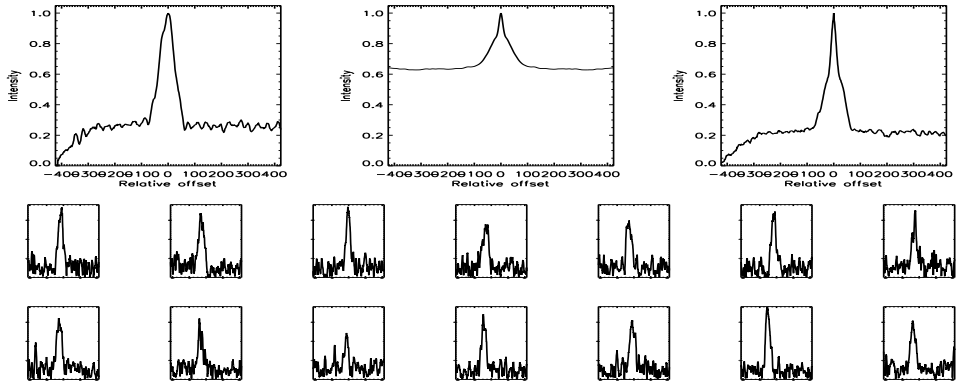

FIGURE B.49: SFP inspection for HD 010086 with S1-W1 on UT 2007/08/16, seq 001

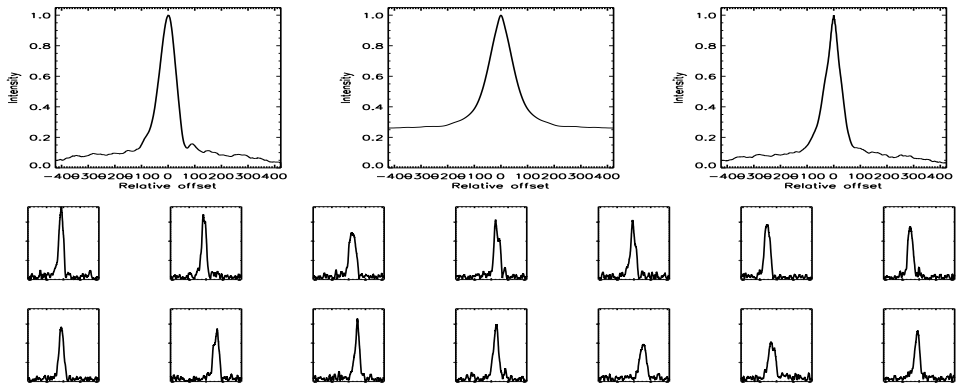

FIGURE B.50: SFP inspection for HD 010476 with S1-E1 on UT 2007/07/29, seq 001

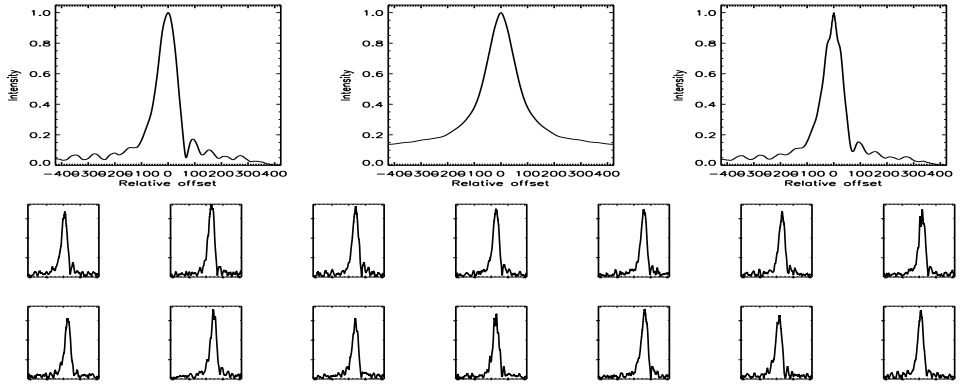

FIGURE B.51: SFP inspection for HD 010476 with S1-E1 on UT 2007/08/16, seq 001

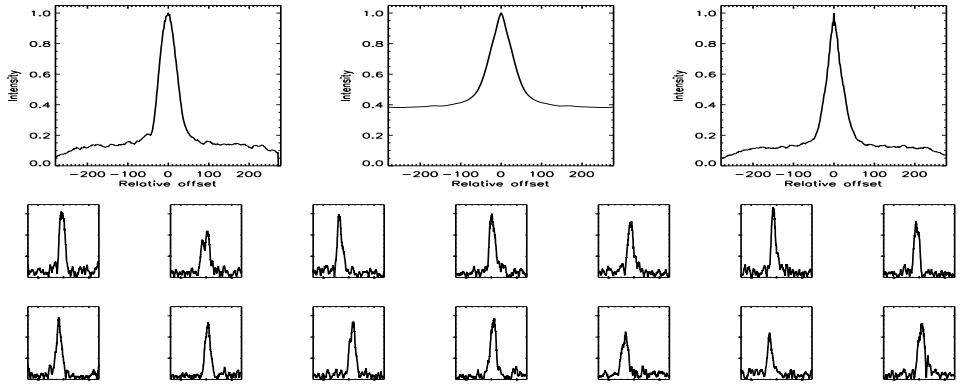

FIGURE B.52: SFP inspection for HD 010476 with S1-W1 on UT 2007/08/14, seq 001

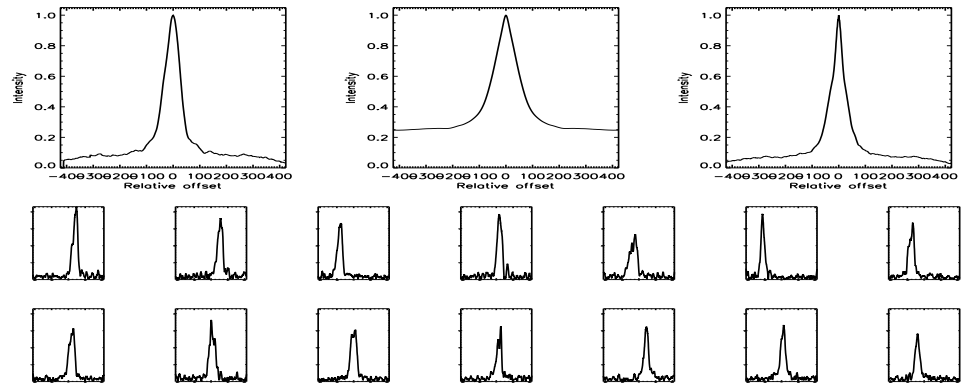

FIGURE B.53: SFP inspection for HD 010780 with S1-E1 on UT 2007/09/16, seq 002

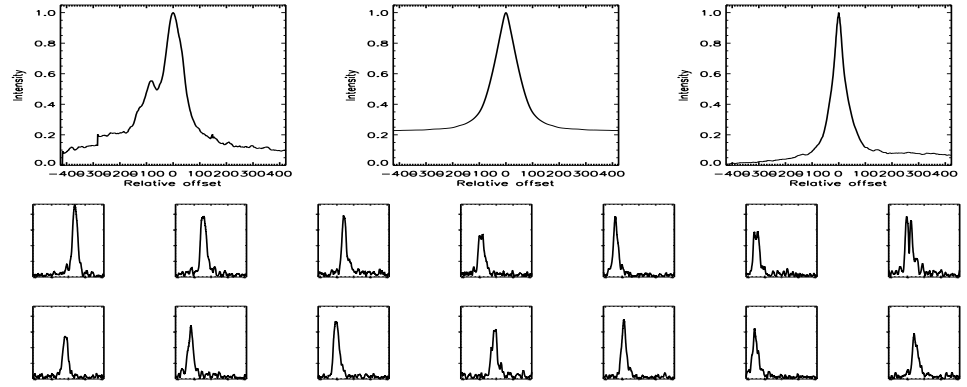

FIGURE B.54: SFP inspection for HD 010780 with S1-W1 on UT 2007/09/16, seq 001

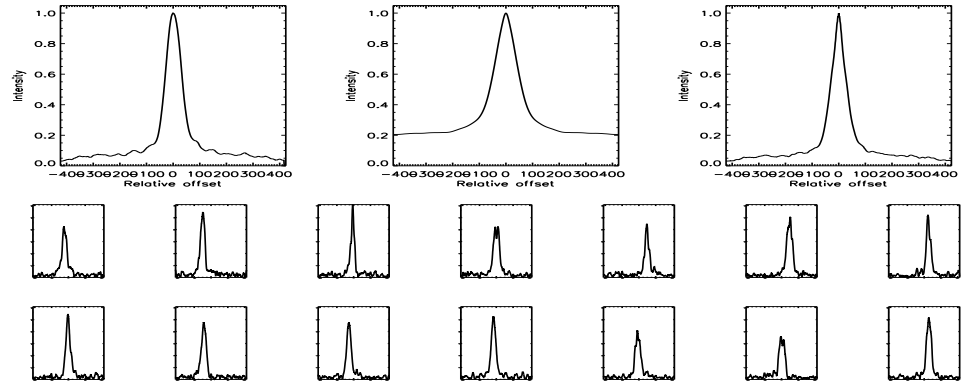

FIGURE B.55: SFP inspection for HD 010780 with S2-E1 on UT 2007/08/20, seq 002

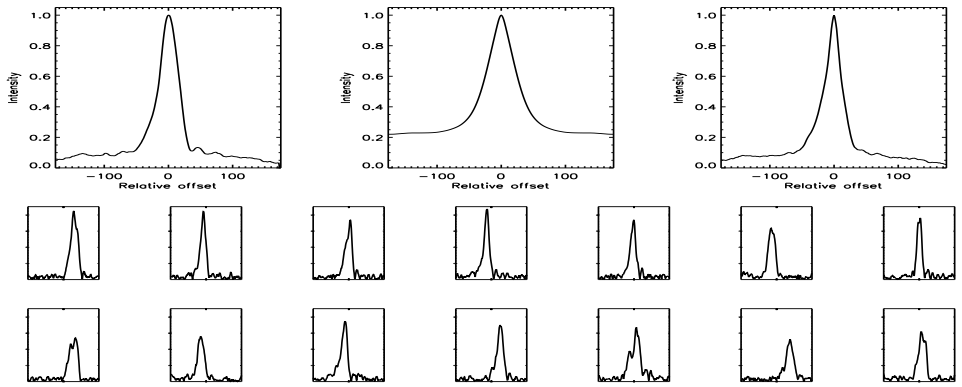

FIGURE B.56: SFP inspection for HD 010780 with S2-W1 on UT 2008/06/24, seq 001

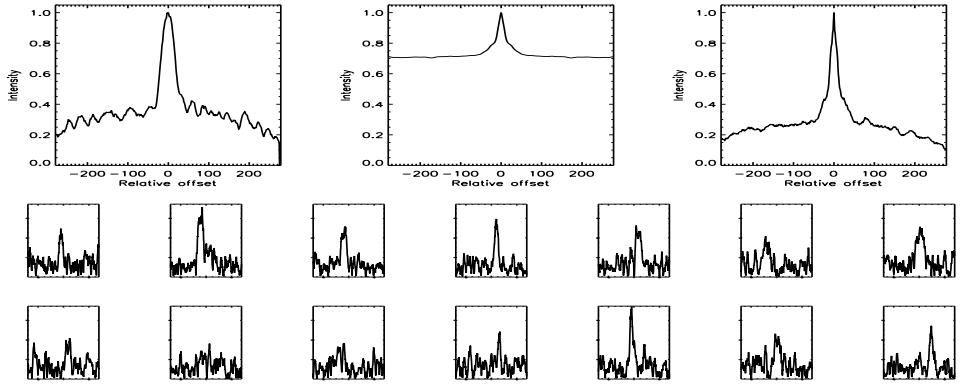

FIGURE B.57: SFP inspection for HD 012051 with S1-E1 on UT 2007/01/26, seq 001

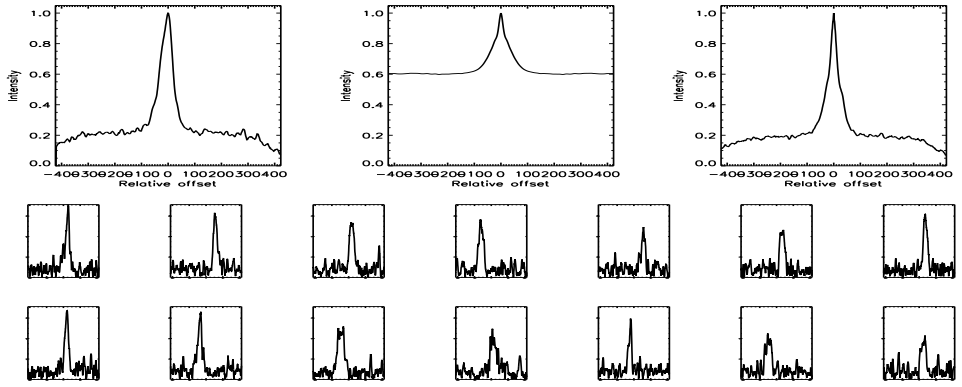

FIGURE B.58: SFP inspection for HD 012051 with S2-E2 on UT 2007/09/18, seq 001

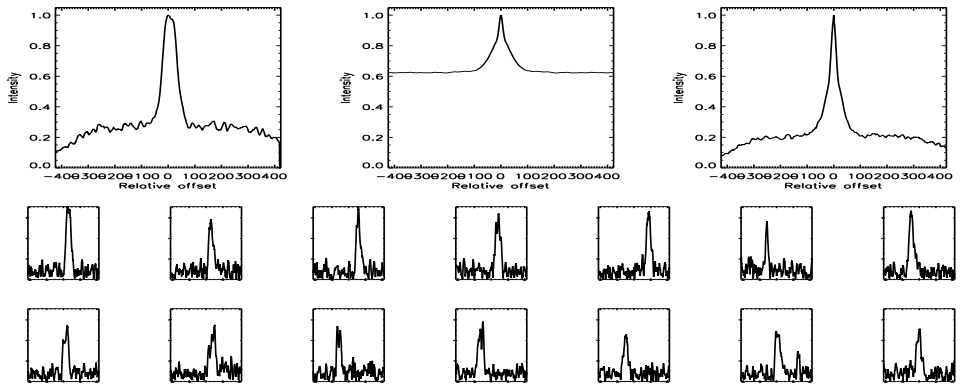

FIGURE B.59: SFP inspection for HD 012051 with S2-E2 on UT 2007/09/18, seq 002

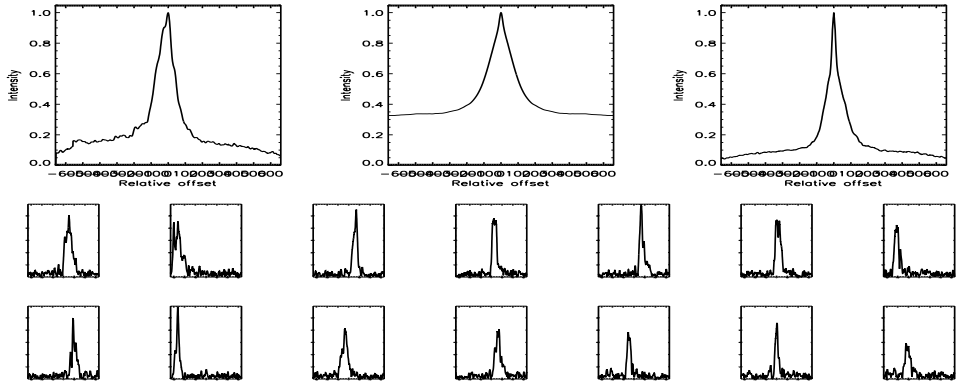

FIGURE B.60: SFP inspection for HD 012051 with S2-W1 on UT 2007/09/17, seq 001

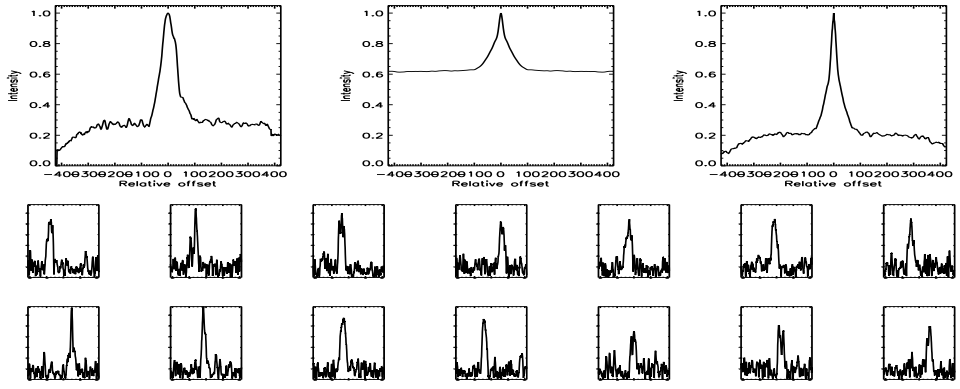

FIGURE B.61: SFP inspection for HD 012846 with S2-E2 on UT 2007/09/18, seq 001

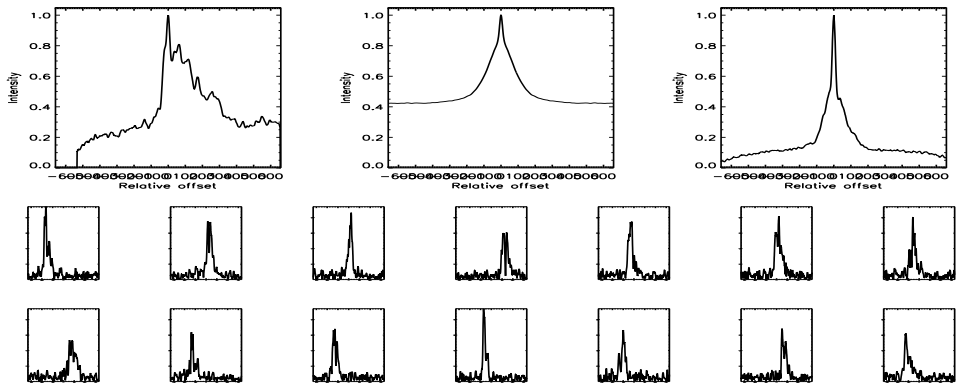

FIGURE B.62: SFP inspection for HD 012846 with S2-W1 on UT 2007/09/17, seq 001

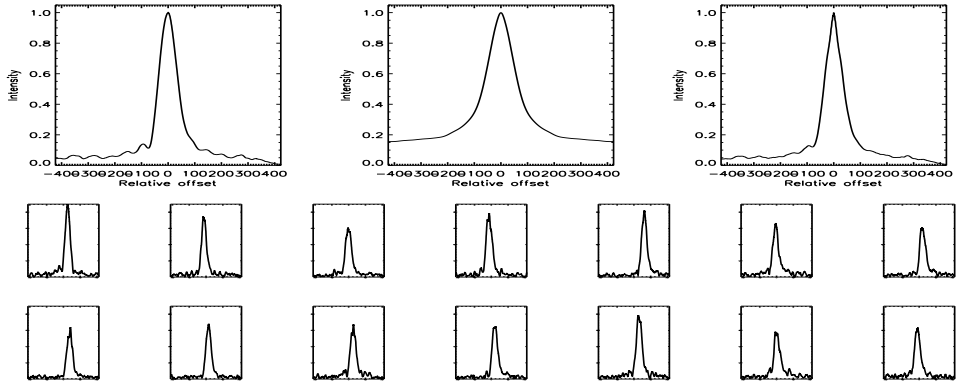

FIGURE B.63: SFP inspection for HD 016160 with S1-E1 on UT 2007/08/15, seq 001

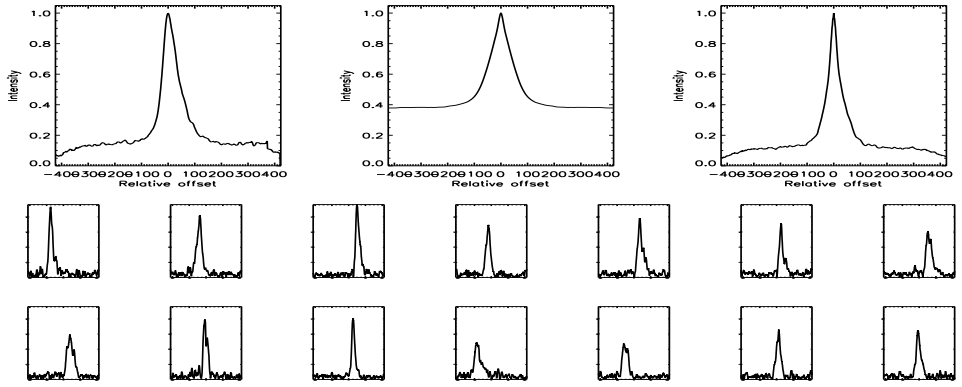

FIGURE B.64: SFP inspection for HD 016160 with S2-E2 on UT 2007/09/18, seq 001

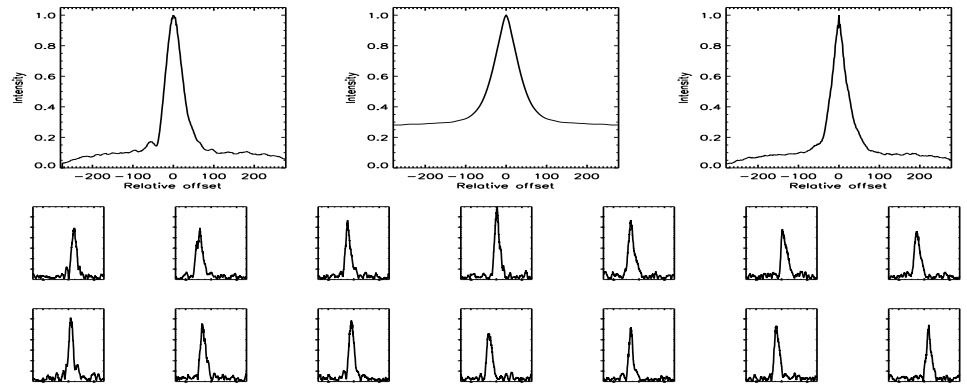

FIGURE B.65: SFP inspection for HD 016160 with S2-W1 on UT 2007/09/17, seq 001

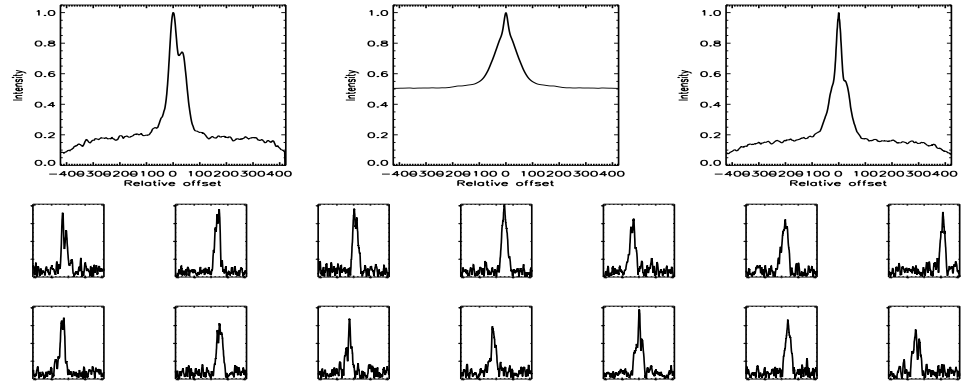

FIGURE B.66: SFP inspection for HD 016287 with S1-E1 on UT 2007/08/15, seq 001

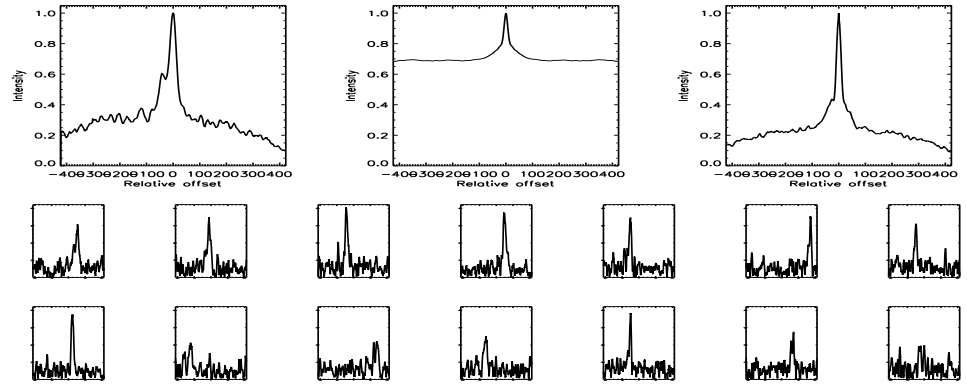

FIGURE B.67: SFP inspection for HD 016287 with S1-E1 on UT 2007/10/31, seq 001

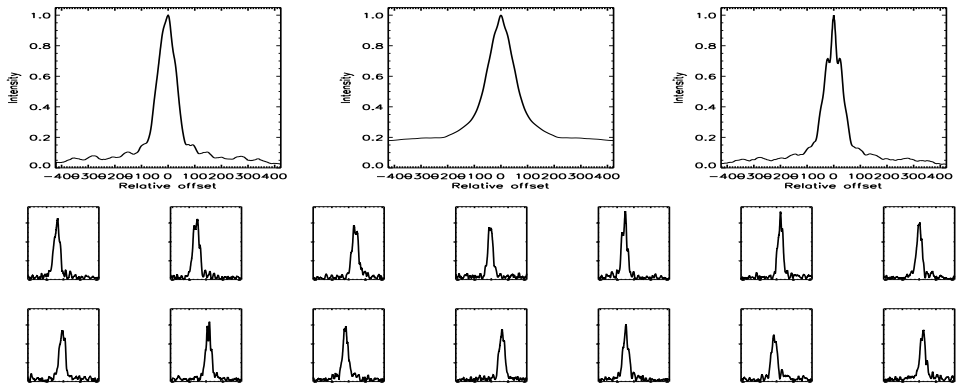

FIGURE B.68: SFP inspection for HD 016673 with S1-E1 on UT 2007/08/15, seq 001

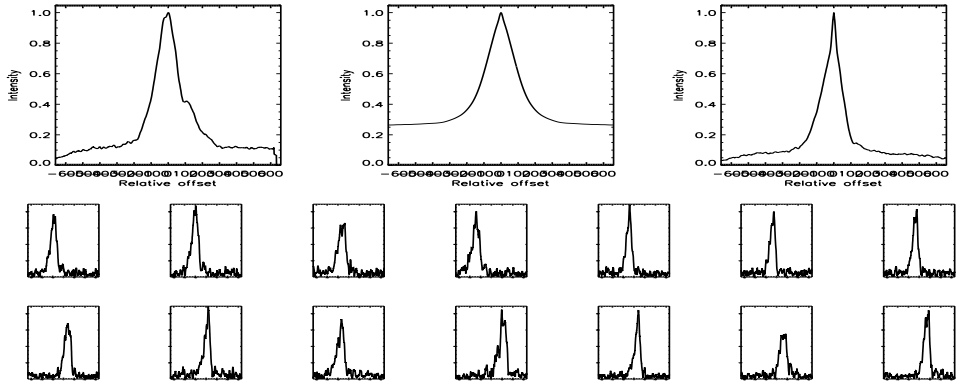

FIGURE B.69: SFP inspection for HD 016673 with S2-E2 on UT 2007/09/27, seq 001

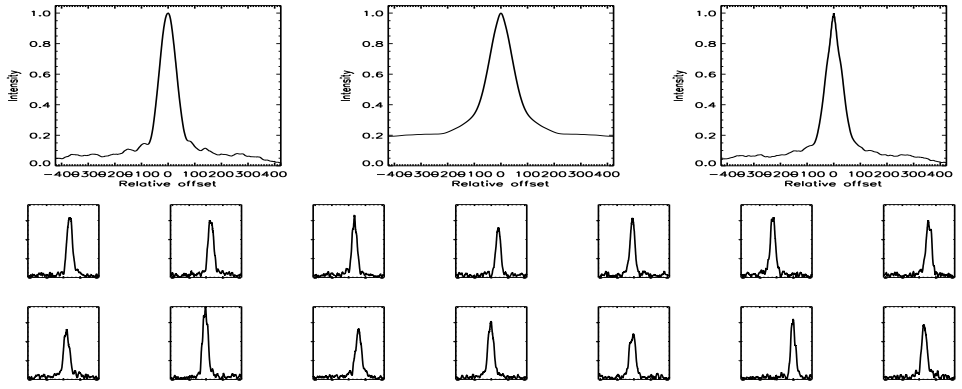

FIGURE B.70: SFP inspection for HD 016765 with S1-E1 on UT 2007/08/15, seq 001

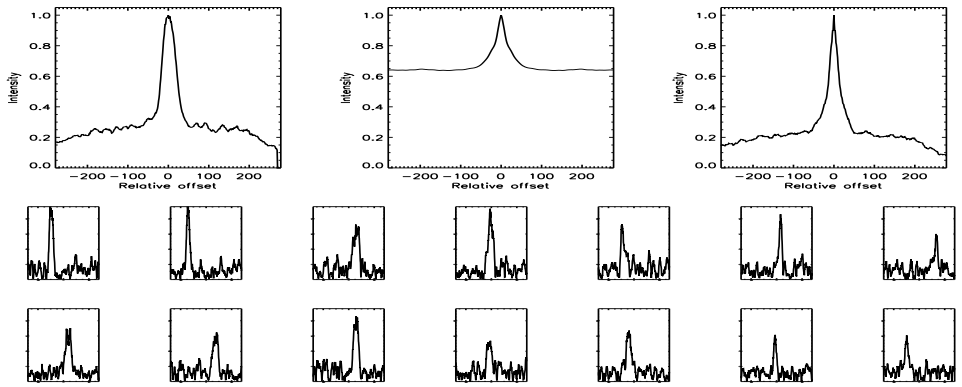

FIGURE B.71: SFP inspection for HD 016765 with S1-E1 on UT 2007/10/31, seq 001

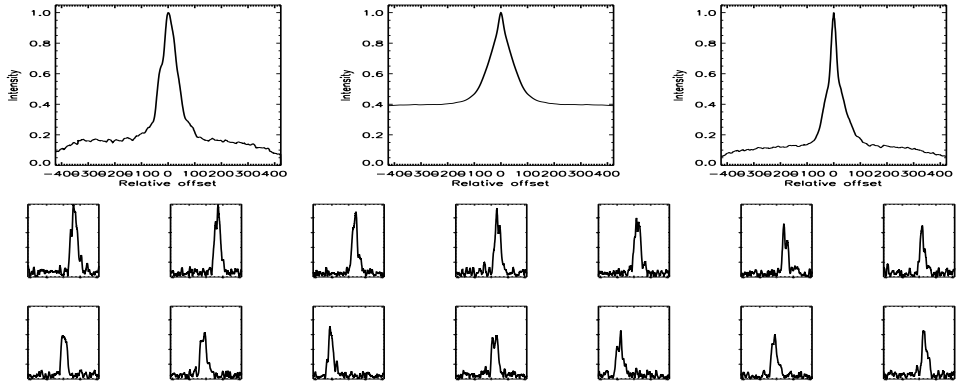

FIGURE B.72: SFP inspection for HD 016765 with S1-W1 on UT 2007/10/31, seq 002

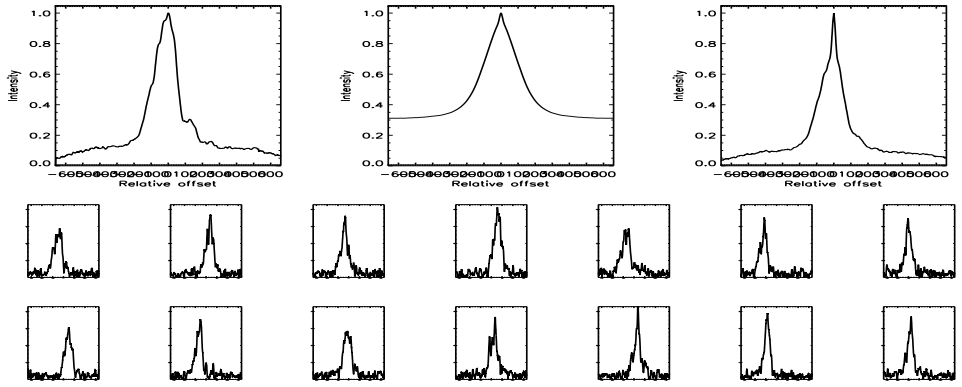

FIGURE B.73: SFP inspection for HD 016765 with S2-E2 on UT 2007/09/27, seq 001

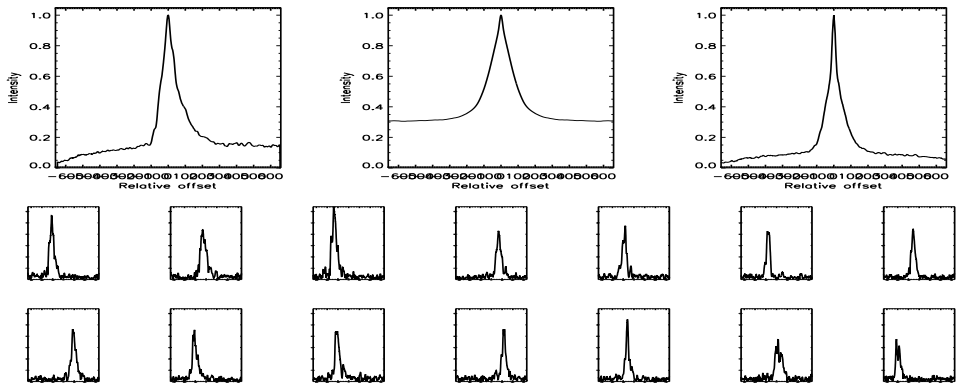

FIGURE B.74: SFP inspection for HD 016765 with S2-W1 on UT 2007/09/17, seq 001

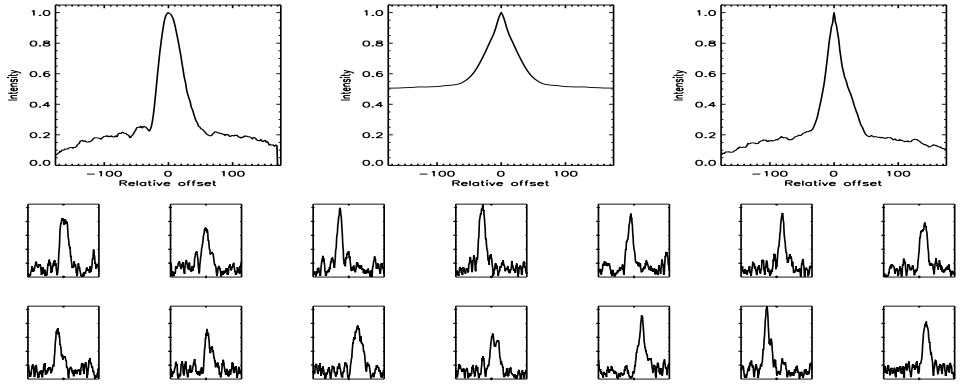

FIGURE B.75: SFP inspection for HD 017382 with S1-W1 on UT 2008/07/07, seq 001

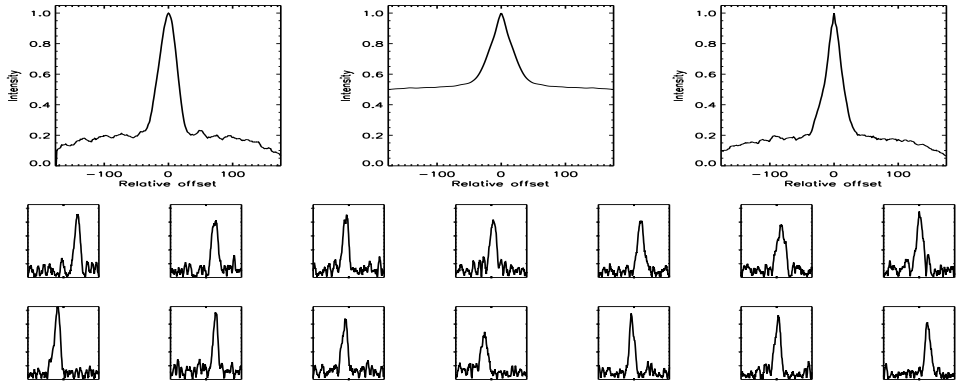

FIGURE B.76: SFP inspection for HD 017382 with S1-W1 on UT 2008/07/08, seq 001

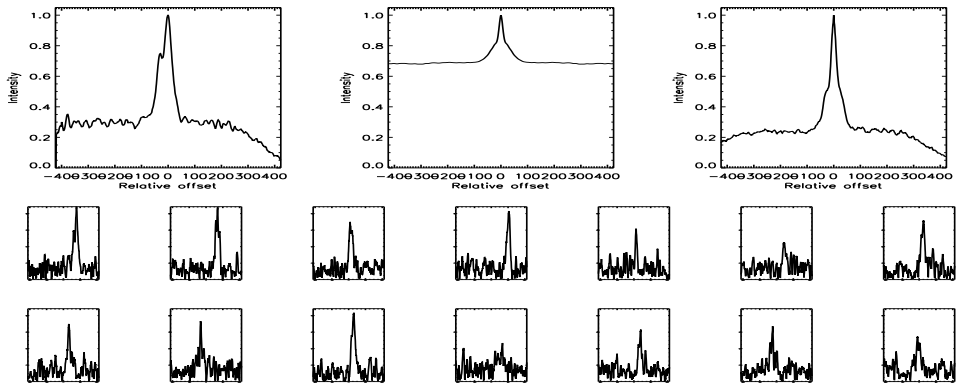

FIGURE B.77: SFP inspection for HD 017382 with S2-E2 on UT 2007/09/18, seq 001

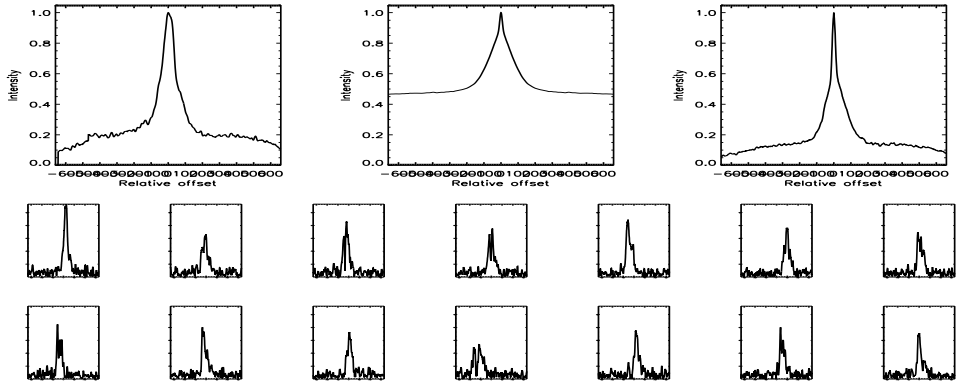

FIGURE B.78: SFP inspection for HD 017382 with S2-W1 on UT 2007/09/17, seq 001

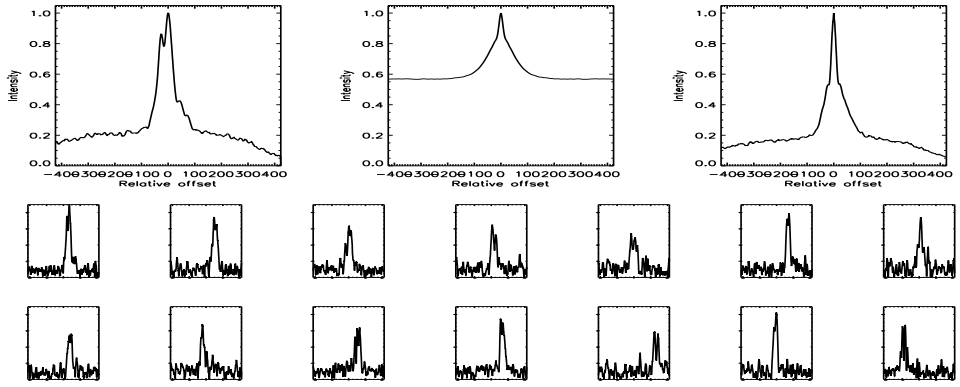

FIGURE B.79: SFP inspection for HD 018143 with S1-E1 on UT 2007/10/31, seq 001

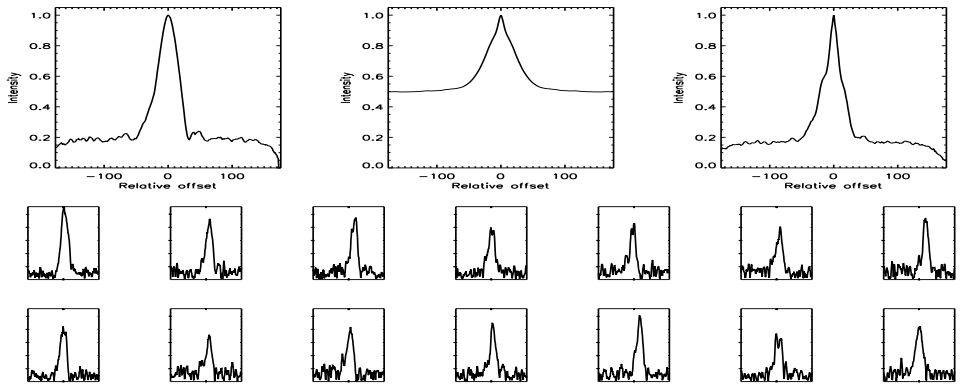

FIGURE B.80: SFP inspection for HD 018143 with S1-E1 on UT 2008/07/23, seq 001

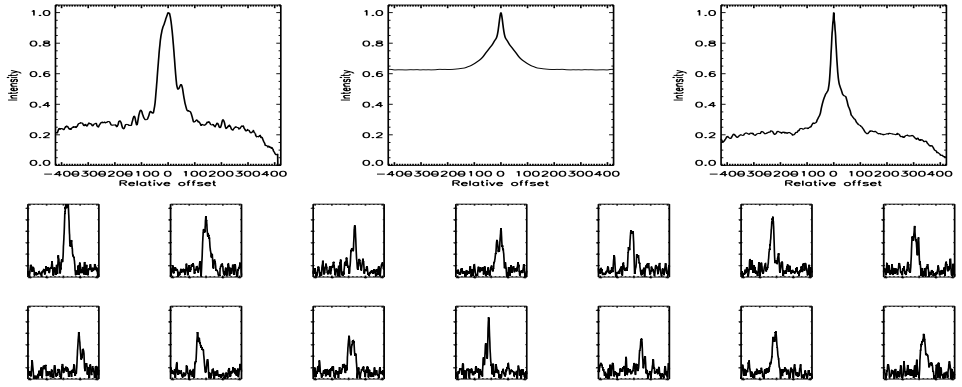

FIGURE B.81: SFP inspection for HD 018143 with S1-W1 on UT 2007/11/01, seq 001

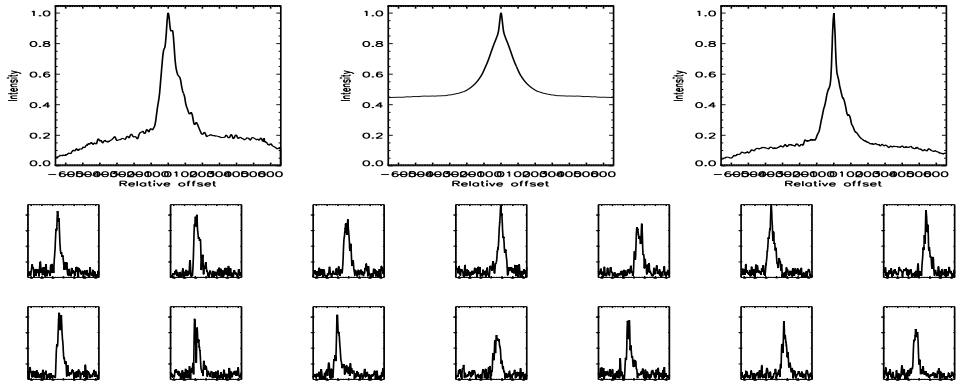

FIGURE B.82: SFP inspection for HD 018143 with S2-W1 on UT 2007/09/17, seq 001

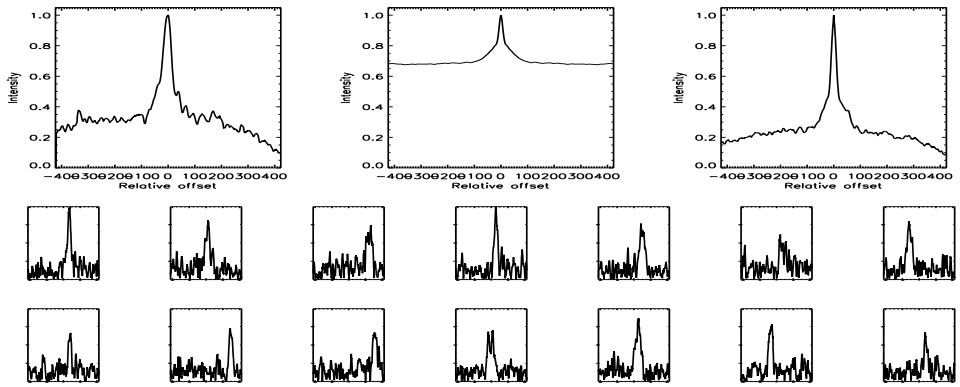

FIGURE B.83: SFP inspection for HD 018632 with S1-E1 on UT 2007/11/01, seq 001

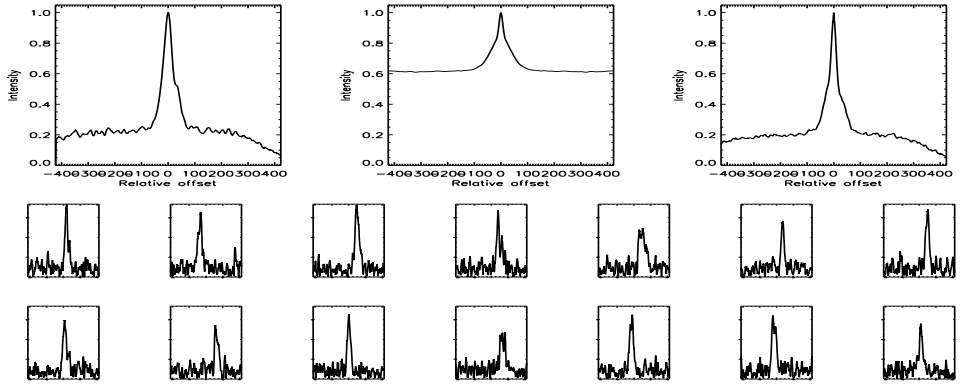

FIGURE B.84: SFP inspection for HD 018632 with S1-W1 on UT 2007/11/01, seq 002

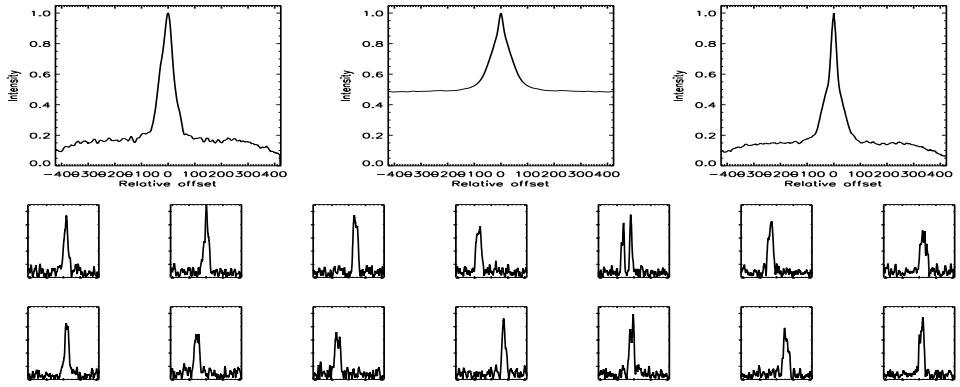

FIGURE B.85: SFP inspection for HD 018757 with S1-E1 on UT 2007/09/16, seq 003

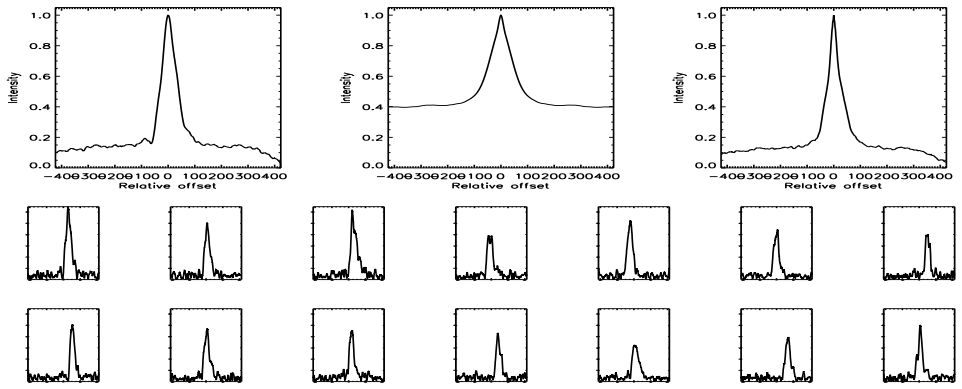

FIGURE B.86: SFP inspection for HD 018757 with S1-W1 on UT 2007/09/16, seq 002

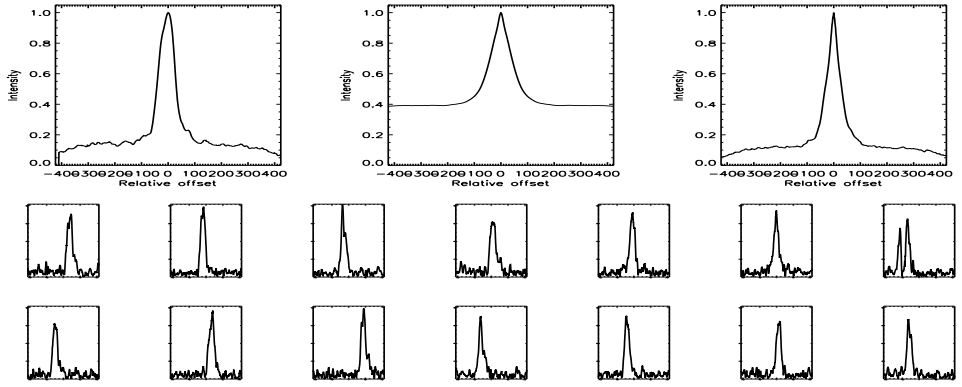

FIGURE B.87: SFP inspection for HD 018757 with S2-E1 on UT 2007/08/20, seq 001

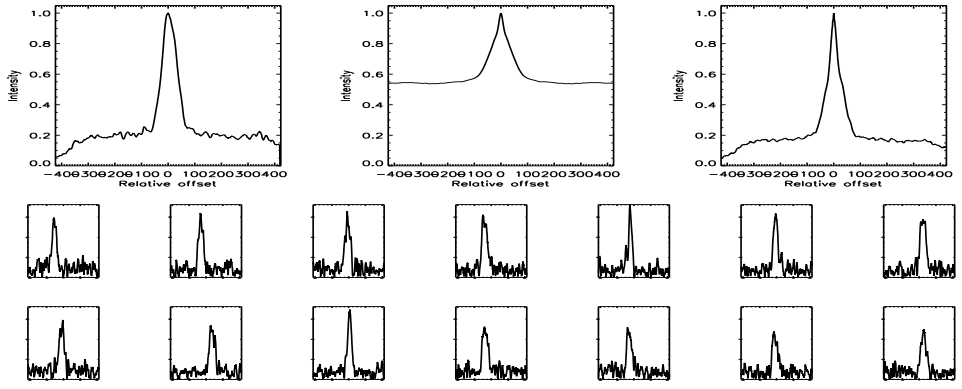

FIGURE B.88: SFP inspection for HD 018803 with S2-E2 on UT 2007/09/18, seq 001

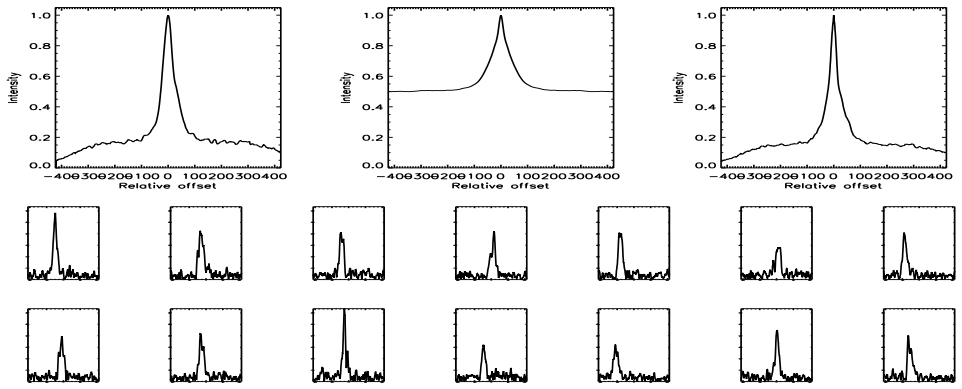

FIGURE B.89: SFP inspection for HD 018803 with S2-W1 on UT 2007/09/17, seq 001

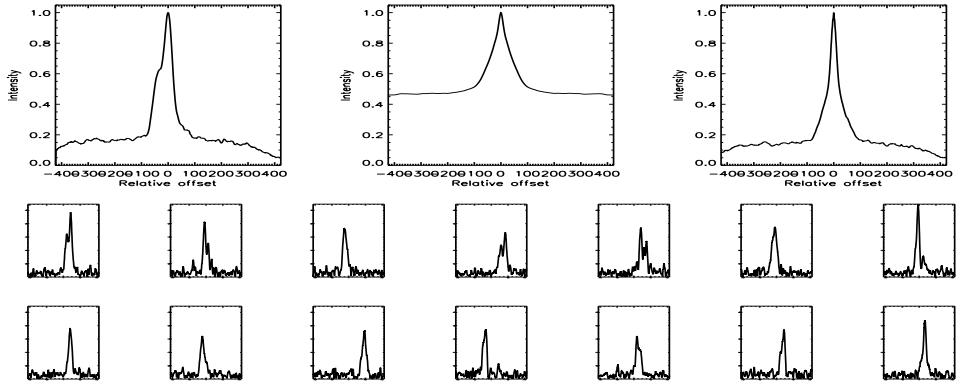

FIGURE B.90: SFP inspection for HD 019994 with S1-E1 on UT 2007/11/01, seq 001

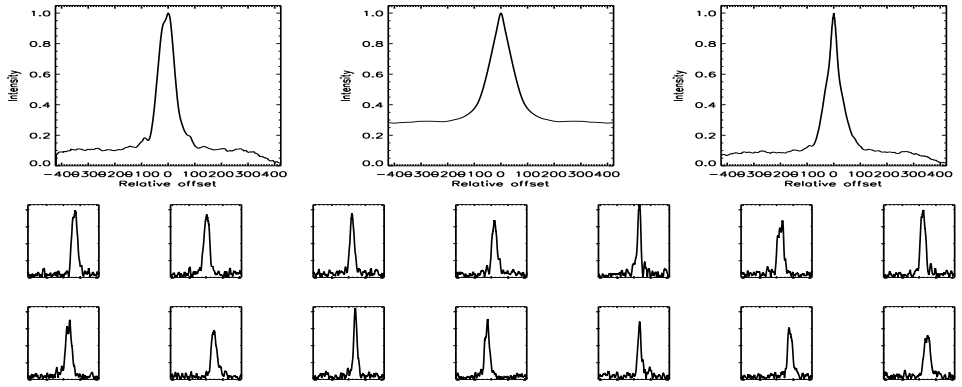

FIGURE B.91: SFP inspection for HD 019994 with S1-W1 on UT 2007/11/01, seq 002

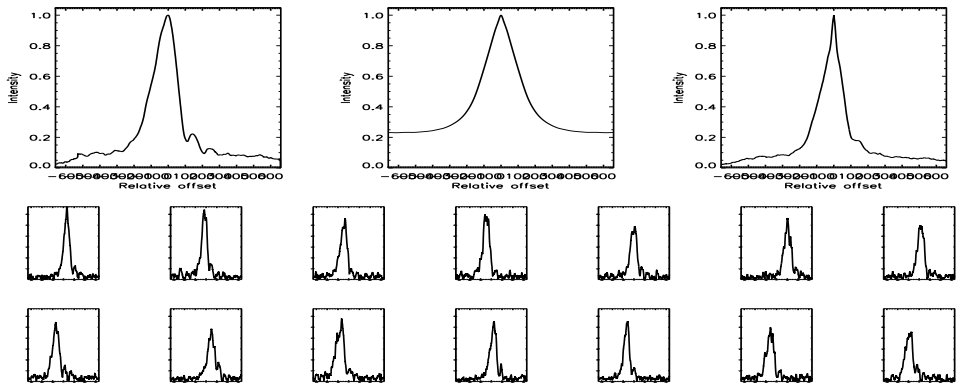

FIGURE B.92: SFP inspection for HD 019994 with S2-E2 on UT 2007/09/27, seq 001

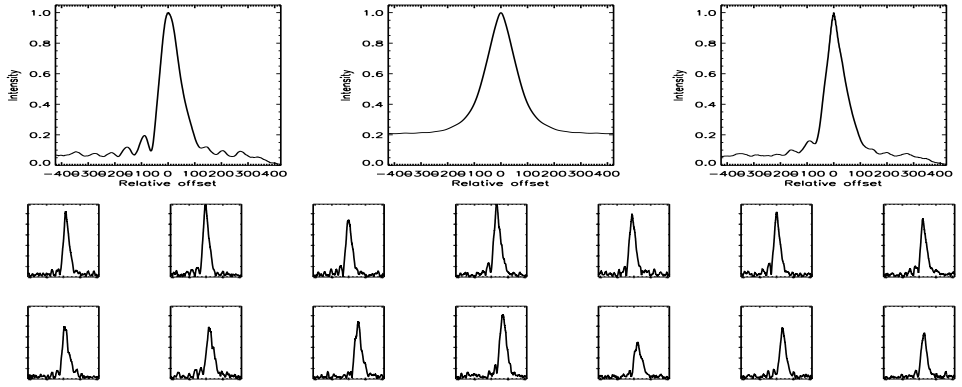

FIGURE B.93: SFP inspection for HD 019994 with S2-E2 on UT 2007/09/27, seq 002

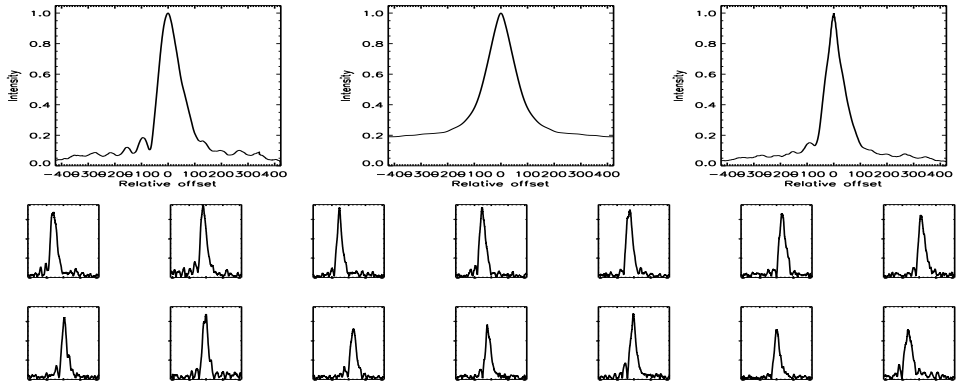

FIGURE B.94: SFP inspection for HD 019994 with S2-E2 on UT 2007/09/27, seq 003

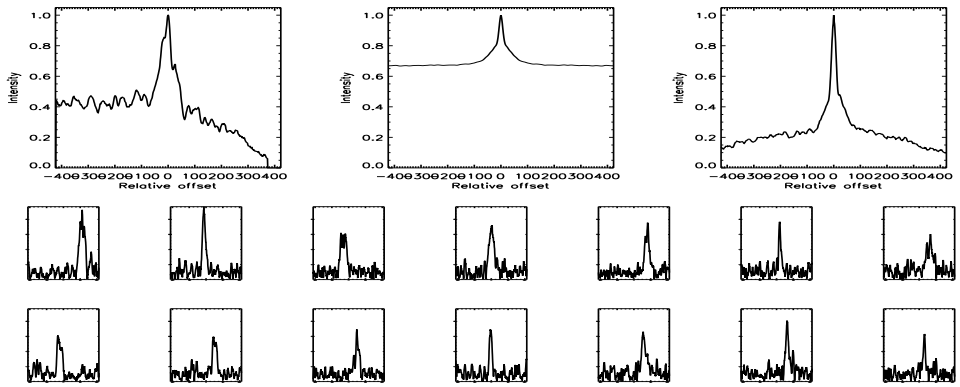

FIGURE B.95: SFP inspection for HD 020165 with S1-E1 on UT 2007/11/01, seq 001

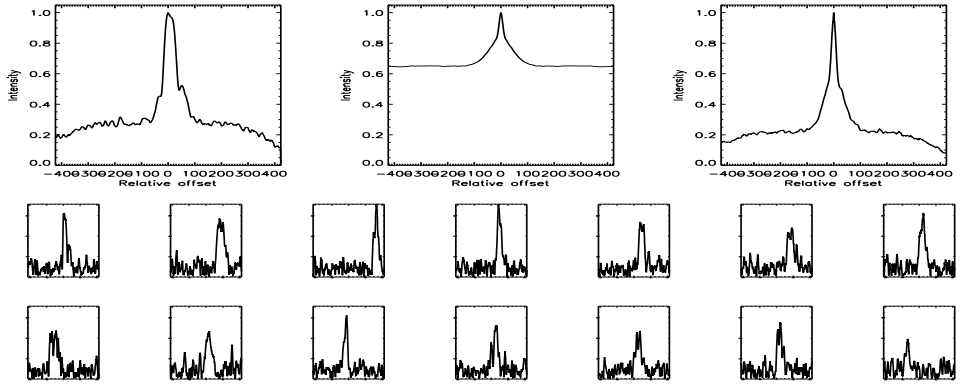

FIGURE B.96: SFP inspection for HD 020165 with S1-W1 on UT 2007/11/01, seq 002

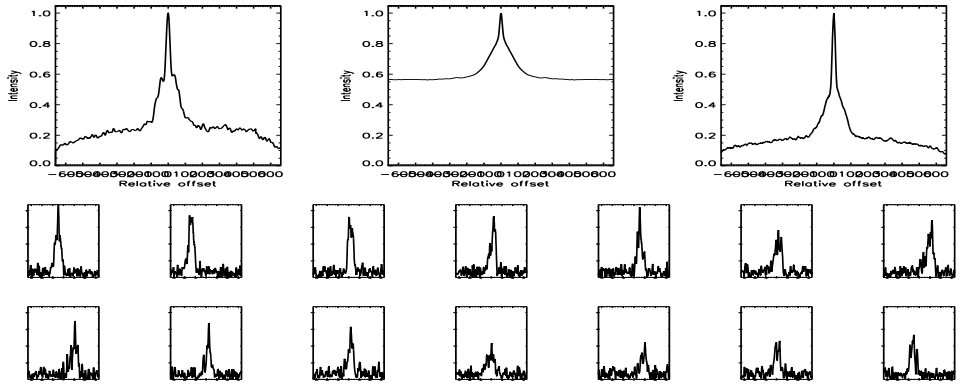

FIGURE B.97: SFP inspection for HD 020619 with S1-E1 on UT 2007/11/01, seq 001

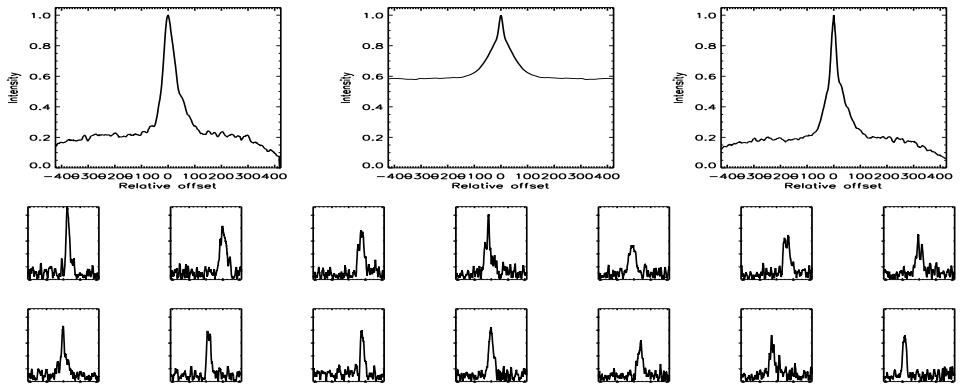

FIGURE B.98: SFP inspection for HD 020619 with S1-W1 on UT 2007/11/01, seq 002

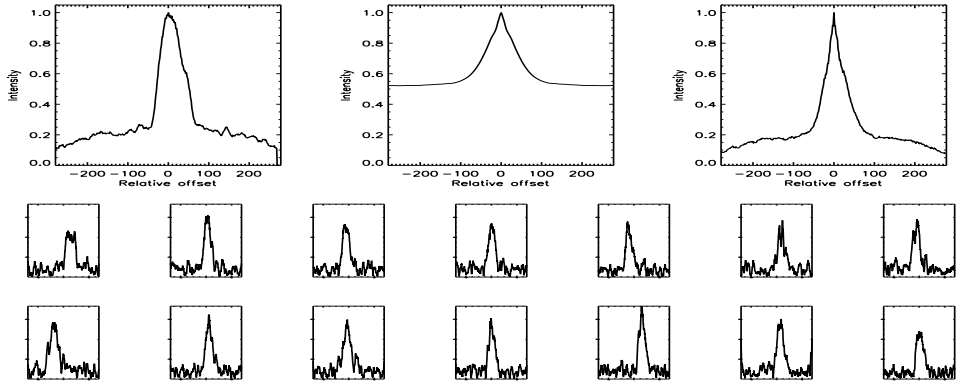

FIGURE B.99: SFP inspection for HD 022049 with S2-E2 on UT 2007/09/27, seq 001

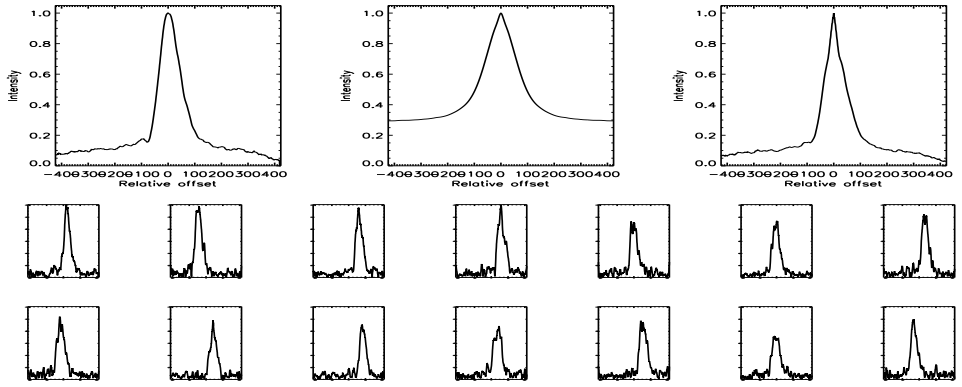

FIGURE B.100: SFP inspection for HD 022049 with S2-E2 on UT 2007/09/27, seq 002

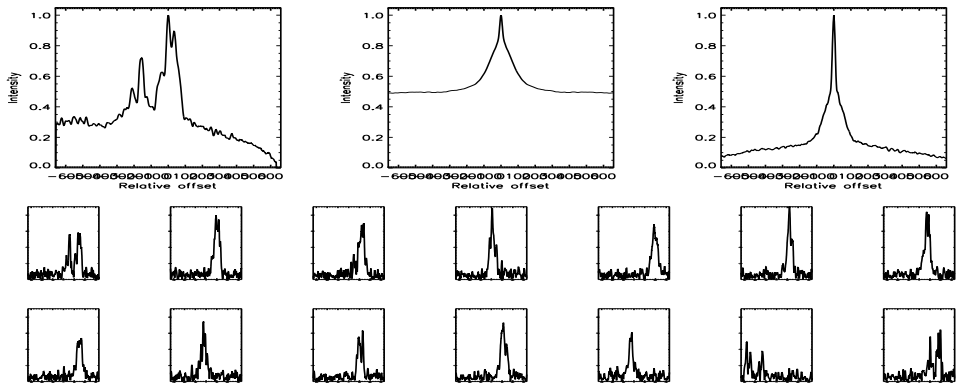

FIGURE B.101: SFP inspection for HD 022879 with S1-E1 on UT 2007/11/01, seq 001

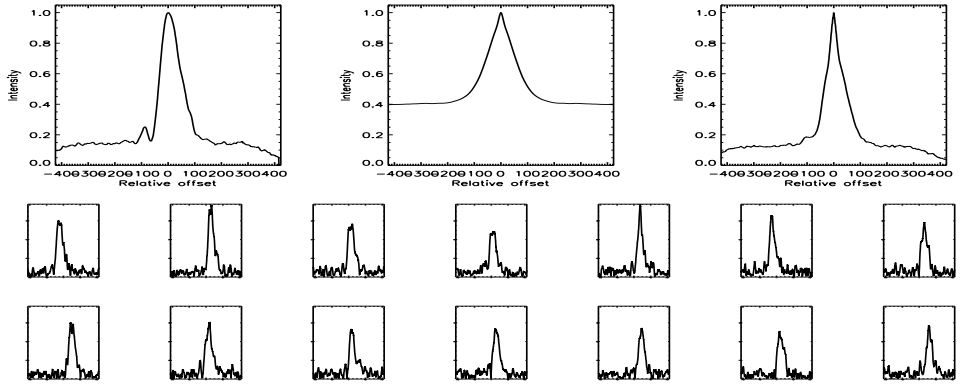

FIGURE B.102: SFP inspection for HD 022879 with S2-E2 on UT 2007/09/27, seq 002

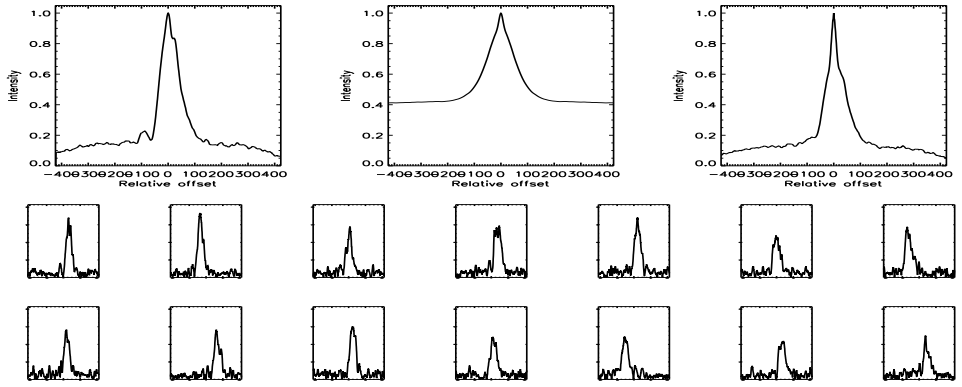

FIGURE B.103: SFP inspection for HD 022879 with S2-E2 on UT 2007/09/27, seq 003

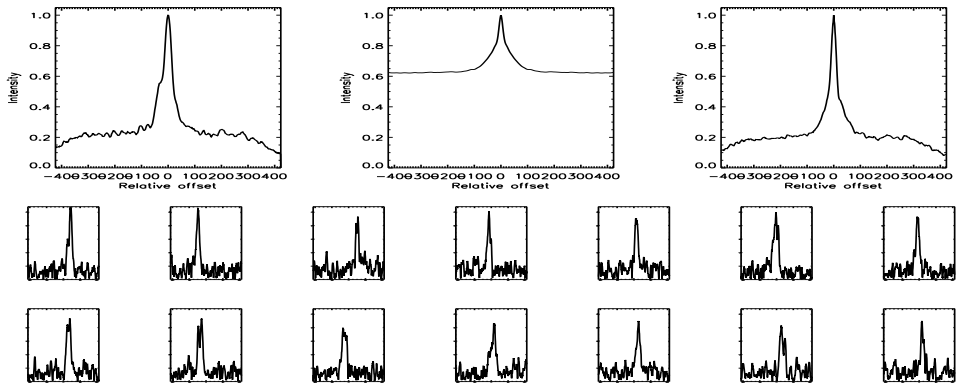

FIGURE B.104: SFP inspection for HD 024238 with S1-E1 on UT 2007/09/16, seq 002

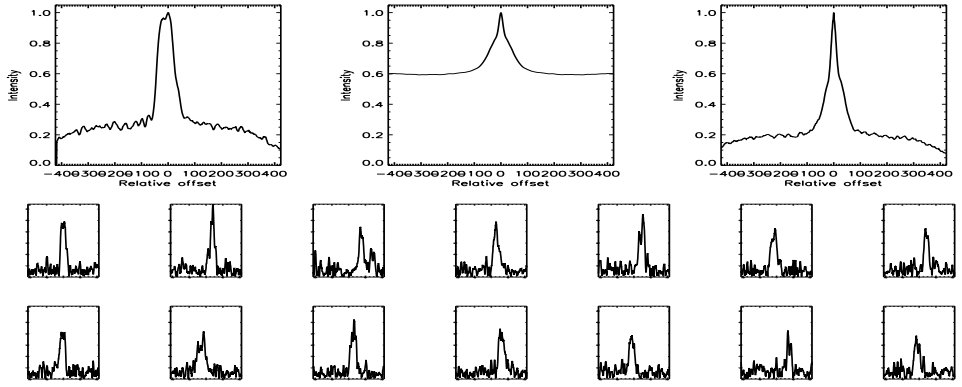

FIGURE B.105: SFP inspection for HD 024238 with S1-W1 on UT 2007/09/16, seq 001

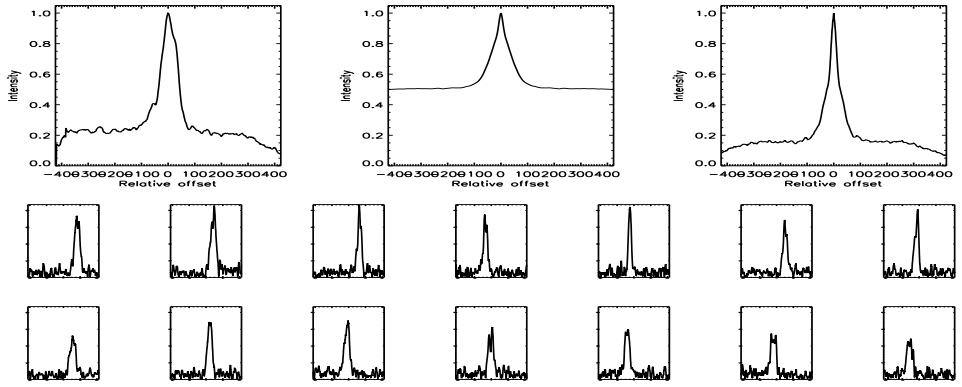

FIGURE B.106: SFP inspection for HD 024409 with S1-E1 on UT 2007/09/16, seq 002

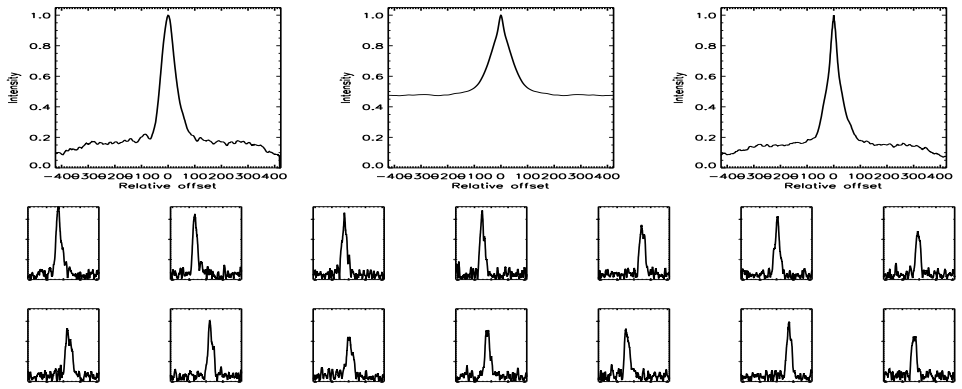

FIGURE B.107: SFP inspection for HD 024409 with S1-W1 on UT 2007/09/16, seq 001

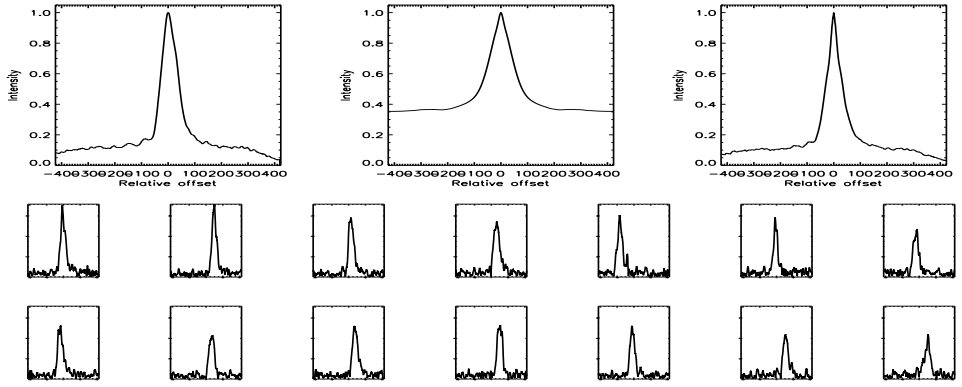

FIGURE B.108: SFP inspection for HD 024409 with S2-E1 on UT 2007/08/20, seq 001

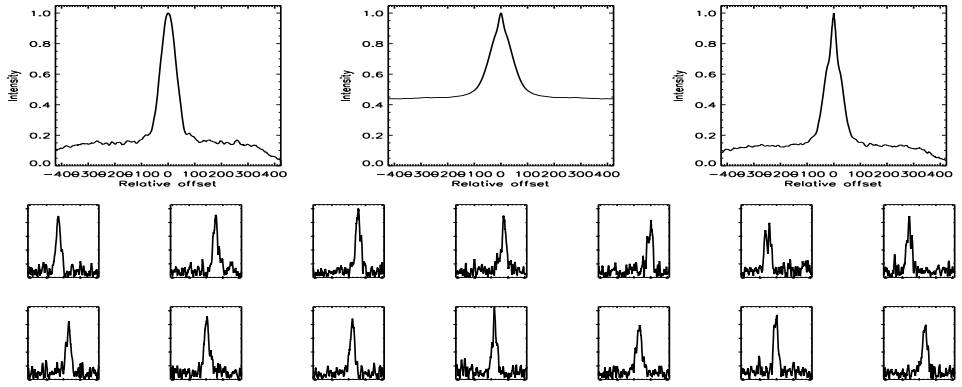

FIGURE B.109: SFP inspection for HD 024496 with S1-E1 on UT 2007/10/31, seq 001

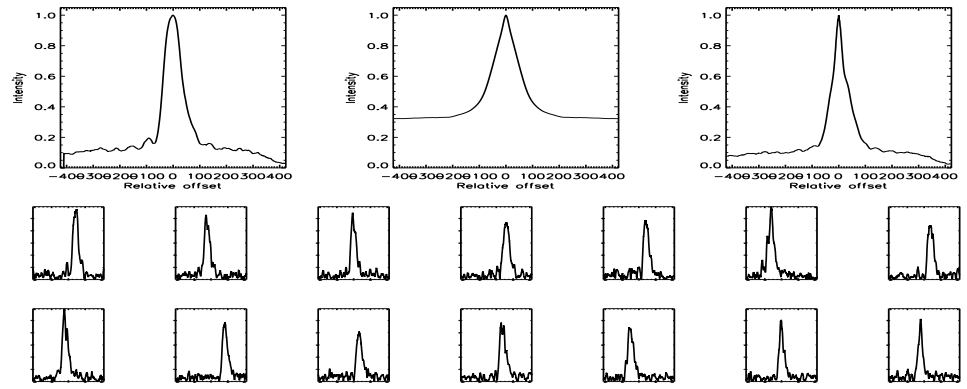

FIGURE B.110: SFP inspection for HD 024496 with S1-W1 on UT 2007/10/31, seq 002

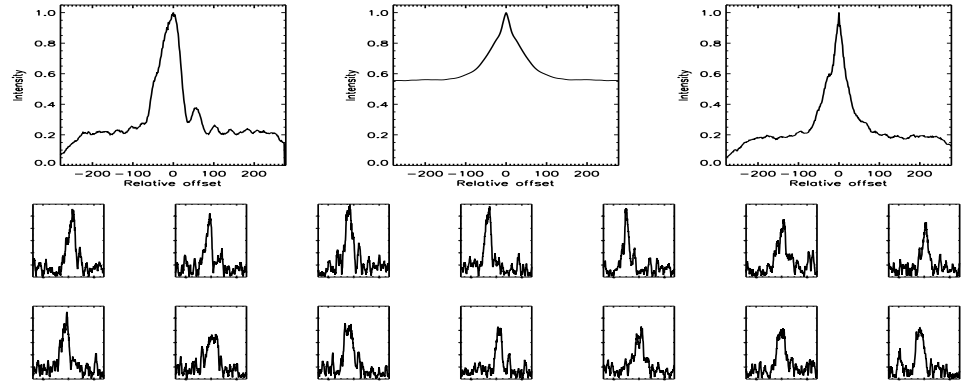

FIGURE B.111: SFP inspection for HD 024496 with S2-E2 on UT 2007/09/26, seq 001

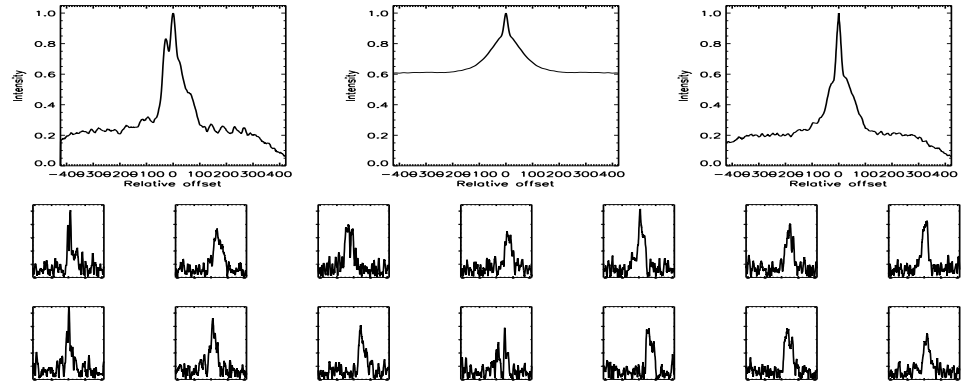

FIGURE B.112: SFP inspection for HD 024496 with S2-E2 on UT 2007/09/27, seq 001

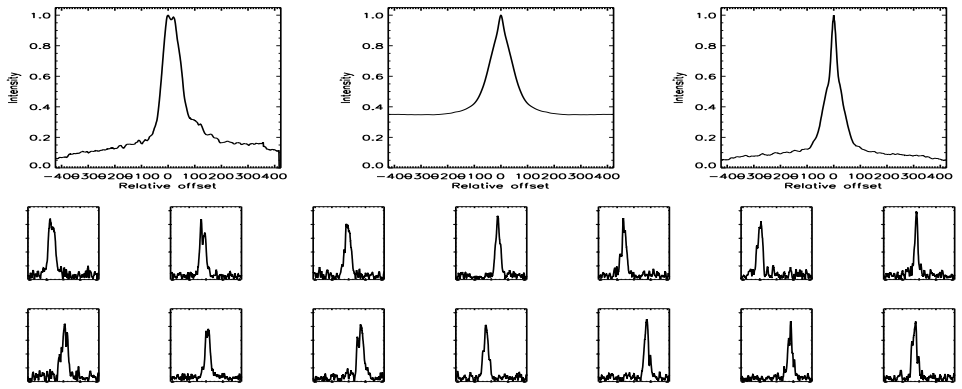

FIGURE B.113: SFP inspection for HD 025457 with S1-E1 on UT 2007/10/31, seq 001

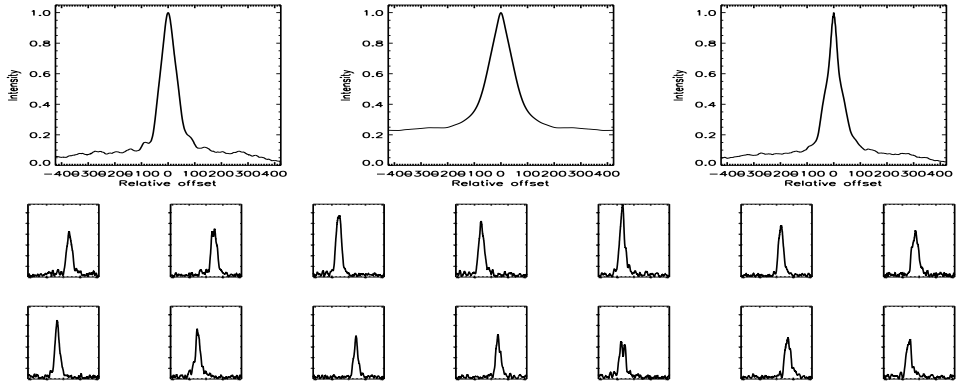

FIGURE B.114: SFP inspection for HD 025457 with S1-W1 on UT 2007/10/31, seq 002

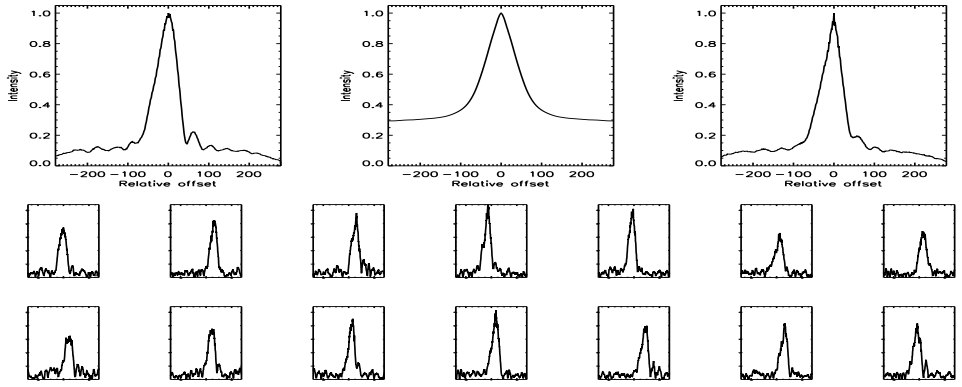

FIGURE B.115: SFP inspection for HD 025457 with S2-E2 on UT 2007/09/26, seq 001

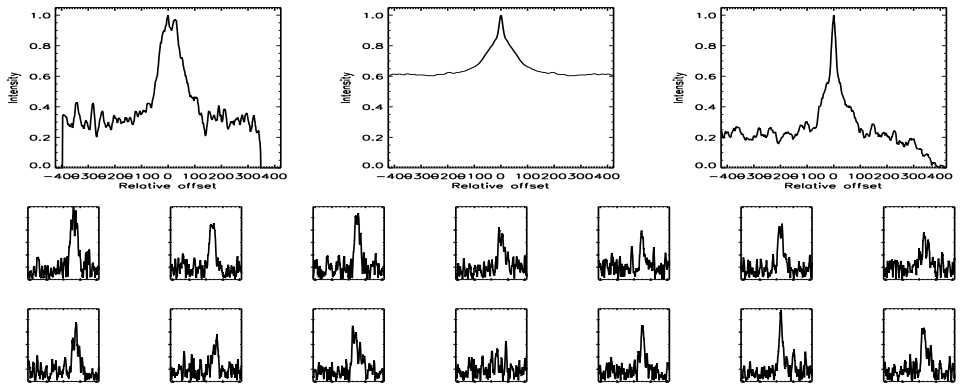

FIGURE B.116: SFP inspection for HD 025457 with S2-E2 on UT 2007/09/27, seq 001

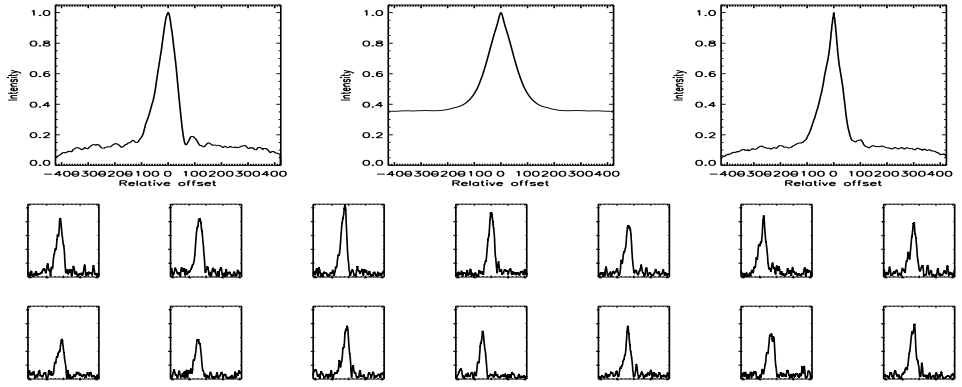

FIGURE B.117: SFP inspection for HD 025457 with S2-E2 on UT 2007/09/27, seq 002

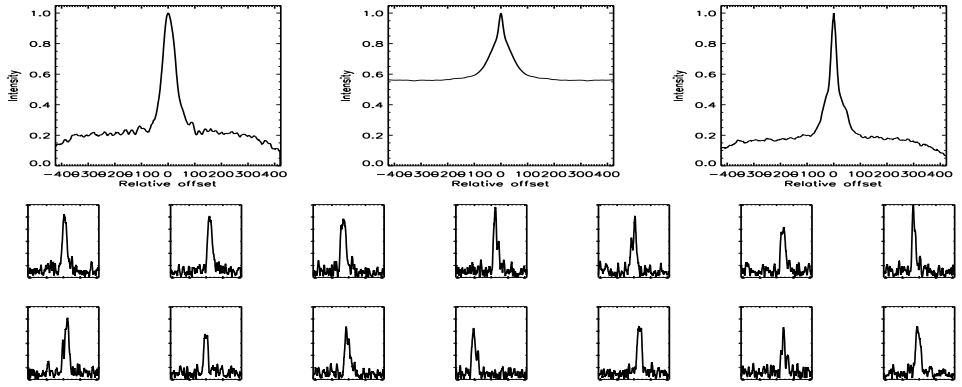

FIGURE B.118: SFP inspection for HD 025665 with S1-E1 on UT 2007/09/16, seq 002

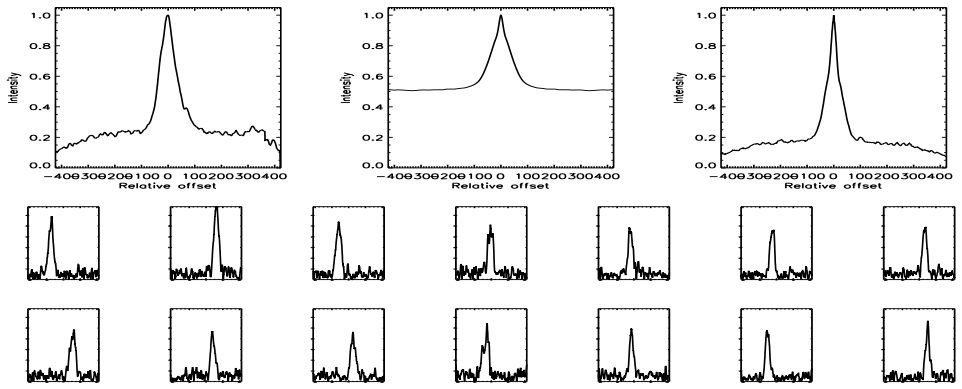

FIGURE B.119: SFP inspection for HD 025665 with S1-W1 on UT 2007/09/16, seq 001

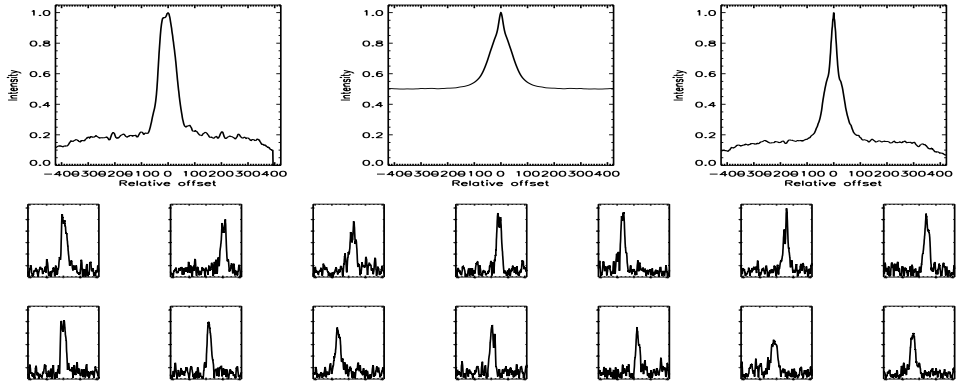

FIGURE B.120: SFP inspection for HD 026913 with S1-E1 on UT 2007/10/31, seq 001

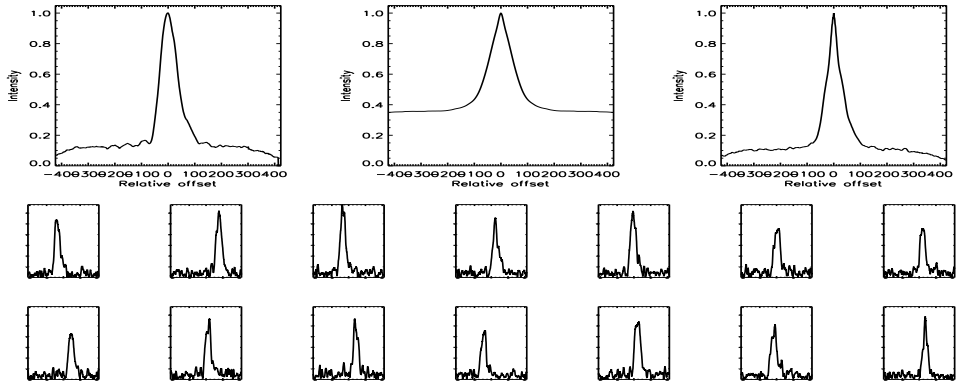

FIGURE B.121: SFP inspection for HD 026913 with S1-W1 on UT 2007/10/31, seq 002

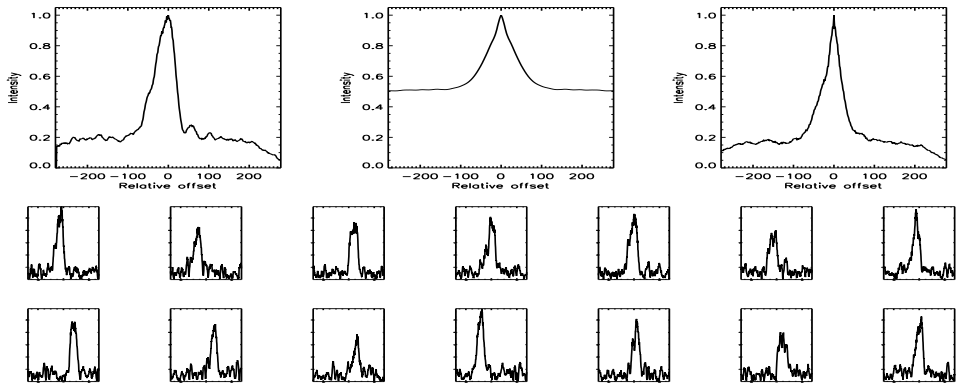

FIGURE B.122: SFP inspection for HD 026913 with S2-E2 on UT 2007/09/26, seq 001

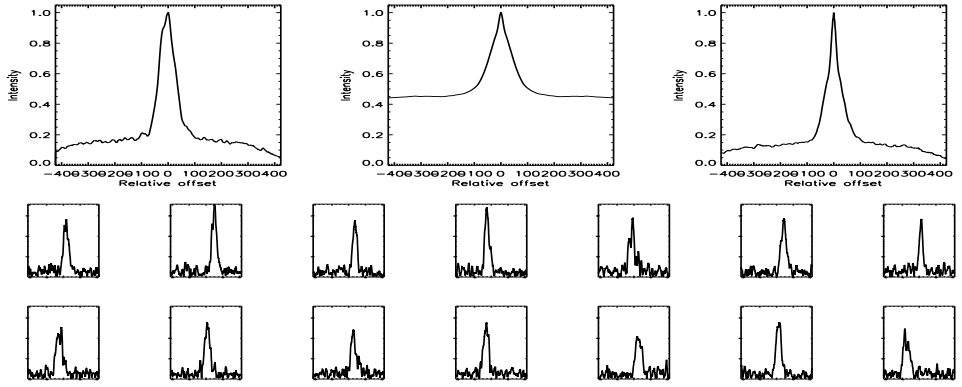

FIGURE B.123: SFP inspection for HD 026923 with S1-E1 on UT 2007/10/31, seq 001

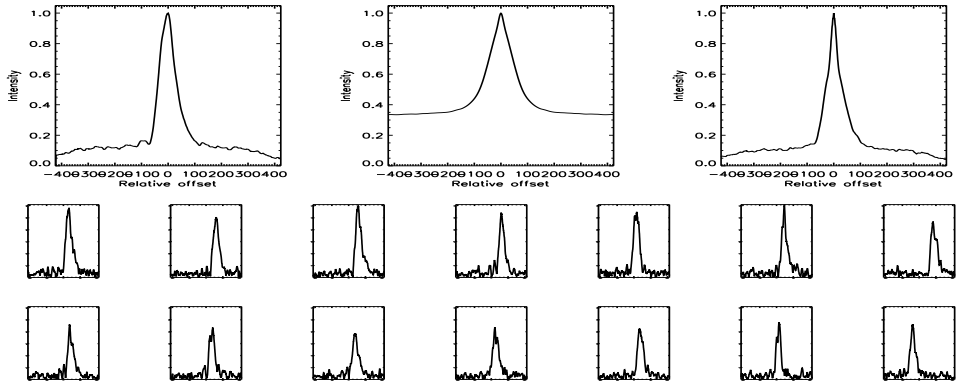

FIGURE B.124: SFP inspection for HD 026923 with S1-W1 on UT 2007/10/31, seq 002

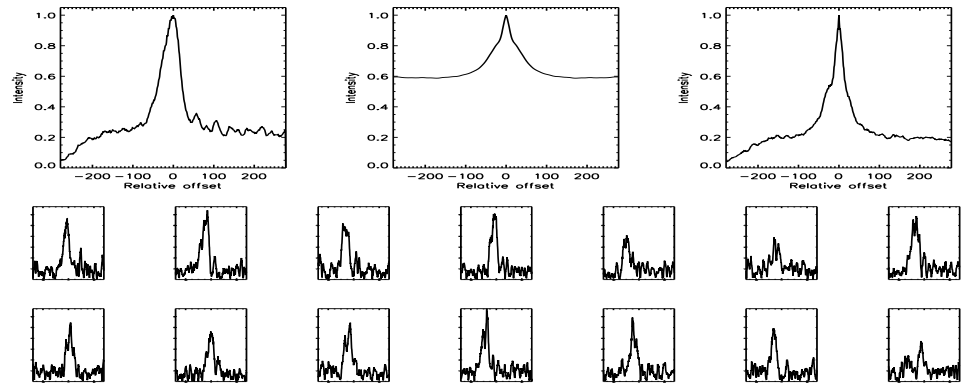

FIGURE B.125: SFP inspection for HD 026923 with S2-E2 on UT 2007/09/26, seq 001

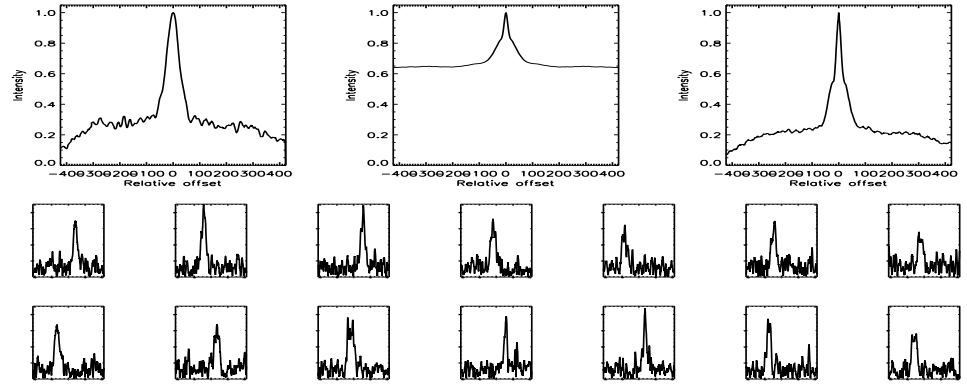

FIGURE B.126: SFP inspection for HD 029883 with S2-E2 on UT 2007/09/18, seq 001

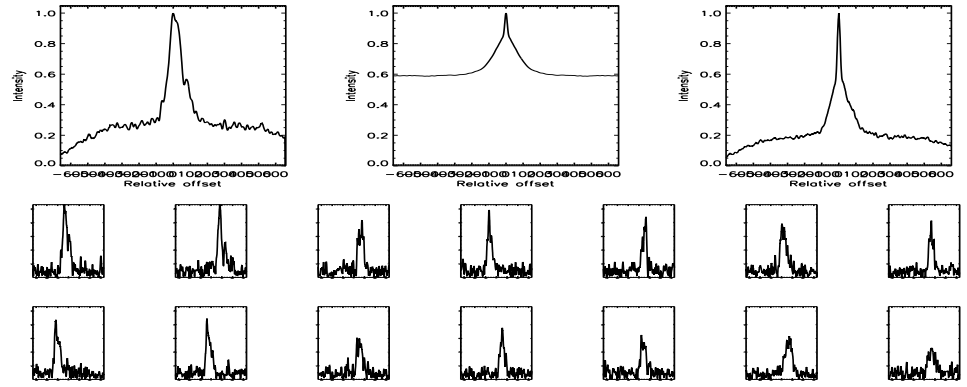

FIGURE B.127: SFP inspection for HD 029883 with S2-W1 on UT 2007/09/17, seq 001

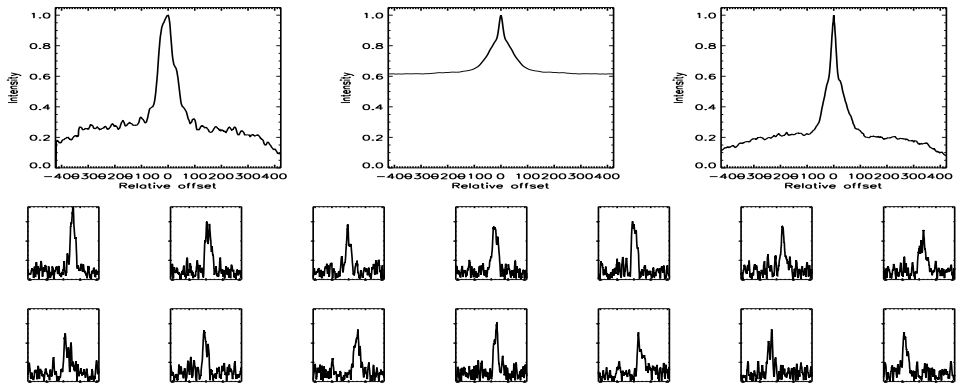

FIGURE B.128: SFP inspection for HD 032850 with S1-E1 on UT 2007/10/31, seq 001

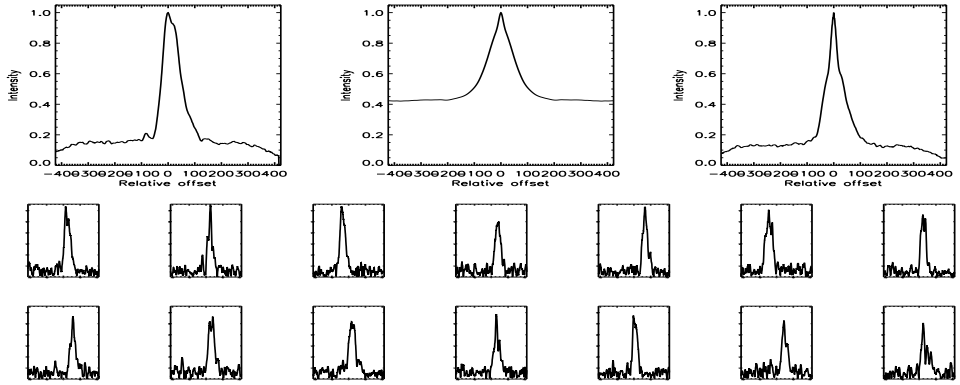

FIGURE B.129: SFP inspection for HD 032850 with S1-W1 on UT 2007/10/31, seq 002

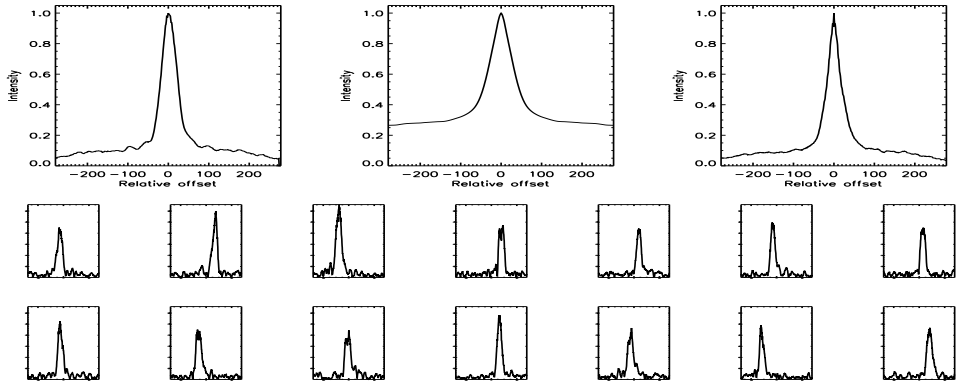

FIGURE B.130: SFP inspection for HD 032923 with S1-E1 on UT 2007/02/25, seq 001

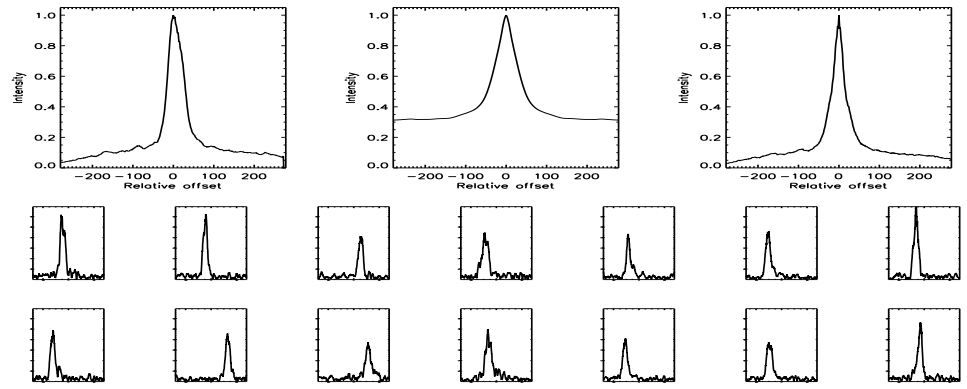

FIGURE B.131: SFP inspection for HD 032923 with S1-E1 on UT 2007/02/25, seq 002

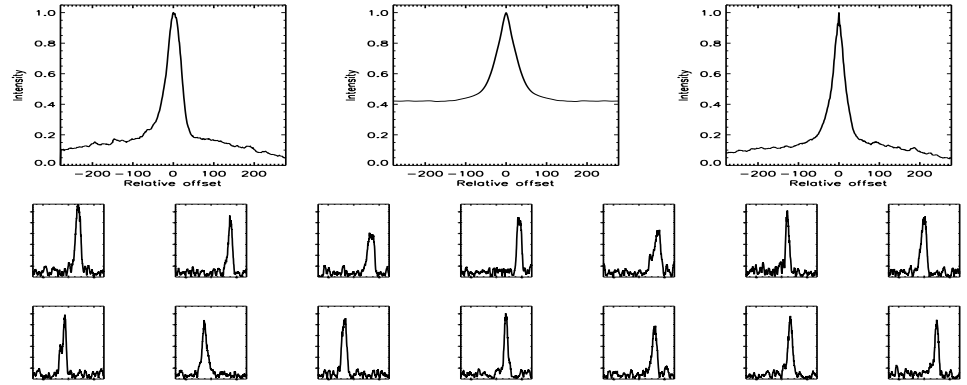

FIGURE B.132: SFP inspection for HD 032923 with S1-E1 on UT 2007/03/11, seq 001

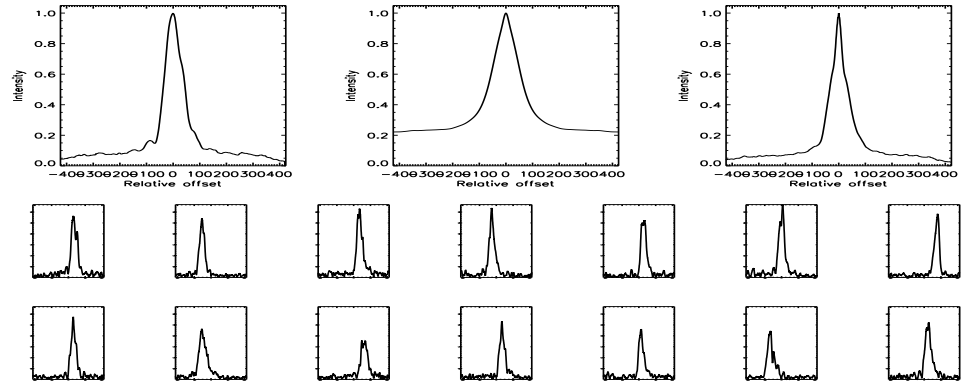

FIGURE B.133: SFP inspection for HD 032923 with S1-E1 on UT 2007/10/31, seq 001

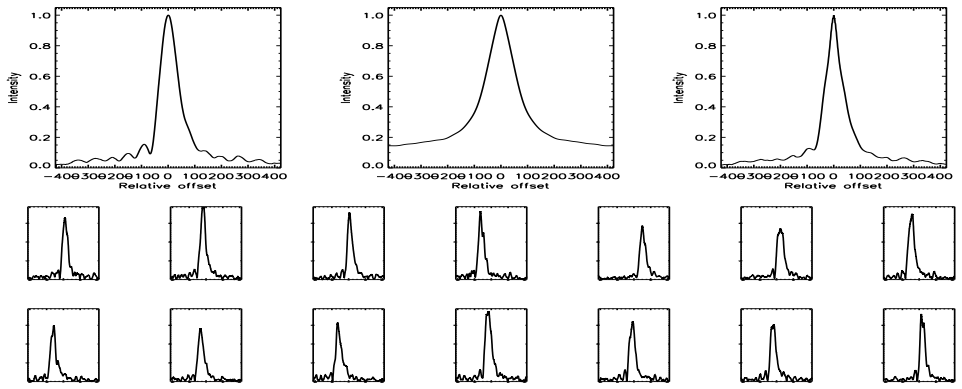

FIGURE B.134: SFP inspection for HD 032923 with S1-W1 on UT 2007/10/31, seq 002

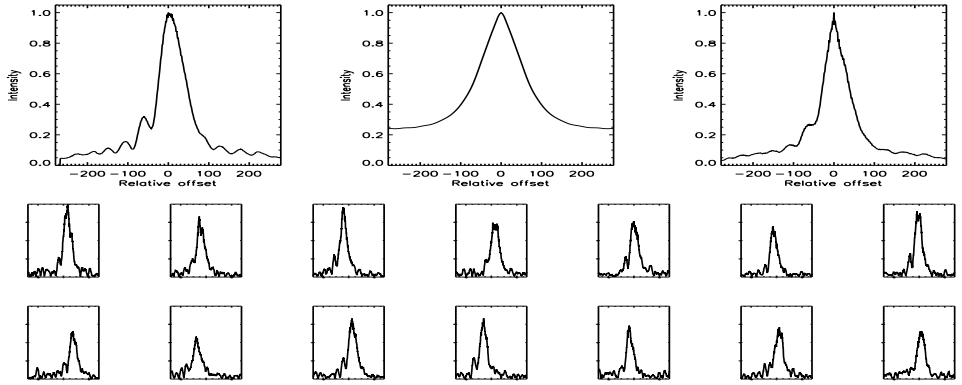

FIGURE B.135: SFP inspection for HD 032923 with S2-E2 on UT 2007/09/26, seq 001

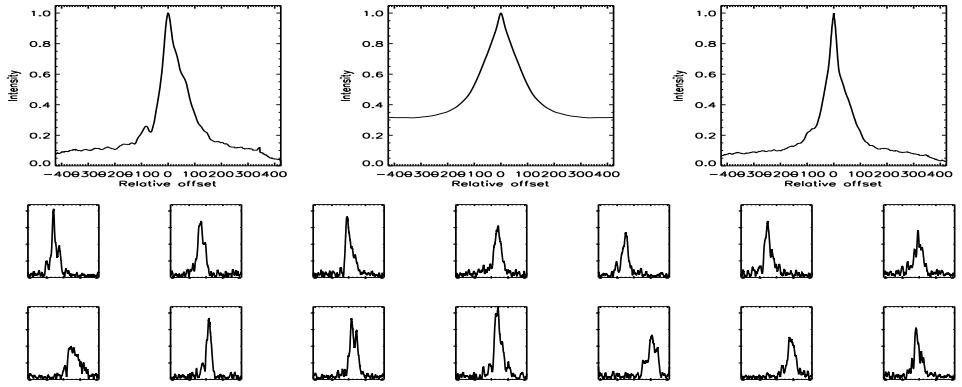

FIGURE B.136: SFP inspection for HD 032923 with S2-E2 on UT 2007/09/27, seq 001

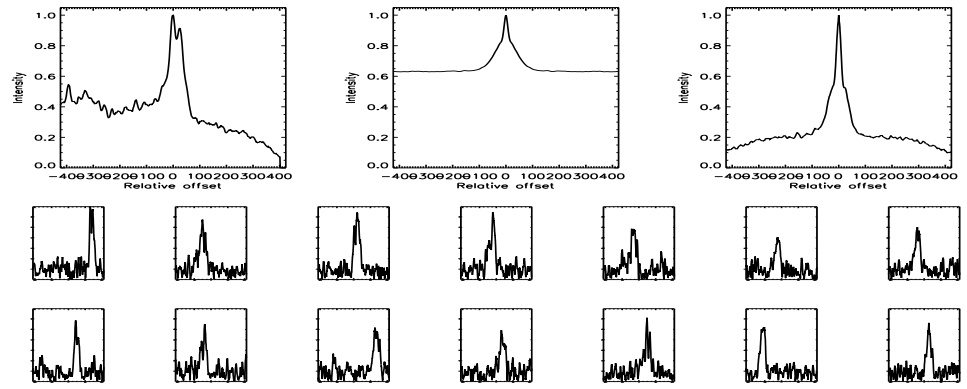

FIGURE B.137: SFP inspection for HD 035112 with S1-E1 on UT 2007/10/31, seq 001

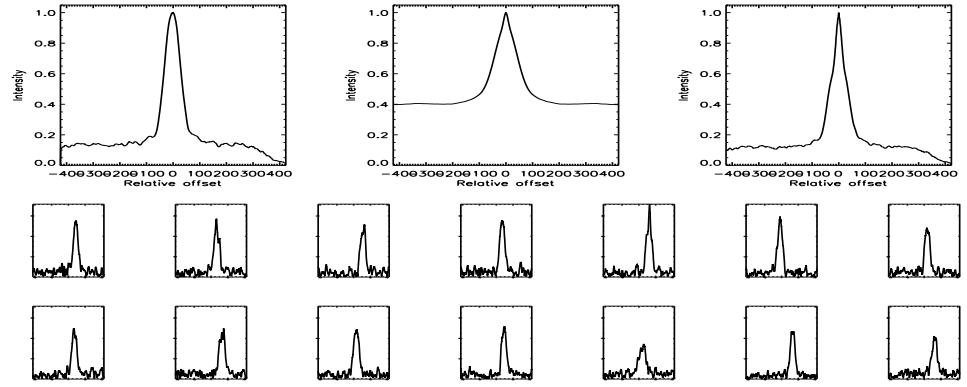

FIGURE B.138: SFP inspection for HD 035112 with S1-W1 on UT 2007/10/31, seq 002

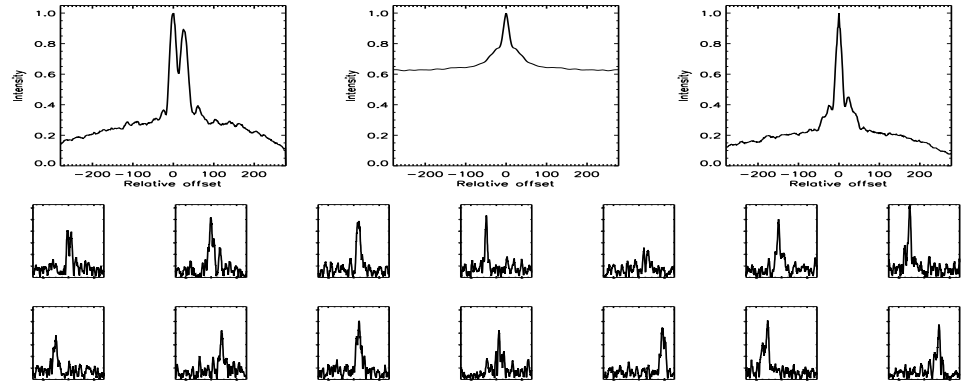

FIGURE B.139: SFP inspection for HD 037008 with S1-E1 on UT 2007/01/25, seq 001

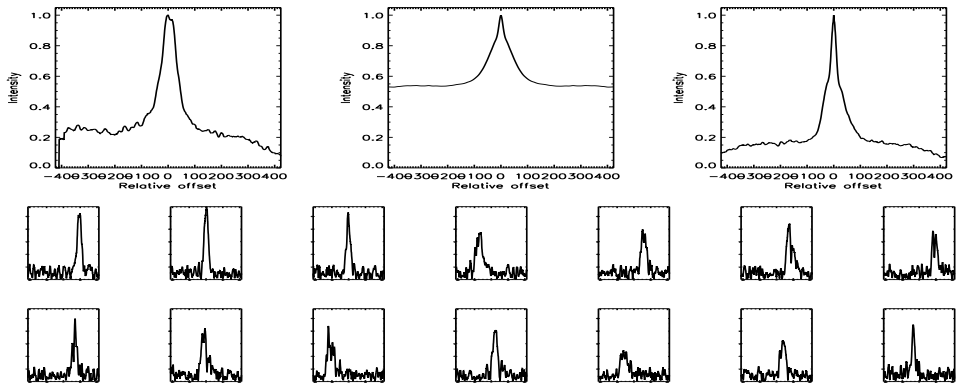

FIGURE B.140: SFP inspection for HD 037008 with S1-W1 on UT 2007/11/01, seq 002

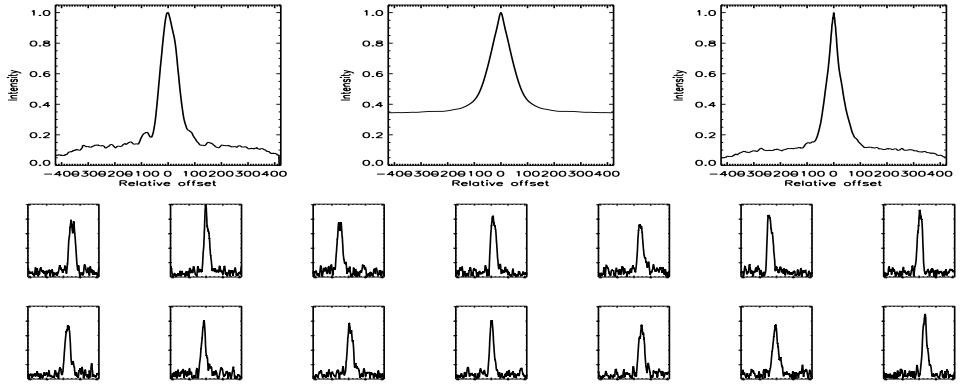

FIGURE B.141: SFP inspection for HD 037008 with S2-E2 on UT 2007/11/19, seq 001

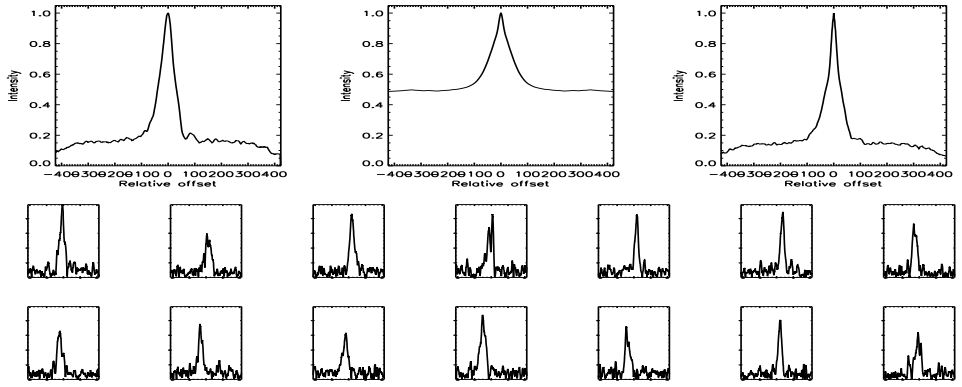

FIGURE B.142: SFP inspection for HD 037008 with S2-E2 on UT 2007/11/19, seq 002

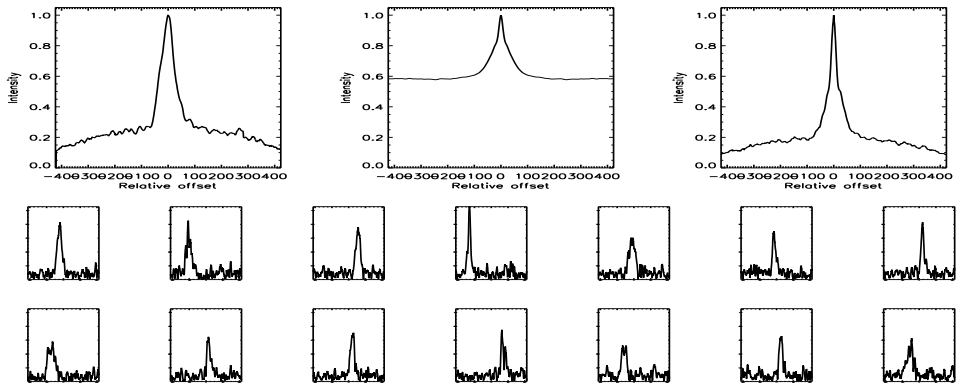

FIGURE B.143: SFP inspection for HD 037008 with S2-E2 on UT 2007/11/27, seq 001

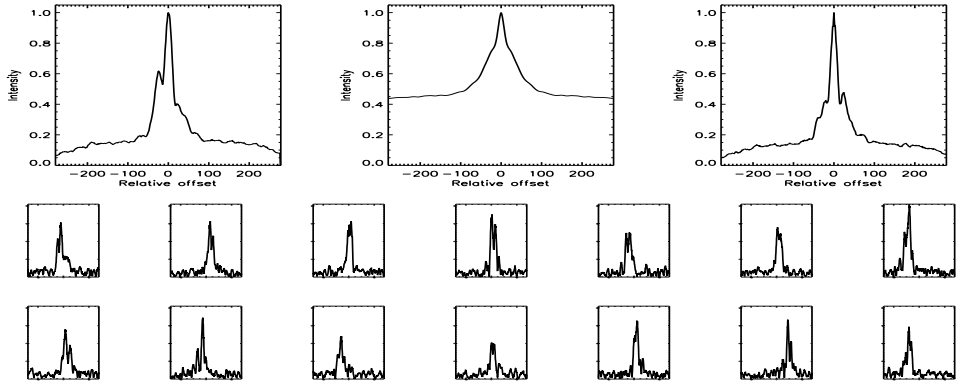

FIGURE B.144: SFP inspection for HD 037394 with S1-E1 on UT 2007/01/25, seq 001

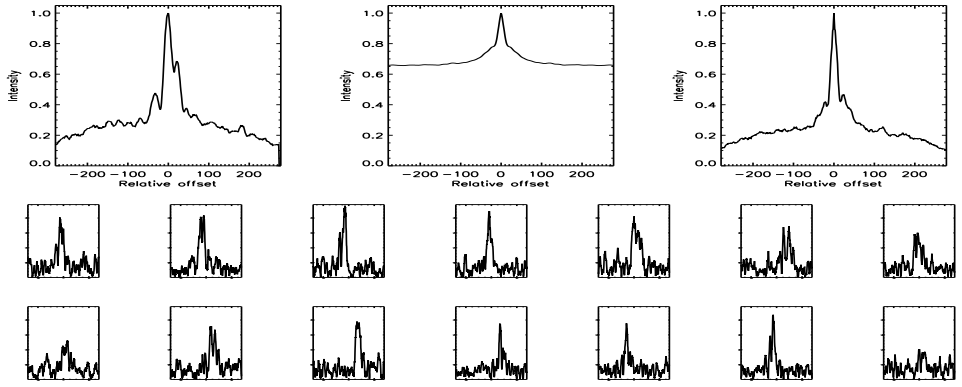

FIGURE B.145: SFP inspection for HD 037394 with S1-E1 on UT 2007/01/26, seq 002

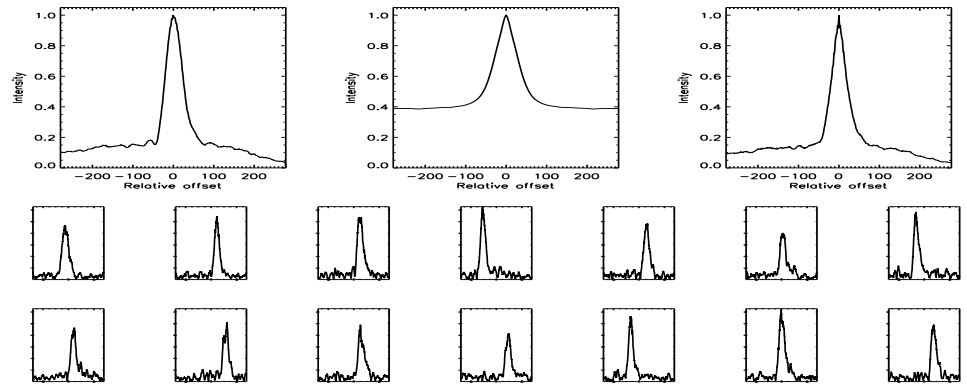

FIGURE B.146: SFP inspection for HD 037394 with S1-E1 on UT 2007/04/14, seq 001

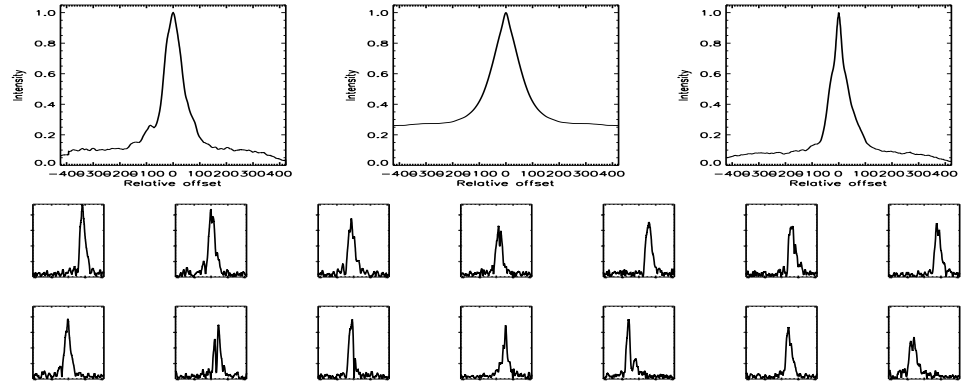

FIGURE B.147: SFP inspection for HD 037394 with S1-W1 on UT 2007/11/01, seq 001

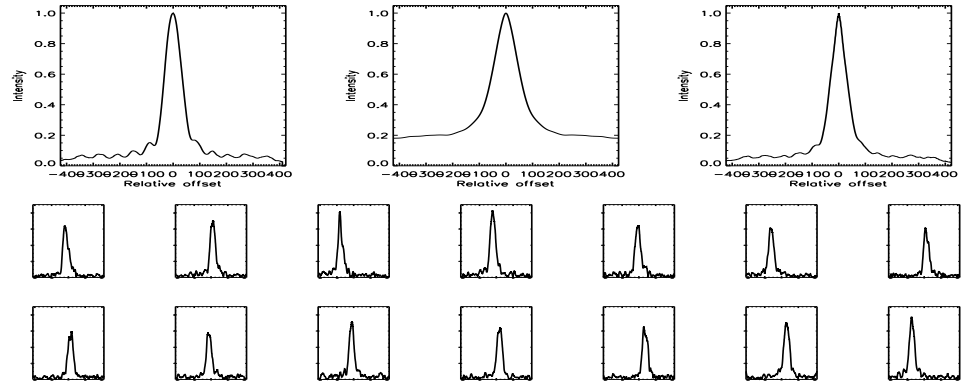

FIGURE B.148: SFP inspection for HD 037394 with S2-E2 on UT 2007/11/19, seq 003

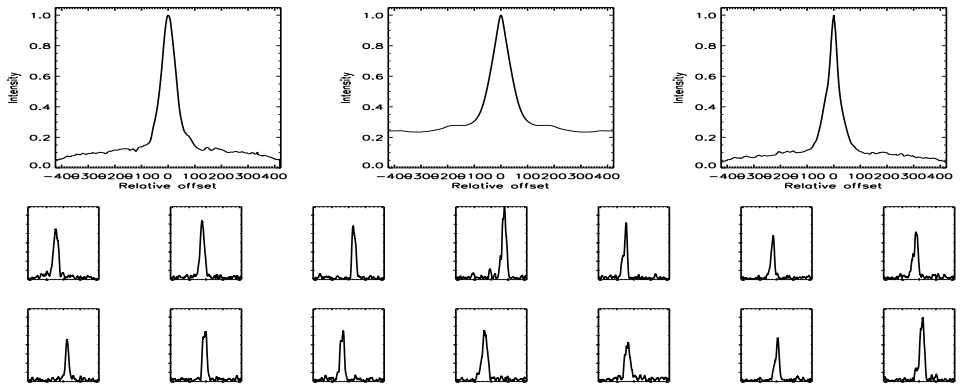

FIGURE B.149: SFP inspection for HD 037394 with S2-E2 on UT 2007/11/19, seq 004

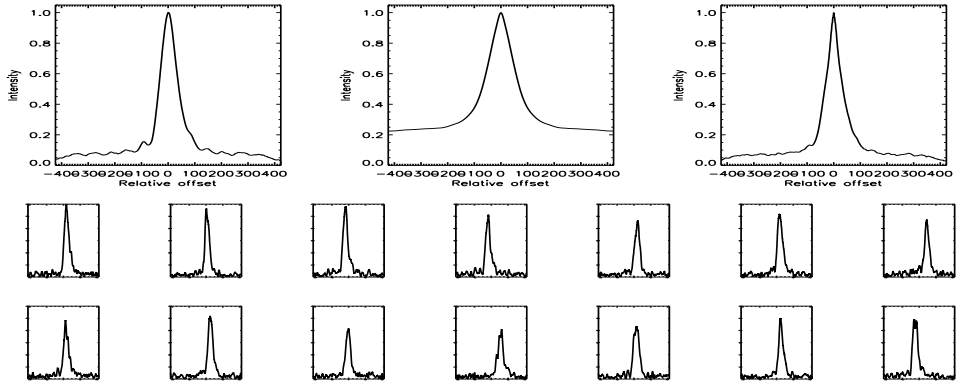

FIGURE B.150: SFP inspection for HD 037394 with S2-E2 on UT 2007/11/19, seq 005

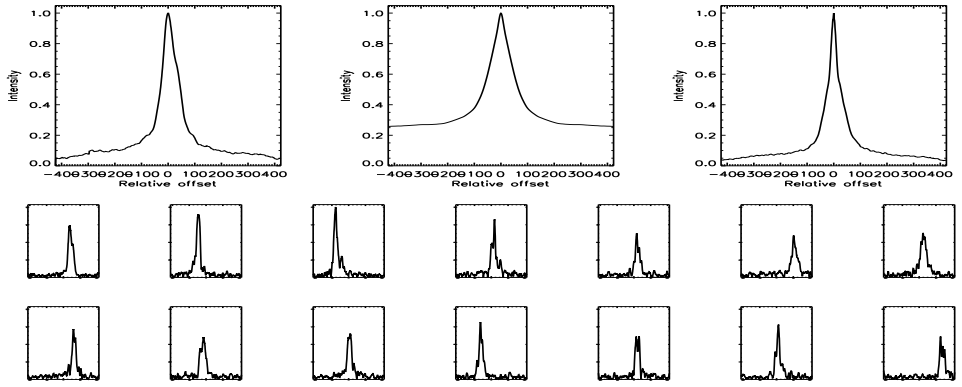

FIGURE B.151: SFP inspection for HD 037394 with S2-E2 on UT 2007/11/27, seq 001

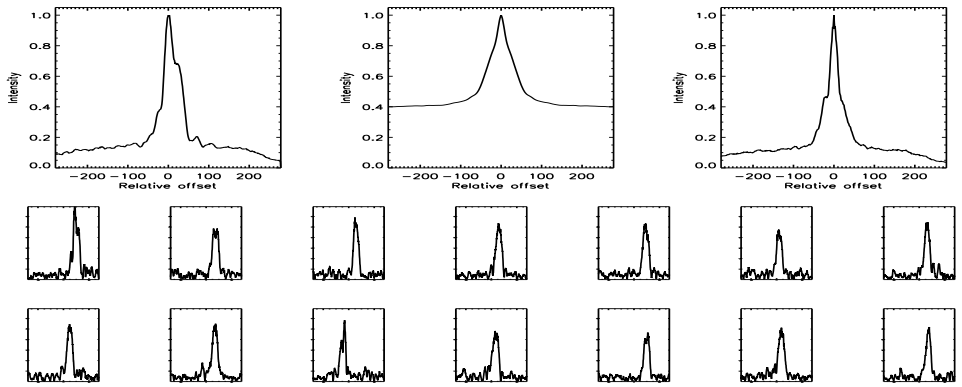

FIGURE B.152: SFP inspection for HD 038230 with S1-E1 on UT 2007/01/25, seq 001

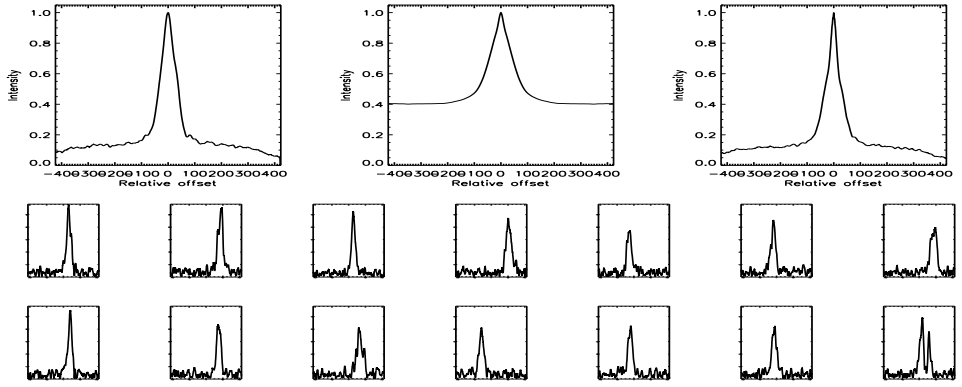

FIGURE B.153: SFP inspection for HD 038230 with S1-W1 on UT 2007/11/01, seq 001

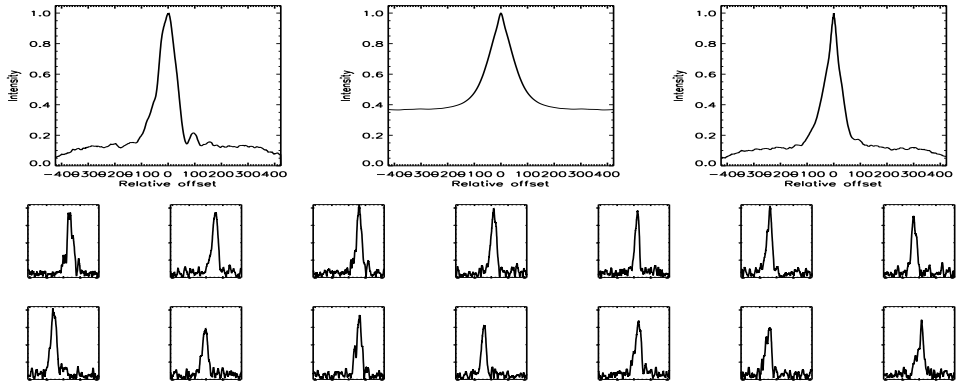

FIGURE B.154: SFP inspection for HD 038230 with S2-E2 on UT 2007/11/19, seq 002

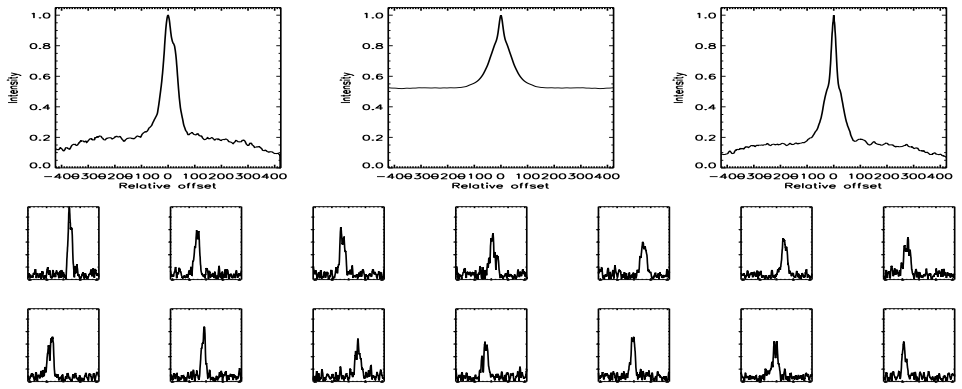

FIGURE B.155: SFP inspection for HD 038230 with S2-E2 on UT 2007/11/27, seq 001

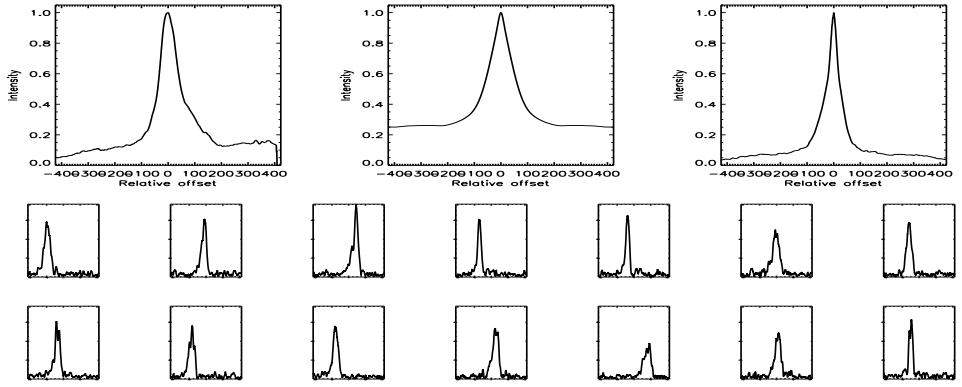

FIGURE B.156: SFP inspection for HD 038858 with S1-E1 on UT 2007/10/31, seq 001

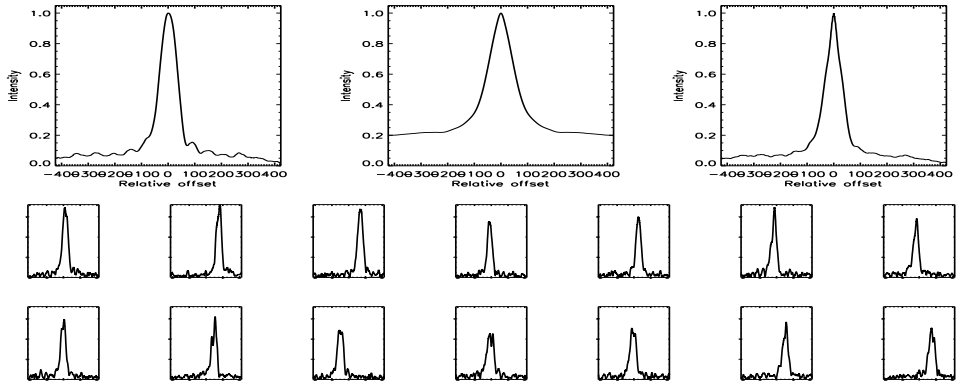

FIGURE B.157: SFP inspection for HD 038858 with S1-W1 on UT 2007/10/31, seq 002

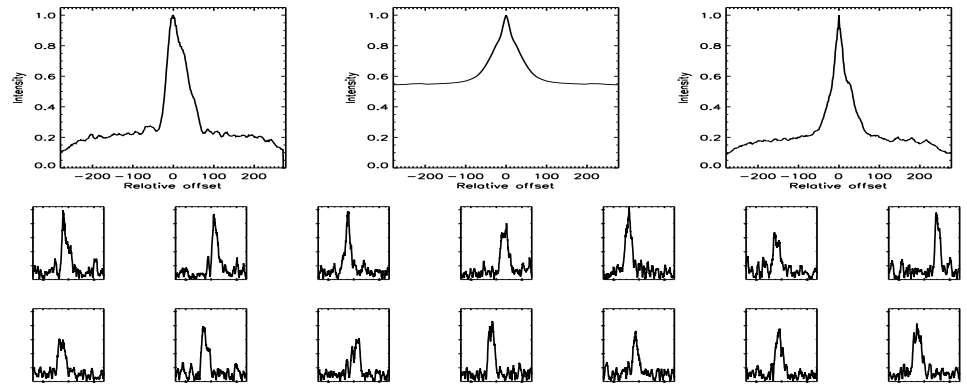

FIGURE B.158: SFP inspection for HD 038858 with S2-E2 on UT 2007/09/26, seq 001

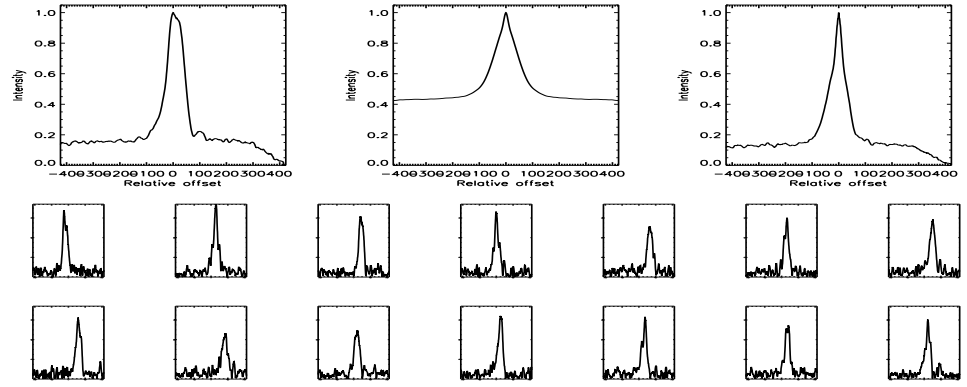

FIGURE B.159: SFP inspection for HD 040397 with S1-W1 on UT 2007/11/01, seq 001

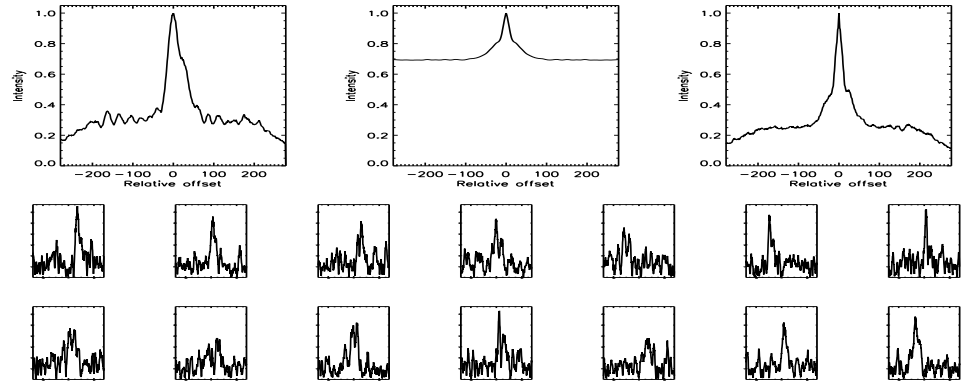

FIGURE B.160: SFP inspection for HD 040397 with S2-E2 on UT 2007/09/26, seq 001

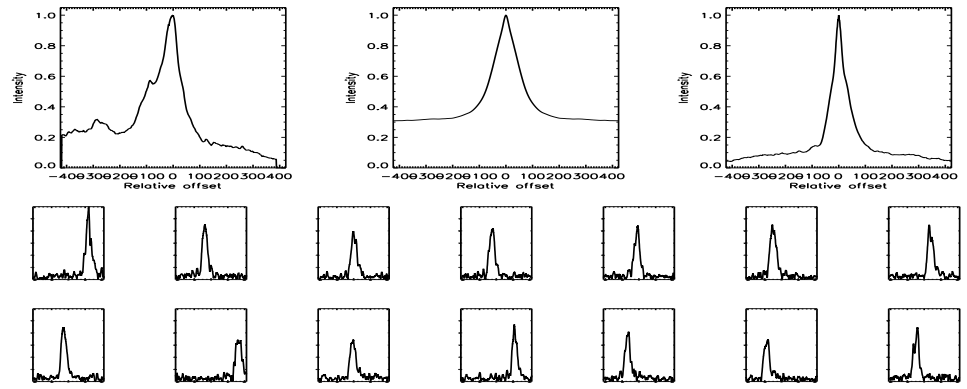

FIGURE B.161: SFP inspection for HD 041593 with S1-E1 on UT 2007/10/31, seq 001

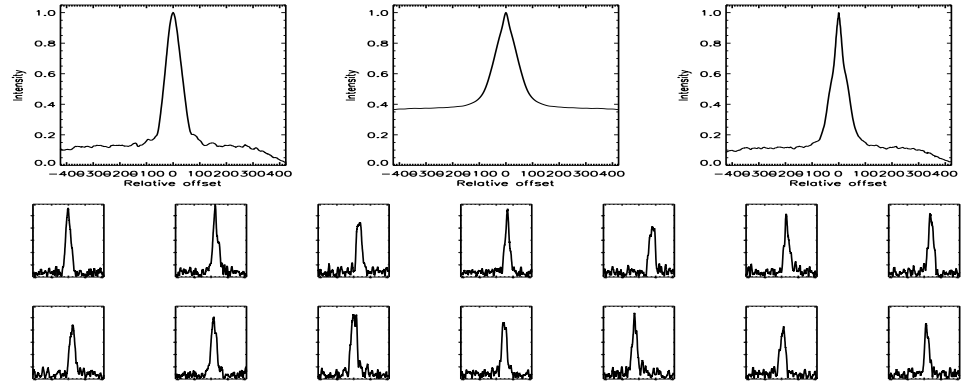

FIGURE B.162: SFP inspection for HD 041593 with S1-W1 on UT 2007/11/01, seq 001

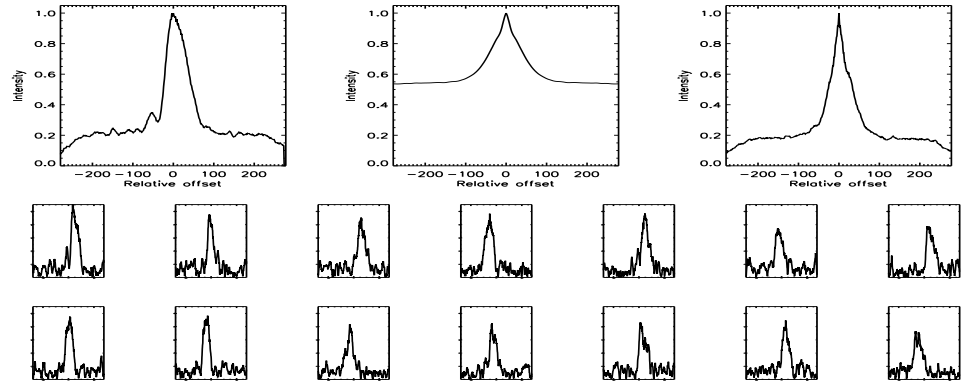

FIGURE B.163: SFP inspection for HD 041593 with S2-E2 on UT 2007/09/26, seq 002

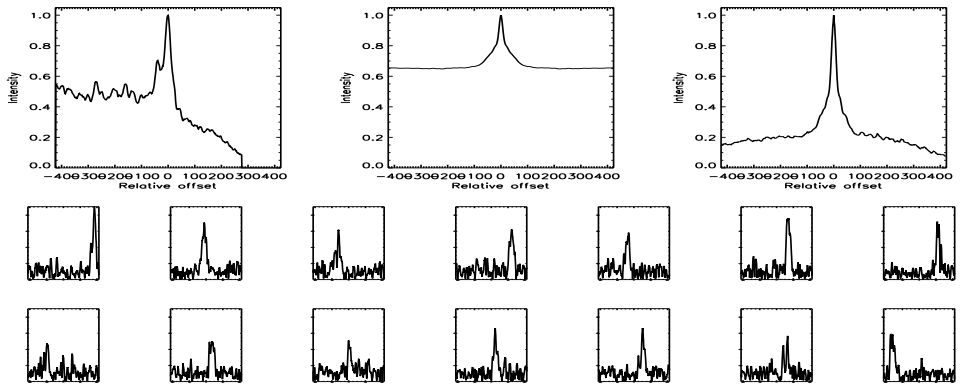

FIGURE B.164: SFP inspection for HD 042618 with S1-E1 on UT 2007/10/31, seq 001

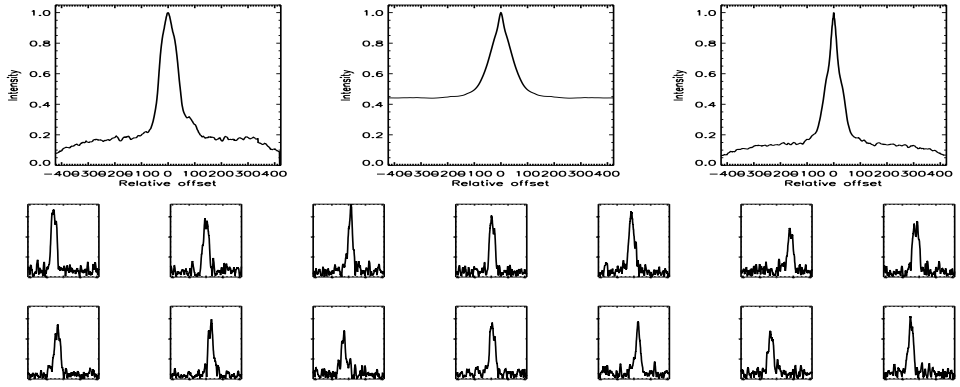

FIGURE B.165: SFP inspection for HD 042618 with S1-W1 on UT 2007/11/01, seq 001

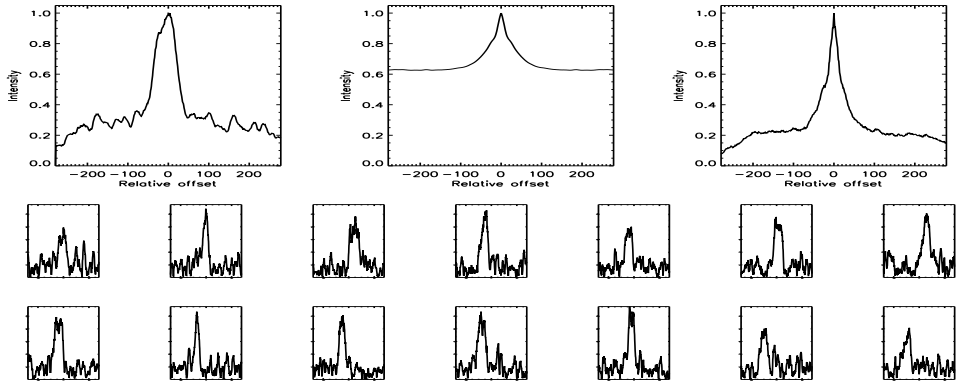

FIGURE B.166: SFP inspection for HD 042618 with S2-E2 on UT 2007/09/26, seq 001

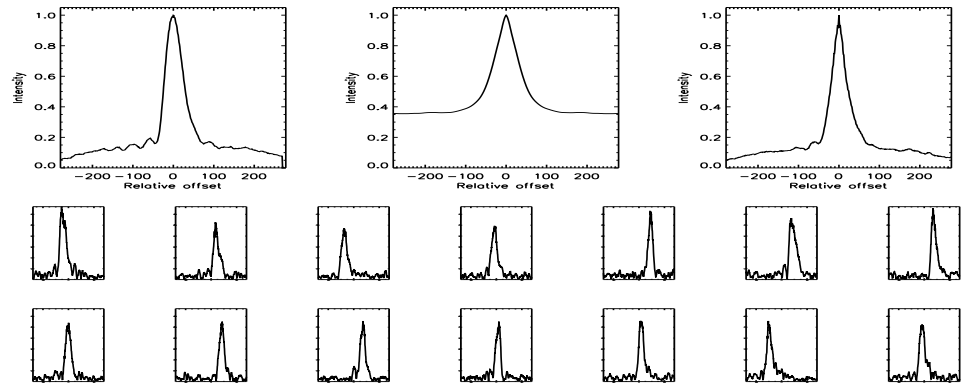

FIGURE B.167: SFP inspection for HD 046588 with S1-E1 on UT 2007/04/14, seq 001

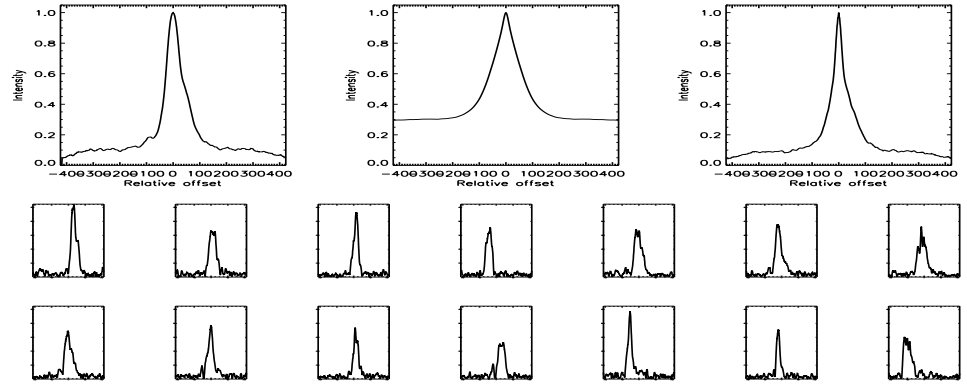

FIGURE B.168: SFP inspection for HD 046588 with S1-E1 on UT 2007/09/16, seq 001

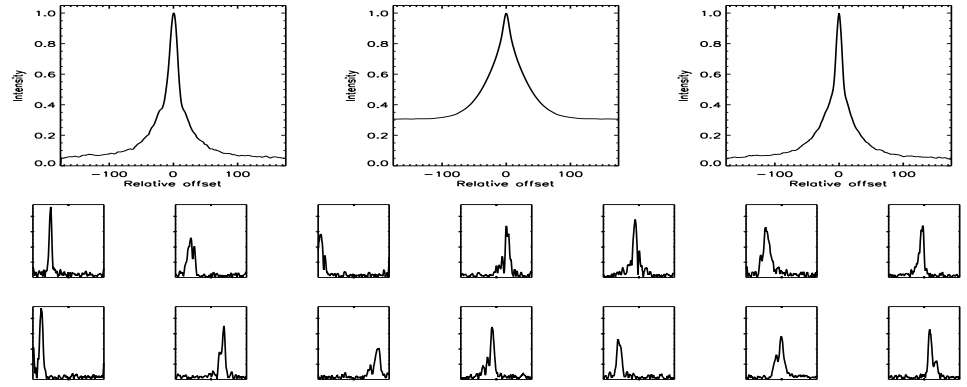

FIGURE B.169: SFP inspection for HD 046588 with S1-W1 on UT 2008/04/26, seq 001

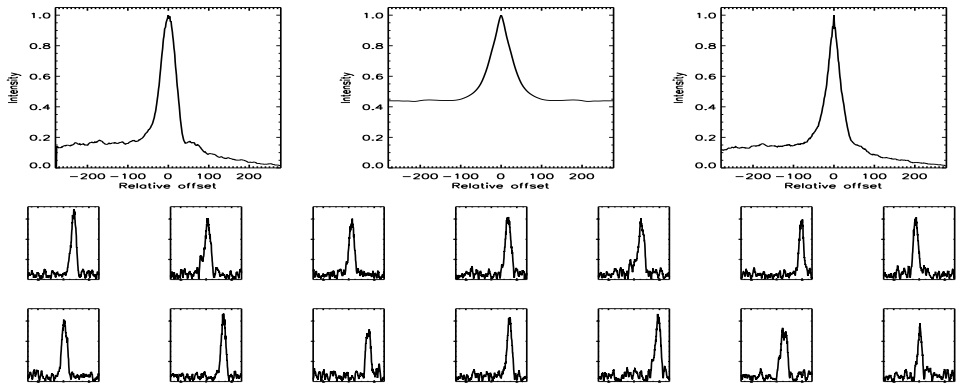

FIGURE B.170: SFP inspection for HD 051419 with S1-E1 on UT 2007/02/05, seq 002

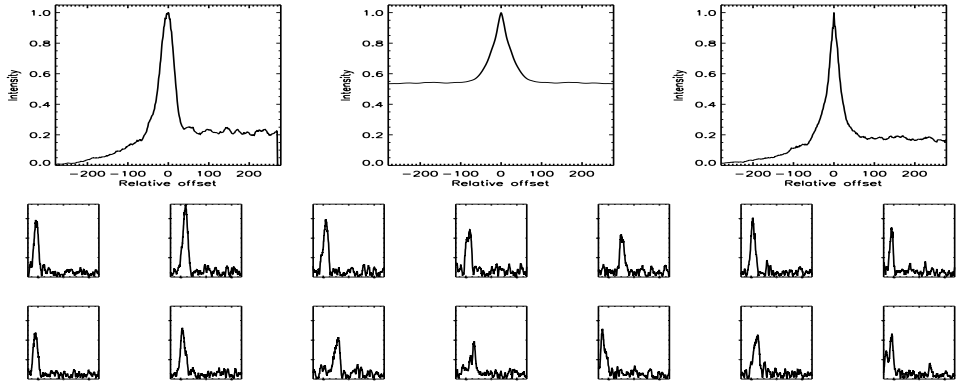

FIGURE B.171: SFP inspection for HD 051419 with S1-E1 on UT 2007/02/05, seq 003

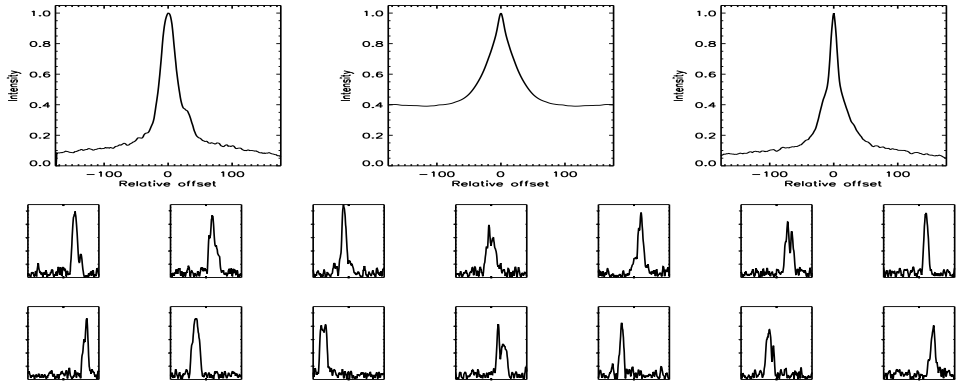

FIGURE B.172: SFP inspection for HD 051419 with S1-W1 on UT 2008/04/26, seq 001

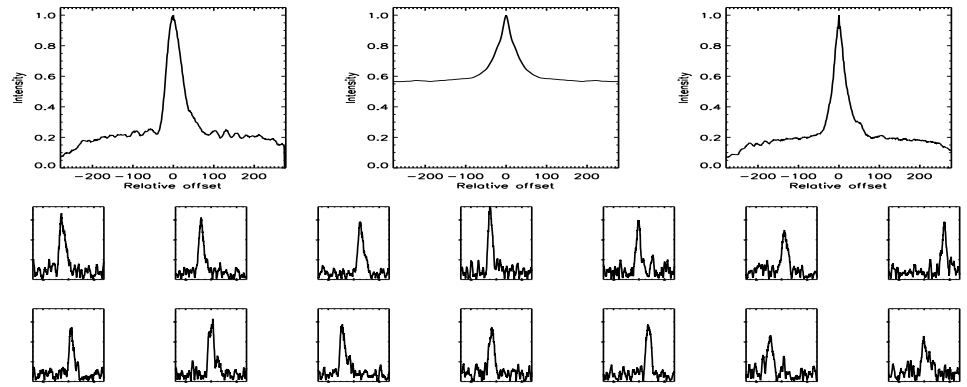

FIGURE B.173: SFP inspection for HD 051866 with S1-E1 on UT 2007/01/25, seq 001

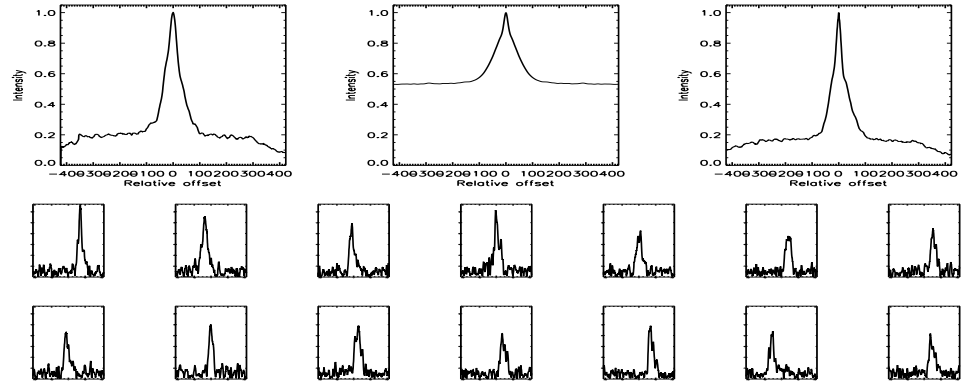

FIGURE B.174: SFP inspection for HD 051866 with S1-W1 on UT 2007/11/01, seq 002

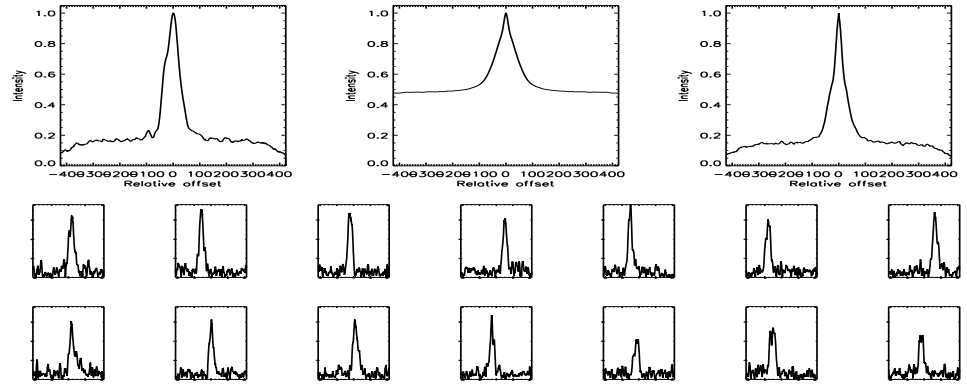

FIGURE B.175: SFP inspection for HD 051866 with S2-E2 on UT 2007/11/19, seq 001

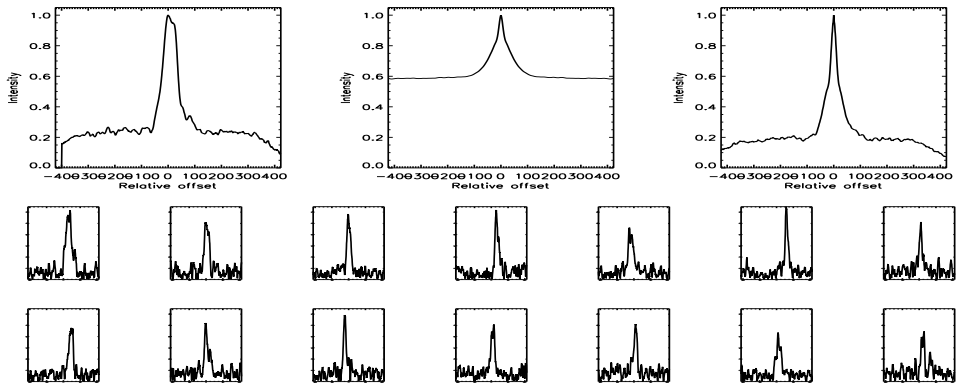

FIGURE B.176: SFP inspection for HD 051866 with S2-E2 on UT 2007/11/19, seq 002

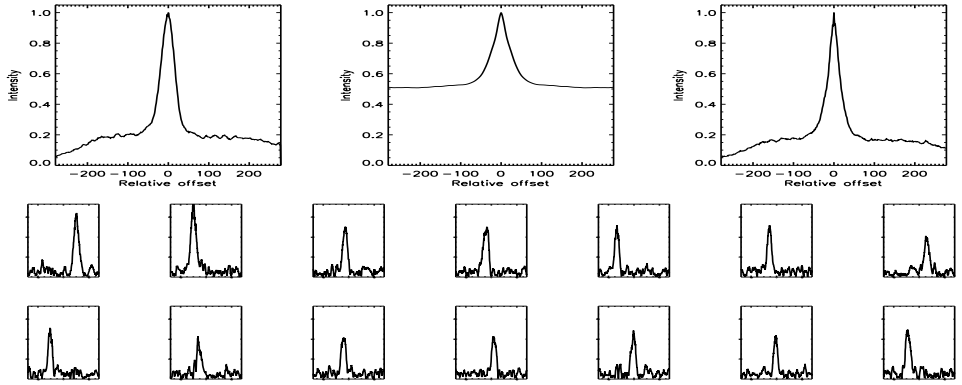

FIGURE B.177: SFP inspection for HD 054371 with S1-E1 on UT 2007/02/04, seq 001

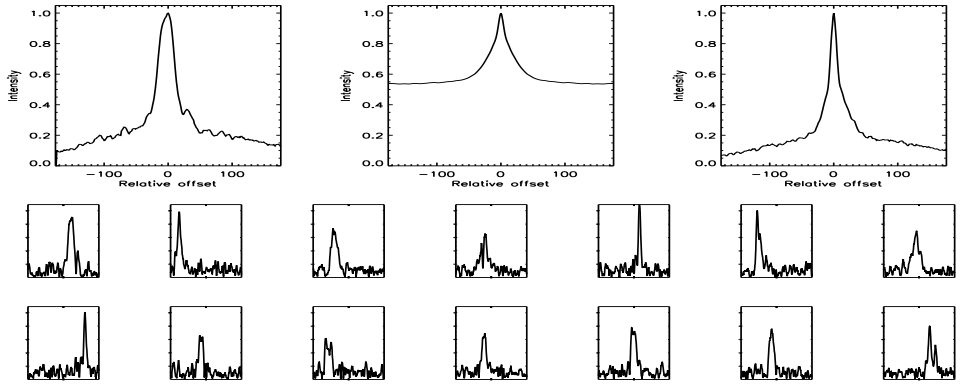

FIGURE B.178: SFP inspection for HD 054371 with S1-E1 on UT 2008/04/25, seq 001

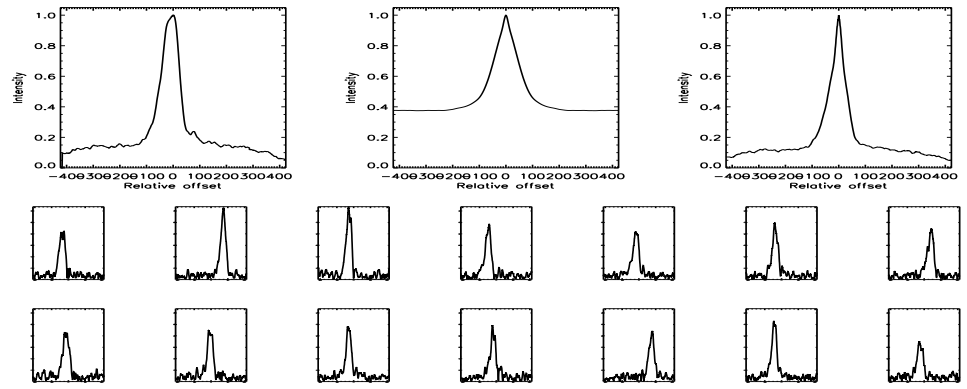

FIGURE B.179: SFP inspection for HD 054371 with S1-W1 on UT 2007/11/01, seq 002

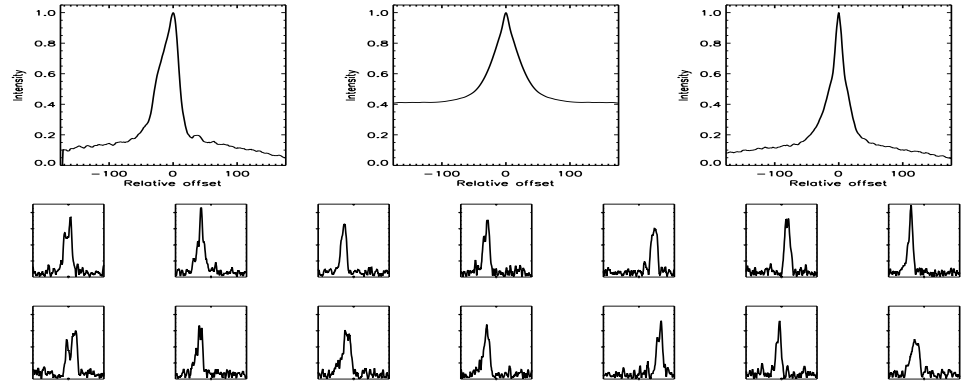

FIGURE B.180: SFP inspection for HD 054371 with S1-W1 on UT 2008/04/26, seq 001

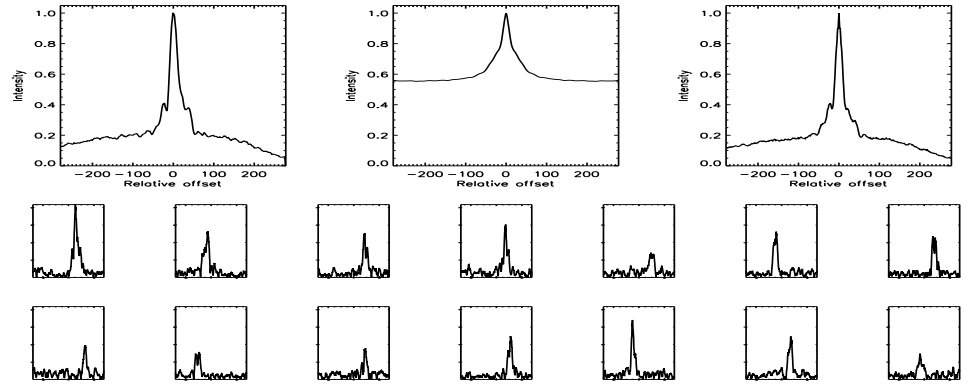

FIGURE B.181: SFP inspection for HD 055575 with S1-E1 on UT 2007/01/26, seq 001

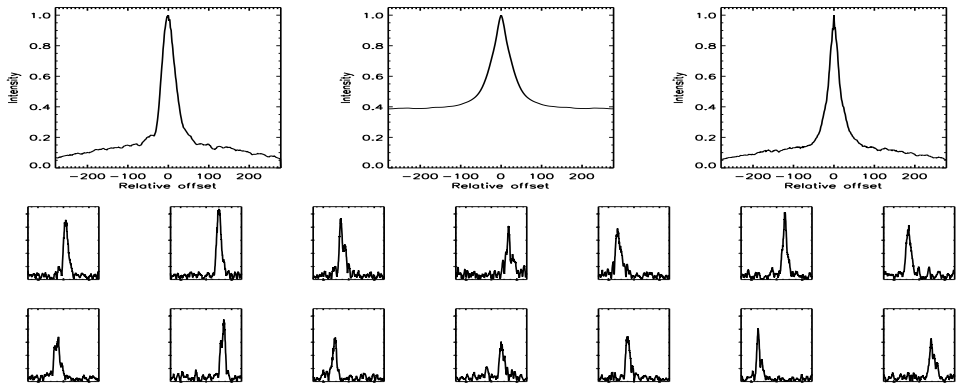

FIGURE B.182: SFP inspection for HD 055575 with S1-E1 on UT 2007/02/03, seq 001

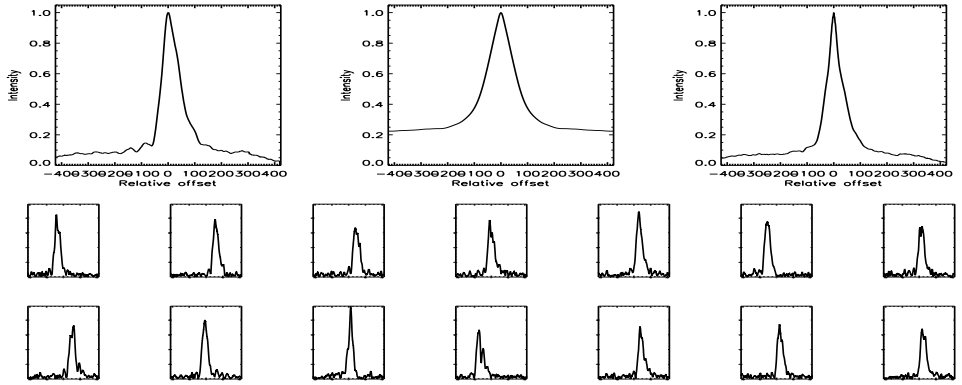

FIGURE B.183: SFP inspection for HD 055575 with S1-W1 on UT 2007/11/01, seq 001

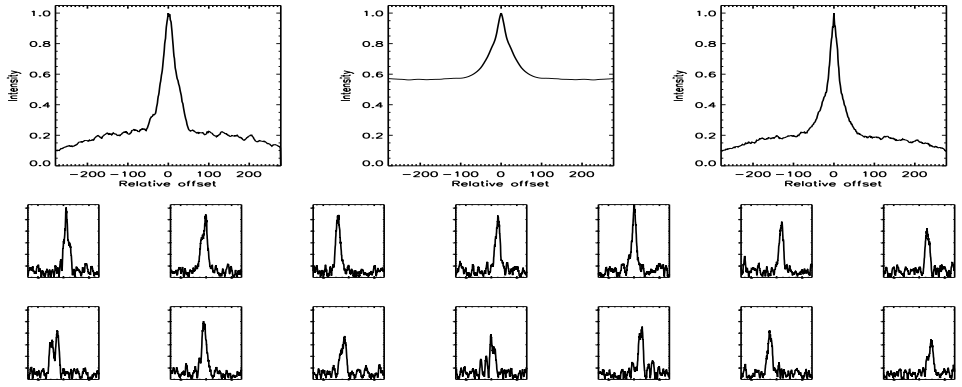

FIGURE B.184: SFP inspection for HD 055575 with S2-E2 on UT 2007/11/20, seq 001

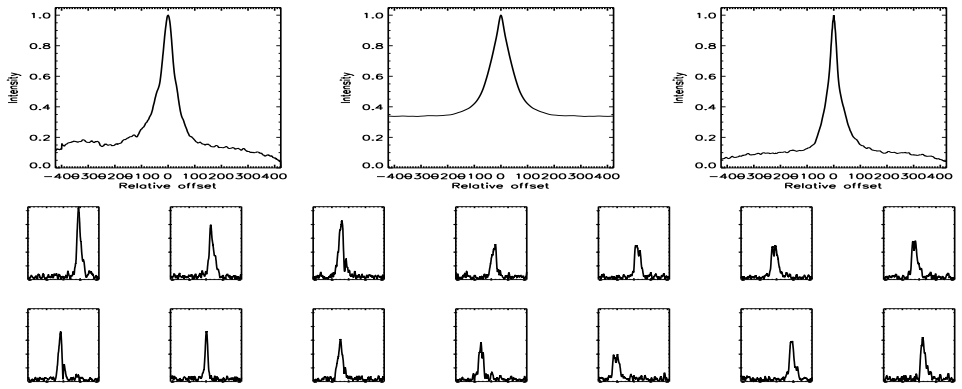

FIGURE B.185: SFP inspection for HD 055575 with S2-E2 on UT 2007/11/27, seq 002

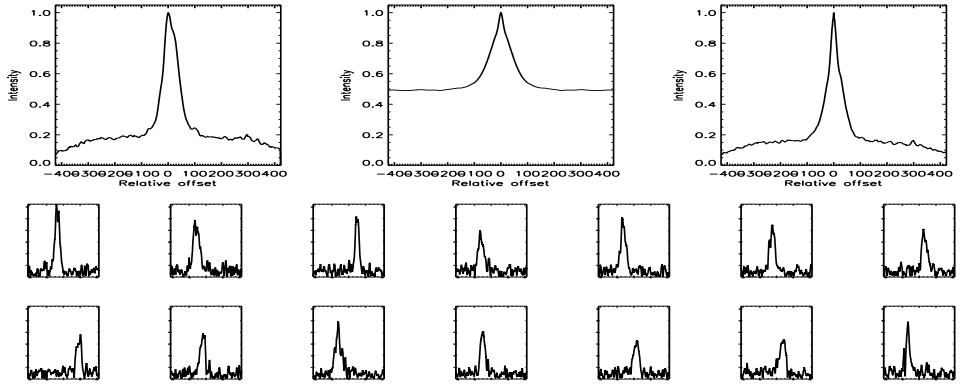

FIGURE B.186: SFP inspection for HD 059747 with S1-W1 on UT 2007/11/01, seq 001

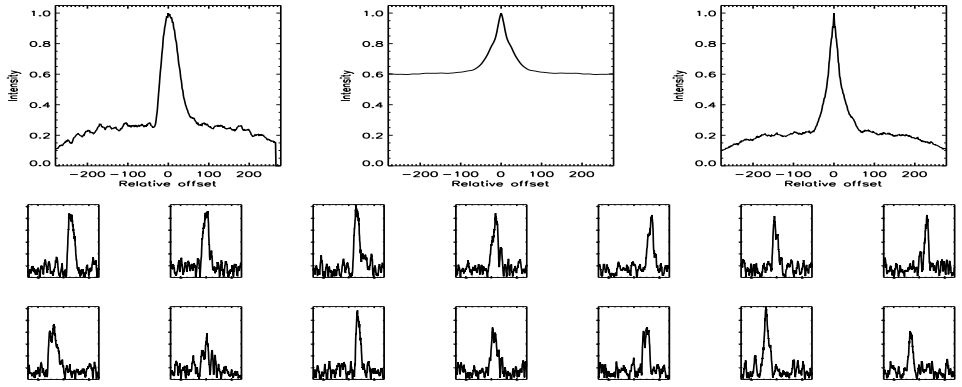

FIGURE B.187: SFP inspection for HD 063433 with S1-E1 on UT 2007/03/20, seq 001

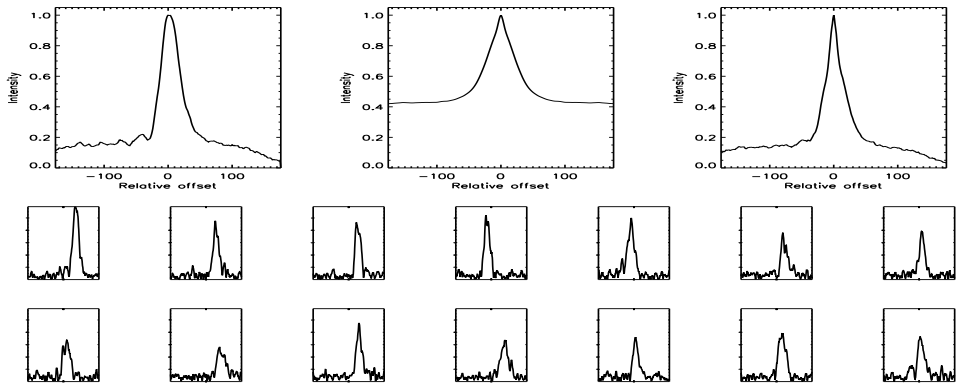

FIGURE B.188: SFP inspection for HD 063433 with S1-E1 on UT 2008/04/13, seq 001

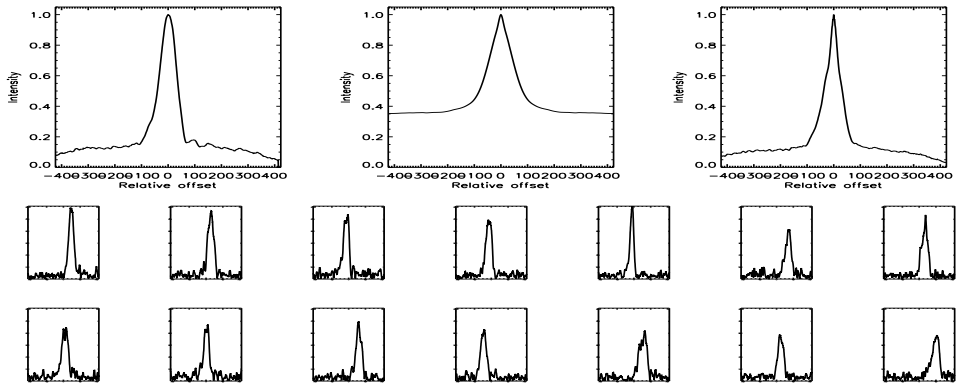

FIGURE B.189: SFP inspection for HD 063433 with S1-W1 on UT 2007/11/01, seq 001

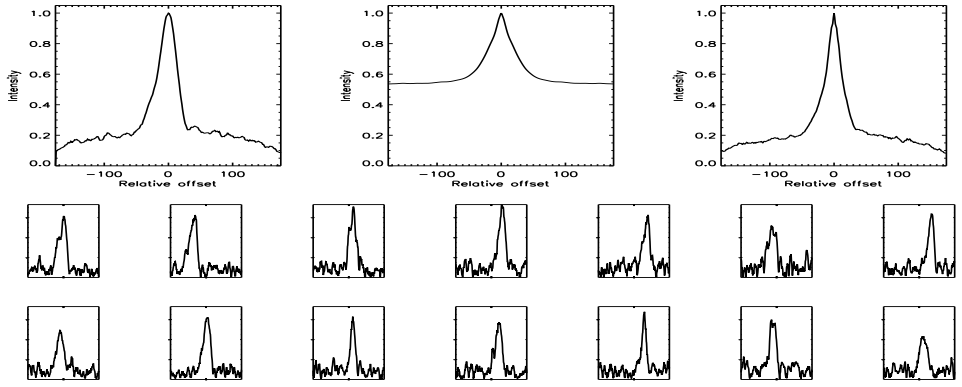

FIGURE B.190: SFP inspection for HD 063433 with S1-W1 on UT 2008/04/12, seq 001

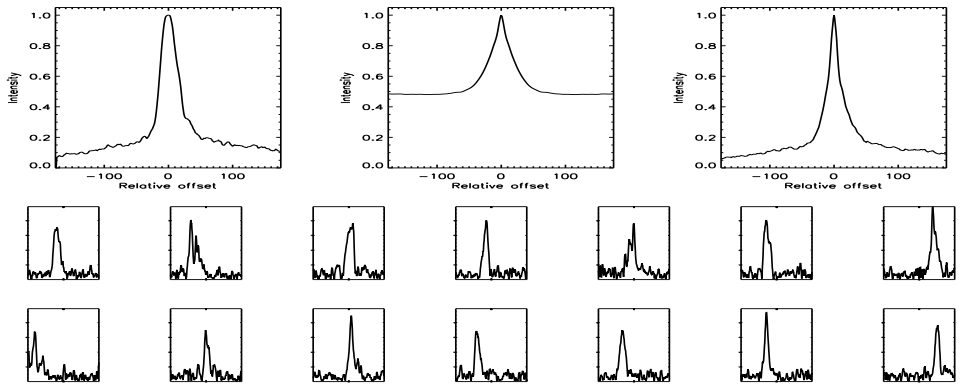

FIGURE B.191: SFP inspection for HD 065430 with S1-W1 on UT 2008/04/26, seq 001

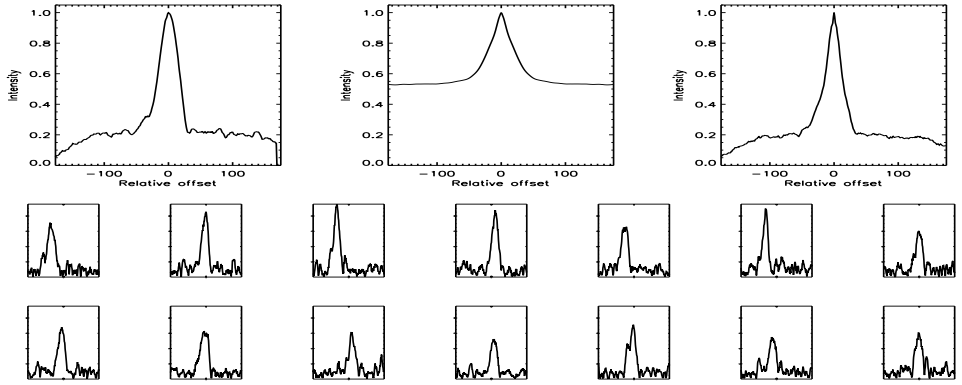

FIGURE B.192: SFP inspection for HD 065583 with S1-E1 on UT 2008/04/13, seq 001

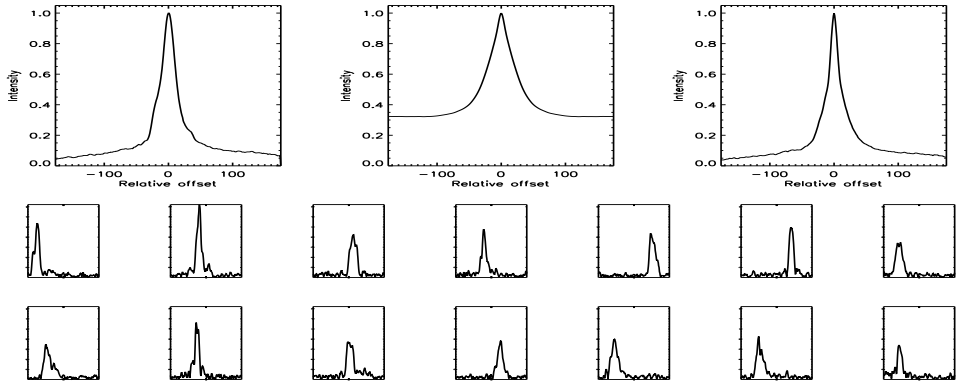

FIGURE B.193: SFP inspection for HD 065583 with S1-W1 on UT 2008/04/26, seq 001

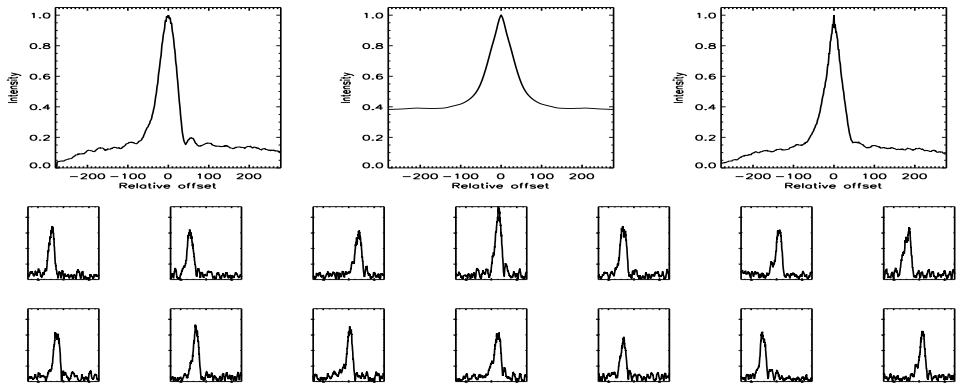

FIGURE B.194: SFP inspection for HD 067228 with S1-E1 on UT 2007/02/06, seq 002

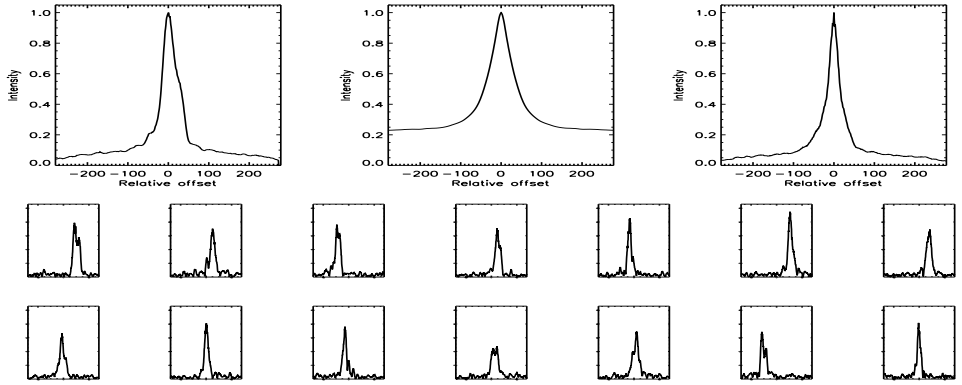

FIGURE B.195: SFP inspection for HD 067228 with S1-E1 on UT 2007/02/25, seq 001

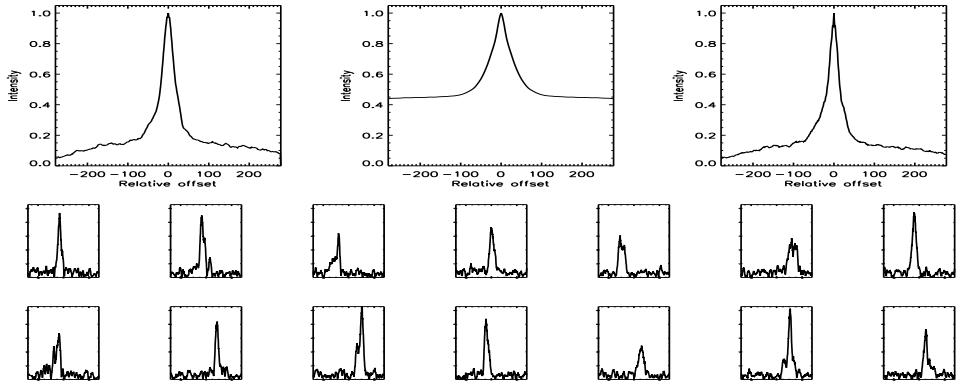

FIGURE B.196: SFP inspection for HD 067228 with S1-E1 on UT 2007/02/25, seq 002

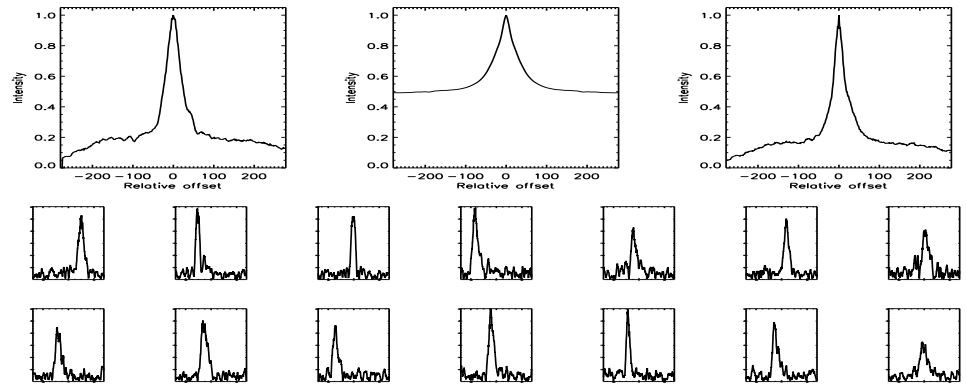

FIGURE B.197: SFP inspection for HD 067228 with S2-E2 on UT 2007/11/29, seq 003

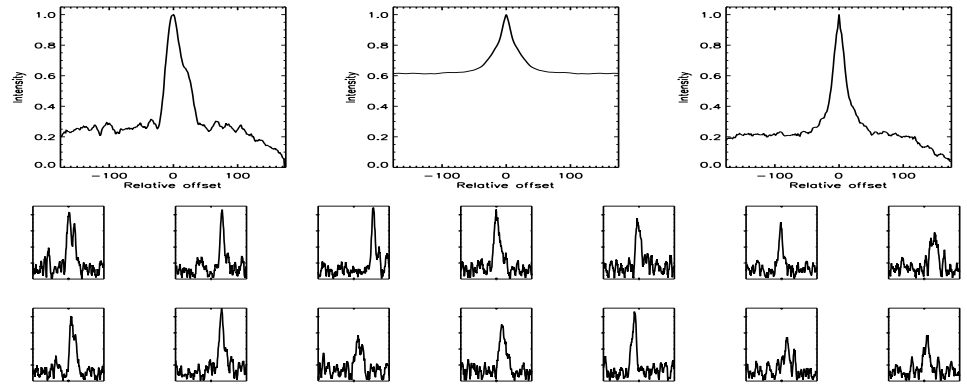

FIGURE B.198: SFP inspection for HD 068017 with S1-E1 on UT 2008/04/13, seq 001

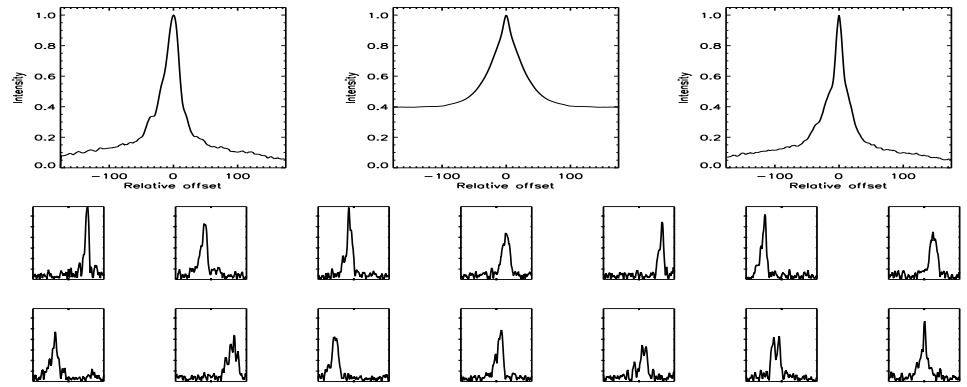

FIGURE B.199: SFP inspection for HD 068017 with S1-E1 on UT 2008/04/25, seq 001

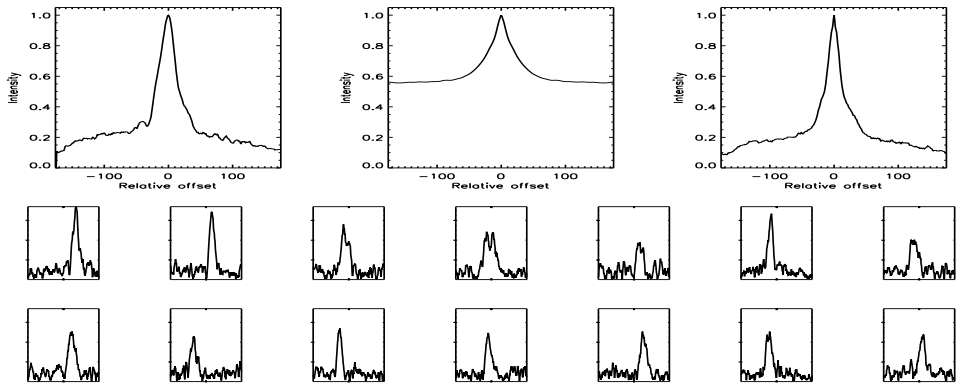

FIGURE B.200: SFP inspection for HD 068017 with S1-W1 on UT 2008/04/12, seq 001

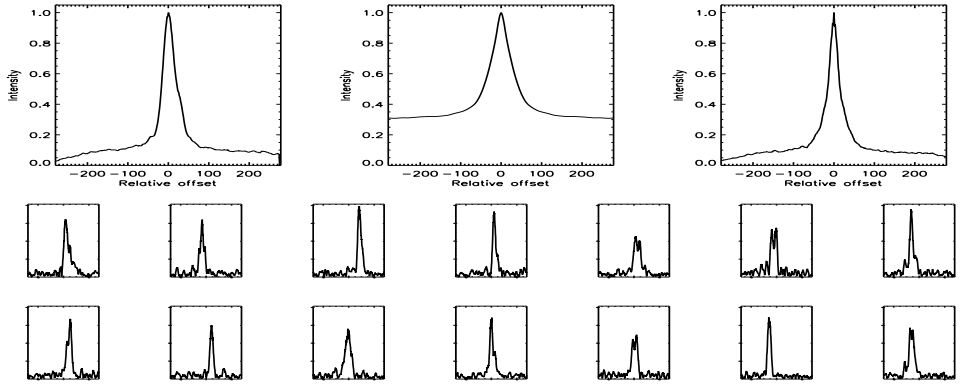

FIGURE B.201: SFP inspection for HD 068255 with S1-E1 on UT 2007/02/25, seq 002

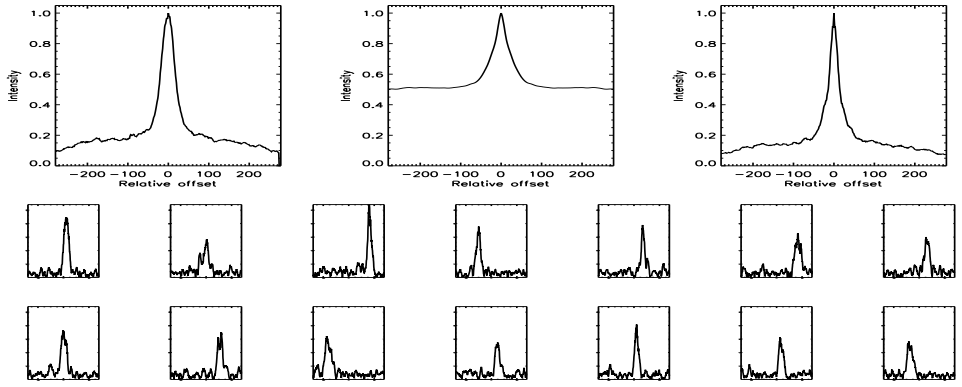

FIGURE B.202: SFP inspection for HD 068255 with S1-E1 on UT 2007/02/25, seq 003

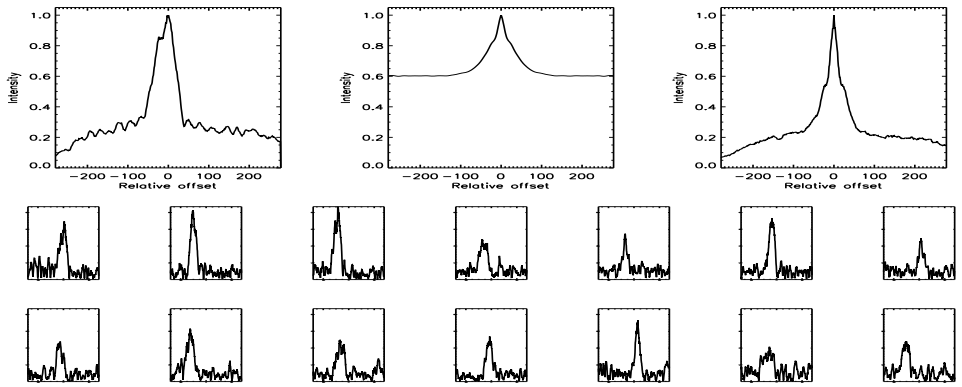

FIGURE B.203: SFP inspection for HD 079096 with S1-E1 on UT 2007/02/06, seq 003

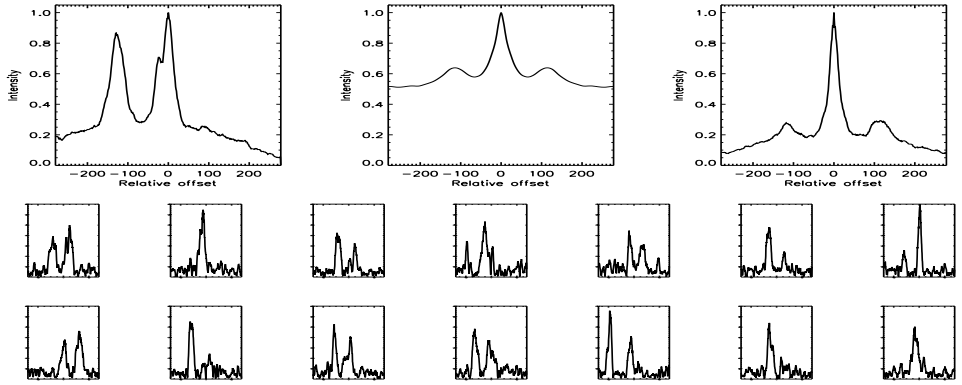

FIGURE B.204: SFP inspection for HD 079096 with S1-E1 on UT 2007/02/25, seq 001

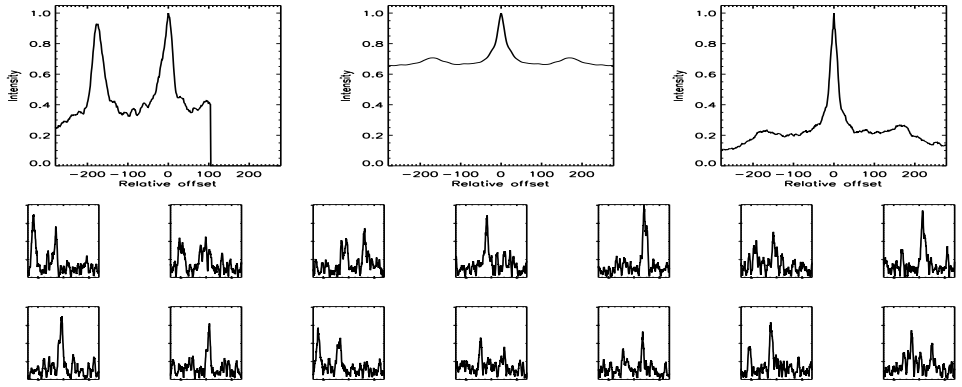

FIGURE B.205: SFP inspection for HD 079096 with S1-E1 on UT 2007/02/25, seq 002

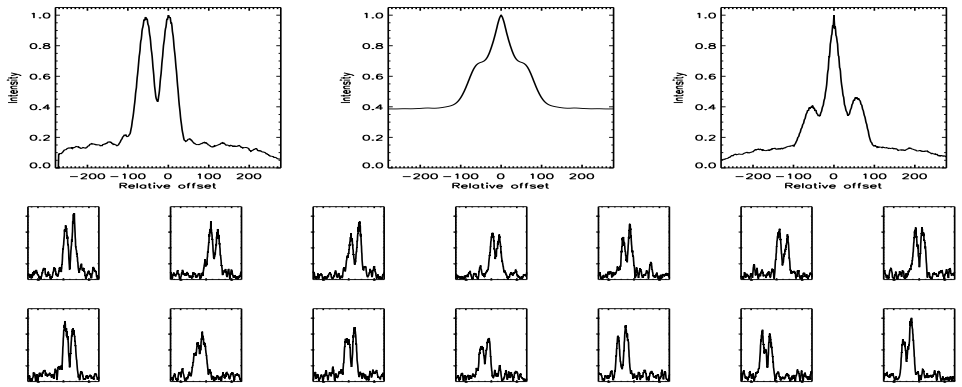

FIGURE B.206: SFP inspection for HD 079096 with S1-E1 on UT 2007/03/09, seq 001

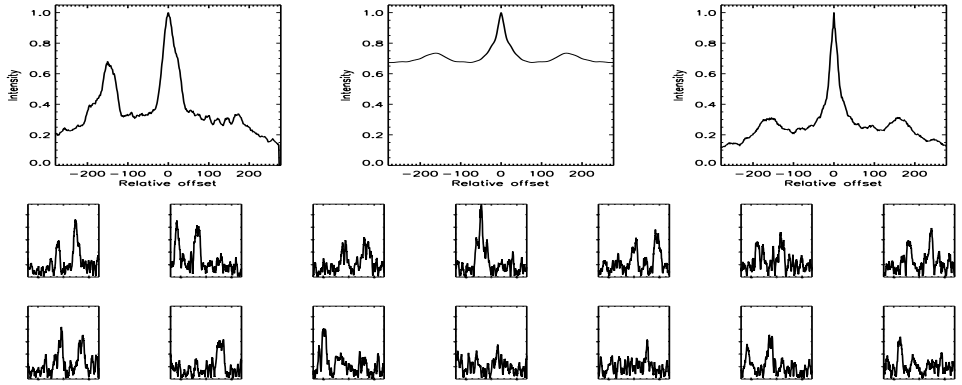

FIGURE B.207: SFP inspection for HD 079096 with S1-E1 on UT 2007/03/09, seq 002

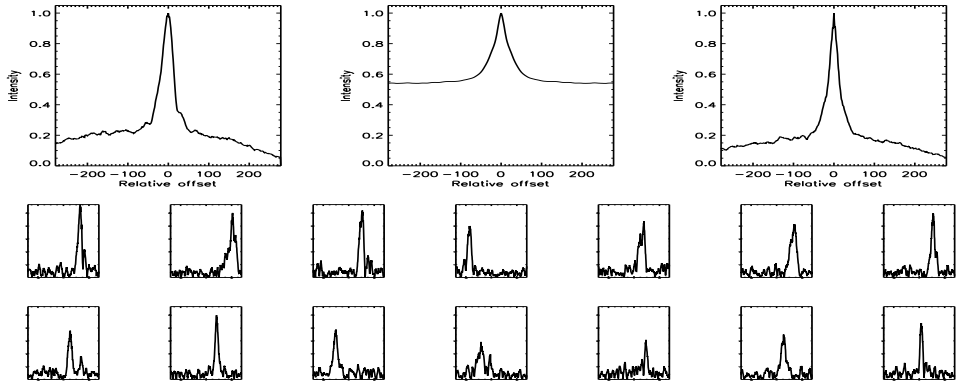

FIGURE B.208: SFP inspection for HD 079096 with S1-E1 on UT 2007/03/10, seq 001

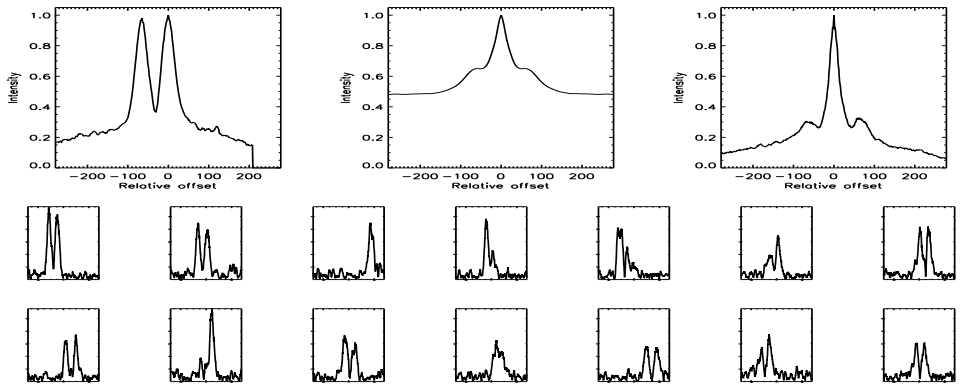

FIGURE B.209: SFP inspection for HD 079096 with S1-E1 on UT 2007/03/11, seq 001

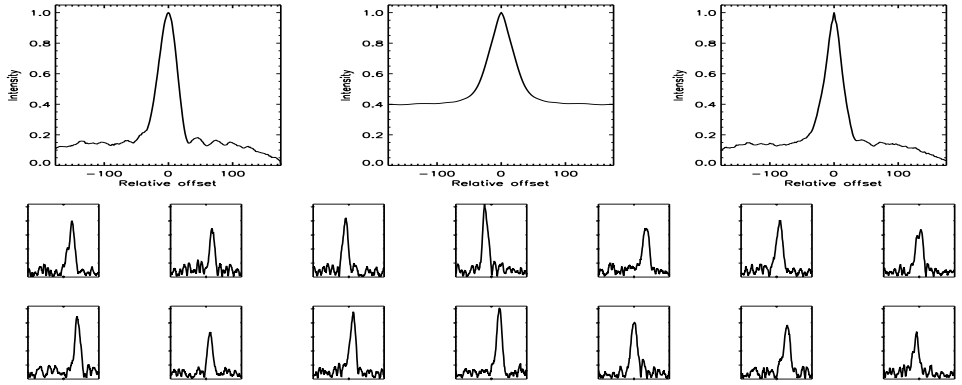

FIGURE B.210: SFP inspection for HD 079096 with S1-E1 on UT 2008/04/14, seq 001

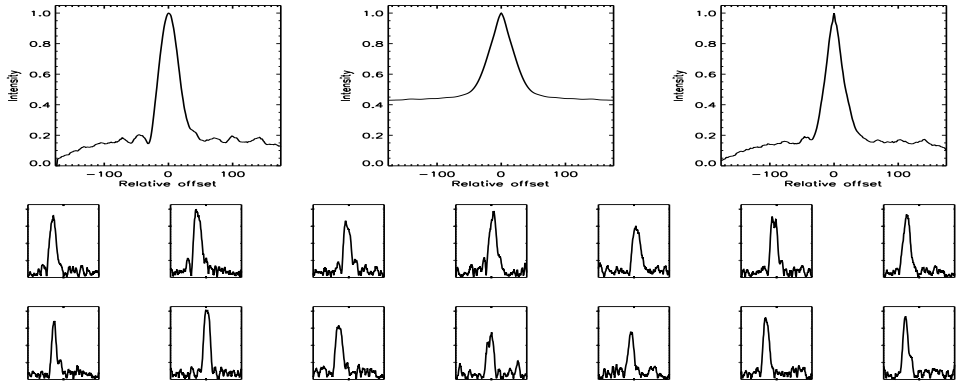

FIGURE B.211: SFP inspection for HD 079096 with S1-E1 on UT 2008/04/14, seq 002

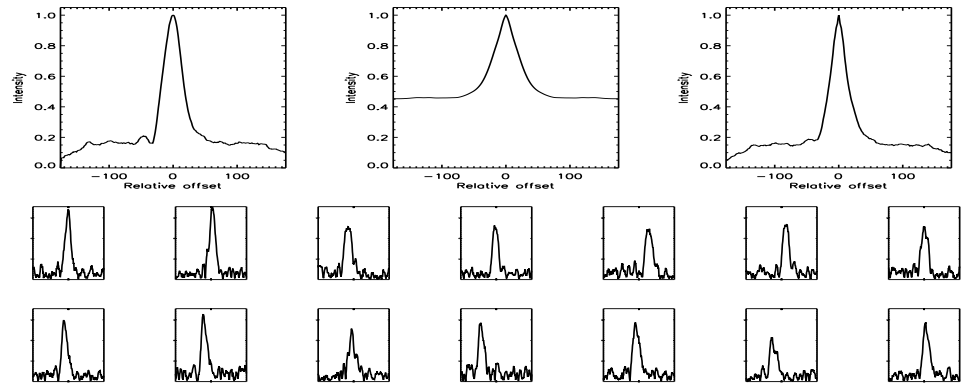

FIGURE B.212: SFP inspection for HD 079096 with S1-E1 on UT 2008/04/14, seq 003

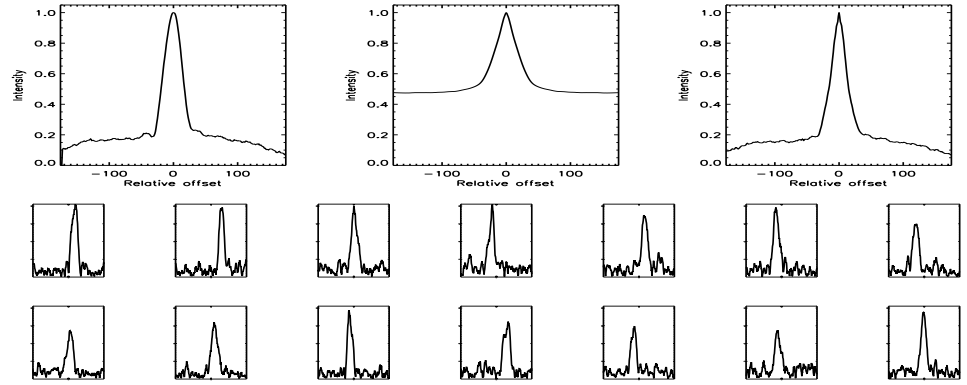

FIGURE B.213: SFP inspection for HD 079096 with S1-W1 on UT 2008/04/12, seq 001

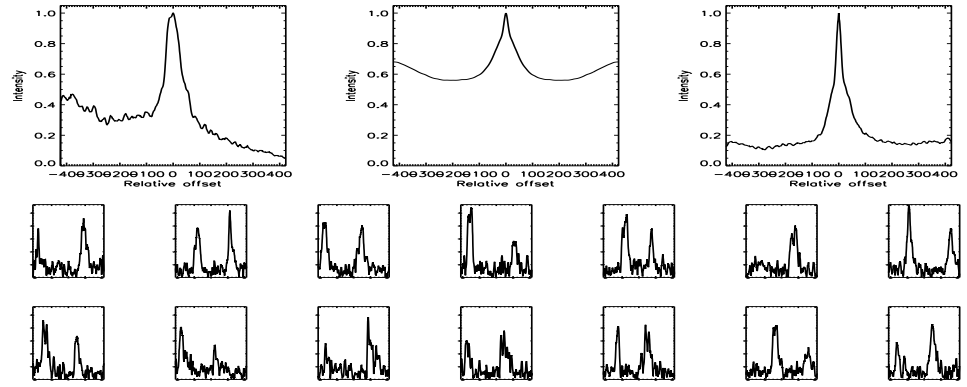

FIGURE B.214: SFP inspection for HD 079096 with S2-E2 on UT 2007/11/29, seq 002

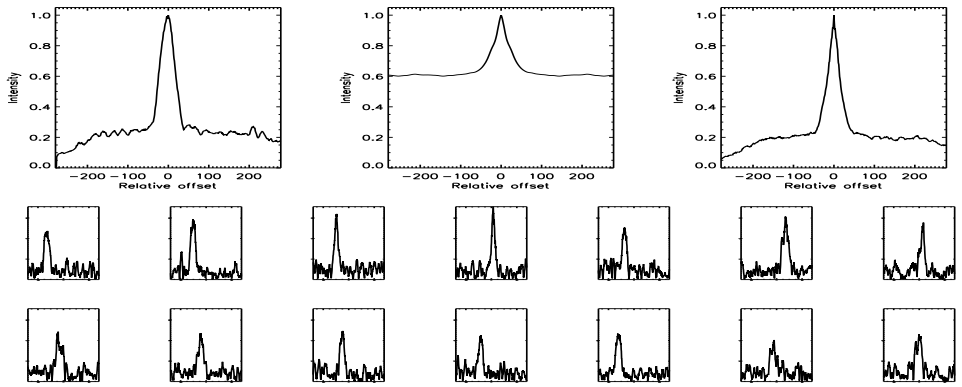

FIGURE B.215: SFP inspection for HD 079969 with S1-E1 on UT 2007/02/06, seq 001

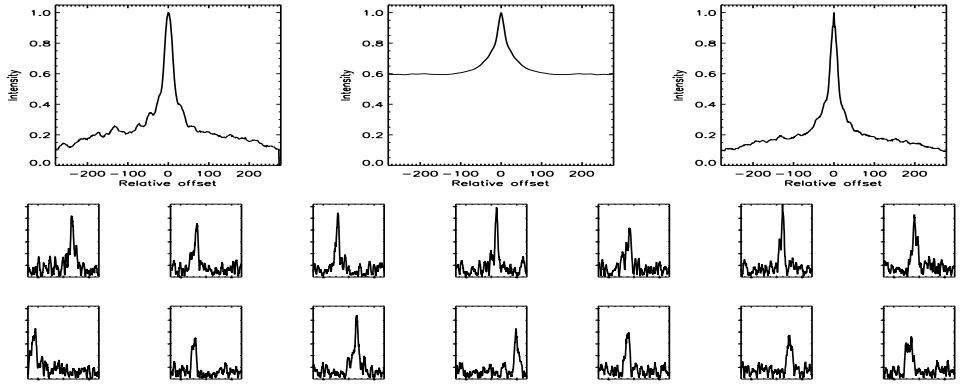

FIGURE B.216: SFP inspection for HD 079969 with S1-E1 on UT 2007/02/25, seq 001

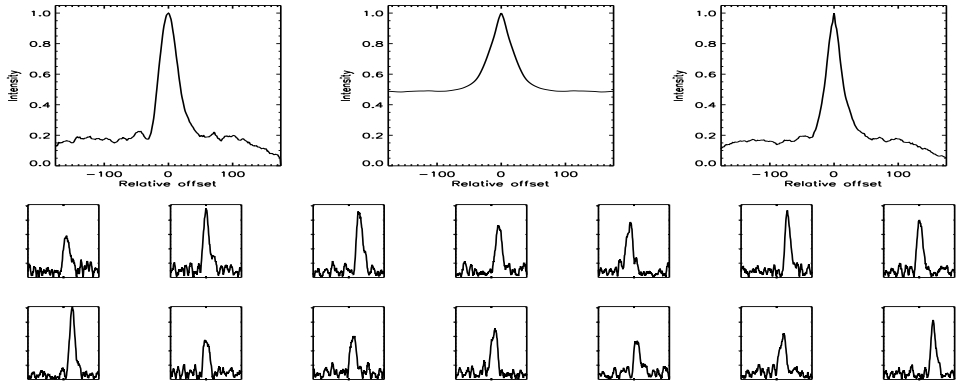

FIGURE B.217: SFP inspection for HD 079969 with S1-E1 on UT 2008/04/13, seq 001

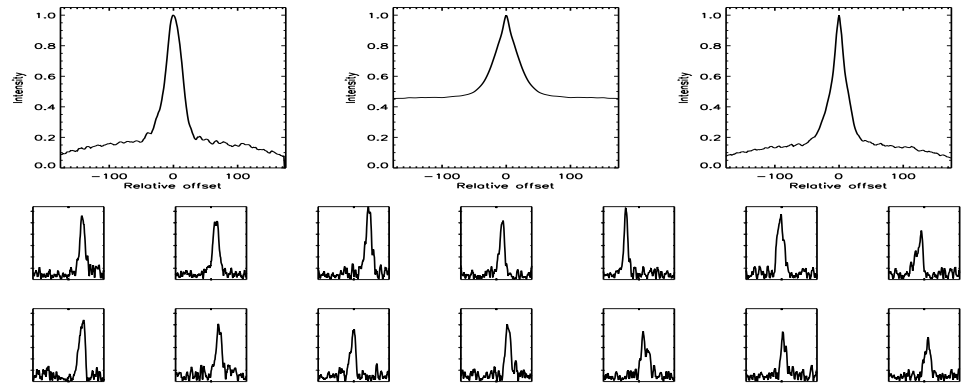

FIGURE B.218: SFP inspection for HD 079969 with S1-W1 on UT 2008/04/12, seq 001

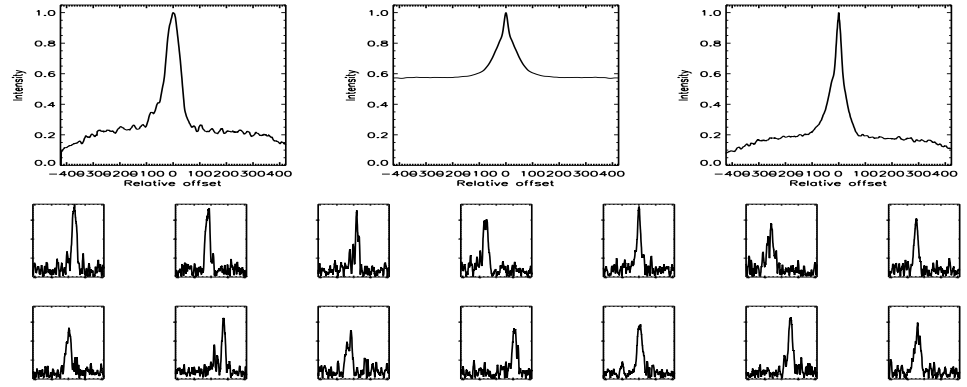

FIGURE B.219: SFP inspection for HD 079969 with S2-E2 on UT 2007/11/29, seq 001

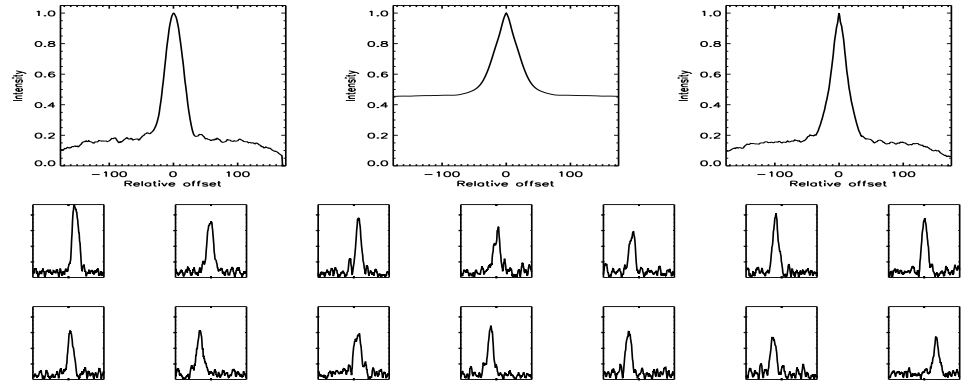

FIGURE B.220: SFP inspection for HD 080715 with S1-E1 on UT 2008/04/13, seq 001

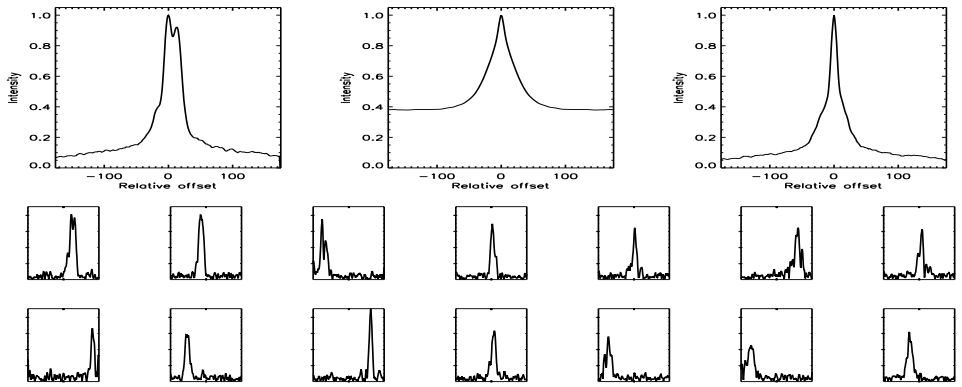

FIGURE B.221: SFP inspection for HD 080715 with S1-W1 on UT 2008/04/26, seq 001

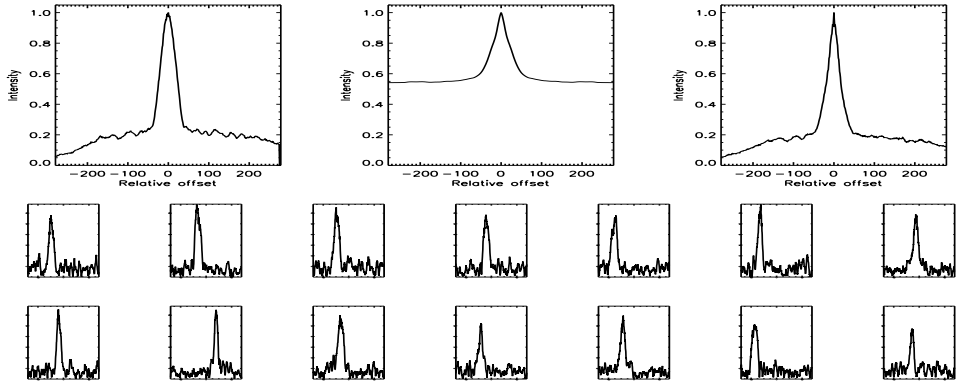

FIGURE B.222: SFP inspection for HD 082443 with S1-E1 on UT 2007/02/06, seq 001

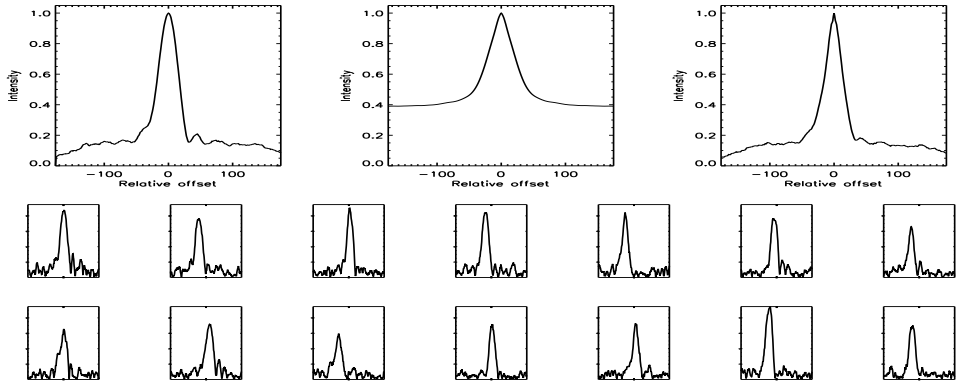

FIGURE B.223: SFP inspection for HD 082443 with S1-E1 on UT 2008/04/13, seq 001

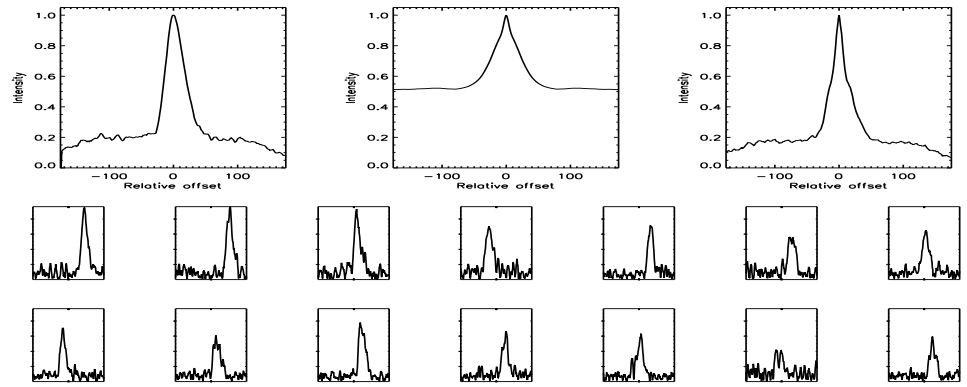

FIGURE B.224: SFP inspection for HD 082443 with S1-E1 on UT 2008/04/13, seq 002

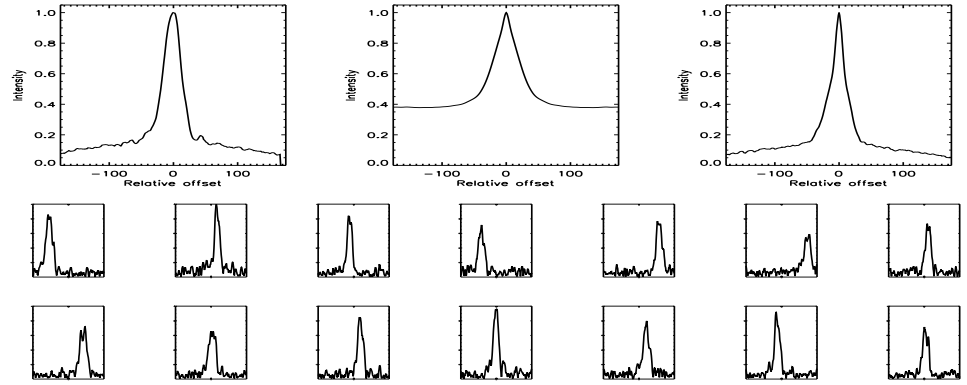

FIGURE B.225: SFP inspection for HD 082443 with S1-W1 on UT 2008/04/12, seq 001

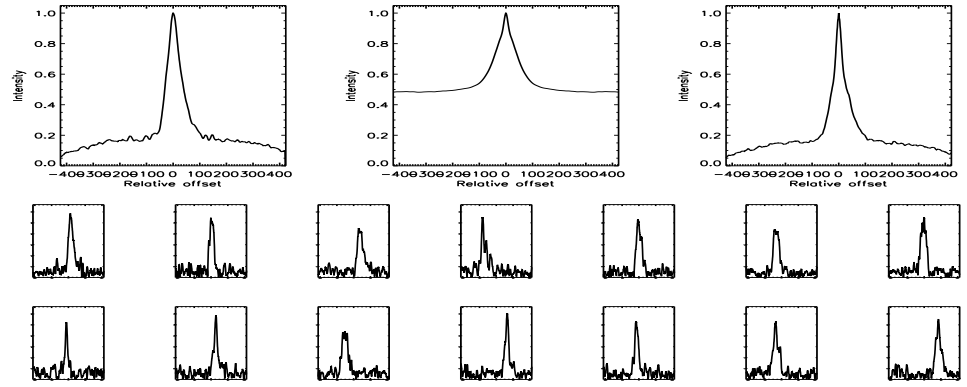

FIGURE B.226: SFP inspection for HD 082443 with S2-E2 on UT 2007/11/29, seq 001

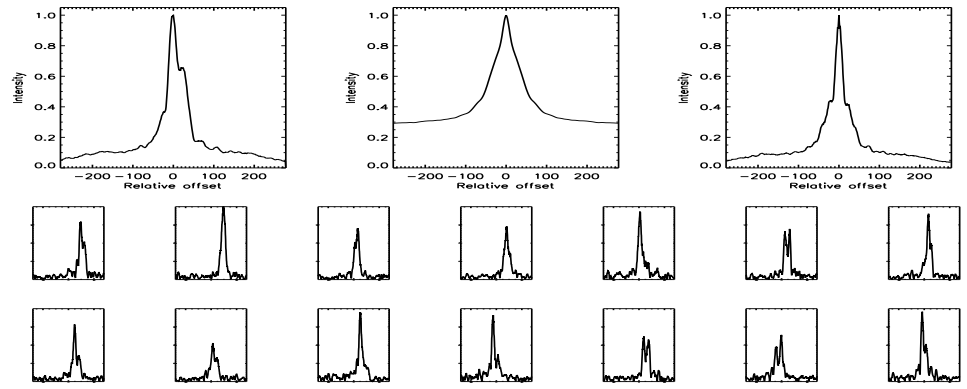

FIGURE B.227: SFP inspection for HD 082885 with S1-E1 on UT 2007/01/26, seq 003

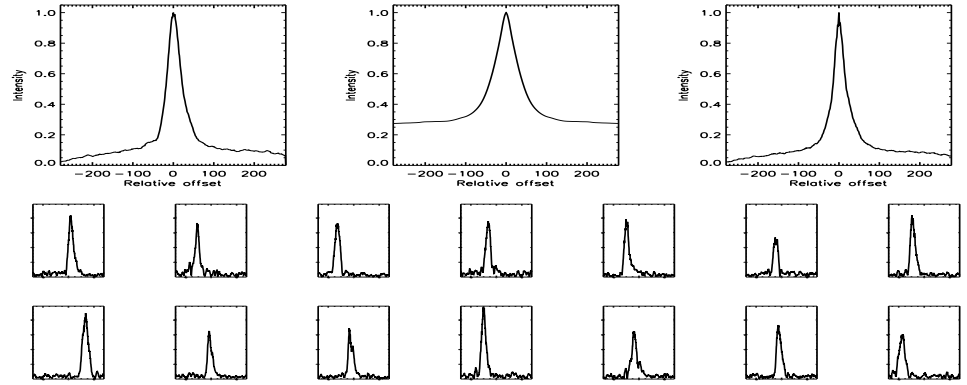

FIGURE B.228: SFP inspection for HD 082885 with S1-W1 on UT 2007/04/24, seq 001

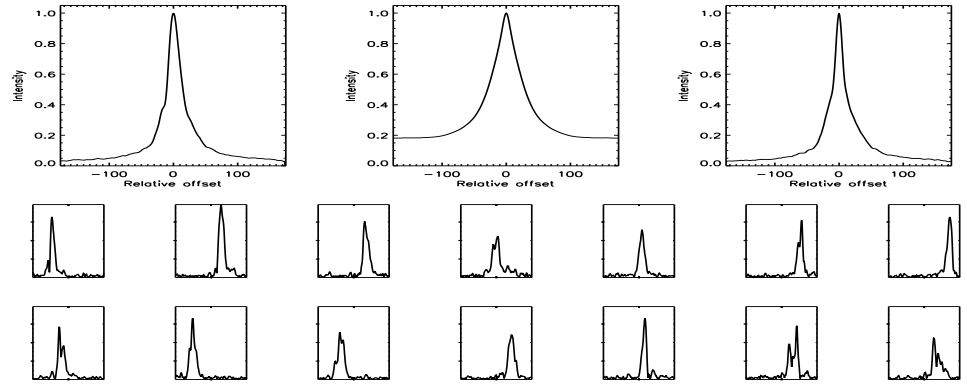

FIGURE B.229: SFP inspection for HD 082885 with S1-W1 on UT 2008/04/26, seq 001

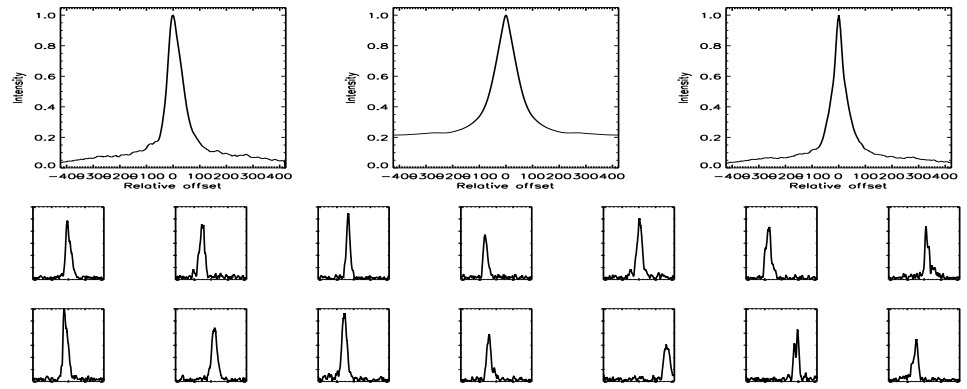

FIGURE B.230: SFP inspection for HD 082885 with S2-E2 on UT 2007/11/29, seq 001

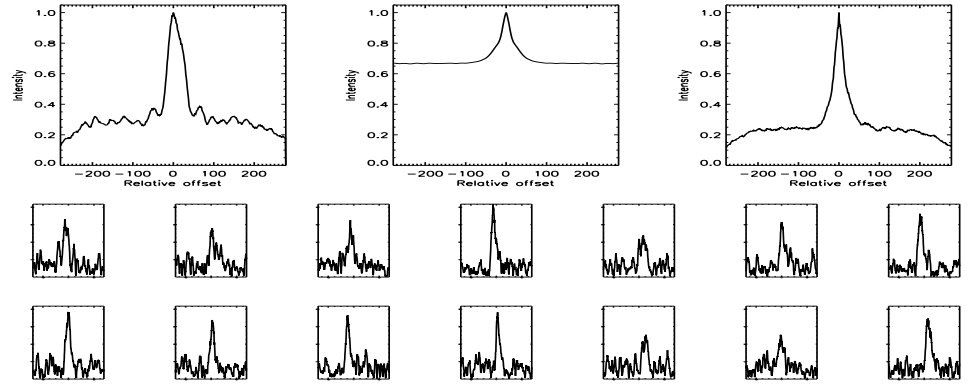

FIGURE B.231: SFP inspection for HD 087883 with S1-E1 on UT 2007/02/06, seq 001

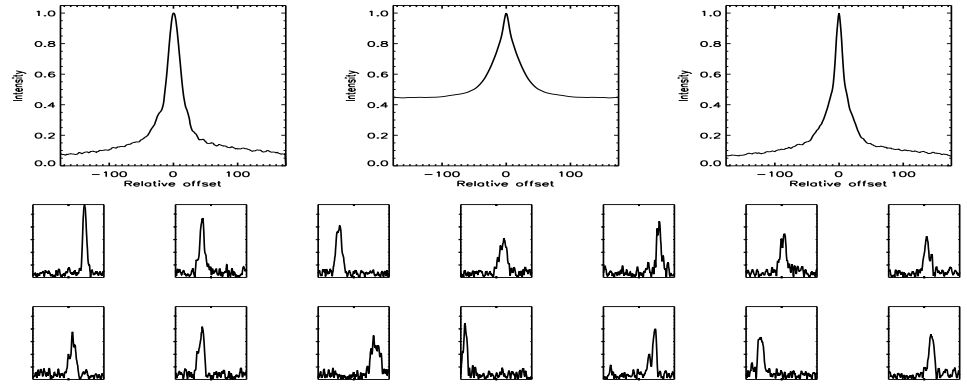

FIGURE B.232: SFP inspection for HD 087883 with S1-W1 on UT 2008/04/26, seq 001

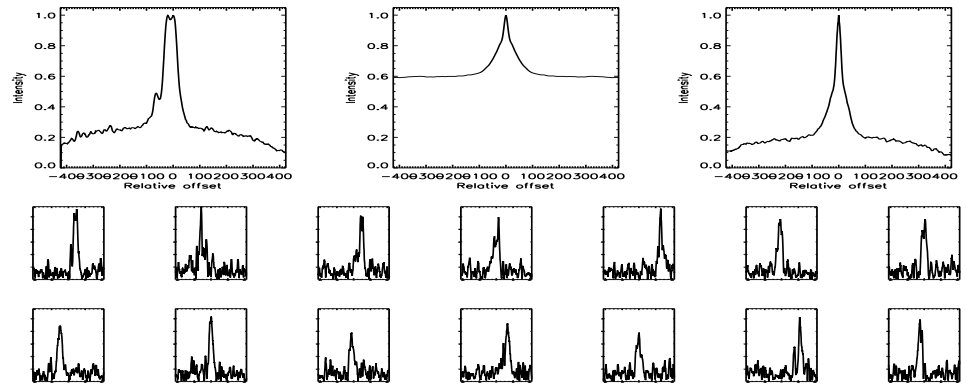

FIGURE B.233: SFP inspection for HD 087883 with S2-E2 on UT 2007/11/29, seq 001

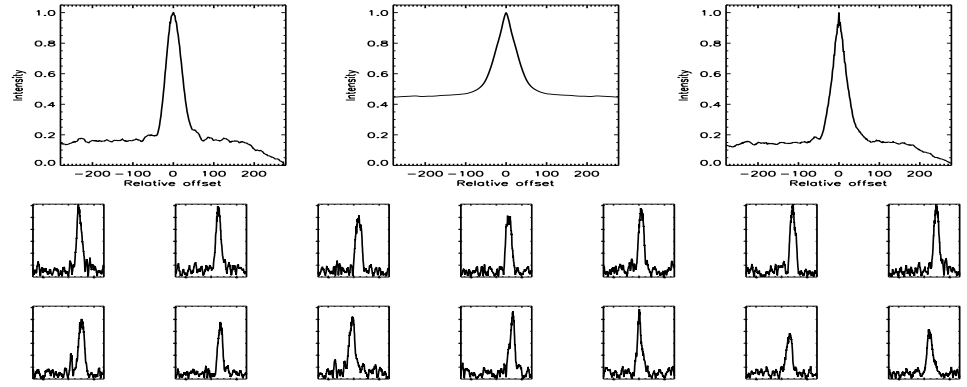

FIGURE B.234: SFP inspection for HD 089269 with S1-E1 on UT 2007/05/17, seq 002

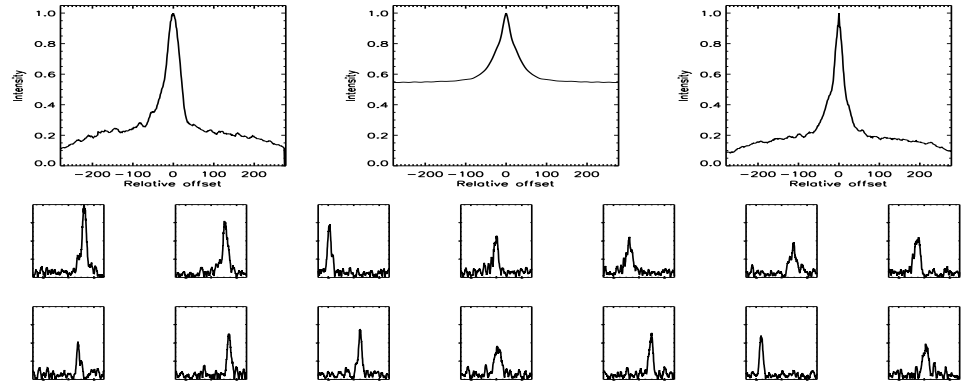

FIGURE B.235: SFP inspection for HD 089269 with S1-W1 on UT 2007/04/24, seq 001

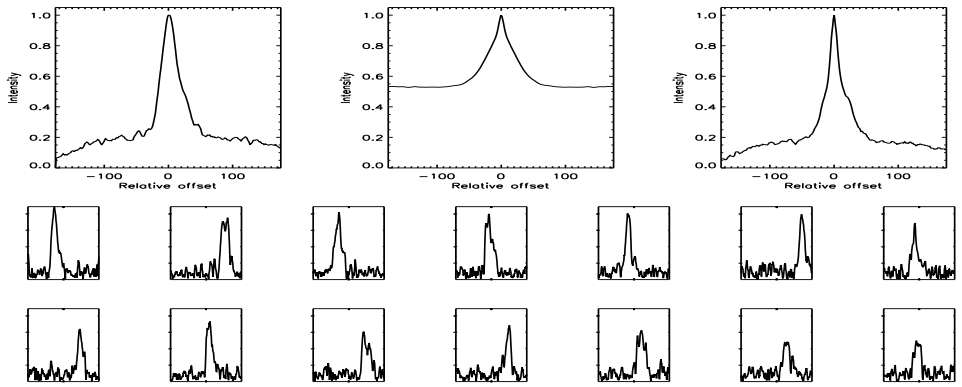

FIGURE B.236: SFP inspection for HD 090343 with S1-E1 on UT 2008/06/25, seq 001

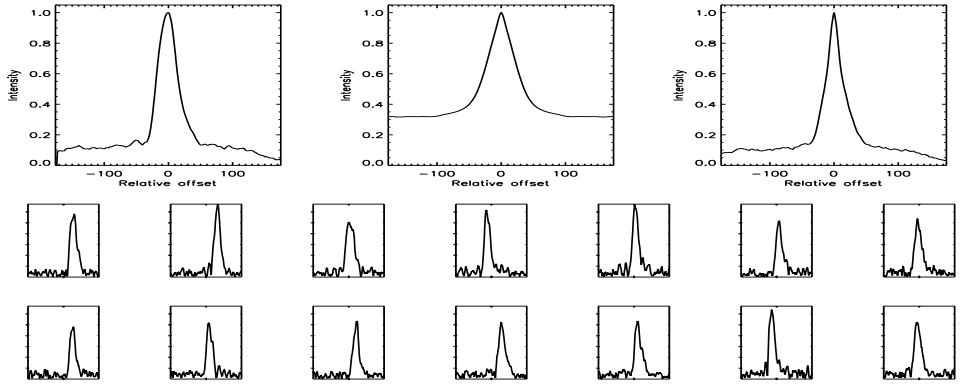

FIGURE B.237: SFP inspection for HD 090343 with S2-W1 on UT 2008/06/24, seq 001

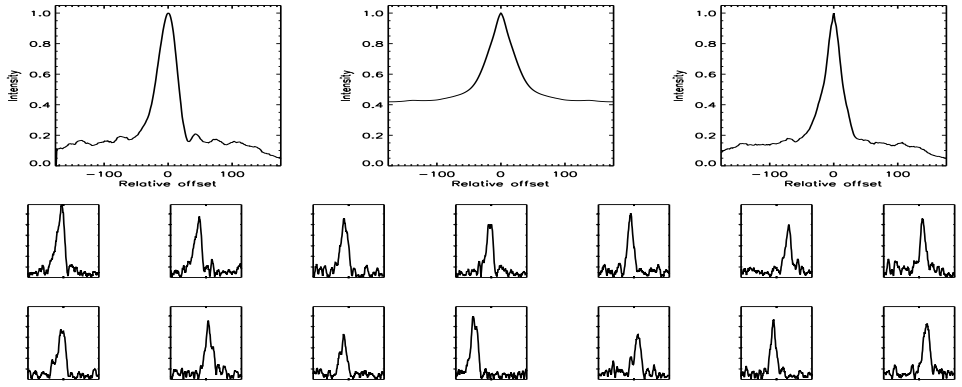

FIGURE B.238: SFP inspection for HD 094765 with S1-E1 on UT 2008/04/14, seq 001

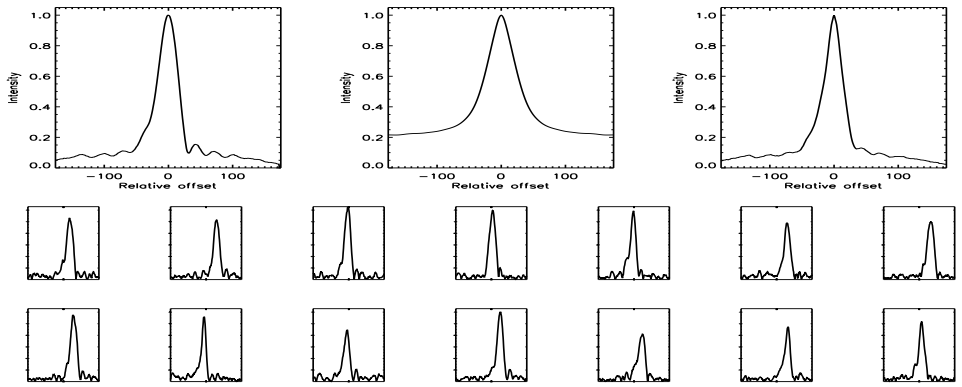

FIGURE B.239: SFP inspection for HD 094765 with S1-W1 on UT 2008/04/15, seq 001

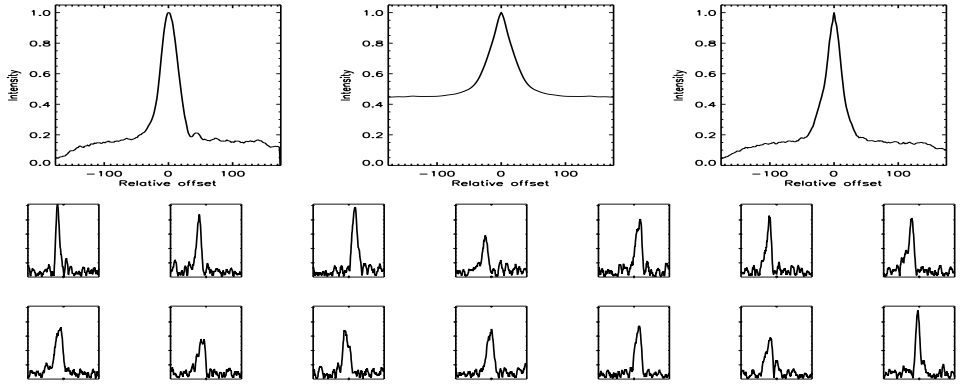

FIGURE B.240: SFP inspection for HD 096064 with S1-E1 on UT 2008/04/14, seq 001

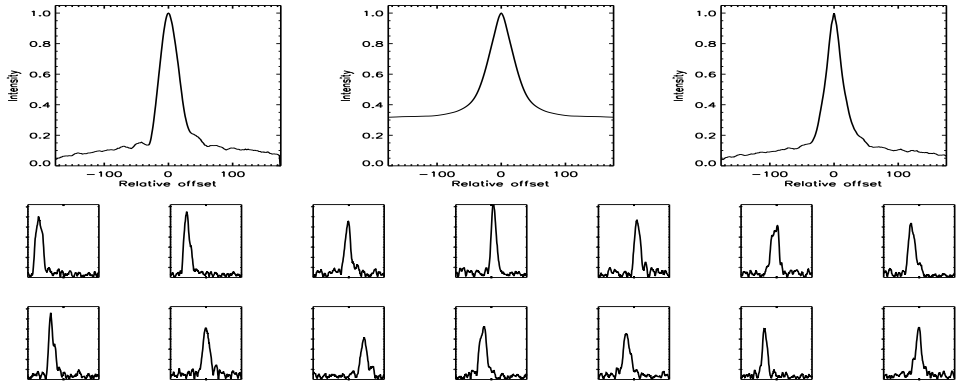

FIGURE B.241: SFP inspection for HD 096064 with S1-W1 on UT 2008/04/15, seq 001

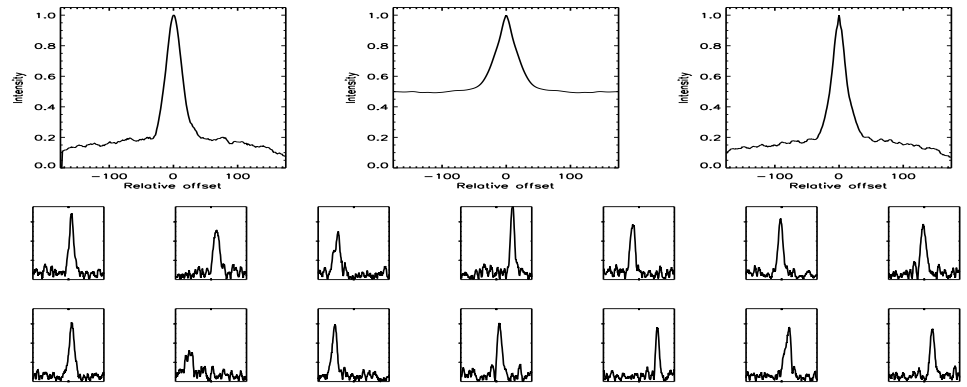

FIGURE B.242: SFP inspection for HD 097334 with S1-E1 on UT 2008/04/12, seq 002

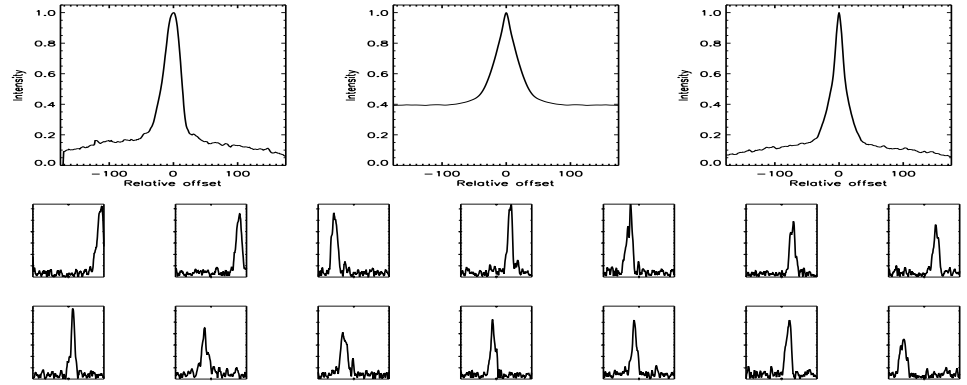

FIGURE B.243: SFP inspection for HD 097334 with S1-W1 on UT 2008/04/12, seq 001

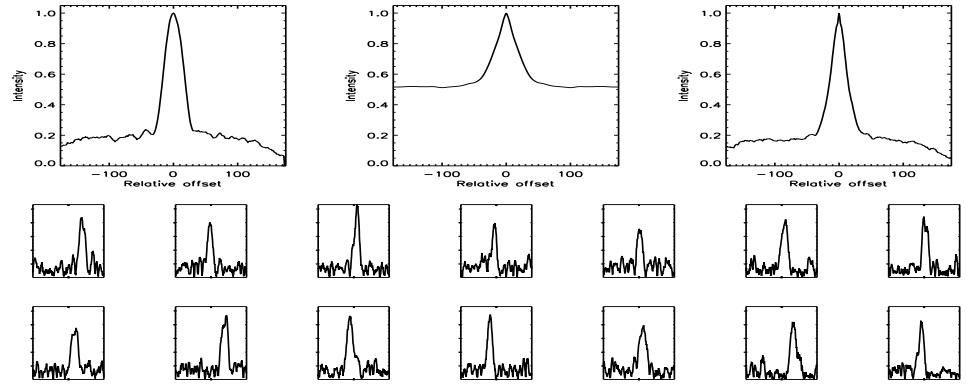

FIGURE B.244: SFP inspection for HD 097658 with S1-E1 on UT 2008/04/13, seq 001

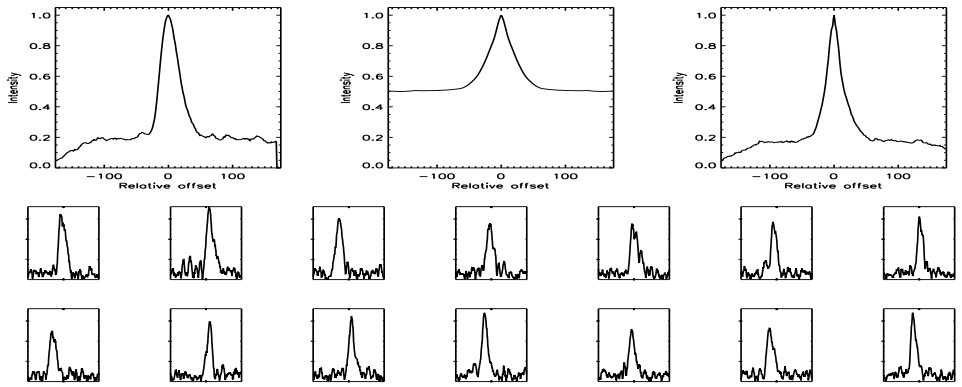

FIGURE B.245: SFP inspection for HD 097658 with S1-E1 on UT 2008/04/14, seq 001

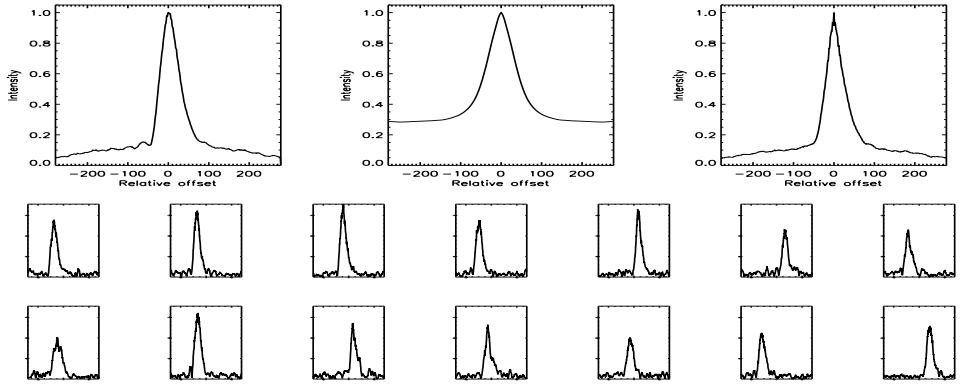

FIGURE B.246: SFP inspection for HD 098230 with S1-E1 on UT 2007/02/06, seq 001

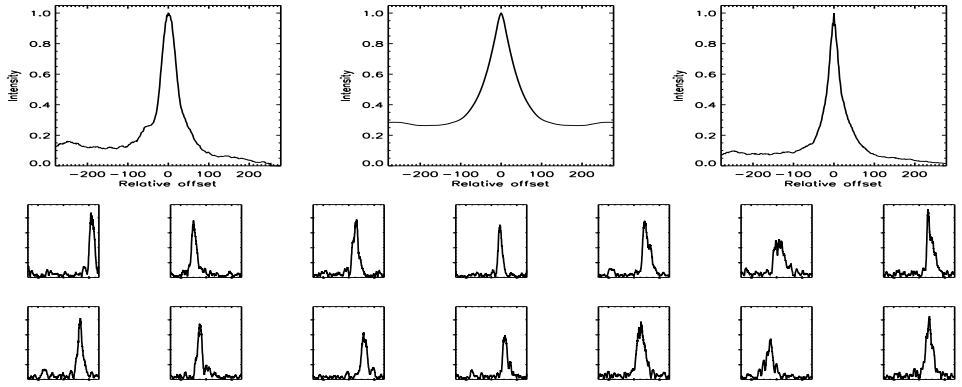

FIGURE B.247: SFP inspection for HD 098230 with S1-E1 on UT 2007/03/08, seq 001

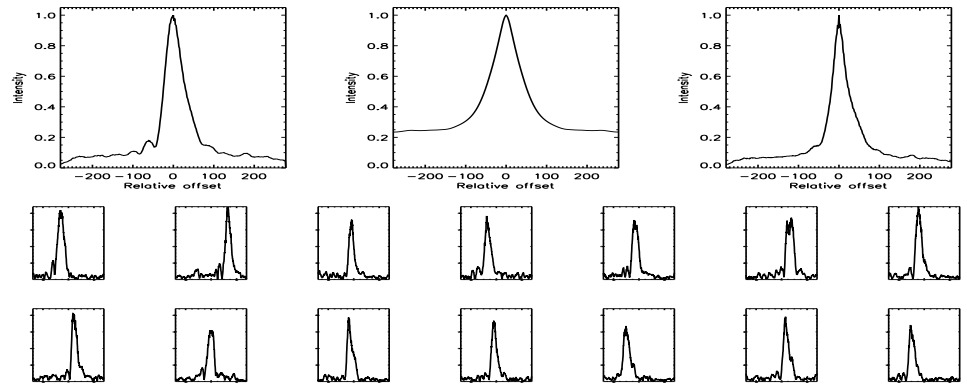

FIGURE B.248: SFP inspection for HD 098230 with S1-E1 on UT 2007/03/08, seq 002

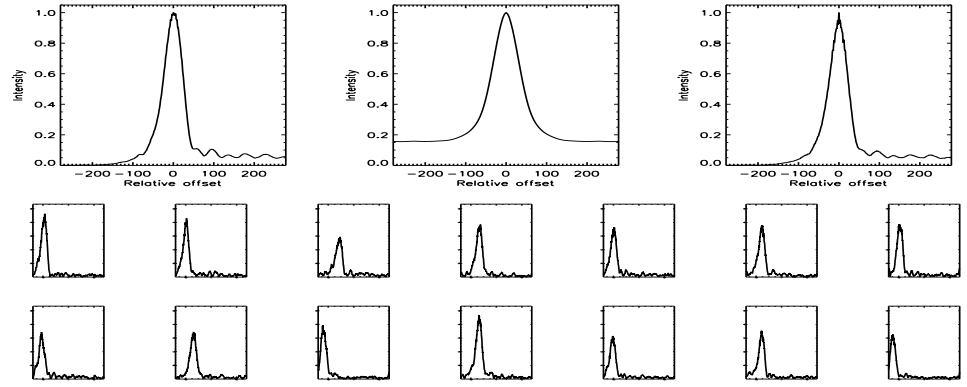

FIGURE B.249: SFP inspection for HD 098230 with S1-E1 on UT 2007/05/17, seq 001

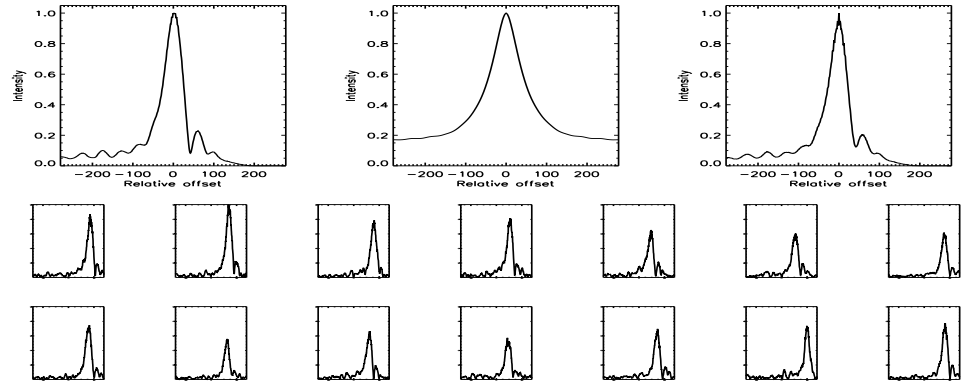

FIGURE B.250: SFP inspection for HD 098230 with S1-E1 on UT 2007/05/17, seq 002

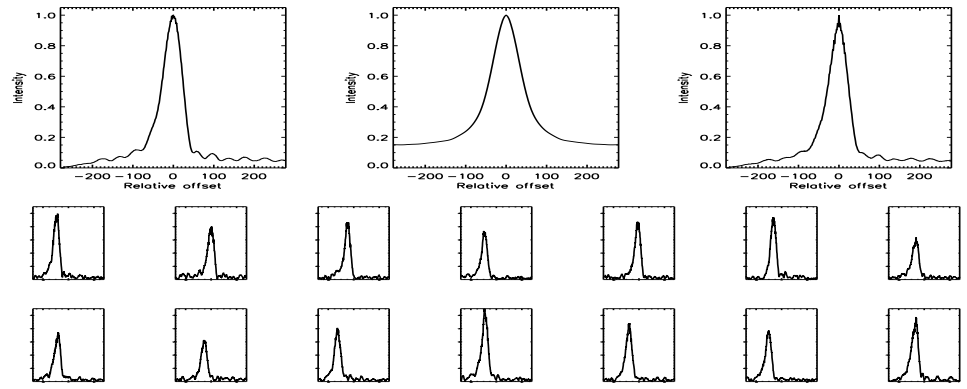

FIGURE B.251: SFP inspection for HD 098230 with S1-E1 on UT 2007/05/17, seq 003

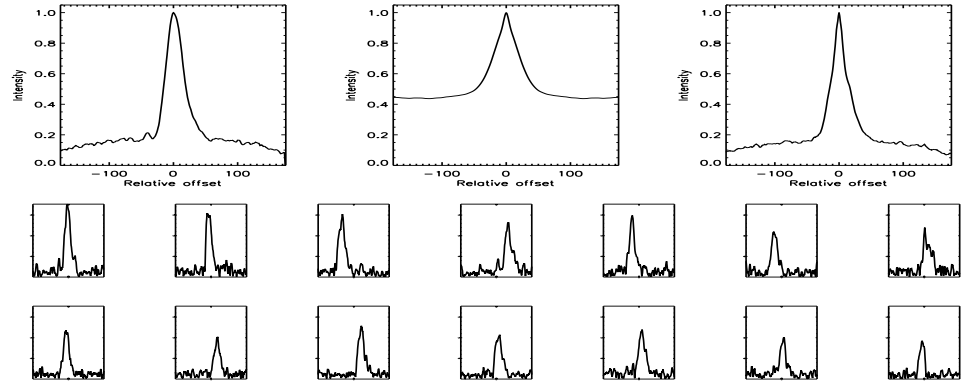

FIGURE B.252: SFP inspection for HD 098230 with S1-E1 on UT 2008/04/13, seq 001

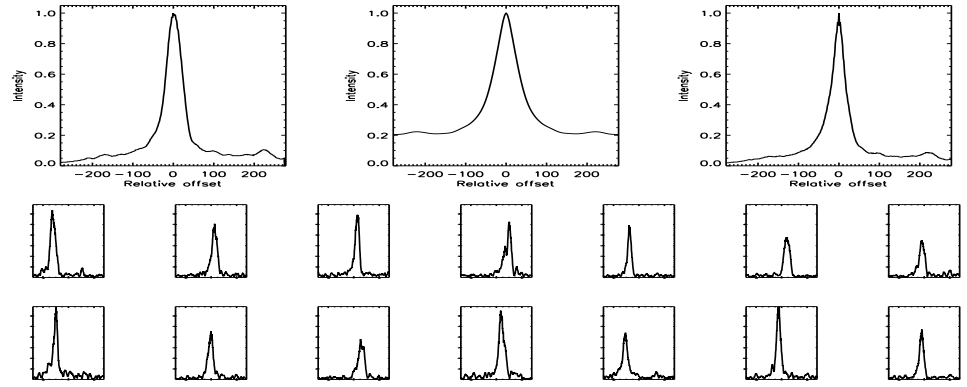

FIGURE B.253: SFP inspection for HD 098230 with S1-W1 on UT 2007/04/24, seq 001

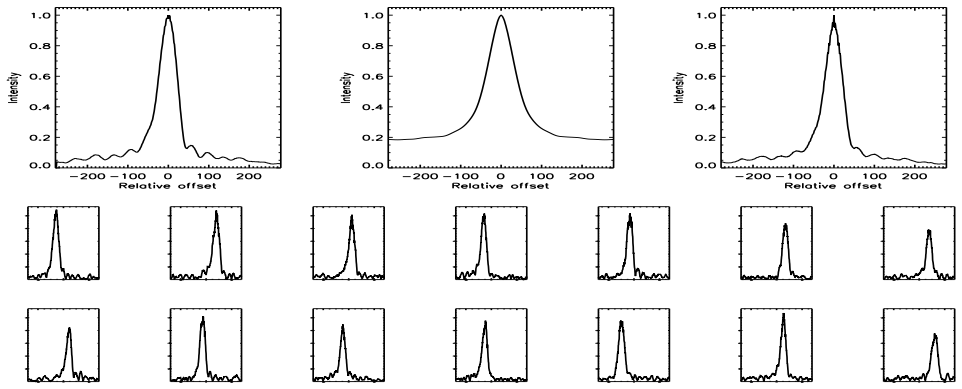

FIGURE B.254: SFP inspection for HD 098230 with S1-W1 on UT 2007/05/28, seq 001

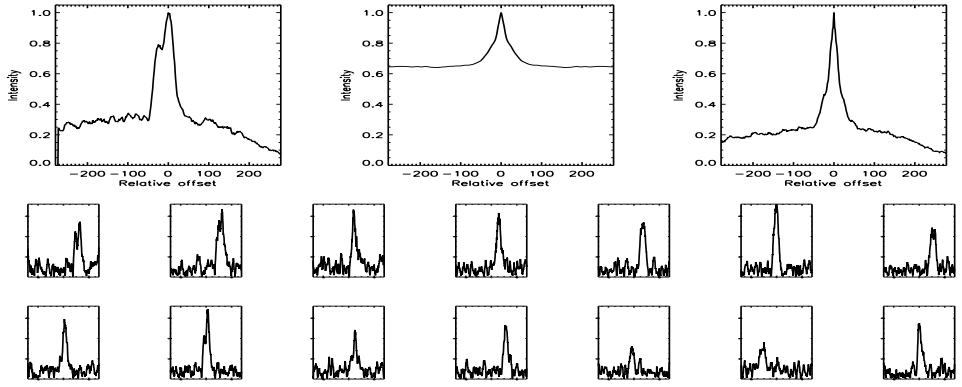

FIGURE B.255: SFP inspection for HD 098230 with S1-W1 on UT 2007/06/01, seq 001

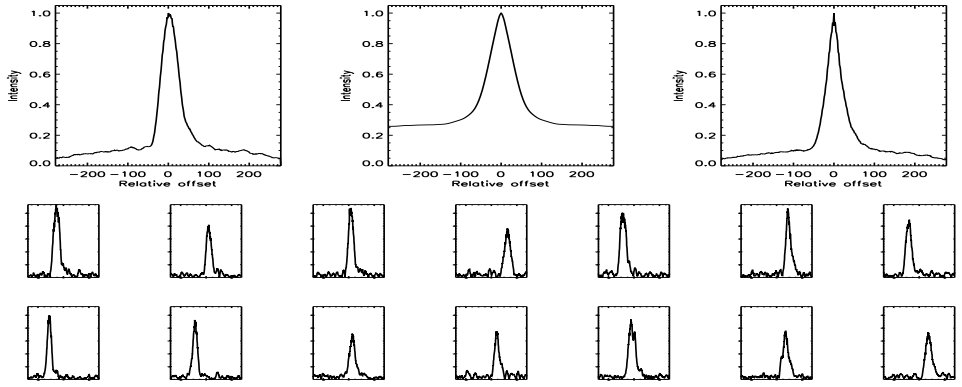

FIGURE B.256: SFP inspection for HD 098230 with S1-W1 on UT 2007/06/01, seq 002

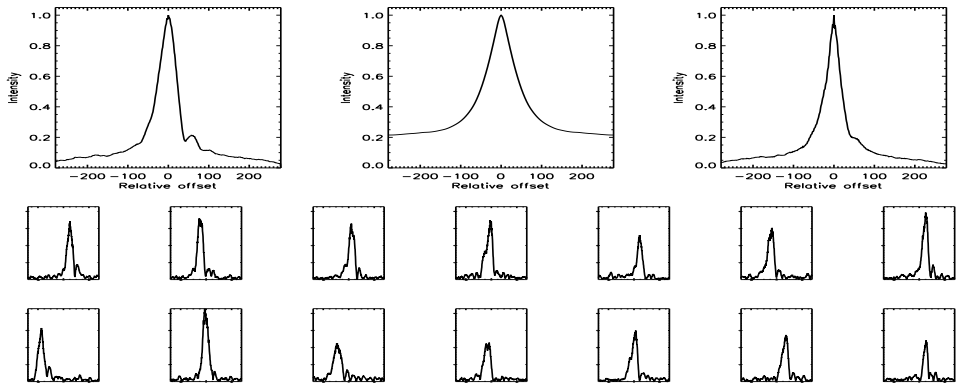

FIGURE B.257: SFP inspection for HD 098230 with S1-W1 on UT 2007/06/01, seq 003

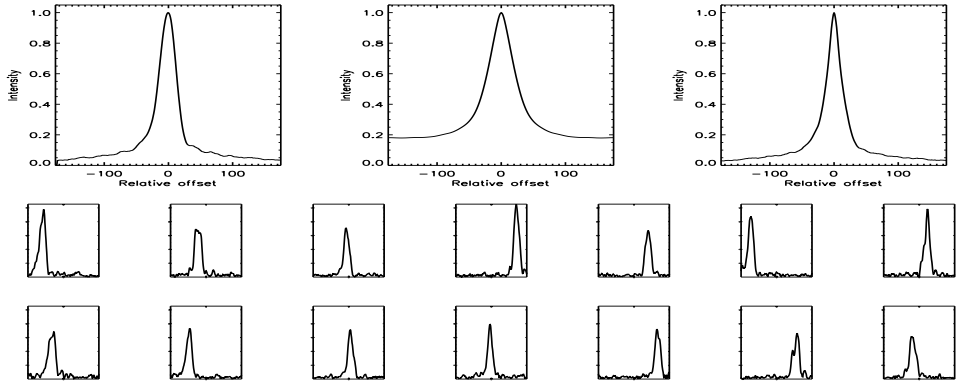

FIGURE B.258: SFP inspection for HD 098230 with S1-W1 on UT 2008/04/12, seq 001

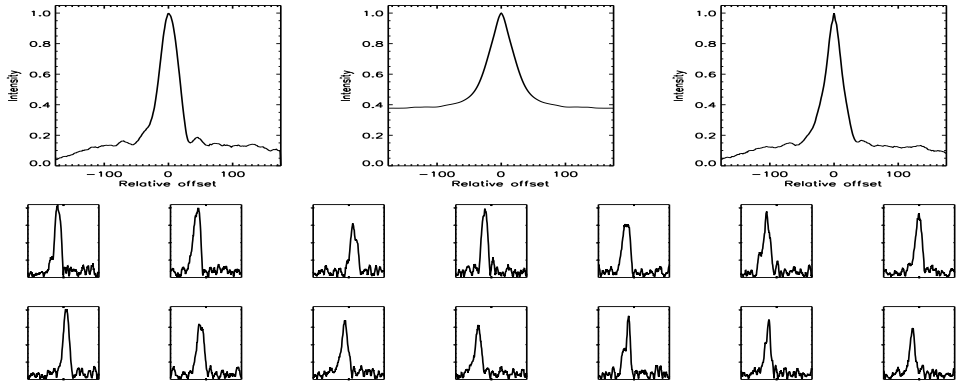

FIGURE B.259: SFP inspection for HD 098281 with S1-E1 on UT 2008/04/14, seq 001

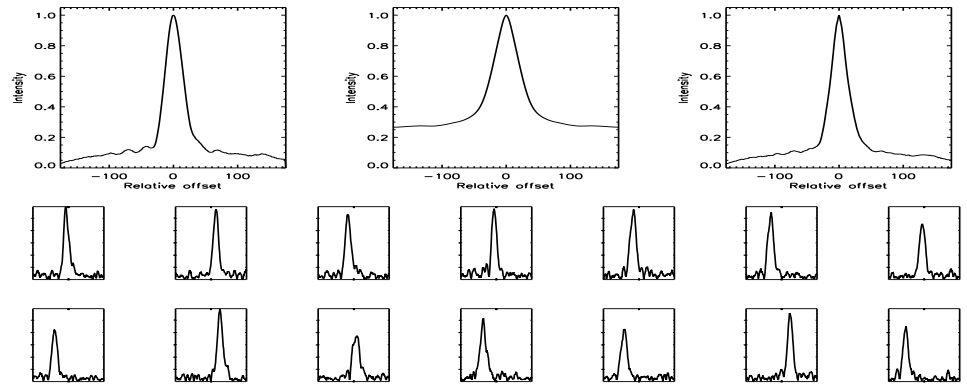

FIGURE B.260: SFP inspection for HD 098281 with S1-W1 on UT 2008/04/15, seq 001

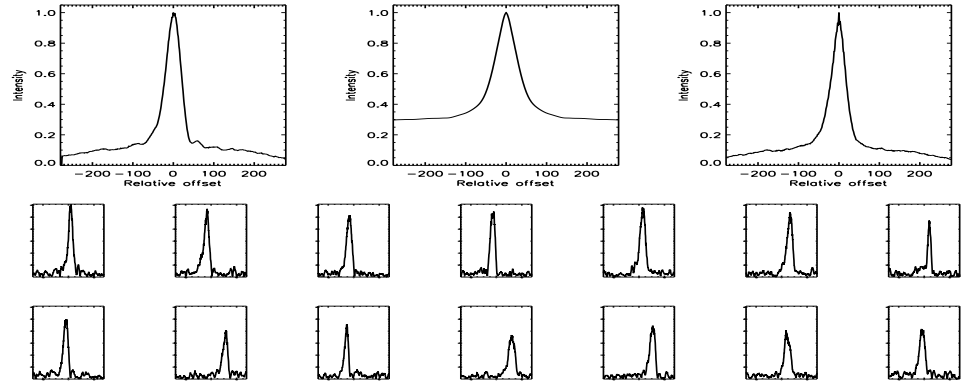

FIGURE B.261: SFP inspection for HD 099028 with S1-E1 on UT 2007/02/06, seq 003

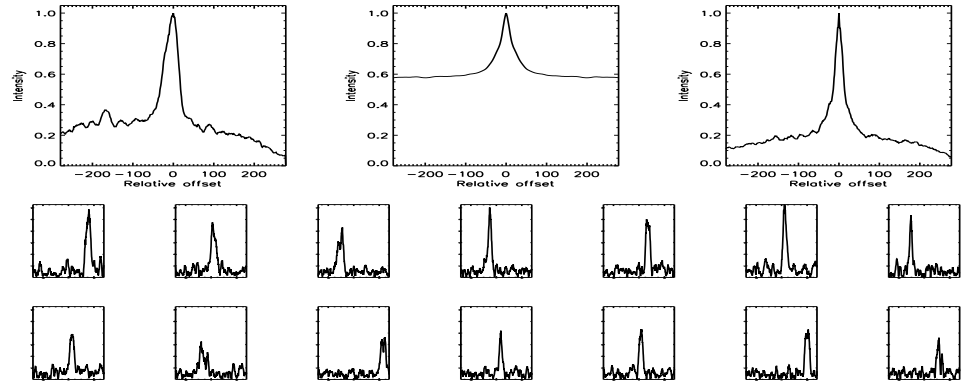

FIGURE B.262: SFP inspection for HD 099491 with S1-E1 on UT 2007/03/08, seq 001

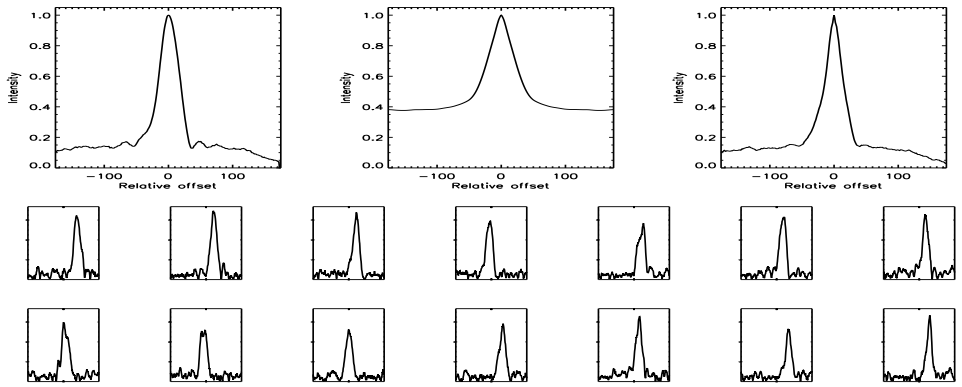

FIGURE B.263: SFP inspection for HD 099491 with S1-E1 on UT 2008/04/14, seq 001

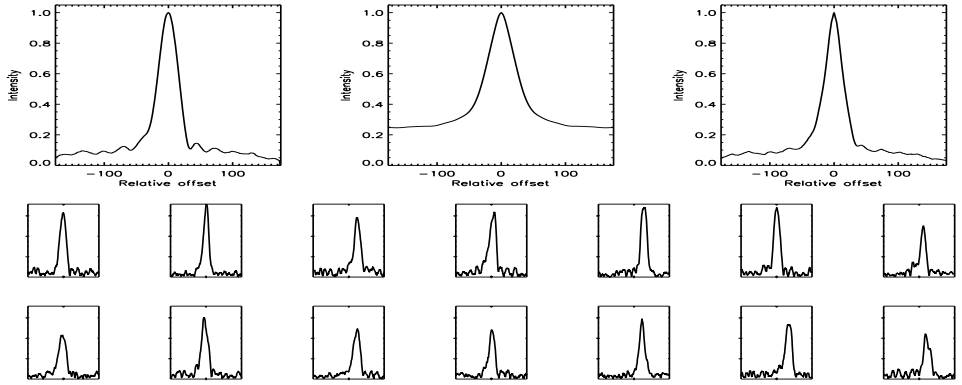

FIGURE B.264: SFP inspection for HD 099491 with S1-E1 on UT 2008/04/14, seq 002

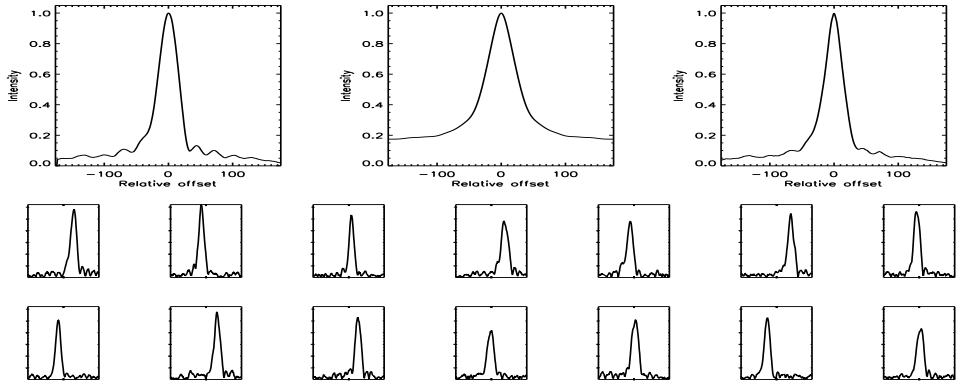

FIGURE B.265: SFP inspection for HD 099491 with S1-W1 on UT 2008/04/15, seq 001

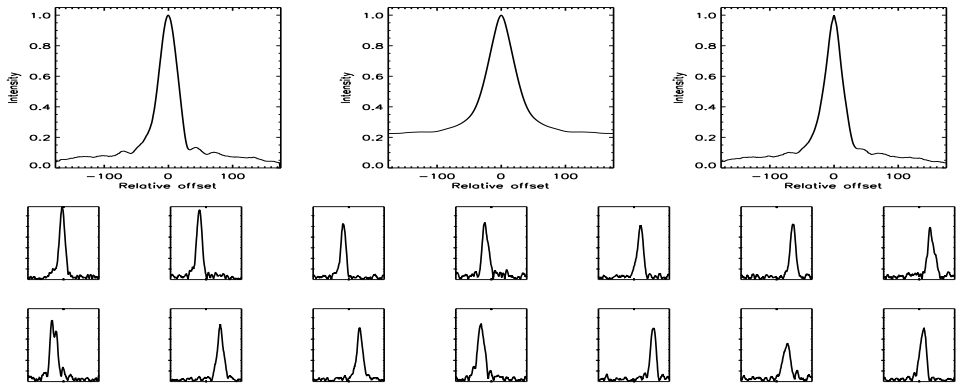

FIGURE B.266: SFP inspection for HD 099492 with S1-W1 on UT 2008/04/15, seq 001

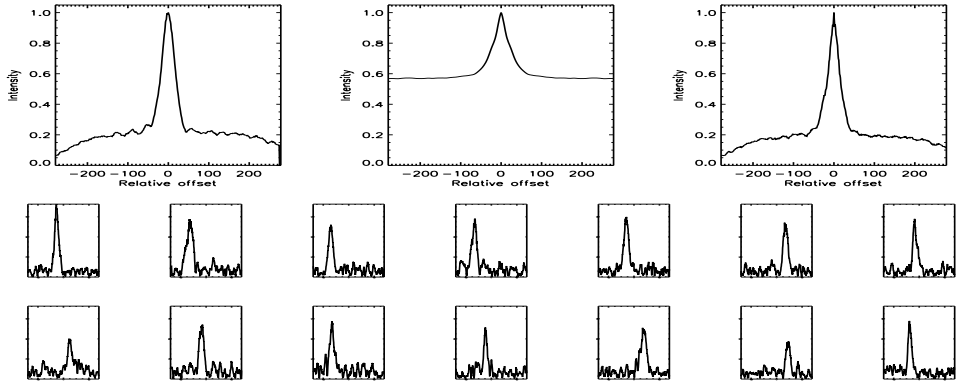

FIGURE B.267: SFP inspection for HD 100180 with S1-E1 on UT 2007/02/06, seq 001

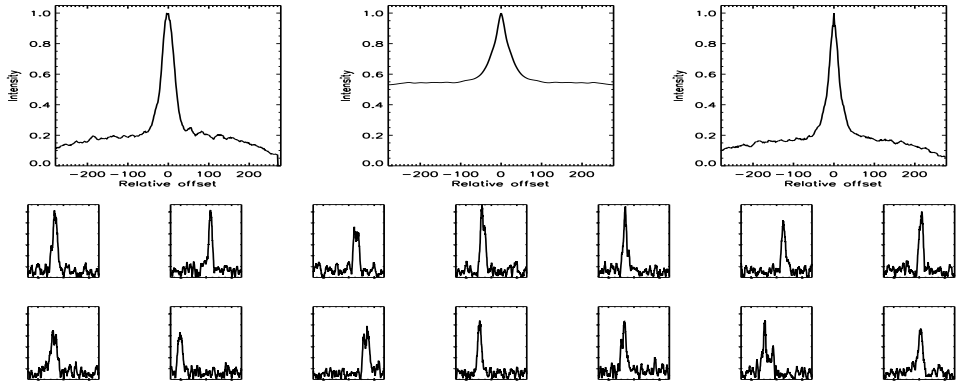

FIGURE B.268: SFP inspection for HD 100180 with S1-E1 on UT 2007/03/08, seq 001

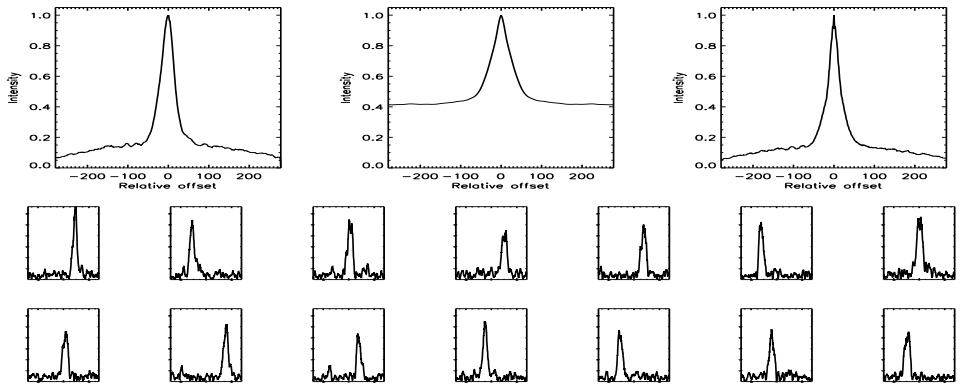

FIGURE B.269: SFP inspection for HD 100180 with S1-W1 on UT 2007/04/24, seq 001

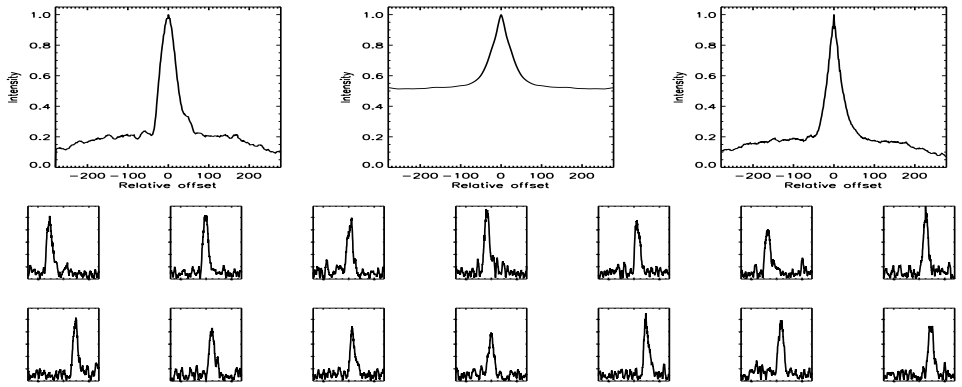

FIGURE B.270: SFP inspection for HD 101177 with S1-E1 on UT 2007/05/17, seq 001

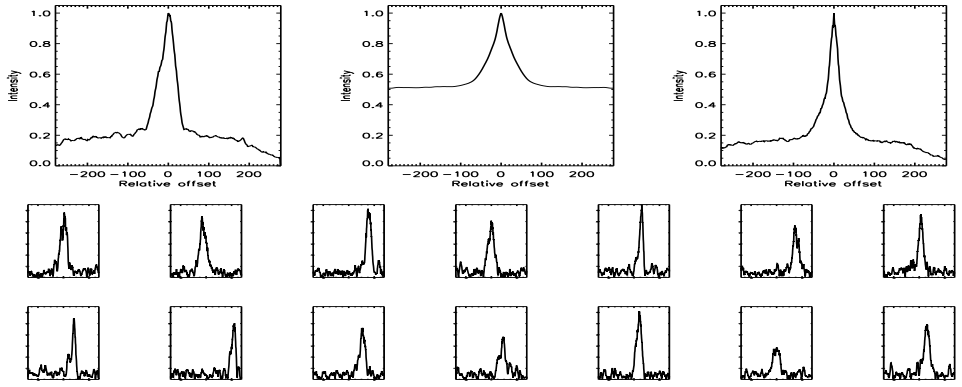

FIGURE B.271: SFP inspection for HD 101177 with S1-W1 on UT 2007/04/24, seq 001

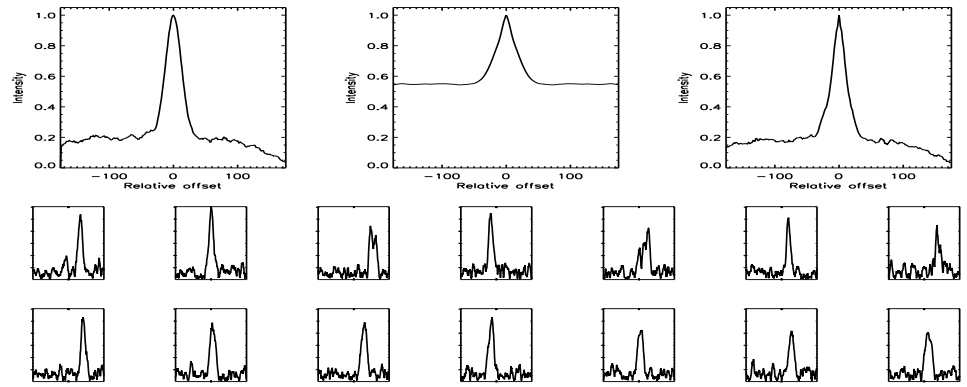

FIGURE B.272: SFP inspection for HD 101206 with S1-E1 on UT 2008/04/12, seq 002

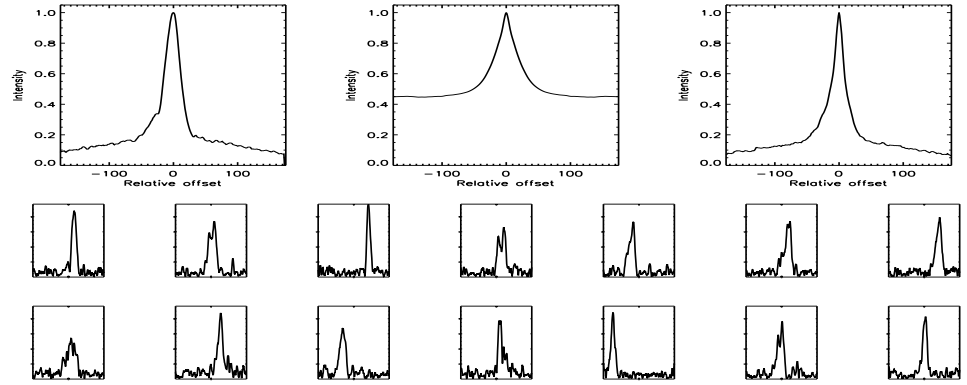

FIGURE B.273: SFP inspection for HD 101206 with S1-W1 on UT 2008/04/12, seq 001

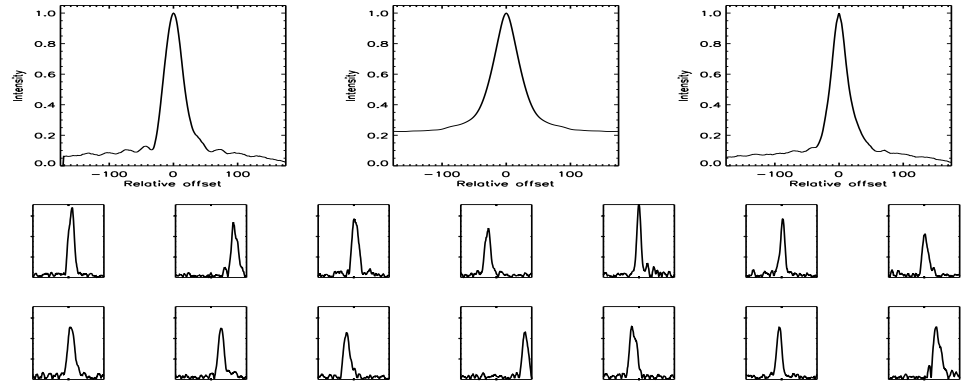

FIGURE B.274: SFP inspection for HD 104304 with S1-E1 on UT 2008/04/14, seq 001

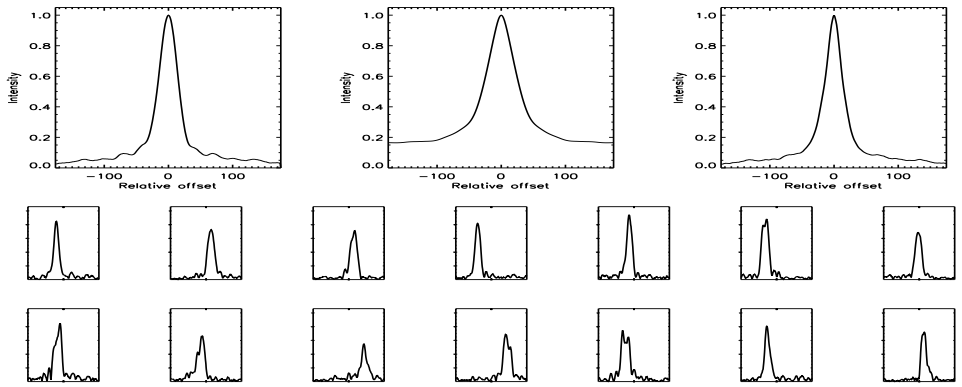

FIGURE B.275: SFP inspection for HD 104304 with S1-W1 on UT 2008/04/15, seq 001

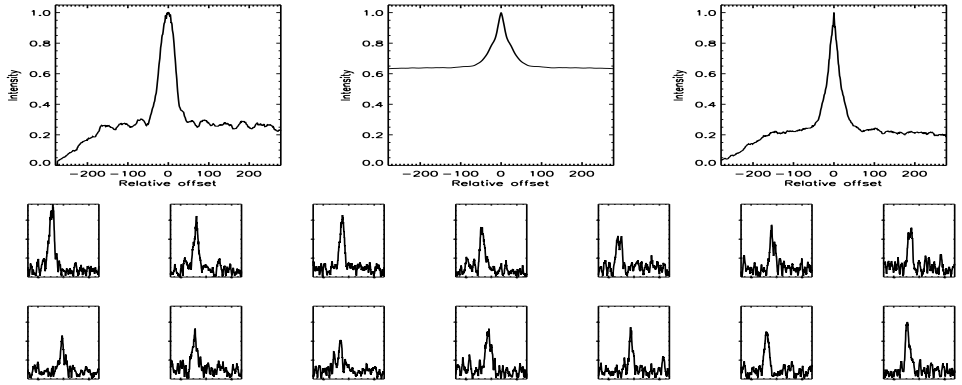

FIGURE B.276: SFP inspection for HD 105631 with S1-E1 on UT 2007/05/17, seq 001

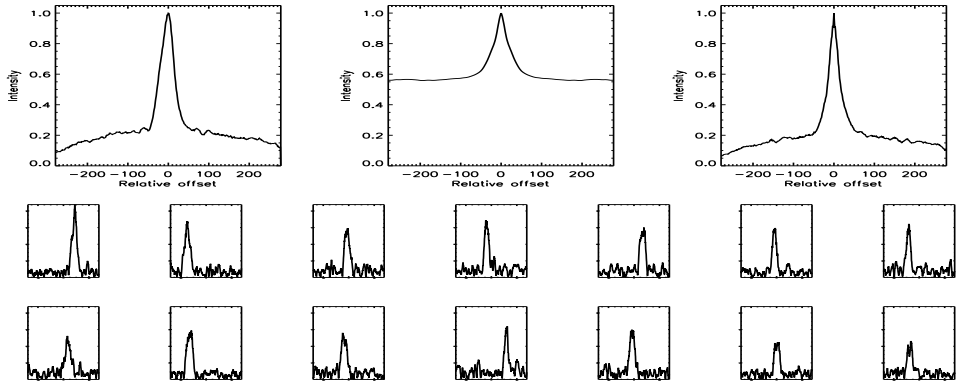

FIGURE B.277: SFP inspection for HD 105631 with S1-W1 on UT 2007/04/24, seq 001

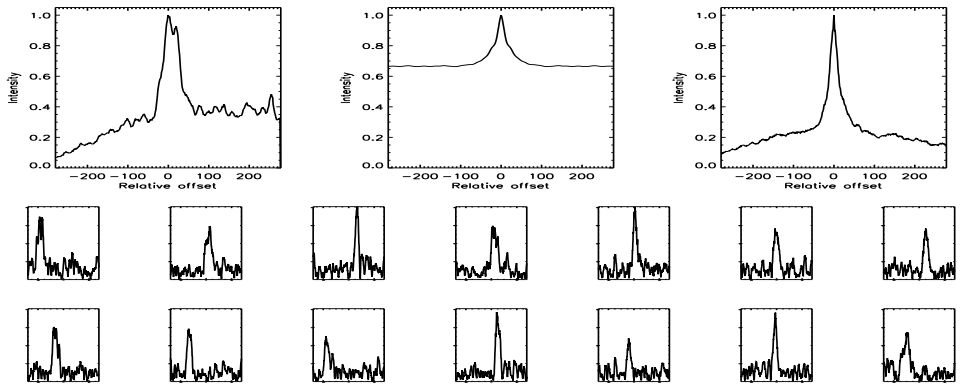

FIGURE B.278: SFP inspection for HD 105631 with S1-W1 on UT 2007/06/01, seq 001

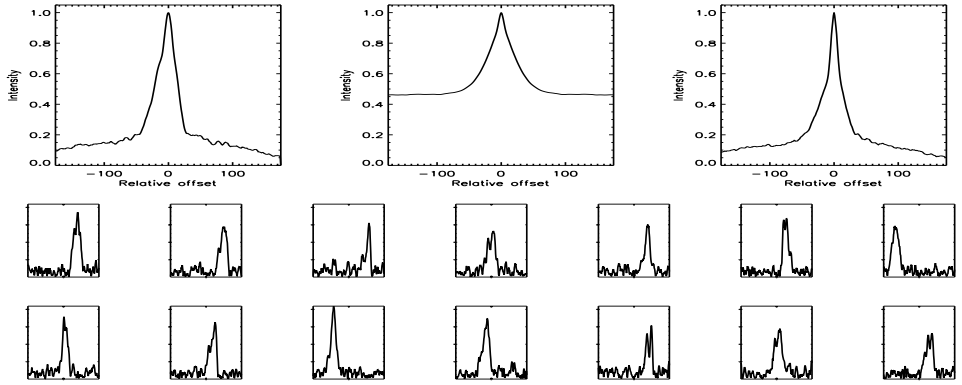

FIGURE B.279: SFP inspection for HD 105631 with S1-W1 on UT 2008/04/26, seq 001

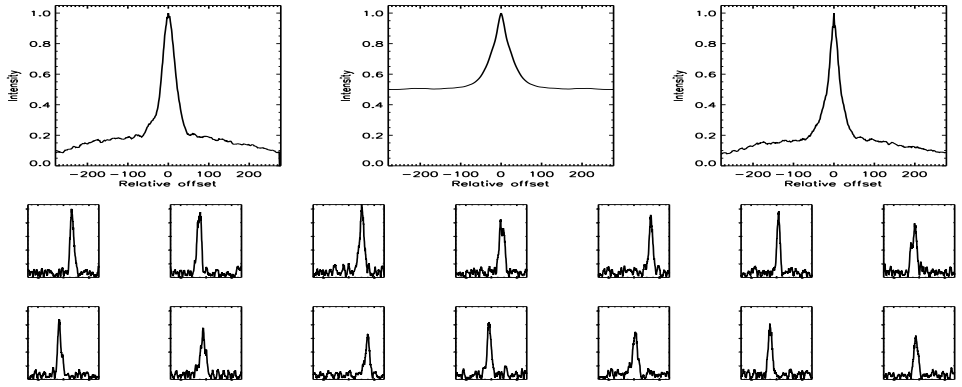

FIGURE B.280: SFP inspection for HD 108954 with S1-E1 on UT 2007/04/11, seq 001

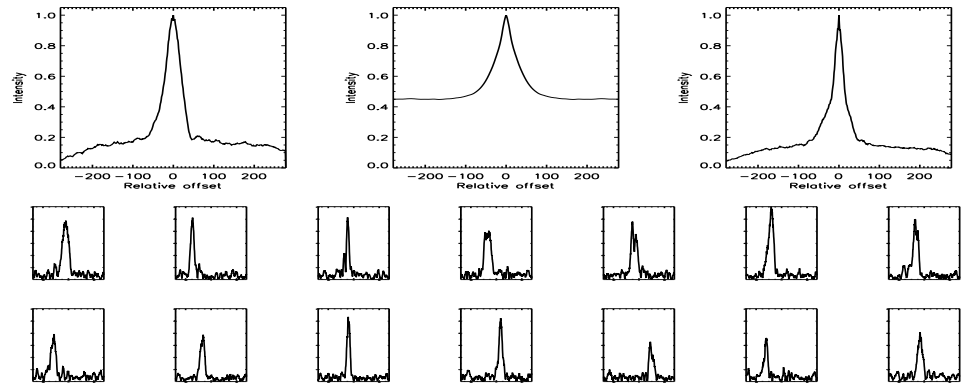

FIGURE B.281: SFP inspection for HD 108954 with S1-E1 on UT 2007/04/11, seq 002

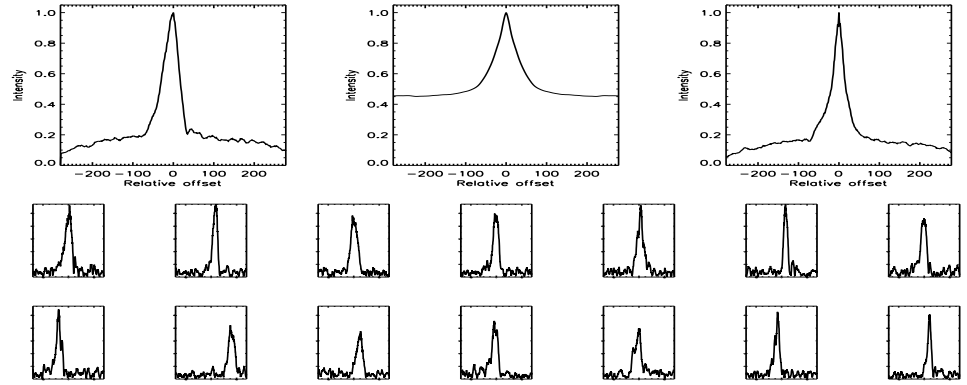

FIGURE B.282: SFP inspection for HD 108954 with S1-W1 on UT 2007/04/24, seq 001

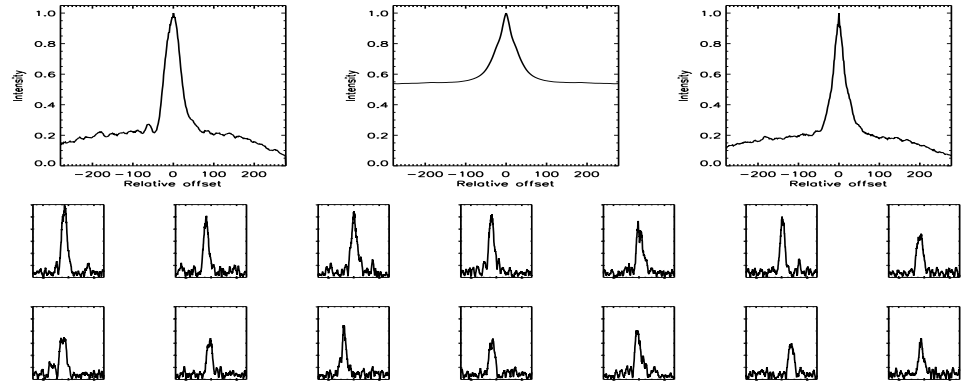

FIGURE B.283: SFP inspection for HD 110833 with S1-E1 on UT 2007/04/14, seq 001

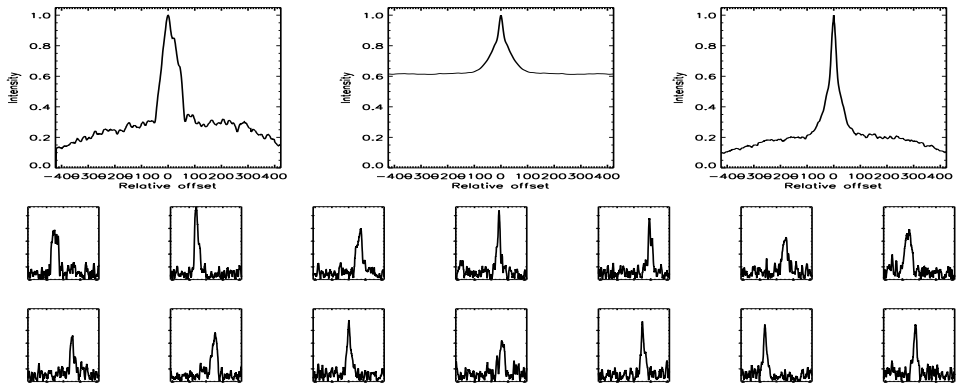

FIGURE B.284: SFP inspection for HD 110833 with S1-E1 on UT 2007/07/28, seq 001

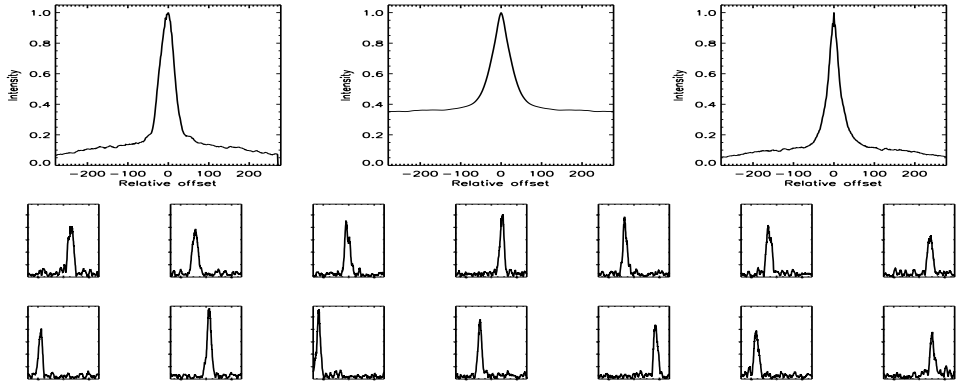

FIGURE B.285: SFP inspection for HD 110833 with S1-W1 on UT 2007/04/17, seq 001

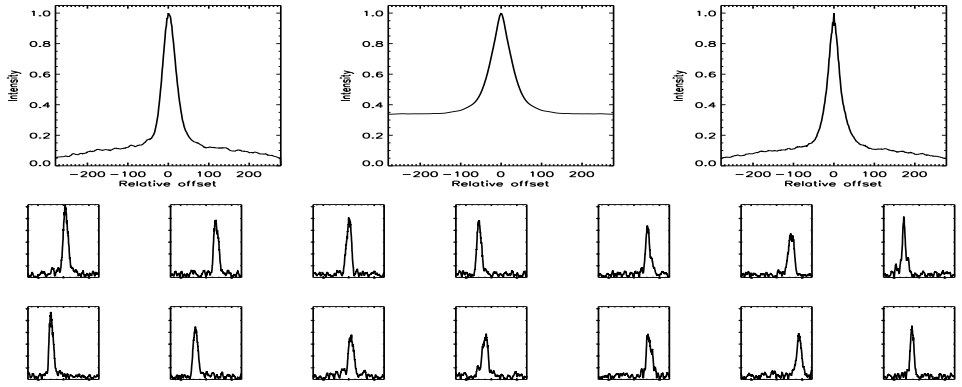

FIGURE B.286: SFP inspection for HD 110833 with S1-W1 on UT 2007/04/17, seq 002

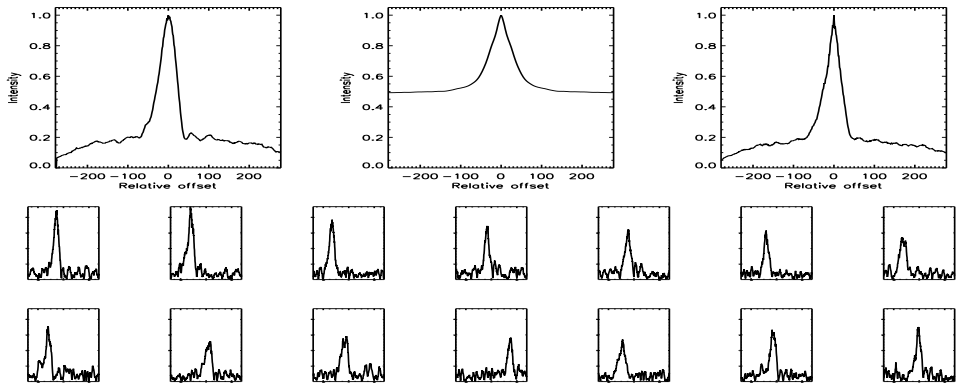

FIGURE B.287: SFP inspection for HD 110833 with S1-W1 on UT 2007/05/28, seq 002

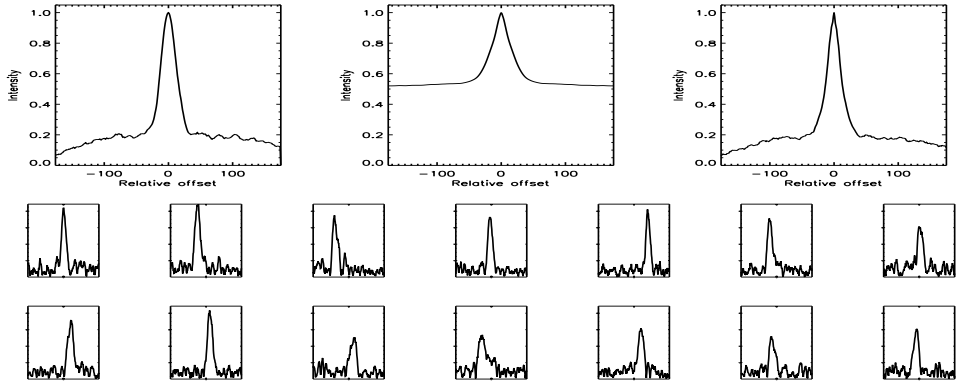

FIGURE B.288: SFP inspection for HD 112758 with S1-E1 on UT 2008/04/14, seq 001

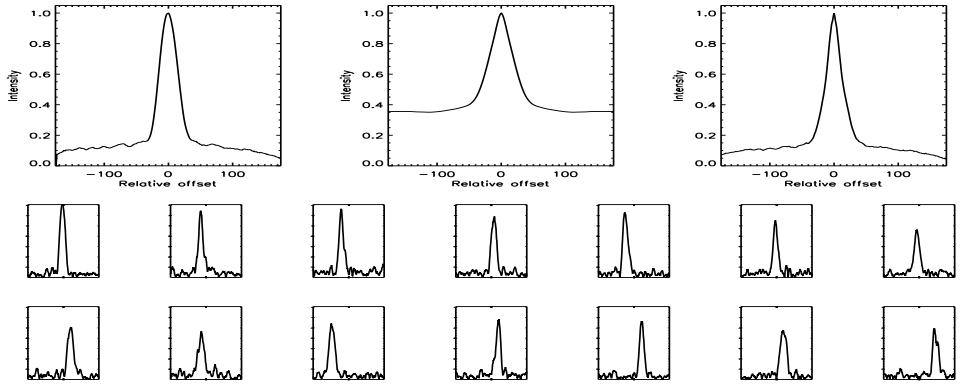

FIGURE B.289: SFP inspection for HD 112758 with S1-W1 on UT 2008/04/15, seq 001

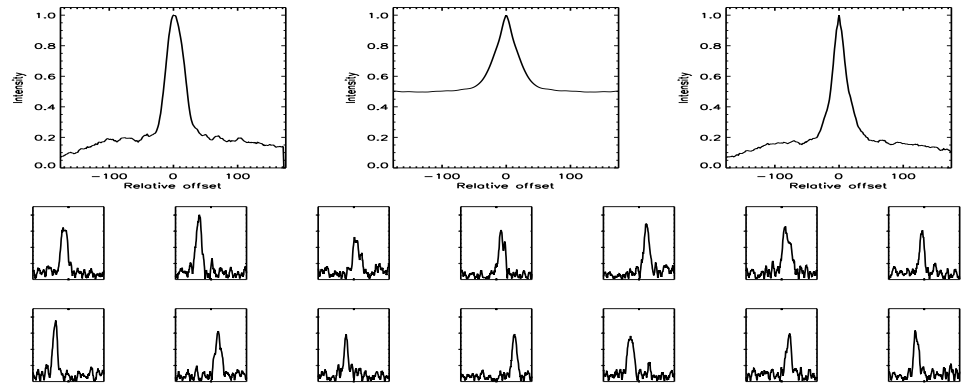

FIGURE B.290: SFP inspection for HD 113449 with S1-E1 on UT 2008/04/14, seq 001

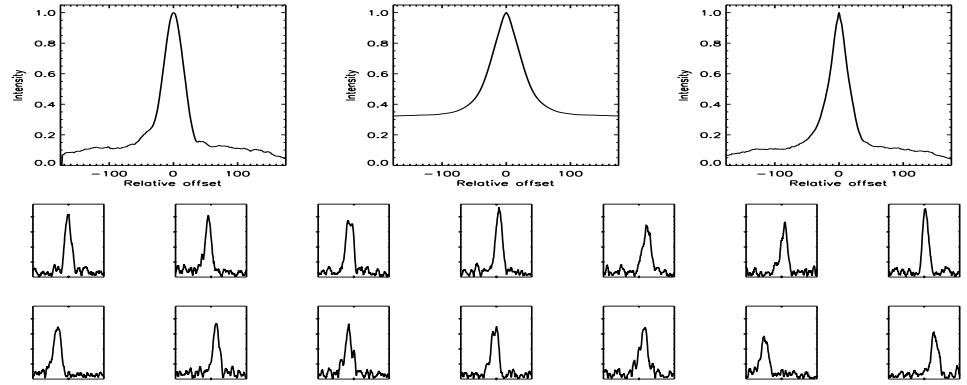

FIGURE B.291: SFP inspection for HD 113449 with S1-W1 on UT 2008/04/15, seq 001

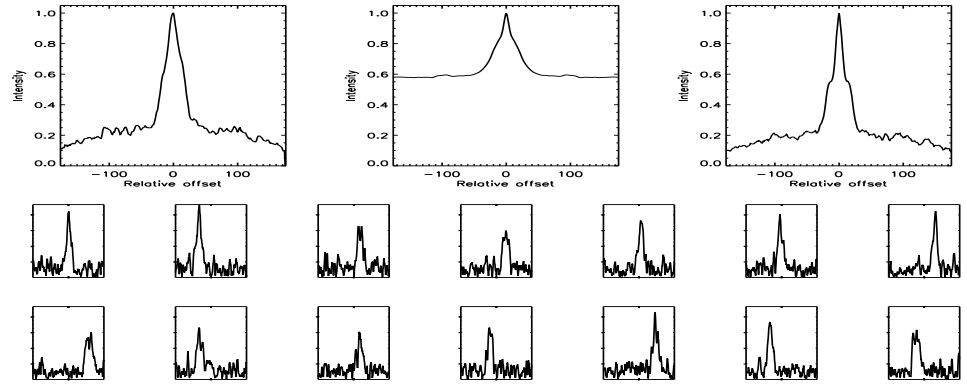

FIGURE B.292: SFP inspection for HD 114783 with S1-E1 on UT 2008/04/13, seq 001

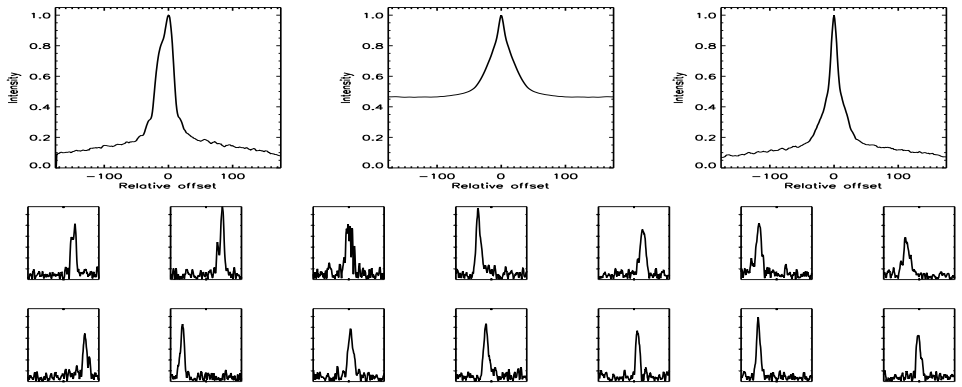

FIGURE B.293: SFP inspection for HD 114783 with S1-E1 on UT 2008/04/25, seq 001

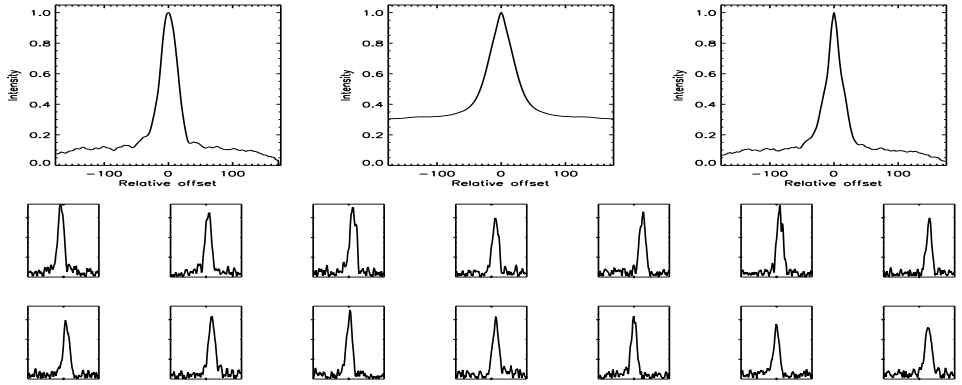

FIGURE B.294: SFP inspection for HD 114783 with S1-W1 on UT 2008/04/13, seq 002

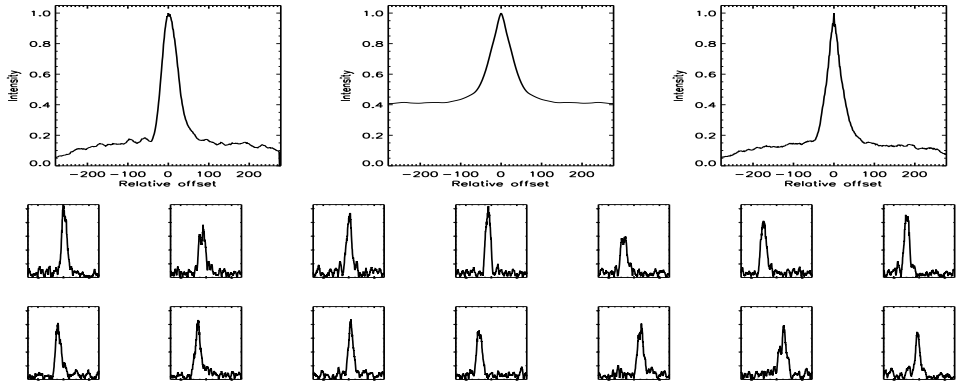

FIGURE B.295: SFP inspection for HD 115404 with S1-E1 on UT 2007/02/06, seq 001

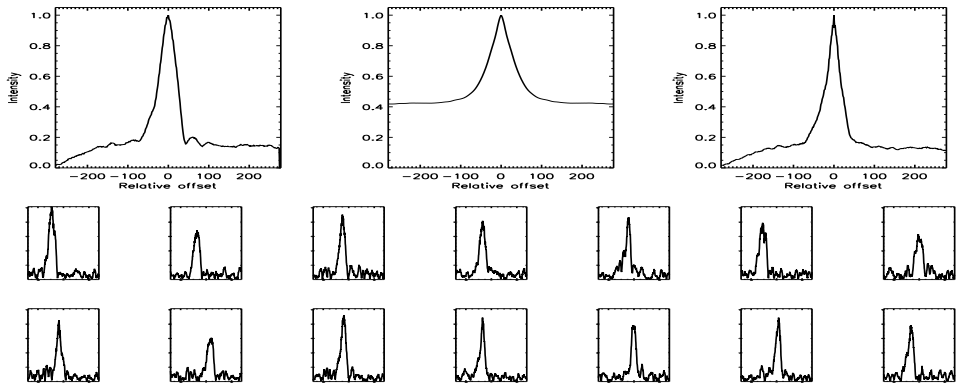

FIGURE B.296: SFP inspection for HD 115404 with S1-E1 on UT 2007/02/06, seq 002

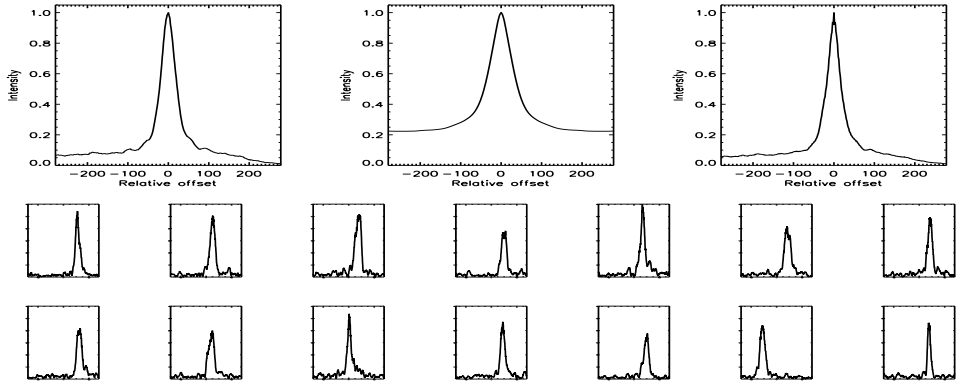

FIGURE B.297: SFP inspection for HD 115404 with S1-E1 on UT 2007/03/08, seq 001

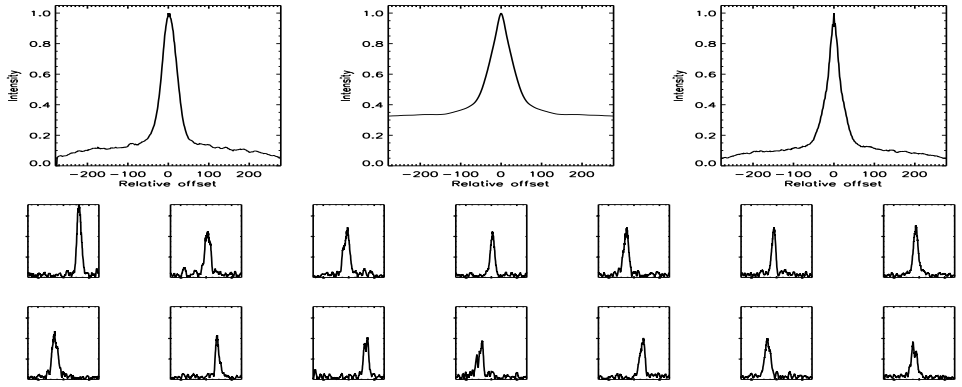

FIGURE B.298: SFP inspection for HD 115404 with S1-W1 on UT 2007/04/24, seq 001

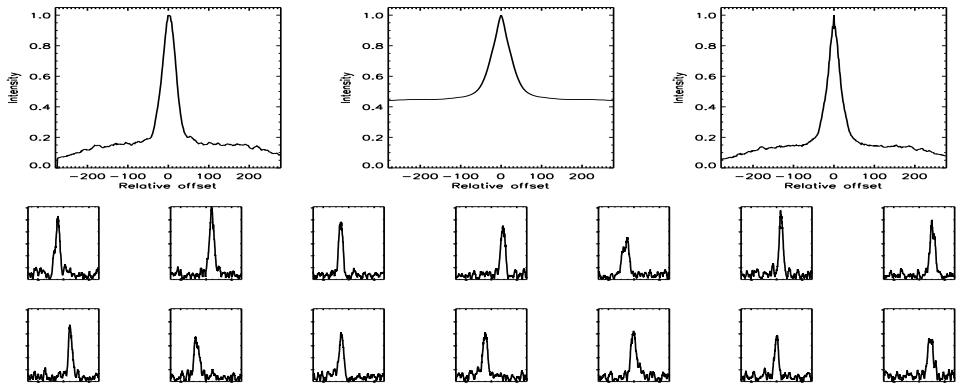

FIGURE B.299: SFP inspection for HD 116442 with S1-E1 on UT 2007/03/12, seq 002

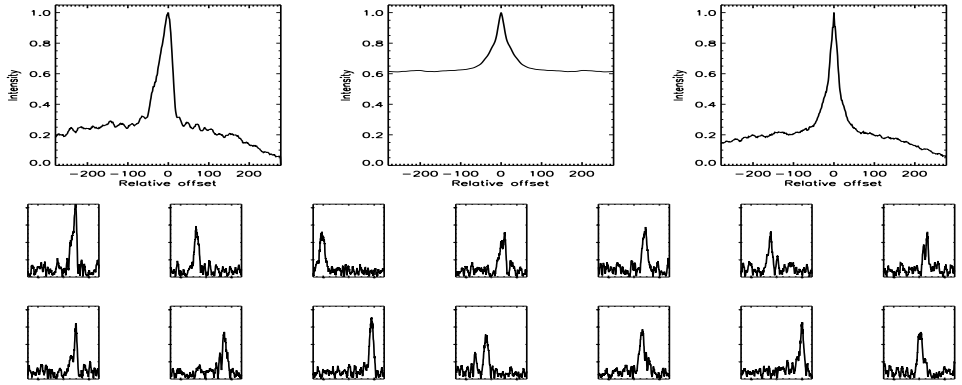

FIGURE B.300: SFP inspection for HD 116442 with S1-W1 on UT 2007/06/01, seq 001

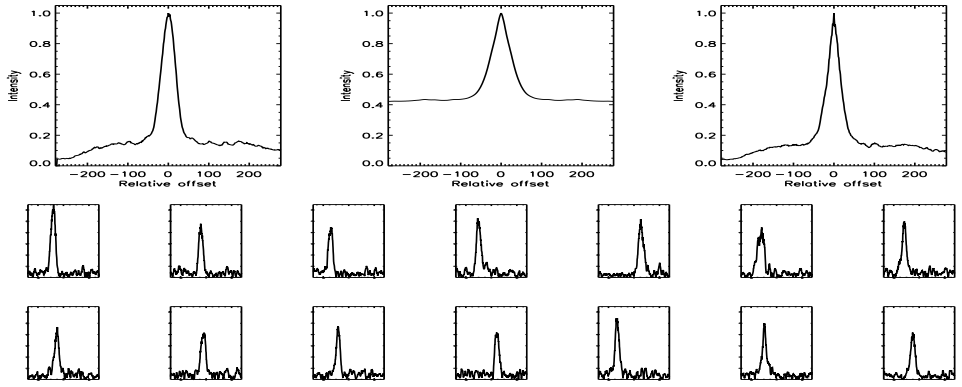

FIGURE B.301: SFP inspection for HD 116443 with S1-E1 on UT 2007/03/12, seq 001

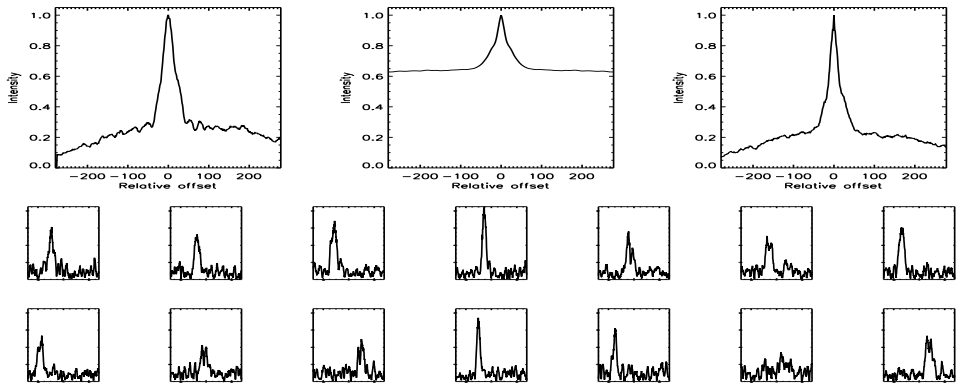

FIGURE B.302: SFP inspection for HD 116443 with S1-W1 on UT 2007/06/01, seq 001

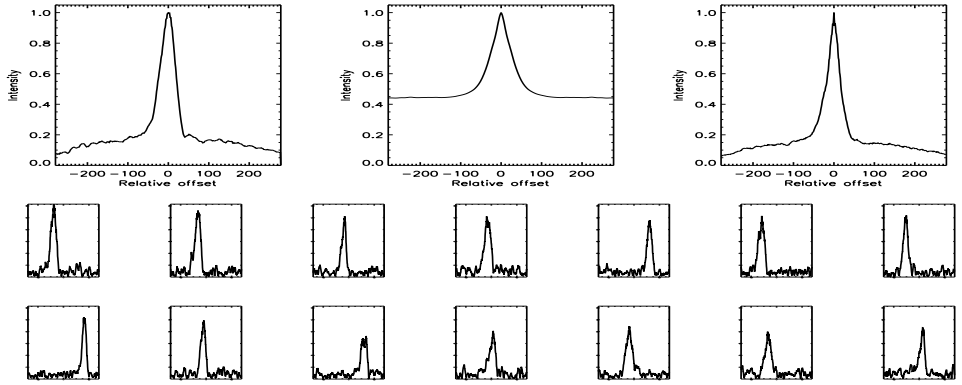

FIGURE B.303: SFP inspection for HD 116956 with S1-E1 on UT 2007/04/03, seq 001

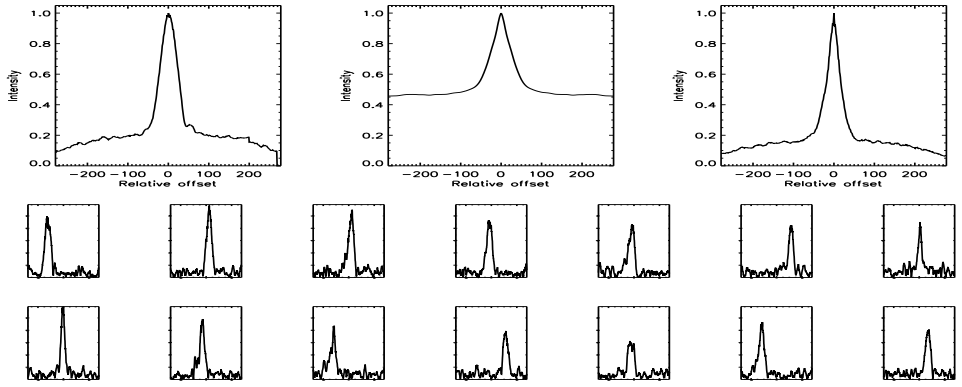

FIGURE B.304: SFP inspection for HD 116956 with S1-E1 on UT 2007/04/03, seq 003

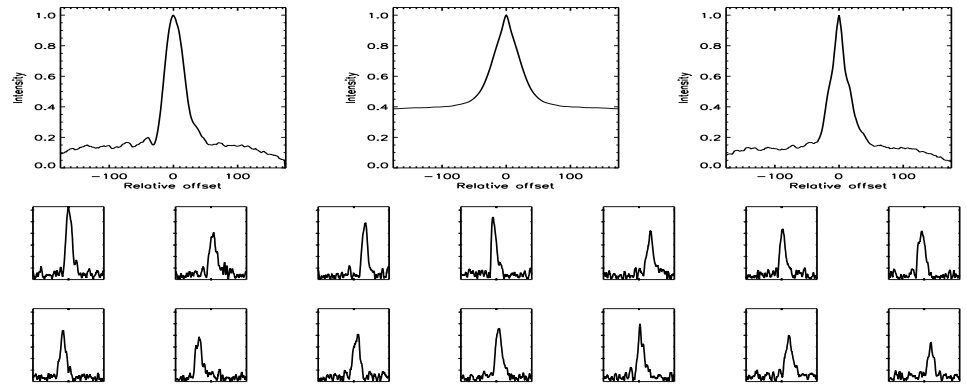

FIGURE B.305: SFP inspection for HD 116956 with S1-E1 on UT 2008/06/25, seq 001

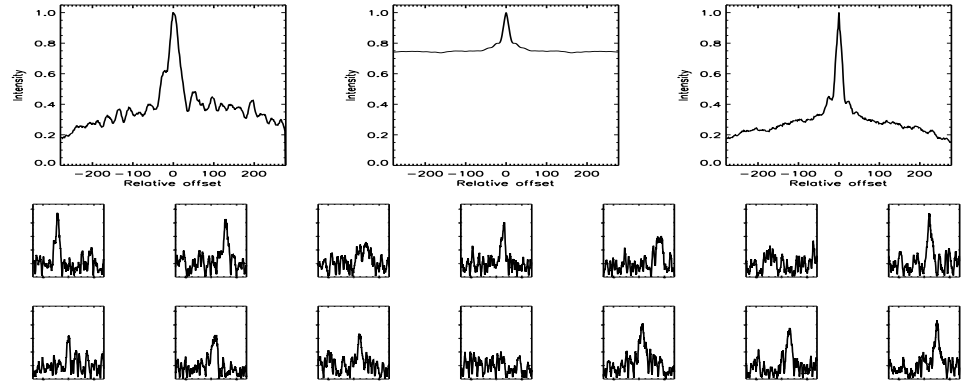

FIGURE B.306: SFP inspection for HD 116956 with S1-W1 on UT 2007/05/28, seq 001

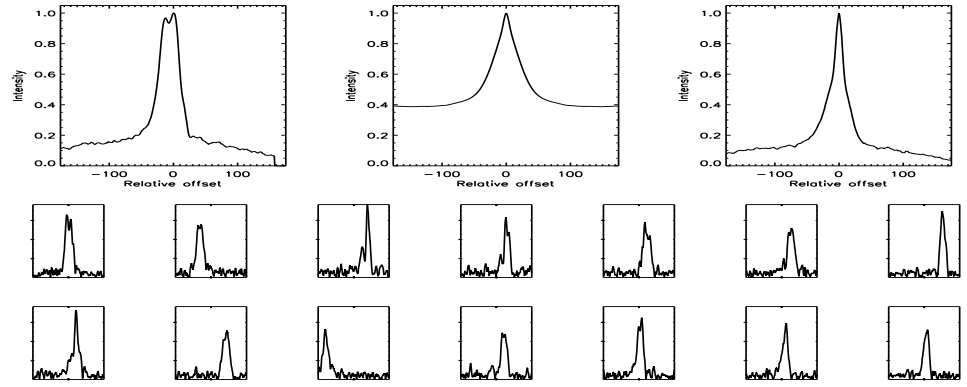

FIGURE B.307: SFP inspection for HD 116956 with S1-W1 on UT 2008/04/26, seq 001

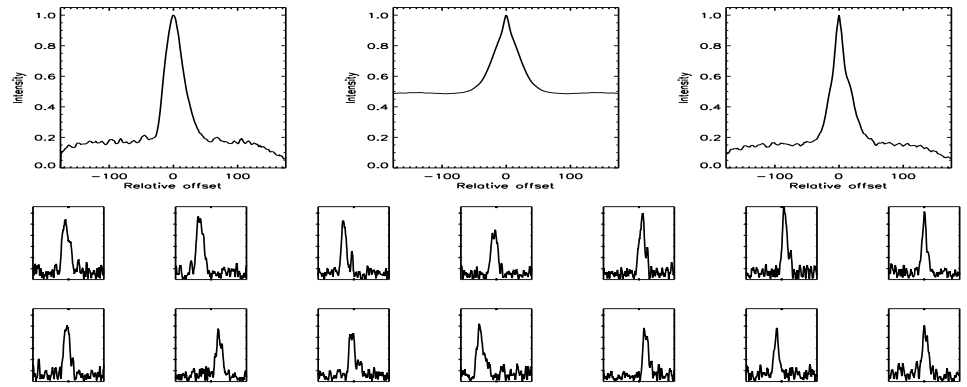

FIGURE B.308: SFP inspection for HD 116956 with S2-W1 on UT 2008/06/24, seq 001

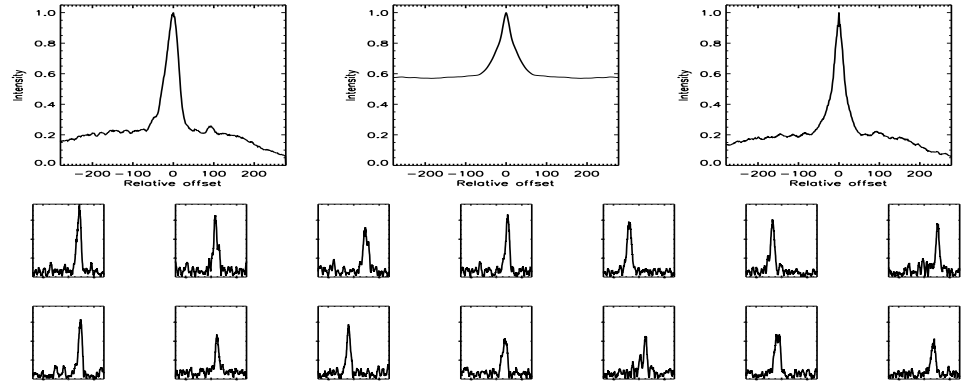

FIGURE B.309: SFP inspection for HD 119332 with S1-E1 on UT 2007/04/03, seq 002

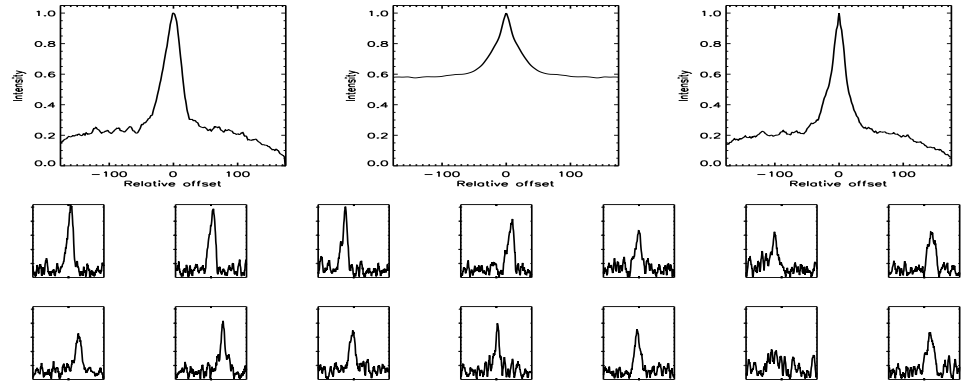

FIGURE B.310: SFP inspection for HD 119332 with S1-E1 on UT 2008/04/12, seq 002

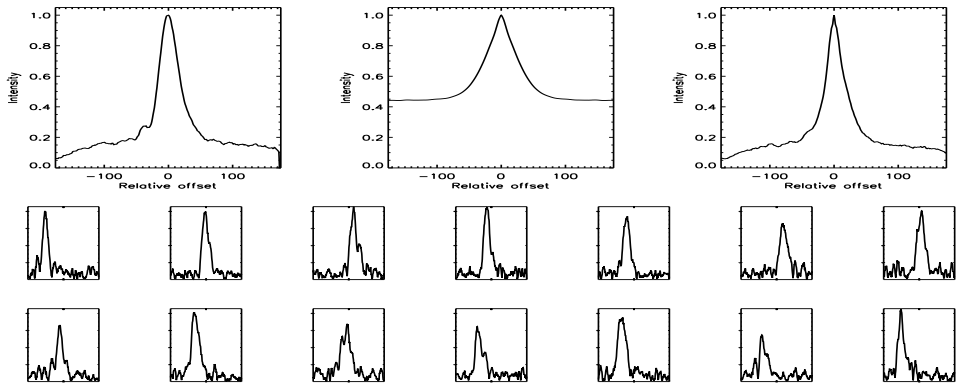

FIGURE B.311: SFP inspection for HD 119332 with S1-W1 on UT 2008/04/12, seq 001

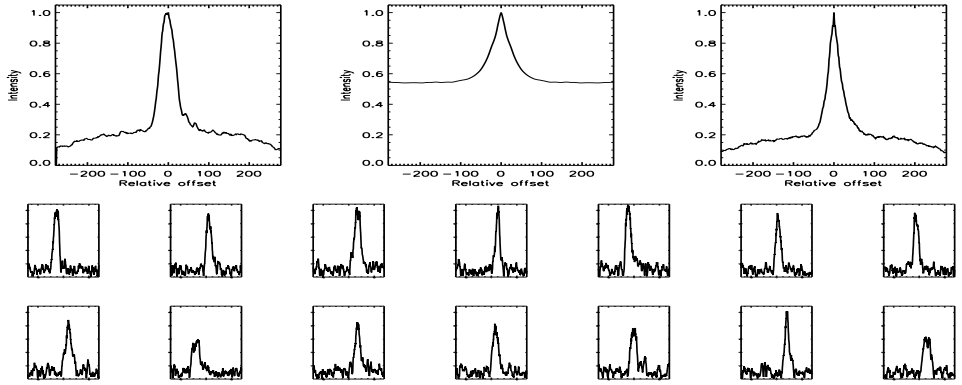

FIGURE B.312: SFP inspection for HD 121560 with S1-E1 on UT 2007/02/05, seq 001

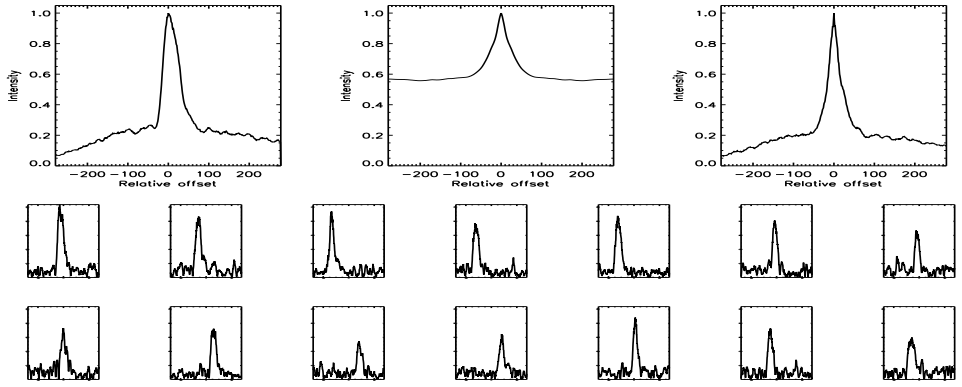

FIGURE B.313: SFP inspection for HD 121560 with S1-E1 on UT 2007/02/05, seq 002

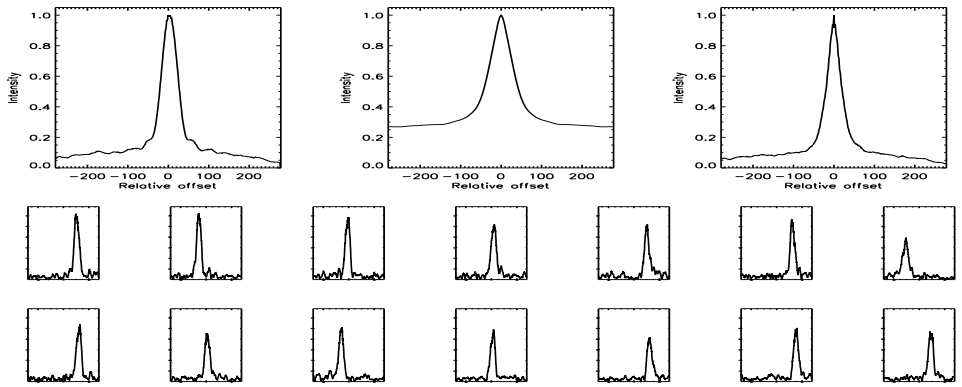

FIGURE B.314: SFP inspection for HD 121560 with S1-E1 on UT 2007/03/08, seq 001

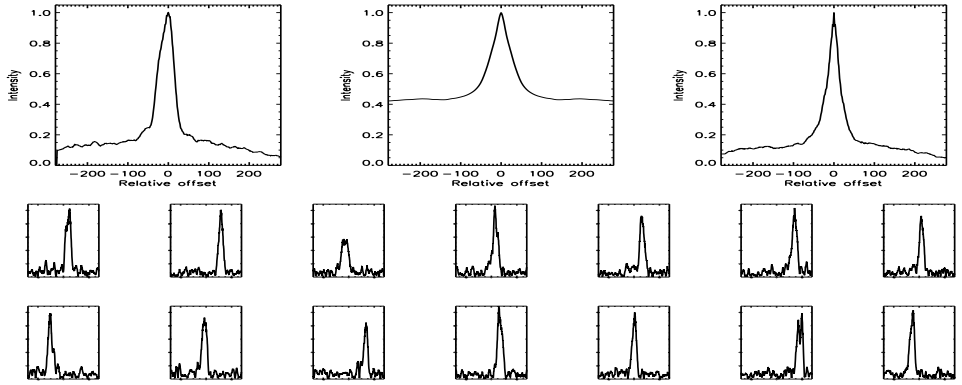

FIGURE B.315: SFP inspection for HD 121560 with S1-W1 on UT 2007/04/24, seq 001

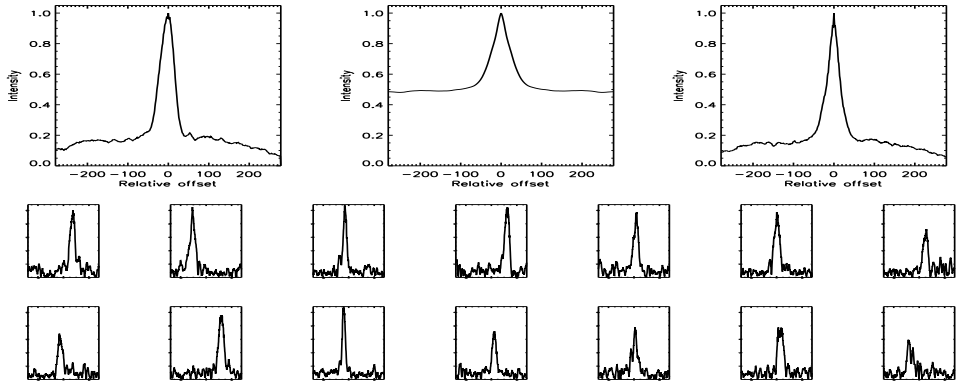

FIGURE B.316: SFP inspection for HD 124292 with S1-E1 on UT 2007/03/12, seq 002

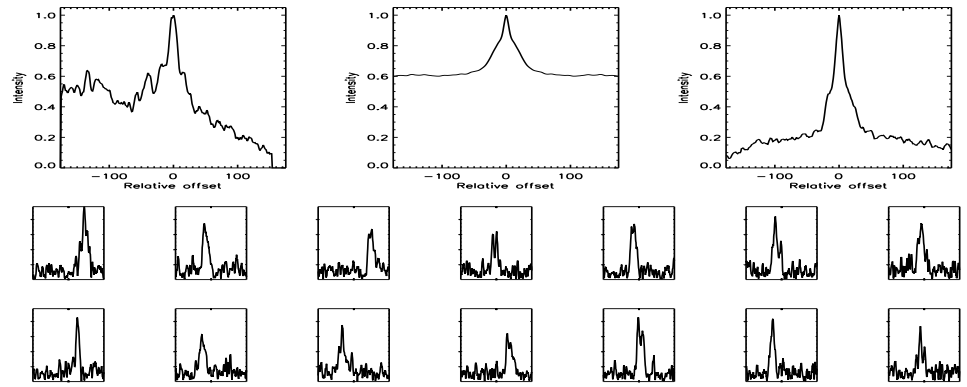

FIGURE B.317: SFP inspection for HD 124292 with S1-E1 on UT 2008/04/13, seq 001

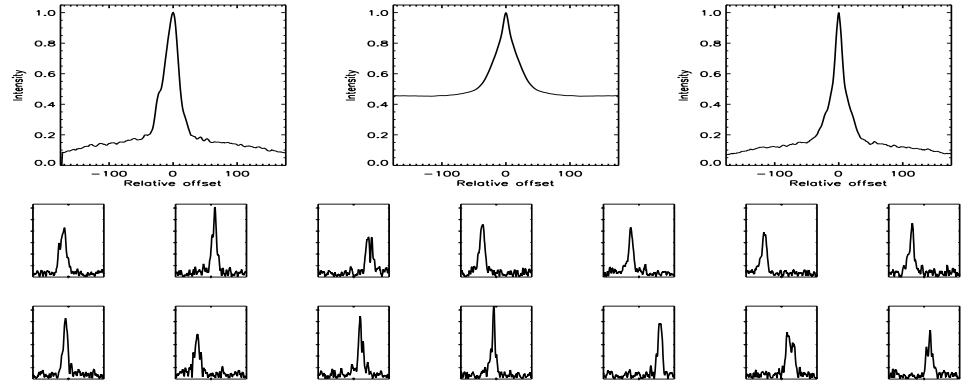

FIGURE B.318: SFP inspection for HD 124292 with S1-E1 on UT 2008/04/25, seq 001

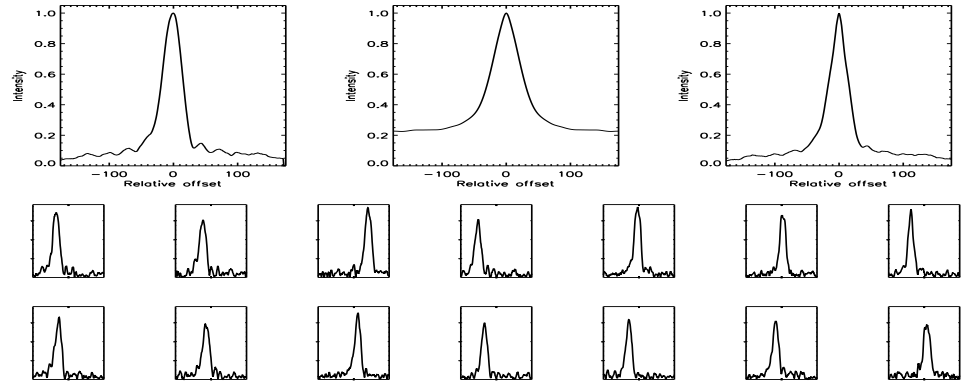

FIGURE B.319: SFP inspection for HD 124292 with S1-W1 on UT 2008/04/13, seq 002

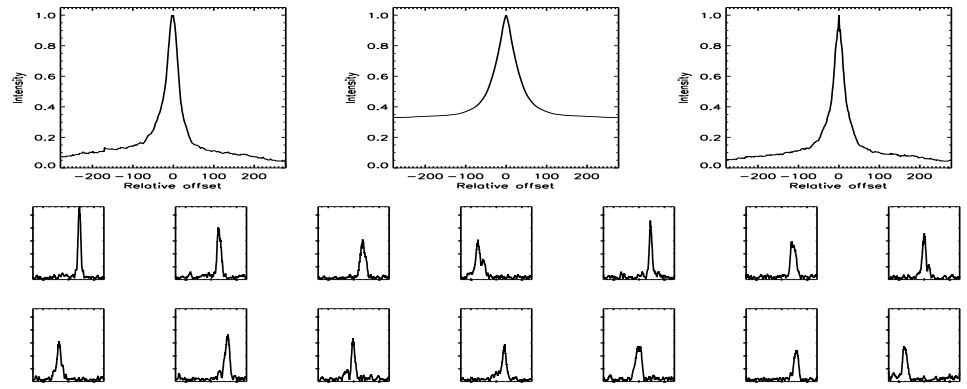

FIGURE B.320: SFP inspection for HD 124850 with S1-E1 on UT 2007/02/16, seq 001

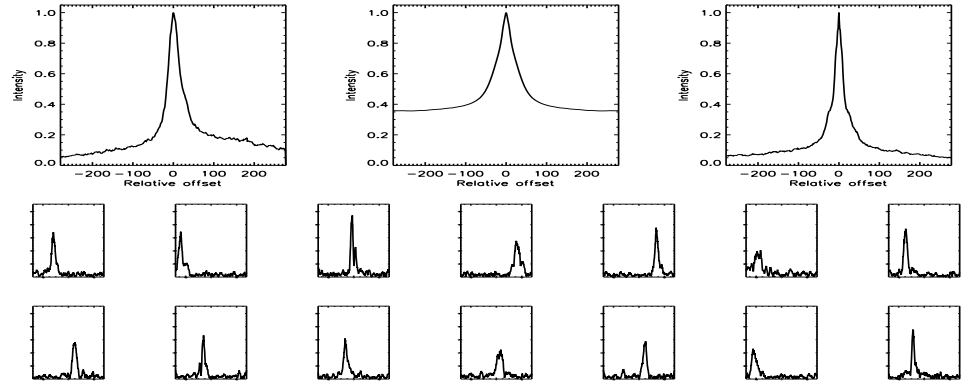

FIGURE B.321: SFP inspection for HD 124850 with S1-E1 on UT 2007/03/23, seq 001

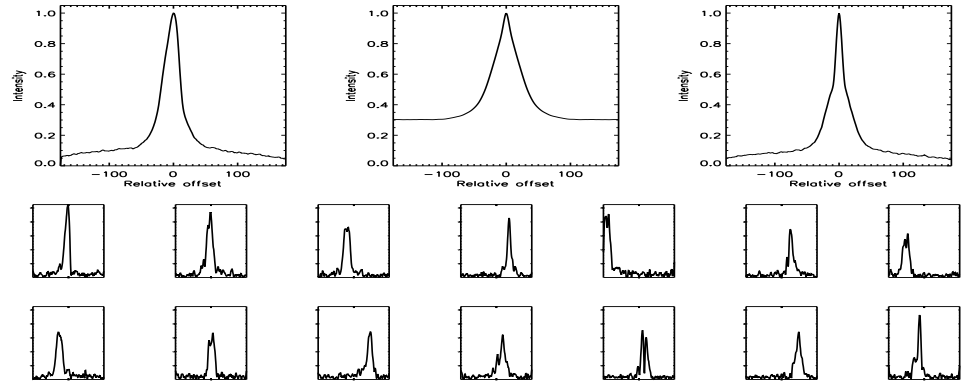

FIGURE B.322: SFP inspection for HD 124850 with S1-E1 on UT 2008/04/25, seq 001

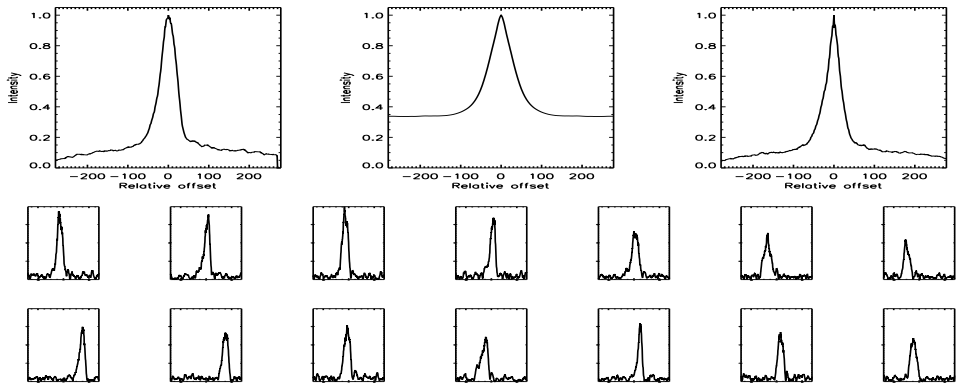

FIGURE B.323: SFP inspection for HD 124850 with S1-E2 on UT 2007/05/31, seq 001

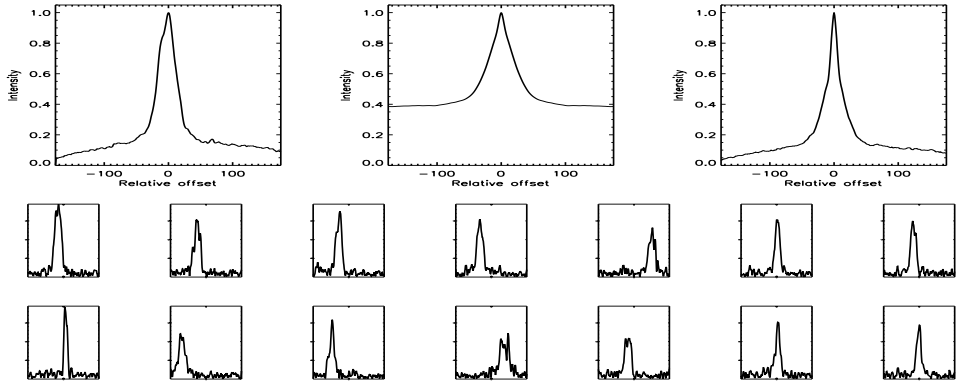

FIGURE B.324: SFP inspection for HD 124850 with S1-E2 on UT 2008/06/08, seq 001

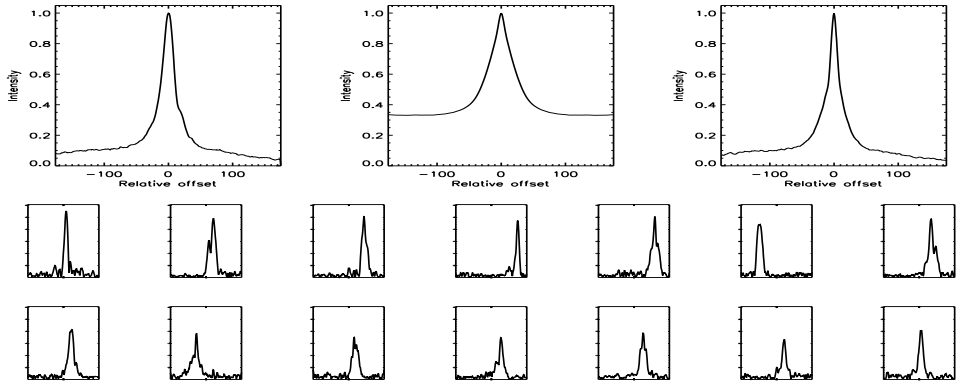

FIGURE B.325: SFP inspection for HD 124850 with S1-E2 on UT 2008/06/08, seq 002

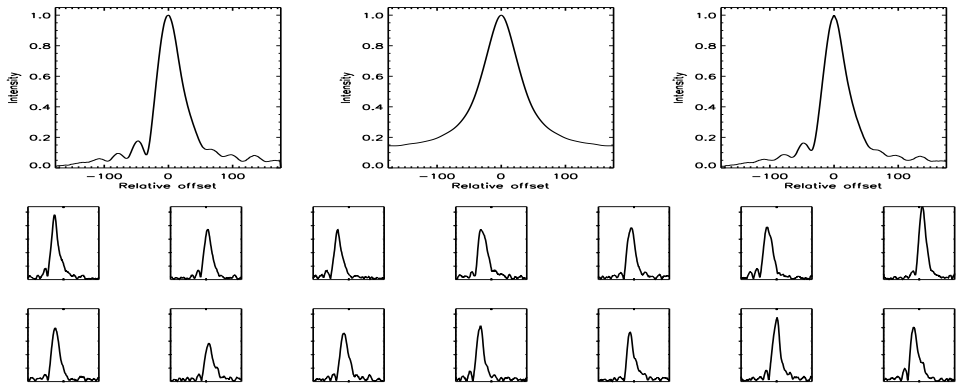

FIGURE B.326: SFP inspection for HD 124850 with S1-W1 on UT 2008/07/08, seq 001

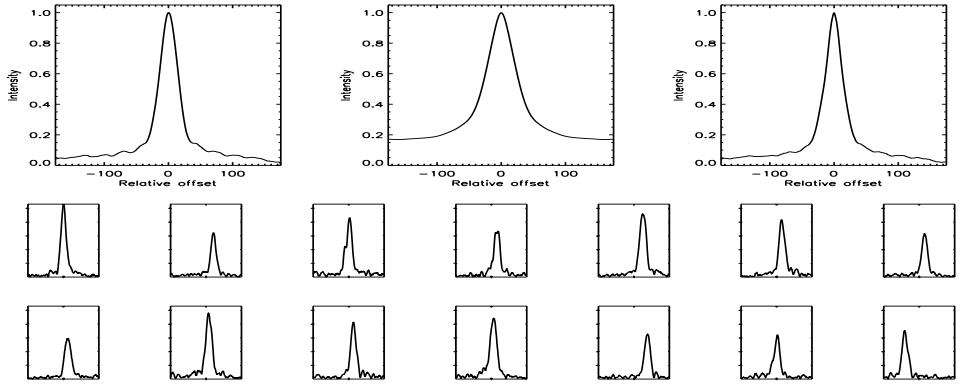

FIGURE B.327: SFP inspection for HD 124850 with S2-W2 on UT 2008/06/09, seq 001

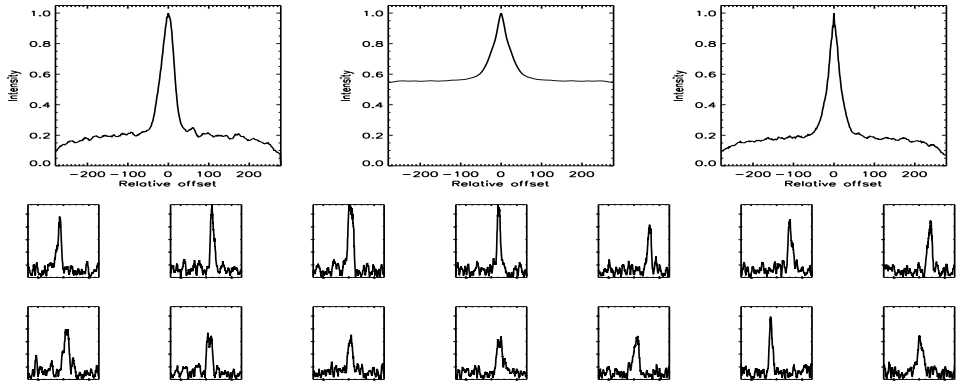

FIGURE B.328: SFP inspection for HD 125455 with S1-E1 on UT 2007/03/12, seq 001

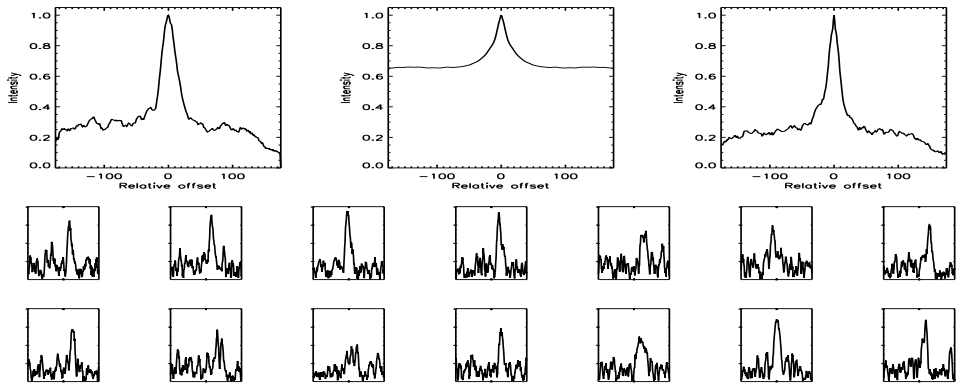

FIGURE B.329: SFP inspection for HD 125455 with S1-E1 on UT 2008/04/14, seq 001

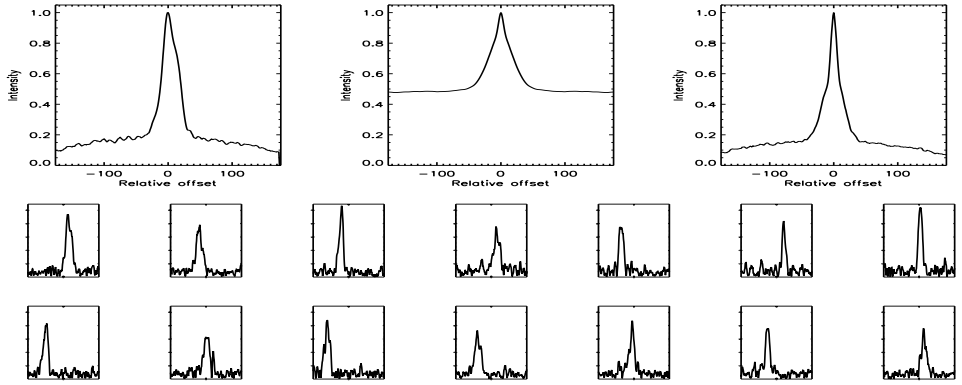

FIGURE B.330: SFP inspection for HD 125455 with S1-E1 on UT 2008/04/25, seq 001

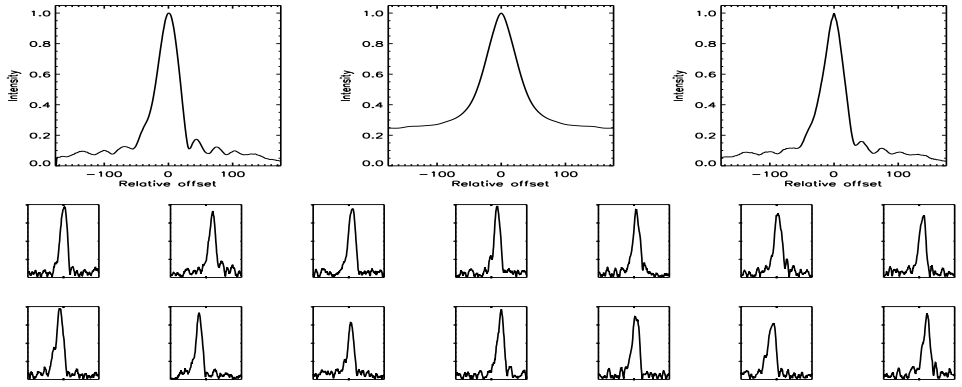

FIGURE B.331: SFP inspection for HD 125455 with S1-W1 on UT 2008/04/14, seq 002

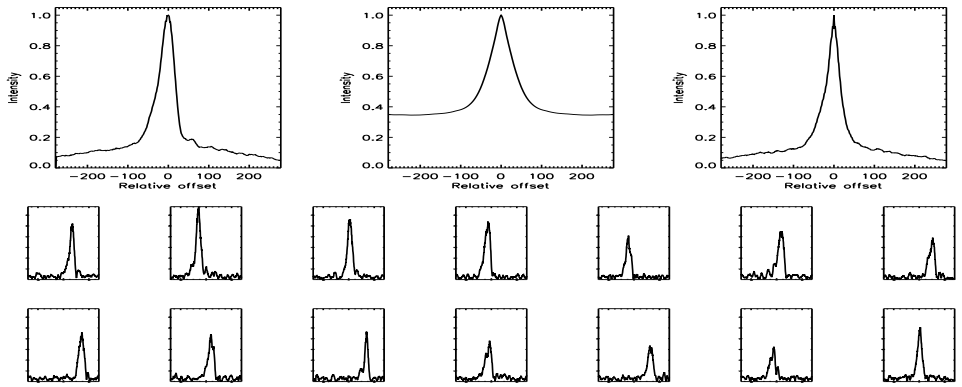

FIGURE B.332: SFP inspection for HD 127334 with E1-W1 on UT 2007/04/26, seq 001

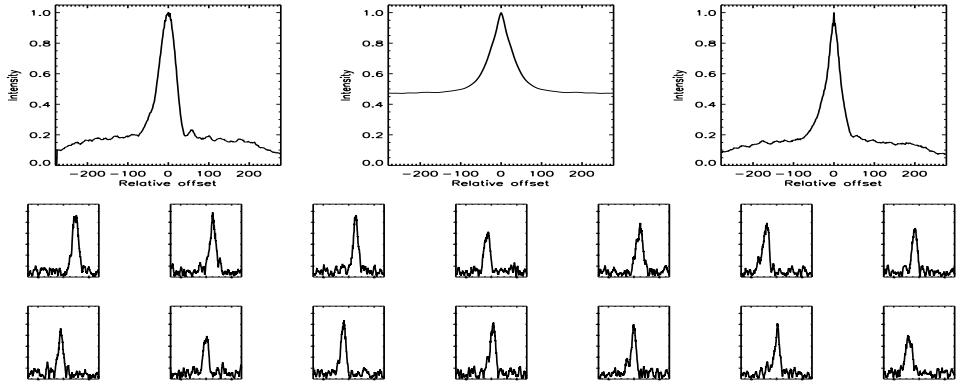

FIGURE B.333: SFP inspection for HD 127334 with S1-E1 on UT 2007/04/14, seq 001

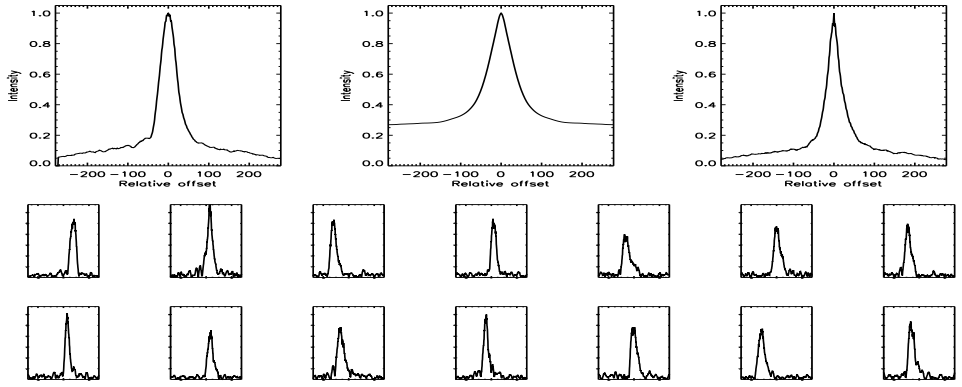

FIGURE B.334: SFP inspection for HD 127334 with S1-W1 on UT 2007/04/17, seq 001

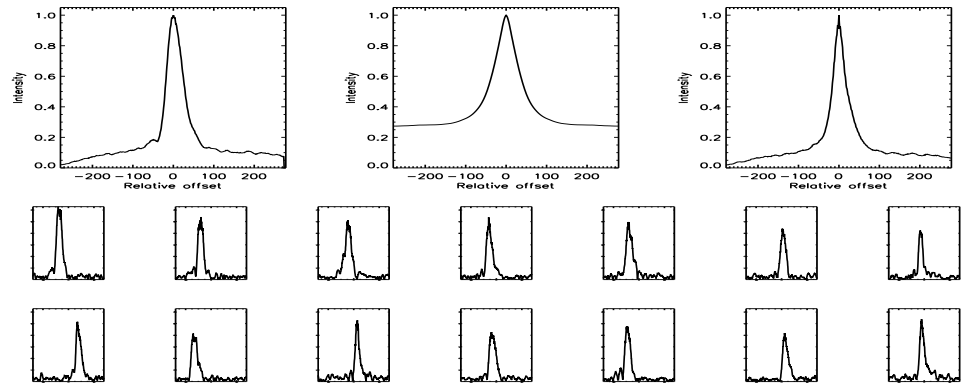

FIGURE B.335: SFP inspection for HD 127334 with S1-W1 on UT 2007/04/17, seq 002

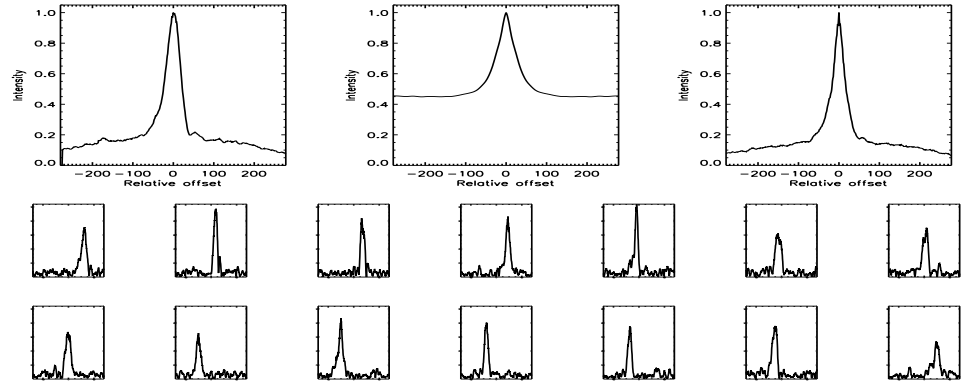

FIGURE B.336: SFP inspection for HD 128165 with E1-W1 on UT 2007/04/26, seq 001

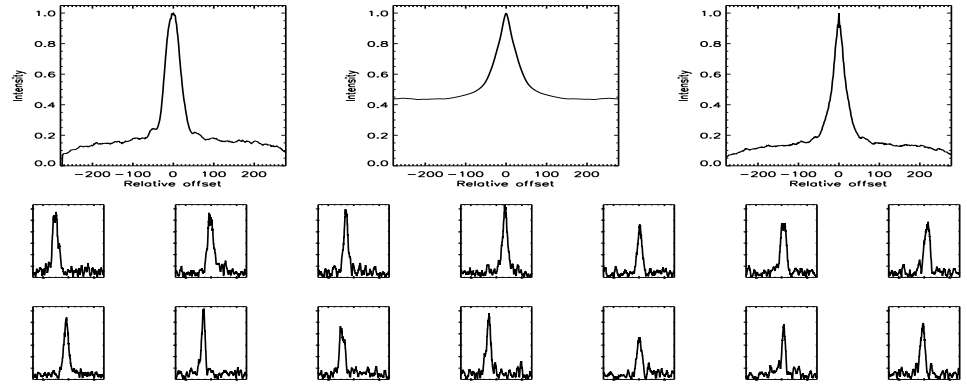

FIGURE B.337: SFP inspection for HD 128165 with S1-E1 on UT 2007/04/14, seq 001

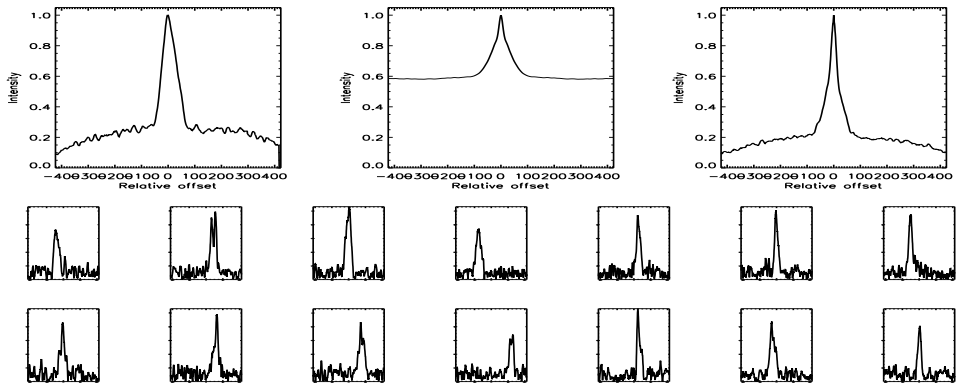

FIGURE B.338: SFP inspection for HD 128165 with S1-E1 on UT 2007/07/28, seq 001

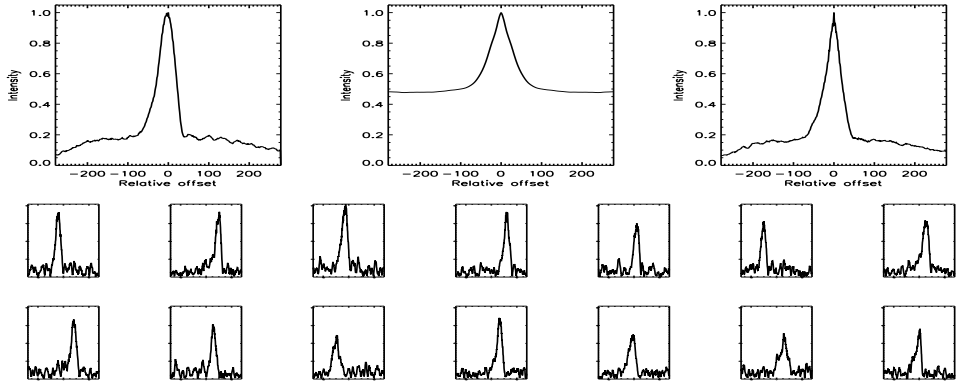

FIGURE B.339: SFP inspection for HD 128165 with S1-W1 on UT 2007/05/28, seq 001

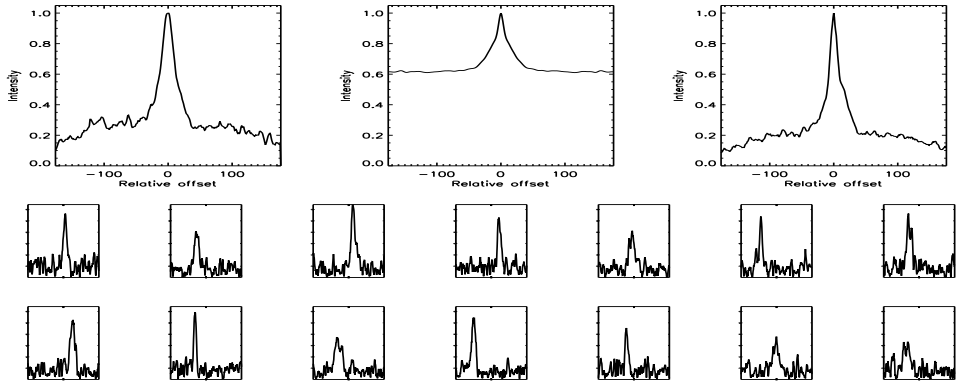

FIGURE B.340: SFP inspection for HD 128311 with S1-E1 on UT 2008/04/13, seq 001

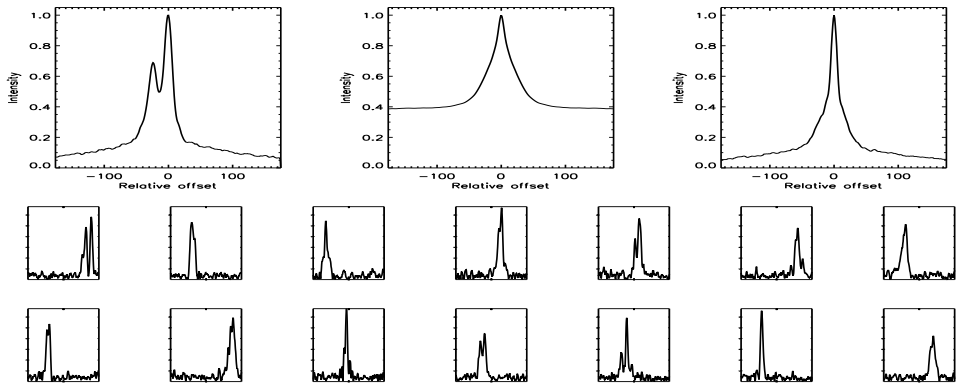

FIGURE B.341: SFP inspection for HD 128311 with S1-E1 on UT 2008/04/25, seq 001

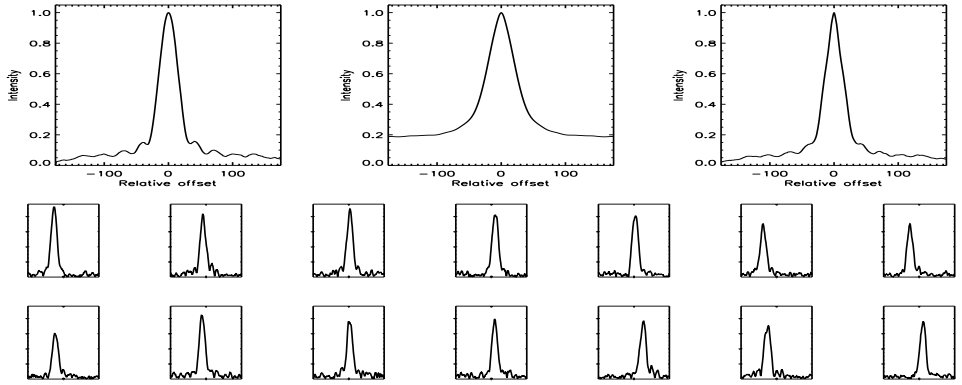

FIGURE B.342: SFP inspection for HD 128311 with S1-W1 on UT 2008/04/13, seq 002

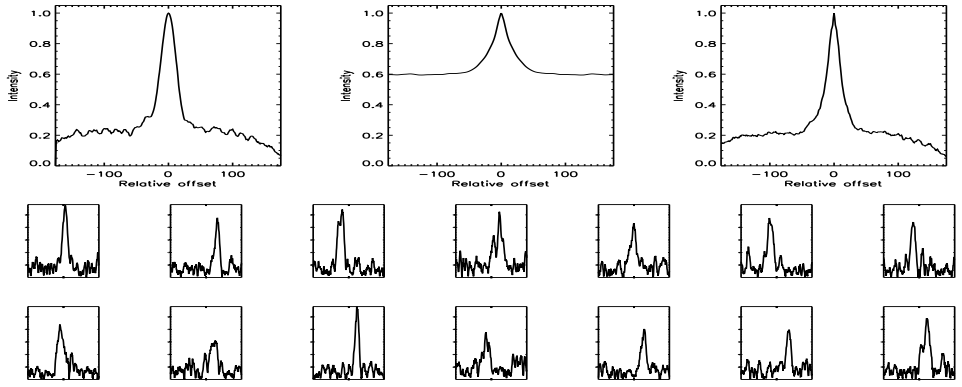

FIGURE B.343: SFP inspection for HD 128642 with S1-E1 on UT 2008/06/25, seq 001

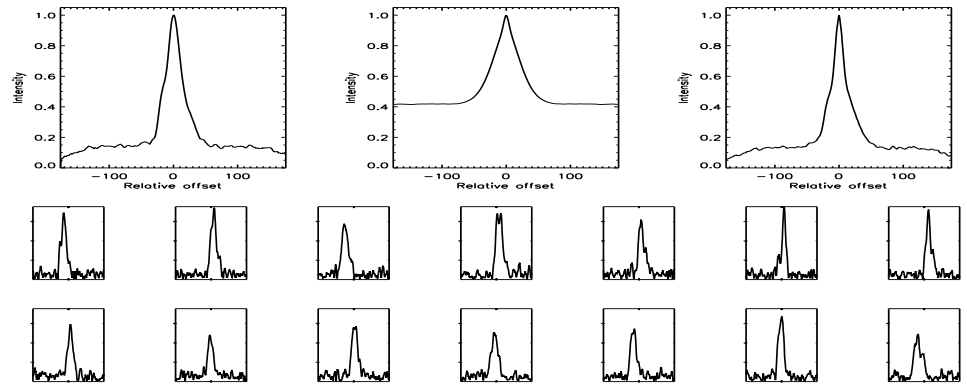

FIGURE B.344: SFP inspection for HD 128642 with S1-E1 on UT 2008/06/25, seq 002

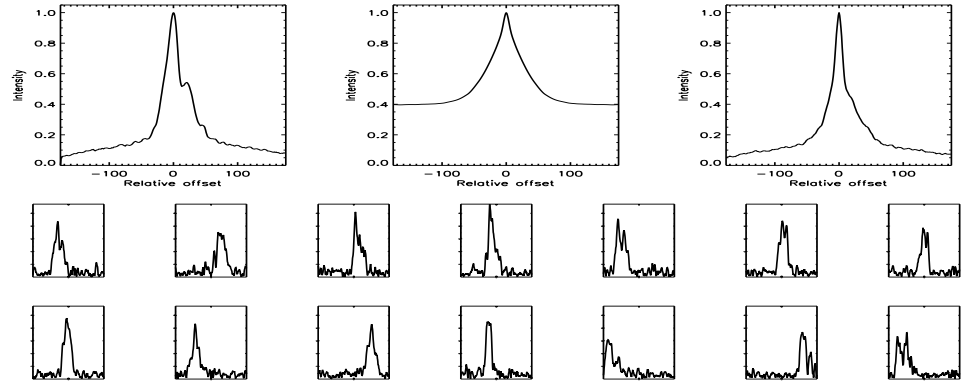

FIGURE B.345: SFP inspection for HD 128642 with S1-W1 on UT 2008/04/26, seq 001

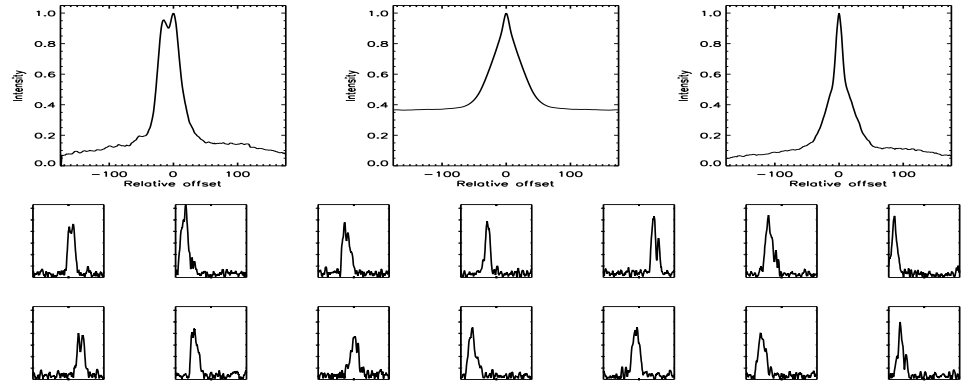

FIGURE B.346: SFP inspection for HD 128642 with S1-W1 on UT 2008/04/26, seq 002

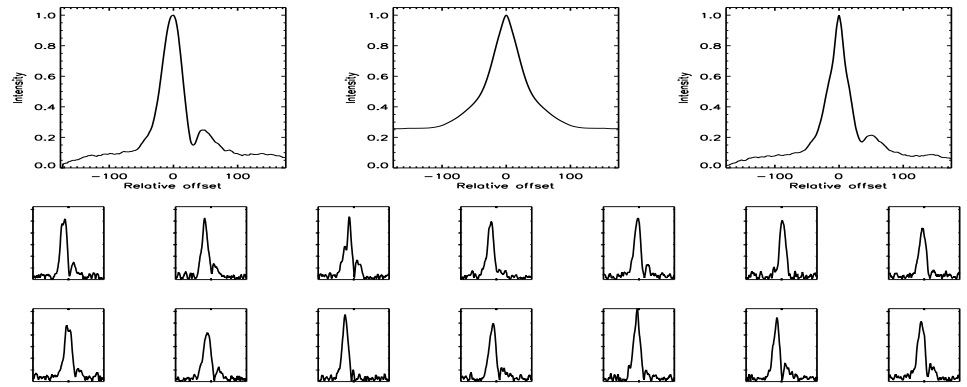

FIGURE B.347: SFP inspection for HD 128642 with S2-W1 on UT 2008/06/24, seq 001

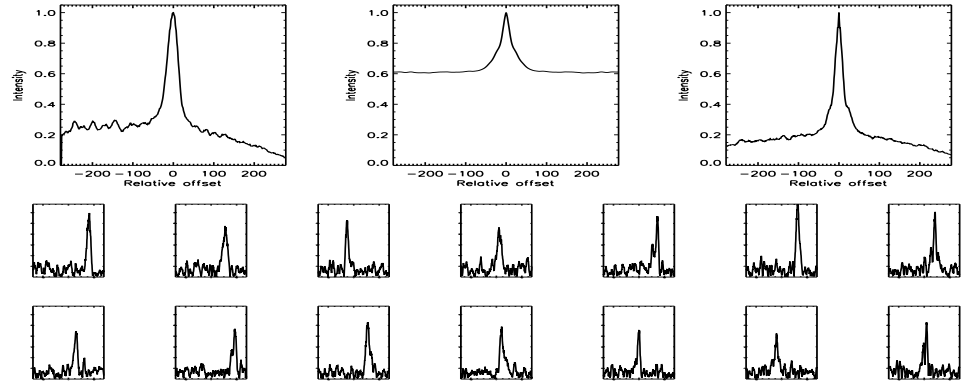

FIGURE B.348: SFP inspection for HD 130004 with S1-E1 on UT 2007/03/10, seq 001

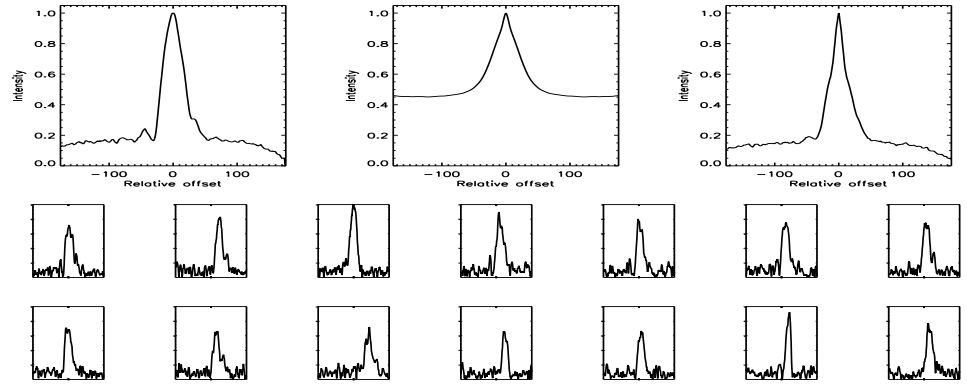

FIGURE B.349: SFP inspection for HD 130004 with S1-E1 on UT 2008/04/13, seq 001

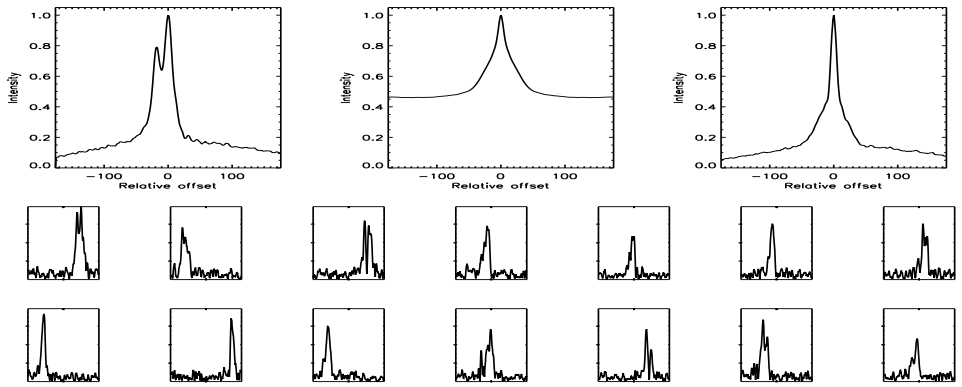

FIGURE B.350: SFP inspection for HD 130004 with S1-E1 on UT 2008/04/25, seq 001

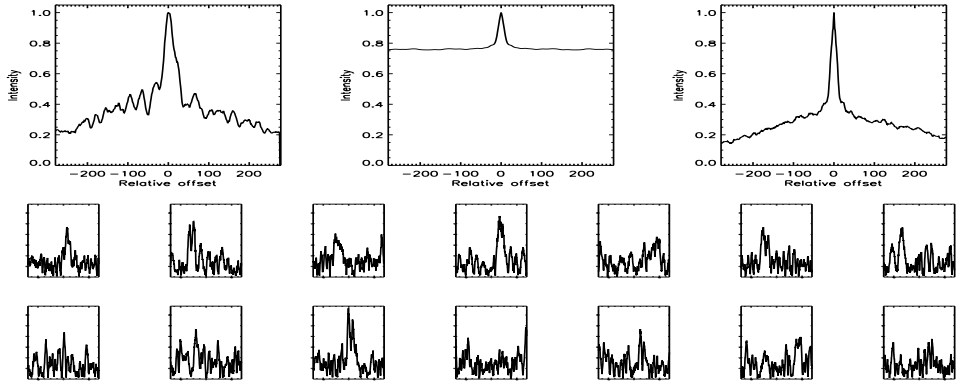

FIGURE B.351: SFP inspection for HD 130004 with S1-W1 on UT 2007/05/28, seq 001

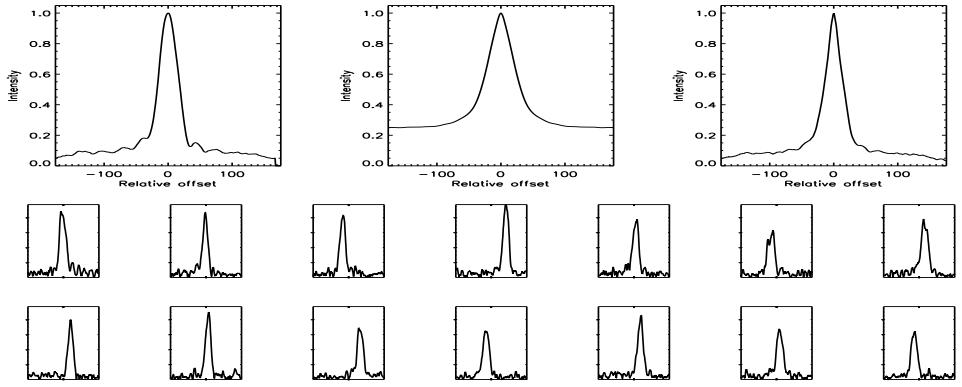

FIGURE B.352: SFP inspection for HD 130004 with S1-W1 on UT 2008/04/13, seq 002

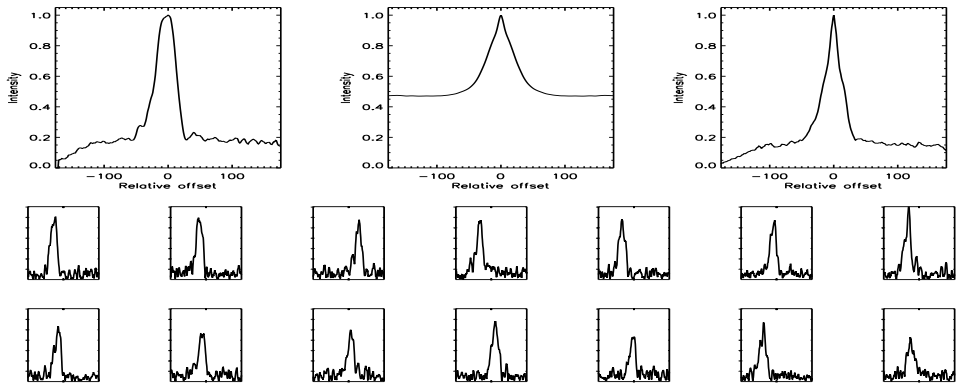

FIGURE B.353: SFP inspection for HD 130307 with S1-E1 on UT 2008/04/13, seq 001

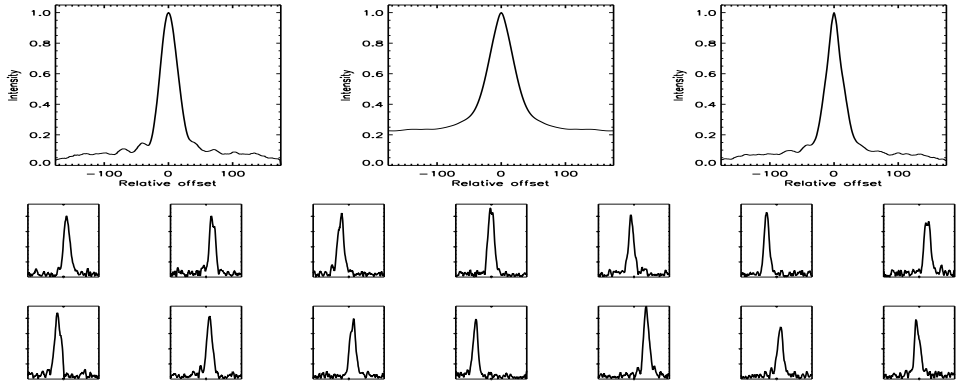

FIGURE B.354: SFP inspection for HD 130307 with S1-W1 on UT 2008/04/13, seq 002

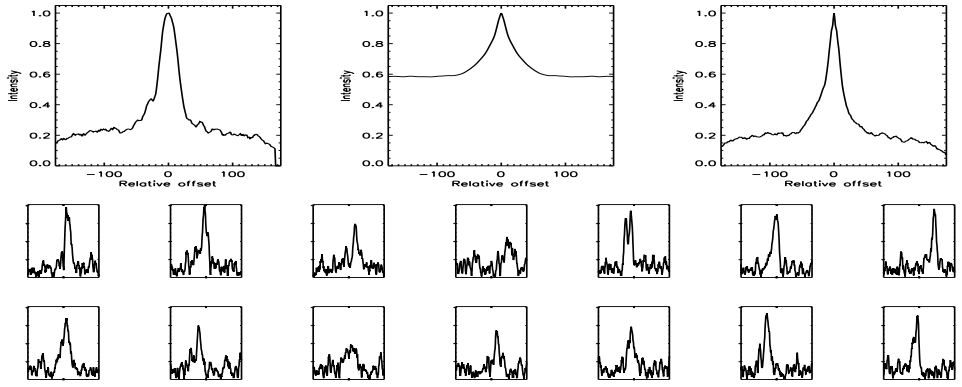

FIGURE B.355: SFP inspection for HD 132142 with S1-E1 on UT 2008/04/12, seq 002

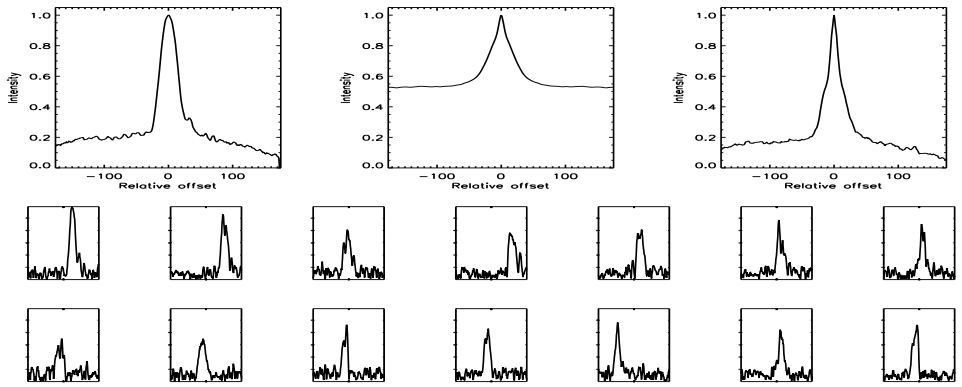

FIGURE B.356: SFP inspection for HD 132142 with S1-E1 on UT 2008/06/25, seq 001

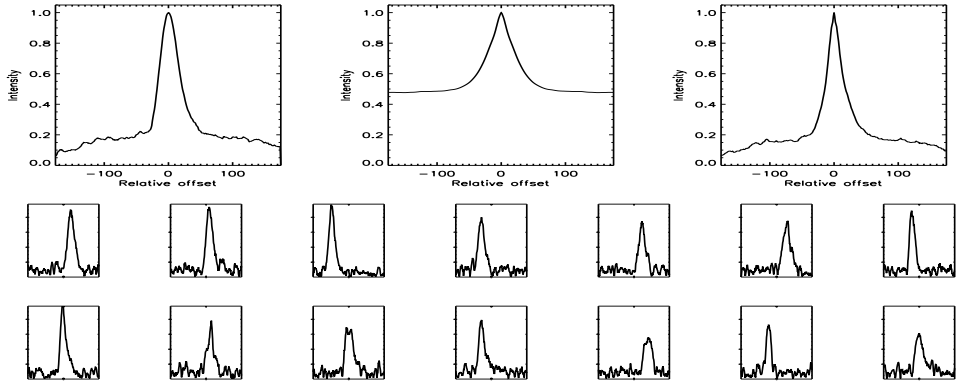

FIGURE B.357: SFP inspection for HD 132142 with S1-W1 on UT 2008/04/12, seq 001

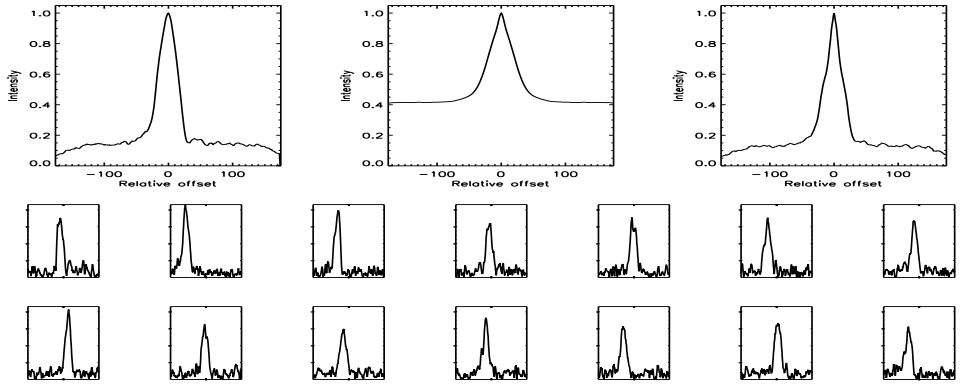

FIGURE B.358: SFP inspection for HD 132142 with S2-W1 on UT 2008/06/24, seq 001

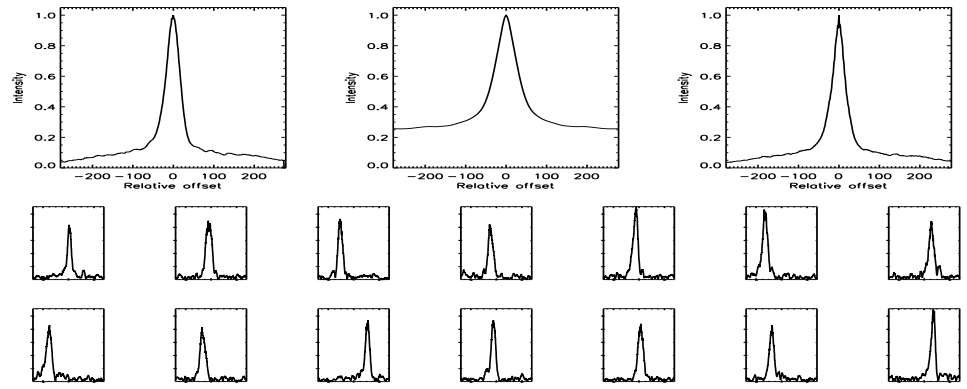

FIGURE B.359: SFP inspection for HD 132254 with E1-W1 on UT 2007/04/26, seq 001

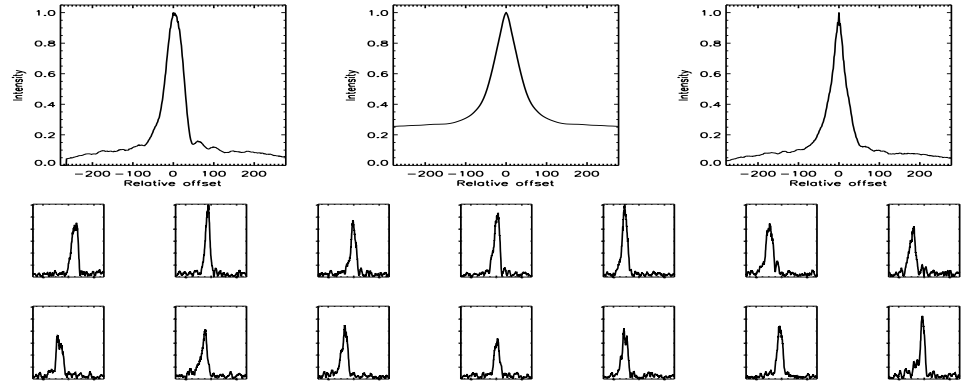

FIGURE B.360: SFP inspection for HD 132254 with S1-E1 on UT 2007/04/11, seq 001

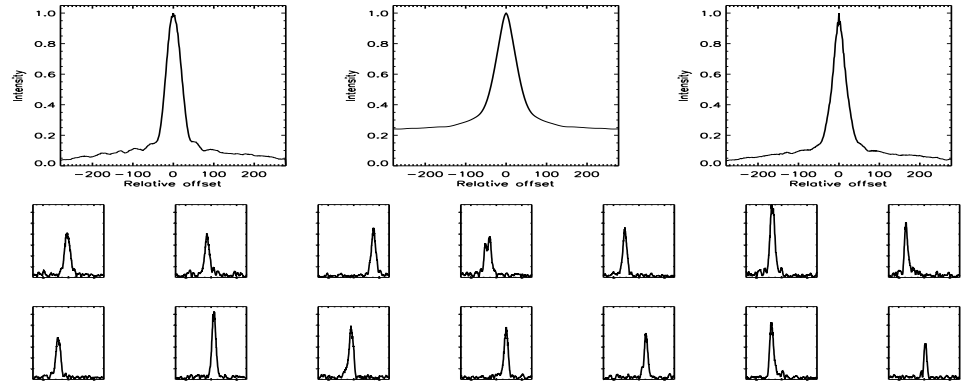

FIGURE B.361: SFP inspection for HD 132254 with S1-W1 on UT 2007/04/24, seq 001

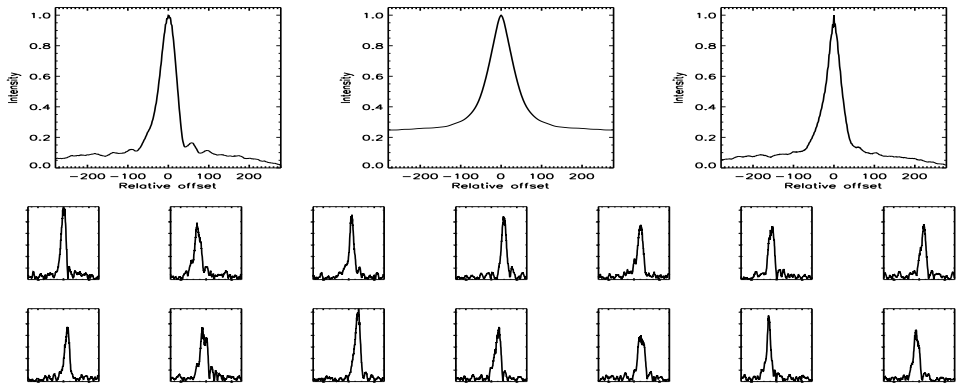

FIGURE B.362: SFP inspection for HD 135204 with S1-E1 on UT 2007/03/08, seq 001

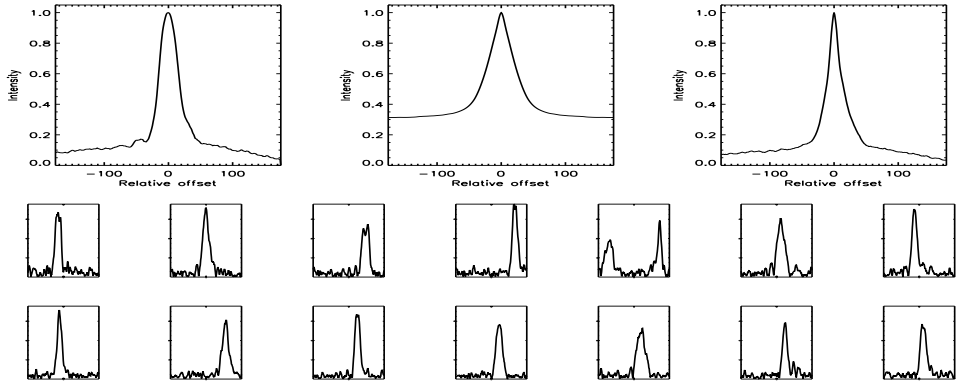

FIGURE B.363: SFP inspection for HD 135204 with S1-E1 on UT 2008/06/23, seq 001

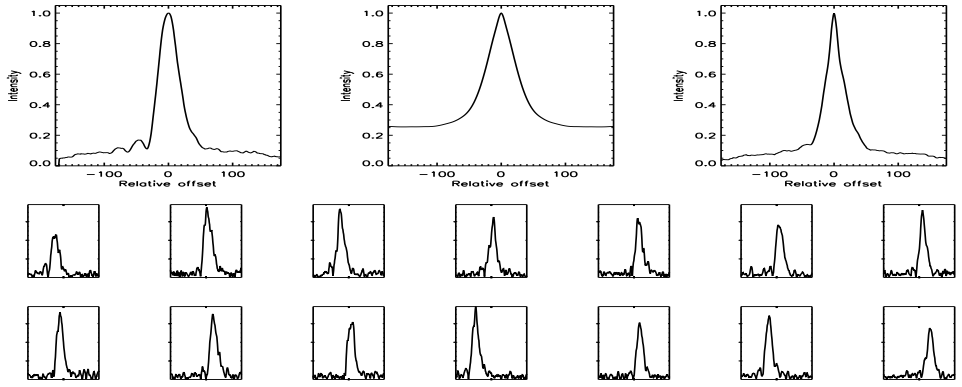

FIGURE B.364: SFP inspection for HD 135204 with S1-E1 on UT 2008/07/05, seq 001

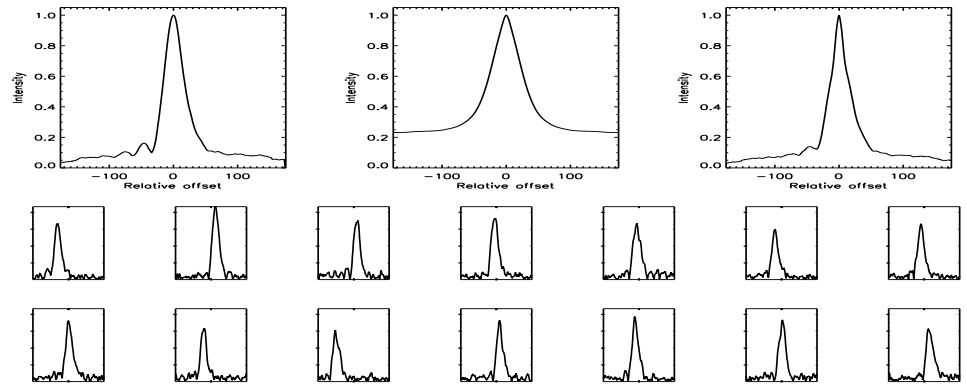

FIGURE B.365: SFP inspection for HD 135204 with S1-E1 on UT 2008/07/05, seq 002

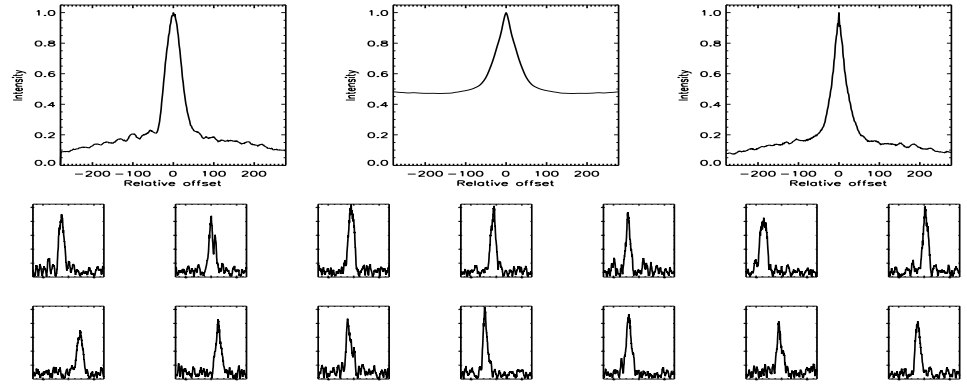

FIGURE B.366: SFP inspection for HD 135204 with S1-E2 on UT 2007/05/31, seq 001

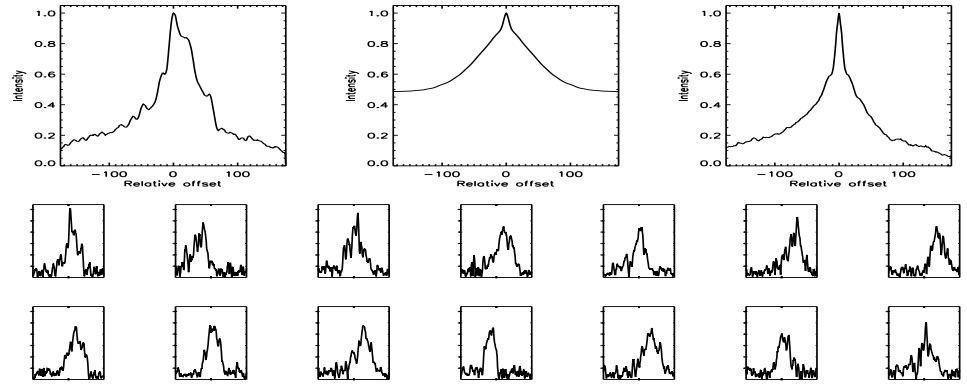

FIGURE B.367: SFP inspection for HD 135204 with S1-W1 on UT 2008/06/22, seq 001

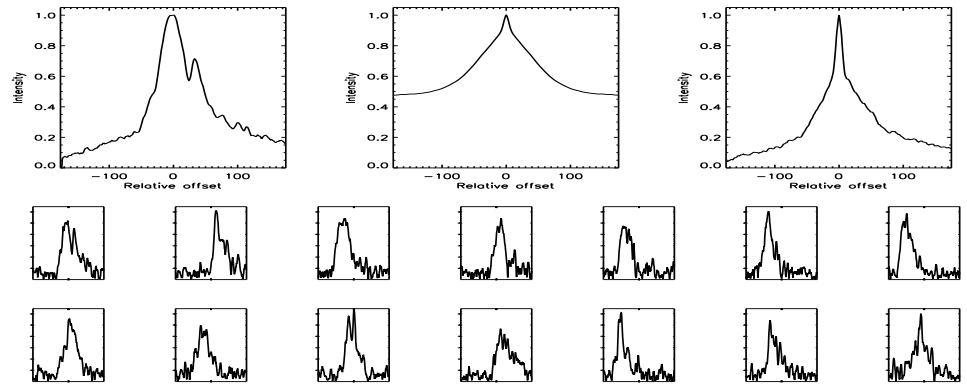

FIGURE B.368: SFP inspection for HD 135204 with S1-W1 on UT 2008/06/22, seq 002

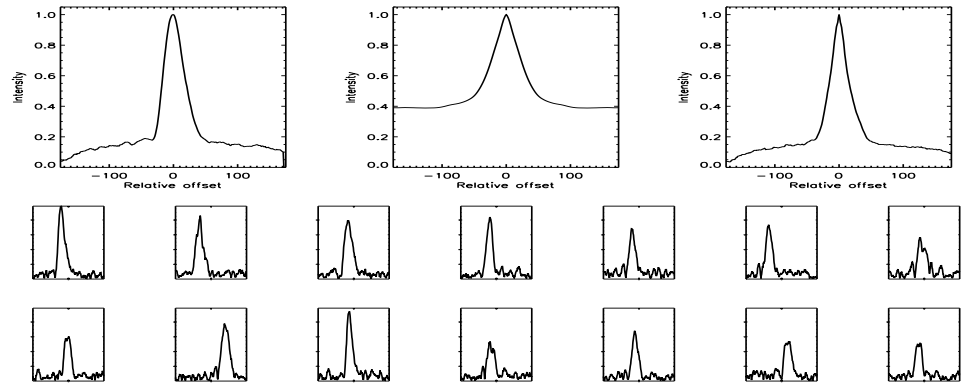

FIGURE B.369: SFP inspection for HD 135204 with S1-W1 on UT 2008/07/08, seq 001

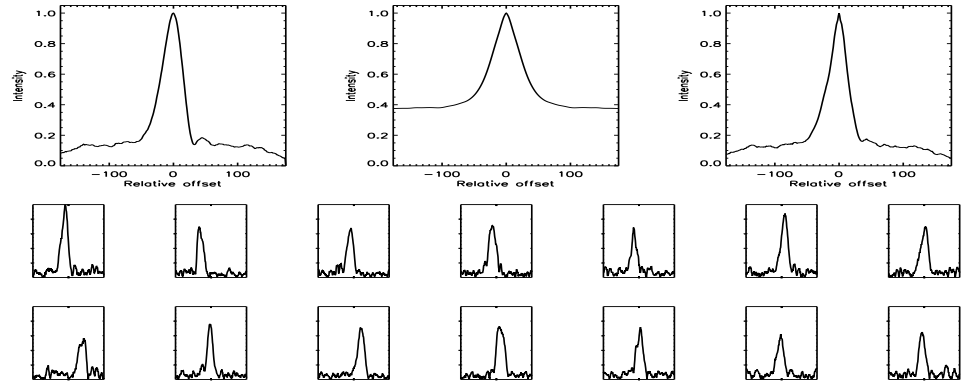

FIGURE B.370: SFP inspection for HD 135204 with S1-W1 on UT 2008/07/08, seq 002

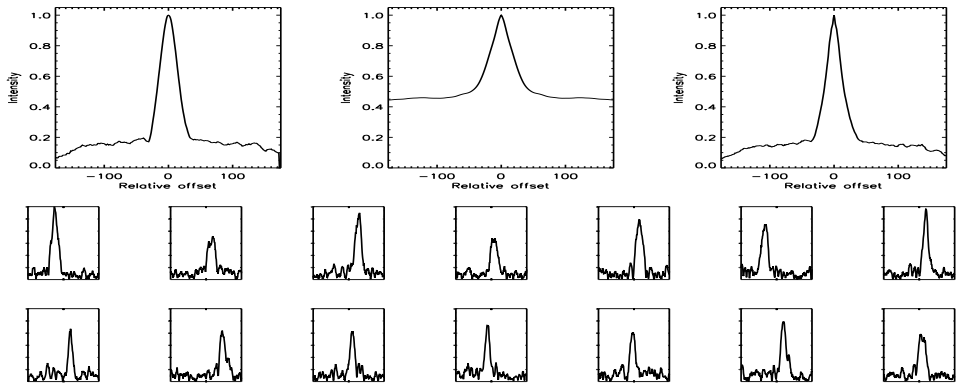

FIGURE B.371: SFP inspection for HD 135204 with S2-W2 on UT 2008/06/09, seq 001

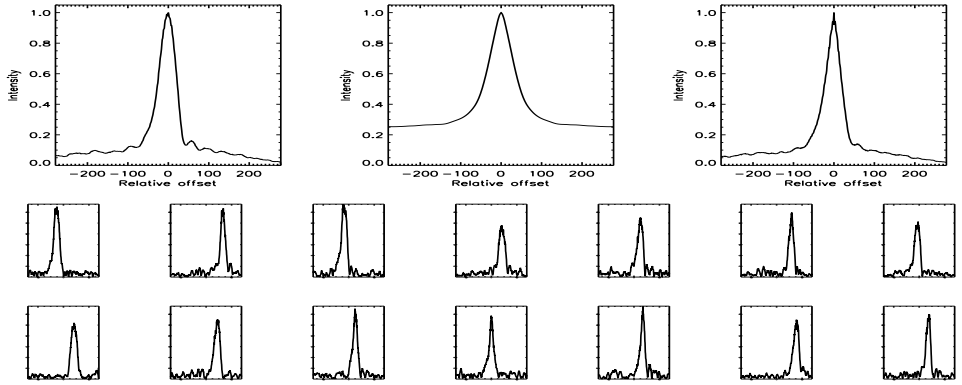

FIGURE B.372: SFP inspection for HD 135599 with S1-E1 on UT 2007/03/08, seq 001

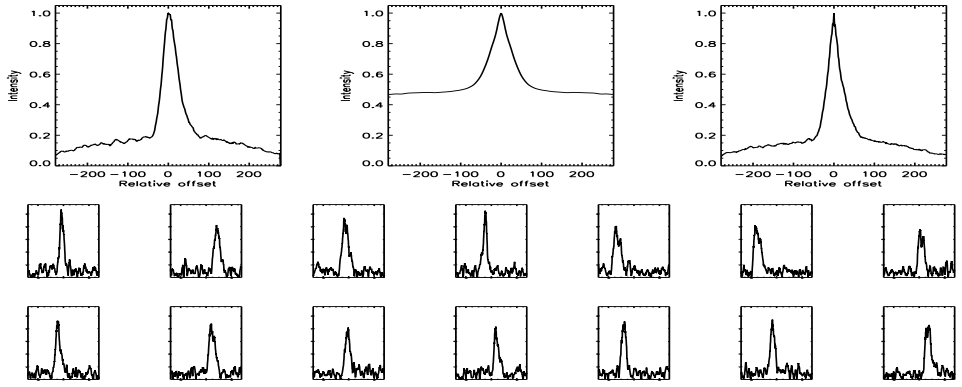

FIGURE B.373: SFP inspection for HD 135599 with S1-E2 on UT 2007/05/31, seq 001

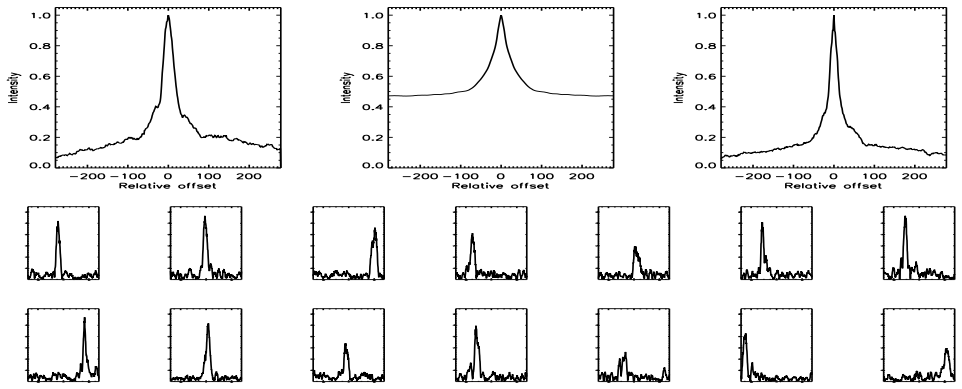

FIGURE B.374: SFP inspection for HD 136202 with S1-E1 on UT 2007/02/16, seq 001

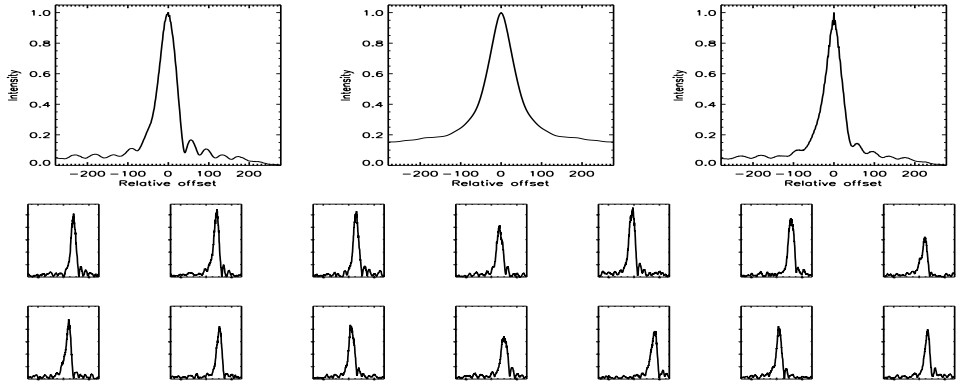

FIGURE B.375: SFP inspection for HD 136202 with S1-E1 on UT 2007/03/08, seq 001

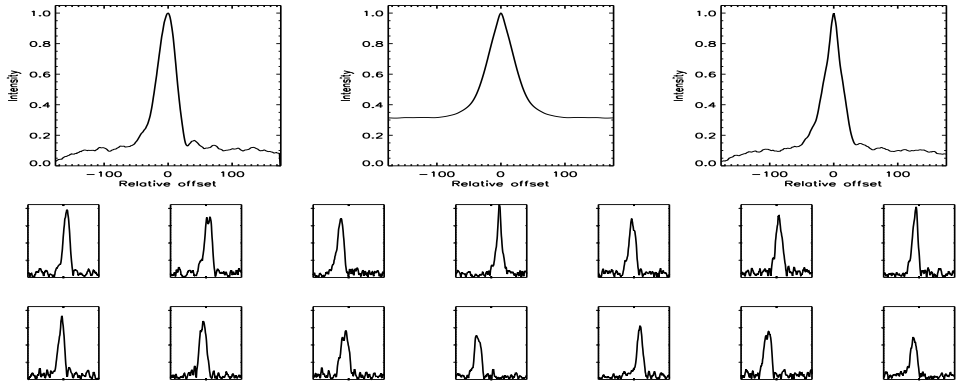

FIGURE B.376: SFP inspection for HD 136202 with S1-E1 on UT 2008/04/13, seq 001

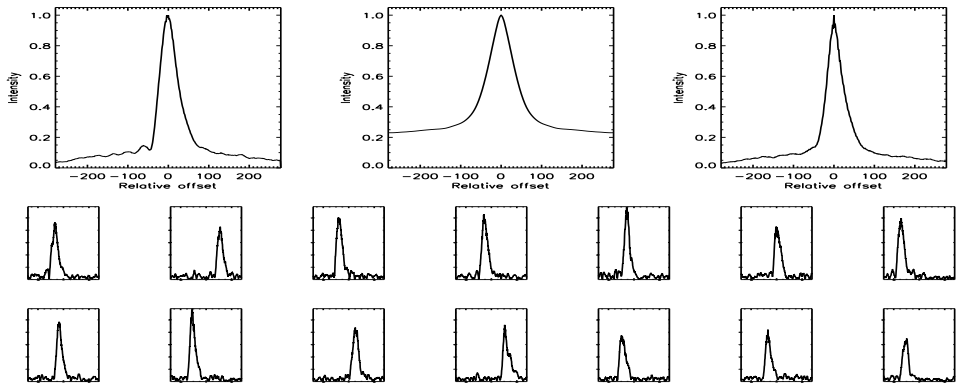

FIGURE B.377: SFP inspection for HD 136202 with S1-E2 on UT 2007/05/31, seq 001

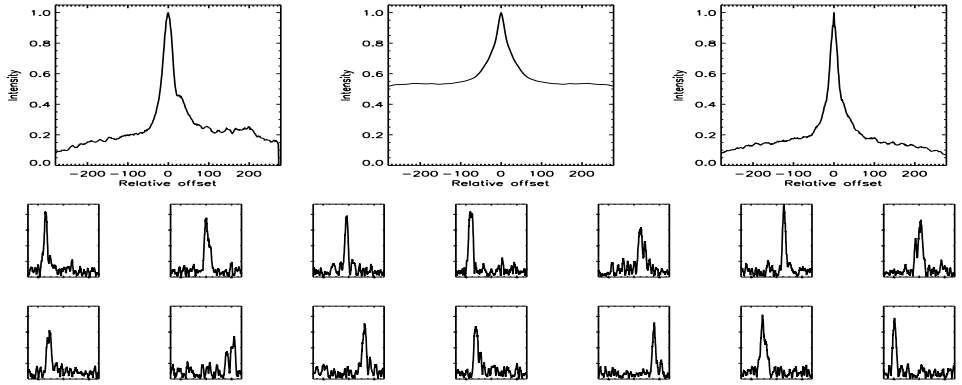

FIGURE B.378: SFP inspection for HD 136202 with S1-E2 on UT 2007/06/01, seq 001

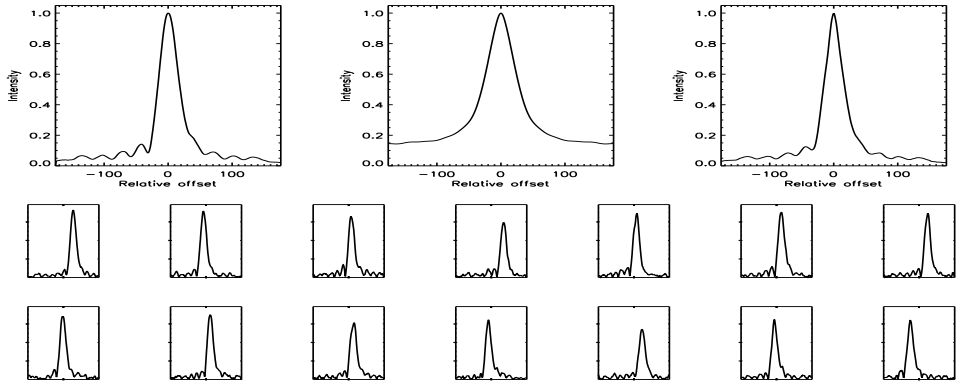

FIGURE B.379: SFP inspection for HD 136202 with S1-W1 on UT 2008/04/13, seq 002

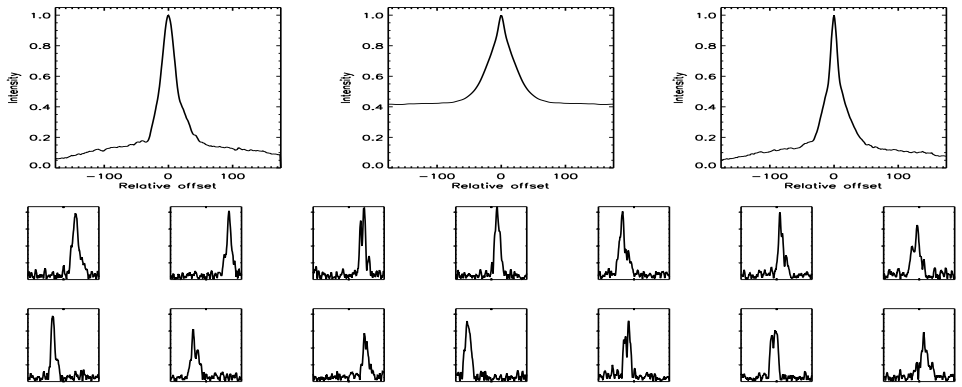

FIGURE B.380: SFP inspection for HD 136713 with S1-E1 on UT 2008/04/25, seq 001

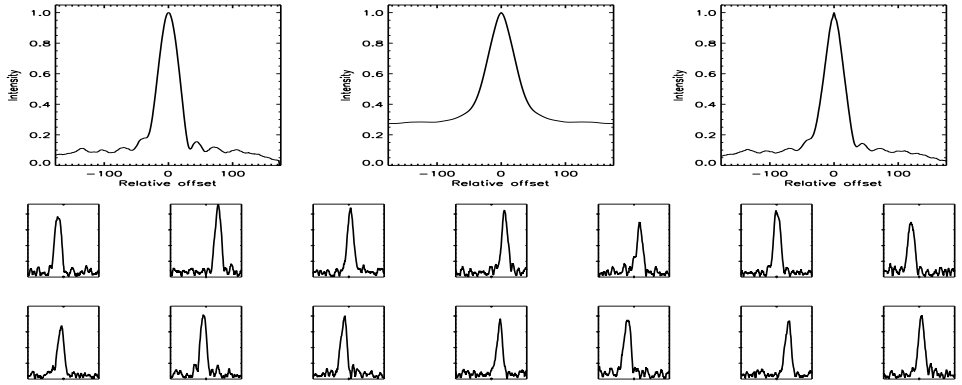

FIGURE B.381: SFP inspection for HD 136713 with S1-W1 on UT 2008/04/14, seq 001

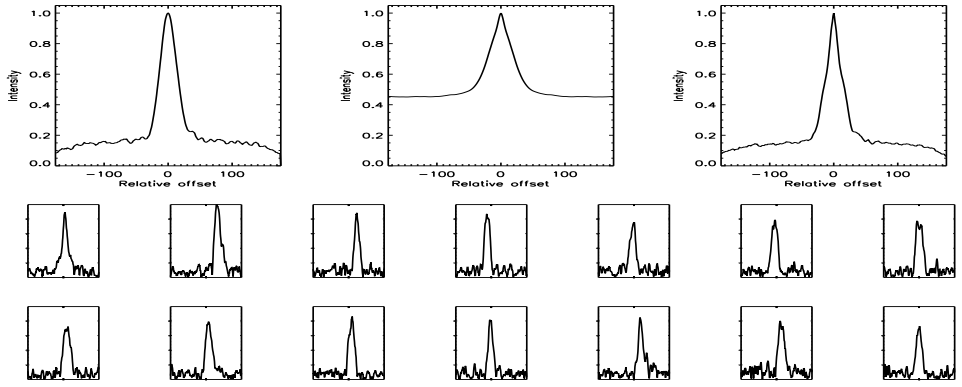

FIGURE B.382: SFP inspection for HD 136923 with S1-E1 on UT 2008/04/13, seq 001

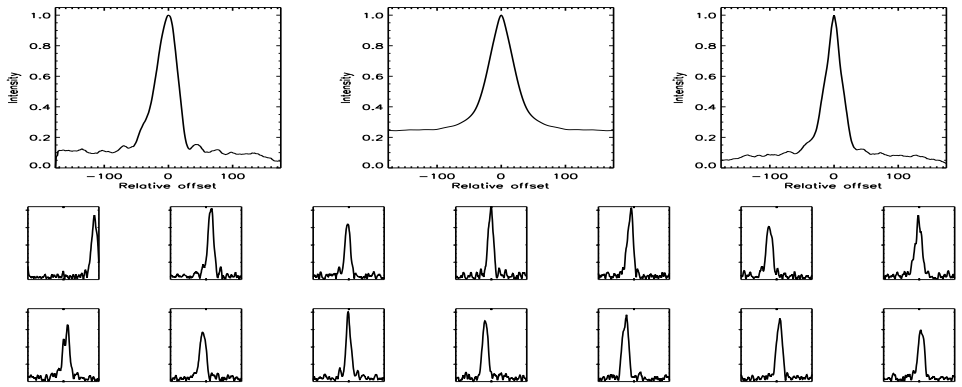

FIGURE B.383: SFP inspection for HD 136923 with S1-W1 on UT 2008/04/13, seq 002

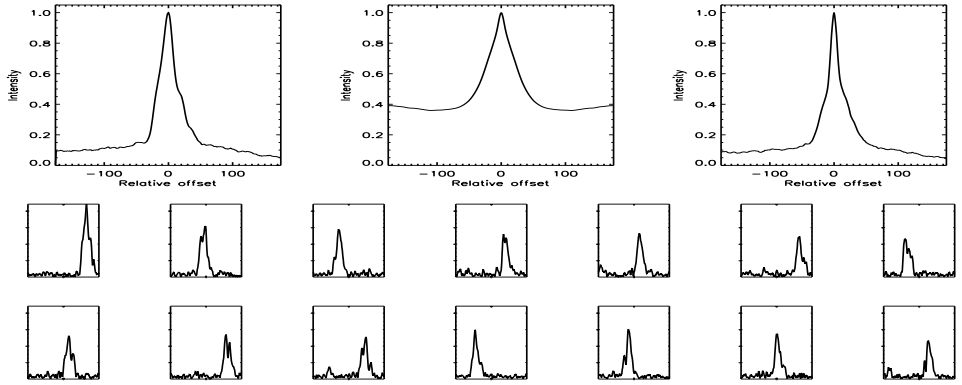

FIGURE B.384: SFP inspection for HD 137763 with S1-E1 on UT 2008/04/25, seq 001

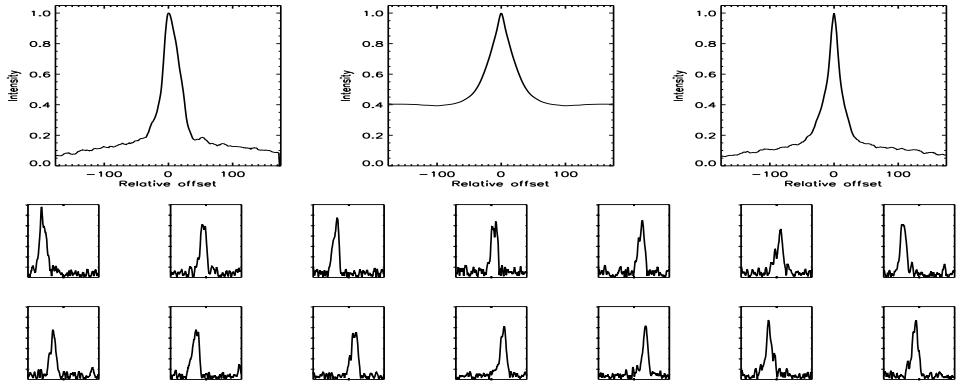

FIGURE B.385: SFP inspection for HD 137763 with S1-E1 on UT 2008/06/23, seq 001

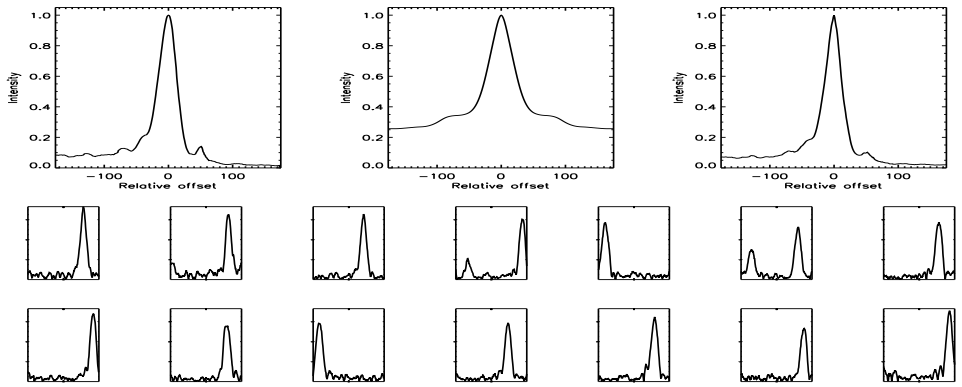

FIGURE B.386: SFP inspection for HD 137763 with S1-W1 on UT 2008/04/14, seq 001

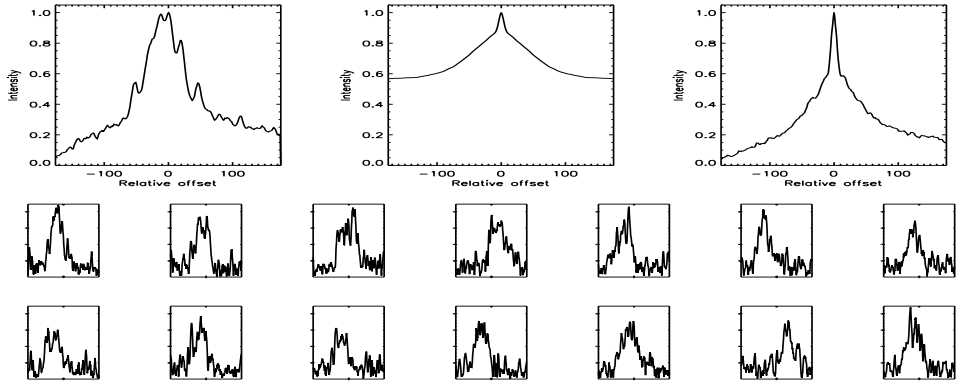

FIGURE B.387: SFP inspection for HD 137763 with S1-W1 on UT 2008/06/22, seq 001

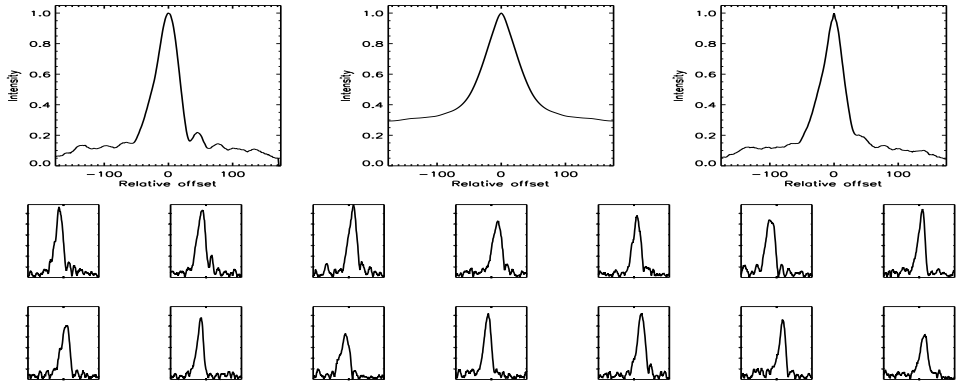

FIGURE B.388: SFP inspection for HD 137763 with S1-W1 on UT 2008/07/07, seq 001

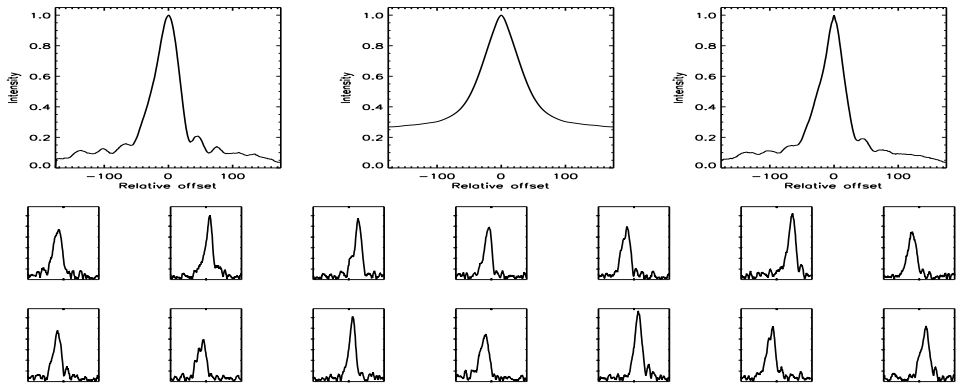

FIGURE B.389: SFP inspection for HD 137763 with S1-W1 on UT 2008/07/07, seq 002

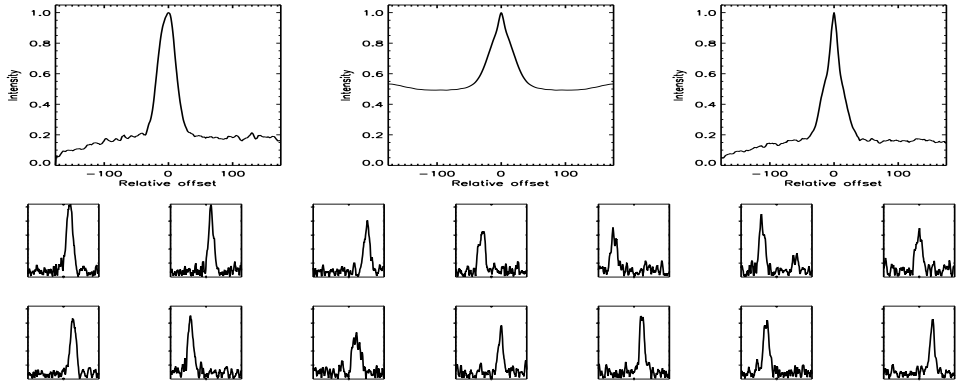

FIGURE B.390: SFP inspection for HD 137763 with S2-W2 on UT 2008/06/09, seq 001

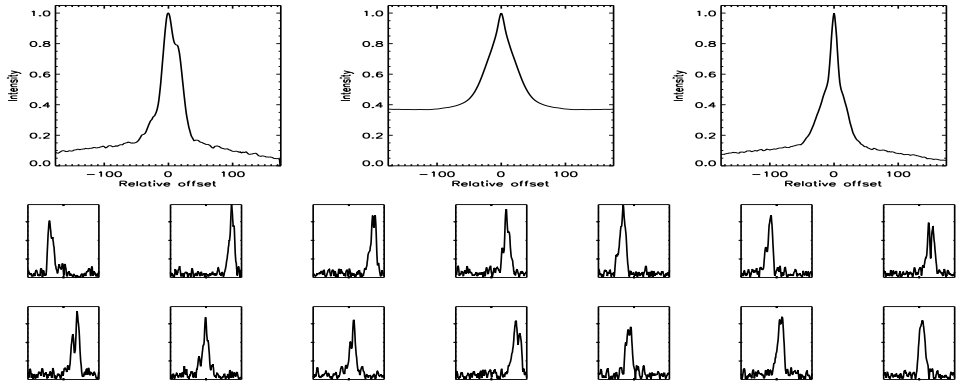

FIGURE B.391: SFP inspection for HD 137778 with S1-E1 on UT 2008/04/25, seq 001

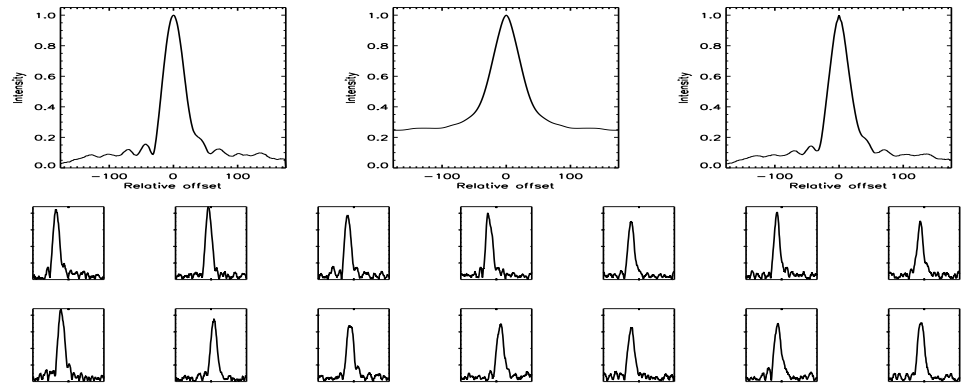

FIGURE B.392: SFP inspection for HD 137778 with S1-W1 on UT 2008/04/14, seq 001

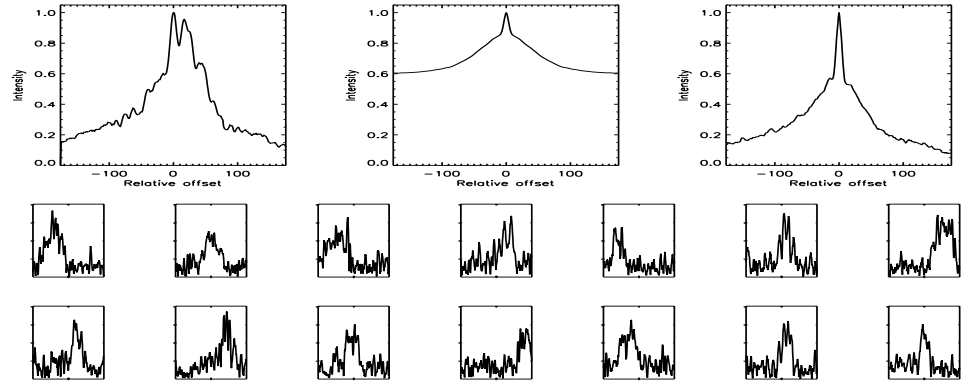

FIGURE B.393: SFP inspection for HD 137778 with S1-W1 on UT 2008/06/22, seq 001

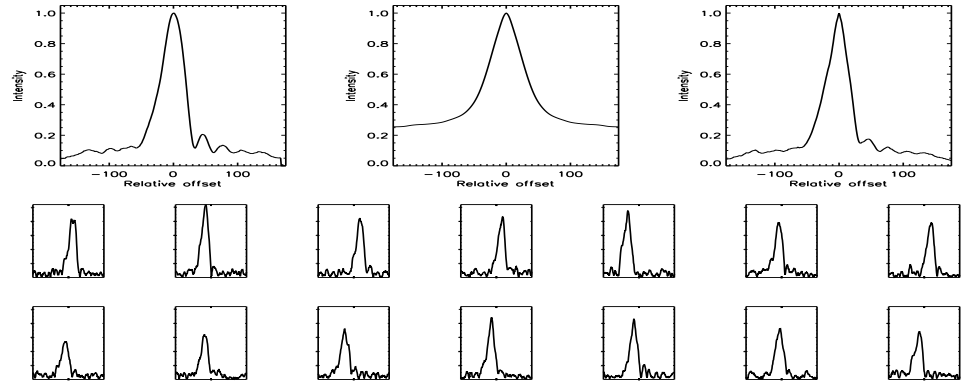

FIGURE B.394: SFP inspection for HD 137778 with S1-W1 on UT 2008/07/07, seq 001

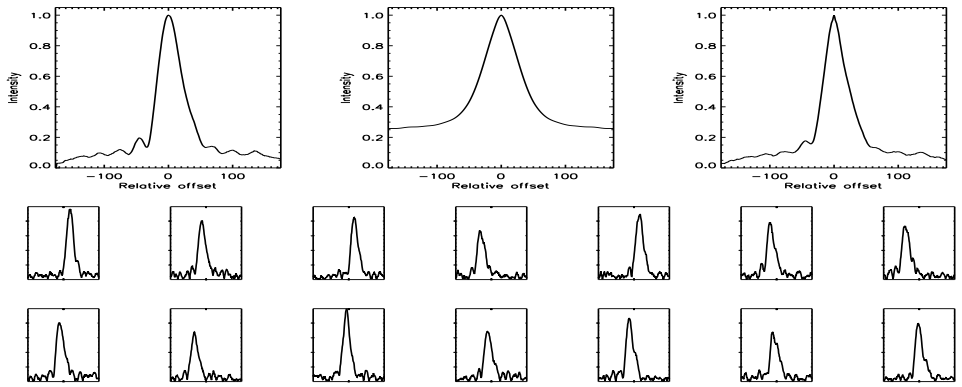

FIGURE B.395: SFP inspection for HD 137778 with S1-W1 on UT 2008/07/07, seq 002

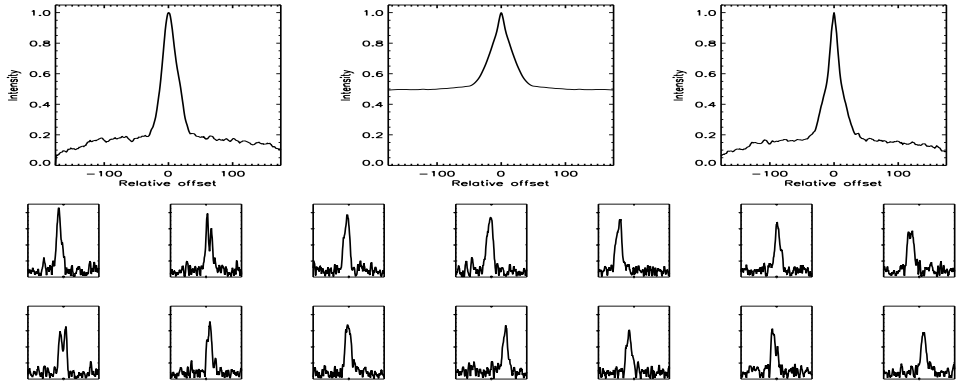

FIGURE B.396: SFP inspection for HD 139323 with S1-E1 on UT 2008/04/12, seq 002

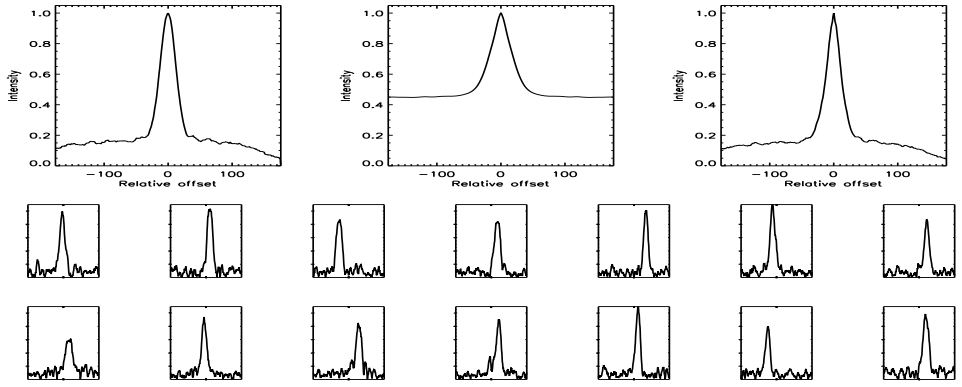

FIGURE B.397: SFP inspection for HD 139323 with S1-W1 on UT 2008/04/12, seq 001

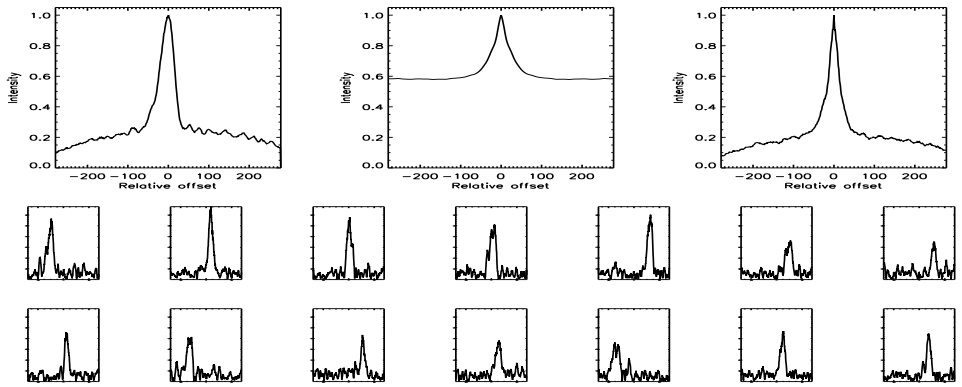

FIGURE B.398: SFP inspection for HD 139341 with E1-W1 on UT 2007/04/26, seq 002

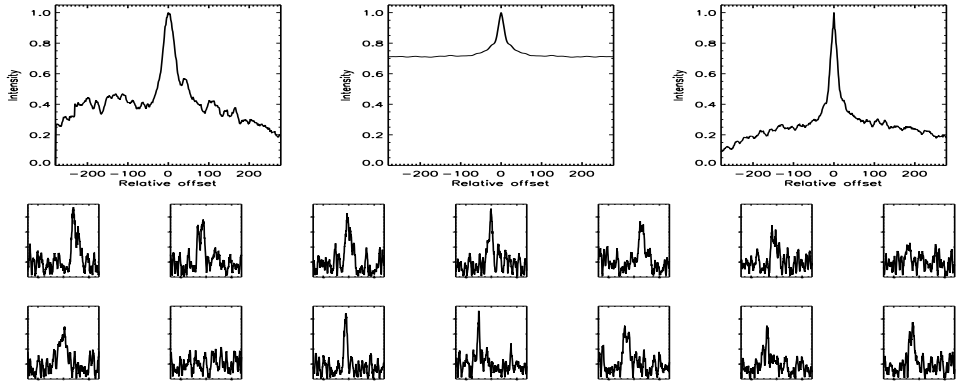

FIGURE B.399: SFP inspection for HD 139341 with S1-E1 on UT 2007/04/14, seq 001

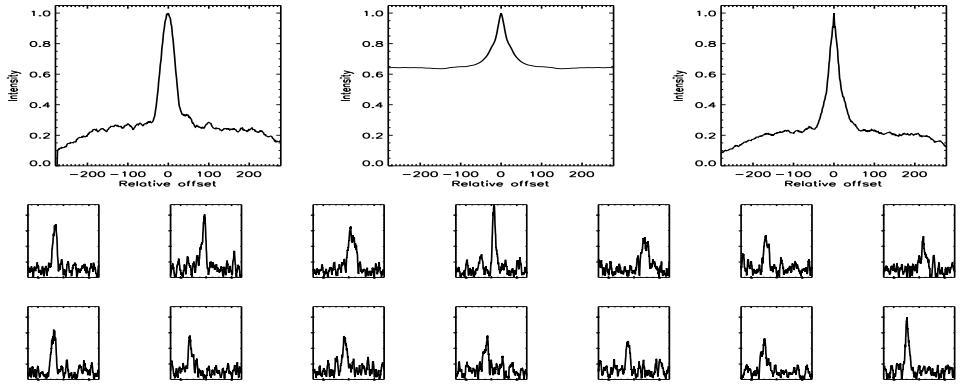

FIGURE B.400: SFP inspection for HD 139341 with S1-W1 on UT 2007/04/17, seq 001

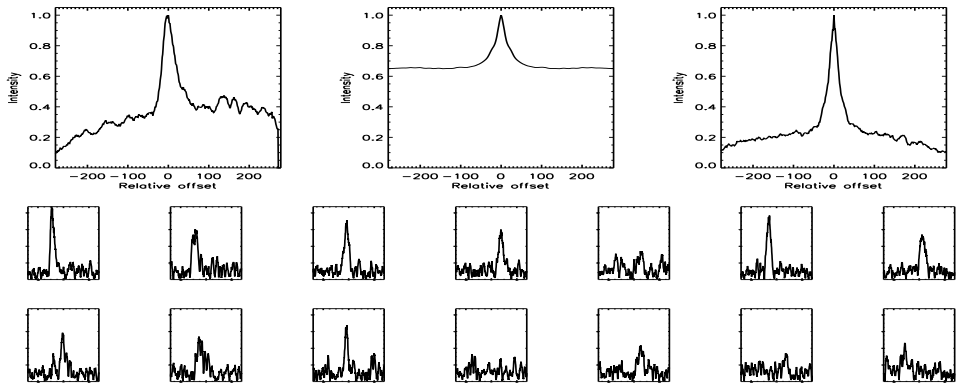

FIGURE B.401: SFP inspection for HD 139341 with S1-W1 on UT 2007/04/17, seq 002

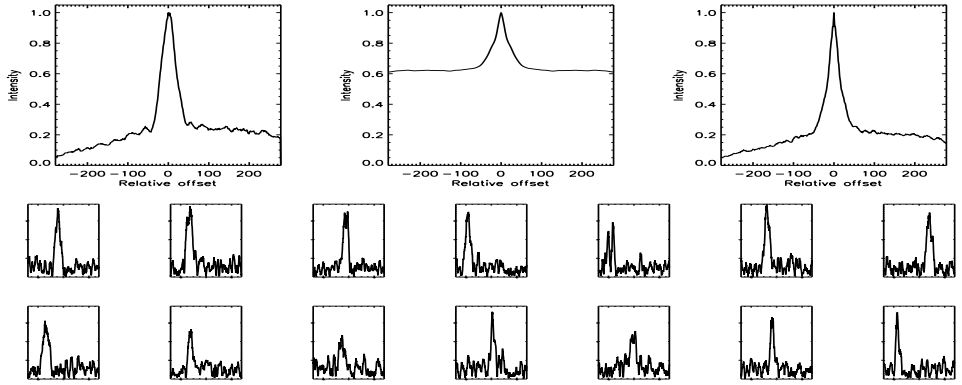

FIGURE B.402: SFP inspection for HD 139341 with S1-W1 on UT 2007/04/17, seq 004

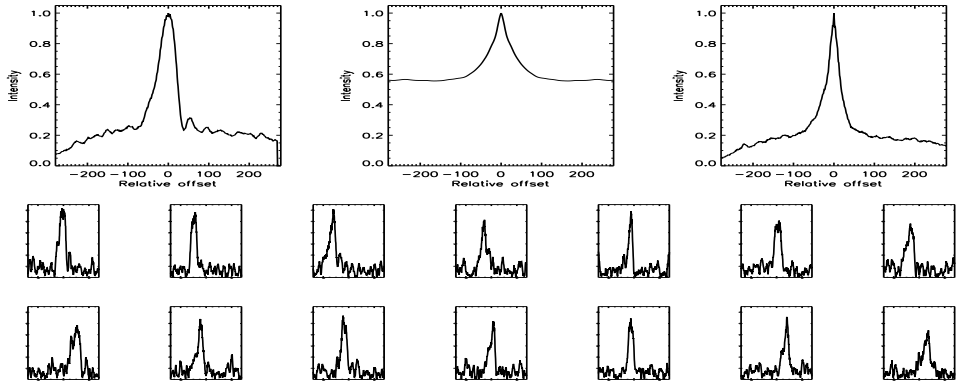

FIGURE B.403: SFP inspection for HD 139777 with S1-E1 on UT 2007/04/14, seq 001

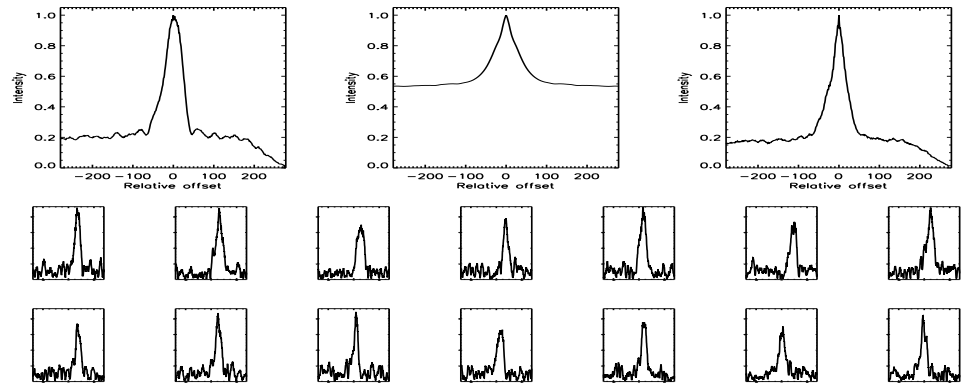

FIGURE B.404: SFP inspection for HD 139777 with S1-W1 on UT 2007/05/28, seq 001

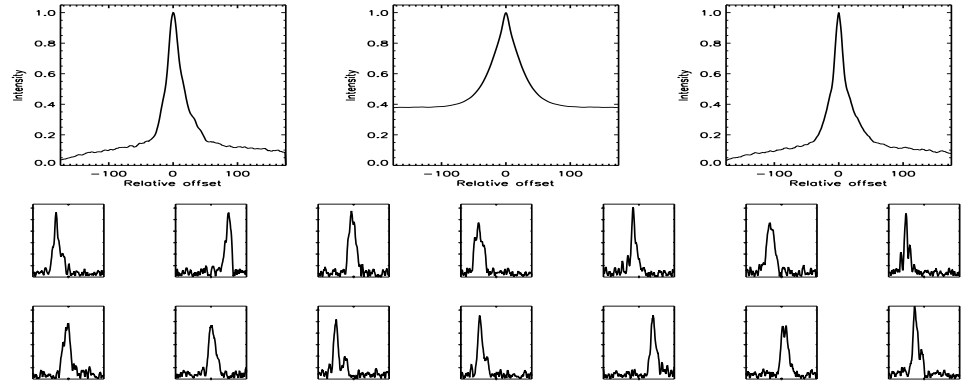

FIGURE B.405: SFP inspection for HD 139777 with S1-W1 on UT 2008/04/26, seq 001

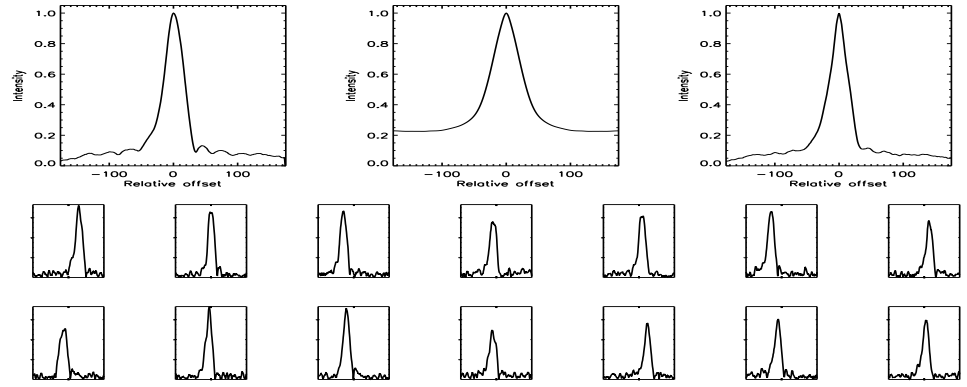

FIGURE B.406: SFP inspection for HD 139777 with S2-W1 on UT 2008/06/24, seq 001

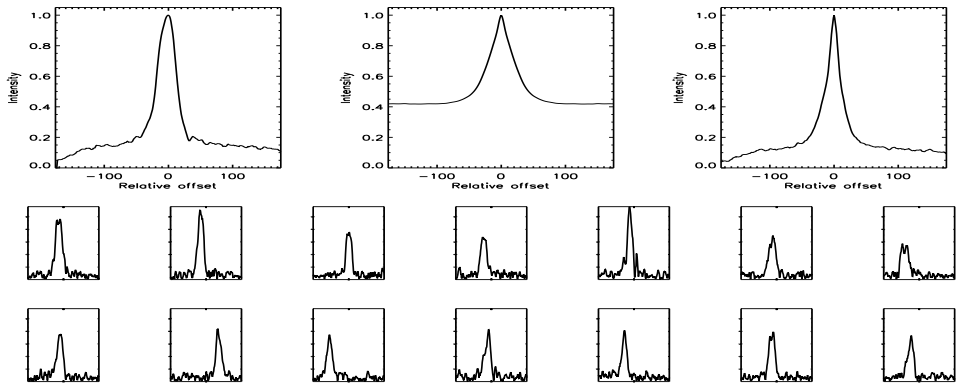

FIGURE B.407: SFP inspection for HD 139813 with S1-E1 on UT 2008/06/25, seq 001

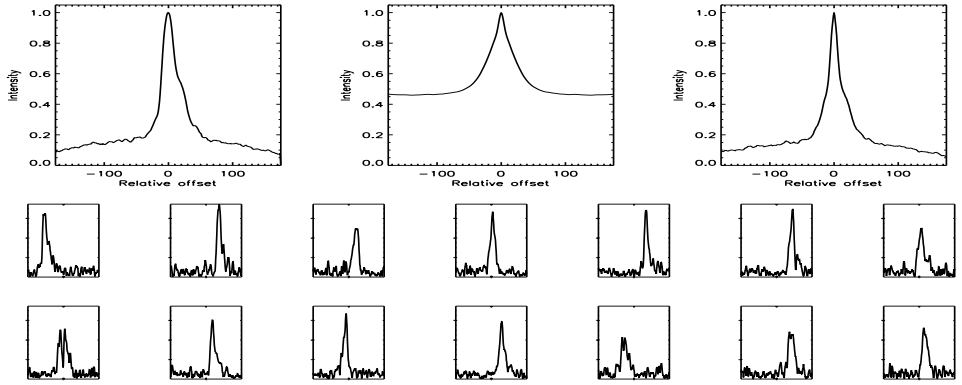

FIGURE B.408: SFP inspection for HD 139813 with S1-W1 on UT 2008/04/26, seq 001

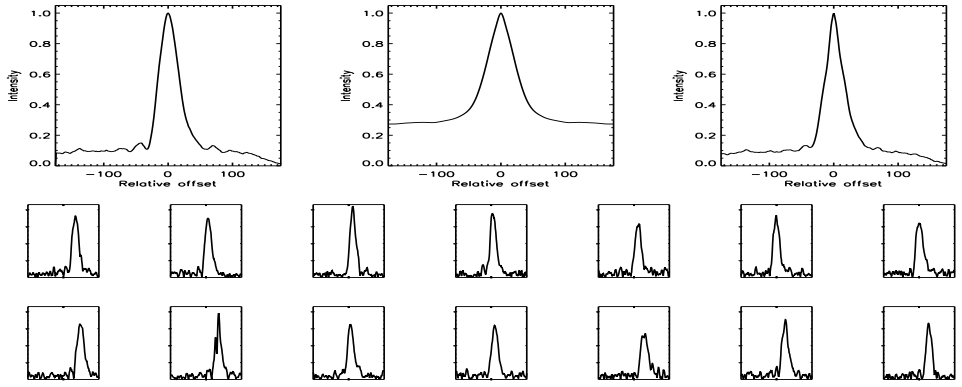

FIGURE B.409: SFP inspection for HD 139813 with S2-W1 on UT 2008/06/24, seq 001

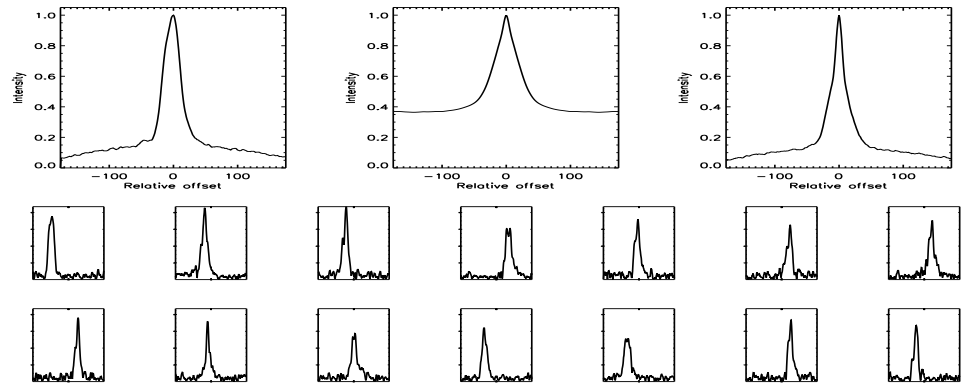

FIGURE B.410: SFP inspection for HD 141272 with S1-E1 on UT 2008/04/25, seq 001

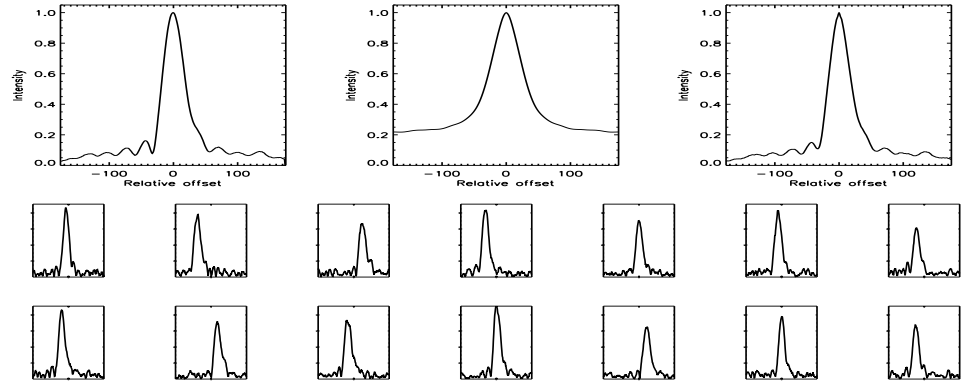

FIGURE B.411: SFP inspection for HD 141272 with S1-W1 on UT 2008/04/14, seq 001

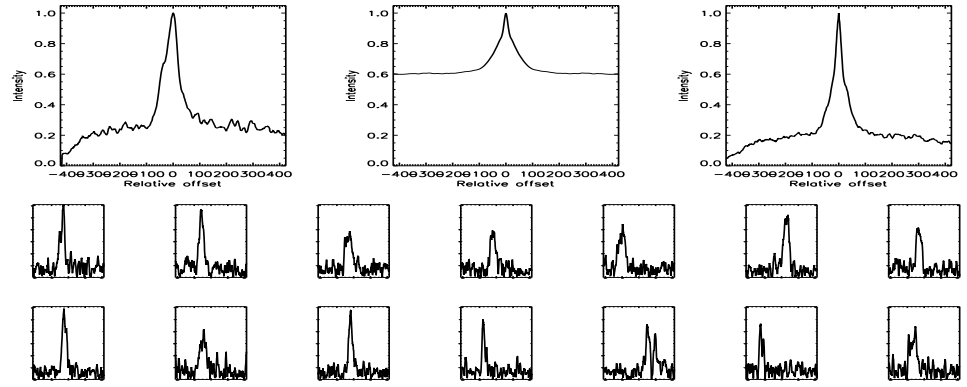

FIGURE B.412: SFP inspection for HD 142267 with S1-E1 on UT 2007/08/15, seq 001

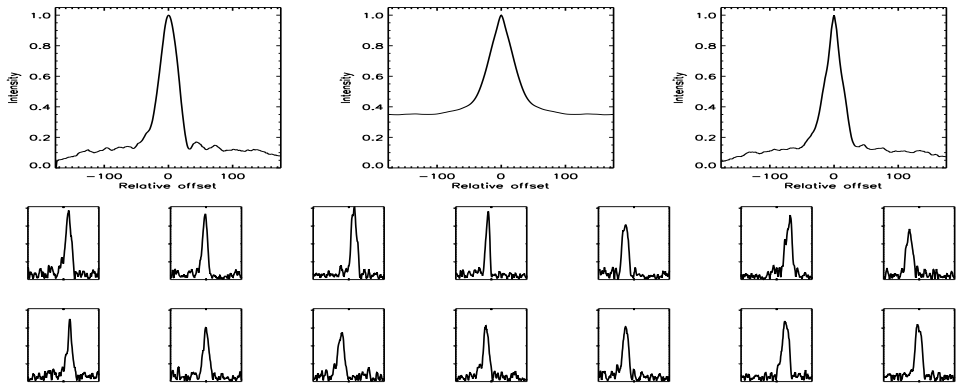

FIGURE B.413: SFP inspection for HD 142267 with S1-E1 on UT 2008/04/13, seq 001

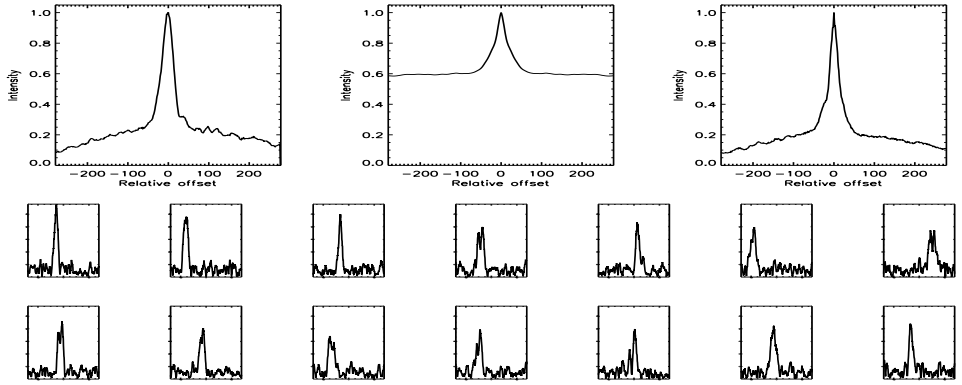

FIGURE B.414: SFP inspection for HD 142267 with S1-E2 on UT 2007/06/01, seq 001

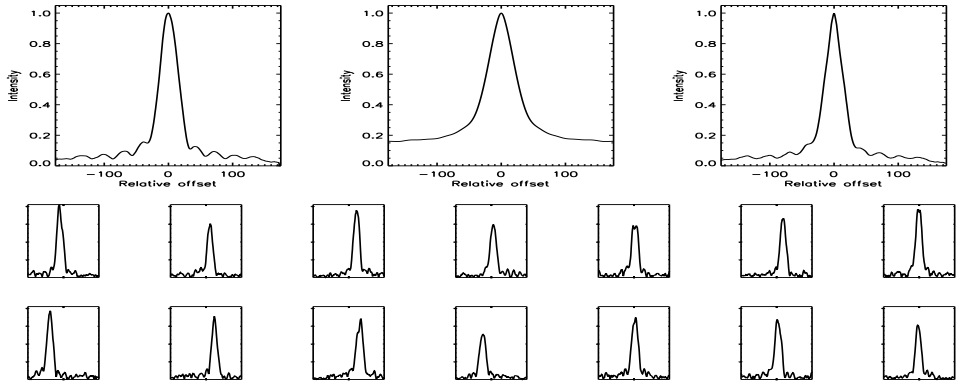

FIGURE B.415: SFP inspection for HD 142267 with S1-W1 on UT 2008/04/13, seq 002

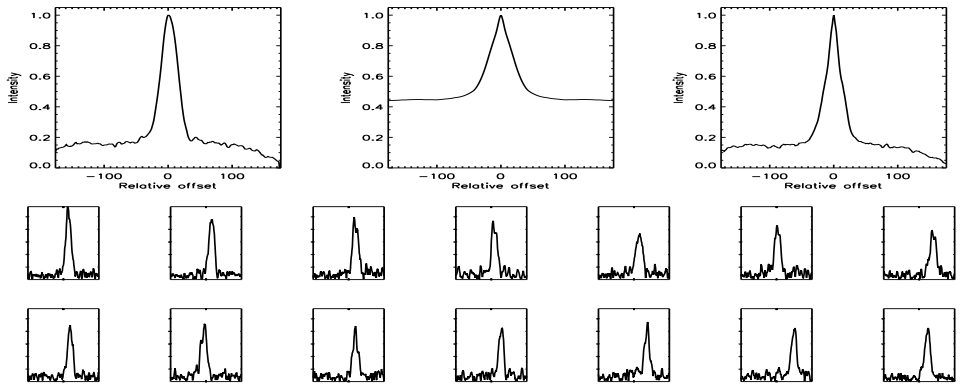

FIGURE B.416: SFP inspection for HD 144287 with S1-E1 on UT 2008/04/13, seq 001

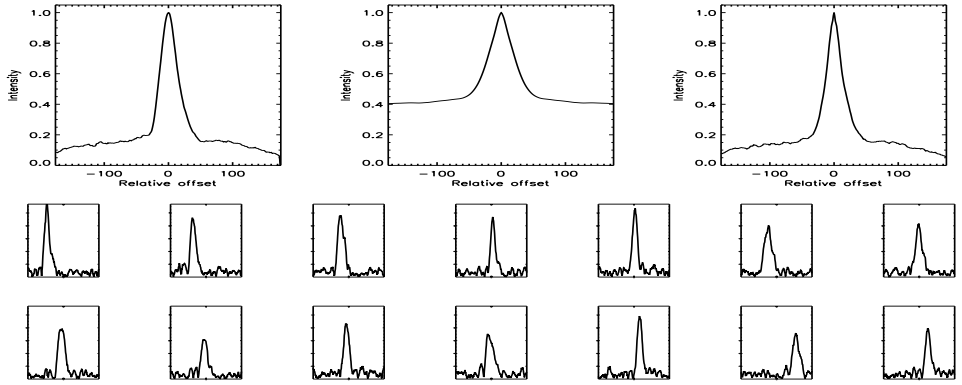

FIGURE B.417: SFP inspection for HD 144287 with S1-W1 on UT 2008/04/12, seq 001

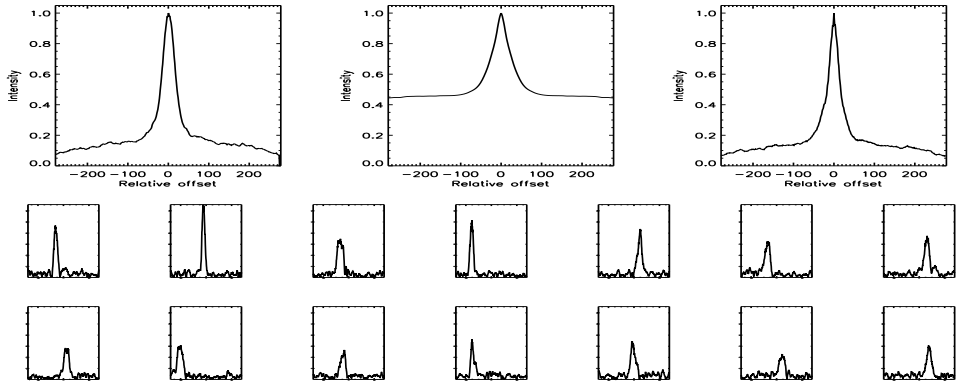

FIGURE B.418: SFP inspection for HD 145675 with E1-W1 on UT 2007/04/26, seq 001

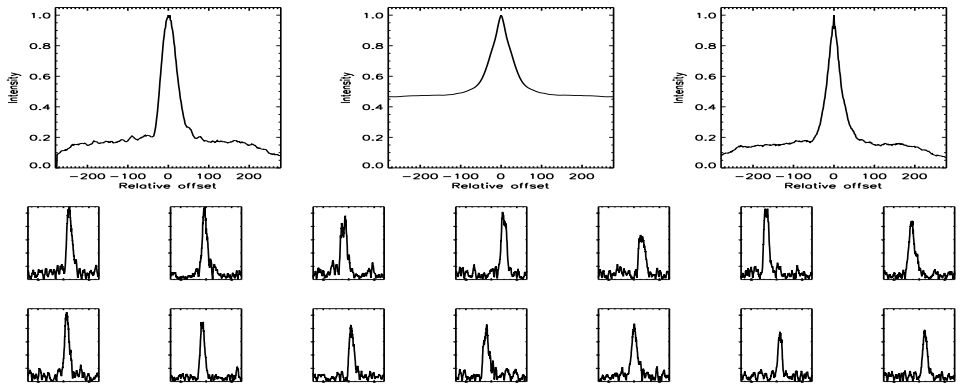

FIGURE B.419: SFP inspection for HD 145675 with S1-E1 on UT 2007/05/17, seq 001

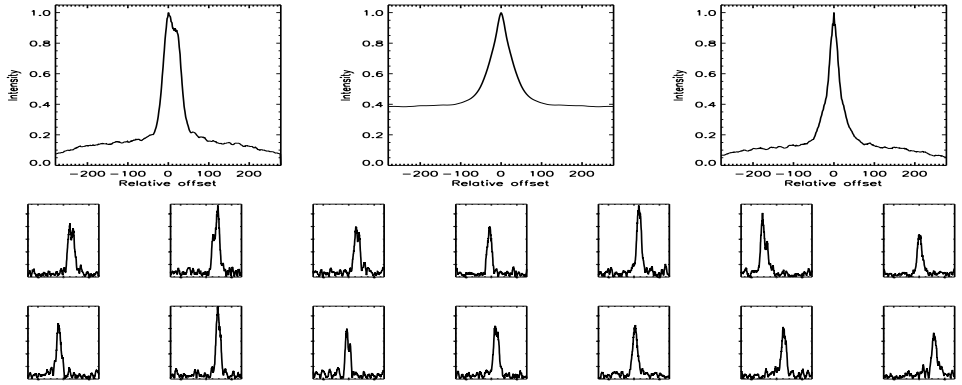

FIGURE B.420: SFP inspection for HD 145675 with S1-W1 on UT 2007/04/24, seq 001

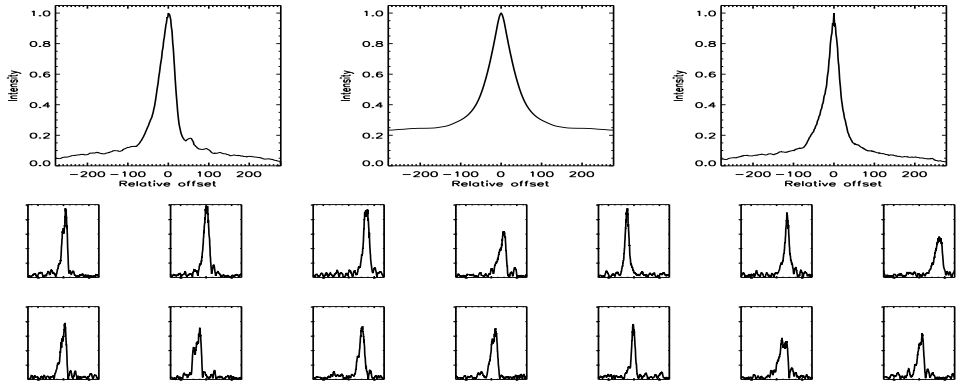

FIGURE B.421: SFP inspection for HD 146233 with S1-E1 on UT 2007/03/08, seq 001

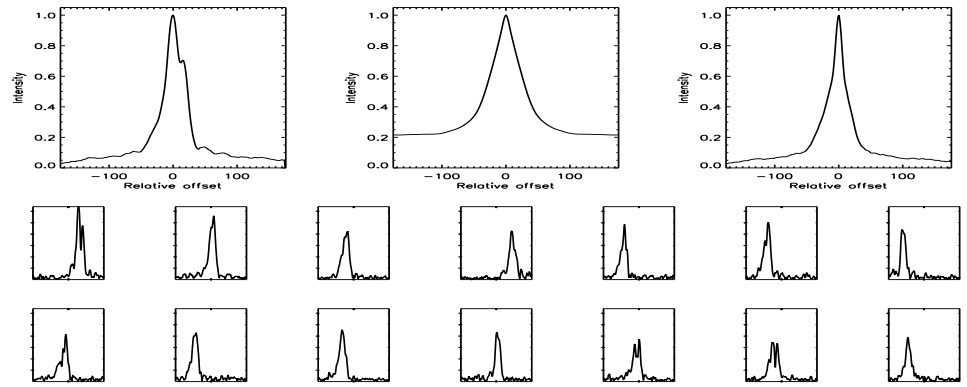

FIGURE B.422: SFP inspection for HD 146233 with S1-E1 on UT 2008/04/25, seq 001

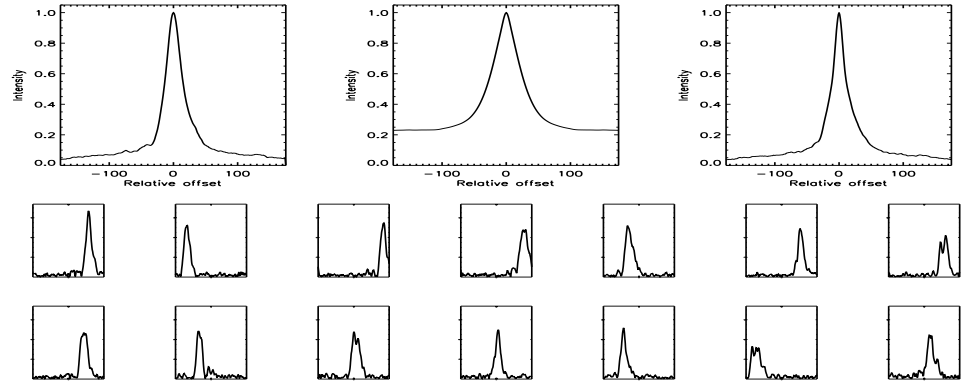

FIGURE B.423: SFP inspection for HD 146233 with S1-E1 on UT 2008/06/23, seq 001

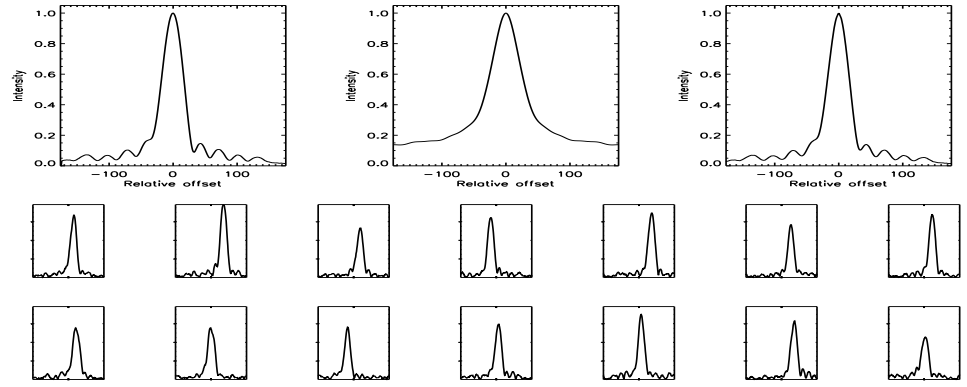

FIGURE B.424: SFP inspection for HD 146233 with S1-W1 on UT 2008/04/14, seq 001

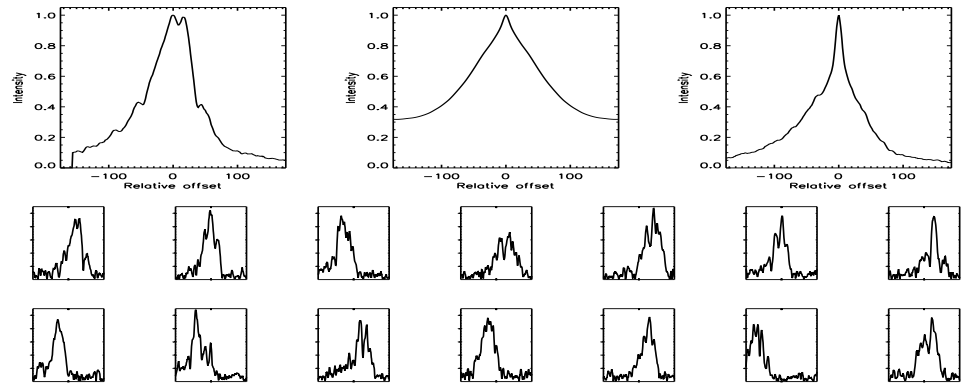

FIGURE B.425: SFP inspection for HD 146233 with S1-W1 on UT 2008/06/22, seq 001

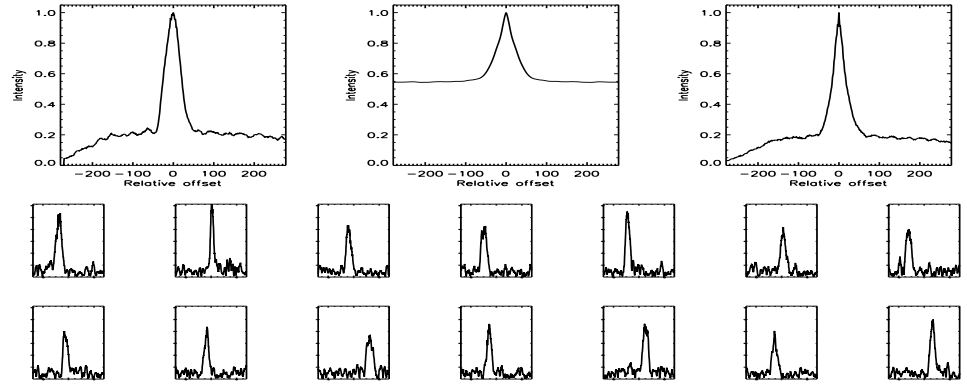

FIGURE B.426: SFP inspection for HD 148653 with S1-E1 on UT 2007/02/04, seq 001

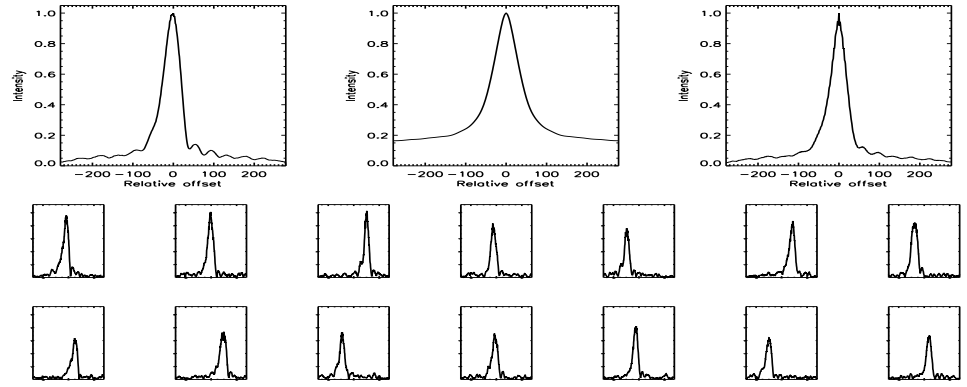

FIGURE B.427: SFP inspection for HD 149661 with S1-E1 on UT 2007/03/08, seq 002

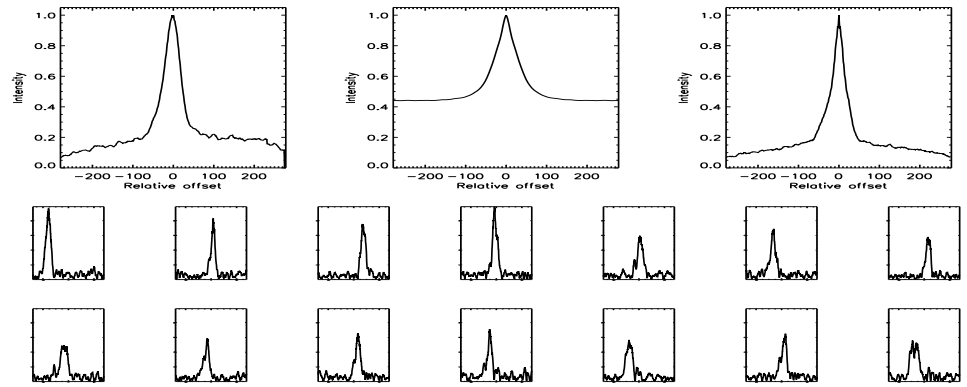

FIGURE B.428: SFP inspection for HD 149661 with S1-E2 on UT 2007/05/31, seq 001

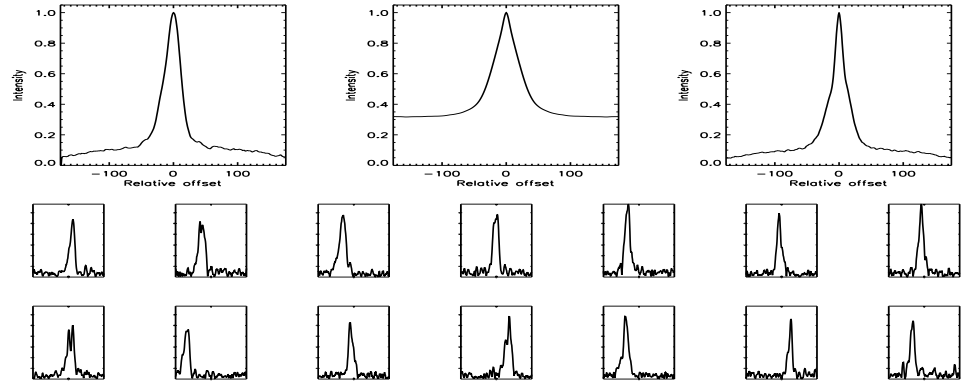

FIGURE B.429: SFP inspection for HD 149806 with S1-E1 on UT 2008/04/25, seq 001

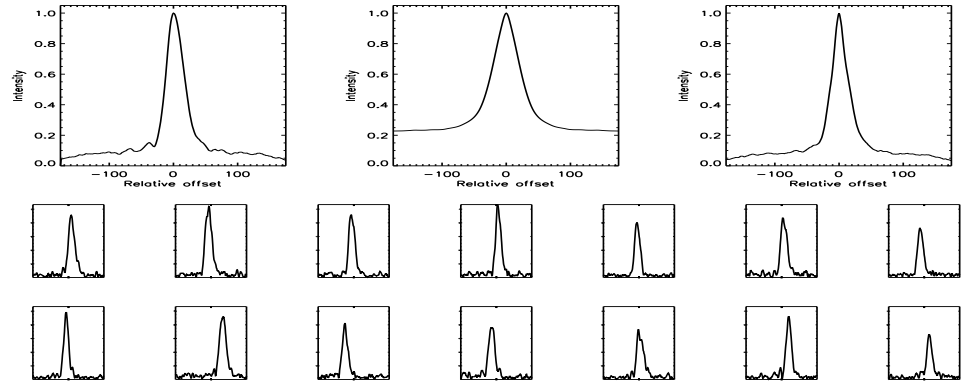

FIGURE B.430: SFP inspection for HD 149806 with S1-W1 on UT 2008/04/13, seq 001

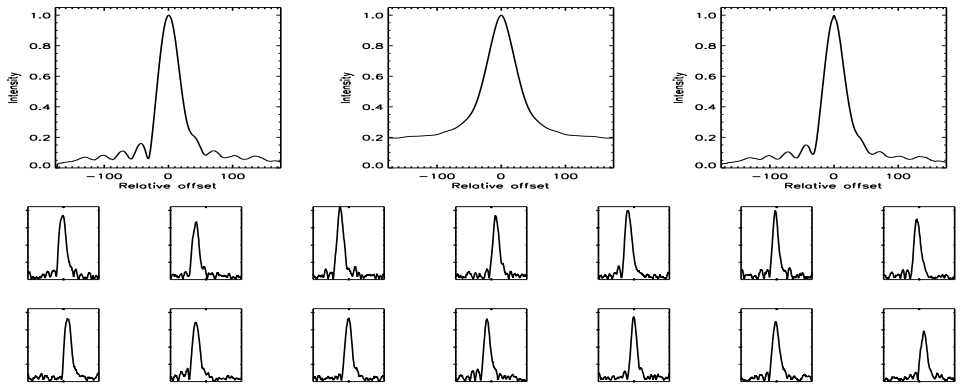

FIGURE B.431: SFP inspection for HD 149806 with S1-W1 on UT 2008/04/14, seq 001

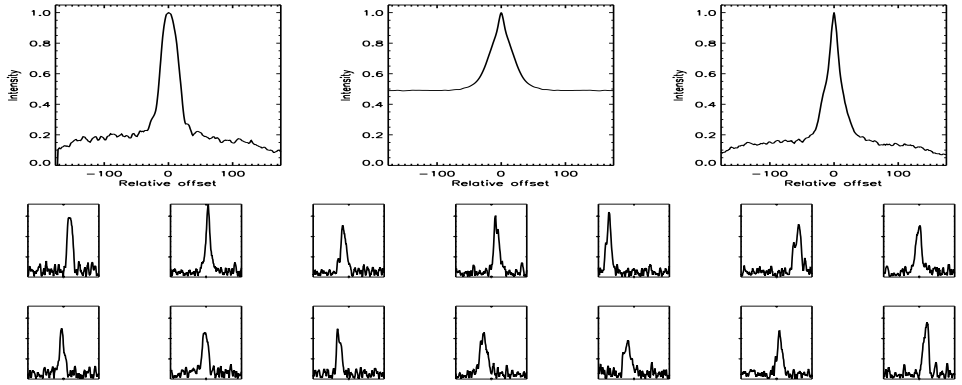

FIGURE B.432: SFP inspection for HD 151541 with S1-E1 on UT 2008/06/25, seq 001

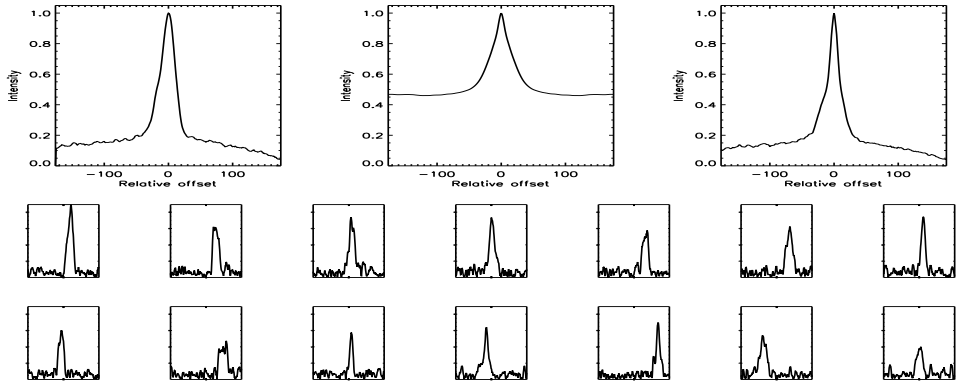

FIGURE B.433: SFP inspection for HD 151541 with S1-W1 on UT 2008/04/26, seq 001

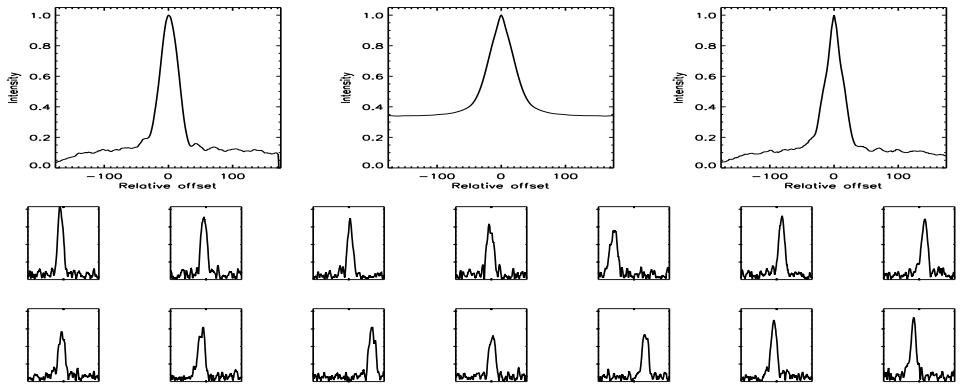

FIGURE B.434: SFP inspection for HD 151541 with S2-W1 on UT 2008/06/24, seq 001

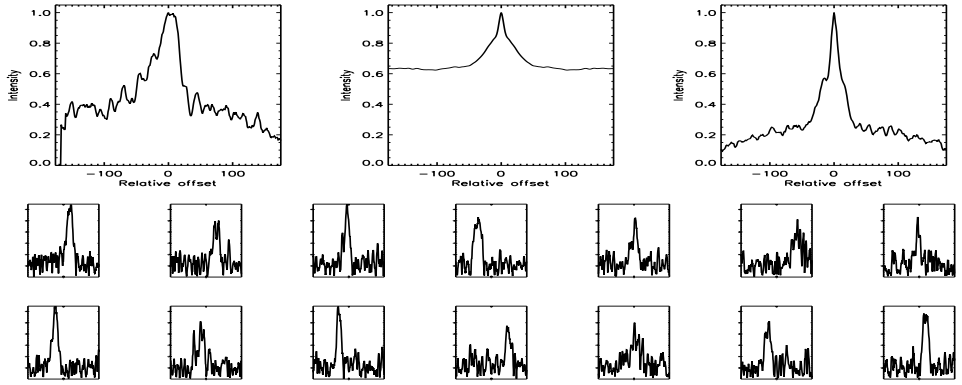

FIGURE B.435: SFP inspection for HD 153557 with S1-E1 on UT 2008/06/25, seq 001

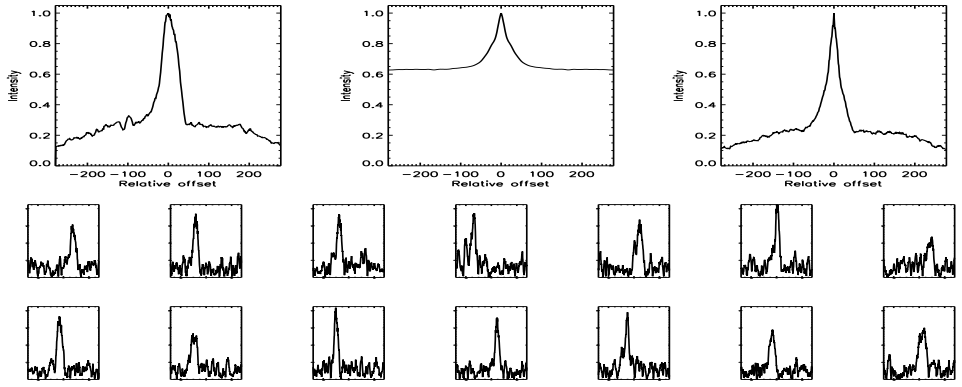

FIGURE B.436: SFP inspection for HD 153557 with S1-W1 on UT 2007/05/30, seq 001

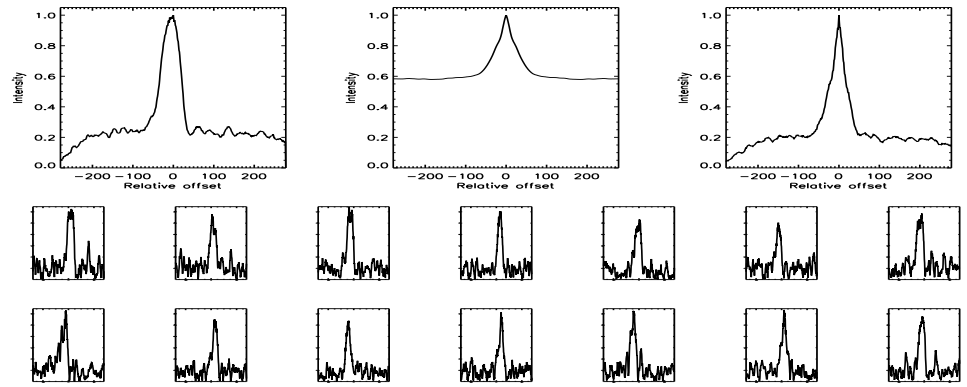

FIGURE B.437: SFP inspection for HD 153557 with S1-W1 on UT 2007/08/21, seq 001

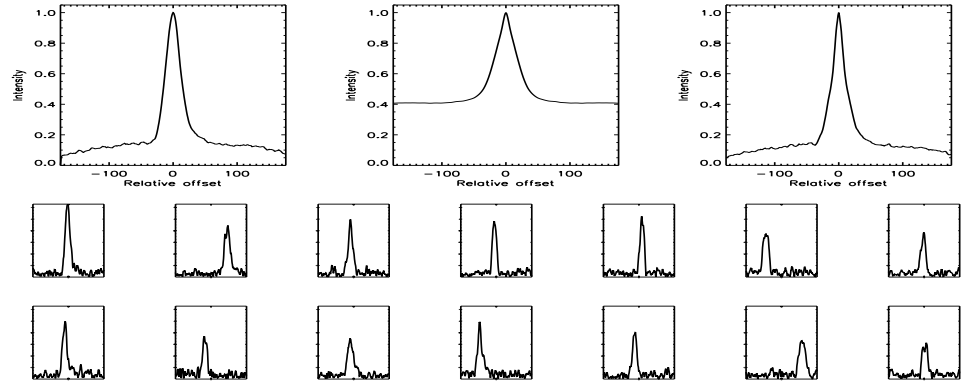

FIGURE B.438: SFP inspection for HD 153557 with S1-W1 on UT 2008/04/12, seq 001

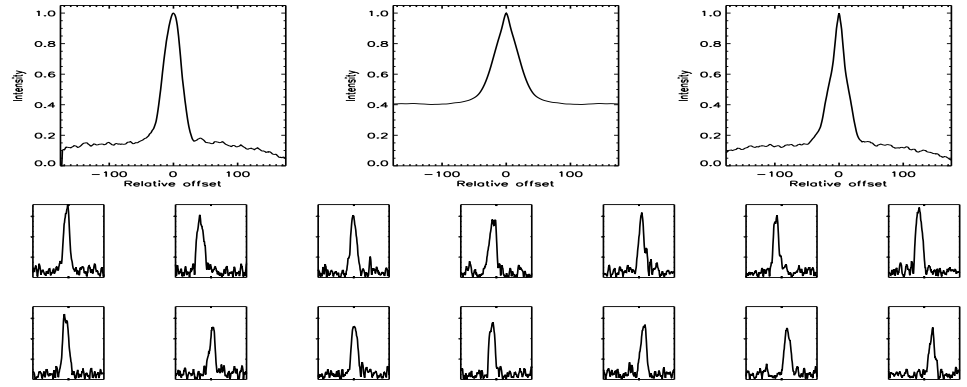

FIGURE B.439: SFP inspection for HD 153557 with S2-W1 on UT 2008/06/24, seq 001

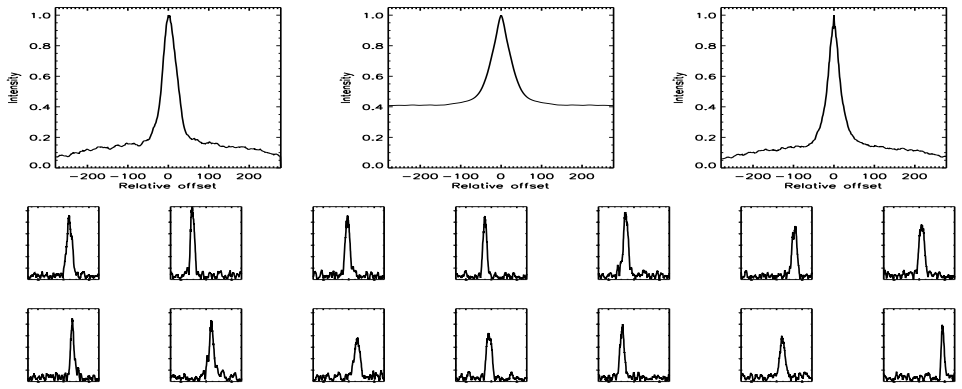

FIGURE B.440: SFP inspection for HD 154345 with E1-W1 on UT 2007/04/26, seq 001

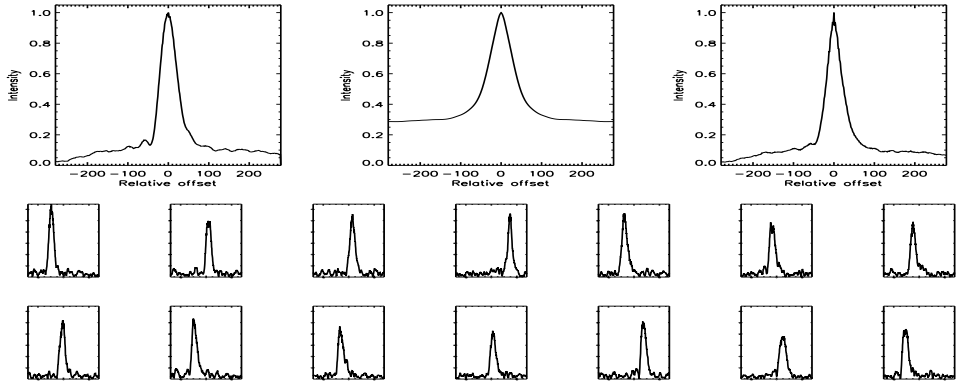

FIGURE B.441: SFP inspection for HD 154345 with S1-E1 on UT 2007/04/14, seq 001

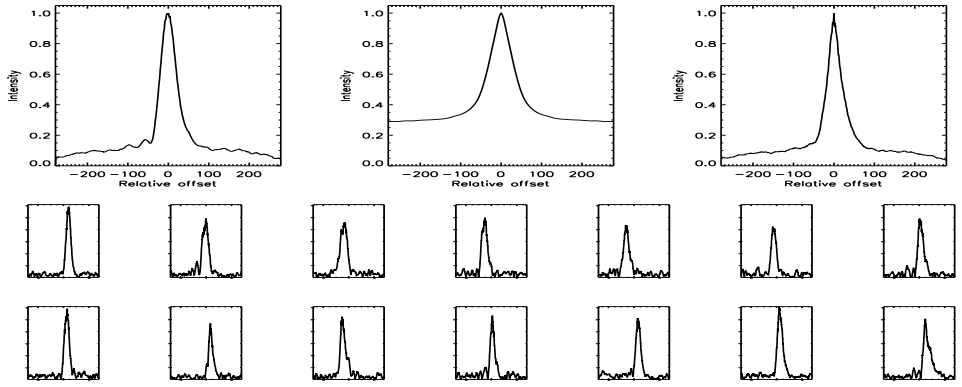

FIGURE B.442: SFP inspection for HD 154345 with S1-W1 on UT 2007/04/17, seq 001

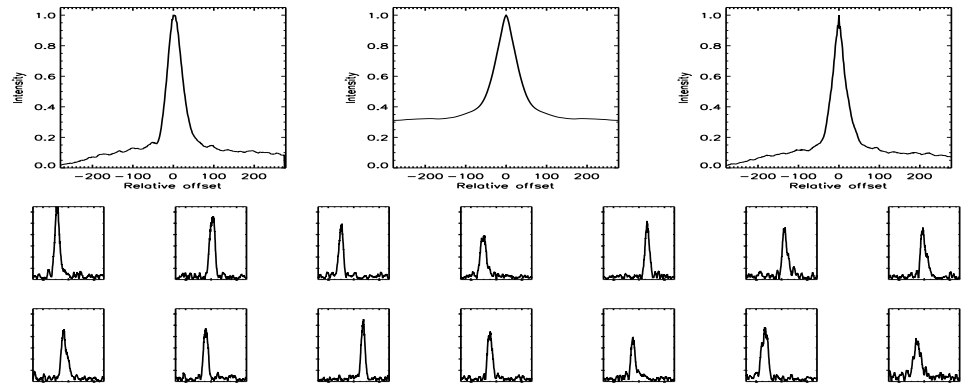

FIGURE B.443: SFP inspection for HD 154345 with S1-W1 on UT 2007/04/17, seq 002

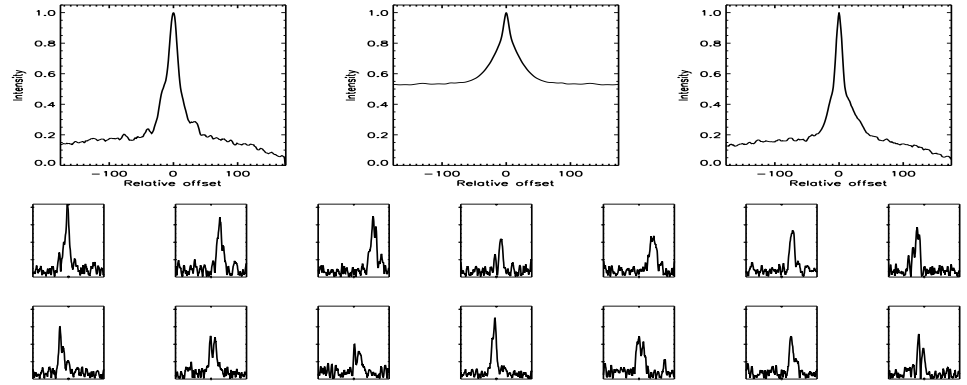

FIGURE B.444: SFP inspection for HD 155712 with S1-E1 on UT 2008/04/25, seq 001

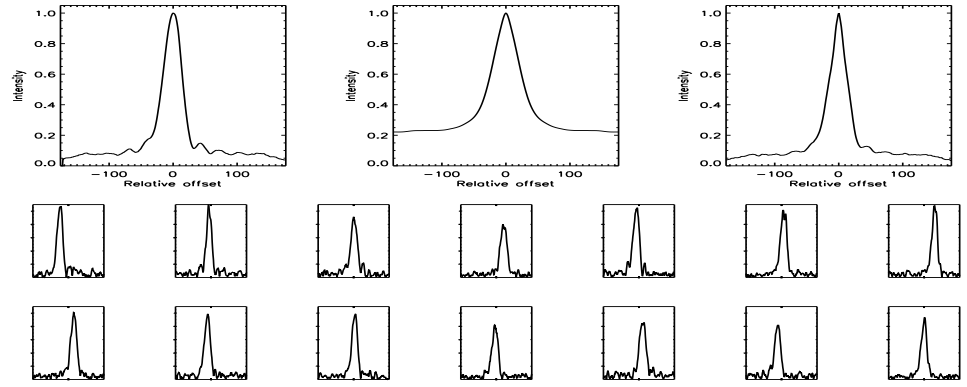

FIGURE B.445: SFP inspection for HD 155712 with S1-W1 on UT 2008/04/13, seq 001

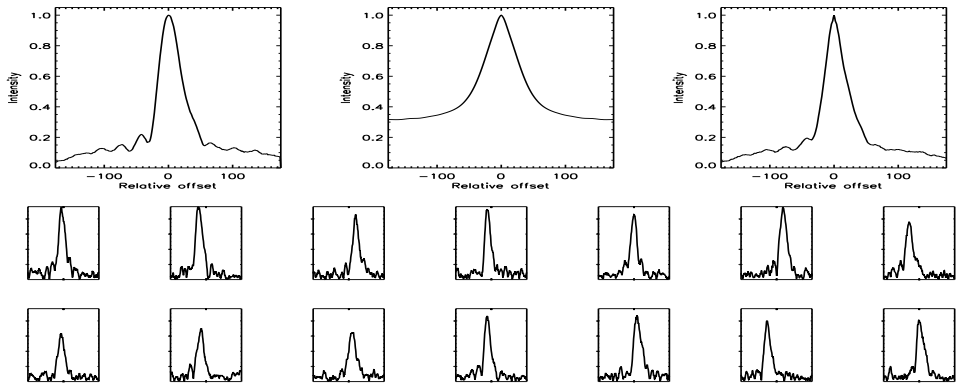

FIGURE B.446: SFP inspection for HD 155712 with S1-W1 on UT 2008/04/14, seq 001

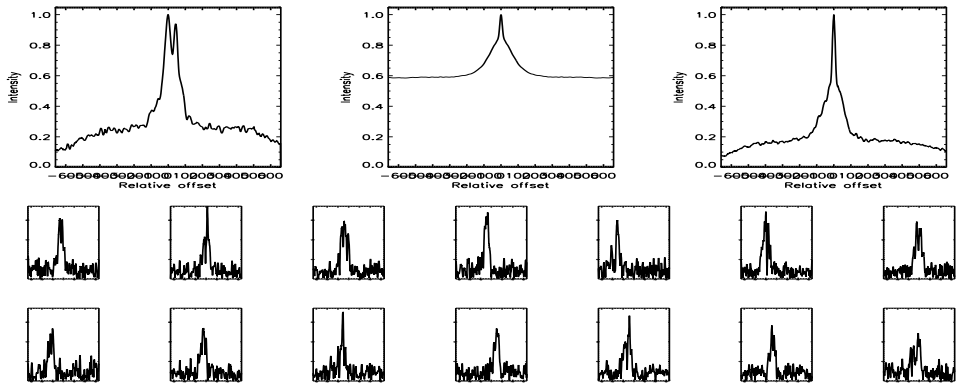

FIGURE B.447: SFP inspection for HD 155712 with S2-W1 on UT 2007/09/17, seq 001

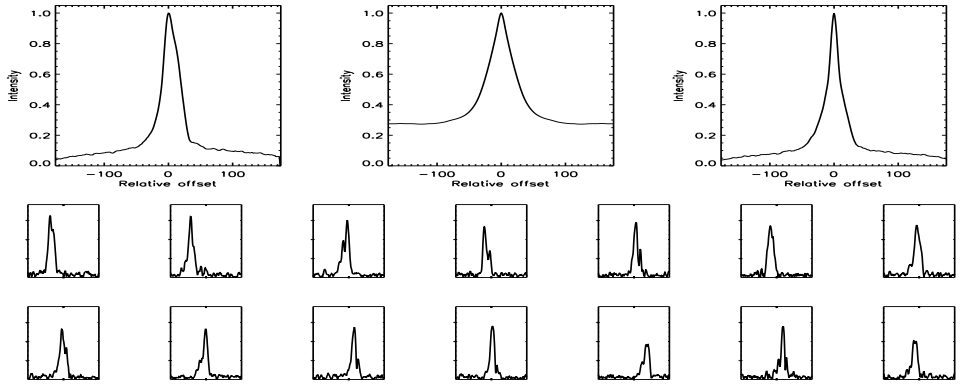

FIGURE B.448: SFP inspection for HD 157347 with S1-E1 on UT 2008/04/25, seq 001

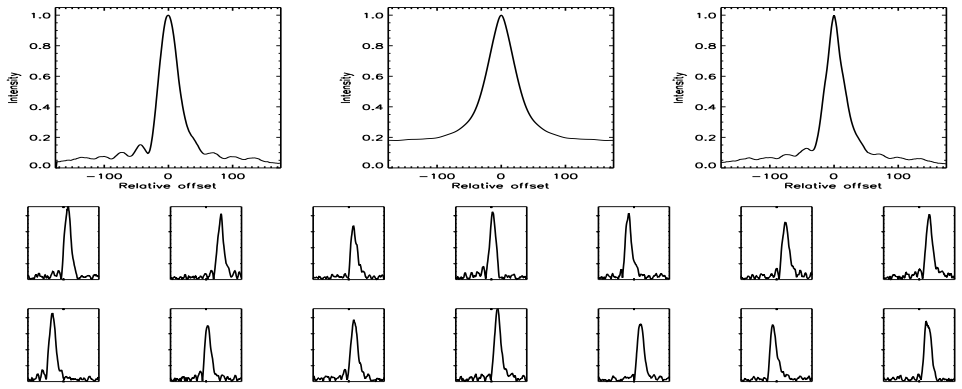

FIGURE B.449: SFP inspection for HD 157347 with S1-W1 on UT 2008/04/13, seq 001

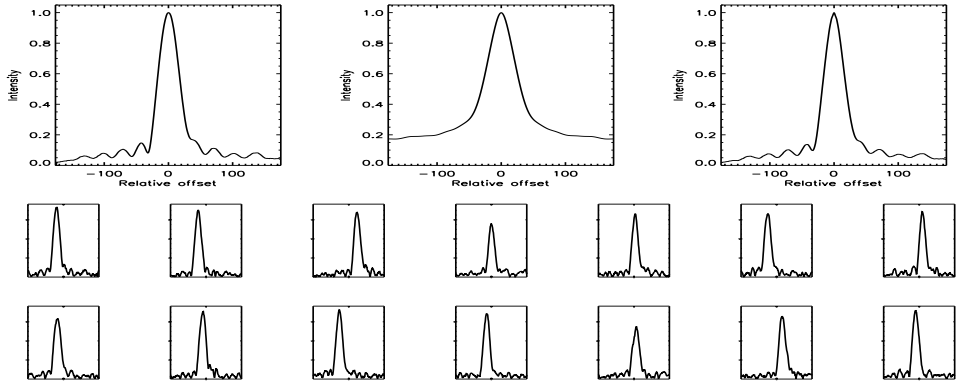

FIGURE B.450: SFP inspection for HD 157347 with S1-W1 on UT 2008/04/14, seq 001

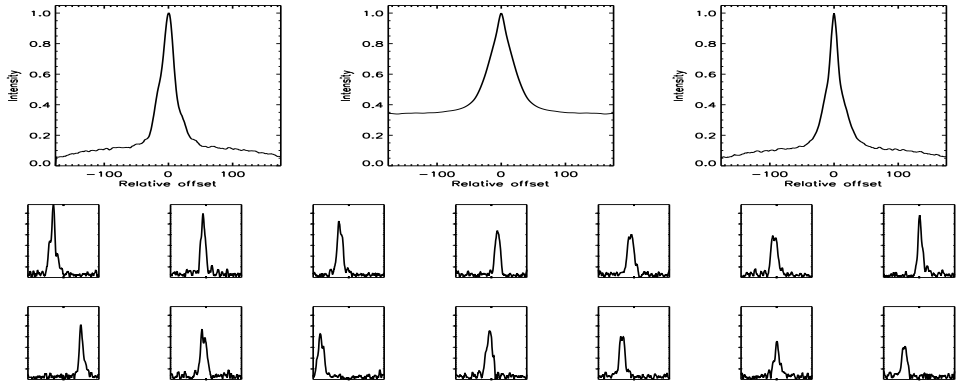

FIGURE B.451: SFP inspection for HD 158614 with S1-E1 on UT 2008/04/25, seq 001

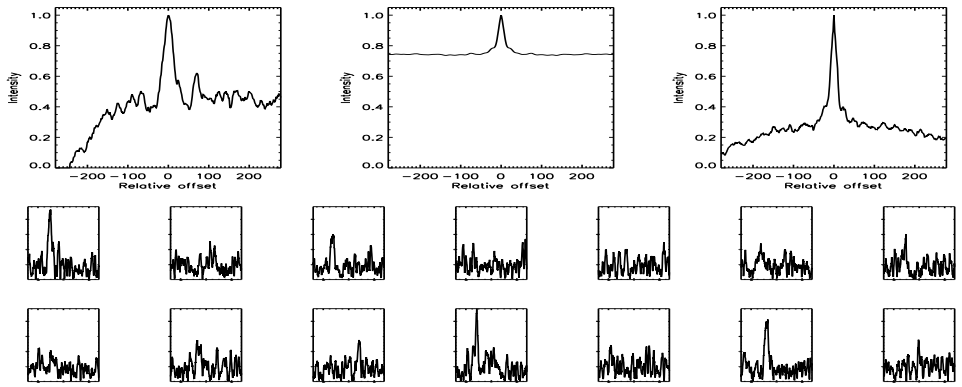

FIGURE B.452: SFP inspection for HD 158614 with S1-E2 on UT 2007/06/01, seq 001

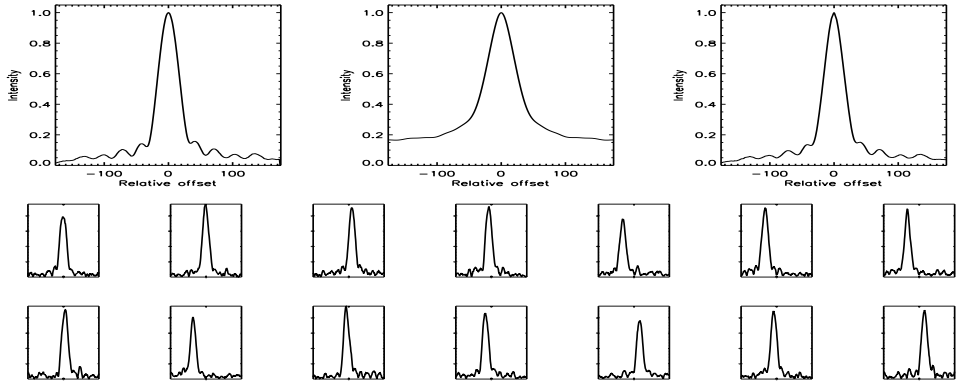

FIGURE B.453: SFP inspection for HD 158614 with S1-W1 on UT 2008/04/14, seq 001

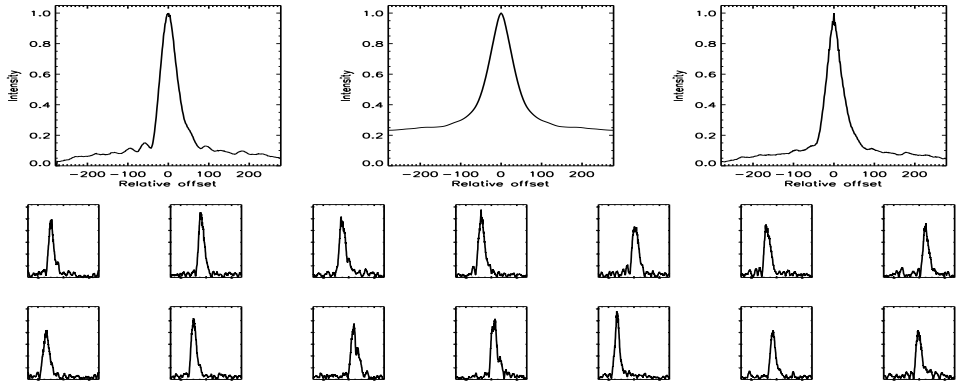

FIGURE B.454: SFP inspection for HD 158633 with S1-E1 on UT 2007/04/14, seq 001

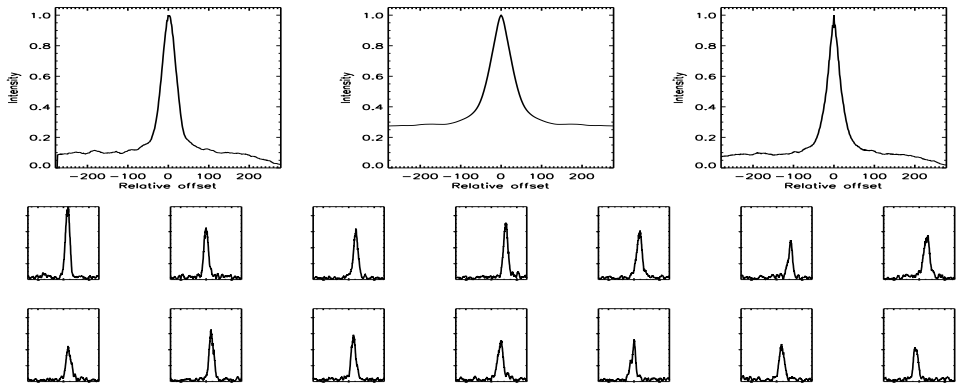

FIGURE B.455: SFP inspection for HD 158633 with S1-W1 on UT 2007/04/17, seq 001

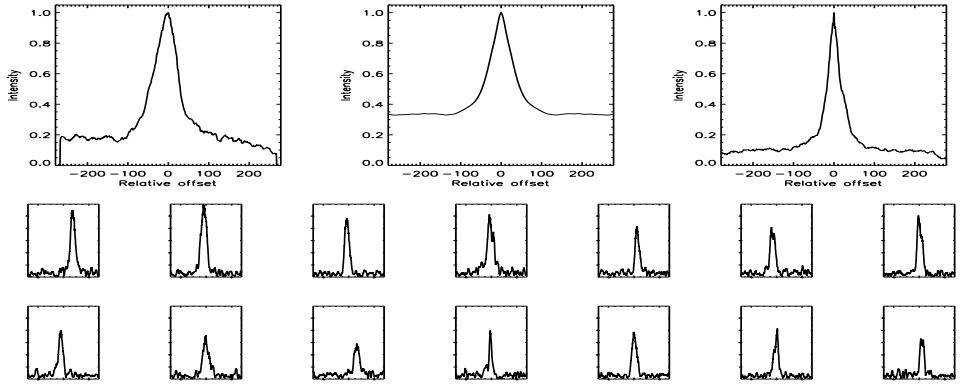

FIGURE B.456: SFP inspection for HD 158633 with S1-W1 on UT 2007/04/17, seq 002

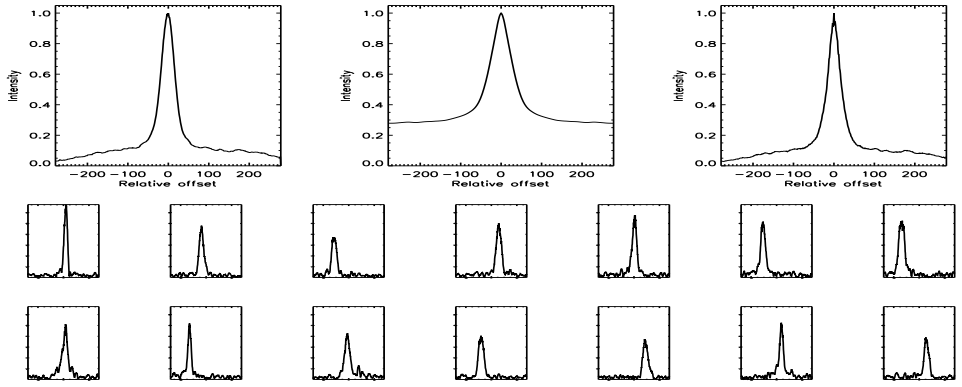

FIGURE B.457: SFP inspection for HD 158633 with S1-W1 on UT 2007/04/17, seq 003

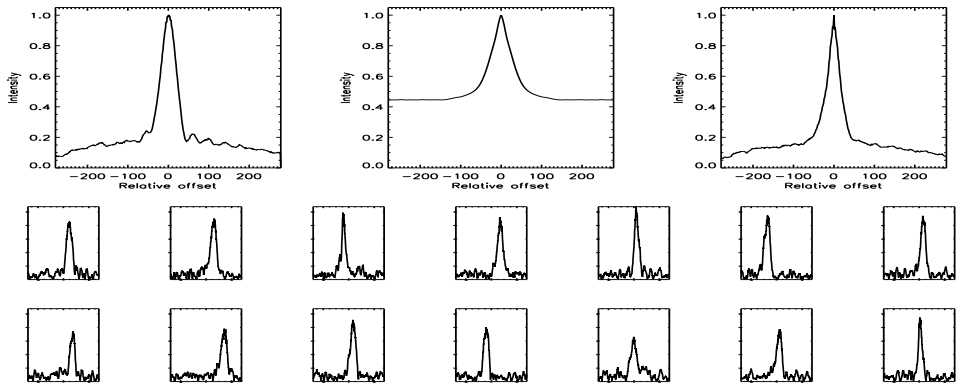

FIGURE B.458: SFP inspection for HD 159062 with S1-E1 on UT 2007/04/14, seq 001

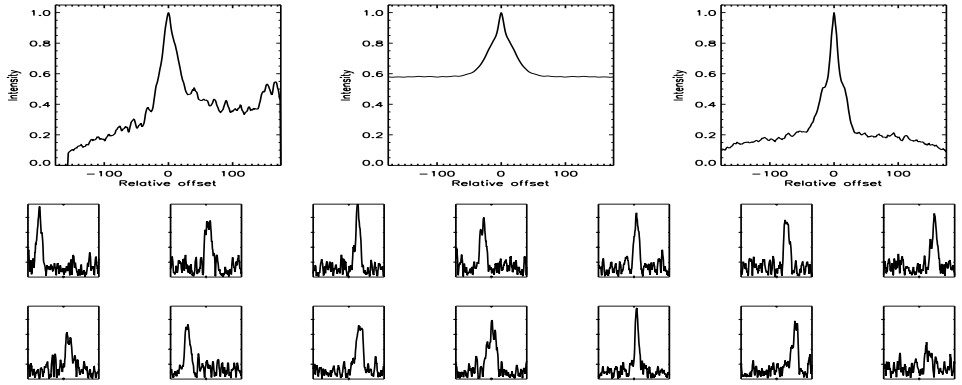

FIGURE B.459: SFP inspection for HD 159062 with S1-E1 on UT 2008/06/25, seq 001

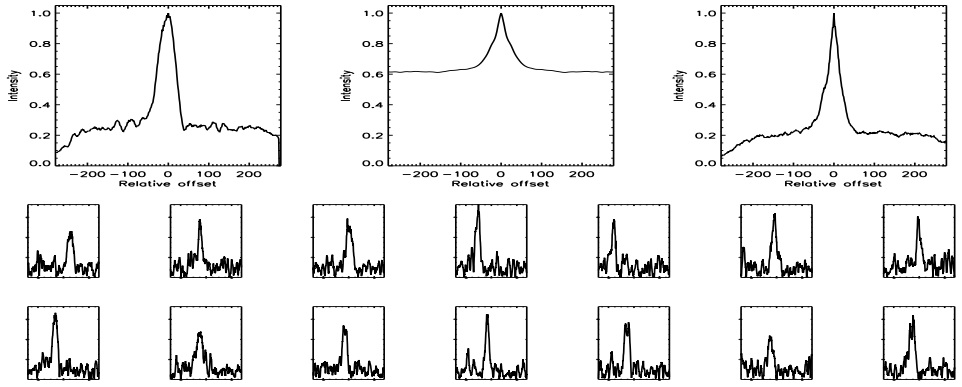

FIGURE B.460: SFP inspection for HD 159062 with S1-W1 on UT 2007/08/21, seq 002

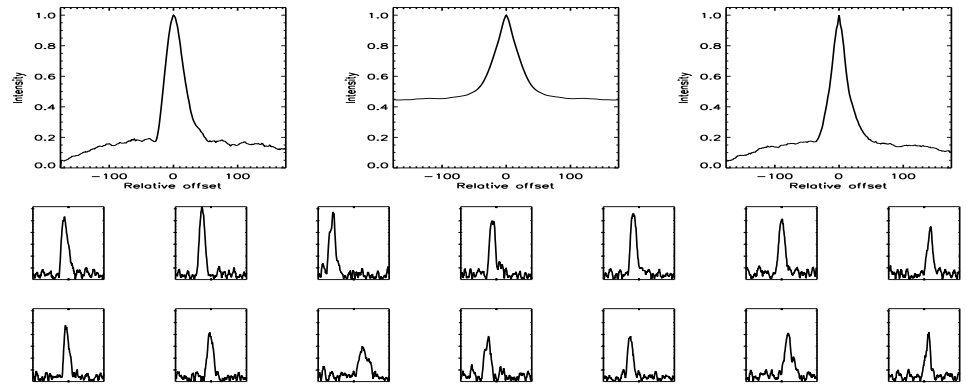

FIGURE B.461: SFP inspection for HD 159062 with S1-W1 on UT 2008/04/12, seq 001

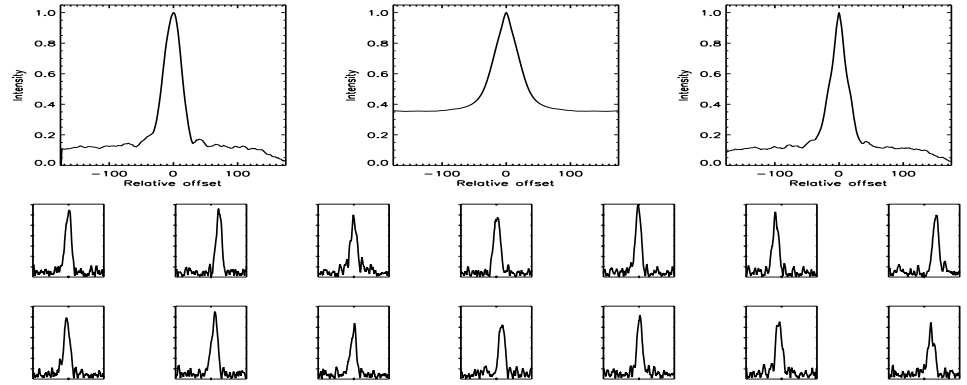

FIGURE B.462: SFP inspection for HD 159062 with S2-W1 on UT 2008/06/24, seq 001

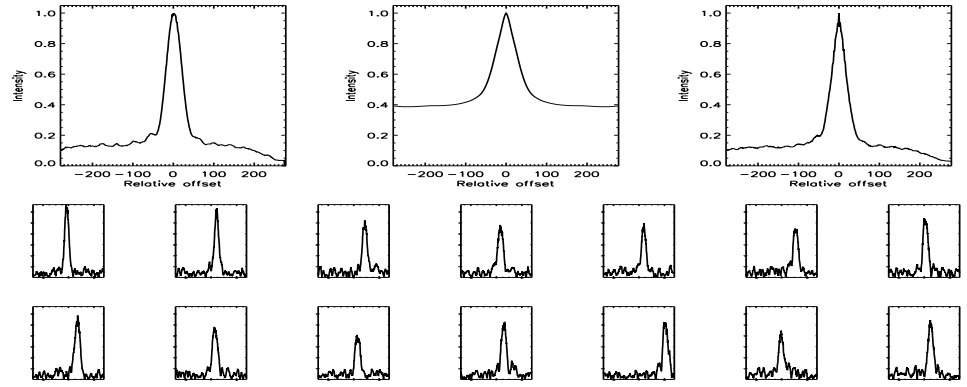

FIGURE B.463: SFP inspection for HD 159222 with S1-E1 on UT 2007/05/17, seq 002

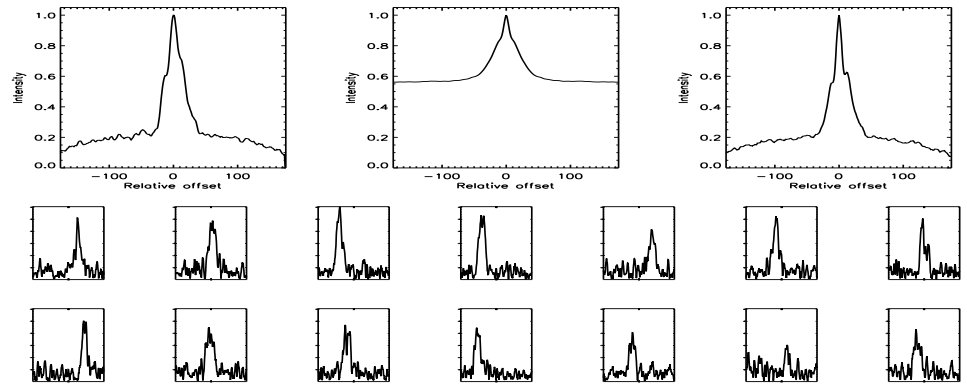

FIGURE B.464: SFP inspection for HD 159222 with S1-E1 on UT 2008/06/26, seq 001

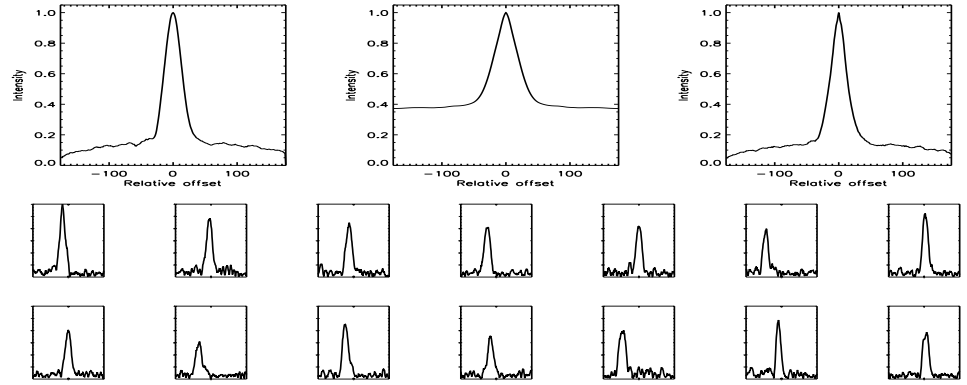

FIGURE B.465: SFP inspection for HD 159222 with S1-W1 on UT 2008/04/12, seq 001

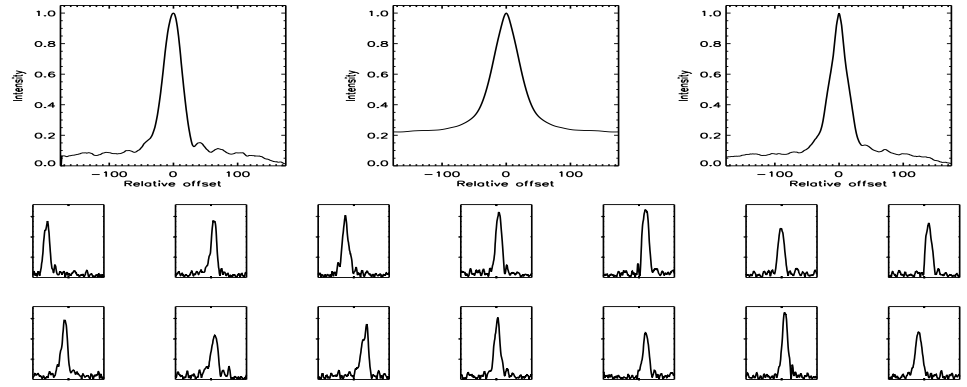

FIGURE B.466: SFP inspection for HD 159222 with S2-W1 on UT 2008/06/24, seq 001

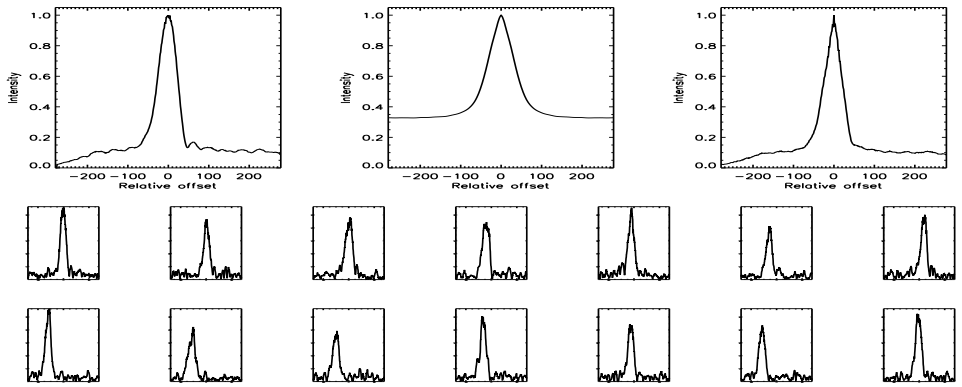

FIGURE B.467: SFP inspection for HD 160346 with S1-E1 on UT 2007/07/22, seq 003

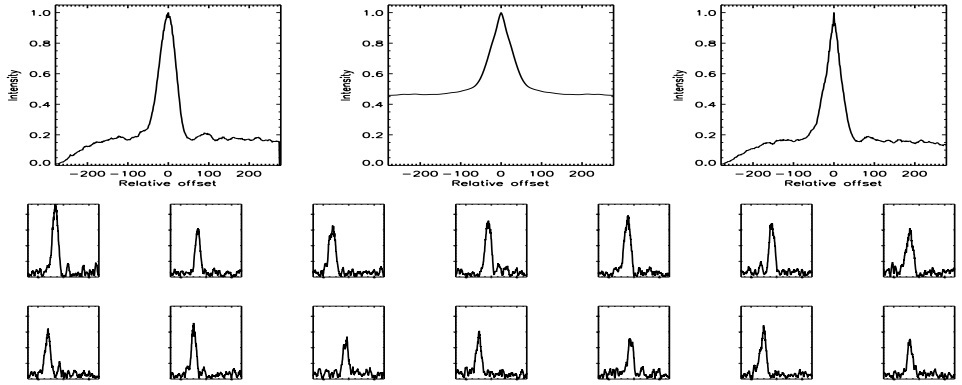

FIGURE B.468: SFP inspection for HD 160346 with S1-W1 on UT 2007/07/22, seq 001

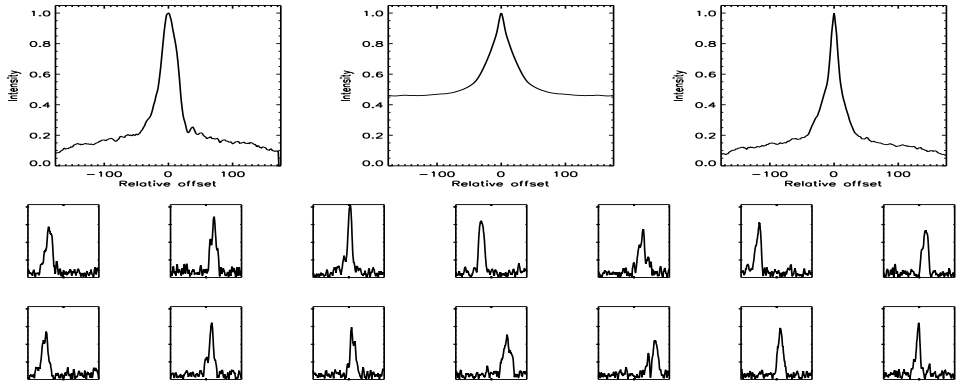

FIGURE B.469: SFP inspection for HD 161198 with S1-E1 on UT 2008/04/25, seq 001

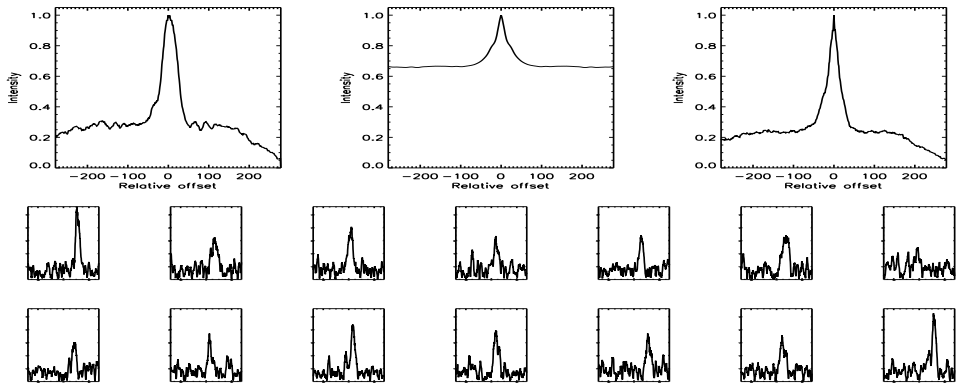

FIGURE B.470: SFP inspection for HD 161198 with S1-W1 on UT 2007/05/30, seq 001

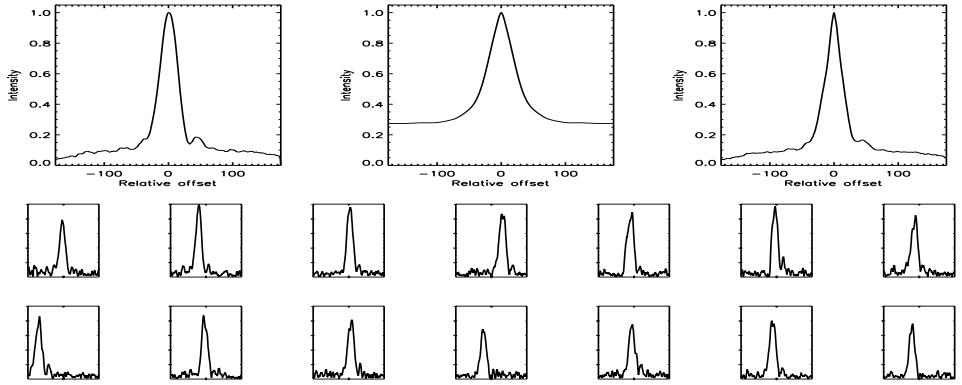

FIGURE B.471: SFP inspection for HD 161198 with S1-W1 on UT 2008/04/13, seq 001

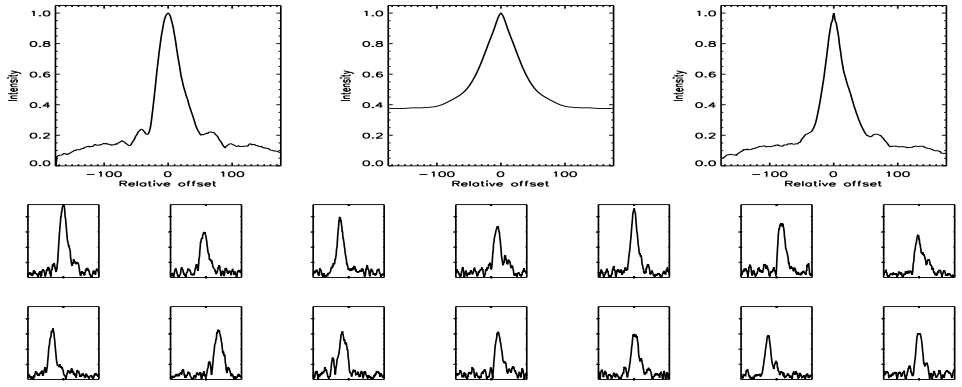

FIGURE B.472: SFP inspection for HD 161198 with S1-W1 on UT 2008/04/14, seq 001

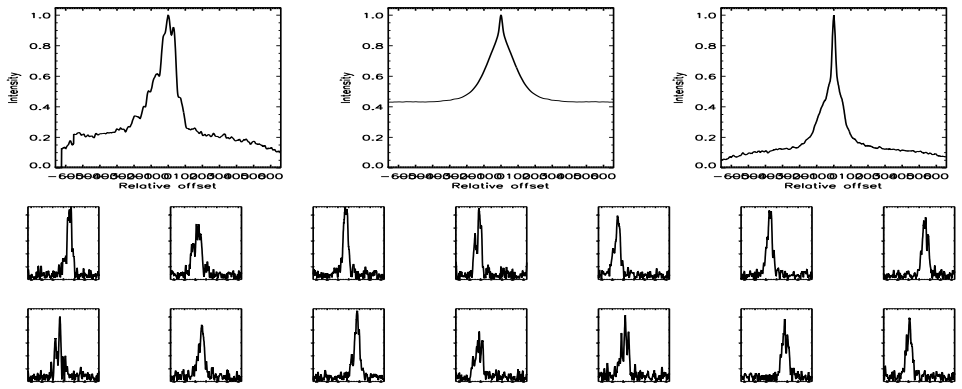

FIGURE B.473: SFP inspection for HD 161198 with S2-W1 on UT 2007/09/17, seq 001

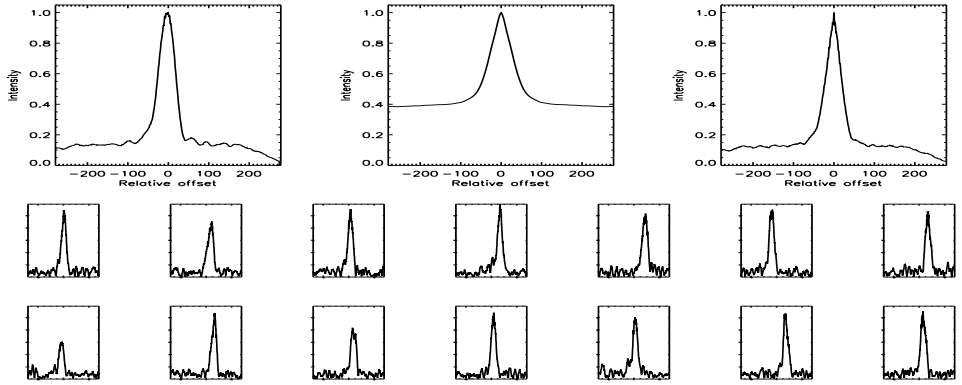

FIGURE B.474: SFP inspection for HD 164922 with S1-E1 on UT 2007/05/17, seq 001

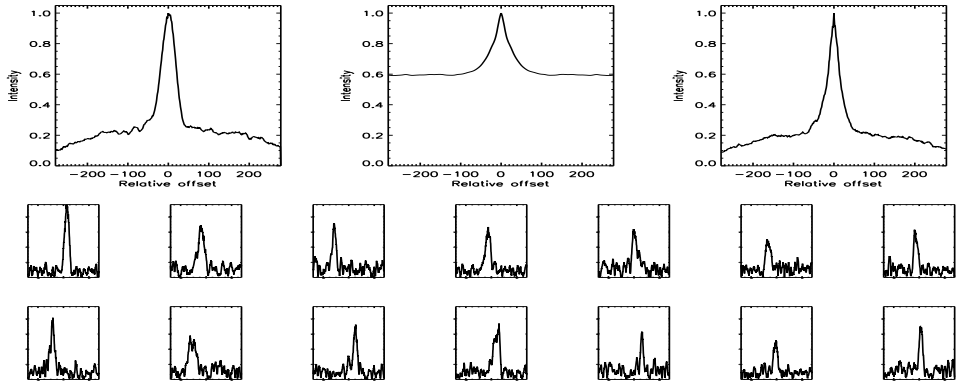

FIGURE B.475: SFP inspection for HD 164922 with S1-E2 on UT 2007/05/31, seq 001

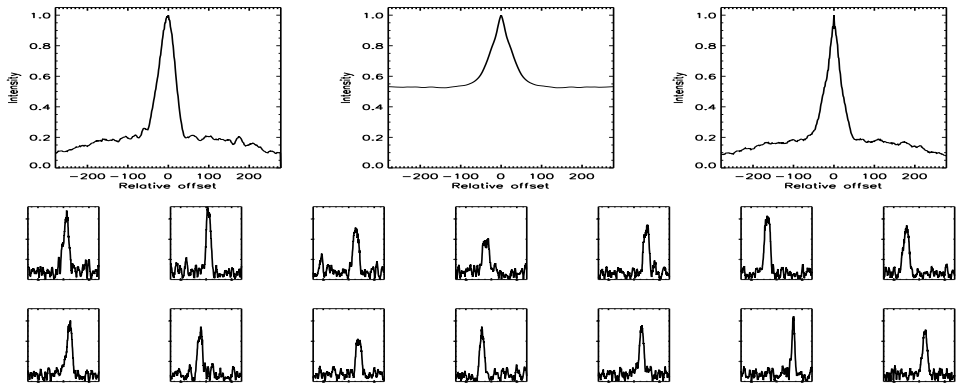

FIGURE B.476: SFP inspection for HD 165401 with S1-E1 on UT 2007/07/22, seq 002

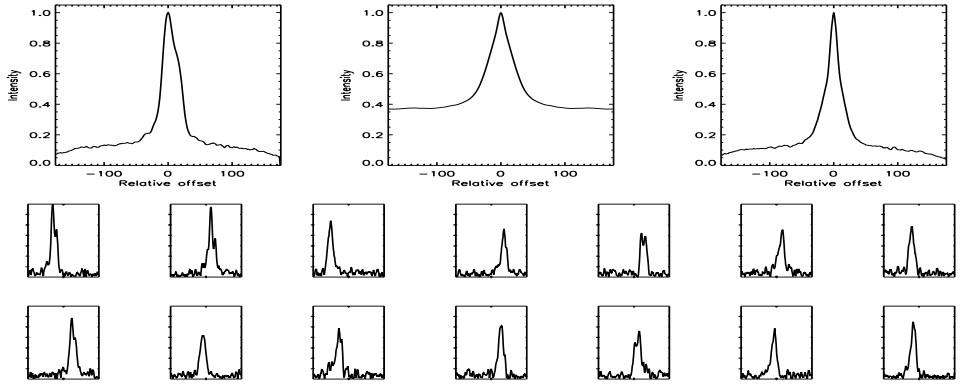

FIGURE B.477: SFP inspection for HD 165401 with S1-E1 on UT 2008/04/25, seq 001

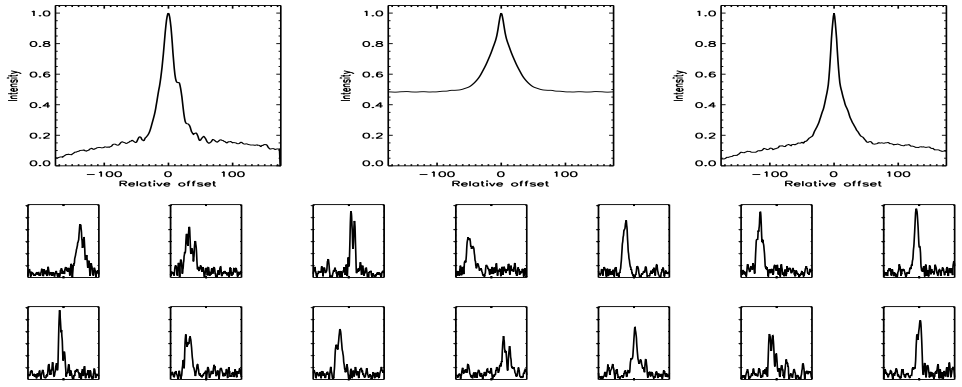

FIGURE B.478: SFP inspection for HD 165401 with S1-E1 on UT 2008/06/21, seq 001

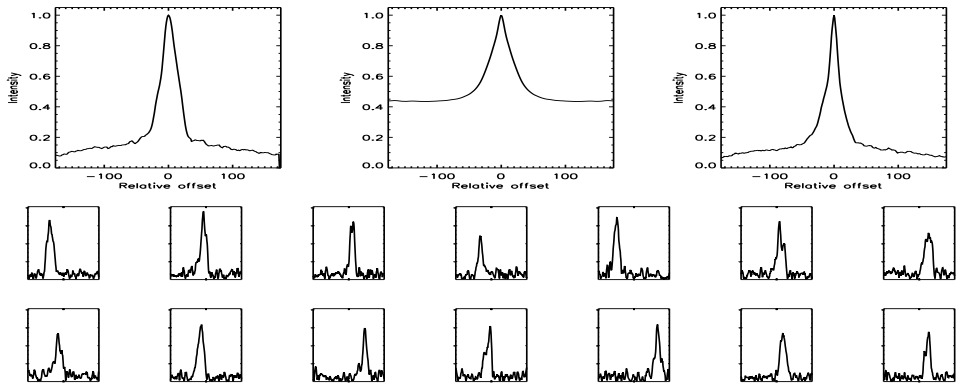

FIGURE B.479: SFP inspection for HD 165401 with S1-E1 on UT 2008/06/23, seq 001

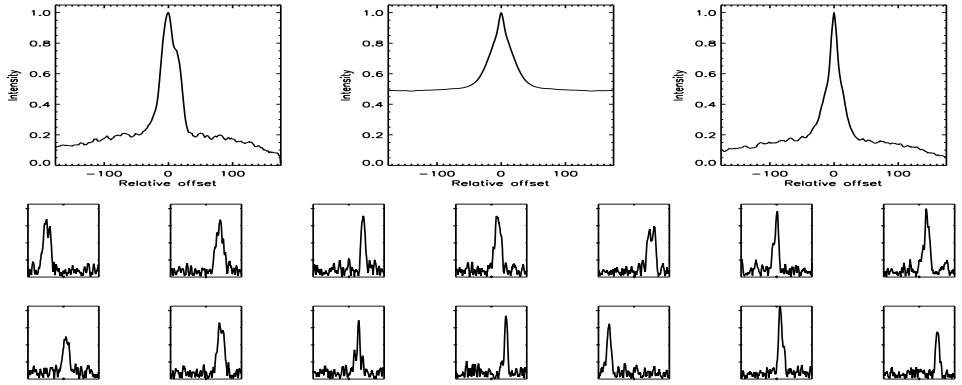

FIGURE B.480: SFP inspection for HD 165401 with S1-E1 on UT 2008/07/05, seq 001

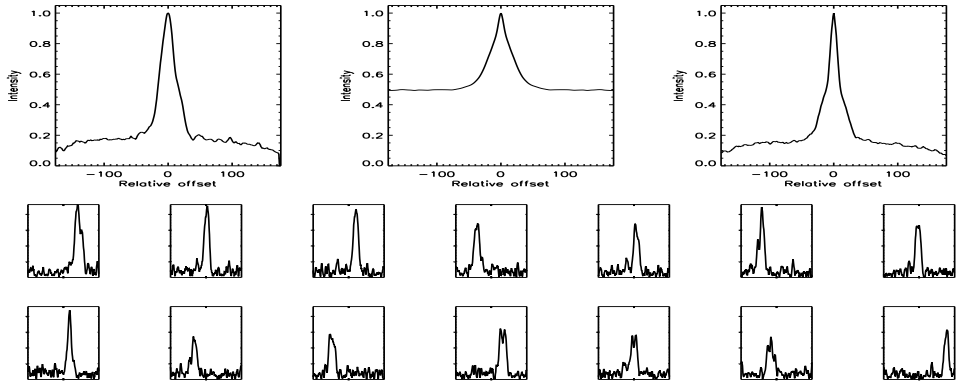

FIGURE B.481: SFP inspection for HD 165401 with S1-E1 on UT 2008/07/05, seq 002

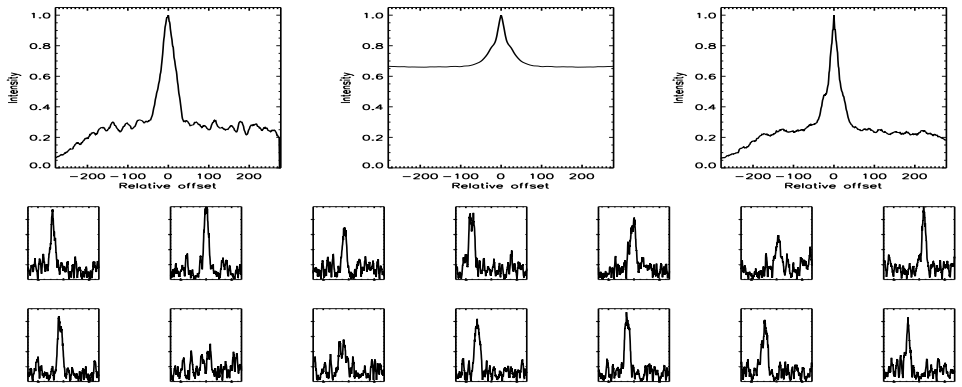

FIGURE B.482: SFP inspection for HD 165401 with S1-W1 on UT 2007/07/22, seq 001

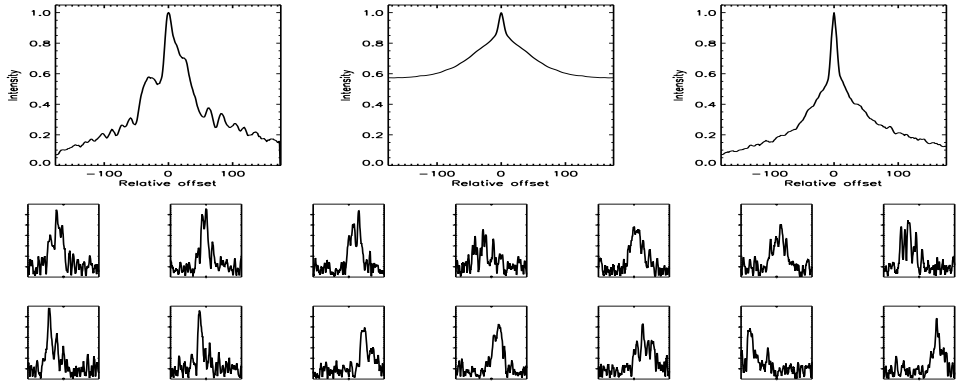

FIGURE B.483: SFP inspection for HD 165401 with S1-W1 on UT 2008/06/22, seq 001

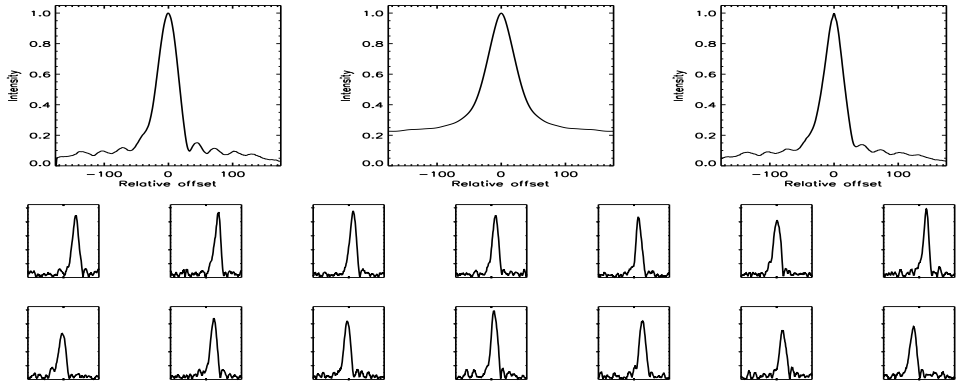

FIGURE B.484: SFP inspection for HD 165401 with S1-W1 on UT 2008/07/07, seq 001

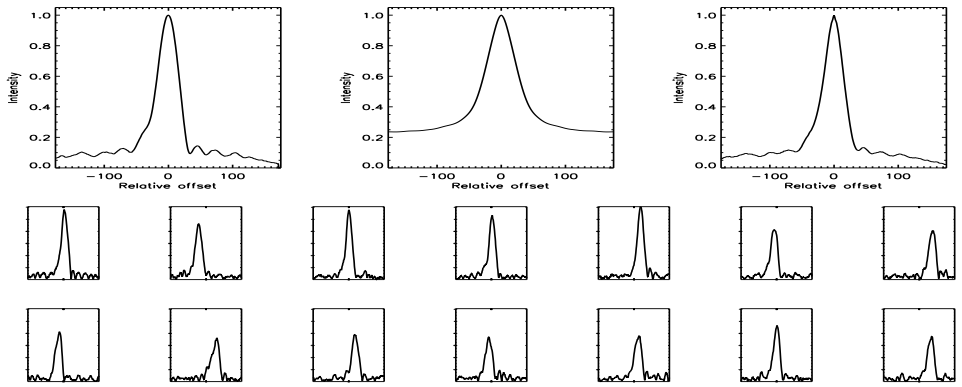

FIGURE B.485: SFP inspection for HD 165401 with S1-W1 on UT 2008/07/07, seq 002

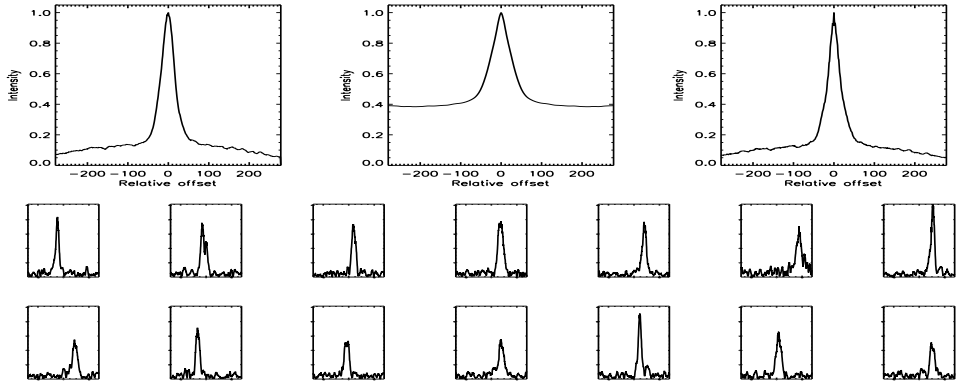

FIGURE B.486: SFP inspection for HD 166620 with E1-W1 on UT 2007/04/26, seq 001

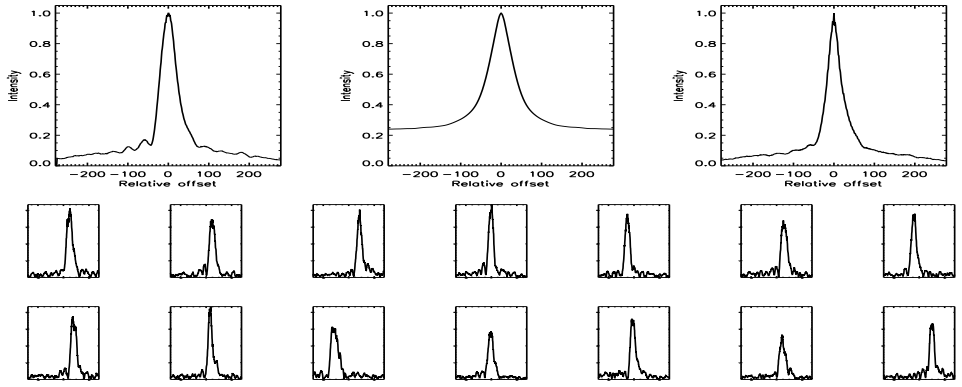

FIGURE B.487: SFP inspection for HD 166620 with S1-E1 on UT 2007/04/14, seq 001

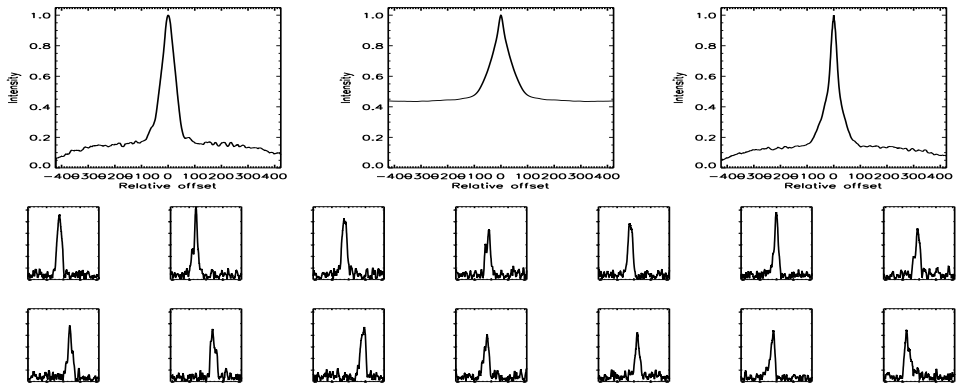

FIGURE B.488: SFP inspection for HD 166620 with S2-E2 on UT 2007/09/18, seq 001

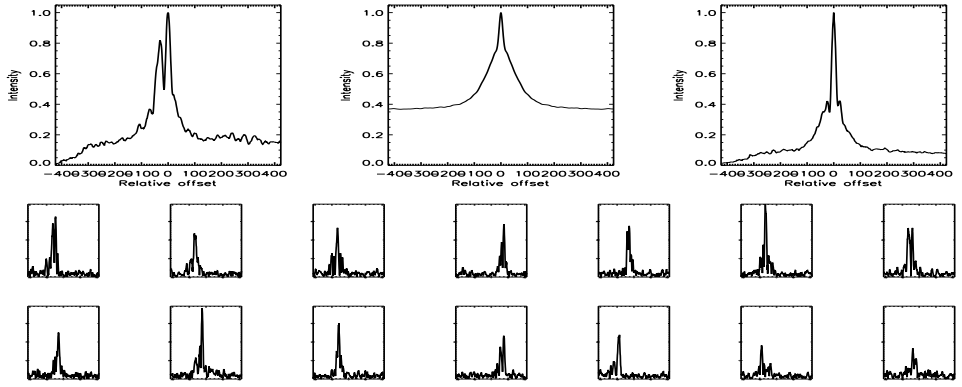

FIGURE B.489: SFP inspection for HD 166620 with S2-W1 on UT 2007/09/17, seq 001

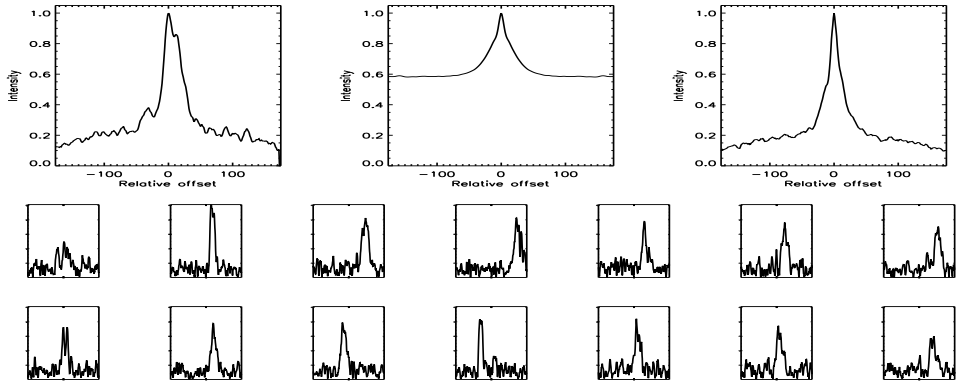

FIGURE B.490: SFP inspection for HD 175742 with S1-E1 on UT 2008/06/21, seq 001

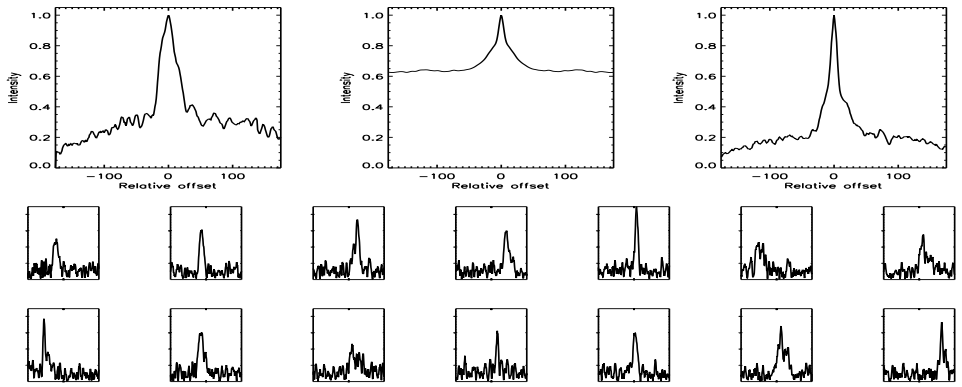

FIGURE B.491: SFP inspection for HD 175742 with S1-E1 on UT 2008/06/23, seq 001

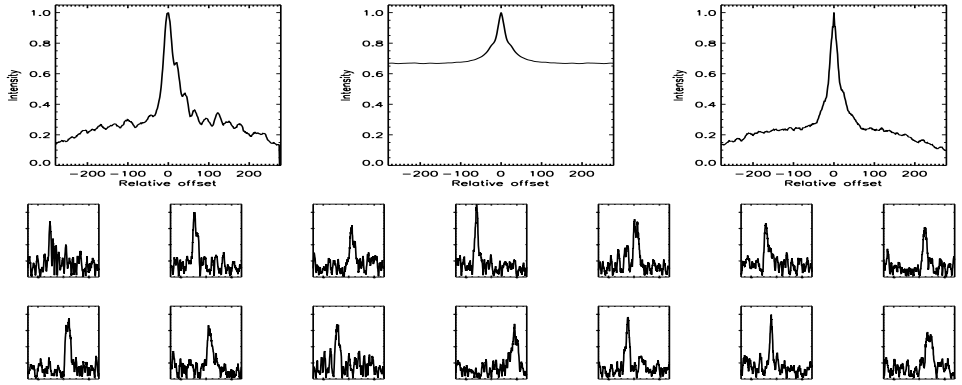

FIGURE B.492: SFP inspection for HD 175742 with S1-E2 on UT 2007/05/29, seq 001

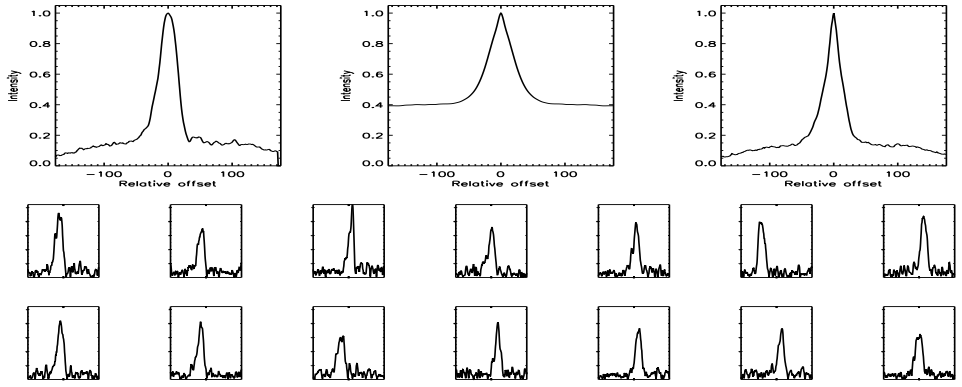

FIGURE B.493: SFP inspection for HD 175742 with S1-W1 on UT 2008/04/13, seq 001

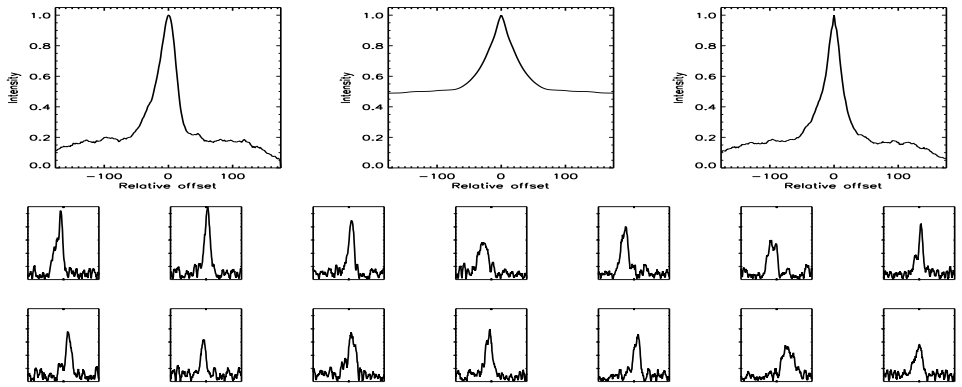

FIGURE B.494: SFP inspection for HD 175742 with S1-W1 on UT 2008/04/14, seq 001

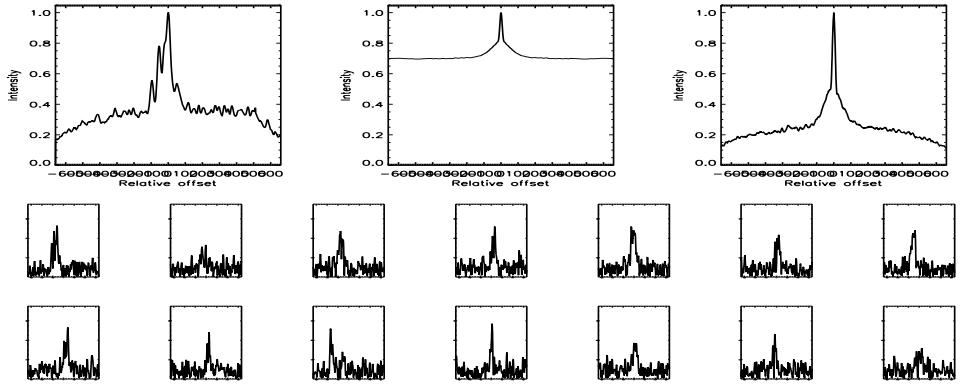

FIGURE B.495: SFP inspection for HD 175742 with S2-E2 on UT 2007/09/18, seq 003

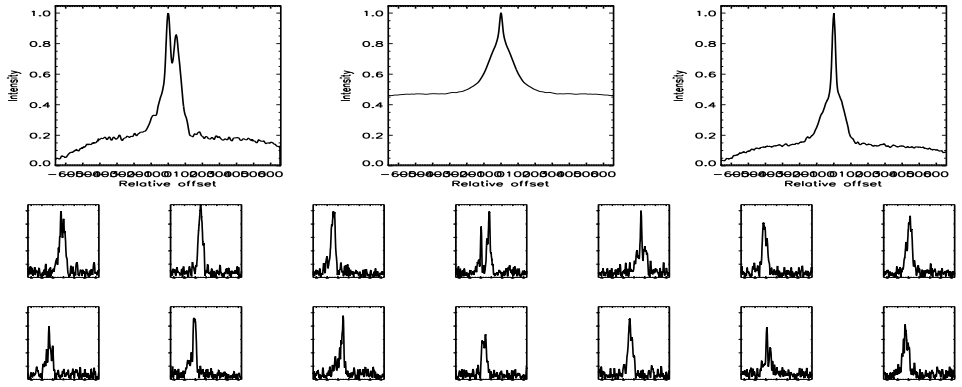

FIGURE B.496: SFP inspection for HD 175742 with S2-W1 on UT 2007/09/17, seq 001

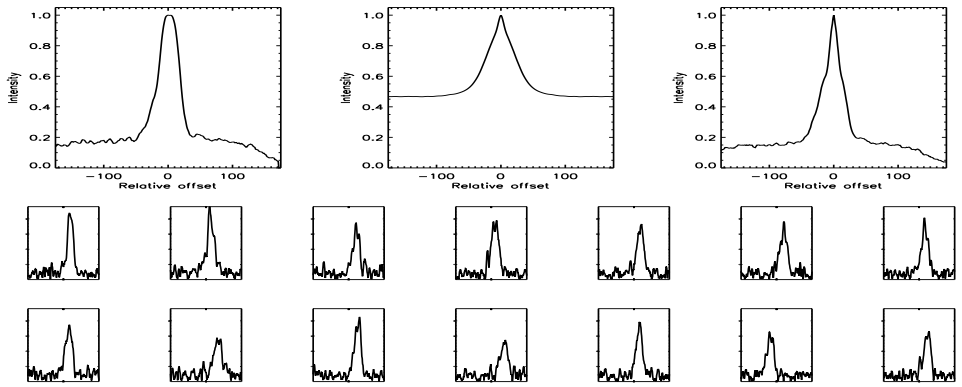

FIGURE B.497: SFP inspection for HD 175742 with S2-W1 on UT 2008/06/24, seq 001

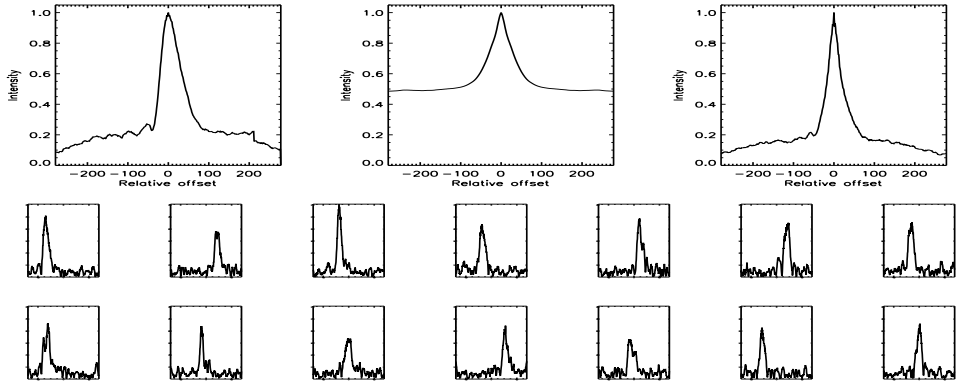

FIGURE B.498: SFP inspection for HD 176377 with S1-E1 on UT 2007/04/14, seq 001

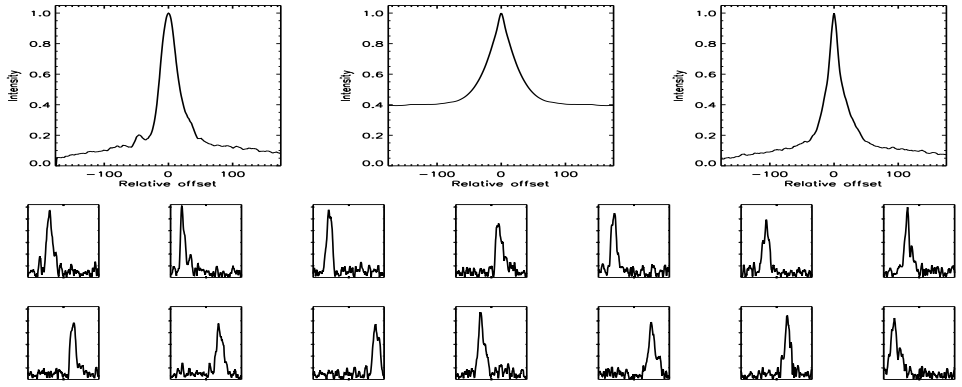

FIGURE B.499: SFP inspection for HD 176377 with S1-E1 on UT 2008/06/21, seq 001

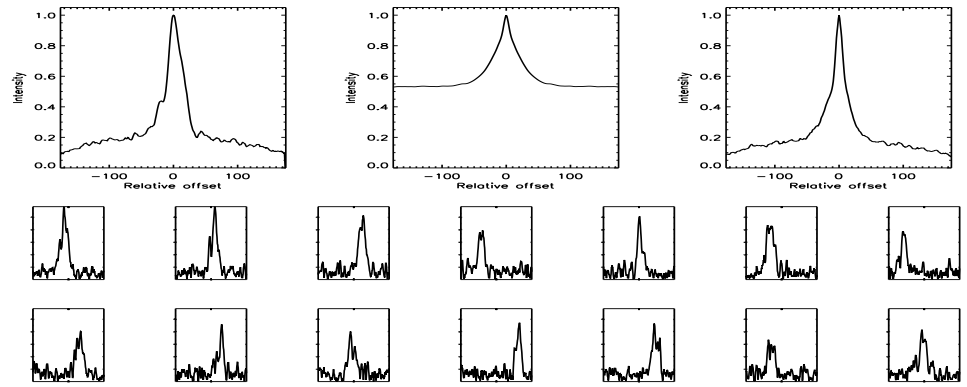

FIGURE B.500: SFP inspection for HD 176377 with S1-E1 on UT 2008/06/23, seq 001

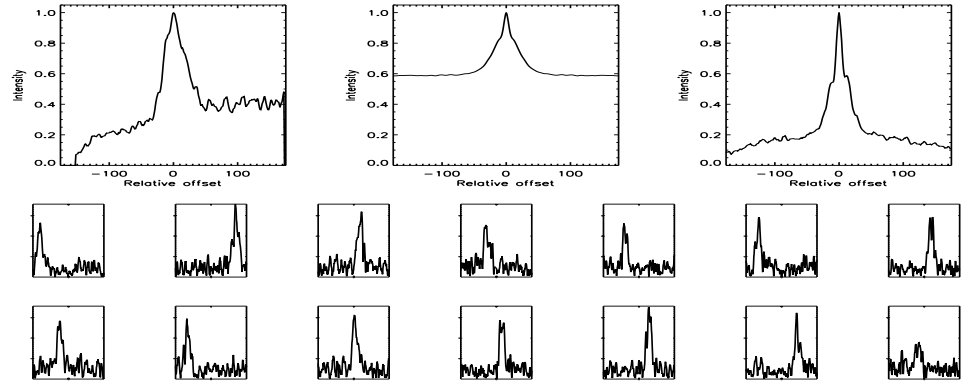

FIGURE B.501: SFP inspection for HD 176377 with S1-E1 on UT 2008/06/26, seq 001

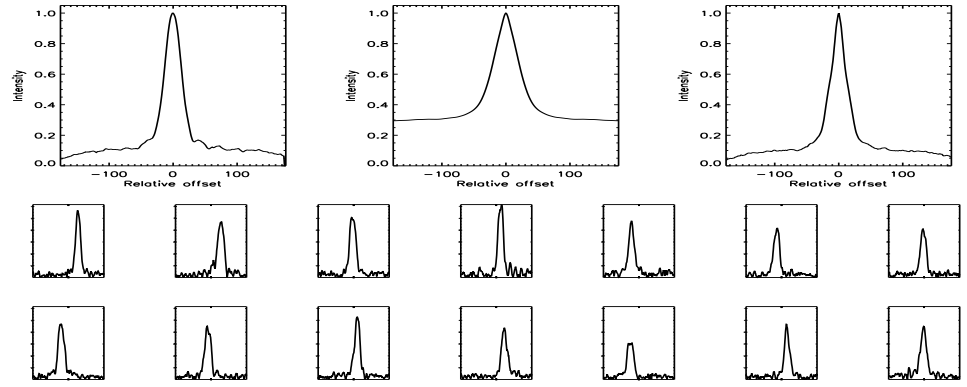

FIGURE B.502: SFP inspection for HD 176377 with S1-W1 on UT 2008/04/13, seq 001

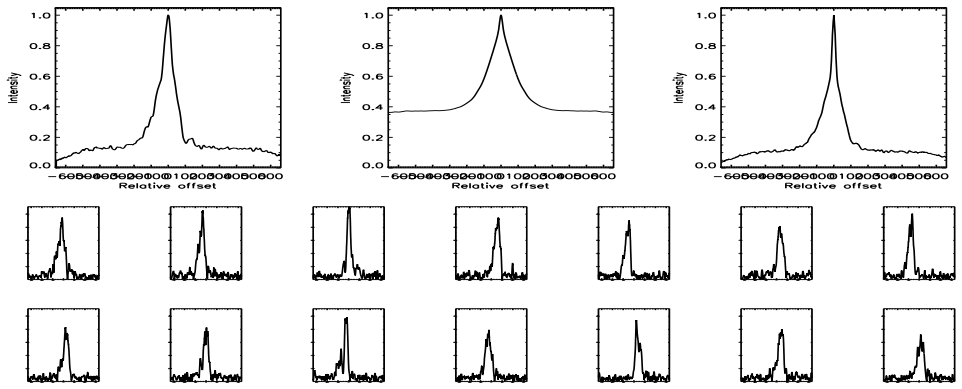

FIGURE B.503: SFP inspection for HD 176377 with S2-W1 on UT 2007/09/17, seq 001

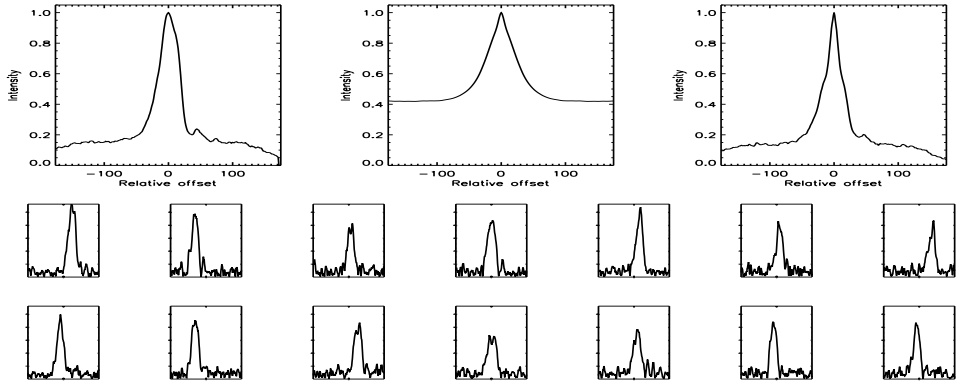

FIGURE B.504: SFP inspection for HD 176377 with S2-W1 on UT 2008/06/24, seq 001

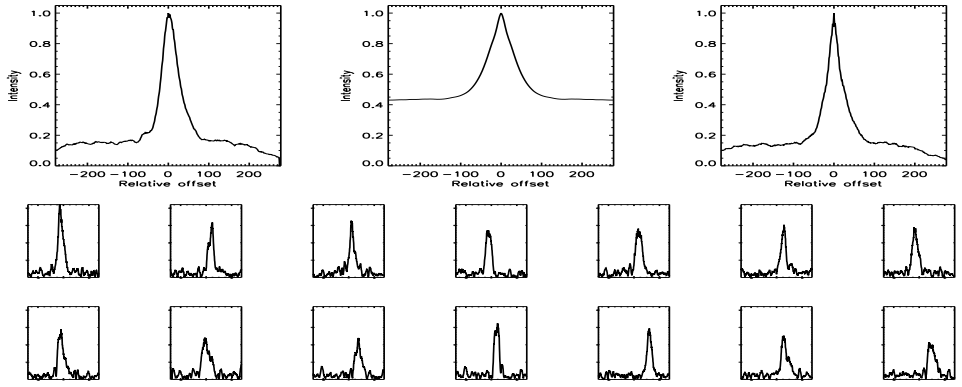

FIGURE B.505: SFP inspection for HD 178428 with S1-E2 on UT 2007/05/29, seq 001

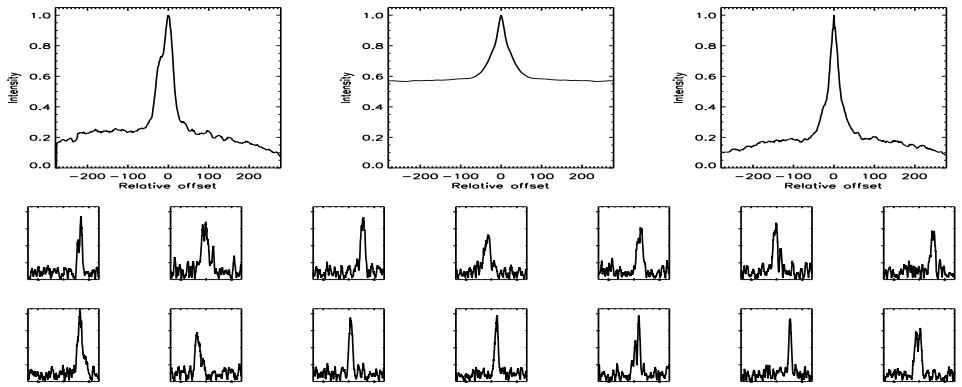

FIGURE B.506: SFP inspection for HD 178428 with S1-E2 on UT 2007/06/01, seq 001

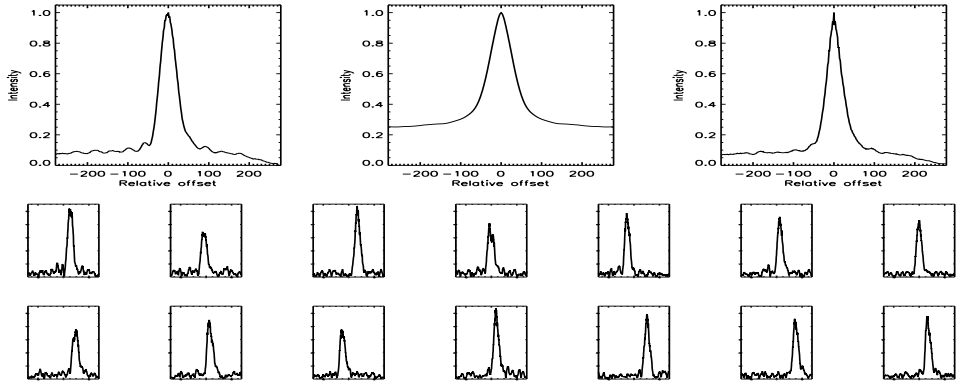

FIGURE B.507: SFP inspection for HD 178428 with S1-W1 on UT 2007/05/30, seq 001

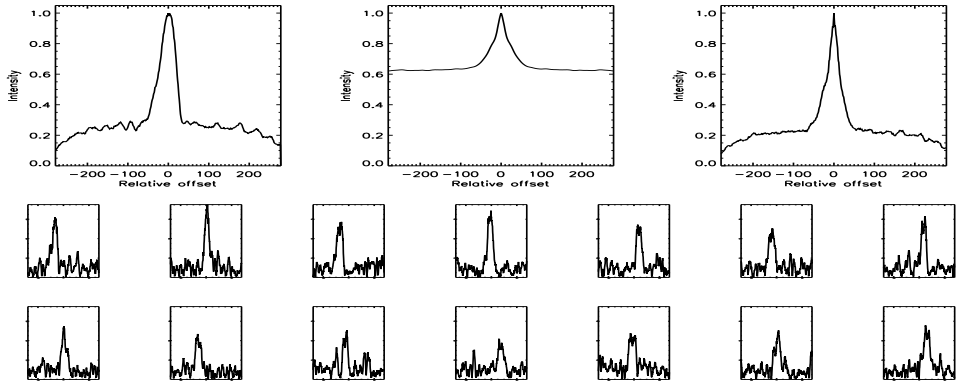

FIGURE B.508: SFP inspection for HD 179957 with S1-E1 on UT 2007/07/25, seq 002

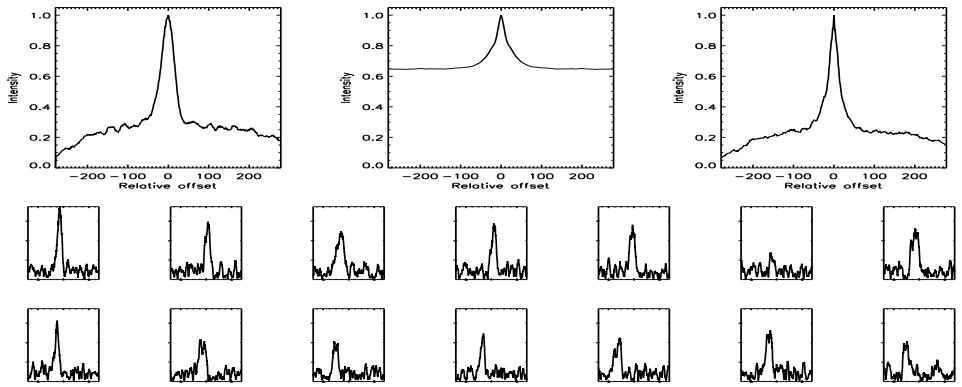

FIGURE B.509: SFP inspection for HD 179957 with S1-W1 on UT 2007/05/30, seq 001

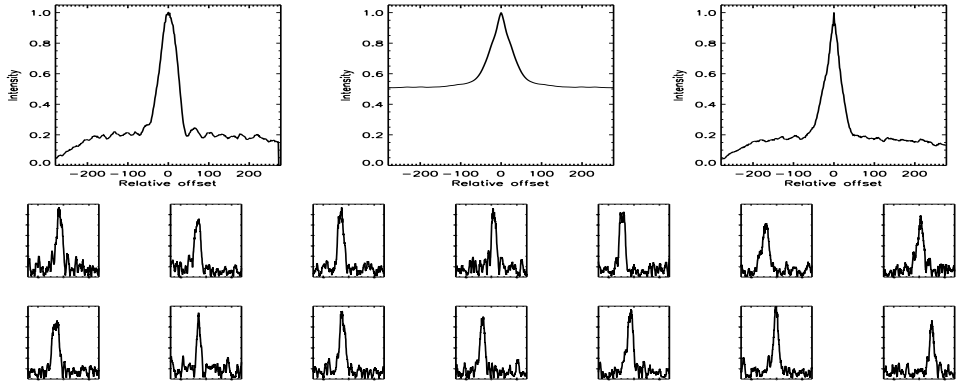

FIGURE B.510: SFP inspection for HD 179957 with S1-W1 on UT 2007/08/18, seq 001

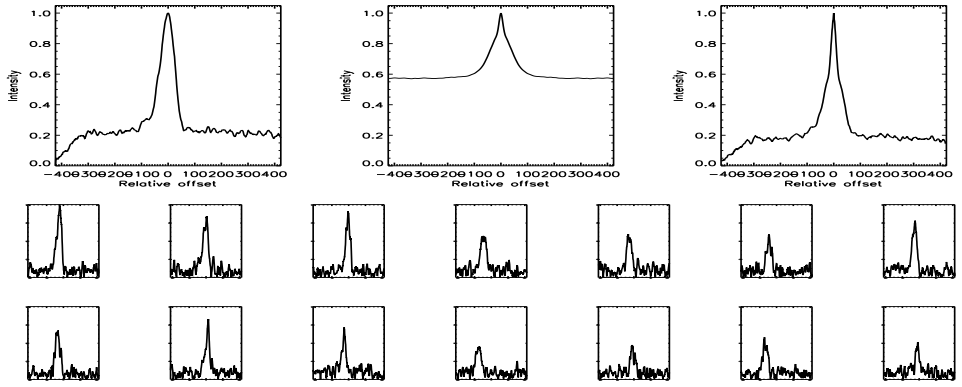

FIGURE B.511: SFP inspection for HD 179957 with S1-W1 on UT 2007/08/21, seq 002

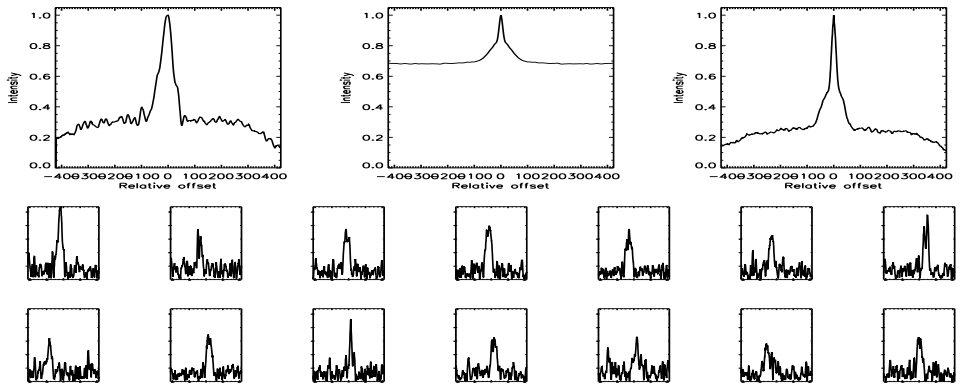

FIGURE B.512: SFP inspection for HD 179957 with S2-E1 on UT 2007/08/20, seq 001

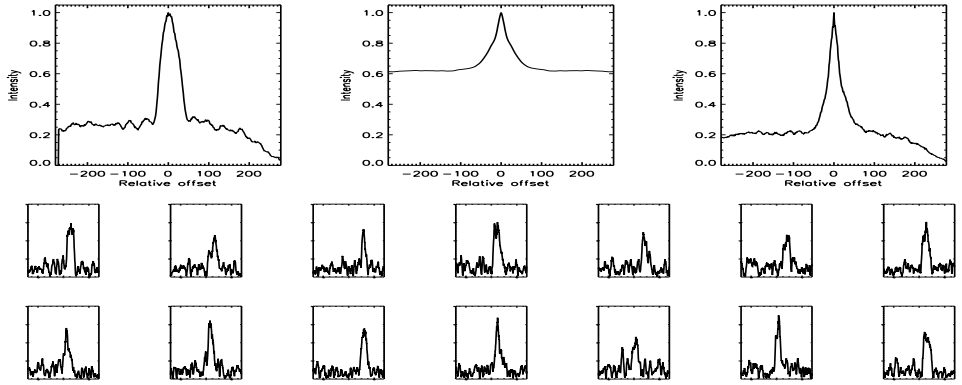

FIGURE B.513: SFP inspection for HD 179958 with S1-W1 on UT 2007/05/30, seq 002

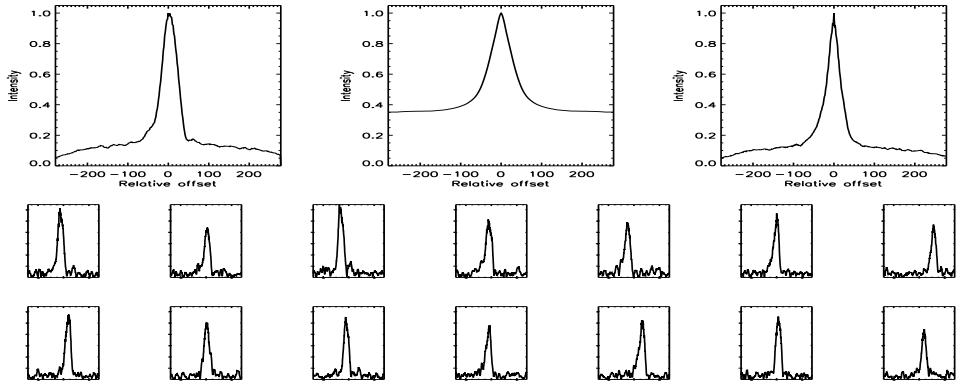

FIGURE B.514: SFP inspection for HD 180161 with S1-E1 on UT 2007/04/14, seq 001

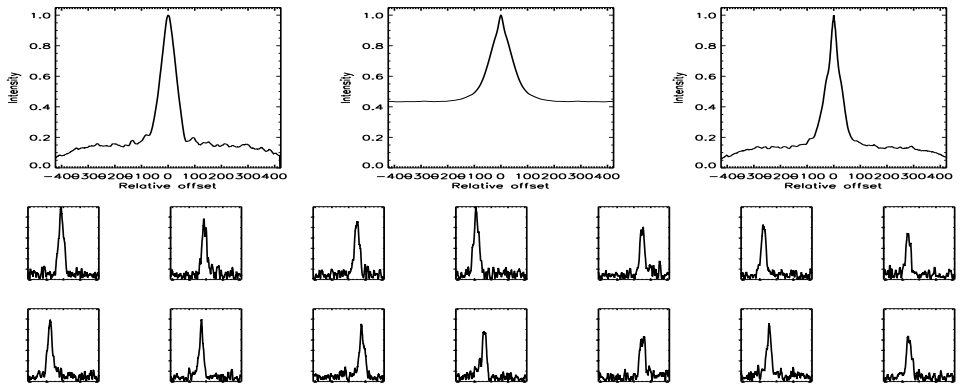

FIGURE B.515: SFP inspection for HD 180161 with S1-E1 on UT 2007/09/16, seq 002

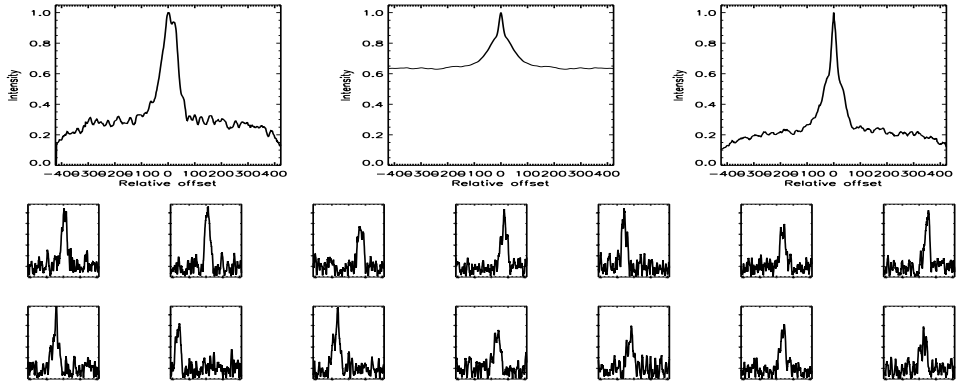

FIGURE B.516: SFP inspection for HD 180161 with S1-W1 on UT 2007/08/21, seq 001

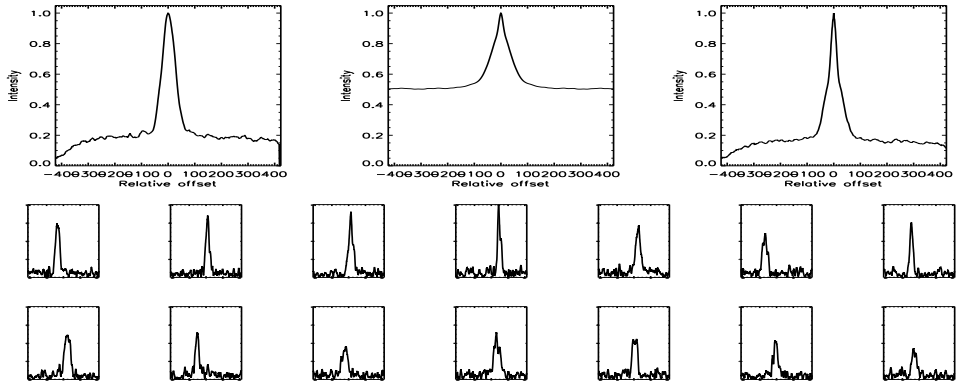

FIGURE B.517: SFP inspection for HD 180161 with S1-W1 on UT 2007/09/16, seq 001

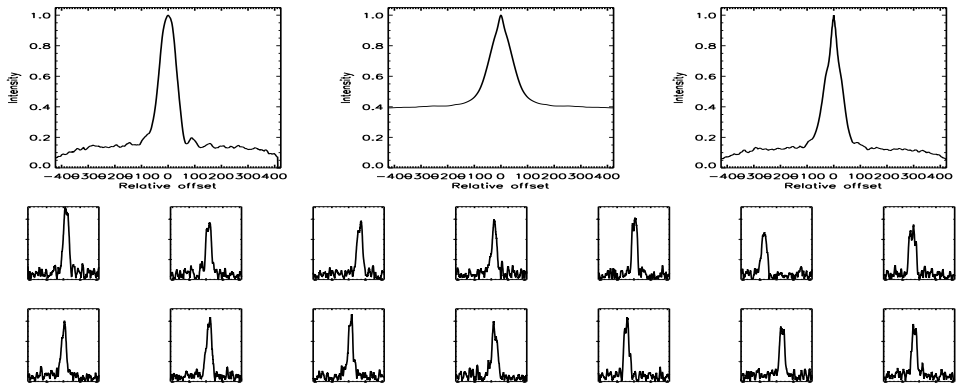

FIGURE B.518: SFP inspection for HD 180161 with S2-E1 on UT 2007/08/20, seq 001

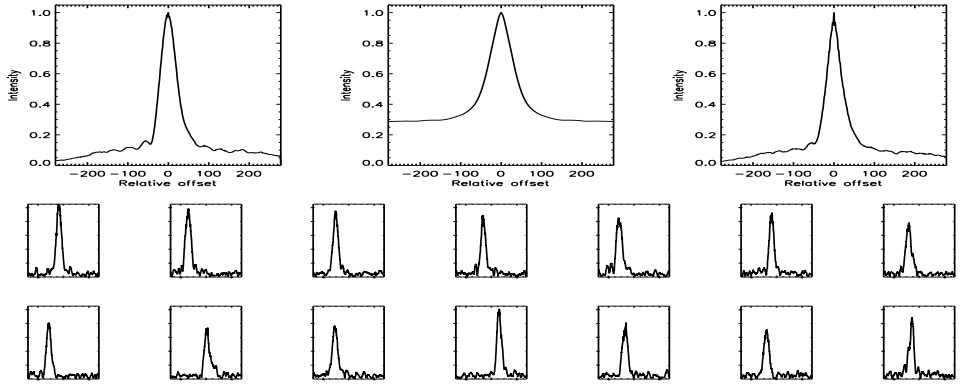

FIGURE B.519: SFP inspection for HD 182488 with S1-E1 on UT 2007/04/14, seq 001

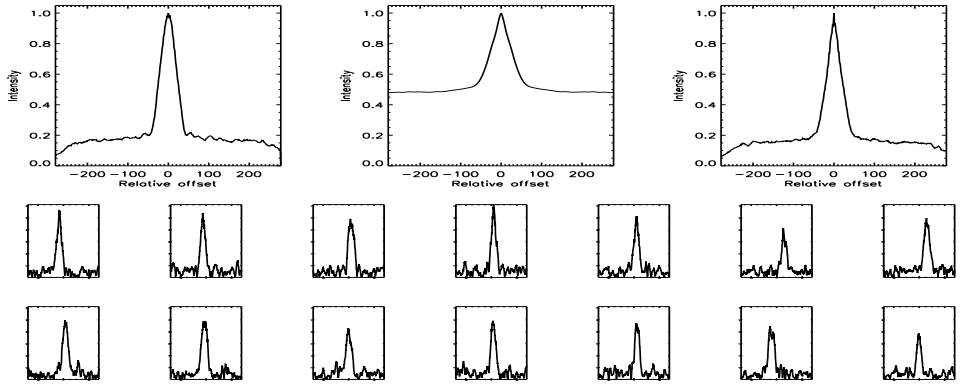

FIGURE B.520: SFP inspection for HD 182488 with S1-W1 on UT 2007/08/18, seq 001

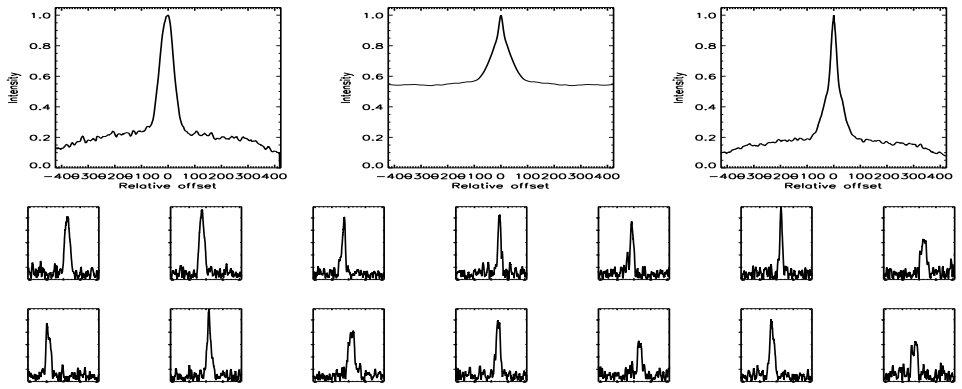

FIGURE B.521: SFP inspection for HD 182488 with S2-E2 on UT 2007/09/18, seq 001

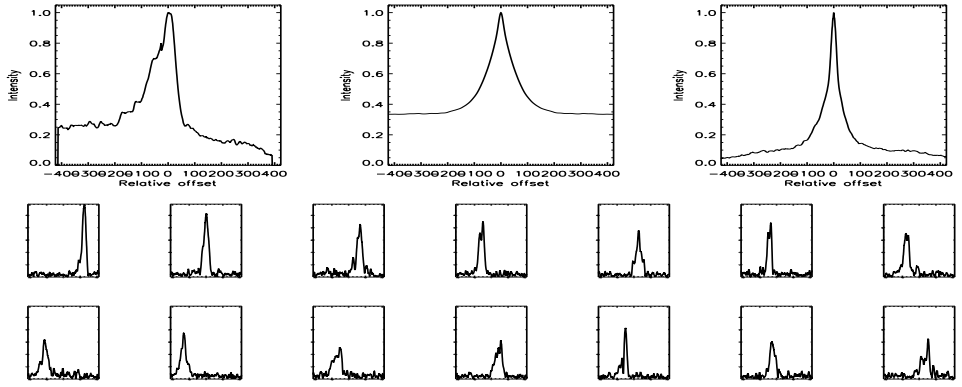

FIGURE B.522: SFP inspection for HD 182488 with S2-W1 on UT 2007/09/17, seq 001

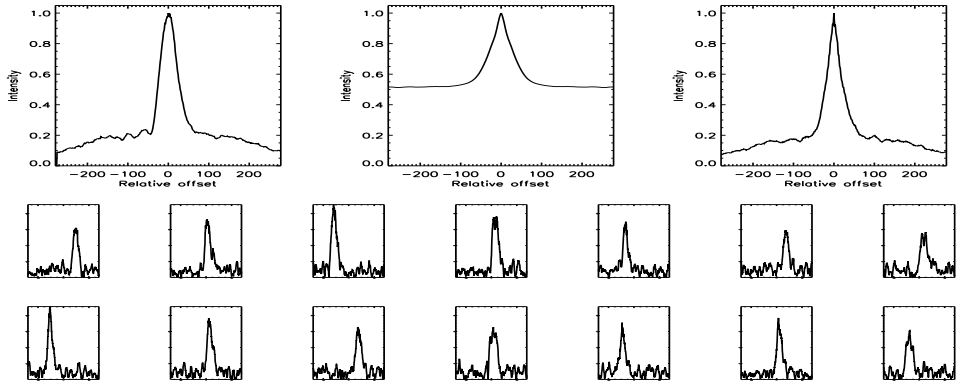

FIGURE B.523: SFP inspection for HD 184385 with S1-E2 on UT 2007/05/29, seq 001

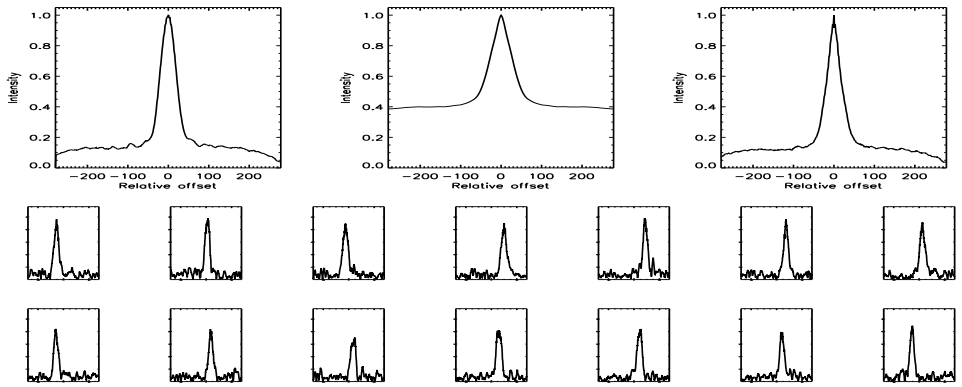

FIGURE B.524: SFP inspection for HD 184385 with S1-W1 on UT 2007/05/30, seq 001

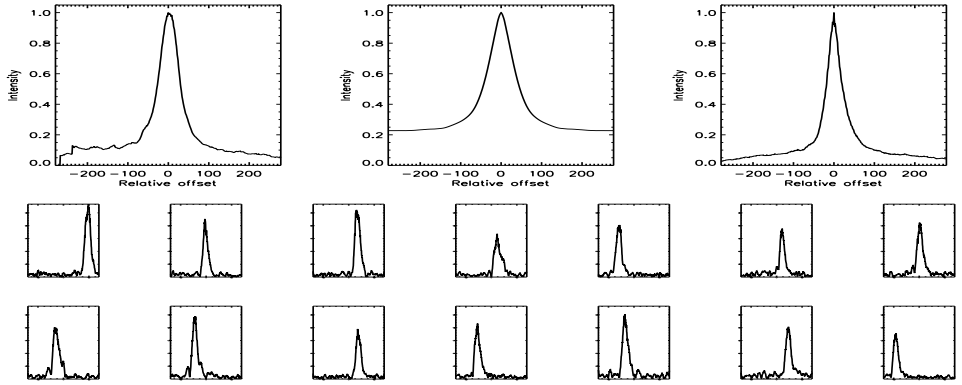

FIGURE B.525: SFP inspection for HD 185144 with E1-W1 on UT 2007/04/26, seq 001

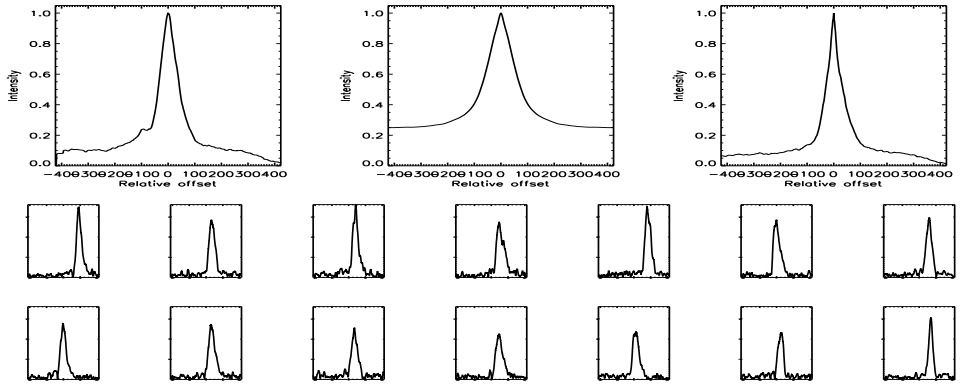

FIGURE B.526: SFP inspection for HD 185144 with S1-E1 on UT 2007/07/28, seq 001

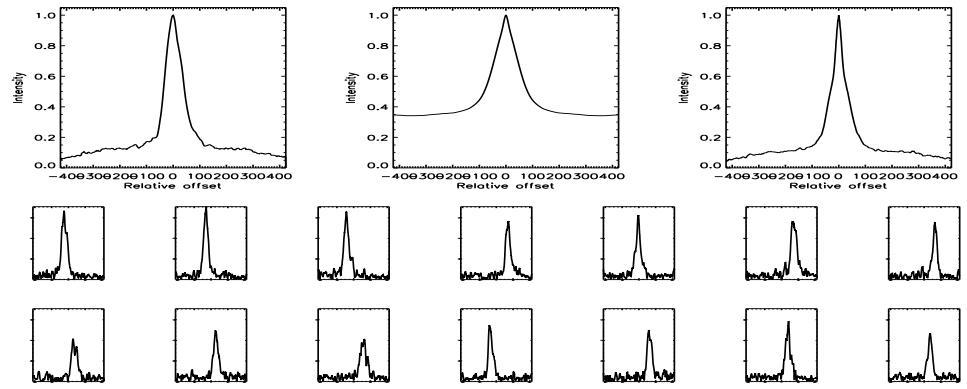

FIGURE B.527: SFP inspection for HD 185144 with S1-E1 on UT 2007/09/16, seq 002

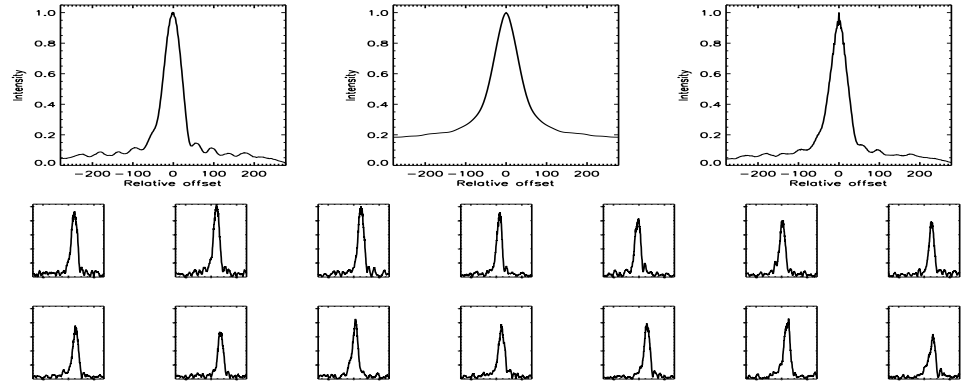

FIGURE B.528: SFP inspection for HD 185144 with S1-W1 on UT 2007/05/28, seq 001

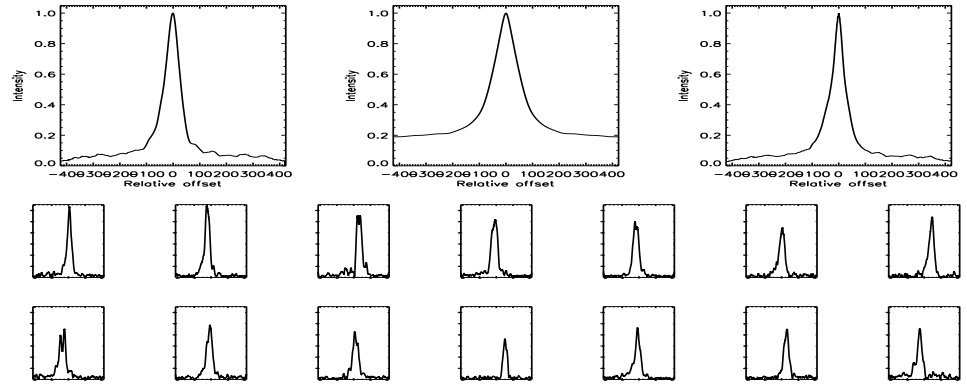

FIGURE B.529: SFP inspection for HD 185144 with S1-W1 on UT 2007/09/16, seq 001

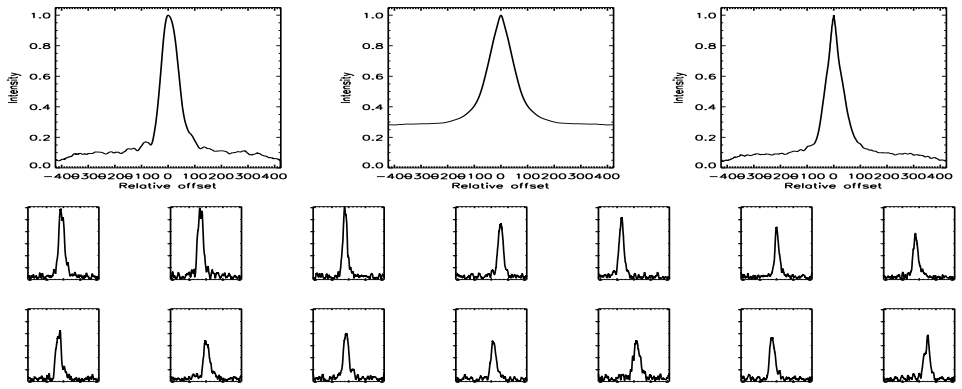

FIGURE B.530: SFP inspection for HD 185144 with S2-E1 on UT 2007/08/20, seq 001

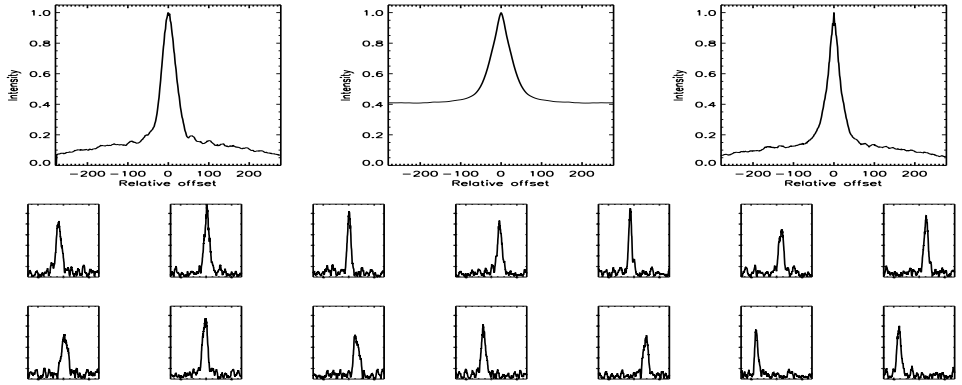

FIGURE B.531: SFP inspection for HD 185414 with S1-E1 on UT 2007/04/14, seq 001

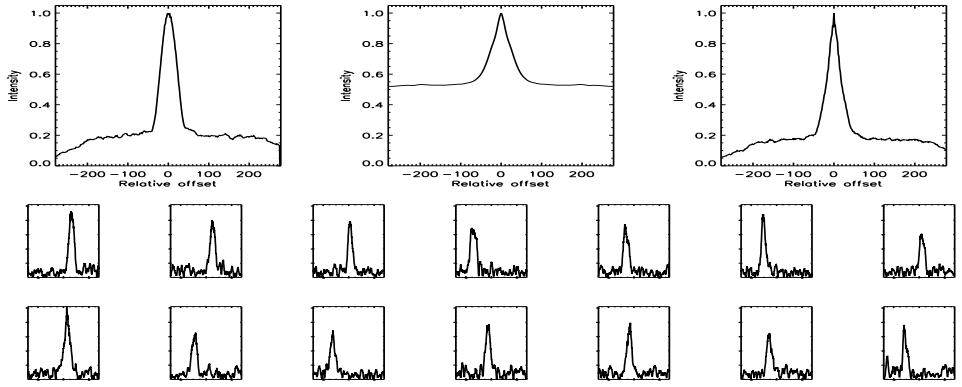

FIGURE B.532: SFP inspection for HD 185414 with S1-W1 on UT 2007/05/28, seq 001

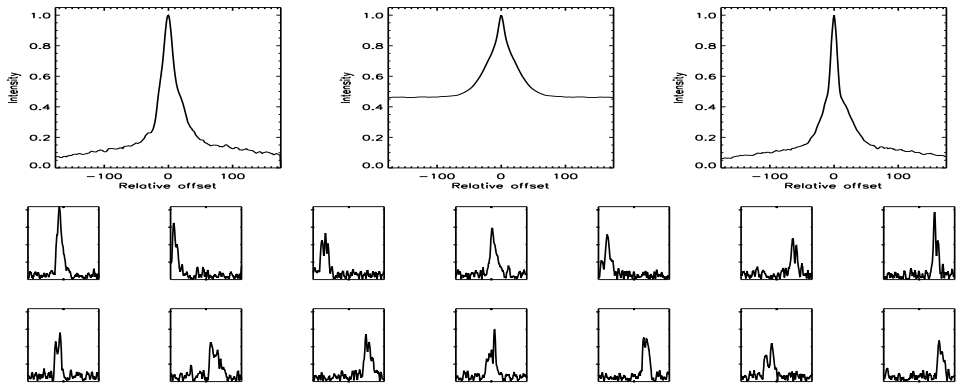

FIGURE B.533: SFP inspection for HD 189340 with S1-E1 on UT 2008/06/21, seq 001

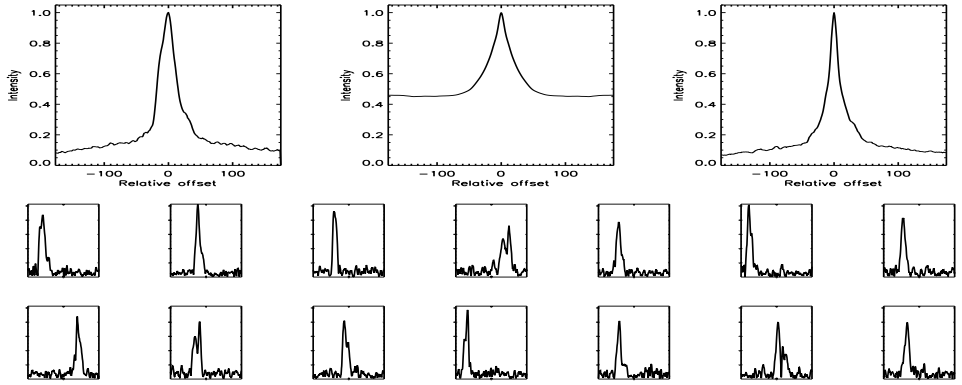

FIGURE B.534: SFP inspection for HD 189340 with S1-E1 on UT 2008/06/23, seq 001

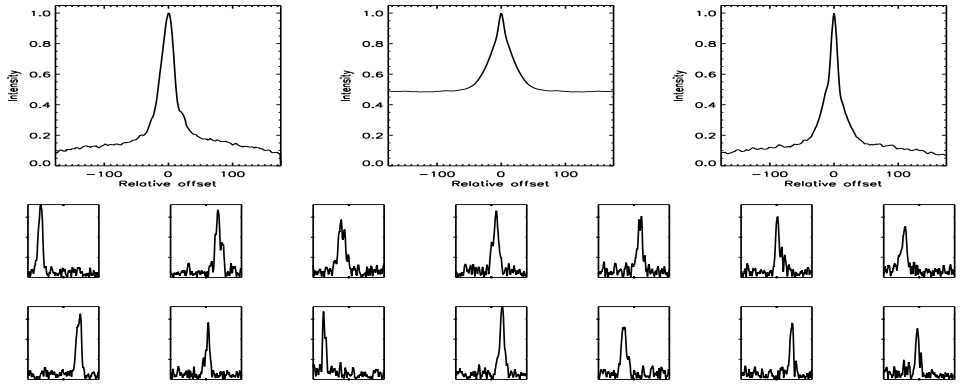

FIGURE B.535: SFP inspection for HD 189340 with S1-E1 on UT 2008/06/23, seq 002

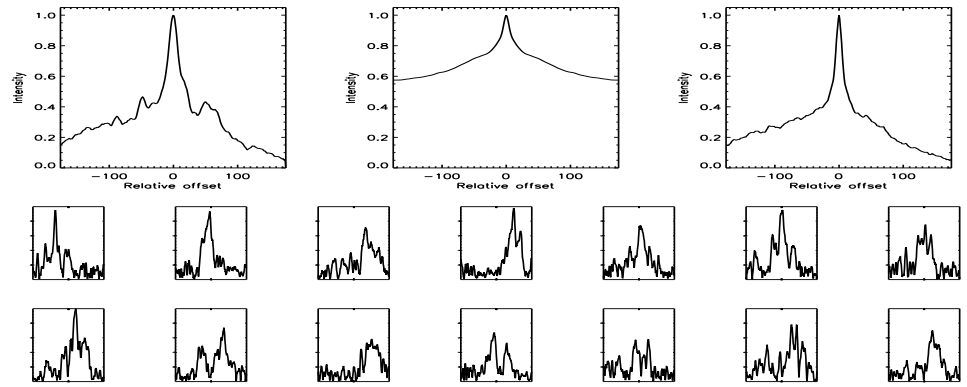

FIGURE B.536: SFP inspection for HD 189340 with S1-W1 on UT 2008/06/22, seq 001

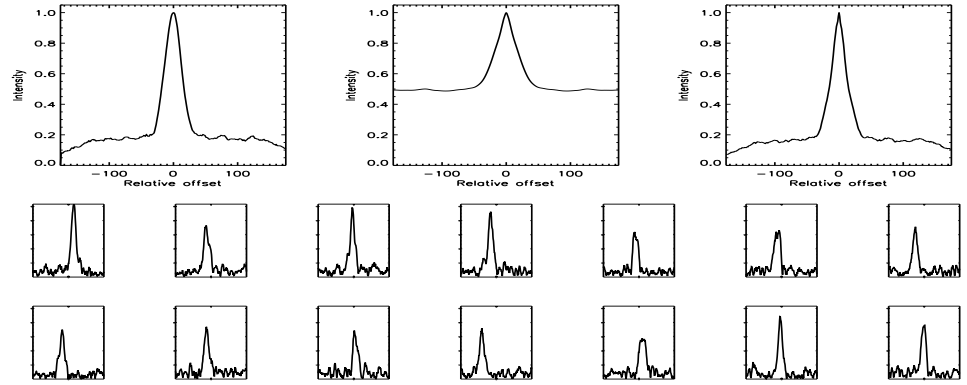

FIGURE B.537: SFP inspection for HD 189340 with S2-W2 on UT 2008/06/09, seq 001

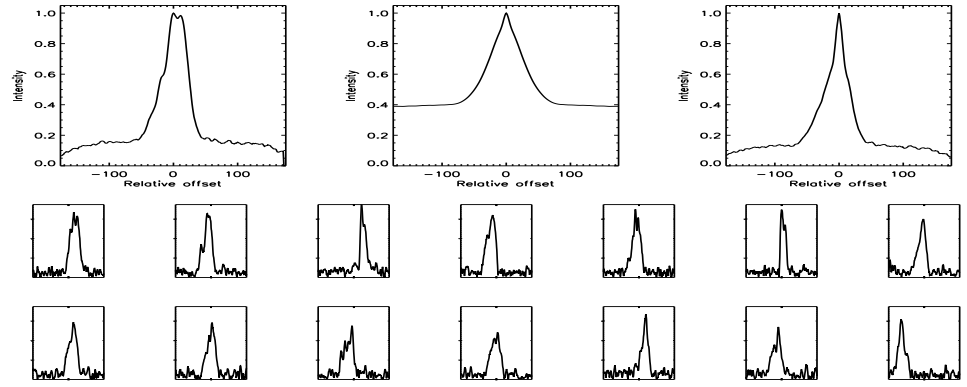

FIGURE B.538: SFP inspection for HD 189340 with S2-W2 on UT 2008/06/09, seq 002

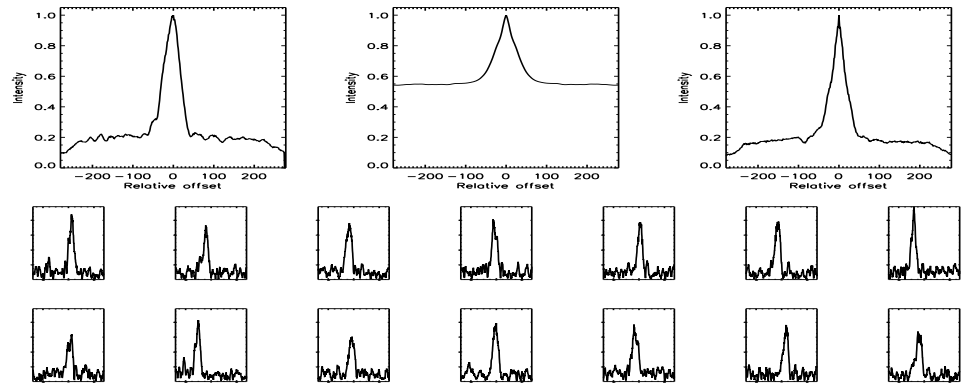

FIGURE B.539: SFP inspection for HD 189733 with S1-E1 on UT 2007/07/24, seq 001

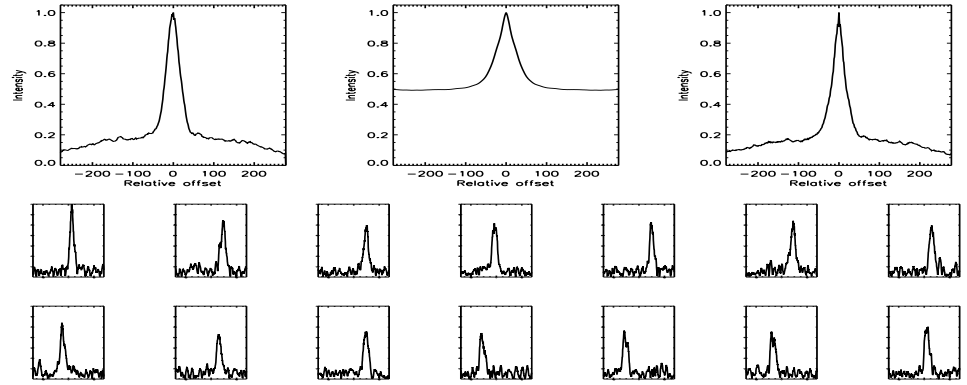

FIGURE B.540: SFP inspection for HD 189733 with S1-W1 on UT 2007/05/30, seq 001

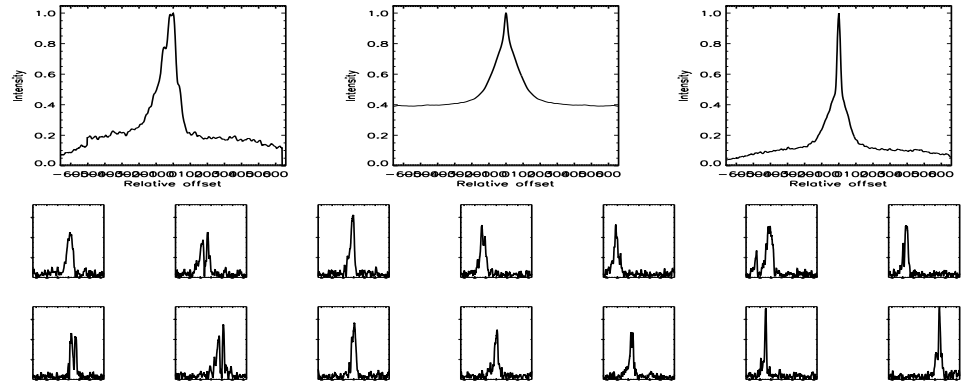

FIGURE B.541: SFP inspection for HD 189733 with S2-W1 on UT 2007/09/17, seq 001

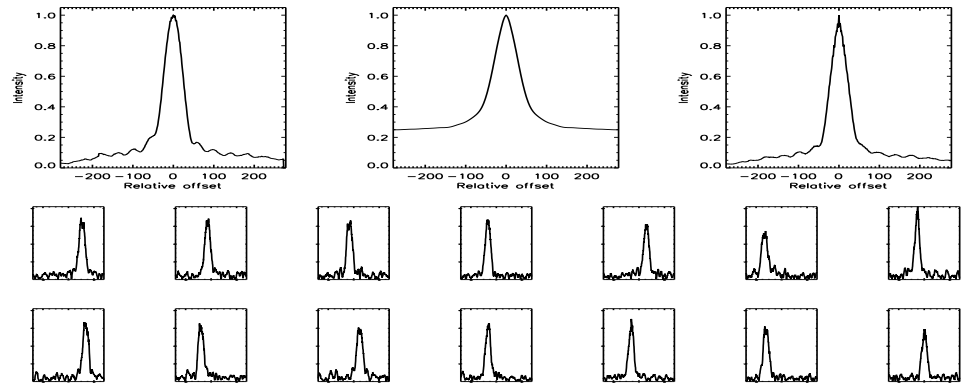

FIGURE B.542: SFP inspection for HD 190067 with S1-E1 on UT 2007/07/22, seq 002

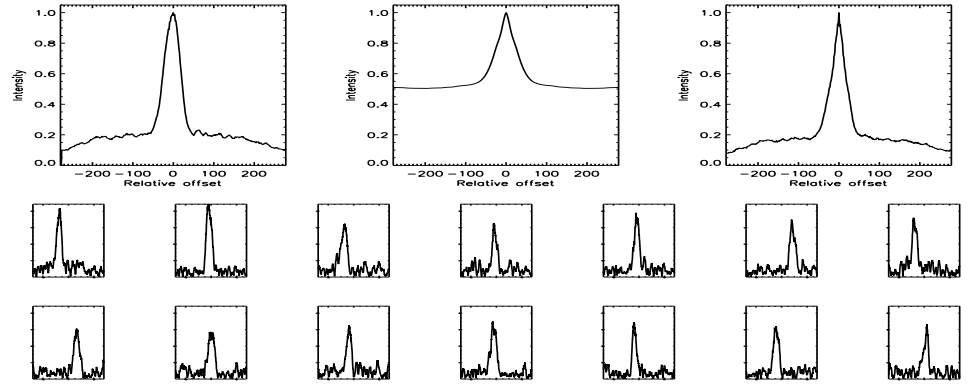

FIGURE B.543: SFP inspection for HD 190067 with S1-E1 on UT 2007/07/24, seq 003

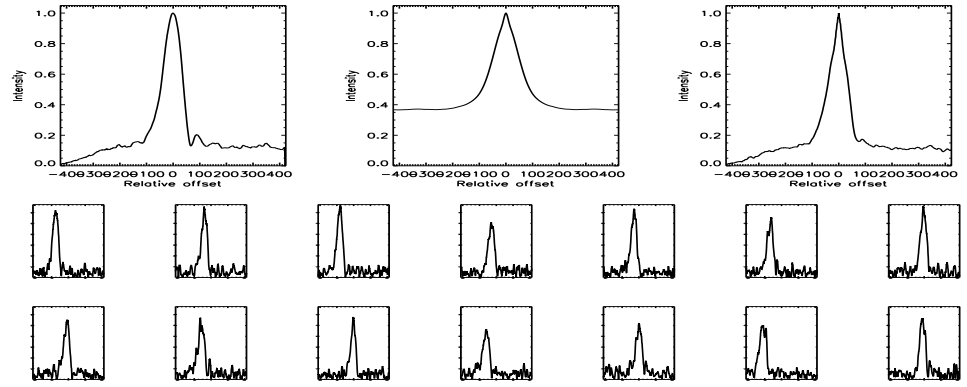

FIGURE B.544: SFP inspection for HD 190067 with S1-W1 on UT 2007/07/22, seq 001

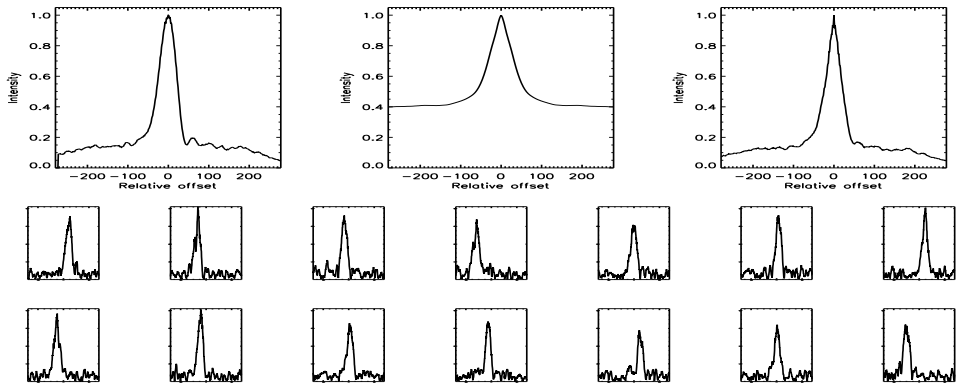

FIGURE B.545: SFP inspection for HD 190404 with S1-E1 on UT 2007/07/24, seq 001

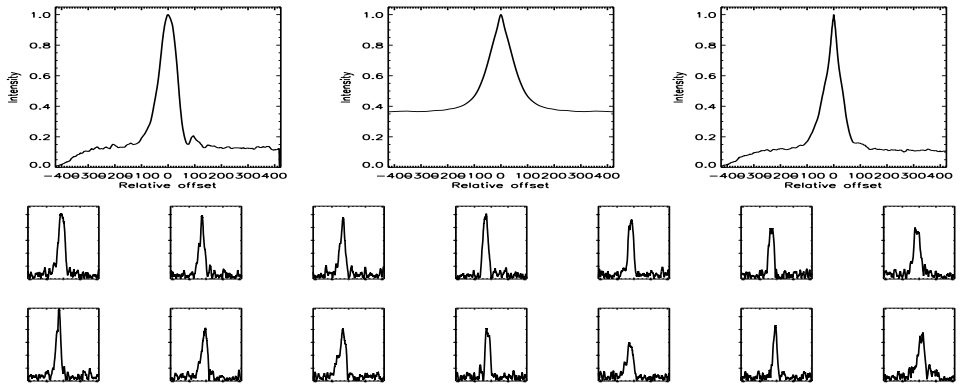

FIGURE B.546: SFP inspection for HD 190404 with S1-W1 on UT 2007/07/24, seq 002

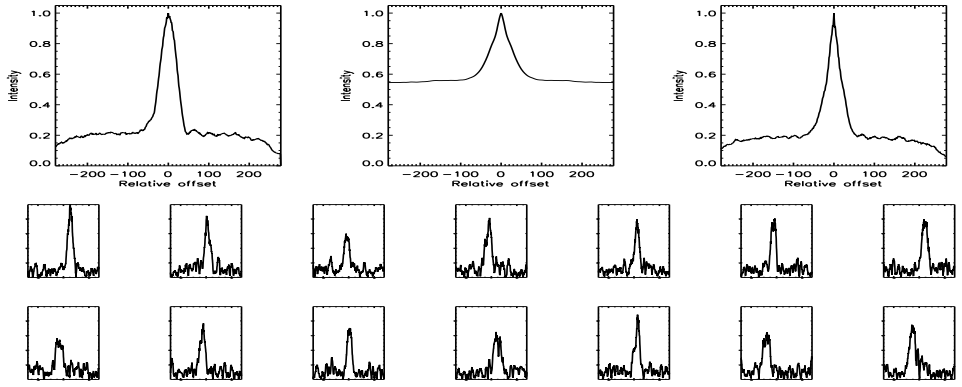

FIGURE B.547: SFP inspection for HD 190470 with S1-E1 on UT 2007/07/24, seq 001

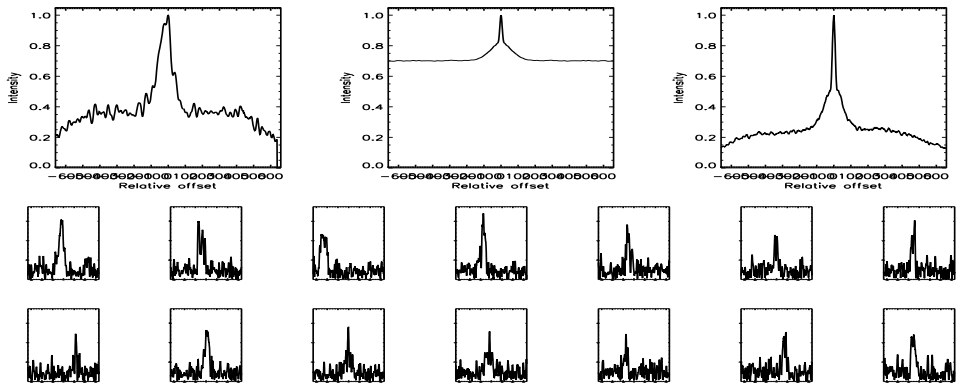

FIGURE B.548: SFP inspection for HD 190470 with S1-E1 on UT 2007/08/18, seq 002

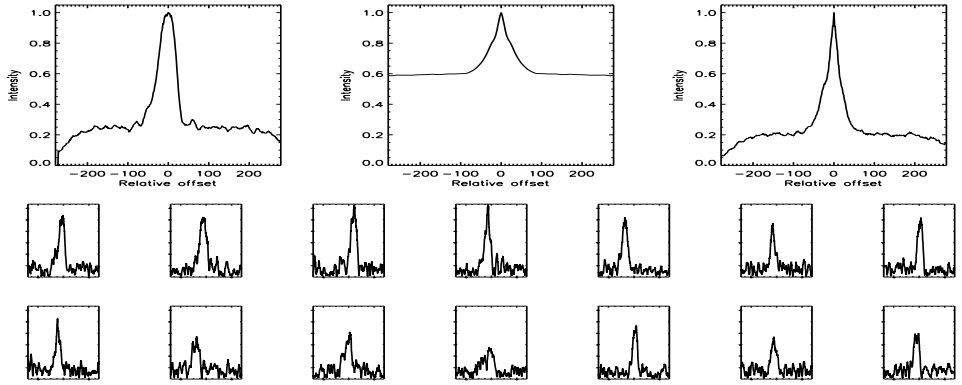

FIGURE B.549: SFP inspection for HD 190470 with S1-W1 on UT 2007/07/24, seq 002

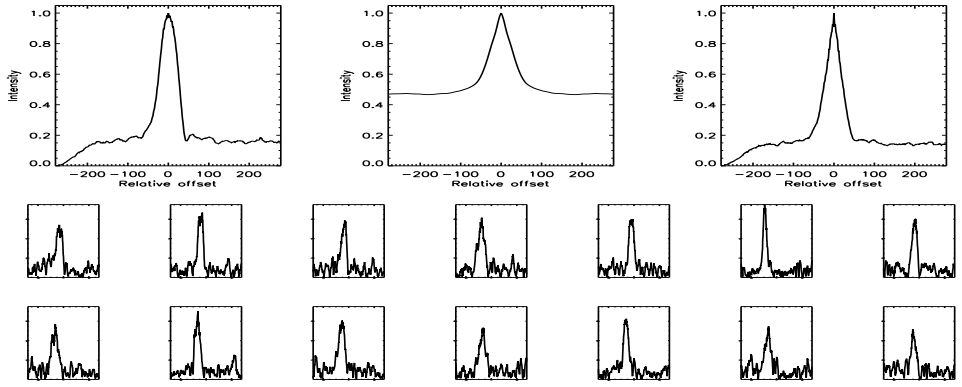

FIGURE B.550: SFP inspection for HD 190470 with S1-W1 on UT 2007/08/17, seq 001

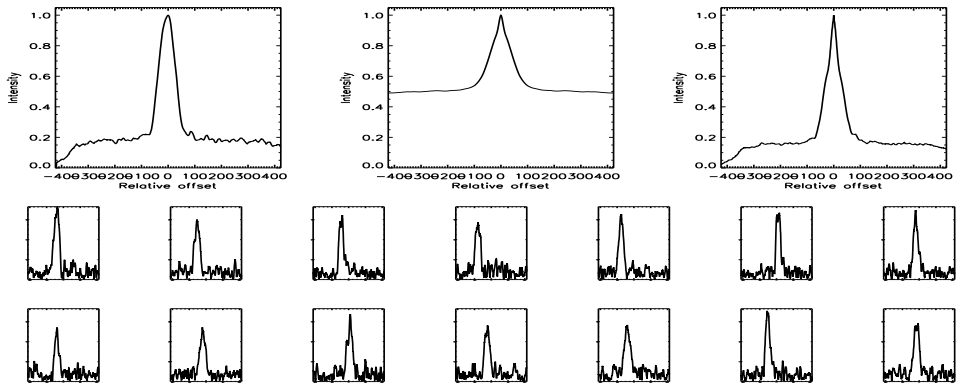

FIGURE B.551: SFP inspection for HD 190470 with S1-W1 on UT 2007/08/18, seq 001

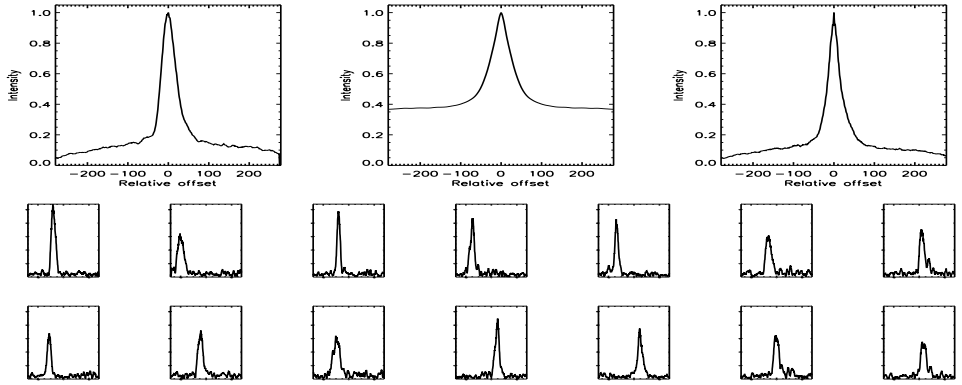

FIGURE B.552: SFP inspection for HD 190771 with S1-E1 on UT 2007/04/14, seq 001

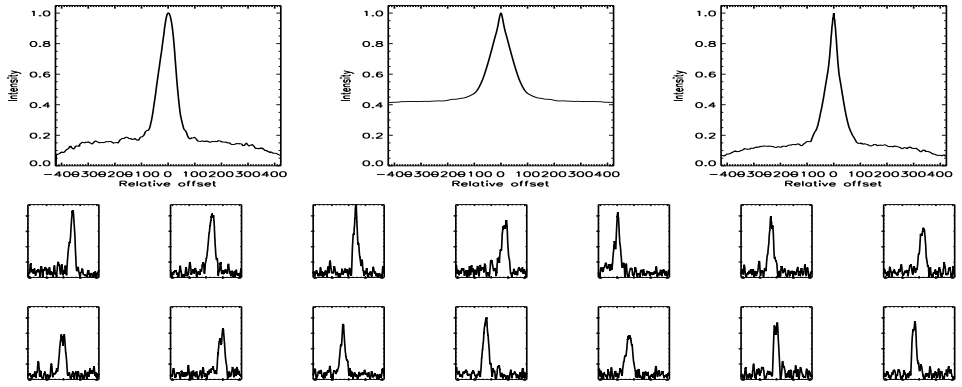

FIGURE B.553: SFP inspection for HD 190771 with S1-E1 on UT 2007/08/18, seq 002

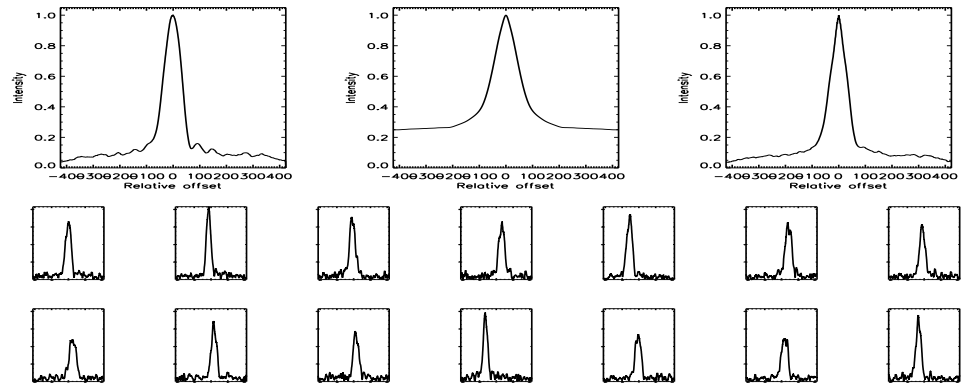

FIGURE B.554: SFP inspection for HD 190771 with S1-W1 on UT 2007/08/18, seq 001

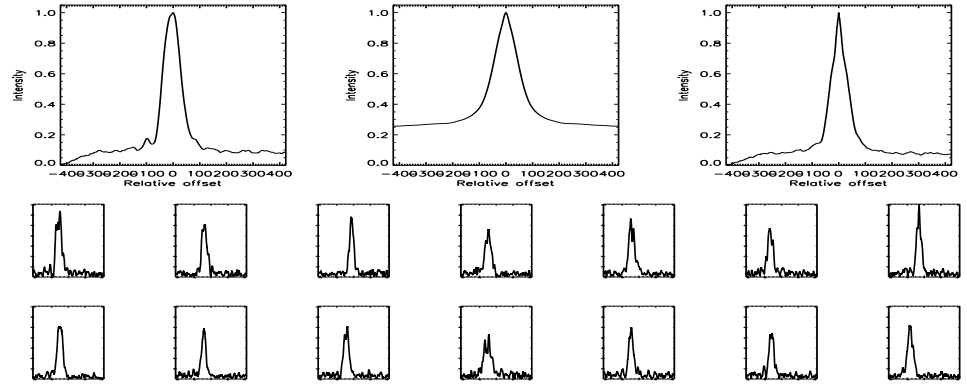

FIGURE B.555: SFP inspection for HD 190771 with S1-W1 on UT 2007/08/21, seq 001

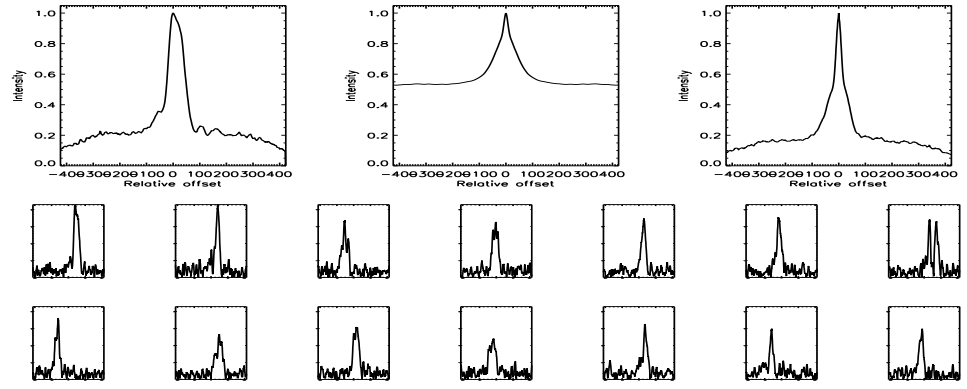

FIGURE B.556: SFP inspection for HD 190771 with S2-E1 on UT 2007/08/20, seq 001

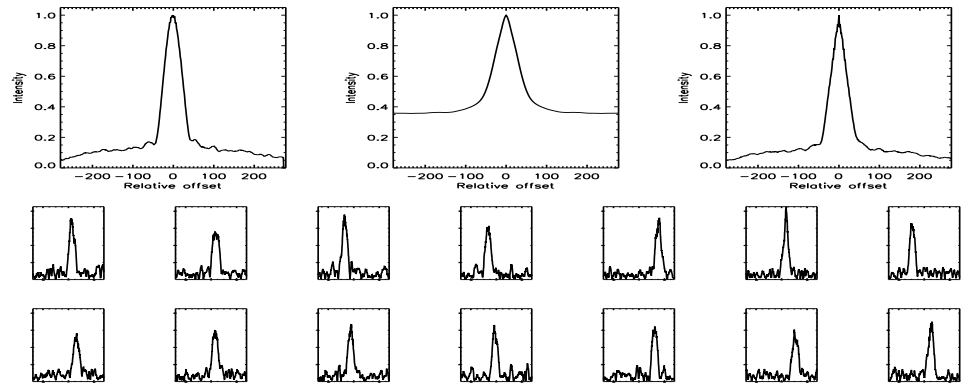

FIGURE B.557: SFP inspection for HD 191499 with S1-E1 on UT 2007/07/22, seq 002

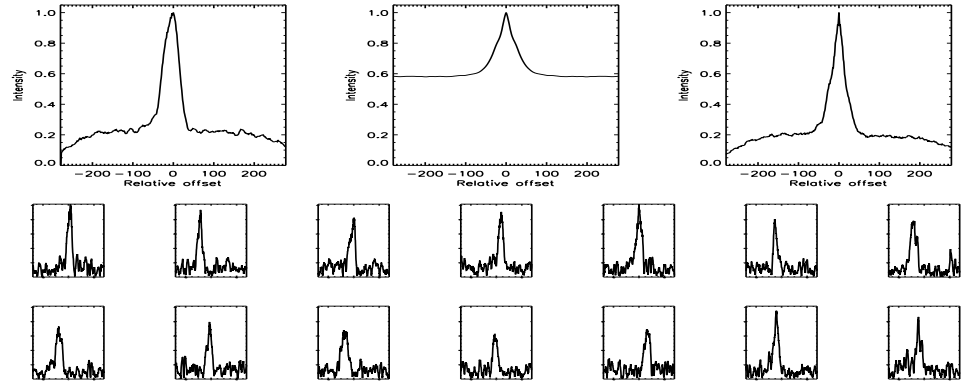

FIGURE B.558: SFP inspection for HD 191499 with S1-E1 on UT 2007/07/24, seq 001

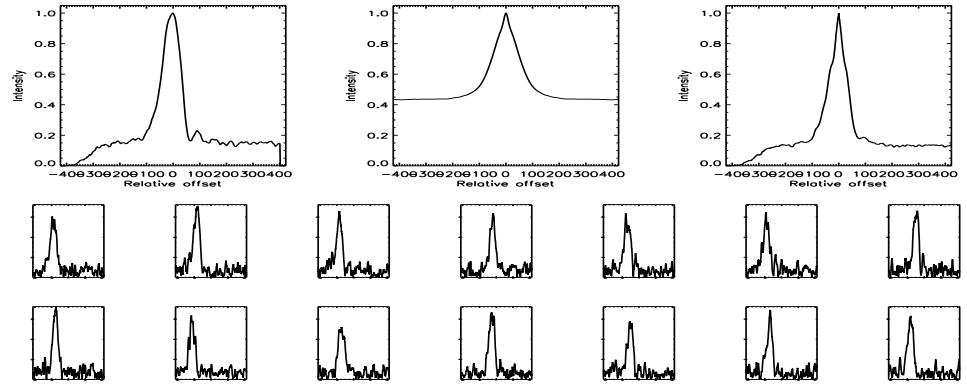

FIGURE B.559: SFP inspection for HD 191499 with S1-W1 on UT 2007/07/22, seq 001

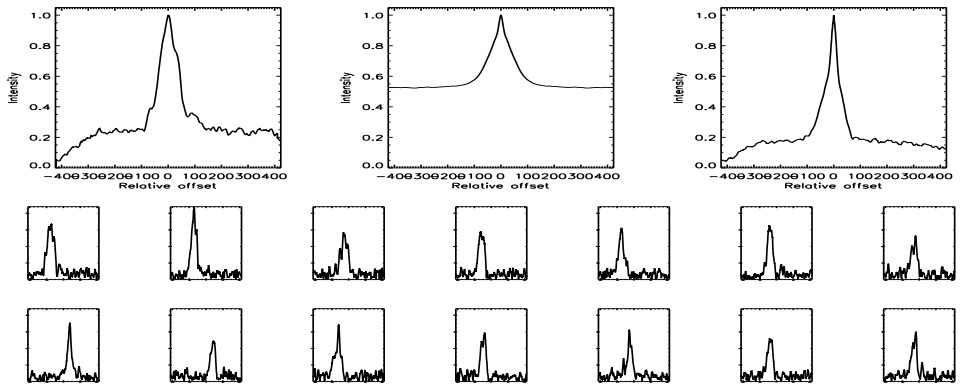

FIGURE B.560: SFP inspection for HD 191499 with S1-W1 on UT 2007/07/24, seq 002

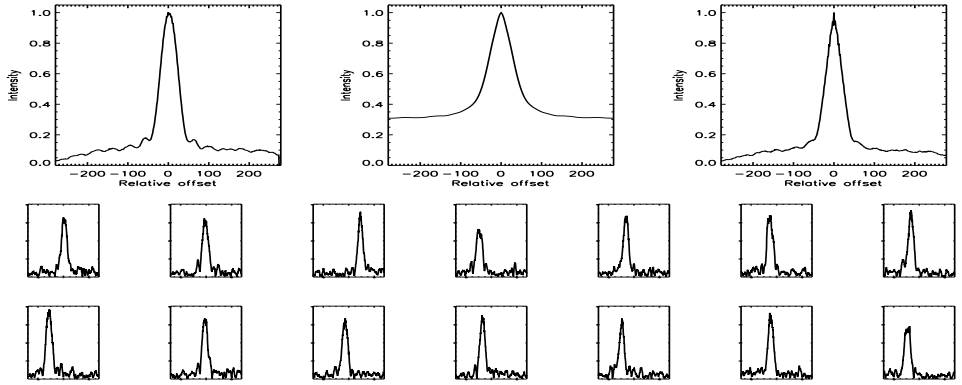

FIGURE B.561: SFP inspection for HD 191785 with S1-E1 on UT 2007/07/22, seq 001

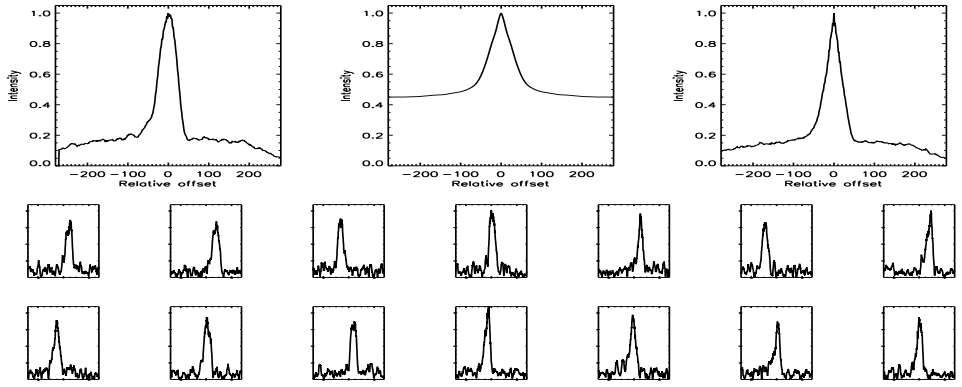

FIGURE B.562: SFP inspection for HD 191785 with S1-E1 on UT 2007/07/24, seq 001

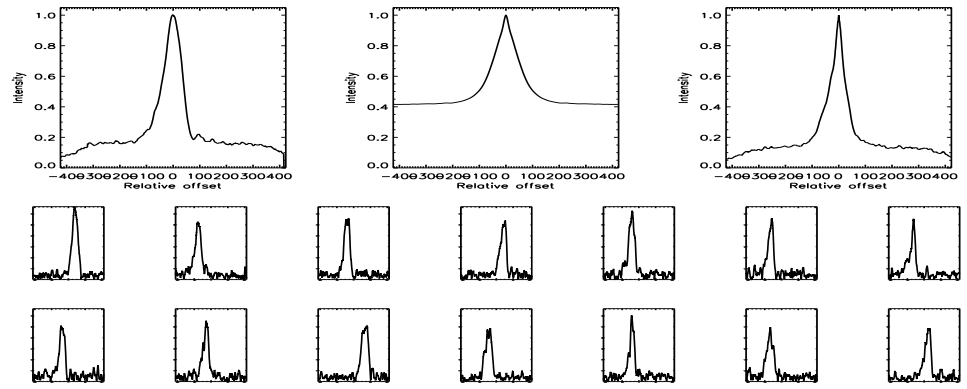

FIGURE B.563: SFP inspection for HD 191785 with S1-W1 on UT 2007/07/24, seq 002

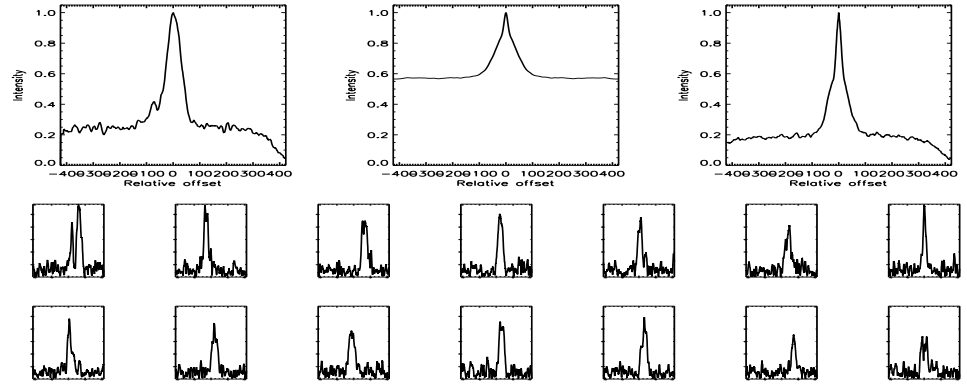

FIGURE B.564: SFP inspection for HD 192263 with S1-E1 on UT 2007/08/15, seq 002

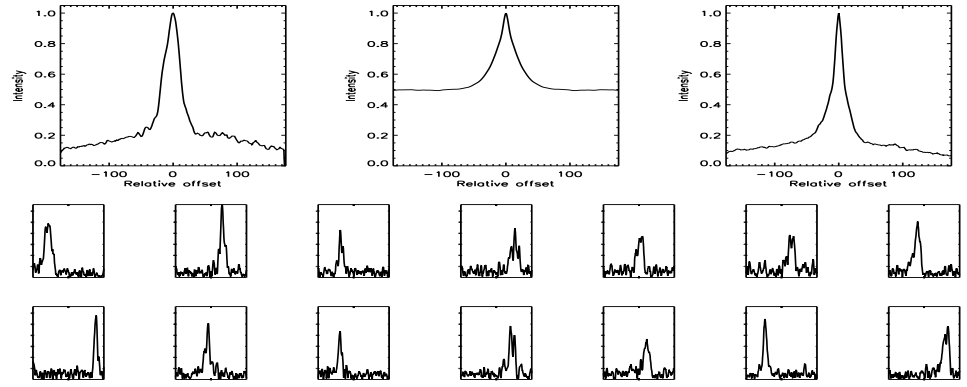

FIGURE B.565: SFP inspection for HD 192263 with S1-E1 on UT 2008/04/25, seq 001

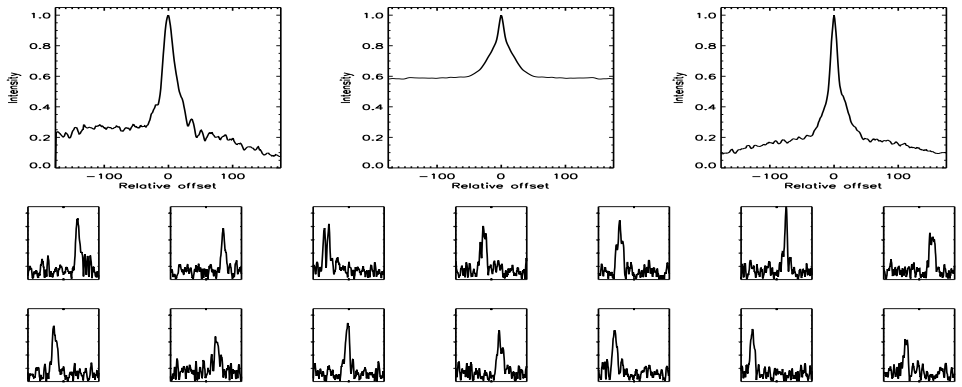

FIGURE B.566: SFP inspection for HD 192263 with S1-E1 on UT 2008/06/23, seq 001

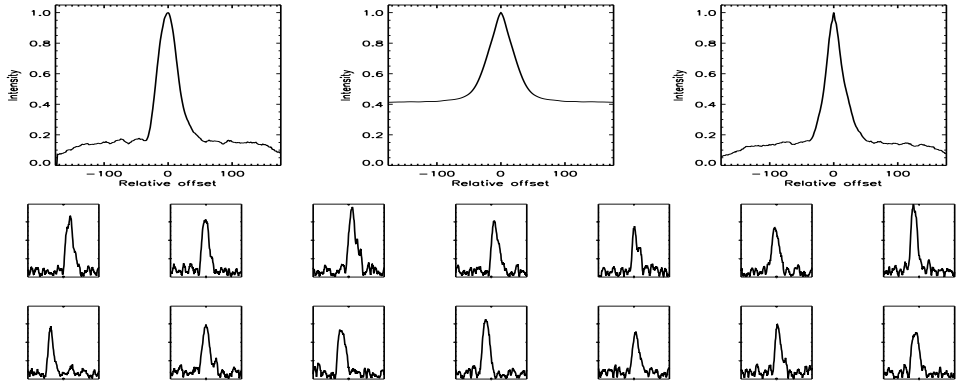

FIGURE B.567: SFP inspection for HD 192263 with S1-E1 on UT 2008/07/06, seq 001

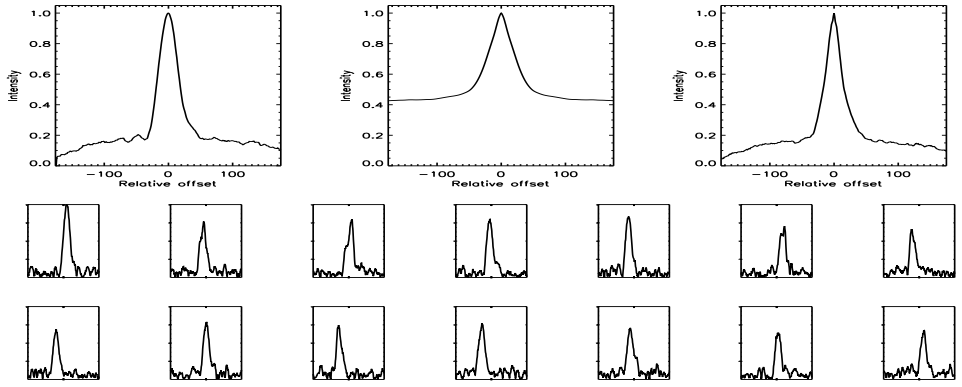

FIGURE B.568: SFP inspection for HD 192263 with S1-E1 on UT 2008/07/06, seq 002

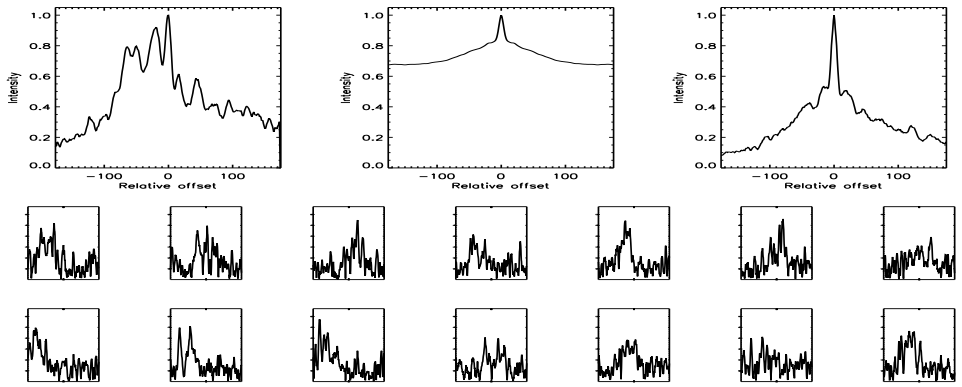

FIGURE B.569: SFP inspection for HD 192263 with S1-W1 on UT 2008/06/22, seq 001

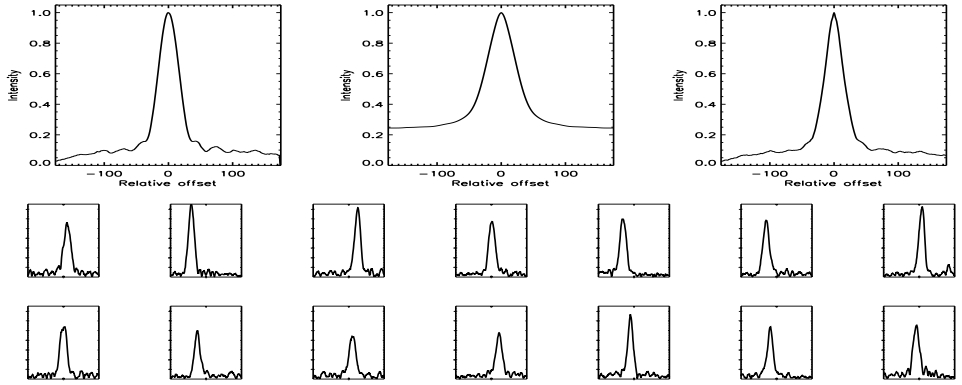

FIGURE B.570: SFP inspection for HD 192263 with S1-W1 on UT 2008/07/07, seq 001

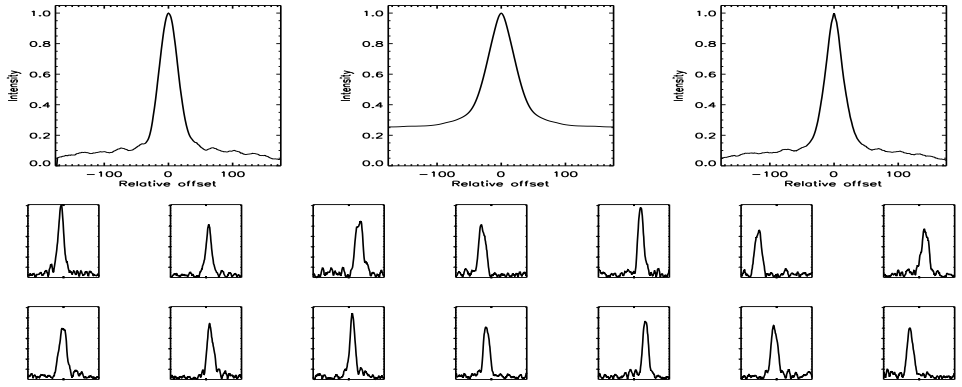

FIGURE B.571: SFP inspection for HD 192263 with S1-W1 on UT 2008/07/07, seq 002

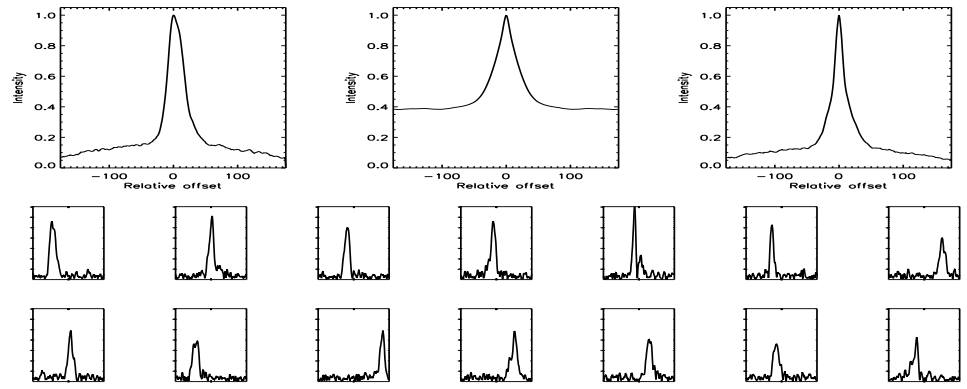

FIGURE B.572: SFP inspection for HD 195564 with S1-E1 on UT 2008/06/23, seq 001

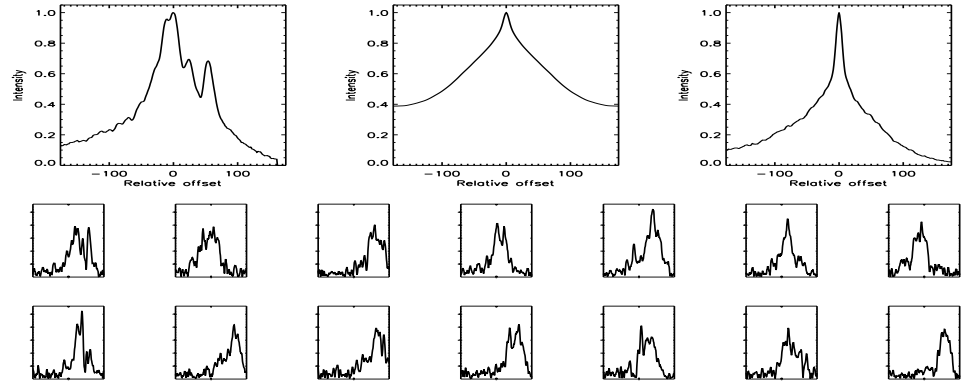

FIGURE B.573: SFP inspection for HD 195564 with S1-W1 on UT 2008/06/22, seq 001

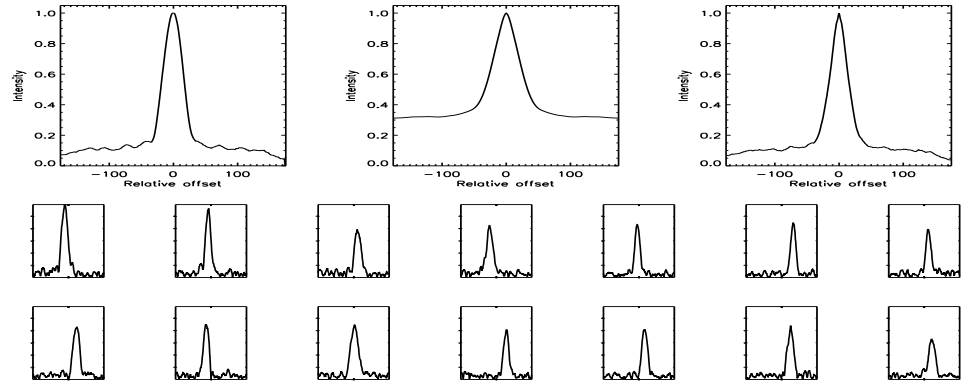

FIGURE B.574: SFP inspection for HD 195564 with S2-W2 on UT 2008/06/09, seq 001

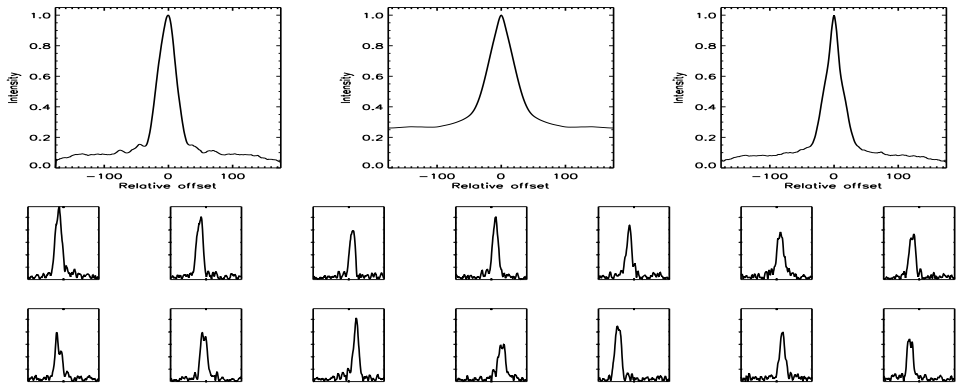

FIGURE B.575: SFP inspection for HD 195564 with S2-W2 on UT 2008/06/09, seq 002

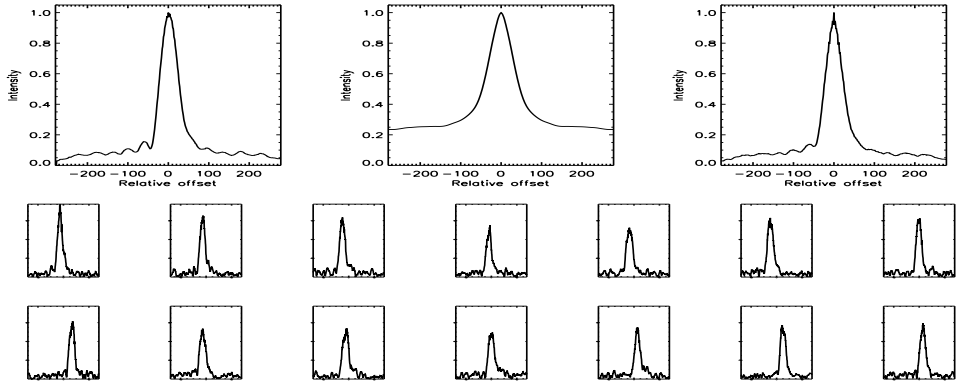

FIGURE B.576: SFP inspection for HD 197076 with S1-E1 on UT 2007/07/22, seq 002

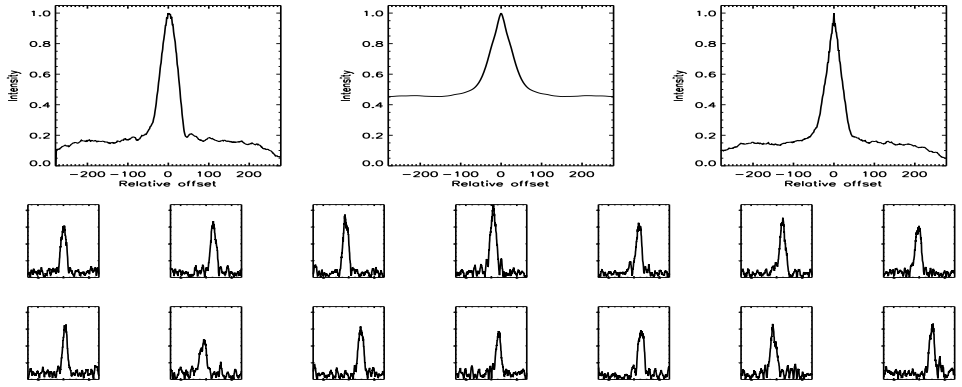

FIGURE B.577: SFP inspection for HD 197076 with S1-E1 on UT 2007/07/24, seq 001

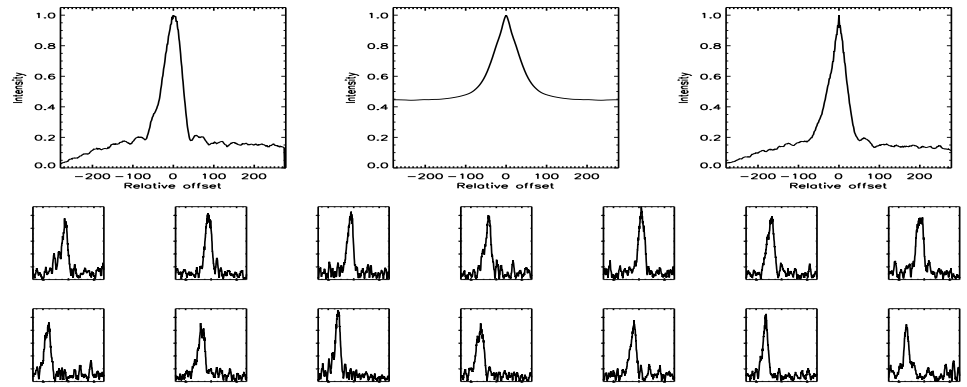

FIGURE B.578: SFP inspection for HD 197076 with S1-W1 on UT 2007/07/22, seq 001

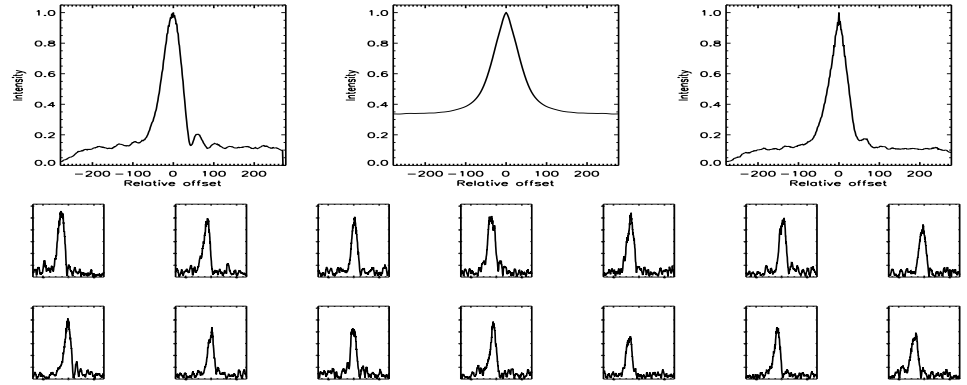

FIGURE B.579: SFP inspection for HD 197076 with S1-W1 on UT 2007/07/24, seq 002

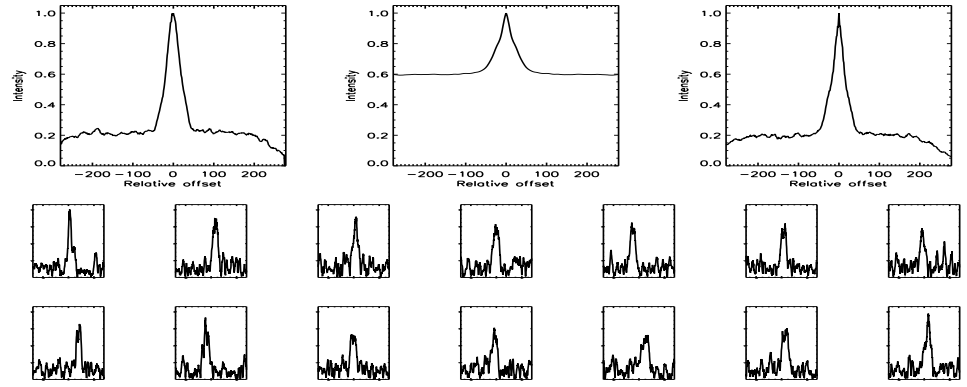

FIGURE B.580: SFP inspection for HD 198425 with S1-E1 on UT 2007/08/14, seq 001

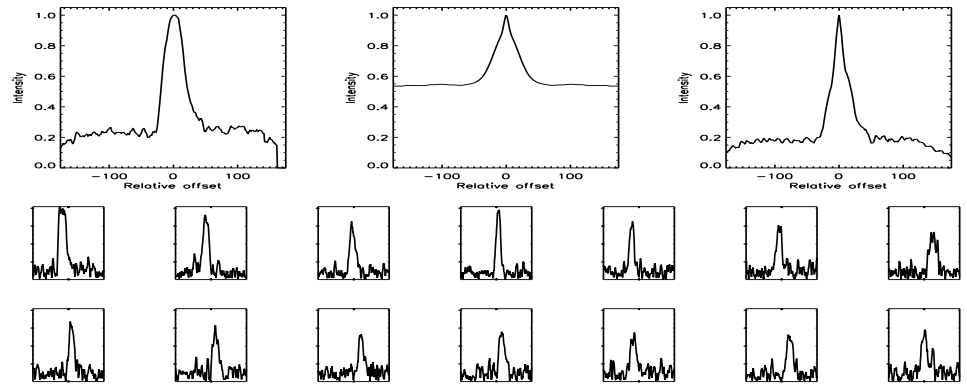

FIGURE B.581: SFP inspection for HD 198425 with S1-E1 on UT 2008/07/23, seq 001

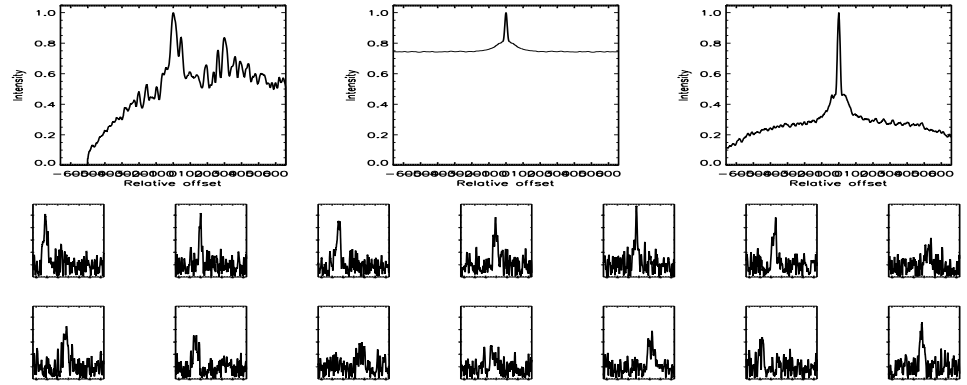

FIGURE B.582: SFP inspection for HD 198425 with S1-W1 on UT 2007/08/17, seq 001

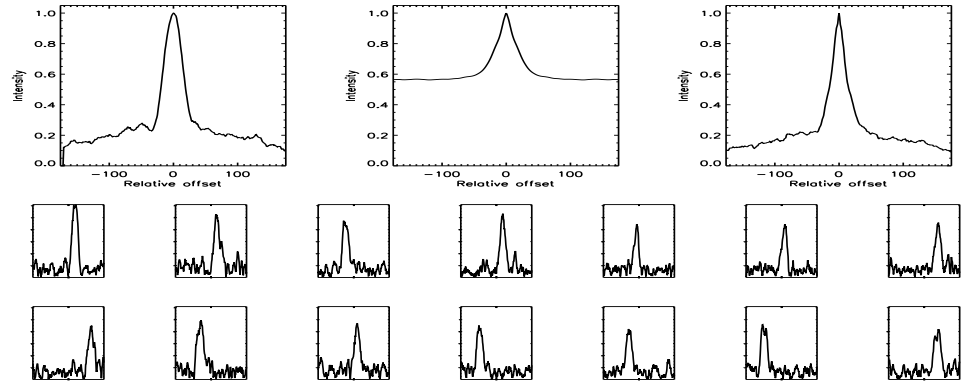

FIGURE B.583: SFP inspection for HD 198425 with S1-W1 on UT 2008/07/08, seq 001

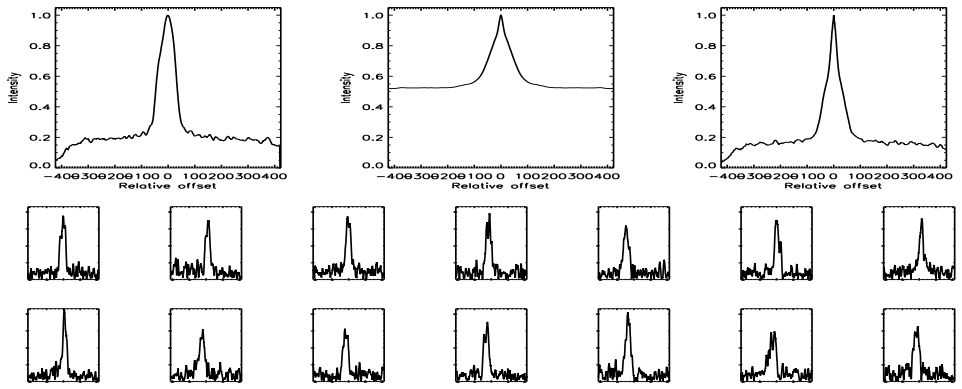

FIGURE B.584: SFP inspection for HD 200560 with S1-E1 on UT 2007/07/28, seq 001

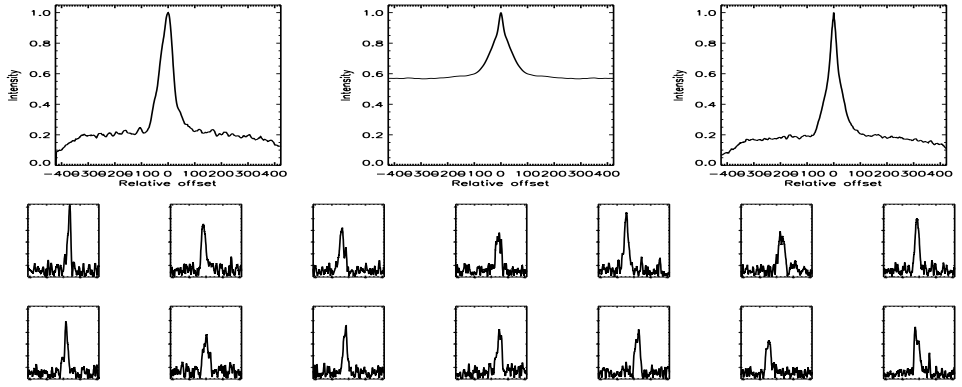

FIGURE B.585: SFP inspection for HD 200560 with S1-E1 on UT 2007/08/18, seq 002

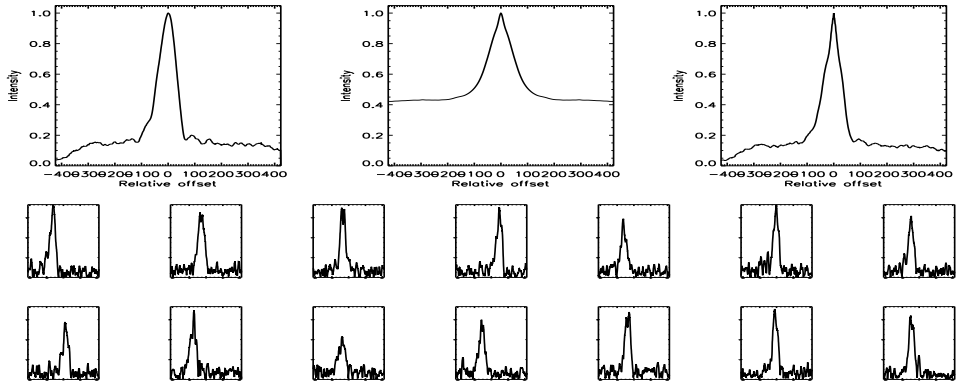

FIGURE B.586: SFP inspection for HD 200560 with S1-W1 on UT 2007/08/18, seq 001

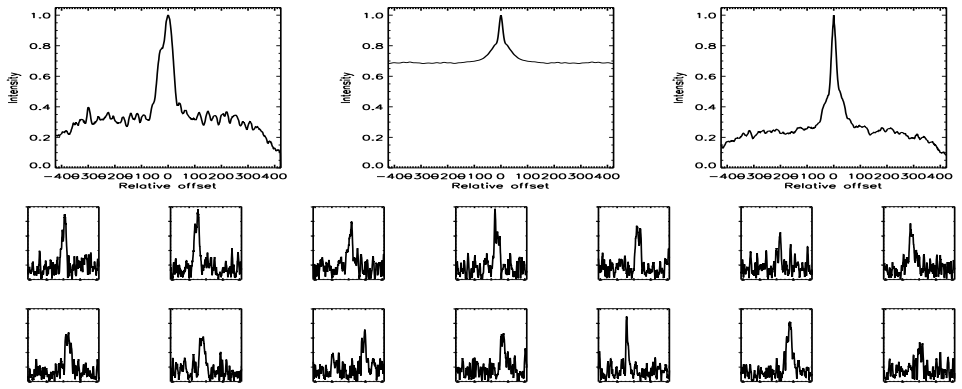

FIGURE B.587: SFP inspection for HD 200560 with S2-E1 on UT 2007/08/20, seq 001

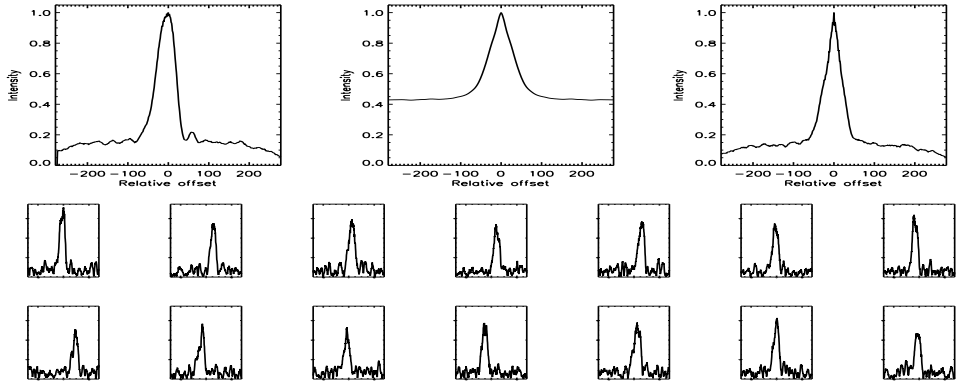

FIGURE B.588: SFP inspection for HD 202751 with S1-E1 on UT 2007/07/22, seq 001

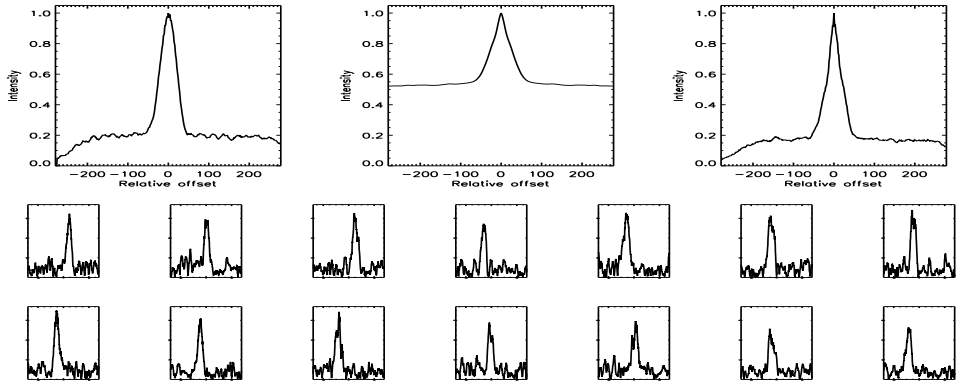

FIGURE B.589: SFP inspection for HD 202751 with S1-W1 on UT 2007/07/24, seq 001

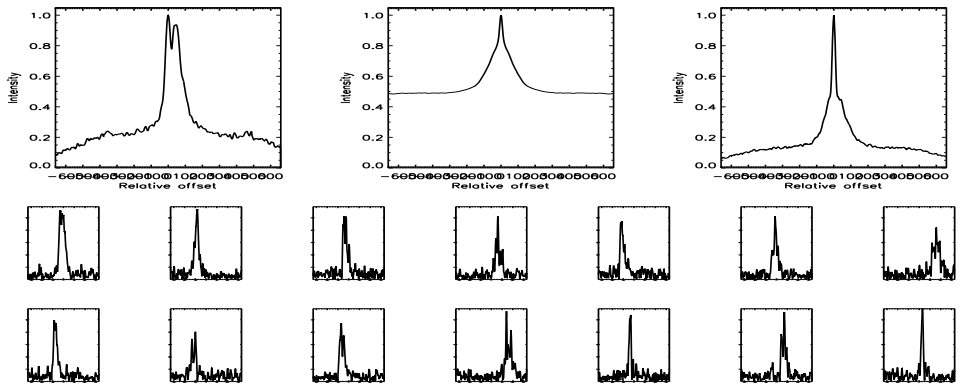

FIGURE B.590: SFP inspection for HD 202751 with S2-W1 on UT 2007/09/17, seq 001

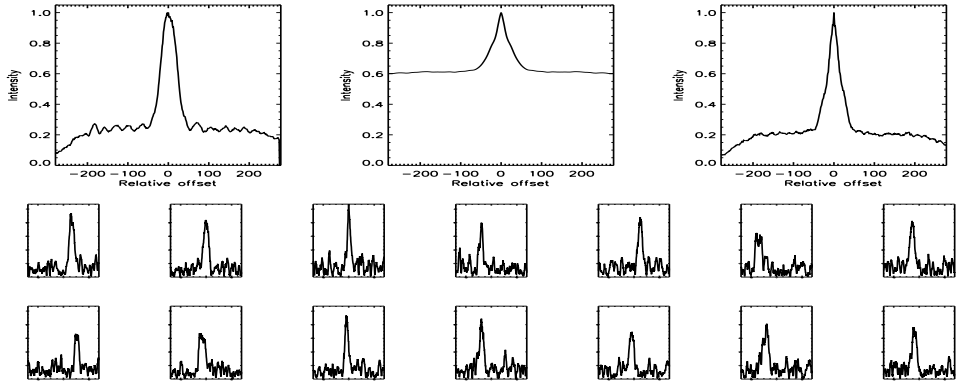

FIGURE B.591: SFP inspection for HD 208038 with S1-E1 on UT 2007/07/24, seq 002

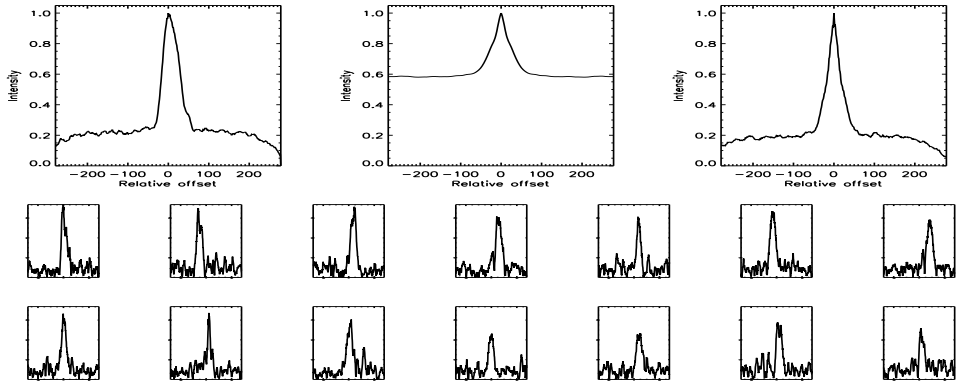

FIGURE B.592: SFP inspection for HD 208038 with S1-E1 on UT 2007/08/14, seq 001

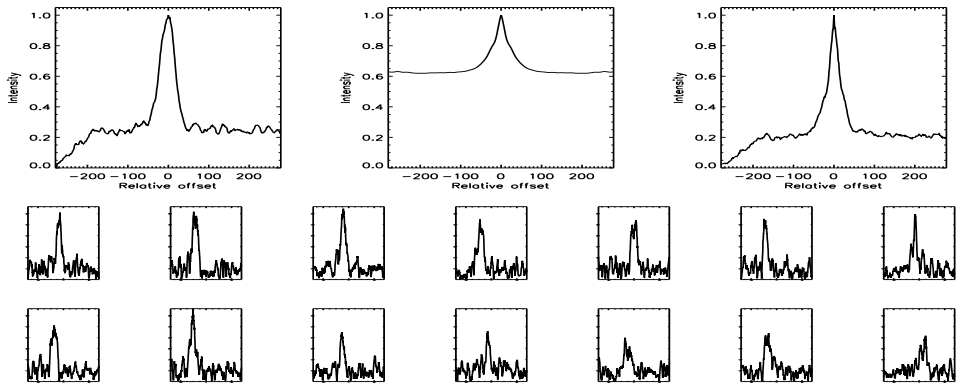

FIGURE B.593: SFP inspection for HD 208038 with S1-W1 on UT 2007/08/14, seq 002

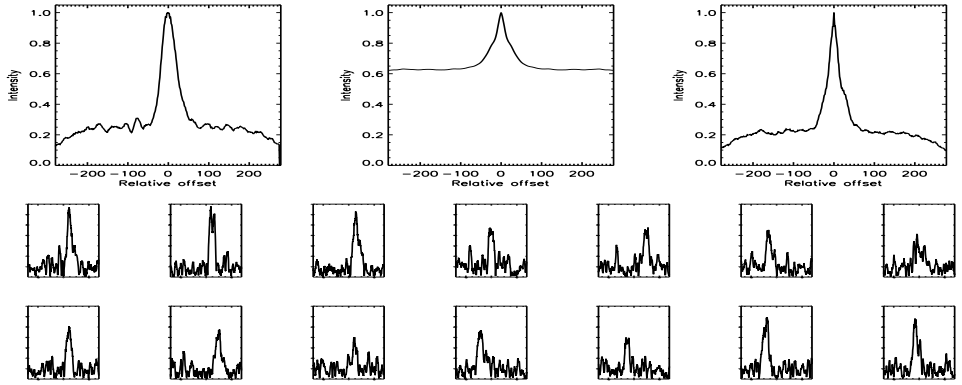

FIGURE B.594: SFP inspection for HD 208313 with S1-E1 on UT 2007/07/25, seq 001

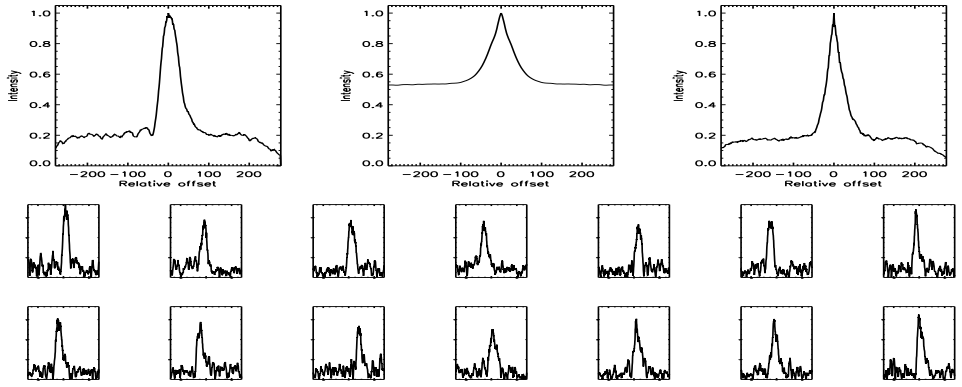

FIGURE B.595: SFP inspection for HD 208313 with S1-E1 on UT 2007/08/14, seq 001

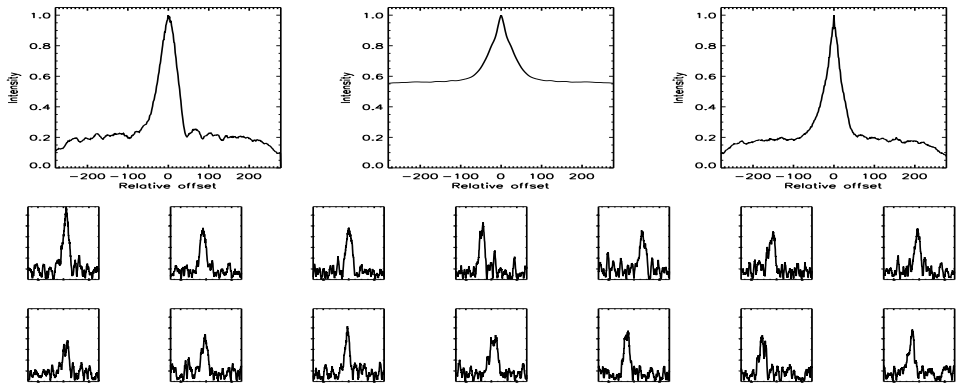

FIGURE B.596: SFP inspection for HD 208313 with S1-W1 on UT 2007/08/14, seq 002

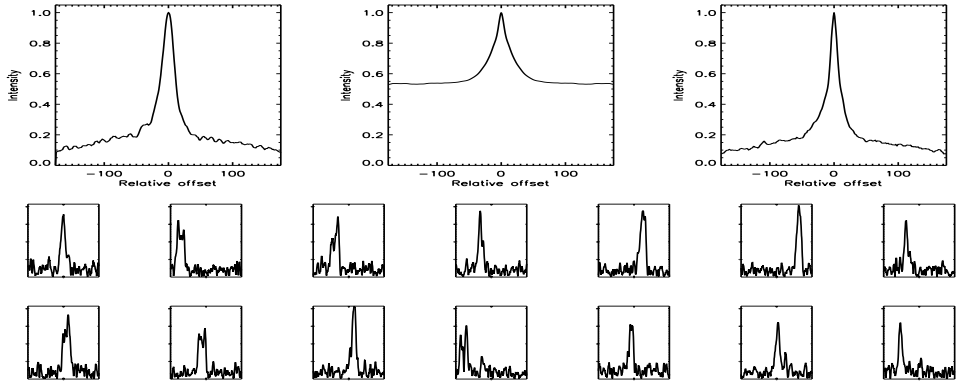

FIGURE B.597: SFP inspection for HD 210277 with S1-E1 on UT 2008/06/23, seq 001

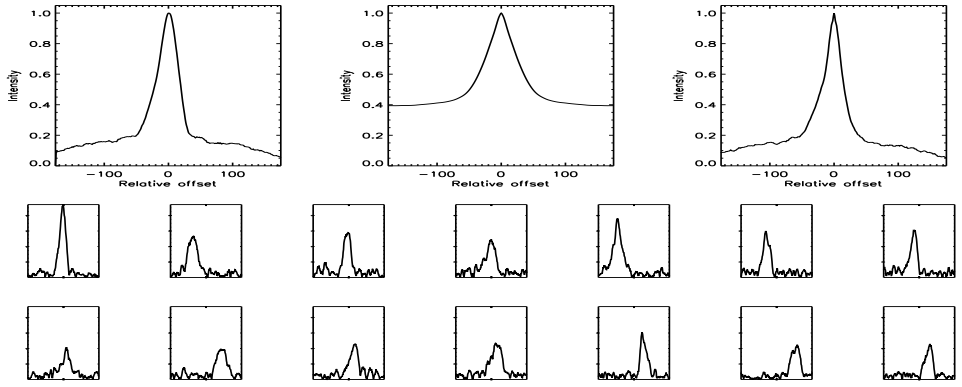

FIGURE B.598: SFP inspection for HD 210277 with S1-E1 on UT 2008/07/06, seq 001

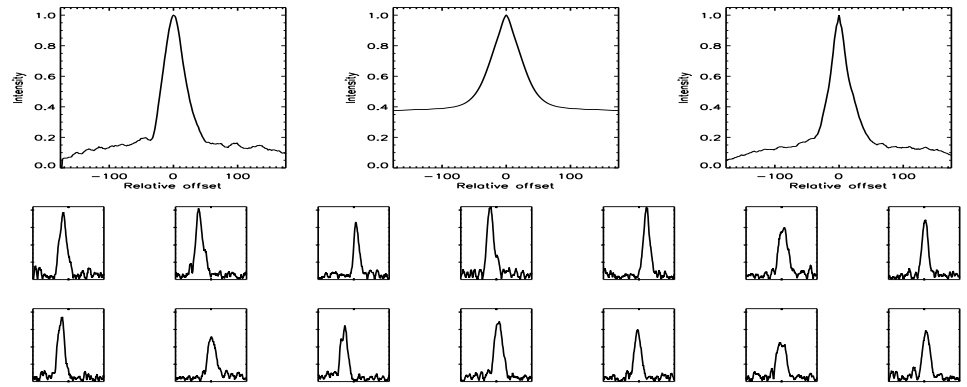

FIGURE B.599: SFP inspection for HD 210277 with S1-E1 on UT 2008/07/06, seq 002

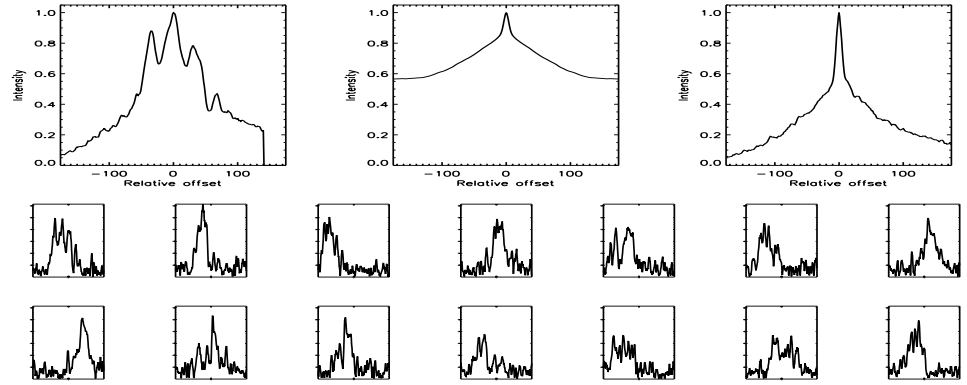

FIGURE B.600: SFP inspection for HD 210277 with S1-W1 on UT 2008/06/22, seq 001

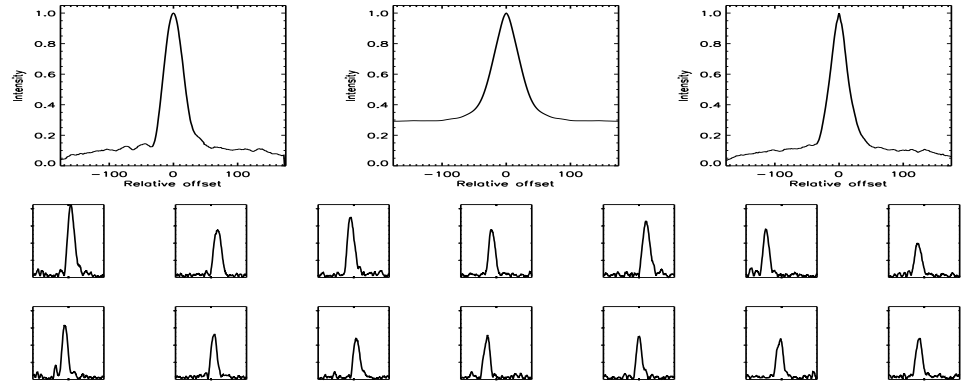

FIGURE B.601: SFP inspection for HD 210277 with S1-W1 on UT 2008/07/07, seq 001

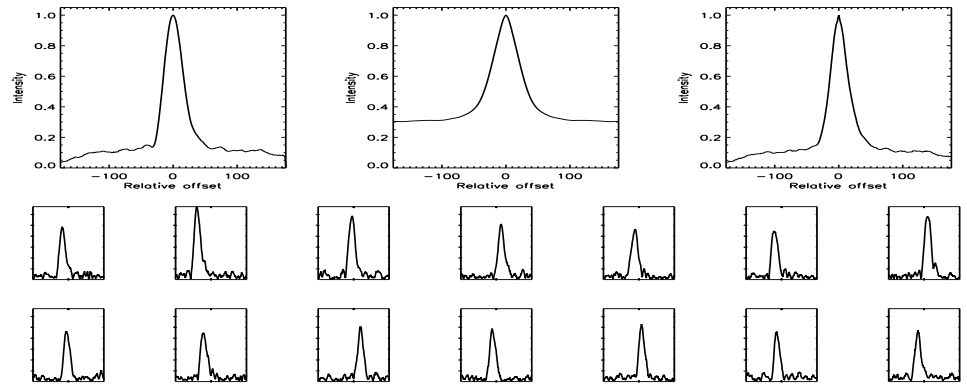

FIGURE B.602: SFP inspection for HD 210277 with S1-W1 on UT 2008/07/07, seq 002

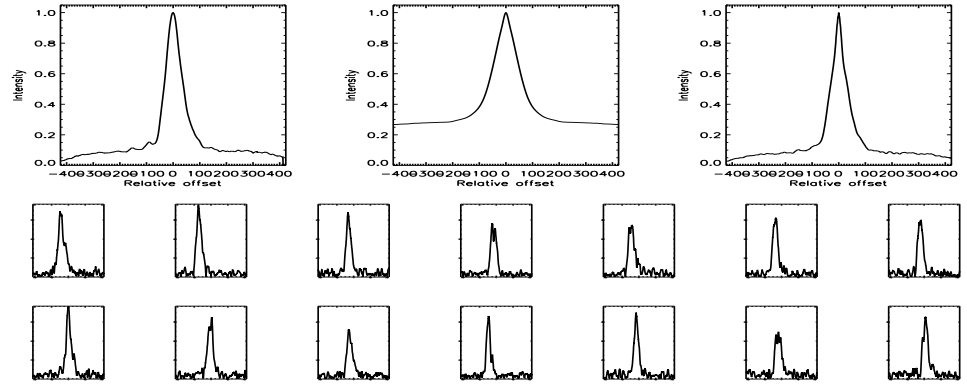

FIGURE B.603: SFP inspection for HD 210277 with S2-W1 on UT 2007/09/17, seq 001

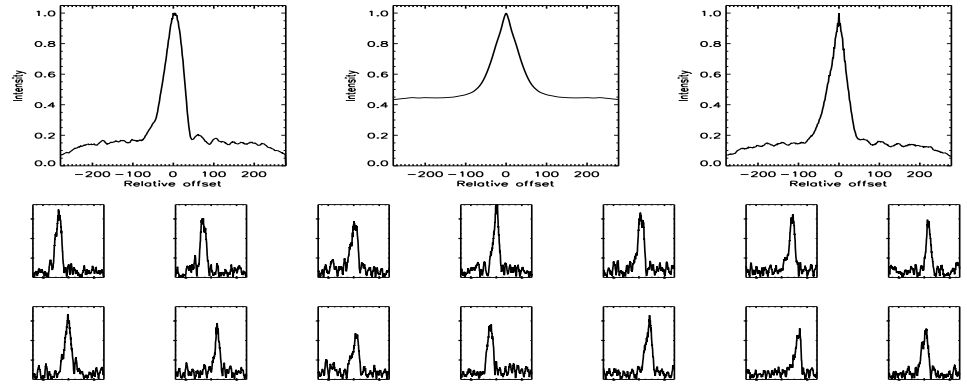

FIGURE B.604: SFP inspection for HD 210667 with S1-E1 on UT 2007/07/26, seq 001

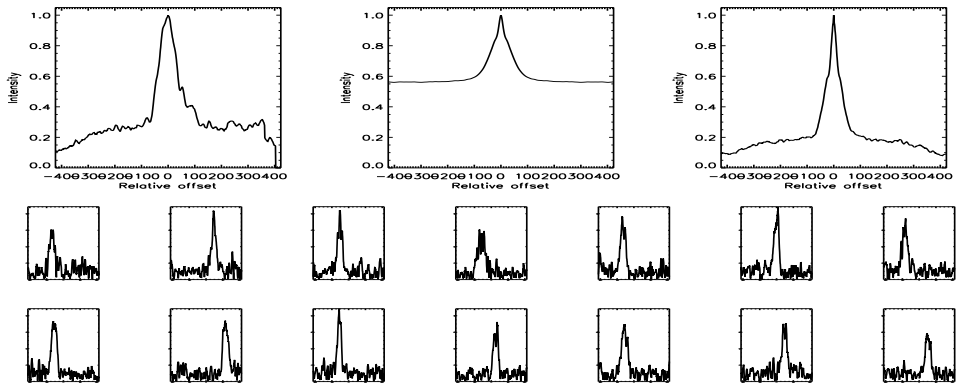

FIGURE B.605: SFP inspection for HD 210667 with S1-E1 on UT 2007/07/28, seq 001

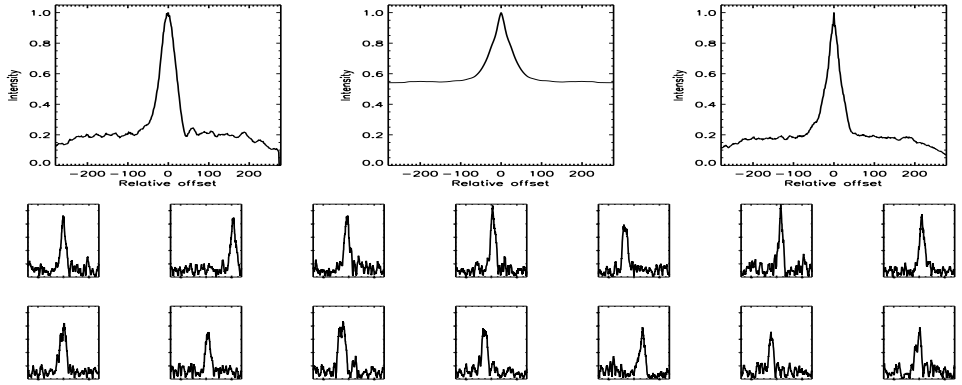

FIGURE B.606: SFP inspection for HD 210667 with S1-W1 on UT 2007/07/26, seq 002

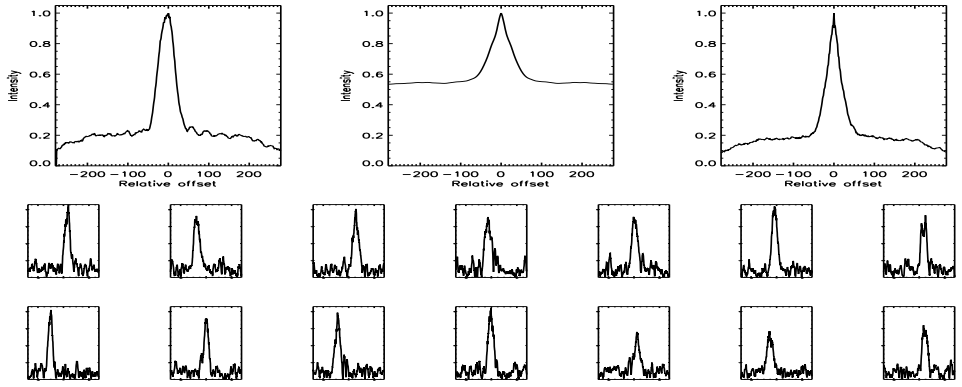

FIGURE B.607: SFP inspection for HD 211472 with S1-E1 on UT 2007/07/26, seq 001

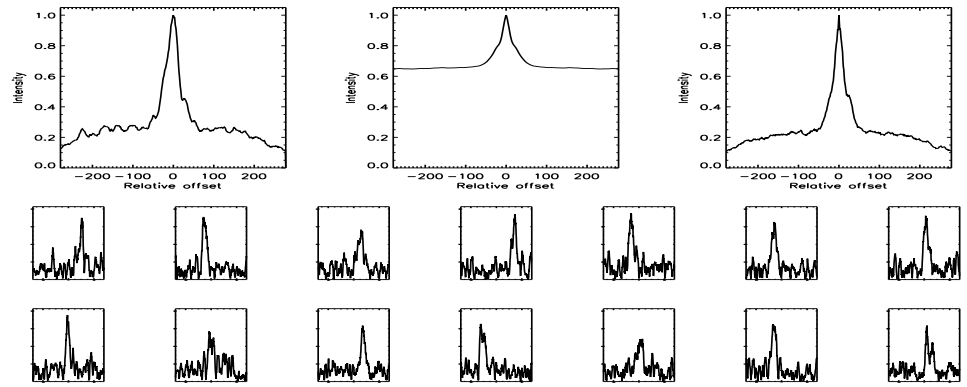

FIGURE B.608: SFP inspection for HD 211472 with S1-E1 on UT 2007/07/28, seq 001

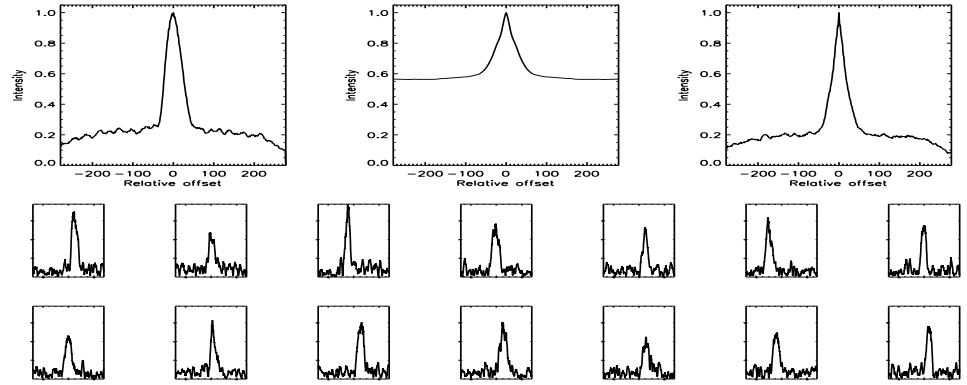

FIGURE B.609: SFP inspection for HD 211472 with S1-W1 on UT 2007/07/26, seq 002

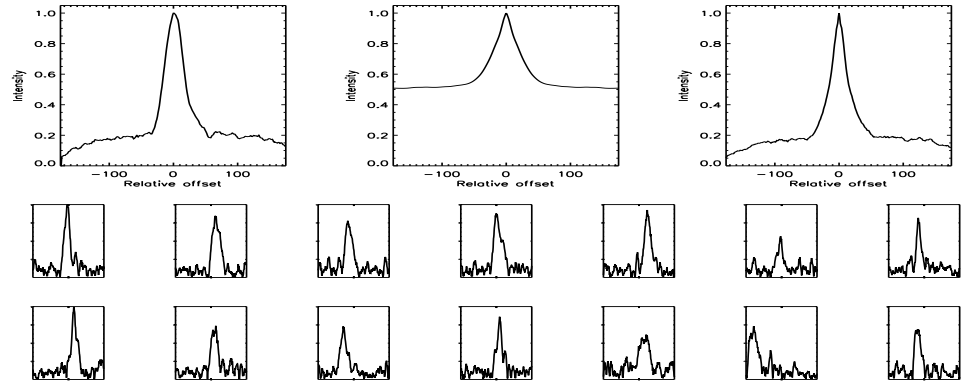

FIGURE B.610: SFP inspection for HD 215152 with S1-E1 on UT 2008/07/06, seq 001

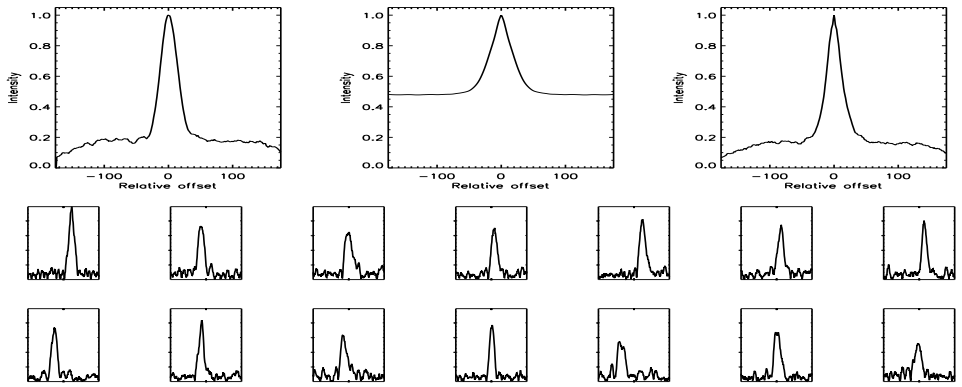

FIGURE B.611: SFP inspection for HD 215152 with S1-W1 on UT 2008/07/07, seq 001

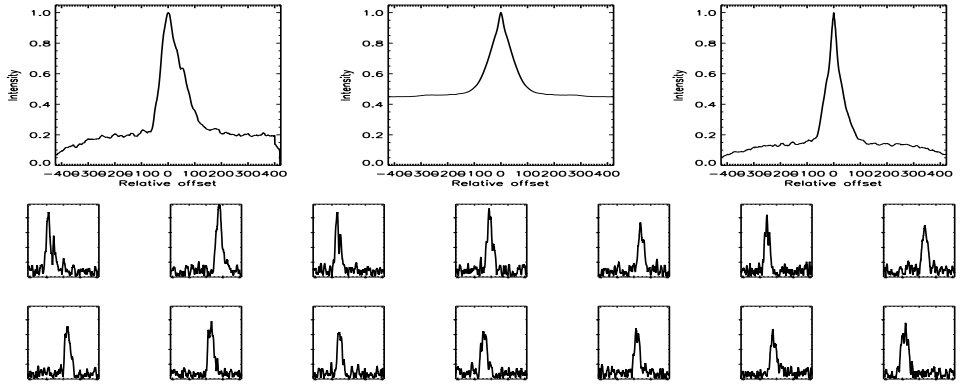

FIGURE B.612: SFP inspection for HD 215152 with S2-W1 on UT 2007/09/17, seq 001

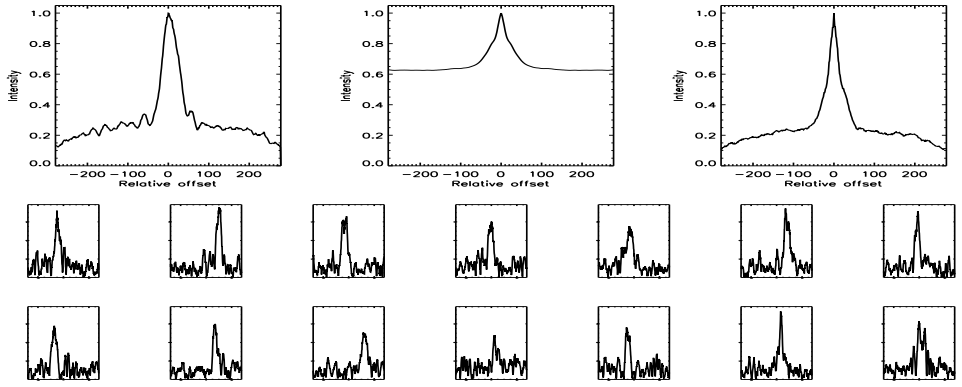

FIGURE B.613: SFP inspection for HD 216520 with S1-E1 on UT 2007/07/26, seq 001

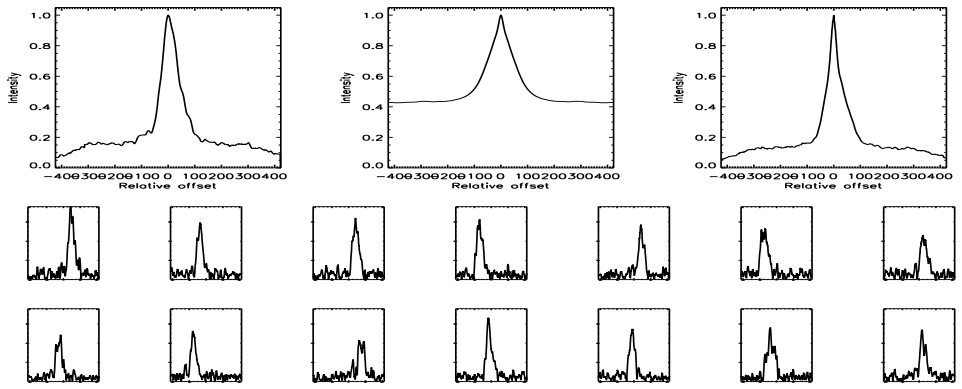

FIGURE B.614: SFP inspection for HD 216520 with S1-E1 on UT 2007/09/16, seq 002

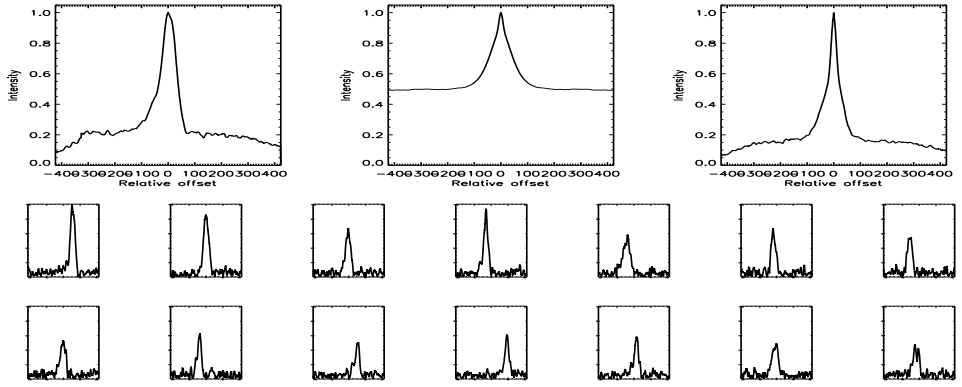

FIGURE B.615: SFP inspection for HD 216520 with S1-W1 on UT 2007/09/16, seq 001

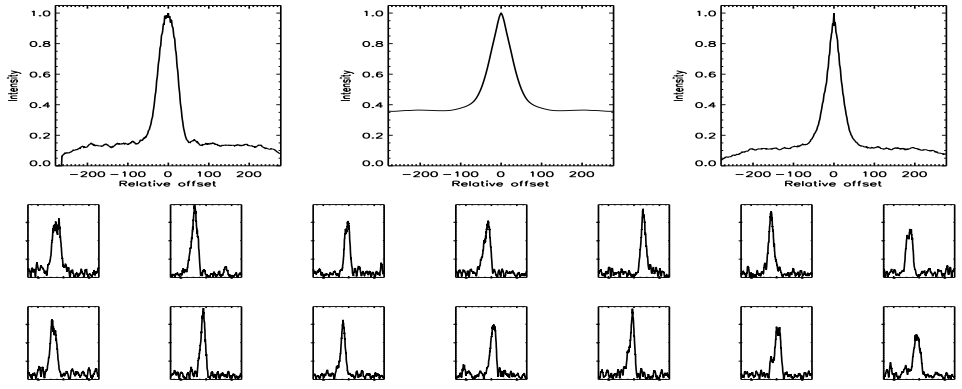

FIGURE B.616: SFP inspection for HD 217107 with S1-E1 on UT 2007/08/14, seq 001

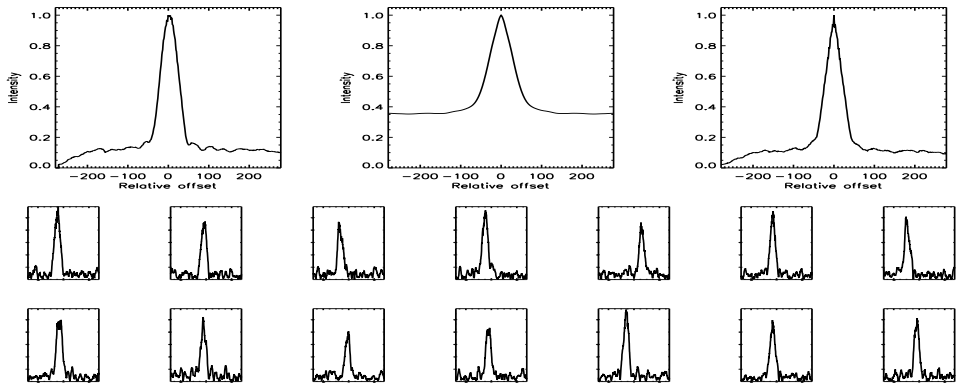

FIGURE B.617: SFP inspection for HD 217107 with S1-W1 on UT 2007/08/14, seq 002

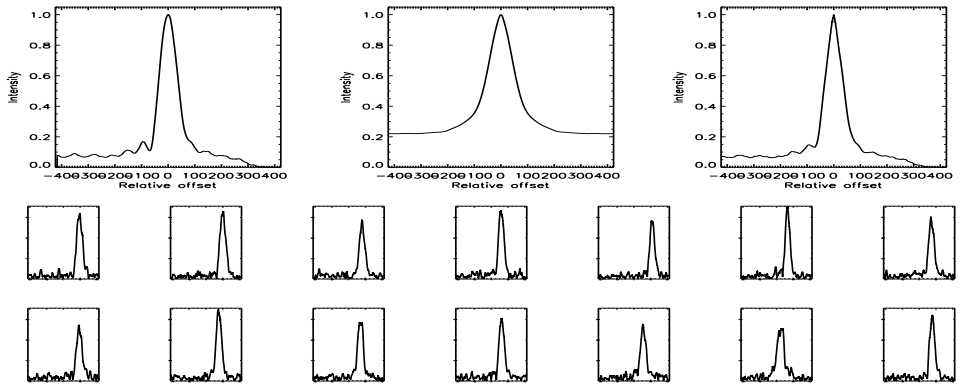

FIGURE B.618: SFP inspection for HD 217813 with S1-E1 on UT 2007/07/22, seq 001

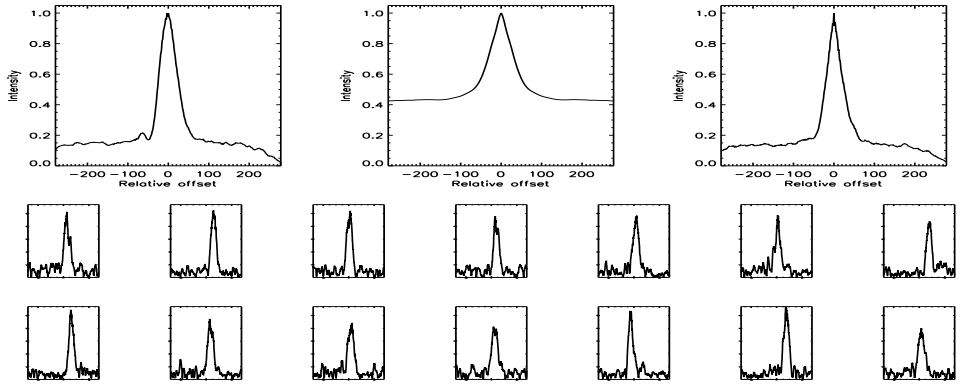

FIGURE B.619: SFP inspection for HD 217813 with S1-E1 on UT 2007/08/14, seq 001

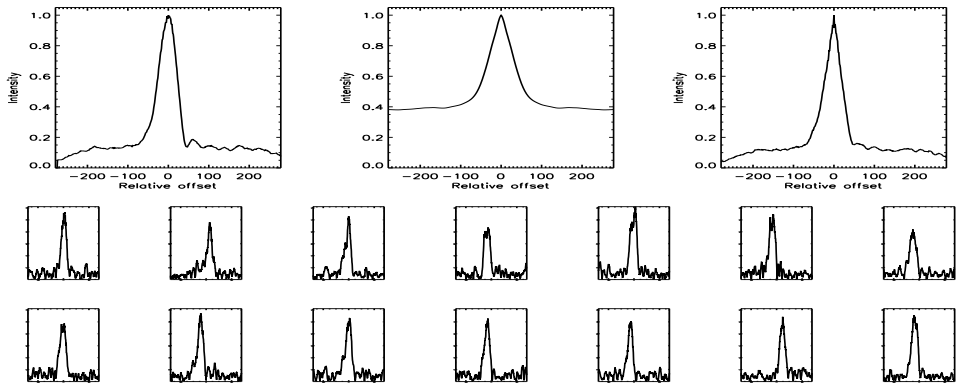

FIGURE B.620: SFP inspection for HD 217813 with S1-W1 on UT 2007/08/14, seq 002

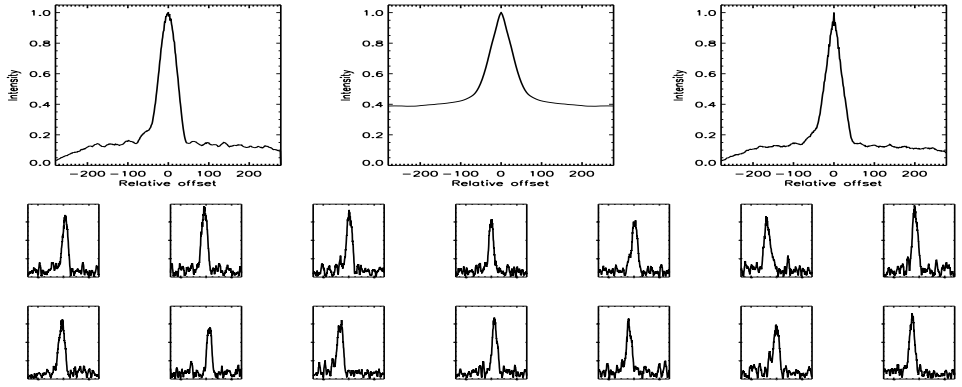

FIGURE B.621: SFP inspection for HD 218868 with S1-E1 on UT 2007/07/26, seq 001

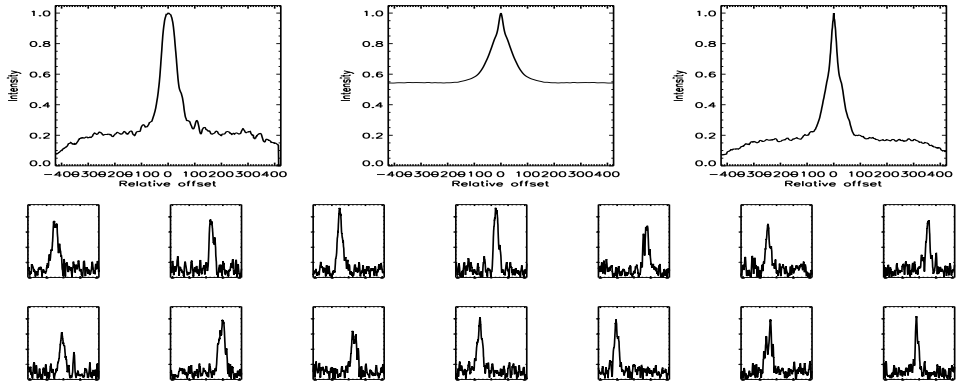

FIGURE B.622: SFP inspection for HD 218868 with S1-E1 on UT 2007/07/28, seq 002

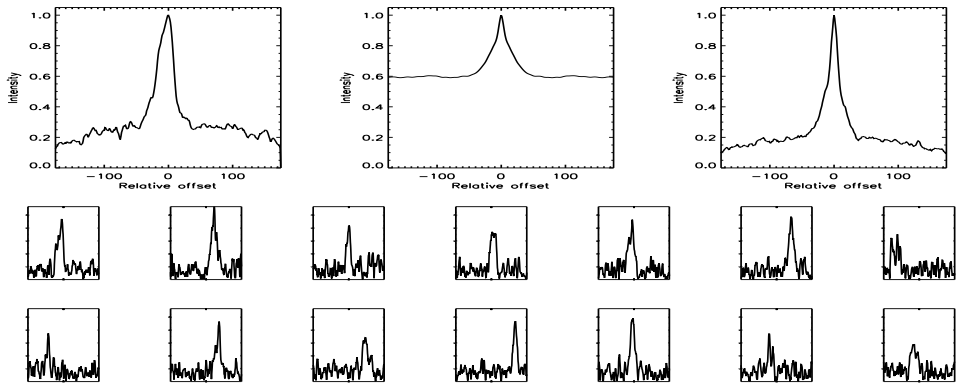

FIGURE B.623: SFP inspection for HD 218868 with S1-E1 on UT 2008/06/25, seq 001

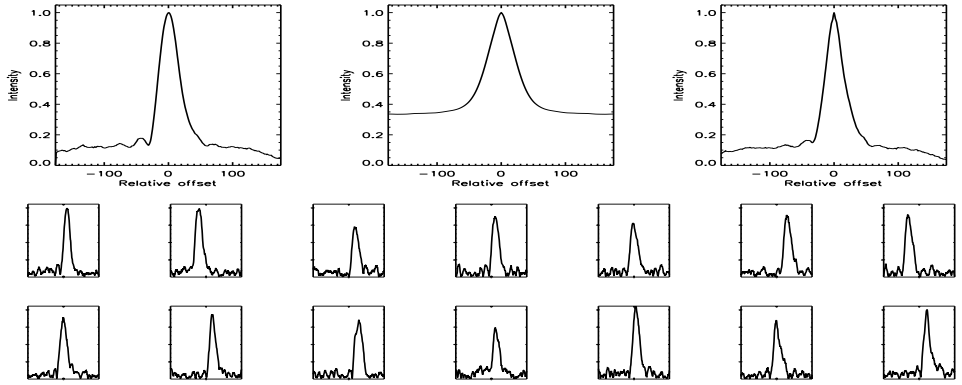

FIGURE B.624: SFP inspection for HD 218868 with S1-E1 on UT 2008/07/21, seq 001

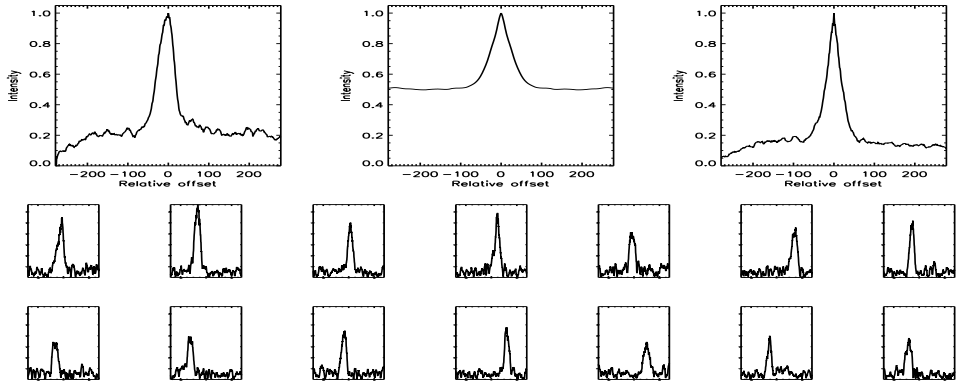

FIGURE B.625: SFP inspection for HD 218868 with S1-W1 on UT 2007/07/26, seq 002

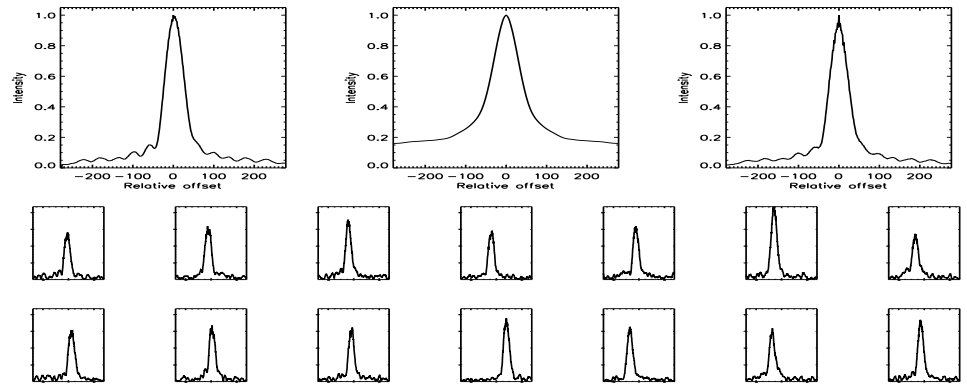

FIGURE B.626: SFP inspection for HD 219134 with S1-E1 on UT 2007/07/26, seq 002

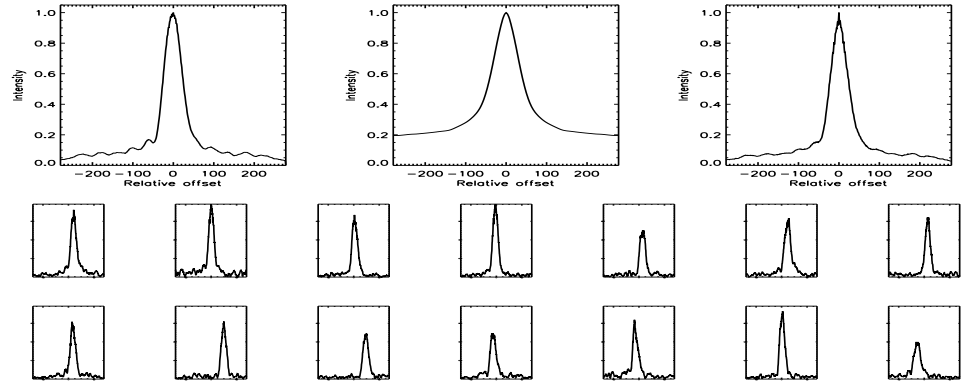

FIGURE B.627: SFP inspection for HD 219134 with S1-W1 on UT 2007/07/26, seq 003

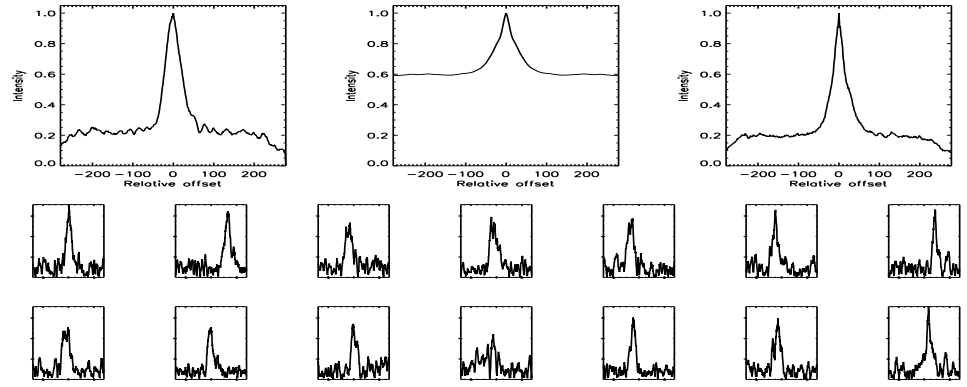

FIGURE B.628: SFP inspection for HD 219538 with S1-E1 on UT 2007/08/14, seq 001

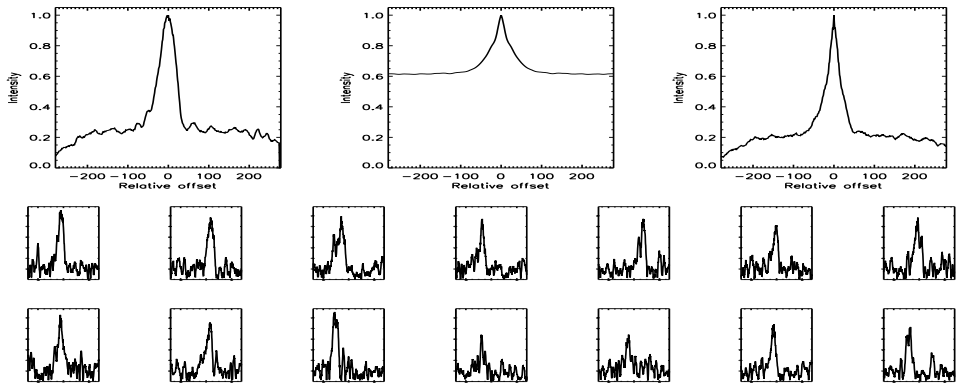

FIGURE B.629: SFP inspection for HD 219538 with S1-W1 on UT 2007/08/14, seq 002

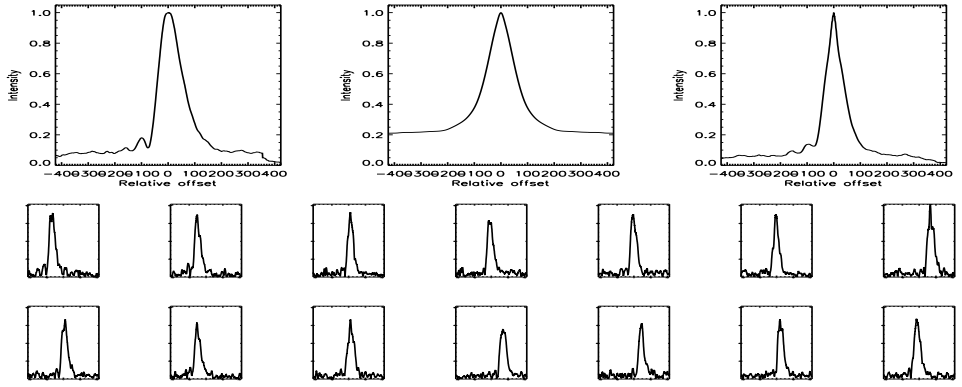

FIGURE B.630: SFP inspection for HD 219623 with S1-E1 on UT 2007/08/18, seq 002

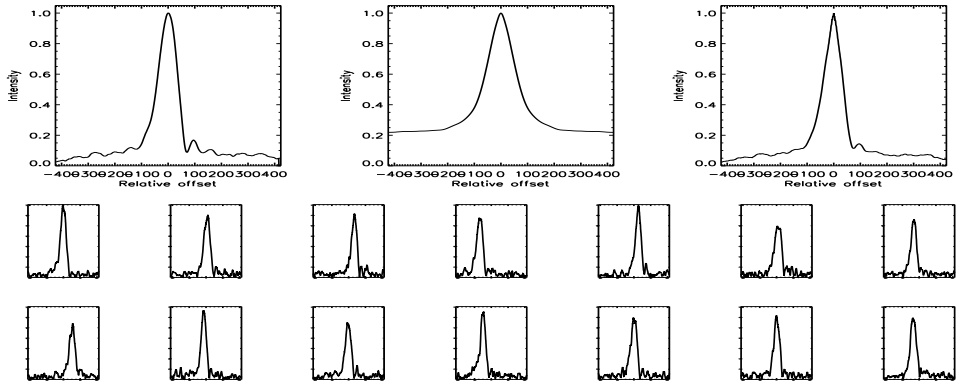

FIGURE B.631: SFP inspection for HD 219623 with S1-W1 on UT 2007/08/18, seq 001

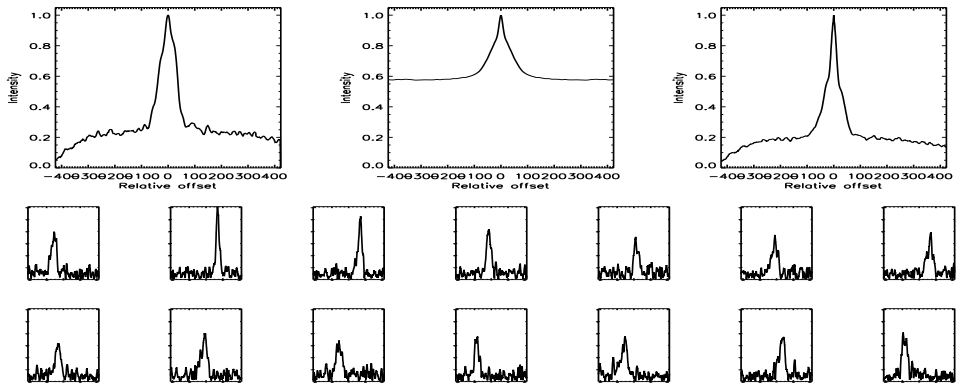

FIGURE B.632: SFP inspection for HD 219623 with S2-E1 on UT 2007/08/20, seq 001

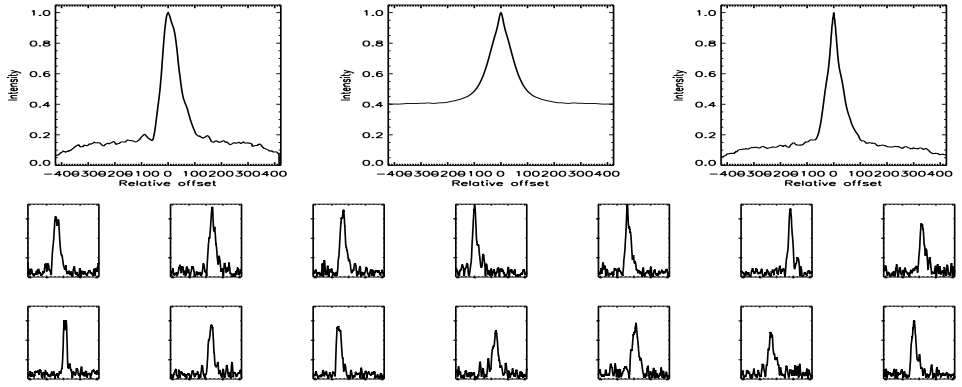

FIGURE B.633: SFP inspection for HD 220140 with S1-E1 on UT 2007/09/16, seq 002

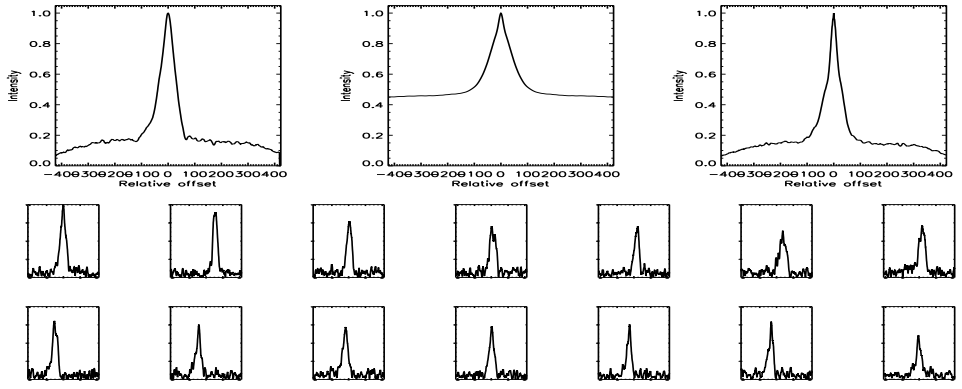

FIGURE B.634: SFP inspection for HD 220140 with S1-W1 on UT 2007/09/16, seq 001

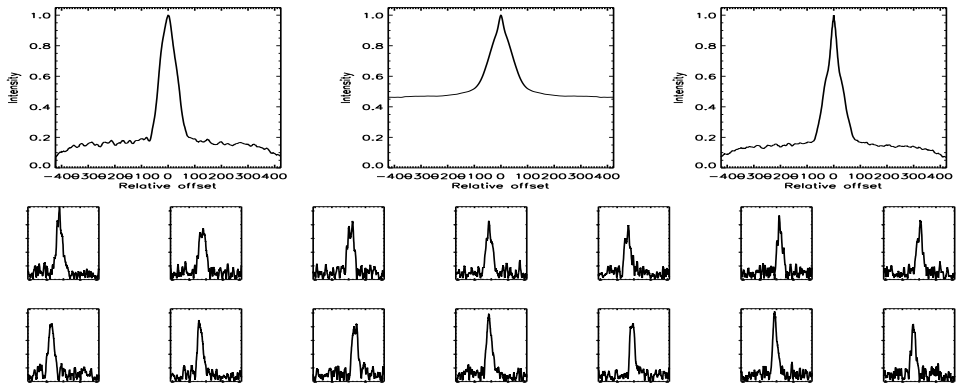

FIGURE B.635: SFP inspection for HD 220182 with S1-E1 on UT 2007/08/18, seq 002

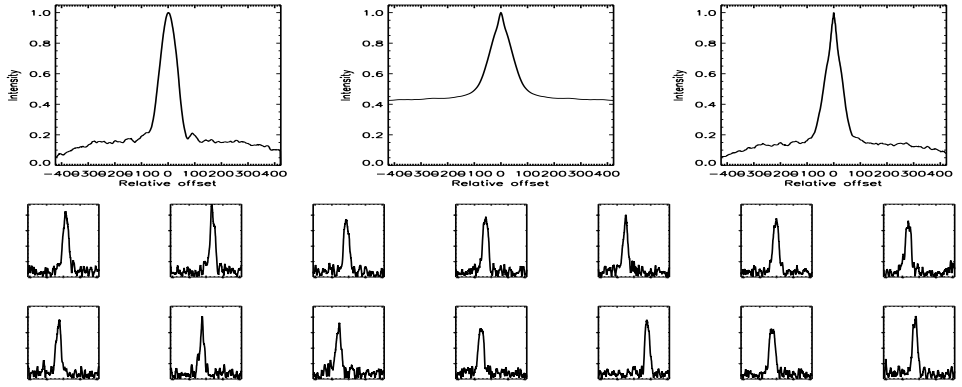

FIGURE B.636: SFP inspection for HD 220182 with S1-W1 on UT 2007/08/18, seq 001

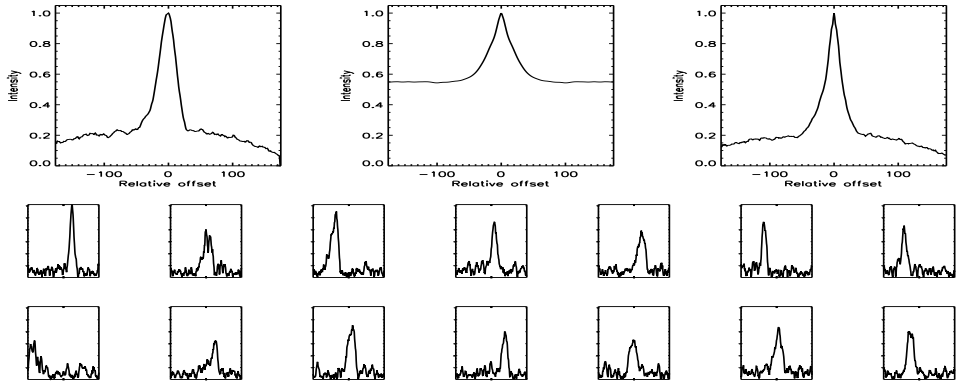

FIGURE B.637: SFP inspection for HD 220339 with S1-E1 on UT 2008/07/06, seq 001

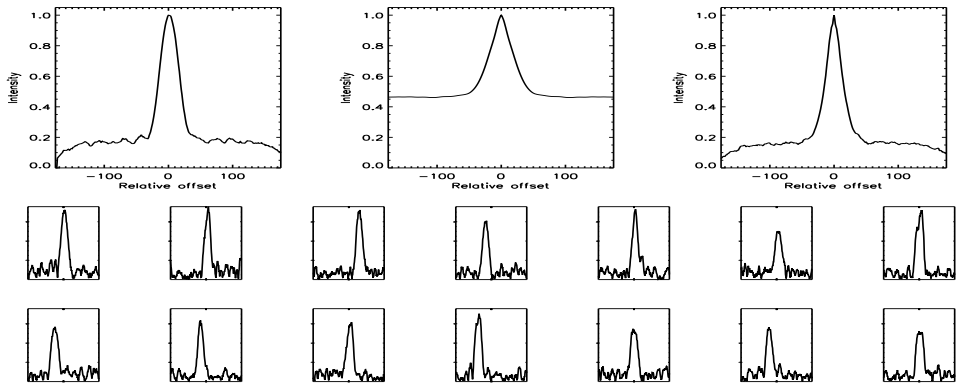

FIGURE B.638: SFP inspection for HD 220339 with S1-W1 on UT 2008/07/07, seq 001

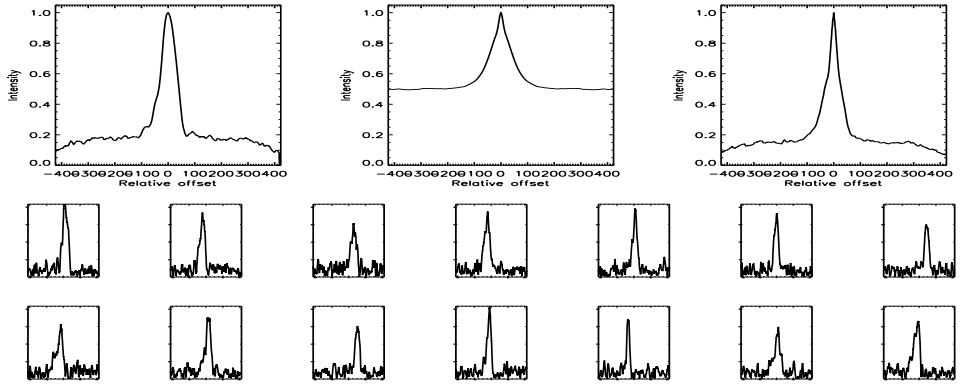

FIGURE B.639: SFP inspection for HD 221354 with S1-E1 on UT 2007/09/16, seq 002

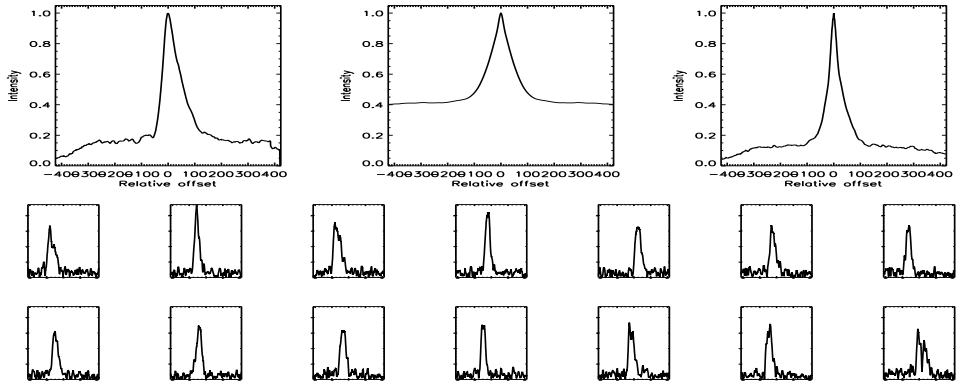

FIGURE B.640: SFP inspection for HD 221354 with S1-W1 on UT 2007/09/16, seq 001

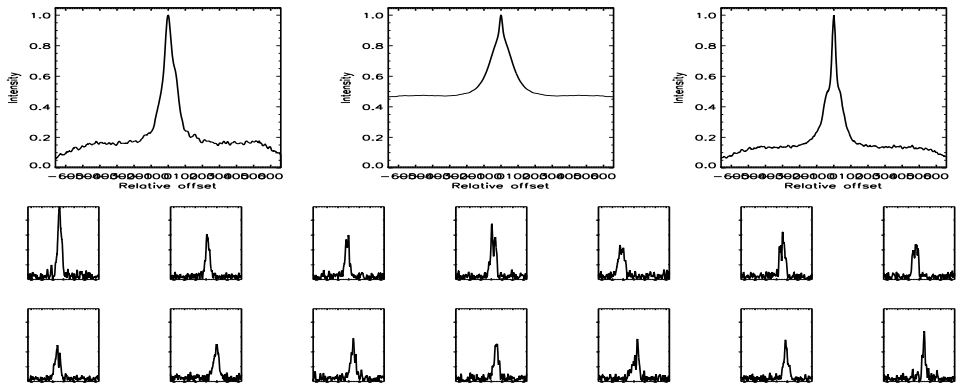

FIGURE B.641: SFP inspection for HD 221354 with S2-E1 on UT 2007/08/20, seq 002

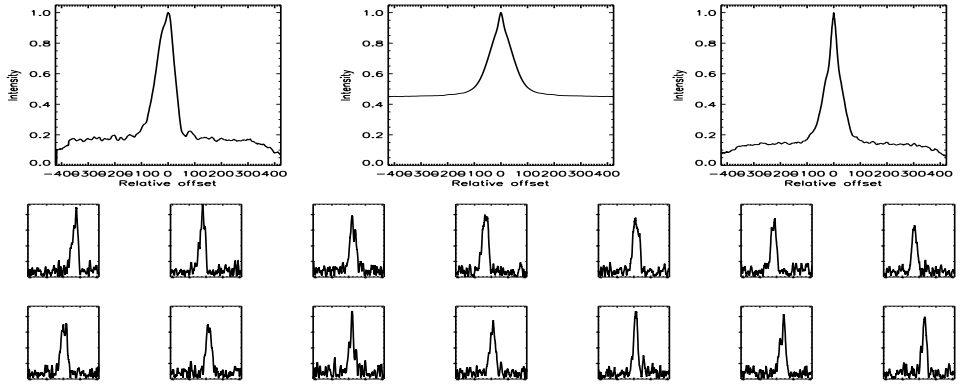

FIGURE B.642: SFP inspection for HD 221851 with S1-E1 on UT 2007/08/18, seq 002

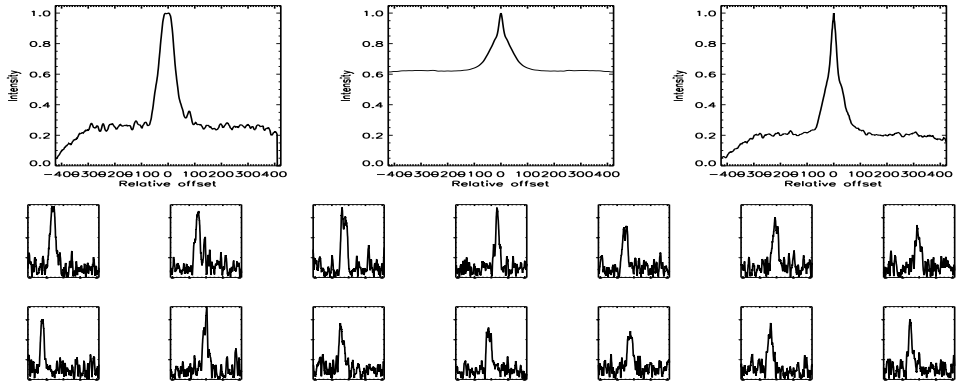

FIGURE B.643: SFP inspection for HD 221851 with S1-W1 on UT 2007/08/18, seq 001

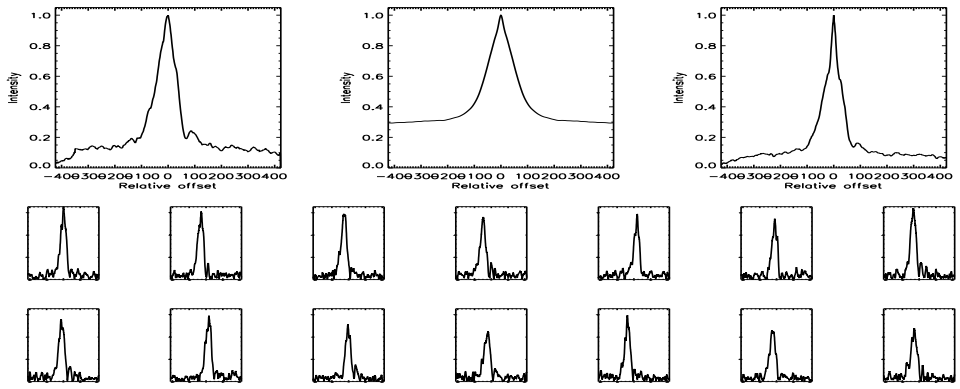

FIGURE B.644: SFP inspection for HD 222143 with S1-E1 on UT 2007/07/27, seq 001

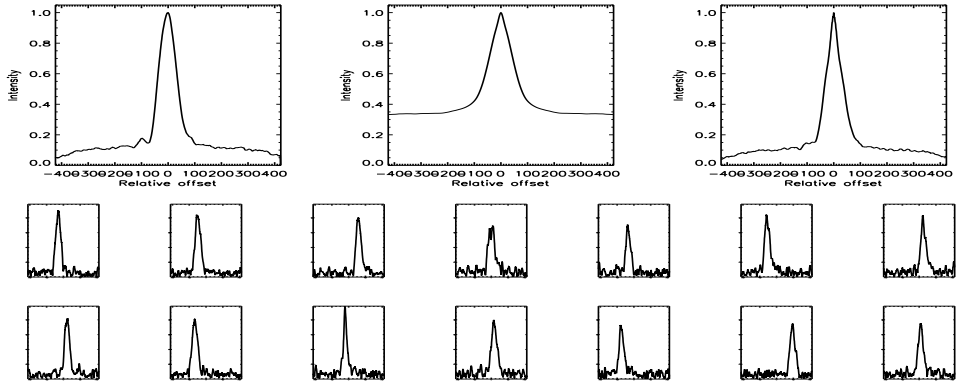

FIGURE B.645: SFP inspection for HD 222143 with S1-E1 on UT 2007/08/18, seq 002

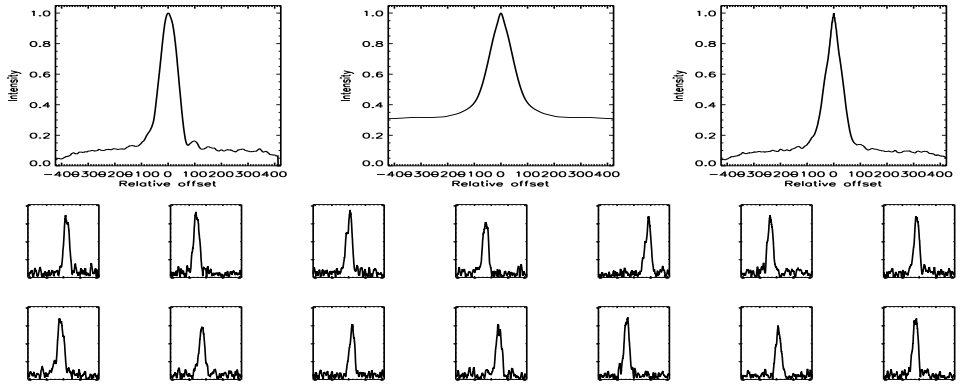

FIGURE B.646: SFP inspection for HD 222143 with S1-W1 on UT 2007/08/18, seq 001

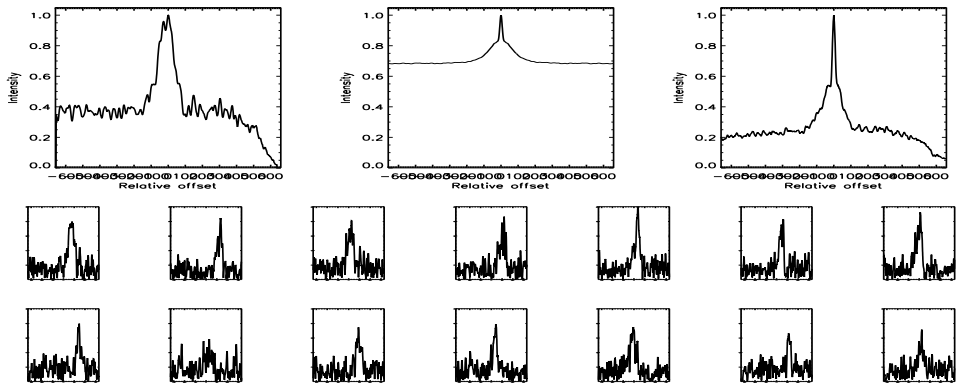

FIGURE B.647: SFP inspection for HD 222143 with S2-E1 on UT 2007/08/20, seq 001

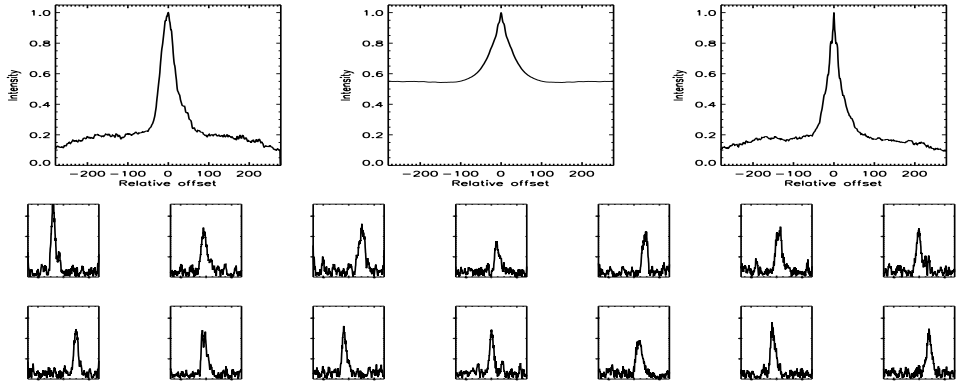

FIGURE B.648: SFP inspection for HD 222404 with S1-E1 on UT 2007/09/16, seq 003

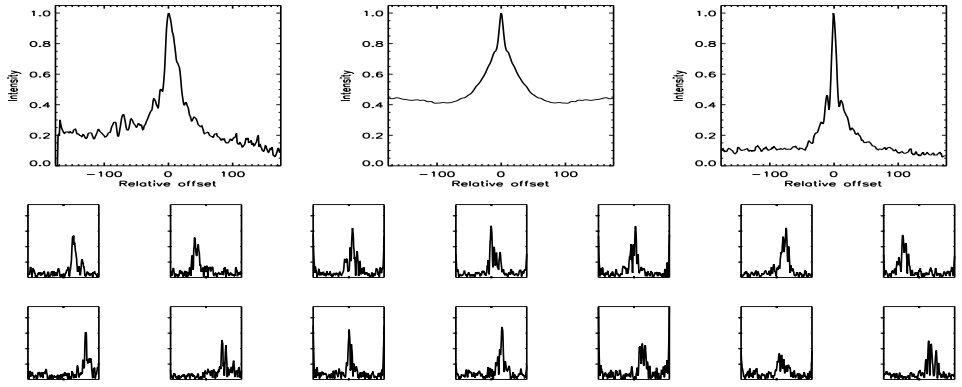

FIGURE B.649: SFP inspection for HD 222404 with S1-E1 on UT 2008/06/25, seq 001

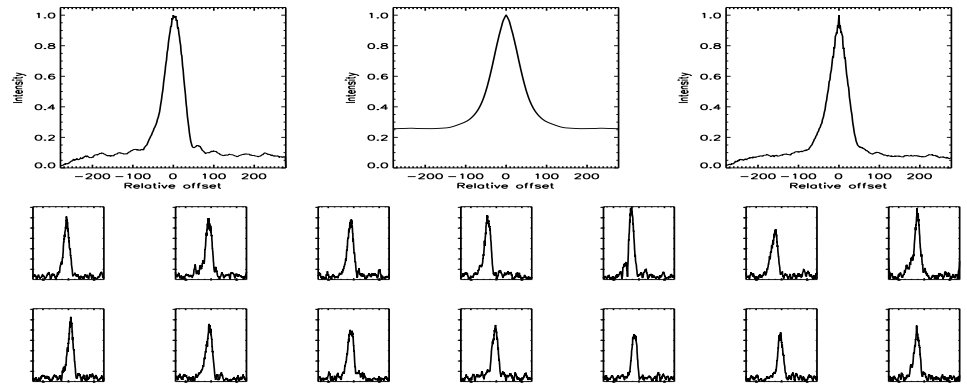

FIGURE B.650: SFP inspection for HD 222404 with S1-W1 on UT 2007/09/16, seq 002

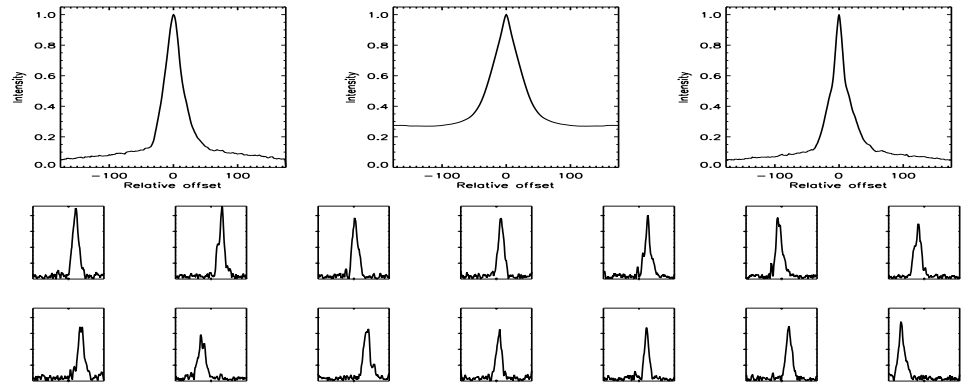

FIGURE B.651: SFP inspection for HD 222404 with S1-W1 on UT 2008/04/26, seq 001

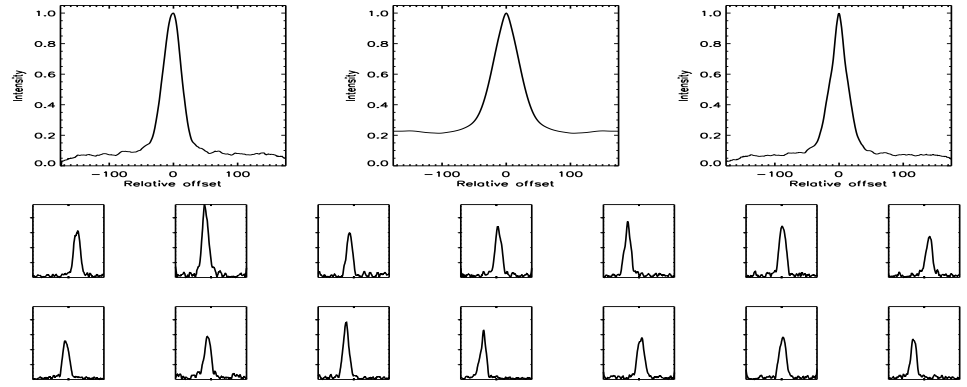

FIGURE B.652: SFP inspection for HD 222404 with S2-W1 on UT 2008/06/24, seq 001

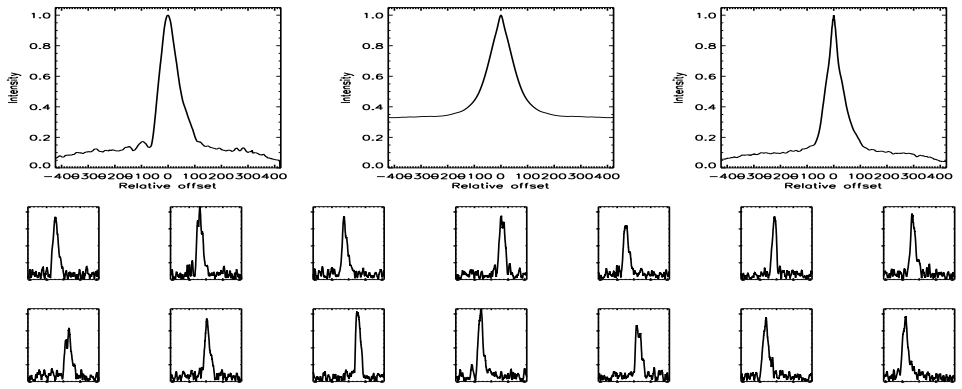

FIGURE B.653: SFP inspection for HD 224465 with S1-E1 on UT 2007/08/18, seq 002

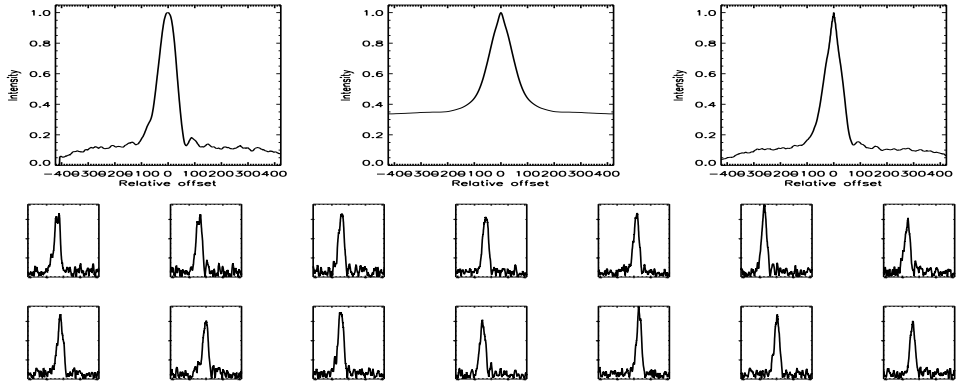

FIGURE B.654: SFP inspection for HD 224465 with S1-W1 on UT 2007/08/18, seq 001

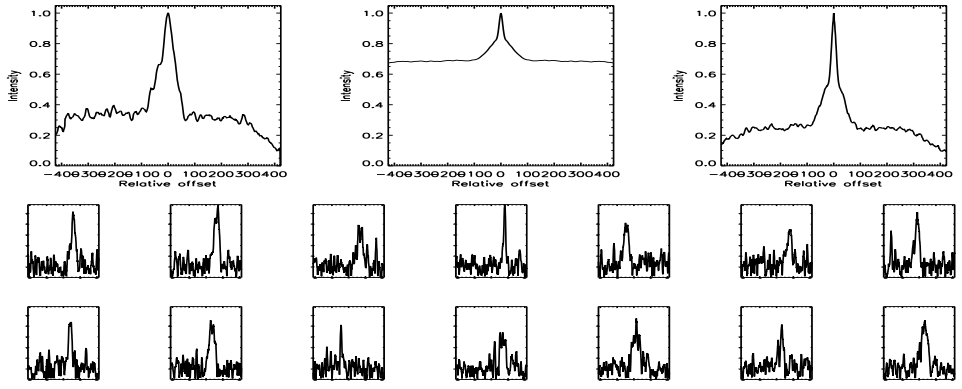

FIGURE B.655: SFP inspection for HD 224465 with S2-E1 on UT 2007/08/20, seq 001

– C –

IDL Programs

This appendix reproduces the IDL codes written for some important aspects of the this project including observation planning and data processing.

C.1 CHARA Observations Planning Tool for Survey Projects

C.1.1 Example Input File

```
;IMPORTANT: DO NOT MODIFY THE FORMATTING OF THIS FILE.
;           ENTER YOUR DATA IN RELEVANT PLACES, BUT LEAVE HEADER LINES
;           AND POSITIONING OF THE DATA ELEMENTS UNCHANGED!
;#########################################################################
;#  INPUT FILE FOR CHARA PLAN (BATCH VERSION)                            #
;#  See comments in IDL program chara_planB.pro for a better             #
;#  description of the program.                                          #
;#  Questions? Contact: Deepak Raghavan (raghavan@chara.gsu.edu)         #
;#########################################################################
;
Observing Date (YYYY/MM/DD): 2007/02/15
Wave Band (K, H): K
Minimum observing time required per target (hours): 1.5

START BASELINE/POP LIST
+--------------+----------------+----------------+
| Baseline     |  POPs Tel 1    |  POPs Tel 2    |
| (e.g. S1-E1) |  (e.g. 1,2,3)  |  (e.g. 1,2,3)  |
| Enter your data below, as many lines as needed |
|              |                |                |
| S1-E1        |  1,2,3,4       |  1,2           |
| S1-W1        |  1             |  1             |
| W1-W2        |  1,2           |  1,2,4         |
|              |                |                |
|              |                |                |
+---END-BP-----+----------------+----------------+

START TARGET LIST (HD number or coordinates & epoch)
Enter HD numbers or coordinates & epoch below, one entry per row:
HD number format: nnnnnn; Coordinate/epoch format: hh:mm:ss.ss +dd:mm:ss.s eeee.ee
224930
00:06:36.78 +29:01:17.4 2000.00
000166
039587
07:29:01.77 +31:59:37.8 2000.00
07:54:34.18 -01:24:44.1 2000.00
160346
217107
```

C.1.2 IDL code

```
;######################################################################
;#  CHARA PLAN (BATCH VERSION)                                        #
;#                                                                    #
;#  An observing prepation tool for the CHARA array                   #
;#  Original Version: January 3, 2007                                 #
;#  Deepak Raghavan (raghavan@chara.gsu.edu)                          #
;#                                                                    #
;#  For a given observing date, filter, set of baselines, POPs, and a #
;#  set of HD numbers, this program will create an output file of the #
;#  subset of targets, baselines, and POPs that can be observed for at#
;#  least a specified number of hours during the night.  A target is  #
;#  considered observable at times between dusk and dawn when its     #
;#  altitude is greater than 30 degrees and the optical path length   #
;#  difference between the two telescopes is less than the maximum    #
;#  range that the OPLE carts can compensate for.                     #
;#  Most of the logic in CHK_AVAIL was borrowed from Jason            #
;#  Aufdenbereg's CHARA_PLAN program, with modifications and          #
;#  enhancements as required.                                         #
;#                                                                    #
;#  Input: Specified in chara_planB.inp (see that file for formatting)#
;#  Output: chara_planB.out                                           #
;#  NOTE: Input file must be in current directory from where you run  #
;#        the IDL program!  The output file will also be created in   #
;#        same directory.                                             #
;#  CAUTION: If a file with same name as output file exists in current#
;#           directory, it will be overwritten!                       #
;#                                                                    #
;#  Maintenance Log:                                                  #
;#  ***************                                                   #
;#     1/25/07  Fixed bug to account for non-consecutive delay/alt avl#
;#        e.g. if delay is avail from 2:00 - 3:30 and then again from #
;#        6:00 - 6:30, the old version assumed avail from 2:00 - 6:30! #
;#                                                                    #
;######################################################################
pro chara_planB  ; CHARA_PLAN_BATCH

;
;  Comon variables to share with chk_avail
;

common CHARA, TELESCOPES, BASELNAME, POPS
common params, year_obs, month_obs, day_obs, wave_band, min_obst


;#
;#  SETUP CHARA CONSTANTS
;#

TELESCOPES = ['S1','S2','E1','E2','W1','W2'] ; Tels are numbered 0 - 5
BASELNAME = ['S1S2','E1E2','W1W2','W2E2','S2W2','S1W2','E1W2','S2E2',$
             'S2W1','W1E2','S1W1','S1E2','S2E1','E1W1','S1E1'] ; Baselines are numbered 0 - 14
POPS = [1,2,3,4,5]

;  Non CHARA-related constants:

MAX_HD = 359083  ; Maximum HD number from 1949 extension of the catalog

;#
;#  READ INPUT FILE TO GET PARAMETERS
;#
openr,1,'./chara_planB.inp'

input = '; '  ; Read and ignore header lines; read first data line
while (NOT EOF(1)) do begin
      readf,1,input
      if (STRMID(input,0,1) NE ';') then BREAK ; First data line found
endwhile

if (EOF(1)) then begin          ; Premature end of file!
   print,'End of input file reached before required data gathered (1)!'
   print,'  Please fix the input file and rerun this program'
   close,1
   goto, done
endif

;
;#  Extract observing date
;
work = strsplit(input,':',/extract)
```

```
if (work(0) NE 'Observing Date (YYYY/MM/DD)') then begin
   print,'Invalid first line of data (after header lines)!'
   print,'  You entered  : ', input
   print,'  Valid example: ', 'Observing Date (YYYY/MM/DD): 2007/02/15'
   print,'  Please fix the input file and rerun this program'
   close,1
   goto, done
endif

work2 = strsplit(work(1),'/',/extract)
year_obs = work2(0) * 1
month_obs = work2(1) * 1
day_obs = work2(2) * 1

;  Validate date: Not perfect, but good enough!
;  If folks are still using this program after 2050, we have BIG problems!
;
if (year_obs LT 2000 OR year_obs GT 2050 OR $
    month_obs LT 1 OR month_obs GT 12 OR $
    day_obs LT 1 OR day_obs GT 31) then begin
   print,'Invalid observing date entered!'
   print,'  You entered date as: ', work(1)
   print,'  It should be in YYYY/MM/DD format'
   print,'  Please fix the input file and rerun this program'
   close,1
   goto, done
endif

;
;#  Extract and validate observing wave band
;
readf,1,input
if (EOF(1)) then begin          ; Premature end of file!
   print,'End of input file reached before required data gathered (2)!'
   print,'  Please fix the input file and rerun this program'
   close,1
   goto, done
endif

work = strsplit(input,':',/extract)
if (work(0) NE 'Wave Band (K, H)') then begin
   print,'Invalid second line of data (after header lines)!'
   print,'  You entered  : ', input
   print,'  Valid example: ', 'Wave Band (K, H): K'
   print,'  Please fix the input file and rerun this program'
   close,1
   goto, done
endif

wave_band = work(1)
rmv_blank,wave_band
if (wave_band NE 'K' AND wave_band NE 'H') then begin
   print,'Invalid Wave Band value entered'
   print,'  You entered: ', wave_band
   print,'  Valid values are K or H'
   print,'  Please fix the input file and rerun this program'
   close,1
   goto, done
endif

;
;#  Extract and validate minimum observing time per target (hours)
;
readf,1,input
if (EOF(1)) then begin          ; Premature end of file!
   print,'End of input file reached before required data gathered (3)!'
   print,'  Please fix the input file and rerun this program'
   close,1
   goto, done
endif

work = strsplit(input,':',/extract)
if (strmid(work(0),0,11) NE 'Minimum obs') then begin
   print,'Invalid third line of data (after header lines)!'
   print,'  You entered  : ', input
   print,'  Valid example: ', 'Minimum observing time required per target (hours): 1.5'
   print,'  Please fix the input file and rerun this program'
   close,1
   goto, done
```

```
endif

min_obst = work(1) * 1.  ; Minimum observing time per target (hours)
if (min_obst LE 0 OR min_obst GE 10) then begin
   print,'Invalid minimum observing time entered'
   print,'  You entered: ', min_obst
   print,'  Value must be greater than zero and less than 10'
   print,'  Default value of 1.5 hours assumed'
   min_obst = 1.5
endif

;#
;#  Extract Baselines & POPs from input list
;#

while (NOT EOF(1)) do begin   ; skip to "start baseline/pop list"
      readf,1,input
      if (STRMID(input,0,10) EQ 'START BASE') then BREAK  ; Start found
endwhile

if (EOF(1)) then begin          ; Premature end of file!
   print,'End of input file reached before required data gathered (4)!'
   print,'  Please fix the input file and rerun this program'
   close,1
   goto, done
endif

i = 0
while (NOT EOF(1)) do begin   ; skip 4 comment lines
      readf,1,input
      i = i + 1
      if (i GE 4) then BREAK  ; 4 lines skipped
endwhile

if (EOF(1)) then begin          ; Premature end of file!
   print,'End of input file reached before required data gathered (5)!'
   print,'  Please fix the input file and rerun this program'
   close,1
   goto, done
endif

;
;  Start gathering baseline/POP data
;
nbr_bl = 0
maxnbl = size(BASELNAME,/dimensions)  ; Get maximum number of baselines possible
inp_tel1a = strarr(maxnbl)
inp_tel2a = strarr(maxnbl)
inp_pop1a = intarr(maxnbl,5)
inp_pop2a = intarr(maxnbl,5)
;
;#  Begin baseline/POP loop
;
while (NOT EOF(1)) do begin

    readf,1,input  ; Read baseline/POP data line
    if (STRMID(input,0,10) EQ '+---END-BP') then BREAK ; end of BL/POP data

    work = strsplit(input,'|',/extract)
    nelem = size(work,/dimensions)
    If (nelem(0) NE 3) then begin
       print,'Invalid baseline,POP data line'
       print,'  You entered  : ', input
       print,'  Valid example: ', '| S1-E1        |  1,2,3,4,5     |  1,2,3,4,5     |'
       print,'  This data line will be ignored'
       CONTINUE ; Skip to next iteration of baseline/POP loop
    endif

;
;   3 elements found as required (baseline, pop1, pop2), so proceed...
;

;
;  Extract and validate telescopes
;
    ibase = work(0)
    rmv_blank,ibase
    ipop1 = work(1)
    rmv_blank,ipop1
```

```
    ipop2 = work(2)
    rmv_blank,ipop2
    if (ibase EQ '' AND ipop1 EQ '' AND ipop2 EQ '') then $
       CONTINUE ; Skip bkank line, go to next iteration of baseline/POP loop

    itel = strsplit(ibase,'-',/extract)
    ntel = size(itel,/dimensions)
    if (ntel(0) NE 2) then begin  ; Two telescopes found?
       print,'Baseline format invalid'
       print,'  You entered  : ', input
       print,'  Valid example: ', '| S1-E1        |  1,2,3,4,5     |  1,2,3,4,5     |'
       print,'  This data line will be ignored'
       CONTINUE ; Skip to next iteration of baseline/POP loop
    endif

    itel1 = itel(0)
    t1 = where(TELESCOPES EQ itel1) ; Set numeric value of Tel 1
    if (t1(0) EQ -1) then begin   ; Invalid Tel 1
       print,'Invalid value for Telescope 1: ', itel1
       print,'  In data line: ', input
       print,'  Valid values are: S1, S2, E1, E2, W1, W2'
       print,'  This data line will be ignored'
       CONTINUE ; Skip to next iteration of baseline/POP loop
    endif

    itel2 = itel(1)
    t2 = where(TELESCOPES EQ itel2) ; Set numeric value of Tel 2
    if (t2(0) EQ -1) then begin   ; Invalid Tel 2
       print,'Invalid value for Telescope 2: ', itel2
       print,'  In data line: ', input
       print,'  Valid values are: S1, S2, E1, E2, W1, W2'
       print,'  This data line will be ignored'
       CONTINUE ; Skip to next iteration of baseline/POP loop
    endif

    if (itel1 EQ itel2) then begin ; Tel 1 & 2 can not be the same!
       print,format='("Telescope 1 and 2 have same value!: ",A2,", ",A2)', itel1, itel2
       print,'  In data line: ', input
       print,'  Choose different telescope values'
       print,'  This data line will be ignored'
       CONTINUE ; Skip to next iteration of baseline/POP loop
    endif

;
;   Extract and validate pop1 & pop2
;
    errdata = 'N'

    for i = 1, 2 do begin  ; Process POP1 and POP2 lists

        ipop = strsplit(work(i),',',/extract)
        npop = size(ipop,/dimensions)
        if (npop(0) LT 1 OR npop(0) GT 5) then begin  ; Invalid number of pops
           print,format='("POP ",I1, " format invalid")', i
           print,'  You entered: ', input
           print,'  Enter upto 5 POPs, comma demilited'
           print,'  This data line will be ignored'
           errdata = 'Y'
           BREAK ; Exit FOR loop and proceed to process next data line
        endif

        for j = 0, 4 do begin ; Always load array with 5 elements (0 fill at end)

            if (j GE npop(0)) then begin  ; Zero fill at end of array
               curpops = [curpops, 0]
               CONTINUE
            endif

            ipop(j) = ipop(j) * 1
            if (ipop(j) LT 1 OR ipop(j) GT 5) then begin ; Invalid pop number
               print,format='("POP number ",I1, " for POP-", I1, " invalid: ",I2)',j+1,i,ipop(j)
               print,'  In data line: ', input
               print,'  POP numbers must be between 1 & 5'
               print,'  This data line will be ignored'
               errdata = 'Y'
               BREAK ; Exit FOR loop and proceed to process next data line
            endif
;
;           Save valid POP in array
```

```
;
            if (j EQ 0) then curpops = ipop(j) $
            else curpops = [curpops, ipop(j)]

        endfor ; for loop for 5 elements ends

        if (errdata EQ 'Y') then BREAK ; Skip to next baseline/POP data

        if (i EQ 1) then curpops1 = curpops $
        else curpops2 = curpops

    endfor  ; for loop for 2 POPs ends

    if (errdata EQ 'Y') then CONTINUE ; Skip to next baseline/POP data

    nbr_bl = nbr_bl + 1
    bli = nbr_bl - 1
    if (nbr_bl GT maxnbl) then begin  ; Can only process 25 baselines
       print,'Cannot process more than 25 valid baseline/POP data lines'
       print,'  Will ignore input: ', input
       CONTINUE ; Skip to next iteration of baseline/POP loop
    endif

    inp_tel1a(bli) = itel1
    inp_tel2a(bli) = itel2
    inp_pop1a(bli,*) = curpops1
    inp_pop2a(bli,*) = curpops2

endwhile
;
;#  END baseline/POP loop
;

if (EOF(1)) then begin          ; Premature end of file!
   print,'End of input file reached before required data gathered (6)!'
   print,'  Please fix the input file and rerun this program'
   close,1
   goto, done
endif

if (nbr_bl EQ 0) then begin          ; No valid baselines found
   print,'No valid baseline/POP found!'
   print,'  Please fix the input file and rerun this program'
   close,1
   goto, done
endif

;#
;#  Extract HD numbers and/or coordinates from input list
;#

while (NOT EOF(1)) do begin   ; skip to "start target list"
      readf,1,input
      if (STRMID(input,0,12) EQ 'START TARGET') then BREAK  ; Start found
endwhile

if (EOF(1)) then begin          ; Premature end of file!
   print,'End of input file reached before required data gathered (7)!'
   print,'  Please fix the input file and rerun this program'
   close,1
   goto, done
endif

i = 0
while (NOT EOF(1)) do begin   ; skip 2 comment lines
      readf,1,input
      i = i + 1
      if (i GE 2) then BREAK  ; 2 lines skipped
endwhile

if (EOF(1)) then begin          ; Premature end of file!
   print,'End of input file reached before required data gathered (8)!'
   print,'  Please fix the input file and rerun this program'
   close,1
   goto, done
endif

;
;  Gather target HD/coords into an array
```

```
;

nbr_tar = 0
restore,'/usr/local/rsi/idl_lib/CHARA_PLAN_V1.2/hipp_ra_dec_hd_spec.sav' ; Restore HIPPARCOS catalog
while (NOT EOF(1)) do begin

      readf,1,input
;
;  If colon found in data, treat as coordinates, else treat as HD number
;
      work = strsplit(input,':',/extract)
      nelem = size(work,/dimensions)
      If (nelem(0) LE 1) then begin    ; HD number as no colon found

         curhd = input * 1.
;
;     Validate HD number range and against HIP catalog
;
         if (curhd LE 0 OR curhd GT MAX_HD) then begin  ; Invalid HD number
            print,'Invalid HD number specified: ', curhd
            print,'  In data line: ', input
            print,'  Valid values are between 1 and ', MAX_HD
            print,'  This data line will be ignored'
            CONTINUE ; Skip to next iteration of HD loop
         endif

         hipind = where(hipp_hd eq curhd)
         if (hipind(0) eq -1) then begin  ; star not in Hipparcos catalog
            print,format='("Cannot find coordinates for HD ",I6," in HIPPARCOS catalog")', curhd
            print,'  In data line: ', input
            print,'  This data line will be ignored'
            CONTINUE ; Skip to next iteration of HD loop
         endif

         irad = hipp_ra(hipind(0))    ; HIP RA in degrees
         idecd = hipp_dec(hipind(0))  ; HIP DEC in degrees
         iepoc = 1991.25              ; Epoch of HIP coordinates


      endif else begin                ; Coordinates entered

         curhd = 0.
         work = strsplit(input,' ',/extract)  ; Extract RA, DEC, Epoch
         nelem = size(work,/dimensions)
         If (nelem(0) LT 3) then begin    ; 3 elements not found (ra, dec, epoch)
            print,'Coordinates format is invalid'
            print,'  You entered  : ', input
            print,'  Valid example: ', '07:01:38.10 +48:22:47.0 2000.0'
            print,'  This data line will be ignored'
            CONTINUE ; Skip to next iteration of target loop
         endif

         ira = work(0)  ; Input RA
         idc = work(1)  ; Input Dec
         iep = work(2)  ; Input Epoch
;
;        Extract RA and convert to decimal degrees
;
         work = strsplit(ira,':',/extract)
         nelem = size(work,/dimensions)
         If (nelem(0) NE 3) then begin    ; 3 elements not found (rah, ram, ras)
            print,'Coordinate RA format is invalid'
            print,'  You entered  : ', input
            print,'  Valid example: ', '07:01:38.10 +48:22:47.0 2000.0'
            print,'  This data line will be ignored'
            CONTINUE ; Skip to next iteration of target loop
         endif

         irah = work(0) * 1
         iram = work(1) * 1
         iras = work(2) * 1.
         if (irah LT 0 or irah GE 24 or iram LT 0 or iram GE 60 or iras LT 0. or iras GE 60.) then b
egin
            print,'Coordinate RA h/m/s value is invalid'
            print,'  You entered  : ', input
            print,'  Hour must be between 0 and 24, minute and second must be between 0 and 60'
            print,'  This data line will be ignored'
            CONTINUE ; Skip to next iteration of target loop
         endif
```

```
         irad = TEN(irah,iram,iras) * 15.  ; Convert from h:m:s to decimal degrees
;
;        Extract DEC and convert to decimal degrees
;
         work = strsplit(idc,':',/extract)
         nelem = size(work,/dimensions)
         If (nelem(0) NE 3) then begin    ; 3 elements not found (dcd, dcm, dcs)
            print,'Coordinate DEC format is invalid'
            print,'  You entered  : ', input
            print,'  Valid example: ', '07:01:38.10 +48:22:47.0 2000.0'
            print,'  This data line will be ignored'
            CONTINUE ; Skip to next iteration of target loop
         endif

         idcd = work(0) * 1
         idcm = work(1) * 1
         idcs = work(2) * 1.
         if (idcd LT -90 or idcd GE +90 or idcm LT 0 or idcm GE 60 or idcs LT 0. or idcs GE 60.) the
n begin
            print,'Coordinate DEC d/m/s value is invalid'
            print,'  You entered  : ', input
            print,'  Degree must be between -90 and +90, minute and second must be between 0 and 60'
            print,'  This data line will be ignored'
            CONTINUE ; Skip to next iteration of HD loop
         endif
         idecd = TEN(idcd,idcm,idcs) ; Convert from d:m:s to decimal degrees
;
;        Extract & validate epoch
;
         iepoc = iep * 1.
         if (iepoc LT 1950. or iepoc GT 2100.) then begin
            print,'Coordinate epoch value is invalid'
            print,'  You entered  : ', input
            print,'  Epoch must be between 1950.0 and 2100.0'
            print,'  This data line will be ignored'
            CONTINUE ; Skip to next iteration of target loop
         endif

     endelse


;
;  Save HD ID and coordinates of the target in array
;
      nbr_tar = nbr_tar + 1
      if (nbr_tar EQ 1) then begin
         inp_hda = curhd
         inp_raa = irad     ; RA in degrees
         inp_deca = idecd   ; HIP DEC in degrees
         inp_epocha = iepoc ; Epoch of HIP coordinates
      endif else begin
         inp_hda = [inp_hda, curhd]
         inp_raa = [inp_raa, irad]
         inp_deca = [inp_deca, idecd]
         inp_epocha = [inp_epocha, iepoc]
      endelse

endwhile  ; End of load HD loop

close,1  ; Close input file

if (nbr_tar EQ 0) then begin          ; No valid targets found
   print,'No valid targets found!'
   print,'  Please fix the input file and rerun this program'
   goto, done
endif


;##
;##   INPUT DATA HAS BEEN OBTAINED. NOW, START PROCESSING!
;##

openw,2,'./chara_planB.out'

;
;  Print parameters & headings
;
printf,2,'CHARA observing report created by CHARA_PLANB on ', SYSTIME()
printf,2,' '
```

```
pdate = string(format='(I4,"/",I2,"/",I2)', year_obs, month_obs, day_obs)
sub_string,pdate,' ','0'  ; Substitute blanks with zeroes
printf,2,format='("Observing Date: ",A10)', pdate
printf,2,format='("Wave Band: ",A1)', wave_band
printf,2,format='("Minimum observing time required per target: ",F5.2," hours")', min_obst
printf,2,format='("Total number of valid targets: ",I4)', nbr_tar
printf,2,' '
printf,2,'                                          Obs     Obs Window Opens     Obs Window Closes
 Max  at      Min  at    Max  at'
printf,2,' HD ID  <=== Coordinates ===>  Epoch    Dur     HA     UT    Alt     HA     UT    Alt
 Alt  UT     Base  UT   Base  UT'
printf,2,'                                          (h)     (h) (hh:mm) (deg)    (h) (hh:mm) (deg)
(deg)         (m)        (m)'
printf,2,' '
;
print,' '
print,format='("Total number of valid targets to process: ",I4)', nbr_tar
;
;  Process each baseline
;
for bli = 0, nbr_bl - 1 do begin

    tel_1 = inp_tel1a(bli)
    tel_2 = inp_tel2a(bli)
    curpops1 = inp_pop1a(bli,*)
    curpops2 = inp_pop2a(bli,*)

    print,' '
    print,'Processing baseline: ', tel_1, '-', tel_2, '  ...'

;
;   Process each POP combination
;
    for pop1i = 0, 4 do begin

       pop_1 = curpops1(pop1i)
       if (pop_1 EQ 0) then CONTINUE ; Skip zero POP

       for pop2i = 0, 4 do begin

          pop_2 = curpops2(pop2i)
          if (pop_2 EQ 0) then CONTINUE ; Skip zero POP

;
;         Process each target
;
;         Print start of Baseline/POP to file
          printf,2,format='("Baseline/POP: ",A2,"(",I1,")-",A2,"(",I1,")")', $
               tel_1, pop_1, tel_2, pop_2
          printf,2,' '

          obsct = 0
          for tari = 0, nbr_tar - 1 do begin

             ra = inp_raa(tari)
             dec = inp_deca(tari)
             epoch = inp_epocha(tari)

             chk_avail, tel_1, tel_2, pop_1, pop_2, ra, dec, epoch, $
                          str_obs_ha, end_obs_ha, str_obs_alt, end_obs_alt, $
                          str_obs_ut, end_obs_ut, min_pbase, min_pbase_ut, $
                          max_pbase, max_pbase_ut, max_alt, max_alt_ut, $
                          nbr_avl_int

             obsfl = 'N'
             for ri = 0, nbr_avl_int - 1 do begin ; process each avaliable interval

              obs_dur = end_obs_ha(ri) - str_obs_ha(ri)
              if (obs_dur GE min_obst) then begin
                obsfl = 'Y'
;
;             Format variables for printing
;
               if (inp_hda(tari) EQ 0.) then phd = ' ' $
               else phd = string(format='(I6)',inp_hda(tari))
               radec, ra, dec, ihr, imin, xsec, ideg, imn, xsc
               pra = string(format='(I2,":",I2,":",F4.1)',ihr,imin,xsec)
               sub_string,pra,' ','0'  ; Substitute blanks with zeroes
;              If deg is 0, and DEC is LT 0, radec returns ideg as 0 and sign with imn!
```

```
               if (ideg EQ 0 AND imn LT 0) then $
                  pdec = string(format='("-",I2,":",I2,":",F4.1)',ideg,abs(imn),xsc) $
               else $
                  pdec = string(format='(I3,":",I2,":",F4.1)',ideg,imn,xsc)
               if (strmid(pdec,0,2) EQ ' -') then pdec = '-0' + strmid(pdec,2,9)
               if (strmid(pdec,0,1) EQ ' ') then pdec = '+' + strmid(pdec,1,10)
               sub_string,pdec,' ','0'  ; Substitute blanks with zeroes
               hms = sixty(str_obs_ut(ri))
               pstr_obs_ut = string(format='(I2,":",I2)',hms(0),hms(1))
               sub_string,pstr_obs_ut,' ','0'  ; Substitute blanks with zeroes
               hms = sixty(end_obs_ut(ri))
               pend_obs_ut = string(format='(I2,":",I2)',hms(0),hms(1))
               sub_string,pend_obs_ut,' ','0'  ; Substitute blanks with zeroes
               hms = sixty(min_pbase_ut(ri))
               pmin_pbase_ut = string(format='(I2,":",I2)',hms(0),hms(1))
               sub_string,pmin_pbase_ut,' ','0'  ; Substitute blanks with zeroes
               hms = sixty(max_pbase_ut(ri))
               pmax_pbase_ut = string(format='(I2,":",I2)',hms(0),hms(1))
               sub_string,pmax_pbase_ut,' ','0'  ; Substitute blanks with zeroes
               hms = sixty(max_alt_ut(ri))
               pmax_alt_ut = string(format='(I2,":",I2)',hms(0),hms(1))
               sub_string,pmax_alt_ut,' ','0'  ; Substitute blanks with zeroes

               printf,2,format='(A6," ",A11,A12,F8.2,F6.2,F8.2,"  ",A5,F6.1,F8.2,"  ",A5, F6.1, F8.1
, " ", A5, I7," ",A5, I5," ",A5)', $
                  phd, pra, pdec, epoch, obs_dur, str_obs_ha(ri), pstr_obs_ut, $
                  str_alt(ri), end_obs_ha(ri), pend_obs_ut, end_obs_alt(ri), $
                  max_alt(ri), pmax_alt_ut, $
                  min_pbase(ri), pmin_pbase_ut, max_pbase(ri), pmax_pbase_ut

             endif   ; end obs window avail

            endfor    ; end of interval loop

            if (obsfl EQ 'Y') then   obsct = obsct + 1

          endfor     ; end of HD loop

            printf,2,' '
            printf,2,format='(I4," objects observable for: ",A2,"(",I1,")-",A2,"(",I1,")")', $
                 obsct, tel_1, pop_1, tel_2, pop_2
            printf,2,' '
            print,format='(I4," objects observable for: ",A2,"(",I1,")-",A2,"(",I1,")")', $
                 obsct, tel_1, pop_1, tel_2, pop_2

        endfor ; end of POP 2 loop

    endfor ; end of POP 1 loop

endfor  ; end of baseline loop

close,2

;
;  Completion message
;
print,' '
print,'All done!  Look in ./chara_planB.out for results'

done:
return
end                ; End of chara_planB

;#################################################################
; END PROGRAM: CHARA_PLAN_B                                      #
;#################################################################


;#########################################################################
;#  CHECK_AVAIL                                                          #
;#                                                                       #
;#  An observing prepation tool for the CHARA array                      #
;#  Deepak Raghavan (raghavan@chara.gsu.edu)                             #
;#  Original Version: January 3, 2007                                    #
;#                                                                       #
;#  For a given observing date, filter, baselines, POPs, RA & DEC (in    #
;#  degrees) along with its equinox epoch (in Besselian Year) of target,#
;#  this program checks if the object is observable and returns the      #
;#  time-window of availablility, along with corresponding parameters    #
```

```
;#  such as hour angle, altitude, and projected baseline information.   #
;#  A target is considered observable at times between dusk and dawn    #
;#  when its altitude is greater than 30 degrees and delay is           #
;#  available within the maximum range to compensate for path length    #
;#  differences between the two telescopes.  Most of the logic in       #
;#  CHK_AVAIL was borrowed from Jason Aufdenbereg's CHARA_PLAN          #
;#  program, with modifications and enhancements as required.           #
;#                                                                      #
;#  Input: Tel_1, Tel_1, POP_1, POP_2, HDNUM                            #
;#  Common variables required: See common blocks below                  #
;#  Output: Nbr_Avl_Int: 0 if star is not available, else contains      #
;#                       the number of intervals avail for obs          #
;#            (e.g. is star is avail 01:30-02:45 and again 06:00-08:00, #
;#             this number will be 2)                                   #
;#          Start & End HA, Alt, and UT, Min & Max proj baseline        #
;#          with corresponding UT times,                                #
;#          all of which are arrays with Nbr_Avl_Int elements.          #
;#                                                                      #
;######################################################################
pro chk_avail, tel_1, tel_2, pop_1, pop_2, ra, dec, epoch, $
               str_obs_ha, end_obs_ha, str_obs_alt, end_obs_alt, $
               str_obs_ut, end_obs_ut, min_pbase, min_pbase_ut, $
               max_pbase, max_pbase_ut, max_alt, max_alt_ut, nbr_avl_int

;
;  Common variables between CHARA_PLAN and this procedure
;
common CHARA, TELESCOPES, BASELNAME, POPS
common params, year_obs, month_obs, day_obs, wave_band, min_obst

;#
;#  SETUP CHARA CONSTANTS
;#
;## THE CHARA CONSTANTS BELOW ARE FROM TELESCOPES.CHARA FILE OBTAINED FROM THEO ON 1/4/2007. DR
;
;  Delays for telescope and pop combinations (in meters)
;                        POP1             POP2            POP3            POP4            POP5
POP_DELAYS = dblarr(6,5)
POP_DELAYS(0,*)= [   0.000000000d0,  36.583816633d0, 73.152000000d0,109.743124329d0,143.089005503d0]
  ; S1
POP_DELAYS(1,*)= [ -36.576000000d0,   0.000000000d0, 36.576000000d0, 73.152000000d0,106.479000000d0]
  ; S2
POP_DELAYS(2,*)= [   0.000000000d0,  36.576000000d0, 73.101581148d0,109.686953167d0,142.999272291d0]
  ; E1
POP_DELAYS(3,*)= [ -73.125000000d0, -36.516000000d0,  0.000000000d0, 36.575000000d0, 69.986000000d0]
  ; E2
POP_DELAYS(4,*)= [ -73.116500000d0, -36.576000000d0,  0.000000000d0, 36.605196000d0, 69.903000000d0]
  ; W1
POP_DELAYS(5,*)= [-143.055000000d0,-106.479000000d0,-69.903000000d0,-33.327000000d0,  0.000000000d0]
  ; W2

;#
;# Differential Airpaths (relative to S1) in meters (note the divide
;  by 1.d6 at the end of the array to convert from microns to meters)
;#
AIRPATH = [0.d0, 4532654.762d0, 15314546.348d0, 26372594.395d0,$
           29129044.683d0, -8668143.182d0]/1.d6  ;S1,S2,E1,E2,W1,W2

OPLE_MAX=88 ; in meters  ; The full length of delay provided by the delay carts

;#
;# CHARA LATITUDE and LONGITUDE (for S1 from telescopes.chara)
;#
S1_LAT  = ten(34.,13.,27.7813d0)*(!pi/180.d0) ; lat. in deg --> radians
S1_LONG = ten(-118.,3.,25.31272d0)*(!pi/180.d0) ;long in deg --> radians

;
;#  X, Y, Z offset for each telescope relative to S1 in meters
;          S1       S2             E1               E2             W1               W2
;
XOFFSET=[0.0d0, -5748393.059d0, 125337986.867d0, 70389114.6d0,-175073611.569d0, -69080651.822d0]/1.d
6
YOFFSET=[0.0d0, 33581340.790d0, 305925736.557d0,269714608.0d0, 216338950.344d0, 199355622.792d0]/1.d
6
ZOFFSET=[0.0d0,   643880.188d0,  -5920522.324d0, -2802196.8d0, -10806621.168d0,    447470.433d0]/1.d
6

;  Non CHARA-related constants:
```

```
DOM = [31,28,31,30,31,30,31,31,30,31,30,31]  ; Days in each month (non-leap year)

;#
;#  SETUP VARIABLES BASED ON INPUT AND CONSTANTS
;#

;
;  Convert observing date to Besselian Year format
;
obs_dt_BY = year_obs
for i = 0,month_obs-2 do obs_dt_BY = obs_dt_BY + DOM(i) / 365.25 ; Add prior month days
obs_dt_BY = obs_dt_BY + day_obs / 365.25 ; Add current month days
if ((year_obs mod 4) EQ 0 AND (year_obs mod 400) NE 0 $
     AND month_obs GT 2) then obs_dt_BY = obs_DT_BY + 1/365.25  ; Account for leap year

;
;  Validate telescopes & baselines, flip telescope order if required
;
t1 = where(TELESCOPES EQ  tel_1) ; Set numeric value of Tel 1
if (t1(0) EQ -1) then begin   ; Invalid Tel 1
   print, "Invalid value for Telescope 1! ", tel_1
   return
endif
t2 = where(TELESCOPES EQ  tel_2) ; Set numeric value of Tel 1
if (t2(0) EQ -1) then begin   ; Invalid Tel 2
   print, "Invalid value for Telescope 2! ", tel_2
   return
endif

;  Find baseline number.  If the telescopes are in flipped order, flip
;  them back and flip the POPs as well.  (e.g. E1S1 should be switched
;  to S1E1

tcomb = tel_1 + tel_2
blnum = where(BASELNAME EQ tcomb) ; Set numeric value of baseline
if (blnum(0) EQ -1) then begin   ; Baseline not found
;  CHECK IF TELS ARE FLIPPED!
   tcomb = tel_2 + tel_1
   blnum = where(BASELNAME EQ tcomb) ; Set numeric value of baseline
   if (blnum(0) EQ -1) then begin   ; Invalid Baseline
      print, "Invalid baseline! ", tcomb
      return
   endif else begin  ; FLIP TELESCOPES TO RIGHT ORDER
      hold_tel = tel_1
      tel_1 = tel_2
      tel_2 = hold_tel
      hold_t = t1
      t1 = t2
      t2 = hold_t
      hold_pop = pop_1  ;  Flip pop when telescopes are flipped!
      pop_1 = pop_2
      pop_2 = hold_pop
   endelse
endif

;
;  Set pop numbers for telescopes 1 & 2
;
pop1 = where(POPS EQ pop_1)
if (pop1(0) EQ -1) then begin   ; Invalid Pop
   print, "Invalid POP for Tel 1! ", pop_1
   return
endif
pop2 = where(POPS EQ pop_2)
if (pop2(0) EQ -1) then begin   ; Invalid Pop
   print, "Invalid POP for Tel 2! ", pop_2
   return
endif

;
;  Compute delay for telescope & pop combination
;
pop_delay = POP_DELAYS(t2,pop2) - POP_DELAYS(t1,pop1)
pop_delay = pop_delay(0) ; Convert to scalar so future math with vectors works!

;
; precess to current epoch
;
wra  = ra
```

```
wdec = dec
precess,wra,wdec,epoch,obs_dt_BY
wra  = wra/15.0d0           ;RA:  degrees ---> hours
wdec = wdec*!pi/180.d0      ;DEC: degrees --->;radians

;#  Following code is largely lifted from CHARA_CONFIG proecdure in
;#  CHARA_PLAN and modified as needed to suit the needs of this
;#  program.  Deepak Raghavan 2007/01/02

;#
;# Return air path difference (in meters) for current baseline

basevec=dblarr(3)
basevec(0) = xoffset(t1) - xoffset(t2) ;east
basevec(1) = yoffset(t1) - yoffset(t2) ;north
basevec(2) = zoffset(t1) - zoffset(t2) ;up
air_diff = AIRPATH(t1) - AIRPATH(t2)
air_diff = air_diff(0) ; Convert to scalar so future math with vectors works!


;#
;# from the WAVEBAND user input, select K or H band
;#

if (wave_band eq 'K') then lam = 2.2*1.e-6  ; wavelength in meters
if (wave_band eq 'H') then lam = 1.6*1.e-6  ; wavelength in meters


;#############################################################################################
;# Compute local mean sidereal time for a given date                                         #
;#############################################################################################
;# We need this to convert hour angles to UT times for a given date
;#
;#  See "Greenwich Mean Sidereal Time GMST" (on Page B6 from the Astronomical Almanac)
;#  under TIME-SCALES: "Relationships between universal and sidereal time"
;#
;# use ASTROLIB idl routine 'juldate' to compute the reduced julian
;# date (RJD)at UT=0h for the users inputs YEAR, MONTH, DAY
;#

juldate,[year_obs,month_obs,day_obs,0,0,0],rjd  ; Zeroes for time

;#
;# Here we follow the Astronomical Almanac Formulae
;# Also see http://aa.usno.navy.mil/faq/docs/GAST.html

tu=(rjd-51545.d0)/36525.d0  ;# Julian centuries of 36525 days since ;J2000.0

;# Greenwich Mean Sidereal Time at Oh UT (in seconds)
gmst= 24110.54841d0 + (8640184.812866d0*tu) + (0.093104d0*tu*tu) + (6.2d-6*tu*tu*tu)

;# Greenwich Mean Sidereal Time in hours
;#
gmst_h=(gmst/3600.d0)
while(gmst_h gt 24) do     gmst_h=gmst_h-24.d0 ; Reduce value to between 0 - 24
while(gmst_h lt 0) do     gmst_h=gmst_h+24.d0

;#
;# Local Mean Sidereal Time in hours at 0h UT (longitude correction)
;#
lmst_h=(gmst/3600.d0)+((S1_LONG*180./!pi)/15.d0)
while(lmst_h gt 24) do lmst_h=lmst_h-24.d0 ; Reduce value to between 0 - 24
while(lmst_h lt 0) do lmst_h=lmst_h+24.d0

;# Compute the hour angle of the target star at Oh UT
;# We use this to compute the UT times which correspond the vector
;# of hour angles constructed below

ha_at_ut_zero=lmst_h-ra  ;HA of star at 0h UT on RJD

;#############################################################################################
; end time calcucations
;#############################################################################################


;#############################################################################################
; Setup vectors to collect informatoin such as UT time, Altitude etc
; for hour angle between -6h and +6h
;#############################################################################################
```

```
mm = 48 ; Size of arrays, one element per 15 minutes

pbasevec=dblarr(mm+1)           ;vector to save projected baselines (in meters)
havec=dblarr(mm+1)              ;vector to save hour angles (in hours)
altvec=dblarr(mm+1)             ;vector to save altitudes   (in degrees)
azvec=dblarr(mm+1)              ;vector to save azimuths    (in degrees)
u_vec=dblarr(mm+1)              ;vector of save U component of spatial frequency (cycles/arcsec)
v_vec=dblarr(mm+1)              ;vector of save V component of spatial frequency (cycles/arcsec)
sfvec=dblarr(mm+1)              ;vector to save spatial frequenices sf = sqrt(u^2 + v^2) (cycles/arc
sec)
pavec=dblarr(mm+1)              ;vector of save position angles (degrees). note: PA=arctangent(U/V)
gdvec=dblarr(mm+1)              ;vector of geometric delays (in meters)


;#
;#  TOP of Hour Angle loop.
;#
for m=0,mm do begin

;#  compute hour angle (in radians)
;#  from m=0,48, ha goes from -6 h to +6 h, one point every 15 minutes.
;#
    ha=(0.25*m-6)*(15.d0*!pi/180.d0) ; hour angle in hours --> radians

;#
;# Compute Altitude at this hour angle (see Page B61, Astrononmical Almanac)
;#
    sin_altitude=sin(wdec)*sin(S1_LAT)+cos(wdec)*cos(ha)*cos(S1_LAT)
    altitude=asin(sin_altitude)*180./!pi ;altitude in degress

;#
;# Compute Azimuth at this hour angle (see Page B61, Astrononmical Almanac)
;#
    sin_azimuth=-1.d0*cos(wdec)*sin(ha)/cos(asin(sin_altitude))
    cos_azimuth= sin(wdec)*cos(S1_LAT)-cos(wdec)*cos(ha)*sin(S1_LAT)
;#
;#  pick the right quadrant for the azimuth!
;#  also convert to degrees from radians
;#
    if(cos_azimuth ge 0 and sin_azimuth ge 0) then azimuth=asin(sin_azimuth)*180./!pi       ;1st Q
    if(cos_azimuth le 0 and sin_azimuth ge 0) then azimuth=180.0-asin(sin_azimuth)*180./!pi ;2nd Q
    if(cos_azimuth le 0 and sin_azimuth le 0) then azimuth=180.0-asin(sin_azimuth)*180./!pi ;3rd Q
    if(cos_azimuth ge 0 and sin_azimuth le 0) then azimuth=360+asin(sin_azimuth)*180./!pi   ;4th Q

;#
;# Compute U,V coordinates for this Hour Angle
;# Mel Dyck's talk  "Interferometry with Two Telescopes" in
;# Principles of Long Baseline Stellar Interferometry (equation 12.1, page 189)
;# both u and v are in cycles/arcsecond
;#

;# U
    u=(basevec(0)*cos(ha) - basevec(1)*sin(S1_LAT)*sin(ha) +$
       basevec(2)*cos(S1_LAT)*sin(ha) )/(206265.*lam)
;# V
    v=(basevec(0)*sin(wdec)*sin(ha) + $
       basevec(1)*(sin(S1_LAT)*sin(wdec)*cos(ha) + cos(S1_LAT)*cos(wdec)) -$
       basevec(2)*(cos(S1_LAT)*sin(wdec)*cos(ha) - sin(S1_LAT)*cos(wdec)))/(206265.*lam)

;#  gdelay =  delay (in meters) for a baseline vector with north,
;# east  (and now north earth and "up") components.  A star in the west will
;# have a positive delay, while a star in the east will be negative delay.
;#
    gdelay= - basevec(0)*cos(wdec)*sin(ha) - $
     basevec(1)*(sin(S1_LAT)*cos(wdec)*cos(ha) - cos(S1_LAT)*sin(wdec))  +$
     basevec(2)*(cos(S1_LAT)*cos(wdec)*cos(ha) + sin(S1_LAT)*sin(wdec))

;#
;# spatial frequency for a symmetric source
;#
    sf=sqrt(u^2 + v^2)

;#
;# projected baseline (in meters)
;#
    pbase=sf*206265.*lam

;#
```

```
;# Position angle (East of North)
;#
    pa=atan(u/v)*180./!pi
;#
;# It's nice to keep the position angle between -60 to 120
;# since the position angle of the projected baseline is same when
;# rotated 180 degrees
;#
;#
    if (pa le -60) then pa=pa+180

;#
;# Save values at this hour angle step into vectors
;#

    havec(m)=ha*180./(!pi*15.)  ;hour angle [in hours]
    u_vec(m)=u                  ;U [in cycles/arcsec]
    v_vec(m)=v                  ;V [in cycles/arcsec]
    sfvec(m)=sf                 ;spatial frequency [in cycles/arcsec]
    pbasevec(m)=pbase           ;projected baselines [in meters]
    pavec(m)=pa                 ;position angle [in degrees]
    altvec(m)=altitude          ;altitude [in degrees]
    azvec(m)=azimuth            ;azimuth [in degrees]
    gdvec(m)=gdelay             ;geometric delay [in meters]

;# BOTTOM of hour angle loop
endfor

;
;#  Compute UT Time corresponding to hour angle
;
gmstvec = havec + wra - ((S1_LONG*180./!pi)/15.d0)
uttime  = (gmstvec-gmst_h)/1.002737


;
;# OPLE Cart Delay Computation
;
;# This will be used to check the times during which the delay carts
;# can move within the possible range to compensate for path length
;# differences for the given baseline, POP, and target

;# the needed delay to be provided by the carts
cart_delay=-0.5*(gdvec-air_diff+pop_delay)

;#
;# Compute dusk and dawn times in terms of LMST and HA
;#
sunpos,rjd,S1_LAT,S1_LONG,tw_dusk,tw_dawn,lmst_dusk,lmst_dawn

ha_dusk = lmst_dusk - wra
ha_dawn = lmst_dawn - wra

if (ha_dawn lt -12) then ha_dawn=ha_dawn+24
if (ha_dawn gt 12) then ha_dawn=ha_dawn-24

if (ha_dusk lt -12) then ha_dusk=ha_dusk+24
if (ha_dusk gt 12) then ha_dusk=ha_dusk-24

;#
;#  Compute indices for which:
;#  ==>  Altitude is greater than 30 degrees (goodalti)
;#  ==>  Cart delay is within maximum limits (gooddelayi)
;#  ==>  Time corresponds to night-time (nighti)
;#  ==>  Satisfies all the above conditions (obsi)
;#
goodalti = where(altvec GT 30.)
gooddelayi = where(cart_delay LE OPLE_MAX/2.0 AND $
                   cart_delay GE -OPLE_MAX/2.d0)
if (ha_dawn GT ha_dusk) then $  ; Dawn time after Dusk
   nighti = where(havec GT ha_dusk AND havec LT ha_dawn) $ ; night = between dusk & dawn
else $                          ; Dusk time after Dawn
   nighti = where(havec GT ha_dusk OR havec LT ha_dawn)    ; night = before dawn or after dusk
;  Same conditions as above for night time are checked below
obsi = where(altvec GT 30. AND $
                    cart_delay LE OPLE_MAX/2.0 AND $
                    cart_delay GE -OPLE_MAX/2.d0 AND $
                    ((ha_dawn GT ha_dusk AND $
                    havec GT ha_dusk AND havec LT ha_dawn) $
```

```
                    OR (ha_dawn LE ha_dusk AND $
                    (havec GT ha_dusk OR havec LT ha_dawn))))

;#  Initialize return parameters

nbr_avl_int = 0
str_obs_ha = 0.
end_obs_ha = 0.
str_obs_alt = 0.
end_obs_alt = 0.
str_obs_ut = 0.
end_obs_ut = 0.
min_pbase = 0.
min_pbase_ut = 0.
max_pbase = 0.
max_pbase_ut = 0.
max_alt = 0.
max_alt_ut = 0.

if (obsi(0) EQ -1) then return  ; Star is not observable at all

;#  Separate out the non-consecutive availability
;#  e.g. if obsi = [4,5,6,7,13,14,15,16,17], set
;#  nbr_avl_int = 2, and
;#  obsi = [[4,5,6],[13,14,15,16,17]]  (2-D array)
t0obsi = obsi
t1obsi = [t0obsi(0)-1,t0obsi]  ; offset array by one element to right
t2obsi = t0obsi - t1obsi
brki = where(t2obsi NE 1)
if (brki(0) EQ -1) then nbr_avl_int = 1 $
else begin
   nbr_avl_int = SIZE(brki,/dimensions)
   nbr_avl_int = nbr_avl_int(0) + 1  ; convert to scalar, add 1
endelse

nt0 = size(t0obsi,/dimensions)
obsi = intarr(nbr_avl_int, nt0)  ; set up obsi as 2-D array of max possible size
obsi = obsi - 1 ; set initial values as -1 (invalid index)
; add element at begining as start of first interval, and at end out to size of array
if (nbr_avl_int EQ 1) then brki = [0, nt0] $
else brki = [0, brki, nt0]

for ti = 0, nbr_avl_int - 1 do begin    ; process each interval
    obsi(ti, 0:(brki(ti+1)-brki(ti)-1)) = t0obsi(brki(ti) : brki(ti+1)-1)
endfor
;##  End of logic to split obsi into arrays of consecutive availabilities!!

str_obs_ha   = fltarr(nbr_avl_int)
end_obs_ha   = fltarr(nbr_avl_int)
str_obs_alt  = fltarr(nbr_avl_int)
end_obs_alt  = fltarr(nbr_avl_int)
str_obs_ut   = fltarr(nbr_avl_int)
end_obs_ut   = fltarr(nbr_avl_int)
min_pbase    = fltarr(nbr_avl_int)
min_pbase_ut = fltarr(nbr_avl_int)
max_pbase    = fltarr(nbr_avl_int)
max_pbase_ut = fltarr(nbr_avl_int)
max_alt      = fltarr(nbr_avl_int)
max_alt_ut   = fltarr(nbr_avl_int)

for ti = 0, nbr_avl_int - 1 do begin ; Return data for each interval
    datai = where(obsi(ti, *) NE -1)
    cobsi = obsi(ti, datai)  ; Current observal indices
    str_obs_ha(ti) = MIN(havec(cobsi), str_obs_i)
    end_obs_ha(ti) = MAX(havec(cobsi), end_obs_i)
    str_obs_i = cobsi(str_obs_i)  ; Get to index of full vector!
    end_obs_i = cobsi(end_obs_i)  ; Get to index of full vector!
    str_obs_alt(ti) = altvec(str_obs_i)
    end_obs_alt(ti) = altvec(end_obs_i)
    str_obs_ut(ti) = uttime(str_obs_i)
    end_obs_ut(ti) = uttime(end_obs_i)
    min_pbase(ti) = MIN(pbasevec(cobsi), min_pbi)
    max_pbase(ti) = MAX(pbasevec(cobsi), max_pbi)
    max_alt(ti) = MAX(altvec(cobsi), max_alti)
    min_pbi = cobsi(min_pbi)  ; Get to index of full vector!
    max_pbi = cobsi(max_pbi)  ; Get to index of full vector!
    max_alti = cobsi(max_alti)  ; Get to index of full vector!
    min_pbase_ut(ti) = uttime(min_pbi)
    max_pbase_ut(ti) = uttime(max_pbi)
```

```
    max_alt_ut(ti) = uttime(max_alti)
endfor

return
end        ; End CHK_AVAIL

;#####################################################################
; END PROGRAM: CHK_AVAIL                                             #
;#####################################################################


;#####################################################################
; PROGRAM: RMV_BLANK                                                 #
;  Eliminate leading, trailing and embedded blanks from a string     #
;  Input: inp_out : The input string                                 #
;  Output: inp_out: The output string with blanks removed            #
;#####################################################################

pro rmv_blank, inp_out

arrsp = strsplit(inp_out,' ',/EXTRACT)
arrsz = size(arrsp,/dimensions)
inp_out = ''
for i = 0, arrsz(0)-1 do inp_out=inp_out+arrsp(i)

return
end

;#####################################################################
; PROGRAM: SUB_STRING                                                #
;  Substitute every occurance of a value with a substitute value     #
;  in a given string                                                 #
;  Input: inp_out : The input string                                 #
;  Input: old_byte: Byte to be substituted (string of length 1)      #
;  Input: new_byte: Substitution value (string of length 1)          #
;  Output: inp_out: The output string with substitutions made        #
;#####################################################################

pro sub_string, inp_out, old_byte, new_byte

len = strlen(inp_out)
new_str = inp_out
for i = 0, len-1 do begin
    if (strmid(inp_out, i, 1) EQ strmid(old_byte,0,1)) then $
       new_str = strmid(new_str, 0, i) + strmid(new_byte,0,1) + $
                 strmid(new_str, i+1, len-i-1)
endfor
inp_out = new_str

return
end

;#####################################################################
; END PROGRAM: SUB_STRING                                            #
;#####################################################################

;#####################################################################
; PROGRAM: PRECESS                                                   #
; Taken directly from CHARA_PLAN. No modifications made DR 1/4/07    #
;#####################################################################

pro precess, ra, dec, equinox1, equinox2, PRINT = print, FK4 = FK4, $
        RADIAN=radian
;+
; NAME:
;       PRECESS
; PURPOSE:
;       Precess coordinates from EQUINOX1 to EQUINOX2.
; EXPLANATION:
;       For interactive display, one can use the procedure ASTRO which calls
;       PRECESS or use the /PRINT keyword.   The default (RA,DEC) system is
;       FK5 based on epoch J2000.0 but FK4 based on B1950.0 is available via
;       the /FK4 keyword.
;
; CALLING SEQUENCE:
;       PRECESS, ra, dec, [ equinox1, equinox2, /PRINT, /FK4, /RADIAN ]
;
; INPUT - OUTPUT:
;       RA - Input right ascension (scalar or vector) in DEGREES, unless the
```

```
;               /RADIAN keyword is set
;       DEC - Input declination in DEGREES (scalar or vector), unless the
;               /RADIAN keyword is set
;
;       The input RA and DEC are modified by PRECESS to give the
;       values after precession.
;
; OPTIONAL INPUTS:
;       EQUINOX1 - Original equinox of coordinates, numeric scalar.  If
;               omitted, then PRECESS will query for EQUINOX1 and EQUINOX2.
;       EQUINOX2 - Equinox of precessed coordinates.
;
; OPTIONAL INPUT KEYWORDS:
;       PRINT - If this keyword is set and non-zero, then the precessed
;               coordinates are displayed at the terminal.    Cannot be used
;               with the /RADIAN keyword
;       FK4   - If this keyword is set, the FK4 (B1950.0) system
;               will be used otherwise FK5 (J2000.0) will be used instead.
;       RADIAN - If this keyword is set and non-zero, then the input and
;               output RA and DEC vectors are in radians rather than degrees
;
; RESTRICTIONS:
;       Accuracy of precession decreases for declination values near 90
;       degrees.  PRECESS should not be used more than 2.5 centuries from
;       2000 on the FK5 system (1950.0 on the FK4 system).
;
; EXAMPLES:
;       (1) The Pole Star has J2000.0 coordinates (2h, 31m, 46.3s,
;               89d 15' 50.6"); compute its coordinates at J1985.0
;
;       IDL> precess, ten(2,31,46.3)*15, ten(89,15,50.6), 2000, 1985, /PRINT
;
;               ====> 2h 16m 22.73s, 89d 11' 47.3"
;
;       (2) Precess the B1950 coordinates of Eps Ind (RA = 21h 59m,33.053s,
;       DEC = (-56d, 59', 33.053") to equinox B1975.
;
;       IDL> ra = ten(21, 59, 33.053)*15
;       IDL> dec = ten(-56, 59, 33.053)
;       IDL> precess, ra, dec ,1950, 1975, /fk4
;
; PROCEDURE:
;       Algorithm from Computational Spherical Astronomy by Taff (1983),
;       p. 24. (FK4). FK5 constants from "Astronomical Almanac Explanatory
;       Supplement 1992, page 104 Table 3.211.1.
;
; PROCEDURE CALLED:
;       Function PREMAT - computes precession matrix
;
; REVISION HISTORY
;       Written, Wayne Landsman, STI Corporation  August 1986
;       Correct negative output RA values   February 1989
;       Added /PRINT keyword      W. Landsman   November, 1991
;       Provided FK5 (J2000.0)  I. Freedman   January 1994
;       Precession Matrix computation now in PREMAT   W. Landsman June 1994
;       Added /RADIAN keyword                         W. Landsman June 1997
;       Converted to IDL V5.0   W. Landsman   September 1997
;-
  On_error,2                                          ;Return to caller

  npar = N_params()
  deg_to_rad = !DPI/180.0D0

   if ( npar LT 2 ) then begin

     print,'Syntax - PRECESS, ra, dec, [ equinox1, equinox2,' + $
               ' /PRINT, /FK4, /RADIAN ]'
     print,'         NOTE: RA and DEC must be in DEGREES unless /RADIAN is set'
     return

  endif else if (npar LT 4) then $
      read,'Enter original and new equinox of coordinates: ',equinox1,equinox2

  npts = min( [N_elements(ra), N_elements(dec)] )
  if npts EQ 0 then $
       message,'ERROR - Input RA and DEC must be vectors or scalars'

  if not keyword_set( RADIAN) then begin
          ra_rad = ra*deg_to_rad     ;Convert to double precision if not already
```

```
          dec_rad = dec*deg_to_rad
  endif else begin
        ra_rad= double(ra) & dec_rad = double(dec)
  endelse

  a = cos( dec_rad )

 CASE npts of                    ;Is RA a vector or scalar?

   1:    x = [a*cos(ra_rad), a*sin(ra_rad), sin(dec_rad)] ;input direction

   else: begin

         x = dblarr(npts,3)
         x[0,0] = a*cos(ra_rad)
         x[0,1] = a*sin(ra_rad)
         x[0,2] = sin(dec_rad)
         x = transpose(x)
         end

   ENDCASE

   sec_to_rad = deg_to_rad/3600.d0

; Use PREMAT function to get precession matrix from Equinox1 to Equinox2

  r = premat(equinox1, equinox2, FK4 = fk4)

  x2 = r#x      ;rotate to get output direction cosines

 if npts EQ 1 then begin                ;Scalar

        ra_rad = atan(x2[1],x2[0])
        dec_rad = asin(x2[2])

 endif else begin               ;Vector

        ra_rad = dblarr(npts) + atan(x2[1,*],x2[0,*])
        dec_rad = dblarr(npts) + asin(x2[2,*])

 endelse

  if not keyword_set(RADIAN) then begin
        ra = ra_rad/deg_to_rad
        ra = ra + (ra LT 0.)*360.D            ;RA between 0 and 360 degrees
        dec = dec_rad/deg_to_rad
  endif else begin
        ra = ra_rad & dec = dec_rad
  endelse

  if keyword_set( PRINT ) then $
      print, 'Equinox (' + strtrim(equinox2,2) + '): ',adstring(ra,dec,1)

  return
end

;#####################################################################
; END PROGRAM: PRECESS                                               #
;#####################################################################

;#####################################################################
; PROGRAM PROGRAM: SUNPOS                                            #
; Taken directly from CHARA_PLAN. No modifications made DR 1/4/07    #
;#####################################################################
;+
; NAME: sunpos
;
;
;
; PURPOSE: compute the position of the sun and return times (UT)
;          for astronomical twilight (both dusk and dawn) & LSMT times too.
;
;"Low precision formulas for the Sun's coordinates and the equation of time"
;From Astronomical Almanac (1989) page C24

;
; CALLING SEQUENCE:
;          sunpos,JD_IN,LAT,LONG,TW_DUSK,TW_DAWN,LMST_DUSK,LMST_DAWN
;
```

```
;
; INPUTS:
;          JD_IN = reduced julian date
;
;          LAT = latitude in radians
;
;          LONG = longitude in radians
;
;
; OPTIONAL INPUTS: none

;
;
; KEYWORD PARAMETERS: none
;
;
; OUTPUTS:

;          TW_DUSK = UT time of dusk (astronomical twilght) after sunset
;                    when zenith distance of the sun is at 120 degrees
;
;          TW_DAWN = UT time of dawn (astronomical twilght) before sunrise
;                    when zenith distance of the sun is at 120 degrees
;
;          LMST_DUSK = Local Mean Sideral Time of dusk
;                    (astronomical twilght: after sunset when zenith
;                    distance of the sun is at 120 degrees)
;
;          LMST_DAWN = Local Mean Sideral Time of dawn
;                    (astronomical twilght: before sunrise when zenith
;                    distance of the sun is at 120 degrees);
;
;
; OPTIONAL OUTPUTS: none
;
;
;
; COMMON BLOCKS: none
;
;
;
; SIDE EFFECTS: none
;
;
;
; RESTRICTIONS: This will probably break if choose the LAT and LONG
;               near or above/below the artic/anarctic circles!
;
; EXAMPLE:
;
;     At CHARA,  25-DEC-1981
;
;   sunpos,44963.5d0, ten(34.,13.,0.)*(!pi/180.d0),$
;        ten(-118.,03.,36.)*(!pi/180.d0),tw_dusk,tw_dawn,lmst_dusk,lmst_dawn
;
;   print,tw_dusk,tw_dawn
;   3.2904176       12.416673
;
;
; MODIFICATION HISTORY:
;
; comments added/improved: 13/feb/04 (jpa)
;
; first version early December 2003 (jpa)
;
;-

pro sunpos,jd_in,lat,long,tw_dusk,tw_dawn,lmst_dusk,lmst_dawn

n_points=96

;intialize vectors
altsun=fltarr(n_points) ;altitude of the sun
time=fltarr(n_points)   ;time in hours
stime=fltarr(n_points)  ;
ra_vec=fltarr(n_points)
ra_h_vec=fltarr(n_points)
dec_vec=fltarr(n_points)
ha_vec=fltarr(n_points)
```

```
lmst_vec=fltarr(n_points)
l_vec=fltarr(n_points)
g_vec=fltarr(n_points)
lambda_vec=fltarr(n_points)

for jj=0,n_points-1 do begin

    hour=jj/4.d0        ;hours run from 0 h to 23.75 h in 0.25 h steps

;    jd=jd_in+0.5+(hour/24.d0)   ;compute RJD for each hour step why
;    the did I add 0.5 here?? looks like a bug to me!

    jd=jd_in+(hour/24.d0)   ;compute RJD for each hour step

;from Almanac formulae
    n=jd-51545.d0

;Mean longitude of Sun, corrected for aberration
    L=280.460d0 + (0.9856474d0*n)

;Mean anomaly
    g=357.528d0 + (0.9856003d0*n)

;put L and g in the range 0 to 360 degrees by adding multiples of 360

    while (L gt 360.d0) do L=L-360.d0
    while (g gt 360.d0) do g=g-360.d0

;Ecliptic longitude
    lambda=L+(1.915d0 * sin(!pi*g/180.d0)) + (0.020 * sin (!pi*2.d0*g/180.d0))

    while (lambda lt 0.d0) do lambda=lambda+360.d0
    while (lambda gt 360.d0) do lambda=lambda-360.d0

;# Obliquity of ecliptic
    epsilon=23.439 - (0.0000004d0*n)

;# right ascension of the ran
    ra=atan(cos(epsilon*!pi/180.d0)*tan(lambda*!pi/180.d0))

    ra_deg=ra*180.d0/!pi

;# R.A. should be in the same quadrant as lambda, but the arctan
;# expression containing the obliquity of the ecliptic may place
;# the R.A. 90 degrees off. adjust R.A. accordingly
;
;# We do this because the R.A. will be discontinuous across lambda
;# quadrants otherwise
;#

    if (lambda ge 0.d0 and lambda le 90.d0) then begin
        while (ra_deg lt 0.d0)  do ra_deg=ra_deg+90
        while (ra_deg gt 90.d0)  do ra_deg=ra_deg-90
    endif

    if (lambda gt 90.d0 and lambda le 180.d0) then begin
        while (ra_deg lt 90.d0)  do ra_deg=ra_deg+90
        while (ra_deg gt 180.d0)  do ra_deg=ra_deg-90
    endif

    if (lambda gt 180.d0 and lambda le 270.d0) then begin
        while (ra_deg lt 180.d0)  do ra_deg=ra_deg+90
        while (ra_deg gt 270.d0)  do ra_deg=ra_deg-90
    endif

    if (lambda gt 270.d0 and lambda le 360.d0) then begin
        while (ra_deg lt 270.d0)  do ra_deg=ra_deg+90
        while (ra_deg gt 360.d0)  do ra_deg=ra_deg-90
    endif

;#RA  of the sun in hours
    ra_h=ra_deg/15.d0

;# RA of the sun in radians
    ra=ra_h*15.d0*!pi/180.d0

;# Declination of the sun in radians
    dec=asin(sin(epsilon*!pi/180.d0)*sin(lambda*!pi/180.d0))
```

```
;# See  GMST (Page B6 from the Astronomical Almanac)
;# TIME-SCALES: "Relationships between universal and sidereal time"

;with reduced JD
    tu=(jd-51545.d0)/36525.d0 ;Julian centuries of 36525 days since ;J2000.0

;# GMST in seconds at 0h UT
    gmst= 24110.54841d0 + (8640184.812866d0*tu) + (0.093104d0*tu*tu) + (6.2d-6*tu*tu*tu)

;Greenwich mean sidereal time in hours
    gmst_h=(gmst/3600.d0)+ (hour*1.00273791d0)

    while(gmst_h gt 24) do gmst_h=gmst_h-24.d0 ;
    while(gmst_h lt 0) do gmst_h=gmst_h+24.d0 ;

;# LMST: local mean sidereal time in hours
    lmst_h=(gmst/3600.d0)+ (hour*1.00273791d0)+long*(180./!pi)/15.d0

;# H.A. of the sun
    ha_h=lmst_h-ra_h

;# H.A. in radians
    ha_rad=(ha_h*15.d0)*!pi/180.d0

;#
;# compute solar altitude
;#
    sin_altitude=sin(dec)*sin(lat)+cos(dec)*cos(ha_rad)*cos(lat)
    altitude=asin(sin_altitude)*180./!pi ;in degrees

;# save variables into vectors at each time step

    altsun(jj)=altitude
    time(jj)=hour
    stime(jj)=lmst_h
    ra_vec(jj) = ra
    ra_h_vec(jj) = ra_h
    dec_vec(jj) = dec*180.d0/!pi
    ha_vec(jj) = ha_h
    lmst_vec(jj) = lmst_h
    L_vec(jj) = L
    g_vec(jj) = g
    lambda_vec(jj) = lambda

endfor

;#
;# zenith distance of the sun in degrees
;#
zd=90.d0-altsun

;#
;# UT of astronomical twilight
;#

k=where(zd ge 108.d0) ; for all zd > 108 degrees = astronomical twilight
j=sort(zd(k))

if (zd(k(j(0))) lt zd(k(j(0))+1)) then begin
;zd is increasing with time so this is dusk
    tw_dusk=interpol(time(k(j(0))-1:k(j(0))),zd(k(j(0))-1:k(j(0))),108.d0)
endif else begin
    tw_dawn=interpol(time(k(j(0)):k(j(0))+1),zd(k(j(0)):k(j(0))+1),108.d0)
endelse

if (zd(k(j(1))) lt zd(k(j(1))+1)) then begin
;zd is increasing with time so this is dusk
    tw_dusk=interpol(time(k(j(1))-1:k(j(1))),zd(k(j(1))-1:k(j(1))),108.d0)
endif else begin
    tw_dawn=interpol(time(k(j(1)):k(j(1))+1),zd(k(j(1)):k(j(1))+1),108.d0)
endelse


;local mean sidereal time of dusk and dawn (in hours)
lmst_dusk=(gmst/3600.d0)+ (tw_dusk*1.00273791d0)+long*(180./!pi)/15.d0
lmst_dawn=(gmst/3600.d0)+ (tw_dawn*1.00273791d0)+long*(180./!pi)/15.d0

while(lmst_dawn gt 24) do lmst_dawn=lmst_dawn-24.d0 ;
while(lmst_dawn lt 0) do lmst_dawn=lmst_dawn+24.d0 ;
```

```
while(lmst_dusk gt 24) do lmst_dusk=lmst_dusk-24.d0 ;
while(lmst_dusk lt 0) do lmst_dusk=lmst_dusk+24.d0 ;


end

;#####################################################################
; END PROGRAM: SUNPOS                                                #
;#####################################################################
```

C.2 Example Output File

```
CHARA observing report created by CHARA_PLANB on Mon Jan 29 16:13:49 2007

Observing Date: 2007/01/21
Wave Band: K
Minimum observing time required per target:  1.50 hours
Total number of valid targets:  138

                                          Obs     Obs Window Opens     Obs Window Closes    Min  at    Max  at
 HD ID  <=== Coordinates ===>  Epoch      Dur     HA     UT    Alt     HA     UT    Alt     Base  UT   Base  UT
                                          (h)     (h) (hh:mm) (deg)    (h) (hh:mm) (deg)    (m)        (m)

Baseline/POP: S1(1)-E1(1)

 10086  01:39:35.8 +45:52:42.0 1991.25  4.00    1.25  02:47  71.5    5.25  06:46  31.1    323 06:46  329 03:47
 12051  01:59:06.5 +33:12:37.9 1991.25  3.75    1.00  02:51  77.5    4.75  06:36  32.1    327 04:06  330 06:36
 19373  03:09:02.9 +49:36:48.6 1991.25  5.50   -0.25  02:47  74.3    5.25  08:16  32.2    318 08:16  326 05:16
 20675  03:21:52.4 +49:04:15.8 1991.25  5.75   -0.50  02:44  74.1    5.25  08:28  32.1    319 08:28  327 05:29
140775  15:45:23.5 +05:26:50.4 1991.25  1.50   -3.75  11:51  30.7   -2.25  13:21  47.5    326 13:21  330 12:21
141795  15:50:48.9 +04:28:39.3 1991.25  1.50   -3.75  11:56  30.1   -2.25  13:26  46.8    325 13:26  330 12:26
142860  15:56:27.0 +15:39:53.0 1991.25  1.75   -4.25  11:32  30.2   -2.50  13:17  51.6    315 11:32  330 13:17
139225  15:36:29.2 +16:07:08.8 1991.25  2.25   -4.25  11:12  30.5   -2.00  13:27  57.5    314 11:12  330 13:12
142860  15:56:27.0 +15:39:53.0 1991.25  1.75   -4.25  11:32  30.2   -2.50  13:17  51.6    315 11:32  330 13:17

   9 objects observable for: S1(1)-E1(1)
```

C.3 SFP Detection

```
pro SFPF, inp_fil, inp_dir, DEBUG=debug, OUTF=outf, DISSERT=dissert

;*************************************************************************
;  CHARA Data Reduction  - Separated Fringe Packet Analysis               *
;                                                                         *
;  Analyze data from CHARA CLASSIC for separated fringe packet binaies.   *
;  NOTE: THIS VERSION USES THE FITS FILES GENERATED BY THE CHARA          *
;        SOFTWARE STARTING 2008 JAN.                                      *
;        For the old IRBRIEF format, see SFPbinary.pro                    *
;                                                                         *
;  Input:  Input File name to reduce (with wildcards)                     *
;          Input Directory name (default value assumed if not specified)  *
;          /DEBUG = Runs in debug mode, stops execution for reviews       *
;          /OUTF = Write output to file                                   *
;          /DISSERT = Suppress individual plots generated for /OUTF       *
;          but generate summary plot for each observation for dissertation.*
;  Input file contains:                                                   *
;          Output of "irbrief" run on Michelson, which creates a text     *
;          file with 3 arrays: Dither mirror position (microns), I_A,     *
;          and I_B - which are the measured intensities on A and B side   *
;          of beam combiner.                                              *
;  Output: Sumamry and detailed plot to help identify a secondary fringe, *
;          if present.                                                    *
;                                                                         *
;  Original Version: Deepak Raghavan    March 26, 2007                    *
;                                                                         *
;  Modifications:                                                         *
;                                                                         *
;     5/21/2007  DR  Added average PS plot for display                    *
;                                                                         *
;                                                                         *
;*************************************************************************


;
;  Check input parameters
;
if (N_PARAMS() EQ 0) then begin
   print, 'Usage: SFPB, inp_fil, inp_dir, /debug'
   print, '/debug is optional, but input file (with wild-cards) is required'
   print, 'if inp_dir is not specified, the default value is used.'
   return
endif

;
;  Define constants
;

DEF_INP_DIR = '~/chara/sfp_data_fit/'  ; Default directory for input data files

;
;  Generate list of files to process based on input parameter
;

if (N_PARAMS() EQ 1) then inp_dir = DEF_INP_DIR
lscmd = string(format='("ls -l ", 2A, " > SFPB.tmp.in")', inp_dir, inp_fil)
spawn, lscmd
openr,7, 'SFPB.tmp.in'
file = ' '
inp = ' '

while (NOT EOF(7)) do begin

      readf,7,inp
      work = strsplit(inp,' ',/extract)
      file = work(8)
      chk_target, file, DEBUG=debug, OUTF=outf, DISSERT=dissert

endwhile

close,7
spawn,'rm -f SFPB.tmp.in'

return
end

;*************************************************************************
;   END OF SFPB                                                           *
;*************************************************************************
```

```
;*****************************************************************************
; CHK_TARGET                                                                 *
;                                                                            *
;   Check specified target for secondary packet and generate the             *
;   diagnostic plots.                                                        *
;                                                                            *
;*****************************************************************************

pro chk_target, curfil, DEBUG=debug, OUTF=outf, DISSERT=dissert

;
;  Define constants
;
MINDATS = 150l        ; Minimum number data scans in input data
L_PASS = 20           ; Wavelength lower-limit for low-pass filter
BW = 30               ; Bandwidth (Hz) on each side of Nominal freq to use for bandpass filtering
MIN_SCW = 1.0         ; Minimum scan weight to identify good SNR scans
jj = 20               ; Index to use for plot of example scans
BASELINES = ['W2-S1', 'W2-S2', 'W2-E1', 'W2-E2', 'W2-W1', 'W1-S1', 'W1-S2', $
             'W1-E1', 'W1-E2', 'E2-S1', 'E2-S2', 'E2-E1', 'E1-S1', 'E1-S2', 'S2-S1']
; Default directory for output data files
if KEYWORD_SET(dissert) then DEF_OUT_DIR = '~/dissert/figures/sfp/' $
else DEF_OUT_DIR = '~/chara/red_data/'


!p.multi = 0
set_plot,'x'    ; default to terminal graphics output
!p.color=0
!p.background=19

;
;  Read FITS file and set header variables
;
fits_open, curfil, fitf
fits_read, fitf, fitdat, fithdr

BefShw = 1 * HDRVAL(fithdr, 'CCSHUTA ')  ; Width of "before" shutter sequence (in number-of-scan uni
ts)
AftShw = 1 * HDRVAL(fithdr, 'CCSHUTB ')  ; Width of "after" shutter sequence (in number-of-scan unit
s)
Wave_Lth = 1.e-6 * HDRVAL(fithdr, 'CCLAMBDA')  ; Wavelength (K band, m)

hd_id = long(STRMID(HDRVAL(fithdr, 'CCSTARHD'), 3))
fsplit = strsplit(curfil,'/', /EXTRACT)
nf = SIZE(fsplit, /DIMENSIONS)
scurfil = fsplit(nf(0)-1)  ; Short file name (w/o dir name)
seq_no = 1 * HDRVAL(fithdr, 'CCNUMBER')
seq_no = strmid(string(format='(I4)',1000+seq_no),1,3)  ; convert to 3 digit string

scope1 = strmid(HDRVAL(fithdr, 'CC_BEAM5'), 0, 2)
scope2 = strmid(HDRVAL(fithdr, 'CC_BEAM6'), 0, 2)
blname = scope1 + '-' + scope2
bl_num = where(blname EQ BASELINES)   ; Baseline number

utdate = HDRVAL(fithdr, 'CCUTDATE')
work   = strsplit(utdate, '-', /EXTRACT)  ; remove '-' separators
obs_yr = work(0)
obs_mo = work(1)
obs_dt = work(2)

uttime = HDRVAL(fithdr, 'CCUTTIME')
work   = strsplit(uttime, ' ', /EXTRACT)  ; remove ' ' separators
obs_hr = work(0)
obs_mn = work(1)
obs_sc = work(2)


;
;  Read dith, I_A, I_B into arrays
;
inpdat = dblarr(3)
dith = reform(fitdat(*,1,*))
I_A  = reform(fitdat(*,2,*))
I_B  = reform(fitdat(*,3,*))

ScanLth = 1 * HDRVAL(fithdr, 'CCNDATA ')      ; Nbr of samples per scan
NbrTotS = 1 * HDRVAL(fithdr, 'CCNSCANS')      ; Total nbr of scans
```

```
NbrDatS = 1 * HDRVAL(fithdr, 'CCDATSCN')      ; Nbr of data scans
SampleInt = 1.d / HDRVAL(fithdr, 'CCSAMPLE')  ; Sample rate in seconds
DithRange = 1.d * HDRVAL(fithdr, 'CCDRANGE')  ; Dither motion range (microns)

;
;  Skip if minimum number fo data scans not found
;

if (NbrDatS LT MINDATS) then begin
   print,format='("Input file: ", 1A)', curfil
   print,format='("Input file has only ", I6, " data scans")', NbrDatS
   print,format='("Minimum ", I6, " lines required, skipping this file")', MINDATS
   return
endif

;
;  PRINT HEADER INFO FOR TARGET
;

;
;  Format date/time for printing
;
put = string(format='(I4,"/",A2,"/",A2," ",A2,":",A2,":",F6.3)', $
      obs_yr, strmid(string(format='(I3)',obs_mo+100),1,2), $
      strmid(string(format='(I3)',obs_dt+100),1,2), $
      strmid(string(format='(I3)',obs_hr+100),1,2), $
      strmid(string(format='(I3)',obs_mn+100),1,2), $
      strmid(string(format='(F7.3)',obs_sc+100.),1,6))

if NOT KEYWORD_SET(dissert) then begin
   print,format='("Input file: ", 1A)', curfil
   print,format='("Reduced (ET): ", 1A)', systime()
   print,format='("HD: ", I6, "  Seq: ", A3, "  Baseline: ", A5, "  Obs Start (UT): ", A23)', $
       hd_id, seq_no, blname, put
endif

;  Set prefix of output file name
outfp = DEF_OUT_DIR + "HD" + strmid(string(format='(I7)',hd_id+1000000), 1, 6) + "_" + $
         strmid(blname,0,2) + strmid(blname,3,2) + "_" + $
         string(format='(I4)', obs_yr) + strmid(string(format='(I3)',obs_mo+100),1,2) + $
         strmid(string(format='(I3)',obs_dt+100),1,2) + "_" + seq_no + "."

if KEYWORD_SET(outf) then begin
   openw,2, outfp+"Header"
   printf, 2, format='("Input file: ", 1A)', curfil
   printf, 2, format='("Reduced (ET): ", 1A)', systime()
   printf, 2, format='("HD: ", I6, "  Seq: ", A3, "  Baseline: ", A5, "  Obs Start (UT): ", A23)', $
              hd_id, seq_no, blname, put
endif

;
;  Set positions for first shutter sequence
;

strbl = BefShw                  ; Index of left shutter seq start
strbd = strbl + BefShw          ; Index of dark start
strbr = strbd + BefShw          ; Index of right shutter seq start

;
;  Set positions for second shutter sequence
;

stral = 4 * BefShw + NbrDatS  ; Start index of left shutter seq
strad = stral + AftShw        ; Start index of dark
strar = strad + AftShw        ; Start index of right shutter seq


Indfss = 4 * BefShw           ; Index of first signal scan (after initial shutter sequence)
Indlss = Indfss + NbrDatS - 1 ; Index of last signal scan (before final shutter sequence)

if NOT KEYWORD_SET(dissert) then begin
   print,format='("    Indfss = ", I6, "    Scan Length = ", I4)', Indfss, ScanLth
   print,format='("    Total Nbr of Scans = ", I4, "   Nbr of Data Scans =", I4)', NbrTotS, NbrDatS
   print,format='("    WvLth (um) = ", F5.3, "   Dither range (um) = ", F8.4, "  Samples per sec = "
, F7.3)', $
               1.e6*Wave_Lth, DithRange, 1.d/SampleInt
endif

if KEYWORD_SET(outf) then begin
```

```
   printf,2,format='("    Indfss = ", I6, "    Scan Length = ", I4)', Indfss, ScanLth
   printf,2,format='("    Total Nbr of Scans = ", I4, "   Nbr of Data Scans =", I4)', NbrTotS, NbrDa
tS
   printf,2,format='("    WvLth (um) = ", F5.3, "   Dither range (um) = ", F8.4, "  Samples per sec
= ", F7.3)', $
                    1.e6*Wave_Lth, DithRange, 1.d/SampleInt
endif

;
;  PLOT SHUTTER POSITIONS TO VERIFY AND CONTINUE
;

plot_x = indgen(1l*NbrTotS*ScanLth, /long)
plot_x = REFORM(plot_x, [ScanLth, NbrTotS])

if NOT KEYWORD_SET(dissert) then begin

   window,1, retain=2, xsize=1000,ysize=300, xpos=0, ypos=500, $
        title=curfil + " " + blname
   plot,plot_x, I_A, Title='Beam A data'
;  Overplot shutter points in gray
   oplot,plot_x(*, BefShw:4l*BefShw-1), I_A(*, BefShw:4l*BefShw-1), color = 12
   oplot,plot_x(*, stral:NbrTotS-BefShw-1),I_A(*, stral:NbrTotS-BefShw-1), $
         color = 12
;  Overplot signal points in blue
   oplot,plot_x(*, Indfss:stral-1), I_A(*, Indfss:stral-1), color = 96

   window,2, retain=2, xsize=1000,ysize=300, xpos=0, ypos=150, $
        title=curfil + " " + blname
   plot,plot_x, I_B, Title='Beam B data'
;  Overplot shutter points in gray
   oplot,plot_x(*, BefShw:4l*BefShw-1),I_B(*, BefShw:4*BefShw-1), color = 12
   oplot,plot_x(*, stral:NbrTotS-BefShw-1),I_B(*, stral:NbrTotS-BefShw-1), $
        color = 12
;  Overplot signal points in blue
   oplot,plot_x(*, Indfss:stral-1), I_B(*, Indfss:stral-1), color = 96

endif


;
;  Plot to output file
;
if KEYWORD_SET(outf) then begin
   set_plot,'ps'
   device,filename=outfp+'InpData.eps',/landscape
   plot, plot_x, I_A, Title='Beam A data', subtitle = curfil + " " + blname
   oplot,plot_x(*, BefShw:4*BefShw-1), I_A(*, BefShw:4*BefShw-1), color = 12
   oplot,plot_x(*, stral:NbrTotS-BefShw-1), I_A(*, stral:NbrTotS-BefShw-1), $
         color = 12
   oplot,plot_x(*, Indfss:stral-1), I_A(*, Indfss:stral-1), color = 96
   plot, plot_x, I_B, Title='Beam B data', subtitle = curfil + " " + blname
   oplot,plot_x(*, BefShw:4*BefShw-1), I_B(*, BefShw:4*BefShw-1), color = 12
   oplot,plot_x(*, stral:NbrTotS-BefShw-1), I_B(*, stral:NbrTotS-BefShw-1), $
        color = 12
   oplot,plot_x(*, Indfss:stral-1), I_B(*, Indfss:stral-1), color = 96
   device,/close   ; close the PS file
   set_plot,'x'    ; revert back to terminal graphics output
   !p.color=0
   !p.background=19
endif

;
;  Calculate dither mirror velocity in m/s
;    Dither step is in microns
;    Time elapsed b/w consecutive dither mirror steps = SampleInt (s)
;    Multiply by 2 due to accont for reflection off mirror
;    (Delta light path = 2 * mirror movement)
;

frdi = fix(ScanLth*0.2) ; As dither velocity is not uniform at edges,
todi = fix(ScanLth*0.8) ; take midle 60%
DithVel = ABS(dith(todi, jj) - dith(frdi, jj)) / (todi-frdi) * 2.d / (SampleInt * 1.e6)  ; jj-th sca
n taken as repr

;
;  Nominal Fringe Frequency
;
```

```
Freq0   = round(DithVel/Wave_Lth)        ; Fringe Freq Calc
FrgFreq = 1 * HDRVAL(fithdr, 'CCDFREQ ')  ; Fringe Freq from FITS

if NOT KEYWORD_SET(dissert) then begin
   print, format = '("Dither mirror velocity = ", F8.6, " mm/s")', $
          DithVel * 1000.d
   print, format = '("Nominal Fringe Frequency: Calc = ", F5.1, ", From FITS = ", F5.1, " Hz")', Fre
q0, FrgFreq
endif

if KEYWORD_SET(outf) then begin
   printf,2,format = '("Dither mirror velocity = ", F8.6, " mm/s")', DithVel * 1000.d
   printf,2,format = '("Nominal Fringe Frequency: Calc = ", F5.1, ", From FITS = ", F5.1, " Hz")', F
req0, FrgFreq
endif


if KEYWORD_SET(debug) then stop,'Review shutter and signal positions, then enter .c to continue' $
else if NOT KEYWORD_SET(dissert) then wait,2

;
;  Calculate and subtract dark (bias) from IA & IB
;

;  Beam A - Calculate dark (bias)
;
darkIAb = MEAN(I_A(*, strbd:strbd+BefShw-1))
sig_darkIAb = STDDEV(I_A(*, strbd:strbd+BefShw-1))
darkIAa = MEAN(I_A(*, strad:strad+AftShw-1))
sig_darkIAa = STDDEV(I_A(*, strad:strad+AftShw-1))
darkA = 0.5*(darkIAb+darkIAa)
sig_darkA = 0.5*(sig_darkIAb+sig_darkIAa)
;
;  Beam B - Calculate dark (bias)
;
darkIBb = MEAN(I_B(*, strbd:strbd+BefShw-1))
sig_darkIBb = STDDEV(I_B(*, strbd:strbd+BefShw-1))
darkIBa = MEAN(I_B(*, strad:strad+AftShw-1))
sig_darkIBa = STDDEV(I_B(*, strad:strad+AftShw-1))
darkb = 0.5*(darkIBb+darkIBa)
sig_darkB = 0.5*(sig_darkIBb+sig_darkIBa)

if NOT KEYWORD_SET(dissert) then begin
   print,format='("    darkA = ", F5.1, "     darkB = ", F5.1)', darkA, darkB
   print,format='("sig_darkA = ", F5.1, " sig_darkB = ", F5.1)', sig_darkA, sig_darkB
endif
if KEYWORD_SET(outf) then begin
   printf,2,format='("    darkA = ", F5.1, "     darkB = ", F5.1)', darkA, darkB
   printf,2,format='("sig_darkA = ", F5.1, " sig_darkB = ", F5.1)', sig_darkA, sig_darkB
endif

I_A = I_A - darkA
I_B = I_B - darkB


;
;   Calculate shutter input factors
;

;  Beam A - Calculate shutter input factors
;
avIAbl = MEAN(I_A(*, strbl:strbl+BefShw-1))
avIAbr = MEAN(I_A(*, strbr:strbr+BefShw-1))
avIAal = MEAN(I_A(*, stral:stral+AftShw-1))
avIAar = MEAN(I_A(*, strar:strar+AftShw-1))
IAS1 = 0.5d*(avIAbl + avIAal)
IAS2 = 0.5d*(avIAbr + avIAar)

;  Beam B - Calculate shutter input factors
;
avIBbl = MEAN(I_B(*, strbl:strbl+BefShw-1))
avIBbr = MEAN(I_B(*, strbr:strbr+BefShw-1))
avIBal = MEAN(I_B(*, stral:stral+AftShw-1))
avIBar = MEAN(I_B(*, strar:strar+AftShw-1))
IBS1 = 0.5d*(avIBbl + avIBal)
IBS2 = 0.5d*(avIBbr + avIBar)

if NOT KEYWORD_SET(dissert) then begin
   print,format='("    IAS1 = ", F5.1, "     IAS2 = ", F5.1)', IAS1, IAS2
```

```
   print,format='("    IBS1 = ", F5.1, "     IBS2 = ", F5.1)', IBS1, IBS2
endif
if KEYWORD_SET(outf) then begin
   printf,2,format='("    IAS1 = ", F5.1, "     IAS2 = ", F5.1)', IAS1, IAS2
   printf,2,format='("    IBS1 = ", F5.1, "     IBS2 = ", F5.1)', IBS1, IBS2
endif

;
;  LOAD DATA SCANS (EXCLUDING SHUTTER SEQ) INTO A 2-D ARRAY
;    j = Scan number 0..NbrDatS-1  (first index)
;    k = Dither steps for each scan 0..ScanLth-1  (second index)
;

SIA =    TRANSPOSE(I_A(*, Indfss:Indlss))
SIB =    TRANSPOSE(I_B(*, Indfss:Indlss))
dither = TRANSPOSE(dith(*, Indfss:Indlss))

;
;  Print dither arrays to verify that slicing of scans is
;  appropriately done.  Should see a clean X in the plot if
;  everything is OK and there is no drift in slicing the scans.
;  A drifting i.e wide X in the plot indicates a problem.
;
if NOT KEYWORD_SET(dissert) then begin
   wset,2
   plot,dither(0,*), title = 'Dither positions to verify scan slicing'
   for j = 1, NbrDatS - 1 do oplot, dither(j,*)
endif

if KEYWORD_SET(debug) then stop,'Review dither positions i.e scan slicing, then enter .c to continue
' $
else if NOT KEYWORD_SET(dissert) then wait,2

;
;  Normalize A & B scans before combining
;

nSIA = SIA / AVG(SIA)
nSIB = SIB / AVG(SIB)

;
;  Combine light from A & B sides for further processing
;  Take average of A & B side, accounting for sign difference
;  as they are 180d out of phase.
;

SigScan = (nSIA - nSIB) / 2.0d  ; Average A & B

;
;  FLIP ALTERNATE SCANS TO ALIGN ALL SCANS IN THE SAME DIRECTION
;
;  Dither mirror moves back and forth while scanning so that each
;  scan is in the opposite ditection of the previous/next scan.
;

jind = indgen(NbrDatS)
jodd = jind(where(jind MOD 2 NE 0))  ; Odd indices

tSigScan = SigScan
for k = 0, ScanLth - 1 do begin
    tSigScan(jodd,k) = SigScan(jodd,ScanLth-1-k)
endfor
SigScan = tSigScan

;
;  PERFORM FT ON SIGNAL TO WORK IN FREQUENCY DOMAIN
;

FSig = dcomplexarr(NbrDatS, ScanLth)

for j = 0, NbrDatS - 1 do begin

    FSig(j,*) = FFT(SigScan(j,*), -1)  ; Fast Fourier transform

endfor

;
;  SETUP THE FREQUENCY ARRAY FOR FFT RESULTS (see IDL help
;  for even and odd numbered arrays).
```

```
;  For even number of elements, freq = [0,1/NT, 2/NT, .. ,(N/2-1)/NT,
;  then mirror image for negative freq]
;  For odd number of elements, freq = [0,1/NT, 2/NT, .. ,(N-1)/2NT,
;  then mirror image for negative freq]
;  e.g. if N=10, T=2s, freq are:
;  [0, 1/20, 2/20, 3/20, 4/20, 5/20, -4/20, -3/20, -2/20, -1/20]
;  if N=9, T=2s, freq are:
;  [0, 1/18, 2/18, 3/18, 4/18, -4/18, -3/18, -2/18, -1/18]
;

nposf = long(ScanLth/2.) + 1l  ; number of positive freq (incl 0)
FTfreq = findgen(nposf)/(ScanLth*SampleInt)
nposi = long((ScanLth+1)/2.) - (indgen(long((ScanLth-1)/2.)) + 1) ; index of repeated frequencies
FTfreq = [FTfreq, -1.d * FTfreq(nposi)]

;
;  IDENTIFY NOISE SCANS (scans without a fringe) AND ELIMINATE THEM
;
;  A scan is considered to contain a fringe when the power in the vicinity
;  of the fringe frequency is greater than the power in the adjoining
;  higher frequency range.  e.g.  for fringe freq = 150 Hz and
;  bandwidth = 30 Hz, power in range (120 - 180 Hz) is compared
;  with power in range (181 - 241 Hz) to assign a scan weight.
;

;  Fringe frequency range & indices:
strfrg = FrgFreq - BW
stpfrg = FrgFreq + BW
xfrg_freqi = where(ABS(FTFreq) LT strfrg OR ABS(FTFreq) GT stpfrg) ; indices outside fringe width
;  Off fringe (high frequency) range & indices:
stroff = FrgFreq + BW + 1
stpoff = stroff + 2*BW
xoff_freqi = where(ABS(FTFreq) LT stroff OR ABS(FTFreq) GT stpoff) ; indices outside high-freq width

scan_wt = fltarr(NbrDatS)  ; Scan Weight (measure of SNR)

uPS = FSig * CONJ(FSig)  ; Unfiltered Power Spectrum

for j = 0, NbrDatS - 1 do begin

    tPS = uPS(j,*)
    tPS(xfrg_freqi) = 0.0d
    tot_frg_pow = TOTAL(tPS)

    tPS = uPS(j,*)
    tPS(xoff_freqi) = 0.0d
    tot_off_pow = TOTAL(tPS)

    scan_wt(j) = (tot_frg_pow - tot_off_pow) / tot_off_pow

endfor

;
;  Select good SNR scans
;
gsi = where(scan_wt GE MIN_SCW)  ; good SNR scan indices
Ngscans = SIZE(gsi, /DIMENSIONS) ; Number of good scans
gSigScan = SigScan(gsi, *)       ; Subset of good scans
FgSig = FSig(gsi, *)             ; Subset of FTs of good scans
guPS = uPS(gsi, *)               ; Subset of unfiltered PS

if NOT KEYWORD_SET(dissert) then begin
   print, format='("Good SNR scans = ", I3, " / ", I4)', Ngscans(0), NbrDatS
endif
if KEYWORD_SET(outf) then begin
   printf,2,format='("Good SNR scans = ", I3, " / ", I4)', Ngscans(0), NbrDatS
endif

if (Ngscans(0) LT jj + 10) then begin  ; Not enough good scans, skip
   if KEYWORD_SET(outf) then $
      printf,2,'Not enough good scans found, skipping target!'
   if NOT KEYWORD_SET(dissert) then $
      stop,'Not enough good scans found, skipping target; enter .c to continue'
   if KEYWORD_SET(outf) then close,2
   return
endif


FSig = FgSig
```

```
SigScan = gSigScan
NScans = Ngscans(0)
uPS = guPS

;
;  Plot histogram of scan weights as a indicator of seeing
;

gsw = scan_wt(gsi)  ; Good (selected) scan weights
swi = sort(gsw)     ; Sort indices in ascending order
avg_wt = AVG(gsw)
sdev_wt = STDDEV(gsw)
if NOT KEYWORD_SET(dissert) then begin
   print, format='("Scan weights: Avg = ", F4.1, "  SDev = ", F4.1)', $
       avg_wt, sdev_wt
endif
if KEYWORD_SET(outf) then $
   printf,2,format='("Scan weights: Avg = ", F5.1, "    SDev = ", F5.1)', $
            avg_wt, sdev_wt

binincr = 1   ; increment of histogram bins
BINARRAY, gsw, binincr, bin, binct

if NOT KEYWORD_SET(dissert) then begin
   wset,2
   maxy = max(binct)+1
   plot, bin, binct, title = 'Histogram of Scan Weights', psym=10, $
      xrange=[0,max(scan_wt)+1], yrange=[0,maxy], $
      xtitle='Scan Weight', ytitle='Number of Scans'
   oplot,[avg_wt,avg_wt],[0,maxy], linestyle=2
   oplot,[avg_wt-sdev_wt, avg_wt+sdev_wt], [1,1], linestyle=2
endif

if KEYWORD_SET(debug) then stop,'Review scan weights, then enter .c to continue' $
else if NOT KEYWORD_SET(dissert) then wait,2



;
;  PERFORM LOW-PASS FILTER TO REMOVE LOW FREQ NOISE
;

lp_freqi = where(ABS(FTfreq) LE L_PASS) ; indices in LP filter
lpfi = dblarr(ScanLth)
lpfi(lp_freqi) = 1  ; Select freq below L_PASS

lpfilt = dcomplexarr(NScans, ScanLth)
LPSig = dcomplexarr(NScans, ScanLth)
lpPS = dcomplexarr(NScans, ScanLth)

for j = 0, NScans - 1 do begin

    lpfilt(j,*) = FFT(FSig(j,*)*lpfi, 1)     ; LP filter (low freq modulation)
    LPSig(j,*) = FFT(FSig(j,*)*(1-lpfi), 1)  ; LP filtered signal (low freq mod taken out)
    lpPS(j,*) = uPS(j,*) * (1-lpfi)          ; LP filtered PS

endfor

if NOT KEYWORD_SET(dissert) then begin
   window,3, retain=2, xsize=350,ysize=550, xpos=300, ypos=250, $
        title=scurfil + " " + blname
   miny = MIN(SigScan(jj,*)) - 0.05 * MIN(SigScan(jj,*))
   maxy = 10 * (MAX(SigScan(jj,*)) - miny)
   plot,[0],[0], title='Example signal scans', xrange=[0,ScanLth-1], $
              yrange=[miny,maxy]
   for jp = 0, 9 do oplot, SigScan(jj+jp,*) + jp*maxy/10
   for jp = 0, 9 do oplot, lpfilt(jj+jp,*) + jp*maxy/10, color=96, thick=2

   window,4, retain=2, xsize=350,ysize=550, xpos=660, ypos=250, $
        title=scurfil + " " + blname
   miny = MIN(FLOAT(LPSig(jj,*))) - 0.05 * MIN(FLOAT(LPSig(jj,*)))
   maxy = 10 * (MAX(FLOAT(LPSig(jj,*))) - miny)
   plot,[0],[0], title='Example LP filtered scans', xrange=[0,ScanLth-1], $
              yrange=[miny,maxy]
   for jp = 0, 9 do oplot,LPSig(jj+jp,*)+jp*maxy/10.
endif

if KEYWORD_SET(debug) then stop,'Review low-pass filtering and enter .c to continue' $
else if NOT KEYWORD_SET(dissert) then wait,2
```

```
;
;  PLOT LOWPASS FILTERED POWER SPECTRUM EXAMPLES AND AVERAGE PS
;

if NOT KEYWORD_SET(dissert) then begin
   wset,3
   minx = FTfreq(0)
   maxx = FTfreq(ScanLth/2-1)
   plot,[0],[0], title='LP filtered PS', xrange=[minx,maxx], $
                 yrange=[-1,11]
   for jp = 0, 9 do oplot, $
       FTfreq(0:ScanLth/2-1), lpPS(jj+jp,0:ScanLth/2-1)/MAX(lpPS(jj+jp,*)) + jp
endif

;
;  Plot average low-pass filtered power spectrum
;

alpPS = dcomplexarr(ScanLth)
for k = 0, ScanLth - 1 do alpPS(k) = AVG(lpPS(*,k))
maxy = MAX(alpPS) * 1.05

if NOT KEYWORD_SET(dissert) then begin
   window,2, retain=2, xsize=500,ysize=300, xpos=510, ypos=80, $
        title=curfil + " " + blname
   plot,FTfreq(0:ScanLth/2-1),alpPS, title='Average Power Spectrum', $
           yrange=[0,maxy]
endif

;
;  Overplot BP filter frequency range
;

low = FrgFreq - BW
high = FrgFreq + BW
xbp_freqi = where(ABS(FTFreq) LT low OR ABS(FTFreq) GT high) ; indices outside BP filter
bpfilt = intarr(ScanLth/2-1)
bpfilt = bpfilt+maxy
bpfilt(xbp_freqi) = 0
if NOT KEYWORD_SET(dissert) then begin
   oplot,FTfreq(0:ScanLth/2-1),bpfilt,linestyle=2
endif

if KEYWORD_SET(outf) then begin
   set_plot,'ps'
   device,filename=outfp+'PS.eps',/landscape
   plot,FTfreq(0:ScanLth/2-1), alpPS, Title='Average Power Spectrum', subtitle = curfil + " " + blna
me
   oplot,FTfreq(0:ScanLth/2-1),bpfilt,linestyle=2
   device,/close   ; close the PS file
   set_plot,'x'    ; revert back to terminal graphics output
   !p.color=0
   !p.background=19
endif

if KEYWORD_SET(debug) then stop, 'Review Power Spectrum and enter .c to continue' $
else if NOT KEYWORD_SET(dissert) then wait,2

;
;  PERFORM BANDPASS FILTERING
;
;  Weight frequencies within "BW" of nominal fringe frequency as 1 and
;  supress frequencies outside this range by weighting as 0.1,
;  then inverse FT to get banpass filtered signal
;

FSig = dcomplexarr(NScans, ScanLth)

for j = 0, NScans - 1 do begin

    FSig(j,*) = FFT(LPSig(j,*), -1)  ; FT the signal to convert to frequency domain

endfor

FSig(*, xbp_freqi) = 0.1d * FSig(*, xbp_freqi)

BPSig = dcomplexarr(NScans, ScanLth)
```

```
for j = 0, NScans - 1 do begin

    BPSig(j,*) = FFT(FSig(j,*), 1)  ; Inverse FT to get BP filtered signal

endfor

;
;  GENERATE FRINGE ENVELOPE
;
;  This is done by  zeroing out negative frequencies on
;  the bandpass filtered FT and taking the modulus of the
;  inverse FT transform
;

negf = where(FTFreq LT 0.)
FSig(*, negf) = 0.0d             ; Zero out negative frequencies

FESig = dcomplexarr(NScans, ScanLth)

for j = 0, NScans - 1 do begin

    FESig(j,*) = FFT(FSig(j,*), 1)             ; Inverse FT to get signal

endfor

FE = 2 * ABS(FESig) ; Twice the mod (twice b/c neg freq suppressed)

miny = MIN(SigScan(jj,*)) - 0.05 * MIN(SigScan(jj,*))
maxy = 10 * (MAX(SigScan(jj,*)) - miny)

if NOT KEYWORD_SET(dissert) then begin
   window,3, retain=2, xsize=350,ysize=550, xpos=300, ypos=250, $
        title=scurfil + " " + blname
   plot,[0],[0], title='Example Scans Before BP filtering', $
                xrange=[0,ScanLth-1],yrange=[miny,maxy]
   for jp = 0, 9 do oplot,LPSig(jj+jp,*)+jp*maxy/10.

   window,4, retain=2, xsize=350,ysize=550, xpos=660, ypos=250, $
        title=scurfil + " " + blname
   plot,[0],[0], title='Example BP filtered Fringes with Envelope', $
               xrange=[0,ScanLth-1],yrange=[miny,maxy]
   for jp = 0, 9 do oplot, BPSig(jj+jp,*) + jp*maxy/10.  ; Plot fringes
   for jp = 0, 9 do oplot, FE(jj+jp,*) + jp*maxy/10., color=240 ; Overplot FE
endif

if KEYWORD_SET(debug) then stop,'Review bandpass filtering & fringe envelopes, then enter .c to cont
inue' $
else if NOT KEYWORD_SET(dissert) then wait,2

;
;  SHIFT INDIVIDUAL FRINGE PEAKS TO ALIGN AND SUM SHIFTED FRINGES
;
;  This is a tool used to detect a secondary fringe
;  Steps:
;  1. Select the scan with maximum fringe weight as standard.
;  2. Shift the peak of this scan to the center
;  3. Cross-correlate each fringe wrt to the standard
;  4. Find maximum of cross correlation function
;  5. Shift scan by this amount plus shift of the standard scan
;  6. Add all shifted scans
;  7. Center the peak of the summed FE and plot
;

gsw = scan_wt(gsi)  ; Scan weight subset of good scans
sgsw = reverse(sort(gsw))  ; sort indices in descending order
bestj = sgsw(0)  ; index of best scan
BestFE = FE(bestj,*)
max = MAX(BestFE, maxi)
ctri = long(Scanlth/2)
sftb = ctri - maxi   ; indices to shift best FE to center
clag = indgen((NScans-2)*2+1) - (NScans-2)  ; max allowed range for c-corr lag
plot_x = INDGEN(ScanLth) - ctri

SCFE = DCOMPLEXARR(ScanLth)  ; Shifted FE
for j = 0, NScans - 1 do begin

    CurFE = FE(j,*)
    ccorr = C_CORRELATE(BestFE, CurFE, clag)
    mxc = max(ccorr, sftc)
```

```
    sfti = sftb - clag(sftc) ; indices to shift by
;   Note: IDL SHIFT routine wraps array around, and we do not want
;   that!  So, manullay zero out padded values.
    sCurFE = SHIFT(CurFE, sfti)
    if (sfti GT 0) then sCurFE(0:sfti-1) = 0. $
    else sCurFE(ScanLth-1+sfti:ScanLth-1) = 0.

    SCFE(*) = SCFE(*) + sCurFE

endfor

SCFE = SCFE / MAX(SCFE)  ; Normalize
;
;  Shift peak to center
;
max = MAX(SCFE, maxi)
sfti = ctri - maxi ; indices to shift by
SCFE = SHIFT(SCFE, sfti)
if (sfti GT 0) then sCFE(0:sfti-1) = 0. $
else SCFE(ScanLth-1+sfti:ScanLth-1) = 0.

if NOT KEYWORD_SET(dissert) then begin
   window, 5, retain=2, xsize=350,ysize=350, xpos=0, ypos=450, $
        title=scurfil + " " + blname
   plot,plot_x,SCFE, title='Cross-corr shifted fringe envelopes', $
        yrange=[0,1]
endif

;
;  AUTO-CORRELATE FRINGE ENVELOPES TO HELP DETECT A SECONDARY FRINGE
;
;  Auto-correlation = Inverse-FT (FT * CONJ(FT))
;  ACor = Sum of auto-correlation of each fringe scan
;

ACor = DCOMPLEXARR(ScanLth)

for j = 0, NScans - 1 do begin

    FFE = FFT(FE(j,*), -1)                       ; FT of Fringe Envelope
    ACor(*) = ACor(*) + FFT((FFE*CONJ(FFE)), 1)  ; Autocorrelation

endfor

ACor = SHIFT(ACor, ctri)  ; Shift to place primary-peak in the center

Acor = Acor / MAX(Acor)  ; Normalize
if NOT KEYWORD_SET(dissert) then begin
   window,3, retain=2, xsize=350,ysize=350, xpos=300, ypos=450, $
        title=scurfil + " " + blname
   plot,plot_x,Acor, title='Autocorrelation of fringe envelopes', $
     yrange=[0,1]
endif

;
;  SHIFT INDIVIDUAL FRINGE PEAKS TO CENTER AND SUM SHIFTED FRINGES
;
;  This is another tool used to detect a secondary fringe
;

SFE = DCOMPLEXARR(ScanLth)  ; Shifted FE
for j = 0, NScans - 1 do begin

    CurFE = FE(j,*)
    max = MAX(CurFE, maxi)
    sfti = ctri - maxi ; indices to shift by
    sCurFE = SHIFT(CurFE, sfti)
    if (sfti GT 0) then sCurFE(0:sfti-1) = 0. $
    else sCurFE(ScanLth-1+sfti:ScanLth-1) = 0.
    SFE(*) = SFE(*) + sCurFE

endfor

SFE = SFE / MAX(SFE)  ; Normalize
if NOT KEYWORD_SET(dissert) then begin
   window,4, retain=2, xsize=350,ysize=350, xpos=660, ypos=450, $
        title=scurfil + " " + blname
   plot,plot_x,SFE, title='Sum of shifted fringe envelopes', $
     yrange=[0,1]
```

```
endif

;
;; Plot the PS version of above 3 plots
;

if KEYWORD_SET(dissert) then begin
   !p.multi = [0, 3, 2, 0, 0]    ; xp x yp panes
   set_plot,'ps'
   device,filename=outfp+'FEsummary.eps',/landscape
   plot,plot_x,SCFE, $ ; title='Cross-corr shifted fringe envelopes', $
;       subtitle = curfil + " " + BASELINES(bl_num), yrange=[0,1]
       charsize=1.8, xthick=4, ythick=4, charthick=4, thick=4, $
       yrange=[0.,1.05], xtickinterval=100, $
       xtitle='Relative offset', ytitle='Intensity'
   plot,plot_x,Acor, $ ; title='Autocorrelation of fringe envelopes', $
;       subtitle = curfil + " " + BASELINES(bl_num), yrange=[0,1]
       charsize=1.8, xthick=4, ythick=4, charthick=4, thick=4, $
       yrange=[0,1.05], xtickinterval=100, $
       xtitle='Relative offset', ytitle='Intensity'
   plot,plot_x,SFE, $ ;title='Sum of shifted fringe envelopes', $
;       subtitle = curfil + " " + BASELINES(bl_num), yrange=[0,1]
       charsize=1.8, xthick=4, ythick=4, charthick=4, thick=4, $
       yrange=[0,1.05], xtickinterval=100, $
       xtitle='Relative offset', ytitle='Intensity'
;
;  Plot 12 strongest FE below this
;
   !p.multi = [14, 7, 4, 0, 0]    ; xp x yp panes
   maxy = MAX(FE, MIN=miny)
   for pp = 0, 13 do begin
       if (pp LT Nscans) then $
          plot, plot_x, FE(sgsw(pp),*), $
;              title = string(format='("FE ",I3)', sgsw(cp)), $
               yrange=[miny,maxy], $
               xcharsize=0.1, xthick=4, ythick=4, charthick=4, thick=4, $
;               xtitle='Relative offset', ytitle='Intensity', $
               xtickinterval=200, ycharsize=0.1, ytickv=['','','','',''], $
               xtickv=['','']
   endfor

   device,/close   ; close the PS file
   set_plot,'x'    ; revert back to terminal graphics output
   !p.color=0
   !p.background=19
   !p.multi = 0

endif


if KEYWORD_SET(debug) then stop, 'Enter .c to see individual fringe envelopes' $
else if NOT KEYWORD_SET(dissert) then WAIT,4

;
;  PLOT INDIVIDUAL FRINGE ENVELOPES
;
;  Plot them in order of scan_wt, descending so that "best"
;  scans are displayed first.
;  Keep Y-axis scale same across all plots to facilitate
;  comparison of the relative strengths of fringe envelopes
;

maxy = MAX(FE, MIN=miny)

if NOT KEYWORD_SET(dissert) then begin

   window, 6, retain=2, xsize=1000,ysize=700, xpos=0, ypos=100, $
        title=curfil + " " + blname
   xp = 7   ; number of panes in X direction
   yp = 6   ; number of panes in Y direction
   !p.multi = [0, xp, yp, 0, 0]    ; xp x yp panes
   ppp = xp * yp   ; plots per page
   npg = fix(NScans / ppp)  ; Number of pages
   if (NScans MOD ppp NE 0) then npg = npg + 1

   for pg = 0, npg - 1 do begin

       for pp = 0, ppp - 1 do begin
```

```
        cp = pg * ppp + pp   ; Current plot
        if (cp LT NScans) then $
            plot, plot_x, FE(sgsw(cp),*), title = string(format='("FE ",I3)', sgsw(cp)), $
                  yrange=[miny,maxy]

       endfor

       if KEYWORD_SET(debug) then  stop, 'Enter .c to go to next page' $
       else WAIT,4
   endfor
   wdelete,6
endif

;
;  Print individual FE to .eps file
;
if KEYWORD_SET(outf) then begin
   !p.multi = [0, xp, yp, 0, 0]    ; xp x yp panes
   set_plot,'ps'
   device,filename=outfp+'FEplots.eps',/landscape
   for pg = 0, npg - 1 do begin
       for pp = 0, ppp - 1 do begin
           cp = pg * ppp + pp   ; Current plot
           if (cp LT NScans) then $
              plot, plot_x, FE(sgsw(cp),*), title = string(format='("FE ",I3)', sgsw(cp)), $
                    yrange=[miny,maxy]
       endfor
   endfor
   device,/close   ; close the PS file
   set_plot,'x'    ; revert back to terminal graphics output
   !p.color=0
   !p.background=19
endif

!p.multi = 0
if KEYWORD_SET(outf) then close,2

if NOT KEYWORD_SET(dissert) then begin
   stop, "Review " + scurfil + " and enter .c to continue"
endif
return
end

;*****************************************************************************
;   END OF CHK_TARGET                                                        *
;*****************************************************************************


;*****************************************************************************
;  This procedure accepts an array,and a bin interval and returns two       *
;  other arrays:                                                            *
;  one with the values of bin intervals, and another with the               *
;  number of elements in original array with values between current         *
;  and next bin interval.  This is useful for plotting histograms.          *
;  Input parameter: inparr, binincr.  Output parameters: bin, binct         *
;*****************************************************************************

pro BINARRAY,inparr,binincr,bin,binct

s = size(inparr)        ; determine size
maxind = s(1) - 1       ; second elemenet of s contains size of 1st dim

iamax = max(inparr, min=iamin)
bin = fix(iamin)                        ; truncate to integer
if (bin LT 0) then bin = bin - 1        ; e.g if bin = -18.2, set to -19

binct = 0
iasort = sort(inparr)

i = 0           ; bin counter
si = 0          ; srt index counter
done = 0
while (done EQ 0) do begin

        binmax = bin(i) + binincr

        while (done EQ 0 and inparr(iasort(si)) LT binmax) do begin

                binct(i) = binct(i) + 1
```

```
                if (si LT maxind) then si = si + 1 $
                else done = 1

        endwhile

        if (done EQ 0) then begin
                bin = [bin, bin(i) + binincr]   ; create next bin
                binct = [binct,0]       ; create next bin count
                i = i + 1               ; incr bin counter
        endif

endwhile

return
end

;*************************************************************************
;   END OF BINARRAY                                                      *
;*************************************************************************



;*************************************************************************
;   FUNCTION HDRVAL
;   For a given header array and a header parameter value interested,
;   return the corresponding parameter value
;   Usage hval = HDRVAL(header, hfld)
;*************************************************************************

function hdrval, hdr, hfld

hval = 'FLD NOT FOUND!'   ; Default error value

for i = 0, N_elements(hdr)-1 do begin

    work = strsplit(hdr(i), "=", /EXTRACT)

    if (work(0) EQ hfld) then begin
       work1 = strsplit(strmid(work(1),1,strlen(work(1))-1), "/", /EXTRACT)
       hval = work1(0)
       work1 = strsplit(work1(0), "'", /EXTRACT)  ; Remove single quotes, if present
       hval = work1(0)
       BREAK

   endif

endfor

return, hval

end
```

C.4 Blinking Archival Images

```
;  Program to blink DSS (or other) fits images to find CPM companions.
;  Original version obtained from W.C.Jao April 2006
;  Modified by Deepak Raghavan
;  Program prerequisites:
;  Obtain fits files in 2 epochs for taregt list
;  Note: To download DSS images from the web, use dss.sub.pl PERL
;        script written by WCJ
;
;  Parameters:
;    fitsdir = Directory containing FITS images
;  Keyword parameters:
;   OUTF = If set, results are appended to OUTFILE

pro fitsblink, fitsdir, OUTF=outf

BL_SIZE = 15  ; Size of image to blink
              ;  If image is larger, program will blink
              ;  image of size BL_SIZE from each corner of larger image
              ;  e.g. if downloaded image is 22' x 22', the code will
              ;  blink 15' x 15' from each corner of the 22' image.
DSS1_RESOL = 1.7  ; arcsec per pixel of DSS1 (lower resol) image
OUTFILE = '~/dss/DSSblinkResults'
DEF_FITSDIR = '/nfs/morgan2/raghavan/dss_images/'

if (N_PARAMS() EQ 0) then  fitsdir = DEF_FITSDIR


lsfits = ('ls ' + fitsdir + '*.fits' + '> ./fitsblink.in')
spawn, lsfits

loadct, 0  ; load B&W color table
!p.color = 255 ; Print white on black
!p.charsize = 1.0

; Load fits file list into array
openr, 1, './fitsblink.in'
data=''
readf, 1, data
fitslist = data
while not eof(1) do begin
      READF, 1, data
      fitslist = [fitslist, data]
endwhile
close,1

;  Set pointer in fits list for starting HIP number
print,'Enter number of stars to process:'
read,nproc
strind = -1
strhip = ' '
while (strind LT 0) do begin
    print,'Enter starting HIP number (Format=HIPnnnnnn):'
    read,strhip
    strind = where(fitslist EQ fitsdir + strhip + '.dss1.fits')
endwhile

openw,2,'./temp.out'
print,'Date/Time Processed   Target    Rotation Primary X/Y pos    Comp X/Y pos   Sep "  Pos-Ang'
if (KEYWORD_SET(outf)) then $
   printf,2,'Date/Time Processed   Target    Rotation Primary X/Y pos    Comp X/Y pos   Sep "  Pos-A
ng'

curnbr = 0
for j = strind(0), strind(0)+nproc*2-1, 2 do begin

    curnbr = curnbr + 1
    parse = strsplit(fitslist(j), "/", /EXTRACT)
    starid = strmid(parse(n_elements(parse)-1),0,9)
    dt = strmid(systime(),20,4)+' '+strmid(systime(),4,16) ; Get curr date/time
    fits_open,fitslist[j], fcb1
    fits_read, fcb1,dss1, header1
    word1  = sxpar(header1, 'DATE-OBS') ; obtain header parameter
    pltscl = sxpar(header1, 'PLTSCALE') ; plate scale in arcsec/mm
    xpixsz = sxpar(header1, 'XPIXELSZ') / 1000. ; X pixel size in mm
    ypixsz = sxpar(header1, 'YPIXELSZ') / 1000. ; Y pixel size in mm
    fits_close, fcb1
    epoch1=strsplit(word1,'T',/EXTRACT) ; split date & time

    fits_open,fitslist[j+1], fcb2
```

```
    fits_read, fcb2, dss2, header2
    word2=sxpar(header2, 'DATE-OBS')
    fits_close, fcb2
    epoch2=strsplit(word2, 'T',/EXTRACT)

;   DSS-1 resolution is 1.7"/pix, while DSS-2 res is 1"/pix
;   The following lines resize DSS-2 image to the size of DSS-1
;   while preserving total flux count
    dss1size=size(dss1,/dimension)

    xdss1size=dss1size[0]
    ydss1size=dss1size[1]
    dss2=frebin(dss2, xdss1size,ydss1size,/total)

;
;   If image size is more than 5% larger than BL_SIZE, blink
;   four quadrants separately of BL_SIZE each
;
    imgpix = fix(BL_SIZE * 60. / DSS1_RESOL)+1 ; Nbr pixels for BL_SIZE
    if (xdss1size LT 1.05 * imgpix) then nquad = 1 $
    else nquad = 4

  for nq = 0, nquad-1 do begin  ; Process each quadrant

    if (nquad EQ 1) then begin
       img1 = dss1
       img2 = dss2
       curstar = starid + '   '
    endif else if (nq EQ 0) then begin
       img1 = dss1(0:imgpix-1, 0:imgpix-1)
       img2 = dss2(0:imgpix-1, 0:imgpix-1)
       curstar = starid + ' ll'
    endif else if (nq EQ 1) then begin
       img1 = dss1(xdss1size-1-imgpix+1:xdss1size-1, 0:imgpix-1)
       img2 = dss2(xdss1size-1-imgpix+1:xdss1size-1, 0:imgpix-1)
       curstar = starid + ' lr'
    endif else if (nq EQ 2) then begin
       img1 = dss1(xdss1size-1-imgpix+1:xdss1size-1, $
                   xdss1size-1-imgpix+1:xdss1size-1)
       img2 = dss2(xdss1size-1-imgpix+1:xdss1size-1, $
                   xdss1size-1-imgpix+1:xdss1size-1)
       curstar = starid + ' ur'
    endif else begin
       img1 = dss1(0:imgpix-1, xdss1size-1-imgpix+1:xdss1size-1)
       img2 = dss2(0:imgpix-1, xdss1size-1-imgpix+1:xdss1size-1)
       curstar = starid + ' ul'
    endelse

    xxtitle='  Object '+ curstar
    title1='Epoch='+string(epoch1[0], format='(A10)')+xxtitle
    title2='Epoch='+string(epoch2[0], format='(A10)')+xxtitle

;   Determine sky level & stdev in the fits images
    sky, img1, skymode1, skysig1,/silent
    sky, img2, skymode2, skysig2,/silent

;   Take the sky out of the fits images
    dss1_r1=img1/skymode1
    dss2_r1=img2/skymode2

;   Identify star pixels where flux gt sky + 3*sky sdev
    dss1starpix=where(img1 gt skymode1 + 3.*skysig1)
    dss2starpix=where(img2 gt skymode2 + 3.*skysig2)

;   Normalize total star flux count for both images
    if (dss1starpix(0) NE -1 AND dss2starpix(0) NE -1) then begin
        totaldss1=total(dss1_r1(dss1starpix))
        totaldss2=total(dss2_r1(dss2starpix))
        dss1_r2=dss1_r1
        dss2_r2=dss2_r1*totaldss1/totaldss2
    endif else begin
        dss1_r2=dss1_r1
        dss2_r2=dss2_r1
    endelse

;   Rotate from -10deg to +10deg to find best match
    angle=findgen(81)*0.25-10.0
    diff=fltarr(81)
    for i=0, 80 do begin
```

```
        newdss2=rot(dss2_r2, angle(i), /interp)
        diff(i)=total((dss1_r2-newdss2)^2)
    endfor

;   Fit gaussian & plot angle vs. goodness of fit
    fitted= gaussfit(angle, diff, AA, nterms=6)
    optrot = AA(1)  ; Optimal rotation in degrees
    window, 3,xsize=300, ysize=300
    plot, angle, diff, psym=4,color=0,background=255, $
          title = 'Optimum rotation = ' + string(optrot,format='(F5.2)') + $
                  ' deg',charsize=0.9,xtitle=curstar
    oplot, angle, fitted,color=0

;   Rotate image 2 by optimum angle to maximize fit
    dss2_r3=rot(dss2_r2, optrot,/interp)

;   Plot image difference to identify CPM
    diffim = dss1_r2 - dss2_r3
    window, 2, xsize=400, ysize=400
    tvim, diffim,/noframe, /rct,title=curstar

;   Plot image 1 & 2, and blink on left-click
    window, 0, xsize=600, ysize=600
    tvim, dss1_r2, /rct,/noframe, title=title1
    xyouts,-40,360,string(format='("Processing ",I3," of ",I3)',curnbr,nproc)
    xyouts,100,-10,'L-Click on image to blink'
    xyouts,100,-20,'Use subtracted image on left & blinking to ID CPM comps'
    xyouts,100,-30,'R-Click on image when done, to capture companion info'
    cursor, readx, ready,3

;
;   If repeatedly blinked, stop on a alternating images after each
;   click. This allows the user to inspect each image closely.
;
    swap = 'n'
    while (!mouse.button eq 1) do begin
       for btimes = 0,14 do begin; blink 15 times for every click
           tvim, dss1_r2, /rct, /noframe, title=title1
           wait, 0.1
           tvim, dss2_r3, /rct, /noframe, title=title2
           wait, 0.1
       endfor
       if (swap EQ 'y') then begin
          tvim, dss1_r2, /rct, /noframe, title=title1
          swap = 'n'
       endif else swap = 'y'
       cursor, readx, ready, 3
    endwhile

;   Collect positions of candidate companions, if any:
;   If primary has no detectable PM, R-click with x & y < 0
;   If primary's PM is marginal, R-click with x > 0 and y < 0
;   If primary's PM is detectable, but no CPM candidate detected,
;   R-click with x < 0 and y > 0
;   If CPM candidates exist, L-click on the primary star, then L-click
;   on every candidate companion.  Then, R-click anywhere when done.

    tvim, dss2_r2, /rct, /noframe, title=title2 ; Display unrot epoch-2
    xyouts,-40,360,string(format='("Processing ",I3," of ",I3)',curnbr,nproc)
    xyouts,-40,-15,'No Pri PM'
    xyouts,-40,-25,'Rclk HERE'
    xyouts,-40,0,'__________'
    xyouts,0,-10,'|',charsize=1.2
    xyouts,0,-17,'|',charsize=1.2
    xyouts,0,-24,'|',charsize=1.2
    xyouts,0,-31,'|',charsize=1.2
    xyouts,0,-38,'|',charsize=1.2
    xyouts,50,-15,'Marginal Primary PM'
    xyouts,50,-25,'   R-Click HERE'
    xyouts,-40,175,'No CPM'
    xyouts,-40,165,'companion'
    xyouts,-40,155,'Rclk HERE'
    xyouts,-40,300,'Can''t proc'
    xyouts,-40,290,'img,R-Clk'
    xyouts,-40,280,'on img-->'
    xyouts,175,-10,'CPM candidate companions exist:'
    xyouts,175,-20,'First, L-Click on primary, then on each candidate'
    xyouts,175,-30,'Finally, R-Click anywhere on image'
    cursor, readx, ready, 3  ; skip or capture primary's position
```

```
    if (!mouse.button EQ 1) then begin ; L-click = capture prim & sec pos

       primx = readx
       primy = ready
       cursor, readx, ready, 3  ; skip or capture primary's position
       if (!mouse.button NE 1) then begin
        print,format='(A22,A12,"  ",F7.2,"  Prim selected, but no comp!")', $
              dt,curstar,optrot
        if (KEYWORD_SET(outf)) then $
            printf,2,format='(A22,A12,"  ",F7.2,"  Prim selected, but no comp!")', $
              dt,curstar,optrot
        endif
        while (!mouse.button eq 1) do begin ; capture candidate positions
           candx = readx
           candy = ready
           nsdist = (candy - primy) * pltscl * ypixsz ; N-S sep in arcsec
           ewdist = (primx - candx) * pltscl * xpixsz ; E-W sep in arcsec
           sep = sqrt(ewdist^2+nsdist^2)  ; Sep in arcsec
           if (ewdist EQ 0. AND nsdist GE 0.) then pa = 0.        $
           else if (ewdist EQ 0. AND nsdist LT 0.) then pa = 180. $
           else if (ewdist GE 0. AND nsdist EQ 0.) then pa = 90.  $
           else if (ewdist LT 0. AND nsdist EQ 0.) then pa = 270. $
           else if (ewdist GT 0. AND nsdist GT 0.) then $
                    pa = atan(ewdist/nsdist)*180./!pi             $
           else if (ewdist GT 0. AND nsdist LT 0.) then $
                    pa = atan(ewdist/nsdist)*180./!pi + 180.      $
           else if (ewdist LT 0. AND nsdist LT 0.) then $
                    pa = atan(ewdist/nsdist)*180./!pi + 180.      $
           else if (ewdist LT 0. AND nsdist GT 0.) then $
                    pa = atan(ewdist/nsdist)*180./!pi + 360.
           print,format='(A22,A12,"  ",F7.2,5F8.2,F7.1)',dt,curstar,$
                 optrot,primx,primy,candx,candy,sep,pa
           if (KEYWORD_SET(outf)) then $
             printf,2,format='(A22,A12,"  ",F7.2,5F8.2,F7.1)',dt,curstar,$
                 optrot, primx,primy,candx,candy,sep,pa
           cursor, readx, ready, 3  ; skip or capture next candidate pos
       endwhile

    endif else begin           ; write no PM or no CPM candidate record

       if (readx LT 0. AND ready LT 0.) then begin

          print,format='(A22,A12,"  ",F7.2,"  No PM for primary detected")' $
                   ,dt,curstar,optrot
          if (KEYWORD_SET(outf)) then $
            printf,2,format='(A22,A12,"  ",F7.2,"  No PM for primary detected")' $
                   ,dt,curstar,optrot

       endif else if (readx GT 0. AND ready LT 0.) then begin

          print,format='(A22,A12,"  ",F7.2,"  Marginal PM for primary, no CPM candidate found")',dt,
curstar,optrot
          if (KEYWORD_SET(outf)) then $
             printf,2,format='(A22,A12,"  ",F7.2,"  Marginal PM for primary, no CPM candidate found"
)',dt,curstar,optrot

       endif else if (readx LT 0. AND ready GT 0.) then begin

          print,format='(A22,A12,"  ",F7.2,"  Primary PM detected, but no CPM candidate found")',dt,
curstar,optrot
          if (KEYWORD_SET(outf)) then $
              printf,2,format='(A22,A12,"  ",F7.2,"  Primary PM detected, but no CPM candidate found
")',dt,curstar,optrot

       endif else begin
          print,format='(A22,A12,"  ",F7.2,"  Error in image! Cannot process")'                    ,d
t,curstar,optrot
          if (KEYWORD_SET(outf)) then $
              printf,2,format='(A22,A12,"  ",F7.2,"  Error in image! Cannot process")'
     ,dt,curstar,optrot

      endelse
  endelse


 endfor

endfor
```

```
close,1
close,2
spawn,'rm -f ./fitsblink.in'
if (KEYWORD_SET(outf)) then spawn,'cat ./temp.out >> ' + OUTFILE
spawn,'rm -f ./temp.out'

end
```

C.5 Deriving a Visual Orbit From Interferometric Visibilities

C.5.1 Deriving the Best-fit Orbit

```
pro OrbFit, dir, nmiter, OUTF=outf, WRITECS=writecs, VSQ=vsq, Csma=csma

;*************************************************************************
;  CHARA Data Reduction  - Fit observed visibilities to visual orbit       *
;                                                                          *
;  Fit the observed visibilities to a visual orbit to obtain orbital       *
;  parameters. This version does brute-force fitting, similar to           *
;  the MathCAD ORBGRID code.                                               *
;                                                                          *
;  Input:  Paramaters:                                                     *
;            dir        - Directory name of star (e.g. hd008997)           *
;            nmiter     - Nbr of million iterations to try                 *
;            /OUTF      - Write results and plot data into utput files     *
;                         if this parameter is set.  Else, write and       *
;                         plot on the screen.                              *
;            /WRITECS   - If set, write CHI-SQ values within 10 of the     *
;                         current minimum value into an output file        *
;                         along with all parameter values for each         *
;                         iteration.  This is used to create 1-D           *
;                         projections of CHI-SQ change for each parameter  *
;                         to determine the -, 2, 3 sigma errors.           *
;            /VSQ       - If set, work with V-squared values & error,      *
;                         If not, work with V values and error.            *
;            /CSMA      - If set, constrain angular sma based on           *
;                         asini, plx, and incl                             *
;                         If not, vary asma as a free parameter.           *
;  Input:  Input file with calibrated visibilities (OrbCalV.inp)           *
;            Space-delimited columns are:                                  *
;               Epoch of observation (same unit as T0 - MJD/JD/HJD)        *
;               Baseline (m)                                               *
;               Baseline angle (degrees)                                   *
;               Visibility (Calibrated)                                    *
;               Visibility error                                           *
;               Wavelength of observation (microns)                        *
;            To have the program ignore a data line, place a semicolon(;)  *
;            in the first column                                           *
;          Input file with ranges of orbital elements (OrbEleM.inp)        *
;            First row is column headings (ignored by the program)         *
;            Columns are:                                                  *
;              Parameter name (ignored by program)                         *
;              Lower limit for parameter                                   *
;              Upper limit for parameter                                   *
;            The parameters MUST be speficied in the following order       *
;              Period (days)                                               *
;              Eccentricity                                                *
;              Epoch of Periastron (same unit as Epoch - MJD/JD/HJD)       *
;              Argument of periapse (lowercase omega)                      *
;              Semi-major axis (mas)                                       *
;              Inclination (deg)                                           *
;              Longitude of ascending node (capital OMEGA)                 *
;              Delta-mag (mag)                                             *
;              Primary's angular diameter (mas)                            *
;              Secondary's angular diameter (mas)                          *
;            For each parameter, specify a range of valid values           *
;            and an increment value.  If the lower and upper limits        *
;            are equal, the parameter is fixed at the lower limit.         *
;                                                                          *
;                                                                          *
;  Original Version: Deepak Raghavan    March 26, 2007                     *
;                                                                          *
;  Modifications:                                                          *
;                                                                          *
;                                                                          *
;*************************************************************************

;
;  Read input parameters
;

COMMON FUNC_ARGS, obsepoch, base, bang, wvlth, vsqf

parname = ["Period ", "Ecc    ", "T0     ", "l-omega", "a      ", $
           "i      ", "C-OMEGA", "d-mag  ", "Prim-D ", "Sec-D  "]

if (N_PARAMS() EQ 0) then begin  ; set default parameter values
   nmiter = 1
endif

openr,1, '~/idl/thesis/vbo_data/' + dir + '/OrbCalV.inp'
```

```
inp = ' '
inpdat = dblarr(5)
maxdata = 1000  ; maximum data points for visib
obsepoch = dblarr(maxdata)
base = dblarr(maxdata)  ; baseline (m)
bang = dblarr(maxdata)  ; baseline orientation angle (deg)
v = dblarr(maxdata)     ; calibrated visib
verr = dblarr(maxdata)  ; visib error
wvlth = dblarr(maxdata) ; wavelength of observation (microns)
i = -1

while (NOT EOF(1)) do begin

      readf,1,inp
      if (STRMID(inp,0,1) NE ";") then begin
          inpdat = STRSPLIT(inp, ' ', /extract)
          i = i + 1
          obsepoch(i) = inpdat(0)
          base(i) = inpdat(1)
          bang(i) = inpdat(2)
          v(i) = inpdat(3)
          verr(i) = inpdat(4)
          wvlth(i) = inpdat(5)
      endif

endwhile
close,1

vsqf = 'n'
if KEYWORD_SET(vsq) then begin  ;  Convert to V-squared values!
   verr = 2*v*verr
   v = v^2
   vsqf = 'y'
endif

;  Trim arrays to actual number of data elements
nv = i
obsepoch = obsepoch(0:nv)
base = base(0:nv)
bang = bang(0:nv)
v = v(0:nv)
verr = verr(0:nv)
wvlth = wvlth(0:nv)

;
;  Read Orbital element parameters
;

;
;  Initialize physical limits for each parameter
;
npar = 10  ; max possible number of free parameters

if KEYWORD_SET(outf) then begin
   openw, 2, '~/idl/thesis/vbo_data/' + dir + '/OrbFitR.tmp'
   printf,2, ' '
   printf,2, format='(3A)', $
   '**********************  ', SYSTIME(), '  ************************'
   printf,2, ' '
endif

openr, 1, '~/idl/thesis/vbo_data/' + dir + '/OrbEleR.inp'
readf, 1, inp  ; Read and ignore header line

inpdat = strarr(4)
i = -1
lowlim = dblarr(npar)
upplim = dblarr(npar)

for i = 0, npar-1 do begin

      readf,1,inp
      inpdat = STRSPLIT(inp, ' ', /extract)
      lowlim(i) = DOUBLE(inpdat(1))
      upplim(i) = DOUBLE(inpdat(2))

endfor
```

```
close,1


totiter = 1.d * nmiter * 1.0e6

print, format='("Total iterations = ", I10, "  started ", 1A)', $
       totiter, SYSTIME()
if KEYWORD_SET(outf) then printf, $
   2, format='("Total iterations = ", I10, "  Nbr visib points = ", I3)', $
       totiter, nv + 1
begt = SYSTIME(1) ; retrieve systime in seconds
begtj = SYSTIME(/JULIAN)

;
;  Setup plot to PS, if required
;
if KEYWORD_SET(outf) then begin
   set_plot,'ps'
   dt = SYSTIME()
   work = STRSPLIT(dt, ' ', /EXTRACT)
   hms = STRSPLIT(work(3), ':', /EXTRACT)
   plotfn = string(format='("~/idl/thesis/vbo_data/",1A,"/OrbFitR_", I4, 2A, "_", 2A, ".ps")', $
            dir, work(4), $
            work(1), strmid(string(format='(I3)', work(2)+100),1,2), $
            hms(0), hms(1))
   device,filename=plotfn, /portrait
endif

if KEYWORD_SET(writecs) then $
   openw, 3, '~/idl/thesis/vbo_data/' + dir + '/OrbFitR.csq'

parm = dblarr(npar)          ; parameter array
bfparm = dblarr(npar)        ; final best-fit parameters
bfidx = 0l                   ; best-fit index
minchisq = 99999999.9d       ; minimum chisq

iter = -1l
while (iter LT totiter) do begin

     iter = iter + 1l
;
;  Generate random values for each parameter within the ranges specified
;
     for ir = 0, npar-1 do begin
         if (lowlim(ir) EQ upplim(ir)) then begin  ; Constant parms
            parm(ir) = lowlim(ir)
         endif else begin
            parm(ir) = lowlim(ir) + $
                       (upplim(ir)-lowlim(ir))* double(RANDOMU(seed))
         endelse
     endfor

;    DR: 3/27/2008
;    Enhancements, per conversation with Latham & Torres
;    a is not a free parameter.  It can be computed using asini from
;    spectroscopy, and i assumed here.  Errors in parallax and asini
;    induce a spread in a values, so process multiple a values.

;  Print progress message only once for iter loop
   piter = 'y'

   if (KEYWORD_SET(csma)) then $
      CalcSma, dir, parm(5), asma, easma, niter $
   else niter = 1

   for ii = 1, niter do begin  ; Process niter values for sma

;     Pick a random value of sma within its 1-sigma error
      if (KEYWORD_SET(csma)) then $
          parm(4) = (asma - easma) + 2.d * easma * double(RANDOMU(seed))

      modelv = calcVis(obsepoch, parm)
      residv = v-modelv
      chisq = TOTAL((residv/verr)^2)
;     Save current data if it is minimum chi-sq
      if (chisq LT minchisq) then begin
         minchisq = chisq
         bfparm = parm
         bfidx = iter
```

```
     endif

;     If chisq is within 10 of the current minimum,
;     write details of current iteration to an output
;     file.  This is used by a subsequent program to
;     create 1-D projections of chi-sq for each
;     parameter to get 1, 2, 3 signam errors
      if (KEYWORD_SET(writecs) AND (chisq LT minchisq + 10.)) $
      then begin
         printf, 3, format='(10F17.9, F10.2)', parm, chisq
      endif

;     Print progress message for long runs (> 10,000 iterations)
      if ((piter EQ 'y') AND (totiter GT 10000.0d) AND $
         (LONG((iter*10/totiter)) NE $
         LONG(((iter-1)*10/totiter)))) then begin
         piter = 'n'
         curt = SYSTIME(1) ; retrieve systime in seconds
         projcmp = SIXTY(((begtj+1.d*totiter/iter*(curt-begt)/ $
                   86400.d + 0.5d) MOD 1.d)*24.d)
         print, format='(I3, "% done in ", I2,2(":",I2),                                    ", p
rojected completion at ", I2, 2(":",I2),                                ", Min chi-sq = ", F6.1)
', $
                iter*100./totiter, SIXTY((curt-begt)/3600.), $
                projcmp, minchisq
      endif

   endfor

endwhile                            ; end of iterations loop

if KEYWORD_SET(writecs) then close, 3

curt = SYSTIME(1) ; retrieve systime in seconds
print, format='(I3, "% done in ", I2,2(":",I2))', $
                100., SIXTY((curt-begt)/3600.)
if KEYWORD_SET(outf) then printf, $
   2, format='("Job completed in ", I2,2(":",I2), ".  Results:")', $
                SIXTY((curt-begt)/3600.)

print, "Results:"
print, format='("Min chisq = ",F9.2, " at index ", I10)', minchisq, bfidx
print, 'Best-fit parameters'

for ip = 0, npar-1 do begin
    if (lowlim(ip) EQ upplim(ip)) then lim = 'f' $
    else if (bfparm(ip) EQ lowlim(ip)) then lim = '<' $
    else if (bfparm(ip) EQ upplim(ip)) then lim = '>' else lim = ' '
    print, format='(A7, "[", 2F17.9, " ] = ", F17.9, 2X, A1)', $
       parname(ip), lowlim(ip), upplim(ip), bfparm(ip), lim
endfor

if KEYWORD_SET(outf) then begin

   printf,2, format='("Min chisq = ",F9.2, " at index ", I10)', $
             minchisq, bfidx
   printf,2, 'Parameter     Lower-Limit      Upper-Limit        Best-Fit-Value  L'
   for ip = 0, npar-1 do begin
      if (lowlim(ip) EQ upplim(ip)) then lim = 'f' $
      else if ((bfparm(ip) - lowlim(ip)) LT (upplim(ip)-lowlim(ip))*0.1) then $
               lim = '<' $
      else if ((upplim(ip) - bfparm(ip)) LT (upplim(ip)-lowlim(ip))*0.1) then $
              lim = '>' else lim = ' '
      printf,2, format='(A7, "[", 2F17.9, " ] = ", F17.9, 2X, A1)', $
             parname(ip), lowlim(ip), upplim(ip), bfparm(ip), lim
   endfor

   close, 2
   spawn, 'cat ~/idl/thesis/vbo_data/' + dir + '/OrbFitR.tmp >> ~/idl/thesis/vbo_data/' + dir + '/Or
bFitR.results'
   spawn, 'rm -f ~/idl/thesis/vbo_data/' + dir + '/OrbFitR.tmp'

endif


;
;  Compute orbital phase and plot data points and best-fit solution
;
T0 = bfparm(2)
```

```
Per = bfparm(0)
orbphs = dblarr(nv+1) ; Define orbphs as same size as epoch
for i = 0, nv do begin
    if (obsepoch(i) GE T0) then orbphs(i) = ((obsepoch(i)-T0) MOD Per) / Per $
    else orbphs(i) = 1. + (((obsepoch(i) - T0) MOD Per) / Per)
endfor
if (KEYWORD_SET(vsq)) then yts = '^2'  else yts = ' '
if (NOT KEYWORD_SET(outf)) then WINDOW, 1, RETAIN=2
plot, [0],[0],xrange=[-0.05,1.05], yrange=[0.,1.2], psym=3, $
      xtitle = 'Orbital Phase', ytitle = 'Calibrated Visibility (V)'+yts, $
      charsize=1.2, xthick=3, ythick=3, charthick=4, thick=4
;
;  IDL OPLOTERR does not accept THICK parameter, so manually plot
;  values and error bars in thick=4
;
;oploterr, orbphs, v, verr, 1, thick=4
oplot, orbphs, v, psym=1, thick=4
for iv = 0, nv do begin
    oplot, [orbphs(iv), orbphs(iv)], [v(iv)-verr(iv), v(iv)+verr(iv)], $
           linestyle=0, thick=4
endfor

modelv = calcVis(obsepoch, bfparm)
oplot, orbphs, modelv, psym=4, thick=4

;
;  Plot Baseline vs. Visib Curve
;
if (NOT KEYWORD_SET(outf)) then WINDOW, 2, RETAIN=2
plot,[-1],[-1], psym=3, $
     xrange=[fix(min(base)-2),fix(max(base)+2)], $
     yrange = [0.,1.2], xtitle = 'Baseline (meters)', $
     ytitle = 'Calibrated Visibility', $
     charsize=1.2, xthick=3, ythick=3, charthick=4, thick=4
;
;  IDL OPLOTERR does not accept THICK parameter, so manually plot
;  values and error bars in thick=4
;
;oploterr, base, v, verr, 1
oplot, base, v, psym=1, thick=4
for iv = 0, nv do begin
    oplot, [base(iv), base(iv)], [v(iv)-verr(iv), v(iv)+verr(iv)], $
           linestyle=0, thick=4
endfor
oplot, base, modelv, psym=4, thick=4

;
;  Print Each obs, with a extra gap separating each night
;
count = 1
countv = INTARR(nv+1)
countv(0) = count
for iv = 1, nv do begin
    if (fix(obsepoch(iv)) EQ fix(obsepoch(iv-1))) then $ ; same night
       count = count + 1 $ ; increment count by 1
    else  $  ; different night
       count = count + 2  ; insert night gap in data
    countv(iv) = count
endfor

if (NOT KEYWORD_SET(outf)) then WINDOW, 3, RETAIN=2
plot,[-1],[-1], psym=3, $
     xrange=[0,count+1], $
     yrange = [0.,1.2], xtitle = 'Observation', $
     ytitle = 'Calibrated Visibility', $
     charsize=1.2, xthick=3, ythick=3, charthick=4, thick=4
;
;  IDL OPLOTERR does not accept THICK parameter, so manually plot
;  values and error bars in thick=4
;
;oploterr, base, v, verr, 1
oplot, countv, v, psym=1, thick=4
for iv = 0, nv do begin
    oplot, [countv(iv), countv(iv)], [v(iv)-verr(iv), v(iv)+verr(iv)], $
           linestyle=0, thick=4
endfor
oplot, countv, modelv, psym=4, thick=4
```

```
;
;  Print visib values in detail file
;
if KEYWORD_SET(outf) then begin
   openw, 3, '~/idl/thesis/vbo_data/' + dir + '/OrbFitR.visib.fit'
   printf,3, format='(1A)', SYSTIME()
   printf,3, format='(5x,"HJD",7x,"Obs V",1A," Err-V","  Calc V",1A,"   O-C")',yts,yts
   for i = 0, nv do begin
     printf, 3, format='(F12.5, F8.3, F8.3, F8.3, F8.3)', $
                obsepoch(i), v(i), verr(i), modelv(i), v(i)-modelv(i)
   endfor
   close, 3
endif

if KEYWORD_SET(outf) then begin
   device,/close   ; close the PS file
   set_plot,'x'    ; revert back to terminal graphics output
endif


return
END


pro CalcSma, hdid, incl, angsma, eangsma, niter

;  For given incl (current iteration value of incl in deg),
;  use asini from spectroscopy and parallax from Hipparcos or other
;  sources to compute & return angular sma and its 1-sigma error in mas.
;  Return an "approriate" nbr of tries of sma within 1-sigma error
;  (see calc below for what is "appropriate")

;  Parameters for the stars from spectroscopic orbit and other refs
;  All spectroscopic elements are from CfA orbits
;  Plx for 146361 is from Les1999, and for all others are from van Leeuwen 2007
thd = ['hd008997', 'hd045088', 'hd146361', 'hd223778']
tplx  = [42.13, 67.89, 43.93, 91.82]  ; mas
teplx = [00.68, 01.53, 00.10, 00.30]  ; mas
tasini  = [18.74, 16.849, 2.8098, 14.622]  ; R_sun from CfA orbit
teasini = [00.11, 00.057, 0.0093,  0.053]  ; R_sun from CfA orbit

fd = where(thd EQ hdid)
if (fd(0) EQ -1) then begin
   print, 'HD ID not found! ', hdid
   incl  = -1.
   eincl = -1.
   niter = -1.
   RETURN
endif else fdi = fd(0)

asini  = tasini(fdi) * 696000./1.496e8  ; Convert to AU
easini = teasini(fdi) * 696000./1.496e8 ; Convert to AU
plx = tplx(fdi)
eplx  = teplx(fdi)

sma = asini / sin(incl*!pi/180.)
esma = SQRT( (easini/sin(incl*!pi/180.))^2. )

angsma = sma * plx
eangsma = angsma * SQRT( (esma/sma)^2. + (eplx/plx)^2. )

;  Do 1 iteration per 0.01 mas uncertainty in angsma.
;  Limit iterations to between 3 and 15
niter = fix(eangsma/0.01)
if (niter LT 3) then niter = 3
if (niter GT 15) then niter = 15

return
END

@~/idl/thesis/CalcVis
```

C.5.2 Example Input File of Calibrated Visibilities

```
;    HJD          Baseline     Base-orient    Visib        Visib-err   Wavelength
; UT 2007-05-17 data
   54237.76327   322.1841535   38.90860753  0.8640769114 0.08580654039   2.1329
   54237.77388   324.5476995   37.30277017  0.9091188593   0.106622512   2.1329
   54237.78419   326.4113232   35.67037403  0.7364975443 0.06168599425   2.1329
   54237.79557   328.0124214   33.78930955  0.7020072262 0.06269439484   2.1329
   54237.80566   329.0755172   32.04316448  0.5845545093 0.05771936068   2.1329
   54237.81631   329.8684988   30.13042126  0.6523913486 0.07643914754   2.1329
   54237.83333   330.540187    26.92415368  0.4680483653 0.05339319801   2.1329
   54237.93189   328.3259477    5.313527934 0.8332661835 0.04919897218   2.1329
   54237.94172   328.1780545    2.98267306  0.774508627  0.05928058711   2.1329
   54237.95385   328.1087726    0.09088828  0.6724026543 0.03818548611   2.1329
   54237.98020   328.4001867  173.8252467   0.2436991552 0.01545608878   2.1329
; UT 2007-05-27 data
   54247.70094   267.8789627   36.65248893  0.8584099682    0.11275264   2.1329
   54247.71566   271.0695809   34.63715219  0.8881816548  0.0796278443   2.1329
   54247.72925   273.4224039   32.64404675  0.8243610105 0.08334095568   2.1329
   54247.74400   275.3865649   30.34974599  0.6693624858 0.09335511181   2.1329
   54247.76088   276.9845969   27.54552975  0.4352274163  0.0577530859   2.1329
; UT 2007-05-29 data
   54249.71443   271.8639639   34.02704177  0.5890979542  0.0525760834   2.1329
   54249.72550   273.6829955   32.38170559  0.5703079435 0.05386102256   2.1329
   54249.73937   275.4838152   30.2106718   0.5748088173 0.06444664595   2.1329
   54249.75079   276.6128202   28.32720157  0.5939382742 0.06269114484   2.1329
   54249.77217   277.9874522   24.59837625  0.3912264245 0.05944668181   2.1329
; UT 2007-07-29 data
   54310.71647   328.6495782   8.516645449  0.6157056247 0.06179587933   2.1329
   54310.72609   328.4076091   6.258141671  0.4050823413 0.05033409499   2.1329
   54310.77554   328.3412799   174.4944247  0.4771855878 0.04980552717   2.1329
   54310.78593   328.5842383   172.0420132  0.5583759033 0.05400055664   2.1329
   54310.79650   328.897506    169.5794852  0.8701816929 0.09978546524   2.1329
```

C.5.3 Example Input File of Orbital Elements

```
Element                  Lower_Limit       Upper_Limit
Period_(P,days)           1.139791343       1.139791503
Eccentricity_(e)          0.000             0.000
Epoch_of_node(T,HJD)      50127.04835       50127.04875
l-omega_(deg)             0.0               0.0
semi-major_axis_(a,mas)   1.19              1.27
inclination_(i,deg)       27.0              29.0
C-OMEGA_(deg)             206.0             210.5
del-mag_(mag)             0.0               0.7
Angular_dia_prim_(mas)    0.45              0.55
Angular_dia_sec_(mas)     0.40              0.50
```

C.5.4 Calculating Interferometric Visibility for Given Parameters

```
FUNCTION calcVis, epoch, P, DEBUG = debug
;*************************************************************************
;  FUNCTION calcVis - Calculate visibility for a given t (independent var) *
;                   and input parameters as below:                         *
;                                                                          *
;     epoch = Epoch of observation (same unit as T0 - MJD/JD/HJD)          *
;     P(0)  = Period (days)                                                *
;     P(1)  = Eccentricity                                                 *
;     P(2)  = Epoch of Periastron (same unit as epoch - MJD/JD/HJD)        *
;     P(3)  = Argument of periapse (lowercase omega)                       *
;     P(4)  = Semi-major axis (mas)                                        *
;     P(5)  = Inclination (deg)                                            *
;     P(6)  = Longitude of ascending node (capital OMEGA)                  *
;     P(7)  = Delta-mag (mag)                                              *
;     P(8)  = Primary's angular diameter (mas)                             *
;     P(9)  = Secondary's angular diameter (mas)                           *
;                                                                          *
;     In addition to the above parameters, this function requires the      *
;     following parameters passed via the COMMON block:                    *
;     COMMON FUNC_ARGS, obsepoch, base, bang, wvlth, vsqf                  *
;       obsepoch = array of epochs of observations                         *
;       base = array of baselines (m) of observations                      *
;       bang = array of baseline orientations (deg) of observations        *
;       wvlth = Wavelength (microns) of observation                        *
;       vsqf = If set to 'y', return V^2, else return V                    *
;                                                                          *
;*************************************************************************

COMMON FUNC_ARGS, obsepoch, base, bang, wvlth, vsqf

;
;  Fitted parameters
;
Per = P(0)
ecc = P(1)
T0 = P(2)
lomega = P(3)
a = P(4)
incl = P(5)
COmega = P(6)
dmag = P(7)
angdiaP = P(8)
angdiaS = P(9)

;
;  Conversion constants
;

d2r = !pi / 180.  ; degrees to radians
r2d = 180./ !pi   ; radians to degrees
m2r = 1.e-3/3600. * d2r  ; mas to radians

;
;  Input epoch could be an array of dates.  Process each element and
;  load results into an array as well
;

nele = SIZE(epoch,/DIMENSIONS)
nele = nele (0)
if (nele EQ 0) then begin
   calcV = 0.d  ; define as scalar
   nele = 1     ; force one iteration of follwoing loop
endif else $
   calcV = dblarr(nele)

for ci = 0, nele-1 do begin

;
;   Lookup baseline and its orientation for current epoch
;

    curt = epoch(ci)
    ti = where(obsepoch EQ curt)
    if (ti EQ -1) then begin
       print, 'Current epoch not found', curt
       ERROR_CODE = -1
       return, 0.
    endif
```

```
    curbase = base(ti)
    curbang = bang(ti)
    curbang = bang(ti)
    curwv = wvlth(ti) / 1000000.d   ; in meters

;
;   Calculate visibilities for the individual stars
;

    besf = !pi * curbase / curwv  ; Besel function factor
    Vprim = 2.d * BESELJ(angdiaP * m2r * besf, 1) / (angdiaP * m2r * besf)
    Vsec = 2.d * BESELJ(angdiaS * m2r * besf, 1) / (angdiaS * m2r * besf)

;
;   CALCULATE ORBITAL PROPERTIES
;


;
;   Mean anomaly
;
    MA = 2*!pi/Per*(curt-T0)
;
;   Eccentric anomaly, solved over 20 iterations
;
    EA = MA + ecc * SIN(MA) + ecc^2 / 2. * SIN(2*MA)  ; Starting value (E3)
    for i = 1, 20 do EA = MA + ecc * SIN(EA)
;
;   True anomaly
;
    TA = 2.d*ATAN(SQRT((1.+ecc)/(1.-ecc))*TAN(EA/2.d))
;
;   Position vector magnitude (radius)
;
    posr = a * (1. - ecc * COS(EA))
    rho = posr * SQRT(1 - SIN(TA+lomega*d2r)^2.*SIN(incl*d2r)^2.)
;
;   Angle of position vector (theta)
;
    ttemp = ABS(ATAN(TAN(TA+lomega*d2r)*COS(incl*d2r)))
    if (SIN(TA+lomega*d2r) GE 0. AND COS(TA+lomega*d2r) GE 0.) then $
       tmo = ttemp
    if (SIN(TA+lomega*d2r) GE 0. AND COS(TA+lomega*d2r) LT 0.) then $
       tmo = !pi - ttemp
    if (SIN(TA+lomega*d2r) LT 0. AND COS(TA+lomega*d2r) GE 0.) then $
       tmo = 2. * !pi - ttemp
    if (SIN(TA+lomega*d2r) LT 0. AND COS(TA+lomega*d2r) LT 0.) then $
       tmo = !pi + ttemp
    if (COS(incl*d2r) GE 0.) then theta = COmega + tmo * r2d $
    else theta = COmega - tmo * r2d
    if (theta GT 360.) then theta = theta - 360.

    beta = 10.^(0.4*dmag)

    if (vsqf EQ 'y') then $ ;  Return V-squared values
       calcV(ci) = 1./(1. + beta)^2 * (beta^2*Vprim^2 + Vsec^2 + $
                   2*beta*Vprim*Vsec* $
             COS(2.*!pi*curbase/curwv*rho*m2r*ABS(COS((theta-curbang)*d2r)))) $
    else $                    ; Return V
       calcV(ci) = 1./(1. + beta) * SQRT(beta^2*Vprim^2 + Vsec^2 + $
                   2*beta*Vprim*Vsec* $
             COS(2.*!pi*curbase/curwv*rho*m2r*ABS(COS((theta-curbang)*d2r))))

;   Print details if called in debug mode
    if KEYWORD_SET(debug) then begin
        print, format='("P, e, T0, lo, a: ", 5F12.4)',P(0:4)
        print, format='("i, CO, dm, diap, dias: ", 5F12.4)',P(5:9)
        print, format='("t, Base, B-ang: ", 3F16.6)', $
                          epoch, curbase, curbang
        print, format='("wavelth: ", E14.6)', curwv
        print, format='("Visib_P, Visib_S: ", 2F14.6)', Vprim, Vsec
        print, format='("MA, EA, TA, TA+2pi: ", 4F16.6)', MA, EA, TA, TA+2*!pi
        print, format='("Posr, rho, theta, beta, TMO: ", 5F12.6)', $
                          posr, rho, theta, beta, tmo
        print, format='("Terms of Visib eq: ", 5F10.6)', $
             beta^2*Vprim^2, Vsec^2, 2*beta*Vprim*Vsec, $
             COS(2.*!pi*curbase/curwv*rho*m2r*ABS(COS((theta-curbang)*d2r))), $
             ABS(COS((theta-curbang)*d2r))
        print, format='("Calculated V = ", F6.3)', calcV
        stop
```

```
    endif

endfor

return, calcV
END
```

C.5.5 Estimating Parameter Uncertainties

```
pro OrbErr, dir, mincs, SEPPS=sepps

;*****************************************************************************
;  CHARA Data Reduction  - Explore parameter space to establish 1, 2, 3    *
;                          sigma errors for each parameter                 *
;                                                                          *
;  Read the parameter/chi-sq data points generated by OrbitFitR.pro        *
;  and create 1-D projections for each parameter. Fit the lower envelope   *
;  of each projection with a curve to get the 1, 2, 3 sigma errors.        *
;                                                                          *
;  Input:  Paramaters:                                                     *
;            mincs   Minimum chi-sq value for these data points from       *
;                    OrbFitR.pro                                           *
;            /SEPPS  If set, generate separate PS file for each param      *
;  Input:  Input file with values of each parameter and corr chi-sq        *
;            (OrbFitR.csq)                                                 *
;            Space-delimited columns are:                                  *
;              Period (days)                                               *
;              Eccentricity                                                *
;              Epoch of Periastron (same unit as Epoch - MJD/JD/HJD)       *
;              Argument of periapse (lowercase omega)                      *
;              Semi-major axis (mas)                                       *
;              Inclination (deg)                                           *
;              Longitude of ascending node (capital OMEGA)                 *
;              Delta-mag (mag)                                             *
;              Primary's angular diameter (mas)                            *
;              Secondary's angular diameter (mas)                          *
;              Chi-square value for current set of parameters              *
;          Input file with ranges of orbital elements (OrbEleR.inp)        *
;            This file is read only to get the limits of each parameter    *
;            in order to set XRANGE for the plots.                         *
;            First row is column headings (ignored by the program)         *
;            Columns are:                                                  *
;              Parameter name (ignored by program)                         *
;              Lower limit for parameter                                   *
;              Upper limit for parameter                                   *
;                                                                          *
;  Output: Plots for each parameter variation for 1, 2, 3 sigma errors     *
;                                                                          *
;  Original Version: Deepak Raghavan    September 10, 2007                 *
;                                                                          *
;  Modifications:                                                          *
;                                                                          *
;                                                                          *
;*****************************************************************************

;
;  Initialize constants and arrays
;
npar = 10  ; max possible number of free parameters
parname = ["Period ", "Ecc    ", "T0     ", "!7x!X!N (degrees)", $
           "!7a!X!N (mas)", "i (degrees)", "!7X!X!N (degrees)", $
           "!7D!X!NK' (magnitude)", "!7H!X!Np", "!7H!X!Ns"]

;
;  Read parameter ranges for use in setting XRANGE for plots
;

inp = ' '
openr, 1, '~/idl/thesis/vbo_data/' + dir + '/OrbEleR.inp'
readf, 1, inp  ; Read and ignore header line

inpdat = strarr(4)
i = -1
lowlim = dblarr(npar)
upplim = dblarr(npar)

for i = 0, npar-1 do begin

      readf,1,inp
      inpdat = STRSPLIT(inp, ' ', /extract)
      lowlim(i) = DOUBLE(inpdat(1))
      upplim(i) = DOUBLE(inpdat(2))

endfor

close,1

;
```

```
;  Setup plot file
;

if (NOT KEYWORD_SET(sepps)) then begin ; Combined PS for all params
   set_plot,'ps'
   device,filename="~/idl/thesis/vbo_data/"+dir+"/OrbErrR.ps", /portrait
endif

for ip = 0, npar-1 do begin

    if (lowlim(ip) EQ upplim(ip)) then CONTINUE  ; skip for fixed parameters

    if (KEYWORD_SET(sepps)) then begin ; Separate PS for each param
       set_plot,'ps'
       device,filename=string(format='("~/idl/thesis/vbo_data/",2A,I1,1A)', $
                dir,"/OrbErrR.",ip,".ps"), $
              /portrait
    endif

;
;  Setup plot area for current parameter
;

    xlow = lowlim(ip)-(upplim(ip)-lowlim(ip))/10.
    xupp = upplim(ip)+(upplim(ip)-lowlim(ip))/10.

    if (ip EQ 0) then $ ; Period axis value format
       plot, [xlow], [mincs-3], xrange=[xlow,xupp], $
             yrange=[mincs-3,mincs+10], psym=3, $
             xtitle = parname(ip), ytitle = '!7v!X!N!U2', $
             charsize=1.2, xthick=3, ythick=3, charthick=4, thick=4, $
             xtickformat='(F8.5)' $
    else if (ip EQ 2) then $  ; T0 axis value format
       plot, [xlow], [mincs-3], xrange=[xlow,xupp], $
             yrange=[mincs-3,mincs+10], psym=3, $
             xtitle = parname(ip), ytitle = '!7v!X!N!U2', $
             charsize=1.2, xthick=3, ythick=3, charthick=4, thick=4, $
             xtickformat='(F9.2)' $
    else $
       plot, [xlow], [mincs-3], xrange=[xlow,xupp], $
             yrange=[mincs-3,mincs+10], psym=3, $
             xtitle = parname(ip), ytitle = '!7v!X!N!U2', $
             charsize=1.2, xthick=3, ythick=3, charthick=4, thick=4

    oplot, [!x.crange(0), !x.crange(1)], [mincs, mincs], linestyle=5, thick=4
    oplot, [!x.crange(0), !x.crange(1)], [mincs+1, mincs+1], $
           linestyle = 5, thick=4
    oplot, [!x.crange(0), !x.crange(1)], [mincs+4, mincs+4], $
           linestyle = 5, thick=4
    oplot, [!x.crange(0), !x.crange(1)], [mincs+9, mincs+9], $
           linestyle = 5, thick=4

;
;   Read parameters & chi-sq values
;

    openr,1, '~/idl/thesis/vbo_data/' + dir + '/OrbFitR.csq'

    inpdat = dblarr(11)
    minchisq = 999999999.9d

    while (NOT EOF(1)) do begin

          readf,1,inpdat
          curpar = inpdat(ip)      ; save current parameter
          curchisq = inpdat(npar)  ; chi-sq is the last column
          if (curchisq LT minchisq) then begin
             minchisq = curchisq
             mincspar = curpar
          endif

          oplot, [curpar], [curchisq], psym=3

    endwhile
    close,1

;    xyouts, !x.crange(0)+(!x.crange(1)-!x.crange(0))/10., mincs-2., $
;            string(format='(A10, " = ", F14.6)', parname(ip), mincspar)
```

```
    if (KEYWORD_SET(sepps)) then begin ; Separate PS for each param
       device,/close   ; close the PS file
       set_plot,'x'    ; revert back to terminal graphics output
    endif


endfor

if (NOT KEYWORD_SET(sepps)) then begin ; Combined PS for all params
   device,/close   ; close the PS file
   set_plot,'x'    ; revert back to terminal graphics output
endif

return
END
```

– D –

Two Suns in the Sky: Stellar Multiplicity in Exoplanet Systems

This chapter reproduces a 2006 Astrophysical Journal publication (Raghavan et al. 2006), which was completed as a part of this thesis effort.

The Astrophysical Journal, 646:523–542, 2006 July 20
© 2006. The American Astronomical Society. All rights reserved. Printed in U.S.A.

TWO SUNS IN THE SKY: STELLAR MULTIPLICITY IN EXOPLANET SYSTEMS

Deepak Raghavan and Todd J. Henry
Center for High Angular Resolution Astronomy and Department of Physics and Astronomy, Georgia State University, P.O. Box 4106, Atlanta, GA 30302-4106; raghavan@chara.gsu.edu

Brian D. Mason
US Naval Observatory, 3450 Massachusetts Avenue NW, Washington, DC 20392-5420

John P. Subasavage, Wei-Chun Jao, and Thom D. Beaulieu
Center for High Angular Resolution Astronomy and Department of Physics and Astronomy, Georgia State University, P.O. Box 4106, Atlanta, GA 30302-4106

and

Nigel C. Hambly
Institute for Astronomy, School of Physics, University of Edinburgh, Royal Observatory, Blackford Hill, Edinburgh EH9 3HJ, Scotland, UK
Received 2005 November 4; accepted 2006 March 29

ABSTRACT

We present results of a reconnaissance for stellar companions to all 131 radial velocity–detected candidate extrasolar planetary systems known as of 2005 July 1. Common proper-motion companions were investigated using the multiepoch STScI Digitized Sky Surveys and confirmed by matching the trigonometric parallax distances of the primaries to companion distances estimated photometrically. We also attempt to confirm or refute companions listed in the Washington Double Star Catalog, in the Catalogs of Nearby Stars Series by Gliese and Jahreiß, in *Hipparcos* results, and in Duquennoy & Mayor's radial velocity survey. Our findings indicate that a lower limit of 30 (23%) of the 131 exoplanet systems have stellar companions. We report new stellar companions to HD 38529 and HD 188015 and a new candidate companion to HD 169830. We confirm many previously reported stellar companions, including six stars in five systems, that are recognized for the first time as companions to exoplanet hosts. We have found evidence that 20 entries in the Washington Double Star Catalog are not gravitationally bound companions. At least three (HD 178911, 16 Cyg B, and HD 219449), and possibly five (including HD 41004 and HD 38529), of the exoplanet systems reside in triple-star systems. Three exoplanet systems (GJ 86, HD 41004, and γ Cep) have potentially close-in stellar companions, with planets at roughly Mercury–Mars distances from the host star and stellar companions at projected separations of $\sim$20 AU, similar to the Sun–Uranus distance. Finally, two of the exoplanet systems contain white dwarf companions. This comprehensive assessment of exoplanet systems indicates that solar systems are found in a variety of stellar multiplicity environments—singles, binaries, and triples—and that planets survive the post–main-sequence evolution of companion stars.

Subject headings: binaries: general — planetary systems — surveys

Online material: machine-readable tables

1. INTRODUCTION

The hunt for planets outside our solar system has revealed 161 candidate planets in 137 stellar systems as of 2005 July 1, with 18 of these systems containing multiple planets. After the initial flurry of "hot jupiter" discoveries—primarily a selection effect due to the fact that (1) the nascent effort was biased toward discovery of short-period systems and (2) massive planets induce more readily detected radial velocity variations—it is now believed that the more massive planets preferentially lie farther away from the primary (Udry et al. 2004; Marcy et al. 2005a), perhaps leaving the space closer to the star for the harder to detect terrestrial planets. Through these discoveries, we are now poised to gain a better understanding of the environments of exoplanet systems and compare them to our solar system.

Our effort in this paper is focused on a key parameter of planetary systems: the stellar multiplicity status of exoplanet hosts. We address questions such as the following: (1) Do planets preferentially occur in single-star systems (like ours), or do they commonly occur in multiple-star systems as well? (2) For planets residing in multiple-star systems, how are the planetary orbits related to stellar separations? (3) What observational limits can we place on disk truncations or orbit disruptions in multistar planetary systems? This study contributes to the broader subjects of planetary system formation, evolution, and stability through a better understanding of the environments of exoplanet systems.

Stellar multiplicity among exoplanet systems was first studied by Patience et al. (2002), who looked at the first 11 exoplanet systems discovered and reported two binaries and one triple system. Luhman & Jayawardhana (2002) conducted an adaptive optics (AO) survey looking for stellar and substellar companions to 25 exoplanet hosts and reported null results. More recently, Eggenberger et al. (2004) and Udry et al. (2004) reported 15 exoplanet systems with stellar companions in a comprehensive assessment, and additional companions have been reported for several specific systems (Mugrauer et al. 2004a, 2004b, 2005). Our effort confirms many of these previously reported systems, reports two new companions, identifies an additional candidate, and recognizes, for the first time, one triple and four binary exoplanet systems (these are known stellar

TABLE 1
EXOPLANET SYSTEMS SEARCHED FOR COMPANIONS

NAME (1)	PROPER MOTION (arcsec yr^{-1}) (2)	PROPER MOTION (deg) (3)	DSS IMAGES Epoch 1 (4)	DSS IMAGES Epoch 2 (5)	TOTAL μ (arcsec) (6)	μ OBSERVABLE? (7)	COMPANIONS CPM (8)	COMPANIONS Other (9)
BD −10 3166	0.183	268.5	1983.29	1992.04	1.602	Yes	...	...
GJ 436	1.211	132.2	1955.28	1996.38	49.770	Yes	...	...
GJ 876	1.174	125.1	1983.76	1989.83	7.116	Yes	...	...
HD 000142	0.577	94.0	1982.87	1996.62	7.933	Yes	...	B
HD 001237	0.438	97.6	1977.77	1997.58	8.676	Yes	...	...
HD 002039	0.080	79.0	1978.82	1997.61	1.503	No	...	...
HD 002638	0.248	205.5	1983.53	1993.85	2.560	Yes	...	...
HD 003651	0.592	231.2	1953.91	1987.65	19.972	Yes	...	...
HD 004203	0.176	134.7	1954.00	1987.65	5.922	Yes	...	...
HD 004208	0.348	64.4	1980.63	1989.74	3.171	No	...	...
HD 006434	0.554	197.8	1976.89	1990.73	7.666	Yes	...	...
HD 008574	0.298	122.1	1949.98	1991.76	12.453	Yes	...	...
HD 008673	0.250	109.8	1954.67	1991.76	9.273	Yes	...	B?
HD 009826	0.418	204.4	1953.71	1989.77	15.073	Yes	B	B
HD 010647	0.198	122.6	1977.92	1997.61	3.898	Yes	...	...
HD 010697	0.115	203.1	1954.89	1986.69	3.657	Yes	...	...
HD 011964	0.441	236.6	1982.63	1991.70	4.003	Yes	B	B
HD 011977	0.105	46.1	1976.67	1987.72	1.160	No	...	...
HD 012661	0.206	211.6	1953.87	1990.87	7.622	No	...	...
HD 013189	0.006	13.3	1954.76	1989.83	0.210	No	...	...
HD 013445	2.193	72.6	1975.85	1988.91	28.646	Yes	...	B
HD 016141	0.464	199.7	1982.79	1997.74	6.937	Yes	...	B?
HD 017051	0.399	56.7	1977.78	1997.81	7.995	Yes	...	...
HD 019994	0.205	109.7	1951.69	1997.84	9.463	Yes	...	B
HD 020367	0.118	241.2	1953.77	1993.72	4.714	Yes	...	...
HD 022049	0.977	277.1	1982.79	1998.97	15.806	Yes	...	...
HD 023079	0.214	244.6	1978.82	1993.96	3.241	Yes	...	...
HD 023596	0.058	68.5	1953.03	1989.76	2.130	No	...	...
HD 027442	0.175	196.0	1983.04	1997.74	2.573	Yes	...	B
HD 027894	0.328	33.8	1983.04	1997.74	4.823	Yes	...	...
HD 028185	0.101	126.7	1982.82	1985.96	0.317	No	...	...
HD 030177	0.067	100.3	1983.04	1997.74	0.985	No	...	...
HD 033636	0.227	127.2	1954.85	1990.81	8.164	Yes	...	...
HD 034445	0.149	184.4	1954.85	1990.82	5.360	Yes	...	...
HD 037124	0.427	190.8	1951.91	1991.80	17.032	Yes	...	...
HD 037605	0.252	167.5	1955.90	1992.06	9.114	Yes	...	...
HD 038529	0.163	209.4	1951.91	1990.87	6.350	Yes	B	...
HD 039091	1.096	16.5	1978.03	1989.99	13.116	Yes	...	...
HD 040979	0.179	148.0	1953.12	1989.83	6.570	Yes	B	B
HD 041004	0.078	327.0	1978.03	1993.96	1.243	Yes	...	B, C
HD 045350	0.069	219.3	1953.19	1986.91	2.326	No	...	...
HD 046375	0.150	130.3	1953.94	1998.88	6.740	Yes	...	B
HD 047536	0.126	59.5	1979.00	1992.99	1.763	Mar	...	...
HD 049674	0.128	164.1	1953.19	1989.86	4.694	Yes	...	...
HD 050499	0.097	314.8	1976.89	1994.21	1.679	No	...	...
HD 050554	0.103	201.2	1956.27	1994.03	3.889	Yes	...	...
HD 052265	0.141	304.8	1983.04	1989.18	0.864	No	...	...
HD 059686	0.087	150.5	1953.02	1989.08	3.137	Mar	...	...
HD 063454	0.045	207.5	1975.94	1992.99	0.767	No	...	...
HD 065216	0.190	320.1	1976.25	1991.13	2.827	No	...	...
HD 068988	0.132	76.1	1954.01	1989.98	4.747	Yes	...	...
HD 070642	0.303	318.1	1976.97	1991.10	4.283	No	...	...
HD 072659	0.150	229.2	1954.97	1992.03	5.559	Yes	...	...
HD 073256	0.192	290.0	1977.22	1991.26	2.697	Mar	...	...
HD 073526	0.173	339.5	1977.06	1991.27	2.459	Mar	...	...
HD 074156	0.202	172.9	1953.02	1991.10	7.692	Yes	...	...
HD 075289	0.229	185.1	1977.06	1991.27	3.255	Yes	...	B
HD 075732	0.539	244.2	1953.94	1998.30	23.908	Yes	B	B
HD 076700	0.308	293.2	1976.26	1991.05	4.558	Yes	...	...
HD 080606	0.047	81.6	1953.13	1995.25	1.979	Yes	B	B
HD 082943	0.174	179.2	1983.36	1987.32	0.689	No	...	...
HD 083443	0.123	169.5	1980.06	1995.09	1.849	No	...	...

TABLE 1—*Continued*

Name (1)	Proper Motion (arcsec yr^{-1}) (2)	Proper Motion (deg) (3)	DSS Images Epoch 1 (4)	DSS Images Epoch 2 (5)	Total μ (arcsec) (6)	μ Observable? (7)	Companions CPM (8)	Companions Other (9)
HD 088133	0.264	182.8	1955.23	1998.99	11.555	Yes	...	...
HD 089307	0.276	261.8	1950.29	1987.32	10.219	Yes	...	...
HD 089744	0.183	220.9	1953.21	1990.23	6.773	No	...	B
HD 092788	0.223	183.2	1982.37	1991.21	1.971	Yes	...	...
HD 093083	0.177	211.6	1980.21	1995.10	2.636	Yes	...	...
HD 095128	0.321	279.9	1955.22	1998.38	13.855	Yes	...	...
HD 099492	0.755	284.7	1955.29	1996.28	30.944	Yes	A	A
HD 101930	0.348	2.5	1987.20	1992.24	1.754	No	...	...
HD 102117	0.094	222.1	1987.20	1992.24	0.474	No	...	...
HD 104985	0.174	122.1	1955.17	1997.11	7.299	Yes	...	...
HD 106252	0.280	175.1	1955.29	1991.27	10.076	Yes	...	...
HD 108147	0.192	251.5	1987.26	1996.30	1.735	No	...	...
HD 108874	0.157	124.7	1955.39	1991.07	5.602	Yes	...	...
HD 111232	0.116	13.9	1987.08	1996.29	1.067	No	...	B?
HD 114386	0.353	203.0	1975.41	1992.25	5.943	Yes	...	...
HD 114729	0.369	213.2	1978.13	1991.21	4.826	Yes	...	B
HD 114762	0.583	269.8	1950.30	1996.30	26.822	Yes	...	B
HD 114783	0.138	274.0	1956.27	1996.23	5.514	Yes	...	...
HD 117176	0.622	202.2	1955.38	1997.35	26.110	Yes	...	...
HD 117207	0.217	250.7	1975.27	1991.21	3.458	Mar	...	...
HD 117618	0.127	168.6	1975.19	1991.23	2.037	No	...	...
HD 120136	0.483	276.4	1954.25	1992.20	18.328	Yes	...	B
HD 121504	0.264	251.5	1987.26	1994.19	1.828	No	...	...
HD 128311	0.323	140.5	1950.28	1989.25	12.588	Yes	...	...
HD 130322	0.191	222.6	1980.22	1996.37	3.085	Yes	...	...
HD 134987	0.400	86.1	1976.42	1991.50	6.034	Yes	...	...
HD 136118	0.126	280.7	1955.30	1992.41	4.676	Yes	...	...
HD 137759	0.019	334.5	1953.46	1995.15	0.792	No	...	...
HD 141937	0.100	76.1	1976.41	1991.61	1.520	No	...	...
HD 142022	0.339	264.7	1977.63	1996.30	6.329	Yes	B	B
HD 142415	0.153	228.1	1988.30	1992.58	0.654	No	...	...
HD 143761[a]	0.798	194.3	1950.28	1994.37	35.182	Yes	...	...
HD 145675	0.326	156.1	1955.23	1991.43	11.802	Yes	...	...
HD 147513	0.073	87.3	1987.39	1993.25	0.428	No	...	B
HD 149026	0.094	304.7	1954.49	1993.33	3.651	Yes	...	...
HD 150706	0.130	132.6	1955.39	1996.54	5.350	Yes	...	B?
HD 154857	0.103	122.4	1987.30	1993.32	0.621	No	...	...
HD 160691	0.192	184.5	1987.70	1992.58	0.938	No	...	...
HD 162020	0.033	140.2	1987.71	1991.68	0.131	No	...	...
HD 168443	0.242	202.3	1978.65	1988.59	2.406	No	...	...
HD 168746	0.073	197.7	1978.65	1988.59	0.726	No	...	...
HD 169830	0.015	356.8	1987.38	1992.41	0.075	No	...	B?
HD 177830	0.066	218.1	1950.46	1992.42	2.770	No	...	...
HD 178911B	0.203	18.6	1955.39	1992.44	7.523	Yes	A	A, C
HD 179949	0.153	131.6	1987.42	1991.62	0.643	No	...	...
HD 183263	0.038	208.2	1950.61	1992.59	1.595	No	...	...
HD 186427	0.212	219.6	1951.53	1991.53	8.679	Yes	A	A, C
HD 187123	0.189	130.7	1952.54	1992.67	7.583	Yes	...	...
HD 188015	0.106	149.4	1953.53	1992.49	4.130	Yes	B	...
HD 190228	0.126	123.7	1953.53	1992.49	4.910	Yes	...	...
HD 190360	0.861	127.5	1953.53	1992.49	33.549	Yes	B	B
HD 192263	0.270	346.4	1951.58	1988.67	10.013	Yes	...	...
HD 195019	0.354	99.2	1951.52	1990.71	13.874	Yes	...	B
HD 196050	0.201	251.4	1977.61	1991.75	2.842	Mar	...	B
HD 196885	0.096	29.7	1953.68	1987.50	3.246	Yes	...	...
HD 202206	0.126	197.7	1977.55	1991.74	1.788	No	...	...
HD 208487	0.156	139.3	1980.55	1995.63	2.353	Mar	...	...
HD 209458	0.034	122.4	1950.54	1990.73	1.366	No	...	...
HD 210277	0.458	169.2	1979.72	1987.79	3.693	Yes	...	...
HD 213240	0.236	214.9	1980.77	1995.65	3.510	Yes	B	B
HD 216435	0.232	110.6	1980.54	1996.62	3.730	No	...	...
HD 216437	0.085	329.5	1978.82	1996.79	1.527	No	...	...
HD 216770	0.290	127.9	1980.78	1995.79	4.354	Yes	...	...

TABLE 1—*Continued*

Name (1)	Proper Motion (arcsec yr^{-1}) (2)	Proper Motion (deg) (3)	DSS Images Epoch 1 (4)	DSS Images Epoch 2 (5)	Total μ (arcsec) (6)	μ Observable? (7)	Companions CPM (8)	Companions Other (9)
HD 217014	0.217	73.7	1954.59	1990.79	7.856	Yes	...	...
HD 217107	0.017	200.7	1982.80	1991.68	0.151	No	...	B?
HD 219449	0.369	92.6	1983.82	1991.76	2.931	Yes	B	B, C
HD 222404	0.136	339.0	1954.73	1992.76	5.172	Yes	...	B
HD 222582	0.183	232.6	1983.54	1989.83	1.152	Yes	B	B
HD 330075	0.254	248.2	1988.45	1995.25	1.725	No	...	...

Note.—Table 1 is also available in machine-readable form in the electronic edition of the *Astrophysical Journal*.
[a] We conclude that this system (ρ CrB) has either a planetary or a stellar companion, but not both. See § 2.3 for more details.

companions, but previously not noted to reside in exoplanet systems).

2. SAMPLE AND COMPANION SEARCH METHODOLOGY

Our sample includes all known exoplanet systems detected by radial velocity techniques as of 2005 July 1. We primarily used the Extrasolar Planets Catalog,[1] maintained by Jean Schneider at the Paris Observatory, to build our sample list for analyses. To ensure completeness, we cross-checked this list with the California & Carnegie Planet Search Catalog.[2] Our sample excludes planets discovered via transits and gravitational lensing, as these systems are very distant, with poor or no parallax and magnitude information for the primaries. In addition, these systems cannot be observed for stellar companions in any meaningful way. We also exclude a radial velocity–detected system, HD 219542, identified by Eggenberger et al. (2004) as an exoplanet system with multiple stars but since confirmed as a false planet detection by its discoverers (Desidera et al. 2004). The final sample comprises 155 planets in 131 systems. This list is included in Table 1 along with companion detection information, as described below.

Several efforts were carried out to gather information on stellar companions to exoplanet stars. To identify known or claimed companions, we checked available sources listing stellar companions: the Washington Double Star Catalog (WDS), the *Hipparcos* Catalog (Perryman et al. 1997), the Catalog of Nearby Stars (CNS; Gliese 1969; Gliese & Jahreiss 1979, 1991), and Duquennoy & Mayor (1991). We also visually inspected the STScI Digitized Sky Survey (DSS) multiepoch frames for the sky around each exoplanet system to investigate reported companions and to identify new common proper-motion (CPM) companion candidates. We then confirmed or refuted many candidates through photometric distance estimates using plate magnitudes from SuperCOSMOS, optical CCD magnitudes from the Cerro Tololo Inter-American Observatory (CTIO) 0.9 and 1.0 m telescopes, and infrared magnitudes from the Two Micron All Sky Survey (2MASS). The origin and status of each companion are summarized in Table 2 and described in § 5.1.

Table 1 lists each target star in our sample, sequenced alphabetically by name, and identifies all known and new companions. Column (1) is the exoplanet host star's name (HD when available, otherwise BD or GJ name). Columns (2) and (3) give the proper-motion magnitude (in arcsec yr^{-1}) and direction (in deg) of the star, mostly from *Hipparcos*. Columns (4) and (5) specify the observational epochs of the DSS images blinked to identify CPM companion candidates. Column (6) lists the total proper motion (in arcsec) of the exoplanet host during the time interval between the two observational epochs of the DSS plates. Column (7) identifies whether the proper motion of the star was detectable in the DSS frames, allowing the identification of CPM candidates. The entries "Yes" and "No" are self-explanatory, and "Mar" identifies that the proper motion was marginally detectable. Systems with very little proper motion or a brief separation between plate epochs could not be searched effectively (see § 2.1). Column (8) specifies companions identified via CPM, and column (9) specifies companions listed in the sources mentioned above or in other refereed papers. A question mark following the companion ID indicates that the source remains a candidate and could not be confirmed or refuted with confidence. The absence of a question mark indicates that the companion is confirmed.

Each reference we used for the companion search is described in the subsections below.

2.1. *STScI Digitized Sky Survey*

We downloaded multiepoch images of the sky around each exoplanet primary from the STScI Digitized Sky Survey (DSS).[3] The images of these surveys are based on photographic data obtained using the Oschin Schmidt Telescope on Palomar Mountain and the UK Schmidt Telescope in Australia. We typically extracted 10′ square images at two epochs centered on an exoplanet host star. The range of time interval between the epochs for a given target is 3.1–46.2 yr. Figure 1 shows a histogram of the number of systems per time interval bin for our sample.

We identified CPM companion candidates by eye, by blinking the two epoch frames. In general, primaries with a total proper motion of $\geq 3''$ were effectively searched, while those with a total proper motion in the range of $2''$–$3''$ were marginally searched, and stars with $\leq 2''$ total proper motion could not be searched for companions using this method. Exceptions to these ranges exist and are due to poorly matched astrometric fields caused by specific issues with the plate images, such as saturation around the primary, distribution of background stars in the frames, brightness of the companion and its proximity to the primary, and the relative rotation between the frames. The $3''$ detection limit corresponds to a proper-motion range of $0''.1$–$1''.0$ yr^{-1} with a median value of $0''.2$ yr^{-1} for the time intervals sampled. In addition, this method favors the detection of wide companions because bright primaries saturate the surrounding region out to many arcseconds and prevent companion detection within a $\sim 15''$–$30''$ radius, depending on source brightness. At the median distance

[1] See http://vo.obspm.fr/exoplanetes/encyclo/catalog.php.
[2] See http://exoplanets.org.
[3] See http://stdatu.stsci.edu/cgi-bin/dss_form.

TABLE 2

EXOPLANET SYSTEMS WITH STELLAR COMPANIONS

Sequence (1)	HD Name (2)	Other Name (3)	Component (4)	R.A. (J2000.0) (5)	Decl. (J2000.0) (6)	π (arcsec) (7)	Distance (pc) (8)	Basis (9)	Spectral Type (10)	Angular Separation (arcsec) (11)	P.A. (deg) (12)	Projected Separation (AU) (13)	$M \sin i$ (M_J) (14)	$a \sin i$ (AU) (15)	e (16)	Sources (17)	References (18)
1.....	000142	GJ 4.2	A	00 06 19.18	−49 04 30.7	0.03900	25.6	T	G1 IV	...	...	...	...	...	...	...	
	000142	...	b	...	...	...	...	...	...	...	...	...	1	0.98	0.38	...	
	000142	...	B	...	...	...	...	...	...	5.4	177	138	...	...	...	WC	1, 2
2.....	009826	υ And	A	01 36 47.84	+41 24 19.7	0.07425	13.5	T	F8.0 V	...	...	...	...	...	...	...	
	009826	...	b	...	...	...	...	...	...	...	...	...	0.69	0.059	0.012	...	
	009826	...	c	...	...	...	...	...	...	...	...	...	1.89	0.829	0.28	...	
	009826	...	d	...	...	...	...	...	...	...	...	...	3.75	2.53	0.27	...	
	009826	...	B	01 36 50.40	+41 23 32.1	...	...	...	M4.5 V	52	150	702	...	...	...	P	2, 3, 4
3.....	011964	GJ 81.1	A	01 57 09.61	−10 14 32.7	0.02943	34.0	T	G5	...	...	...	...	...	...	...	
	011964	...	b	...	...	...	...	...	...	...	...	...	0.11	0.229	0.15	...	
	011964	...	c	...	...	...	...	...	...	...	...	...	0.7	3.167	0.3	...	
	011964	...	B[a]	01 57 11.07	−10 14 53.2	...	...	...	...	29.7	133	1010	...	...	...	PWC	5, 6
4.....	013445	GJ 86	A	02 10 25.93	−50 49 25.4	0.09163	10.9	T	K1 V	...	...	...	...	...	...	...	
	013445	...	b	...	...	...	...	...	...	...	...	...	4.01	0.11	0.046	...	
	013445	...	B	...	...	...	...	...	WD	1.93	119	21	...	...	...	O	7, 8, 9
5.....	019994	GJ 128	A	03 12 46.44	−01 11 46.0	0.04469	22.4	T	F8.5 V	...	...	...	...	...	...	...	
	019994	...	b	...	...	...	...	...	...	...	...	...	2	1.3	0.2	...	
	019994	...	B	...	...	...	...	...	M	2.5	213	56	...	...	...	WCD	10, 11, 12, 13
6.....	027442	ϵ Ret	A	04 16 29.03	−59 18 07.8	0.05484	18.2	T	K2 IVa	...	...	...	...	...	...	...	
	027442	...	b	...	...	...	...	...	...	...	...	...	1.28	1.18	0.07	...	
	027442	...	B[a]	...	...	...	...	...	...	13.8	36	251	...	...	...	WCI	14, 15
7.....	038529	HIP 27253	A	05 46 34.91	+01 10 05.5	0.02357	42.4	T	G4 V	...	...	...	...	...	...	...	16
	038529	...	b	...	...	...	...	...	...	...	...	...	0.78	0.129	0.29	...	
	038529	...	c	...	...	...	...	...	...	...	...	...	12.7	3.68	0.36	...	
	038529	...	B[b]	05 46 19.38	+01 12 47.2	...	28.7	C	M3.0 V	284	305	12042	...	...	...	P	
8.....	041004	HIP 28393	A	05 59 49.65	−48 14 22.9	0.02324	43.0	T	K1 V	...	...	...	...	...	...	...	
	041004	...	b	...	...	...	...	...	...	...	...	...	2.3	1.31	0.39	...	
	041004	...	B	05 59 43.81	−48 12 11.9	...	...	...	M2.5 V	0.5	176	22	...	...	...	WH	4, 17, 18, 19
	041004	...	C	...	...	...	...	...	...	...	...	...	18.4	0.016	0.08	...	18, 19
9.....	040979	BD +44 1353	A	06 04 29.95	+44 15 37.6	0.03000	33.3	T	F8	...	...	...	...	...	...	...	
	040979		b	...	...	...	...	...	...	...	...	...	3.32	0.811	0.23	...	
	040979	BD +44 1351	B	06 04 13.02	+44 16 41.1	...	15.2	P	K5	192	290	6394	...	...	...	P	4, 16, 20, 21
10.....	046375	HIP 31246	A	06 33 12.62	+05 27 46.5	0.02993	33.4	T	K0 V	...	...	...	...	...	...	...	
	046375		b	...	...	...	...	...	...	...	...	...	0.249	0.041	0.04	...	
	046375		B[a]	06 33 12.10	+05 27 53.2	...	26.4	C	...	9.4	308	314	...	...	...	WI	22, 23
11.....	075289	HIP 43177	A	08 47 40.39	−41 44 12.5	0.03455	28.9	T	G0 V	...	...	...	...	...	...	...	
	075289	...	b	...	...	...	...	...	...	...	...	...	0.42	0.046	0.054	...	
	075289	...	B	08 47 42.26	−41 44 07.6	...	...	...	...	21.5	78	621	...	...	...	O	24
12.....	075732	55 Cnc	A	08 52 35.81	+28 19 50.9	0.07980	12.5	T	K0 IV–V	...	...	...	...	...	...	...	
	075732	...	e	...	...	...	...	...	...	...	...	...	0.045	0.038	0.174	...	
	075732	...	b	...	...	...	...	...	...	...	...	...	0.784	0.115	0.020	...	
	075732	...	c	...	...	...	...	...	...	...	...	...	0.217	0.24	0.44	...	
	075732	...	d	...	...	...	...	...	...	...	...	...	3.92	5.257	0.327	...	
	075732	...	B	08 52 40.85	+28 18 59.0	...	8.7	C	M4	84	130	1050	...	...	...	PWCD	4, 12, 25, 26, 27
13.....	080606	HIP 45982	A	09 22 37.57	+50 36 13.4	0.01713	58.4	T	G5	...	...	...	...	...	...	...	
	080606	...	b	...	...	...	...	...	...	...	...	...	3.41	0.439	0.927	...	
	080607	HIP 45983	B	09 22 39.73	+50 36 13.9	...	...	...	G5	20.6	269	1203	...	...	...	PWH	4, 28

TABLE 2—*Continued*

Sequence (1)	HD Name (2)	Other Name (3)	Component (4)	R.A. (J2000.0) (5)	Decl. (J2000.0) (6)	π (arcsec) (7)	Distance (pc) (8)	Basis (9)	Spectral Type (10)	Angular Separation (arcsec) (11)	P.A. (deg) (12)	Projected Separation (AU) (13)	$M \sin i$ (M_J) (14)	$a \sin i$ (AU) (15)	e (16)	Sources (17)	References (18)
14.....	089744	HIP 50786	A	10 22 10.56	+41 13 46.3	0.02565	39.0	T	F8 IV	...	...	...	...	...	...	...	
	089744	...	b	...	...	...	...	...	...	...	...	...	7.99	0.89	0.67	...	
	089744	...	B	10 22 14.87	+41 14 26.4	...	...	...	L0 V	63.0	48	2456	...	...	...	O	29, 30
15.....	099492	GJ 429B	B	11 26 46.28	+03 00 22.8	0.05559	18.0	T	K2 V	...	...	...	...	...	...	...	
	099492	...	b	...	...	...	...	...	...	...	...	...	0.122	0.119	0.05	...	
	099491	GJ 429A	A	11 26 45.32	+03 00 47.2	0.05659	17.7	T	K0 IV	28.6	150	515	...	...	...	PWHC	31
16.....	114729	HIP 64459	A	13 12 44.26	−31 52 24.1	0.02857	35.0	T	G3 V	...	...	...	...	...	...	...	
	114729	...	b	...	...	...	...	...	...	...	...	...	0.82	2.08	0.31	...	
	114729	...	B	13 12 43.97	−31 52 17.0	...	...	...	...	8.05	333	282	...	...	...	O	32
17.....	114762	HIP 64426	A	13 12 19.74	+17 31 01.6	0.02465	40.6	T	F9 V	...	...	...	...	...	...	...	
	114762	...	b	...	...	...	...	...	...	...	...	...	11.02	0.3	0.25	...	
	114762	...	B	...	...	...	...	...	...	3.26	30	132	...	...	...	O	3, 4
18.....	120136	τ Boo	A	13 47 15.74	+17 27 24.9	0.06412	15.6	T	F6 IV	...	...	...	...	...	...	...	
	120136	...	b	...	...	...	...	...	...	...	...	...	4.13	0.05	0.01	...	
	120136	...	B	...	...	...	...	...	...	2.87	31	45	...	...	...	WCD	3, 4, 12
19.....	142022	GJ 606.1	A	16 10 15.02	−84 13 53.8	0.02788	38.9	T	G8/K0 V	...	...	...	...	...	...	...	
	142022	...	b	...	...	...	...	...	...	...	...	...	4.4	2.8	0.57	...	
	142022	...	B	16 10 25.34	−84 14 06.7	...	...	...	K7 V	20.4	130	794	...	...	...	PWC	33, 34
20.....	147513	GJ 620.1	A	16 24 01.29	−39 11 34.7	0.07769	12.9	T	G5 V	...	...	...	...	...	...	...	
	147513	...	b	...	...	...	...	...	...	...	...	...	1	1.26	0.52	...	
	147513	...	B	16 23 33.83	−39 13 46.1	0.07804	12.8	T	WD	345	245	4451	...	...	...	C	13, 35
21.....	178911B	HIP 94076B	B	19 09 03.10	+34 35 59.5	0.02140	46.7	T	G5	...	...	...	...	...	...	...	
	178911B	...	b	...	...	...	...	...	...	...	...	...	6.292	0.32	0.124	...	
	178911	HIP 94076	A	19 09 04.38	+34 36 01.6	0.02042	49.0	T	G1 V J	16.1	82	789	...	...	...	PWH	4, 36, 37, 38, 39
	178911	...	C[c]	...	...	...	...	...	...	0.1	21	4.9	...	...	...	W	
22.....	186427	16 Cyg B	B	19 41 51.97	+50 31 03.1	0.04670	...	...	G3 V	...	...	...	...	...	...	...	
	186427	...	b	...	...	...	...	...	...	...	...	...	1.69	1.67	0.67	...	
	186408	16 Cyg A	A	19 41 48.95	+50 31 30.2	0.04625	21.6	T	G1.5 V J	39.8	313	860	...	...	...	PWC	2, 3, 4, 40, 41
	186408	...	C[c]	...	...	...	...	...	...	3.4	209	73	...	...	...	W	
23.....	188015	HIP 97769	A	19 52 04.54	+28 06 01.4	0.01900	52.6	T	G5 IV	...	...	...	...	...	...	...	
	188015	...	b	...	...	...	...	...	...	...	...	...	1.26	1.19	0.15	...	
	188015	...	B[b]	19 52 05.51	+28 06 03.7	...	46.9	C	...	13	85	684	...	...	...	P	
24.....	190360	GJ 777	A	20 03 37.41	+29 53 48.5	0.06292	15.9	T	G7 IV–V	...	...	...	...	...	...	...	
	190360	...	c	...	...	...	...	...	...	...	...	...	0.057	0.128	0.01	...	
	190360	...	b	...	...	...	...	...	...	...	...	...	1.502	3.92	0.36	...	
	190360	...	B	20 03 26.58	+29 51 59.5	...	18.5	P	M4.5 V	179	234	2846	...	...	...	PWC	4, 5, 16, 42
25.....	195019	HIP 100970	A	20 28 18.64	+18 46 10.2	0.02677	37.3	T	G3 IV–V	...	...	...	...	...	...	...	
	195019	...	b	...	...	...	...	...	...	...	...	...	3.43	0.14	0.05	...	
	195019	...	B	...	...	...	...	...	...	3.5	330	131	...	...	...	W	4, 5, 43, 44
26.....	196050	HIP 101806	A	20 37 51.71	−60 38 04.1	0.02131	46.9	T	G3 V	...	...	...	...	...	...	...	
	196050	...	b	...	...	...	...	...	...	...	...	...	3	2.5	0.28	...	
	196050	...	B	20 37 51.85	−60 38 14.9	...	...	...	...	10.9	175	510	...	...	...	O	32
27.....	213240	HIP 111143	A	22 31 00.37	−49 25 59.8	0.02454	40.8	T	G0/G1 V	...	...	...	...	...	...	...	
	213240	...	b	...	...	...	...	...	...	...	...	...	4.5	2.03	0.45	...	
	213240	...	B	22 31 08.26	−49 26 56.7	...	41.8	C	M5.0 V	95.8	127	3909	...	...	...	P	32

TABLE 2—*Continued*

Sequence (1)	HD Name (2)	Other Name (3)	Component (4)	R.A. (J2000.0) (5)	Decl. (J2000.0) (6)	π (arcsec) (7)	Distance (pc) (8)	Basis (9)	Spectral Type (10)	Angular Separation (arcsec) (11)	P.A. (deg) (12)	Projected Separation (AU) (13)	$M \sin i$ (M_J) (14)	$a \sin i$ (AU) (15)	e (16)	Sources (17)	References (18)
28.....	219449	GJ 893.2	A	23 15 53.49	−09 05 15.9	0.02197	45.5	T	K0 III	...	...	...	...	...	...	...	
	219449	...	b	...	...	...	...	...	...	...	...	...	2.9	0.3	–	...	
	219430	...	B[a]	23 15 51.00	−09 04 42.7	...	42.4[d]	C	K8 V J	49.4	313	2248	...	...	...	PWC	6, 45
	219430	...	C[a,e]	...	...	...	42.4[d]	C	...	0.4	101	18	...	...	...	W	
29.....	222404	γ Cephei	A	23 39 20.85	+77 37 56.2	0.07250	13.8	T	K1 III	...	...	...	...	...	...	...	
	222404	...	b	...	...	...	...	...	...	...	...	...	1.59	2.03	0.2	...	
	222404	...	B	...	...	...	...	...	...	...	...	...	...	20.3	0.39	H	4, 46, 47, 48, 49
30.....	222582	HIP 116906	A	23 41 51.53	−05 59 08.7	0.02384	42.0	T	G5	...	...	...	...	...	...	...	
	222582	...	b	...	...	...	...	...	...	...	...	...	5.11	1.35	0.76	...	
	222582	...	B[a]	23 41 45.14	−05 58 14.8	...	32.1	C	M3.5 V	113	302	4746	...	...	...	PW	6
							Candidate (Unconfirmed) Stellar Companions										
31.....	008673	HIP 6702	A	01 26 08.78	+34 34 46.9	0.02614	38.3	T	F7 V	...	...	...	...	...	...	...	
	008673	...	b	...	...	...	...	...	...	...	...	...	14	1.58	–	...	
	008673	...	B	...	...	...	...	...	...	0.1	78	3.8	...	...	...	W	
32.....	016141	HIP 12048	A	02 35 19.93	−03 33 38.2	0.02785	35.9	T	G5 IV	...	...	...	...	...	...	...	
	016141	...	b	...	...	...	...	...	...	...	...	...	0.23	0.35	0.21	...	
	016141	...	B	02 35 19.88	−03 33 43.9	...	...	...	...	6.2	188	222	...	...	...	O	32
33.....	111232	HIP 62534	A	12 48 51.75	−68 25 30.5	0.03463	28.9	T	G8 V	...	...	...	...	...	...	...	
	111232	...	b	...	...	...	...	...	...	...	...	...	6.8	1.97	0.2	...	
	111232	...	B	...	...	...	...	...	...	...	...	...	...	...	...	H	13
34.....	150706	GJ 632	A	16 31 17.59	+79 47 23.2	0.03673	27.2	T	G0	...	...	...	...	...	...	...	
	150706	...	b	...	...	...	...	...	...	...	...	...	1	0.82	0.38	...	
	150706	...	B	...	...	...	...	...	...	...	...	...	...	...	...	H	50
35.....	169830	HIP 90485	A	18 27 49.48	−29 49 00.7	0.02753	36.3	T	F9 V	...	...	...	...	...	...	...	
	169830	...	b	...	...	...	...	...	...	...	...	...	2.88	0.81	0.31	...	
	169830	...	c	...	...	...	...	...	...	...	...	...	4.04	3.6	0.33	...	
	169830	...	B[f]	18 27 48.65	−29 49 01.6	...	...	...	...	11	270	399	...	...	...	...	
36.....	217107	HIP 113421	A	22 58 15.54	−02 23 43.4	0.05071	19.7	T	G8 IV–V	...	...	...	...	...	...	...	
	217107	...	b	...	...	...	...	...	...	...	...	...	1.37	0.074	0.13	...	
	217107	...	c	...	...	...	...	...	...	...	...	...	2.1	4.3	0.55	...	
	217107	...	B	...	...	...	...	...	...	0.3	156	6	...	...	...	W	51, 52

NOTES.—Planet data are from the Exoplanet Encyclopedia Web site, http://vo.obspm.fr/exoplanetes/encyclo/catalog.php. Table 2 is also available in machine-readable form in the electronic edition of the *Astrophysical Journal*.

[a] Known companion, but first identification of the star as a companion to an exoplanet host.

[b] New stellar companion reported by this work.

[c] Separation and position angle are listed with respect to component A. A and C have been referred to as Aa and Ab, respectively, in other publications, but we follow a consistent naming convention, using uppercase letters to represent stars and lowercase letters to denote planets.

[d] Photometry obtained is for the BC pair. Distance estimate assumes identical binary components.

[e] Separation and position angle are listed with respect to component B.

[f] New candidate companion reported by this work, via Kevin Apps.

REFERENCES.—(1) Bailey 1900; (2) Lowrance et al. 2002; (3) Patience et al. 2002; (4) Eggenberger et al. 2004; (5) Allen et al. 2000; (6) Zacharias et al. 2004; (7) Els et al. 2001; (8) Mugrauer & Neuhäuser 2005; (9) Queloz et al. 2000; (10) Smyth 1844; (11) Hale 1994; (12) Duquennoy & Mayor 1991; (13) Mayor et al. 2004; (14) Jessup 1955; (15) Holden 1966; (16) Lepine & Shara 2005; (17) See 1897; (18) Zucker et al. 2003; (19) Zucker et al. 2004; (20) Hog et al. 1998; (21) Halbwachs 1986; (22) Soulie 1985; (23) Urban et al. 1998; (24) Mugrauer et al. 2004a; (25) van Altena et al. 1995; (26) Dahn et al. 1988; (27) Marcy et al. 2002; (28) Naef et al. 2001; (29) Wilson et al. 2001; (30) Mugrauer et al. 2004b; (31) Marcy et al. 2005b; (32) Mugrauer et al. 2005; (33) Luyten 1979; (34) Eggenberger et al. 2006; (35) Wegner 1973; (36) McAlister et al. 1987b; (37) Balega et al. 2004; (38) Hartkopf et al. 2000; (39) Zucker et al. 2002; (40) Turner et al. 2001; (41) Cochran et al. 1997; (42) Naef et al. 2003; (43) Hough 1887; (44) Fischer et al. 1999; (45) Wilson 1953; (46) Mason et al. 2001; (47) Campbell et al. 1988; (48) Griffin et al. 2002; (49) Hatzes et al. 2003; (50) Halbwachs et al. 2003; (51) McAlister et al. 1987a; (52) Mason et al. 1999.

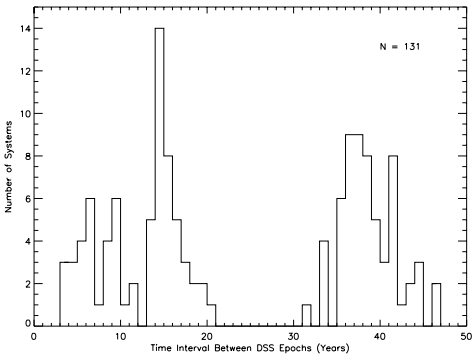

FIG. 1.—Histogram of time intervals between DSS epochs for the exoplanet sample.

of 35.6 pc for our sample, this translates to a minimum projected distance of ~500–1000 AU. However, some bright companions can be picked up much closer, due to twin diffraction spikes or an anomalous point-spread function (PSF) compared to other stars in the field. For an outer limit, the 10′ image gives us a radius of 5′, which translates to a projected distance of ~10,000 AU for the median distance of the exoplanet sample. This is of the order of magnitude of the canonical limit for gravitational binding, although Poveda et al. (1994) listed several companions with separations larger than this.

Of the 131 systems, 82 had easily detectable proper motions and hence were searched effectively for CPM companions, 7 had marginal proper motions, and 42 systems had no detectable proper motions. Of the 82 systems searched effectively, 15 definite CPM companions were confirmed (one per system), and 67 had no CPM companions detected within the search region outlined above. However, in 12 (plus 3 candidates) of these 67 systems, close companions were identified by other sources. In 3 (plus 3 candidates) of the 49 marginal or unsearched systems, companions were reported by other sources. These additional companions could not be detected by our method due to saturation around the primary and/or a short time baseline between the DSS image pair.

2.2. *Washington Double Star Catalog* (*WDS*)

The WDS catalog[4] is the world's most comprehensive database of multiple stars. However, it is a catalog of doubles, not binaries, so it explicitly contains an unknown number of nonphysical chance alignments. Table 3 lists 20 WDS entries that are not gravitationally bound to the exoplanet host, but rather are field stars, listed in WDS ID sequence (col. [1]). Column (2) is the HD identifier of the star. Column (3) is the component suffix

[4] See http://ad.usno.navy.mil/wds.

TABLE 3
WDS ENTRIES THAT ARE NOT GRAVITATIONALLY BOUND COMPANIONS

WDS ID (1)	HD Name (2)	Component (3)	θ (deg) (4)	ρ (arcsec) (5)	Epoch (6)	Number (7)	Notes (8)
00394+2115	003651	...	80	167.6	1997	9	1
01368+4124	009826	AB	128	114.0	1909	1	1
01368+4124	009826	AC	289	273.6	1991	7	1
03329−0927	022049	...	143	0.0	1975	1	2
11268+0301	099492	AC	187	90.5	1937	3	1
13284+1347	117176	AB	127	268.6	2002	13	1
13284+1347	117176	AC	263	325.5	1923	1	1
13573−5602	121504	...	55	36.2	1999	32	3
15249+5858	137759	...	50	254.8	2002	12	4
16010+3318	143761	...	49	135.3	2002	22	1
19091+3436	178911	Aa-C	130	60.0	1944	1	1
20140−0052	192263	A-BC	102	73.1	2003	19	1
20140−0052	192263	AD	244	71.3	1921	1	1
20140−0052	192263	BC-D	65	23.5	1998	8	1
20283+1846	195019	AC	72	70.9	1998	11	1
20283+1846	195019	AD	97	84.5	1998	2	1
20399+1115	196885	...	6	182.9	2000	13	1
22310−4926	213240	...	359	21.9	1999	7	1
23159−0905	219449	AD	274	80.4	1924	6	1
23159−0905	219449	BC-E	341	19.7	1924	6	1

NOTES.—Cols. (1), (3), and (7) are listed here exactly as in the WDS catalog. Cols. (4), (5), and (6) correspond to the most recent observation. All data are as of 2005 June 20. Certain pairs of multiple systems omitted from this table are confirmed to be gravitationally bound companions (01368+4124AD, 11268+0301AB, 19091+3436Aa and Aa-B, 20283+1846AB, and 23159−0905A-BC and BC). One omitted pair (20140−0052BC) has several speckle observations (Jonckheere 1911, 1917, 1944; Vanderdonck 1911; Van Biesbroeck 1960) and several failed attempts (van den Bos 1949, 1960, 1963; Couteau 1954; Baize 1957) and is hence inconclusive. Col. (8) notes: (1) DSS multiepoch plates do not show CPM for WDS entry. In fact, proper motion of the primary star causes change in separation and position angle, indicating that the "companion" is a background star. (2) Primary star is ϵ Eri, the well-studied exoplanet system. WDS listing is based on a single speckle measure by Blazit et al. (1977). This system has been observed 13 other times and no companion was resolved (McAlister 1978; Hartkopf & McAlister 1984; Oppenheimer et al. 2001). (3) Primary's $\mu = 0\farcs264\ \mathrm{yr}^{-1}$ at 251° from *Hipparcos* is not detectable in DSS plates. For the WDS companion, SuperCOSMOS lists $\mu = 0\farcs013\ \mathrm{yr}^{-1}$ at 91°, clearly not matching the primary's. (4) Primary does not show detectable proper motion in DSS plates. Planet discovery paper, Frink et al. (2002), refuted the WDS entry based on distance estimate to WDS entry and proper-motion comparisons.

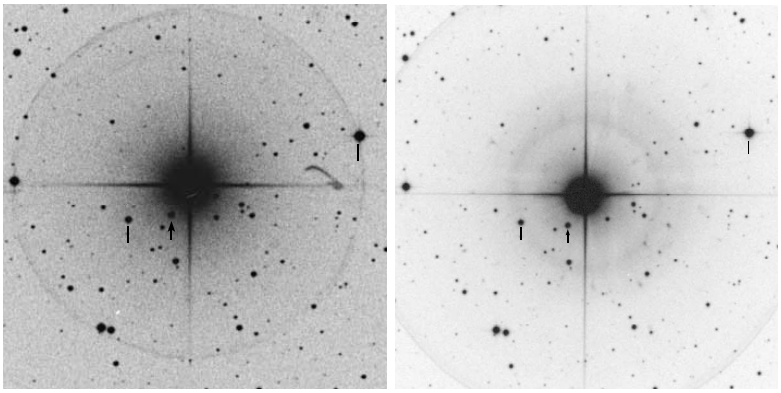

FIG. 2.—DSS images from two epochs for HD 9826. The 10′ square images have north up and east to the left. WDS lists components B and C (marked by lines), which are background stars. WDS component D (marked by an arrow), however, is a CPM companion. The primary's $\mu = 0''.42\ \mathrm{yr}^{-1}$ at 204°.

of the pair, as it appears in the WDS catalog, for which position angle, separation, and epoch of the most recent observation are listed in columns (4), (5), and (6). Column (7) is the number of observations listed in the WDS. Note that a few of these "companions" have many observations, but they are not true companions. Column (8) identifies the specific method used to refute the WDS entry.

Figure 2 shows an example for HD 9826. The lines mark two WDS entries that do not share the primary's high proper motion and hence are background stars. On the other hand, the known CPM companion (marked by an arrow) is easily identifiable in these images.

2.3. *Hipparcos Catalog*

As most of the exoplanet systems are close to the Sun (128 of the 131 are within 100 pc), the *Hipparcos* Catalog[5] provides fairly reliable distances and some photometric data for these systems. The catalog also notes some stellar companions, identified by field H59 as component solutions ("C" flag), accelerated proper motions ("G" flag), or orbital solutions ("O" flag). In total, *Hipparcos* identified stellar companions in nine exoplanet systems, four each with C and G flags, and one with the O flag. Five of the nine *Hipparcos* companions were independently confirmed, one (HD 38529c) is a close brown dwarf, and two (both G flags) remain as candidates. The ρ CrB system (HD 143761) has an O flag and contains a companion that is a planet (Noyes et al. 1997; Zucker & Mazeh 2001) or a star (Gatewood et al. 2001; Pourbaix & Arenou 2001; Halbwachs et al. 2003), but not both.

2.4. *Catalog of Nearby Stars*

Among our sample of 131 stars, 39 are listed in the CNS. We reviewed the earlier versions of the catalog (Gliese 1969; Gliese & Jahreiss 1979, 1991), as well as the consolidated information on the Web.[6] The catalog identifies any known companions and lists separation, position angle, and references in the notes section. Twelve stars from our sample have companions listed in the CNS, and every one of them was confirmed by other sources to be a true companion.

2.5. *Duquennoy & Mayor*

The Duquennoy & Mayor (1991) G Dwarf Survey specifically looked at multiplicity among solar-type stars in the solar neighborhood using radial velocity techniques. This is an ideal reference for our sample because searches for exoplanet systems have focused on such systems. Duquennoy & Mayor (1991) identified target stars as single-line, double-line, or line width spectroscopic binaries, or spectroscopic binaries with orbits. Only three stars from our sample have companions listed in this reference, and each of these was confirmed by other sources to be a true companion.

3. PHOTOMETRIC DISTANCE ESTIMATES FOR COMPANION CANDIDATES

In addition to the proper-motion investigation, we collected archival 2MASS and SuperCOSMOS photometry and new CCD photometry that allowed us to compute distance estimates to companion candidates, as described below. Table 4 summarizes the photometry data, as well as the distance estimates computed. Column (1) is the star's name, and column (2) contains the spectral type identified as part of this work (see § 4). Columns (3), (4), and (5) are the *BRI* plate magnitudes from SuperCOSMOS, followed by the *VRI* CCD magnitudes observed by us at the CTIO 0.9 and 1.0 m telescopes in columns (6), (7), and (8). Column (9) gives the number of observations available for the *VRI* photometry. This is followed by 2MASS JHK_s photometry in columns (10), (11), and (12). Columns (13), (14), and (15) are the estimated plate photometric distance, total error of this estimate, and the number of color relations used in computing this estimate. Columns (16), (17), and (18) similarly list the CCD distance estimate, total error, and the number of color relations used.

3.1. *2MASS Coordinates and Photometry*

We used the 2MASS Web database, accessed via the Aladin interactive sky atlas[7] (Bonnarel et al. 2000), to obtain equinox

[5] See http://www.rssd.esa.int/Hipparcos/HIPcatalogueSearch.html.
[6] See http://www.ari.uni-heidelberg.de/aricns.
[7] See http://aladin.u-strasbg.fr/aladin.gml.

TABLE 4
Observations and Computed Distances

Name (1)	Spectral Type (2)	Plate Magnitudes B (3)	R (4)	I (5)	CCD Magnitudes V (6)	R (7)	I (8)	Number of Observations (9)	Infrared Magnitudes J (10)	H (11)	K_s (12)	D_{plt} (pc) (13)	Error (pc) (14)	Number of Relations (15)	D_{CCD} (pc) (16)	Error (pc) (17)	Number of Relations (18)
Exoplanet Host Without Parallax																	
BD −10 3166	...	9.90	8.80	8.08	10.03	9.59	9.19	1	8.61	8.30	8.12	33.8	8.8	1	66.8	10.0	1
Confirmed Companions																	
HD 038529B	M3.0 V	13.81	11.84	10.05	13.35	12.29	10.98	3	9.72	9.04	8.80	31.8	9.0	11	28.7	4.8	12
HD 040979B	...	9.92	8.72	...	...	...	...	...	7.27	6.79	6.69	15.2	4.0	3	...	...	...
HD 046375B	...	...	...	...	11.80	11.01	9.80	3	8.70	8.08	7.84	...	...	...	26.4	6.0	12
HD 075732B	...	13.14	11.53	...	13.26	11.91	10.24	2	8.56	7.93	7.67	14.5	4.6	6	8.7	1.4	12
HD 188015B	...	...	...	...	...	15.54	13.91	1	12.09	11.59	11.34	...	...	...	46.9	9.5	7
HD 190360B	...	15.30	12.35	...	...	...	...	...	9.55	9.03	8.71	18.5	6.2	6	...	...	...
HD 213240B	M5.0 V	...	...	...	17.40	15.96	14.13	1	12.36	11.74	11.47	...	...	...	41.8	6.5	12
HD 219449BC	Early K	...	...	...	9.17	8.57	8.05	1	7.31	6.84	6.69	...	...	...	29.9	4.7	6
HD 222582B	M3.5 V	15.25	13.16	11.41	14.49	13.33	11.83	1	10.39	9.81	9.58	35.1	9.3	11	32.1	5.0	12
Candidate Companions																	
HD 169830B	...	...	...	...	14.35	13.62	12.39	1	10.16	9.50	9.35	...	...	...	29.2	23.4	12
Refuted Candidate Companions																	
BD −10 3166 #1	M5.0 V	14.71	13.36	11.78	14.43	13.03	11.22	1	9.51	8.97	8.64	16.4	10.1	11	12.5	2.0	12
HD 033636 #1	M1.0 V	20.56	18.17	...	19.31	18.43	17.37	1	16.26	15.63	15.16	608.5	162.9	6	738.9	162.3	12
HD 041004 #1	M0.5 V–VI	18.90	16.87	15.76	17.89	16.91	16.05	1	15.06	14.50	14.16	414.0	119.1	11	557.4	103.3	9
HD 072659 #1	M3.0 V	20.21	18.05	16.43	18.91	18.02	16.53	1	15.31	14.67	14.30	293.0	82.5	11	368.6	99.2	12
HD 114783 #1	Early K	10.60	9.32	8.92	9.78	9.31	8.90	2	8.32	7.90	7.79	20.2	5.4	3	54.0	9.3	2

J2000.0 coordinates for the companion candidates, the epoch of observation, and J, H, and K_s photometry. The errors in JHK_s were almost always less than 0.05 mag and were typically 0.02–0.03 mag. Notable exceptions are three distant and faint refuted candidates listed in Table 4, HD 33636 #1 (errors of 0.14, 0.15, null at JHK_s, respectively), HD 41004 #1 (0.05, 0.06, and 0.07 mag), and HD 72659 #1 (0.05, 0.06, and 0.07 mag).

3.2. *SuperCOSMOS Plate Photometry and Distance Estimates*

We obtained optical plate photometry in B_J, R_{59F}, and I_{IVN} bands (hereafter *BRI*) from the SuperCOSMOS Sky Survey (SSS) scans of Schmidt survey plates (Hambly et al. 2001b). The SSS plate photometry is calibrated by means of a network of secondary standard-star sequences across the entire sky, with the calibration being propagated into fields without standards by means of the ample overlap regions between adjacent survey fields. The external accuracy of the calibrations is ± 0.3 mag in individual passbands (Hambly et al. 2001a); however, the internal accuracy in colors (e.g., $B-R$, $R-I$) is much better, being typically 0.1 mag for well-exposed, uncrowded images. We used point-source photometric measures in all cases.

Photometric distance estimates were then derived using these SSS plate magnitudes, combined with 2MASS JHK_s by fitting various colors to M_{K_s}-color relations from Hambly et al. (2004). Results for 11 companion candidates are given in Table 4. Errors quoted from this procedure include internal and external errors. Internal errors represent the standard deviation of distance estimates from the suite of M_{K_s}-color relations. External errors represent a measure of the reliability of the relations for stars of known distance, which is estimated to be 26% in Hambly et al. (2004).

3.3. *CCD Photometry Observations and Distance Estimates*

Because of the relatively large photometric distance errors associated with photographic plate photometry, we obtained optical CCD photometry for one exoplanet host and 13 companion candidates (given in Table 4) in the $V_J R_{KC} I_{KC}$ bands (hereafter *VRI*) using the CTIO 0.9 and 1.0 m telescopes during observing runs in 2003 December, 2004 June, September, and December, 2005 August and December, and 2006 March as part of the SMARTS (Small and Moderate Aperture Research Telescope System) Consortium. For the 0.9 m telescope, the central quarter of the 2048×2046 Tektronix CCD camera was used with the Tek 2 *VRI* filter set. For the 1.0 m telescope, the Y4KCam CCD camera was used with the Harris 1 4mts *VR* and kc 1 4mts *I* filter set. Standard stars from Graham (1982), Bessel (1990), and Landolt (1992) were observed through a range of air masses each night to place measured fluxes on the Johnson-Kron-Cousins *VRI* system and to calculate extinction corrections.

Data were reduced using IRAF via typical bias subtraction and dome flat-fielding, using calibration frames taken at the beginning of each night. In general, a circular aperture $14''$ in diameter was used to determine stellar fluxes in order to match apertures used by Landolt (1992) for the standard stars. In cases of crowded fields, an appropriate aperture $2''$–$12''$ in diameter was used to eliminate stray light from close sources and aperture corrections were applied. For one target (HD 169830B), we used Gaussian fitting via an IDL program to the PSF tail of a bright nearby source to eliminate its effects and completed the photometry on the target using the IDL APER routine. The same approach was performed on two of our standard stars to correct for zero-point difference between IDL and IRAF magnitudes. As discussed in Henry et al. (2004), photometric errors are typically ± 0.03 mag or less, which includes both internal and external errors. The only exceptions with larger errors were distant and faint refuted candidates HD 33636 #1 (errors of 0.06, 0.04, and 0.04 mag at V, R, and I, respectively) and HD 72659 #1 (0.10, 0.05, and 0.03 mag), new companion HD 188015B (0.05 and 0.04 mag at R and I, respectively), and new candidate HD 169830B (0.12, 0.09, and 0.13 mag). The errors for HD 188015B and HD 169830B are high due to the uncertainties introduced by the large-aperture corrections and, for HD 169830B, PSF fitting as well.

Photometric distances were obtained using the *VRI* magnitudes along with 2MASS JHK_s and fitting various colors to M_{K_s}-color relations from Henry et al. (2004). The results for these companion candidates are given in columns (16)–(18) of Table 4. Errors quoted from this procedure include internal and external errors. Internal errors represent the standard deviation of distance estimates from the suite of M_{K_s}-color relations. External errors represent a measure of the reliability of the relations for stars of known distance, which is estimated to be 15% in Henry et al. (2004).

4. SPECTROSCOPIC OBSERVATIONS

New spectra of nine companion candidates were obtained during observing runs in 2003 October and December, 2004 March and September, and 2005 January at the CTIO 1.5 m telescope as part of the SMARTS Consortium. The Ritchey-Chrétien spectrograph and Loral 1200×800 CCD detector were used with grating 32 in our red setup and grating 09 in our blue setup, which provided 8.6 Å resolution and wavelength coverage over 6000–9500 Å in the red and 3800–6800 Å in the blue. Data reduction consisted of background subtraction, spectrum extraction, and wavelength and flux calibrations in IRAF after standard bias subtraction, flat-fielding, and illumination corrections were applied. Standard dome flats were used for flat-fielding and calibration frames were taken at the beginning of each night. Fringing at wavelengths longer than 7000 Å is common in data from this spectrograph; however, it is typically removed fully by flat-fielding, and no further steps were needed to remove the fringes. Spectral types for stars observed in the red wavelength regime, listed in Table 4, were assigned using the ALLSTAR program as described in Henry et al. (2002). RECONS types have been assigned using a set of standard comparison stars from the RECONS database, a library of $\sim$500 M0.0 V–M9.0 V spectra. Only rough spectral types were assigned based on our blue spectra by comparing features in our spectra with standard stars in Jacoby et al. (1984).

5. RESULTS

Table 2 is a compendium of the 30 exoplanet systems confirmed to have two or more stellar components, listed in coordinate sequence. At the end of the table, six additional systems are listed that may be stellar multiples, although these have not yet been confirmed. Column (1) lists a sequence number of the exoplanet system matching the value plotted in Figure 5, and columns (2) and (3) list the HD name and an alternate name of the exoplanet host and companion stars. Column (4) lists stellar (A, B, C, . . .) or planetary components (b, c, d, . . .). Columns (5) and (6) list the right ascension and declination of stars at epoch 2000.0, equinox J2000.0. For stars listed in *Hipparcos* (all primaries and a few companions), we used the *Hipparcos* 1991.25 epoch coordinates and proper motions to compute the coordinates listed. For fainter stars not observed by *Hipparcos*, we used 2MASS coordinates at the epoch of observation and converted the coordinates to epoch 2000.0 using proper motions from SuperCOSMOS or NLTT (Luyten 1979),[8] if available.

[8] Also available via the VizieR Online Data Catalog I/98A.

When the proper motion of a companion was not available, we used the primary's *Hipparcos* proper motion. In some instances, 2MASS coordinates were not available for the companions, and in these instances, the coordinates of the companions are not listed. However, in all but three of these cases, the separation and position angle of the companion from the primary are listed in columns (11) and (12). The three exceptional cases (one confirmed and two candidates), where neither coordinates nor separations from the primaries are known, are all *Hipparcos* G flags and hence close astrometric binaries. Column (7) lists the trigonometric parallax from *Hipparcos*, in arcseconds. Columns (8) and (9) list the distance, in pc, and its basis on either trigonometric parallax, if available (coded as "T"), calculated CCD photometric distance using relations from Henry et al. (2004) (coded as "C"), or calculated plate magnitude distance from SuperCOSMOS using relations from Hambly et al. (2004) (coded as "P"). If both plate and CCD distance estimates are available, only the more reliable CCD distance is listed. Column (10) lists the spectral type from Gray et al. (2003), the planet discovery paper, or other references for the primary and from our spectroscopic observations or other references for the companion. Columns (11) and (12) list the angular separation (in arcsec) and position angle (in deg) of stellar companions with respect to the exoplanet host. For companions listed in WDS, these are typically the most recent entry in WDS; otherwise, they are the values listed in the companion discovery paper. For new companions, these astrometry values are our measurements from our CTIO or the DSS images. Column (13) lists the projected spatial separation (and is therefore a lower limit at the epoch of plate observation) of companion stars with respect to their primaries, in AU. Column (14) gives the $M \sin i$ in Jupiter masses for planets. Columns (15) and (16) list the $a \sin i$ (in AU) and eccentricity of the orbits. Column (17) specifies the sources used to detect the companion stars. The codes are as follows: "P" represents a CPM detection using the multiepoch DSS images; "W" represents a companion listing in the WDS catalog; "H" represents a *Hipparcos* catalog companion identification; "C" represents a companion identification in the CNS catalog; "D" represents a companion identification in Duquennoy & Mayor (1991); "I" represents confirmation via our recent *VRI* images taken to verify CPM; and "O" represents that the companion was not found by any of the above means but reported in one or more refereed papers. Finally, column (18) lists relevant references relating to stellar companions. We have chosen not to list the individual planet discovery papers as references, unless they identify a stellar companion.

5.1. *Notes for Each Multiple System*

5.1.1. *New, Known, or Confirmed Companion Systems*

HD 142.—This close binary (separation 5″.4) is listed in WDS and CNS. While this pair was first resolved at Harvard College Observatory in 1894 (Bailey 1900), the separation and $\Delta m \simeq 5$ make this a difficult object. It was found at approximately the same position six times from 1894 to 1928. It then remained unmeasured for 72 yr until it became evident in 2MASS in 2000 at approximately the same position angle. Given the primary's $\mu = 0''.58$ yr^{-1} due east and the long time lapse between the 1928 WDS observation and our image of 2004, a background star would easily have been detected, but we found a blank field at its expected position. This system was mentioned in Lowrance et al. (2002) as a single planet in a multiple-star system.

HD 9826.—This CPM pair is clearly identified in DSS images but not listed in any of the other sources checked. Lowrance et al. (2002) identified this as the first system discovered with multiple planets and multiple stars. It was also mentioned in Patience et al. (2002) and Eggenberger et al. (2004) as an exoplanet primary having a stellar companion.

HD 11964.—This CPM pair is clearly identified in DSS images and listed in WDS and CNS. Allen et al. (2000) listed this as a wide binary system in a catalog of 122 binaries identified via CPM from a sample of 1200 high-velocity, metal-poor stars. The primary's $\mu = 0''.441$ yr^{-1} at 237° from *Hipparcos*, and the companion's $\mu = 0''.444$ yr^{-1} at 236° (Zacharias et al. 2004), a good match. Our work is the first identification of this as a stellar companion to a planetary system.

HD 13445.—Els et al. (2001) reported the discovery of this close companion (1″.72 ± 0″.2 separation) via AO imaging, incorrectly identifying the companion as a T dwarf based on its colors. The recent publication of Mugrauer & Neuhäuser (2005) identified this companion as a cool white dwarf based on its spectrum, claiming the first white dwarf discovery in a planetary system. However, HD 147513 was in fact the first white dwarf discovery in a planetary system, reported by Mayor et al. (2004). There are now two known systems with evidence of planets surviving the post–main-sequence evolution of a stellar companion, with this one being the closest known white dwarf companion to an exoplanet host (at a projected separation of just 21 AU, similar to the Sun–Uranus distance).

HD 19994.—WDS lists 14 observations for this companion. This pair was first resolved by Admiral Smyth in 1836 with a 6 inch refractor (Smyth 1844). It has been resolved 15 times since then, most recently by Hale (1994), who also calculated a 1420 yr orbit for this pair. While there is some hint of curvilinear motion in the data, the orbit is certainly preliminary. This companion is also listed in CNS and Duquennoy & Mayor (1991). Several references have identified this as a stellar companion to a planetary system (Lowrance et al. 2002; Mayor et al. 2004; Eggenberger et al. 2004; Udry et al. 2004).

HD 27442.—WDS and CNS list this companion at 13″.8 separation at 36°. It was first resolved in 1930 by Jessup (1955) and measured again by Holden (1966) almost 35 years later at approximately the same position. Our short-exposure *VRI* images taken at CTIO in 2004 September identified a source about 13″ away at 34°, consistent with the observations of almost 75 years ago. Given the primary's $\mu = 0''.175$ yr^{-1}, this can be confirmed as a companion. Our work is the first identification of this as a stellar companion to a planetary system.

HD 38529.—This CPM pair was discovered by us using DSS images. The primary's $\mu = 0''.163$ yr^{-1} at 209° from *Hipparcos*, and the companion's $\mu = 0''.162$ yr^{-1} at 204° from Lepine & Shara (2005)[9] and 0″.158 yr^{-1} at 208° from SuperCOSMOS. Figure 3 includes two DSS images showing the primary and the companion. Our CCD photometric distance estimate of 28.7 ± 4.8 pc is consistent with our spectral identification of M3.0 V and matches the primary's distance of 42 pc within 3 σ. At our request, spectroscopic observations of the companion were obtained by G. Fritz Benedict in 2004 February using the McDonald Observatory 2.1 m telescope and Sandiford Cassegrain echelle spectrograph (McCarthy et al. 1993). The data were reduced and one-dimensional spectra were extracted using the standard IRAF `echelle` package tools. The radial velocity was determined by cross-correlating the spectra of the star with that of an M2 dwarf (GJ 623) template using the IRAF task `fxcor`. The adopted radial velocity for the GJ 623 primary (it is a binary) was −29.2 km s^{-1}, given the orbital phase at which the template was secured and a

[9] Also available via the VizieR Online Data Catalog I/298.

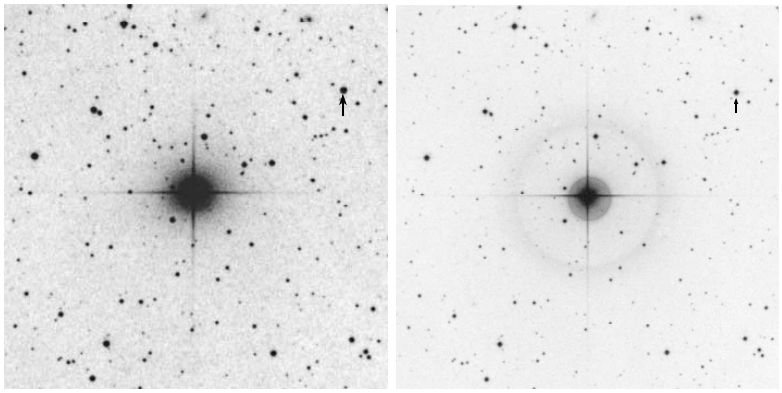

FIG. 3.—New stellar companion to exoplanet host HD 38529. The 10′ square DSS images have north up and east to the left. The companion, marked by arrows, is at an angular separation of 284″ at 305° from the primary, which is at the center of the images.

systemic velocity of −27.5 km s^{-1}, from Marcy & Moore (1989). HD 38529B's radial velocity was measured to be 26.26 ± 0.10 km s^{-1}. This is roughly consistent with the primary's radial velocity of 30.21 km s^{-1} (Nidever et al. 2002), and the odds of two unassociated stars having such similar velocities are low. However, discrepancies in radial velocities and photometric distances could indicate that the new companion is a double. The projected separation of the primary to the new companion(s) is ~12,000 AU, which is extreme for a gravitationally bound system, although Poveda et al. (1994) listed a few wide binaries with even greater separations. This primary also has a *Hipparcos* G flag listing, which was recently used by Reffert & Quirrenbach (2006) to conclude that the substellar companion "c" is actually a brown dwarf of mass $37^{+36}_{-19}\,M_J$.

HD 41004.—A companion is listed in WDS and annotated in *Hipparcos* with a C flag, indicating a linear relative motion of components, implying either an orbital period that is several times the length of the *Hipparcos* observing interval (3.3 yr) or stars that are not physically linked. At a separation of 0.″5 and a $\Delta m = 3.67$ (from *Hipparcos*), the identification of a close companion is difficult, but there are other such *Hipparcos* observations (similar separation and Δm) that were independently confirmed. For example, T. J. J. See measured a close large Δm pair, known as SEE 510 (HIP 86228), with the Lowell 24 inch (0.61 m) telescope in 1896 (See 1897). This pair, lost for nearly 100 yr, was recovered by *Hipparcos* at about the same position (0.″2, Δm = 1.8). While SEE 510 is not morphologically identical to HD 41004, we believe that it is comparably difficult, and so we accept the *Hipparcos* identification of a companion to HD 41004. This system was mentioned in Eggenberger et al. (2004) as a stellar companion in an exoplanet system. Further, Zucker et al. (2003) listed the radial velocity for the primary as 42.5 ± 0.01 km s^{-1} and found the companion to be a double, with a velocity range of 34–48 km s^{-1} (±0.56 km s^{-1}) over 103 observations. They derived an orbital solution for the BC pair, concluding that the orbit is nearly circular with $a \sin i = 0.016$ AU and that the low-mass companion has a minimum mass of $18.4 M_J$. Zucker et al. (2004) derived orbital elements of the possible M dwarf–brown dwarf pair and concluded that this is a unique system with each stellar component of a visual binary having a low-mass companion in orbit around it: one a planet, and the other a possible brown dwarf. Note that the projected separation between A and B is just 22 AU, similar to the separation of the Sun and Uranus.

HD 40979.—This CPM pair is clearly identified in DSS images. The primary is 33 pc away with $\mu = 0.''179$ yr^{-1} at 148° (from *Hipparcos*). The companion, BD +44 1351, has a very similar $\mu = 0.''179$ yr^{-1} at 148° from Lepine & Shara (2005) and 0.″180 yr^{-1} at 148° from Hog et al. (1998). Halbwachs (1986) identified this CPM pair, listing the companion as a K5 star. Eggenberger et al. (2004) identified this as a stellar companion to a planetary system, noting that physical association of this pair has been confirmed via radial velocity measurements. However, our plate photometric distance estimate to the companion is 15.2 ± 4.0 pc (based on only three colors), not a very good match with the primary, although the error is large. This discrepancy could be due to the poor quality of the photometric distance estimate (due to the blue colors of the companion) or perhaps because the companion is an unresolved double.

HD 46375.—WDS lists this 9.″4 separation companion at 308°. We took short exposure frames at CTIO in 2004 September, which identified a companion at a separation of 10″ at 310°, consistent with the WDS observation. The first published resolution of this pair made by Soulie (1985) in 1984 has also been confirmed by 2MASS images. Reanalysis of Astrographic Catalogue data (Urban et al. 1998) has added an observation at about the same secondary position in 1932, thereby confirming that it has the same proper motion. Our CCD photometric distance estimate of 26.4 ± 6.0 pc is within 2 σ of the primary's distance of 33.4 pc from *Hipparcos*. We therefore conclude that this is a physical pair. This work is the first identification of this as a stellar companion to a planetary system.

HD 75289.—This CPM candidate was detected by Mugrauer et al. (2004a) and confirmed by their photometry and spectroscopy. While the companion is seen in the epoch 2 DSS image, CPM could not be established by our method due to saturation of the region around the primary in the epoch 1 image.

HD 75732.—This CPM pair is easily identified in DSS images and matches entries in WDS, CNS, and Duquennoy &

Mayor (1991). The primary has $\mu = 0\farcs539$ yr^{-1} at 244° and $\pi = 0\farcs07980 \pm 0\farcs00084$, from *Hipparcos*. Our CCD photometric distance estimate to the companion is 8.7 ± 1.4 pc, a match within 3 σ. The companion's $\mu = 0\farcs540$ yr^{-1} at 244° and $\pi = 0\farcs0768 \pm 0\farcs0024$ from the Yale Parallax Catalog (van Altena et al. 1995) and $0\farcs0757 \pm 0\farcs0027$ from Dahn et al. (1988) are all consistent with the primary's. This system is listed in Eggenberger et al. (2004) as a stellar companion to a planetary system. The primary star, more commonly known as 55 Cnc, has four reported planets, so this system is the most extensive solar system with a stellar companion, which is at a projected distance of more than 1000 AU. The discrepancy in photometric distance could hint that the companion is an unresolved double.

HD 80606.—This CPM pair is easily identified in DSS images and matches entries in WDS and *Hipparcos*. The primary's $\mu = 0\farcs047$ yr^{-1} at 82° and $\pi = 0\farcs01713 \pm 0\farcs00577$, from *Hipparcos*. The parallax has a large error due to the close companion. The companion is HD 80607, spectral type G5, $\mu = 0\farcs043$ yr^{-1} at 79°, and *Hipparcos* lists an identical parallax. This companion was listed by Eggenberger et al. (2004) as a stellar companion to a planetary system.

HD 89744.—This companion was reported as a candidate by Wilson et al. (2001) based on spectroscopic observations, and they identified it as a massive brown dwarf of spectral type L0 V. Companionship was subsequently confirmed astrometrically by Mugrauer et al. (2004b). This faint companion is not seen in the DSS images.

HD 99492.—This CPM pair is easily identified in DSS images and matches entries in WDS, *Hipparcos*, and CNS. Component B (the exoplanet host) has $\mu = 0\farcs755$ yr^{-1} at 285° and $\pi = 0\farcs05559 \pm 0\farcs00331$, from *Hipparcos*. Component A is HD 99491 with spectral type K0 IV, $\mu = 0\farcs749$ yr^{-1} at 284°, and $\pi = 0\farcs05659 \pm 0\farcs00140$, from *Hipparcos*. These match HD 99492's values well and confirm the pair as physical.

HD 114729.—This CPM candidate was detected recently by Mugrauer et al. (2005) and confirmed by their photometry and spectroscopy. It could not be detected using DSS frames due to saturation of the region around the primary.

HD 114762.—This close companion was discovered using high-resolution imaging (Patience et al. 2002). It was also mentioned by Eggenberger et al. (2004) as a stellar companion to a planetary system. The "planet," with $M \sin i = 11.0 M_J$, may in fact be a star in a low-inclination orbit (Cochran et al. 1991; Fischer & Valenti 2005).

HD 120136.—This close companion is listed in WDS (53 observations), CNS, and Duquennoy & Mayor (1991). The primary's $\mu = 0\farcs483$ yr^{-1} at 276° from *Hipparcos*. CNS lists the companion as GJ 527B, and SIMBAD gives its $\mu = 0\farcs480$ yr^{-1} at 274°, a good match to the primary's. This system has been recognized as a stellar companion to an exoplanet system (Patience et al. 2002; Eggenberger et al. 2004).

HD 142022.—This CPM pair (GJ 606.1AB) is easily identified in DSS images and matches entries in WDS and CNS. The companion's spectral type is K7 V. The NLTT catalog lists identical μ for both components, $\mu = 0\farcs320$ yr^{-1} at 269° (Luyten 1979).

HD 147513.—This companion is listed in CNS and was the first white dwarf found in an exoplanet system (Mayor et al. 2004). The primary's $\mu = 0\farcs073$ yr^{-1} at 87° and $\pi = 0\farcs07769 \pm 0\farcs00086$, from *Hipparcos*. The companion is HIP 80300, type DA2 (Wegner 1973), with matching *Hipparcos* values of $\mu = 0\farcs076$ yr^{-1} at 90° and $\pi = 0\farcs07804 \pm 0\farcs00240$.

HD 178911.—This is a triple-star system with one known planet. The wide CPM pair (AC-B) is clearly seen in DSS images. The $6.3 M_J$ planet orbits HD 178911B, while HD 178911AC is a close binary, first resolved by McAlister et al. (1987b) with the Canada-France-Hawaii Telescope (CFHT). This pair has since been resolved 10 more times, most recently with the 6 m telescope of the Special Astrophysical Observatory in Zelenchuk in 1999 (Balega et al. 2004). Hartkopf et al. (2000) present an orbital solution with a 3.5 yr period based on speckle observations, and Tokovinin et al. (2000) present a full orbital solution using spectroscopic and interferometric data. The multiplicity of this system has been previously identified (Zucker et al. 2002; Eggenberger et al. 2004). From *Hipparcos*, HD 178911AC's $\mu = 0\farcs200$ yr^{-1} at 14° and $\pi = 0\farcs02042 \pm 0\farcs00157$ and the companion's $\mu = 0\farcs203$ yr^{-1} at 19° and $\pi = 0\farcs02140 \pm 0\farcs00495$, a match within the errors, confirming a physical association.

HD 186427.—This is a triple-star system with one known planet. The wide CPM pair (AC-B) is clearly seen in DSS images. The planet orbits 16 Cyg B (HD 186427), while 16 Cyg A (HD 186408) is a close binary, first resolved by Turner et al. (2001) with the AO system on the Hooker 100″ telescope and independently confirmed by IR imaging by Patience et al. (2002) with the Keck 10 m and Lick 3 m. In the five total observations, the position of the secondary has not changed much. However, they span less than 2 yr of time and little motion would be expected at a projected separation of 73 AU. The multiplicity of this system has been previously identified (Patience et al. 2002; Lowrance et al. 2002; Eggenberger et al. 2004). From *Hipparcos*, 16 Cyg A's $\mu = 0\farcs217$ yr^{-1} at 223° and $\pi = 0\farcs04625 \pm 0\farcs00050$ and the planet host's $\mu = 0\farcs212$ yr^{-1} at 220° and $\pi = 0\farcs04670 \pm 0\farcs00052$, a match within the errors, confirming a physical association.

HD 188015.—This new companion was detected by us as a CPM candidate and confirmed via CCD photometry. The primary's $\pi = 0\farcs01900 \pm 0\farcs00095$ and $\mu = 0\farcs106$ yr^{-1} at 149°, from *Hipparcos*. The companion, 13″ away from the primary at 85°, does not have proper motion listed in SuperCOSMOS or NLTT, but our CCD photometric distance of 46.9 ± 9.5 pc matches the primary's distance within 1 σ and hence confirms this as a companion. Figure 4 includes two DSS images showing the primary and the companion.

HD 190360.—This CPM pair is easily identified in DSS images and matches entries in WDS and CNS. The primary is GJ 777A with spectral type G7 IV–V and $\mu = 0\farcs861$ yr^{-1} at 127° from *Hipparcos*. The companion is GJ 777B with spectral type M4.5 V and $\mu = 0\farcs860$ yr^{-1} at 127° (Lepine & Shara 2005). Our plate photometric distance estimate of 18.5 ± 6.2 pc is a good match with the primary's trigonometric parallax distance of 15.9 pc. This system has been recognized as a binary and as an exoplanet primary with a stellar companion (Allen et al. 2000; Naef et al. 2003; Eggenberger et al. 2004).

HD 195019.—WDS is the only source listing this close binary at a separation of 3″.5 at 330°. The close pair, first resolved by Hough (1887) with an 18 inch refractor, has moved 7° in position angle and closed in from 4″.5 to 3″.5 in separation in 12 observations over 107 yr. This transition has not been smooth, no doubt due to $\Delta m = 4$, making observations a challenge. The typical measurement errors of micrometry, coupled with slow motion, make characterization difficult. It was identified as a binary in Allen et al. (2000) and recognized as a stellar companion to an exoplanet system in Eggenberger et al. (2004).

HD 196050.—This CPM candidate was detected recently by Mugrauer et al. (2005) and confirmed by their photometry and spectroscopy. It could not be detected using DSS frames due to saturation of the region around the primary.

HD 213240.—This CPM pair was identified by us using DSS images. The primary's $\mu = 0\farcs236$ yr^{-1} at 215° and $\pi = 0\farcs02454 \pm 0\farcs00081$, from *Hipparcos*. The companion's

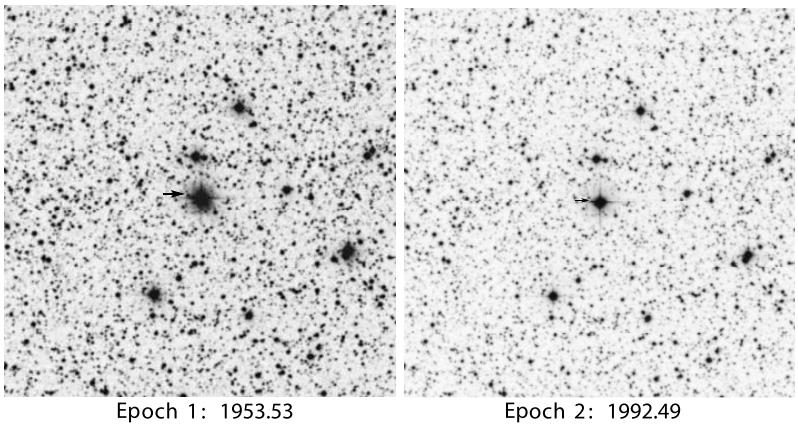

FIG. 4.—New stellar companion to exoplanet host HD 188015. The 10′ square DSS images have north up and east to the left. The companion, marked by arrows, is at an angular separation of 13″ at 85° from the primary, which is the bright source at the center of the images.

$\mu = 0\farcs229$ yr^{-1} at 214° from SuperCOSMOS is a good match. Our CCD photometric distance of 41.8 ± 6.5 pc is consistent with our spectral type identification of M5.0 V and is a good match to the primary's trigonometric parallax distance of 40.8 pc. This new companion identification in an exoplanet system was recently reported by Mugrauer et al. (2005) during the writing of this paper.

HD 219449.—A CPM companion is easily detected in the DSS images and is matched by WDS and CNS entries. WDS lists the secondary as a tight binary (0.″4 separation at 101°). The primary's $\mu = 0\farcs369$ yr^{-1} at 93° and $\pi = 0\farcs02197 \pm 0\farcs00089$, from *Hipparcos*. The companion binary has $\mu = 0\farcs377$ yr^{-1} at 91° from NLTT and $0\farcs385$ yr^{-1} at 96° from Zacharias et al. (2004), both good matches to the primary. NLTT also lists the companion's spectral type as K8 V. Our CCD photometric distance of 29.9 ± 4.7 pc is for the BC pair, and we predict an actual distance of 42.4 pc (assuming identical spectral types), which is a good match to the primary (45.5 pc). Radial velocities from Wilson (1953) are -26.4 ± 0.9 km s^{-1} for the primary and -25 ± 5 km s^{-1} for the secondary, also a match within the errors. Our approximate spectral identification as an early K type is consistent with the photometric distances. This work recognizes, for the fist time, that this exoplanet system resides in a triple-star system.

HD 222404.—This companion is listed in *Hipparcos* with a G flag, indicating a close astrometric binary. While some speckle searches have failed to detect a companion (e.g., Mason et al. 2001), the companion has been detected via radial velocity efforts and identified as a stellar companion in an exoplanet system (Campbell et al. 1988; Griffin et al. 2002; Eggenberger et al. 2004). The semimajor axes of the planet and stellar companions with respect to the primary place them at Sun–Mars and Sun–Uranus separations, respectively.

HD 222582.—This CPM pair is easily seen in DSS images and is listed in the WDS. The primary's $\mu = 0\farcs183$ yr^{-1} at 233° and $\pi = 0\farcs02384 \pm 0\farcs00111$, from *Hipparcos*. The secondary's $\mu = 0\farcs180$ yr^{-1} at 231° from NLTT, $0\farcs186$ yr^{-1} at 230° from SuperCOSMOS, and $0\farcs187$ yr^{-1} at 232° from Zacharias et al. (2004) are all good matches to the primary. Our CCD photometric distance of 32.1 ± 5.0 pc matches the primary's distance of 42.0 pc within 2 σ. Our spectral type of M3.5 V is consistent with the photometric distance estimates. This pair, resolved by Luyten in 1960, was noted to have a common proper motion. This work confirms the gravitational relationship via CPM, photometry, and spectroscopy and is the first identification of this stellar companion to an exoplanet system.

5.1.2. *Candidate Companion Systems*

HD 8673.—WDS is the only source listing a close companion, at 0.″1 separation. Resolved by Brian Mason in 2001 as part of a survey of nearby G dwarfs for duplicity, this unpublished observation has yet to be confirmed. The projected stellar separation of 3.8 AU is just over twice the planet/brown dwarf projected separation of 1.6 AU and dynamical instability is likely. Alternatively, given the large $M \sin i = 14 M_J$ for the "planet," it is possible that it is actually a star in a near face-on orbit ($i \leq 10°$) and that the radial velocity and speckle observations are of the same object.

HD 16141.—This CPM candidate was recently detected by Mugrauer et al. (2005) at a separation of 6.″2, and they plan follow-up observations to confirm it. We could not detect the companion using DSS frames due to saturation of the region around the primary.

HD 111232.—This companion is mentioned only in *Hipparcos* and is listed with a G flag, indicating that the proper motion was best fitted with higher order terms. Mason et al. (1998) conducted a specific search for a companion using optical speckle but did not find any. Their effort should have picked up companions with $\Delta V \lesssim 3$ and separations 0.″035–1.″08.

HD 150706.—This companion is mentioned only in *Hipparcos* and is listed with a G flag, indicating that the proper motion was best fitted with higher order terms. Halbwachs et al. (2003) reported this as a single star based on two CORAVEL radial velocity surveys that yielded statistical properties of main-sequence binaries with spectral types F7–K and with periods up to 10 yr.

HD 169830.—A candidate companion was detected by Kevin Apps as a close 2MASS source with 11″ separation at 265° (K. Apps 2005, private communication). Our CCD photometric distance estimate for the companion is 29 ± 23 pc, consistent

with the primary's distance of 36 pc, but the large error in our estimate prevents confirmation. The large error is likely due to the uncertainty in our and 2MASS photometry, caused by the close, bright primary and the proximity of the companion to the primary's diffraction spike. While 2MASS lists errors of 0.04 mag for JHK_s, it notes that the photometry is contaminated by a nearby bright source. Also, the J magnitude from DENIS is 0.36 mag brighter than the 2MASS value, indicating a larger uncertainty. The low proper motion ($0\farcs015$ yr^{-1}) of the primary prevents confirmation via CPM. While we believe that the evidence strongly indicates that this is a true companion, we cannot confirm it until we obtain a spectrum or other conclusive evidence.

HD 217107.—Only WDS lists this close companion with $0\farcs3$ separation at 156°. Proper motion of the primary is not detectable in DSS images. This pair has been resolved only twice (McAlister et al. 1987a; Mason et al. 1999) 15 yr apart, and the lack of additional resolutions of this bright pair seems to indicate that a large magnitude difference may be preventing additional detections. Given the two reported planets with $a \sin i = 0.1$ and 4.3 AU, this companion at a projected separation of just 6 AU would likely induce dynamical instability. Explanations for this include the possibility that this is an unrelated star with a chance alignment and/or that the wider "planet" is actually a stellar companion with a face-on orbit.

5.2. *Refuted Candidates: CPM Alone Does Not Confirm Companionship*

As CPM is often used to detect gravitationally bound companions, we list here five exceptions that, upon follow-up analyses, turned out to be unrelated field stars rather than true companions. In three of these instances (HD 33636, HD 41004, and HD 72659) we found proper motions in DSS plates to be an acceptable match by eye, but photometric distances indicated that each candidate was a distant field star. In the cases of BD −10 3166 and HD 114783, photometric distances did not provide a conclusive answer, but plotting these on an M_V versus $B - V$ curve of a sample of *Hipparcos* stars allowed us to refute them.

BD −10 3166 is the only exoplanet primary without a *Hipparcos* parallax. We derived a CCD photometric distance of 66.8± 10.0 pc, but that is based on just one color because the object is on the blue end of the M_{K_s}-color relations described in Henry et al. (2004). The companion candidate, LP 731-076, is $17''$ from the primary at 217° (in the DSS1, epoch 1983.29 image) and appears to have a matching proper motion. The two stars were identified by Luyten (1978) as a CPM pair and recently recovered in SuperCOSMOS data by R. Jaworski (2005, private communication). In SuperCOSMOS, the primary's $\mu = 0\farcs189$ yr^{-1} at 252° and the candidate's $\mu = 0\farcs202$ yr^{-1} at 242°. The candidate has a published photometric distance of 11.6 ± 0.8 pc (Reid et al. 2002), which is consistent with our photometric distance estimate of 12.5 ± 2.0 pc and our spectral type listed in Table 4. In order to get a better distance estimate to the primary, we plotted 285 stars from *Hipparcos* on an M_V versus $B - V$ diagram. The stars were selected based on distance (parallax greater than $0\farcs05$), quality of parallax (error less than 10%), luminosity class (main sequence only), and $B - V$ value of greater than 0.5. Fitting the primary's $B - V$ of 0.84 from Ryan (1992) to the least-squares fit curve through the *Hipparcos* data yields a distance estimate of 68 pc, consistent with our photometric distance estimate and too large to be associated with the candidate companion. This is an interesting example of a close ($17''$ separation) CPM pair for which distance estimates to both components are of the same order of magnitude, but the components seem to be unrelated.

HD 33636 has $\mu = 0\farcs227$ yr^{-1} at 127° and $\pi = 0\farcs03485 \pm 0\farcs00133$ (29 pc) from *Hipparcos*. The faint CPM candidate at a separation of $220''$ at 250° (in the DSS POSS2/UKSTURed, epoch 1990.81 image) was refuted by us after obtaining a CCD photometric distance of 739 ± 162 pc. Our spectrum, although noisy, allows us to estimate the spectral type to be M1.0 V, which indicates a large distance consistent with the photometric estimate.

HD 41004 has $\mu = 0\farcs078$ yr^{-1} at 327° and $\pi = 0\farcs02324 \pm 0\farcs00102$ (43 pc), from *Hipparcos*. The faint CPM candidate at a separation of $145''$ at 335° (in the DSS POSS2/UKSTURed, epoch 1993.96 image) was refuted by us after obtaining a CCD photometric distance of 557 ± 103 pc. We estimate the spectral type to be M0.5, although the luminosity class is uncertain: it could be a dwarf or a subdwarf. The candidate's $\mu = 0\farcs046$ yr^{-1} at 6° from SuperCOSMOS is not a good match to the primary.

HD 72659 has $\mu = 0\farcs150$ yr^{-1} at 229° and $\pi = 0\farcs01947 \pm 0\farcs00103$ (51 pc), from *Hipparcos*. The candidate, at a separation of $195''$ at 165° (in the DSS POSS2/UKSTURed, epoch 1992.03 image), was refuted by us after obtaining a CCD photometric distance of 369 ± 99 pc. Our spectral identification as M3.0 V is consistent with this photometric distance. SuperCOSMOS lists the CPM candidate's $\mu = 0\farcs066$ yr^{-1} at 199°, showing that proper motion is not a good match.

HD 114783 is another CPM pair that looks like it may be physical but is not. From *Hipparcos*, the primary has $\mu = 0\farcs138$ yr^{-1} at 274° and from SuperCOSMOS, the candidate companion (at a separation of $240''$ at 47° in the DSS POSS2/UKSTURed, epoch 1996.23 image) has $\mu = 0\farcs184$ yr^{-1} at 281°. The primary's distance from the *Hipparcos* parallax is 20.4 pc. Our plate photometric distance estimate for the companion is 20.2 ± 5.2 pc based on only three colors. However, using CCD photometry, we get a distance of 54.0 ± 9.3 pc, based on only two colors. The candidate companion is CCDM J13129−0213AB, a binary (listed in the WDS with a separation of $2\farcs0$ at 28°), and hence its actual distance is greater than photometrically indicated. We plotted the primary on the M_V versus $B - V$ diagram using *Hipparcos* data as described above, and it falls close to the main-sequence fit, indicating that it is likely a single star. The candidate companion, based on its $B - V$ of 1.10, yields a distance of 36 pc, using the *Hipparcos* plot, but its actual distance will be greater because it is a binary. Our spectra for the two stars show very similar absorption lines, although the continuum seems to indicate that the candidate companion is slightly redder. Given that the spectral types are close and that the candidate companion is a binary while the primary appears to be single, we can only explain the large ΔV (primary $V = 7.56$, and candidate companion $V = 9.78$) by adopting significantly different distances to the two stars. Hence, we conclude that this is not a gravitationally bound pair, despite the compelling proper-motion match.

6. DISCUSSION

Our findings indicate that 30 (23%) of the 131 exoplanet systems have confirmed stellar companions and 6 more (5%) have candidate companions. Given the constraints of our search (any new companions we detected had to be widely separated from primaries with high proper motion), these numbers should be regarded as lower limits. This point is confirmed by a recent paper, Mugrauer et al. (2005), which reported four new companions in exoplanet systems, of which we had independently identified only one (HD 213240B). Several interesting properties are revealed by this comprehensive assessment.

Three of the exoplanet systems (HD 178911, 16 Cyg B, and HD 219449) are stellar triples and are arranged similarly: a

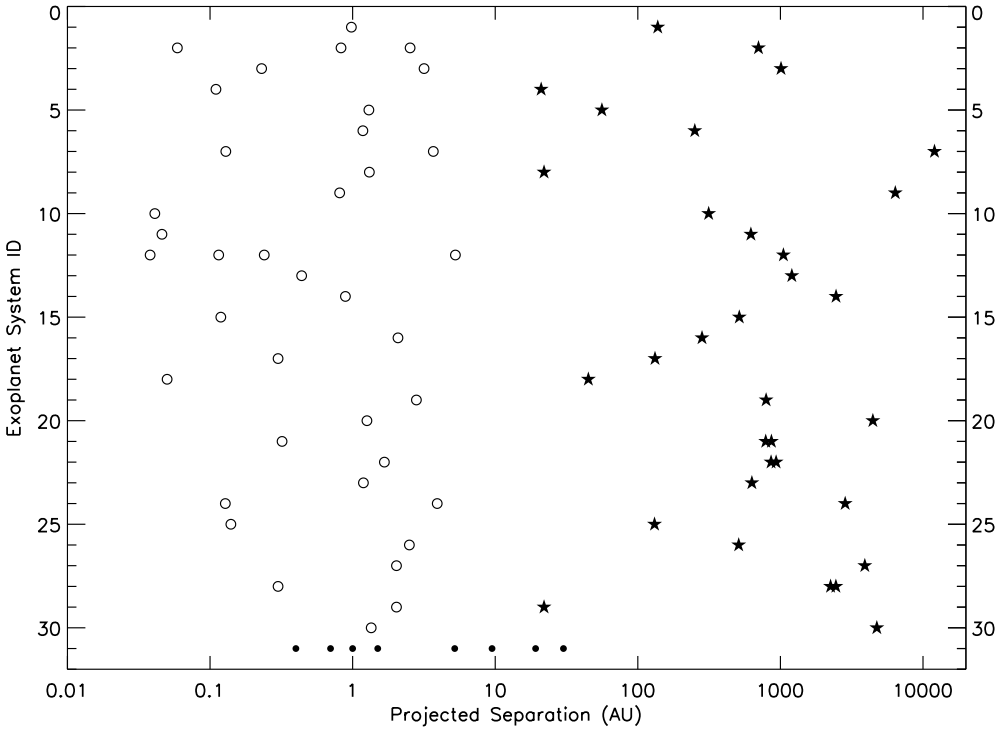

FIG. 5.— Orbits of planets and stars in exoplanet systems with stellar companions. The exoplanet host stars are at a position of 0 AU. Open circles represent planets, and stars represent stars. Points will tend to move right because of orbital inclination and projection effects. Separations between the components of the three binary companions are exaggerated to be able to distinguish the binary components on the plot. For comparison, the positions of the eight planets of our solar system are shown at the bottom as filled circles.

single planet orbits close to one star and there is a distant, tight binary. In each system, the three stars are all of the same spectral class (G for HD 178911 and 16 Cyg, and K for HD 219449). We find it curious that all three triple systems contain stars of comparable mass (i.e., systems such as a G dwarf exoplanet host with an M dwarf binary are not seen). Could this be due to a selection effect (i.e., faint companions are not as well studied for multiplicity), or does this say something about the angular momentum distribution in star-forming regions? Only a comprehensive survey of all companions for duplicity can lead us to an answer.

It is interesting to note that recent exoplanet discoveries are predominantly found in single-star systems. Of the first 102 radial velocity–detected exoplanet systems, 26 (26%) have confirmed stellar companions. In contrast, only 4 (14%) of the latest 29 systems have confirmed stellar companions. Even though we are dealing with small number statistics, we believe that this change is significant and worthy of further examination. Our first inclination was that recent planet detections are at larger projected semimajor axes and hence favor single systems because stellar companions would have to be even farther out to provide the uncorrupted "single" systems sought by radial velocity programs. However, we found no correlation between the timing of exoplanet reporting and its projected semimajor axis. Thus, we are not able to explain this curiosity at this point and simply identify it for further examination.

Exoplanet hosts are deficient in having stellar companions when compared to a sample of field stars. Our updated results for stellar counts in the exoplanet sample yield a single : double : triple : quadruple percentage of 79:21:2:0 for confirmed systems, and 72:24:4:0 considering candidates. While these are lower limits for multiplicity, they are significantly lower than the Duquennoy & Mayor (1991) results of 57 : 38 : 4 : 1 for multiples with orbits, and 51 : 40 : 7 : 2 considering candidates. This is certainly due in part to the fact that planet searches specifically exclude known close binaries from their samples (e.g., Vogt et al. 2000) and further eliminate any new binaries detected via radial velocity. We currently do not have enough detailed information about the exoplanet search target selection process to say whether the different multiplicity ratios are entirely due to selection effects or are indicative of planetary disk instability and reduced planet formation in binary-star systems.

6.1. *Planetary and Stellar Orbits in Multiple-Star Systems*

Figure 5 shows the $a \sin i$ of planetary companions and projected separations of the stellar companions for the 30 confirmed exoplanets that reside in multiple-star systems. The *Y*-axis shows

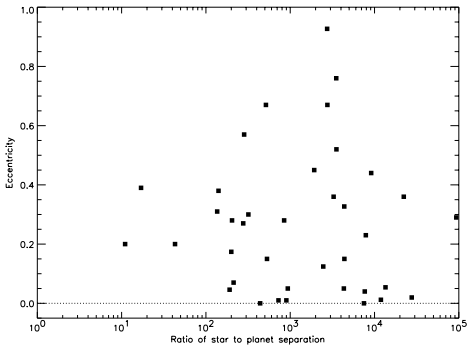

FIG. 6.—Eccentricity of planetary orbits as a function of proximity of the stellar companion. The ratio is computed using projected stellar separation and $a \sin i$ of the planetary orbit.

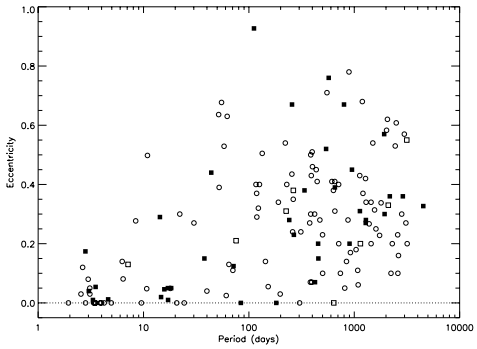

FIG. 7.—Period-eccentricity diagram for planets orbiting single stars (*open circles*) and planets in systems with more than one star (*open squares*: candidate multiplicity; *filled squares*: confirmed multiplicity).

the sequence number of the exoplanet system as listed in column (1) of Table 2. The figure clearly indicates the presence of separate planetary and stellar orbit regimes for the data currently available. All planets are within 6 AU, and all stars are at a projected separation of greater than 20 AU from the exoplanet host. Note that all points in the figure can potentially move right because (1) planets are plotted at a separation of $a \sin i$ and (2) stars are plotted based on their projected separations (although a few could move left if they have been caught near apastron in their orbits). The continued search for wider orbit planets will answer the question of whether this is simply due to selection effects or if this says something significant about planetary disk truncation in multiple-star systems.

55 Cnc (HD 75732), an extensive extrasolar system with four reported planets, has the widest projected planetary orbit with an $a \sin i$ of 5.3 AU. It is noteworthy that such an extensive exoplanet system also has a stellar companion, at a projected separation of 1050 AU. This provides direct evidence of the stability of protoplanetary disks in multiple-star systems such as to allow formation and sustenance of multiple planets, at least as long as the separation between the stars is sufficiently large. This system can also provide an observational constraint for evaluating theoretical models of disk stability and solar system evolution.

The smallest projected separation for a stellar companion is 21 AU for GJ 86, closely followed by 22 AU for HD 41004 and γ Cep. Each system has only one reported planet, with $a \sin i$ of 0.1, 1.3, and 2.0 AU, respectively. This may be evidence that a sufficiently close stellar companion will disrupt the protoplanetary disk, truncating planet formation at a few AU from the primary.

Several studies have investigated the theoretical stability of planetary orbits in multiple-star systems (e.g., Holman & Wiegert 1999; Benest & Gonczi 2003), deriving ratios of orbital semimajor axes of the planet and stellar companions for various values of mass ratio and eccentricity of the stellar orbits. Our work provides observational constraints based on all known exoplanets in multiple-star systems. Of the 30 confirmed exoplanets in multiple-star systems, only 3 have a ratio of stellar to planetary projected separation of less than 100. The lowest ratio is 11, for γ Cep (HD 222404). Although numerical simulations demonstrate the stability of orbits for much smaller separation ratios [e.g., for $m_2/(m_1 + m_2) = 0.5$ and $e = 0.1$, the minimum ratio of stellar and planetary orbital semimajor axes is about 4 from Holman & Wiegert 1999], no planets have yet been observed in this regime. This could be attributed to the selection effect of close binaries being excluded from planet searches, as described above. However, this could also provide evidence for protoplanetary disk truncation by a close stellar companion, preventing planet formation in systems with separation ratios close to the limits permitted by numerical simulations.

Every exoplanet system so far discovered in a multiple-star system has an S-type (satellite-type) orbit, where the planet orbits one of the stars. This is not surprising because current radial velocity searches for exoplanets exclude close binaries (e.g., Vogt et al. 2000). While the formation and stability of planets in P-type (planet-type) orbits, where a planet orbits the center of mass of a binary- or multiple-star system, have been theoretically demonstrated (Holman & Wiegert 1999; Boss 2005; Musielak et al. 2005), they have not yet been observationally supported. However, Correia et al. (2005) have raised the interesting possibility that the $2.4 M_J$ outer planet around HD 202206 may in fact have formed in a circumbinary disk around the primary and the closer $17 M_J$ minimum-mass object.

6.2. *Stellar Companions Might Influence Eccentricity of Planetary Orbits*

Eccentricities of exoplanet orbits are significantly higher than those of planets in our solar system (Marcy et al. 2005a). Takeda & Rasio (2005) investigated whether the Kozai mechanism can explain this entirely and concluded that other effects are also at play. We investigated the potential impact of close stellar companions on the eccentricity of planetary orbits, as these would have a greater gravitational influence on the planet's orbit and potentially reduce the period of Kozai cycles. Figure 6 shows the eccentricity of the planetary orbits as a function of the ratio of projected stellar separations to the $a \sin i$ of planetary orbits and does not conclusively demonstrate any relationship. However, even though three data points do not provide conclusive evidence, it is interesting to note that the systems with ratios under 100 have a minimum eccentricity of 0.2, while larger ratio systems have lower eccentricities.

We also looked at the relationship between period and eccentricity of planetary orbits in systems with and without stellar companions. Figure 7 shows the eccentricity of planetary orbits

versus the orbital period. Planet orbits in systems with confirmed stellar companions are represented by filled squares, orbits with candidate stellar companions are represented by open squares, and orbits in single-star systems are denoted by open circles. Udry et al. (2004) and Eggenberger et al. (2004) presented similar plots and concluded that all of the planets with a period $P \lesssim 40$ days orbiting in multiple-star systems have an eccentricity smaller than 0.05, whereas longer period planets found in multiple-star systems can have larger eccentricities. Our updated results show that this conclusion is no longer strictly true. The latest planet reported around 55 Cnc, designated with suffix e, has a period of 2.81 days and an eccentricity of 0.17. Also, we report HD 38529 as a multiple-star system, which was assumed to be a single-star system in Udry et al. (2004). Planet HD 38529b has a period of 14.31 days and an eccentricity of 0.29. It appears that single-star and multiple-star planetary systems have similar period-eccentricity relationships.

7. CONCLUSIONS

Our comprehensive investigation of 131 exoplanet systems reveals that 30 (23%) of these have stellar companions, an increase from 15 reported in previous such comprehensive efforts (Eggenberger et al. 2004; Udry et al. 2004). We report new stellar companions to HD 38529 and HD 188015 and identify a candidate companion to HD 169830. Our synthesis effort, bringing together disparate databases, recognizes, for the first time, five additional stellar companions to exoplanet hosts, including one triple system. A by-product of our CPM investigation is the determination that 20 of the WDS entries for exoplanet hosts are not gravitationally bound to their "primaries" but are chance alignments in the sky. Some interesting examples in the inventory of multiple-star exoplanet systems include the following: (1) at least three and possibly five exoplanet systems are stellar triples (see § 6); (2) three systems (GJ 86, HD 41004, and γ Cep) have planets at roughly Mercury–Mars distances and potentially close-in stellar companions at projected separations similar to the distance between the Sun and Uranus ($\sim$20 AU); and (3) two systems (GJ 86 and HD 147513) have white dwarf companions. These results show that planets form and survive in a variety of stellar multiplicity environments. We hope that this compendium of stellar multiples in exoplanet systems will provide a valuable benchmark for future companion searches and exoplanet system analyses.

We wish to thank Charlie Finch and Jennifer Winters for their supporting work in this effort. We also thank G. Fritz Benedict and Jacob Bean for obtaining and reducing the radial velocity data for HD 38529B. We are grateful to Geoff Marcy and Kevin Apps for reviewing our draft and providing useful suggestions and to the anonymous referee, who provided detailed comments based on a thorough review. The photometric and spectroscopic observations reported here were carried out under the auspices of the SMARTS (Small and Moderate Aperture Research Telescope System) Consortium, which operates several small telescopes at CTIO, including the 0.9, 1.0, and 1.5 m. T. J. H.'s Space Interferometry Mission grant supported some of the work carried out here. This effort used multiepoch images from the Digitized Sky Survey, which was produced at the Space Telescope Science Institute under US Government grant NAG W-2166. This work also used data products from the Two Micron All Sky Survey, which is a joint project of the University of Massachusetts and the Infrared Processing and Analysis Center/California Institute of Technology, funded by the National Aeronautics and Space Administration and the National Science Foundation. In addition, this work used data from the SuperCOSMOS Sky Survey, the *Hipparcos* catalog, and SIMBAD databases.

REFERENCES

Allen, C., Poveda, A., & Herrera, M. A. 2000, A&A, 356, 529
Bailey, S. I. 1900, Harvard Ann., 32, 296
Baize, P. 1957, J. des Obs., 40, 165
Balega, I., Balega, Y. Y., Maksimov, A. F., Pluzhnik, E. A., Schertl, D., Shkhagosheva, Z. U., & Weigelt, G. 2004, A&A, 422, 627
Benest, D., & Gonczi, R. 2003, Earth Moon Planets, 93, 175
Bessel, M. S. 1990, A&AS, 83, 357
Blazit, A., Bonneau, D., Koechlin, L., & Labeyrie, A. 1977, ApJ, 214, L79
Bonnarel, F., et al. 2000, A&AS, 143, 33
Boss, A. P. 2005, BAAS, 207, 84.03
Campbell, B., Walker, G. A. H., & Yang, S. 1988, ApJ, 331, 902
Cochran, W. D., Hatzes, A. P., Butler, R. P., & Marcy, G. W. 1997, ApJ, 483, 457
Cochran, W. D., Hatzes, A. P., & Hancock, T. J. 1991, ApJ, 380, L35
Correia, A. C. M., Udry, S., Mayor, M., Laskar, J., Naef, D., Pepe, F., Queloz, D., & Santos, N. C. 2005, A&A, 440, 751
Couteau, P. 1954, J. des Obs., 37, 37
Dahn, C. C., et al. 1988, AJ, 95, 237
Desidera, S., Gratton, R. G., Endl, M., Claudi, R. U., & Cosentino, R. 2004, A&A, 420, L27
Duquennoy, A., & Mayor, M. 1991, A&A, 248, 485
Eggenberger, A., Mayor, M., Naef, D., Pepe, F., Queloz, D., Santos, N. C., Udry, S., & Lovis, C. 2006, A&A, 447, 1159
Eggenberger, A., Udry, S., & Mayor, M. 2004, A&A, 417, 353
Els, S. G., Sterzik, M. F., Marchis, F., Pantin, E., Endl, M., & Kürster, M. 2001, A&A, 370, L1
Fischer, D. A., Marcy, G. W., Butler, R. P., Vogt, S. S., & Apps, K. 1999, PASP, 111, 50
Fischer, D. A., & Valenti, J. 2005, ApJ, 622, 1102
Frink, S., Mitchell, D. S., Quirrenbach, A., Fischer, D. A., Marcy, G. W., & Butler, R. P. 2002, ApJ, 576, 478
Gatewood, G., Han, I., & Black, D. C. 2001, ApJ, 548, L61
Gliese, W. 1969, Veröff. Astron. Rech.-Inst. Heidelberg, 22, 1
Gliese, W., & Jahreiss, H. 1979, Bull. Cent. Donnees Stellaires, 16, 92
———. 1991, The Astronomical Data Center CD-ROM: Selected Astronomical Catalogs, Vol. 1, ed. L. E. Brotzmann & S. E. Gesser (Greenbelt: NASA GSFC)
Graham, J. A. 1982, PASP, 94, 244
Gray, R. O., Corbally, C. J., Garrison, R. F., McFadden, M. T., & Robinson, P. E. 2003, AJ, 126, 2048
Griffin, R. F., Carquillat, J.-M., & Ginestet, N. 2002, Observatory, 122, 90
Halbwachs, J. L. 1986, A&AS, 66, 131
Halbwachs, J. L., Mayor, M., Udry, S., & Arenou, F. 2003, A&A, 397, 159
Hale, A. 1994, AJ, 107, 306
Hambly, N. C., Henry, T. J., Subasavage, J. P., Brown, M. A., & Jao, W. 2004, AJ, 128, 437
Hambly, N. C., Irwin, M. J., & MacGillivray, H. T. 2001a, MNRAS, 326, 1295
Hambly, N. C., et al. 2001b, MNRAS, 326, 1279
Hartkopf, W. I., & McAlister, H. A. 1984, PASP, 96, 105
Hartkopf, W. I., et al. 2000, AJ, 119, 3084
Hatzes, A. P., Cochran, W. D., Endl, M., McArthur, B., Paulson, D. B., Walker, G. A. H., Campbell, B., & Yang, S. 2003, ApJ, 599, 1383
Henry, T. J., Subasavage, J. P., Brown, M. A., Beaulieu, T. D., Jao, W., & Hambly, N. C. 2004, AJ, 128, 2460
Henry, T. J., Walkowicz, L. M., Barto, T. C., & Golimowski, D. A. 2002, AJ, 123, 2002
Hog, E., Kuzmin, A., Bastian, U., Fabricius, C., Kuimov, K., Lindegren, L., Makarov, V. V., & Roeser, S. 1998, A&A, 335, L65
Holden, F. 1966, Publ. Univ. Michigan Obs., 9, 185
Holman, M. J., & Wiegert, P. A. 1999, AJ, 117, 621
Hough, G. W. 1887, Astron. Nachr., 116, 273
Jacoby, G. H., Hunter, D. A., & Christian, C. A. 1984, ApJS, 56, 257
Jessup, M. K. 1955, Publ. Univ. Michigan Obs., 11, 1
Jonckheere, R. 1911, MNRAS, 72, 45
———. 1917, MmRAS, 61, 1
———. 1944, J. des Obs., 27, 11

Landolt, A. U. 1992, AJ, 104, 340
Lepine, S., & Shara, M. M. 2005, AJ, 129, 1483
Lowrance, P. J., Kirkpatrick, J. D., & Beichman, C. A. 2002, ApJ, 572, L79
Luhman, K. L., & Jayawardhana, R. 2002, ApJ, 566, 1132
Luyten, W. J. 1978, Univ. Minnesota Proper Motion Survey 50
———. 1979, New Luyten Catalogue of Stars with Proper Motions Larger than Two Tenths of an Arcsecond (NLTT) (Minneapolis: Univ. Minnesota)
Marcy, G., Butler, R. P., Fischer, D., Vogt, S., Wright, J. T., Tinney, C. G., & Jones, H. R. A. 2005a, Prog. Theor. Phys. Suppl., 158, 24
Marcy, G. W., Butler, R. P., Fischer, D. A., Laughlin, G., Vogt, S. S., Henry, G. W., & Pourbaix, D. 2002, ApJ, 581, 1375
Marcy, G. W., Butler, R. P., Vogt, S. S., Fischer, D. A., Henry, G. W., Laughlin, G., Wright, J. T., & Johnson, J. A. 2005b, ApJ, 619, 570
Marcy, G. W., & Moore, D. 1989, ApJ, 341, 961
Mason, B. D., Hartkopf, W. I., Holdenried, E. R., & Rafferty, T. J. 2001, AJ, 121, 3224
Mason, B. D., Henry, T. J., Hartkopf, W. I., Ten Brummelaar, T., & Soderblom, D. R. 1998, AJ, 116, 2975
Mason, B. D., et al. 1999, AJ, 117, 1890
Mayor, M., Udry, S., Naef, D., Pepe, F., Queloz, D., Santos, N. C., & Burnet, M. 2004, A&A, 415, 391
McAlister, H. A. 1978, PASP, 90, 288
McAlister, H. A., Hartkopf, W. I., Hutter, D. J., & Franz, O. G. 1987a, AJ, 93, 688
McAlister, H. A., Hartkopf, W. I., Hutter, D. J., Shara, M. M., & Franz, O. G. 1987b, AJ, 93, 183
McCarthy, J. K., Sandiford, B. A., Boyd, D., & Booth, J. 1993, PASP, 105, 881
Mugrauer, M., & Neuhäuser, R. 2005, MNRAS, 361, L15
Mugrauer, M., Neuhäuser, R., Mazeh, T., Alves, J., & Guenther, E. 2004a, A&A, 425, 249
Mugrauer, M., Neuhäuser, R., Mazeh, T., Guenther, E., & Fernández, M. 2004b, Astron. Nachr., 325, 718
Mugrauer, M., Neuhäuser, R., Seifahrt, A., Mazeh, T., & Guenther, E. 2005, A&A, 440, 1051
Musielak, Z. E., Cuntz, M., Marshall, E. A., & Stuit, T. D. 2005, A&A, 434, 355
Naef, D., et al. 2001, A&A, 375, L27
———. 2003, A&A, 410, 1051
Nidever, D. L., Marcy, G. W., Butler, R. P., Fischer, D. A., & Vogt, S. S. 2002, ApJS, 141, 503
Noyes, R. W., Jha, S., Korzennik, S. G., Krockenberger, M., Nisenson, P., Brown, T. M., Kennelly, E. J., & Horner, S. D. 1997, ApJ, 487, L195
Oppenheimer, B. R., Golimowski, D. A., Kulkarni, S. R., Matthews, K., Nakajima, T., Creech-Eakman, M., & Durrance, S. T. 2001, AJ, 121, 2189
Patience, J., et al. 2002, ApJ, 581, 654
Perryman, M. A. C., et al. 1997, The *Hipparcos* and Tycho Catalogues (ESA SP-1200; Noordwijk: ESA)
Pourbaix, D., & Arenou, F. 2001, A&A, 372, 935
Poveda, A., Herrera, M. A., Allen, C., Cordero, G., & Lavalley, C. 1994, Rev. Mex. AA, 28, 43
Queloz, D., et al. 2000, A&A, 354, 99
Reffert, S., & Quirrenbach, A. 2006, A&A, 449, 699
Reid, I. N., Kilkenny, D., & Cruz, K. L. 2002, AJ, 123, 2822
Ryan, S. G. 1992, AJ, 104, 1144
See, T. J. J. 1897, Astron. Nachr., 142, 43
Smyth, W. H. 1844, Cycle of Celestial Objects (London: J. W. Parker)
Soulie, G. 1985, A&AS, 61, 17
Takeda, G., & Rasio, F. A. 2005, ApJ, 627, 1001
Tokovinin, A. A., Griffin, R. F., Balega, Y. Y., Pluzhnik, E. A., & Udry, S. 2000, Astron. Lett., 26, 116
Turner, N. H., Brummelaar, T. A. t., McAlister, H. A., Mason, B. D., Hartkopf, W. I., & Roberts, L. C. 2001, AJ, 121, 3254
Udry, S., Eggenberger, A., Mayor, M., Mazeh, T., & Zucker, S. 2004, Rev. Mex. AA Conf. Ser., 21, 207
Urban, S. E., Corbin, T. E., Wycoff, G. L., Martin, J. C., Jackson, E. S., Zacharias, M. I., & Hall, D. M. 1998, AJ, 115, 1212
van Altena, W. F., Lee, J. T., & Hoffleit, E. D. 1995, Yale Trigonometric Parallaxes (4th ed.; New Haven: Yale Univ. Obs.)
Van Biesbroeck, G. 1960, Publ. Yerkes Obs., 9, Pt. 2, 1960
van den Bos, W. H. 1949, Union Obs. Circ., 5, 312
———. 1960, Publ. Yerkes Obs., 9, Pt. 1, 1960
———. 1963, AJ, 68, 582
Vanderdonck, J. 1911, MNRAS, 72, 45
Vogt, S. S., Marcy, G. W., Butler, R. P., & Apps, K. 2000, ApJ, 536, 902
Wegner, G. 1973, MNRAS, 163, 381
Wilson, J. C., Kirkpatrick, J. D., Gizis, J. E., Skrutskie, M. F., Monet, D. G., & Houck, J. R. 2001, AJ, 122, 1989
Wilson, R. E. 1953, General Catalogue of Stellar Radial Velocities (Washington, DC: Carnegie Inst. Washington)
Zacharias, N., Urban, S. E., Zacharias, M. I., Wycoff, G. L., Hall, D. M., Monet, D. G., & Rafferty, T. J. 2004, AJ, 127, 3043
Zucker, S., & Mazeh, T. 2001, ApJ, 562, 549
Zucker, S., Mazeh, T., Santos, N. C., Udry, S., & Mayor, M. 2003, A&A, 404, 775
———. 2004, A&A, 426, 695
Zucker, S., et al. 2002, ApJ, 568, 363

– E –

The Visual Orbit σ^2 Coronae Borealis

The following pages reproduce the Astrophysical Journal publication, Raghavan et al. (2009), that, based on the work done as part of this thesis, presented a revised spectroscopic orbit and a new visual orbit for σ^2 CrB.

The Astrophysical Journal, 690:394–406, 2009 January 1 doi:10.1088/0004-637X/690/1/394
© 2009. The American Astronomical Society. All rights reserved. Printed in the U.S.A.

THE VISUAL ORBIT OF THE 1.1 DAY SPECTROSCOPIC BINARY σ^2 CORONAE BOREALIS FROM INTERFEROMETRY AT THE CHARA ARRAY

Deepak Raghavan[1], Harold A. McAlister[1], Guillermo Torres[2], David W. Latham[2], Brian D. Mason[3], Tabetha S. Boyajian[1], Ellyn K. Baines[1], Stephen J. Williams[1], Theo A. ten Brummelaar[4], Chris D. Farrington[4], Stephen T. Ridgway[5], Laszlo Sturmann[4], Judit Sturmann[4], and Nils H. Turner[4]
[1] Center for High Angular Resolution Astronomy, Georgia State University, P.O. Box 3969, Atlanta, GA 30302-3969, USA; raghvan@chara.gsu.edu
[2] Harvard-Smithsonian Center for Astrophysics, 60 Garden Street, Cambridge, MA 02138, USA
[3] US Naval Observatory, 3450 Massachusetts Avenue NW, Washington, DC 20392-5420, USA
[4] The CHARA Array, Mount Wilson Observatory, Mount Wilson, CA 91023, USA
[5] National Optical Astronomy Observatory, P.O. Box 26732, Tucson, AZ 85726-6732, USA
Received 2008 May 27; accepted 2008 August 28; published 2008 December 1

ABSTRACT

We present an updated spectroscopic orbit and a new visual orbit for the double-lined spectroscopic binary σ^2 Coronae Borealis (CrB) based on radial velocity measurements at the Oak Ridge Observatory in Harvard, MA and interferometric visibility measurements at the Center for High Angular Resolution Astronomy (CHARA) Array on Mount Wilson in California. σ^2 CrB is composed of two Sun-like stars of roughly equal mass in a circularized orbit with a period of 1.14 days. The long baselines of the CHARA Array have allowed us to resolve the visual orbit for this pair, the shortest-period binary yet resolved interferometrically, enabling us to determine component masses of $1.137 \pm 0.037\ M_\odot$ and $1.090 \pm 0.036\ M_\odot$. We have also estimated absolute V-band magnitudes of $M_V(\text{primary}) = 4.35 \pm 0.02$ and $M_V(\text{secondary}) = 4.74 \pm 0.02$. A comparison with stellar evolution models indicates a relatively young age of 0.1–3 Gyr, consistent with the high-Li abundance measured previously. This pair is the central component of a quintuple system, along with another similar-mass star, σ^1 CrB, in a ∼730-year visual orbit, and a distant M-dwarf binary, σ CrB C, at a projected separation of ∼10′. We also present differential proper motion evidence to show that components C & D (ADS 9979C & D) listed for this system in the Washington Double Star Catalog are optical alignments that are not gravitationally bound to the σ CrB system.

Key words: binaries: spectroscopic – stars: fundamental parameters – stars: individual (σ^2 Coronae Borealis) – techniques: interferometric

1. INTRODUCTION

σ Coronae Borealis (CrB) is a hierarchical multiple system 22 pc away. Its primary components, σ^1 CrB (HR 6064; HD 146362) and σ^2 CrB (HR 6063; HD 146361), are in a visual orbit with a preliminary period of ∼900 years (Scardia 1979), of which the latter is an RS CVn binary with a circularized and synchronized orbit of 1.139-day period (Strassmeier & Rice 2003, SR03 hereafter). In addition to these three solar-type stars, the Washington Double Star Catalog[6] (WDS) lists three additional components for this system. WDS components C and D were resolved 18″ away at 103° in 1984 (Popović 1986) and 88″ away at 82° in 1996 (Courtot 1996), respectively. We will show in Section 6 that both these components are optical alignments that are not gravitationally bound to the σ CrB system. Finally, WDS component E (σ CrB C, HIP 79551), which was resolved 635″ away at 241° in 1991 by *Hipparcos* (Perryman & ESA 1997), was identified as a photocentric-motion binary by Heintz (1990). The parallax and proper motion listed for this star in van Leeuwen (2007), the improved *Hipparcos* results based on a new reduction of the raw data, match the corresponding measures for σ^2 CrB within the errors, confirming a physical association.

SR03 presented photometric evidence in support of a rotation period of 1.157 ± 0.002 days for both components of σ^2 CrB, the central pair of this system. They explained the 0.017-day difference between the rotation and orbital periods as differential surface rotation. Bakos (1984) estimated an orbital inclination of 28°, assuming component masses of $1.2\ M_\odot$ based on spectral types. SR03 subsequently adopted this inclination to obtain component masses of $1.108 \pm 0.004\ M_\odot$ and $1.080 \pm 0.004\ M_\odot$, but these masses are based on circular reasoning, and the errors are underestimated as they ignore the uncertainty in inclination. Several spectroscopic orbits have been published for this pair (Harper 1925; Bakos 1984; Duquennoy & Mayor 1991; SR03), enabling the spectroscopic orbital elements to be well constrained. We present an updated spectroscopic solution based on these prior data and our own radial velocity measurements (Sections 2.1 and 4.1). Our visual orbit leverages these spectroscopic solutions and derives all orbital elements for this binary (Section 4.2), leading to accurate component masses (Section 5.1).

This work utilizes a very precise parallax measure for this radio-emitting binary obtained by Lestrade et al. (1999) using very long baseline interferometry (VLBI). Their parallax of 43.93 ± 0.10 mas is about 10 times more precise than the *Hipparcos* catalog value of 46.11 ± 0.98 mas and 12 times more precise than the van Leeuwen (2007) measure of 47.35 ± 1.20 mas. The Lestrade et al. value is 2.2σ and 2.9σ lower than the *Hipparcos* and van Leeuwen measures, respectively. To check for systematic offsets, we compared the parallaxes for all overlapping stars in these three sources. While the difference in parallax is most significant for σ^2 CrB, we found no systematic differences. Moreover, Lestrade et al. performed statistical checks to verify the accuracy of their measure, so we adopt their parallax to derive the physical parameters of the component stars (Section 5).

[6] http://ad.usno.navy.mil/wds/

The Center for High Angular Resolution Astronomy (CHARA) Array's unique capabilities, facilitated by the world's longest optical interferometric baselines, have enabled a variety of astrophysical studies (e.g., McAlister et al. 2005; Baines et al. 2007; Monnier et al. 2007). This work utilizes the Array's longest baselines to resolve the 1.14-day spectroscopic binary, the shortest-period system yet resolved. While this is the first visual orbit determined using interferometric visibilities measured with the CHARA Array, the technique described here has regularly been employed for longer-period binaries using other long-baseline interferometers (e.g., Hummel et al. 1993; Boden et al. 1999). The σ^2 CrB binary has a projected angular separation of about 1.1 mas in the sky, making it easily resolvable for the CHARA Array, which has angular resolution capabilities in the K' band down to about 0.4 mas for binaries.

2. SPECTROSCOPIC MEASUREMENTS

Spectroscopic observations of σ^2 CrB were conducted at the Harvard-Smithsonian Center for Astrophysics (CfA) with an echelle spectrograph on the 1.5 m Wyeth reflector at the Oak Ridge Observatory in the town of Harvard, MA. A total of 46 usable spectra were gathered from 1992 May to 1999 July, each of which covers a single echelle order (45 Å) centered at 5188.5 Å and was recorded using an intensified photon-counting Reticon detector (see Latham 1992). The strongest lines in this window are those of the Mg I b triplet. The resolving power of these observations is $\lambda/\Delta\lambda \approx 35{,}000$, and the nominal signal-to-noise ratios (S/Ns) range from 21 to 94 per resolution element of 8.5 km s^{-1}.

Radial velocities were obtained using the two-dimensional cross-correlation algorithm TODCOR (Zucker & Mazeh 1994). Templates for the cross-correlations were selected from an extensive library of calculated spectra based on model atmospheres by R. L. Kurucz[7] (see also Nordström et al. 1994; Latham et al. 2002). These calculated spectra cover a wide range of effective temperatures ($T_{\rm eff}$), rotational velocities ($v \sin i$ when seen in projection), surface gravities ($\log g$), and metallicities. Experience has shown that radial velocities are largely insensitive to the surface gravity and metallicity adopted for the templates. Consequently, the optimum template for each star was determined from extensive grids of cross-correlations varying the temperature and rotational velocity, seeking to maximize the average correlation weighted by the strength of each exposure. The results we obtain, adopting $\log g = 4.5$ and solar metallicity[8] for both stars, are $T_{\rm eff} = 6050$ K and $v \sin i = 26$ km s^{-1} for the primary, and $T_{\rm eff} = 5870$ K and $v \sin i = 26$ km s^{-1} for the secondary. Estimated uncertainties are 150 K and 1 km s^{-1} for the temperatures and projected rotational velocities, respectively. Template parameters near these values were selected for deriving the radial velocities. The typical uncertainty for the velocities is 1 km s^{-1} for both stars.

The stability of the zero point of our velocity system was monitored by means of exposures of the dusk and dawn sky, and small run-to-run corrections were applied in the manner described by Latham (1992). Additional corrections for systematics were applied to the velocities as described by Latham et al. (1996) and Torres et al. (1997) to account for residual blending effects. These corrections are based on simulations with artificial composite spectra processed with TODCOR in the same way as the real spectra. The final heliocentric velocities and their 1σ errors are listed in Table 1, along with the corresponding epochs of observation, $O - C$ residuals, and orbital phase.

The light ratio between the components was estimated directly from the spectra following Zucker & Mazeh (1994). After corrections for systematics analogous to those described above, we obtain $\ell_{\rm s}/\ell_{\rm p} = 0.67 \pm 0.02$ at the mean wavelength of our observations (5188.5 Å). Given that the stars have slightly different temperatures, a small correction to the visual band was determined from synthetic spectra integrated over the V passband and the spectral window of our observations. The corrected value is $(\ell_{\rm s}/\ell_{\rm p})_V = 0.70 \pm 0.02$.

The visual companion σ^1 CrB was also observed spectroscopically at the CfA with the same instrumental setup. We obtained 18 observations between 1996 June and 2004 August. The stellar parameters were determined with a procedure similar to that used for σ^2 CrB, and yielded $T_{\rm eff} = 5950 \pm 100$ K and $v \sin i = 3 \pm 2$ km s^{-1}, for an adopted $\log g = 4.5$ and solar metallicity (see Footnote 8). Radial velocities were obtained with standard cross-correlation techniques using a template selected according to the above parameters. These measurements give an average velocity of -14.70 ± 0.11 km s^{-1}, with no significant variation within the observational errors. We use this radial velocity to unambiguously determine the longitude of the ascending node for the wider $\sigma^1 - \sigma^2$ CrB visual orbit (Section 5.4).

2.1. Historical Data Sets

In addition to our own, four other radial-velocity data sets have been published in the literature (Harper 1925; Bakos 1984; Duquennoy & Mayor 1991; SR03). Except for the more recent one, the older data are generally of lower quality and contribute little to the mass determinations, but they do extend the time coverage considerably (to nearly 86 years, or 27,500 orbital cycles), and can be used to improve the orbital period. Because of our concerns over possible systematic differences among different data sets, particularly in the velocity semiamplitudes but also in the velocity zero points, we did not simply merge all these observations together indiscriminately, but instead we proceeded as follows. We considered all observations simultaneously in a single least-squares orbital fit, imposing a common period and epoch of maximum primary velocity in a circular orbit, but we allowed each data set to have its own velocity semiamplitudes ($K_{\rm p}$, $K_{\rm s}$) as well as its own systematic velocity zero-point offset relative to the reference frame defined by the CfA observations. Additionally, we included one more adjustable parameter per set to account for possible systematic differences between the primary and secondary velocities in each group. These were statistically significant only in the observations by SR03. Relative weights for each data set were determined by iterations from the rms residual of the fit, separately for the primary and secondary velocities. The resulting orbital period is $P = 1.139791423 \pm 0.000000080$ days, and the time of maximum primary velocity nearest to the average date of the CfA observations is $T = 2{,}450{,}127.61845 \pm 0.00020$ (HJD). We adopt this ephemeris for the remainder of the paper.

[7] Available at http://cfaku5.cfa.harvard.edu

[8] SR03 have reported a metallicity for σ^2 CrB of [Fe/H] = −0.37 with an uncertainty no smaller than 0.1 dex, and Nordström et al. (2004) reported the value [Fe/H] = −0.24 based on Strömgren photometry. Metallicity determinations for double-lined spectroscopic binaries are particularly difficult, and both of these estimates are likely to be affected at some level by the double-lined nature of the system. However, the visual companion (σ^1 CrB) is apparently a single star, and has an accurate spectroscopic abundance determination by Valenti & Fischer (2005) giving [Fe/H] = -0.06 ± 0.03, and another by Fuhrmann (2004) giving [Fe/H] = -0.064 ± 0.068. The near-solar metallicity from these determinations is considered here to be more reliable.

Table 1
Radial Velocities of σ^2 CrB

HJD (2,400,000+)	RV_p (km s^{-1})	RV_s (km s^{-1})	σ_{RV_p} (km s^{-1})	σ_{RV_s} (km s^{-1})	$(O-C)_p$ (km s^{-1})	$(O-C)_s$ (km s^{-1})	Orbital Phase
48764.6474	6.88	−36.45	2.68	2.84	−1.72	−0.87	0.193
48781.6495	35.46	−64.08	2.99	3.16	1.15	−1.68	0.109
48810.6618	−69.00	46.22	1.16	1.23	0.47	0.37	0.564
48813.6236	18.25	−46.52	1.19	1.26	−0.89	0.06	0.162
48820.6185	−31.35	5.07	1.61	1.71	0.24	−1.27	0.299
48822.6494	41.46	−69.41	1.32	1.40	0.97	−0.55	0.081
48826.5581	−74.53	52.87	1.19	1.26	−0.38	2.13	0.510
48828.6849	−56.96	31.25	1.37	1.45	−0.33	−1.21	0.376
48838.5942	43.01	−71.62	1.15	1.22	0.62	−0.79	0.070
50258.6759	48.63	−75.42	1.43	1.51	0.73	1.17	0.984
50260.6371	−31.00	4.33	0.85	0.90	−0.66	−0.71	0.704
50263.6316	−42.68	17.76	0.83	0.88	0.40	−0.56	0.332
50266.6225	46.61	−73.03	0.99	1.04	0.74	1.43	0.956
50269.7633	−27.25	2.84	0.99	1.05	0.53	0.47	0.711
50271.6269	−46.41	23.01	0.95	1.01	1.46	−0.31	0.346
50275.6464	29.47	−57.26	0.97	1.03	−0.22	0.33	0.873
50285.6440	−49.95	26.91	0.90	0.95	0.84	0.54	0.644
50287.6352	−60.98	37.03	0.89	0.94	−0.45	0.51	0.391
50292.5697	−23.39	−1.49	1.02	1.08	0.90	−0.22	0.721
50295.6335	−65.17	39.49	0.79	0.83	−0.72	−1.13	0.409
50298.5502	46.99	−75.36	0.71	0.75	0.03	0.24	0.968
50300.5553	−22.15	−4.43	0.80	0.85	−0.21	−0.70	0.727
50302.6499	−69.55	44.72	0.84	0.89	−0.23	−0.98	0.565
50346.5051	46.86	−76.63	0.92	0.97	0.65	−1.81	0.041
50348.5107	4.35	−29.89	0.99	1.04	−1.77	3.10	0.801
50350.5649	−63.76	38.37	0.81	0.86	−1.83	0.39	0.603
50352.4779	−24.23	−1.41	0.79	0.84	0.74	−0.84	0.281
50356.4742	−0.04	−26.85	0.79	0.84	−1.27	1.05	0.787
50358.4740	−72.84	50.15	0.77	0.81	−0.68	1.49	0.542
50361.4826	13.31	−40.12	0.80	0.85	0.79	−0.45	0.182
50364.4624	1.84	−29.15	0.86	0.91	−2.54	2.04	0.796
50374.4574	−70.50	44.94	0.85	0.90	−1.26	−0.67	0.565
50379.4665	45.29	−73.75	0.82	0.87	−0.99	1.14	0.960
50383.4500	−70.47	48.43	0.84	0.89	1.34	0.13	0.455
50385.4760	−6.74	−19.80	0.81	0.86	−0.54	0.35	0.232
50388.4407	15.96	−44.52	0.92	0.97	−1.63	0.45	0.833
50391.4280	−71.44	49.52	0.81	0.86	0.32	1.28	0.454
50590.7488	−41.53	17.65	0.98	1.04	0.68	0.24	0.329
50619.6791	−26.78	3.14	1.05	1.11	1.06	0.72	0.711
50846.9255	39.45	−68.48	0.90	0.95	0.06	−0.78	0.087
51216.9001	−35.81	12.55	1.98	2.09	1.52	0.23	0.685
51246.7808	36.69	−66.52	2.01	2.13	−0.06	−1.57	0.901
51279.6859	−5.90	−19.52	2.51	2.65	−0.71	1.68	0.770
51341.7199	6.97	−33.48	1.77	1.87	−0.33	0.75	0.196
51374.6086	44.93	−73.34	2.01	2.12	−0.16	0.31	0.051
51374.6112	45.14	−74.26	3.08	3.26	0.34	−0.91	0.054

3. INTERFEROMETRIC MEASUREMENTS

Interferometric visibilities for σ^2 CrB were measured during 2007 May–July at the CHARA Array's six-element long-baseline interferometer located in Mount Wilson, CA (ten Brummelaar et al. 2005). The Array uses the visible wavelengths 480–800 nm for tracking and tip/tilt corrections, and the near-infrared K' (2.13 μm) and H (1.67 μm) bands for fringe detection. The 26 visibility measurements used in the final orbit determination, listed in Table 2, were obtained in the K' band on the S1–E1 and S1–E2 two-telescope baselines spanning projected baselines of 268–331 m. The interference fringes were obtained using the pupil-plane "CHARA Classic" beam combiner. While some of the data were obtained via on-site observing at Mount Wilson, the bulk of the data were gathered at the Arrington Remote Operations Center (AROC; Fallon et al. 2003) located on the Georgia State University campus in Atlanta, GA. Following the standard practice of time-bracketed observations, we interleaved each target visibility measurement with those of a calibrator star (HD 152598) in order to remove instrumental and atmospheric effects. For further details on the observing practice and the data reduction process, refer to McAlister et al. (2005).

We selected HR 6279 (HD 152598), an F0V star offset from σ^2 CrB by 8.°3, as the calibrator based on its small estimated angular diameter and its apparent lack of any close companions. We obtained photometric measurements for this star in the Johnson UBV bands from Grenier et al. (1985) and Perryman & ESA (1997), and JHK_S bands from the Two Micron All Sky Survey[9] (2MASS) and transformed them to calibrated

[9] http://www.ipac.caltech.edu/2mass

Table 2
Interferometric Visibilities for σ^2 CrB

HJD (2,400,000+)	Measured V	σ_V	Model V	$(O-C)_V$	u (m)	v (m)	Hour Angle (h)
54237.763	0.864	0.086	0.783	0.081	202.4	250.7	−2.24
54237.774	0.909	0.107	0.775	0.134	196.7	258.2	−1.99
54237.784	0.736	0.062	0.759	−0.022	190.3	265.2	−1.74
54237.796	0.702	0.063	0.729	−0.027	182.4	272.6	−1.46
54237.806	0.585	0.058	0.688	−0.103	174.6	278.9	−1.22
54237.816	0.652	0.076	0.625	0.027	165.6	285.3	−0.97
54237.833	0.468	0.053	0.474	−0.006	149.7	294.7	−0.56
54237.932	0.833	0.049	0.833	0.001	30.4	326.9	1.82
54237.942	0.775	0.059	0.791	−0.017	17.1	327.7	2.05
54237.954	0.672	0.038	0.672	0.001	0.5	328.1	2.34
54237.980	0.244	0.015	0.247	−0.004	−35.3	326.5	2.98
54247.701	0.858	0.113	0.887	−0.029	159.9	214.9	−3.08
54247.716	0.888	0.080	0.863	0.025	154.1	223.0	−2.73
54247.729	0.824	0.083	0.785	0.040	147.5	230.2	−2.40
54247.744	0.669	0.093	0.644	0.025	139.1	237.6	−2.05
54247.761	0.435	0.058	0.430	0.005	128.1	245.6	−1.64
54249.714	0.589	0.053	0.621	−0.032	152.1	225.3	−2.63
54249.726	0.570	0.054	0.609	−0.039	146.6	231.1	−2.36
54249.739	0.575	0.064	0.573	0.002	138.6	238.1	−2.03
54249.751	0.594	0.063	0.524	0.070	131.3	243.5	−1.75
54249.772	0.391	0.059	0.376	0.015	115.7	252.8	−1.24
54310.716	0.616	0.062	0.526	0.090	48.7	325.0	1.49
54310.726	0.405	0.050	0.410	−0.005	35.8	326.4	1.72
54310.776	0.477	0.050	0.454	0.023	−31.5	326.8	2.91
54310.786	0.558	0.054	0.619	−0.061	−45.5	325.4	3.16
54310.797	0.870	0.100	0.745	0.125	−59.5	323.5	3.42

flux measurements using the methods described in Colina et al. (1996) and Cohen et al. (2003). We then fitted these fluxes to spectral energy distribution models,[10] yielding an angular diameter of 0.467 ± 0.013 mas for HD 152598, corresponding to $T_{\rm eff} = 7150$ K and $\log g = 4.3$. This diameter estimate results in a predicted calibrator visibility of $V_{\rm cal} = 0.858 \pm 0.008$ at our longest baseline of 330 m, contributing roughly 1% error to the calibrated visibilities. This error is included in our roughly 10% total visibility errors listed in Table 2, along with the epoch of observation (at mid-exposure), the target star's calibrated visibility, the predicted visibility for the best-fit orbit, the $O-C$ visibility residual, the baseline projections along the east–west (u) and north–south (v) directions, and the hour angle of the target.

4. DETERMINATION OF THE ORBIT

Consistent with prior evidence of a synchronized orbit (SR03), we adopt a circular orbit ($e \equiv 0$, $\omega \equiv 0$) with the orbital period (P) and epoch of nodal passage (T) from Section 2.1 for the spectroscopic and visual orbit solutions presented below.

4.1. Spectroscopic Orbital Solutions

Our measured radial velocities enable us to derive the three remaining spectroscopic orbital elements, namely, the center-of-mass velocity (γ) and the radial velocity semi-amplitudes of the primary and secondary ($K_{\rm p}$ and $K_{\rm s}$, respectively). To check for consistency with prior efforts, we used the velocities published in SR03 to derive a second orbital solution. The calculated radial velocities for the derived orbits are shown in Figures 1 and 2 (the solid and dashed curves for the primary and secondary, respectively) along with the measured radial velocities and residuals for the primary (filled circles) and secondary (open circles). The corresponding orbital solutions are presented in Table 3 along with the related derived quantities. For comparison purposes, we have also included the values presented in SR03, which are consistent with our orbit generated using their velocities. However, the orbit obtained using our velocities is statistically different from that obtained using SR03 velocities. While the primary's velocity semi-amplitude matches within the errors between these two solutions, the secondary's differs by over 5σ, resulting in a 4σ difference in the mass ratios.

One possible explanation of the difference in the orbital solutions could be the velocity residuals for the orbit using SR03 data (Figure 2), which show an obvious pattern for both components. Those observations were obtained on four nights over a five-day period. To further examine these patterns, we display the residuals for each of the four nights in Figure 3, as a function of time. Clear trends are seen on each night, which are different for the primary and secondary components and have peak-to-peak excursions reaching 4 km s^{-1} in some cases, significantly larger than the velocity errors of 0.1–1.2 km s^{-1} (SR03). On some, but not all, nights there appears to be a periodicity of roughly 0.20–0.25 days. The nature of these trends is unclear, particularly because this periodicity is much shorter than either the orbital or the rotational periods. Instrumental effects seem unlikely, but an explanation in terms of the considerable spottedness of both stars is certainly a distinct possibility. The Doppler imaging maps produced by SR03 show that both components display a very patchy distribution of surface features covering the polar regions. Individual features coming in and out of view as the stars rotate could easily be the cause of the systematic effects observed in the radial velocities, and the effects would not necessarily have to be the same on both stars, just as observed. Slight changes in the spots from one night to the next could account for the different patterns

[10] The model fluxes were interpolated from the grid of models from R. L. Kurucz, available at http://cfaku5.cfa.harvard.edu

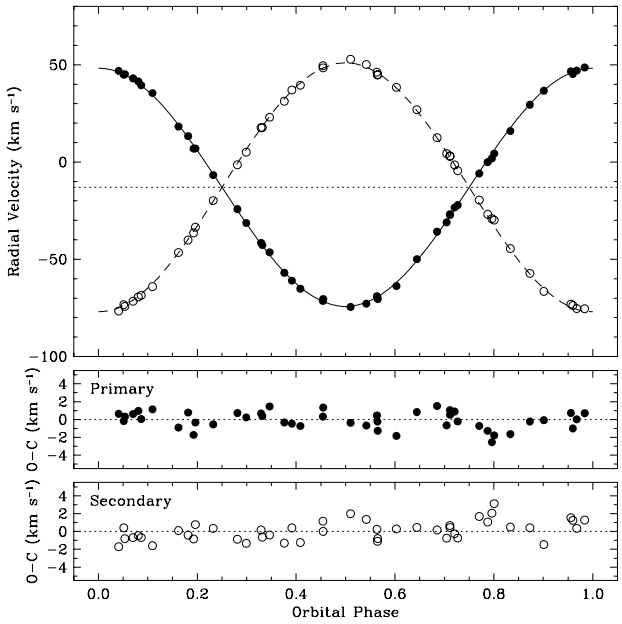

Figure 1. Our radial velocities and the orbital fit for σ^2 CrB (top panel) and the primary and secondary residuals (bottom panels). The filled circles represent the primary and the open circles represent the secondary component. The corresponding orbital elements are listed in Table 3.

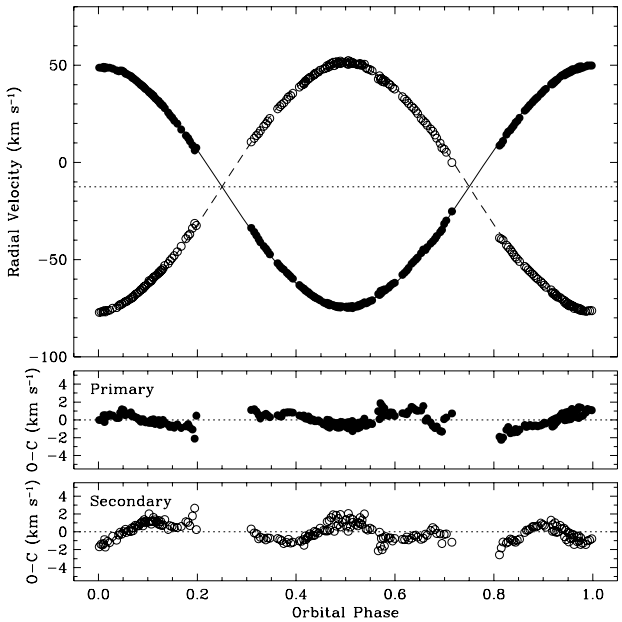

Figure 2. Same as Figure 1, but based on SR03 radial velocities.

Table 3
Spectroscopic Orbital Solutions for σ^2 CrB

Element	This Work	SR03 Velocities[a]	SR03 Results
Orbital elements			
P (days)	1.139791423 ± 0.000000080[b]	1.139791423 ± 0.000000080[b]	1.1397912 (adopted)
T (HJD-2,400,000)[c]	50, 127.61845 ± 0.00020[b]	50, 127.61845 ± 0.00020[b]	50,127.6248[d]
e	0.0[e]	0.0[e]	0.0[e]
ω (deg)	0.0[e]	0.0[e]	0.0[e]
γ (km s^{-1})	−13.03 ± 0.11	−12.58 ± 0.05	−12.3 ± 0.06
K_p (km s^{-1})	61.25 ± 0.21	61.31 ± 0.06	61.34 ± 0.06
K_s (km s^{-1})	63.89 ± 0.22	62.90 ± 0.08	62.91 ± 0.08
Derived quantities			
$M_p \sin^3 i$ ($M_\odot$)	0.11818 ± 0.00092	0.11461 ± 0.00032	0.1147
$M_s \sin^3 i$ ($M_\odot$)	0.11329 ± 0.00086	0.11170 ± 0.00027	0.1118
$q \equiv M_s/M_p$	0.9586 ± 0.0047	0.9746 ± 0.0016	0.975 ± 0.002
$a_p \sin i$ (10^6 km)	0.9600 ± 0.0033	0.96085 ± 0.00097	0.96138 ± 0.00093
$a_s \sin i$ (10^6 km)	1.0014 ± 0.0035	0.98592 ± 0.00126	0.9861 ± 0.0012
$a \sin i$ ($R_\odot$)	2.8181 ± 0.0068	2.7971 ± 0.0023	2.798 ± 0.002
Other quantities pertaining to the fit			
N_{obs}	46	217	217
Time span (days)	2610	5.4	5.4
σ_p (km s^{-1})[f]	1.04	0.74	0.71
σ_s (km s^{-1})[f]	1.10	0.97	...

Notes.
[a] Our orbital solution using SR03 velocities.
[b] Determined using all published velocities (see Section 2.1).
[c] T is the epoch of maximum primary velocity.
[d] The value from SR03 has been shifted by an integer number of cycles to the epoch derived in this work, for comparison purposes.
[e] Circular orbit adopted.
[f] RMS residual from the fit.

seen in Figure 3. The relatively large amplitude of the residual variations raises the concern that they may be affecting the velocity semi-amplitudes of the orbit, depending on the phase at which they occur. We do not see such trends in the CfA data, perhaps because our observations span a much longer time (more than 7 years, and ∼2200 rotational cycles), allowing for spots to change and average out these effects. We therefore proceed on the assumption that possible systematic effects of this nature on K_p and K_s are lessened in the CfA data.

4.2 The Visual Orbit Solution

The basic measured quantity from an interferometric observation is *visibility*, which evaluates the contrast in the fringe pattern obtained by combining starlight wave fronts from multiple apertures, filtered through a finite bandwidth. For a single star of angular diameter θ, the interferometric visibility V for a uniform disk model is given by

$$V = \frac{2J_1(\pi B\theta/\lambda)}{\pi B\theta/\lambda}, \quad (1)$$

where J_1 is the first-order Bessel function, B is the projected baseline length as seen by the star, and λ is the observed bandpass central wavelength. The interferometric visibility for a binary, where the individual stars have visibilities V_p (primary) and V_s (secondary) per Equation (1), is given by

$$V = \frac{\sqrt{\left(\beta^2 V_p^2 + V_s^2 + 2\beta V_p V_s \cos((2\pi/\lambda)\mathbf{B}\cdot\mathbf{s})\right)}}{1+\beta}, \quad (2)$$

where β is the primary to secondary flux ratio, $\mathbf{B}$ is the projected baseline vector as seen by the binary, and $\mathbf{s}$ is the binary's angular-separation vector in the plane of the sky.

Using our measured interferometric visibilities and the above equations, we are able to augment the spectroscopic orbital solutions to derive a visual orbit for σ^2 CrB. Adopting the period and epoch of nodal passage from Section 2.1, we now derive the parameters that can only be determined astrometrically: angular semimajor axis (α), inclination (i), and longitude of the ascending node (Ω). We also treat the K'-band magnitude difference as a free parameter in order to test evolutionary models.

For a circular orbit, the epoch of periastron passage (T_0) is replaced by the epoch of ascending nodal passage (T_{node}), defined as the epoch of fastest secondary recession, in the visual orbit equations (Heintz 1978). Accordingly, we translate the T value listed in Section 2.1 by one-half of the orbital period to determine the epoch of the ascending nodal passage as T_{node} = 2,450,127.04855 ± 0.00020 (HJD) for use in our visual orbit solution. The 1σ errors of this and other adopted parameters listed in Table 4 have been propagated to our error estimates for the derived parameters.

The angular diameters of the components are too small to be resolved by our K'-band observations. We therefore estimate these based on the components' absolute magnitudes and temperatures as described below. We first estimate the Johnson V-band magnitude of σ^2 CrB using its *Tycho*-2 magnitudes of B_T = 6.262 ± 0.014 and V_T = 5.620 ± 0.009 and the relation $V_J = V_T - 0.090(B_T - V_T)$ from the Guide to the *Tycho*-2 Catalog. Then, using the V-band flux ratio from Section 2 and the Lestrade et al. (1999) parallax, we obtain absolute magnitudes of M_V = 4.35 ± 0.02 for the primary and M_V = 4.74 ± 0.02 for the secondary. These magnitudes lead to linear radius estimates of 1.2 $R_\odot$ for the primary and 1.1 $R_\odot$ for the secondary using the tabulation of stellar physical parameters in Popper (1980) and

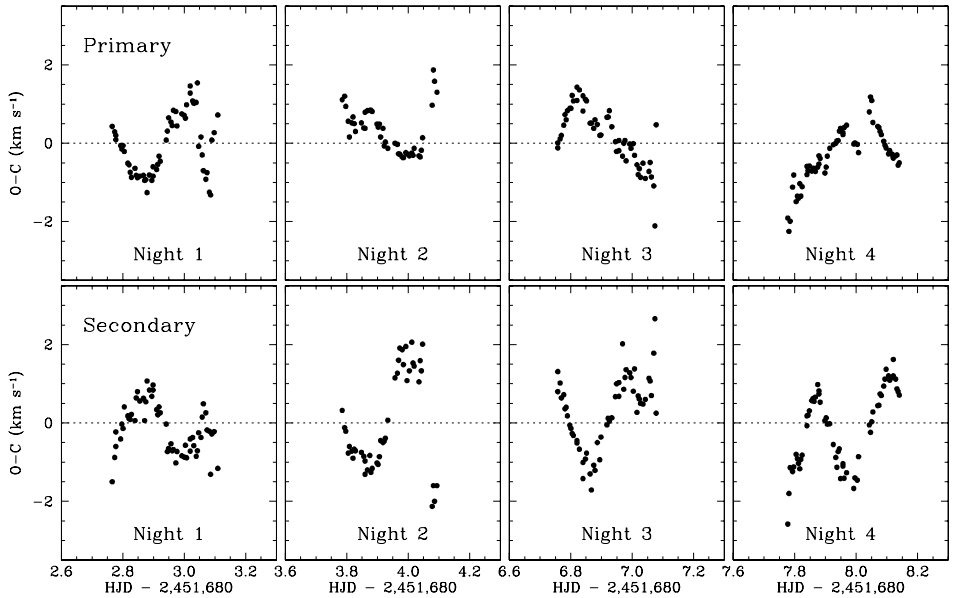

Figure 3. Residuals for the individual nights' velocities from SR03.

Andersen (1991). Finally, using the Lestrade et al. (1999) parallax, we adopt component angular diameters of $\theta_p = 0.50$ mas and $\theta_s = 0.45$ mas, propagating a 0.05 mas uncertainty in these values for deriving the uncertainty of our orbital elements. Diameter estimates using the temperatures of the components from Section 2 are consistent with these values.

We conduct an exhaustive search of the parameter space for the unknown parameters mentioned, namely, α, i, Ω, and $\Delta K'$. The orbital inclination is constrained by the $a \sin i$ from spectroscopy, the free-parameter α, and the Lestrade et al. (1999) parallax. We impose this constraint during our exploration of the parameter space along with its associated 1σ error. We explore the unknown parameters over many iterations, by randomly selecting them between broad limits and using Equation (2) to evaluate the predicted binary visibility for the baseline and binary positions at each observational epoch. The orbital solution presented here represents the parameter set with the minimum χ^2 value when comparing the predicted and measured visibilities.

Figure 4 shows the measured visibilities (plus signs) with vertical error bars for each of the 26 observations, along with the computed model visibilities (diamonds), and Table 2 lists the corresponding numerical values of the observed and model visibilities along with the residuals of the fit. Table 4 summarizes the visual orbit parameters for σ^2 CrB from our solution and Figure 5 plots the visual orbit in the plane of the sky. As seen in Figure 5, we have a reasonably good phase coverage from our observations.

As mentioned in Section 4.1, star spots can create systematic effects in the data obtained on this binary. These effects are especially significant for data obtained over a short time baseline, as seen for the SR03 spectroscopic solution. While our interferometric data span 73 days, allowing for some averaging of these effects, the bulk of the data used were obtained over 12 days, justifying an exploration of this effect. Specifically, the separation between the stars derived from our visibility data would represent the separation of the centers of light rather than that of mass. As discussed in Hummel et al. (1994), heavily spotted stars will incur a systematic shift in the center

Table 4
Visual Orbit Solution for σ^2 CrB

Orbital Parameter	Value
Adopted values	
Period (days)	1.139791423 ± 0.000000080[a]
T_{node} (HJD-2,400,000)[b]	50, 127.04855 ± 0.00020
e	0.0[c]
ω (deg)	0.0[c]
θ_p (mas)	0.50 ± 0.05[d]
θ_s (mas)	0.45 ± 0.05[d]
Visual orbit parameters	
α (mas)	1.225 ± 0.013
i (deg)	28.08 ± 0.34
Ω (deg)	207.93 ± 0.67[e]
$\Delta K'$	0.19 ± 0.19
Reduced χ^2	0.61[f]

Notes.
[a] See Section 2.1.
[b] This is the epoch of the ascending node, defined as the epoch of maximum secondary velocity, and accordingly is one-half period less than the value in Table 3 (see Section 4.2).
[c] Circular orbit adopted.
[d] See Section 4.2.
[e] This value suffers from a 180°ambiguity due to the cosine term in Equation (2).
[f] The low χ^2 indicates that our error estimates for visibility are conservative.

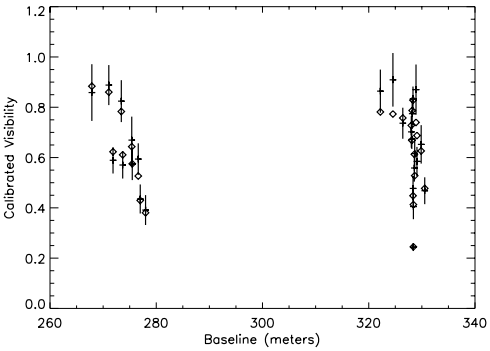

Figure 4. Calibrated visibility measurements for σ^2 CrB vs. the projected baseline. The plus signs are the calibrated visibilities with vertical error bars, and the diamonds are the calculated visibilities for the best-fit orbit. Table 2 lists the numeric values corresponding to this plot.

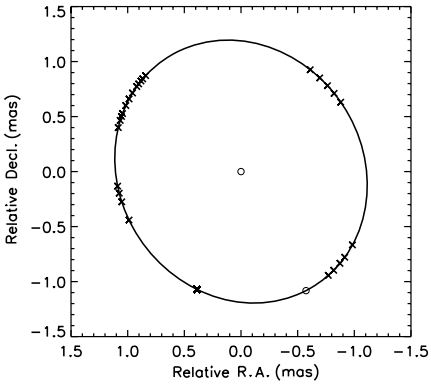

Figure 5. Visual orbit of σ^2 CrB. The open circles mark the positions of the two components at the epoch of ascending nodal passage, and the X marks identify the secondary's calculated positions at the epochs of visibility measurement.

of light from rotational and orbital motions, perhaps inducing an additional uncertainty in the orbital elements derived. We assume a spot-induced change in the angular semimajor axis of 2% of the primary's diameter, or 0.01 mas. This is less than the uncertainty of our derived semimajor axis, and at our baselines of 270–330 m translates to a 0.005–0.011 change in the visibility. While the uncertainties of our measured visibilities are an order of magnitude larger than this, we ran a test orbital fit by adding a 0.010 uncertainty to the visibility errors as a root-sum-squared. While, as expected, the χ^2 of the fit improved, the values and uncertainties of the derived parameters remained unchanged, leading us to conclude that this effect, while real, is too small to affect our results.

We determine the 1, 2, and 3σ uncertainties of each visual orbit parameter using a Monte Carlo simulation approach. We compute the orbital fit for 100,000 iterations, where for each iteration, we randomly select the adopted parameters within their respective 1σ intervals and the model parameters around their corresponding best-fit solution, generating a multi-dimensional χ^2 "surface." Then, we project this surface along

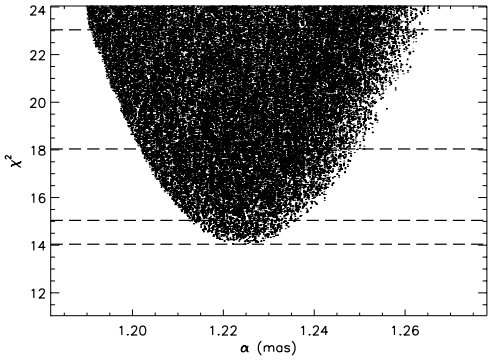

Figure 6. χ^2 distribution around the best-fit solution for the angular semimajor axis (α). The bottom dashed line corresponds to the minimum χ^2 value, and the others mark a deviation of 1, 4, and 9 units above the minimum, corresponding to 1, 2, and 3-σ errors.

each parameter axis, resulting in the plots shown in Figures 6–9. The figures show the χ^2 distribution around the best-fit orbit and enable estimation of 1, 2, and 3σ errors for each parameter based on a χ^2 deviation of 1, 4, and 9 units, respectively, from its minimum value. The horizontal dashed lines in the figures from bottom to top mark the minimum χ^2 value and those corresponding to 1, 2, and 3σ errors, and Table 4 lists the corresponding numerical 1σ errors of the model parameters.

5. PHYSICAL PARAMETERS

5.1. Component Mass Estimates

Our angular semimajor axis obtained from interferometry translates to 0.0279 ± 0.0003 AU or 5.99 ± 0.07 $R_\odot$ using the Lestrade et al. (1999) parallax. Newton's generalization of Kepler's third law then yields a mass sum of 2.227 ± 0.073 $M_\odot$ for the pair, and using the mass ratio from our spectroscopic solution of 0.9586 ± 0.0047, we get individual component masses of 1.137 ± 0.037 $M_\odot$ and 1.090 ± 0.036 $M_\odot$ for the primary and secondary, respectively. As noted in Section 4.1, the SR03 velocities yield a significantly different mass ratio of 0.9746 ± 0.0016, but this 4σ difference is not enough to influence the mass estimates significantly. The uncertainty in our masses is dominated by the cubed semimajor axis factor in estimating the mass sum, resulting in about a 3% uncertainty in mass sum corresponding to a 1% uncertainty in the semimajor axis. The high precision of the mass ratio from the spectroscopic solution results in final masses of 3% uncertainty as well. Component mass estimates using the SR03 velocities are 1.128 ± 0.037 and 1.099 ± 0.036, in excellent agreement with the masses using our velocities. These masses along with other physical parameters derived are listed in Table 5.

5.2. Radii of the Components

Assuming synchronous and co-aligned rotation of spherical components, reasonable given the short orbital period and evidence from SR03 of unevolved stars contained within their Roche limits, we can estimate the component radii from the measured spectroscopic $v \sin i$. As mentioned in Section 2, our spectra yield $v \sin i = 26 \pm 1$ km s^{-1} for both the primary and secondary. These values and uncertainties are identical to

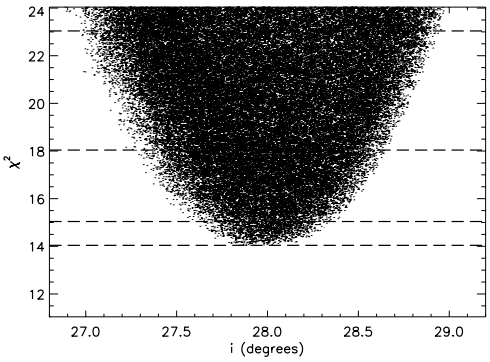

Figure 7. Same as Figure 6, but for the orbital inclination (i).

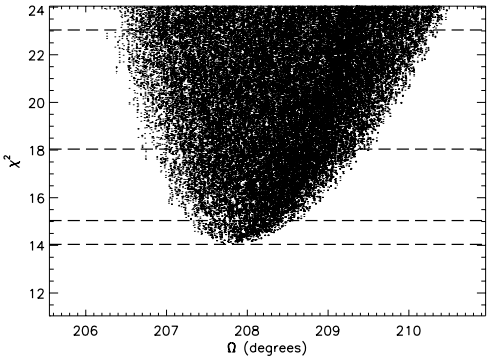

Figure 8. Same as Figure 6, but for the longitude of the ascending node (Ω).

those in SR03. Using the inclination from our visual orbit, and adopting the orbital period from spectroscopy as the rotational period, we get identical component radii of $1.244 \pm 0.050\ R_\odot$ for the primary and secondary. This translates to an angular diameter of 0.509 ± 0.020 mas for each component using the Lestrade et al. (1999) parallax, in excellent agreement with our adopted diameter for the primary and a 1σ variance for the secondary, given our associated 0.05 mas errors for these values. These radii estimates, along with the effective temperatures from Section 2

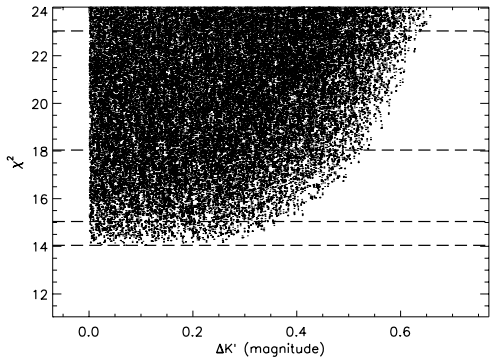

Figure 9. Same as Figure 6, but for the K'-band magnitude difference ($\Delta K'$).

and the relation $L \propto R^2\, T_{\rm eff}^4$, lead to a luminosity ratio of 0.89 ± 0.16. Alternatively, using bolometric corrections from Flower (1996) of $\mathrm{BC_p} = -0.038 \pm 0.017$ and $\mathrm{BC_s} = -0.064 \pm 0.020$ corresponding to the components' effective temperatures, the V-band flux ratio of 0.70 ± 0.02 from spectroscopy translates to a total luminosity ratio of 0.68 ± 0.20, a 1σ variance from the estimate above. Conversely, our estimates of effective temperature and luminosity ratio require a radius ratio of 0.88 ± 0.14, again at a 1σ variance from the 1.00 ± 0.06 estimate from the identical $v \sin i$ values of the components.

5.3. Absolute Magnitudes and Ages

We allowed the K'-band magnitude difference to be a free parameter for our visual orbit fit, obtaining $\Delta K' = 0.19 \pm 0.19$, consistent with the 0.18 estimate from the mass–luminosity relations of Henry & McCarthy (1993).[11] The uncertainty in $\Delta K'$ is large because visibility measurements of nearly equal mass, and hence nearly equal brightness, pairs are relatively insensitive to the magnitude difference of the components (Hummel et al. 1998; Boden et al. 1999). Using Equation (2), we have verified that a 10% change in $\Delta K'$ for σ^2 CrB results in only 0.1% change in visibility. This, along with the poor-quality K magnitude listed in 2MASS (for σ^2 CrB, $K = 4.052 \pm 0.036$, but flagged as a very poor fit), thwart any attempts to use these magnitudes for

[11] The relations from Henry & McCarthy are for $0.5\ M_\odot \leqslant$ Mass $\leqslant 1.0\ M_\odot$. We consider it safe to extrapolate out to our estimated masses of slightly larger than $1.0\ M_\odot$.

Table 5
Physical Parameters for σ^2 CrB

Physical Parameter	This Work		SR03 Spectroscopy[a]		SR03 Results	
	Primary	Secondary	Primary	Secondary	Primary	Secondary
$a\ (R_\odot)$	5.99 ± 0.07		5.99 ± 0.07		...	
Mass ($M_\odot$)	1.137 ± 0.037	1.090 ± 0.036	1.128 ± 0.037	1.099 ± 0.036	1.108 ± 0.004[b]	1.080 ± 0.004[b]
Radius ($R_\odot$)	1.244 ± 0.050	1.244 ± 0.050	1.244 ± 0.050	1.244 ± 0.050	1.14 ± 0.04	1.14 ± 0.04
$T_{\rm eff}$ (K)	6050 ± 150	5870 ± 150	6000 ± 50	5900 ± 50	6000 ± 50	5900 ± 50
$M_{\rm V}$ (mag)	4.35 ± 0.02	4.74 ± 0.02	4.45 ± 0.02	4.61 ± 0.02	4.61 ± 0.07	4.76 ± 0.07
$M_{\rm K}$ (mag)	2.93 ± 0.09	3.12 ± 0.11	...	...	...	...

Notes.
[a] These parameters use the SR03 spectroscopic results such as flux ratio, rotational velocities, and radial velocities, but use the Lestrade et al. (1999) parallax, *Tycho*-2 magnitudes, and our visual orbit.
[b] As noted in Section 1, these uncertainties are unrealistically small.

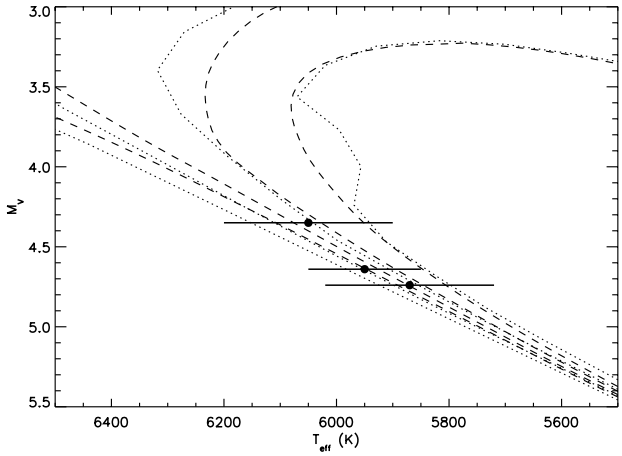

Figure 10. Position of the Sun-like components of σ CrB on the H–R diagram. The points from top to bottom are σ^2 CrB primary, σ^1 CrB, and σ^2 CrB secondary. The isochrones are from the Yonsei–Yale (dotted) and Victoria–Regina (dashed models) for 0.5, 1.5, 3.0, and 5.0 Gyr ages (left to right) for solar metallicity stars.

checking stellar evolution models. However, we can revert to *V*-band photometry to explore this topic.

In Section 4.2, we derived the absolute *V*-band magnitudes of the components of σ^2 CrB as $M_V = 4.35 \pm 0.02$ for the primary and $M_V = 4.74 \pm 0.02$ for the secondary. For σ^1 CrB, we similarly use the *Tycho*-2 magnitudes and the Lestrade et al. (1999) parallax to obtain $M_V = 4.64 \pm 0.01$. SR03 had a smaller magnitude difference for the components of σ^2 CrB, and the corresponding results using their spectroscopy are also included in Table 5 along with the values from their paper. Figure 10 plots these three stars on a Hertzsprung–Russell (H–R) diagram using our magnitude and temperature estimates, along with isochrones for 0.5, 1.5, 3.0, and 5.0 Gyr ages (left to right) from the Yonsei–Yale isochrones (dotted, Yi et al. 2001) and the Victoria–Regina stellar evolution models (dashed, VandenBerg et al. 2006) for solar metallicity (see Footnote 8).

Wright et al. (2004) estimate an age of 1.8 Gyr for σ^1 CrB based on chromospheric activity, and Valenti & Fischer (2005) estimate an age of 5.0 Gyr from spectroscopy with limits of 2.9–7.8 Gyr based on 1σ changes to $\log L$. SR03 identify a much lower age, of a few times 10^7 years, by matching pre-main-sequence evolutionary tracks and point to their higher Li abundance as supporting evidence. While abundance determinations in double-lined spectroscopic binaries are particularly difficult and more prone to errors, the high-Li abundance of 2.60 ± 0.03 (SR03) for the slow-rotating single-lined companion σ^1 CrB does argue for a young system. Each point along the isochrones plotted in Figure 10 corresponds to a particular mass, allowing us to use our mass estimates for the components of σ^2 CrB to further constrain the system's age. Our mass, luminosity, and temperature estimates indicate an age for this system of 0.5–1.5 Gyr, with a range of 0.1–3 Gyr permissible within 1σ errors.

5.4. Mass Estimate of σ^1 CrB

Our mass estimates for the components of σ^2 CrB allow us to constrain the mass of the wider visual companion σ^1 CrB as well. Scardia (1979) presented an improved visual orbit for the AB pair based on 886 observations spanning almost 200 years of observation, yielding $P = 889$ years, $a = 5''.9$, $i = 31°.8$, $e = 0.76$, and $\Omega = 16°.9$. However, he did not publish uncertainties for these parameters, and given the long period, his less than one-third phase coverage leads to only a preliminary orbital solution, albeit one that convincingly shows orbital motion of the pair. He further uses parallaxes available to him to derive a mass sum for the AB system of 3.2 $M_\odot$. We used all current WDS observations, adding almost 200 observations since Scardia (1979), to update this orbit and obtain uncertainties for the parameters. Our visual orbit is presented in Figure 11, along with the Scardia orbit for comparison, and Table 6 lists the derived orbital elements. Adopting the Lestrade et al. (1999) parallax of the A component, we estimate a mass sum of 3.2 ± 0.9 $M_\odot$, resulting in a B-component mass estimate of 1.0 $M_\odot$, consistent with its spectral type of G1 V (Gray et al. 2003). Valenti & Fischer (2005) estimate a mass of 0.77 ± 0.21 $M_\odot$ based on high-resolution spectroscopy, but we believe that they systematically underestimate their uncertainty by overlooking the $\log e$ factor in converting from uncertainty in $\log L$ to uncertainty in *L*. Using the $\log e$ factor, we followed their methods for obtaining a mass estimate of 0.77 ± 0.44 $M_\odot$. The mass error is dominated by the uncertainty of the Gliese & Jahreiß (1991) parallax used by Valenti & Fischer (2005). Adopting the higher precision Lestrade et al. (1999) parallax of the primary, we follow their method, and using the $\log e$ factor, get a mass estimate of 0.78 ± 0.11 $M_\odot$. This mass is too low for the spectral type (as well as our own estimate of the effective temperature; see Section 2) and the expectation from the visual orbit.

Table 6
Visual Orbit Solution for $\sigma^1 - \sigma^2$ CrB

Orbital Parameter	Value
P (years)	726 ± 62
T_0 (BY)	1825.2 ± 1.5
e	0.72 ± 0.01
ω (deg)	237.3 ± 6.8
α (arcsec)	5.26 ± 0.35
i (deg)	32.3 ± 4.1
Ω (deg)	28.0 ± 0.5

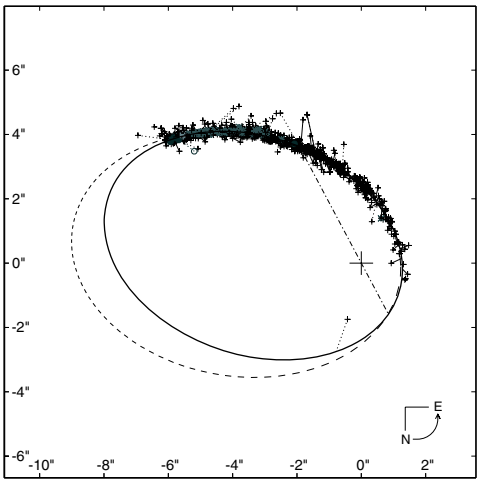

Figure 11. Visual orbit of the wider $\sigma^1 - \sigma^2$ CrB (AB) system based on all measures in the WDS. The plus signs indicate micrometric observations, the asterisks indicate photographic measures, open circles indicate eyepiece interferometry, and the filled circles represent speckle interferometry. The solid curve is our orbit fit and the dashed curve is the Scardia (1979) orbit. $O - C$ lines connect each measure to its predicted position along the orbit. The big plus at the origin indicates the position of the primary and the dot-dashed line through it is the line of nodes. Scales are in arcseconds, and the curved arrow at the lower right corner by the north and east direction indicators shows the direction of orbital motion.

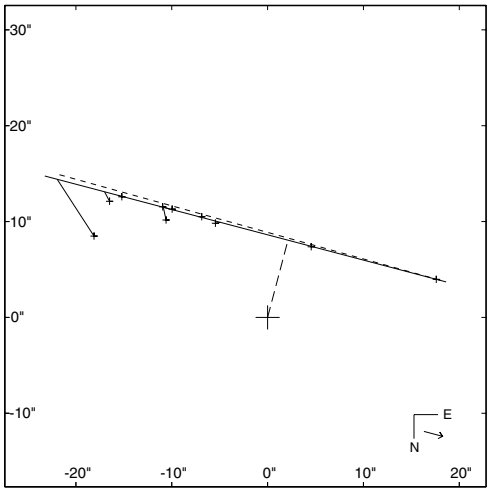

Figure 12. Relative separation between σ^2 CrB and ADS 9979C based on 10 resolutions of the pair from 1832 to 1984. The plus signs indicate micrometric observations. The $O - C$ lines connect each measure to its predicted position along the linear fit (thick solid line). The thick dashed line is the predicted movement based on the differential proper motions. The long dashed line connected to the origin indicates the predicted closest apparent position. The scale is in seconds of arc. An arrow in the lower right corner by the north and east direction indicators shows the direction of motion of the star.

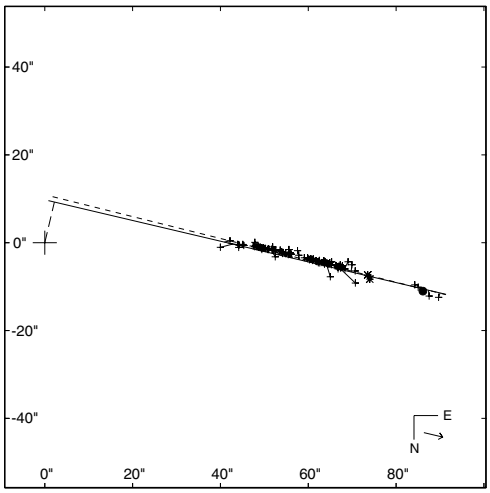

Figure 13. Same as Figure 12, but for ADS 9979D based on 106 resolutions of the pair from 1825 to 1996. The asterisks indicate photographic measures and the filled circles represent *Tycho* measures.

A possible contamination of the secondary's spectral type from the 7″ distant primary is unlikely, as determined by Richard Gray at our request from new spectroscopic observations (R. Gray 2008, private communication).

The inclination and longitude of the ascending node for this visual orbit are similar to those of the inner (σ^2 CrB) orbit, suggesting coplanarity. For the outer visual orbit, we can use our radial velocity estimate for σ^1 CrB, our derived systemic velocity for σ^2 CrB, and the speckle observations to unambiguously determine the longitude of the ascending node as $\Omega = 28\overset{\circ}{.}0 \pm 0\overset{\circ}{.}5$. Using the equation for the relative inclination of the two orbits (ϕ) from Fekel (1981), we get $\phi = 4\overset{\circ}{.}7$ or $60\overset{\circ}{.}3$, given the 180° ambiguity in Ω for the inner orbit, confirming coplanarity as a possibility.

6. THE WIDE COMPONENTS: OPTICAL OR PHYSICAL?

In addition to the three solar-type stars, the WDS lists three additional components for σ CrB. We present evidence to show that WDS components C and D are optical alignments, while component E, itself a binary, is a physical association. WDS component C (ADS 9979C), measured 18″ away at 103° in 1984 (Popović 1986), has a proper motion of $\mu_\alpha = -0\overset{''}{.}016$ yr^{-1} and $\mu_\delta = -0\overset{''}{.}015$ yr^{-1} (Jeffers et al. 1963), significantly different from that of σ^2 CrB of $\mu_\alpha = -0\overset{''}{.}26364 \pm 0\overset{''}{.}00091$ yr^{-1} and $\mu_\delta = -0\overset{''}{.}09259 \pm 0\overset{''}{.}00129$ yr^{-1} from van Leeuwen (2007). Similarly, component D, measured 88″ away at 82° in 1996 (Courtot 1996) and clearly seen by us as a field star by blinking the multi-epoch STScI Digitized Sky Survey[12] (DSS) images, has a proper motion of $\mu_\alpha = +0\overset{''}{.}004$ yr^{-1} and $\mu_\delta = -0\overset{''}{.}017$ yr^{-1} (Jeffers et al. 1963), again significantly different from that of σ^2 CrB. As a confirmation of the optical alignment, we compare in Figures 12 and 13 the observed separations of components C and D, respectively, from the primary with the corresponding expected values based

[12] http://stdatu.stsci.edu/cgi-bin/dss_form

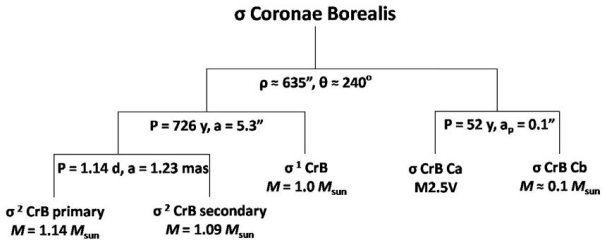

Figure 14. Mobile diagram of σ CrB and some of its properties. The Ca–Cb pair is WDS component E, while WDS components C & D are not gravitationally bound to the σ CrB system (see Figures 12 and 13, and the text in Section 6). a_p for the Ca–Cb pair is the photocentric semimajor axis.

on their proper motions. The solid line is a linear fit to the published measurements from the WDS and the dashed line is the expected separation based on differential proper motion. The excellent agreement between the two lines for both components confirms them as field stars.

WDS component E (σ CrB C, HIP 79551) is widely separated from the primary at 635″, translating to a minimum physical separation of over 14,000 AU using the Lestrade et al. (1999) parallax. Despite its wide separation, this component appears to be physically associated with σ CrB based on its matching parallax of $\pi = 45.40 \pm 3.71$ mas and proper motion of $\mu_\alpha = -0\farcs26592 \pm 0\farcs00299$ yr^{-1} and $\mu_\delta = -0\farcs08363 \pm 0\farcs00368$ yr^{-1} (van Leeuwen 2007). While seemingly extreme for gravitationally bound systems, physical association has been demonstrated for pairs with separations out to 20,000 AU (e.g., Latham et al. 1991; Poveda et al. 1994). σ CrB C has a spectral classification of M2.5V (Reid et al. 1995), apparent magnitude of $V = 12.24$ (Bidelman 1985), and has itself been identified as a photocentric motion binary with an unseen companion of 0.1 $M_\odot$ in a 52 year orbit (Heintz 1990). Perryman & ESA (1997) also identify this star as a binary of type "X" or stochastic solution, implying a photocenter wobble for an unresolved star, but for which the *Hipparcos* data are not sufficient to derive an orbit.

7. CONCLUSION

Augmenting our radial velocity measurements with published values, we obtain a coverage of nearly 86 years or 27,500 orbital cycles, resulting in a very precise ephemeris of $P = 1.139791423 \pm 0.000000080$ days and $T = 2{,}450{,}127.61845 \pm 0.00020$ (HJD) and a robust spectroscopic orbit for σ^2 CrB. Using the CHARA Array, we have resolved this 1.14 day spectroscopic binary, the shortest-period system yet resolved, and derived its visual orbit. The resulting component masses are 1.137 ± 0.037 $M_\odot$ and 1.090 ± 0.036 $M_\odot$ for the primary and secondary, respectively. Our spectroscopy supports prior efforts in estimating the same $v \sin i$ values for both components, which assuming a synchronized, co-aligned rotation results in equal radii of 1.244 ± 0.050 $R_\odot$ for both components. The corresponding radius ratio is consistent within 1σ with its estimate using the components' temperatures and flux ratio from spectroscopy. We have also shown that this binary resides in a hierarchical quintuple system, composed of three close Sun-like stars and a wide M-dwarf binary. The wider visual orbit companion, σ^1 CrB, is about 7″ away in a 726-year visual orbit with $i = 32\fdg3$, which appears to be coplanar with the inner orbit. A comparison of the mass and absolute magnitude estimates of σ^1 CrB and σ^2 CrB with current stellar evolution models indicates a young age for the system of 0.1–3 Gyr, consistent with the relatively high Li abundance previously measured. Finally, the widest member of this system is an M-dwarf binary, σ CrB C, at a minimum separation of 14,000 AU. Figure 14 depicts the system's hierarchy in a pictorial form.

We thank Andy Boden and Doug Gies for their many useful suggestions that improved the quality of this work, and Richard Gray for making new observations at our request to confirm the spectral typing of the components. The CfA spectroscopic observations of σ^1 CrB and σ^2 CrB used in this paper were obtained with the help of J. Caruso, R. P. Stefanik, and J. Zajac. We also thank the CHARA Array operator P. J. Goldfinger for obtaining some of the data used here and for her able assistance of remote operations of the Array from AROC. Research at the CHARA Array is supported by the College of Arts and Sciences at Georgia State University and by the National Science Foundation (NSF) through NSF grant AST-0606958. G.T. acknowledges partial support for this work from NSF grant AST-0708229 and NASA's MASSIF SIM Key Project (BLF57-04). This research has made use of the SIMBAD literature database, operated at Centre de Données Astronomiques de Strasbourg, France, and of NASA's Astrophysics Data System. This effort used multi-epoch images from the Digitized Sky Survey, which was produced at the Space Telescope Science Institute under U.S. Government grant NAG W-2166. This publication also made use of data products from the 2MASS, which is a joint project of the University of Massachusetts and the Infrared Processing and Analysis Center/California Institute of Technology, funded by NASA and the NSF.

REFERENCES

Andersen, J. 1991, A&A Rev., 3, 91
Baines, E. K., van Belle, G. T., ten Brummelaar, T. A., McAlister, H. A., Swain, M., Turner, N. H., Sturmann, L., & Sturmann, J. 2007, ApJ, 661, L195
Bakos, G. A. 1984, AJ, 89, 1740
Bidelman, W. P. 1985, ApJS, 59, 197
Boden, A. F., et al. 1999, ApJ, 527, 360
Cohen, M., Wheaton, W. A., & Megeath, S. T. 2003, AJ, 126, 1090
Colina, L., Bohlin, R. C., & Castelli, F. 1996, AJ, 112, 307
Courtot, J.-F. 1996, Obs. et Travaux, 47, 47
Duquennoy, A., & Mayor, M. 1991, A&A, 248, 485
Fallon, T., McAlister, H. A., & ten Brummelaar, T. A. 2003, in Proc. SPIE 4838, Interferometry for Optical Astronomy II, ed. W. A. Traub (Bellingham, WA: SPIE), 1193
Fekel, F. C., Jr. 1981, ApJ, 246, 879
Flower, P. J. 1996, ApJ, 469, 355

Fuhrmann, K. 2004, AN, 325, 3
Gliese, W., & Jahreiß, H. 1991, in The Astronomical Data Center CD-ROM: Selected Astronomical Catalogs, Vol. I, ed. L. E. Brotzmann & S. E. Gesser (Greenbelt, MD: NASA/Astronomical Data Center, Goddard Space Flight Center)
Gray, R. O., Corbally, C. J., Garrison, R. F., McFadden, M. T., & Robinson, P. E. 2003, AJ, 126, 2048
Grenier, S., Gomez, A. E., Jaschek, C., Jaschek, M., & Heck, A. 1985, A&A, 145, 331
Harper, W. E. 1925, Publications of the Dominion Astrophysical Observatory Victoria, 3, 225
Heintz, W. D. 1978, Double Stars (Dordrecht: Reidel),, 32
Heintz, W. D. 1990, AJ, 99, 420
Henry, T. J., & McCarthy, D. W. 1993, AJ, 106, 773
Hummel, C. A., Armstrong, J. T., Quirrenbach, A., Buscher, D. F., Mozurkewich, D., Elias, N. M., & Wilson, R. E. 1994, AJ, 107, 1859
Hummel, C. A., Armstrong, J. T., Quirrenbach, A., Buscher, D. F., Mozurkewich, D., Simon, R. S., & Johnston, K. J. 1993, AJ, 106, 2486
Hummel, C. A., Mozurkewich, D., Armstrong, J. T., Hajian, A. R., Elias, N. M., II, & Hutter, D. J. 1998, AJ, 116, 2536
Jeffers, H. M., van den Bos, W. H., & Greeby, F. M. 1963, Publications of the Lick Observatory (Mount Hamilton, CA: Univ. of California, Lick Obs.)
Latham, D. W. 1992, in ASP Conf. Ser. 32, IAU Coll. 135, Complementary Approaches to Double and Multiple Star Research, ed. H. A. McAlister & W. I. Hartkopf (San Francisco, CA: ASP), 110
Latham, D. W., Davis, R. J., Stefanik, R. P., Mazeh, T., & Abt, H. A. 1991, AJ, 101, 625
Latham, D. W., Nordström, B., Andersen, J., Torres, G., Stefanik, R. P., Thaller, M., & Bester, M. 1996, A&A, 314, 864
Latham, D. W., Stefanik, R. P., Torres, G., Davis, R. J., Mazeh, T., Carney, B. W., Laird, J. B., & Morse, J. A. 2002, AJ, 124, 1144
Lestrade, J.-F., Preston, R. A., Jones, D. L., Phillips, R. B., Rogers, A. E. E., Titus, M. A., Rioja, M. J., & Gabuzda, D. C. 1999, A&A, 344, 1014
McAlister, H. A., et al. 2005, ApJ, 628, 439
Monnier, J. D., et al. 2007, Science, 317, 342
Nordström, B., Latham, D. W., Morse, J. A., Milone, A. A. E., Kurucz, R. L., Andersen, J., & Stefanik, R. P. 1994, A&A, 287, 338
Nordström, B., et al. 2004, A&A, 418, 989
Perryman, M. A. C., ESA 1997, ESA Special Publication, 1200 (Noordwijk: ESA)
Popović, G. M. 1986, Bull. Obs. Astron. Belgrade, 136, 84
Popper, D. M. 1980, ARA&A, 18, 115
Poveda, A., Herrera, M. A., Allen, C., Cordero, G., & Lavalley, C. 1994, RevMAA, 28, 43
Reid, I. N., Hawley, S. L., & Gizis, J. E. 1995, AJ, 110, 1838
Scardia, M. 1979, Astron. Nachr., 300, 307
Strassmeier, K. G., & Rice, J. B. 2003, A&A, 399, 315,(SR03)
ten Brummelaar, T. A., et al. 2005, ApJ, 628, 453
Torres, G., Stefanik, R. P., Andersen, J., Nordström, B., Latham, D. W., & Clausen, J. V. 1997, AJ, 114, 2764
Valenti, J. A., & Fischer, D. A. 2005, ApJS, 159, 141
VandenBerg, D. A., Bergbusch, P. A., & Dowler, P. D. 2006, ApJS, 162, 375
van Leeuwen, F. 2007, *Hipparcos*ll, the New Reduction of the Raw Data (Dordrecht: Springer)
Wright, J. T., Marcy, G. W., Butler, R. P., & Vogt, S. S. 2004, ApJS, 152, 261
Yi, S., Demarque, P., Kim, Y.-C., Lee, Y.-W., Ree, C. H., Lejeune, T., & Barnes, S. 2001, ApJS, 136, 417
Zucker, S., & Mazeh, T. 1994, ApJ, 420, 806